GEOSCIENCE AUSTRALIA RECORD 2003/19

PETROLEUM GEOLOGY OF THE BASS BASIN – INTERPRETATION REPORT

An Output of the Western Tasmanian Regional Minerals Program

Jane E. Blevin (Compiler)
Geoscience Australia
Petroleum and Marine Division

WITH CONTRIBUTIONS BY

Jane E. Blevin, Chris J. Boreham and Kathe R. Trigg, Geoscience Australia

Aaron Cummings, Ric Daniel, John Kaldi, Simon Lang, Nick Lemon, Rob Root and Peter Tingate, National Centre for Petroleum Geology and Geophysics, University of Adelaide

Alan D. Partridge, Biostrata Pty Ltd.

Canberra Australia 2003

Geoscience Australia

Chief Executive Officer: Neil Williams

Department of Industry, Tourism & Resources

Minister for Industry, Tourism & Resources: The Hon Ian Macfarlane MP
Parliamentary Secretary: The Hon Warren Entsch MP
Secretary: Mark Paterson

© Commonwealth of Australia 2003

This work is copyright. Apart from any fair dealings for the purposes of study, research, criticism or review, as permitted under the *Copyright Act*, no part may be reproduced by any process without written permission. Inquiries should be directed to the Communications Unit, Geoscience Australia, GPO Box 378, Canberra City, ACT, 2601

ISSN: 1448-2177
ISBN: 0 642 46777 3

Bibliographic references:

Blevin, J. (Compiler), 2003. Petroleum Geology of the Bass Basin – Interpretation Report, An Output of the Western Tasmanian Regional Minerals Program. Geoscience Australia, Record 2003/19.

Boreham, C., 2003. Petroleum geochemistry of source rocks, oils and gases. In: Blevin, J. (Compiler), Petroleum Geology of the Bass Basin – Interpretation Report, An Output of the Western Tasmanian Regional Minerals Program, Geoscience Australia, Record 2003/19.

Geoscience Australia has tried to make the information in this product as accurate as possible. However, it does not guarantee that the information is totally accurate or complete. **Therefore, you should not rely solely on this information when making a commercial decision.**

Geoscience Australia Website: www.ga.gov.au

TABLE OF CONTENTS

EXECUTIVE SUMMARY vii

1. INTRODUCTION
1.1 Regional setting and aims of the Bass Basin study 1
1.2 Western Tasmanian Regional Minerals Program 1

2. EXPLORATION HISTORY
2.1 Hydrocarbon accumulations and petroleum systems 5
2.2 Previous exploration 6
2.3 Exploration risks 7
2.4 2002 Acreage Release Areas 7
2.5 2003 Acreage Release Areas 8

3. TECTONIC EVOLUTION
3.1 Key points 17
3.2 Basin structure and regional tectonic setting 17
3.3 Redefinition of basin boundaries and basin nomenclature 19
3.4 Basin structural elements 20
3.5 Basin evolution 22

4. ACCOMMODATION CYCLES AND SEQUENCE STRATIGRAPHY
4.1 Key points 43
4.2 Methods and timescales 43
4.3 Sequences mapped and nomenclature 44
4.4 Accommodation cycles 45
4.5 Otway Megasequence 46
4.6 Durroon Megasequence 47
4.7 Bass Megasequence 48
4.8 Aroo Sequence 53
4.9 Demons Bluff Sequence 55
4.10 Torquay Sequence 56
4.11 Nature and distribution of igneous rocks 59

5. PETROLEUM GEOCHEMISTRY OF SOURCE ROCKS, OILS AND GASES
5.1 Key points 85
5.2 Introduction 85
5.3 Aims, samples and methods 86
5.4 Source rock geochemistry 88
5.5 Petroleum generation and expulsion 91
5.6 Kinetics of petroleum generation 92
5.7 Oil geochemistry 92
5.8 Gas geochemistry 93
5.9 Conclusions 95

6. GEOHISTORY AND MATURITY MODELLING
6.1 Key points 125
6.2 Introduction 125
6.3 Previous studies 126
6.4 Database and methods 126
6.5 Geothermal gradients and heatflow 128
6.6 Thermal modelling 129
6.7 Results from default thermal history models 131
6.8 Palaeoheatflow modelling of the Durroon-1 well 132
6.9 Subsidence modelling 134
6.10 Timing of hydrocarbon generation and expulsion 135
6.11 Conclusions 136

7. HYDROCARBON SEAL EVALUATION
7.1 Key points 167
7.2 Methodology 168
7.3 Water saturation 169
7.4 Interpretation of seal capacity 171

8. DIAGENESIS OF HYDROCARBON RESERVOIRS
8.1 Key points 175
8.2 Dataset and previous work 176
8.3 Stratigraphy and depositional history 176
8.4 Diagenetic history 177
8.5 Thermal setting 182
8.6 Summary 183

9. DEPOSITIONAL ENVIRONMENTS AND FACIES ANALYSIS
9.1 Key points 209
9.2 Depositional setting 210
9.3 Facies interpretations and descriptions 210
9.4 Relationship between facies and reservoir quality 214
9.5 Relationship between facies and seal capacity 215

10. PETROLEUM SYSTEMS AND PLAY ANALYSIS
10.1 Key points 239
10.2 Exploration risks 239
10.3 Source rocks 241
10.4 Reservoir rocks 243
10.5 Seals 244
10.6 Play concepts 245

11. ACKNOWLEDGEMENTS 253

12. REFERENCES 255

APPENDICES - VOLUME II (CD-ROM ONLY)

APPENDIX A. List of petroleum exploration wells in the Bass Basin (Jane Blevin, Geoscience Australia)

APPENDIX B: List of horizons interpreted in the Bass Basin wells (Jane Blevin, Geoscience Australia)

APPENDIX C. Biostratigraphy Reports (Alan Partridge, Biostrata Pty Ltd.)

- **C1.** Palynological analysis of Eocene interval 1380 to 2036 m in Cormorant-1, Bass Basin
- **C2.** Palynological review of Upper Cretaceous units in Durroon-1, Bass Basin
- **C3.** Palynological analysis of Eocene interval 1390 to 2036 m in King-1, Bass Basin
- **C4.** Quantitative palynological analysis of Paleocene to Middle Eocene interval Konkon-1, Bass Basin
- **C5.** Quantitative palynological analysis of eleven cuttings samples from 2266 to 3115 m in Koorkah-1, Bass Basin
- **C6.** Quantitative palynological analysis of Eastern View and Demons Bluff Groups in Poonboon-1, Bass Basin
- **C7.** Palynological analysis of Oligocene sandstones in Squid-1, Bass Basin
- **C8.** Bass Basin palynological project, unravelling a Late Cretaceous to Eocene geological history of large palaeolakes, coastal lagoons and marine bays

APPENDIX D. List of core and cuttings from the Bass Basin analysed for organic geochemistry (Chris Boreham, Geoscience Australia)

APPENDIX E. Vitrinite-inertinite reflectance and fluorescence (VRF™ or VIRF) results for Cormorant-1 and Pelican-5 (Jane Newman, Newman Pty Ltd.)

APPENDIX F. Palynology of coals and claystones from Cormorant-1 and Pelican-5 used for oil-source correlations (Mike Macphail, Australian National University)

APPENDIX G. List of oil and gases in the Bass Basin analysed for this study (Chris Boreham, Geoscience Australia)

APPENDIX H. Small Angle Neutron Scattering (SANS) study on low-ash coals from Cormorant-1 and Pelican-5 (Andrzej Radlinski, Alan Hinde and Chris Boreham, Geoscience Australia)

APPENDIX I. Organic petrology of selected samples from the Bass Basin (Alan Cook, Keiraville Konsultants Pty Ltd.)

APPENDIX J. Uncorrected bottom hole temperature data for Bass Basin wells (Aaron Cummings and Peter Tingate, National Centre for Petroleum Geology and Geophysics)

APPENDIX K. Kinetic modelling of Pelican-5 (Aaron Cummings, National Centre for Petroleum Geology and Geophysics)

APPENDIX L. Mercury injection capillary pressure test results and analytical equipment (Ric Daniel and John Kaldi, National Centre for Petroleum Geology and Geophysics)

APPENDIX M. Core photos of selected wells in the Bass Basin (Simon Lang and Rob Root, National Centre for Petroleum Geology and Geophysics)

EXECUTIVE SUMMARY

The Bass Basin is a moderately explored Cretaceous to Cainozoic intracratonic rift basin on Australia's southeastern margin, underlying the shallow seabed between Tasmania and the Victorian mainland (Bass Strait; Figure 1). The basin contains proven commercial reserves of gas and condensate that are soon to be developed (Yolla gas field, Origin Energy Resources Ltd-operated BassGas Project). Other discoveries in the basin include the White Ibis and Pelican gas fields. To date, the 32 wells drilled have targeted Upper Cretaceous to Middle Eocene reservoirs within fault blocks and anticlinal structures. The targeted succession comprises interbedded fluvio-deltaic and lacustrine sandstones, siltstones and shales. The principal source rocks in the Bass Basin are interbedded coals (ranging from 5 to 25 m thick) and lacustrine shales of early Palaeogene age. Geochemical analyses show these source rocks have generated liquid and gaseous hydrocarbons, with the coals being the dominant source for the liquids (Boreham et al., 2003).

As part of the Commonwealth-funded *Western Tasmanian Regional Minerals Program*, Mineral Resources Tasmania (MRT) initiated a collaborative study of the Bass Basin, in partnership with Geoscience Australia (GA) and the National Centre for Petroleum Geology and Geophysics (NCPGG). Commercial inputs into the project were sought from Biostrata Pty Ltd, SRK Consulting, Fugro MCS and CSIRO. The aim of this work was to enhance the petroleum prospectivity of the northern and western regions of offshore Tasmania through an improved understanding of basin geology, an analysis of petroleum systems elements (source rocks, reservoirs and seals), and enhanced access to basic datasets critical to the exploration industry.

This Record presents the results of the geological, geochemical and biostratigrahic studies. Additional reports and data covering other objectives of the Western Tasmanian Regional Minerals Program (WTRMP) are outlined in Table A1. The key findings of the WTRMP Bass Basin study include:

Petroleum Geochemistry and Geohistory Modelling

- The Bass Basin is prospective for oil and gas generation in areas where adequate quantities of coaly source rocks of early Palaeogene age are buried to depths of approximately 2450 m (onset of oil generation) to 3200 m (2700 to 3200 m onset of oil expulsion/primary migration). The main gas window lies at approximately 3650 m in the Pelican Trough.
- Geochemical analyses have yielded strong evidence that Paleocene to Early Eocene coals have sourced the oil and gas at the Yolla, Pelican and Cormorant accumulations.
- The pattern of hydrocarbon charge indicates generation in the main troughs with migration to structures within the depocentre and along the flanks. Oil migration was followed by gas charge, which has displaced some accumulations. A later phase of oil and water migration below the "Demons Bluff" regional seal during the late Palaeogene to early Neogene is suggested.
- A broad decrease in geothermal gradient occurs from the northwest of the basin towards the southeast.

- The main source rocks linked to hydrocarbon accumulations within the basin entered the oil generation window just prior to and following the deposition of the "Demons Bluff" regional seal.

Geology and Petroleum Systems

- Identification of six Basin Phases and related megasequences/supersequences that correlate to three periods of extension, a rift-transition phase, and two subsidence phases. The complex nature of facies relationships across the basin is attributed to the (mostly) terrestrial setting of the basin until the Middle Eocene, multiple phases of extension, strong compartmentalisation of the basin due to underlying basement fabric, and differential subsidence during extension and early subsidence phases. The "Eastern View Coal Measures" (or "Eastern View Group") has been subdivided into three megasequences (Durroon, Bass and Aroo megasequences). A further three component sequences have been recognised within the Bass Megasequence (Furneaux, Tilana and Narimba sequences). Basin boundaries have also been redefined using seismic and potential field datasets.
- A well audit has identified four main areas of exploration risk (Trigg et al., 2003): a) invalid tests due to artefacts or poor data quality; b) trap integrity and seal risk; c) reservoir quality; and, d) lack of adequate hydrocarbon charge.
- Results of MICP analyses of selected potential seal facies indicate that the average column height of oil is 605 m (density 0.735g/cc) and the average column height of gas is 262 m (density 0.1 g/cc). Facies of lower shoreface, fluvial overbank and lagoonal mudstones show the highest seal capacity. The single sample of the regional sealing facies "Demons Bluff" mudstone showed poor seal capacity.
- A sequence of diagenetic events has been integrated from a range of studies. The lack of marine influence is the key difference between reservoirs of the Bass and Gippsland basins. Early cementation is beneficial in that intergranular porosity is preserved during loading and compaction. Dissolution of the carbonate cement at a later stage results in effective secondary intergranular porosity and permeability. Porosity and permeability is overestimated in some samples due to micro-intragranular porosity in clays.
- Facies analyses indicate the highest ranking reservoir facies are coarse-grained sandstones within fluvial channels, with secondary ranking facies of coarse-grained lacustrine shoreface and foreshore sandstones.
- Biostratigraphic studies have identified lacustrine cycles during the Late Cretaceous to Middle Eocene (Partridge, 2002; Appendix C). Integration with geological data indicate these lakes developed during times of increased accommodation.
- The "Demons Bluff" regional seal was deposited in bay and shallow marine environments during a regional transgressive event. Intraformational seals with potentially high sealing capabilities include mudstones within the *L. balmei* to *N. asperus* zones.
- Optimum play conditions exist within coarse-grained fluvial channel belt sandstones or lacustrine shoreline and deltaic facies sealed by lacustrine deposits within the *L. balmei* zone (Tilana and lower Narimba sequences). Higher risk plays occur within fine-grained lacustrine or coastal lagoon shoreface facies, or in compositionally immature coarse-grained alluvial fan and proximal facies.

Other related outputs from the Western Tasmanian Regional Mineral Program include:

- Well audit report of petroleum exploration wells in the Bass Basin (CD-ROM, Geoscience Australia Record 2003/11).
- Reprocessed seismic data from Surveys T69A and T70A along western Tasmania (Sorell Basin), available in SEG-Y format, with navigation and velocity data included (CD-ROM, Geoscience Australia Record 2003/6).
- Regional potential field study of the Bass Basin, commissioned by Geoscience Australia in support of the WTRMP (CD-ROM, Geoscience Australia Record 2003/4).
- Compilation and review of biostratigraphic data from the Bass Basin (CD-ROM, Geoscience Australia Record 2003/7).
- Basic geological data compilation from the Bass Basin (including bathymetry, gravity and magnetic images; and Excel format downloads of open-file biostratigraphy, porosity/permeability, geochemistry and checkshot data) (CD-ROM, Geoscience Australia Record 2003/17).
- Bass Basin GIS Project (CD-ROM, Geoscience Australia Record 2003/18).

For further information on the Western Tasmanian Regional Mineral Program, Petroleum Program Outputs, please contact Carol Bacon, Managing Geologist, Mineral Resources Tasmania, (03) 6233-8326.

1. INTRODUCTION

J. Blevin, Geoscience Australia

1.1 REGIONAL SETTING AND AIMS OF THE BASS BASIN STUDY

The Bass Basin is a moderately explored Cretaceous to Cainozoic intracratonic rift basin on Australia's southeastern margin (Figure 1.1). The basin contains proven commercial reserves of gas and condensate that are soon to be developed (Yolla gas field, Origin Energy Resources Ltd-operated BassGas Project). Other discoveries in the basin include the White Ibis and Pelican gas fields. To date, the 32 exploration wells have targeted Upper Cretaceous to Middle Eocene reservoirs within fault blocks and anticlinal structures. The targeted succession comprises interbedded fluvio-deltaic and lacustrine sandstones, siltstones and shales. The principal source rocks in the Bass Basin are interbedded coals (ranging from 5 to 25 m thick) and lacustrine shales of Palaeogene age. Geochemical analyses show these source rocks have generated liquid and gaseous hydrocarbons, with the coals being the dominant source for the liquids (Boreham et al., 2003). Volcanic rocks are common throughout the basin as sills and flows, often associated with large rift faults and accommodation zones. Petroleum exploration of the Bass Basin began in 1965. Of the 32 wells drilled, only four contain commercial to sub-economic accumulations. A review of exploration wells has identified four main areas of risk (Trigg et al., 2003): a) invalid tests due to artefacts or poor data quality; b) trap integrity and seal risk; c) reservoir quality; and, d) lack of adequate hydrocarbon charge.

Under the auspices of the Commonwealth-funded Western Tasmanian Regional Minerals Program (WTRMP; Section 1.2), Mineral Resource Tasmania sponsored and coordinated a study of the Bass Basin. Modules of the work program were undertaken at Geoscience Australia (seismic and well log interpretation, basin mapping, petroleum geochemistry), the National Centre for Petroleum Geology and Geophysics (geohistory modelling, reservoir, seal and facies analyses), and through a commercial contract with Biostrata Pty Ltd (biostratigraphic analyses). Most of the results of the Bass Basin study are presented in this Record. Other products associated with the Bass Basin and the WTRMP are shown in Table 1.1.

Collectively, the study aimed to address the following objectives:

- improving prospectivity and reduce exploration risk though a better understanding of basin forming processes, particularly those relating to hydrocarbon generation and entrapment; and,
- upgrading the quality and access to exploration data (including seismic reprocessing programs, biostratigraphic and geochemical databases).

1.2 WESTERN TASMANIAN REGIONAL MINERALS PROGRAM

In 1998, the Commonwealth Government of Australia established the Regional Minerals Program to encourage a coordinated regional approach to minerals development (Woodward-Clyde, 1999). The Western Tasmanian Regional Minerals Program (WTRMP) forms part of this program and is a tripartite agreement

between the Commonwealth and Tasmanian Governments and the Minerals Industry. The program covers the areas of western and northern Tasmania as far east as the River Tamar, including the offshore Bass and Sorell basins (Figure 1.2). The WTRMP is coordinated by Mineral Resources Tasmania (MRT) in conjunction with a Management Committee consisting of representatives from the Minerals Industry in Tasmania, MRT and the Commonwealth Department of Industry, Tourism and Resources.

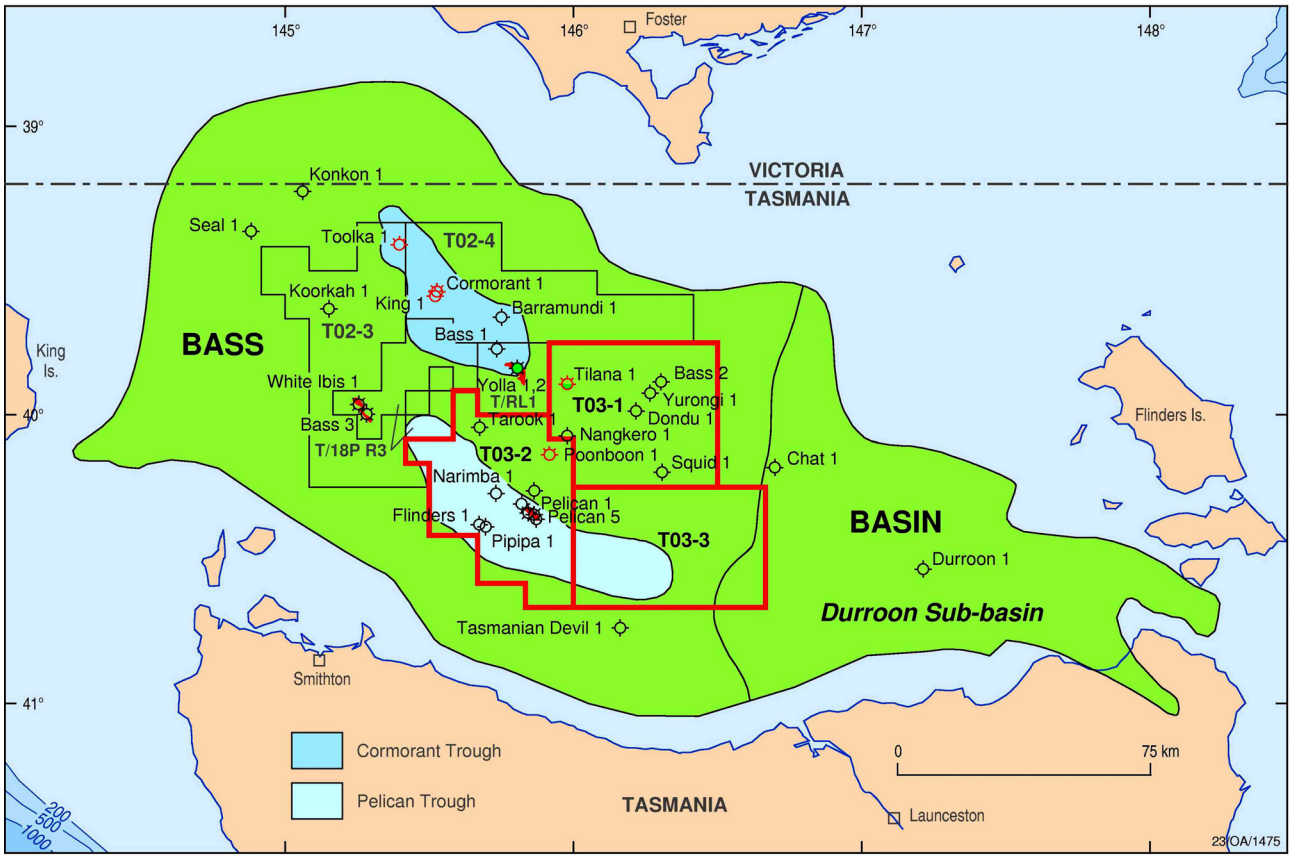
The aims of the WTRMP include addressing the uncertainty over the pricing and forms of available energy – issues which are critical to the expansion of existing facilities and the development of new projects that will further utilise the wealth of northwestern Tasmania. In September 2000, as part of this initiative, MRT sought external consultation to scope projects that could assist in the implementation of recommendations contained in the Final Regional Development Plan (http://www.mrt.tas.gov.au). The result was a series of proposed studies aimed at enhancing prospectivity and encouraging exploration in the northwest Tasmania offshore region (Fardon, 2000). These studies included the following topics: 1) sequence stratigraphy of the Bass Basin; 2) the effects of volcanics and coals on seismic data; 3) biostratigraphic review of the Bass Basin; 4) thermal maturation modelling of the Bass and Sorell basins; 5) study of reservoir quality in the Bass Basin; 6) reprocessing of seismic data in the Sorell Basin; and, 7) updated palaeogeographic maps of the Bass Basin (Fardon, 2000). In addition, the recommendations recognised the importance of ready access to basic geological datasets to explorers in the region.

In early 2001, MRT established a collaborative project to address the recommendations of Fardon (2000). The collaborative partners included MRT, Geoscience Australia (GA), and the National Centre for Petroleum Geology and Geophysics (NCPGG). Services were also sought through commercial contracts with Biostrata Pty. Ltd., SRK Consulting and Fugro Multi Client Services (formerly Seismic Australia). The results of this work are now available as a series of reports and basic data downloads (Table 1.1). This Geoscience Record addresses the research topics 1 to 5, and 7, as outlined by Fardon (2000). Reprocessed seismic data (Fardon, 2000; research topic 6) is now available as Geoscience Australia Record 2003/6 (Fleming and Blevin, 2003). For further information on this or other WTRMP products, please contact Mineral Resources Tasmania, or the Sales Centre, Geoscience Australia (http://www.ga.gov.au).

Table 1.1 List of products produced as part of the Western Tasmanian Regional Minerals Program. These products are available through Mineral Resources Tasmania, or the Sales Centre, Geoscience Australia (02 6249-9519). These products are available at the cost of transfer.

Product Format	Title	Publication Number
CD-ROM, Hardcopy	Petroleum geology of the Bass Basin – interpretation report	Geoscience Australia Record 2003/19
CD-ROM	Regional potential field interpretation report, Bass Basin	Geoscience Australia Record 2003/4
CD-ROM	Western Tasmania regional seismic data, selected reprocessed lines from seismic surveys T69A and T70A	Geoscience Australia Record 2003/6
CD-ROM	Review and compilation of open file micropalaeontology and palynology data from offshore Tasmania	Geoscience Australia Record 2003/7
CD-ROM	An audit of petroleum exploration wells in the Bass Basin, 1965-1999	Geoscience Australia Record 2003/11
CD-ROM	Bass Basin, basic data compilation (including bathymetry, gravity and magnetic images; biostratigraphy, porosity, permeability, geochemistry, checkshot, deviation and seismic navigation data)	Geoscience Australia Record 2003/17
CD-ROM	Bass Basin GIS Project	Geoscience Australia Record 2003/18

Figure 1.1 Location map of the Bass Basin and adjacent region, southeastern Australia. The basin outline, permits, well and field locations, including the 2002 (black) and 2003 (red) Acreage Release areas, are also shown.



2. EXPLORATION HISTORY

J. Blevin and K. Trigg, Geoscience Australia

The Bass Basin is a moderately explored basin with 32 wells drilled since 1965 (Figure 2.1). The basin has a drilling density of approximately one well per 1,320 km^2. Similar to other basins along the Australia's southern margin, exploration has occurred in phases. Two areas in the western Bass Basin were gazetted as part of the 2002 Release of Offshore Petroleum Exploration Areas, and a further three were released in 2003 offshore acreage release round (Figure 2.1). There is one current permit, T/18P (R3), operated by Origin Energy Resources Limited, and one retention lease, T/RL1, also held by Origin Energy Resources Limited.

2.1 HYDROCARBON ACCUMULATIONS AND PETROLEUM SYSTEMS

The hydrocarbons discovered to date on the southern margin of Australia have been assigned to the Austral Petroleum Supersystem based on the age of their source rocks and common tectonic history (Austral A3; Edwards et al., 1999). In the Bass Basin, exploration drilling has confirmed hydrocarbon accumulations at Yolla, Pelican, White Ibis and Cormorant, reservoired in sands of Paleocene to Eocene age (*L. balmei* to *M. diversus* zones). At present, only the accumulation at Yolla is being considered for commercialisation ($400M Origin Energy-operated BassGas Project; The Australian Financial Review, 2002). The project will produce natural gas and liquids from the Yolla field that will be piped under Bass Strait and processed in a new plant to be built near Lang Lang, southeastern Victoria (Wood, 2003). The project is expected to come on-line in the third quarter of 2004 (Wood, 2003).

The Bass Basin oils and gases have a terrestrial source affinity and are geochemically similar to the Gippsland Basin oils (Summons, 1996). The Yolla-1 oil is a medium-gravity (46° API) crude with a correspondingly high wax content, whereas the Cormorant-1 oil is a heavy crude (21° API) as a result of biodegradation (Edwards et al., 1999). Geochemical analyses of the hydrocarbons indicate an input of predominantly land-plant material to the source kerogens, and there is no evidence of marine organic matter (Edwards et al., 1999).

Previous authors (e.g., Nicholas et al., 1981; Miyazaki, 1995) have suggested that liquid hydrocarbons were generated from disseminated organic matter within carbonaceous claystones, while gases were sourced mainly from coaly facies. However, recent oil-to-source correlations undertaken as part of this study (Chapter 5; Boreham et al., 2003) have shown that the oils were sourced from Tertiary coals, particularly those concentrated within the Middle to Early Eocene succession. Oils in the basin are a single oil population (Yolla and Pelican accumulations), while in-reservoir biodegradation of the Cormorant oil has resulted in its statistical classification as a separate oil family (Chapter 5; Boreham et al., 2003). Recent fluid inclusions studies (Kempton et al., 2002) have identified palaeo-oil zones at Yolla-1 and Cormorant-1, along with suspected zones at King-1 and Pelican-5. In addition, several potential palaeo-hydrocarbon zones were

identified at Yurongi-1, Chat-1, Seal-1, Tilana-1 and Squid-1. These zones are characterised by aqueous inclusions containing small amounts of oil (Kempton et al., 2002). Overall, the pattern of hydrocarbon distribution in the basin shows that hydrocarbon generation has occurred in the Cormorant, Yolla and Pelican troughs with migration into structures within those depocentres and on the adjacent flanks.

2.2 PREVIOUS EXPLORATION

Commercial exploration of the Bass Basin began in the early 1960s with permits awarded to Hematite Petroleum Pty Ltd (BHP) and Esso Exploration and Production Australia Ltd (Esso) (Robinson, 1974; Smith, 1986). Bass-1, the first well in the basin, was drilled by Esso in 1965. Esso's subsequent exploration program included 15 wells drilled over the ensuing nine year period from 1966 to 1974. During this exploration phase, gas and condensate accumulations were discovered at Pelican-1 and Pelican-2, while numerous gas shows were recorded at Bass-3, Pelican-3, Poonboon-1, Toolka-1, and Aroo-1. Several thin pay zones were encountered within the Eastern View Group at Cormorant-1, including a 2 m oil column, and 2 m and 3 m gas and condensate columns (Ozimic et al., 1986). Hematite Petroleum Pty Ltd drilled a further four wells between 1974 and 1978, however no further hydrocarbon discoveries were made. The stratigraphic terms in the following exploration review reflect the nomenclature used at the time of drilling (Figure 2.2).

Yolla-1, drilled in 1985 by Amoco Australia Petroleum Company, was sited as a crestal test of the Eastern View Group within a four-way dip and fault-closed structure. Light oil and associated gas shows were recorded in sands at the "Top Eastern View Group". Wireline pressure tests (RFTs) and logs indicated the presence of at least three separate gas columns within sandstones of the Eastern View Group. Final log analysis indicates that Yolla-1 encountered approximately 30 m of net gas pay over a 278 m interval (Lennon et al., 1999). In addition, the well penetrated a gross hydrocarbon column of 31 m (wet gas cap of 20.4 m overlying a 10.6 m oil leg). The stacked hydrocarbon accumulations within the Eastern View Group at Yolla are sealed by relatively thick and laterally continuous intraformational shales that were deposited in a lacustrine environment (Lennon et al., 1999).

In 1998, Boral Energy Resources Ltd and partners drilled two wells in the central Bass Basin – Yolla-2 and White Ibis-1. Both wells encountered gas columns in the Paleocene to Lower Eocene succession, with liquids-rich gas recovered from reservoirs in wireline tests (Lennon et al., 1999). Yolla-2 was an appraisal well that confirmed a resource of between 450 to 600 billion cubic feet of liquids-rich gas and 70 million barrels of oil in place (OIP). The White Ibis-1 well, located in exploration permit T/18P, was a crestal test over a large basement high updip of Bass-3. Formation pressure data suggests the presence of a thin oil rim, with the well encountering a gas accumulation estimated at 85 BCF of oil and gas in place (OGIP).

Barramundi-1, drilled by GLOBEX Far East in 1999, is the most recent well in the Bass Basin. The well tested a faulted rollover structure with closure at the top of the Eocene succession. A large AVO anomaly corresponding to interpreted thick sands was interpreted (pre-drill) as evidence of a valid hydrocarbon accumulation (Crist et al., 2001). No commercial quantities of hydrocarbons were encountered during drilling

at Barramundi-1. Failure of the well was attributed to breaching of the trap during Miocene inversion which resulted in faulting and fracturing of the overlying Demons Bluff regional seal.

2.3 EXPLORATION RISKS

As part of the Western Tasmanian Regional Minerals Program (WTRMP), Geoscience Australia undertook an audit of all 32 wells drilled in the basin since 1965. The well audit is available as a separate report (Trigg, et al., 2003; Trigg and Blevin, 2003) through Mineral Resources Tasmania or Geoscience Australia (see Table 1.1). Details of the wells drilled in the Bass Basin from 1965 to 1999 are summarised in Table 2.1.

The outcome of the well audit showed four main areas of exploration risk (Trigg et al., 2003; Trigg and Blevin, 2003): a) invalid tests due to artefacts or poor data quality; b) trap integrity and seal risk; c) reservoir quality; and, d) lack of hydrocarbon charge. Work undertaken as part of the WTRMP study aimed to provide a better understanding of these factors to reduce the perception of risk (Chapters 3 to 10).

2.4 2002 ACREAGE RELEASE AREAS

Areas T02-3 and 4 are located in western Bass Strait, north of Tasmania and east of King Island (Figure 2.1). They comprise 40 and 38 graticular blocks, respectively. The release areas cover approximately 2680 (T02-3) and 2550 km^2 (T02-4), for a total area of approximately 5230 km^2. Water depths across both areas are less than 75 metres. The release areas are adjacent to current exploration permit T/18P (R3) operated by Origin Energy Resources Limited, and retention lease T/RL1, also held by Origin Energy Resources.

The 2002 Release Areas (T02-3 and T02-4) are located in the western part of the Bass Basin. Area T02-3 includes the Koorkah-1 and Toolka-1A wells, while Area T02-4 includes the King-1, Cormorant-1 and Barramundi-1 wells. A number of exploration wells with strong hydrocarbon shows surround the current release areas (Table 2.1), including the Yolla gas field located south of T02-4. Play types in the 2002 Release Areas are likely to be related to reactivated rift structures such as inversion anticlines and faulted controlled traps, with primary targets within the Eastern View Group.

Area T02-3

Koorkah-1 targeted Upper Cretaceous to Lower Eocene sandstones of the Eastern View Group. Post-drill interpretations show that the primary objective sandstones had low porosity and permeability due to diagenetic processes. Sediments at Koorkah-1 were thermally immature to marginally mature and deemed to be gas-prone. Traces of free oil evident from 2,400 m to TD were apparently derived from a deeper mature source rock that was relatively rich in resinite.

Toolka-1A was drilled in 1974 to evaluate the stratigraphic equivalents of the Middle Eocene hydrocarbon-bearing sands encountered nearby at Cormorant-1. The discontinuous nature of these sands resulted in only minor oil and gas shows being recorded. The anticlinal structure drilled at Toolka-1A was deemed to be a valid test, with the failure of the well attributed to lean source rocks and lack of reservoir sands.

A 'flat spot anomaly' has been identified on intersecting seismic lines in the western part of Area T02-3 (Das and Lemon, 2000a). This anomaly has the seismic characteristics of a gas-liquid contact, with a two-way time structure map showing that its occurrence coincides with an elongate, northeast/southwest-trending faulted anticline at the Eastern View Group stratigraphic level (Das and Lemon, 2000a). The anomaly covers approximately 40 km^2 and has a maximum structural relief of about 40 milliseconds two-way time. More detailed amplitude-versus-offset (AVO) analysis is needed to fully understand the nature of these seismic features, and to assess their validity as indicators of in-place hydrocarbon accumulations.

Area T02-4

Drilled in the central Bass Basin during 1970, Cormorant-1 encountered significant oil, gas and condensate shows within the Eastern View Group (Figure 2.3). The Cormorant structure is a large, northwest-southeast trending anticline that formed as a result of Miocene compression. Several pay zones were encountered within the Eastern View Group, including a 2 m oil column, and 2 m and 3 m gas and condensate columns. The lack of an economic accumulation at Cormorant-1 was attributed to ineffective seal and late development of the trapping structure.

King-1 was drilled in 1992 as a follow-up to Cormorant-1. The well targeted basal Eocene fluvial sands (*N. asperus* spore/pollen zone) of the Eastern View Group in a crestal position on the previously defined Cormorant anticlinal structure. Although the target sands were water saturated at King-1, they displayed excellent reservoir characteristics (porosities of 20 to 30% and permeabilities of 0.7 mD to 1D). The King-1 structure was found to be valid, and potential source rocks were assessed as mature, with encouraging hydrocarbon shows. Possible reasons for failure include poor migration pathways into the structure from mature Paleocene source rocks and possible fault breaching of the Demons Bluff top seal.

2.5 2003 ACREAGE RELEASE AREAS

Areas T03-1, -2 and -3 are located in the Bass Strait region, north of Tasmania and west of Flinders Island (Figure 1). Each release area consists of 40 graticular blocks, covering areas of approximately 2670 km^2 (T03-1), 2665 km^2 (T03-2), and 2660 km^2 (T03-3). Water depths across the areas are less than 75 metres. The release areas are adjacent to current exploration permit T/18P (R3) operated by Origin Energy Resources Limited, and retention lease T/RL1, also held by Origin Energy Resources.

The 2003 Release Areas are located in the central part of the Bass Basin. Area T03-2 overlies the Pelican gas field, which was discovered by Esso in 1970. A number of exploration wells with strong hydrocarbon shows surround the current release areas, including the Yolla field located to the west of T03-1. Play types in the area include rotated fault blocks with drape closure (Figure 2.4), and anticlinal structures that formed in shallower strata during Miocene compression. A host of stratigraphic plays also exist, but these are unlikely to be primary targets. Descriptions of the structures and drilling results from exploration wells in the 2003 Release Areas are presented in Table 2.1 – these include: Area T03-1/Tilana-1, Nangkero-1, Bass-2,

Yurongi-1, Dondu-1 and Squid-1; and, Area T03-2/Tarook-1, Poonboon-1, Narimba-1, Flinders-1, Pipipa-1, and Pelican-1 to -5 wells (including the Pelican gas field). No wells have been drilled in T03-3.

Table 2.1 Drilling results and hydrocarbon occurrences in the Bass Basin.

Well Name, Operator and Year	Play Type and Target Horizon(s)	Results	Comments
Aroo-1 Hematite Petroleum 1974	Drape over basement high; Paleocene to Early Eocene sands	P&A Fluorescence, minor gas shows	Structural interpretation inaccurate due to the presence of volcanic rocks near target horizons.
Barramundi-1 Globex Far East 1999	Faulted rollover; Paleocene to Early Eocene sands	P&A CO^2 shows	Failure due to breach of regional seal.
Bass-1 Esso E & P Australia 1965	Carbonate reef complex	P&A No shows	Pre-drill interpreted reef structure was invalid. Intersected volcanic section of pyroclastic material.
Bass-2 Esso E & P Australia 1966	Anticlinal structure; Early Eocene sands	P&A No shows	No seal facies; igneous intrusion near TD.
Bass-3 Esso E & P Australia 1966	Anticlinal structure over basement fault block; Mid-Eocene sands	P&A Minor gas	Minor gas shows between 2054.05 to 2055.57 m. Deeper section was water wet. Later drilling of White Ibis-1 in 1998 showed that Bass-3 was not optimally located over the structure.
Chat-1 Bridge Oil Ltd 1986	Faulted dependent closure; Eocene and younger	P&A No shows	Lack of hydrocarbon charge; volcanics intersected near TD.
Cormorant-1 Esso E & P Australia 1970	Anticlinal structure; Paleocene to Early Eocene sands	P&A Minor gas and oil legs	Several pay zones encountered within the Eastern View Group, including a 2 m oil column, and 2 m and 3 m gas and condensate columns. Failure caused by ineffective seal due to late stage reactivation of trap.
Dondu-1 Esso E & P Australia 1973	Anticlinal structure; Paleocene to Early Eocene sands	P&A No shows	Dispersed minor gas shows associated with coals. Good reservoir quality sands above 2743 m.
Durroon-1 Esso E & P Australia 1972	Fault block with updip closure; Early Cretaceous	P&A No shows	No structural closure, lack of seal facies, variable porosity and permeability
Flinders-1 SAGASCO Resources 1992	Fault block; Early Eocene sands	P&A No shows	Water saturated; igneous intrusion near primary objective.
King-1 SAGASCO Resources 1992	Anticlinal structure; Paleocene to Early Eocene sands	P&A Fluorescence, gas shows, trace oil	Water saturated reservoir.
Konkon-1 Esso E & P Australia 1973	Four-way dip closed structure; Paleocene to Early Eocene sands	P&A No shows	Lack of reservoir and regional seal units.
Koorkah-1 Amoco Australia Exploration 1985	Anticlinal structure; Paleocene to Early Eocene sands	P&A No shows	Poor reservoir quality, possible lack of hydrocarbon charge.
Nangkero-1 Hematite Petroleum 1974	Fault block with overlying drape closure; Early to Middle Eocene sands	P&A No shows	Good reservoir and seal rocks encountered.
Narimba-1 Esso E & P Australia 1973	Anticlinal structure; Early Eocene	P&A No shows	Lack of hydrocarbon charge.

Pelican-1 Esso E & P Australia 1970	Anticlinal structure; Maastrichtian to Early Paleocene sands	P&A Gas and condensate discovery	Non-commercial accumulation with 12 gas/condensate-bearing sands between 2471 and 3162 m KB.
Pelican-2 Esso E & P Australia 1970	Anticlinal structure; Maastrichtian to Early Paleocene sands	P&A Gas and condensate	Appraisal well of gas/condensate discovery at Pelican-1. 16 gas/ condensate-bearing sands between 2272 and 3066 m KB.
Pelican-3 Esso E & P Australia 1972	Fault block; Late Paleocene sands	P&A Minor gas shows, weak fluorescence	Hydrocarbon-bearing sands encountered at Pelican-1 and -2 (Lower *M. diversus*) were absent at Pelican-3.
Pelican-4 Hematite Petroleum 1979	Anticlinal structure; Maastrichtian to Early Paleocene sands	P&A Gas and condensate shows	Further appraisal of gas/condensate-bearing sands at Pelican-1 and -2. Also aimed to test flow characteristics of reservoirs – however sands were too tight to conduct production tests. Three main gas/condensate-bearing intervals encountered, with minor gas and fluorescence recorded in thinner beds.
Pelican-5 Amoco Australia Exploration 1985	Faulted anticlinal structure; Maastrichtian to Early Eocene sands	P&A Gas and condensate flows (DST)	Further testing of Pelican structure. Six DSTs with 2 flows. Log evaluation indicates moveable hydrocarbons at various levels from 2750 to 4050 m KB. Low permeability reservoirs encountered.
Pipipa-1 Hematite Petroleum 1982	Faulted anticlinal structure; Early Eocene sands	P&A Trace gas, weak fluorescence	Good reservoir and seal rocks encountered. Water saturated.
Poonboon-1 Esso E & P Australia 1972	Anticlinal structure, drape over fault block; Late Paleocene to Eocene sands	P&A No shows	Good reservoir and seal rocks encountered. Water saturated. Minor gas kicks associated with coals.
Seal-1 Bridge Oil Ltd 1986	Anticlinal structure; Paleocene to Early Eocene sands	P&A No shows	Lack of hydrocarbon charge (access to mature source rocks).
Squid-1 Weaver Gas & Oil Corporation Australia 1984	Faulted anticlinal structure and overlying Oligocene sand lens; Late Cretaceous to Eocene sands	P&A No shows	Minor gas kicks associated with coals.
Tarook-1 Esso E & P Australia 1972	Low relief anticlinal structure; Early to Middle Eocene sands	P&A No shows	Good reservoir and seal rocks encountered.
Tasmanian Devil-1 Weaver Gas & Oil Corporation Australia 1984	Tilted fault block; Eocene and older sands	P&A No shows	Strata penetrated was significantly different to pre-drill prediction.
Tilana-1 Amoco Australia Exploration 1985	Anticlinal structure; Late Cretaceous to Eocene sands	P&A Minor oil and gas shows	Fluorescence recorded over intervals 3081 to 3096, 3260 and 3573 m KB. Overmature sediments may be due to local intrusions. Target sands had low permeability and porosity.
Toolka-1 Esso E & P Australia 1974	Anticlinal structure; Paleocene to Early Eocene sands	P&A Gas shows, Minor oil	Discontinuous reservoir sands.
White Ibis-1 Boral Energy Resources 1998	Anticlinal structure; Paleocene to Early Eocene sands	P&A Gas discovery	Suspended gas discovery.
Yolla-1 Amoco Australia Exploration 1985	Faulted basement high with dip and fault closure; Paleocene to Early Eocene sands	Suspended Condensate, gas and oil discovery	Production due to come on-line in 2004 (Origin Energy operated BassGas Project).

Yolla-2 Premier Oil Australasia 1998	Appraisal well of Yolla-1 downdip along anticline	P&A Gas shows	Successful in evaluating the Yolla accumulation.
Yurongi-1 Esso E & P Australia 1973	Anticlinal structure; Late Paleocene to Eocene sands	P&A No shows	Good reservoir and seal rocks encountered.

Figure 2.1 Location map of the Bass Basin and adjacent region, southeastern Australia. The basin outline, permits, well and field locations, including the 2002 (black) and 2003 (red) Acreage Release areas, are also shown.

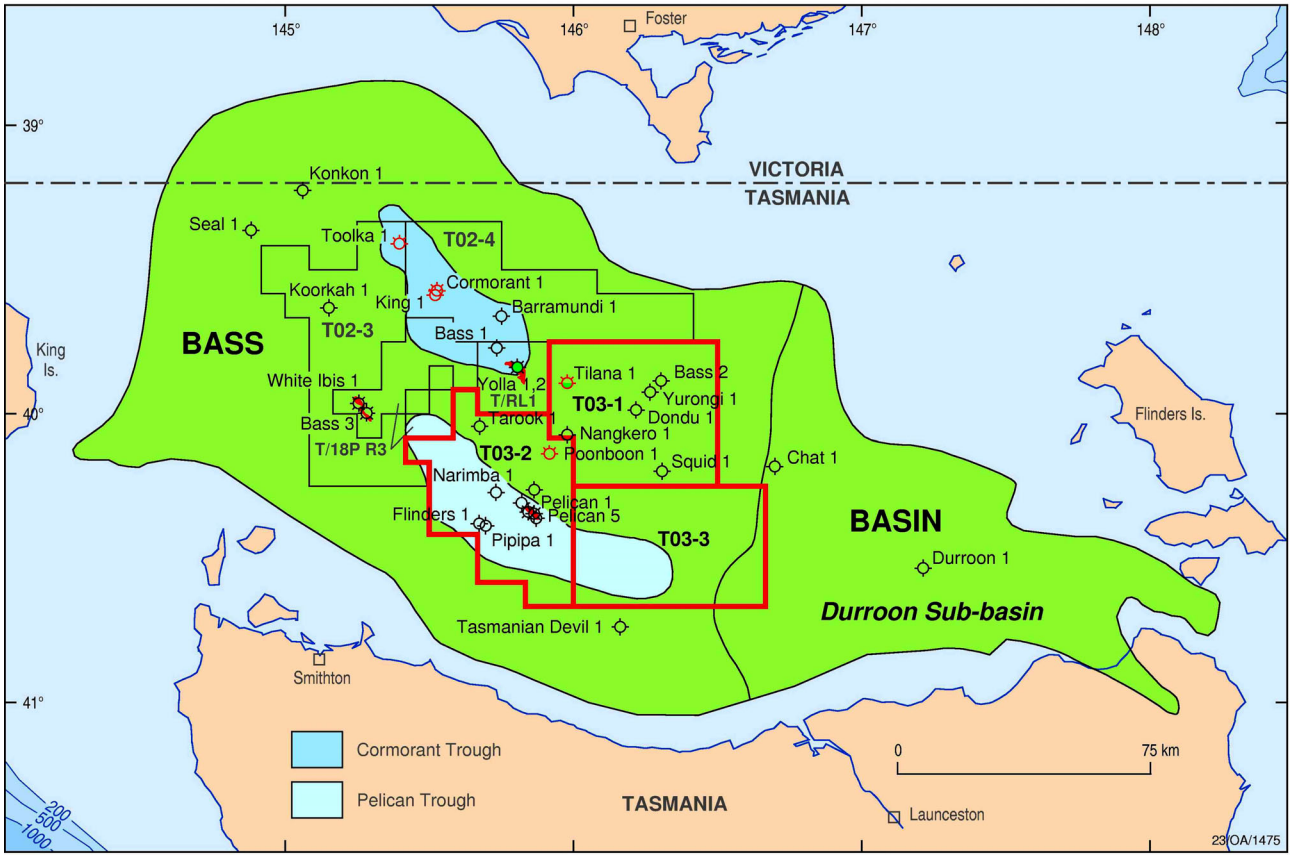


Figure 2.2 Generalised stratigraphy of the Bass Basin (after Lennon et al., 1999), including hydrocarbon accumulations and shows.

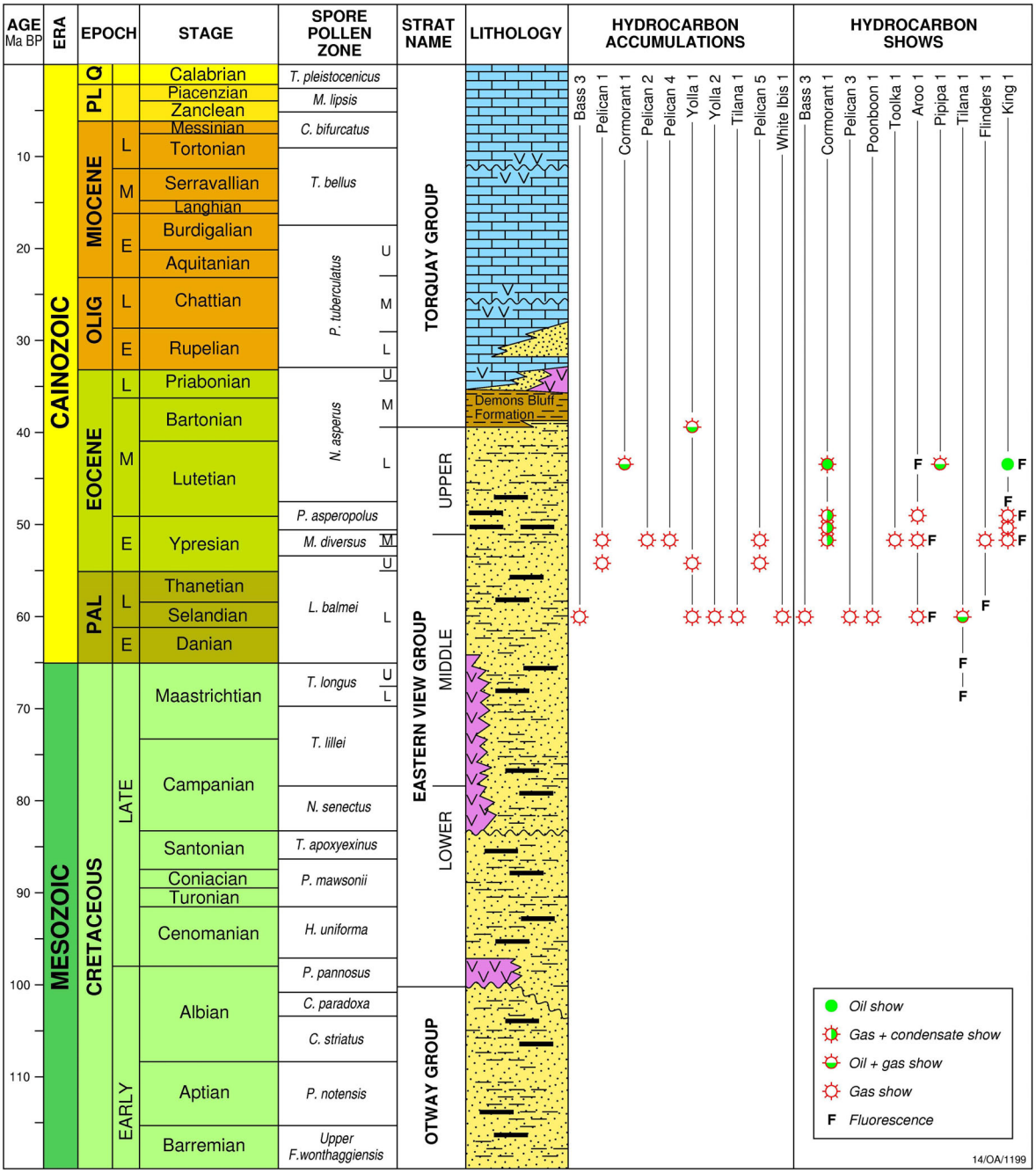


Figure 2.3 Seismic line across the Cormorant Anticline in the northwestern Bass Basin. The anticline formed as a result of Miocene compression. Cormorant-1 was drilled into a minor crestal collapse graben, and encountered several pay zones within the Eastern View Group, including a 2 m oil column, and 2 m and 3 m gas and condensate columns. The well also intersected several volcanic horizons (Late Oligocene, 0.68 ms TWT; sill at 1.99 ms TWT). This seismic image is used with the permission of Fugro MCS.

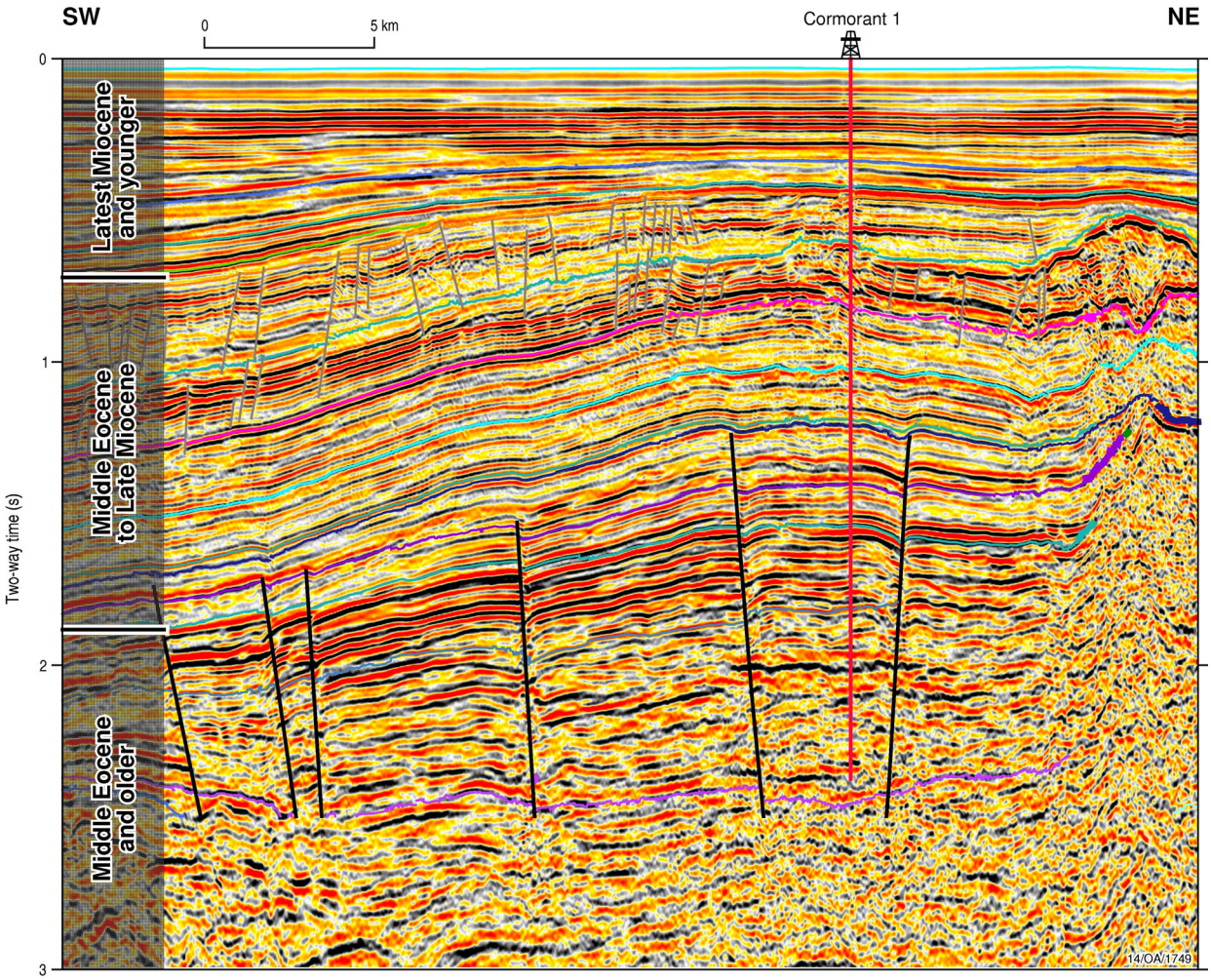
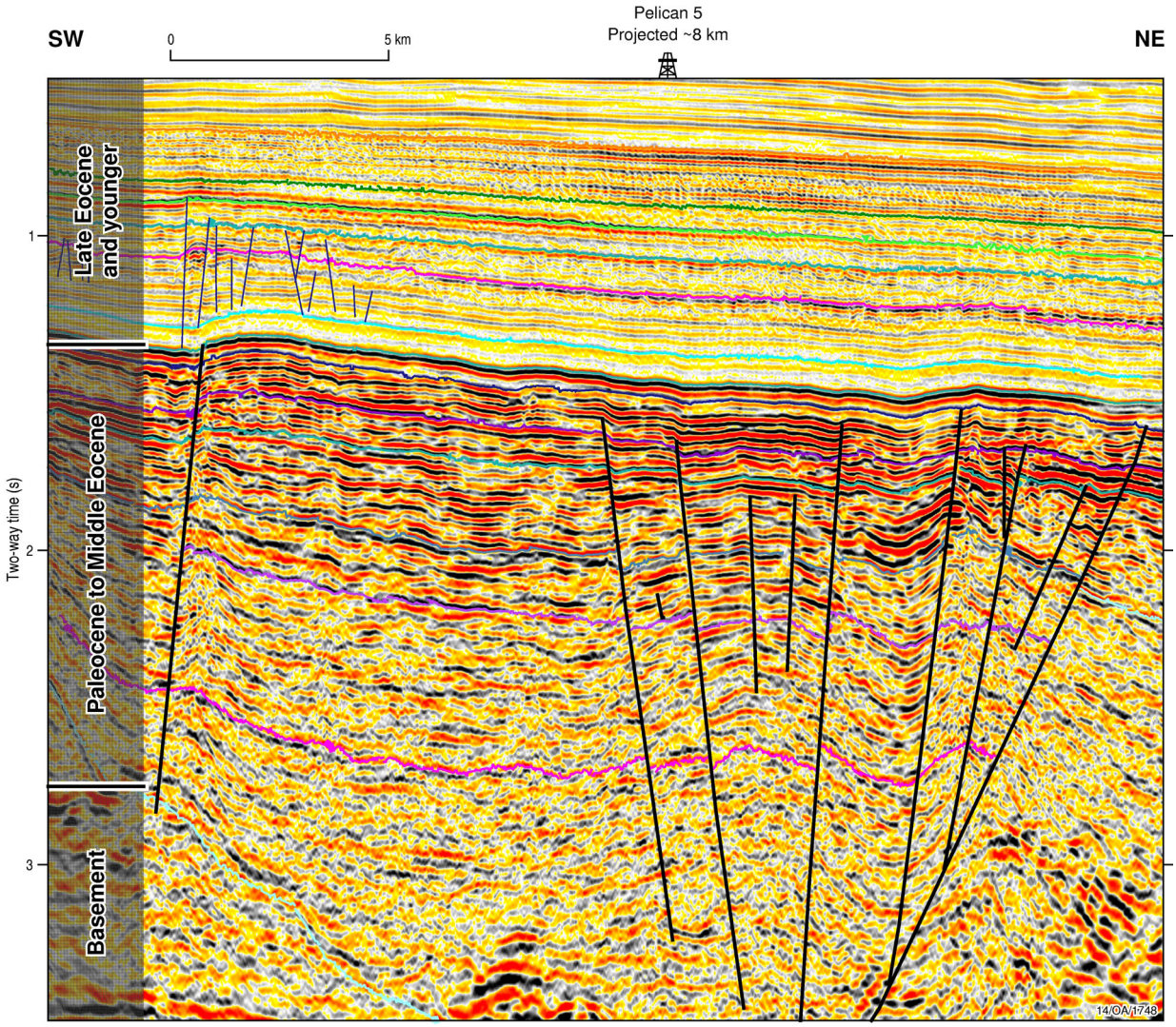


Figure 2.4 Seismic line across the Pelican Trough in Release Area T03-2. Exploration well Pelican-5 was drilled into a crestal collapse structure within the handing well, and is projected for correlation purposes. This seismic image is used with the permission of Fugro MCS.



3. TECTONIC EVOLUTION

J. Blevin, Geoscience Australia

3.1 KEY POINTS

- The formation of the Mesozoic Bass Basin was strongly controlled by the fabric of Proterozoic and Palaeozoic basement terranes that underlie the basin. In the western Bass Basin, basement rocks are Proterozoic fold belt metasediments, while in the east, the basin is underlain by metasediments and granitic intrusions of the Palaeozoic Lachlan Fold Belt.
- The Bass Basin is dissected by a north-to-northeast-trending accommodation structure – the Chat Accommodation Zone. A change in rift polarity is observed across this zone. The Chat-1 well was drilled near this accommodation zone and intersected dolerites at total depth.
- The formation of the Chat Accommodation Zone was probably controlled by an underlying terrane boundary within basement, possibly the boundary between the Proterozoic and Palaeozoic fold belts. The zone sub-divides the Bass Basin into the Durroon Sub-basin (east) and the Cape Wickham Sub-basin (west).
- The Mesozoic Bass Basin formed through multiple periods of upper crustal extension associated with three main regional events: a) rifting in the Southern Margin Rift System (Stagg et al., 1990) to the west; b) rifting associated with the formation of the Tasman Basin to the east; and, c) prolonged separation, fragmentation and clearance between the Australian and Antarctic plates along the western margin of Tasmania.
- The amount and rate of subsidence varied across the basin, particularly between the Cape Wickham and Durroon sub-basins. Structural elements within the Cape Wickham Sub-basin also experienced different subsidence histories.
- Three phases of extension are recognised based on seismic mapping and well log interpretations. It is likely that the latest stage of extension was the result of far-field stresses and was oblique in orientation. The late Early Eocene to Middle Eocene was a time of rift-transition, when it appears that the effects of intra-plate stresses progressively waned from east to west, as Antarctica moved further south relative to the west Tasmanian margin.
- Most of the coaly source rocks now typed to liquid hydrocarbon generation (Chapter 5; Boreham et al., 2003) were deposited during the period of late Early Eocene to Middle Eocene rift-transition.
- A combination of factors including multiple rift events, a complex basement fabric, differential subsidence, and deposition within a terrestrial landlocked basin (until the Middle Eocene) has resulted in complex facies relationships across the basin.

3.2 BASIN STRUCTURE AND REGIONAL TECTONIC SETTING

The Bass Basin is a northwest-trending, intracratonic rift basin that underlies the Bass Strait region between northern Tasmania and southern Victoria (Figure 3.1). The basin covers an area of approximately 42,000 km^2, and is separated from the Otway Basin to the west and northwest by the King Island High, and from

the Gippsland Basin to the northeast by Flinders Island and the Bassian Rise. The orientation of rift-related extensional stresses in the Bass Basin has been proposed as north-northeast, resulting in a series of west to northwest-striking basement-controlled normal faults offset along strike by northeast-trending accommodation zones (Etheridge et al., 1985; Young et al., 1991; Gunn et al., 1996; Lennon et al., 1999). In the Otway Basin, Hill et al. (1994) suggest that Early Cretaceous extension may have been broadly north-south across an area with pre-existing northeast and northwest basement fabrics. The Bass Basin is characterised by a half-graben structural style, with tilted Palaeozoic and Proterozoic basement blocks showing large scale offset along northeast and southwest dipping normal faults. Fault throws are in the order of 3 to 5 km, with the total sedimentary succession (syn-rift and post-rift) reaching thicknesses of 8 to 10.5 km (Williamson et al., 1987). The deepest depocentres in the basin have been informally named the Cormorant, Yolla, and Pelican troughs (Lennon et al., 1999). The structural style of the eastern Bass Basin differs significantly, and this eastern region has been referred to as the Durroon Basin or Sub-basin (Baillie and Pickering, 1991; Das and Lemon, 2000b).

The rifted margins of eastern and southern Australia formed during multiple periods of extension associated with the fragmentation and dispersal of Gondwana in the Late Jurassic to early Palaeogene (Veevers and Ettreim, 1988; Veevers et al., 1991). Along with the flanking Otway, Gippsland and Sorell basins, the Bass Basin was initiated in the Late Jurassic to Early Cretaceous (Tithonian-Barremian) as part of the Southern Rift System (SRS; Stagg et al., 1990; Willcox and Stagg, 1990; Etheridge et al., 1985). This major rift system extended from Broken Ridge in the west, to the South Tasman Rise in the east. Extension during the Jurassic and Early Cretaceous resulted in the formation of a series of west-northwesterly trending continental rift basins along the southern margin of Australia and a series of north-northwest trending transtensional basins along the western margin of Tasmania. The amount of upper crustal extension varied between basins of the SRS, with relatively thick, early syn-rift sediments of Late Jurassic to earliest Cretaceous age preserved in half-graben systems in the Bight Basin (Eyre, inner Recherche, eastern Ceduna and Duntroon sub-basins; Totterdell et al., in press) and western onshore Otway and Gippsland basins. There is presently no direct evidence of Jurassic age sediments in the Bass Basin, although the prolific extrusion of dolerites across central Tasmania is thought to mark the onset of rifting. Other research has suggested the onset of rifting in the Bass Basin may have occurred as late as Early Cretaceous along with extensive associated volcanism (Gleadow and Duddy, 1980).

This phase of upper crustal extension preceded the eventual breakup between the Australian and Antarctic plates off the Bight Basin in the latest Santonian to earliest Campanian (83 Ma; Sayers et al., 2001). In the eastern Otway-Sorell basins region, oceanic crust was probably not generated until the Eocene (Moore et al., 1992; Norvick and Smith, 2001). The onset of regional thermal subsidence has been inferred as diachronous (Mutter et al., 1985; Moore et al., 1992), progressing east from the Bight Basin and eventually jumping south along the Tasman Fracture Zone, leaving Tasmania attached to the Australian craton (Hill et al., 1994). After separation, the transform margin along the Tasman Fracture Zone underwent severe shear deformation as the Antarctic plate moved southward relative to the Australian plate. This deformation

continued to affect the southernmost part of the South Tasman Rise until the Early Miocene (chron 6B, 23 Ma) when the Southeast Indian Ridge axis cleared from the western edge of the South Tasman Rise (Royer and Rollet, 1997). These far-field stresses related to prolonged separation of the continents continued to affect existing structures in the Bass Basin until the latest Eocene, coincident with the opening of the Southern Gateway (Exon et al., 2001).

In the incipient southern Tasman Basin to the east of the Bass Basin, seafloor spreading began at about 83 Ma (earliest Campanian, chron 33), approximately coeval with southern margin breakup, in a west-southwest direction (Hayes and Ringis 1973; Weissel and Hayes 1977; Shaw 1978). Extension preceding Tasman breakup began approximately 10 m.y. earlier in the Turonian (Symonds et al., 1996), resulting in deposition of the Turonian to Santonian age Emperor and Golden Beach megasequences in the Gippsland Basin (Norvick and Smith, 2001), and similar age syn-rift megasequences in the Durroon Sub-basin (Baillie and Pickering 1991; Blevin, 2001; Cummings et al., 2002). Royer and Rollet (1997) identified the oldest magnetic anomaly (chron 34) in the Tasman Basin just north of the East Tasman Plateau, indicating that spreading may have commenced slightly earlier in the southernmost Lord Howe Rise. Although extension progressed to breakup and seafloor spreading in Southern Ocean and Tasman basins, the Bass Basin and the adjacent Torquay Sub-basin remained 'failed rift' basins where breakup did not occur.

3.3 REDEFINITION OF BASIN BOUNDARIES AND BASIN NOMENCLATURE

The boundaries of the Bass Basin have been remapped using seismic and potential field data to more accurately reflect the distribution of the main depocentres (Figures 3.1 and 3.2). This outline is defined by a series of northwest-trending basin edge faults and depositional hinges. Latest Miocene to Recent highstand sediments extend beyond this boundary onto shallow basement, but are not considered highly prospective for petroleum exploration.

In the southwest, the basin margin is a northeast-dipping flexural ramp that forms the hanging wall to a northwest-striking normal fault near the Bass-3 and White Ibis-1 wells (Figure 3.3). Although seismic data is limited, there is some indication (at the end of lines) that small half graben also occur to the east of King Island (Figure 3.3). However, given the size and shallow nature of these features, it is unlikely that they are prospective for petroleum exploration. These half graben show some similarity to the King Island Sub-basin of the Sorell Basin, where Clam-1 was drilled.

The northwestern edge of the Bass Basin is difficult to define in both location and nature due to the presence of thick volcanics that degrade data quality (Figures 3.2 and 3.4). The prominence of volcanic material at or near the seabed masks seismic penetration below 200 m depth. Potential field datasets are similarly affected and cannot be reliably used to determine the extent of the basin. However, based on the presence of a large inversion structure over which Cormorant-1 and King-1 were drilled, it is likely that this margin is formed by a steeply dipping, northwest-striking normal fault that dips to the southwest.

The prominent effects of volcanism appear to lessen east of the Yolla-1 and Tilana-1 wells. From Yurongi-1 to just west of Chat-1, the basin margin is defined by a east – west striking normal fault, although there is significant lateral offset on this fault segment. A prominent change in the polarity of the rift basin occurs just north of Chat-1. Here, the basin margin changes from a faulted edge (as seen near Yurongi-1) to a southwesterly-dipping ramp margin. This accommodation zone can be mapped southward across the basin to west of the Tasmanian Devil-1 well (Figure 3.2), where a similar change in basin polarity is observed. The west-southwesterly extent of the basin is defined by onshore mapping and outcrop (Moore et al., 1984). The onshore extension of the Bass Basin has been called the Boobyalla Sub-basin (Moore et al., 1984), however this area is now considered the easternmost part of the Durroon Sub-basin. The most southerly boundary of the Durroon Sub-basin is a northeast-dipping normal fault. Seismic mapping has now shown that significant inversion occurred along this margin in the Cenomanian and Late Miocene.

The accommodation zone defined here by the change in rift polarity marks the boundary between the "western" and "eastern" depocentres of the Bass Basin. The eastern depocentre was previously named the Durroon Basin (Baillie and Pickering, 1991). This name was later modified to the Durroon Sub-basin, in recognition of the similar structural history between the two depocentres, suggesting that a separate basin status (or hierarchy) was not warranted. That view is supported by the mapping undertaken during this study. The new name "Cape Wickham Sub-basin" is proposed to described the western depocentres of the Bass Basin. Cape Wickham occurs on the northernmost tip of King Island; it lies in Tasmanian waters, and marks the most westerly extent of the Bass Basin (Figure 3.1). The boundary between the Durroon and Cape Wickham sub-basins is recognised as a structural accommodation zone marked by a change in rift polarity.

3.4 BASIN STRUCTURAL ELEMENTS

The Bass Basin has been described as a system of multiple northwest-trending, inter-linked half graben (Etheridge et al, 1985; Gunn et al., 1996; Lennon et al., 1999). The integration of basement geology and mapping of the depocentres has helped to clarify the nature of structural elements within the basin. Lennon et al. (1999) defined the Cormorant, Yolla and Pelican troughs as the deepest depocentres within the Bass Basin (Figure 3.2). Two adjacent areas where sediments were significantly thinner were called the Tertiary platforms (Lennon et al., 1999). Some modification has been made to the Lennon et al. (1999) definition of structural elements – mainly, in the Pelican Trough, the Tertiary Platform area near Yurongi-1 and Dondu-1, and the introduction of the White Ibis Trough (Figure 3.2). In addition, the accommodation zone that sub-divides the basin into the Cape Wickham and Durroon sub-basins is recognised as a fundamental structural and depositional hinge that controlled sedimentation from the Late Cretaceous onwards.

The Pelican Trough is defined by a west – northwest-striking normal fault that dips to the southwest. Pelican-1, -2, -3 and -5 and Narimba-1 were drilled on a crestal collapse structure that formed in syn-tectonic sediments deposited over the hanging wall (Figure 3.5). The Pelican Trough dies-out along strike towards the White Ibis-1 and Bass-3 wells. The eastern end of the Pelican Trough also dies-out along strike,

although the bounding fault is eventually truncated by the accommodation zone between the Durroon and Cape Wickham sub-basins. The new name "White Ibis Trough" is proposed for the half graben that lies northeast of the White Ibis-1 and Bass-3 wells. This is consistent with other nomenclature proposed for the basin (Lennon et al., 1999) which uses the names of wells that either intersect the type sections within the trough (e.g., Pelican and Cormorant wells), or are positioned near basement structures that define the trough (e.g., Yolla and White Ibis wells).

The separation of the Cormorant and Yolla troughs as shown by Lennon et al. (1999) recognises the offset along strike and possible change in polarity of the rift faults in this area. The structural complexity in this part of the Mesozoic basin suggests that it is located over a major boundary between basement terranes. East of Yolla-1, the strike of basement faults within the central basin switch from a north-northwest to northwest orientation. The area defined by these northwest trending faults and the accommodation zone to the east has been termed the Tertiary Platform by Lennon et al. (1999). This term "Tertiary Platform" suggests potentially low prospectivity due to a lack of thick Palaeogene sediments (i.e., potential source rocks). However, mapping undertaken during this study suggests that basement beneath the Tertiary Platform can be mapped considerably deeper than proposed by Lennon et al. (1999). It is clear from seismic data and the stacking patterns interpreted from well logs at Yurongi-1, Dondu-1 and Tilana-1 that subsidence (or accommodation) was much slower in this part of the basin, particularly during the Paleocene and Early Eocene. However, a thick Late Cretaceous to earliest Palaeogene section can be interpreted to lie above basement. There is no suggestion of inversion or uplift to account for the thinner Cainozoic section, and it is interpreted that this area is underlain by a stable basement block that was not affected by upper crustal deformation during the early Palaeogene.

The location of the accommodation zone that separates the Durroon and Cape Wickham sub-basins was also strongly influenced by underlying basement fabric. As the Chat-1 well was drilled within this zone (Figure 3.6), the name Chat Accommodation Zone (CAZ) is proposed for the structure. An interpretation of basement from potential field data was commissioned by Geoscience Australia during the early stages of the Bass Basin study. The results (Teasdale et al., 2001, 2003) indicate that the Mesozoic basin geometry was strongly controlled by the proposed Moyston-Tamar Fault Zone, a northwest-trending basement fracture system (Figure 3.7). However, seismic mapping that followed the Teasdale et al. (2001, 2003) study shows that there are probably multiple splays off the fracture zone, some of which may trend northwest. In particular, the change in rift polarity that is observed along the northern basin margin could be due to a splay off the fracture zone, or alternatively, a boundary between accreted terranes within the Lachlan Fold Belt. Two parallel northeast-trending seismic lines from either side of the CAZ show the change in rift polarity (Figures 3.8 and 3.9).

East of the Chat Accommodation Zone, the Durroon Sub-basin has a distinctly different structural style to the western part of the Bass Basin (Baillie and Pickering, 1991). Here, the half-graben structures are narrower and more intensely faulted (Figure 3.10). The underlying basement fabric was also likely to have influenced

the geometry of the rift structures. While the Cape Wickham Sub-basin overlies Proterozoic fold belt metasediments, the Durroon Sub-basin overlies sediments and intruded granites of the Palaeozoic Lachlan Fold Belt. It is also apparent from potential field and other evidence that the Early-Middle Jurassic dolerites that cover much of central Tasmania also extend to areas under the Cretaceous Durroon Sub-basin. The dolerite intersected at total depth in Chat-1 has been submitted for isotope dating by the argon/argon technique, however results were unavailable at the time of publication.

3.5 BASIN EVOLUTION

Due to its regional tectonic setting between two major rift systems, the Bass Basin was affected by multiple episodes of upper crustal extension and compression, driven by both inter- and intra-plate stresses. Structural development was further influenced after breakup along the central Southern Margin by the prolonged fragmentation and clearance of Antarctica along western Tasmania. The fact that the Bass Basin is underlain by basement of differing fabric has also influenced the different structural styles observed within the overlying Mesozoic rift basin. Stresses across the basin are likely to have been partioned by the Chat Accommodation Zone, which is clearly a basement-controlled feature. Basement character also played a role in the different post-rift subsidence histories observed between the Cape Wickham and Durroon sub-basins. On its margins, the Bass Basin is flanked by basement buttresses forming the King Island High to the west-northwest, and the Bassian Rise to the northeast. These features acted to focus and partition Cretaceous and Cainozoic compressional stress along the northern, eastern and western margins of the Bass Basin.

From the integration of well logs and regional seismic mapping, at least three broad phases of upper crustal extension, spanning the Early Cretaceous to the Early Eocene, can be recognised in the Bass Basin (Figure 3.11). These basin phases are correlated to megasequences or supersequences (first and second-order cycles of deposition; Chapter 4). The first phase of rifting occurred during the ?Barremian to earliest Cenomanian (Otway Rift Phase), as part of a broader phase of extension that affected the eastern part of the southern margin (Otway-Sorell region). The second phase of rifting during the Turonian to Campanian was associated with extensional stresses that preceded Tasman Basin breakup (Durroon Rift Phase). Although mapping of the deeper syn-tectonic section in the western Bass Basin is difficult (due to depth of burial), the early Otway Rift Phase appears to have affected most of the Bass Basin, while the effects of the Tasman rift phase are more pronounced in the Durroon and central Cape Wickham sub-basins. The Durroon Sub-basin ceased to be tectonically active in the mid-Campanian, with sediments from the Late Cretaceous until the Miocene deposited under conditions of post-rift thermal subsidence. The third phase of extension focused on the central and western regions of the Bass Basin, particularly structures within the Pelican and Cormorant troughs (Bass Rift Phase; Smit, 1988). This final phase of upper crustal extension may have been related to propagated far-field, intra-plate stresses associated with the prolonged clearance of the Antarctic and Australian plates, and therefore was probably highly oblique to the existing rift-bounding faults. This phase of extension resulted in successive reactivation of existing Lower Cretaceous half-graben structures during the Campanian to Late Maastrichtian, the Late Maastrichtian to Early Paleocene, and again during the Late Paleocene to Early Eocene.

Seismic and well log interpretations have shown that each of the structural elements of the Bass Basin is different in its evolution. During the early phases of extension when the rate of tectonic-driven subsidence was high, sedimentation in the evolving depocentres was probably more uniform, although somewhat geographically focused within the axis of the depocentre. As tectonic subsidence slowed and became more focused in the central and western parts of the basin, sedimentation patterns began to diverge. Tectonic processes ceased to affect the Durroon Sub-basin from the late Campanian onward. In the central Bass Basin, many faults were active until the Late Paleocene, while in the western part of the basin faulting continued until the Middle Eocene. It is during this period of basin evolution (Campanian to Middle Eocene) that sediments show the greatest diversity in facies type, depositional environment and thickness. The stratigraphy of the Bass Basin is presented in Chapter 4.

Early Cretaceous Extension – Rift Phase 1: Otway Rift Phase

Durroon-1 is the only well in the Bass Basin to intersect sediments of Early Cretaceous age (Figure 3.10). Correlation between the well and seismic data is difficult because of the steep dip of the beds intersected. The well is also located over a basement block where the onlapping beds have thinned, and some erosion related to footwall uplift has occurred. Durroon-1 intersected two syn-tectonic sequences – an Early Cretaceous (Aptian to Albian) succession (Otway Megasequence) and a mid-to-Late Cretaceous succession (Turonian to mid-Campanian, Durroon Megasequence – see below). The Otway Megasequence syn-rift succession overlies basement, and is itself the pre-rift section to the later Turonian to mid-Campanian syn-rift succession (Durroon Megasequence; Figures 3.10 and 3.12). Sediments of the Early Cretaceous rift phase (Durroon-1) are distinctly similar in their lithic and volcanogenic character to equivalent age sediments in the Otway Basin (Eumeralla Formation). However, in the Otway Basin, the Eumeralla Formation has been identified as a largely post-rift succession ("Otway Syn-rift/Post-rift Megasequence 3"; Norvick and Smith, 2001). In some instances, the Otway Megasequence in the Durroon Sub-basin appears as a relatively flat-lying succession overlying Palaeozoic basement (i.e., no apparent evidence of syn-tectonic deposition). However, structural restorations of the Otway Megasequence by Cummings et al. (2002; personal communication, 2003) have shown its deposition to be fault-controlled.

Mapping of the syn-rift sediments of the Otway Phase beyond the Durroon Sub-basin is problematic. This is mainly due to an increased depth of burial (poor imaging) and lack of penetration in the Cape Wickham Sub-basin. The patchy distribution of the Otway Phase syn-tectonic sediments suggest that the effects of extension across the broader Bass Basin were limited and probably resulted in formation of isolated shallow half graben. Only during the subsequent phase of extension (Durroon Phase) did the fault segments propagate and link to form more continuous rift features. Interpretation of the Durroon-1 succession indicates the dominance of sand-rich fluvial systems with a significant input of volcanic sediment during this period of basin evolution (Chapter 4).

Turonian to mid-Campanian Extension – Rift Phase 2: Durroon Rift Phase

The Turonian to mid-Campanian Durroon Rift Phase is related to upper crustal extension that preceded breakup and spreading in the Tasman Basin to the east. Although extension probably affected most of the Bass Basin, the effect is most clearly observed in the Durroon Sub-basin. The Durroon Rift Phase is also poorly documented through drilling, although Durroon-1 does provide clear evidence to date this phase of basin development (Figure 3.10 and 3.12). Seismic correlation away from the Durroon-1 well provides more extensive evidence of this syn-rift package, and suggests episodic pulses of fault movement punctuated by short intervening periods of erosion (Figure 3.13). Although several syn-rift wedges are observed on seismic data around the Durroon-1 well, only the "top of Durroon Megasequence" can be correlated westward beyond the Chat Accommodation Zone. New biostratigraphic analyses undertaken as part of this study (Partridge 2002; Appendix C) provide evidence of lacustrine environments within the developing basin (Chapter 4). It is proposed that during deformation, fault segments and associated half graben that were initiated during the previous Otway Phase propagated to form a system of interlinked rift depocentres. Correlation with the Durroon-1 well indicates that extension ceased between 75 and 78 Ma following breakup in the Tasman Basin during the latest Santonian to early Campanian. At the end of the Durroon Rift Phase, the Durroon Sub-basin underwent an extended phase of slow post-rift subsidence.

Late Cretaceous to Early Palaeogene Extension – Rift Phase 3: Bass Rift Phase

While extension in the Durroon Sub-basin ceased in the mid-Campanian, extension continued to episodically affect the central and western parts of the Bass Basin. This coincided with continuing tectonic activity in parts of the Otway Basin and across much of the Sorell Basin along western Tasmania. The age of breakup off the Otway Basin has been suggested as Maastrichtian, although the oldest seafloor lineaments are only Early-Middle Eocene in age (Norvick and Smith, 2001). Final separation and clearance between the Antarctic and Australian plates did not occur until the Late Eocene, signaled by the subsequent opening of the Southern Gateway at around 33 Ma (Exon et al., 2001).

The integration of seismic and well log interpretations clearly shows that the Bass Rift Phase encompasses a series of "pulses" of far-field, upper crustal extension (growth faults). This is probably because the Bass Basin failed to breakup at the end of the Otway and Durroon rift phases, and the locus of extensional stresses associated with fragmentation of the Otway-Sorell-South Tasman Rise region moved progressively further away from the Bass Basin with time. This is reflected in the waning magnitude of each successive event (or "pulse") in Rift Phase 3. In addition, far-field tectonic stresses probably became more oblique through time, such that by the end of Rift Phase 3, only select faults of particular orientations were affected. These events have been consolidated into a single rift/basin phase (and corresponding megasequence) in recognition that they affected only the Cape Wickham Sub-basin (i.e., not the Durroon Sub-basin), and collectively equate to the recognised timeframe of a tectonic cycle (i.e., 20 Ma yrs). The localised nature of these events (and accommodation) has meant that sediments deposited during the Bass Rift Phase vary widely in facies type, environment and thickness. Partridge (2002, Appendix C) has recognised the

widespread development of lacustrine environments across the northern and central Cape Wickham Sub-basin during this time (Chapter 4).

Three unconformity-bounded sequences related to episodes of growth faulting are recognised within the Bass Rift – the Furneaux Sequence (mid-Campanian to late Maastrichtian), Tilana Sequence (late Maastrichtian to mid-Late Paleocene), and Narimba Sequence (mid-Late Paleocene to late Early Eocene). The Furneaux Sequence uses the nomenclature of Maung et al. (1993) who subdivided the Eastern View Coals Measures into two broad lithostratigraphic units based on the abundance of coal. Evidence of the Furneaux rift episode is derived mainly from seismic mapping between the Durroon and Cape Wickham sub-basins. Sediments from only the uppermost part of the Furneaux Sequence have been penetrated by drilling in the western Bass Basin (Lower and Upper *F. longus zones*; Koorkah-1, Poonboon-1, and Tilana-1). Here, the syn-rift nature of the Furneaux Sequence is apparent on seismic data. By contrast, in the Pelican Trough (Pelican-5), later faulting has obscured the syn-rift nature of the sequence (Figure 3.5).

The overlying Tilana Sequence correlates to a basinward thickening wedge of sediment of latest Maastrichtian to Late Paleocene age. Unlike the underlying Furneaux Sequence, the Tilana Sequence does not consistently display stratal geometries indicative of strong syn-tectonic growth (Figure 3.14). However, much of this sequence is heavily affected by (post-depositional) igneous intrusions. The emplaced volcanic material and associated fluids have laterally invaded porous or fractured strata of a coaly/sandy nature. The intrusions mask the original stratal geometry of the sequence on seismic data, resulting in chaotic, high-amplitude and low-frequency reflections throughout the affected succession. Faults controlling deposition of the Tilana Sequence appear to be reactivated older faults of the underlying Cretaceous rift. Towards the upper part of the Tilana Sequence as growth fault-related movement slowed, accommodation was probably heavily influenced by sediment loading and compaction which continued until the latest Paleocene.

The upper part of the Bass Rift Phase (Narimba episode) is more confidently documented by both drilling and seismic correlation. This episode of faulting was probably largely oblique and driven by far-field stresses. Only some faults bounding the Pelican, Yolla and Cormorant troughs were most affected, with growth accommodated by reactivation of the underlying Cretaceous rift faults. The Narimba-1 well intersected over 900 m of latest Paleocene to Early Eocene syn-tectonic sediments in the Pelican Trough. In areas unaffected by reactivation (Poonboon-1, Dondu-1), this succession is less than 150 m thick. The Narimba rift phase was probably oblique in orientation to existing structures, and resulted in the selected reactivation of the early rift faults depending on their orientation. The key period of fault movement, constrained by well and seismic correlations, occurred from the latest Late Paleocene (intra-Upper *L. balmei* zone) until the late Early Eocene (base Upper *M. diversus* zone). The "expanded" syn-tectonic section has also been intersected at Cormorant-1 and in the western Cape Wickham Sub-basin (Koorkah-1, Toolka-1A and Konkon-1).

Early to Middle Eocene Post-Rift Sag – Subsidence Phase 1: Aroo Sequence

From the late Early Eocene until the Middle Eocene (Upper *M. diversus* to intra-Lower *N. asperus* zones) basin-scale tectonic activity waned, marking the transition from rift to post-rift conditions. Many faults within the basin succession terminate at or near the "Base Upper *M. diversus*" or "Base *P. asperopolus*" horizons on seismic data. However, it is clear from well log and seismic correlations that there was not a synchronous end to tectonic activity, thus the nature of this basin phase differs slightly across the basin. In parts of the basin that were not affected by the preceding Narimba rift phase (Poonboon-1, Dondu-1), the transition to post-rift conditions may have begun earlier (possibly Late Paleocene). The deposition of coaly facies increased from the latest Paleocene to Middle Eocene in response to a reduction in the rate of accommodation (the transition from rift to post-rift subsidence). The concentration of coals within this megasequence is clearly observed on seismic data (high amplitude, low frequency). Minor contractional events recorded during this phase are important in the formation of hydrocarbon traps.

Post-Rift Sag – Subsidence Phase 2: Demons Bluff Supersequence

The base of Subsidence Phase 2 in the western Bass Basin is correlated in wells to an unconformity within the Lower *N. asperus* spore/pollen zone. Seismically, this megasequence shows extensive development of fluvial channels and lateral variations in the seismic reflection character within the lower section, grading upward to more uniform bedding and thin progradational units along the basin margin. Biostratigraphic evidence indicates the occurrence of widespread shallow lacustrine environments (Partridge, 2002; Appendix C). Subsidence Phase 2 also coincides with the slow onset of a post-rift transgression that began with fluctuations in base level before any marine influence commenced in the basin. There are multiple localised unconformities within this megasequence, reflecting the low gradient within the former basin depocentres. Widespread marine flooding of the basin occurred during the late Middle Eocene with the deposition of the "Demons Bluff" shale facies (formerly the "Eocene Shale"). Shallow bay to open marine conditions continued until the time of a sea level fall in the mid-Oligocene.

Post-Rift Sage – Subsidence Phase 3: Torquay Supersequence

A sea-level fall in the mid-Oligocene (approximately at the Early/Late Oligocene boundary) resulted in the formation of a regional unconformity across the Bass Basin. This unconformity correlates to the most continuous seismic horizon observed within the basin. By this time, any relicts of the underlying basin topography were buried beneath the fine-grained sediments of the Demons Bluff Supersequence, and the basin was flat and featureless. A rise in eustatic sea level resulted in flooding of the basin in the Late Oligocene and the onset of deposition of fine-grained shallow marine clastic sediment (siltstone and marl). Increasingly open marine conditions developed in the Middle Miocene signaled by the deposition of bioclastic carbonates.

Polygonal faulting is widespread throughout the basin (Das, 2001), but generally only affects fine-grained sediments of Late Oligocene to Early Miocene age (Figure 3.15). From the Miocene to Pliocene, the Australian craton was placed into compression following arc collision 3500 km to the north. The long-distance transmission of these compressional stresses through the lithosphere (Hill et al., 1995) resulted in

multiple periods of Neogene (mid-Miocene) contraction in southeastern Australia (Etheridge et al., 1985; Young et al., 1991; Hill et al., 1995). The western and northwestern margins of the Bass Basin were affected by these contractional events, with large-scale anticlines formed within the syn- and post-rift successions from Miocene through Pliocene time. Several of these structures have been targeted for drilling (e.g., Cormorant-1; Figure 3.15). Similar stresses in the Gippsland Basin resulted in the formation of an en-echelon series of northeast-soutwest trending anticlinal structures on east-west striking Early Cretaceous normal faults (Young et al., 1991). Etheridge et al. (1985) proposed that Neogene inversion occurred along inferred northeast-southwest trending transfer faults throughout the Bass Strait region, rather than by inversion of extensional faults. The Bass Basin and adjacent areas of mainland Tasmania and Victoria have been affected by multiple periods of volcanic activity during the post-rift phases of basin evolution. Offshore, these events are marked by the widespread emplacement of intrusive and extrusive rocks, particularly in the southern and western parts of the basin in association with large-scale faults and accommodation zones (Figures 3.4 and 3.15).

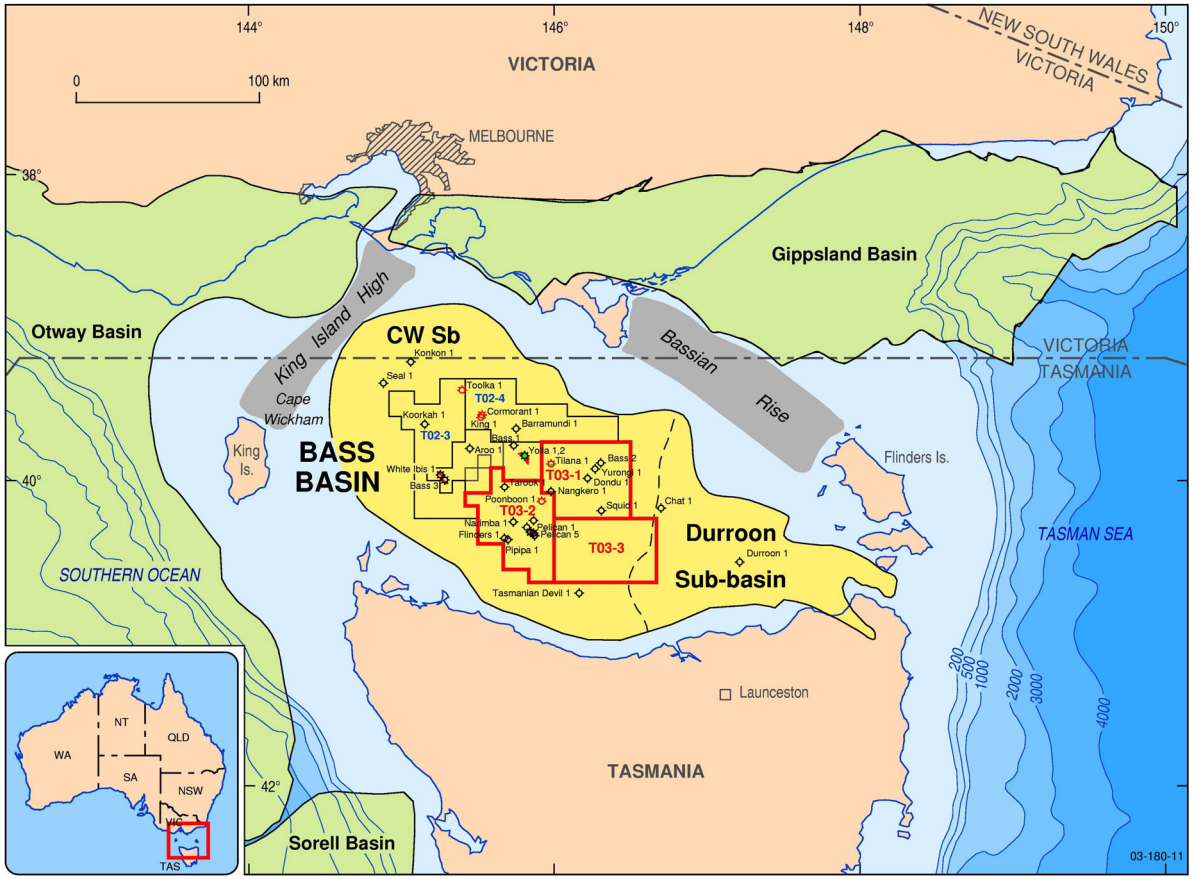


Figure 3.1 Regional map showing the location of the Bass Basin, Bassian Rise, King Island High and surrounding basins (Gippsland, Otway and Sorell basins). The location of Bass Basin wells, fields and the 2003 and 2002 Offshore Acreage Release areas are also shown. Note the location of Cape Wickham on the northeastern tip of King Island, the Cape Wickham Sub-basin (CW Sb; western Bass Basin) and the Durroon Sub-basin (eastern Bass Basin).

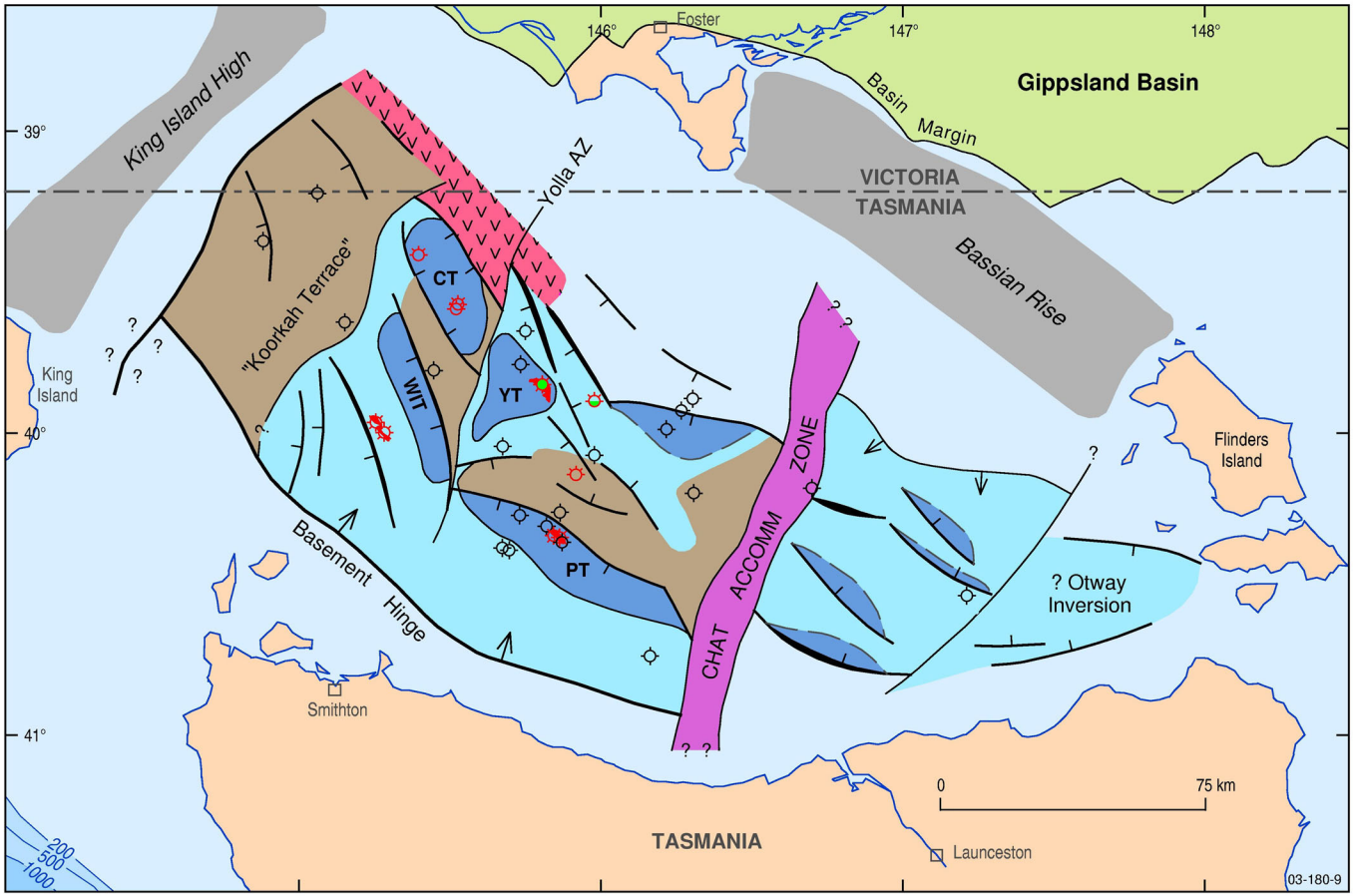


Figure 3.2 Regional map showing the location of tectonic elements and generalised basement fault trends in the Bass Basin. The location of the main Cretaceous half graben in the Cape Wickham Sub-basin are shown by the Cormorant (CT), Yolla (YT), White Ibis (WIT) and Pelican troughs (PT). The Chat Accommodation Zone (CAZ) marks the boundary between the Cape Wickham and Durroon sub-basins. Note the change in overall rift polarity across the CAZ. Early Cretaceous depocentres in the Durroon Sub-basin are generalised (see Baillie and Pickering, 1991 for detailed fault trends). Informal names used here include the Koorkah Terrace and Yolla Accommodation Zone (YAZ).

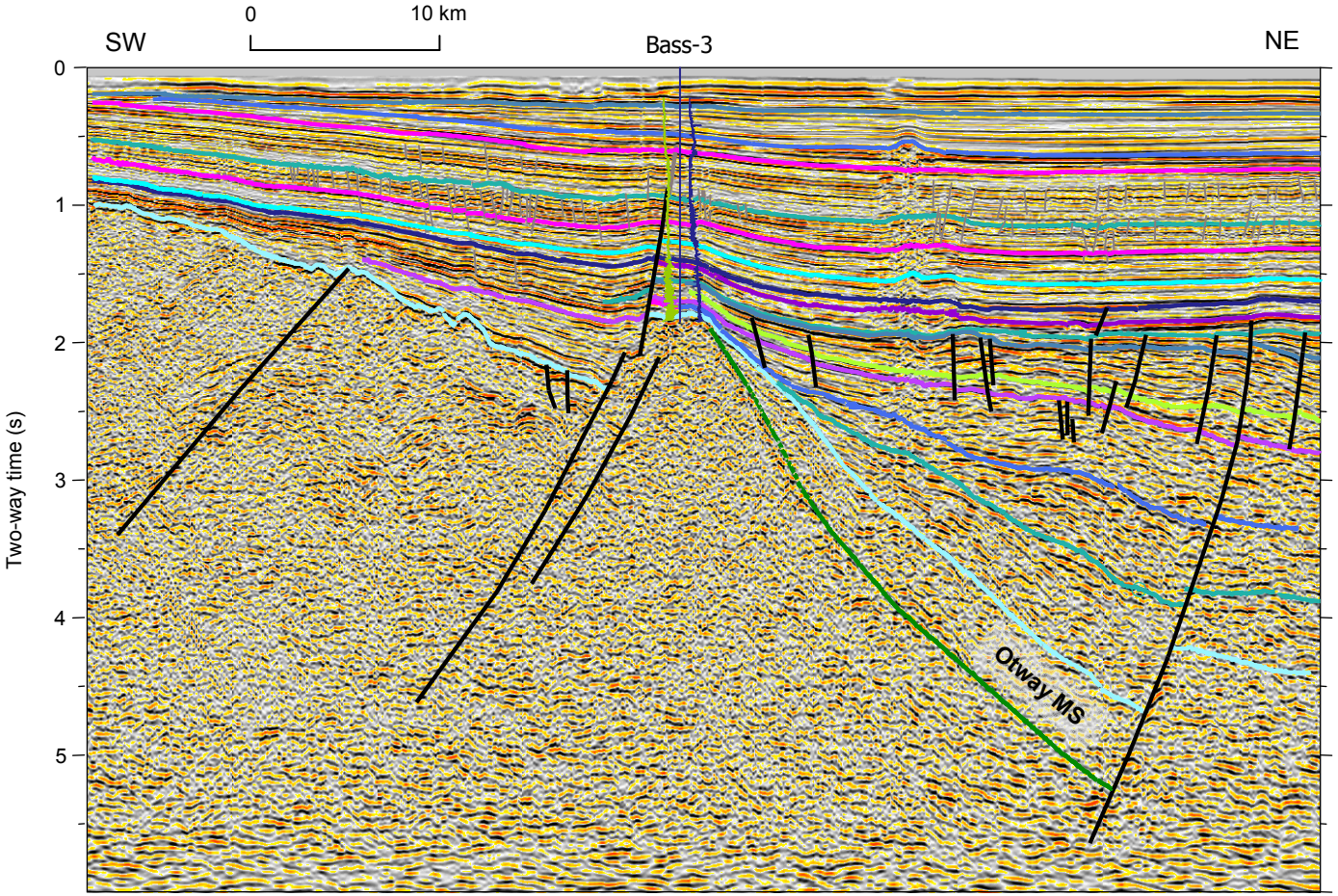


Figure 3.3 Geoscience Australia seismic line in the western Bass Basin showing the hinged nature of the southern basin boundary. Note the location of the Bass-3 well situated at the crest of a basement fault block (footwall), and the thickening of mid-Cretaceous to Early Eocene sediments (towards the northeast). The Otway Megasequence has been interpreted below the "Base-2" horizon (light blue). Also note the volcanic intrusion northeast of the Bass-3 well extending into Late Miocene and younger sediments. The seismic image used in this figure is published with the permission of Fugro MCS.

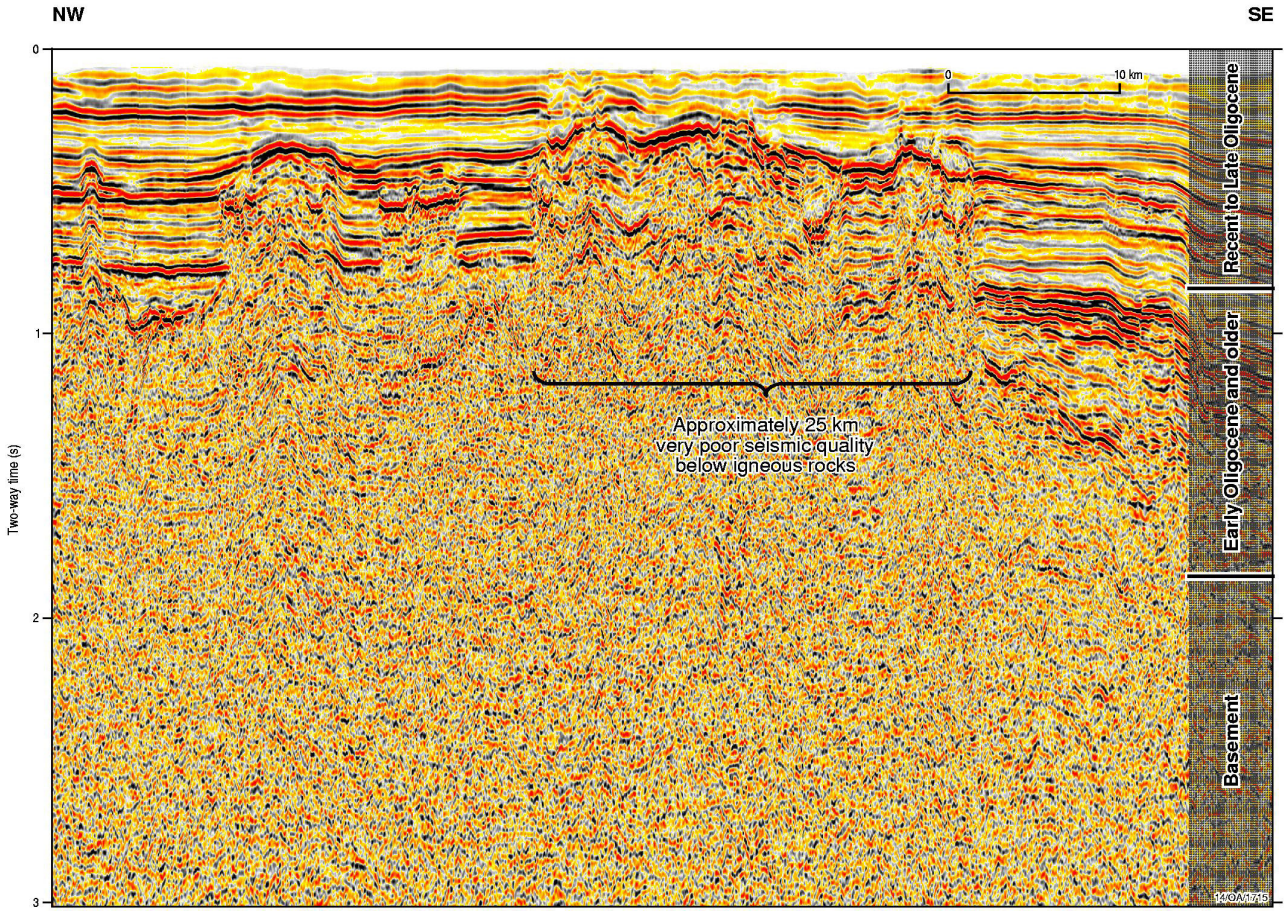


Figure 3.4 Geoscience Australia seismic line in the Bass Basin showing the occurrence of volcanic intrusions and extrusions into Late Oligocene and younger sediments along the northwestern basin boundary. The volcanics obscure the faulted nature of the margin and the overall thickness of the underlying succession. This seismic image is published with the permission of Fugro MCS.

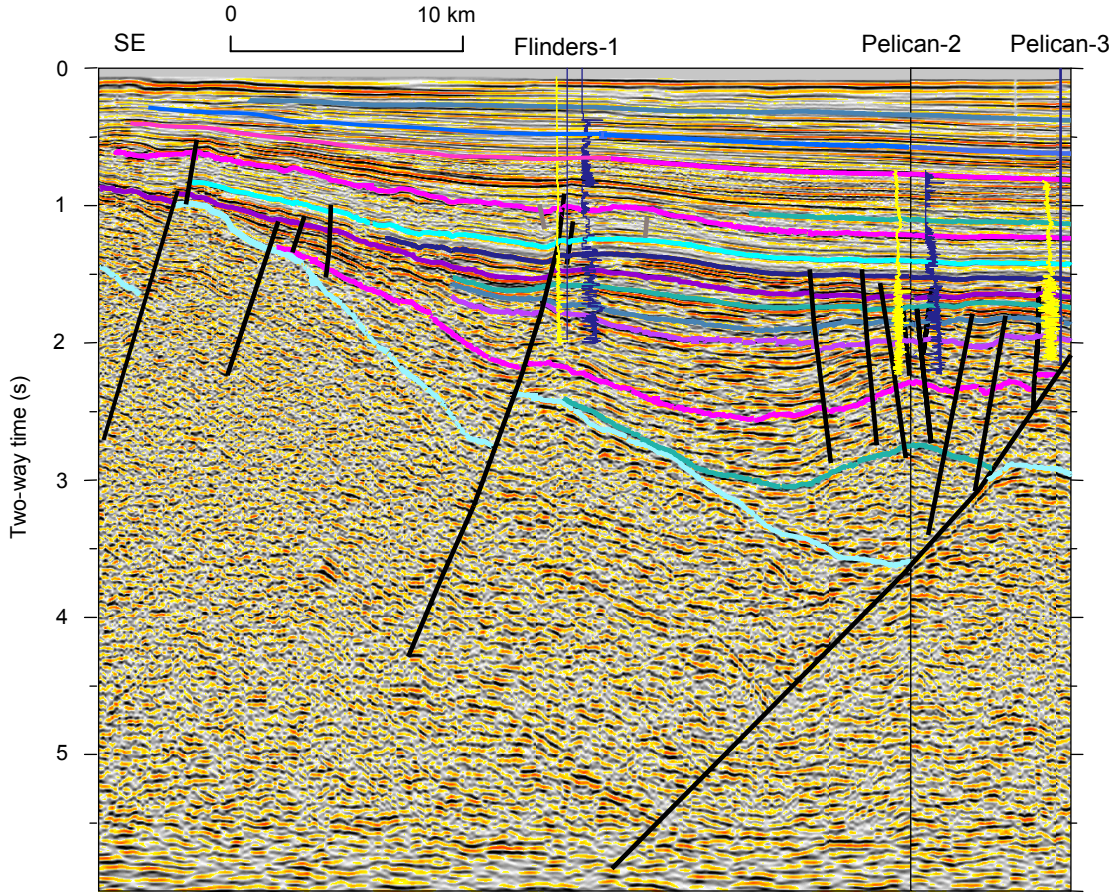


Figure 3.5 Geoscience Australia seismic line across the Pelican Trough in the southern-central Bass Basin. The section shows the location of the Pelican-2, -3 and Flinders-1 wells. The Pelican wells drilled into a crestal collapse structure within the hanging wall of the Pelican Trough, while Flinders-1 is located updip over a footwall block. Structural closure at the Flinders-1 well extends well into the Late Miocene section (pink horizon at approximately 0.65 s TWT), while trap formation in the Pelican Trough mainly occurred during the Eocene. See Figure 2.4 for a more detailed section across the Pelican Trough. This seismic image is published with the permission of Fugro MCS.

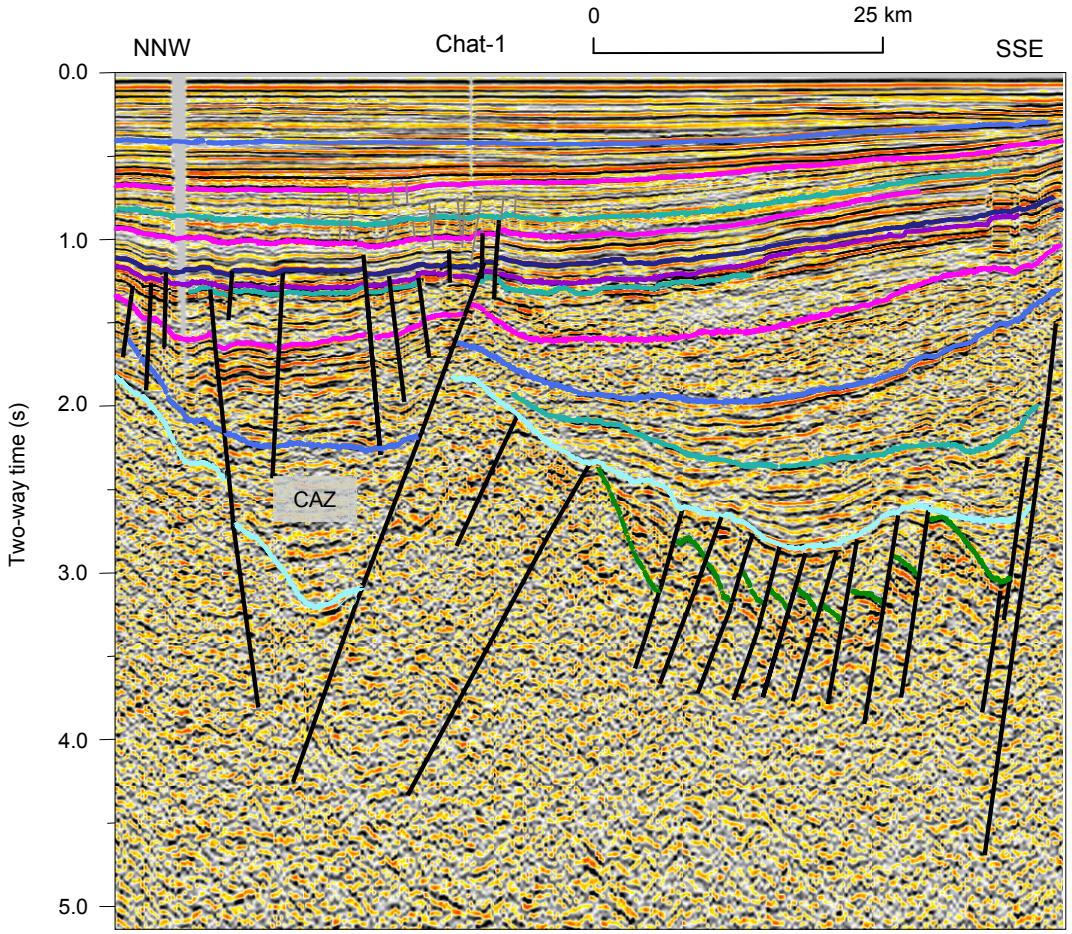


Figure 3.6 Geoscience Australia seismic line across the Chat Accommodation Zone (CAZ). Chat-1 was drilled in the Durroon Sub-basin over an uplifted basement block near the CAZ. The well intersected Cainozoic to Upper Cretaceous sediments before reaching total depth in a dolerite of interpreted mid-Jurassic age. Note the thickening of Palaeogene and younger sediments from east (Durroon Sub-basin) to west (Cape Wickham Sub-basin). This seismic image is published with the permission of Fugro MCS.

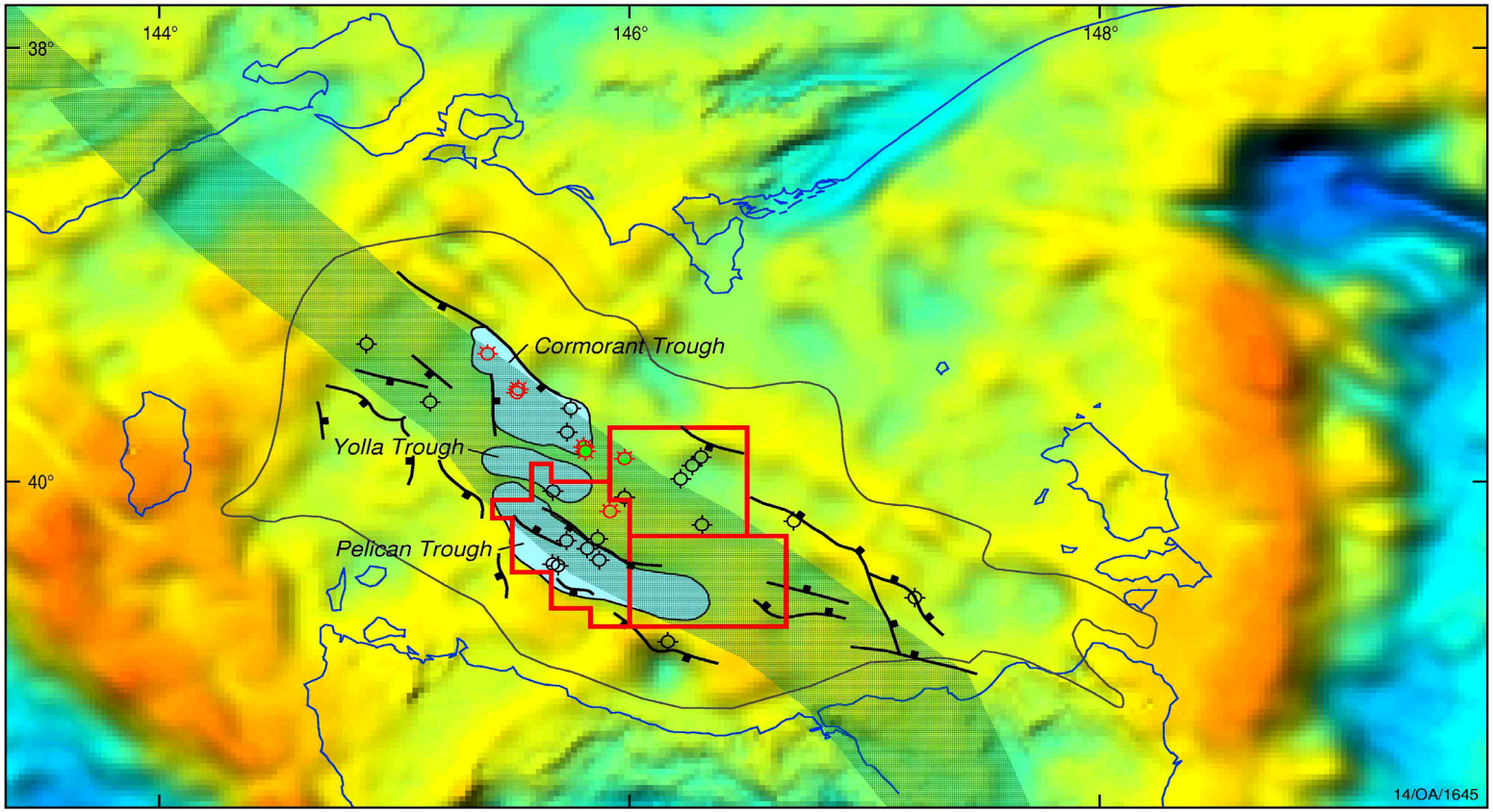


Figure 3.7 Free-air gravity map of the Bass Basin showing the approximate location of a basement fracture zone (shaded area) interpreted to underlie the Bass Basin (Teasdale et al., 2001, 2003). The major bounding faults and depocentres of the Bass Basin are after Lennon et al. (1999). Exploration wells and the 2003 Acreage Release Areas are also shown.

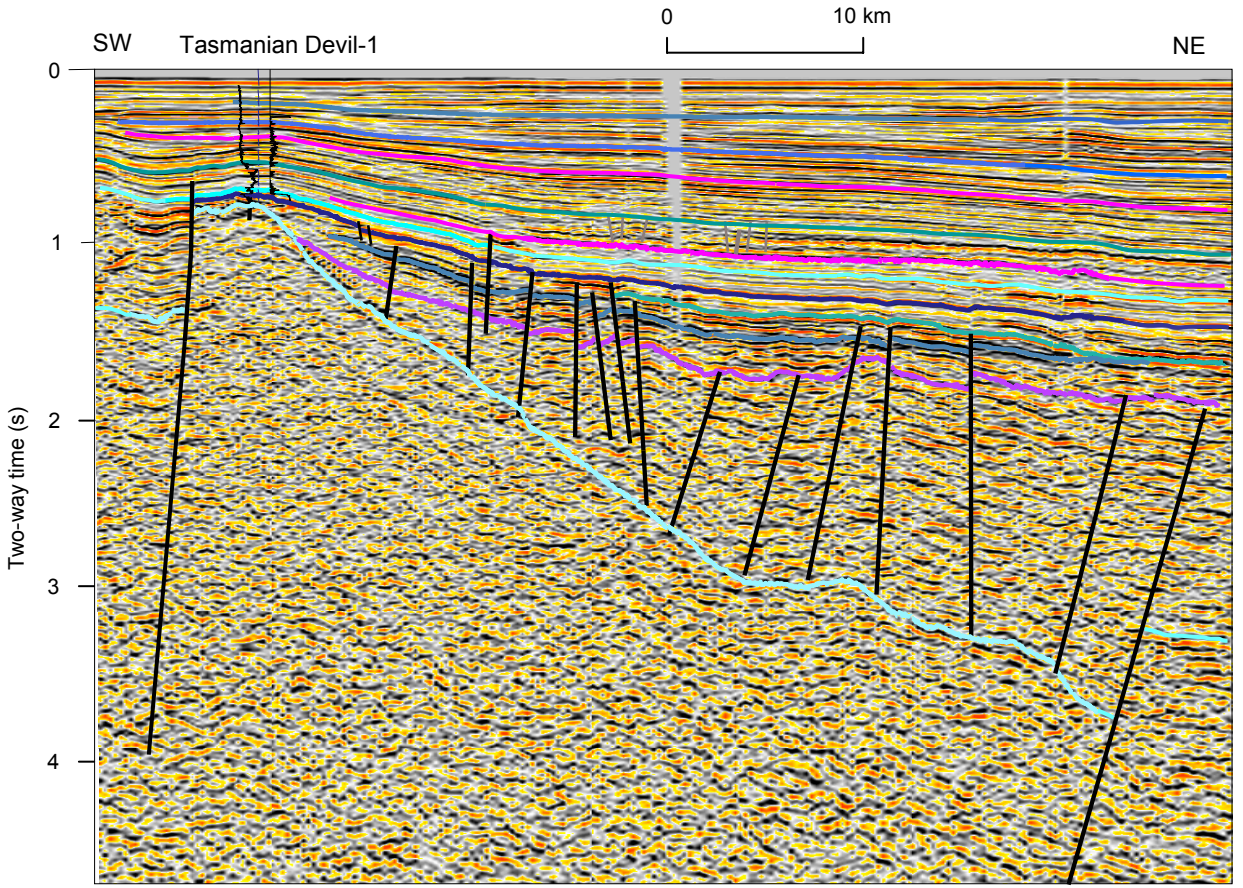


Figure 3.8 Geoscience Australia seismic line across the southern margin of the Bass Basin. The section has been highly decimated to show the nature of major northwest-striking normal faults that dip to the southwest (towards northern Tasmania). This line lies to the west of the Chat Accommodation Zone (CAZ) in the Cape Wickham Sub-basin (near the Pelican Trough). This seismic image is published with the permission of Fugro MCS.

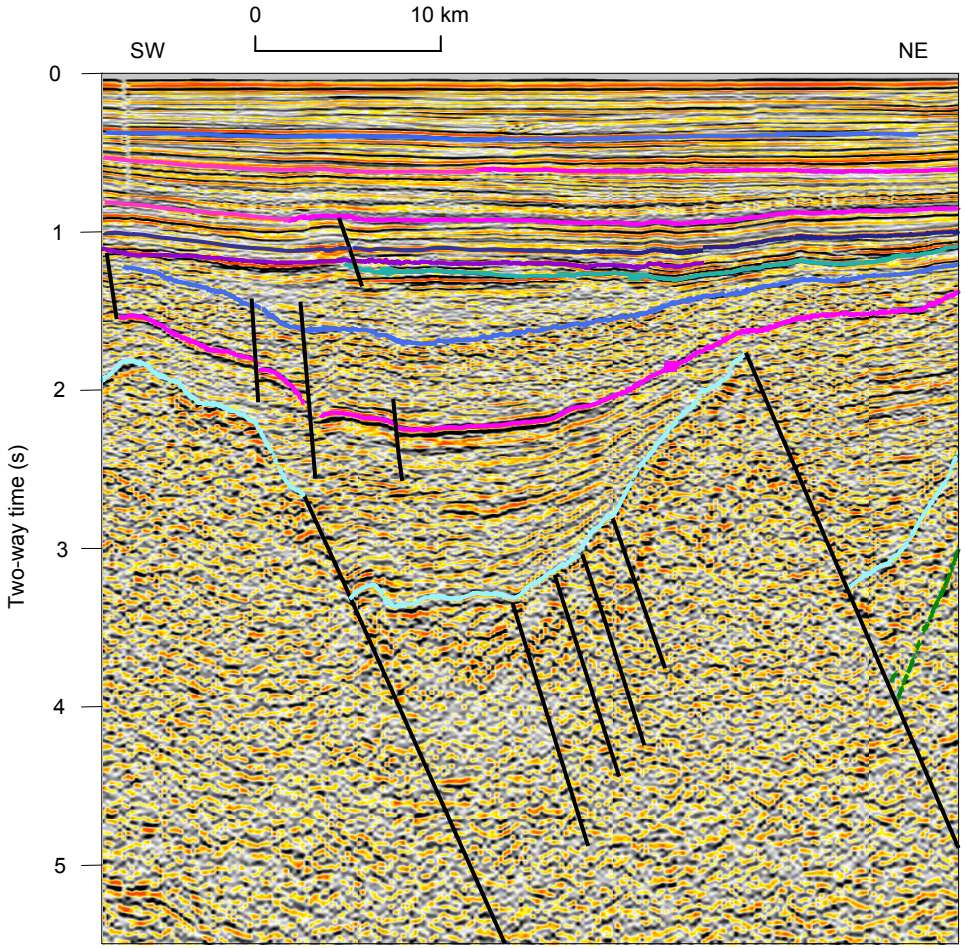


Figure 3.9 Geoscience Australia seismic line across the southeastern margin of the Bass Basin. The section has been highly decimated to show the nature of basin margin and major northwest-striking normal faults that dip to the northeast (towards Flinders Island and the Bassian Rise). This line lies to the east of the Chat Accommodation Zone (CAZ) in the Durroon Sub-basin. This seismic image is published with the permission of Fugro MCS.

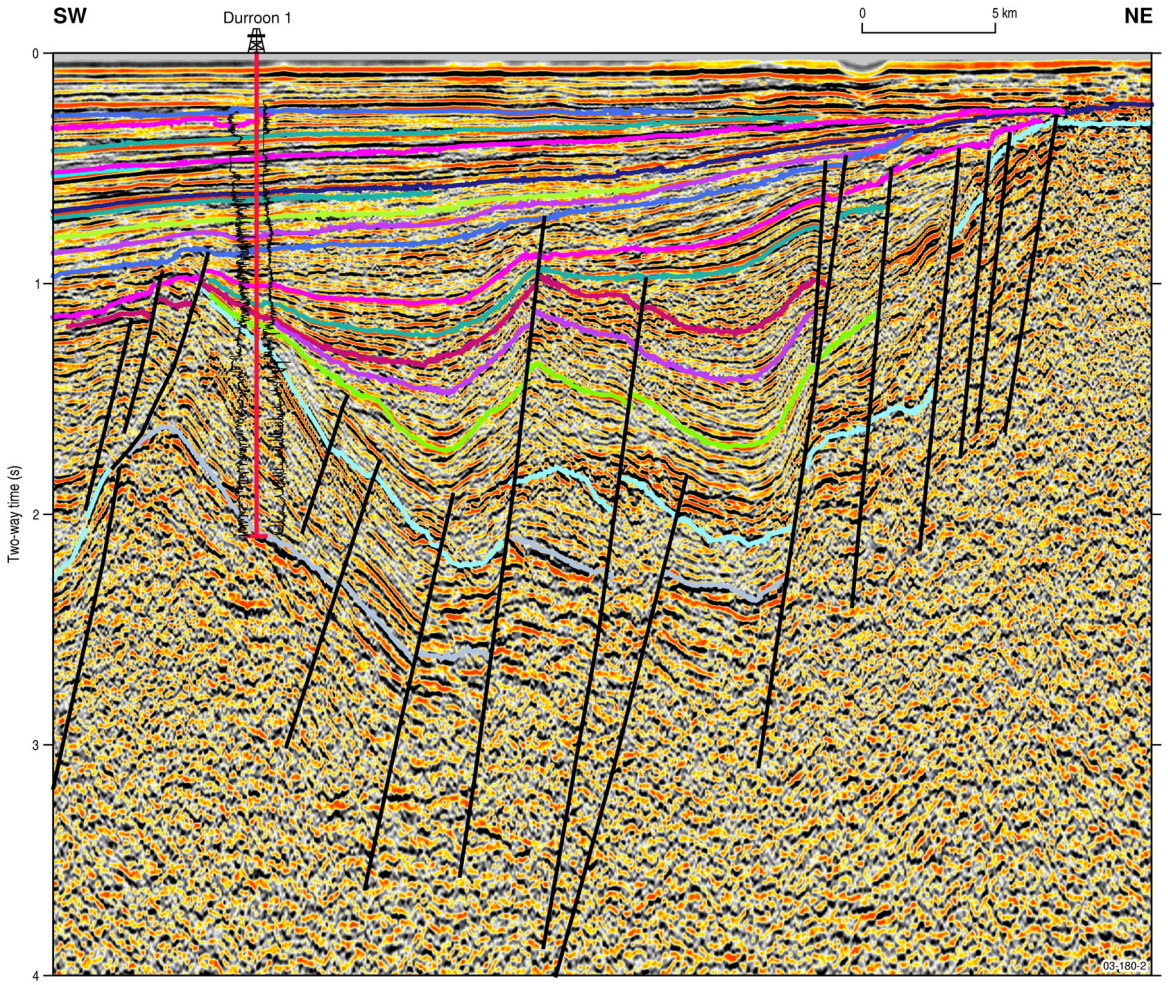
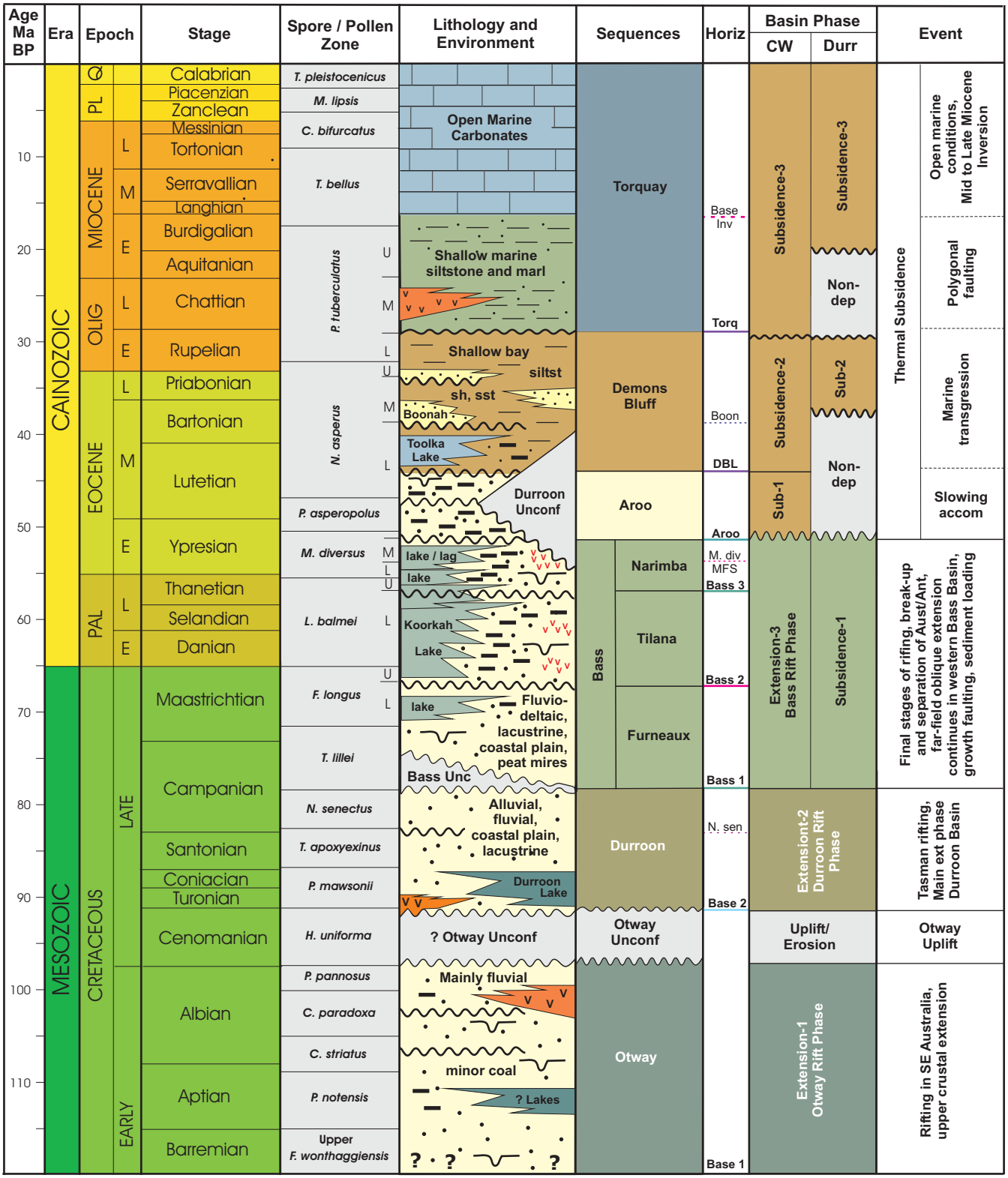


Figure 3.10 Geoscience Australia seismic line across the Durroon Sub-basin showing the structural style of the depocentre and the location of the Durroon-1 well over a faulted footwall block. The well penetrated two syn-tectonic successions of Early Cretaceous (Otway Megasequence) and Late Cretaceous (Durroon Megasequence) age. An interpretation of this line is shown in Figure 3.12. This seismic image is published with the permission of Fugro MCS.

Figure 3.11 Stratigraphic correlation chart for the Bass Basin showing the relationship between lithostratigraphy, sequence stratigraphy, basin phases, events and horizons mapped. The basin phases are shown in detail for the Cape Wickham (CW) and Durroon (Durr) sub-basins. The timescale is from Young and Laurie (1996), with modifications to spore/pollen zones from Partridge (2001).



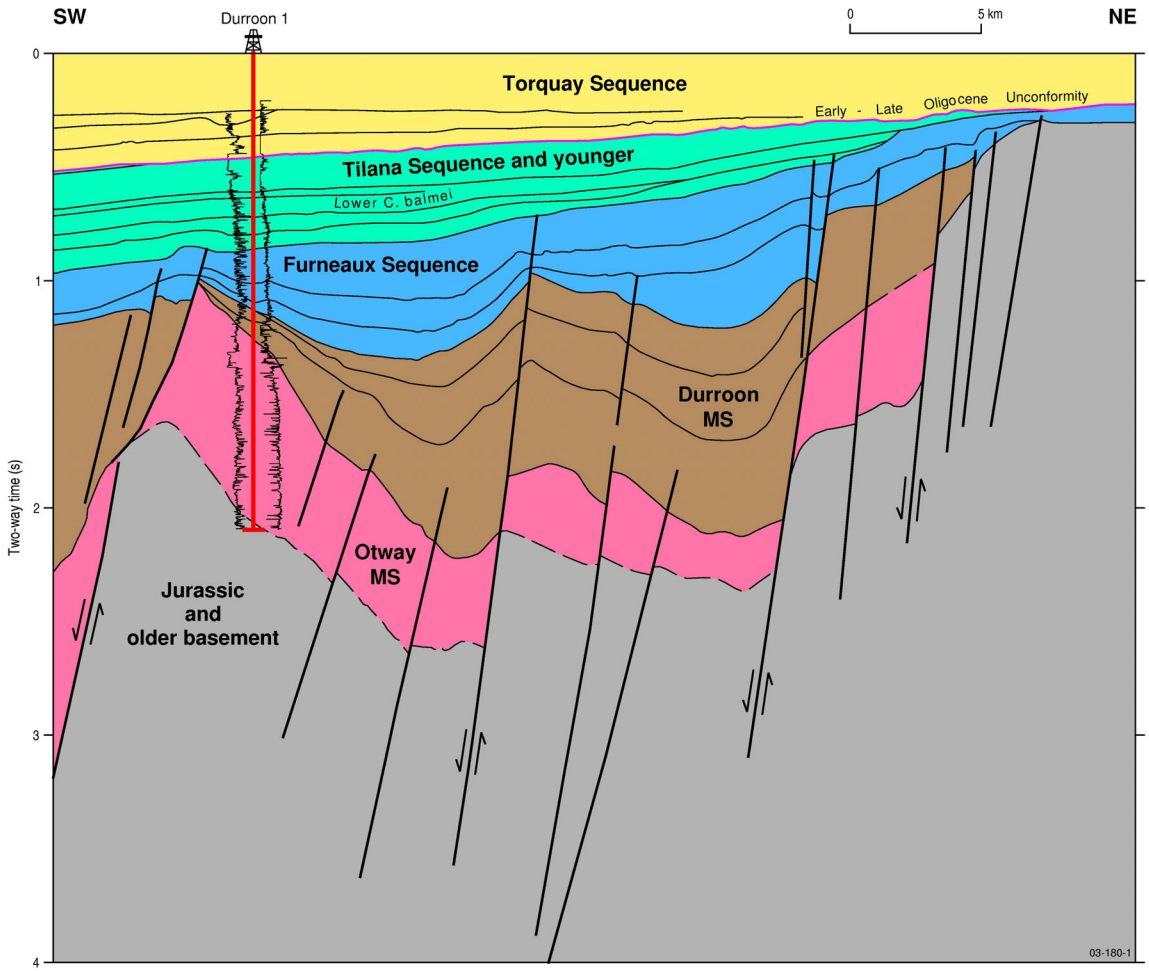


Figure 3.12 A geoseismic section across across the Durroon Sub-basin (see Figure 3.10) showing the structural style of the depocentre and the location of the Durroon-1 well over a faulted footwall block. The well penetrated two syn-tectonic successions of Early Cretaceous (Otway Megasequence) and Late Cretaceous (Durroon Megasequence) age.

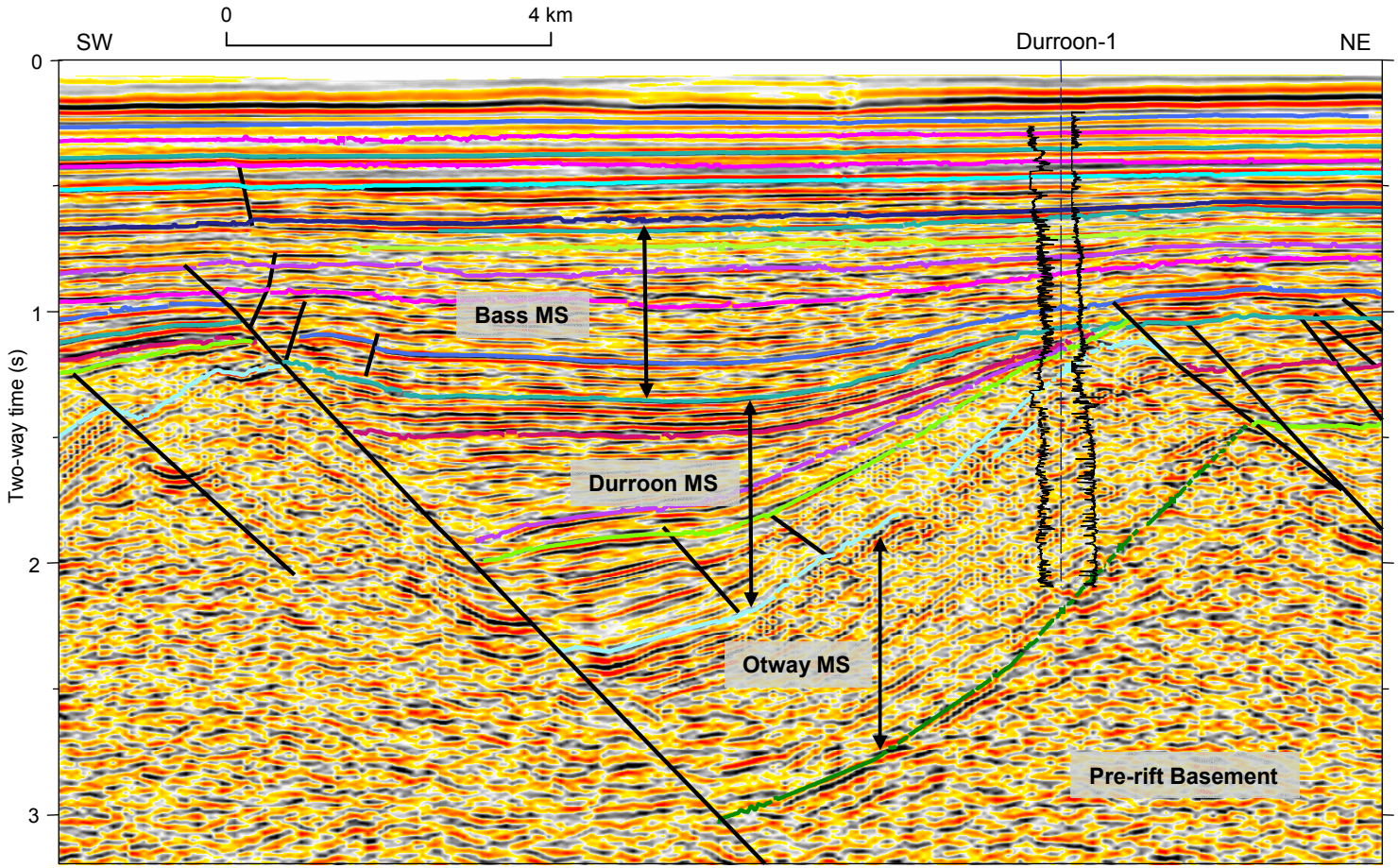


Figure 3.13 Geoscience Australia seismic line across part of the Durroon Sub-basin. This section shows in more detail the syn-tectonic successions intersected at the Durroon-1 well: the Early Cretaceous Otway Megasequence (Rift Phase 1) and the overlying early Late Cretaceous Durroon Megasequence (Rift Phase 2). In the Durroon Sub-basin, the Late Cretaceous Bass Megasequence is largely a sag-related succession deposited during post-rift subsidence. This seismic image is published with the permission of Fugro MCS.

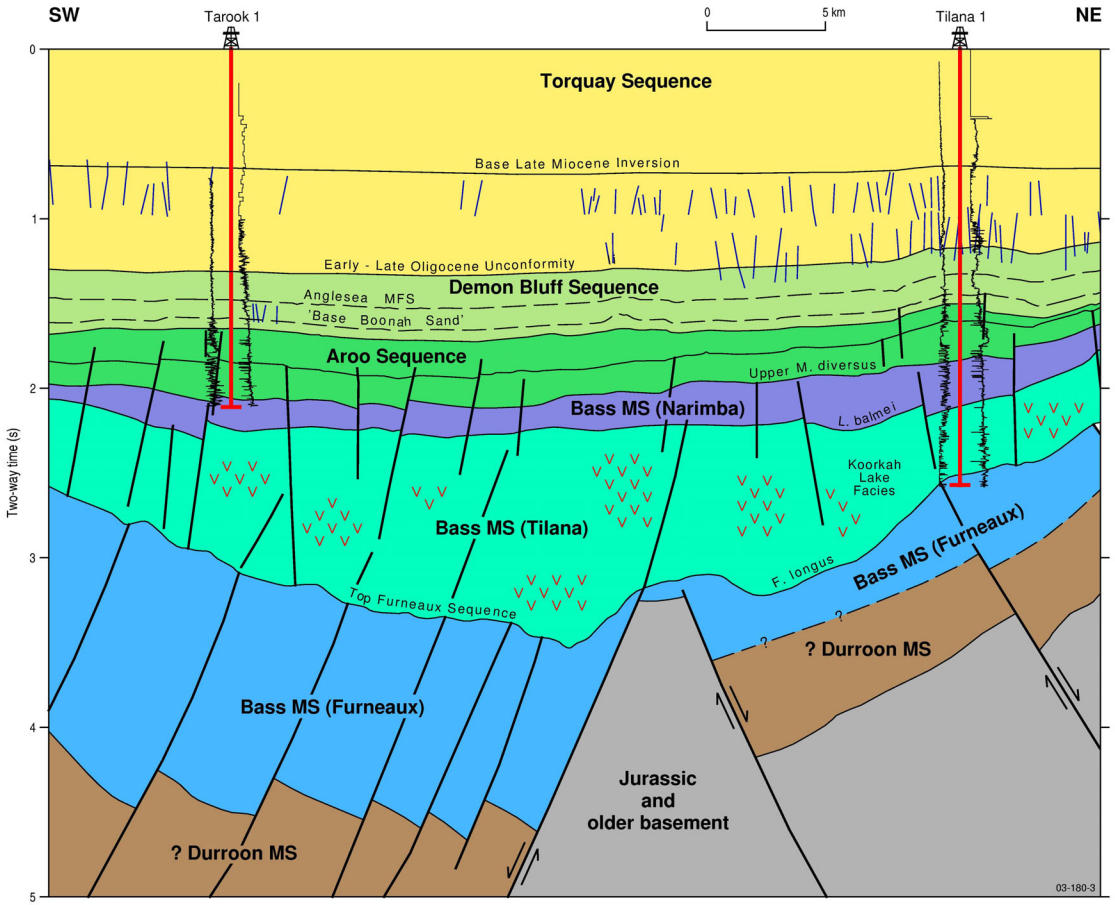


Figure 3.14 Diagrammatic cross-section across the central Bass Basin showing the syntectonic nature of the Durroon and Bass sequences (Furneaux, Tilana and Narimba sequences), and the overlying post-rift successions of Aroo, Demons Bluff and Torquay sequences. The stratal geometry and faults controlling the deposition of the Tilana Sequence are obscured due to the prolific intrusion of volcanics into the succession. The Narimba Sequence shows only minimal growth on this section.

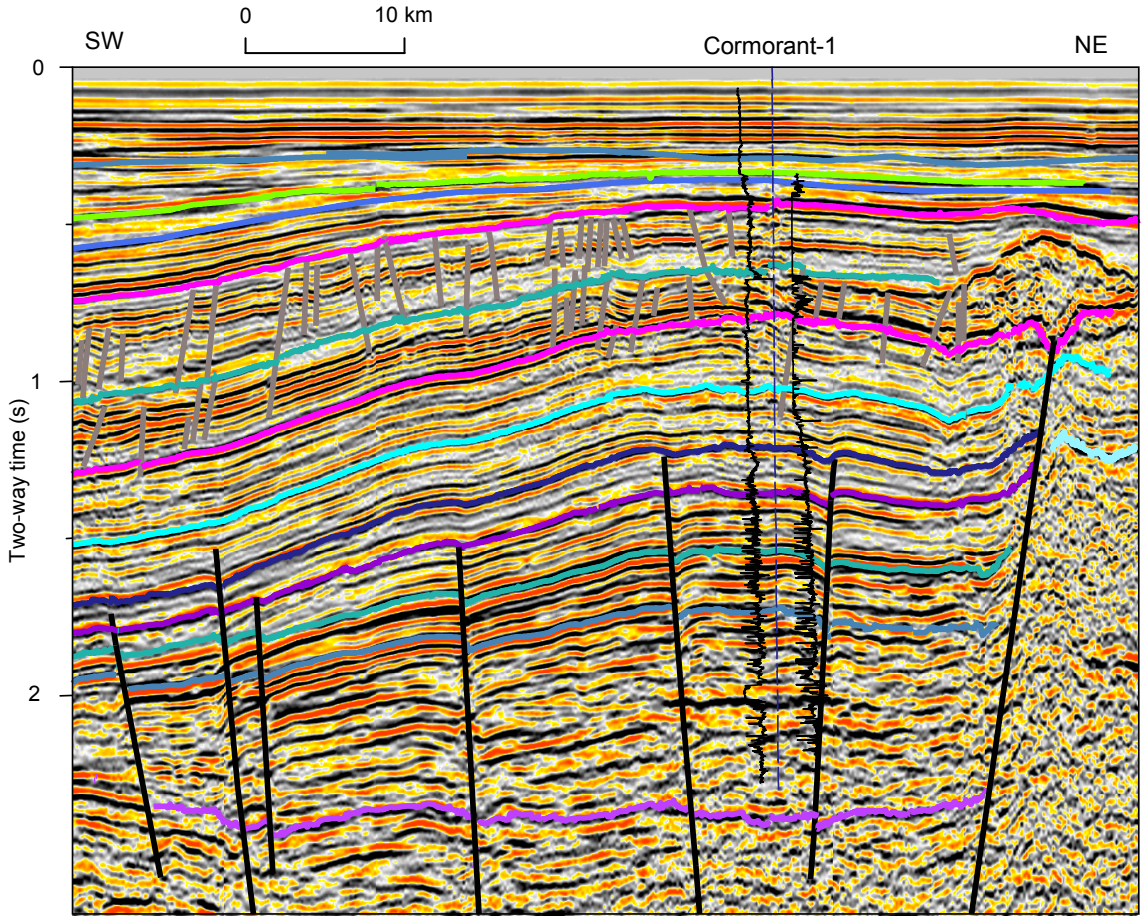


Figure 3.15 Geoscience Australia seismic line across the Cormorant Anticline. The anticline is an inversion structure that formed against the northwestern margin of the basin. The syn-inversion succession at Cormorant-1 has been dated as late Middle Miocene and younger. Cormorant-1 well drilled a minor graben within the crestal collapse structure, and intersected minor oil and gas legs in the Palaeogene succession. High-amplitude, cross-cutting volcanic intrusions seen near 2.00 s TWT were intersected by the well. In addition, a large volcanic mound is observed to the north of Cormorant-1. The mound overlies the mid-Oligocene unconformity and maybe associated with basinward polygonal faulting. This seismic image is published with the permission of Fugro MCS.

4. ACCOMMODATION CYCLES AND SEQUENCE STRATIGRAPHY

J. Blevin and K. Trigg, Geoscience Australia
S. Lang, National Centre for Petroleum Geology and Geophysics
A. Partridge, Biostrata Pty Ltd.

4.1 KEY POINTS

- The integration of biostratigraphy, sequence and seismic stratigraphy to identify accommodation cycles and related environments has resulted in a sub-division of the Bass Basin stratigraphic succession. Six depositional sequences – mainly megasequences and supersequences – are recognised and correlated to phases of tectonic activity and eustatic fluctuation.
- Three megasequences are related to phases of rift-related extension. Evidence of the initial rift phase (Otway Megasequence) is only clearly observed in the Durroon Sub-basin and in the southwestern Cape Wickham Sub-basin (near Bass-3/White Ibis-1 wells).
- The second rift phase (Durroon Megasequence) is pervasive throughout the Bass Basin, although a full succession of this megasequence was only penetrated in the Durroon Sub-basin.
- The third-rift phase (Bass Megasequence) is also pervasive throughout the basin, but appeared to affect only particular depocentres such as the Pelican, Cormorant and Yolla troughs. Here, expanded syn-tectonic growth sections have been intersected (Narimba-1). There is wide variation in facies type, environment and thickness of the Bass Megasequence due to differential rates of subsidence. Three component sequences have been recognised with the Bass Megasequence (Furneaux, Tilana and Narimba sequences). Each sequence correlates to discrete periods of increased accommodation.
- The shift from rift-to-post-rift conditions (Subsidence Phase 1 – Aroo Megasequence) was signaled by waning subsidence rates and an increasing brackish influence. A wide variation in facies types, environments and thicknesses is also observed within this megasequence. The frequency and thickness of coals began to increase during the deposition of this megasequence, lasting from Early Eocene until the mid-Middle Eocene. A slow down in subsidence rates allowed the aggradation of coaly facies and indicates there was a balance between accommodation, sediment supply and peat production.
- The most important megasequences for petroleum generation and trapping are the Bass and Aroo megasequences. Accommodation has controlled the stacking of oil-prone coaly facies, while the increasing marine influence has provided an early cement to fluvial and deltaic sandstone reservoirs. Optimal conditions for seal deposition occurred during lacustrine cycles in the Late Cretaceous to Early Eocene, and the mid-Eocene.

4.2 METHODS AND TIMESCALES

A dataset of geophysical well logs, biostratigraphic and seismic data was interpreted and integrated using principles of seismic and sequence stratigraphy to define a broad-scale basin framework. Petrophysical logs

from 29 of the 32 wells in the Bass Basin were interpreted and correlated via synthetic seismograms (generated using Geoquest software) to a 4,000+ km regional seismic grid (Fig. 4.1). The grid included reprocessed industry data (licensed through Fugro MCS) and reprocessed deep seismic data acquired by Geoscience Australia during 1990-92 (Geoscience Australia Surveys 40, 82 and 90). Seismic images used as figures in this report are published with the permission of Fugro MCS.

A modified version of the Geoscience Australia (formerly AGSO) Phanerozoic Timescale and Biozonation Chart (Young and Laurie, 1996) was used as the reference timescale for this study (Figures 4.2a and 4.2b). The Mesozoic portion of the biozonation scheme is based on Helby et al. (1987), with modifications to age boundaries provided by subsequent radiometric analyses. Further modifications to the timescale were made to incorporate changes to biozonations boundaries as published by Partridge (2001). These changes affected biozones within the Albian to Late Paleocene age range. The present study incorporates the new biostratigraphic work commissioned by Geoscience Australia, on behalf of Mineral Resources Tasmania under the funding auspices of the Western Tasmanian Regional Minerals Program. The work was undertaken by Dr. Alan Partridge, Biostrata Pty Ltd on selected well intervals to address specific scientific questions relating to depositional environment (including processing for microplankton and other evidence indicative of marine influence) and evidence of cyclicity. In addition, the sampling program targeted gaps in the drilled section at key wells. Overall, intervals within seven wells were studied (Cormorant-1, King-1, Konkon-1, Koorkah-1, Poonboon-1, Squid-1 and Durroon-1) – the full reports of these analyses are included as Appendices C1 to C8 of this Record (which includes a Summary Report). A new stratigraphic chart for the Bass Basin proposed by Partridge (2002) summarises this work (Figure 4.3).

4.3 SEQUENCES MAPPED AND NOMENCLATURE

A total of 15 seismic horizons were mapped throughout the seismic grid (Appendix B). These horizons include megasequence and sequence boundaries, as well as multiple marker horizons within sequences. Consistent with a sequence stratigraphic approach, the *bases of sequences* were mapped throughout the seismic grid. Most horizons mapped correlate to unconformities within the stratigraphic succession, although in some instances (particularly in the uppermost Torquay marine succession) some horizons mark lithologic changes such as marl-to-carbonate facies. The approach used in this study aimed to understand the tectonostratigraphic nature of the basin succession, and to overcome difficulties often experienced in regional lithostratigraphic correlations in a terrestrial basin system. Further descriptions of facies and palaeo-environmental interpretations of selected intervals are presented in Chapter 9 and Appendix C.

There are several published nomenclature schemes for the Bass Basin stratigraphic succession (Robinson, 1974; Smith, 1986; Williamson et al., 1987; Maung, et al., 1993; Hill et al., 1995; Lennon et al., 1999). Most vary in their sub-division and use of the terms "Eastern View Coal Measures" (Lennon et al., 1999) and "Eastern View Group" (Smith, 1986; Maung et al., 1993). The most recent scheme (Lennon et al., 1999; Figure 4.2b) divided the entire Bass Basin stratigraphic succession into three broad lithostratigraphic units -

the Torquay Group, the Eastern View Coal Measures (includes Upper, Middle and Lower sub-divisions) and the Otway Group (Figure 4.3).

An aim of this study has been to subdivide the stratigraphic succession into tectonically-controlled cycles of deposition (megasequences) and, in particular, to recognise depostional cycles within the "Eastern View Group". Adopting existing names (such as the "Eastern View Coal Measures") into a new sequence stratigraphic framework is useful, particularly where there is some correlation between lithostratigraphy and the new sequences identified. However, in the case of the Bass Basin, many of the names in use were drawn from type sections in other basins (e.g., the Eastern View Coals Measures was identified in the Torquay Basin – Raggatt and Crespin, 1952, 1955; then applied to the Bass Basin – Brown, 1976). To avoid confusion, new names have been adopted for sequences where type sections have been identified.

4.4 ACCOMMODATION CYCLES

The Bass Basin contains sediments ranging in age from Early Cretaceous to Recent. Jurassic dolerites, Palaeozoic and older sediments are present within the pre-rift basement blocks that floor the Mesozoic basin. The Bass Basin formed as an intra-cratonic rift basin within the shallow basement ridge system that underlies the present-day Bass Strait. As continental breakup and seafloor spreading bypassed this region, the Bass Basin did not progress to become a passive margin basin, as occurred in the flanking Otway, Sorell and Gippsland basins. From the Early Cretaceous to Middle Eocene, much of Bass Basin sedimentary succession was deposited in terrestrial to marginal marine environments. Sediments eroded from the basin flanks and adjacent highlands were deposited in fluvial and lacustrine environments in the developing rift basin as part of an internal drainage system. Widespread marine flooding of the basin did not occur until the late Middle Eocene, with deepening marine environments dominating from the Late Miocene onwards.

The regional tectonic setting of the Bass Basin between two major rift systems (Southern Rift System and Tasman Basin) has meant that the basin was subjected to complex inter- and intra-plate stresses and multiple periods of upper crustal extension prior to seafloor spreading in the adjacent basins. The basin was particularly influenced by the prolonged process of separation that occurred between Australia and Antarctica during the Paleocene to Late Eocene. It is also suggested that a fundamental basement boundary underlies the Bass Basin (Chapter 3). This boundary may have acted to partition stresses and further influence the nature of tectonically-driven accommodation cycles. Although the present-day geometry of the Bass Basin appears to have evolved as a series of linked, relatively simple half graben, regional chronostratigraphic correlations now show that cycles and rates of accommodation varied between individual depocentres. This scenario, together with the difficulty in correlating terrestrial facies of limited lateral extent, has meant that lithology-based correlations are difficult. In addition, the lack of significant time gaps in the stratigraphic succession suggests that deposition across the basin has been more-or-less continuous, particularly from the Late Cretaceous onward. The overall succession is riddled with multiple third- and four-order unconformities, often of local extent.

Six regional-scale basin phases and associated megasequences and sequences have been identified (Chapter 3). Factors that controlled the complex facies relationships observed in the basin have been discussed in Chapter 3. Three megasequences are related to phases of extension. Evidence of the initial rift phase (Otway Megasequence) is only clearly observed in the Durroon Sub-basin and in the southwestern Cape Wickham Sub-basin (near Bass-3 and White Ibis-1). The second rift phase (Durroon Megasequence) is pervasive throughout the Bass Basin, although the full succession of sediments of this megasequence was only penetrated in the Durroon Sub-basin. The third-rift phase (Bass Megasequence) is also pervasive throughout the basin, but appeared to affect only particular depocentres where expanded syn-tectonic growth sections have been intersected (Narimba-1). There are wide variations in facies type, environment and thickness of the Bass Megasequence due to differential rates of subsidence. The rift-to-post-rift phase of basin evolution (Subsidence Phase 1 – Aroo Sequence) signaled a shift to waning subsidence rates and increasing brackish influence. Wide variations in facies types, environments and thicknesses are also observed within this sequence. The Demons Bluff and Torquay sequences were deposited during subsequent periods of post-rift thermal subsidence (Subsidence Phases-2 and -3). Multiple episodes of margin uplift, inversion and volcanic intrusion/extrusion affected the basin during the deposition of the Subsidence Phase-3 sequence. These effects are often localised and they have not been identified as separate basin phases. Presented below is a summary of the megasequences/sequences and accommodation cycles determined from this study.

4.5 OTWAY MEGASEQUENCE

Durroon-1 was the only well in the Bass Basin to intersect Early Cretaceous sediments of the Otway Megasequence (Baillie and Pickering, 1991; Figures 4.4 and 4.5; Table 4.1). Durroon-1 intersected two syn-tectonic sequences – an Early Cretaceous, 1452 m thick succession of Aptian to late Albian age sediments (Otway Megasequence), overlain by a 374 m thick syn-rift succession of Turonian to Mid-Campanian age (Durroon Megasequence – see below). These sequences are separated by a 36 m thick basaltic unit. The Early Cretaceous (Otway Megasequence) syn-rift succession overlies basement, and is itself the pre-rift to the later Turonian to mid-Campanian syn-rift succession (Figure 4.4; Durroon Megasequence). The Otway Megasequence is the chronostratigraphic equivalent of the post-rift Eumeralla Formation in the Otway Basin, and the post-rift Upper Strzelecki Group in the Gippsland Basin, as defined by Norvick and Smith (2001). The age and stratal geometries of the early Otway Megasequence suggest that it was deposited during a period of slow subsidence within a low relief trough, possibly during the initiation of the rift basin, but prior to the onset of rapid upper crustal extension. Strong truncation at the "top" of the Otway Megasequence is observed on footwall fault blocks (Baillie and Pickering, 1991), suggesting that a moderate amount of uplift occurred during fault movement prior to deposition of the overlying Durroon Megasequence.

The Otway Megasequence consists of a stacked succession of blocky, fluvial channel sands with thin, coaly overbank-floodplain shales (Figure 4.5). These sediments bear a strong lithological similarity to the Eumeralla Formation in the Otway Basin. Overall, organic-rich facies are typically thin, although the frequency of coals increases in uppermost 650 m of the sequence. Potential sealing facies are limited to thin

(<10 m thick) intraformational shales interbedded with the coals. A single core of lithic sandstone had a measured porosity of 6 to 10%, and permeability of 0.07 to 0.74 md (Core Laboratories Inc., 1985).

Table 4.1 Otway Megasequence (Rift Phase 1)

Age:	Aptian to latest Albian (?possibly Barremian – inferred)
Top:	Late Albian, *P. pannosus* (Otway Unconformity)
Base:	Aptian, *C. hughesii* (approximate *P. notensis* equivalent)
Type Section:	Durroon-1
Formation Equivalent:	Otway Group Equivalent (Lennon et al., 1999)
Dominant Lithology:	Sandstones with volcanogenic clastics and minor coal
Environment:	Fluvio-deltaic
Unconformities:	Multiple (Intra-*C. striatus*, Intra-*C. paradoxa*)
Sequence Character:	Aggradational stacked channel sands, multiple (6) transgressive-regressive cycles
Aerial Extent:	Limited to early trough/s and half graben in the Durroon Sub-basin. May lie deeply buried in similar structures in the Cape Wickham Sub-basin.
Play Elements:	Probably variable prospectivity; mostly lean source rocks, although some intervals with higher source potential (98 to 112 Ma; Chapter 5); moderate reservoir quality, only minor intraformational sealing facies

4.6 DURROON MEGASEQUENCE

Durroon-1 was the only well in the Bass Basin to intersect a complete stratigraphic succession of early Late Cretaceous age of the Durroon Megasequence (Figures 4.4 and 4.5; Table 4.2). Chat-1, Koorkah-1 and Pelican-5 penetrated strata of similar mid-Campanian age (*T. lillei* spore/pollen zone), but recent work by Partridge (2002) has shown the zone at Koorkah-1 to be younger (i.e., *F. longus* in age and thus not part of the Durroon Megasequence). Elsewhere in the basin, this sequence is imaged on seismic data where it lies deep within the depocentres. Only two wells have tested plays within the Durroon Megasequence (Durroon-1 and Chat-1).

In the Durroon-1 well, the megasequence consists of approximately 36 m of basalt, overlain by 374 m of shale, siltstone and sandstone of Turonian to mid-Campanian age. Informally, Baillie (cited by Partridge, 2002) proposed the following lithostratigraphic subdivision of the Durroon Megasequence: "Furneaux Group" (1544 - 1646 m), "Durroon Formation" (1370 - 1544 m), and the "Boobyalla Formation" (1235 - 1370 m). The Durroon Formation was later formally proposed by Smith (1986) for the shaley section lying between 1374 and 1545 m. Recent biostratigraphic work by Partridge (2002; Appendix C) on the Durroon Formation suggests deposition in a distal, probably deep, freshwater lacustrine environment (Figure 4.6). These facies contain a moderate to high abundance of non-marine microplankton and abundant *Dilwynites* and *Araucariacites* pollen. The Durroon Formation is the chronostratigraphic equivalent of the youngest part of

the Kipper Shale in the Gippsland Basin. Deposition in a lacustrine environment is consistent with the tectonostratigraphic interpretation of these facies as tectonically-controlled rift lakes. Partridge (2002; Figure 4.6; Appendix C) has not identified Santonian (*T. apoxyexinus* spore/pollen zone) sediments in the Durroon-1 well. However, sediments of this age have been interpreted on seismic data, with absence at the well due to stratigraphic pinchout (onlap) onto steeply dipping footwall blocks.

In contrast to the underlying Otway Megasequence, the Durroon Megasequence shows strong syn-tectonic growth of strata against the bounding normal faults (Figure 4.4). This indicates that the main phase of rift-related accommodation occurred during a relatively short-lived period of upper crustal extension lasting from the Turonian to mid-Campanian, associated with rifting in the Tasman Basin to the east. In the Gippsland Basin, this event is recorded by the syn-rift Emperor and rift-transition Golden Beach megasequences (Norvick and Smith, 2001). Due to depth of burial and its association with volcanic material in the western Bass Basin, only the "top" of the sequence can be confidently picked on seismic data.

Table 4.2 Durroon Megasequence (Rift Phase 2)

Age:	Turonian to mid-Campanian
Top:	Mid-Campanian, intra- *T. lillei* spore/pollen zone
Base:	Early Turonian, *P. mawsonii* spore/pollen zone (zone not present in well succession, but inferred from seismic interpretations); overlies the Otway Unconformity
Type Section:	Durroon-1
Formation Equivalent:	Lower Eastern View Coal Measures/Durroon Formation (Lennon et al., 1999)
Dominant Lithology:	Basal volcanic rocks, overlain by sandstones that grade upward to shales and siltstones
Environment:	Fluvio-deltaic to lacustrine, syn-rift lakes and associated marginal environments
Unconformities:	Multiple minor unconformities, probably related to high-order changes in the rate of accommodation or sediment supply; intra-*T. apoxyexinus*; intra-*N. senectus* zones
Sequence Character:	Basal channel sandstones (blocky), maximum flooding surface with lacustrine shales overlain by lacustrine deltaic sands
Aerial Extent:	Widespread across the half graben of the Durroon Sub-basin (seismically mapped, although difficult well tie due to steepness of dipping beds). Probably lies deeply buried in the Cape Wickham Sub-basin, but difficult to map.
Play Elements:	Low source potential (Chapter 5), although only one well has fully tested the sequence to determine source potential; moderate to poor reservoir quality, possible lacustrine sealing facies to alluvial and lacustrine deltaic sands

4.7 BASS MEGASEQUENCE

The mid-Campanian to late Early Eocene Bass Megasequence (Tables 4.3, 4.4 and 4.5) has been subdivided into three second- or third-order sequences based on the recognition of significant bounding unconformities

and intervals of syn-tectonic growth: **Furneaux** (mid-Campanian to latest Maastrichtian), **Tilana** (latest Maastrichtian to late Late Paleocene) and **Narimba Sequences** (latest Paleocene to late Early Eocene). The megasequence and its sequence components can be difficult to map seismically across the basin due to significant lateral changes in facies, seismic character and overall unit thickness (300 to >2500 m). During this period of basin evolution, region-scale tectonic processes were waning and the locus of accommodation shifted between different structural elements within the basin. Pelican-5 is the only well to penetrate all three sequences (Figure 4.7). Unfortunately, intense faulting within the Pelican Trough has meant that it is difficult to confidently map the sequence boundaries beyond this structure (Figure 4.8). Other wells with significant sections are Narimba-1, Poonboon-1, Tilana-1, Aroo-1, and Koorkah-1. The Bass Megasequence is roughly correlative to the "Middle Eastern View Coal Measures" of Lennon et al. (1999; Figure 4.2b), although subdivisions within the unit have not been previously documented.

The Furneaux Sequence encompasses the mid-Campanian (intra-*T. lillei* zone) to latest Maastrichtian (Near base Upper *F. longus* zone; Table 4.3) succession. The sequence is well imaged on seismic data in the central and western basin, around the Poonboon-1, Tilana-1 and Tarook-1, and Koorkah-1 and Toolka-1A wells (Figure 4.9). The upper sequence boundary was penetrated at Koorkah-1 (2955 m) and Pelican-5 (3695 m), but lies below TD in the other wells. Seismic interpretation suggests that the Furneaux Sequence was deposited as a syn-rift succession as a result of reactivation of older Early Cretaceous extensional faults (Figure 4.9). The sequence is heavily intruded by volcanic material and associated fluids (Tilana-1; Figure 4.10), and has undergone mild inversion during the latest Cretaceous. The Furneaux Sequence is the chronostratigraphic equivalent of the upper part of the syn-rift Sherbrook Group in the Otway Basin (Norvick and Smith, 2001). Where penetrated, the sequence ranges from interbedded fluvio-deltaic sandstones and freshwater lacustrine shales (Koorkah-1), to fluvio-deltaic sandstones and thin interbedded overbank or delta plain shales and coals (Pelican-5). The upper sequence boundary is marked by an angular unconformity, and is approximately coeval with Maastrichtian breakup in the flanking Otway Basin.

Table 4.3 Bass Megasequence: Furneaux Sequence (Rift Phase 3)

Age:	Mid-Campanian to Late Maastrichtian
Top:	mid-Late Maastrichtian, near base of Upper *F. longus* spore/pollen zone
Base:	Mid-Campanian, lower intra-*T. lillei* zone (only intersected in a few wells; some confusion on *T. lillei* picks in wells drilled during the 1980s – Koorkah-1).
Type Section:	Koorkah-1, Pelican-5
Formation Equivalent:	Part of the Middle Eastern View Coal Measures (Lennon et al., 1999)
Dominant Lithology:	Interbedded sandstone, siltstone and shale, with lacustrine shale and minor coal
Environment:	Fluvio-deltaic with minor freshwater lacustrine influence
Unconformities:	Minor within Lower *F. longus* spore/pollen zone
Sequence Character:	Overall transgressive – regressive cycle with multiple higher-order cycles within

Aerial Extent:	Across most of the Bass Basin, deeply buried except along the basin margins
Play Elements:	Transgressive-regressive cycles provide good stacking of reservoir and seal facies

The Tilana Sequence encompasses the latest Maastrichtian (near base Upper *F. longus* zone) to latest Paleocene (near base Upper *L. balmei* zone) succession. Seismic correlations suggest that deposition of the Tilana Sequence was controlled by a combination of reactivation of underlying Early Cretaceous faults, tectonic subsidence, sediment loading and compaction (Figure 4.9). Some areas of the basin appear to have been unaffected by increased subsidence during this time (Poonboon-1) suggesting that rates of accommodation varied significantly between the different rift segments. This variation in accommodation is clearly shown in the thickness and range of facies types deposited.

Biostratigraphic work undertaken by Partridge (2002) for the WTRMP focused on the evaluation of Late Cretaceous to Eocene facies in Koorkah-1, Poonboon-1 and Konkon-1 (Appendices C4, C5 and C6). These analyses show the occurrence of lagoonal, freshwater and brackish lacustrine environments across the Bass Basin from the latest Maastrichtian to late Early Eocene (Figures 4.11 and 4.12). The "Lower Koorkah" lake cycle (base Upper *F. longus* to base Upper *L. balmei* zones) generally correlates with the Tilana Sequence, while the "Upper Koorkah" lake cycle (Upper *L. balmei* to base Upper *M. diversus* zones) correlates with the overlying Narimba Sequence (Figures 4.9 and 4.11). Koorkah-1, Tilana-1 and Aroo-1 are type sections of these facies. The wells show basal fluvial channels sandstones overlain by thick (100+ m), freshwater lacustrine shales, grading upward to progradational lacustrine deltaic and shoreface sandstones capped by thin coal beds (Figure 4.11). Unfortunately, no cores were available to determine seal capacity of the lacustrine shales (MICP analysis; Chapter 7), but the thickness and widespread nature of these facies suggest good sealing capability. Geochemical analysis show moderate source potential (Chapter 5).

The Koorkah Lake facies are best developed in areas where fault-controlled subsidence rates were moderate to high (4.13). In contrast to the strongly aggradational and progradational nature of the Koorkah Lake facies, deltaic-to-lower coastal plain facies characterise areas like the "Tertiary Platform" (Lennon et al., 1999), where only minimal subsidence occurred. Here, the equivalent age facies are thinly bedded successions of fluvio-deltaic sandstones, floodplain shales and peat mire coals (Figure 4.14; Poonboon-1). Significantly, the geochemical characterisation of interbedded coals and shales undertaken for this project (Chapter 5) identified two instances of hydrogen-rich coals. The oldest occurrence was noted at Poonboon-1 (3042 m), and suggests that while lakes occupied the deeper areas of the basin, oil-prone coals were forming on the fringing floodplains and peat mires. This scenario is depicted in a palaeogeographic map of the Bass Basin (Figure 4.15), and potentially upgrades the prospectivity of the margins where subsidence rates were low and potential oil-prone coals accumulated.

Similar to the underlying Furneaux Sequence, the Tilana Sequence is also associated with extensive volcanic activity (probably both syn- and post-depositional; Figure 4.9). Selected intervals within the thick succession of "volcanic rock" penetrated at Tilana-1 have been re-examined in thin section. This has shown that some

of the rocks are highly fractured, lithic sandstones cemented by basaltic material (A. Lambeck, T. Dance, Geoscience Australia, personal communication, 2003). This intrusion of volcanic material into the sandstones is thought to reflect the initial high porosity. While this process has destroyed porosity and permeability, the sills could act as effective seals. Similarly, where unaffected by volcanic intrusions, the lacustrine deltaic sandstones should have good reservoir qualities (Koorkah-1).

Table 4.4 Bass Megasequence: Tilana Sequence (Rift Phase 3)

Age:	Latest Maastrichtian to latest Paleocene
Top:	Late Paleocene, near base of Upper *L. balmei* spore/pollen zone
Base:	Late Maastrichtian, near base Upper *F. longus* spore/pollen zone
Type Section:	Koorkah-1, Tilana-1, Aroo-1
Formation Equivalent:	Part of the Middle Eastern View Coal Measures (Lennon et al., 1999)
Dominant Lithology:	Fluvio-deltaic sandstones, floodplain shales and coals. Lacustrine shale with interbedded lacustrine deltaic sandstones and minor coal.
Environment:	Fluvio-deltaic, floodplain and freshwater lacustrine
Unconformities:	Minor unconformity within Lower *L. balmei* spore/pollen zone
Sequence Character:	Overall transgressive – regressive cycle with multiple higher-order cycles within
Aerial Extent:	Across most of the Cape Wickham Sub-basin, thinning in the Durroon Sub-basin
Other:	Transgressive-regressive lacustrine cycles provide good stacking of reservoir and seal facies; associated coals fringing the lakes provide source rocks (Poonboon-1).

The latest Late Paleocene to late Early Eocene Narimba Sequence is the youngest sequence within the Bass Megasequence. The Narimba Sequence was deposited across most of the Bass Basin as a result of the reactivation of select Early Cretaceous rift faults. Seismic interpretations show that significant growth occurred in the Pelican, Yolla and Cormorant troughs (Smit, 1988; Lennon et al., 1999) over the interval defined by "base Upper *L. balmei* " to "base Upper *M. diversus* ". A similarly thick section is encountered at Squid-1 just west of the accommodation zone. As tectonic stresses during this period were largely oblique and far-field, much of the basin was unaffected by significant fault movement (thinner sections were penetrated at Poonboon-1, Nangkero-1, Dondu-1 and Yurongi-1). As a result, the Narimba Sequence shows the broadest range in lithology and facies types, environments and thickness across the Cape Wickham Sub-basin.

Narimba-1 is the type section for the syn-tectonic facies of the Narimba Sequence (Figure 4.16). The well penetrated an 800+ m thick succession of aggradational fluvio-deltaic to floodplain sandstones, shales and thin coals beds. A combination of high rates of accommodation and a steady supply of sandy sediment feeding down the flanks of the rift from northern Tasmania account for the unusually high rate of sedimentation in the Pelican Trough. Similarly high accommodation rates existed in the Cormorant and Yolla troughs. At Poonboon-1, where subsidence rates were lower, equivalent age facies consists of <400 m of

thinly bedded shale, sandstone and coal deposited in lacustrine, lower delta plain and peat mire environments (Figure 4.14). Biostratigraphic analysis (Partridge, 2002) indicate the onset of brackish influence in these wells within the lowermost part of the Upper *L. balmei* succession. The Narimba Sequence is equivalent to the "Upper Koorkah" lake facies identified by Partridge (2002) in Koorkah-1.

While the facies and thicknesses of the Narimba Sequence vary widely, there is one distinct event that can be correlated in almost every well in the basin - a maximum flooding surface (MFS) within the Lower *M. diversus* succession (Figure 4.17). At Poonboon-1, this flooding surface marks the turnaround from transgressive (fining-upward and retrogradational cycles) to regressive facies (largely progradational cycles) within the Narimba Sequence. In this example, coals are rarer in the lower transgressive succession, but became increasingly more frequent and thicker in the regressive succession (Poonboon-1, Dondu-1). This pattern of facies stacking also has direct significant for petroleum exploration. A transgressive shale from 2342.0 m (Upper *L. balmei* zone) at Dondu-1 yielded the highest measured seal capacity of the 15 samples analysed for this study (1395 m/ maximum oil column height, 567 m/maximum gas column height; Chapter 7). In Pelican-5, coals sampled just above the MFS (2800 m) were determined to be hydrogen-rich (HI = 406.5 mg hydrocarbons/gTOC) and have a higher sulphur content (2.46%), while shales within at the MFS could be characterised as "oil shales" (Chapter 6; Boreham et al., 2003).

In the westernmost part of the Bass Basin, Lower Cretaceous rifts also underwent reactivation and moderate extension during deposition of the Narimba Succession. Toolka-1A is located within a shallow half graben and penetrated the entire syn-tectonic succession (Figure 4.13). This well recorded an "intermediate example" between the higher (Narimba-1) and lower (Poonboon-1) rates of accommodation observed across the basin. Both the "Upper Koorkah" and "Lower Koorkah" lake facies are recognised in the well. The "Lower Koorkah" succession (Tilana Sequence) at Toolka-1A is a 418 m thick (2264 - 2682 m), monotonous shale deposited in a moderately deep rift lake environment. The overlying "Upper Koorkah" lake facies (1917 - 2264 m) indicate a shallower lake setting, with prograding lacustrine-deltaic sandstones capped by moderately thick coals (2 to 8 m thick). The upward increase in coals is clearly evident on seismic data.

Table 4.5 Bass Megasequence: Narimba Sequence (Rift Phase 3)

Age:	Late Paleocene to mid-Early Eocene
Top:	mid-Early Eocene, base of Upper *M. diversus* spore/pollen zone
Base:	Late Paleocene, near base Upper *L. balmei* spore/pollen zone
Type Sections:	Localised syn-tectonic facies usually occur over the interval defined by intra-Lower *L. balmei* to base Upper *M. diversus* zones. The expanded section is related to reactivation of selected growth faults within the Pelican, Yolla and Cormorant troughs. In areas unaffected by fault movement, slower rates of subsidence prevailed. Narimba-1: Lower *L. balmei* to base Upper *M. diversus* zones – expanded terrestrial fluvial section due to growth faulting

	Nangkero-1: *L. balmei* to base *M. diversus* zones – terrestrial fluvial 'condensed section' due to slow subsidence
Formation Equivalent:	Uppermost part of the Middle Eastern View Coal Measures (Lennon et al., 1999)
Dominant Lithology:	Narimba-1: sandstones, shales with thin coals at the top of progradational units Nangkero-1: thinly bedded sandstones, shales and coal Koorkah-1: lacustrine mudstone with shoreface and prograding deltaic sandstones and minor coal
Environment:	Narimba-1: fluvio-deltaic to delta-plain with only minor lacustrine influence Nangkero-1: mostly fluvial-deltaic Koorkah-1 and Aroo-1: freshwater to brackish lacustrine or lagoonal
Unconformities and other markers:	Intra-Lower *M. diversus* "maximum flooding surface" (in many wells, signaling maximum accommodation or rise in base level)
Sequence character:	Variable with environment; aggradational to progradational
Aerial extent:	Across most of the Bass Basin but variable thickness (<100 to 900+ m)
Play elements:	Lacustrine mudstones are excellent intraformational seals; Lacustrine progradational and shoreface sands have variable reservoir quality; Hydrogen-rich coals deposited during transgressive cycle (Poonboon-1) possible with lacustrine association.

4.8 AROO SEQUENCE

The late Early Eocene to early Middle Eocene Aroo Sequence (base Upper *M. diversus* to Intra-Lower *N. asperus* zones; Table 4.6) marks the period when large-scale tectonic activity had ceased across most the Bass Basin (Subsidence Phase 1). Many faults that experienced significant movement throughout the evolution of the basin terminated at either the 'Base Upper *M. diversus*" or "Base *P. asperopolus*" horizons. The shift from rift-to-post-rift conditions was signaled by waning subsidence rates and an increasing brackish influence. The frequency and thickness of coals began to increase during the deposition of this sequence, beginning in late Early Eocene and lasting until the mid-Middle Eocene. A slow down in subsidence rates was accompanied by the proliferation of peat mires in broad floodplain environments and along the fringing margins of localised, shallow lakes. The aggradation of coaly facies indicates there was a balance between accommodation, sediment supply and peat production. The lower sequence boundary at Nangkero-1 and Dondu-1 (base Upper *M. diversus* zone) is marked by distinctively thick coals that are 10 and 25 m thick, respectively.

In the Cormorant and Yolla troughs, sedimentation rates were marginally higher during this period. This was probably due to a combination of factors, most likely higher compaction rates (within the underlying syn-tectonic succession) and the fact that these structures were the locus of recent tectonic activity. At Cormorant-1 and Yolla-1, the lower boundary of the Aroo Sequence is difficult to recognize, suggesting that accommodation rates varied only slightly across this boundary. However, as noted elsewhere in basin, the

frequency and thickness of coals increases within the Aroo Sequence in the Cormorant and Yolla troughs, occurring mainly as thin coals that cap short-cycles of coarsening-upward progradation. Palynological evidence suggest the existence of lagoonal to restricted marine conditions in the Cormorant Trough (Partridge, 2002; Appendix C). In contrast, mainly fluvial conditions persisted in the Pelican Trough and along southern margin of the Bass Basin. Here, sand-dominated fluvial systems migrated from northern Tasmania across the low relief flank of basin depocentre. Coals are present in this succession, but thinner and less frequent in the Pelican Trough.

There are a number of significant surfaces within the Aroo Sequence, including a lower-order unconformity in the latest Early Eocene (near the "base of *P. asperopolus*" zone; 2297 m at Pelican-5), and a regional flooding surface in the early Middle Eocene (near the boundary between the *P. asperopolus* to Lower *N. asperus* zones). The flooding surface coincides with a change from coastal plain and deltaic environments, to lagoonal-brackish conditions, as recorded by palynological evidence in Cormorant-1 (Partridge, 2002; Appendix C).

Table 4.6 Aroo Megasequence (Subsidence Phase 1)

Age:	late Early Eocene to mid-Middle Eocene
Top:	Middle Eocene, intra-Lower *N. asperus* spore/pollen zone
Base:	Early Eocene, base Upper *M. diversus* spore/pollen zone
Type Section:	Cormorant-1, Tarook-1, Bass-1, Pelican-3, Yurongi-1, Dondu-1, Chat-1
Formation Equivalent:	Upper Eastern View Coal Measures (Lennon et al., 1999)
Dominant Lithology:	Cormorant-1: mainly siltstone/shale with thin interbeds of sand and coal Pelican-5: stacked channel sandstones with shale and thin coal Yurongi-1, Dondu-1: thick sandstones and coal
Environment:	Fluvio-deltaic, shallow lacustrine and lagoonal-to-restricted marine surrounded by peat mires (central and western basin). Fluvial environments dominated in the southern basin.
Unconformities and other markers:	Latest Early Eocene unconformity (base *P. asperopolus* zone), followed by flooding surface in the early Middle Eocene (boundary between *P. asperopolus* and *N. asperus* zones).
Sequence Character:	Trend from sand-rich to coal-rich is observed in correlation of wells from east to west. This reflects localised continued subsidence in the palaeo-depocentres such as the Cormorant and Yolla troughs, while fluvial systems continued to dominate in the southern part of the basin. Cormorant and Yolla troughs: Aggradation to progradational cycles capped by thin coals (lacustrine delta and shoreface sands).
Aerial Extent:	Widespread across the Bass Basin, but variable in thickness and facies type.
Play Elements:	Excellent source potential in coals, good reservoirs in fluvial sands.

4.9 DEMONS BLUFF SEQUENCE (SUBSIDENCE PHASE 2)

The Middle Eocene to Early Oligocene Demons Bluff Sequence is an overall transgressive-regressive succession that was deposited during a later stage of thermal subsidence (Table 4.7; Subsidence Phase 2). The Demons Bluff Sequence contains formation-based units such as the "Boonah Sand", Anglesea Formation and the regional sealing facies of the "Demons Bluff Formation", that have been described by previous workers (Figure 4.3). The base of the sequence (intra-Lower *N. asperus* zone) is clearly defined by thick channels sands at wells such as Pelican-3 (2048 m) and Narimba-1 (2048 m) on the margins the Pelican Trough. In the central and northern Bass Basin, the boundary is also well defined by thick sandstone units as seen at Poonboon-1 (2169 m), Aroo-1 (2255 m), Yurongi-1 (1490 m) and Dondu-1 (1889 m). Similar to the underlying Aroo Sequence, the basal boundary of the Demons Bluff Sequence is difficult to distinguish in the Cormorant and Yolla troughs, as well as in the western basin near Koorkah-1 and Toolka-1A. In these areas, it is suggested that the boundary is marked by a "correlative conformity" where deposition continued more-or-less uninterrupted due to locally higher rates of subsidence. Regional mapping on seismic data suggests that by the Middle Eocene, the depocentres of the former rift basin were buried and most of the rift-related topographic was obscured. The flanks of the basin were emergent and fluvial systems continued to feed sediment into low-lying areas. The former basin was relatively flat and featureless, except for subtle topographic lows which formed locally over areas of most recent tectonic activity (Cormorant and Yolla troughs; westernmost Bass Basin).

It was during this period in the Middle Eocene (Lower *N. asperus* zone), that Toolka Lake formed in the western Bass Basin (Partridge, 2002; Appendix C). Unlike the Upper Cretaceous to Paleocene Koorkah Lake, which was deeper and primarily confined to fault-controlled topographic lows, Toolka Lake covered a much wider area and was probably shallower (Figure 4.13). Recent palynological work has shown that Toolka Lake had a brackish influence (Figure 4.18; Cormorant-1; Partridge, 2002; Appendix C). Well log correlations suggest that the aerial extend of Toolka Lake expanded and contracted through time, with two lacustrine cycles recognised. The Toolka Lake succession has a distinctive stratal character on seismic data (Figure 4.19). Figure 4.20 depicts the palaeogeographic setting of the basin during the time of the Toolka Lake cycles. At times of maximum extent, the lake covered the deepest part of the western and central Bass Basin, with a proposed marine influence from the west/northwest (Partridge, 2002; Appendix C). Lacustrine shales and thin lacustrine deltaic and shoreface sands are recognised in wells such as Toolka-1A, Cormorant-1 and Koorkah-1. Fringing peat mires, lower delta plain, and fluvial-to-upper delta plain environments dominated the central and western parts of the basin (Figure 4.20).

In the late Middle Eocene (base Middle *N. asperus* zone), a fall in base-level resulted the demise of Lake Toolka and incision of the fluvial systems across the former lake. The fluvial sandstones that mark this boundary are known as the "Boonah Sand" (Figures 4.2a and 4.3). While this unit varies significantly in thickness, it is present across most of the Bass Basin and is the uppermost reservoir within the basin succession ("top reservoir"). The upper boundary of the "Boonah Sand" is a maximum flooding surface (MFS) that correlates to the base of the "Anglesea Formation", a shallow bay siltstone/shale facies. The

"Anglesea MFS" (intra-Middle *N. asperus* zone) is very distinct in wells in the central and southern Bass Basin, such as Pelican-5 (1749 m; Figure 4.7) and Dondu-1 (1622 m). However, mapping of this surface across the basin shows that the relationship between the "Boonah Sand" and the "Anglesea MFS" is more complex than a single, base wide flooding event. Several minor flooding surfaces can be identified below the "Anglesea MFS" that is so clearly seen in wells within the central and southern parts of the basin. This is useful in understanding the progradational nature of some of the underlying "Boonah Sand" facies. From the late Middle Eocene until the mid-Oligocene, the basin was under deepening marine influence. During this time, up to 350 m of siltstones and shales were deposited - including the regional sealing facies of the "Demons Bluff Formation".

Table 4.7 Demons Bluff Sequence (Subsidence Phase 2)

Age:	Middle Eocene to mid-Oligocene
Top:	Boundary between Early and Late Oligocene, I1/I2 planktic foraminifera zone
Base:	Middle Eocene, intra-Lower *N. asperus* spore/pollen zone
Type Section:	Pelican-3, Narimba-1, Konkon-1, Poonboon-1, Yurongi-1, Cormorant-1
Formation Equivalent:	Demons Bluff Formation and lower Torquay Group (Lennon et al., 1999)
Dominant Lithology:	channel and progradational sandstones, marine shales
Environment:	Lowstand fluvio-deltaic and shallow lacustrine systems (Toolka Lake) surrounded by peat mires, grading upward to shallow marine environments
Unconformities and other markers:	Base Middle *N. asperus* zone unconformity ("Base Boonah Sand"); intra-Middle *N. asperus* zone maximum flooding surface ("Anglesea MFS").
Sequence Character:	Overall transgressive-regressive cycle. Mostly aggradational with some progradation.
Aerial Extent:	Widespread across the Bass Basin, deposition in the Durroon Sub-basin recommenced after extended hiatus
Play Elements:	Good reservoir in fluvial sands and high potential for lacustrine shale sealing facies; regional sealing unit of the "Demons Bluff" shale.

4.10 TORQUAY SEQUENCE

An unconformity at the Early/Late Oligocene boundary is recorded in all wells throughout the Bass Basin. On seismic data, this unconformity correlates to the most regionally extensive surface (strong peak) that can be mapped confidently across the entire basin. The spatial extent and prominence of this surface suggest that it is related to a major fall in sea level (mid-Oligocene). By this time, any relicts of the underlying deep basin topography had been buried beneath the fine-grained sediments of the Demons Bluff Sequence, and the former basin depocentre was virtually flat and featureless. This scenario is supported by "flattened" seismic sections that show minimal palaeotopography in the basin at this time. Deposition of the Torquay Sequence (Table 4.8) commenced after a rise in eustatic sea level flooded the basin during the Late Oligocene,

bringing the onset of fine-grained shallow marine clastic sedimentation (siltstones and marls). Increasingly open marine conditions developed in the Middle Miocene, signaled by the deposition of bioclastic carbonates.

Precise dating of the Torquay Sequence is somewhat problematic due to a lack of biostratigraphic analyses (primarily planktonic foraminifera), as well as inconsistencies within the available data. The inconsistency within the dataset appears to be related to different authors and vintages of analyses. Overall, the best age control for the Torquay Sequence comes from Narimba-1 and the Pelican wells, while the foraminifera zones identified at Koorkah-1 are inconsistent and considered less reliable. The youngest sediments dated within the basin were recorded in Bass-3 (at 450 m) as latest Middle Miocene in age (planktonic foraminifera Zone C). Subsea coring by Blom and Alsop (1988) has shown a relatively thick succession (>36 m) of Late Pleistocene to Holocene sediments in Bass Strait.

Four prominent seismic horizons within the Torquay Sequence succession can be mapped regionally (listed from oldest to youngest): Base Torquay, Torquay-1, Torquay-2 and Torquay-3. Each horizon is correlated in wells to either higher-order sequence boundaries within the Torquay Sequence, or late-stage structural movements. Polygonal faulting is widespread throughout the basin (Das, 2001; Figure 4.21), but generally only affected ultrafine-grained sediments of Late Oligocene to Early Miocene age. Within the main basinal area, two sets of layer-bounded polygonal faults are recognised: Polygonal Fault Set-1 is bounded by horizons Base Torquay and Torquay-1, while Polygonal Fault Set-2 is bounded by surfaces within the Torquay-1 succession (mapped locally as Torquay-1A/base and Torquay-1C/top). The occurrence of polygonal faults is strongly facies controlled, thus variations to the distinct layer-bound fault sets are observed near the basin margins where lateral lithological changes occur. In the main basin, the thickness of the unfaulted sedimentary succession between the two polygonal-fault sets varies widely. Where this unit is in excess of 150 m thick, a strong separation of the polygonal fault sets is observed. In instances where the intervening unit is thinner, the two fault-sets are often linked, with some faults from the lowermost set propagating upward. The occurrence of polygonal faulting is often recognisable by the 'noisy' nature of the sonic logs over affected intervals.

Polygonal faults are believed to be formed through the process of syneresis (Cartwright and Dewhurst, 1998), and thus not necessarily related to regional tectonic events. In the Bass Basin, there appears to be some temporal coincidence between the formation of polygonal faults and the emplacement of volcanic material (Figure 4.21). For example, near Cormorant-1 a prominent volcanic mound is observed on seismic data to intrude and overlie the Base Torquay horizon. Sediments of the Torquay-1 succession onlap the margins of the mound, suggesting that emplacement of these volcanic rocks occurred during early Late Oligocene to latest Early Miocene – approximately coeval with the formation of faults within Polygonal Fault Set-1. While volcanic emplacement may have locally influenced some faults (perhaps through proximal heating), the ubiquitous nature of the polygonal faults across the basin suggest their formation was largely unrelated.

Multiple periods of Cainozoic contraction have been recognised in the Bass Basin (Young et al., 1991; Hill et al., 1994; Hill et al., 1995). These contractional events formed large scale anticlines within the syn- and post-rift successions. Sediments in the western and northwestern parts of the basin were most affected by these events. Middle to Late Miocene inversion of the Paleocene to Early Miocene succession at Cormorant-1 resulted in the largest single post-rift structure in the basin – the Cormorant Anticline (Figures 2.3 and 4.21). Cormorant-1 and King-1 tested the trapping capability of this structure, with multiple oil shows recorded during drilling through the inverted section. Recent work undertaken by Geoscience Australia and CSIRO (Kempton et al., 2002), has revealed a palaeo-oil zone near 2800 m depth in Cormorant-1 (Lower *M. diversus* zone), suggesting the Miocene inversion event breached an existing oil accumulation. More subtle structures resulting from Miocene contraction occur along the northern margin of the basin, extending as far east as Dondu-1. The onset of contraction in the Bass Basin can be constrained at the Cormorant-1 and Konkon-1 wells where the syn-inversion succession is penetrated. At Cormorant-1, movement began during the early-Middle to mid-Middle Miocene (Torquay-2, planktonic foraminifera zones E1/D2), and probably ended during the Late Miocene. The precise end of contractional deformation is uncertain due to lack of age dating in Cormorant-1, although regional correlations of the Torquay-4 horizon (top of syn-inversion succession) to Bass-3 show this horizon to be younger than latest Middle Miocene.

Along the southern margin of the Bass Basin, inversion structures within the basinal succession (similar to the Cormorant Anticline) are generally absent. However, mapping of sedimentary packages around Bass-3 suggests that from the early Middle Miocene onward contractional stresses resulted in basement uplift at the margins of the basin (see Figure 3.3). The difference in strain between the northern and southern Bass Basin probably reflects the geometry of the basement fault – the Cormorant Anticline occurs in the hanging wall of a steeply-dipping normal fault, while the southern edge of the basin is a flexural ramp margin.

To the west, in the Torquay Sub-basin of the Otway Basin, contraction that began in the Middle Miocene continued through the Pliocene and persisted into Recent times. In the Bass Basin, the area to west of Konkon-1 and Seal-1 also shows evidence of a similar post-Miocene inversion history. The basement ridge that separates the Torquay Sub-basin from the Bass Basin is known as the King Island High. This feature is a high-standing basement block, although it was likely to have been a less prominent feature in pre-Middle Miocene times. That is, the Miocene and younger inversion has enhanced the magnitude of the structure and possibly masked a inter-basinal link between the Torquay Sub-basin and the western Bass Basin in pre-Miocene times. Partridge (2002, Appendix C) suggests that the marine flooding of the Bass Basin during the Cainozoic occurred via a passage to the west. This scenario has also been suggested by Maung et al. (1999), with "flattened" seismic sections (along strike of the King Island High) supporting this hypothesis.

Table 4.8 Torquay Sequence (Subsidence Phase 3)

Top:	Holocene (seabed)
Base:	Boundary between Early and Late Oligocene, I1/I2 planktic foraminifera zone
Type Section:	Tarook-1, Aroo-1, Cormorant-1, Narimba-1 and the Pelican wells

Formation Equivalent:	Torquay Group (Lennon et al., 1999)
Dominant Lithology:	Late Oligocene to mid-Miocene succession consists of argillaceous sediments (shale, marl, siltstone, up to 650 m thick); late-Middle Miocene and younger sediments are mostly calcarenites (860 m thick)
Environment:	Shallow marine shelf later deepening to open marine
Unconformities:	Tectonic inversion from the mid-Middle Miocene to the early Late Miocene resulted in sub-aerial exposure of areas adjacent to the basin margins (Cormorant-1)
Sequence Character:	Overall transgressive – regressive cycle with multiple higher-order cycles
Aerial Extent:	Across the basin, thicker in Cape Wickham Sub-basin, thinner in Durroon Sub-basin
Play Elements:	Regional loading facies for source rocks of the upper Bass and Aroo megasequences

4.11 NATURE AND DISTRIBUTION OF IGNEOUS ROCKS

A. Cummings, National Centre for Petroleum Geology and Geophysics

J. Blevin, Geoscience Australia

The Bass Basin and adjacent areas of mainland Tasmania and Victoria have been affected by multiple periods of volcanic activity during the several phases of basin evolution. Offshore, these events are marked by the widespread emplacement of intrusive and extrusive rocks, particularly in the southern and western parts of the basin in association with large-scale faults and accommodation zones. Intrusive and extrusive igneous rocks ranging from Early Cretaceous to Late Miocene age occur throughout the Bass Basin.

Early Cretaceous Volcanoclastic Sediments (Otway Megasequence)

The Aptian-Albian Otway Megasequence, as intersected at Durroon-1, consists of volcanolithic sandstone and slightly carbonaceous siltstone interbedded with rare conglomerate and thin coal seams (Williamson et al., 1985). This unit bears close lithological similarities to the Otway Group and Upper Strzelecki Group of the Otway and Gippsland basins, respectively. The volcanoclastic material is thought to have derived principally from ignimbritic volcanoes situated along the Lord Howe Rise (Bryan et al., 1997). Input of volcanic sediment into the Bass Strait region from mid-Barremian to Albian time was so great that the volume of continentally derived sediment appears to have been as low as 25% (Norvick and Smith, 2001).

Middle Cretaceous Volcanics (Otway and Durroon megasequences)

The Durroon-1 well intersected a 100+ m thick succession of highly altered amygdaloidal olivine basalt, interbedded with clastic sediment. This volcanic succession overlies the Barremian to Albian Otway Megasequence, and is directly overlain by the Cenomanian to Campanian Durroon Megasequence. The volcanics can be observed on seismic data across much of the Durroon Sub-basin, often in the form of flows, mounds, and cones situated in close proximity to major faults (Edgerley and Taylor, 1990). A lack of well

control and poor seismic resolution at depth has meant that the extent of these mid-Cretaceous volcanic rocks is poorly constrained west of the Durroon Sub-basin. Mid-Cretaceous volcanism appears to have been related to upper crustal extension associated with the onset of rifting in the Tasman Basin. Basaltic flows intersected at Durroon-1 represent a number of episodes of volcanism, separated by the deposition of clastic sediment derived from the uplifted half-graben shoulders and margins of the basin.

Late Cretaceous to Paleocene Volcanics (Bass Megasequence)

Campanian to Paleocene volcanic rocks have been intersected at Aroo-1, Bass-2, Chat-1, Tilana-1, Yolla-1 and Yolla-2. The distribution of these wells suggests that volcanism during this period was confined to central and northeastern regions of the Bass Basin. However, the full extent of volcanism cannot be precisely determined, as many wells were not drilled deep enough to penetrate the full succession (Baillie, 1993). Late Cretaceous to Paleocene volcanics are difficult to define on seismic data as reflections are typically parallel to the overlying coals in the Bass Megasequence.

A new petrographic examination of well intervals that intersected volcanic rocks has recently been undertaken (T. Dance and A. Lambeck, pers. comm., 2003). Some of these samples show that "volcanic" intervals, as described in well completion reports, are not wholly volcanic in origin. Instead, the rocks consist of medium-to-coarse grained quartzose sandstones that were subsequently intruded by volcanic fluids. These hot fluids have altered the quartz grains and, upon cooling, have acted to cement the rock. This evidence, together with other geophysical evidence from seismic data, suggest that intrusive magmas and associated fluids were emplaced upward into the stratigraphic succession, and then often migrated laterally along porous or fractured strata (primarily sandstones and coals). This could explain the close association and the apparent interbedded nature of the volcanic, sandstone and coaly strata. Occurrences of sills, such as that intersected at Cormorant-1 (2413 to 2469 m), show a slight discordance to the regional strata and increased amplitudes on seismic data (see Figure 2.3). Coal beds and volcanic intrusions/extrusions often show a similar high-amplitude seismic character that decreases in "brightness" laterally along the bed.

Other Upper Cretaceous to Paleocene volcanic suites are composed largely of fine grained amygdaloidal basaltic flows, some displaying weathered tops, interbedded with minor sandstone, siltstone and shale units. Samples collected from drilling indicate the volcanics have undergone varying degrees of alteration, possibly due to prolonged exposure between flows. Petrographic analyses of the volcanic units suggest that the composition of the mafic flows ranges from alkali olivine basalt, to basanite and picrite. Volcanic units of this age have proved difficult to date using conventional geochronology, as alteration has significantly reduced the effectiveness of K/Ar dating. However, palynofloras from within the volcanic suite place the volcanics within the age range of late Cretaceous to Paleocene (~ 55-75 Ma) (Baillie, 1993).

Oligocene to Miocene Volcanics (Torquay Megasequence)

Oligocene to Miocene volcanics are widespread throughout the central and northeastern regions of the Bass Basin (Figure 4.21). Both intrusive bodies and extrusive volcanics are observed on seismic data. Late

Oligocene to Miocene compressional events led to the strike-slip reactivation of a number of pre-existing structures throughout the Bass Basin (Smit, 1988). Large basement-involved faults with significant displacement appear to have been preferentially reactivated. Strike-slip movement along these structures resulted in the development of north-south oriented zones of pop-up and pull-apart flower structures (Smit, 1988). During the Early Miocene, extensive volcanism occurred in the western half of the basin and multiple volcanic complexes of this age are clearly recognisable on seismic data. Intrusions of this age appear to be related to the distribution of the reactivated structures, where faults acted as feeder conduits for the extrusion of volcanic material (Lennon et al., 1999).

Miocene volcanic sequences were intersected at Bass-1, Tilana-1 and Yolla-1. Volcanic mounds and cones are observed on seismic data within the central and northwestern regions of the basin. Evidence from Bass Basin seismic data, and analogue studies of volcanics of similar composition within western Victoria, suggest the main eruption centres were probably scoria cones located along active faults that acted as feeder conduits (Faustmann, 1995). Volcanic facies intersected by wells within the Bass Basin include olivine basalt flows and highly weathered pyroclastics. This indicates a combination of magmatic and phreatomagmatic volcanism was active during this period. The marine setting of the basin during Cainozoic volcanic episodes would have provided an abundance of water to react with the rising magma, enhancing the likelihood of explosive volcanism (Faustmann, 1995). The variation observed in seismic velocities within the Miocene volcanics may be related to facies changes within the volcanic pile (Faustmann, 1995). This variation poses a significant complication for the correction of seismic pull-up and push-down for depth conversion and the accurate interpretation of exploration targets beneath the volcanic units and intrusive bodies (Taylor, 2001).

Miocene intrusive bodies have been encountered at Cormorant-1, Flinders-1, Koorkah-1, Seal-1, Squid-1, Tilana-1, Toolka-1A and Yolla-1. Intrusive bodies are common in the Bass and Aroo megasequences, varying in thickness from a few meters to over 150 m (Tilana-1). Intrusives appear on seismic sections as prominent reflections, often terminating at major faults. Petrographic analysis of Miocene sills show that composition of the mafic intrusions varies from dolerite at Flinders-1, Seal-1, Yolla-1 and Koorkah-1, to olivine gabbro and syenite at Cormorant-1, and alkali olivine basalt at Squid-1.

Cainozoic volcanism within the Bass Basin appears to be both temporally and spatially extensive. The presence of multiple periods of volcanism of a similar mafic composition over such a significant period of time suggests that the source of volcanism may be hotspot related. Tertiary mafic intrusions (alkali basalts) from King Island appear to be enriched in TiO_2 and contain a comparatively small Zr/Nb ratio. This composition indicates a strong affinity to "oceanic intraplate basalts" such as those from Hawaii (Streit, 1994). Primitive mantle normalised abundance patterns for incompatible and insoluble elements from King Island Cainozoic mafic intrusions also suggest a similar affinity to a plume-related source. The relationship of plume related volcanism to regionally elevated geotherms is discussed further in Chapter 6.

Figure 4.1 Location map of seismic lines interpreted for the Bass Basin study. These seismic lines include reprocessed data from Geoscience Australia Surveys 40, 82 and 90 (blue), and selected reprocessed industry lines (yellow) licensed through Fugro MCS. The total grid coverage is approximately 4,000 line kms.

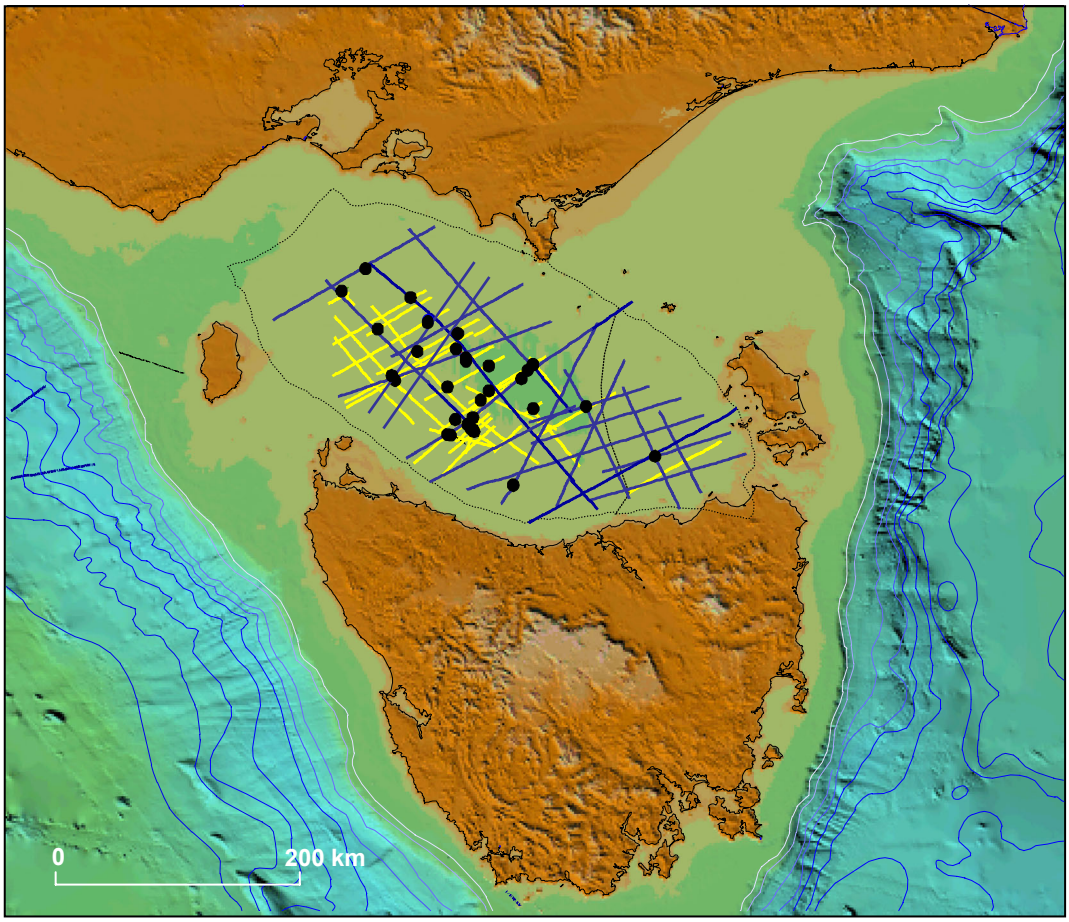


Figure 4.2a Stratigraphic correlation chart for the Bass Basin showing the relationship between age, lithostratigraphy, sequence stratigraphy, basin phases, tectonic events and horizons mapped. The basin phases are shown in detail for the Cape Wickham (CW) and Durroon (Durr) sub-basins. The time scale is from Young and Laurie (1996), with modifications to spore/pollen zones from Partridge (2001).

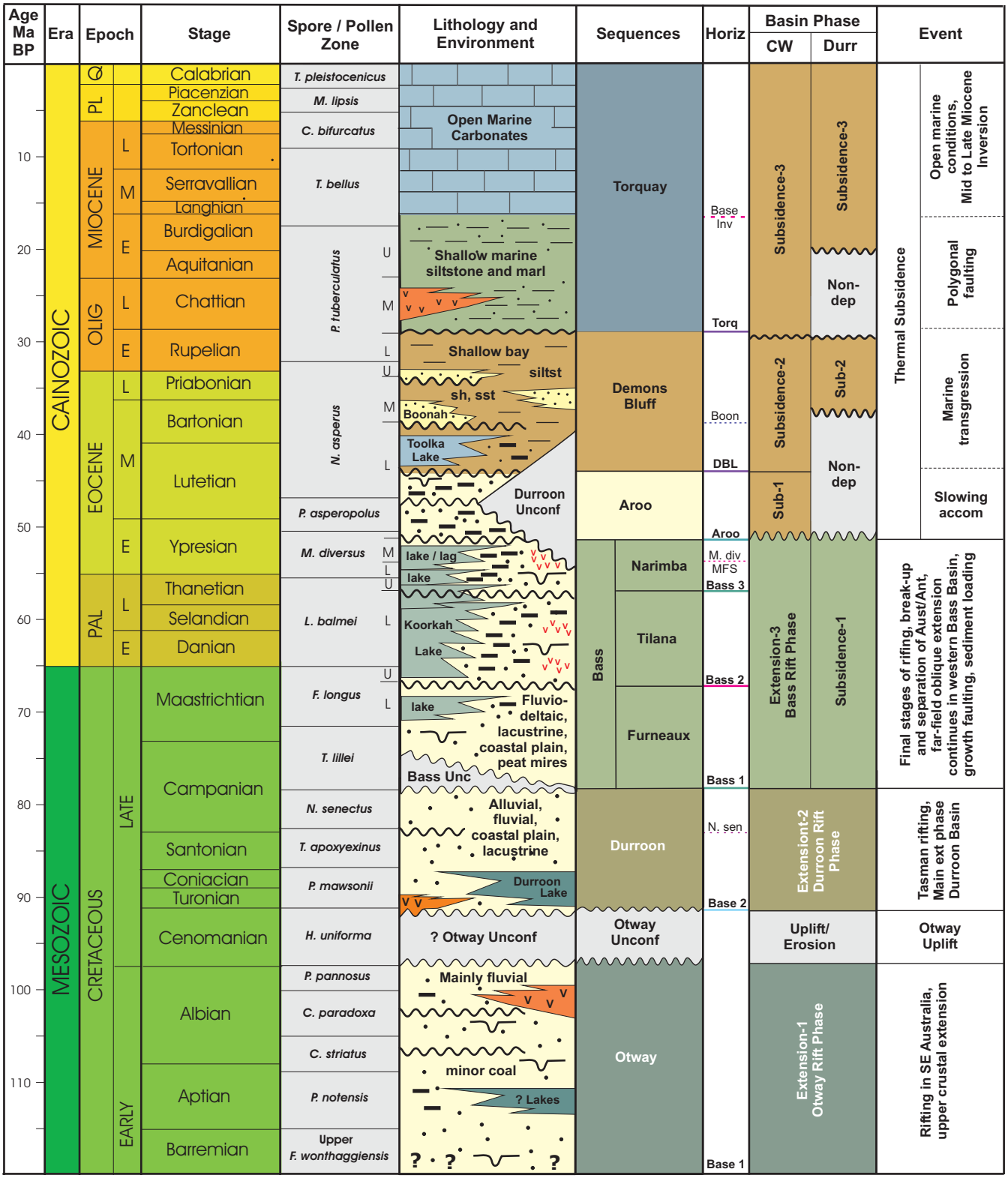
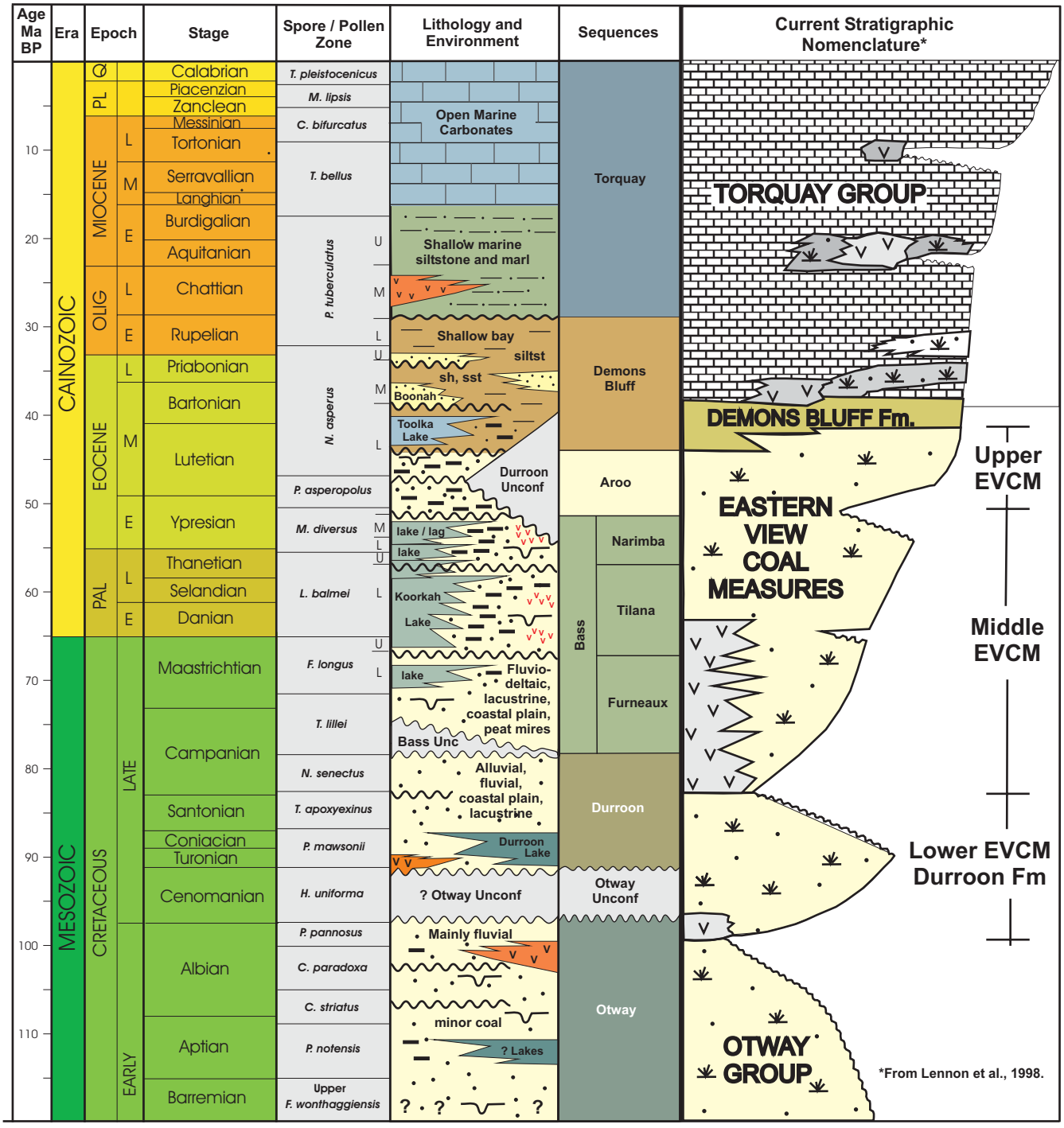


Figure 4.2b Stratigraphic correlation chart for the Bass Basin showing the relationship between the stratigraphic nomenclature scheme of Lennon et al. (1999) and the framework proposed in this report. The time scale is from Young and Laurie (1996), with modifications to spore/pollen zones from Partridge (2001).



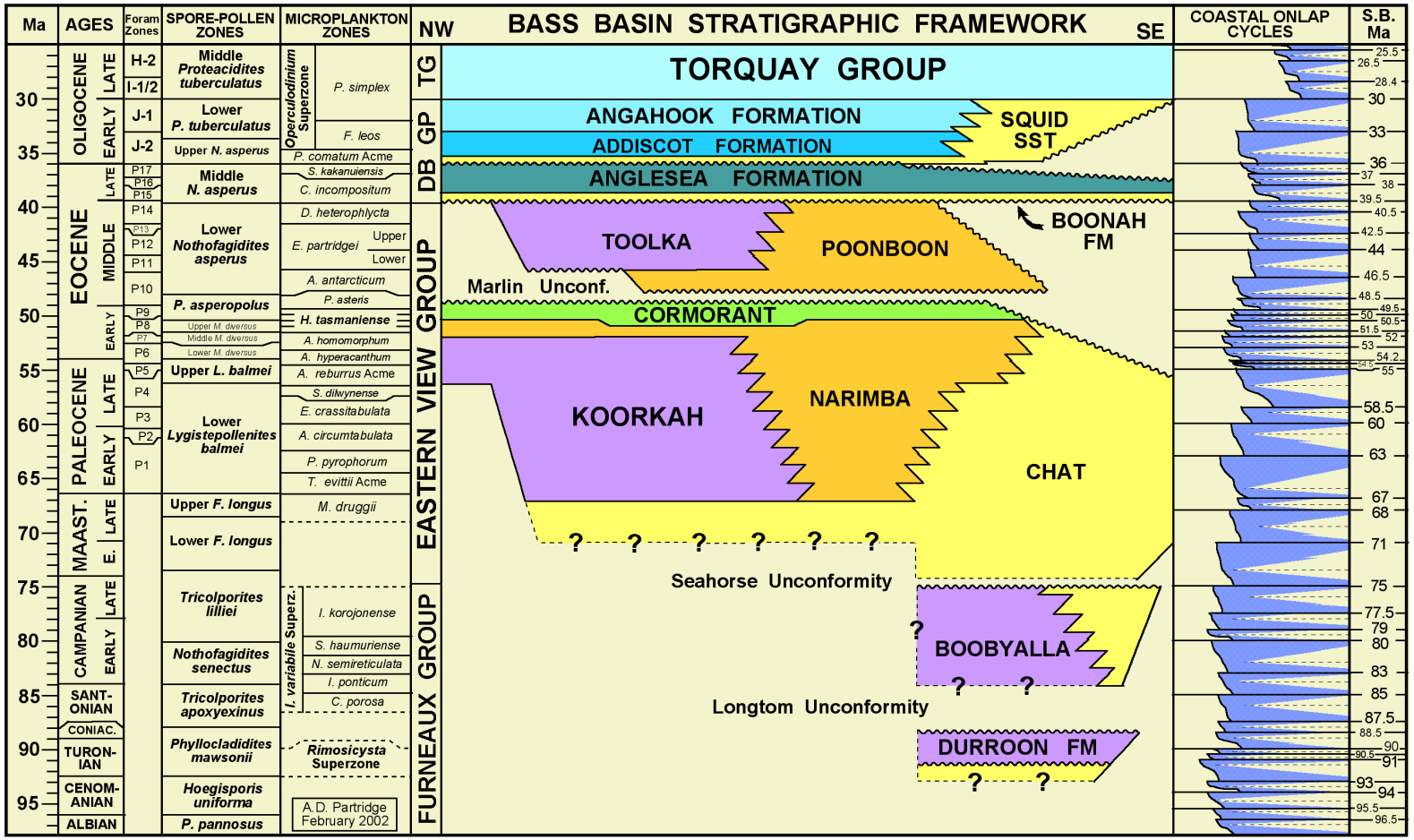


Figure 4.3 Proposed stratigraphic framework for the Bass Basin based on the biostratigraphic analysis and log correlations of Partridge (2002; Appendix C). The palynological zones and correlation to timescale of Haq et al. (1988) is adapted from Partridge (1999). Informal group names used include the Furneaux Group, Eastern View Group, Demons Bluff Group (DB GP) and the Torquay Group (TG). This framework was modified to produced the correlation charts as shown in Figures 4.2a and 4.2b.

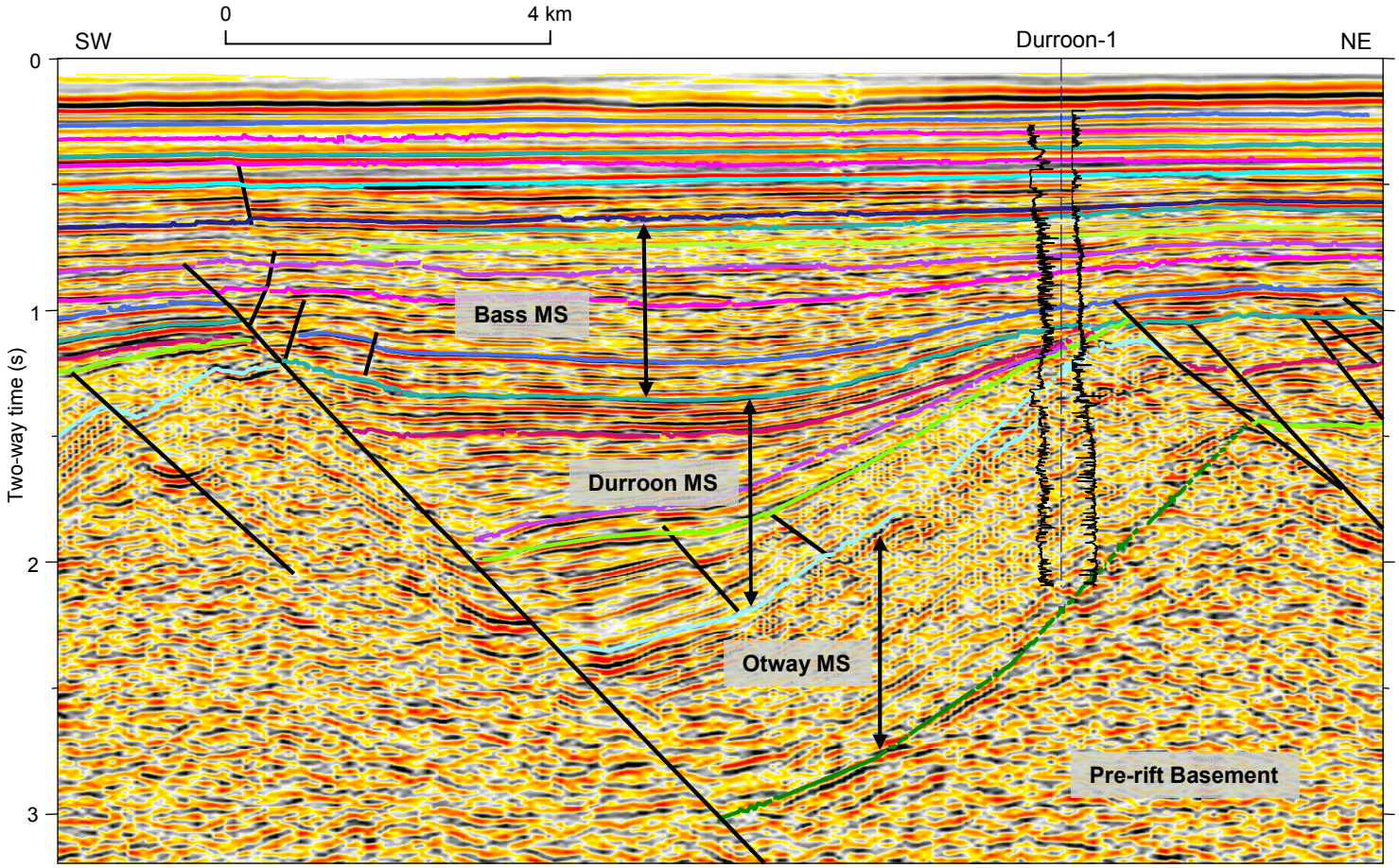
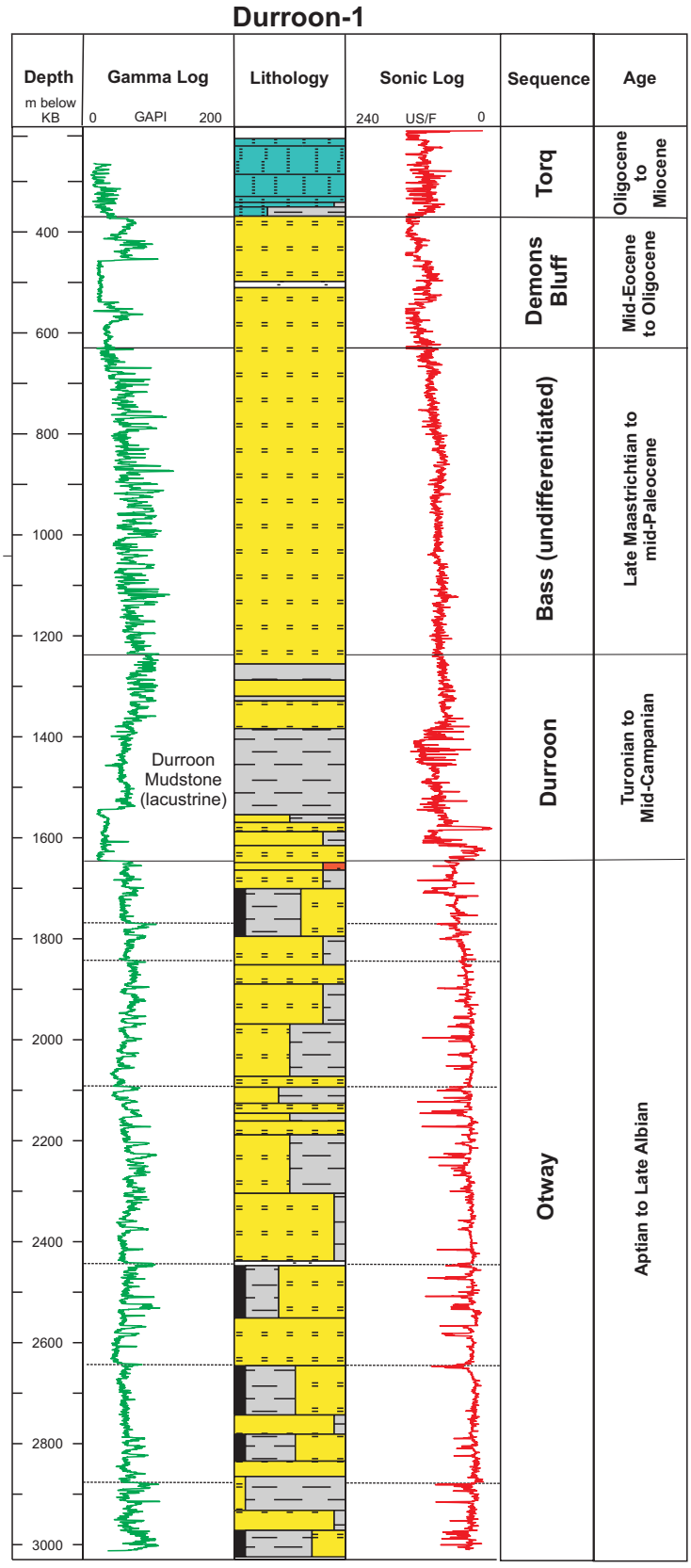


Figure 4.4 Geoscience Australia seismic line across part of the Durroon Sub-basin. This section shows in more detail the syn-tectonic successions intersected at the Durroon-1 well: the Early Cretaceous Otway Megasequence (Rift Phase 1) and the overlying early Late Cretaceous Durroon Megasequence (Rift Phase 2). In the Durroon Sub-basin, the Late Cretaceous Bass Megasequence is largely a sag-related succession deposited during post-rift subsidence. This seismic image is published with the permission of Fugro MCS.

Figure 4.5 Well logs (gamma and sonic) for the Durroon-1 well in the Durroon Sub-basin. The well intersected two syn-rift successions - the Early Cretaceous Otway Megasequence, and the Late Cretaceous Durroon Megasequence. Ages and interpreted sequences, as well as minor unconfomrities within the Otway Megasequence, are shown.



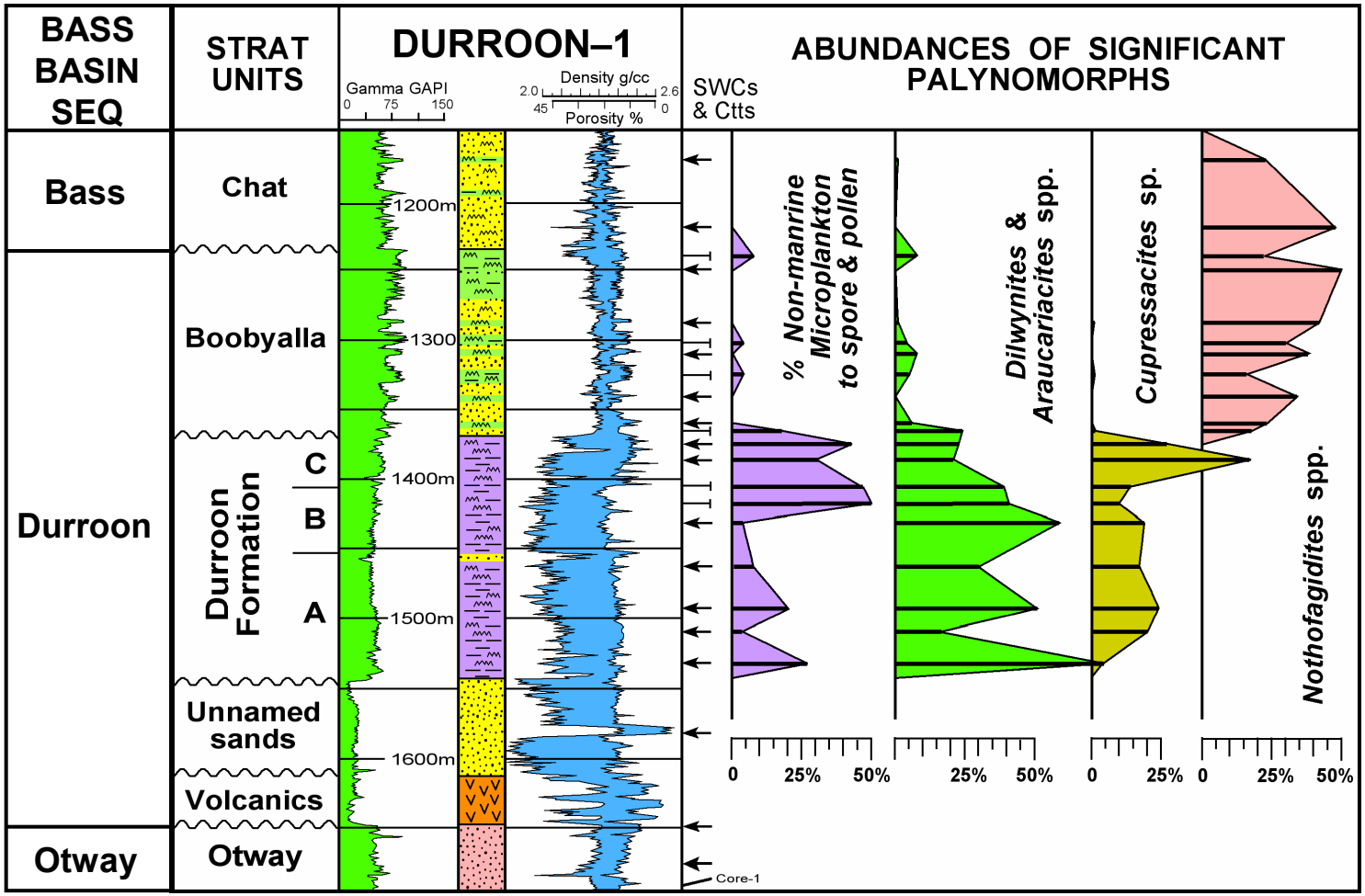
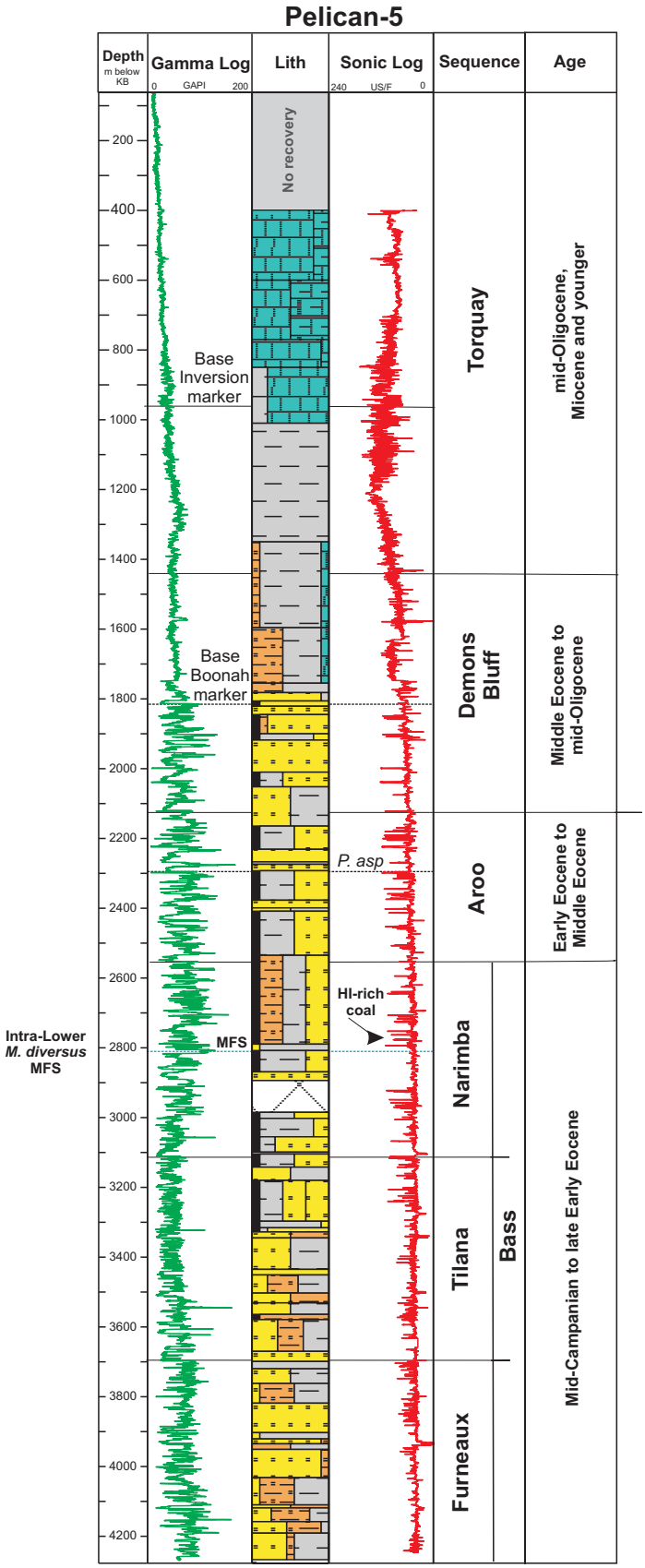


Figure 4.6 Well logs and abundances of significant palynomorphs for samples from Durroon-1 over the interval (1140 to 1670 m; Partridge, 2002). Lithostratigraphic units refer to terms used in Figure 4.3, while sequence names relate to nomenclature proposed in Figure 4.2.

Figure 4.7 Well logs (gamma and sonic) for the Pelican-5 well in the Pelican Trough. The well intersected a complete succession of the Bass Megasequence (Furneaux, Tilana and Narimba sequences). Note the occurrence of a hydrogen-rich coal at 2792 m, above the Intra-Lower M. diversus MFS at 2808 m.



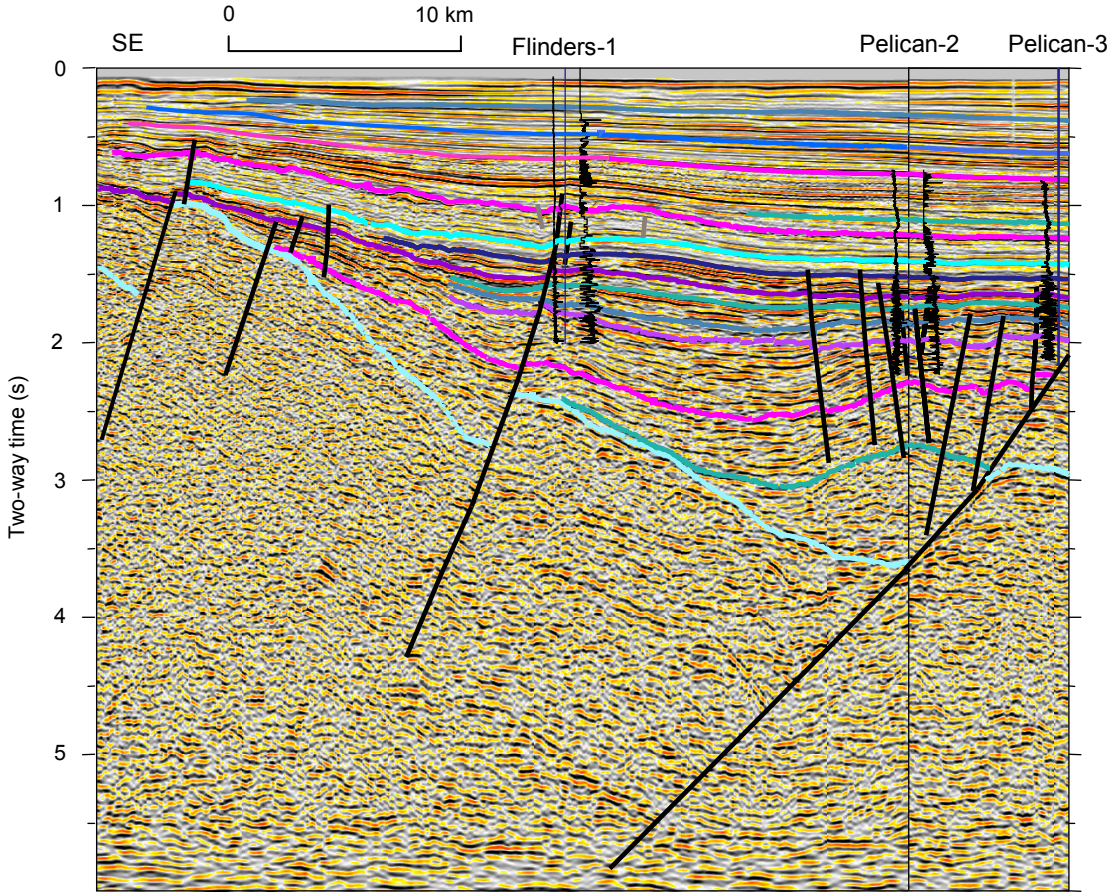


Figure 4.8 Geoscience Australia seismic line across the Pelican Trough in the central Bass Basin. The Pelican wells were drilled into a crestal collapse structure within the hanging wall of the Pelican Trough. Deformation of the deeper sedimentary succession has meant that it is difficult to confidently correlate horizons within the Bass Megasequence away from the Pelican Trough. This seismic image is published with the permission of Fugro MCS.

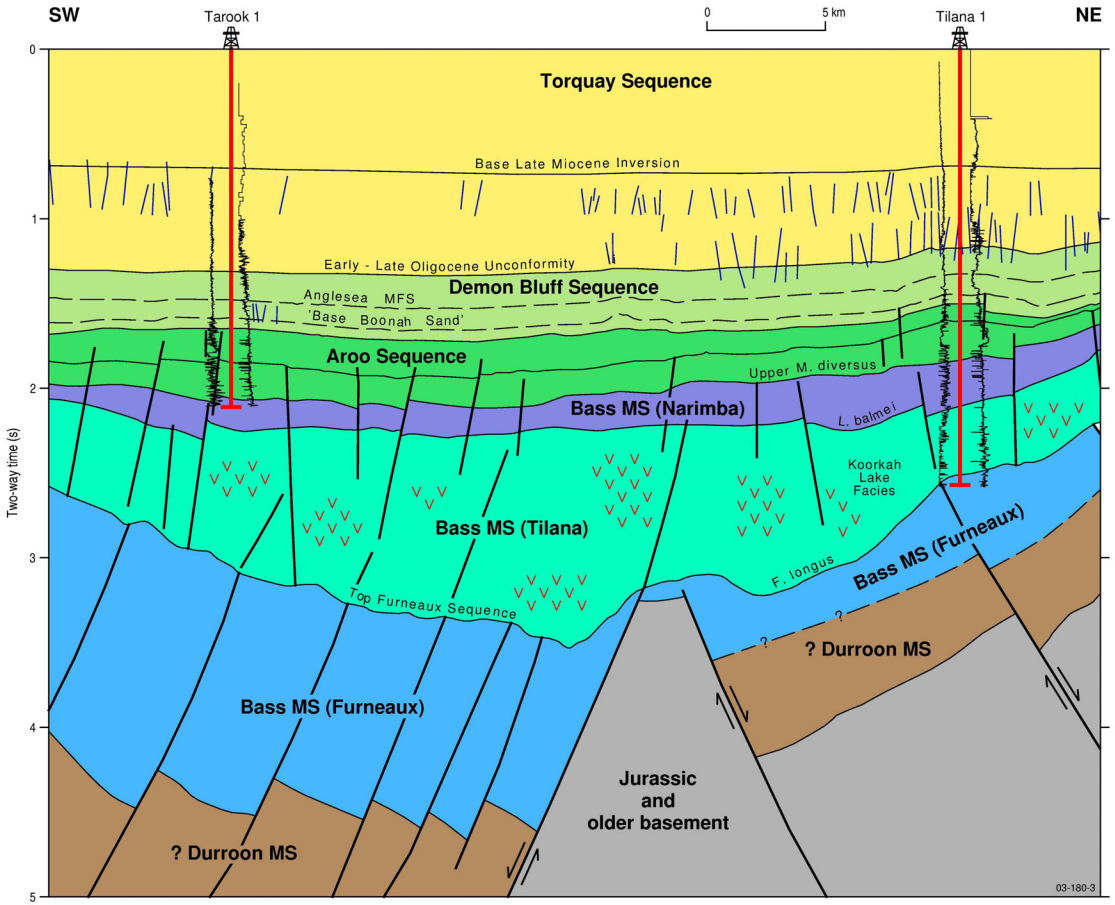
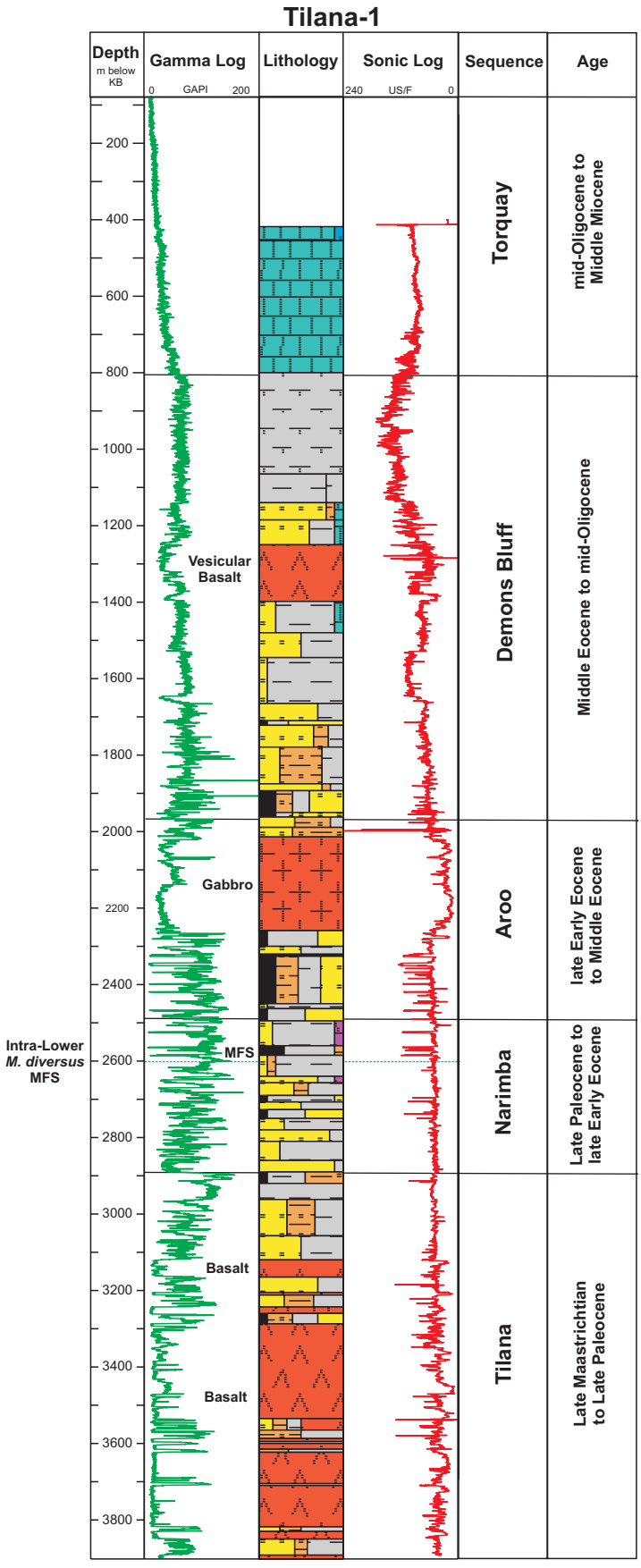


Figure 4.9 Diagrammatic cross-section across the central Bass Basin showing the syn-tectonic nature of the Durroon and Bass sequences (Furneaux, Tilana and Narimba sequences), and the overlying post-rift successions of Aroo, Demons Bluff and Torquay sequences. The stratal geometry and faults controlling the deposition of the Tilana Sequence are obscured due to the prolific intrusion of volcanics into the succession. The Narimba Sequence shows only minimal growth on this section.

Figure 4.10 Well logs (gamma and sonic) for the Tilana-1 well in the central Bass Basin. The well intersected multiple intervals of intrusive and extrusive volcanic rocks. The thick basaltic succession below 3100 m consists of basaltic flows and Paleocene sandstones cemented by intruded volcanic fluids.



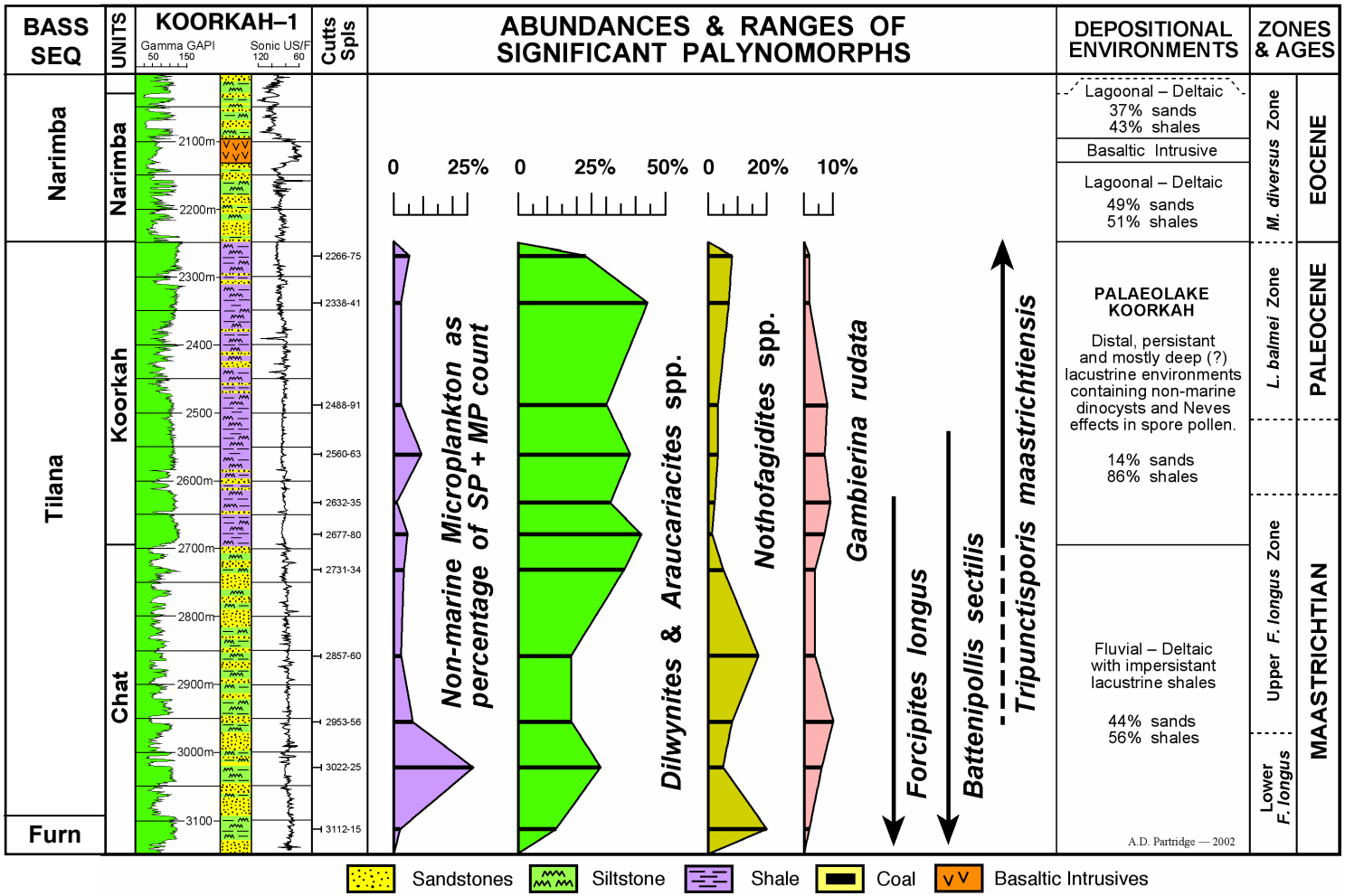


Figure 4.11 Well logs, abundances and ranges of significant palynomorphs for Maastrichtian to Paleocene samples from Koorkah-1 over the interval (2030 to 3140 m; Partridge, 2002). Lithostratigraphic units refer to terms used in Figure 4.3, while sequence names relate to nomenclature proposed in Figure 4.2.

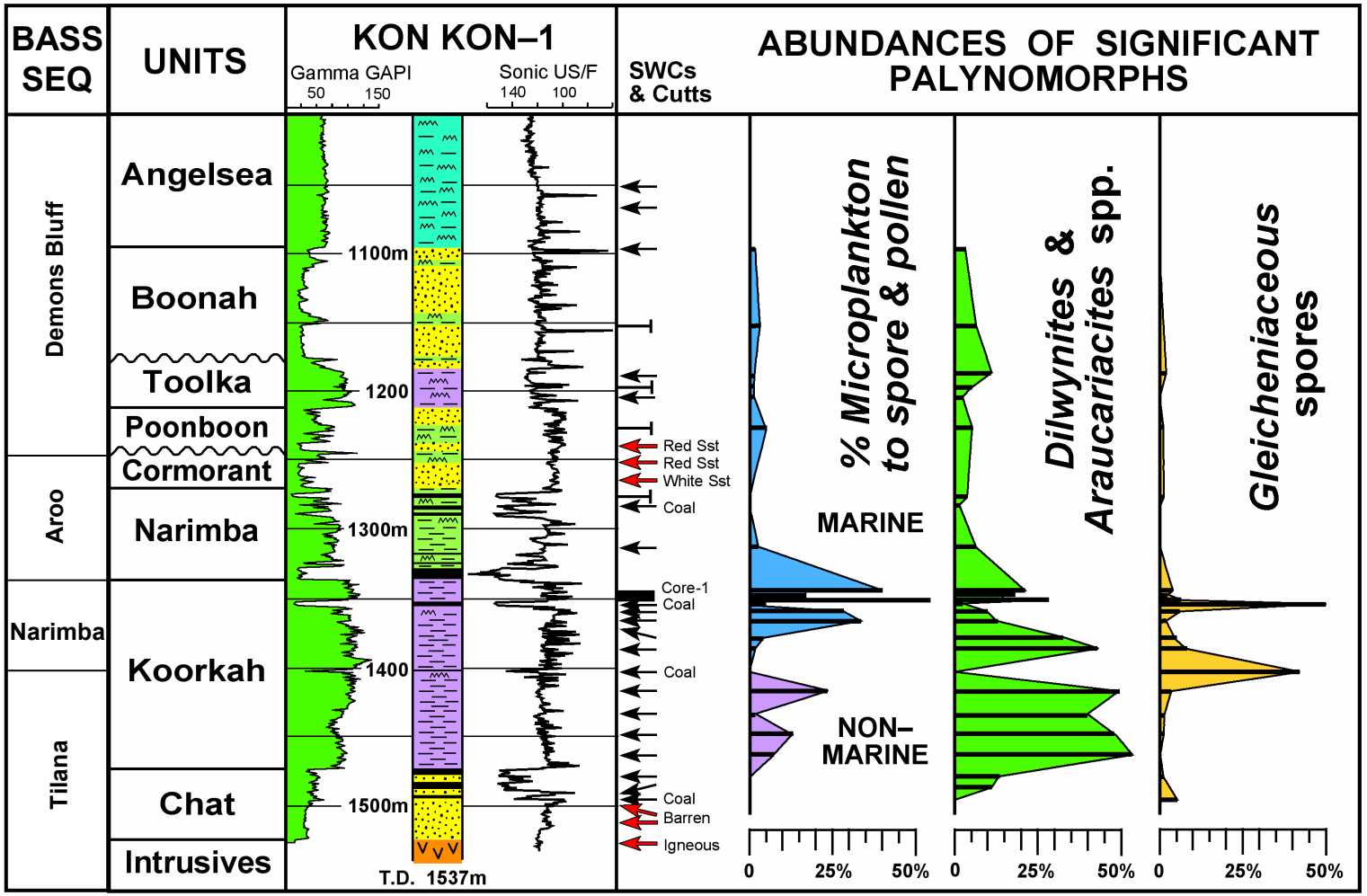


Figure 4.12 Well logs, abundances and ranges of significant palynomorphs for Paleocene to Eocene samples from Konkon-1 over the interval (1000 to 1537 m; Partridge, 2002). Lithostratigraphic units refer to terms used in Figure 4.3, while sequence names relate to nomenclature proposed in Figure 4.2.

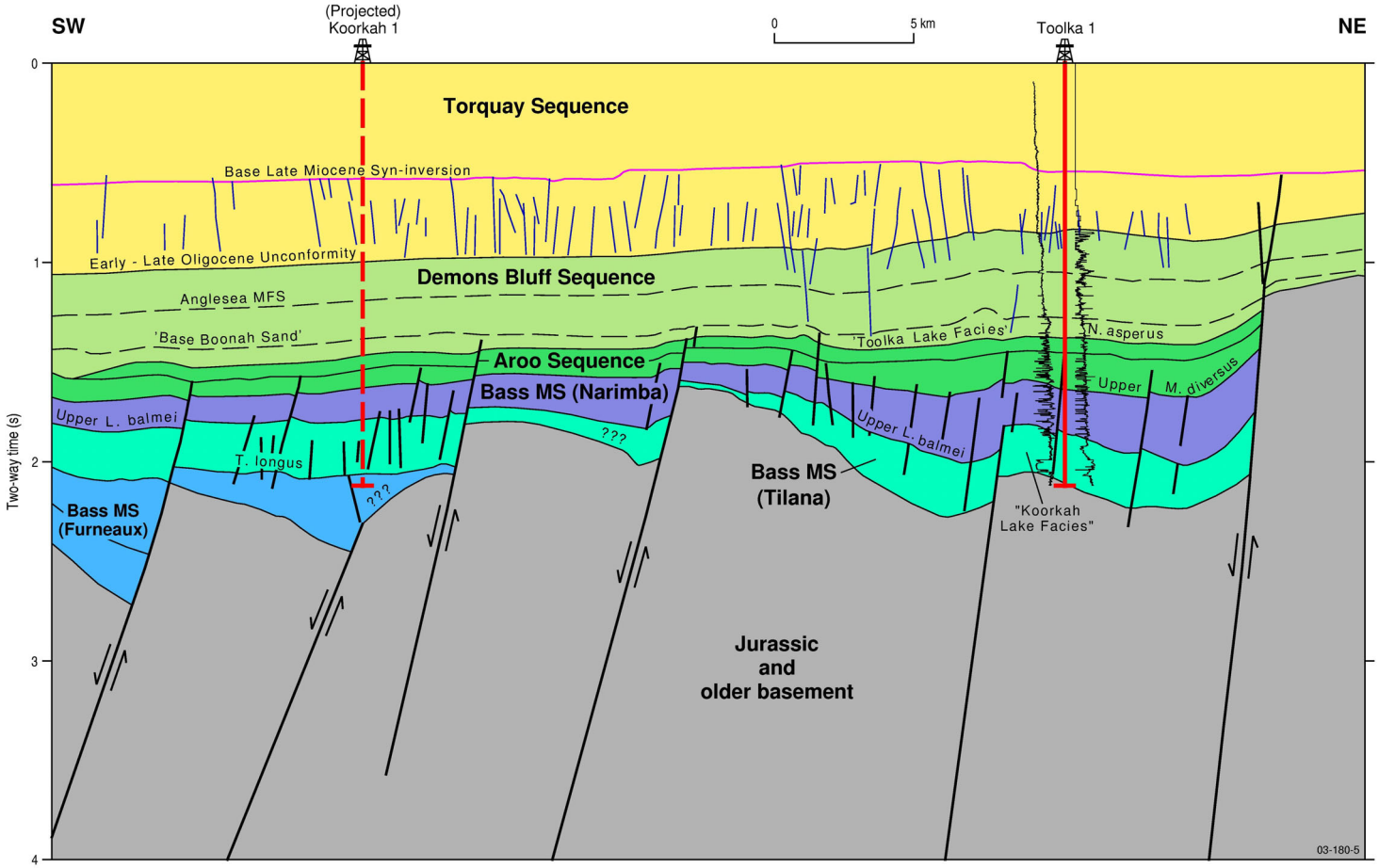
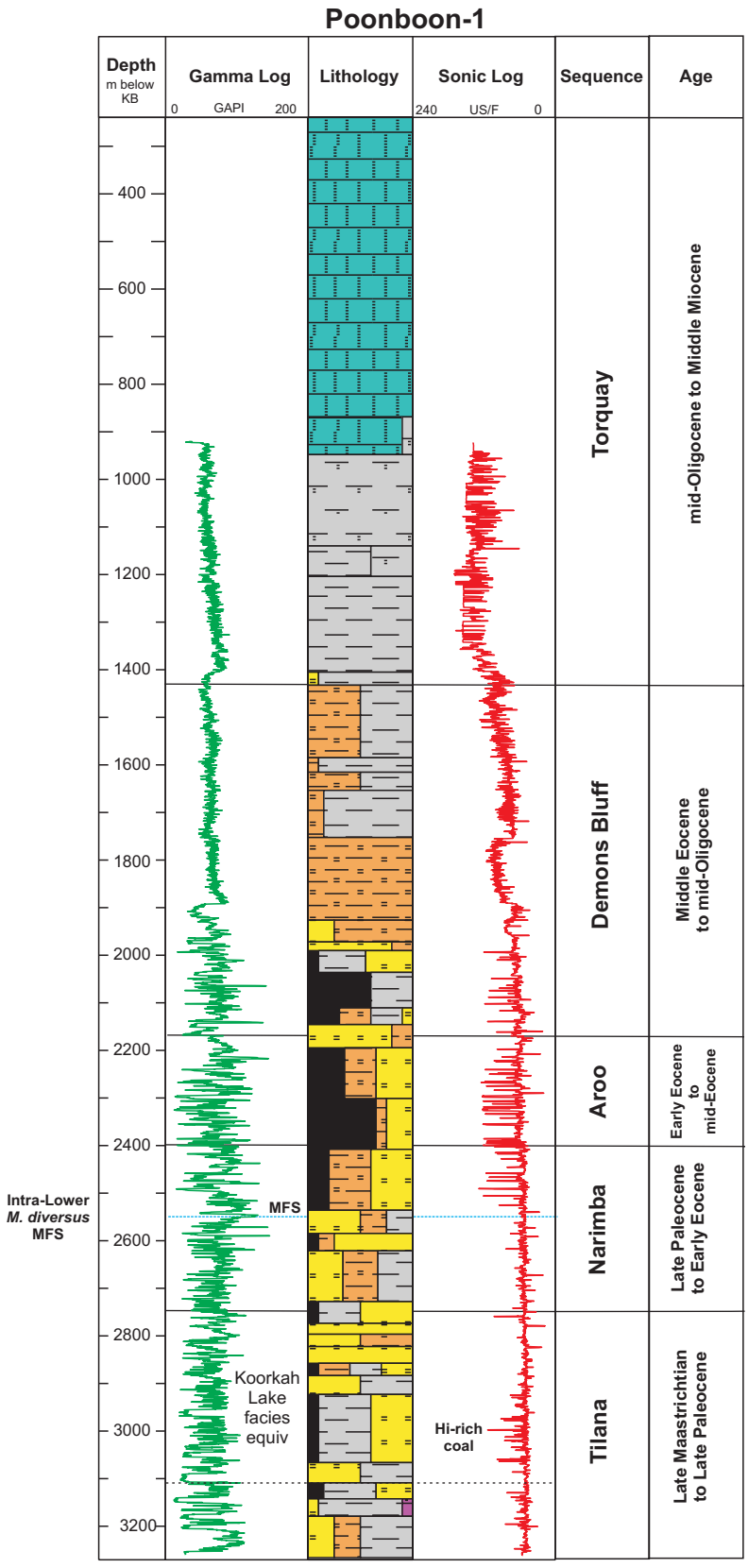


Figure 4.13 Diagrammatic cross-section across the western Bass Basin (near the Toolka-1A and Koorkah-1 wells) showing the syn-tectonic nature of the Bass Megasequence. Growth faulting during the Late Cretaceous to Late Paleocene controlled the development of localised depocentres where deepwater lakes formed (Koorkah Lake). By contrast, the development of Toolka Lake was less influenced by tectonic processes, with the resulting lake being shallower and more widespread than the earlier Koorkah Lake.

Figure 4.14 Well logs (gamma and sonic) for the Poonboon-1 well in the central Bass Basin. The well intersected a lower delta plain to lacustrine succession of Paleocene to Eocene age (Koorkah Lake equivalent facies). The Narimba Sequence is approximately 400 m thick, while in the Pelican Trough this syn-tectonic succession reaches thicknesses of up to 1200 m.



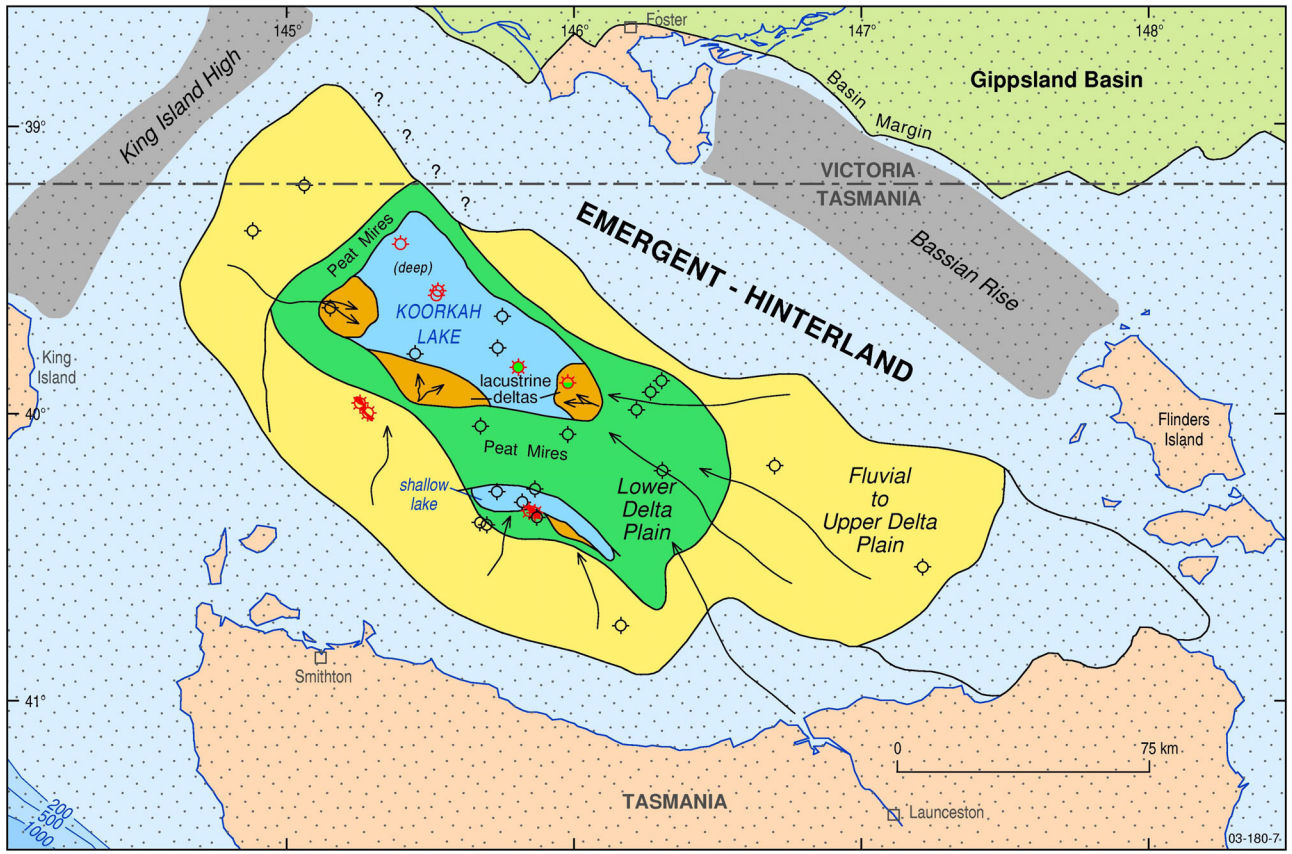


Figure 4.15 Generalised palaeogeographic map showing the maximum extent of Lake Koorkah (Partridge, 2002; Tilana and Narimba sequences). During the lake highstand, deepwater lacustrine shales and lacustrine shoreface/deltaic sands were deposited in mainly faulted-controlled depocentres, while peat mires fringed the margins of the lakes. Hydrogen-rich coals of this age were detected at Poonboon-1 (Chapter 5). The lakes were absent in the Durroon Sub-basin, where mainly fluvial environments dominated during the Late Cretaceous to the early Palaeogene.

Figure 4.16 Well logs (gamma and sonic) for the Narimba-1 in the Pelican Trough. The well intersected an expanded (syn-tectonic) section of the Narimba Sequence (base Upper L. Balmei to base Upper M. diversus zones).

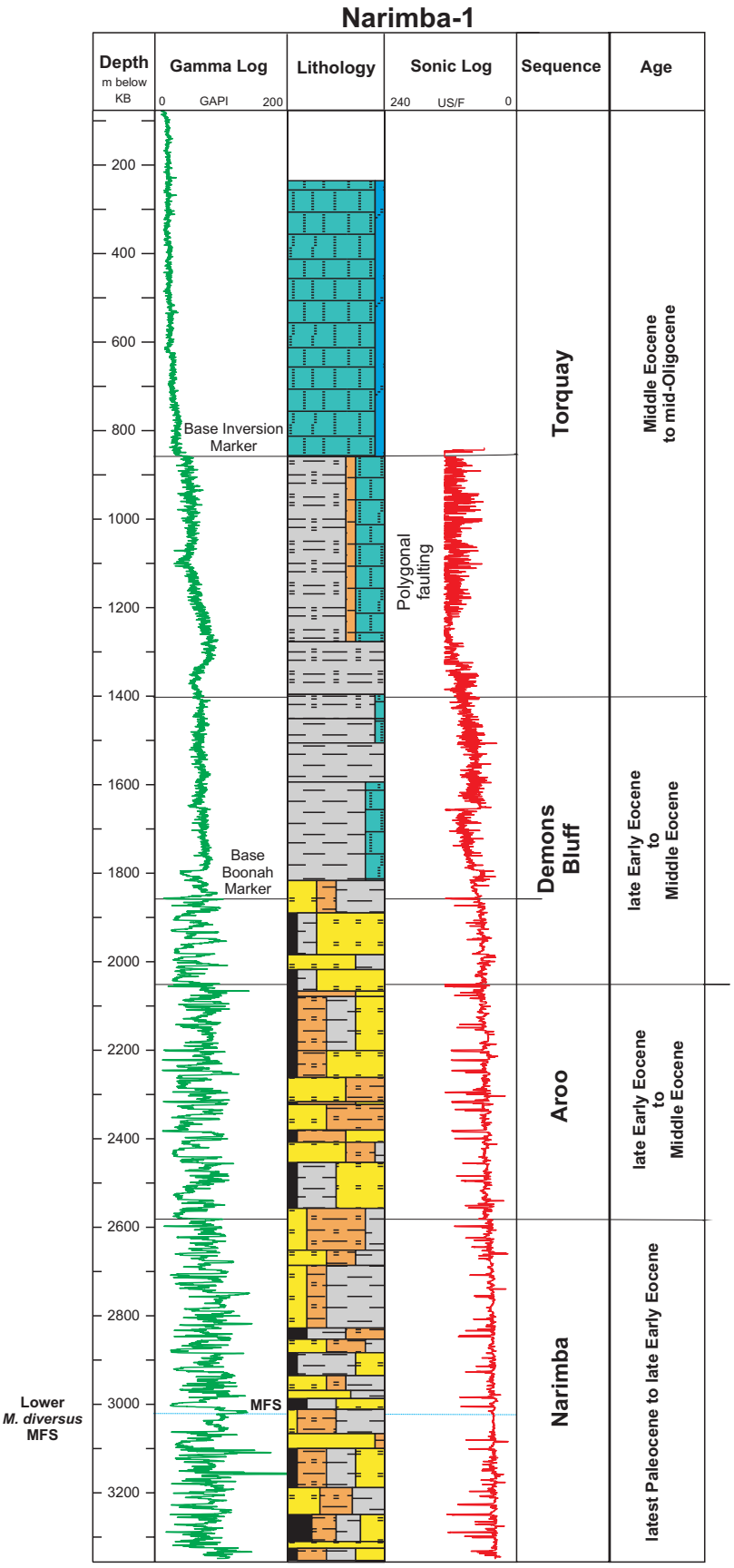
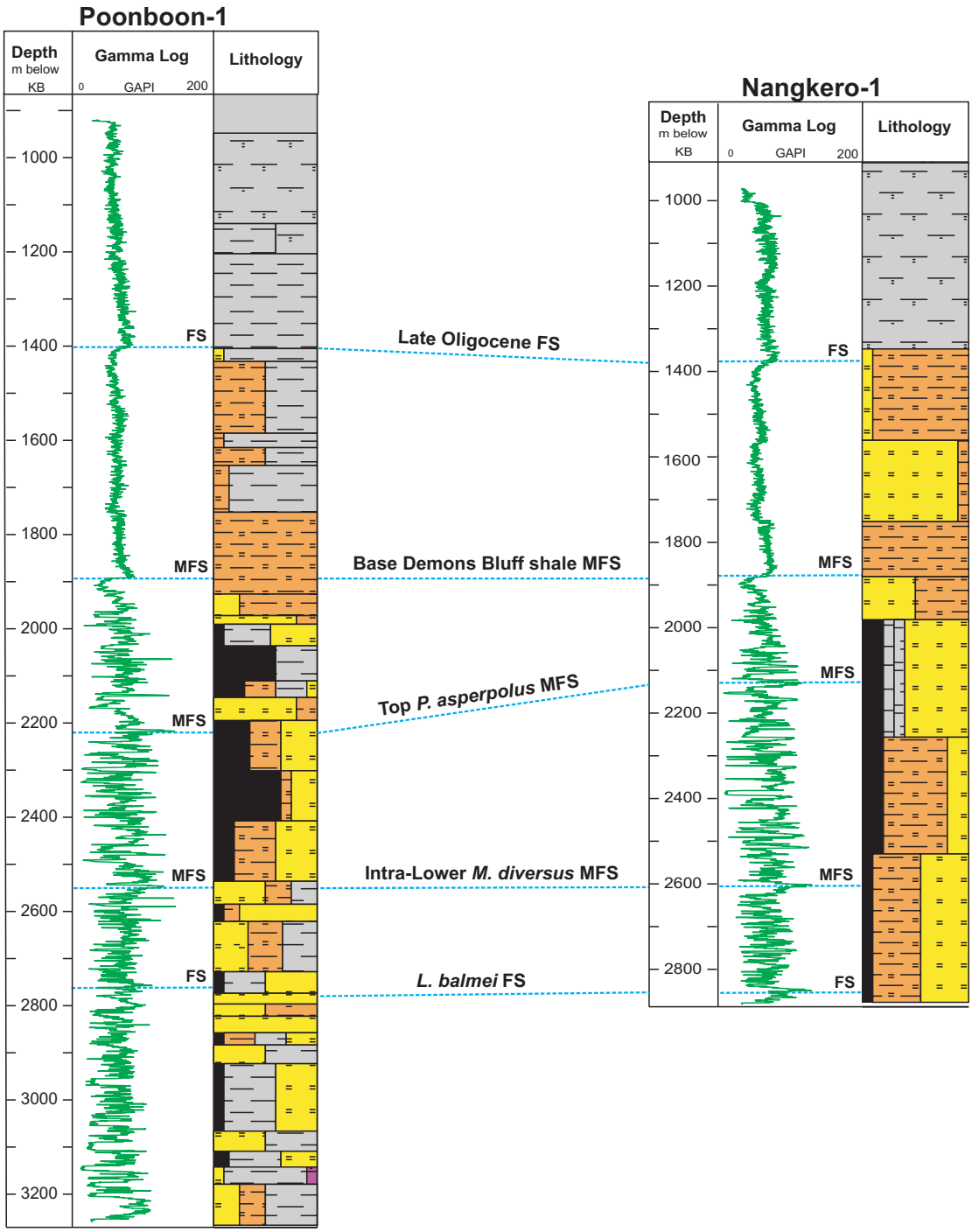


Figure 4.17 Well logs (gamma) for the Poonboon-1 and Nangkero-1 wells in the central Bass Basin showing the correlation of multiple flooding surfaces in the Early Eocene to Late Oligocene succession. MICP analyses indicate that the shales near the Lower M. diversus MFS have a the high seal capacity (1400 m; Chapter 7) of the 15 samples analysed. Shales of the Demons Bluff FS are the regional sealing facies for the Bass Basin succession.



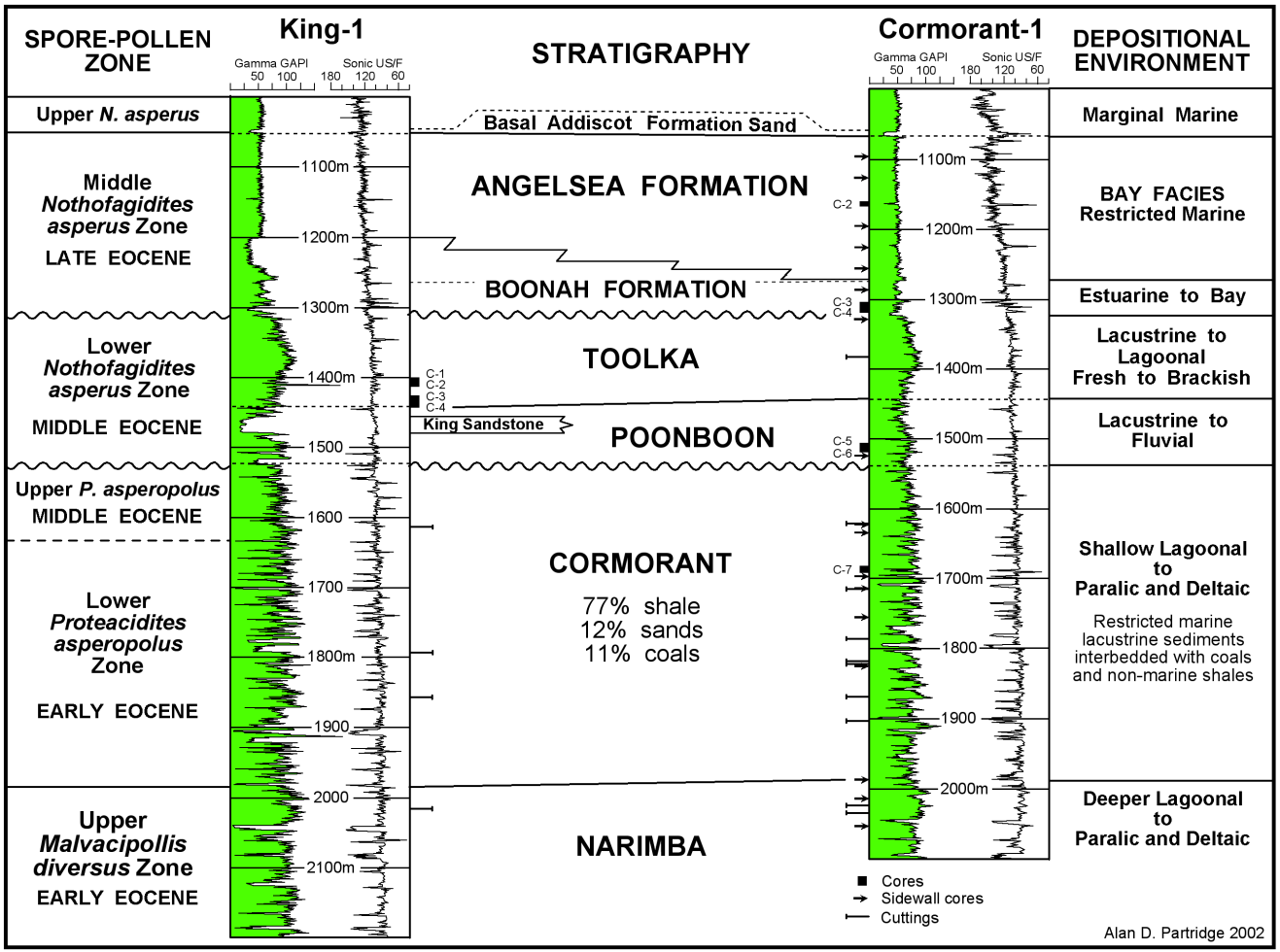


Figure 4.18 Palynological and log correlation between King-1 and Cormorant-1 **(**Partridge, 2002), showing the occurrence of lacustrine, shallow lagoonal and paralic/deltic environments during the Eocene in the northwestern Bass Basin. Lithostratigraphic units refer to terms used in Figure 4.3.

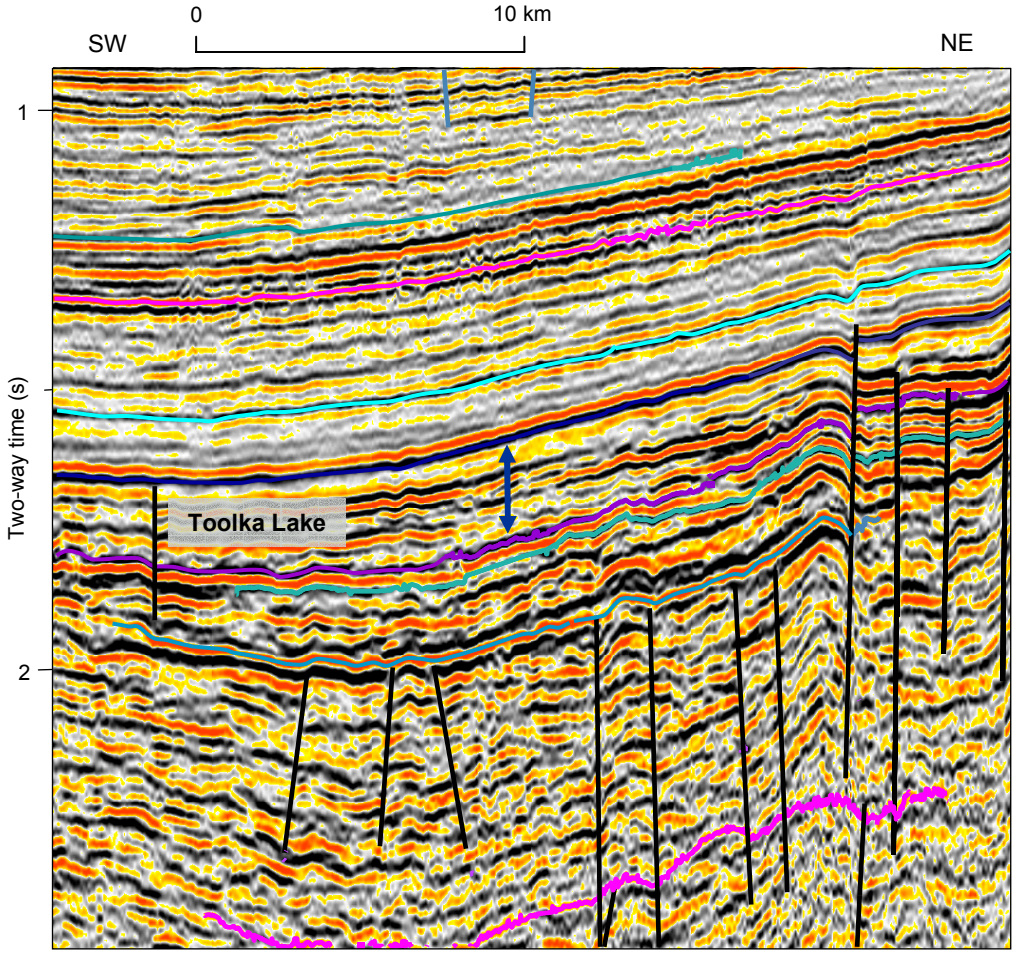


Figure 4.19 Geoscience Australia seismic line across the central Bass Basin showing the geometry and stratal character of the Toolka Lake succession. The dark blue horizon marks the "Base of the Boonah Sand". This figure is published with the permission of Fugro MCS.

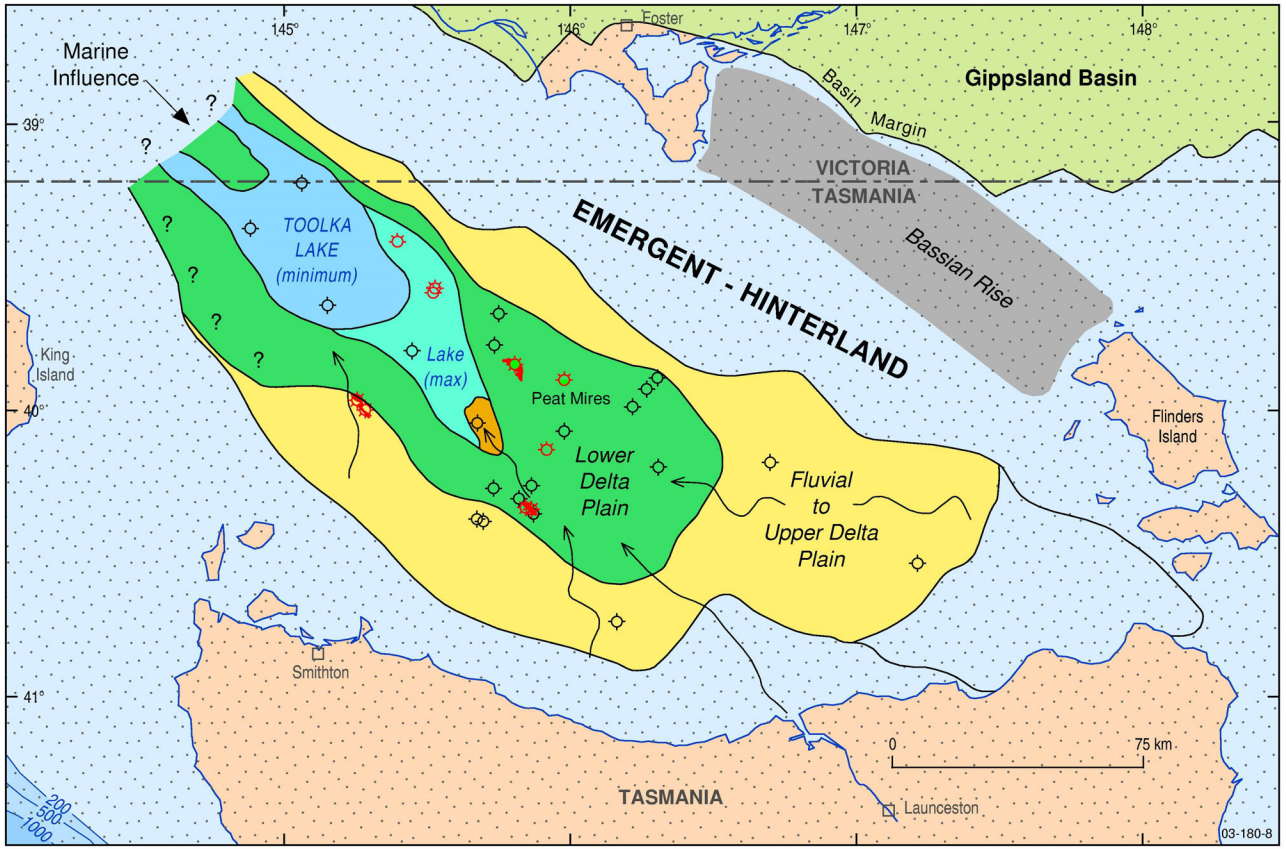


Figure 4.20 Generalised palaeogeographic map showing the minimum and maximum extents of Lake Toolka (Partridge, 2002; Aroo Sequence; Lower to Middle *N. asperus*). During the Middle Eocene lake highstand, shallow water lacustrine shales and lacustrine shoreface/deltaic sands were deposited in broad, low-relief depocentres while peat mires fringed the margins of the lakes. A lagoonal influence was detected in areas to the northwest. The lakes were absent in the Durroon Sub-basin, where mainly fluvial environments dominated from the Late Cretaceous to early Palaeogene.

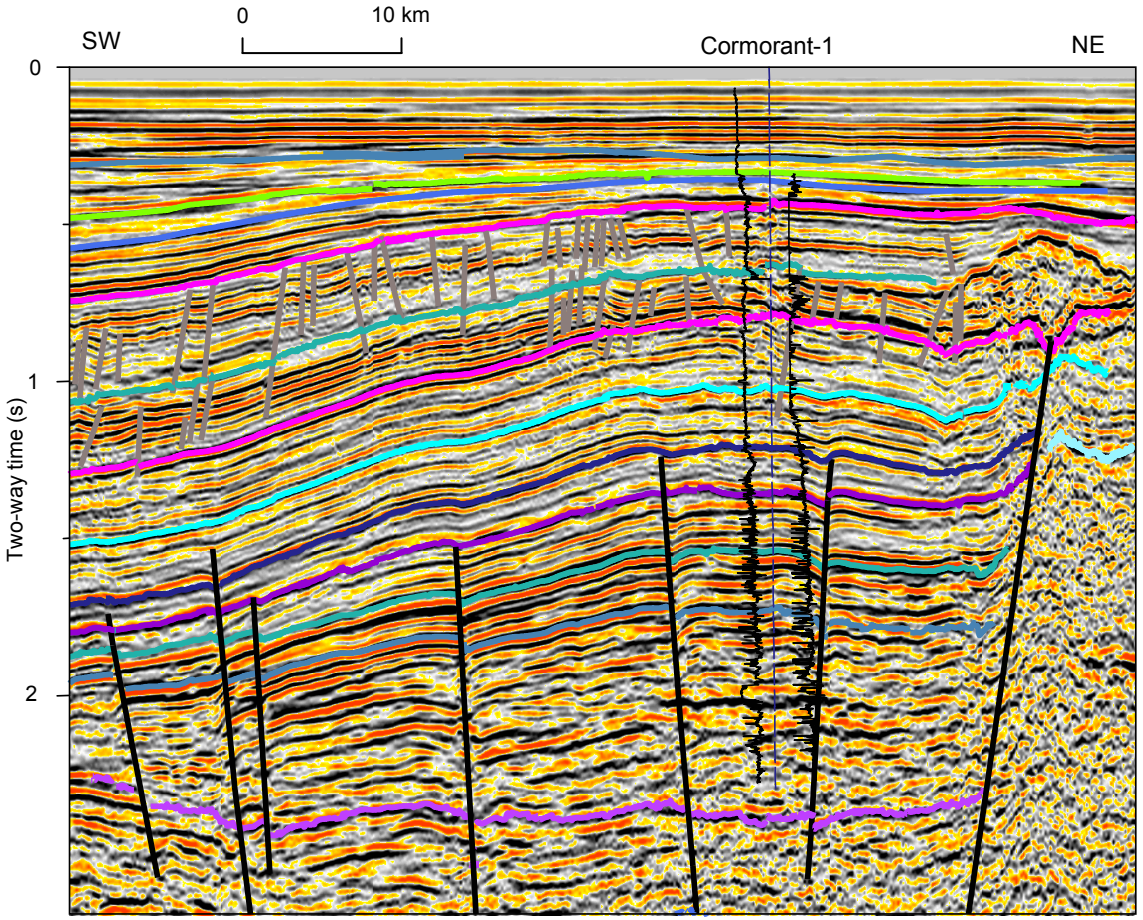


Figure 4.21 Geoscience Australia seismic line across the Cormorant Anticline. The anticline is an inversion structure that formed against the fault bounding the northwestern margin of the basin. The syn-inversion succession at Cormorant-1 has been dated as late Middle Miocene and younger. High-amplitude, cross-cutting volcanic intrusions seen near 2.00 s TWT were intersected by the well. In addition, a large volcanic mound is observed to the north of Cormorant-1. The mound overlies the mid-Oligocene unconformity and maybe associated with basinward polygonal faulting within the Late Oligocene to Late Miocene strata. This seismic image is published with the permission of Fugro MCS.

5. PETROLEUM GEOCHEMISTRY OF SOURCE ROCKS, OILS AND GASES

C. Boreham, Geoscience Australia

5.1 KEY POINTS

- Potential oil-prone source rocks in the Bass Basin are Palaeogene coals, mainly concentrated in the Early to Middle Eocene succession, with Hydrogen Indices (HI) up to 500 mg hydrocarbons/gTOC, while associated disseminated organic matter in claystones is mainly gas prone.
- Maturity is sufficient for oil and gas generation, with vitrinite reflectance (VR) up to 1.8% at the base of Pelican-5. Igneous intrusions, mainly within Paleocene, Oligocene and Miocene sediments, produced localised elevated maturity up to 5% VR.
- Key events in the process of petroleum generation and migration from effective source rocks are:
  - onset of oil generation occurred at a VR of 0.65% (2450 m in Pelican-5)
  - onset of expulsion (primary migration) occurred at a VR of 0.75% (2700 to 3200 m in Bass Basin; 2850 m in Pelican-5)
  - main oil window occurred between VR of 0.75% and 0.95% (2850 to 3300 m in Pelican-5)
  - main gas window occurred at VR>1.2% (>3650 m in Pelican-5).
- Coals and claystones show a range in laboratory-generated chemical kinetic properties, which when applied to the geological timeframe, translates to an approximate 500 m range in the onset of primary migration.
- Oils in the Bass Basin are a single oil population sourced mainly from Early Eocene to Paleocene coals. Biodegradation of the Cormorant oil results in a statistically separate oil family compared to the Pelican and Yolla crudes.
- Much better oil-to-source correlations are found between the oils and the coals, than the claystones.
- Gases in the Bass Basin are wet and high in CO_2 content. The CO_2 is sourced from igneous intrusions.
- Gaseous hydrocarbons have a similar source to oils, but are generated over a wider maturity range. White Ibis-1 gas is of higher maturity than Yolla-2 gas.

5.2 INTRODUCTION

Situated in offshore southeastern Australia, the Bass Basin is a minor terrestrial oil and gas province. It lies to the southwest of the Gippsland Basin, which is Australia's premier petroleum province. Oil and gas in the Gippsland Basin are sourced from terrestrial organic matter (Moore et al., 1992, Boreham et al., 2001). The oil in the Bass Basin is typically paraffinic with oil in shallower reservoirs undergoing significant alteration by biodegradation (Edwards et al., 1999). Biomarker and carbon isotopic data (Edwards et al., 1999), and the lack of a significant potential marine source rock over most of the basin (Miyazaki, 1995) indicate that the oil is sourced primarily from terrestrial organic matter within the Late Cretaceous to Eocene Bass, Aroo and lower Demons Bluff sequences (Eastern View Group). Miyazaki (1995) suggested that disseminated organic

matter within the carbonaceous claystones are the main effective source rocks for oil, while gas is the primary expulsion product from the associated coals. The latter is based on the concept that oil initially generated from the coal over a maturity range of 0.6 to 1.4% vitrinite reflectance (VR) would remain 'absorbed' within the organic matrix. Subsequent expulsion of gas from the coal would only have occurred at higher maturities when oil-to-gas cracking became significant (Miyazaki, 1995).

In the Bass Basin, there is a critical need for more detailed information on the spatial variations in petroleum potential, gas:condensate ratios (GCR), gas:oil ratios (GOR) and maturation characteristics within organic-rich rocks to help identify the potential source(s) for the oil and gas. Previous interpretations of vitrinite reflectance profiles and bulk geochemical parameters, such as Rock-Eval and extractable organic matter (bitumen) content, were undertaken at a regional scale within the Bass Basin (Miyazaki, 1995). This approach did not allow for stratigraphic variations in source rock characteristics to be fully addressed.

5.3 AIMS, SAMPLES AND METHODS

The geochemistry program undertaken as part of the WTRMP aimed to address fundamental questions related to hydrocarbon generation in the Bass Basin, in particular:

- are some coals and claystones more oil-prone than others, and if so, is it possible to predict their distribution?
- what are the respective contributions of coals and associated carbonaceous lithologies to oil and gas generation and expulsion?
- is there evidence that oil is expelled from coal?
- can gas-oil-source correlations be established in the basin?
- are there variations in chemical kinetics for kerogen degradation that would cause source rocks to mature (i.e., generate and expel hydrocarbons) at different temperatures, and can the distribution of these rocks be predicted?

ORGCHEM, Geoscience Australia's Oracle-based organic geochemistry database (http://www.ga.gov.au), was the source for the bulk Rock Eval and vitrinite reflectance data interpreted for this study, while top and base ages (Ma) over the depth interval of the sample were estimated using STRATDAT (Geoscience Australia's Oracle-based biostratigraphy database). This data was complied from well completion reports submitted under the *Petroleum Submerged Lands Act (PSLA) 1967,* and destructive analysis reports submitted to Geoscience Australia by external agencies following analyses of sediments sampled at Geoscience Australia's Core and Cuttings Repository (Canberra).

Additional cores and cuttings were sampled as part of this study and are listed in Appendix D. Coals with a low percentage of ash (<20 % ash) were separated from other lithologies using a heavy liquid of density 1.5 (Sykes, 2001). Standard coal analyses were undertaken by CRL Energy Ltd, Lower Hutt, and ACIRL Ltd, Sydney, following international and in-house standard procedures. These analyses included: proximate

analysis (moisture, ash and volatile matter), elemental analysis (C, H, N), total sulphur, forms of sulphur (sulphate, pyritic and organic) and calorific value. This suite of analyses allows determination of both coal type (on a chemical basis) and rank, while sulphur contents provide a record of the degree of marine influence within the coal-forming environment. Rock Eval and total organic carbon (TOC) were determined using a Rock Eval 6 instrument. Bulk chemical kinetic parameters were calculated from the Rockin™ software by processing Rock Eval S2-rate data collected at 1, 2, 5, 10 and 15^{o}C/min to give a discrete distribution of activation energy (Ea) and a single frequency factor (Arrhenius constant, A). Additionally, gas-to-oil ratios were applied to each individual Ea using the stepwise-pyrolysis gas chromatography mass spectrometry method described in Boreham et al. (1999).

Vitrinite-inertinite reflectance and fluorescence (VRF™ or VIRF) measurements on Cormorant-1 and Pelican-5 (Appendix E) were performed using the procedures described in Newman (1997) and Newman et al. (2000). Quantitative grain fluorescence (QGF) and grains-with-oil-inclusions (GOI™) analyses were determined using the procedures of Liu et al. (2001) and Eadington et al. (1996), respectively. Palynological analysis using procedures described in Boreham et al. (2002) was undertaken on a representative split of the sample used for geochemistry (Appendix F). In all cases, pollen spores and other acid-resistant plant microfossils were extracted using the same standard oxidation and filtration techniques designed to eliminate fines with maximum diameters of less than 5 μm.

Natural gases were obtained for Yolla-1 and While Ibis-1, and oil samples were collected from Cormorant-1, Yolla-1 and Pelican-1 and -2 (Appendix G). Molecular and carbon isotopic compositions of individual gaseous components were compiled from public domain sources such as open-file well completion and literature reports (Geoscience Australia's ORGCHEM database) together with new analyses undertaken by Geoscience Australia's Isotope and Organic Geochemistry Laboratory using analytical procedures described in Boreham and de Boer (1998). All carbon isotope values are reported in the δ^{13}C notation:

$$\delta = \frac{R_{sample} - R_{standard}}{R_{standard}} \times 1000 \left({}^{o}/_{oo} \right)$$

where the standard is PDB limestone with $R_{standard} = {}^{13}C/{}^{12}C = 0.011237$.

All the isotope analyses were run in duplicate with a reproducibility of ± 0.3 ‰. Errors on the molecular composition of the hydrocarbon components analysed by gas chromatography-thermal conductivity detector are of the order of ± 0.05 %.

Gas chromatography-mass spectrometry of the saturated hydrocarbons from oils and source rock extracts using selected ion monitoring (GCMS-SIR) and compound specific carbon isotopic analysis of the *n*-alkanes (isolated from 5Å molecular sieve adducts) by gas chromatography-combustion-isotope ratio mass spectrometry (GC-C-IRMS) were conducted according to Boreham and Summons (1999).

5.4 SOURCE ROCK GEOCHEMISTRY

Geochemical data (Rock Eval, TOC and vitrinite reflectance) are available for 28 exploration wells in the Bass Basin (includes all wells except Barramundi-1, King-1, White Ibis-1 and Yolla-2). These data were partitioned into the following age intervals in order to reflect recognised subdivisions within the stratigraphic succession (Chapter 4):

- >73 Ma (Campanian and older);
- 73-65 Ma (Maastrichtian);
- 65-53 Ma (Paleocene to earliest Eocene, *L. balmei* zone);
- 53-50.5 Ma (Early Eocene, *M. diversus* zone);
- 50.5-47.5 Ma (late Early Eocene to Middle Eocene, *P. asperopolus* zone);
- 47.5-38 Ma (Middle Eocene, Lower *N. asperus* zone);
- 38-35 Ma (Middle to Late Eocene, Middle *N. asperus* Zone; and,
- <35 Ma (latest Eocene and younger, Upper *N. asperus* and younger zones).

Source Richness and Quality

Figure 5.1 shows the plot of TOC versus age for 28 wells in the Bass Basin. Figures 5.2 to 5.9 show these samples subdivided into the specific age intervals. Figure 5.1 shows that the coals (TOC>40%) are clearly concentrated within specific time intervals. The Upper Cretaceous to Eocene succession is the dominant coal-bearing section, while intervals within the Early Eocene to early Middle Eocene section (Upper *L. balmei* to *P. asperopolus* zone) have the greatest concentration of coal (Figures 5.1, 5.5 and 5.6; Bass-1, Cormorant-1, Dondu-1 Konkon-1, Nangkero-1, Narimba-1, Pelican-2, -4, -5, Poonboon-1, Squid-1, Tarook-1, Toolka-1A, Yolla-1 and Yurongi-1). Minor coal occurrences are seen within the Albian (Figure 5.2; Durroon-1), Paleocene (Figure 5.4; Chat-1, Nangkero-1, Narimba-1, Pelican-2, -5 and Poonboon-1), and Middle Eocene sections (Figure 5.7; Bass-1, -3, Cormorant-1, Dondu-1, Flinders-1, Pelican-2, -4, -5, Poonboon-1, Toolka-1A and Yurongi-1), and in the Middle Miocene marine succession (Figure 5.9; Pipipa-1).

Using a TOC value of 2% as the lower limit for an effective source rock containing disseminated organic matter, it is clear that the Cenomanian to Campanian succession has limited source potential (Figure 5.1b; 98-73 Ma). Such an extended period of poor quality source rock development did not occur again until the Oligocene to Middle Miocene (Figure 5.1b; 35-15 Ma). Although potential source rocks exist with sufficient disseminated organic matter (TOC>2%) at other time periods (Figure 5.1), the critical issue is source quality. This is addressed here using a plot of S2 verses TOC (Figures 5.2 to 5.9), where the slope of a line projected from the sample values to the origin (zero TOC and zero S2) is a measure of the Hydrogen Index (HI). For samples with low TOC (<3%), projection to non-zero TOC can be used to account for the mineral matrix effect, which would otherwise lead to a suppressed HI owing to forced projection through zero TOC (Boreham et al., 2002).

Using HI (mg hydrocarbons/gTOC) ranges of >300, 200-300, 100-200 and <100 to indicate oil potential, gas with minor oil potential, gas (wet) potential, and minor gas to no source potential, respectively, the following summations can be made for each time interval:

>73 Ma (Campanian and older)

- Generally poor source potential, except for some good to excellent oil potential in organic-rich sediments from the Aptian-Albian (average HI=300) in Durroon-1 (Figure 5.2);

73-65 Ma (Maastrichtian)

- Good to excellent oil potential in organic-rich Maastrichtian sediments in Chat-1 (average HI=370), and isolated samples from Bass-3 and Pelican-5. All other samples with TOC>2% show, at best, gas potential (Figure 5.3);

65-53 Ma (*L. balmei* zone)

- The Paleocene to earliest Eocene succession has a good representation in the overall dataset with 21 of the 28 wells having analytical data. The coal at 2678 m in Poonboon-1 shows the greatest oil potential with an HI of approximately 500. Oil potential of coaly clastic rocks (TOC>10%, Figure 5.4a) is shown at Nangkero-1 (average HI=400) and at Pelican-5 (average HI=320), while similar organic-rich sediments at Nangkero-1 (average HI=235) show limited oil potential. All other wells have no oil potential. Sediments with TOC <10% (Figure 5.4b), display reduced oil potential with the bulk of the data having HI<300. The exceptions are Bass-2 (1500 m) and in Pelican-5.

53-50.5 Ma (*M. diversus* zone)

- The majority of the wells (23) have analytical data over the Early Eocene interval indicative of a high oil potential. Several wells contain coaly sediments with HI>300 (Figure 5.5a; Chat-1, Cormorant-1, Nangkero-1, Pelican-2, -4, -5, Poonboon-1, Tilana-1, Toolka-1A and Yurongi-1), while maximum HI's of 519 and 482 occur in Pelican-4 and Poonboon-1 at 2701 m and 2430 m, respectively. The carbonaceous clastic rocks (TOC<10 %; Figure 5.5b) have lower hydrocarbon potential with only samples from Pelican-5, Squid-1 (2645 m) and Yolla-1 (2300 m) showing significant liquids potential.

50.5-47.5 Ma (*P. asperopolus* zone)

- Source rocks in the late Early Eocene to early Middle Eocene interval are geochemically similar to the Early Eocene rocks. Twenty-two wells have geochemical data (Figure 5.6), and at least half show major oil potential in the coaly sediments with HI>300 (Figure 5.6a; Bass-1, -2, Cormorant-1, Nangkero-1, Narimba-1, Pelican-2, -4, -5, Tarook-1 and Yolla-1). Only the Pelican-5 well shows major oil potential in organically-lean rocks with TOC<10 % (Figure 5.6b).

47.5-38 Ma (Lower *N. asperus*)

- The Middle Eocene interval is represented in 21 wells with oil-prone source quality (HI>300) occurring in the coaly sediments from approximately half of the wells (Figure 5.7a; Aroo-1, Bass-1, -2, -3, Cormorant-1, Pelican-2, -4, -5, Poonboon-1 and Yurongi-1). Samples from Bass-3 (1787 m) and Pelican-4 (1890 m) have the greatest oil potential, with HI>450 (Figure 5.7a). A poorer source quality is evident for sediments with TOC<10 % with only those from Bass-1 and Pelican-5 at 1952.3 m and 2063 m, respectively, having oil potential (Figure 5.7b).

38-35 Ma (Middle *N. asperus* zone)

- The mainly Late Eocene interval, encompassing the shaley regional sealing facies of the Demons Bluff Sequence ("Eocene Shale"), shows no oil potential in any of the 17 wells intersected (Figure 5.8). In rocks with adequate organic richness to be considered potential source rocks (TOC>2%), only minor gas potential is evident (Figure 5.8; Squid-1 at 1840 m, Yolla-1 at 1765 m)

<35 Ma (Upper *N. asperus* zone and younger)

- The latest Late Eocene and younger age interval is sampled in 12 wells. However, only two organic-rich samples have hydrocarbon potential. Bass-1 at 631 m (HI=178) and Pipipa-1 at 599 m (HI=117) show wet gas and minor gas potential, respectively.

Source Maturity

In the Bass Basin there is a large database of vitrinite reflectance measurements available in the public domain that has been compiled in GA's ORGCHEM database. However, it is well documented that vitrinite reflectance can vary widely depending on the laboratory and analyst. It can also suffer from vitrinite suppression, especially when the vitrinite maceral is strongly associated with hydrogen-rich exinite maceral. The question of reliability of vitrinite reflectance data in the Bass Basin was addressed by new vitrinite reflectance measurements using only normal vitrinite identified using a vitrinite-inertinite reflectance and fluorescence (VRF™) approach (Figure 5.10; Newman, 1997; Newman et al., 2000). Cormorant-1 and Pelican-5 were chosen for analysis as they are in different depocentres and both cover a wide maturity range to total depth. Both wells are currently at their maximum depth of burial. The VRF data show that coal and associated disseminated organic matter in claystones have the same VR, indicating that reflectance measurements are independent of mineral content (Appendix E). Furthermore, the new VR data are comparable with the existing VR data (Figure 5.11), suggesting that existing data can be used with a high degree of confidence.

Figures 5.12 and 5.13 show vitrinite reflectance plotted against depth and age for 28 wells in the Bass Basin. Vitrinite reflectance measurements range from 0.3 to 4.9%, indicating a range from immature to highly overmature sediments within the low metamorphic grade. Intervals with high to extremely high maturity zones (VR>1.5 %) are not necessarily the deepest samples analysed in the wells (except at Pelican-5), suggesting an external, localised heating has supplemented the geothermal gradient. This profile is consistent with the observed influence of igneous intrusions in sediments lying between 1500 and 2500 m depths (Figure 5.12), with ages ranging from Paleocene to Late Miocene (Figure 5.13). In Pelican-5, there is

a smooth increase in vitrinite reflectance with depth, with a maximum VR=1.77 % recorded at the base of the well (Figure 5.11).

Based on a vitrinite reflectance of 0.75% as the threshold for primary migration from the source rock (see below), only Aroo-1, Cormorant-1, Durroon-1, Flinders-1, Koorkah-1, Narimba-1, Pelican-1, -5, Tilana-1 and Yolla-1 have reached that critical maturity. This occurs between 2700 and 3200 m within Eocene or older sediments, while the end of the main phase of oil expulsion (0.95% VR) occurs between 3200 and 3500 m (Figure 5.13).

5.5 PETROLEUM GENERATION AND EXPULSION

The key maturity horizons in the pathway of kerogen transformation to petroleum are: a) the onset of oil generation; b) the onset of expulsion from the source rock (primary migration or critical moment in the petroleum system); c) the oil window; and, d) the onset of gas generation and expulsion. The latter is problematic as gas is generated throughout the oil window over which there is a transition from wet to dry gas in the overmature region. Here, field data using the estimated maturities of the reservoired fluids, analysis of the residual petroleum potential of source rocks (Rock Eval), and the change in pore space geometry and fluid composition (Small Angle Neutron Scattering, SANS; Appendix H) allow a good estimation of these key horizons.

Figure 5.14 shows the depth plot of Hydrogen Index (HI) and Bitumen Index (BI) for low-ash coals in the Pelican-5 well, which was chosen as its shows the greatest maturity range (excluding igneous intrusions) from immature to overmature. The coals form a rather homogeneous set dominated mainly by gymnosperm remains (Appendix F). For HI, a measure of the residual petroleum potential, there is an 'evolution' from fairly constant HI=250 (minor oil potential) in coals shallower than 2450 m, to a rapid increase in HI, which maximises at 440 (major oil potential), at 2850 m. This is followed by an initially sharp decrease in HI and continual decay. Similar trends have recently been documented in New Zealand coals of similar age (Sykes, 2001). Like the New Zealand trends, the Bass Basin trends are interpreted to indicate the onset of oil generation at 2450 m and the onset of expulsion at 2850 m, corresponding to VR of 0.65% and 0.75%, respectively, using the best-fit curve for the VR profile in Figure 5.11.

The main oil window is defined from 0.75% to 0.95% VR (2850 to 3300 m in Pelican-5; Figure 5.11) using methylphenanthrene-based (MPI) chemical maturity parameters for the Pelican and Yolla oils (Table 5.1). The response of BI (residual free hydrocarbons in the coal) is slightly different to HI with a rapid increase up to the onset of expulsion (2850 m) maximising to a constant value to 3650 m (1.2% VR), followed by a steady decrease. The constantly high value in BI represents a steady-state maintenance of maximum oil saturation, while decreasing BI below 3650 m corresponds either to a more efficient expulsion of residual liquids due to a higher gas:oil ratio for the primary generated hydrocarbons or the beginning of oil-to-gas cracking, or a combination of both. Support for the above comes from a SANS analysis on the low-ash coals

in Pelican-5 (Figure 5.15; Appendix H). Filling of pore space with oil is evident between 2400 m to 2800 m where the scattering intensity is at its minimum and remains constant due to constant oil saturation.

5.6 KINETICS OF PETROLEUM GENERATION

Oil and gas generation from organic matter in source rocks is a kinetic process controlled by the time-temperature history. Individual source rocks have their own specific chemical kinetics, which can be determined in the laboratory and applied to the geological timeframe (Boreham et al., 1999; see Chapter 6). Plotted here (Figure 5.16) is the proportion of organic matter transformed versus temperature for a simple linear temperature increase of 1^{o}C/Ma for representative coals (claystones also plot with the range of the coals) in the Bass Basin, together with a calculated vitrinite reflectance (Burnham and Sweeney, 1989). A VR of 0.75% (onset of expulsion) correlates to a transformation ratio (TR) between 0.2 to 0.3 for the range of kinetic parameters for the immature coals (Figure 5.16), whereas by the end of the main phase of oil generation between 50% and 65% of the reactive kerogen has been transformed to oil and gas with a fairly constant gas:oil ratio 0f 0.2.

5.7 OIL GEOCHEMISTRY

Oil-Oil Correlation

To clarify the intra-basinal relationships between the Bass Basin oils and inter-basinal relationships with other oils in the region (Gippsland and Otway basins), a multivariant statistical analysis was employed involving a wide range of GC, GCMS and carbon isotope parameters (Table 5.2). Such an approach has previously been shown to group together chemically-related populations and families of oils that also have geological significance (AGSO and GeoMark Research, 1996; Boreham and Summons, 1999; Boreham et al., 2002, Geoscience Australia and GeoMark Research, 2002). Using the parameters in Table 5.2 and unpublished data (Geoscience Australia and GeoMark Research, 2002), hierarchical cluster analysis (Einsight^{TM} software) was used to generate the dendrograms displayed in Figure 5.17.

Confidence in the statistical approach is supported by the oil population associations (Figure 5.17) following those previously identified within the Austral Petroleum Supersystem for oils from the Otway and Bass basins (Edwards et al., 1999). Furthermore, the set of geochemical variables clusters in geochemically recognisable groups (Figure 5.17), reflecting primary source and depositional environment controls. Thus, the land plant inputs are directly associated with higher %29 sterane, and the Pr/Ph and oleanane contents with stronger bacterial reworking (C31 hopane content). The %27, %28, 29/H, 28/H are associated with minor algal and marine influences, the tricyclic and tetracyclic parameters reflect the changing bacterial communities, while the carbon isotopes, the main distinguishing feature between Bass Basin oils and the other oils, are a fundamental control reflecting inputs from different plant communities.

Oils from the Gippsland Basin separate into two main populations, indicating different generation and preservation histories (Geoscience Australia and GeoMark Research, 2002), while the three main oil populations observed in the Otway Basin (Figure 5.17) reflect multiple source rock organic facies of Late

Jurassic to Early Cretaceous age (Edwards et al., 1999; Geoscience Australia and GeoMark Research, 2002). Furthermore, there is only a weak association between oils from the different basins, suggesting a difference in the nature of terrestrial organic facies between (and also within) the basins.

The Bass Basin oil population (A3 petroleum system of Edwards et al., 1999) shows two families of oils, one family represented by the Pelican and Yolla oils, and the other by the Cormorant oil (Figure 5.17). However, it is suggested that the Cormorant-1 oil was generated from the same source rock facies as the other Bass Basin oils and that in-reservoir alteration has perturbed various geochemical parameters (Edwards et al., 1999). Biodegradation has resulted in depletion in the carbon isotopes due to removal of all *n*-alkanes and various aromatic hydrocarbons, lower Pr/Ph as a result of preferential removal of pristane, selective removal of the higher molecular weight homologues in the tricyclics, and the loss of lower molecular weight hopanes and steranes. The source rock facies for the Bass Basin oils appears to be uniform considering the closer associations shown between Yolla and Pelican oils than between oils from the same well (Figure 5.17). These subtle differences most likely reflect slight maturity differences and alteration effects associated with migration fractionation (Boreham and Summons, 1999)

Oil-Source Correlation

In order to establish inter-relationships between the Bass Basin oils and potential source rocks, a multivariant statistical analysis (Einsight™ software) was employed using biomarker ratios based on diterpane, triterpane, hopane and sterane contents in the saturated hydrocarbon fractions (Table 5.2). Good reproducibility of the analytical protocol is indicated by the close correlation between repeat analyses for the Gippsland basin oils from Halibut-A1 and West Seahorse-1 (Figure 5.18).

The potential source rocks analysed include coals and claystones from Cormorant-1 and Pelican-5, while the oils were from Cormorant-1, Pelican-1, -2 and Yolla-1. Good correlation (correlation coefficient >0.6) with Pelican and Yolla crudes is only seen for coals from Pelican-5 at depths >3000 m. This is consistent with the depth range of the oil window in Pelican-5 (Figure 5.14). A slightly weaker correlation is obtained between Cormorant-1 crude and coals from both Pelcian-5 (2791 m) and Cormorant-1 (2758 and 2941 m). However, biodegradation of the Cormorant-1 crude may have masked a closer correlation. The correlation between the coals and different depocentres in the Bass Basin suggests that there is a wide distribution of a rather uniform source rock facies. Claystones in Cormorant-1 and Pelican-5 do not show any correlation with the oils. Thus, this is the first demonstration of a good oil-source correlation involving Australian coal as the source rock for oil (Boreham and Powell, 1994; Powell and Boreham, 1994).

5.8 GAS GEOCHEMISTRY

Molecular and Carbon Isotopic Composition

For the wet gases from the Bass Basin, the relative proportions of methane (C_1) to wet gas (C_2-C_5 hydrocarbons), represented by the ratio % C_1/C_1-C_5 in Figure 5.19, shows an average of 85.6% for White

Ibis-1 and 87% for Yolla-2. Thus, the Bass Basin gases have a similar wet gas content to average Gippsland Basin gases (85%), while gases from the Otway Basin are, on average (93%), drier (Boreham et al., 2001).

The range in carbon isotopic composition of the individual gaseous hydrocarbons in 'unaltered' natural gases from Australian sedimentary basin is shown in Figure 5.20 (Boreham et al., 2001). The wide carbon isotopic range, 16‰ for methane reducing to 8‰ for *n*-pentane (Figure 5.20), is very significant and enables deconvolution of inter-related factors and processes that can control the carbon isotopic composition in gases. Natural gases that fall outside the normal carbon isotopic range for their respective individual basins (Figure 5.20) have been influenced by very high maturities, have multiple sources or have undergone secondary alteration within the reservoir (Boreham et al., 2001).

The similar carbon isotopic composition and relatively limited isotopic range (<2‰) for gases from the Bass and Gippsland basins (Figure 5.20) suggests that gases in each basin were generated from similar organic facies or from multiple sources that are isotopically similar. The wider isotopic range in gases from the Otway Basin shows that gases were generated from multiple source rock horizons that are isotopically distinct (Figure 5.20; Boreham et al., 2001)

Source and Maturity of Gases

Source and maturity are the primary control on hydrocarbon composition and carbon isotopes, which are at times difficult to deconvolute (Boreham et al., 2001). The approximately linear relationship between the carbon isotopic composition of the individual linear gaseous hydrocarbons and the reciprocal of the carbon number (Figure 5.21; natural gas plot of Chung et al., 1988), is further evidence of a single source input to the Bass Basin gases.

The maturity influence on carbon isotopic composition has a theoretical basis wherein the carbon isotopic difference between individual gas components decreases with increasing maturity (James, 1983, 1990). Thus, by plotting the carbon isotopic differences, source controls are effectively eliminated or considerably reduced (James, 1983, 1990). Such an approach is shown in Figure 5.22, which plots the isotopic differences between methane and ethane against propane and ethane, together with their theoretical maturity relationship developed by James (1983). Using this approach, maturities with vitrinite reflectance >1.5% are required for the effective source rocks for gas reservoired at White Ibis-1 and Yolla-2 wells (Figure 5.22). Similar high maturities are predicted for natural gases in the adjacent Gippsland and Otway basins. However, for terrestrial organic matter sources, the approach in Figure 5.22 can overestimate gas maturities (James, 1990), albeit to different extents depending on organic facies, which currently cannot be effectively quantified (Boreham et al., 2001). Nevertheless, gas maturity is generally higher than maturity of accompanying liquid hydrocarbons (Moore et al., 1992; Edwards et al., 1999; Geoscience Australia and GeoMark Research, 2002) indicating that gas and oil were generated at different times from the same source rocks.

Of the non-hydrocarbon gases in the Bass Basin, nitrogen contents are low (max. 2 mole%) while hydrogen is found at trace levels (0.04 mole%) and helium is below the detection limit (Table 5.3). Carbon dioxide is the most abundant with a very high 20 mole% in Yolla-2 (Table 5.3), although much higher CO_2 contents occur in the Gippsland (54 mole% at Gunter-1) and Otway (99 mole% at Caroline-1) basins (Boreham et al., 2001). An appreciation of the origin of CO_2 can be demonstrated using the relationship between molecular and carbon isotopic compositions (Figure 5.23). The Bass Basin gases plot within the band between -3 and -10‰ and are considered to be derived from an inorganic igneous and/or mantle source (Smith and Pallasser, 1996; Boreham et al., 2001). The pervasive magmatic intrusions within the Bass Basin are undoubtedly the source of the CO_2 gas.

Gas and Oil Correlation

The combination of carbon isotopic compositions of the gaseous hydrocarbons and the *n*-alkanes of oil has proven to be most effective in gas-oil correlation studies (Boreham et al., 2001). Figure 5.24 shows the C_1-C_{30} extended *n*-alkane carbon isotopic profile for gases and oils in the Bass Basin, together with representative gas-oil pairs from the Gippsland Basin. The similar range in $\delta^{13}C$ (< 2‰ for C_{7+} *n*-alkanes of the same carbon number) for the White Ibis-1 and Yolla-1 oils suggests an origin from very similar source rock facies. The consistent depletion in ^{13}C (isotopically light) in the C_{7+} *n*-alkanes for the shallower oil from Yolla-1 (1830 m) is consistent with reservoir spill-fill with an earlier generated, lower maturity liquid. However, the stacked liquids at Yolla-1 have similar maturities based on chemical maturity parameters (Table 5.1) despite vertical separation of 1000 m. Alternatively, this could indicate multiple sourcing from slightly different terrestrial source facies. Compared to the Gippsland Basin hydrocarbons, the Bass Basin C_{2+} *n*-alkanes are consistently 1 to 2 ‰ depleted in ^{13}C (Figure 5.24).

In order to understand the relationship of the gas to the oil, use is made of the position and shape of the extended *n*-alkane carbon isotope profile. A relatively 'smooth' continuum in the carbon isotopic data from the linear C_4-C_5 wet gas components through to the low molecular weight (< C_9) *n*-alkanes in the oil, as is the case for the Yolla-2 gas/Yolla-1 oil pair, indicates that the gas and the liquid hydrocarbons are genetically related, most likely generated from the same source. Maturity estimates indicate that the gas was generated at a slightly higher maturity compared to the oil. Obviously, this maturity difference is relatively isotopically insensitive and does not result in carbon isotopic discrimination in the low molecular weight hydrocarbons. On the other hand, the increase in ^{13}C content (isotopically heavy) for the wet gas components in White Ibis-1 is, most likely, a result of a much higher maturity source rock at the time of primary gas expulsion than in the case of the Yolla-2 gases.

5.9 CONCLUSIONS

- Coals and associated organic matter in claystones (TOC>2%) show good to excellent source rock richness; coal facies dominate in the Early Eocene to early Middle Eocene (Upper *L. balmei* to *P. asperopolus* zone).

- Coals show good source quality for oil with HIs up to 500 mg hydrocarbons/gTOC, while claystones are mainly gas-prone.
- Campanian and older sediments generally have very low source potential, except for some good to excellent oil potential in organic-rich sediments from the Aptian-Albian (average HI=300) in Durroon-1.
- Maastrichtian sediments showing good to excellent oil potential occur in organic-rich facies in Chat-1 and isolated samples from Bass-3 and Pelican-5. All other samples with TOC>2% show some gas potential.
- Paleocene (65-53 Ma; *L. balmei* zone) sediments show oil potential (HI>300) in coals from Poonboon-1, Nangkero-1, Pelican-5 while those from Nangkero-1 have wet gas potential. Only claystones in Bass-2 and Pelican-5 show oil potential (TOC<10%).
- Early Eocene (53-50.5 Ma; *M. diversus* zone) coals consistently show the highest oil potential in Chat-1, Cormorant-1, Nangkero-1, Pelican-2, -4, -5, Poonboon-1, Tilana-1, Toolka-1A and Yurongi-1. The carbonaceous clastic rocks have lower hydrocarbon potential (TOC<10%), with only samples from Pelican-5, Squid-1 and Yolla-1 showing major liquids potential.
- Latest Early Eocene to early Middle Eocene (50.5-47.5 Ma; *P. asperopolus* zone) coals show oil potential in Bass-1, -2, Cormorant-1, Nangkero-1, Narimba-1, Pelican-2, -4, -5, Tarook-1 and Yolla-1. Only the Pelican-5 well shows major oil potential in the organically-leaner rocks with TOC<10%.
- Middle Eocene (47.5-38 Ma; Lower to Middle *N. asperus* zone) coals are oil-prone at Aroo-1, Bass-1-, -2, -3, Cormorant-1, Pelican-2, -4, -5, Poonboon-1 and Yurongi-1. A poorer source quality is evident for sediments with TOC<10%, with only those from Bass-1 and Pelican-5 having oil potential.
- The mainly Late Eocene (38-35 Ma; nominally marine "Demons Bluff shale") sediments have no oil potential and only minor gas potential at Squid-1.
- The latest Late Eocene and younger (<35 Ma; Upper *N. asperus* zone and younger) sediments contain no oil-prone organic matter, although there is limited wet gas and minor gas potential at Bass-1 and Pipipa-1.
- Vitrinite reflectance data indicate that potential source rocks have attained maturities sufficient for oil and gas generation with highest VR values of 1.8% at the base of Pelican-5 attained through burial. Igneous intrusions in Paleocene, Oligocene and younger sediments have elevated localised VR values up to 5.0%.
- Key 'thresholds' in petroleum generation and expulsion were defined in Pelican-5, using a combination of SANS, Rock Eval and chemical maturity parameters for the Bass Basin oils: onset of oil generation, onset of oil expulsion (primary migration), and onset of gas generation occurs at 2450 m, 2850 m and 3650 m, respectively. This corresponds to vitrinite reflectance thresholds of 0.65%, 0.75% and 1.2%, respectively. The main oil window is defined between 0.75% and 0.95% VR (2850 to 3300 m in Pelican-5) based on oil maturity.
- Laboratory-generated chemical kinetic parameters for Paleocene to Eocene coals have identified end-member labile and resistant organic facies. Extrapolation to the geological timeframe results in an approximately 500 m depth range for primary migration, depending on the choice of kinetic parameters. Furthermore, approximately 20-30% of the organic matter needs to be transformed to petroleum before an oil-wet pore space is capable of supporting primary migration from coal.

- Oil-oil correlation in the Bass, Gippsland and Otway basins using GC, isotopes and biomarkers has shown:
  - A single Bass Basin oil population (the Cormorant-1 oil was affected by biodegradation);
  - A uniform terrestrial source rock facies for Bass oils;
  - Distinct oil families for each of the different basins in the Bass Strait region;
- Oil-source correlations using biomarkers (diterpanes, triterpanes, hopanes and steranes) between Bass Basin oils and coals and claystones from Cormorant-1 and Pelican-5 have shown:
  - A good oil-to-source correlation was obtained between oils and coals, but claystones do not show as strong a link.
  - Coals below 2750 and 3000 m (Early Eocene to Paleocene) in Cormorant-1 and Pelican-5, respectively, can be correlated with Bass Basin oils. This is in agreement with depth (and maturity) intervals defined for expulsion from effective source rocks.
- Gas composition and carbon isotopic comparisons between gases and liquids has shown:
  - A high CO_2 content in Bass Basin gases that is derived from inorganic (igneous) sources.
  - Bass Basin gases (and oils) are isotopically light (depleted in ^{13}C) compared to Gippsland Basin hydrocarbons.
  - Yolla gases are associated with Yolla oils, and both were generated from the same source and at similar maturities.
  - White Ibis gases were generated at a higher maturity than Yolla gases.

Table 5.1 Chemical maturity parameters for oils from the Bass Basin.

Well	Pelican-1	Pelican-2	Cormorant-1	Yolla-1	Yolla-1
Geoscience Australia No.	2001950	2001951	10037	10036	10035
DNR-1	8.61	7.89	0.36	0.77	10.00
TNR-1	1.18	0.86	0.36	0.82	1.29
TNR-2	0.77	0.46	0.54	0.47	0.73
TeNR	0.77	0.45	0.51	0.48	0.68
MPI -1	0.80	0.55	0.31	0.76	0.84
Rc-1	0.88	0.73	0.58	0.86	0.90

DNR-1 = 26-+27-)/15-dimethylnaphthalene
TNR-1 = 236-/(146- + 135-)trimethylnaphthalene
TNR-2 = 136-/(136- + 125-)trimethylnaphthalene
TeNR = 1367-/(1367- + 1256)tetramethylnaphthalene
MPI-1 = 1.5*(3- + 2-)methylphenenatrene/(phenanthrene*rf+ (9- + 1-)methylphenenthrene) where rf = 0.83 (response factor relative to methylphenanthrenes in GCMS)
Rc-1 =0.6*MPI + 0.4 (Radke and Welte 1983)

Table 5.2 OilMod™ parameters based on GC, carbon isotopes and biomarkers collected on oils and potential source rocks.

GA No.	Well	Top, metres	Type	19T/23T	24T/23T	Tet/23T	29H/30H	OL/30H	31R/30H	%27	%28	%29	kaur/phyll	ipim/phyll	19-ipim/ipim	labd/phyll	fich/phyll	bery/phyll
10037	Cormorant-1	1500	FIT 6	15.30	1.61	10.59	0.64	0.03	0.54	6.6	26.8	66.6	0.15	1.69	1.05	0.21	0.54	0.90
19999150	Pelican-1	3161.4		4.66	0.52	1.87	0.69	0.11	0.19	17.4	30.0	52.6	0.11	0.64	1.72	0.32	0.22	0.91
19999151	Pelican-2	2879.5	FIT 1	8.40	0.51	6.26	0.62	0.04	0.24	16.1	25.9	58.0	0.12	1.02	0.97	0.44	0.32	1.04
10036	Yolla-1	1830	DST 2	0.98	0.31	3.62	0.71	0.03	0.43	10.3	30.4	59.3	0.15	1.59	0.21	0.19	0.24	1.22
10035	Yolla-1	2824	DST 1	0.22	0.47	1.80	0.55	0.04	0.19	13.1	31.5	55.4	0.11	0.89	0.20	0.24	0.25	1.08
20010071	Cormorant-1	2340.9	coal (cutt)	8.25	0.53	3.90	0.96	0.03	0.45	13.5	28.6	57.9	0.20	0.77	3.64	0.11	0.68	0.90
20010072	Cormorant-1	2758.5	coal (cutt)	15.12	0.30	15.75	0.56	0.02	0.17	7.7	26.0	66.3	0.13	0.33	2.34	0.07	0.26	0.24
20010073	Cormorant-1	2990.1	clyst (cutt)	2.28	0.38	1.97	0.77	0.03	0.39	25.2	22.6	52.2	0.18	0.42	2.53	0.20	0.44	0.94
20010374	Cormorant-1	2941.4	coal (cutt)	10.17	0.40	12.98	0.53	0.02	0.13	11.7	28.0	60.2	0.10	0.52	1.46	0.08	0.23	0.31
20010380	Pelican-5	2592	coal (cutt)	4.67	0.93	5.39	1.09	0.01	0.54	11.6	34.7	53.8	0.41	1.60	1.01	0.24	0.49	2.05
20010051	Pelican-5	2640	clyst (cutt)	7.37	0.73	5.06	1.67	0.01	0.69	7.7	26.5	65.8	0.22	0.93	0.86	0.13	0.25	0.43
20010052	Pelican-5	2791.9	coal (core)	16.31	1.88	37.52	0.79	0.01	0.38	10.0	22.5	67.5	0.14	0.99	0.80	0.07	0.28	0.22
20010053	Pelican-5	2792.1	clyst (core)	4.72	0.30	8.03	0.70	0.02	0.26	22.1	22.6	55.2	0.18	0.63	1.03	0.15	0.43	0.50
20010054	Pelican-5	3015	clyst (cutt)	2.28	0.12	4.90	0.74	0.02	0.28	20.2	27.5	52.3	0.17	5.20	0.18	0.39	0.25	0.48
20010384	Pelican-5	3063	coal (cutt)	4.47	0.40	5.92	0.63	0.02	0.23	12.4	30.9	56.7	0.14	1.52	0.90	0.28	0.25	0.59
20010385	Pelican-5	3162	coal (cutt)	9.06	0.43	14.46	0.58	0.04	0.30	11.1	25.9	63.0	0.17	2.03	0.59	0.29	0.27	1.96
20010055	Pelican-5	3399	clyst (cutt)	1.66	0.44	2.07	0.60	0.02	0.34	18.3	29.7	52.0	0.23	3.87	0.46	0.38	0.29	1.10

19T/23T = ratio of C19 tricyclic to C23 tricyclic
24T/23T = ratio of C24 tricyclic to C23 tricyclic
Tet/23T = ratio of C24 tetracyclic to C23 tricyclic
29H/30H = ratio of C29 abhopane to C30 abhopane
Ol/30H = ratio of oleanane to C30 abhopane
31R/30H = ratio of C31 abhopane 22R to C30 abhopane
%27 = percentage of C27 abb 20S to sum C27, C28, C29 abb 20S steranes
%28 = percentage of C28 abb 20S to sum C27, C28, C29 abb 20S steranes
%29 = percentage of C29 abb 20S to sum C27, C28, C29 abb 20S steranes
kaur/phyll = a-kaurane/b-phyllocladane
ipim/phyll - *iso*-pimarane/b-phyllocladane
19-ipim/ipim - 19-nor-pimarane/*iso*-pimarane
labd/phyll - b-labdane/b-phyllocladane
fich/phyll = fichtilite/b-phyllocladane
bery/phyll = beryene/b-phyllocladane

Table 5.3 Molecular and carbon isotopic composition of gases from the Bass Basin.

Well Name	White Ibis -1	White Ibis -1	Yolla -2	Yolla -2
Geoscience Australia No.	**20009241**	**20009247**	**20009248**	**20009250**
Sample Depth - Top (m)	2015.2	2048.5	2802.0	2815.0
Molecular composition (mole %)				
CH4	72.33	78.57	72.07	20.42
C2	5.96	6.05	6.52	17.46
C3	3.61	2.34	2.55	6.95
i-C4	1.63	0.70	0.39	1.24
C4	1.38	0.76	0.63	2.09
i-C5	0.97	0.36	0.17	0.54
C5	0.69	0.21	0.17	0.66
C6+	3.30	0.56	0.49	1.18
CO2	8.16	8.13	16.72	48.50
N2	1.97	2.32	0.30	0.92
Carbon isotopic composition ($^{o}/_{oo}$ PDB)				
CH4	-37.20	-37.02	-36.85	-36.86
C2	-27.21	-27.03	-29.16	-29.03
C3	-26.73	-26.27	-27.95	-27.86
i-C4	-27.71	-26.99	-28.17	-28.03
C4	-26.13	-25.70	-27.20	-27.02
i-C5	-26.34	-25.47	-27.19	-27.11
C5	-25.98	-25.17	-26.75	-26.74
CO2	-4.36	-4.83	-5.40	-6.86

Figure 5.1 Age (Ma) plot of total organic matter (S2-TOC) for a) all data, and b) sediments with TOC<10%.

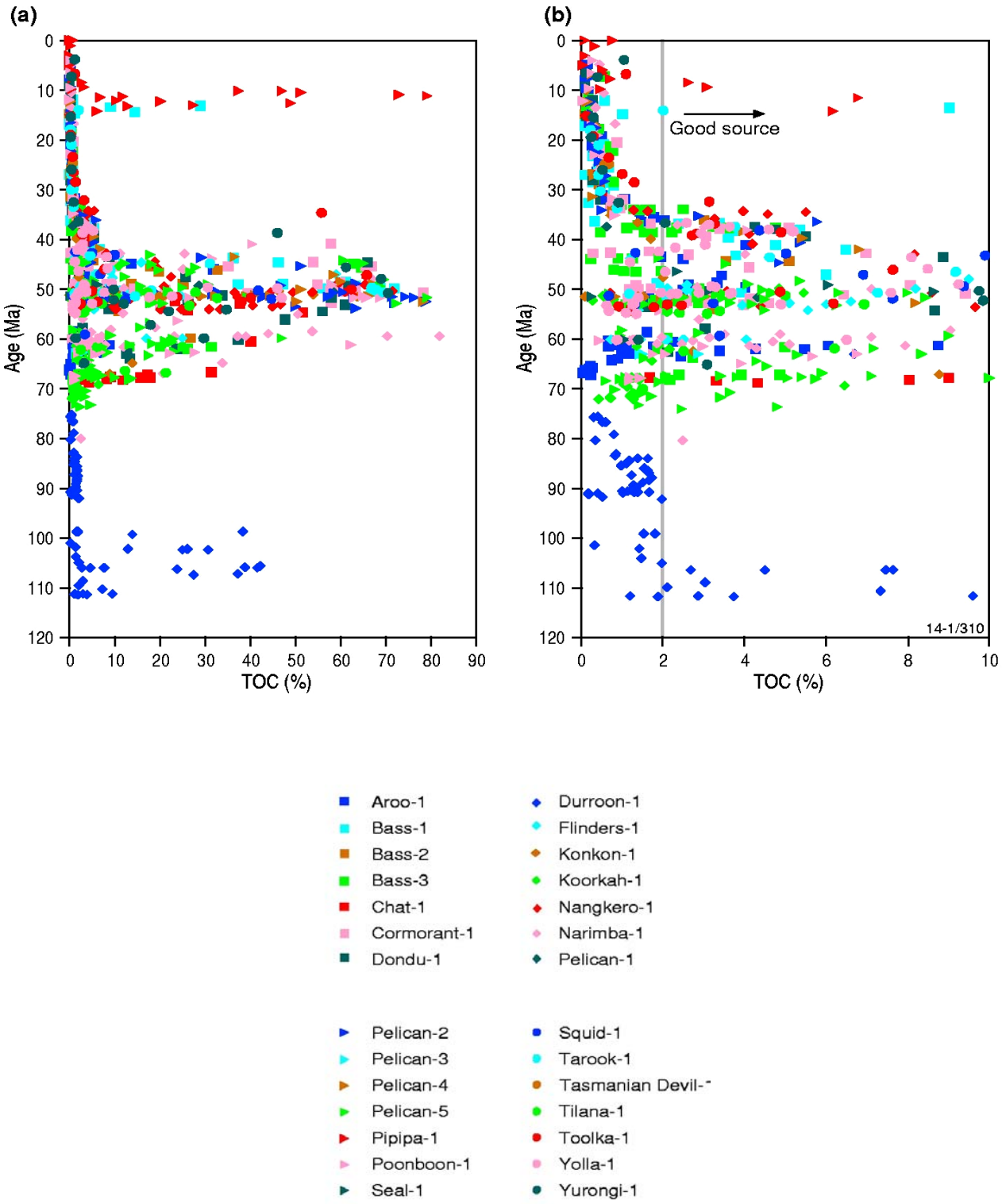


Figure 5.2 Specific age interval (>73 Ma)—S2-TOC plot for a) all data, and b) sediments with TOC<10%.

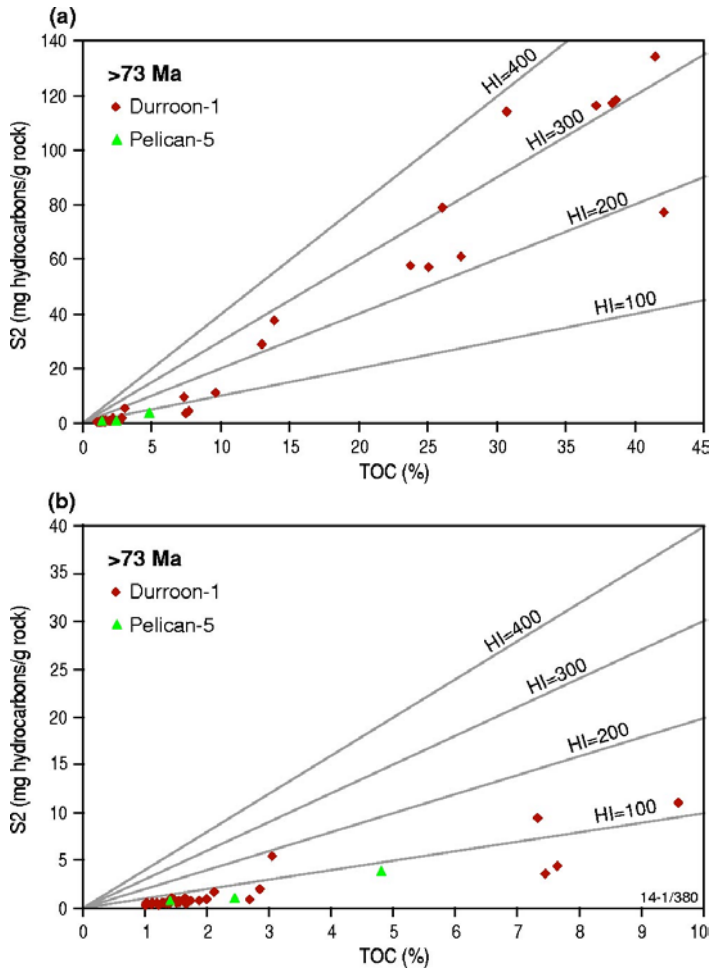


Figure 5.3 Specific age interval (73-65 Ma)—S2-TOC plot for a) all data, and b) sediments with TOC<10%.

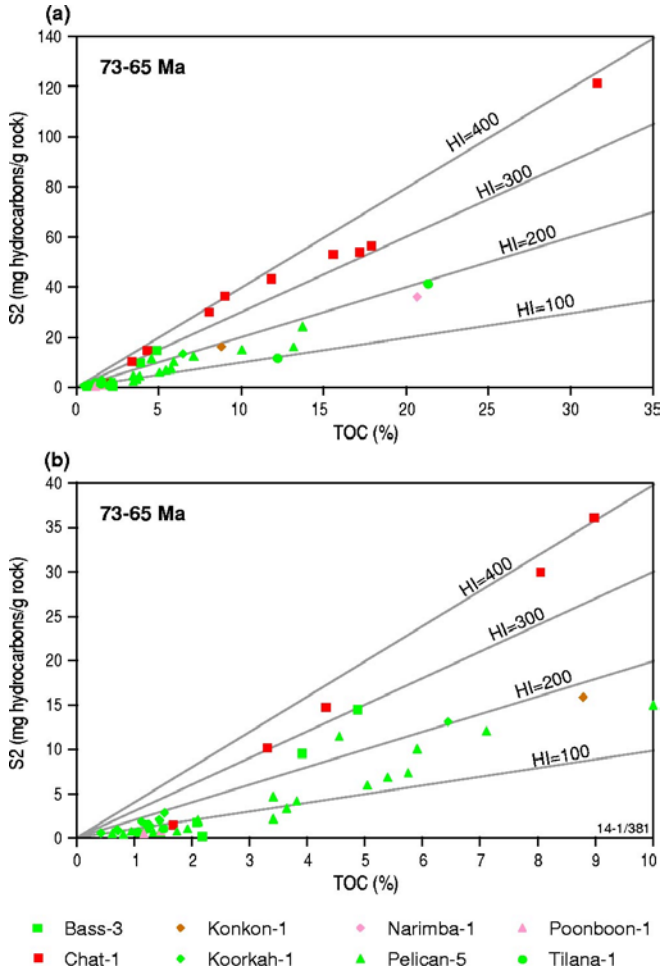


Figure 5.4 Specific age interval (65-53 Ma)—S2-TOC plot for a) all data, and b) sediments with TOC<10%.

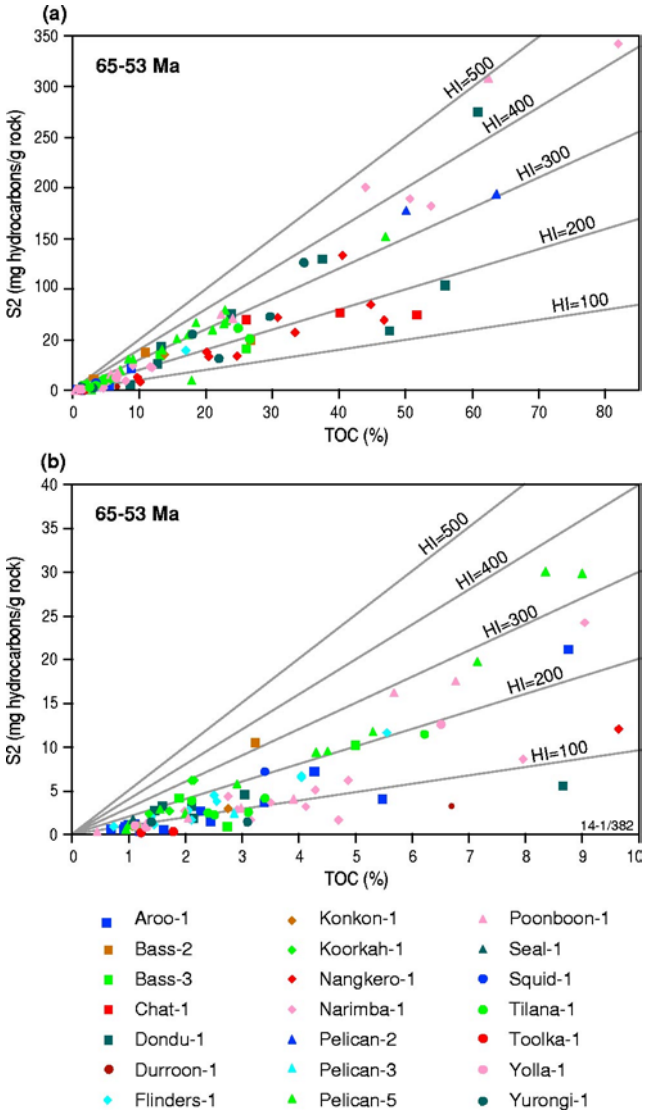


Figure 5.5 Specific age interval (53-50.5 Ma)—S2-TOC plot for a) all data, and b) sediments with TOC<10%.

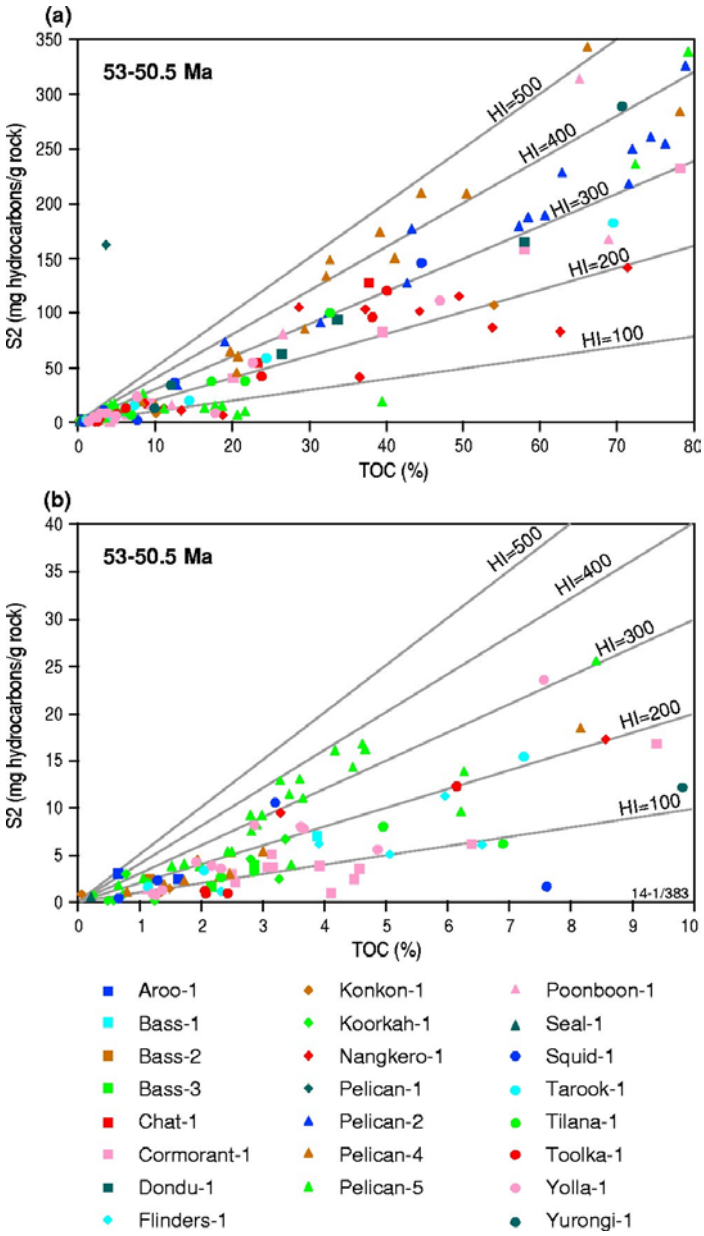


Figure 5.6 Specific age interval (50.5-47.5 Ma)—S2-TOC plot for a) all data, and b) sediments with TOC<10%.

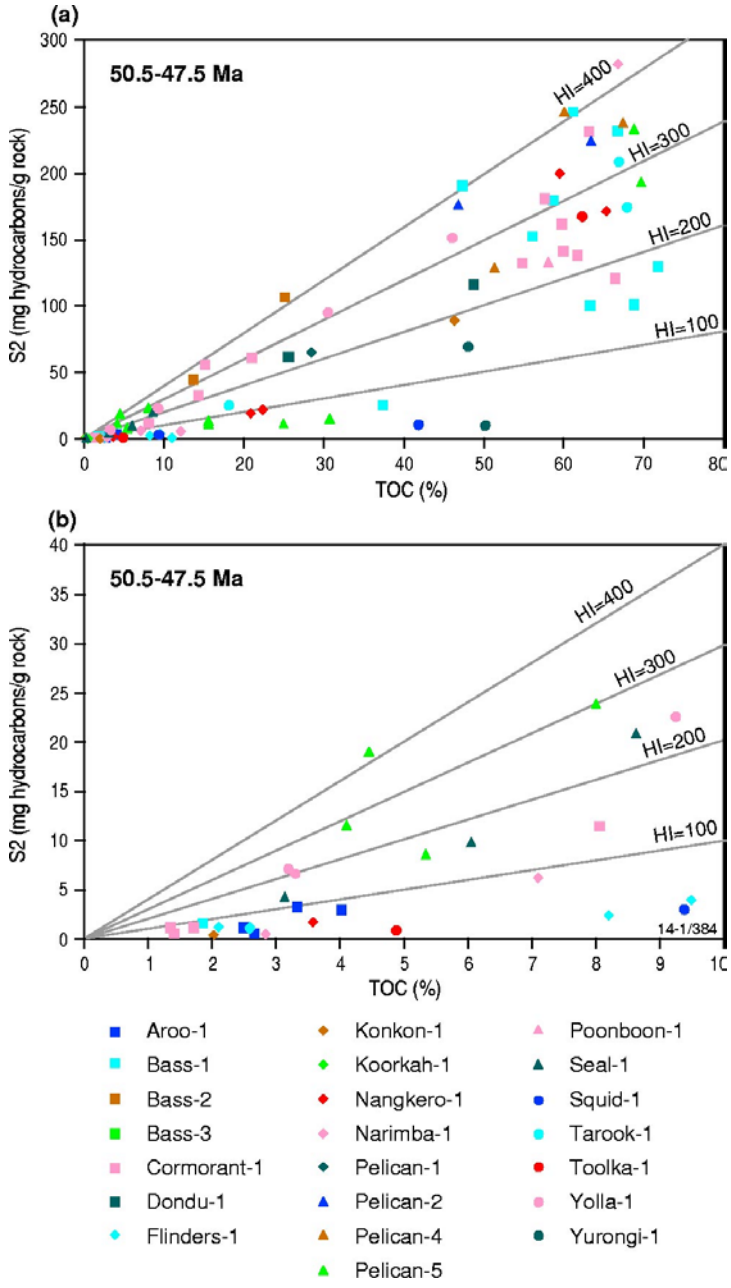


Figure 5.7 Specific age interval (47.5-38 Ma)—S2-TOC plot for a) all data, and b) sediments with TOC<10%.

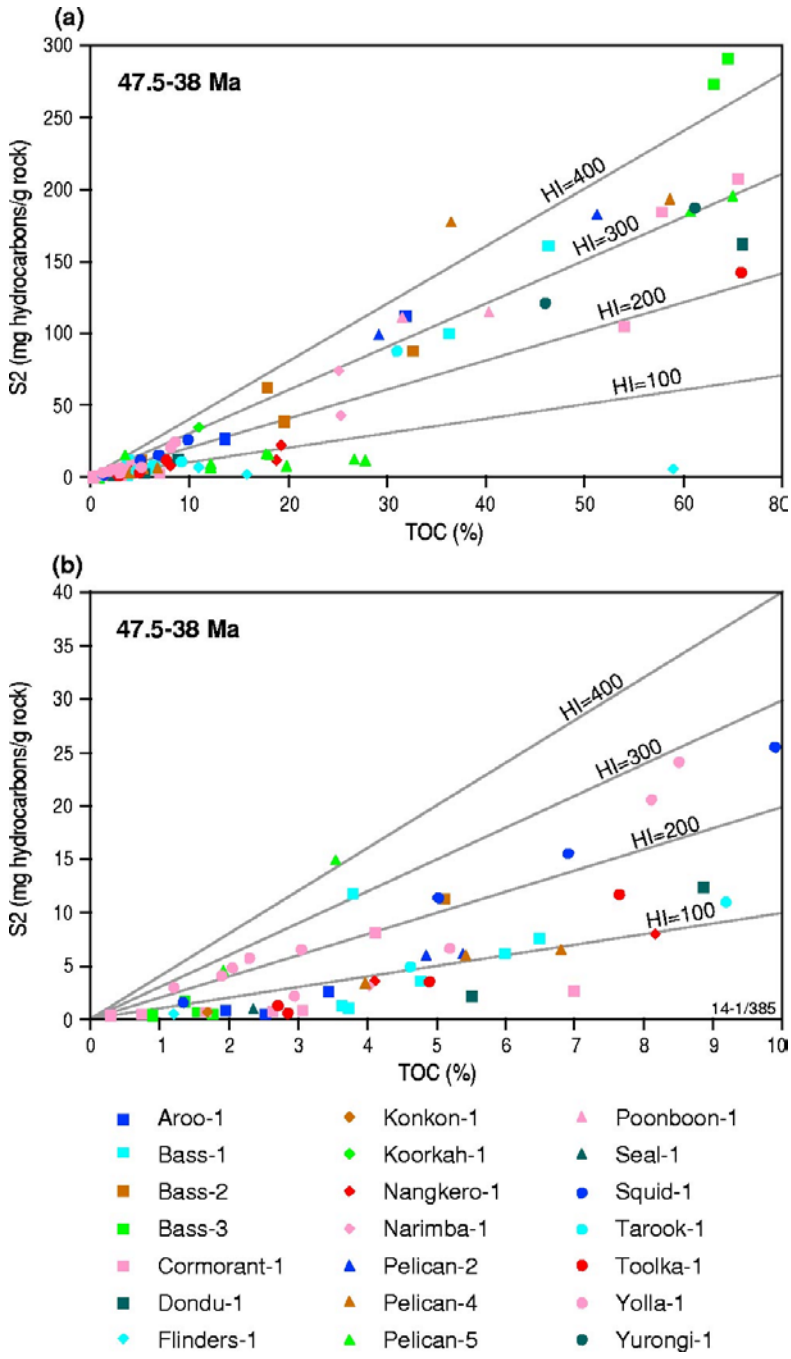


Figure 5.8 Specific age interval (38-35 Ma)—S2-TOC plot for data.

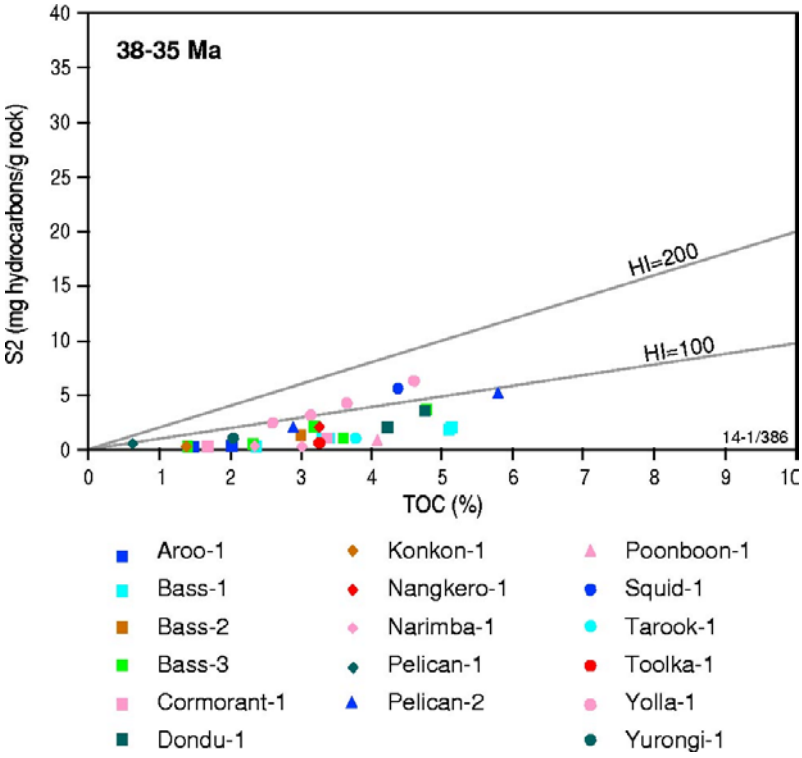


Figure 5.9 Specific age interval (<35 Ma)—S2-TOC plot for a) all data, and b) sediments with TOC<10%.

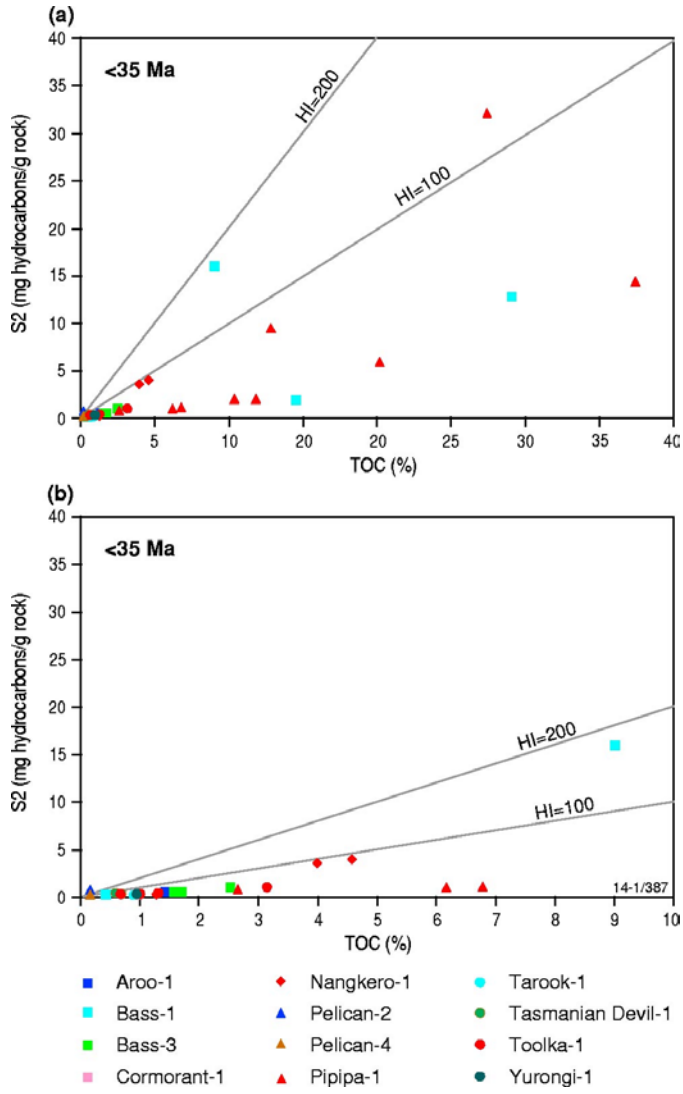


Figure 5.10 VIRF measurements on Pelican-5 sediment showing the identification of perhydrous vitrinite, normal vitrinite and inertinite.

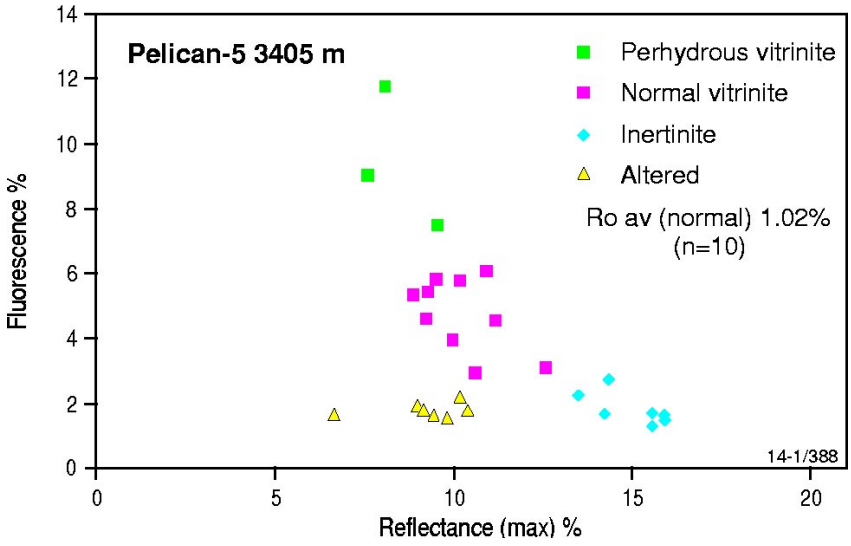


Figure 5.11 Plot of vitrinite reflectance versus depth for sediments from Cormorant-1 and Pelican-5.

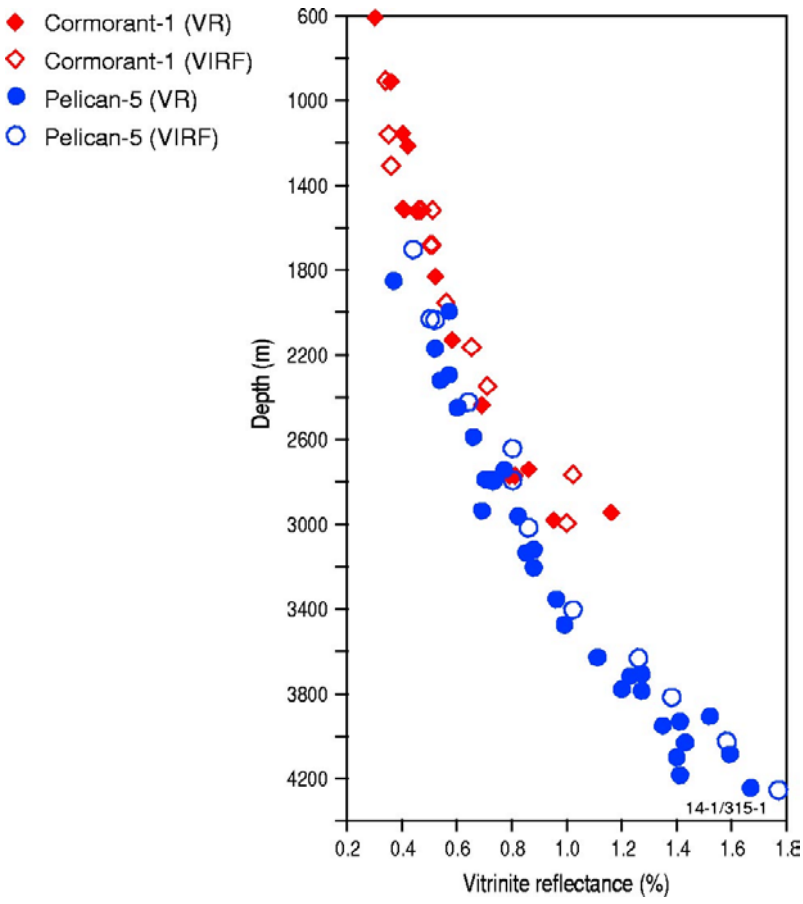


Figure 5.12 Plot of vitrinite reflectance versus age for wells in the Bass Basin.

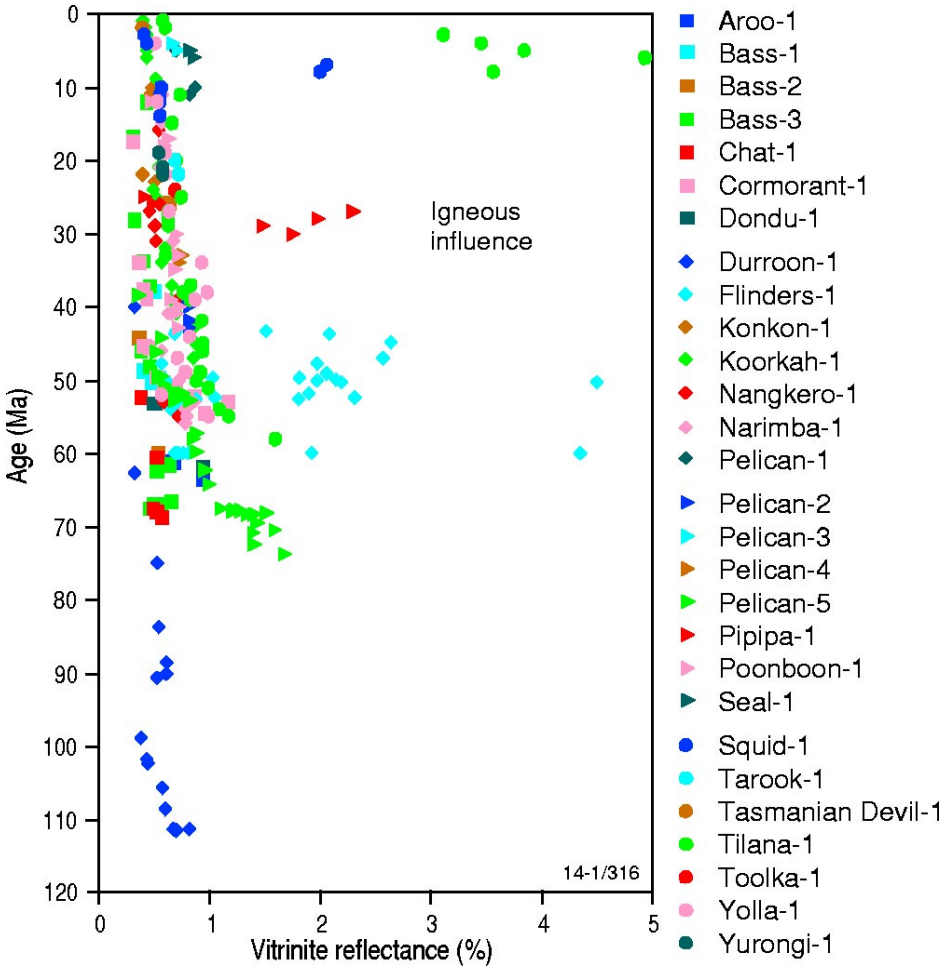


Figure 5.13 Plot of vitrinite reflectance versus depth for wells in the Bass Basin.

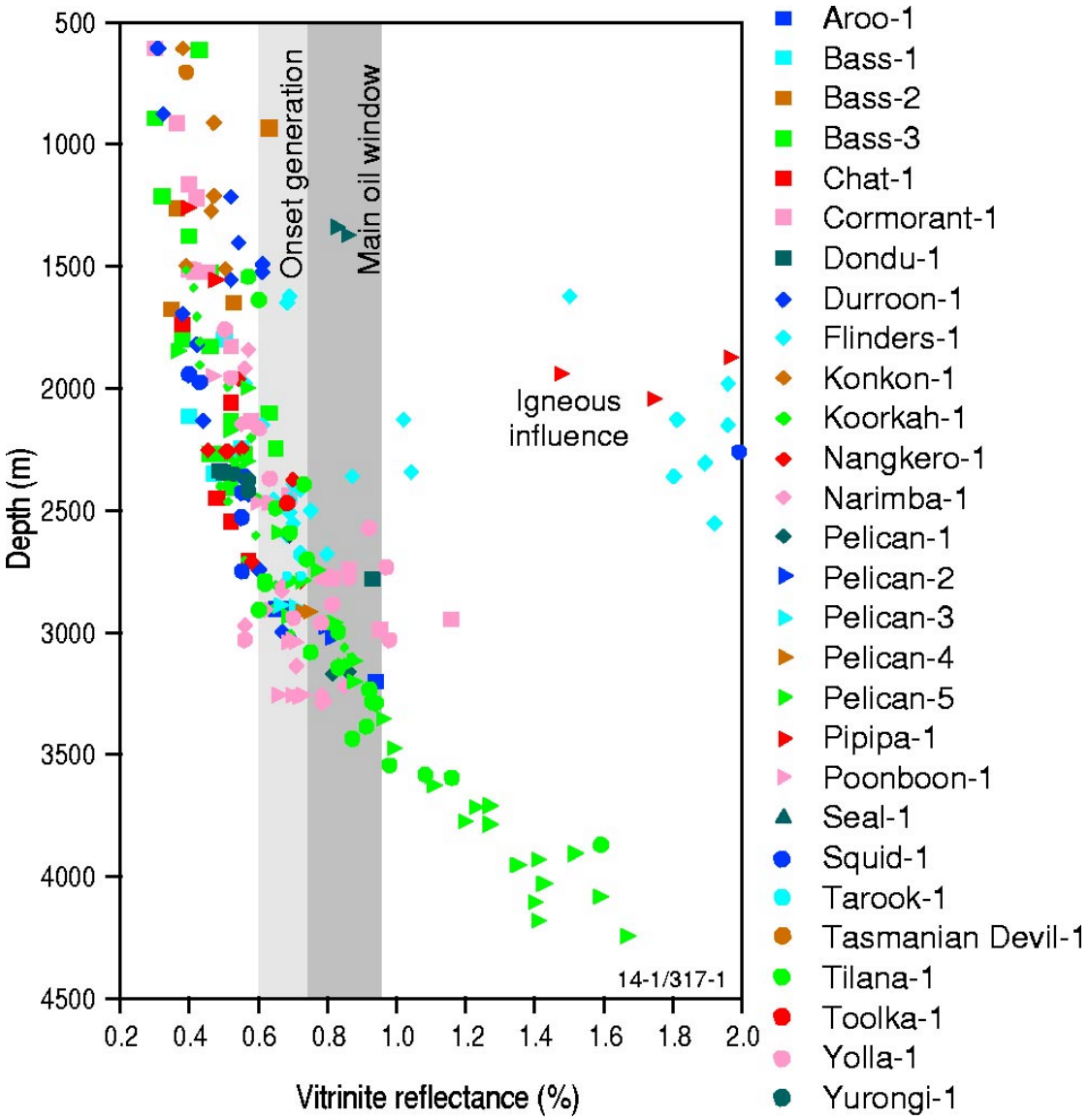


Figure 5.14 Depth plot of Hydrogen Index (HI) and Bitumen Index (BI) for low-ash coals in Pelican-5.

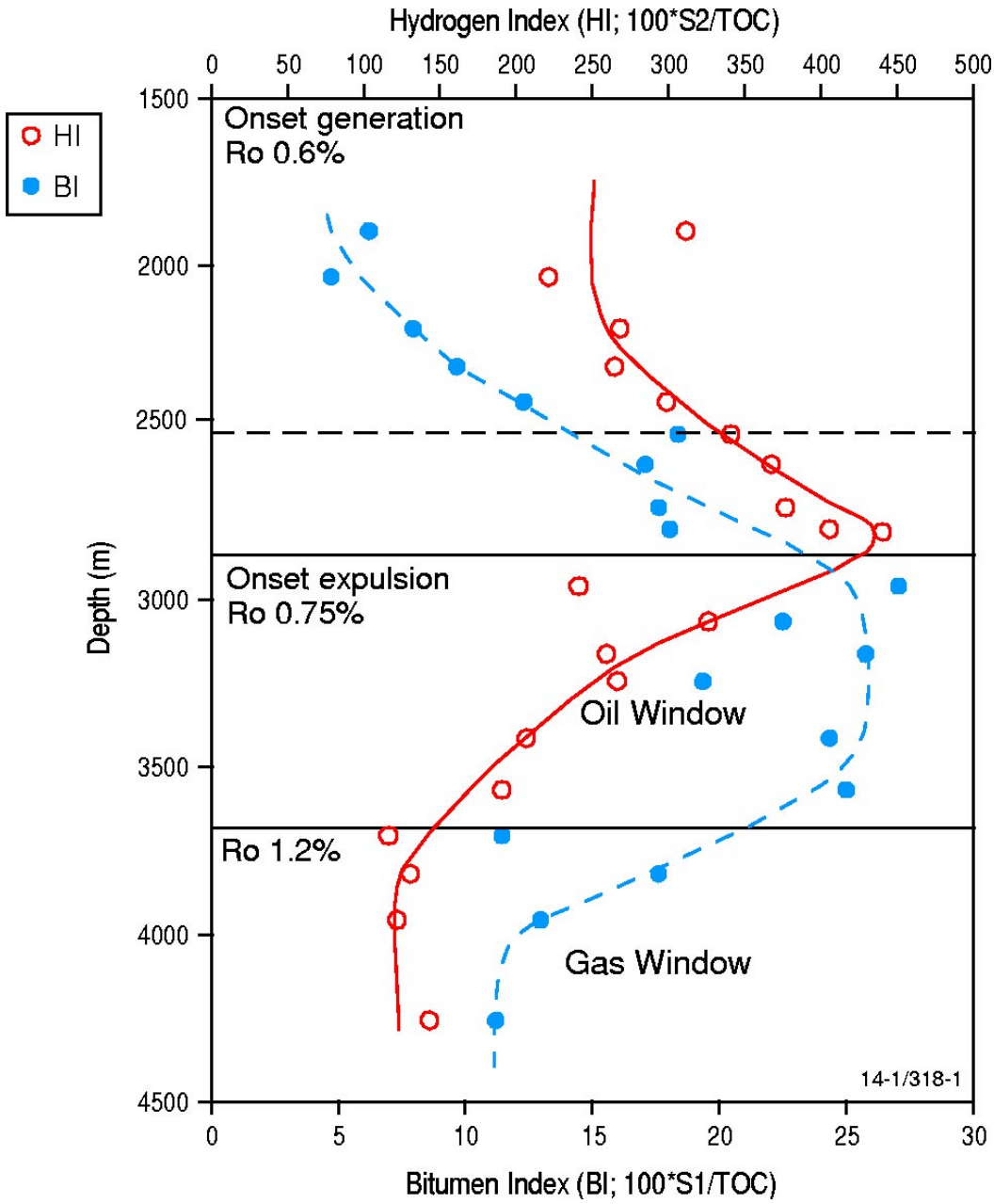


Figure 5.15 Small Angle Neutron Scattering (SANS) results for coals from Pelican-5 showing (a) the calculated pore number density (proportional to the pore size distribution) for three micropore sizes (100Å = 0.01 μm). Note the marked decrease of the pore number density within the depth range 2400 to 2600 m, and (b) the variation of the scattering intensity with depth for mean micropore size 0.025 μm ± 50%.

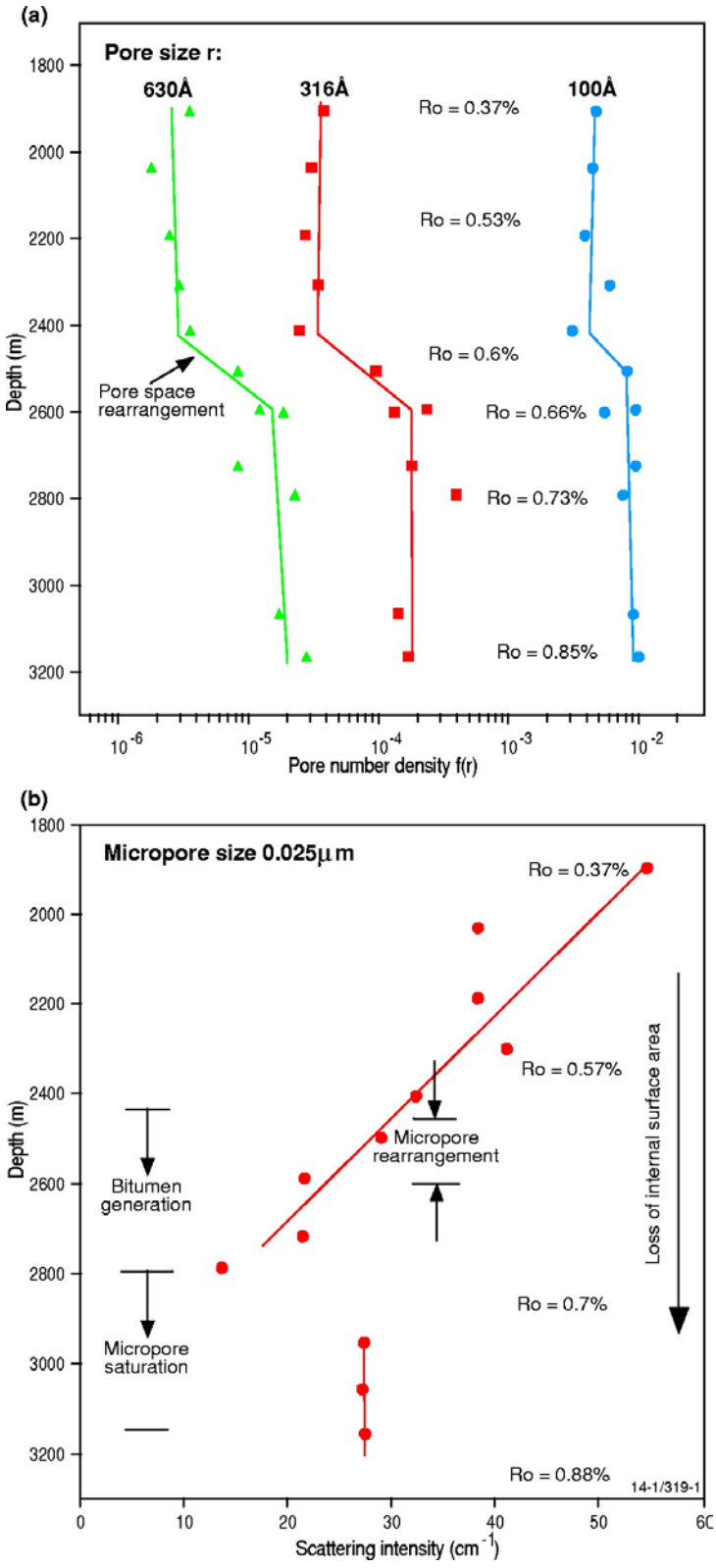


Figure 5.16 Plot of temperature (°C) versus kerogen transformation ratio (TR) and calculated vitrinite reflectance (VR) for a heating rate of 1 °C/Ma.

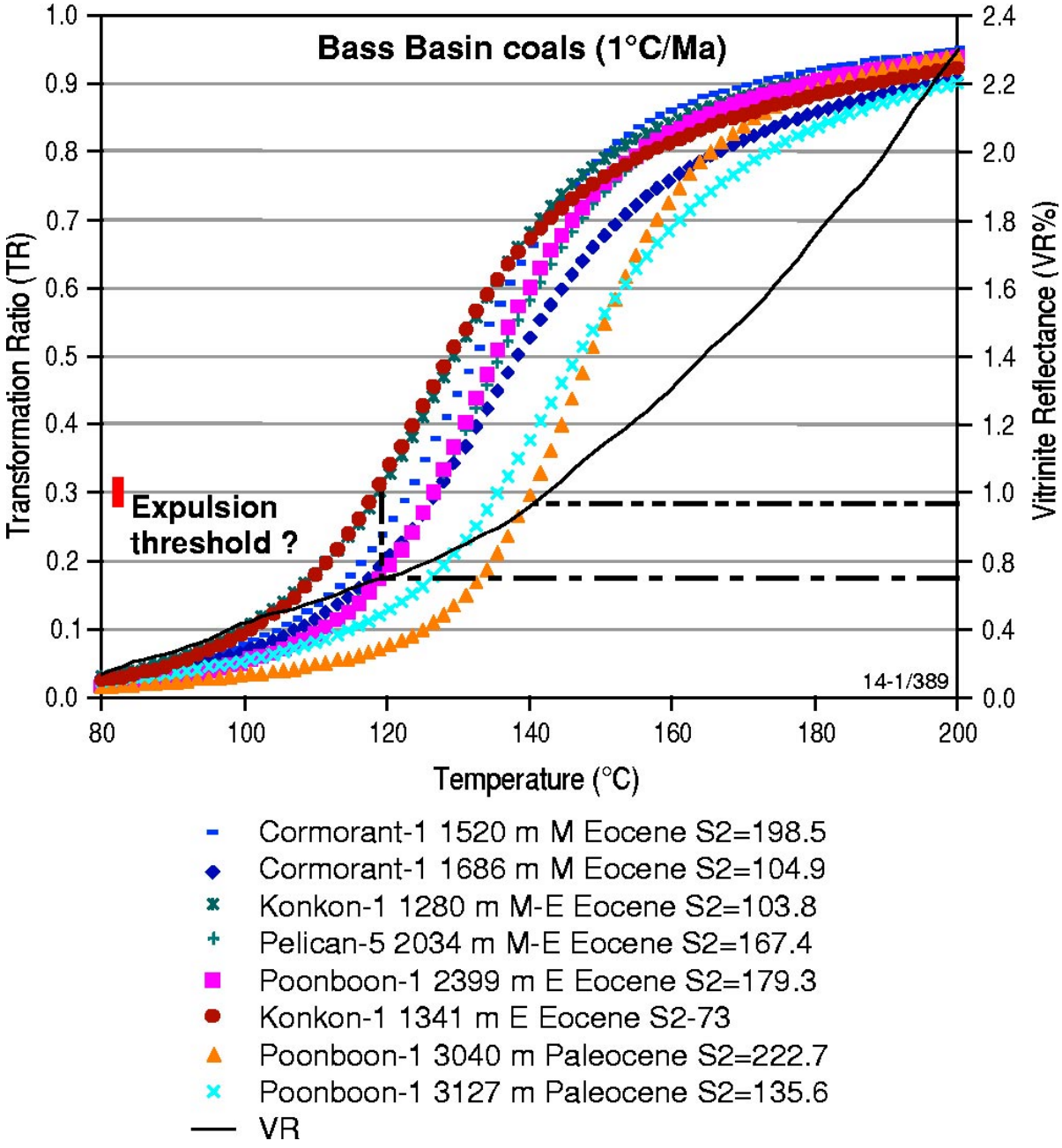


Figure 5.17 Dendrograms resulting from hierarchical cluster analysis using samples and the variables in Table 5.1. Oils from the Bass Basin include those from Cormorant-1, Pelican-1 and –2, and Yolla-1, oils from the Gippsland Basin are represented by Bream, Cobia, Dolphin, Fortescue, Halibut, Kingfish, Kipper, Luderick, Mackeral, Marlin, Perch, Snapper, Sunfish, Tarwhine, Tuna and Wirrah (Geoscience Australia and GeoMark Research, 2002), while oils from the Otway Basin include Haselgrove, Haselgrove South, Katnook, Killanoola, Lindon, Nunga Mia, Port Campbell, Redman, Sawpit, Windermere, Wynn (Edwards et al., 1999; Geoscience Australia and GeoMark Research, 2002). Note: A = Austral Petroleum Supersystem; A1, A2, A3 petroleum systems; A1- F2 freshwater lacustrine facies; A1- F3 = fluvio-lacustrine facies.

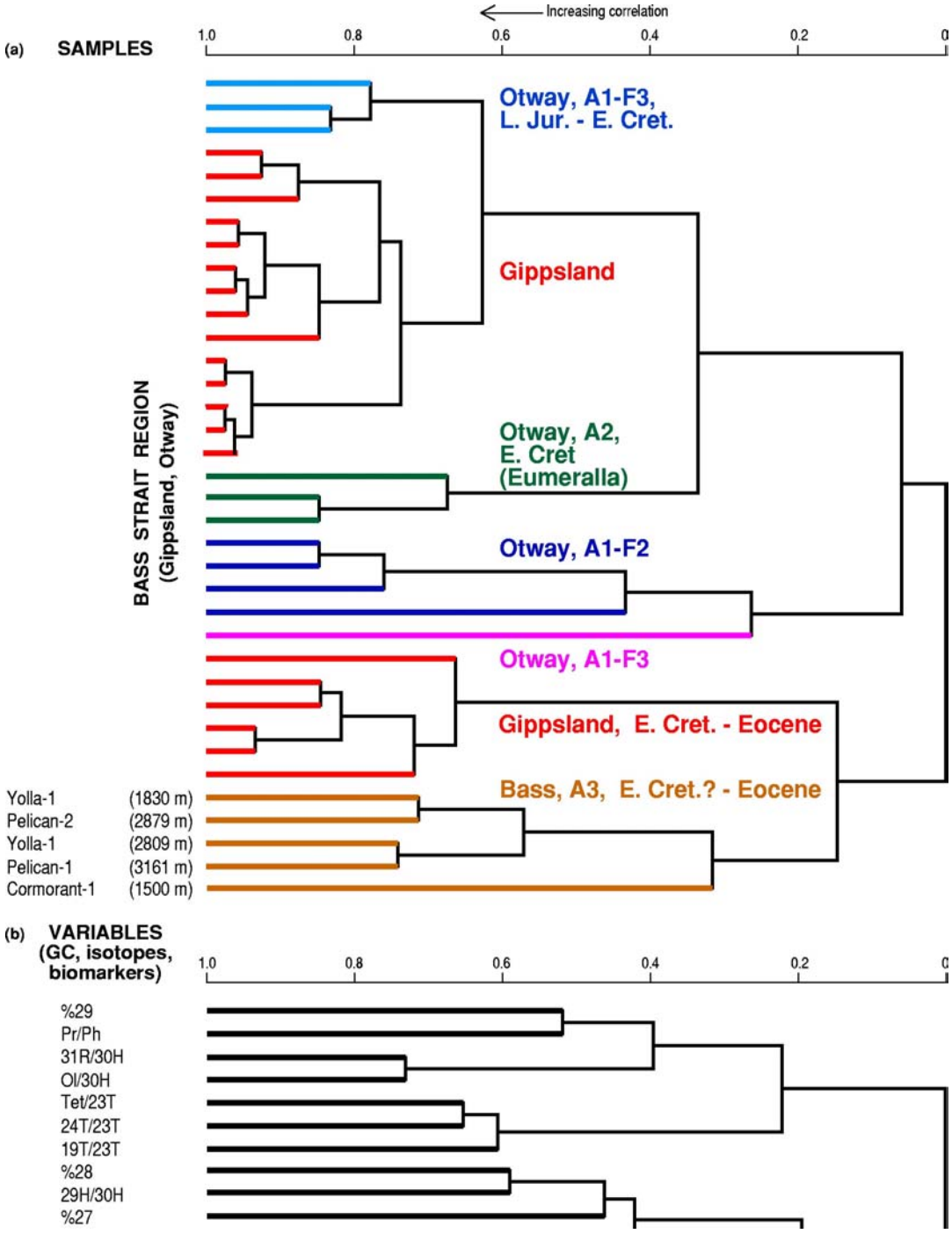


Figure 5.18 Dendrograms resulting from hierarchical cluster analysis using the samples and variables in Table 5.1. The potential source rocks are coals and claystones from Cormorant-1 and Pelican-5. Oils from the Bass Basin include those from Cormorant-1, Pelican 1 and –2, and Yolla-1, while oils from the Gippsland Basin are representative of the compositional extremes seen in Gippsland crudes (Geoscience Australia and GeoMark Research, 2002).

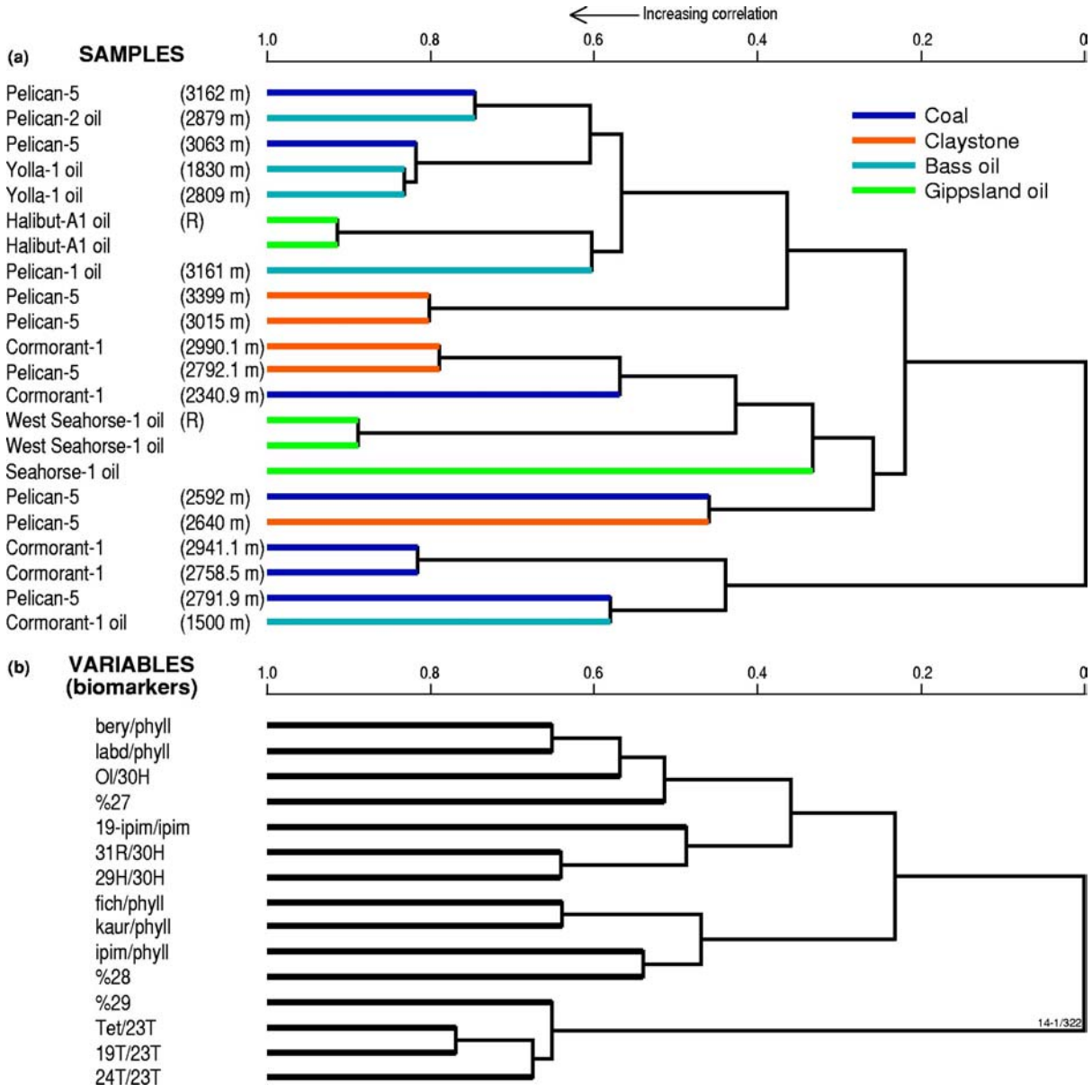


Figure 5.19 Hydrocarbon composition of Bass Basin natural gases expressed as a plot of percentage methane%/(methane% + ethane% + propane% + *iso*- & *n*-butane% + *iso* & *n*-pentane%) versus ethane%/propane% (100 * $\%C_1/\%C_1\text{-}C_5$ vs $\%C_2/\%C_3$). Also plotted are the compositions of gases from the adjacent Gippsland, Otway and other Australian sedimentary basins (Boreham et al., 2001).

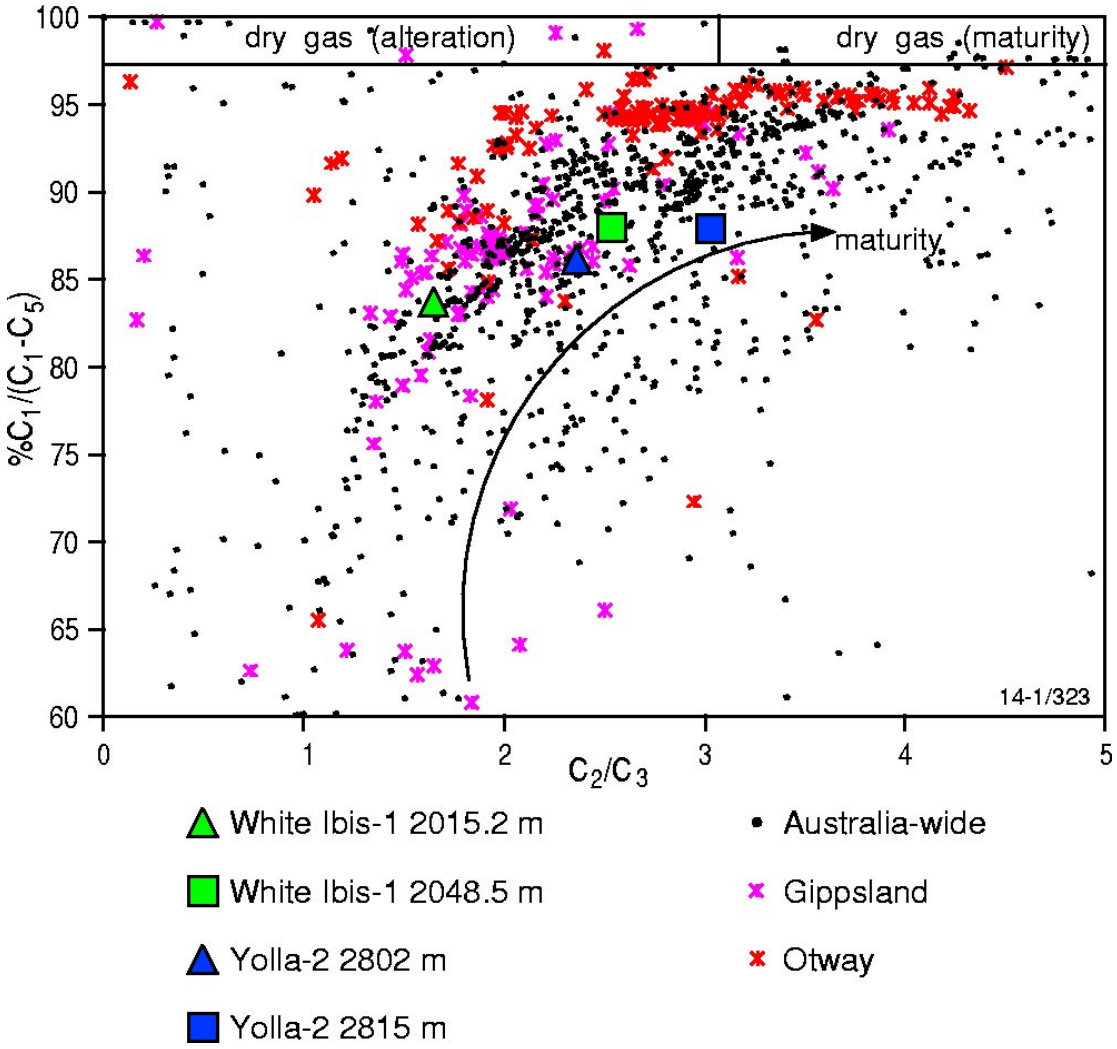


Figure 5.20 Plot of carbon isotopic composition of individual C_1-C_5 gaseous hydrocarbons from the Bass Basin. Also plotted are the carbon isotopic range for unaltered natural gases from Gippsland, Otway and other Australian sedimentary basins (Boreham et al., 2001).

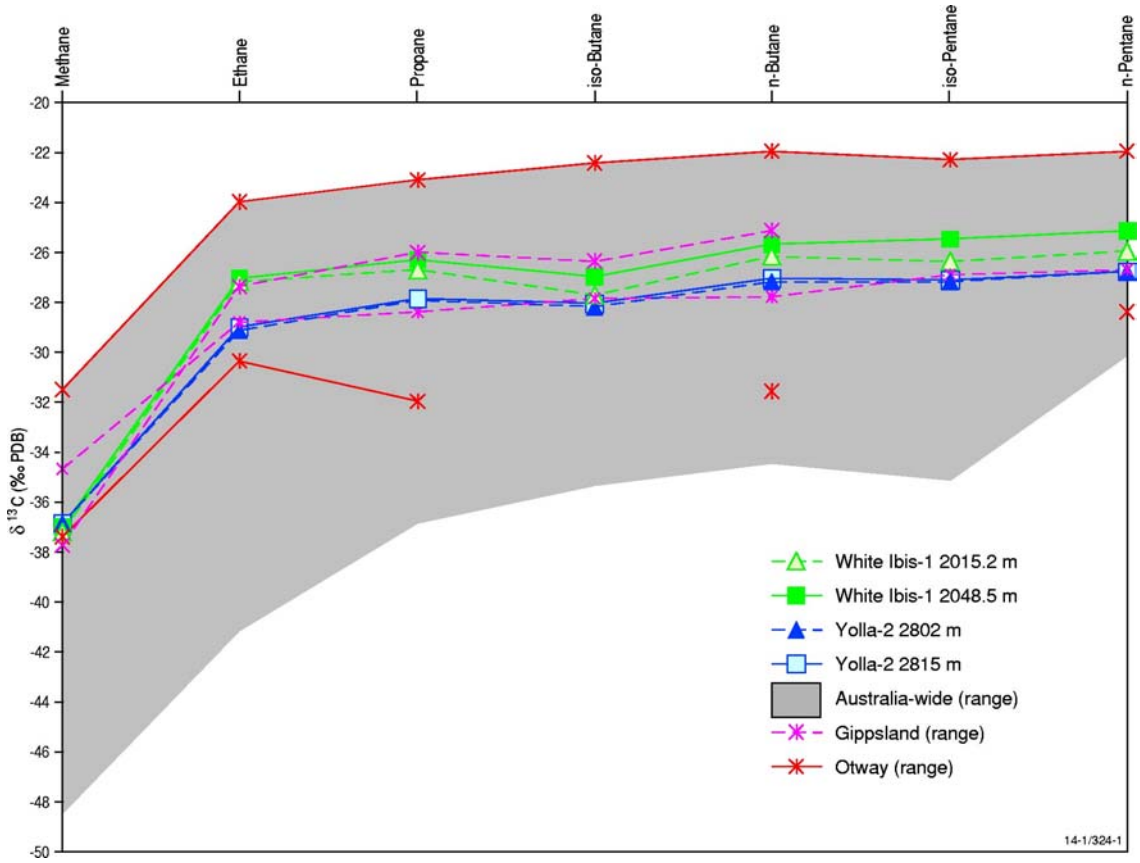


Figure 5.21 Natural gas plot (Chung *et al.*, 1988) for natural gases from the Bass Basin.

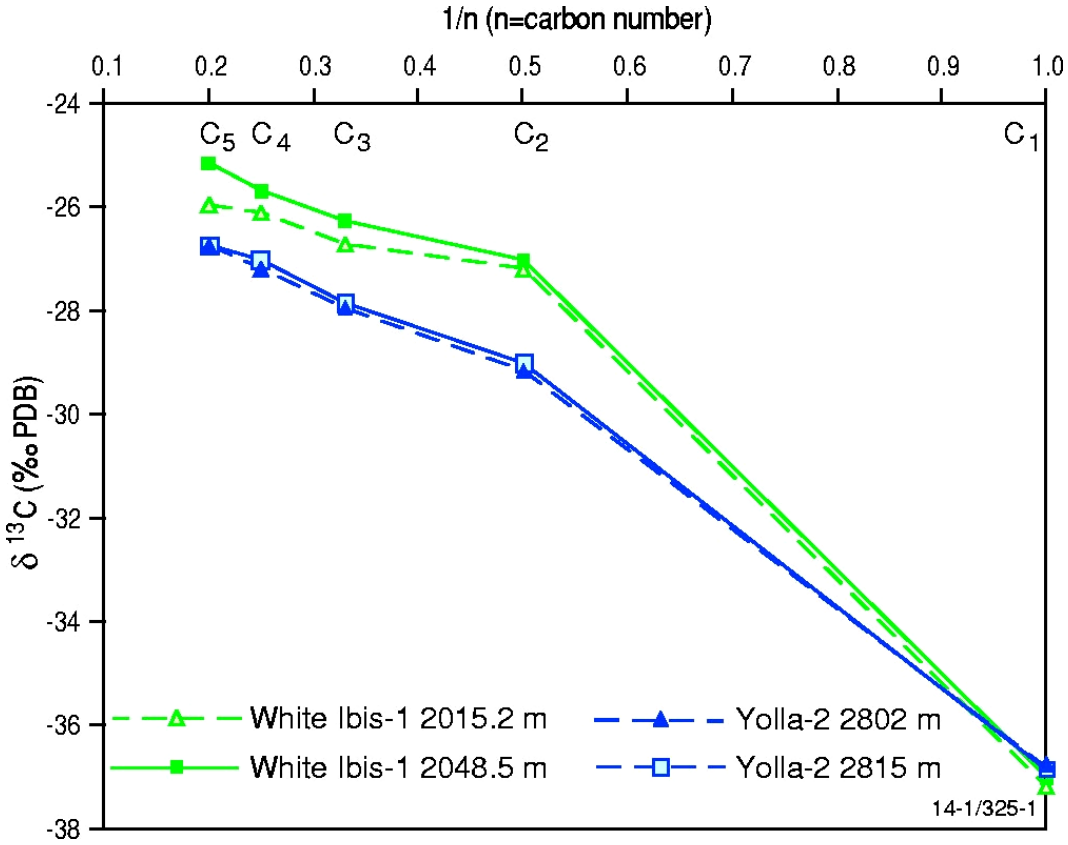


Figure 5.22 Plot of carbon isotopic difference between $\delta^{13}C_{methane}$ and $\delta^{13}C_{ethane}$ versus the carbon isotopic difference between $\delta^{13}C_{ethane}$ and $\delta^{13}C_{propane}$ for natural gases from the Bass Basin. Also plotted are the isotopic differences of gases from Gippsland, Otway and other Australian sedimentary basins (Boreham et al., 2001). Note the predicted evolution of carbon isotopic difference with maturity (numbers refer to Ro %) according to James (1990).

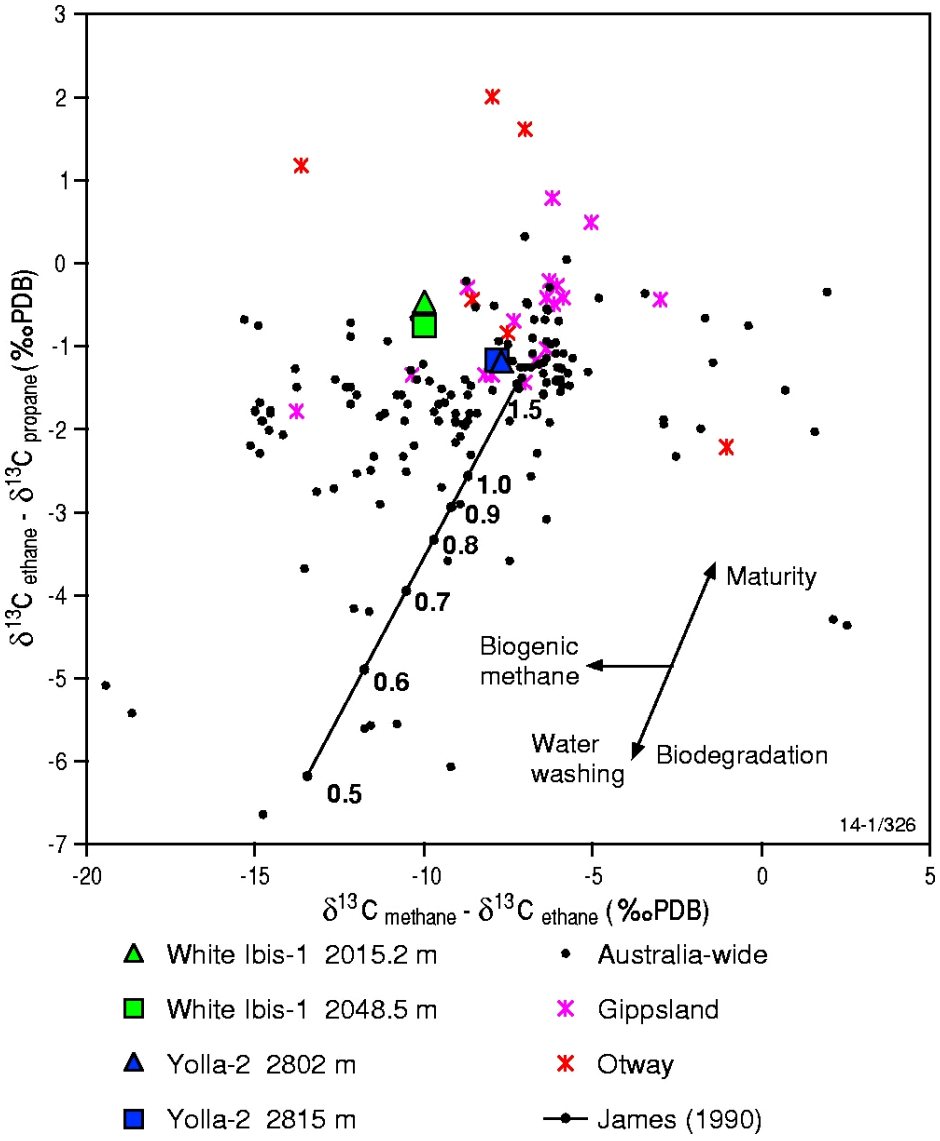


Figure 5.23 Plot of carbon isotopic composition of CO_2 versus molecular percentage of CO_2 for natural gases from the Bass Basin. Also plotted are the corresponding data for gases from Gippsland, Otway and other Australian sedimentary basins (Boreham et al., 2001). Note that the grey-fill depicts the isotopic range of an inorganic source.

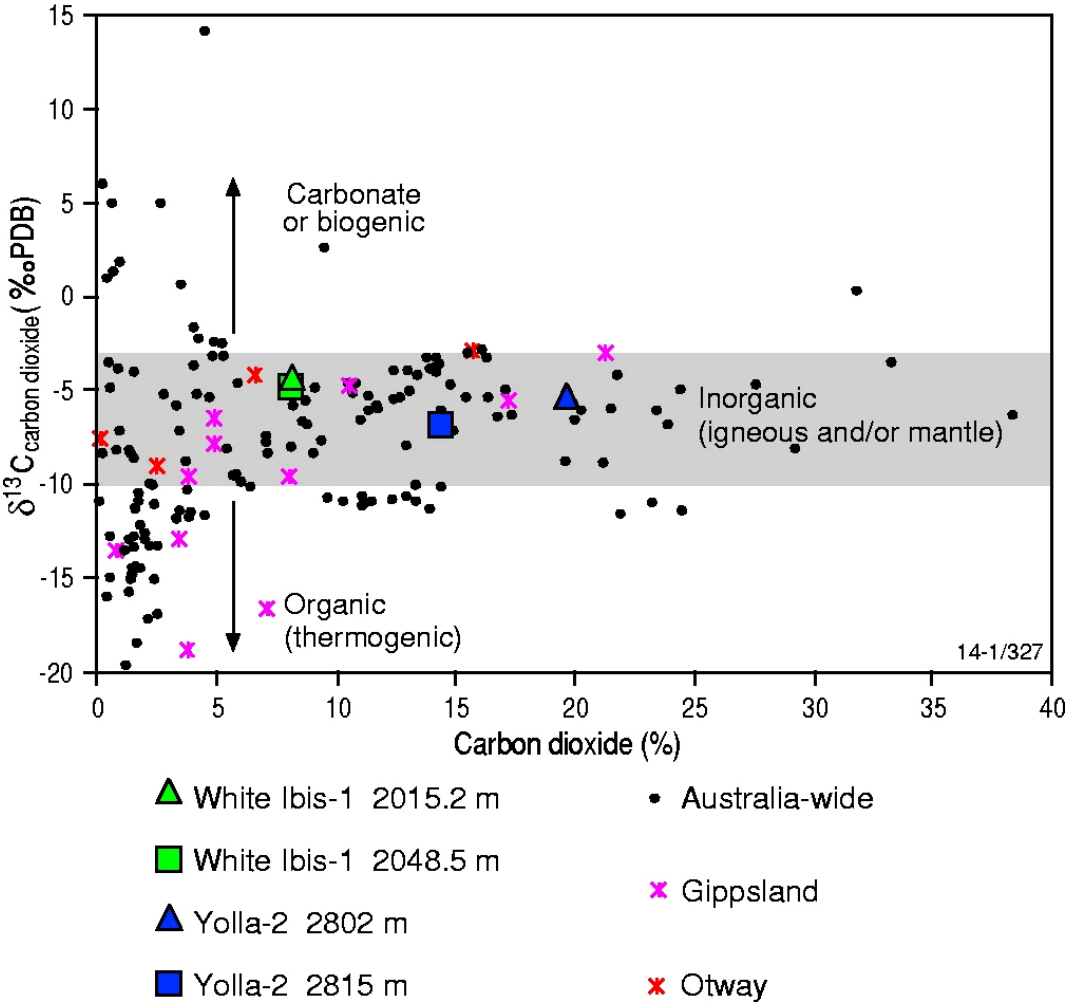
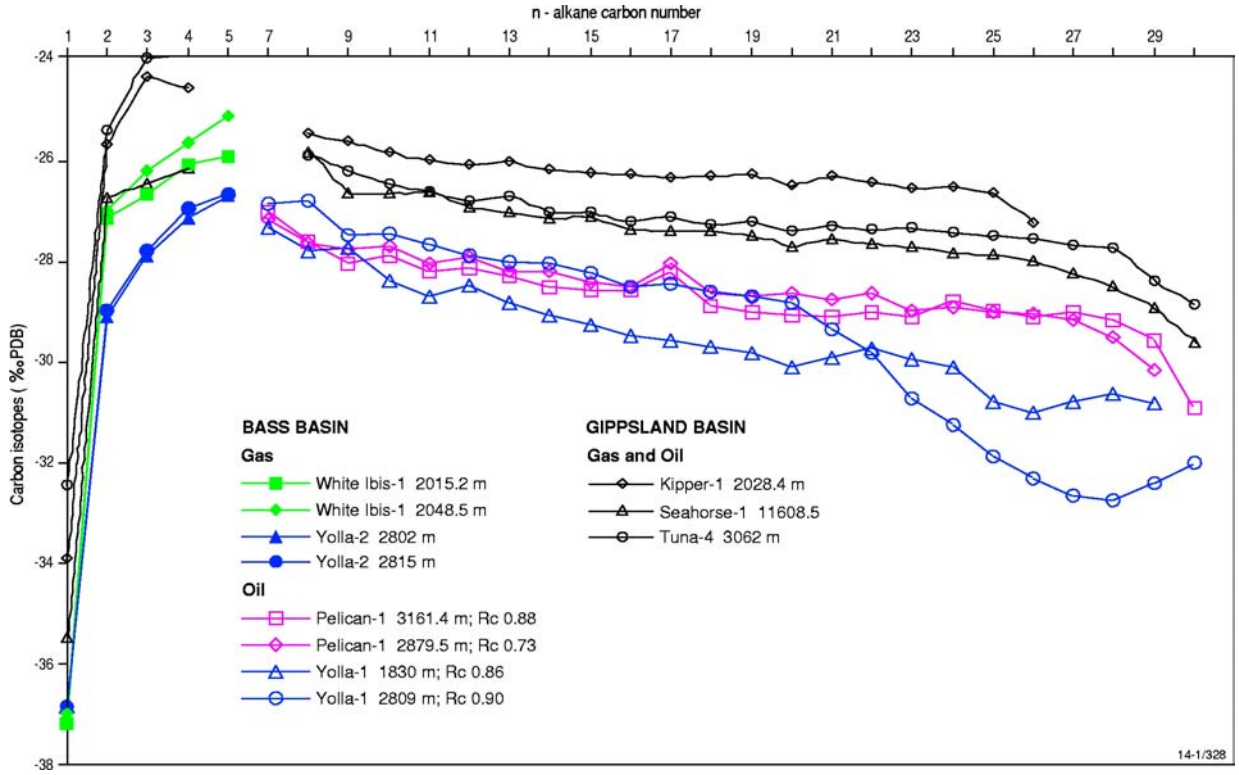


Figure 5.24 Carbon isotopic composition of individual C_1-C_{30} *n*-alkanes for gases and oils from the Bass Basin. Also plotted are representative gases and oils from the Gippsland Basin (Boreham et al., 2001).



6. GEOHISTORY AND MATURITY MODELLING

A. Cummings and P. Tingate, National Centre for Petroleum Geology and Geophysics

6.1 KEY POINTS

- Geothermal gradients within the Bass Basin vary from 3.3°C/100m in the Pelican Trough, to up to 6.5°C/100m at Konkon-1. A broad decrease in geothermal gradient occurs from the northwest of the basin towards the southeast. A similar pattern is reflected in calculated heatflow values.
- 'Default Thermal History' (DTH) models of 13 wells from the Bass Basin indicate that the Late Cretaceous to Recent section is experiencing maximum temperatures today. The majority of wells show a strong correlation between measured and predicted VR profiles.
- DTH models of Koorkah-1, Chat-1, and Durroon-1 display elevated calculated VR profiles with respect to measured VR values, indicating they may have been subjected to a recent heating event (< 2 Ma).
- Burial geohistory diagrams of the wells studied indicate a consistent rate of subsidence and sedimentation from the Late Cretaceous to the present, reflecting the post-rift depositional setting.
- The defined source rocks linked to hydrocarbon accumulations within the Bass Basin (Paleocene to Early Eocene coals) entered the oil generation window just prior to and following deposition of the Demons Bluff shale, and after the major trap forming structural events of the Late Cretaceous and Early Eocene. Paleocene to Early Eocene units continued to pass into the oil expulsion window during and after Miocene structural reactivation events.
- The base of the Pelican-5 well (~ 67 Ma, Maastrichtian) entered the main gas generation window (1.15 – 2.6 %Ro) around the start of the Miocene (~23 Ma). Paleocene to Early Eocene source rock intervals have not entered the main gas generation window. However, deeper undrilled sediments of the Durroon Megasequence (Tasman Rift Phase) may have entered the main gas generation window as early as the Paleocene.

6.2 INTRODUCTION

Successful drilling within the Bass Basin has shown that effective petroleum systems have been active within the region. Geochemical analyses of oils indicate they were sourced predominantly from Paleocene to Early Eocene coals, while gaseous hydrocarbons show a similar source to oils but were generated over a wider maturity range (Chapter 5; Boreham et al., 2003). The aim of this study was to examine thermal and maturation history throughout the Bass Basin in order to constrain the timing of hydrocarbon generation and expulsion. This study draws from the preliminary results of a broader PhD project on the Bass Basin (A. Cummings, in prep.). Key questions that need to be addressed in order to better understand petroleum migration within the Bass Basin include:

- What are the present day thermal conditions within the basin?

- What can we tell of past thermal conditions through the use of palaeothermometers?
- What is the timing of hydrocarbon generation and expulsion from the defined source rock units relative to deposition of the regional seal; and,
- How has Cainozoic structural reactivation within the region affected the distribution of hydrocarbons?
-

This chapter presents the results of 1-D thermal maturation modelling of thirteen key wells and four synthetic well sections throughout the Bass Basin. Modelling was carried out using the 1-D basin modelling software package BasinMod^{TM} (Version 4.2, Platte River Associates). The thirteen wells were modelled using a "Default Thermal History" (DTH) based on the preserved stratigraphy and constant temperature conditions through time (based on present). Using the calculated maturity profiles for the 13 wells, the distribution and timing of hydrocarbon generation throughout the basin was examined. Four pseudowell sections were constructed from detailed seismic mapping of key basin depocentres. The pseudowells were used to examine the subsidence and maturation history through deeper, undrilled sections within the Bass Basin. An investigation of palaeoheatflow was undertaken in the Durroon-1 well, the results of which were applied to the pseudowell sections. Maturity windows and kinetic parameters used were those defined specifically for the Bass Basin by Geoscience Australia (Chapter 5; Boreham et al., 2003).

6.3 PREVIOUS STUDIES

Detailed investigation into the burial and thermal geohistory of the Bass Basin was first undertaken in the early 1980s with the advent of basin modelling computer software (Deighton, 1981; Nicholas et al., 1981; Middleton, 1982). Deighton (1981) noted that prime exploration targets for mature source rock units were Early Eocene and older sequences of the Eastern View Coal Measures (EVCM). It was also shown that many wells drilled within the basin terminated above or just within the predicted maturity zone. Etheridge et al. (1984, 1985) analysed a synthetic well section through the central region of the basin (close to Bass-1), concluding that late Cretaceous and Paleocene source rocks became mature for oil (VR = 0.6%) towards the end of the Oligocene. Williamson and Pigram (1986) completed thermal maturity analysis on 16 wells throughout the Bass Basin and proposed that the Upper Cretaceous EVCM has been mature since Late Eocene times (40 Ma), after the major period of structural activity within the basin had ceased. Russell and Baillie (1989) presented a detailed analysis of present-day thermal conditions, testing the use of vitrinite reflectance as an absolute palaeogeothermometer. They concluded that many of the well sections within the basin have undergone significant cooling of the sedimentary sequence below maximum palaeotemperature (between 40 and 80^{o}C). A review of petroleum prospectivity within the Bass Basin (Miyazaki, 1993) provides an excellent compilation and overview of open file data acquired up until the early 1990s. SAGASCO (Knowles et al., 1994) undertook detailed thermal maturity modelling of Flinders-1, Pelican-5 and a synthetic well within the Pelican Trough. They also investigated the effects of localised Tertiary igneous activity on the vitrinite reflectance profile shown in the Flinders-1 well.

6.4 DATABASE AND METHODS

Data used in this report were compiled from various open file sources. Data for geohistory input, including stratigraphic and lithological information, bottom hole temperature (BHT) and drill stem test (DST) temperature data, measured vitrinite reflectance and other thermal history parameters were collected from open file well completion reports (WCRs), and government reports. Detailed stratigraphic and structural mapping of open file seismic data was incorporated into the study, to constrain the position of unconformities within the Tertiary sequence and to estimate the thickness of eroded sections. Localised source rock kinetic and maturity data, defined specifically for this study of the Bass Basin, was provided by Geoscience Australia (Chapter 5; Boreham et al., 2003). The zone of initial oil generation was taken as 0.65 to 0.75 % Ro, oil expulsion 0.75 to 1.2 % Ro and main gas generation 1.2 to 2.6 % Ro.

Vitrinite reflectance data were compiled for 28 wells throughout the Bass Basin. In addition, a further 27 samples from 11 wells (core and cuttings) were collected from Geoscience Australia's core and cuttings repository and submitted for vitrinite reflectance analysis by Keiraville Konsultants Pty Ltd (Appendix I; Cook, 2002). Sampling was targeted where coal and shale sequences were indicated on geophysical logs and where previous sampling for vitrinite reflectance was lacking. Apatite fission track analysis (AFTA) data the Durroon-1 well (Duddy 1992) was used to investigate palaeoheatflow.

Measured downhole temperatures provide valuable data for the estimation of present-day temperature profiles within wells. An accurate estimation of *in situ* formation temperature is essential for rigorous thermal history calibration and maturity modelling (Waples, 1998). Due to the cooling effects of mud circulation while drilling, log derived temperatures must always be corrected (increased) to approximate true formation temperatures. Unfortunately, within the Bass Basin the quality of subsurface temperature data is highly variable and in many cases bottom hole temperature (BHT) data have not been recorded in sufficient detail for thorough analysis (BHT uncorrected data, Appendix J). Russell and Baillie (1989) undertook a detailed investigation into the correction of BHT data from Bass Basin wells using a number of published techniques. BHTs were re-corrected as part of this study using a recent correction technique (Waples and Ramly, 2001).

The technique described by Waples and Ramly (2001) incorporates a statistically derived empirical correction for single BHT measurements and Horner plot corrected measurements based on subsurface temperature data from the Malay Basin. Where sufficient information was available, including time since circulation data (TSC) and mud circulation times, BHT data from Bass Basin wells were corrected using standard Horner plots (Horner Corrected BHT) and then further corrected using the Waples and Ramly (2001) method. Where mud circulation times were not available, Horner plots were constructed for each well using assumed mud circulation times of 1, 2, 3 and 4 hours. The four corrected temperatures were then averaged (Averaged Horner Corrected BHT). This averaged Horner corrected temperature was then further corrected using the Waples and Ramly (2001) method. For older wells where multiple temperature readings at the same depth were not recorded (e.g. Bass-1, -2, and -3), single BHT data points were corrected using the Waples and Ramly (2001) method (Single Corrected BHT). The temperature correction methods outlined

above have been successful in correcting BHTs to approximate measured DST temperatures throughout the basin (Figure 6.1, Table 6.1).

Estimates of present day seafloor temperatures were calculated based on a present average ocean surface temperature of 15°C that is reduced by 4°C/100m through the water column (Waples et al., 1992). Using this method, it appears that water-sediment interface temperatures vary between 11.6°C (~85m water depth) and 12.6°C (~60m water depth) throughout the basin. Due to the minor variation, an average sea-bottom temperature of 12°C was used for all wells modelled. For modelling, it was assumed that the palaeosurface temperature had remained constant at the estimated present day temperature.

Vitrinite reflectance data are typically presented as either mean random reflectance or mean maximum reflectance. For the purpose of general modelling, both types of reflectance values can be used (Kaiko, 1988; Sweeney and Burnham, 1990). Vitrinite reflectance data from some wells could not be identified as being either mean random or mean maximum reflectance data, as there was insufficient accompanying information. Therefore, the available vitrinite reflectance data was entered as it was reported, without any distinction being made between the two forms of vitrinite reflectance measurements. Kinetic modeling of Pelican-5 well is shown in Appendix K.

One-dimensional thermal maturation modelling of wells within the Bass Basin was carried out using BasinMod™ (Version 4.2, Platte River Associates, Inc) to constrain the timing of hydrocarbon generation and migration. Vitrinite reflectance values were calculated using the Lawrence Livermore National Laboratories (LLNL) kinetics option. Defined stratigraphic units within wells were expressed as a combination of eight pure lithologies, whereby lithology mixes were based on data from cuttings descriptions, composite well logs and log interpretation. BasinMod™ default values were used as inputs for initial porosity, density, grain size, matrix thermal conductivity and matrix thermal capacity. Porosity-depth relationships were modelled using the Middleton (1982) compaction option. Palaeo-water depths used were those outlined by Deighton (1981) or were estimated using foraminiferal data compiled from well completion reports.

6.5 GEOTHERMAL GRADIENTS AND HEATFLOW

The regional variation of geothermal gradients calculated from corrected BHT data is shown in Figure 6.2. Geothermal gradients vary from 3.3°C/100 m at Pelican-2 and Pelican-3, up to 6.5°C/100 m at Konkon-1, with a mean basin gradient of 4.7°C/100 m. A broad decrease in geothermal gradient is observed from the northwestern sector of the basin toward the Durroon Sub-basin. Gradients appear elevated on structural highs and are reduced along the central axis of the basin where the post-rift sequence is thickest.

Heatflow values were calculated at each well location, based on preserved stratigraphy and present-day temperature conditions (Table 1). Simple steady state conduction was assumed where heatflow (Q), is a product of thermal conductivity (k) and geothermal gradient (dT/DZ)(Gretener, 1982).

$$Q = K \times dT/dZ$$

Figure 6.3 shows the areal distribution of calculated heatflow values throughout the basin. It shows a similar trend to the gradient map, where heatflow decreases towards the southeast and along the central axis of the basin.

6.6 THERMAL MODELLING

Thermal modelling was undertaken using the method outlined by Waples et al. (1996), and Duddy and Erout (2001). In order to investigate possible differences in thermal history across the basin, thirteen wells were modelled (Figures 6.4 and 6.5) assuming simple progressive burial through time, non-deposition at all time breaks in stratigraphy and a constant heatflow through time (based upon current temperature conditions). This simple model, termed a 'default thermal history' (DTH), forms a basis from which more detailed investigations into past temperature conditions can be assessed.

Vitrinite reflectance profiles were calculated (Maturity VR LLNL) using a default thermal history scenario and the Falvey and Middleton (1982) compaction option. Calculated VR profiles were then compared to the measured vitrinite reflectance data from each well (Figure 6.5). Comparison of measured and calculated data highlights three situations within DTH models of Bass Basin wells:

- Calculated VR < measured VR
- Calculated VR = measured VR
- Calculated VR > measured VR

It is necessary to investigate the reasons why some data are in accordance with present day thermal conditions and others are not (Figure 6.5).

Where calculated VR < measured VR

A number of wells, including Seal-1, Toolka-1A, Yolla-1, Tilana-1, Nangkero-1, Flinders-1, and Durroon-1, contain intervals where measured VR values are higher than the calculated VR profile. Elevated VR values in Seal-1, Yolla-1, Tilana-1, and Flinders-1 are in close proximity to Miocene igneous intrusions (Figure 6.5) that occur sporadically through the Cainozoic succession in the Bass Basin. Measured VR samples lying proximal to intrusive bodies appear to approach a background reflectance profile, where calculated VR is approximately equal to the measured values.

Elevated VR measurements from samples in both Toolka-1A and Nangkero-1 do not appear to be associated with localised igneous activity. Recent petrographic analysis of cuttings samples from both wells indicates that 'frypanning effects' are a common feature in coal samples collected from cuttings. This may explain the anomalously high VR values observed within these wells (Cook, 2002). "Frypanning" is the term given to a process where cuttings samples are heated during the initial drying process to excessive temperatures

whereby the organic matter oxidises. Rims and cracks within the coal grains display a higher reflectance when they have been affected by frypanning. Conversely, the cores of affected grains often show lower VR values, possibly due to migration of tars into the coals. This makes it difficult to determine the original reflectance of the vitrinite. Cook (2002) observed frypanning within cuttings samples from Aroo-1, Nangkero-1, Tarook-1, and Toolka-1A. Thus, care should be taken when using VR data derived from these four wells, and other wells within the Bass Basin where less detailed petrographic analysis has been undertaken.

The elevation of VR measurements from the Durroon Mudstone (Chapter 4) within the Durroon-1 well do not appear to be related to either localised igneous intrusions, or the effects of frypanning (Figure 6.5). Duddy (1992) indicated that elevated measured VR values observed in samples from the Durroon Mudstone are high due to the effects of oxidation. The VR values estimated from Thermal Alteration Index (TAI) data from the same level appear to be far lower and are in accordance with other samples from the well.

Where calculated VR = measured VR

When a measured VR value is equal to the calculated value predicted from a default thermal history model, it indicates that the sample has not been exposed to palaeotemperatures higher than present temperatures since deposition (Duddy and Erout, 2001). Following the technique proposed by Kaiko (1998), a well was considered to be currently experiencing maximum temperature if the calculated VR profile could be made to correspond to the measured VR profile by adjusting the BHT by no more than ±10 % of the initial corrected BHT value. This allows for any divergence in maturity estimates that may occur from the use of corrected BHT's, and also accounts for possible variation between plotting measured random reflectance and measured maximum reflectance (Ro_{Max} = 1.066 x Ro_{Random}; Ting, 1978; Kaiko, 1998).

Calculated Ro profiles within Seal-1, Cormorant-1, Bass-3, Aroo-1, Yolla-1, Tilana-1, Nangkero-1, Flinders-1, and Pelican-5 appear to approximate measured VR profiles (Figure 6.5). This indicates that stratigraphic sections intersected by these wells are currently experiencing maximum temperature, apart from localised departures associated with intrusions. Any thermal variation due to uplift and erosion that may have occurred in the past has been overprinted by present-day thermal conditions. In this situation, additional thermal history data (e.g., Apatite Fission Track Analysis/AFTA, VR, biomarkers) from these well locations cannot reveal further details to constrain the background thermal history (Duddy and Erout, 2001).

Where calculated VR > measured VR

Koorkah-1, Chat-1 and Durroon-1 all contain measured VR values that are lower than what is predicted from their respective default thermal history models (Figure 6.5). If we assume that both measured VR data and subsurface temperature data are correct, present thermal conditions within these wells may be the result of a relatively recent heating event. Such a thermal increase would need to have occurred after 2 Ma to prevent measured VR reaching equilibrium with present day conditions (Kaiko, 1998).

Another explanation may be that present day temperature conditions have been overestimated through the overcorrection of BHT data. In addition, measured VR values may underestimate the true maturity for reasons including the presence of caved material within cuttings samples, misidentification of true in-situ vitrinite, or the suppression of reflectance in certain organic macerals (Duddy and Erout, 2001). Recent VRF studies however, indicate that VR suppression within the basin appears to be limited (Boreham et al., 2003; Chapter 5). The corrected BHT data and measured VR data at Koorkah-1 and Chat-1 are considered to be accurate, suggesting that a recent heating event is likely.

Irrespective of the reasons for the elevated calculated VR profiles within Koorkah-1, Chat-1 and Durroon-1 (based upon DTH models), the rocks intersected by these wells appear to be experiencing maximum temperature conditions today.

6.7 RESULTS FROM DEFAULT THERMAL HISTORY MODELS

DTH models of the 13 wells studied indicate the Late Cretaceous to Recent section within the Bass Basin has not been exposed to palaeotemperatures any higher than the present temperatures since deposition (excluding the effects of localised igneous activity). The majority of wells show a strong correlation between measured and calculated VR profiles, indicating they are at maximum temperature (Figure 6.5). DTH models for Koorkah-1, Chat-1, and Durroon-1 display elevated calculated maturity profiles with respect to measured values, indicating they may have been subjected to a recent heating event (< 2 Ma). All three wells are located towards the margins of the basin (Figure 6.4).

Maps were constructed showing the areal distribution of VR across the basin, based upon calculated VR profiles from DTH models (Figures 6.6 to 6.12). As the maps were constructed from calculated VR profiles (to investigate regional background VR trends), the localised effects of igneous intrusions on VR have been ignored. However, the effects of localised igneous activity should be considered when undertaking smaller scale investigations of hydrocarbon generation and expulsion, as intrusive bodies are common within Cainozoic succession.

The distribution of calculated VR across the Bass Basin highlights the following points (Figures 6.6 to 6.12):

- Depth to the oil generation window (0.65% Ro) varies between ~1.6 and 2.4 km below seafloor. The top of the defined oil window is deepest in the central region of the basin, and shallowest towards the northwest, where geothermal gradients are highest (Figure 6.6). The average depth to the oil generation window within the basin is 2.0 km below seafloor.
- Depth to the onset of oil expulsion (0.75% Ro) varies between ~2.3 and 3.0 km below seafloor, and is deepest in the central part of the basin, shallowing towards the northwest (Figure 6.7). The average depth to the oil expulsion window within the basin is 2.6 km below seafloor.
- Average VR across the Bass Basin at 2000 m is approximately 0.57%, varying between 0.48 and 0.65% (Figure 6.8). VR shows a broad increase towards the west of the basin where Seal-1, Bass-3, Yolla-1 and Flinders-1 have entered the oil generation window at this depth.

- Average VR across the Bass Basin at 2500 m is approximately 0.70%, varying between 0.62% and 0.78% (Figure 6.9). All lithologies at 2500 m across the basin appear to have entered the defined oil generation window. However, a few wells, including Seal-1, Bass-3, and Yolla-1, are greater than 0.75% Ro implying that they are within the oil expulsion window (>0.75% Ro).
- The Middle to Late Eocene succession (Middle *N. asperus* zone; top of the "Eastern View Group" and base of the regional sealing unit, the Demons Bluff Formation) has a basin-wide average VR of 0.43%. Ranging between 0.3% and 0.56%, sediments of late Middle Eocene age and younger are immature for oil generation across the basin (Figure 6.10).
- The top of the Bass Megasequence (base Upper *M. diversus*; top of the "Middle Eastern View Group") has an average VR across the basin of 0.59%, just below the defined oil generation window of 0.6 %. VR at this level varies between ~ 0.3% to 0.69%. Figure 6.11a shows that the top of the Bass Megasequence ("Middle Eastern View Group") has entered the oil generation window in a north-south oriented zone, directly overlying the Cormorant, Yolla and Pelican Troughs, within the central axis of the basin.
- The top of the Paleocene (top Lower *L. balmei;* top of the Tilana Sequence) has an average VR across the basin of 0.71%, within the defined oil generation window. VR at the top Paleocene level varies between ~ 0.3% and 0.95%. Figure 6.12a shows that the top of the Paleocene has entered the oil generation window within the central region of the basin. Within the central axis of the basin, the top Paleocene level has entered the defined oil expulsion window (> 0.75%Ro).

6.8 PALAEOHEATFLOW MODELLING OF THE DURROON-1 WELL

A DTH model for Durroon-1 has been presented (Figure 6.5) using present day temperature conditions defined by a corrected BHT of 114^{o}C at 3021.5 m (all depths measured below KB), a geothermal gradient of 34.7^{o}C/km, and a heat flow value of 73.1 mW/m^{2}. Durroon-1 is the only well within the Bass Basin to intersect both the Early Cretaceous Otway Megasequence and the Late Cretaceous Durroon Megasequence (Chapter 4). As such, modelling Durroon-1 provides an opportunity to investigate palaeoheatflow throughout the major rifting events that influenced basin development.

While BHT, TAI, VR and AFTA data are available for the well, data quality is highly variable and is consistent with a number of thermal history scenarios. Despite the issues relating to data quality, a number of "end-member" scenarios can be defined, whereby further palaeothermal indicator analysis (VR or AFTA) by future workers may provide further clarification.

Duddy (1992) outlined a comprehensive assessment of thermal history data from the Durroon-1 well, including AFTA data for three samples from the depths 1696 m (L4-116), 2560 m (L4-117), and 3023 m (L4-118) within the Otway Megasequence. Duddy (1992) emphasised that the results of the AFTA data were tentative, as compositional kinetic factors were not fully taken into account, coupled with uncertainties in the estimation of subsurface temperatures. Important aspects of the Durroon-1 thermal history are given below:

- The maximum present temperature defined by the AFTA sample at 3023 m is 90°C (Duddy 1992), suggesting that the present day heat flow value estimated from a corrected BHT value of 114.25°C at 3023 m (used for DTH model), is too high or has risen to that level within the last 2 Ma.
- AFTA age data from the deepest sample (3023 m) suggests that the sample had experienced palaeotemperatures after deposition that were sufficient to totally, or near totally, erase fission tracks in all apatites (Duddy, 1992). A minimum temperature of at least 120°C would be required to do this (as compared to a revised present temperature of 90°C or 114°C at 3023 m) (Figure 6.6).
- There is some evidence from the AFTA data that cooling from maximum palaeotemperature occurred between ~90 and 100 Ma, following early Cretaceous deposition of the Otway Megasequence and the outpouring of mid-Cretaceous basalt (Duddy, 1992) (Figure 6.6). The timing of cooling is consistent with the onset of significant structural extension across the region, related to the initial phase of Tasman rifting (Cummings et al., 2002). Seismic mapping indicates that approximately 300 m of erosion took place at the well location during this period.
- VR data are variable throughout the well section (Figures 6.5 and 6.6), providing equivocal palaeotemperature information. The predicted VR profile from the DTH model overestimates most measured values throughout the Early Cretaceous section, however it significantly underestimates values measured in the "Durroon Mudstone". As mentioned above, these samples are considered to be elevated due to the effects of oxidation (Duddy, 1992).

Two palaeoheatflow models were implemented to analyse the Durroon-1 data (Figure 6.13). Palaeoheatflow models were modified from a regional model outlined by Duddy and Erout (2001), and modelled to fit measured AFTA and VR data from Durroon-1. Heatflow prior to the Tasman rifting event was estimated at approximately 90 mW/m^2 and was elevated to 120 mW/m^2 with the onset of Tasman Rifting around 95 Ma. Heatflow then declined until approximately 65 Ma where it remained constant through to present day (~ 73 mW/m^2). The second palaeoheatflow model involves a reduction in heat flow to approximately 57 mW/m^2 at 65 Ma through to 2 Ma, when heat flow increased rapidly to the present temperature conditions of 73 mW/m^2. Palaeoheatflow model 1 (Figure 6.13) shows a similar calculated VR profile to the DTH (Figure 6.5). The calculated VR profile defined by palaeoheatflow model 2 (Figure 6.13) involving a recent heating event, shows a greater correlation with measured VR samples.

In summary, thermal history models based on the current AFTA and VR data from the Durroon-1 well are equivocal. VR data are consistent with a maximum temperature at present day (DTH model), whereas the thermal history indicated by AFTA data implies a cooling of 10 to 35°C in the mid-Cretaceous (Duddy, 1992). To constrain the thermal history of Durroon-1, a more extensive suit of VR data must be collected and new AFTA samples must be examined using more recent compositional kinetic parameters. Unfortunately, additional VR sampling from the Durroon-1 well could not be incorporated into this study due to a lack of available samples.

6.9 SUBSIDENCE MODELLING

Burial geohistory diagrams were constructed for the 13 wells modelled within the Bass Basin, using the Middleton (1982) decompaction option, palaeo-water depths derived from palaeontological data and uplift amounts estimated from seismic mapping (Figures 6.14a to 6.14d). All wells within the Bass Basin, apart from Durroon-1, were drilled wholly within the Campanian to Recent succession. As such, subsidence curves for most wells within the Bass Basin display a consistent rate of subsidence and sedimentation from the Late Cretaceous to the present, reflecting their post-rift depositional setting.

An increase in the rate of burial is observed from the Early to Middle Eocene within most subsidence models across the basin (Figure 6.15). While sediment accumulation within the basin was largely controlled by regional post-rift thermal subsidence processes from the Campanian onwards, subsidence along the central axis of the basin appears to be related to intermittent periods of sinistral transtension associated with the continued separation of Australia from Antarctica along the "Tasman-Antarctic Shear" to the west of Tasmania (Cummings et al., 2002; Hill et al., 2001). Deposition of the potentially oil-prone Middle to Early Eocene coaly source rocks correlates with the enhanced rate of subsidence within central regions of the basin during this period of structural reactivation.

The onset of fast sea-floor spreading in the Southern Ocean, coupled with the collision of the northern edge of the Australian Plate with Southeast Asia led to compression across many regions of Australia during the mid-to-Late Cainozoic (Smit, 1988; Etheridge et al., 1991). Within the Bass Basin, Late Oligocene to Miocene compression led to the strike-slip reactivation of a number of pre-existing structures. Structural inversion was restricted to the northern margin of the basin and was particularly focused within the Cormorant Trough (Figure 6.16).

Four pseudowells were constructed to investigate subsidence within the major long-lived basin depocentres (Figures 6.16 and 6.17). Three pseudowells were constructed within the three major troughs along the central axis of the basin, the Cormorant, Yolla and Pelican troughs (Figure 6.4). The Cormorant Trough and Pelican Trough models were extended at depth from the Cormorant-1 and Pelican-5 wells respectively (Figure 6.16). A pseudowell was also constructed through the deepest section of the "Boobyalla Half-graben" (Baillie and Pickering, 1991), situated within the Durroon Sub-basin (Figure 6.17).

Subsidence patterns within the Cormorant, Yolla and Pelican troughs show an enhanced rate of subsidence from the Cenomanian to the Campanian (Figures 6.16 and 6.17). The increased accommodation rate during this period is due to basin-wide extension associated with the Tasman rifting event (Cummings et al., 2002). An increase in the rate of accommodation is also evident from the Paleocene to the Early-Middle Eocene. Increased subsidence is considered to be the result of transtensional reactivation of earlier rift structures within the central axis of the Bass Basin. The subsidence curve for the "Boobyalla Half-graben" highlights the impact of Tasman Rifting on development of accommodation space within the southeastern region of the basin (Figure 6.17). In general, the development of accommodation space within the central axis of the Bass

Basin appears to have been largely controlled by post-rift thermal sag process, whereas towards the southeast (Durroon Sub-basin), the dominant influence was Late Cretaceous rift-related subsidence.

6.10 TIMING OF HYDROCARBON GENERATION AND EXPULSION

The timing of hydrocarbon generation and expulsion within the Bass Basin has been investigated through the use of the DTH models from thirteen wells (Figure 6.15). Through the use of the maturation history diagrams, maps were constructed displaying the regional variation of VR for key periods of development within the basin. Boreham et al. (2003; Chapter 5) showed that the dominant oil-prone source rocks found within the Bass Basin are the Palaeogene coals, in particular, those found within Middle to Early Eocene sequences across the basin. To investigate the basin-wide maturation history of this source rich sequence, regional VR distribution maps were constructed for the top of the Middle *M. diversus* zone (top of the Narimba Sequence, "Middle Eastern View Group"; Figure 6.11) and the top of the Lower *L. balmei* zone (top of the Tilana Sequence, Figure 6.12). Where appropriate, areal VR distribution maps for these horizons have been reconstructed to the time when the regional sealing unit was deposited (~34 Ma) and the period when Cainozoic structural reactivation was greatest (~15 Ma, Middle Miocene).

Thermal-maturity plots based on the DTH models indicate that the base of the Eocene sequence (top Lower *L. balmei*, top of Tilana Sequence) was largely immature for oil generation during deposition of the "Demons Bluff" regional sealing unit around 34 Ma (Figures 6.12c). However, this horizon does appear to have entered the oil generation window (> 0.6% Ro) within the centre of the Cormorant Trough and in the vicinity of Tilana-1. By 15 Ma, the base of the Eocene succession had entered the oil generation window along the central axis of the basin, in the Cormorant, Yolla and Pelican troughs (Figure 6.12b). In addition, the deepest regions of the Pelican and Cormorant troughs appear to have entered the oil expulsion window (> 0.75% Ro). Today the base of the Eocene succession lies within the oil generation window across a significant proportion of the basin (Figure 6.12a). Oil expulsion from the base of the Eocene succession appears to have been restricted to a central north-south zone along the axis of the basin, within the Cormorant, Yolla and Pelican troughs.

Prior to 15 Ma, the top of the Middle *M. diversus* zone (top of the Bass Megasequence, top Middle Eastern View Group) had not entered the oil generation window (> 0.6% Ro) (Figure 6.11b). However, the top of the Middle *M. diversus* zone appears to have entered the oil generation window in the central part of the basin within recent times (Figure 6.11a).

Source rock intervals defined for each well by Boreham et al. (2003; Chapter 5) appear to have entered the oil generation window within the central axis of the basin. Maturity models for wells within the central part of the Bass Basin indicate that the Paleocene succession entered the oil generation window following deposition of the "Demons Bluff" regional sealing unit (~ 36 to 40 Ma). Therefore, the source rocks linked to major oil accumulations within the basin appear to have entered the oil generation window following

deposition of regional sealing units, and after the major trap forming structural events of the Late Cretaceous and Early Eocene.

To investigate the timing of hydrocarbon generation and expulsion from deeper undrilled sequences within the basin, maturation histories were defined for the four pseudowell sections modelled (Figures 6.16 and 6.17). A palaeoheatflow model defined for the Durroon-1 well (Model 1) was applied to all four models, incorporating a rapid increase in heatflow during the deposition of Cenomanian to Campanian units, followed by constant heatflow (present levels) from ~ 65 Ma to the present (Figure 6.13).

Within the Cormorant, Yolla and Pelican troughs, the Otway Megasequence appears to have passed through the oil and gas generation windows during the Late Cretaceous deposition of the overlying Durroon Megasequence (Tasman Rift Phase; "Lower Eastern View Group") (Figures 6.16 and 6.17). The Cenomanian to Campanian Durroon Megasequence passed into the oil generation window soon after deposition. It passed completely into the gas generation window by the Eocene within the Cormorant Trough, but maintained a longer residence time within the oil generation and expulsion windows (until the Miocene) within the Yolla and Pelican troughs.

Within the Durroon Sub-basin, the Otway Megasequence passed into the oil and gas generation window during the rapid deposition of overlying Durroon Megasequence (Tasman Rift Phase) (Figure 6.17). Following this high heatflow event, the Otway and Durroon megasequences appear to have failed to reach adequate temperatures to restart hydrocarbon generation (Figure 6.17).

6.11 CONCLUSIONS

- Geothermal gradients within the Bass Basin vary from 3.3^{o}C/100m in the Pelican Trough, up to 6.5^{o}C/100m at Konkon-1. A broad decrease in geothermal gradient occurs from the northwest of the basin towards the southeast. A similar pattern is reflected in calculated heatflow values.
- 'Default Thermal History' (DTH) models of 13 wells from the Bass Basin indicate that the Late Cretaceous to Recent succession is experiencing maximum temperatures today. The majority of wells show a strong correlation between measured and predicted VR profiles.
- DTH models of Koorkah-1, Chat-1, and Durroon-1 display elevated calculated VR profiles with respect to measured VR values, indicating they may have been subjected to a recent heating event (< 2 Ma).
- Igneous intrusions within the Cainozoic succession produced localised elevated maturity above regional profiles defined by calculated VR profiles. Future work involving smaller scale investigations of hydrocarbon generation should consider the impact of igneous activity on hydrocarbon generation within the basin.
- The distribution of VR across the Bass Basin, based on calculated VR profiles (DTH models, ignoring localised igneous events) highlights the following:
    - Depth to the oil generation window (0.65% Ro) varies between ~1.6 and 2.4 km below seafloor. The average depth to the oil generation window across the basin is 2.0 km below seafloor.

- Depth to the oil expulsion window (0.75% Ro) varies between ~2.3 and 3.0 km below seafloor. The average depth to the oil expulsion window across the basin is 2.6 km below seafloor.
- The base of the "Demons Bluff" regional sealing facies is immature for oil generation across the basin, with an average calculated VR of 0.43%.
- The top of the Middle *M. diversus* zone (top of the Narimba Sequence, top "Middle Eastern View Group") has an average VR across the basin of 0.59%. The top of this zone has entered the oil generation window in a north-south oriented region, directly overlying the Cormorant, Yolla, and Pelican troughs.
- The top of the Lower *L. balmei* zone (top Paleocene) has an average VR across the basin of 0.71%, within the defined oil generation window. The top of the Paleocene sequence has entered the oil generation window within the central area of the basin, and the oil expulsion window along a north-south oriented central axis of the basin.

- Thermal history models based on current AFTA and VR data from the Durroon-1 well are equivocal. VR data are consistent with a maximum temperature at present day (DTH model), whereas the thermal history indicated by AFTA data implies a cooling of 10 to 35^{o}C in the mid-Cretaceous (Duddy, 1992). To constrain palaeoheatflow from the Durroon-1 well, a more extensive suite of VR data and revised AFTA analysis is required.
- Burial geohistory diagrams of the wells studied indicate a consistent rate of subsidence and sedimentation from the Late Cretaceous to the Recent, reflecting the post-rift depositional setting.
- The timing of hydrocarbon generation and expulsion within the Bass Basin, as defined by the DTH models from thirteen wells across the basin indicates:
  - The base of the source-rich (oil-prone) Early Eocene coal sequences entered the oil generation window (> 0.65% Ro) after deposition of the "Demons Bluff" regional sealing facies (~ 34 Ma).
  - By the Middle Miocene (~ 15 Ma), significant structural reactivation was occurring. The base of the Eocene succession entered the oil generation window along the central axis of the basin during the Middle Miocene, while in the deepest regions of the Cormorant, Yolla and Pelican Troughs, sediments entered the oil expulsion window (> 0.75% Ro).
  - Prior to 15 Ma, the top of the Middle *M. diversus* succession (top of the Narimba Sequence, "top Middle Eastern View Group") had not entered the oil generation window. However, today the top of the Middle *M. diversus* succession appears to have entered the oil generation window in the central part of the basin.
- The defined source rocks linked to hydrocarbon accumulations within the Bass Basin (Early Eocene to Paleocene coals) entered the oil generation window just prior to and following deposition of the regional sealing units, and after the major trap forming structural events of the Late Cretaceous and Early Eocene. These units continued to pass into the oil expulsion window during and after Miocene structural reactivation events within the basin.
- Pseudowell reconstructions and a defined palaeoheatflow model (Model 1, Figure 6.13) indicate that the Otway Megasequence passed through the oil and gas generation windows in deeper parts of the

Bass Basin (Cormorant, Yolla, and Pelican troughs) during the Late Cretaceous, prior to deposition of the regional sealing units.

- The largely undrilled Durroon Megasequence (Tasman Rift Phase, "Lower Eastern View Group") appears to have entered the oil generation window soon after deposition. The sequence passed completely into the gas generation window by the Eocene within the Cormorant Trough, but maintained a longer residence time within the oil generation/expulsion windows (to the Miocene) within the Yolla and Pelican troughs (based on defined palaeoheatflow, Model 1, Figure 6.13).

Table 6.1 Bass Basin Bottom Hole Temperature (BHT) summary

	KB	Water Depth	Total Depth (KB)	BHT Depth	Highest	Horner Corr.	Waples & Ramly (2001)	Geothermal Gradient
Well Name	**m**	**m**	**m**	**m**	**BHT °C**	**BHT °C**	**Corr. BHT**	**°C/100m**
Aroo-1	9.8	76.2	3652.11	3652.10	138.89	145	-	3.73
Bass-1	9.4	80.8	2349.40	2349.40	96.70	-	138.72	5.61
Bass-2	9.4	85.3	1800.45	1800.45	72.20	-	101.3	5.24
Bass-3	9.4	61.6	2433.80	2433.83	97.80	-	140.05	5.42
Chat-1	25.3	81.4	3107.00	3107.00	104.40	110.24	125.02	3.77
Cormorant-1	30.5	73.2	3000.80	3000.76	114.40	124.16	138.76	4.38
Dondu-1	9.8	79.5	2927.00	2926.99	126.70	146.26	162.03	5.29
Durroon-1	9.8	68.6	3024.23	3021.50	91.11	-	114.25	3.47
Flinders-1	22.3	69.3	2718.80	2718.80	126.10	132.18	146.56	5.12
King-1	22	72.8	2225.00	2122.00	102.20	108.34	112.01	4.93
Konkon-1	9.8	70.1	1537.10	1537.11	69.90	-	107.13	6.53
Koorkah-1	22.5	67.6	3146.20	3146.15	131.70	140.86	148.33	4.46
Nangkero-1	9.8	69.8	2877.30	2877.31	97.80	102.49	114.88	3.68
Narimba-1	9.8	77.1	3353.70	3353.71	138.90	147.3	177.23	5.06
Pelican-1	30.48	76.5	3178.50	-	-	-	-	?
Pelican-2	30.5	77.7	3068.10	3068.12	92.20	93.31	110.66	3.33
Pelican-3	9.8	80.2	2905.00	2799.00	95.60	105.85	102	3.32
Pelican-4	25	77.4	3050.70	3050.74	115.60	148.07	171.25	5.40
Pelican-5	22.3	77.4	4267.00	4267.20	177.80	179.33	179.09	4.01
Pipipa-1	21	73	2115.00	2115.01	86.10	96.26	107.79	4.74
Poonboon-1	9.8	78.9	3258.30	3258.31	120.00	124.15	145.49	4.21
Seal-1	25.3	64.6	1669.00	1669.00	74.40	83.49	98.95	5.51
Squid-1	22.3	80.5		-	-	-	-	?
Tarook-1	9.8	79.6	2773.70	2773.68	94.40	118.07	150.38	5.16
Tas Devil-1	21.9	73.8		-	-	-	-	?
Tilana-1	22.3	82	3900.20	3900.22	115.60	120.79	138.68	3.34
Toolka-1A	9.8	78.6	2714.90	2714.85	106.70	108.87	119.05	4.08
White Ibis-1				-	-	-	-	-
Yolla-1	11	79.5	3347.00	3347.01	143.30	157.51	173.69	4.97
Yolla-2				-	-	-	-	-
Yurongi-1	9.8	81.7	3438.40	2438.40	105.60	113.13	124.96	4.81

Single Corrected BHT
Averaged Horner Corrected BHT
Horner Corrected BHT

Figure 6.1 Plot of measured (uncorrected) and corrected temperatures with depth in Pelican-5 and Yolla-1. Bottom Hole Temperatures (BHT) were corrected by the methods established by Waples and Ramly (2001). Note that corrected BHT values are consistent with the temperature profile of the DST data.

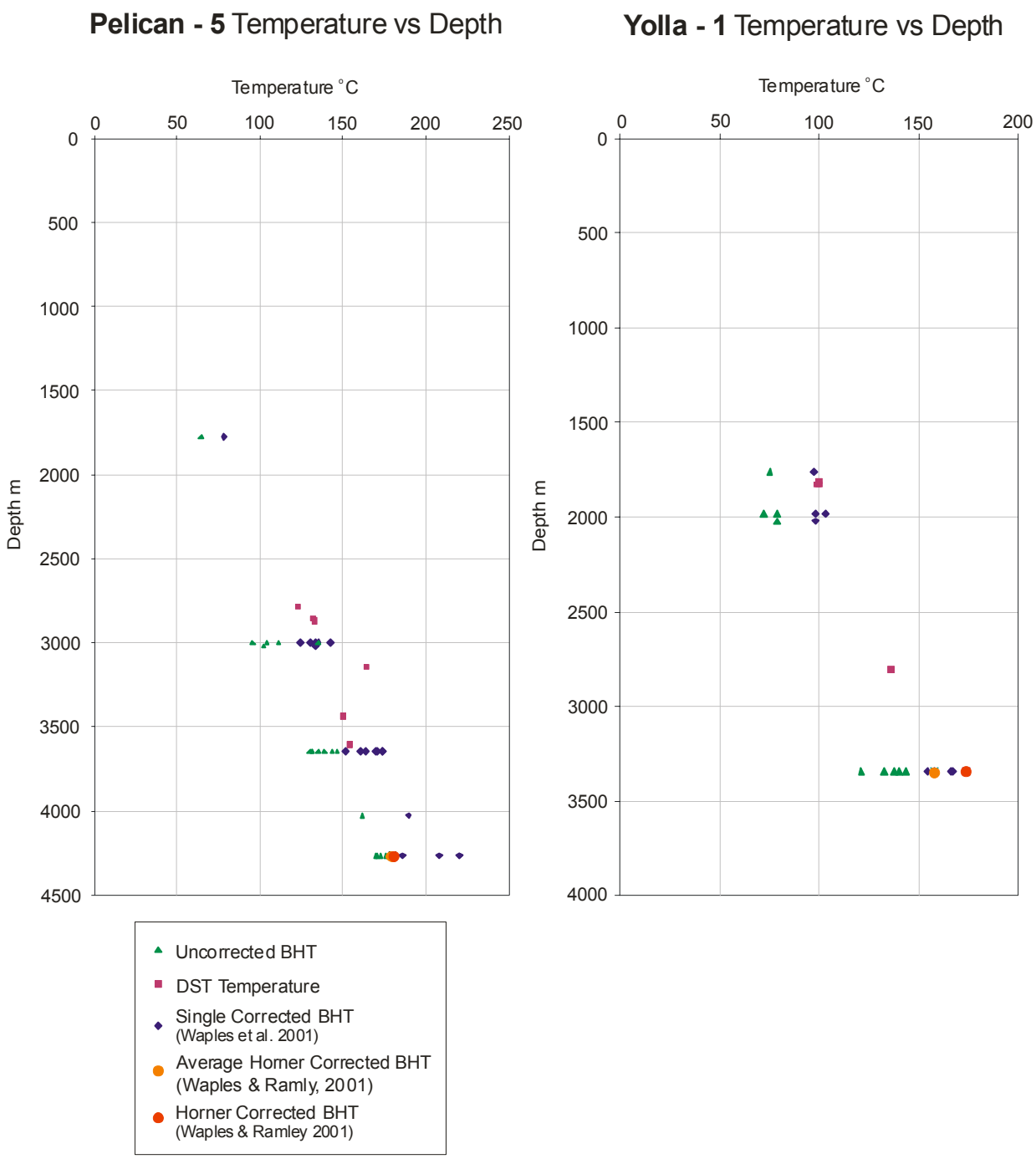


Figure 6.2 Areal distribution of geothermal gradients (coloured circles), generalised structure (modified from Lennon et al., 1999) and basement (Teasdale et al., 2001).

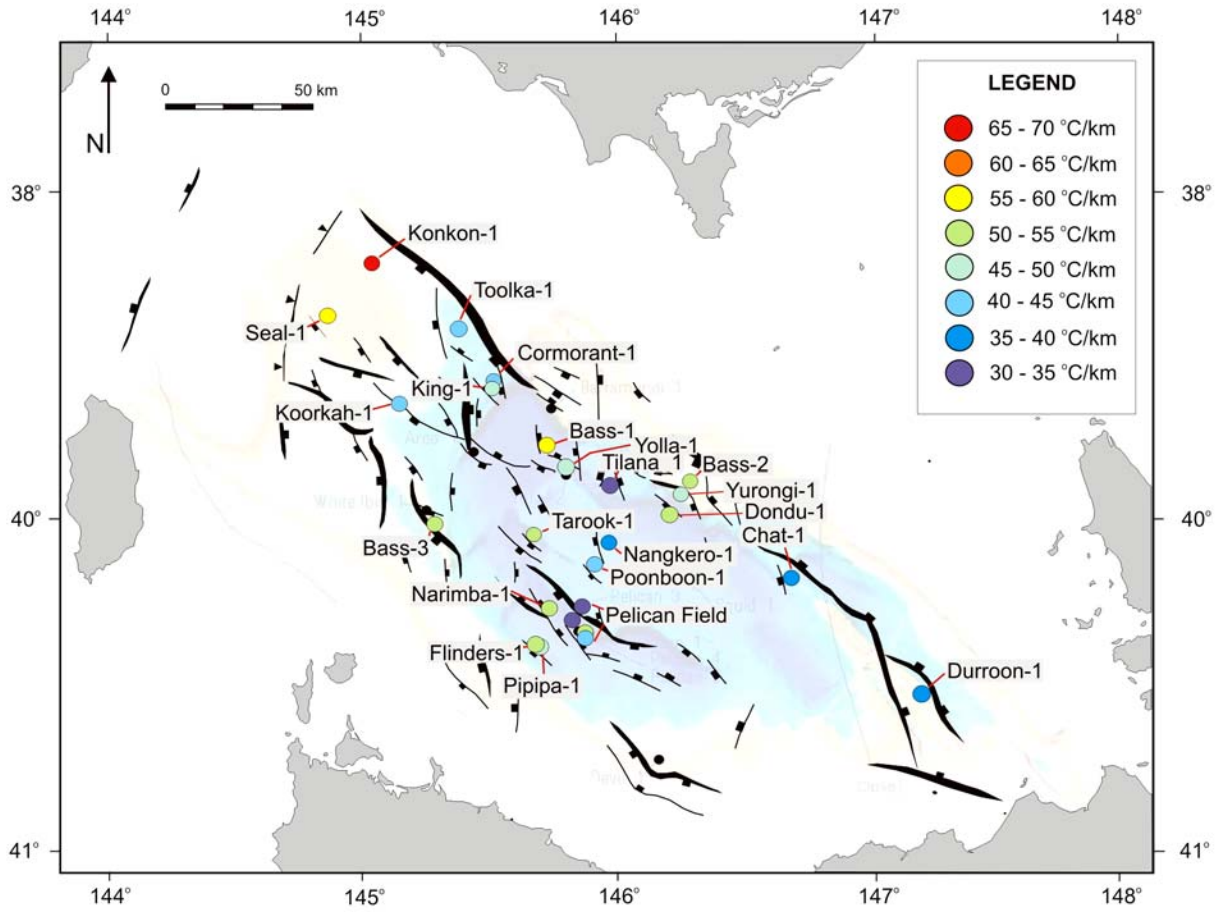


Figure 6.3 Areal distribution of heatflow values (coloured circles). Generalised structure map modified from Lennon et al. (1999) and Teasdale et al. (2001).

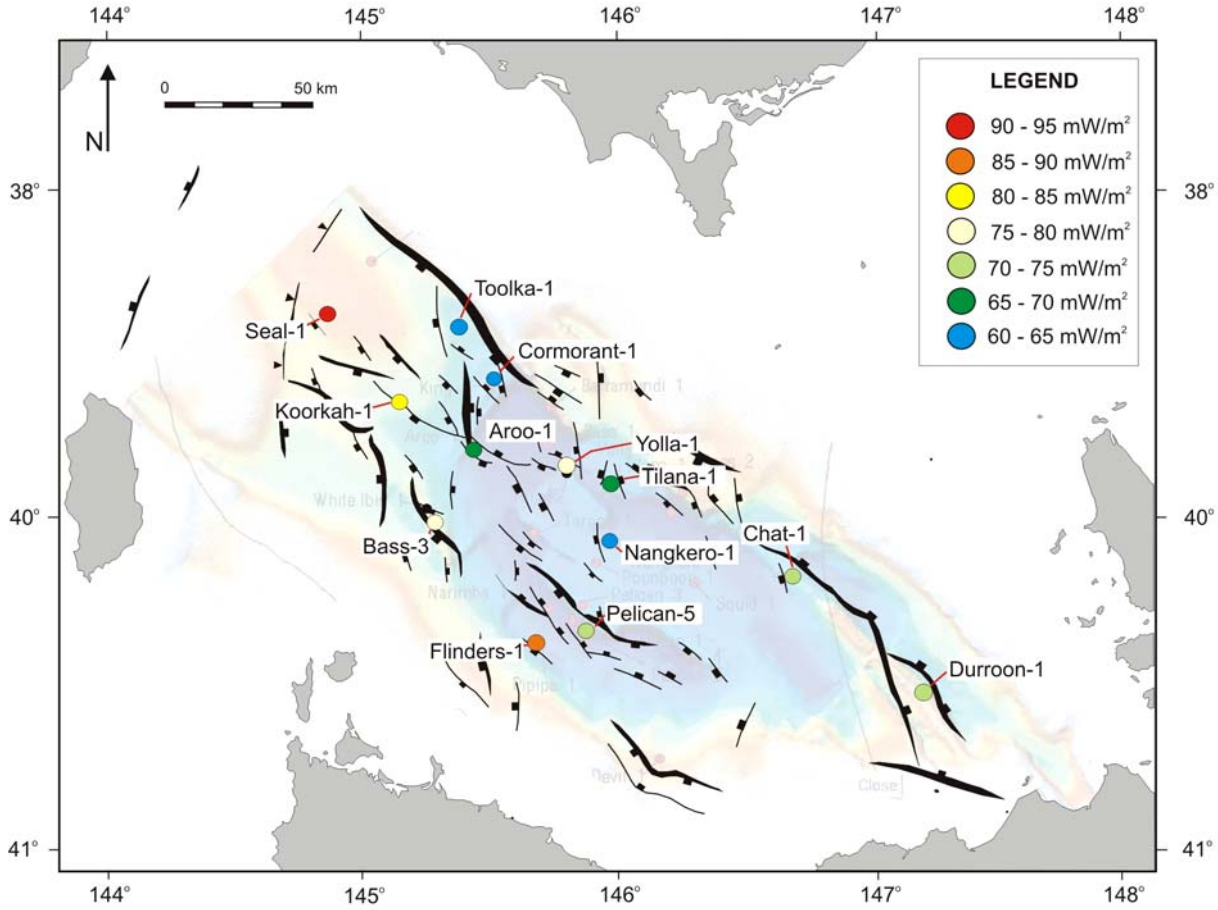


Figure 6.4 Location of wells and pseudowells studied (map modified from Lennon et al., 1999).

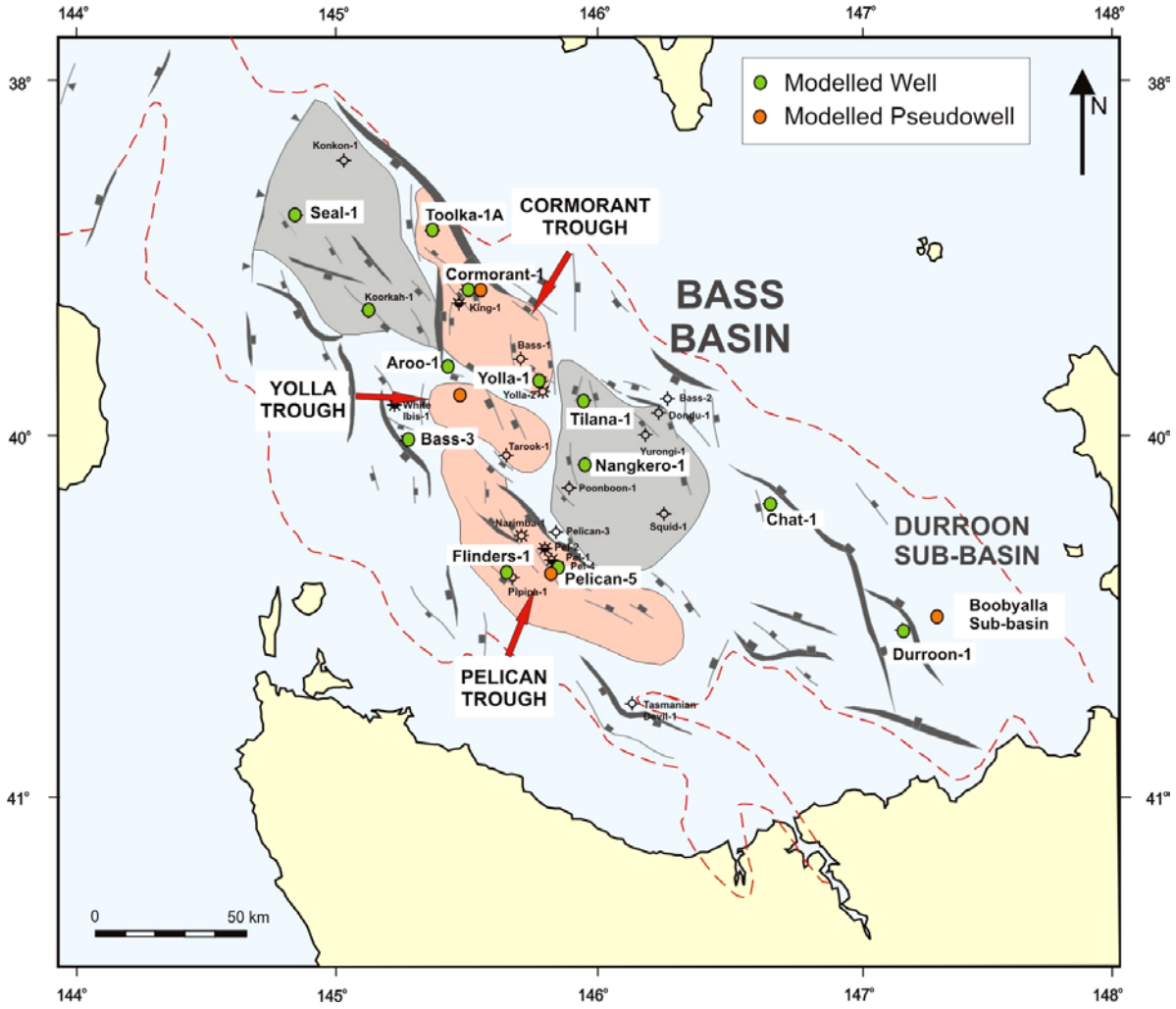


Figure 6.5a Maturity depth plots for Default Thermal History (DTH) models (constant heatflow through time).

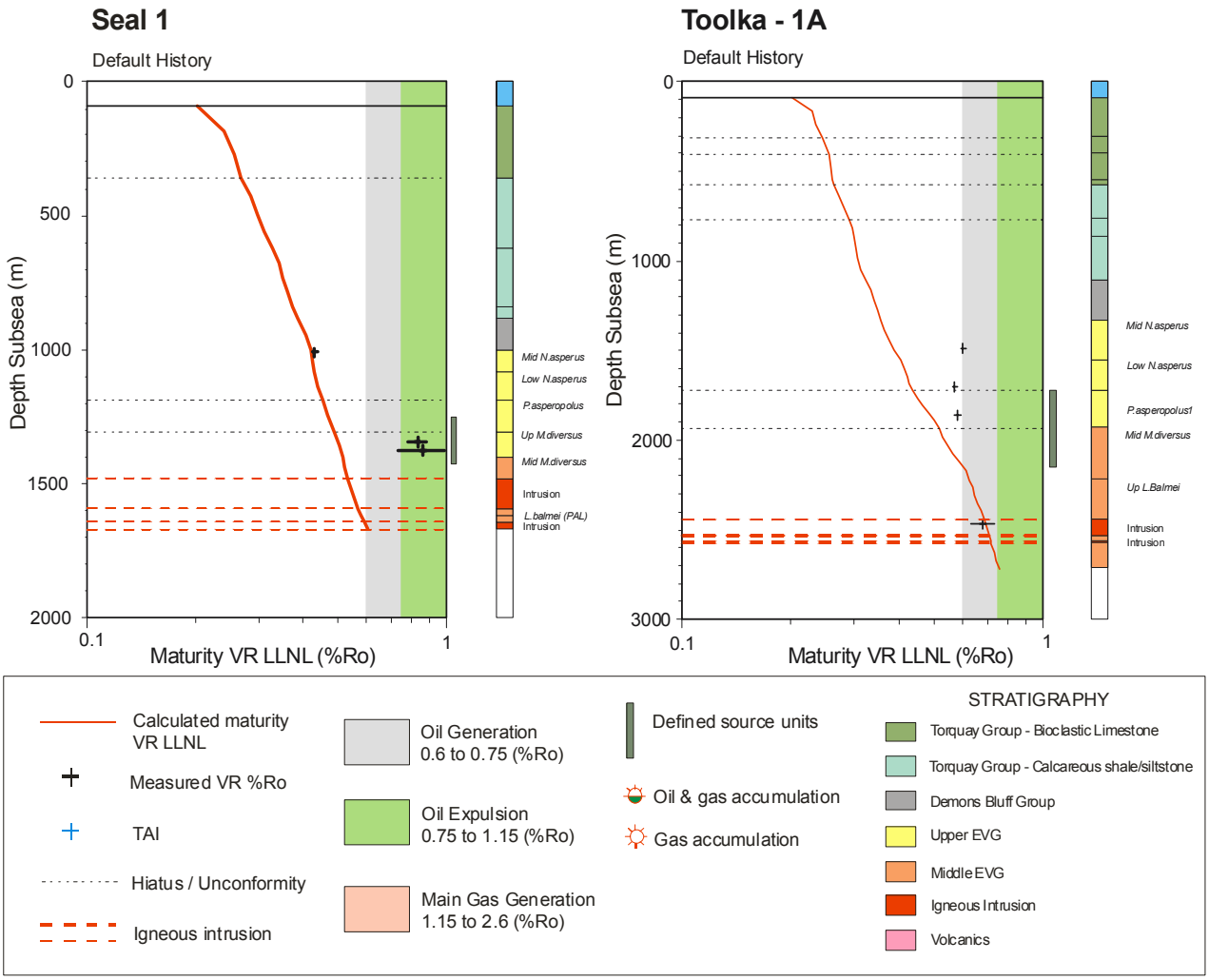


Figure 6.5b Maturity depth plots for Default Thermal History (DTH) models (constant heatflow through time).

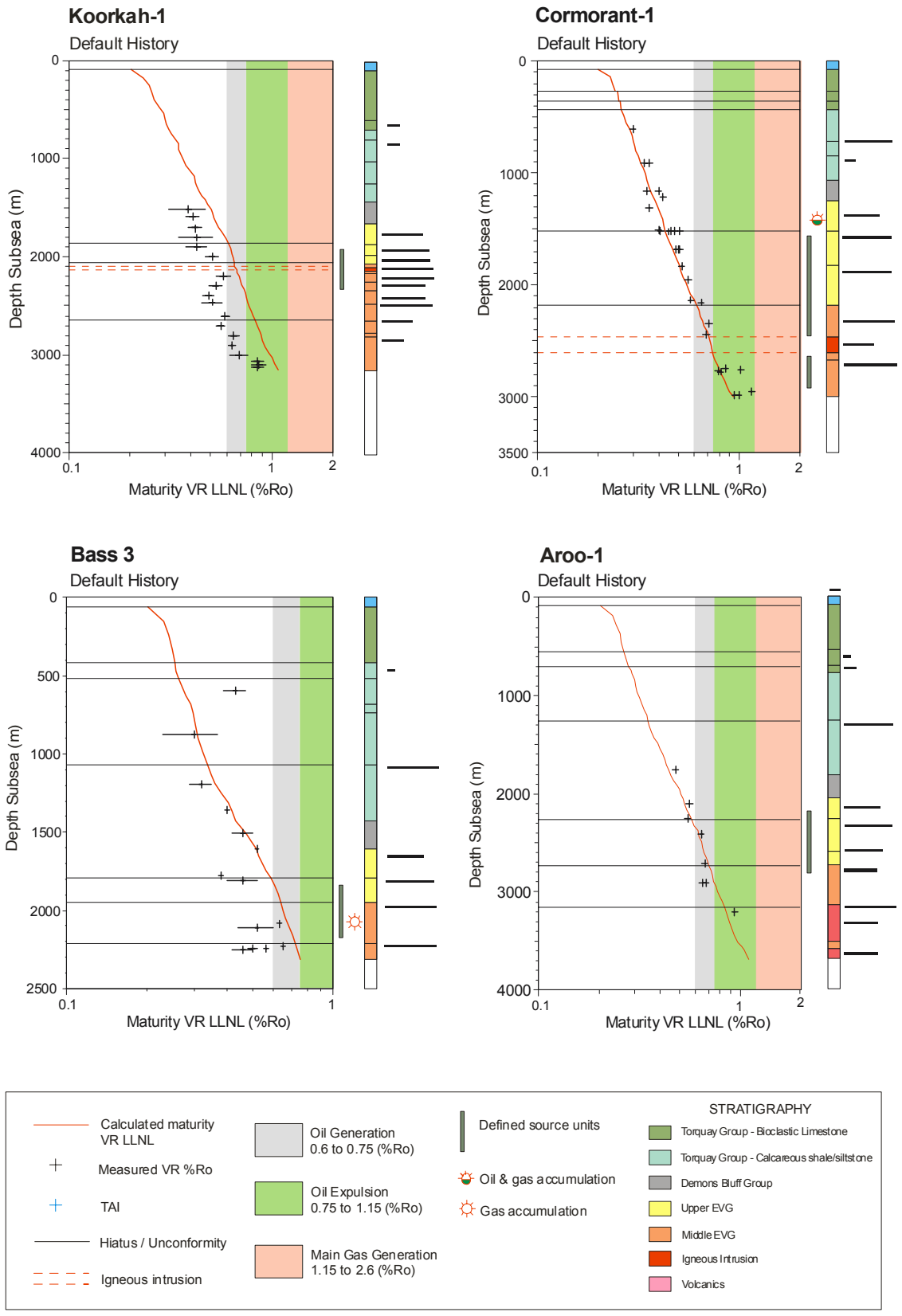


Figure 6.5c Maturity depth plots for Default Thermal History (DTH) models (constant heatflow through time).

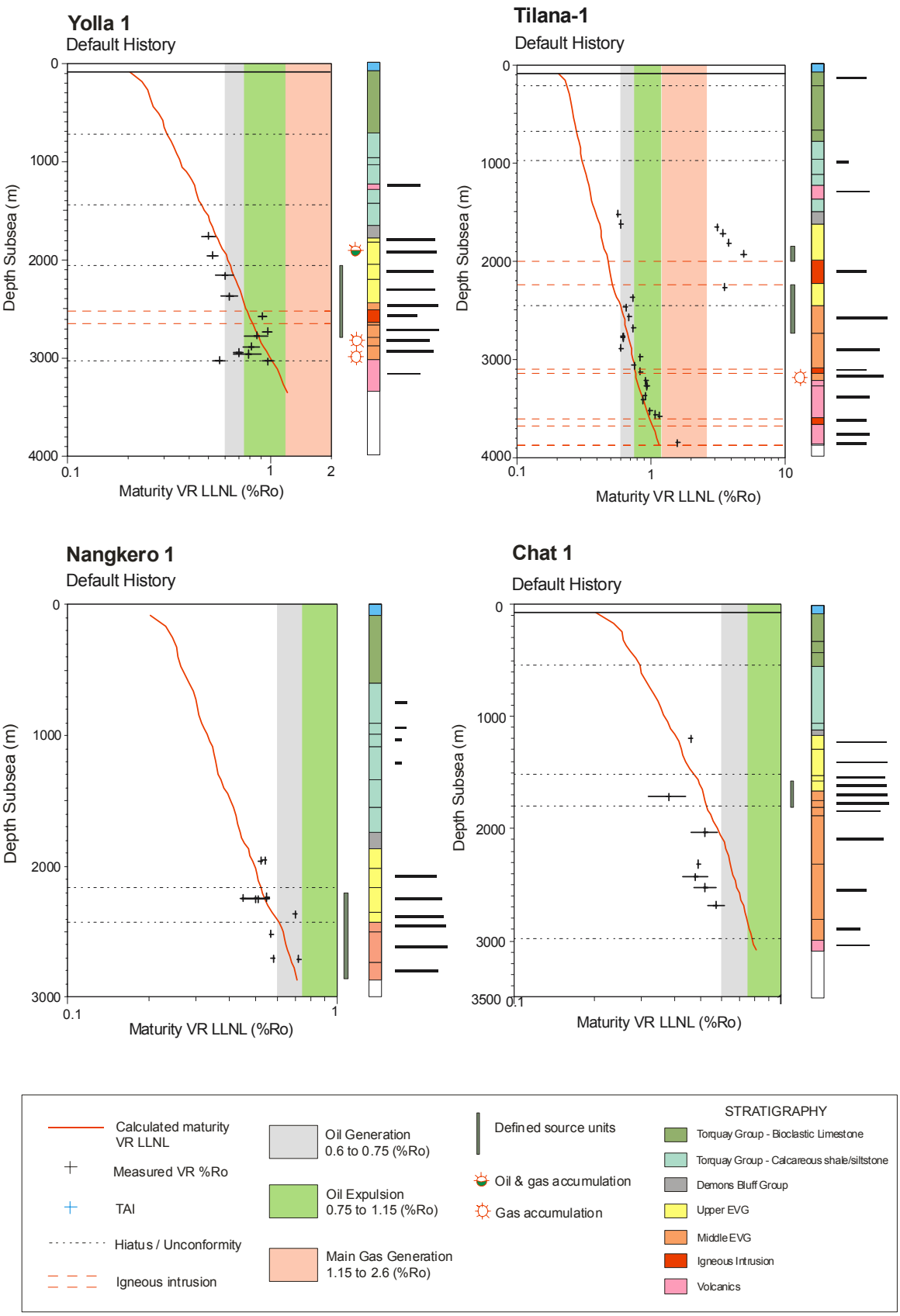


Figure 6.5d Maturity depth plots for Default Thermal History (DTH) models (constant heatflow through time).

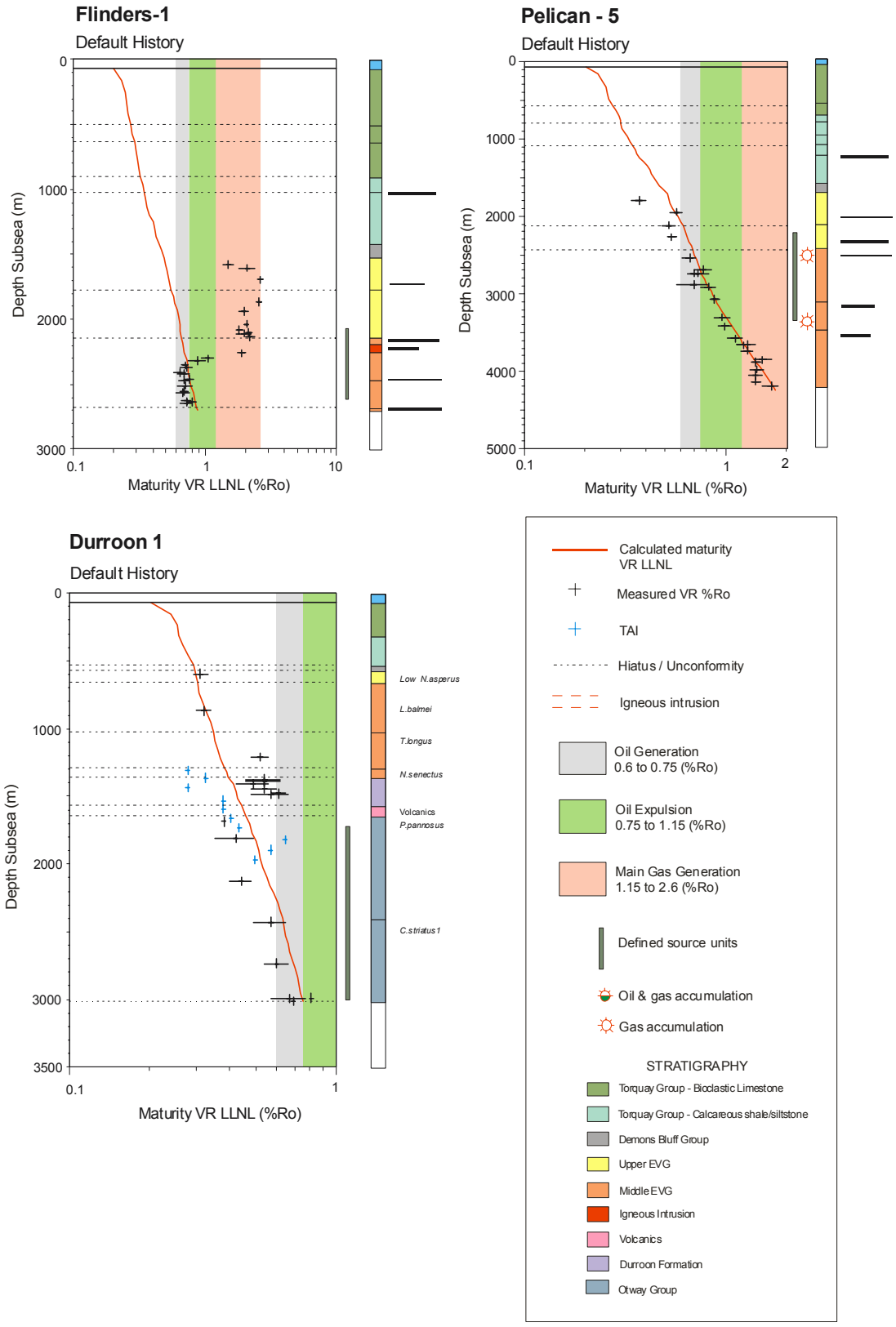


Figure 6.6 Depth at metres below seafloor (mbsf) to the 0.6% Ro isoreflectance surface (map modified from Lennon et al., 1999).

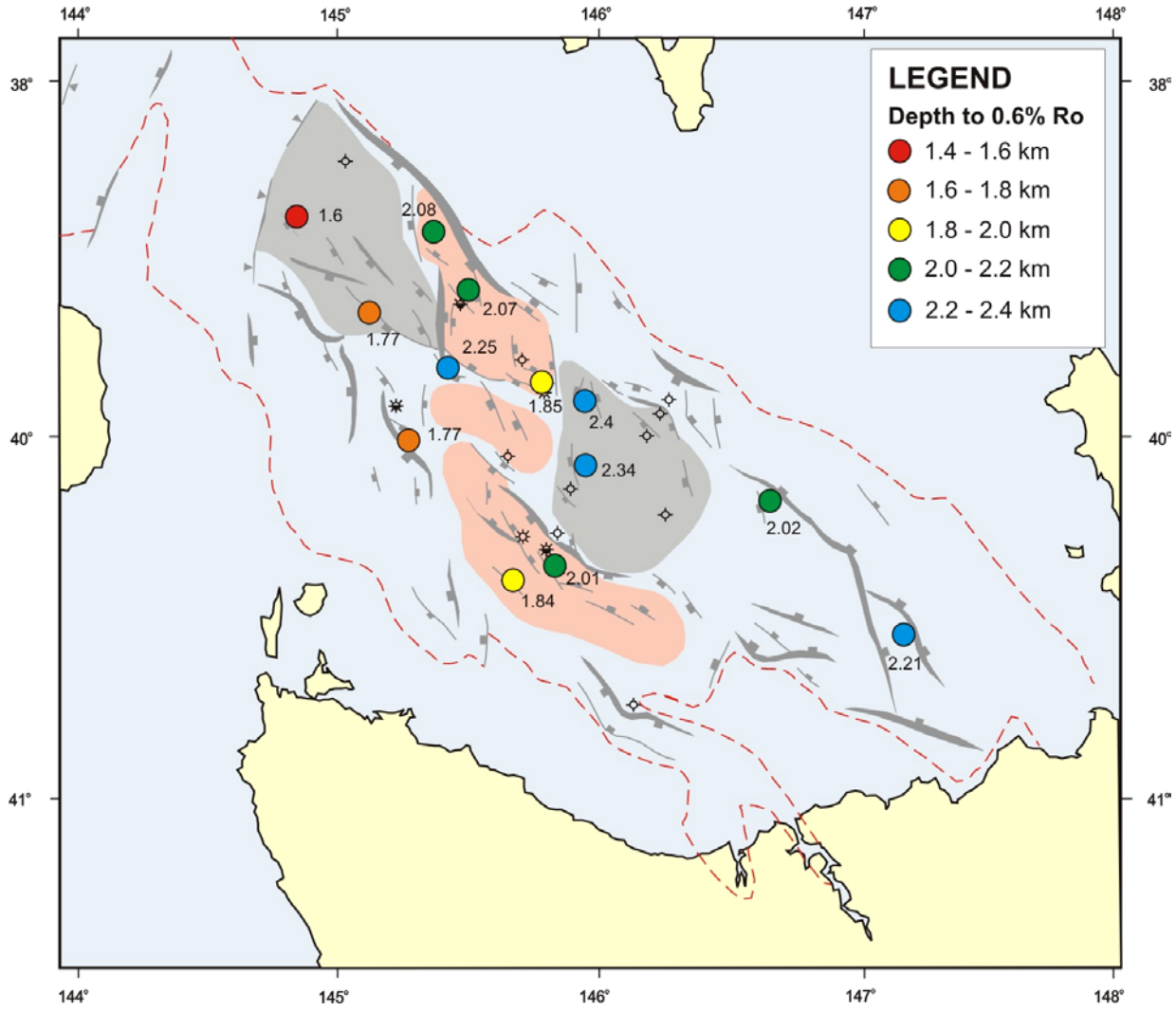


Figure 6.7 Depth (mbsf) to the 0.75% Ro isoreflectance surface (map modified from Lennon et al., 1999).

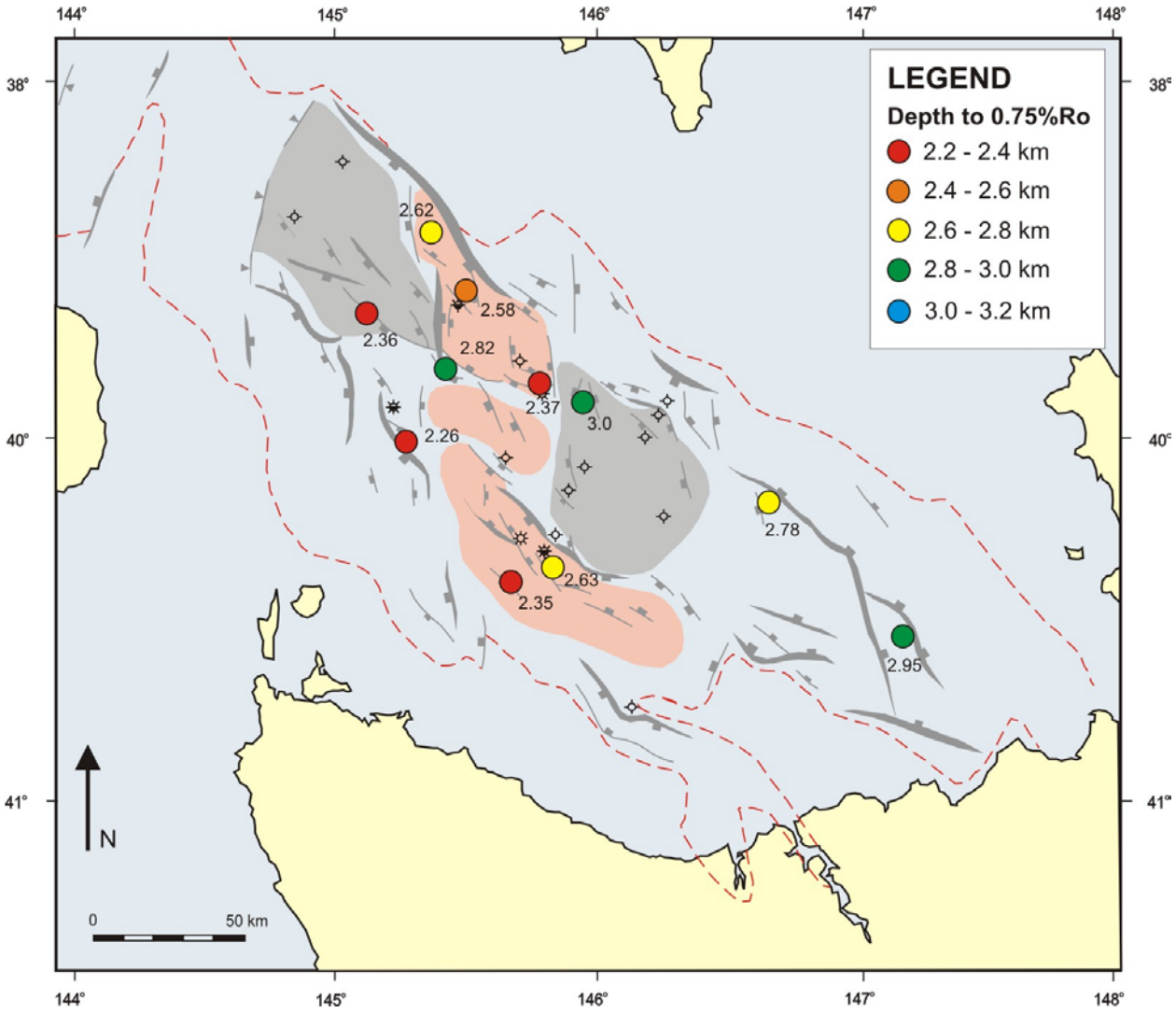


Figure 6.8 Areal variation in calculated maturity at 2000 mbsf (map modified from Lennon et al., 1999).

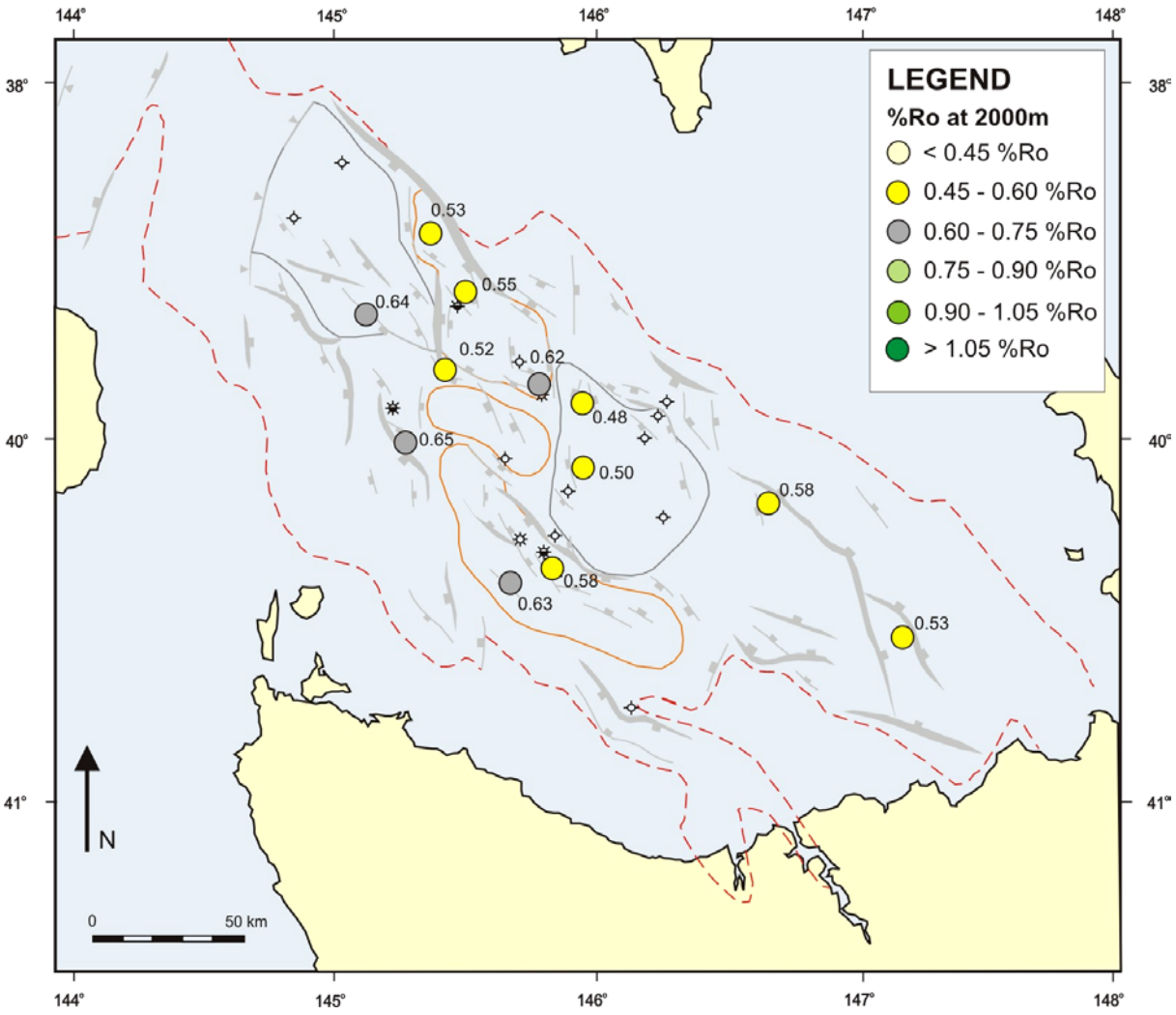


Figure 6.9 Areal variation in calculated maturity at 2500 mbsf (map modified from Lennon et al., 1999).

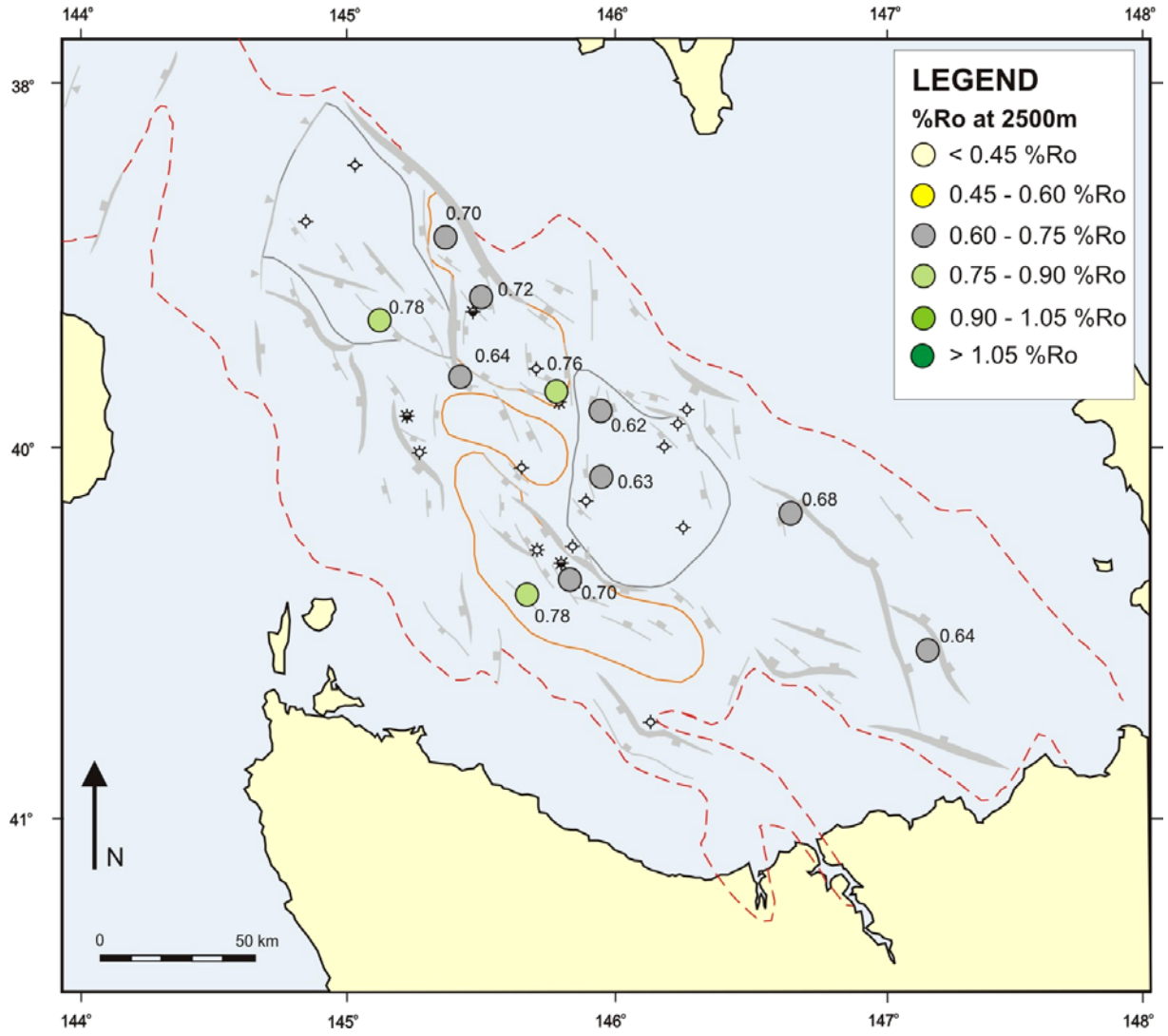


Figure 6.10 Areal variation in calculated maturity at the top of the Middle Eocene (top of the EVG; map modified from Lennon et al., 1999).

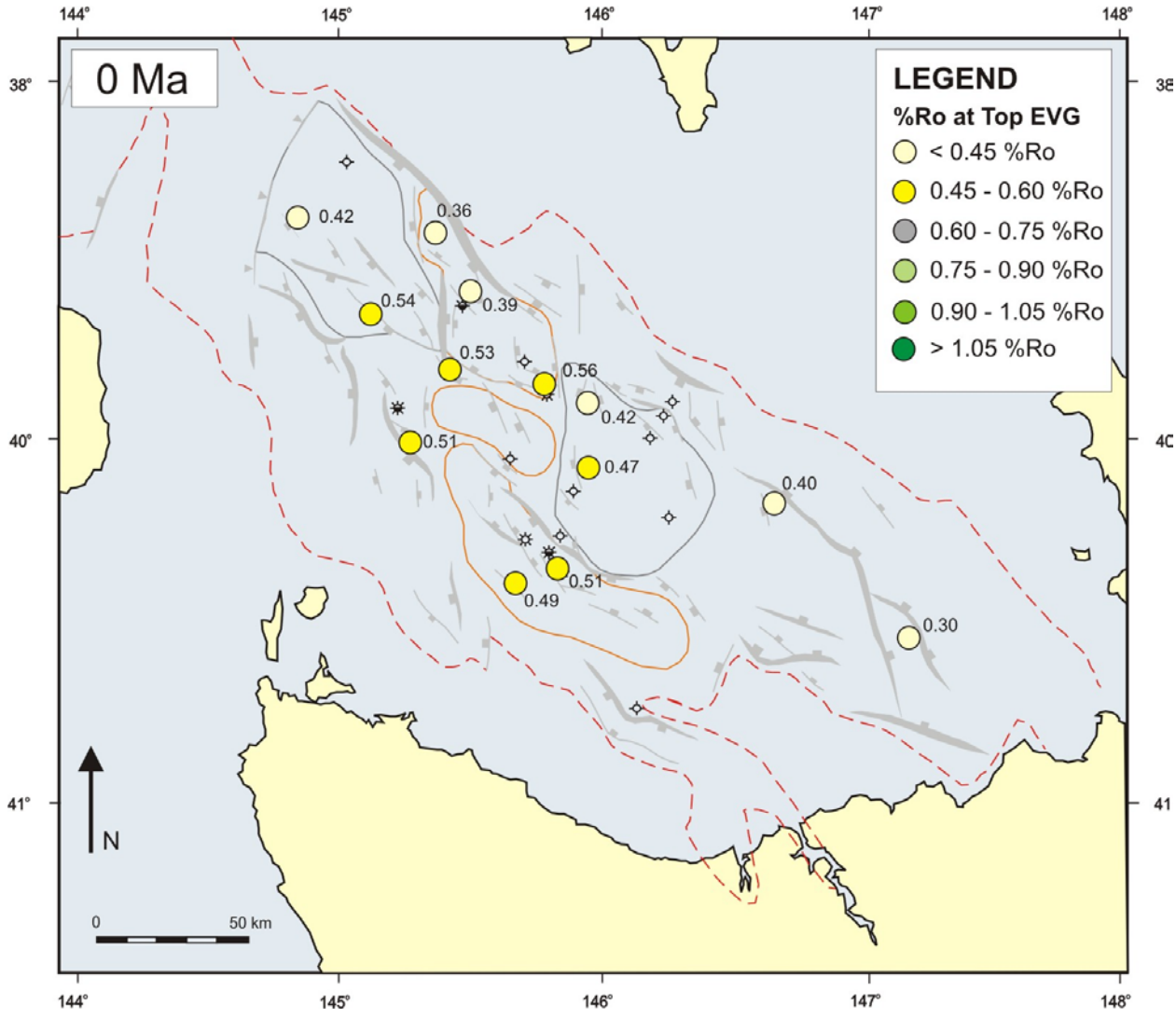


Figure 6.11a Areal variation in calculated maturity at the top Narimba Sequence (top of Middle EVG; top Middle *M. diversus* zone; map modified from Lennon et al., 1999).

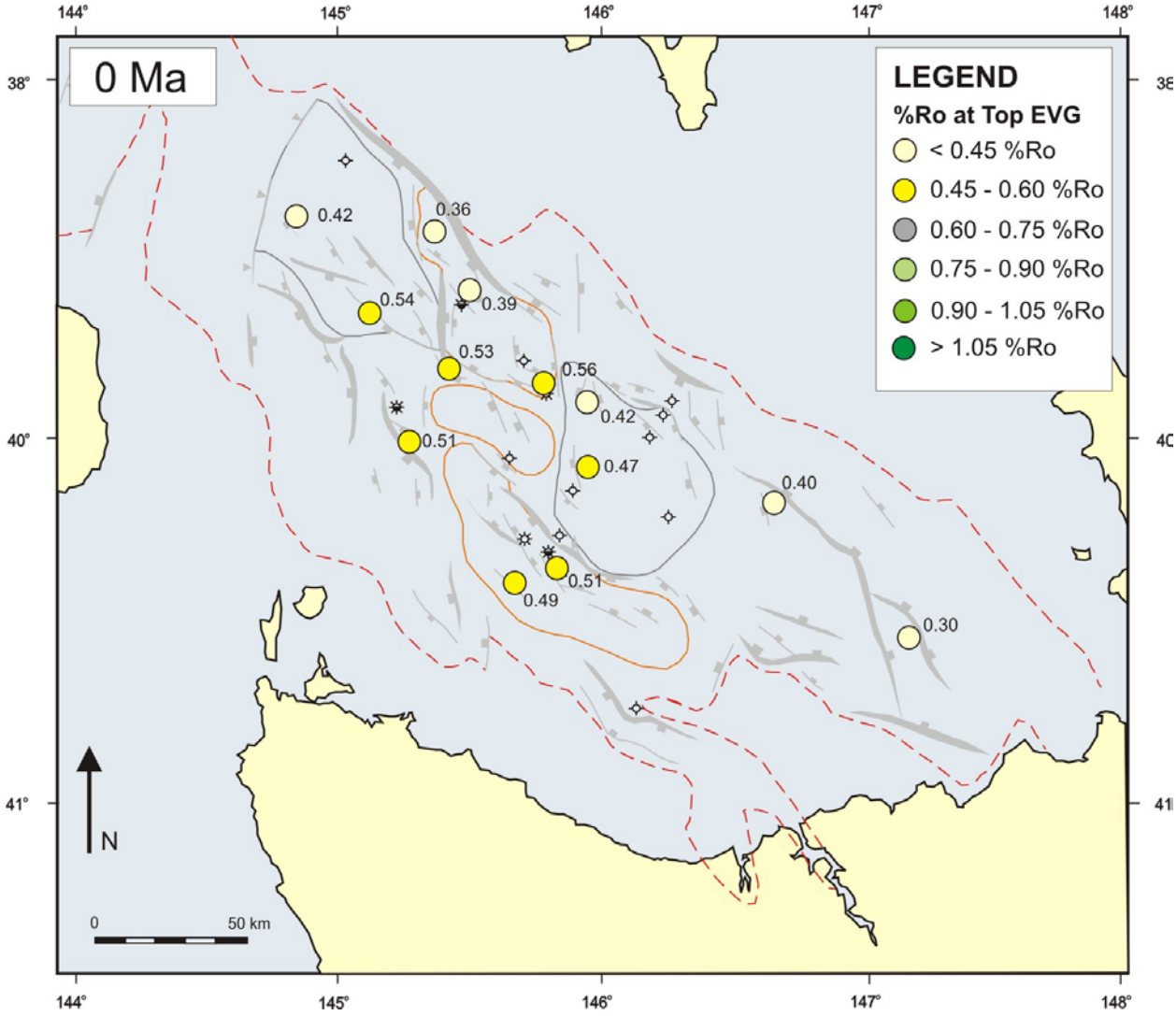


Figure 6.11b Areal variation in calculated maturity at the top of the Narimba Sequence at 15 Ma (top Middle EVG; top Middle *M. diversus* zone; map modified from Lennon et al., 1999).

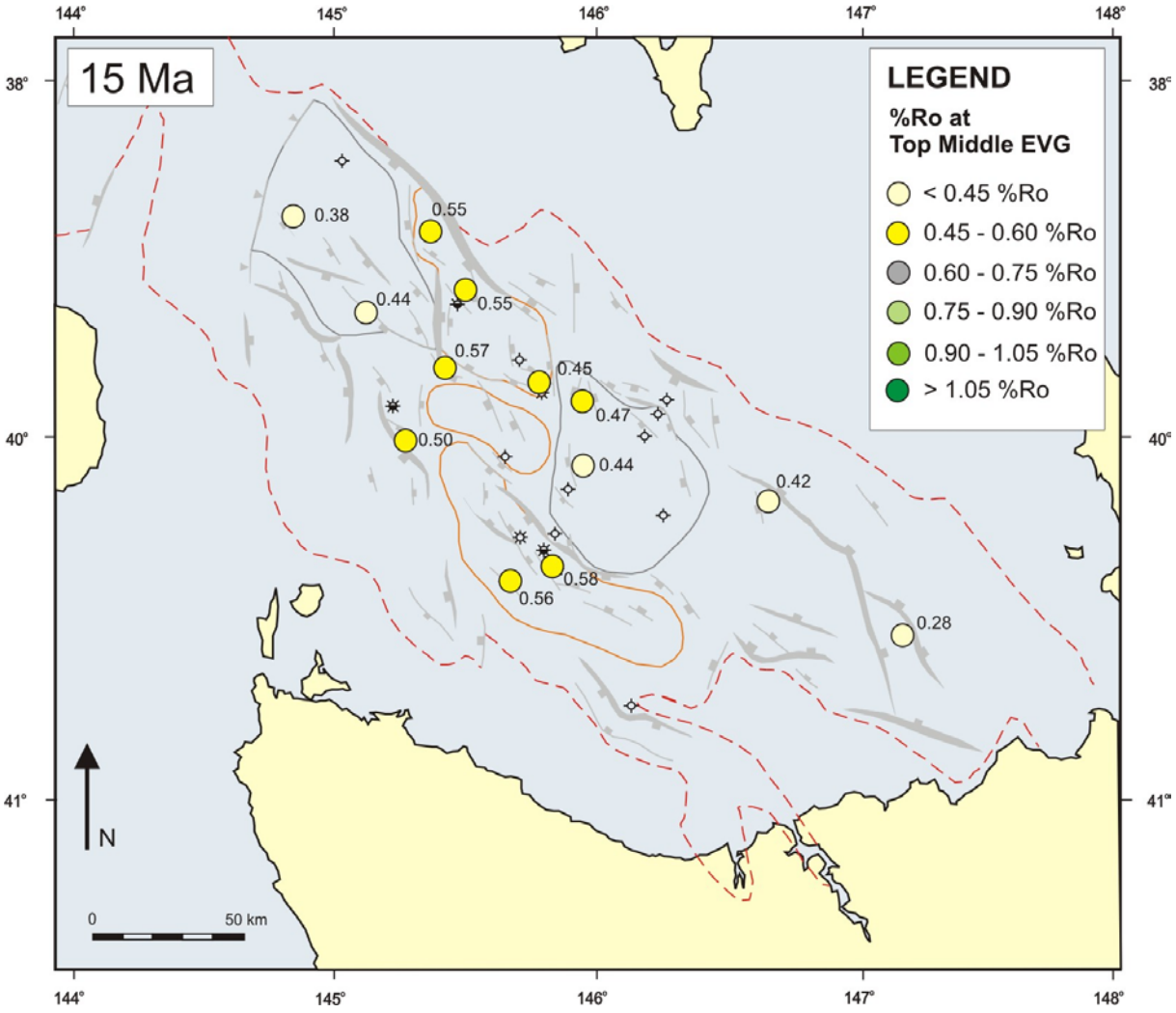


Figure 6.12a Areal variation in calculated maturity at the top Paleocene (top Lower *L. balmei* zone; map modified from Lennon et al., 1999).

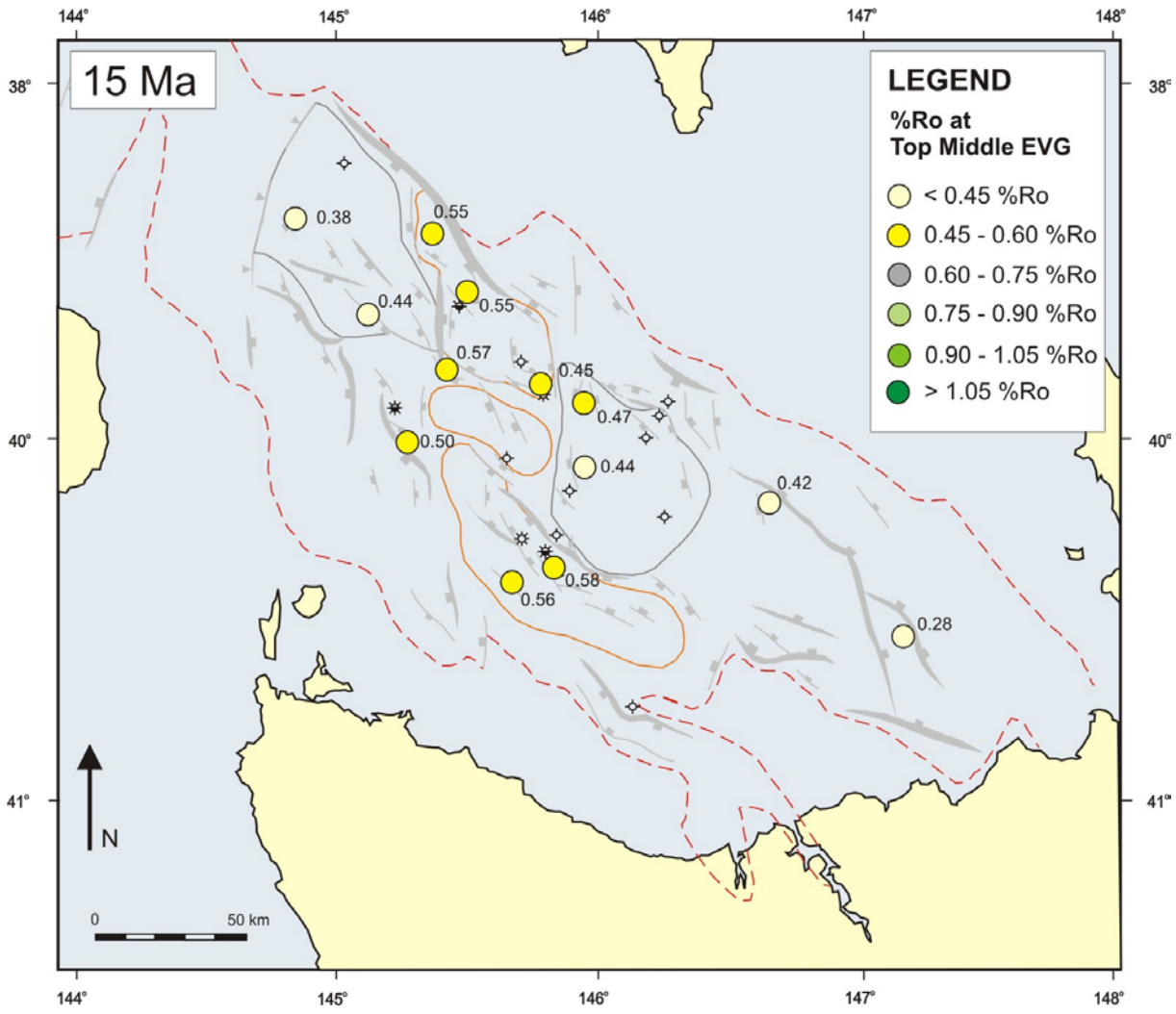


Figure 6.12b Areal variation in calculated maturity at the top of the Narimba Sequence at 15 Ma (Middle EVG; top of Middle *M. diversus* zone; map modified after Lennon et al., 1999).

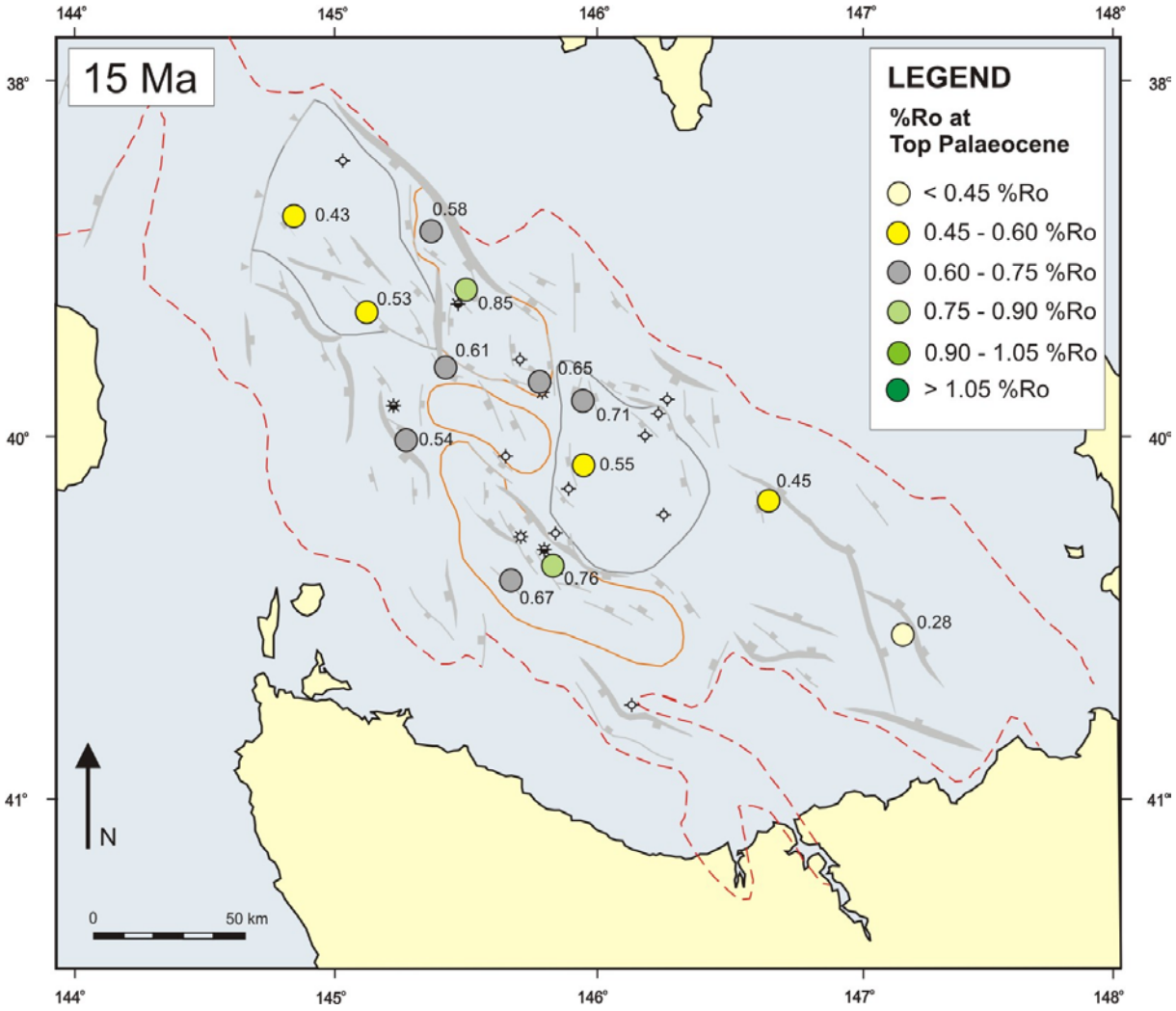


Figure 6.12c Areal variation in calculated maturity at the Narimba Sequence at 34 Ma (top Middle EVG; top of Middle *M. diversus* zone; map modified after Lennon et al., 1999).

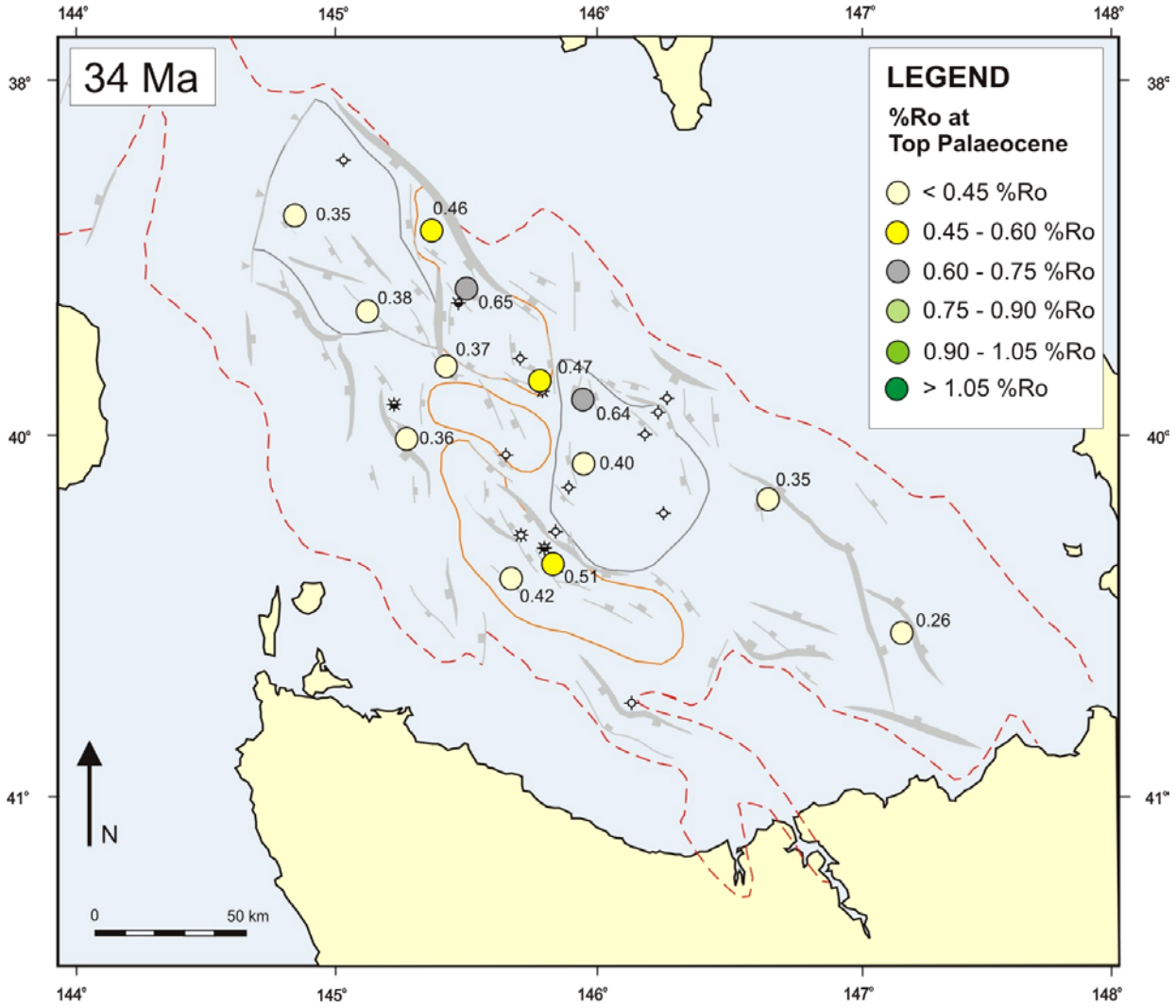


Figure 6.13 a) Palaeo-heatflow models derived from regional tectonic model. Model 1 shows a rapid increase in heatflow due to the Durroon Rift Phase (Tasman Rifting), followed by constant heatflow from the Paleocene onwards. Model 2 includes lower heatflow from the Paleocene and a late-stage heating event. b) Temperature through time with AFTA thermal history solution for sample L4-118 (3023 m) from Durroon-1. c) Maturity depth plots for palaeo-heatflow Models 1 and 2.

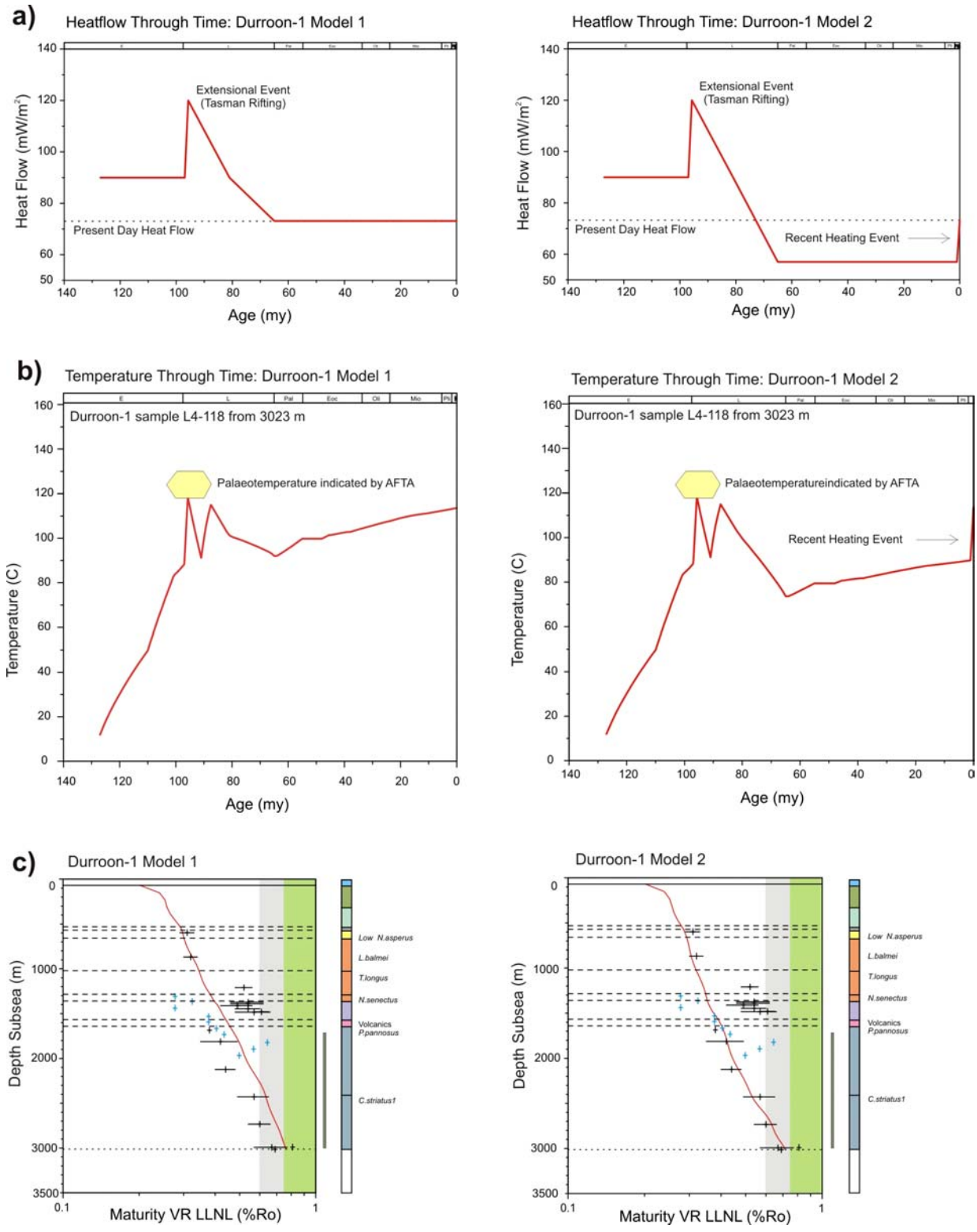


Figure 6.14a Default burial history and maturity models for wells studied, derived from the preserved stratigraphy. Amounts of uplift were estimated from seismic mapping.

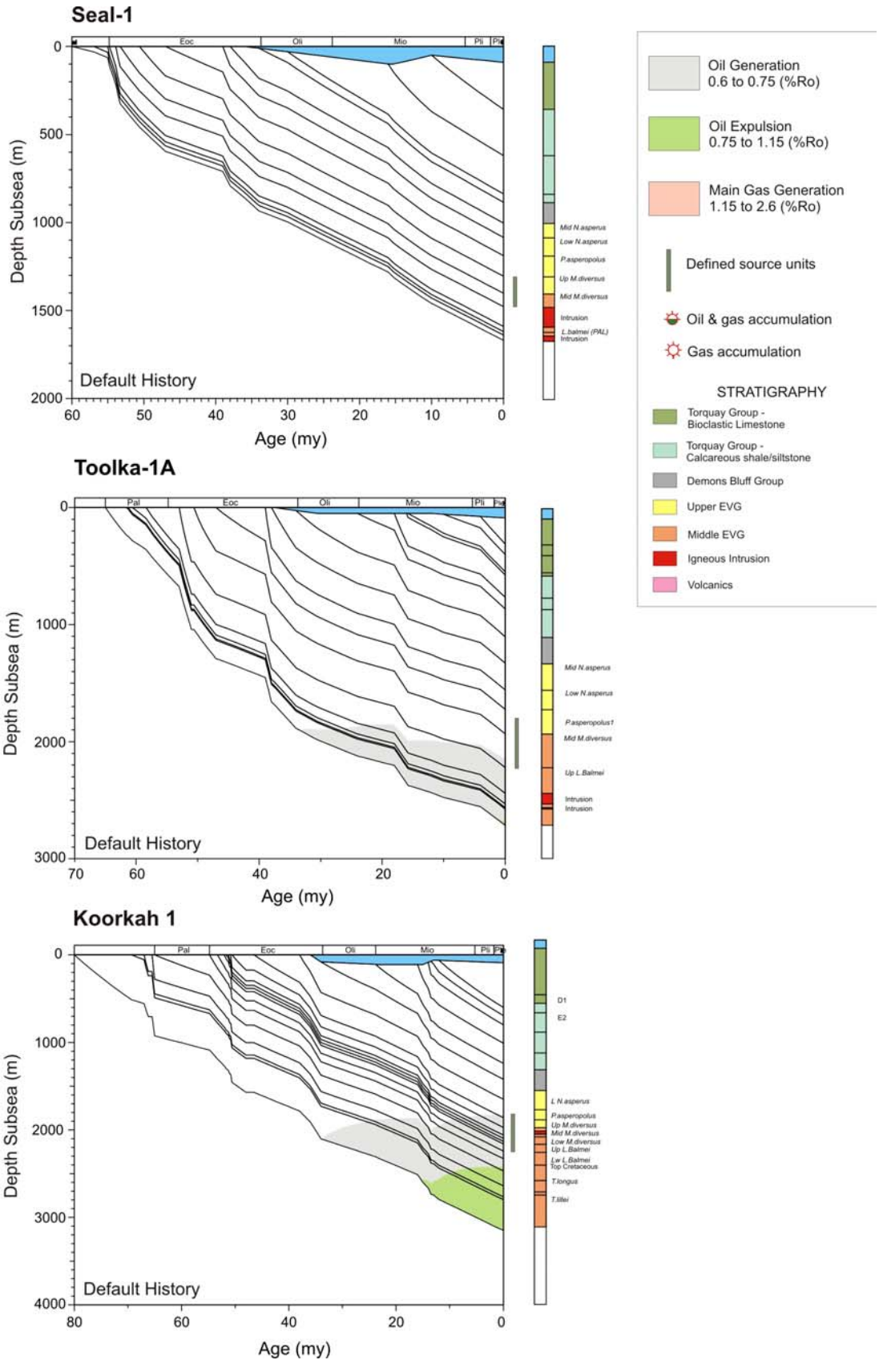


Figure 6.14b Default burial history and maturity models for wells studied, derived from the preserved stratigraphy. Amounts of uplift were estimated from seismic mapping.

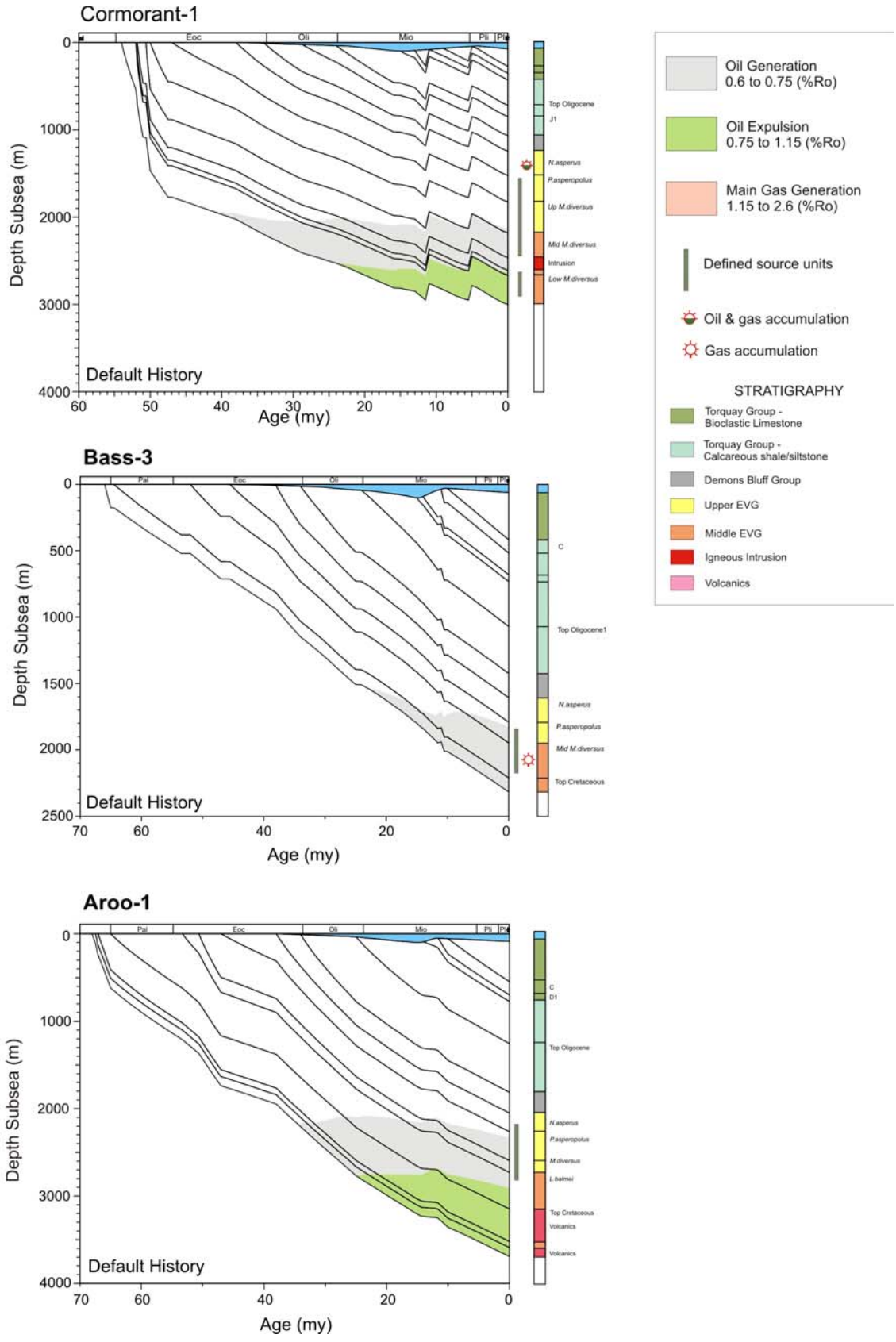


Figure 6.14c Default burial history and maturity models for wells studied, derived from the preserved stratigraphy. Amounts of uplift were estimated from seismic mapping.

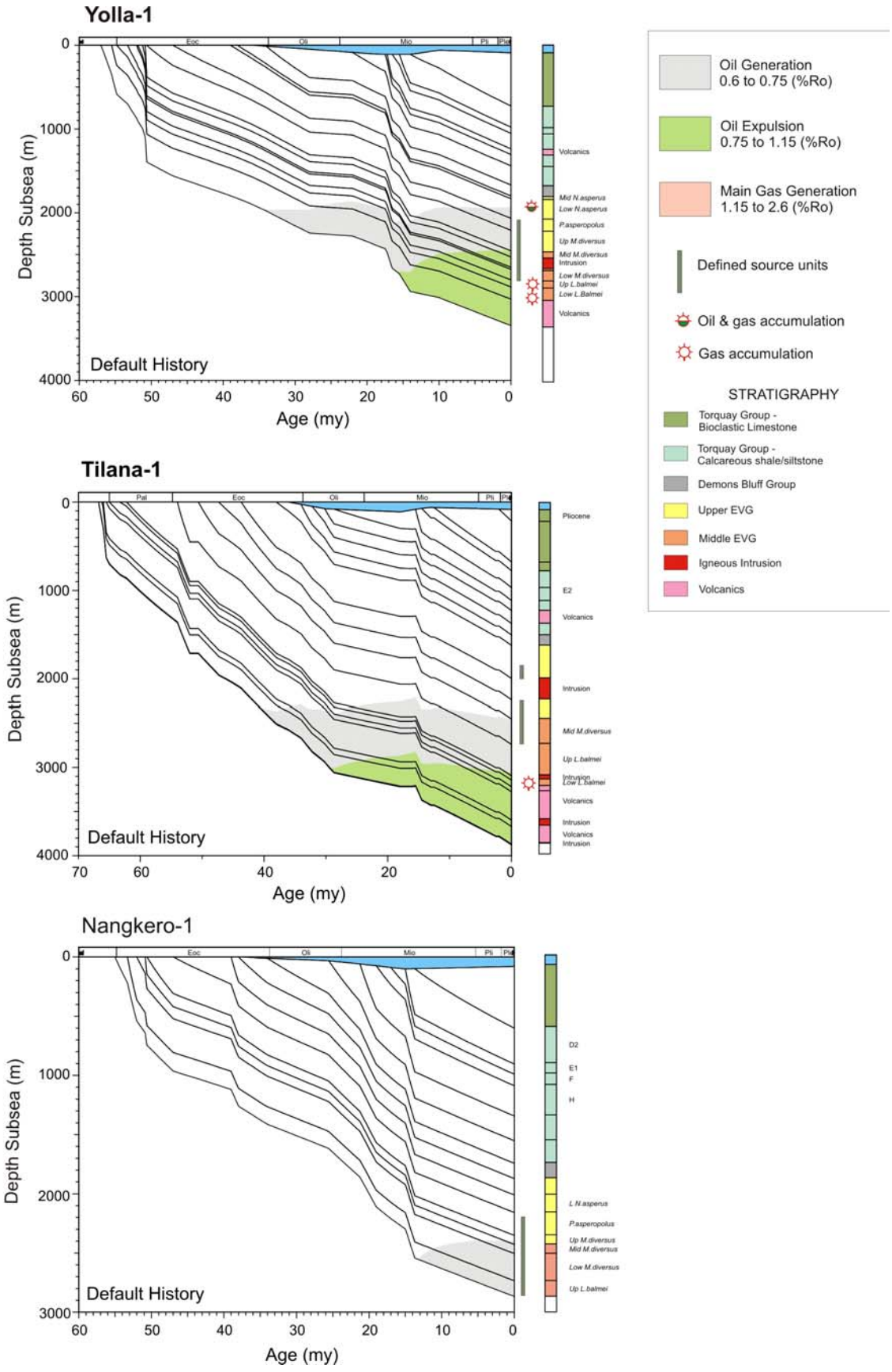


Figure 6.14d Default burial history and maturity models for wells studied, derived from the preserved stratigraphy. Amounts of uplift were estimated from seismic mapping.

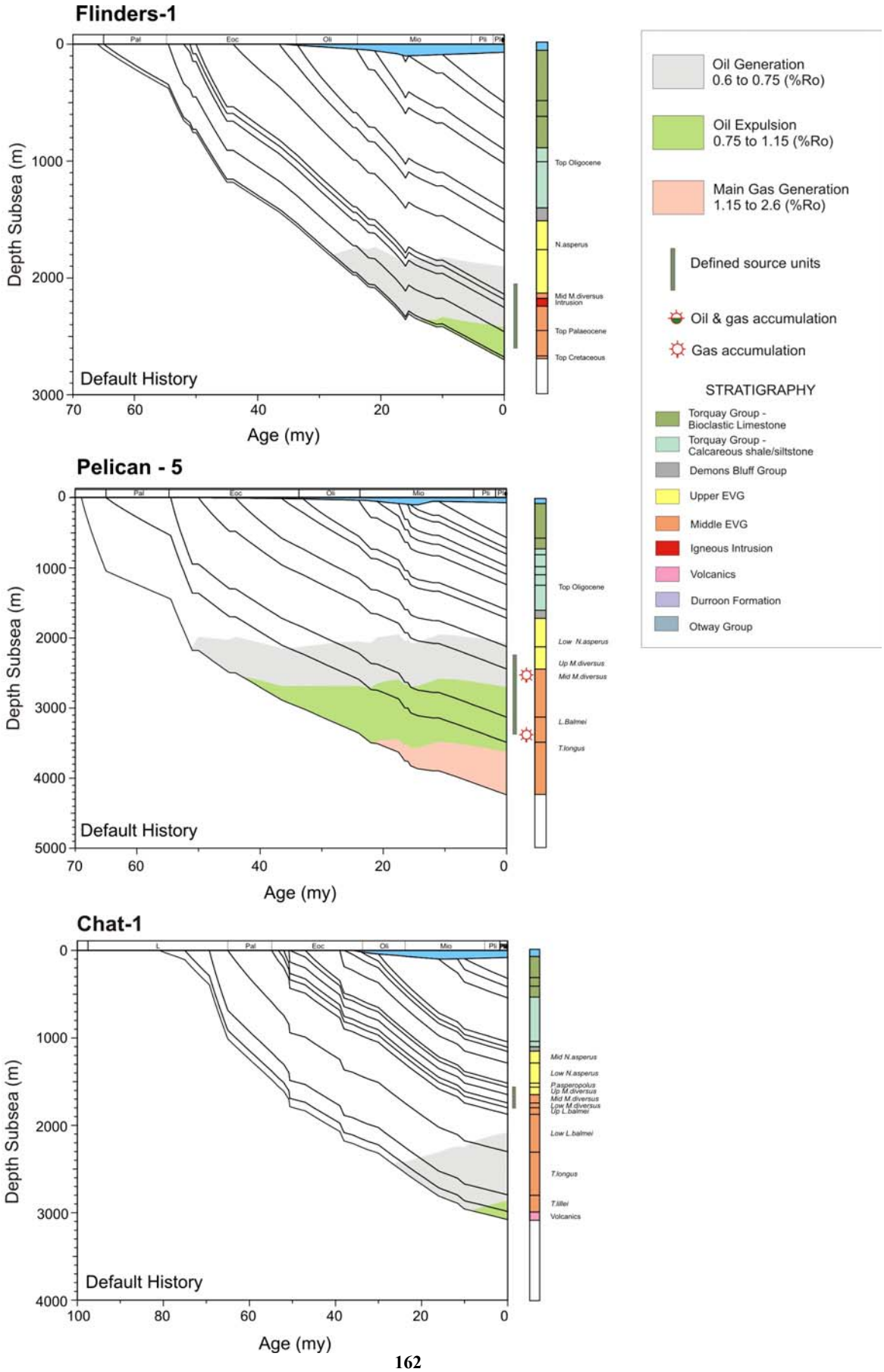


Figure 6.15 A) Subsidence and maturity curve based on Default Thermal History (DTH) for Durroon-1. B) Subsidence and maturity curve based on palaeo-heatflow Model 1 (see Figure 6.6). C) Subsidence and maturity curve based on palaeo-heatflow Model 2 (see Figure 6.6). The amount of mid-Cretaceous uplift was estimated from seismic mapping.

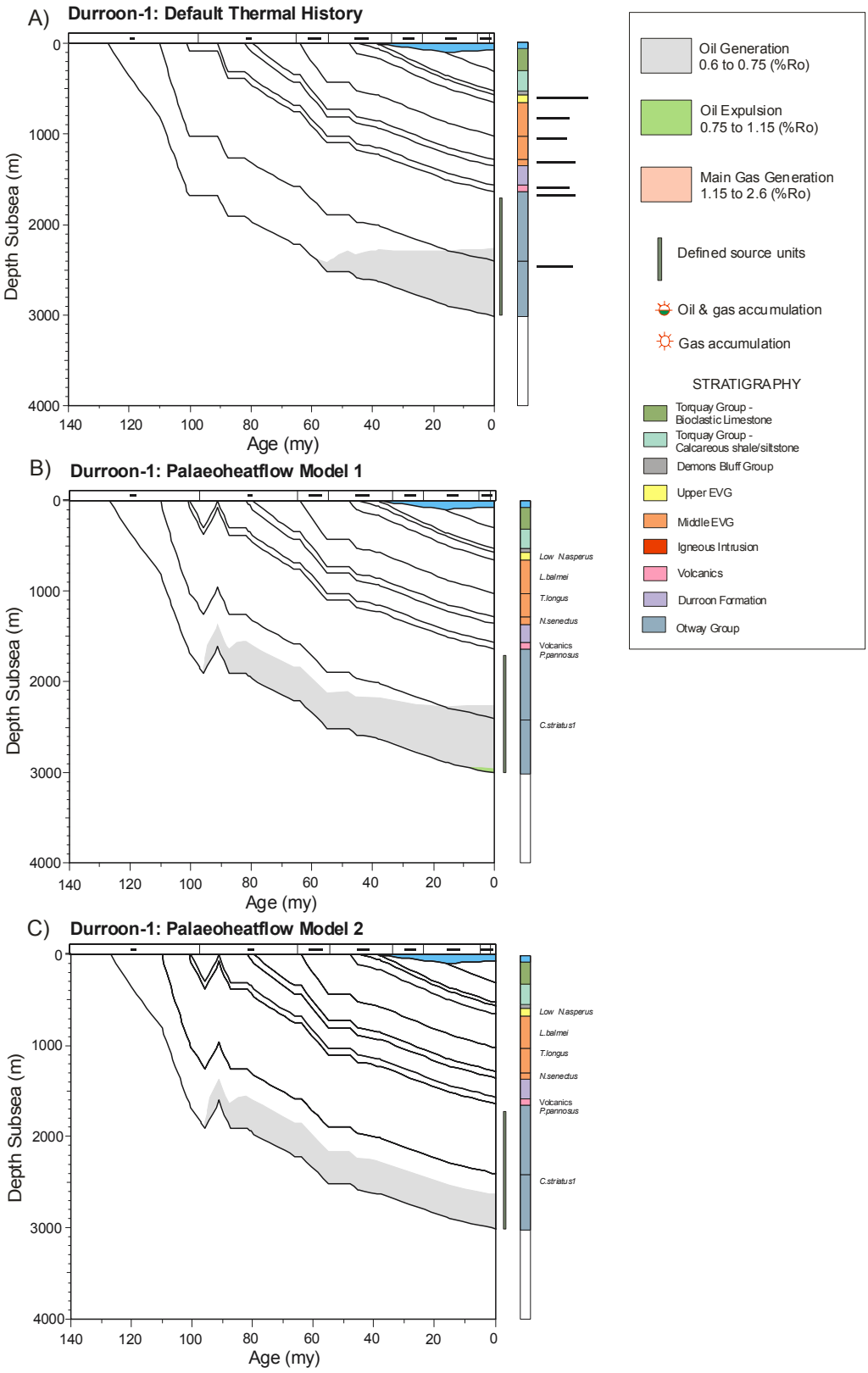


Figure 6.16 Subsidence and maturity curves for pseudowells in the Cormorant and Pelican troughs (extended at depth below Cormorant-1 and Pelican-5 wells with seismic control). Palaeo-heatflow defined from Durroon-1 Model 1 (see Figure 6.6). See Figure 6.4 for pseudowell locations.

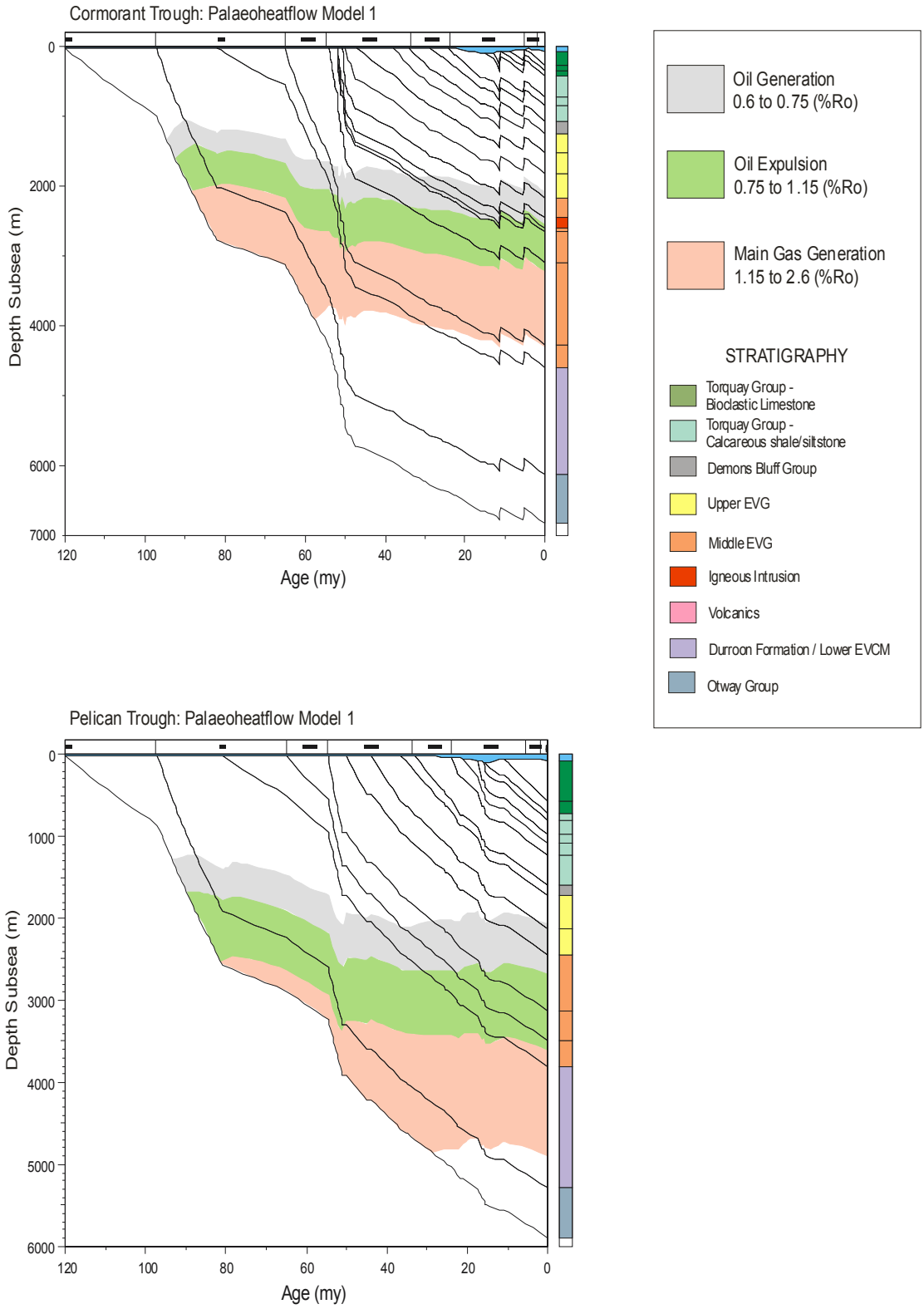
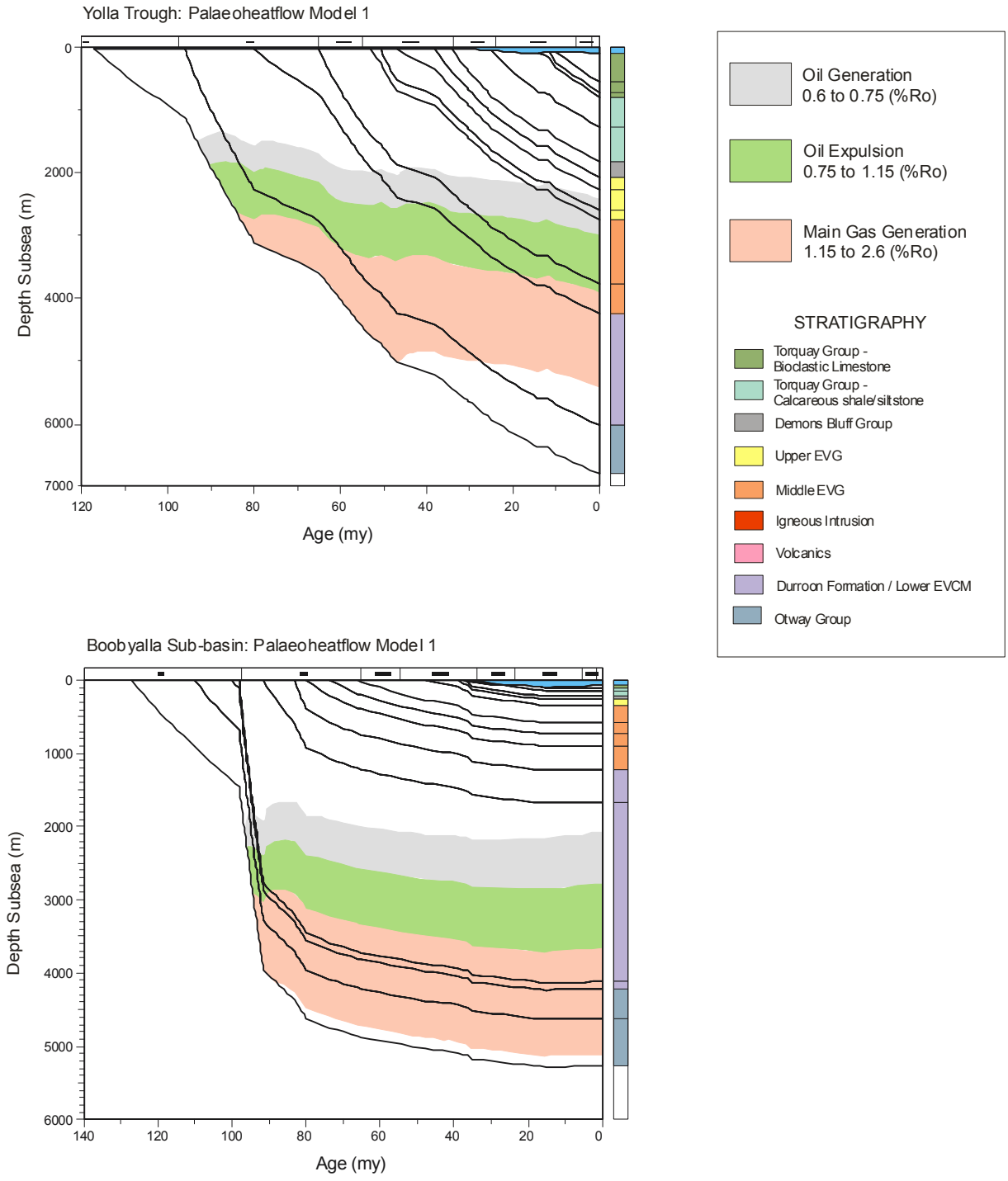


Figure 6.17 Subsidence and maturity curves for Yolla Trough and Durroon Sub-basin pseudowells (defined from seismic mapping). Palaeo-heatflow defined from Durroon-1 Model 1 (see Figure 6.6). See Figure 6.4 for pseudowell locations.



7. HYDROCARBON SEAL EVALUATION

R. Daniel, J. Kaldi and R. Root, National Centre for Petroleum Geology and Geophysics

7.1 KEY POINTS

The National Centre for Petroleum Geology and Geophysics (NCPGG) conducted a study to determine the seal capacity of 15 samples from eight wells in the Bass Basin, offshore Tasmania. The aim of the study was to assess the sealing capacity of the selected mudstones and siltstones by Mercury Injection Capillary Pressure (MICP) Porosimetry. The samples were taken from cores of potential sealing facies that ranged in age from Late Cretaceous to Late Eocene. Samples were collected as part of the facies analyses phase of the Bass Basin study (see Chapter 9 and Appendix M for core descriptions and environmental interpretations). Sensitivities to variations in contact angle, IFT and subsurface fluid density were included in the analysis. Capillary pressure results were used to determine seal capacities (hydrocarbon height retention), as well as pore-throat size distributions and height above free water (HAFWL) versus water saturation (Sw). Hydrocarbon column heights for oil and gas were calculated for each sample. A cross plot of depositional environments (Chapter 9) and seal capacities with varying sensitivities indicates that environments containing facies with significant sealing capacity are: a) lower and upper shoreface; b) interdistributary bays; c) lagoons; and d) stacked crevasse channels.

The sensitivities, in turn, were averaged for each sample for both oil and gas hydrocarbons. An average sealing capacity of all samples, based on the sensitivities for both oil and gas, were also plotted (Appendix L). The average column height of oil above freewater level for all samples is 605 metres (density 0.735g/cc) and a column height of 262 metres for gas (density 0.1 g/cc). The highest oil column (>1400 m) is supported by muds from the lower shoreface in Dondu-1 (2342 m). Lagoonal muds from Cormorant-1 (1999 m) will support an ~1140m column of oil, while the abandoned fluvial channel fills from Durroon-1 (3021 m) and Tilana-1 (2800 m) support >700m oil column. Coastal plain, fluvial overbank and back barrier berm deposits are the least significant sealing lithologies in this study, supporting <200 m oil columns. Details on the operation and quality control of the porosimeter, as well as a complete set of analytical results, are included in Appendix L.

Table 7.1 Samples from Bass Basin wells analysed by MICP.

Well Name	Depth, metres	Sample type	Rock type
Bass-2	1164	Core	Carbonaceous laminated siltstone/mudstone
Bass-2	1262	Core	Carbonaceous laminated siltstone
Cormorant-1	1999	Core	Laminated mudstone
Cormorant-1	2231	Core	Very-fine grained sandstone/siltstone

Dondu-1	2342	Core	Carbonaceous mudstone/siltstone
Durroon-1	3021	Core	Mudstone, very-fine grained sandstone
Pelican-5	2863	Core	Siltstone/sandstone
Pelican-5	2890	Core	Laminated siltstone
Poonboon-1	2474	Core	Carbonaceous laminated siltstone
Poonboon-1	2689	Core	Very-fine grained sandstone
Poonboon-1	3035	Core	Siltstone
Poonboon-1	3259	Core	Mudstone
Tilana-1	1667	Core	Carbonaceous siltstone, very-fine grained sandstone
Tilana-1	2800	Core	Carbonaceous mudstone
Yolla-2	3039	Core	Siltstone, very-fine grained sandstone

7.2 METHODOLOGY

Capillary Pressure

The samples were analysed using the Mercury Injection Capillary Pressure (MICP) techniques described in Appendix L. MICP involves forcing a non-wetting fluid (mercury) into the pore system of a cleaned and dried core sample. The mercury displaces the wetting phase (air) that initially saturated the pores within the rock. Surface forces oppose the entrance of the mercury and pressure must be exerted to enable the mercury to enter the pores and thereby displace the air (Purcell, 1949). The smaller the pore throats, the greater the pressure required for the mercury to enter the rock. Mercury saturation is commonly plotted as a function of mercury injection pressure.

Capillary pressure can be expressed as the relationship:

1. $Pc = 2\sigma \cos \theta / r$

Where: Pc = Capillary Pressure (psi)
σ = interfacial tension (dynes/cm)
θ = contact angle (degrees)
r = radius of capillary (microns)

MICP plots of sidewall cores and cuttings samples are presented in the first two graphs in each set of analyses (Appendix L). These display the data in a lognormal format from 0 – 60,000 psi against volume of mercury injected into the sample (the lognormal format is useful for differentiating data points in the low-pressure regime when analysing reservoir lithologies). The second graph displays plots of pressure against volume of mercury injected as a percentage (this is used for calculating the water saturation graphs) (Appendix L).

Using the following data for the air mercury system from Vavra et al. (1992), capillary pressure data were converted to effective pore throat size:

Air/mercury contact angle (θa/m) = 140°, and
interfacial tension (σa/m) = 480 dynes/cm.
σ(a/m) cos θ(a/m)= 370
1 cm = 10,000 µm, (microns)
1 psi = 69035 dynes/cm2

Solving for r in equation (1) results in the following relationship of capillary pressure to pore throat size:

1 psi = (approx.) 100 microns
10 psi = (approx.) 10 microns
100 psi = (approx.) 1 micron
1000 psi = (approx.) 0.1 micron

The cumulative pore-throat size distributions for the samples are presented in the third figure of the sample analysis set as lognormal size distribution (Appendix L).

7.3 WATER SATURATION

While MICP studies done solely for the purpose of determining pore throat radius and pore throat size distribution are valuable, there is even greater benefit in using these analyses to relate the rock types to saturations as a function of height above the FWL. The mercury/air capillary pressure system is used to replicate static distribution of hydrocarbons in the subsurface. The initial pressure at which the mercury first displaces the air is referred to as "displacement pressure" (Pd). In the subsurface, buoyancy pressure drives hydrocarbon (the non-wetting phase) movement and forces it into the pore throats of a rock, displacing water (the wetting phase). Buoyancy is simply the density difference between hydrocarbon and brine multiplied by the column height and a constant (k) gravitational factor, which is 0.433. The greater the column thickness, the greater the buoyancy pressure driving the hydrocarbon.

Pd in the reservoir system is the pressure at which hydrocarbon first entered the pore system by displacing the water. Different rocks with different pore throat sizes will have different displacement pressures and different saturations as a function of height (h) above the free water level (FWL). Thus, in any given reservoir section, the lowest indication of live (vs residual) hydrocarbon in a particular rock type approximates the displacement pressure (Pd) for that rock. The Pd can thus be considered as the hydrocarbon – water contact *for that particular rock type*. It should be remembered that a reservoir may have several hydrocarbon water contacts (as a function of pore properties controlled by rock type), but will have only one FWL. It is therefore of significance to determine the FWL.

In order to do this, capillary pressure data must first be converted to height above free water level information by using the equation:

2. $P_{cb/o} = h(\rho b - \rho o) \times 0.433$

   Where: $P_{cb/o}$ = Capillary Pressure (psi) reservoir brine/oil system

   h = height (in ft.)

   ρb = brine density (gm/cc)

   ρo = oil density (gm/cc)

In order to use the capillary pressure relationships to interpret real subsurface data in such a way, the data must first be converted from the air/mercury system used in the laboratory to the hydrocarbon/brine system in the reservoir. Laboratory analyses of fluid samples from well completion reports indicate the following reservoir fluid parameters for the wells:

Gas Density - 0.1 gm/cc

Oil Density – 0.735 to 0.797 gm/cc

Brine Density – 1.01- 1.05 gm/cc

No measurements for Contact Angle and Interfacial Tensions were available, so based on existing data from other samples in the region the following values were considered reasonable:

System	Contact angle (θ)	Interfacial tension (σ)
Brine/oil	5	15 dynes/cm
Brine/gas	0°	30 dynes/cm
Air/mercury	140°	485 dynes/cm

Once the capillary pressure values have been converted to h (height in feet), a plot of height versus mercury (non-wetting phase) saturations can be constructed. However, conversion of mercury (non-wetting phase) to hydrocarbon (non-wetting phase) will now result in a height versus hydrocarbon saturation plot. Since water (wetting phase) saturation is more commonly used in the oil and gas industry, the non-wetting phase

saturation needs to be converted to water (wetting-phase) saturation (Schowalter, 1979). This is done using the simple conversion:

3. Sw = 1 - Snw

   Where: Sw = wetting phase (water) saturation

   Snw = non-wetting phase (hydrocarbon) saturation

   Combining equations 2 and 3 results in a plot of height (above FWL)

   versus water saturation.

Saturation height functions were calculated using input parameters of the brine and hydrocarbon densities indicated in well completion reports. The conversion was run using a brine density value (1.01 gm/cc) and the oil density (0.735 to 0.797 gm/cc), and the Sw versus height functions were plotted on the fourth and fifth graph (linear and semi log formats, respectively) for each sample analysis (Appendix L). The height versus water saturation curves for each well were also plotted on a single graph for comparison, both in linear and semi-log plot (Appendix L).

7.4 INTERPRETATION OF SEAL CAPACITY

Table 7.1 presents a summary of average (oil and gas) heights determined for each of the 14 samples analysed. A summary of the water saturation curves for the samples from the Bass Basin is presented in Appendix L as a series of composite coloured graphs of normal (linear) and lognormal parameters. The average hydrocarbon height and displacement pressure is highlighted on each graph (Appendix L). The lognormal graphs are more definitive as a result of larger scale values in the lower height range. Sensitivities used for the study were determined from Bass Basin well completion reports, corroborated with data from adjacent areas.

The threshold or displacement pressure in the samples from the Bass Basin averages 5760 psia at 605 metres above free water level before it leaks off. This means that the sealing lithology will support a 605 metre column of oil with a density of ~ 0.735 gm/cc (or a 262 metre column of gas with a density of 0.1 gm/cc)

The results and interpretation of the analyses on sediments from the these wells (Table 7.1) can be viewed in terms of minimum hydrocarbon heights that can be supported by the sealing lithologies. The seal lithological samples were derived from a variety of depositional environments (Chapter 9), including: shelf, lower shoreface, foreshore-upper shoreface, back barrier lagoon/lake, lacustrine/marine shelf, back barrier berm, coastal plain, interdistributary bay/lake, interdistributary swamp/marsh, fluvial channel, fluvial overbank, stacked crevasse channel, fluvial overbank, and crevasse splays/channels.

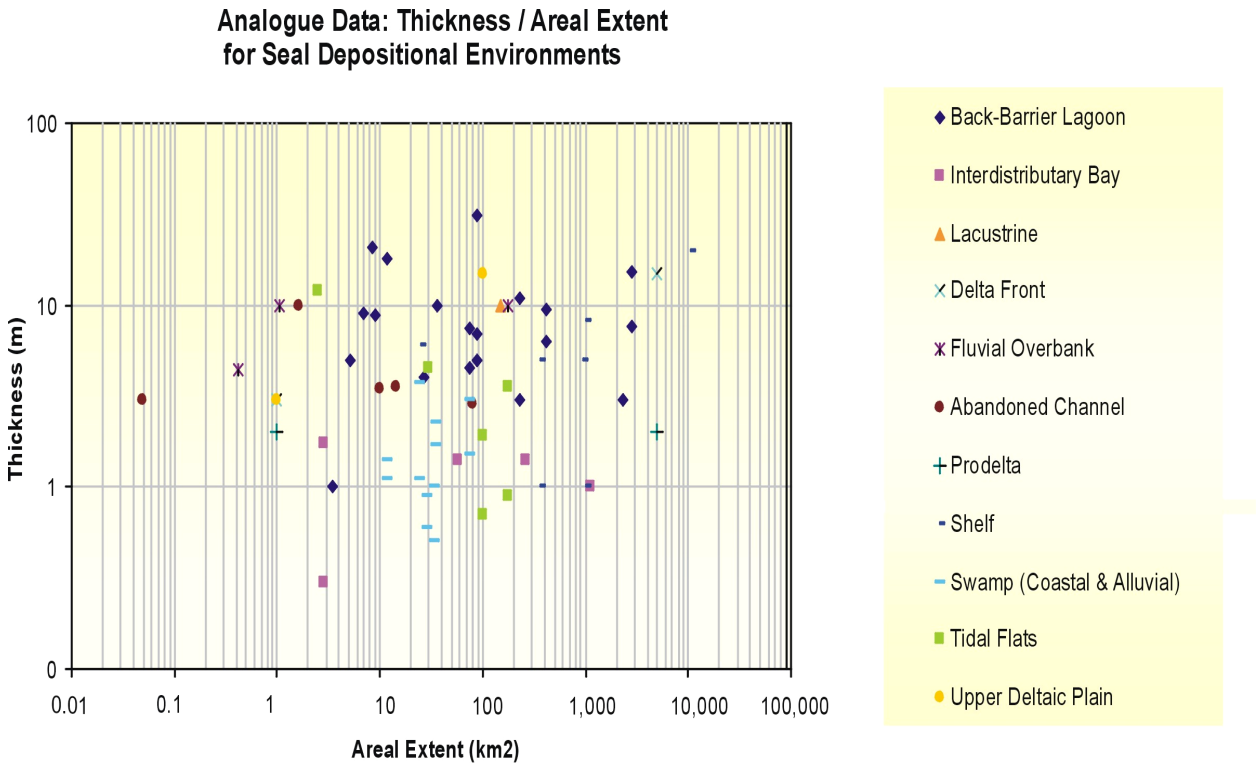
Plots of length versus width and area versus thickness of ancient and modern analogues of seal depositional environments (mudstone and siltstone lithologies) are presented in Figure 7.1. These diagrams highlight the spatial extent of the various depositional environments attributed to the potential sealing lithologies analysed in this study. Significant seal depositional environments determined from this study are lower shoreface (muds), lagoons (silty muds) and abandoned channel fill (silty muds). Based on modern and ancient analogues, the areal distributions of these environments are estimated at >1,000 km^2, 10-1000 km^2 and 1 km^2, with thicknesses of 1-30 m, 1-50 m and 5-10 m, respectively (Figure 7.1).

Table 7.1 Average hydrocarbon (oil and gas) heights for 15 samples from the Bass Basin.

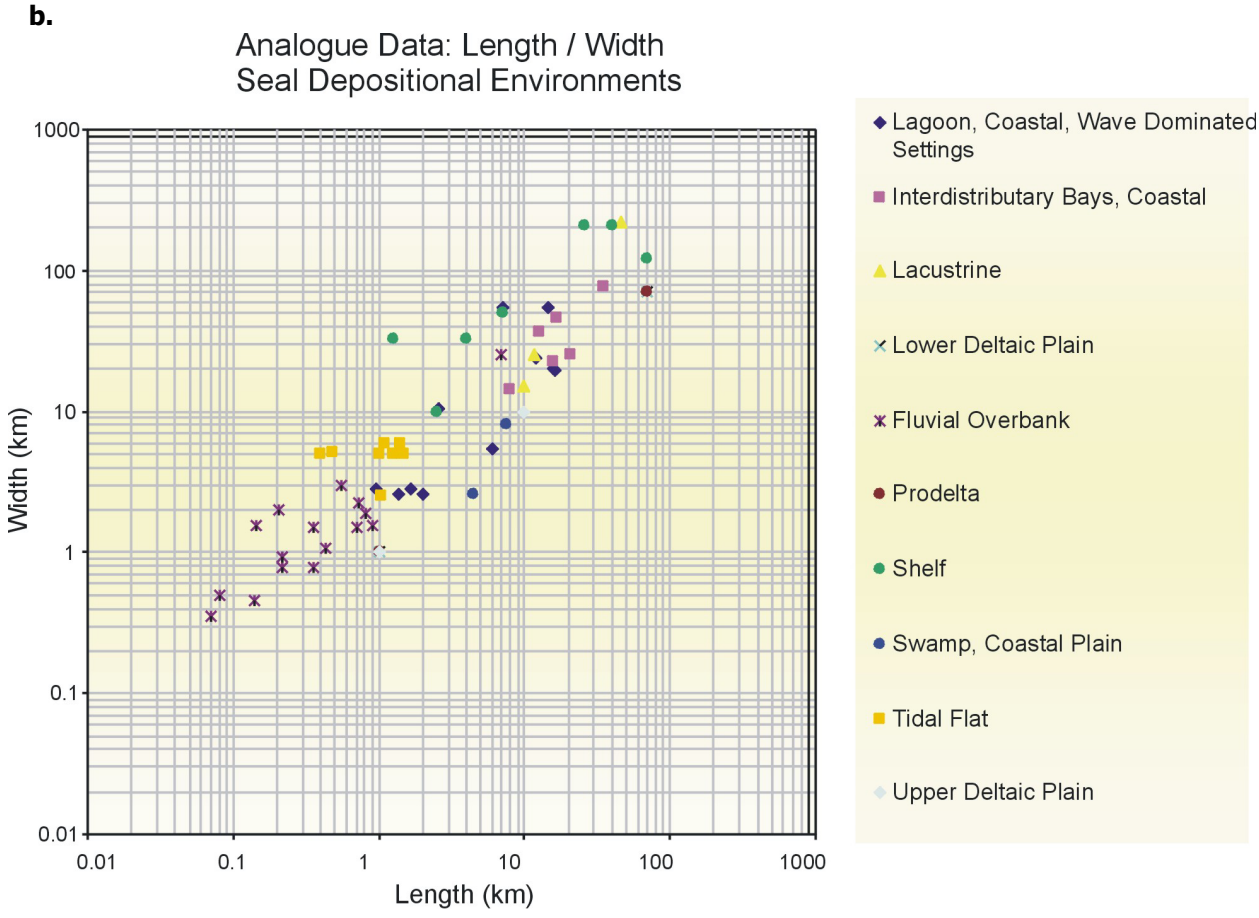
Sample, Depth and Environment	OIL WCR Data	OIL 46API, 1.01 brine	OIL 57API, 1.01 brine	OIL 61API, 1.01 brine	OIL 49API (av), 1.05 brine	Average Oil Height (m)	GAS 0.1g/c 15/0	GAS 0.1g/c 30/0	Average Gas Height (m)
Bass-2 1164.5 m Shelf	389	474	389	367	379	400	111	223	167
Bass-2 1261 m Coastal plain	160	169	142	135	154	152	44	88	66
Cormorant 1 1999.3 m Lagoon	1157	1344	1103	1040	1075	1144	316	631	474
Cormorant-1 2231.6 m Interdistributary bay	806	936	768	725	749	797	220	440	330
Dondu-1 2342 m Lower shoreface	1515	1609	1320	1246	1287	1395	378	756	567
Durroon-1 3021.9 Stacked crevasse channel	1073	1139	935	882	911	988	268	535	402
Pelican-5 2863.8 m Interdistributary bay	723	759	645	614	750	698	209	417	313
Pelican-5 2890.8 m Upper shoreface	882	927	788	750	916	853	255	509	382
Poonboon-1 2474 m Fluvial overbank	193	201	177	170	266	201	68	135	102
Poonboon-1 2689 m Back barrier berm	99	103	91	87	136	103	35	69	52
Poonboon-1 3035 m Interdistributary swamp	387	401	354	341	532	403	135	271	203
Poonboon-1 3259.8 Lacustrine	545	565	499	481	749	568	191	381	286
Tilana-1 1667 m	4	5	4	4	5	4	1	3	2
Tilana-1 2800 m Fluvial channel	947	998	838	795	911	898	259	518	389
Yolla-2 3039.5 m Fluvial overbank	578	406	474	447	462	473	136	271	204
Average	631	669	568	539	619	605	175	350	262

Figure 7.1 Plots showing the relationships between a) thickness and areal extent, and b) length and width for seal depositional environments (based on analogue data).

a.



b.



8. DIAGENESIS OF HYDROCARBON RESERVOIRS

N. Lemon*, National Centre for Petroleum Geology and Geophysics

**Present address: Santos Ltd, Santos House, 91 King William Street, Adelaide SA 5000*

8.1 KEY POINTS

- The lack of marine influence is one of the main differences between the reservoirs of the Bass and Gippsland basins. The Gippsland reservoirs are commonly clean, coarse, well sorted marine shoreline sands, while many of the Bass Basin reservoirs are silty, fluvial channels sands and lacustrine delta sands. The better reservoir sands in the Bass Basin are those where some marine influence is apparent.
- Cross plots of porosity against permeability, grainsize and various petrographic parameters show a series of cut off values below which good reservoir quality is unlikely. Permeability becomes negligible below 12% plug porosity. Observable thin section porosity is zero below 12% plug porosity. The cause of this discrepancy is due to the amount of microporosity within the abundant tightly-packed kaolin. Permeability drops below effective values in sandstones of smaller than medium grain size.
- A sequence of diagenetic events determined by previous authors has been updated. Early siderite cementation and compaction were accompanied by the first stage of quartz cementation. Dolomite cementation followed in parts of the succession where carbonate was available. Dolomite was subsequently replaced by ankerite in the deeper parts of the section. Dissolution porosity is the main form of porosity seen at depth.
- Cathodoluminescence reveals that the quartz cementation history was long and complex. A major pulse of quartz cementation took place after some dissolution of carbonate. It was accompanied by extensive alteration of feldspars to kaolinite and precipitation of kaolinite in adjacent pores. A late dissolution phase removed more dolomite, ankerite and siderite to create some porosity, but also allowed late compaction to reduce those pore spaces. Later illite formation diminished some permeability, but this was primarily a function of temperature and the depth of burial.
- Maps of heat flow determined from corrected bottom hole temperatures show considerable variation across the basin. This is particularly evident in the areas known to have been the focus of later volcanic activity. Steep lateral temperature gradients are apparent across the Pelican Field and several diagenetic events, such as the onset of illite formation, occur at shallower depths where the heat flow was raised.
- Reservoir quality in the Bass Basin is a function of the maturity of the original sediment, grain size, the degree of marine influence, depth of burial, heat flow and level within the stratigraphic succession. Silt-free sediments were more likely to develop and retain high quality reservoir properties. Only sandstones of medium grain size or larger were likely to retain effective reservoir quality. Marine influence during sedimentation removed silt and provided some carbonate that acted

as an early cement until removed by later dissolution processes. Raised temperatures facilitated the growth of illite which damaged permeability. All the favourable factors for high quality reservoir development were combined in the upper parts of the "Eastern View Group" (Aroo Megasequence), which fortuitously underlies the regional sealing facies of the "Demons Bluff shale".

8.2 DATASET AND PREVIOUS WORK

Sandstones of the Upper Cretaceous to Middle Eocene age 'Eastern View Group' (EVG) are the main hydrocarbon-bearing reservoirs in the Bass Basin. Previous studies of the diagenetic history of these intervals have been summarised from published material (Baillie et al., 1991; Cubitt, 1992; Meszoly et al., 1986; Zampatti, 1991), and supplemented with new evidence and interpretations to formulate the diagenetic history of the basin. This new evidence draws heavily on understanding key mineral relationships in thin section utilising transmitted light microscopy and cathodoluminescence microscopy (CL). Scanning Electron Microscope (SEM) micrographs and X-ray Diffraction (XRD) scans of all samples were also available through previous research projects undertaken at the National Centre for Petroleum Geology and Geophysics (NCPGG), University of Adelaide (Zampatti, 1991; Cubitt, 1992).

In addition, Baillie and Bacon (1989) presented results of a systematic study of depositional environments and reservoir quality of the Eastern View Group based on cores from exploration wells in the Bass Basin. This systematic approach was subsequently applied to additional wells in the basin (Baillie et al., 1991), and used by Zampatti (1991) and Cubitt (1992) in research projects at the NCPGG. Collectively, these reports provide consistent coverage of most core material available until the end of 1992, and form the basis for this report.

8.3 STRATIGRAPHY AND DEPOSITIONAL HISTORY

Coals of the Eastern View Group (also know as the "Eastern View Coal Measures"; EVCM) were deposited across the Bass Basin area (Figure 8.1). This succession shows indications of subaqueous sedimentation in the northwestern part of the basin. Sedimentation in this region was probably largely lacustrine with periods of marine influence occurring from late Middle Eocene onwards. Marine dinoflagellates are rarely observed in sediments of the EVG. Sandstone-capped, coarsening-upwards profiles overlying flaser bedded muddy sandstones, as seen in the Dondu-1 core (Figure 8.2; Baillie et al., 1991) are attributed to lake shoreline deposition.

Baillie et al. (1991) followed the informal subdivision of the failed rift part of the succession suggested by Robinson (1974), Smith (1986) and Williamson et al. (1987). They subdivided the Eastern View Group into a lower section of Late Cretaceous to Middle Eocene age comprising interbedded mudstone, sandstone, minor coal and volcanics, and an upper mainly Eocene interval, sandier and more coal-rich than below. Lennon et al. (1999) identify lower, middle and upper subdivisions, with a Cenomanian to Coniacian interval below a thick interval of volcanics in the middle EVG. These authors also use the "Eastern View Coal Measures" (EVCM) terminology rather than the "Eastern View Group" determination.

Coal percentage maps for time slices identified on palynological data were presented by Baillie and Bacon (1989) and Baillie et al. (1991). These show the coals were very patchy during the Cretaceous, but spread across the basin from the south during the Early Eocene, before contracting to the southern end of the basin by the Late Eocene. Baillie et al. (1991) used the nature of the coals and their contacts with the underlying rocks to suggest that the peat swamps were located on upper and lower delta plains marginal to large lakes.

8.4 DIAGENETIC HISTORY

A series of alteration, cementation, dissolution and compaction events have overprinted the sediments of the Eastern View Group in the Bass Basin (Table 8.1; Figure 8.3). Of these event, the precipitation and subsequent dissolution of dolomite, the formation of kaolinite and late compaction were the key modifiers of reservoir quality in the EVG. The events described here are similar to those described from the Permian coal measures succession in the Cooper Basin of South Australia and Queensland (Schulz-Rojahn and Phillips, 1989; Rezaee et al., 1997). The reducing conditions induced by the abundant organic matter, together with organic acids and generation of carbon dioxide formed during maturation of the abundant kerogen, were major controlling influences in both cases. The difference in the Bass Basin was the marginal marine influence that added additional carbonate to the succession.

A key factor in the diagenetic history observed by Cubitt (1992) was that the best reservoir characteristics in the EVG were in the Paleocene (lower *L. balmei* zone) sands of the "Middle EVG" (Lennon et al., 1999). Figure 8.1 shows the stratigraphic distribution of hydrocarbon recovered in the Bass Basin. Although the major reserves are in the upper part of the EVG, there are a number of occurrences in the Paleocene section, trapped by intraformational seals of the EVG. Cubitt (1992) reported porosities of 10-15% in places at this stratigraphic level. Whether those porosities were a function of the depth of burial, the temperature reached, or the nature of the sediments was not determined.

The study by Baillie et al. (1991) concentrated on the Lower EVG, as earlier work had suggested that sediments of the Upper EVG were thermally immature and that the muddy succession inhibited vertical migration of hydrocarbons. A purely statistical look at the reservoir quality in the Paleocene interval of the EVG is summarised by a series of cross plots produced by Baillie et al. (1991) from data relating specifically to Pelican-1 and Tilana-1 (Figure 8.4).

A plot of plug porosity against plug permeability shows a relatively tight "straight line relationship", and that permeability drops below 1 millidarcy (mD) at around 12% porosity. This drop in permeability is due to the abundance of kaolinite. Kaolinite booklets fill much of the primary pore space and replace feldspar grains. While the microporosity between the booklets is registered during routine core analysis on plugs, the kaolinite virtually blocks flow through the rock. Sandstones with less than 1 mD are unlikely to be effective reservoirs. A plot of thin section porosity against plug porosity (Figure 8.4) confirms the microscopic nature

of the porosity. Micropores are not easily recorded during examination of a thin section under transmitted light. The cross plot shows thin section porosity is negligible when plug porosity is still around 11-12%.

The plot of plug permeability against grainsize shows that the reservoir becomes ineffective (below 1 mD) when the grain size drops below medium sand sized. This appears to correspond with a drop in porosity as illite increases, but this is not a direct relationship. There is more total illite in the finer grained samples, present in the silty, muddy matrix. The porosity drop is a function of compaction facilitated by the clays and attendant organic matter, not by the precipitation of an illite cement. Similarly, the plot of plug permeability against thin section illite is a *de facto* representation of a grain size effect.

Each of the events listed in Table 8.1 and its likely distribution and influence in the basin is discussed with reference to the figures in the following section. The figures are a pictorial representation of the diagenetic events. Thin sections were chosen to show the biggest range of diagenetic events and to provide a direct comparison between similar environments of deposition (Figure 8.3).

Siderite Micrite

The earliest cementation event in the EVG is the precipitation of micritic siderite. Fine, golden crystals of micritic siderite rim the quartz and feldspar framework grains (Figure 8.5). Siderite ($FeCO_3$) contains ferrous iron (2^+ oxidation state) that requires reducing conditions to precipitate. Figure 8.5 shows the occurrence of abundant siderite within a siltstone layer and abundant organic matter associated with the finer sediment fractions. Figure 8.6, images collected only 0.5 mm from the edge of the lamina depicted in Figure 8.5, shows less siderite around the framework grains. The amount of siderite shown in Figure 8.7, two millimetres from the silty layer, is further from the silt fraction and associated organic matter. The micritic siderite is corrosive and etches the silicate framework grains.

Siderite Spar and Microspar

The micritic siderite provides a focal point for the precipitation of later siderite, which became coarser grained and less coloured (clearer) as the diagenetic history progressed. Microspar siderite grows on the micrite, eventually progressing to sparry siderite where porosity permits. In some cases, microspar siderite grows within altered and deformed grains. Figure 8.8 shows microspar siderite within a deformed muscovite flake. The lack of alignment of the siderite crystals suggests that they formed after the compactional deformation of the muscovite. The sparry types of siderite formed over an extended period of the diagenetic history of the EVG. The siderite deeply etched the quartz and feldspar grains to produce a distinctive scalloped edge to the grains.

Early Compaction

The silty layers within the EVG provide evidence of the earliest compaction event. Figure 8.9 shows stylolites that developed around organic matter. This relationship indicates that the organic matter and clays, which resided together within the sediment, catalysed the dissolution of silicate minerals. The organic matter was

insoluble, and therefore became concentrated along the dissolution seams. The clusters of siderite micrite are globular and do not appear to have been effected by compaction. The lack of compaction could indicate that either the early cement supported the rock against compaction, or that micritic cementation postdated compaction. While there is no clear evidence in the samples investigated, although other studies of coaly fluvial sediments indicate that siderite tends to form at or near the surface within the soil profile, usually before the rock has been buried or compacted.

Feldspar Dissolution

Cubitt (1992) and Baillie et al. (1991) described feldspar dissolution as a significant diagenetic process within the EVG sediments. While dissolution has occurred, it appears to be far less important than feldspar alteration in the modification of EVG reservoirs. The emplacement of dolomite cement etched silicate grains and had a particularly strong effect the feldspars grains (Figures 8.10 and 8.11). The subsequent dissolution of the carbonate phase created secondary porosity in the then skeletal feldspar grains. Feldspar dissolution is also implied by the relationships observed in Figure 8.12. For siderite spar to occur as a substrate below kaolinite indicates that the altered feldspar (in a composite granitic grain with quartz) must first have been dissolved.

Dolomite Cement

Some shallower samples from the EVG show complete cementation by dolomite. Meszoly et al. (1986) described these shallow carbonate cements as the "Bass Type", as distinct from the "Pelican Type", where dolomite was dissolved and kaolin precipitated in deeper parts of the basin. Figure 8.7 shows the that porosity which remained after early siderite cementation was later occluded by brightly luminescing dolomite. The bright colours under CL imply that the dolomite has a low iron content with respect to trace amounts of manganese which excite the CL response. The lack of colour banding in the dolomite (Figure 8.10) implies that the dolomite may have recrystallised. Faint banding in other samples (Figure 8.11) suggests that growth banding is present, although the distinction between early and later dolomite cements is minimal. The banding is of the order expected, with the brightest cement (lowest iron) rimming the substrate grains, and the slightly darker (a trace more iron) filling the remaining porosity. Dolomite cement is reported by Meszoly et al. (1986) and Cubitt (1992) as being more common in the coarser grained sandstones. This is not surprising, as the finer grain sizes may well have had pores occluded by siderite micrite or by early compaction induced by clays and organic matter. The emplacement of dolomite cement has deeply etched the framework silicate grains, quartz and particularly feldspar.

Ankerite Cement

Baillie et al. (1991) did not report dolomite in the samples they studied. Their work concentrated on samples from farther down in the EVG succession, and this may well be the reason for not recording dolomite. Ankerite, the ferroan form of dolomite, often forms after dolomite, at a greater depth or higher temperature. Increased temperature and depth of burial facilitate the dewatering of mudstones which released iron into the groundwater. The iron was then available for inclusion in the crystal structure of carbonates that form at

those levels. The high iron content of ankerite suppresses the CL response, so that these crystals appear black (Figure 8.13).

Previous studies of the diagenesis in the Bass Basin have reported strong evidence of dolomite dissolution. Figure 8.13 shows the ragged edges of dolomite crystals where secondary pores have been created prior to the emplacement of kaolinite cement. Many of the framework quartz grains at depth in the EVG show irregular edges from dissolution of carbonate. Figure 8.14 shows a good example of the scalloped edges produced when carbonate, which had previously etched the grains, is removed. If the dissolution were the result of aggressive formation waters, then all surfaces in the rock would have been attacked. The current evidence suggests that deep etching is sporadic with some grains untouched (Figure 8.14).

Quartz Cement

Cathodoluminescence (CL) is the key tool in understanding quartz cementation, with Figure 8.14 providing an excellent example of its use. The framework quartz grains are divided by colour. Those with a blue tint are, in this case, of igneous origin and show limited internal strain. Grains with a red and brown tint are of metamorphic origin and show a higher level of internal strain. These grains show only a thin overgrowth rim or a drusy surface, if present at all. The high level of strain means that the quartz is more susceptible to dissolution. The igneous grains, however, have a thick coating of overgrowth cement.

Early compaction has cracked some of the grains and the first phase of quartz cementation has healed these fractures. This is often a two-way relationship, as the compaction which cracked the grains also produced some of the silica that healed the fractures through pressure solution at the grain to grain contacts. Subtle banding is seen in the thick quartz cements. Figure 8.14 shows traces of kaolinite cement, all of which postdate the quartz cement and some of which filled the etched holes left by removal of a patchy carbonate cement. Despite the relationships observed in Figure 8.14, most of the quartz cement seen in samples from the EVG is intergrown with kaolinite booklets (Figure 8.15). Kaolinite, which responds with a bright mid-blue colour under CL, shows a jagged contact with all the dark purplish quartz overgrowths on the framework grains. The intergrowth of the two minerals indicates they were co-genetic. The most common reaction that produces both kaolinite and quartz at the same time is the alteration of feldspar. This can occur either under the influence of carboxylic acids produced during the maturation of kerogen, or under the influence of an excess of carbon dioxide, also probably a product of kerogen maturation.

Kaolinite Cement

As described previously, kaolinite formed at the same time as the majority of the quartz cement in the EVG. Patches of densely packed kaolinite booklets match the size and shape of framework grains (Figure 8.16). These are interpreted to be altered feldspar grains. Where these patches opened to original primary pores, more kaolin has grown, although these areas show some slightly different characteristics, such as larger booklet size or less dense packing. The kaolinite formed by alteration of the feldspars postdates the formation of micritic siderite, some sparry siderite, some quartz cement and feldspar dissolution. Pore-filling

kaolinite postdates dolomite dissolution, postdates most alteration kaolin and is co-genetic with the majority of each quartz overgrowth. Figure 8.17 shows several of the relationships of large patches of kaolin with quartz overgrowths and with dolomite and its dissolution.

The formation of kaolinite from the alteration or dissolution of feldspar has been frequently reported in the literature, often in the context of the development of secondary porosity (e.g., Siebert et al. 1984). Surdam et al. (1984) proposed a series of reaction pathways dependent on the balance of carboxylic acids and carbonic acid, i.e., the concentration of carbon dioxide. There was most likely a plentiful supply of carboxylic acids as a result of the kerogen maturation in the EVG, such that early feldspar alteration was likely to follow that process. Surdam et al. (1986) suggested that the result would be dissolution of feldspar. As alkalinity increased and carbon dioxide remained in the system, aluminium ions would be immobilised and the products of the feldspar reaction (kaolin) would remain in the rock. At high concentrations of carbon dioxide, feldspars would alter without the need for carboxylic acids.

Rock Fragmentation Alteration

Few of the rock fragments in the framework grain suite have retained their original mineralogy. Most fragments are now a mixture of kaolinite and illite. Figure 8.18b shows the characteristic speckled nature of this clays mixture under crossed polarised light. Once the rock fragments have been altered, they become soft and ductile. In this state they are easily compacted to block pore throats, and in many cases, completely block all porosity and impede permeability (Figure 8.18). This stage of compaction probably occurred progressively as the grains were altered. It is expected that the alteration of rock fragments was coincident with the alteration of feldspars, as kaolin is the main product in both instances.

Siderite Dissolution

Siderite dissolution is difficult to prove as there are no rocks that show dissolution with all siderite removed. However, circumstantial evidence shows porosity at depths well below that where primary pores are expected to be closed. These pores are often an amalgam of smaller pores that are the size and shape of areas/grains of micritic siderite and sparry siderite. Some dolomite and ankerite may have remained at these depths, but most of the dolomite was dissolved by the time pore-filling kaolinite was emplaced. Siderite is present in the tight areas depicted in Figures 8.18 and 8.19, but is absent from the open pores in those images. Siderite dissolution is brought about by low pH conditions, such as induced by an increase in carbon dioxide or carboxylic acids.

Late Compaction

Evidence that a late compaction phase postdated thick quartz cementation is shown in Figures 8.19 and 8.20. In Figure 8.19, a quartz grain with an overgrowth has a concavo-convex contact with another grain with its own overgrowth. The occurrence of overgrowth within the concave area is evidence of late compaction. Similarly, in Figure 8.20, a partly altered muscovite grain is wrapped around a quartz grain with a distinct overgrowth. The overgrowth is not complete along that contact as the softer grain probably

prevented growth along the contact margin. Compaction after the quartz overgrowth has resulted in the soft grain being wrapped around parts of the quartz grain.

The driving mechanism for late compaction appears to have been the dissolution of siderite and other carbonate phases that persisted in the rock to that stage. Dissolution was a significant event in that it created secondary pores at a depth where primary porosity is usually absent. The development of secondary pores was patchy and related to the amount of carbonate that was present. Similarly, the amount of late compaction was patchy and it destroyed most of the secondary pores. Effective secondary porosity is therefore a result of the percentage of pores created and the amount that were subsequently destroyed by compaction.

Late carbonate dissolution and compaction appear to be depth related, and the best examples are observed in the Pelican field. Heat flow and temperature contours are very tight in this area, with high temperatures and rapid lateral changes induced by igneous intrusives. The high temperatures may have played a part in carbonate dissolution by driving the maturation of kerogen to produce carbon dioxide. Alternatively, the intrusions themselves could have been responsible for dissolution through degassing and release of carbon dioxide into formation waters. Carbon dioxide released by the degassing of volcanics has been reported by Lennon et al. (1999). Carbon dioxide acts to facilitate the dissolution of carbonate cements, and could have been a key mechanism that brought about late compaction and the development of secondary porosity.

Illite Growth

This study did not recognise the late development of pore-lining and pore-bridging fibrous illite because the samples were not analysed under the Scanning Electron Microscope (SEM). However, previous studies that used the SEM (Baillie et al. 1991; Cubitt, 1992) proved conclusively the occurrence of late illite formation. Illite was observed within the pores and as small fibres attached to kaolin booklets (Baillie, et al., 1991). In these instances, illite fibres are likely to have significantly reduced permeability, even if their effect on porosity reduction was minimal.

8.5 THERMAL SETTING

Many of the diagenetic processes identified by previous authors and in this report are directly or indirectly dependent on elevated temperatures. Heat flow in the Bass Basin has been locally influenced by the occurrence of volcanic and intrusive rocks and by subsequent tectonic episodes. Downthrown extensional blocks and later uplift during inversion have also created rapid lateral changes in temperature. Figure 8.21 plots the distribution of heat flux through the basin as measured by an assessment of the bottom hole temperatures. There is a strong gradient from high temperatures in the southern basin, to lower temperatures along the northeast margin of the basin. A perturbation in this trend occurs in the vicinity of Dondu-1, Yolla-1 and Bass-2, and appears to be related to the localised occurrence of volcanic rocks (Lennon et al., 1999).

Wells that intersect intrusive sills, such as Yolla-1 and Koorkah-1 (Cubitt, 1992), show an increase in vitrinite reflectance profiles for up to 150 m on either side of the intrusion. Other local perturbations could be related to intrusions and volcanics rocks that occur nearby, but are not necessarily intersected by wells (Figure 8.21). A map of the temperature variations at 1000 m below sea level (Figure 8.22), shows the combined influence of structural movements, differences in thermal conductivity and possibly local intrusions. There is a very steep temperature gradient across the Pelican field, although this trend may be partly due to data distribution.

The raised temperatures localised over the Pelican field have meant that several of the diagenetic effects described in this report occur at shallower depths than elsewhere in the basin. Enhancement of reservoir qualities through dissolution of carbonate phases, especially siderite, occurs higher in the section (Cubitt, 1992). As previously mentioned, carbonate dissolution is brought about by the acidic conditions associated with raised carbon dioxide levels, either by maturation of kerogen or by degassing of nearby volcanics and intrusives. However, not all the events are positive in terms of reservoir quality. Through the transformation of smectite and potash alteration of kaolinite, illite growth is facilitated by high temperatures. Illite is particularly damaging to permeability as the fibrous growths of this mineral fringe the grains and bridge across pore throats. There is a balance between the creation of pore space through dissolution and the destruction of permeability through illite growth, as both are related to increased temperatures.

Figure 8.23 shows the temperature distribution across the basin at a particular choronostratigraphic interval (*P. asperopolus* zone). The *P. asperopolus* zone lies just above the top of the upper *L. balmei* zone, the stratigraphic level where many of the hydrocarbons are reservoired (Figure 8.1). High temperatures and a horizontal temperature gradient are evident over the Pelican field, as well as in the subsea depth map (Figures 8.22 and 8.23). While this may have degraded reservoir conditions in the Pelican field, several hydrocarbon shows were detected at this chronostratigraphic level in Poonboon-1, Bass-3 and Yolla-1, all of which are currently at lower temperatures. Clearly, temperature alone has not controlled reservoir quality.

8.6 SUMMARY

The Bass Basin has been a focus for hydrocarbon exploration since the discovery of giant oil and gas fields in the adjacent Gippsland Basin. Exploration success, however, has been more elusive in the Bass Basin despite a number of tantalising shows and smaller fields. These discoveries have been reservoired in the Upper Cretaceous to Eocene Eastern View Group (EVG) succession. The most promising hydrocarbon occurrences are concentrated in sandstones of *N. asperus* and Upper *L. balmei* age.

One of the main differences between the reservoirs of the Bass and Gippsland basins is the lack of marine influence. The Gippsland Basin reservoirs are commonly clean, coarse, well-sorted marine shoreline sands, while many of the Bass Basin reservoirs are silty, fluvial channels sands and lacustrine deltaic sands. The better reservoir sands in the Bass Basin are those where some marine influence is apparent.

Cross plots of porosity against permeability, grainsize and various petrographic parameters show a series of cut off values below which good reservoir quality is unlikely. Permeability becomes negligible below 12% plug porosity. Similarly, observable thin section porosity is zero below 12% plug porosity. The reason for these observations is the amount of microporosity preserved within abundant tightly-packed kaolin. Permeability drops below effective values in sandstones with grain sizes smaller than medium.

The sequence of diagenetic events has largely been determined by previous authors (Baillie, et al., 1991; Cubitt, 1992; Meszoly et al., 1986; Zampatti, 1991), however changes in their order have been highlighted by this study. Early siderite cementation and compaction were accompanied by the first stage of quartz cementation. Dolomite cementation followed in parts of the basin where carbonate was available. Dolomite was subsequently replaced by ankerite in the deeper parts of the stratigraphic succession. All authors report the dissolution of dolomite and ankerite. Dissolution porosity is the main type of porosity observed at depth. Cathodoluminescence studies have revealed that the quartz cementation process was both long and complex. A major phase of quartz cementation occurred after some dissolution of carbonate. It was accompanied by extensive alteration of feldspars to kaolinite and the precipitation of kaolinite in adjacent pore spaces. A late dissolution phase further removed dolomite, ankerite and siderite. This late dissolution phase resulted in some increase in porosity, but also allowed a reduction in pore space due to late compaction. There was some late illite formation which diminishes permeability, but this process appears to have been a function of temperature and depth of burial.

Maps of heat flow (determined from corrected bottom hole temperatures) show considerable variation across the basin. This variation is evident in areas affected by volcanic activity. Steep lateral temperature gradients are apparent across the Pelican field, and several diagenetic processed, such as the onset of illite formation, occurred at shallower depths where the localised heat flow was raised. It is likely that other variations in the heat flow gradient also occur due to igneous activity, however data density is insufficient to clearly define this trend.

Reservoir quality in the Bass Basin is a function of the maturity of the original sediment, the grainsize, the degree of marine influence in the sediment, the depth of burial and the heat flow, and stratigraphic level. Present-day good quality reservoirs were originally free of silt. Only sandstones of medium grain size or larger are likely to have retained effective reservoir quality to the present day. Marine influence during deposition acted to remove silt from the sediment, and provide carbonate to act as an early cement that could subsequently be removed through dissolution. Raised temperatures that facilitated the growth of illite has damaged permeability. The best conditions for reservoir development and preservation occurred in sediments of the "Upper EVG", just below the regional sealing facies of the "Demons Bluff" shale.

Table 8.1 Stratigraphic column for the Bass Basin, including information on hydrocarbon accumulations and shows. A reference column from Lennon et al. (1999) is also shown.

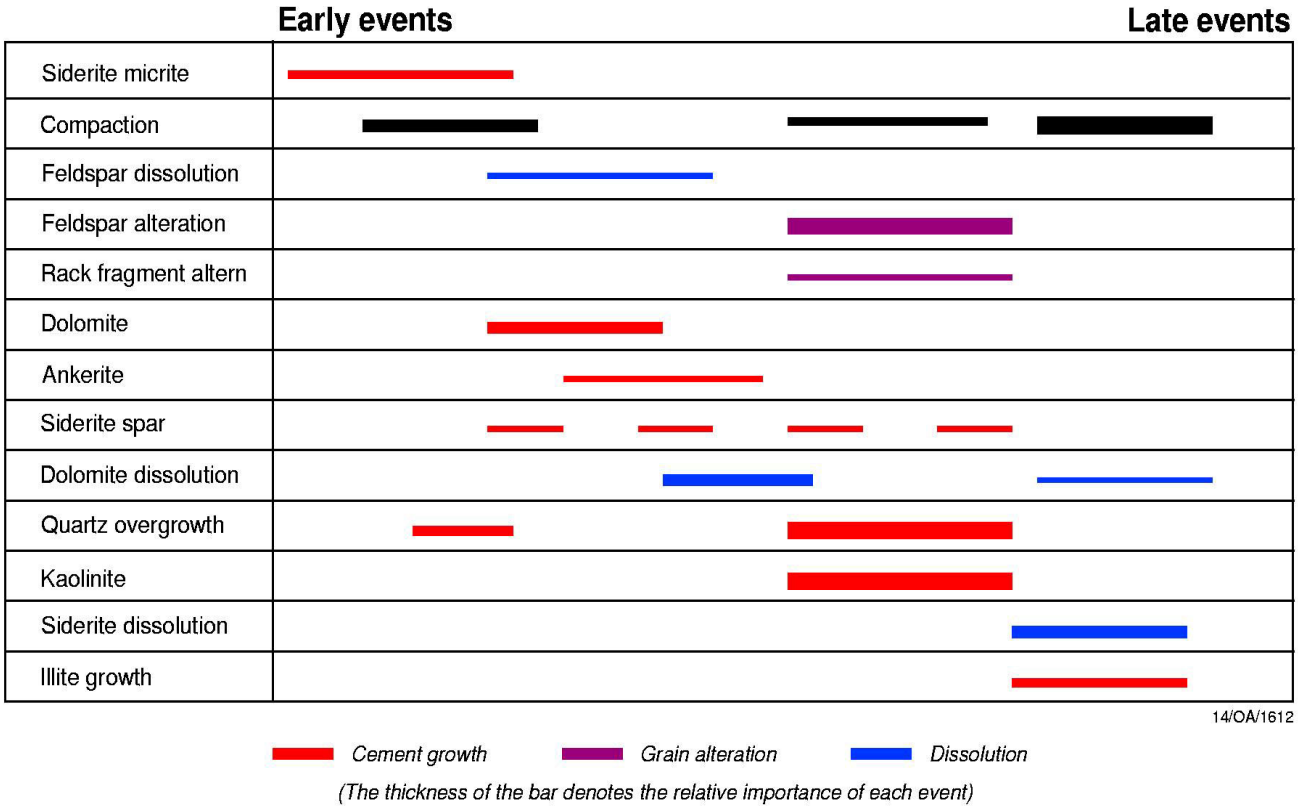


Figure 8.1 Stratigraphic chart for the Bass Basin using the nomenclature scheme of Lennon et al. (1999). The distribution of hydrocarbon accumulations and shows are indicated.

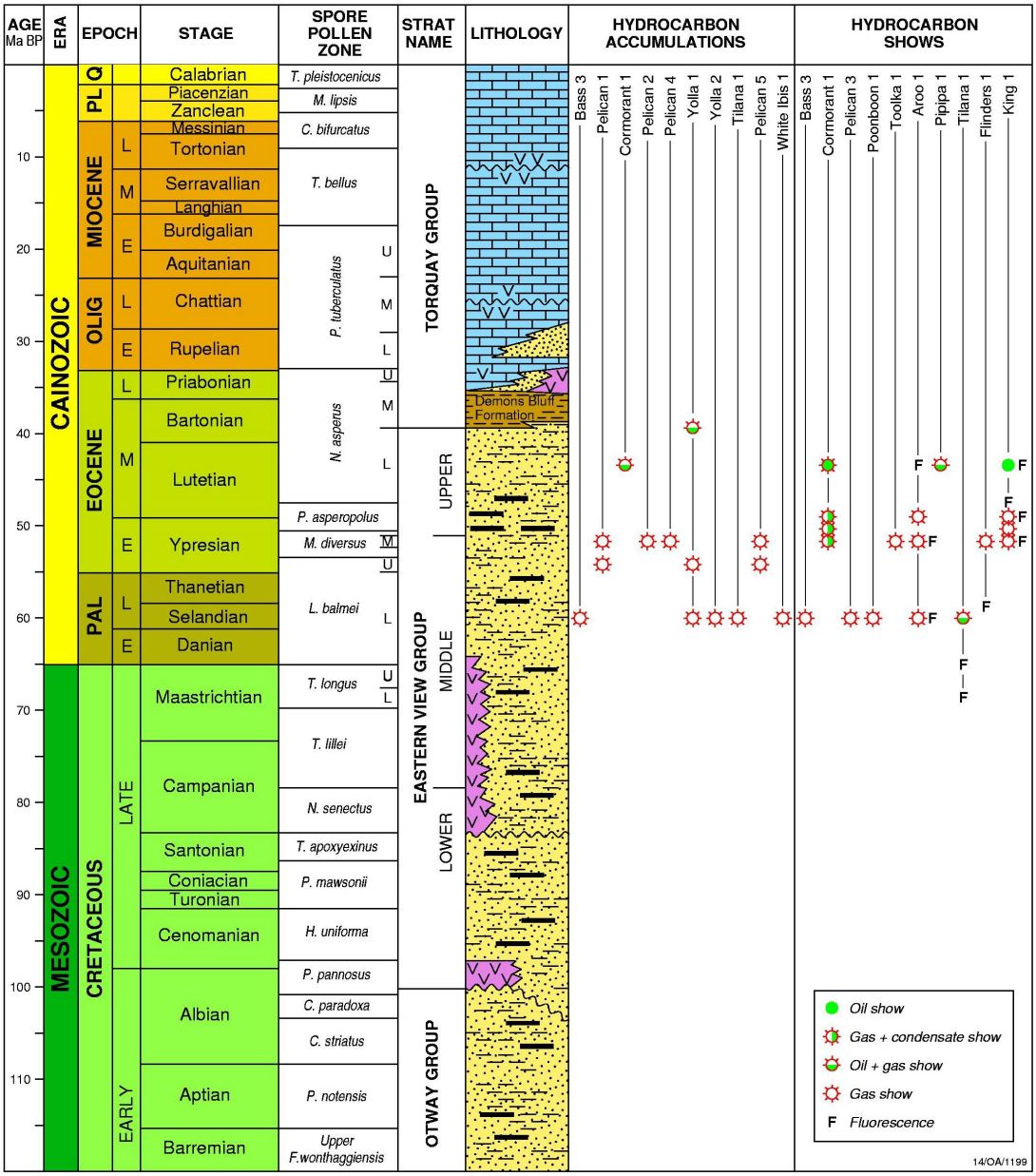


Figure 8.2 The core intervals logged by Baillie et al. (1991). The coarsening-upwards cycle in Dondu-1 is interpreted as a lake shoreline deposit. Coal-topped fining-upward intervals, such as Pelican-1 (Core 4), are interpreted as meandering fluvial systems. Flaser bedded units are probably lacustrine, while the core at Poonboon-1 probably represents deposition of stacked fluvial channels.

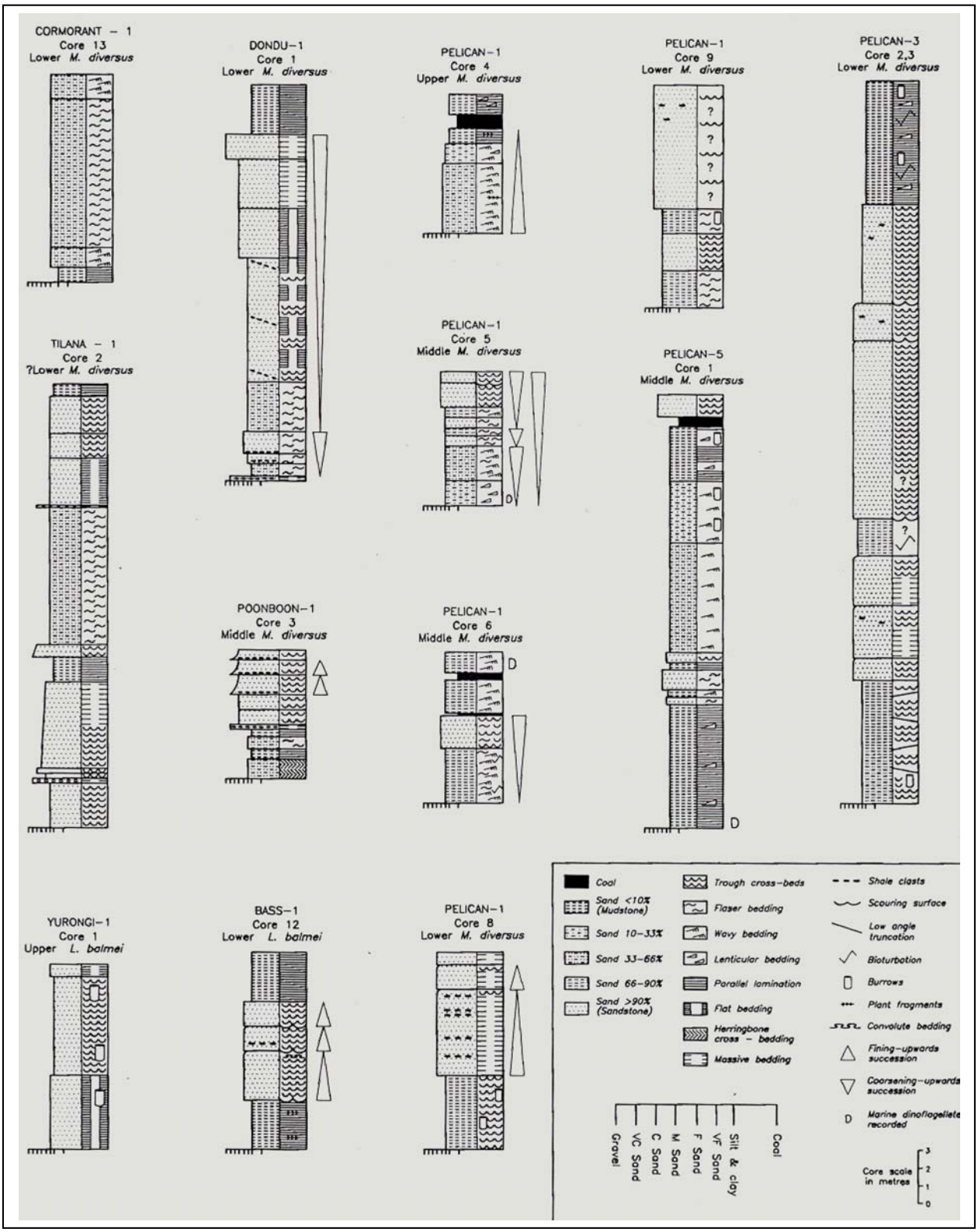
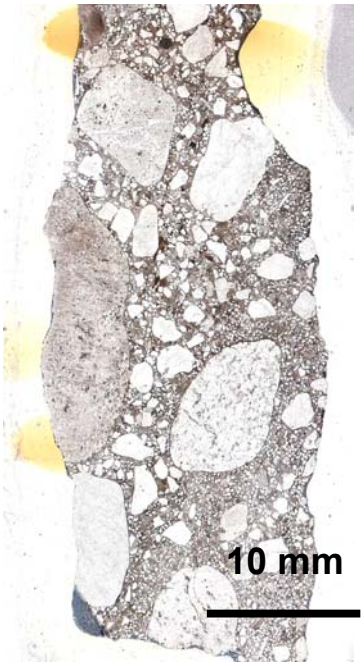


Figure 8.3 Scans of **t**hin sections to illustrate the nature of diagenetic events in the Bass Basin. Sediments in Bass-1 shows weak bioturbation, while Bass-2 is a bedded conglomerate. Dondu-1 has silty-to-very fine-grained sand interbedded with coarse to very coarse sand. The two mud rip-up conglomerates were chosen to show different diagenetic effects at different locations within the same environment of deposition. The deep Cormorant-1 sample shows ripple cross lamination.



Bass 1
2108.54 m



Bass 2
1441.26 m



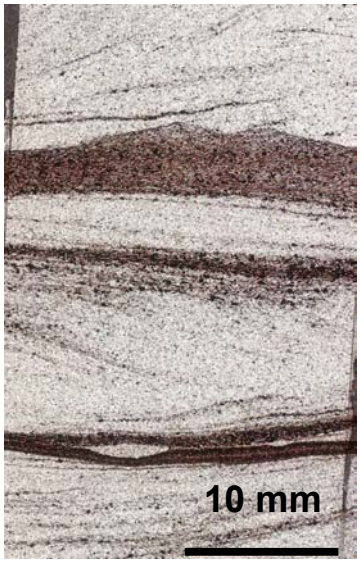
Dondu-1
2349 m



Cormorant-1
2640.2 m



Pelican-1
2896.15 m



Cormorant-1
2773.0 m

Figure 8.4 Core plug and petrographic data from Pelican-1 and Tilana-1 (from Baillie et al., 1991).

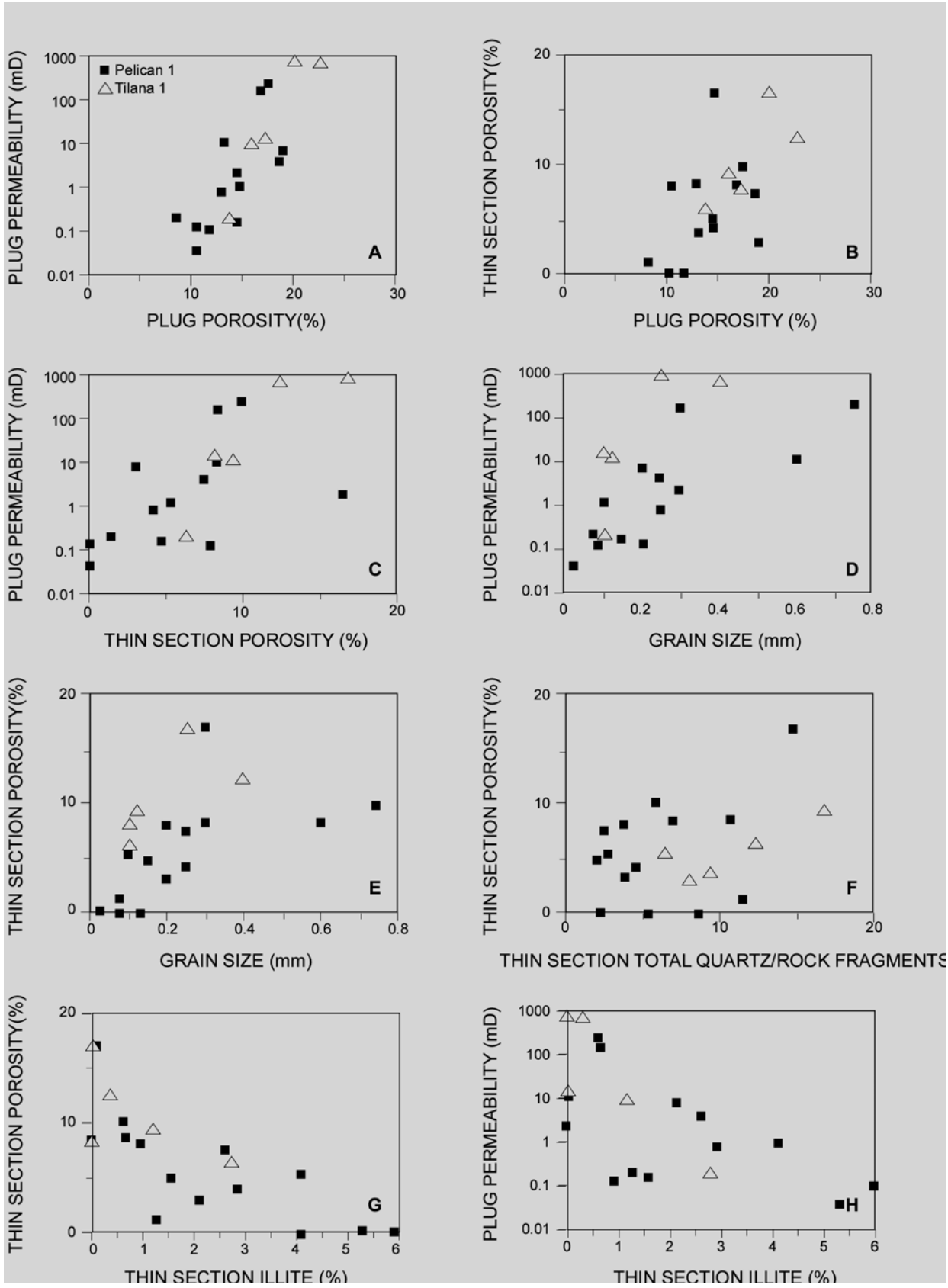


Figure 8.5 Cormorant-1, 2773 m. Photomicrographs of a ripple cross-laminated, interbedded carbonaceous siltstone and very fine sandstone. The images show abundant micritic to microspar siderite, the first cementation stage. The reducing conditions associated with the organic matter allow the siderite to grow. Stylolites are common with dissolution encouraged by the organic matter and clay. Other compaction indicators are the deformed muscovite flakes and complete lack of porosity.

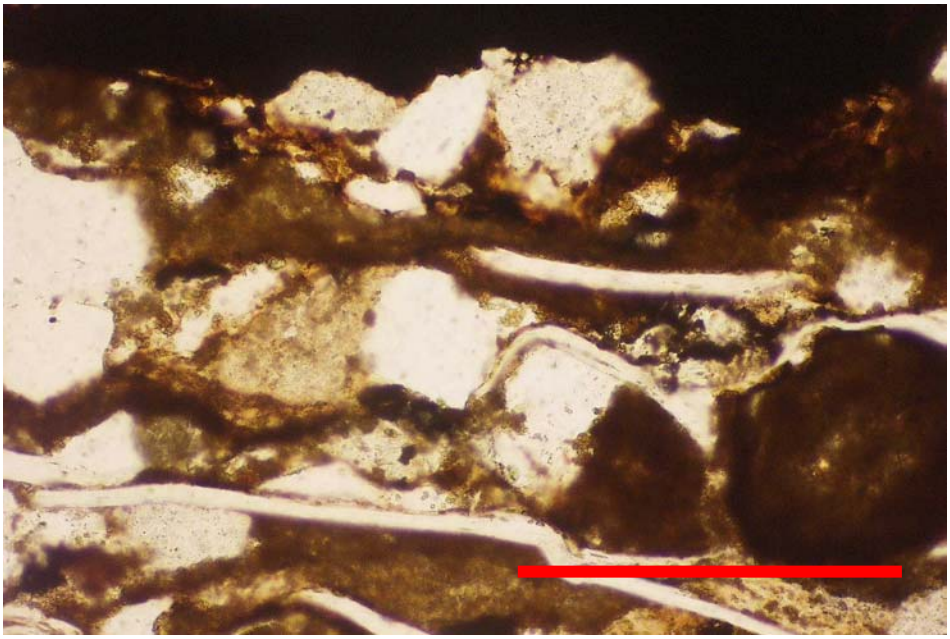


Figure 8.5a Plane polarised light (Scale bar 0.2mm)

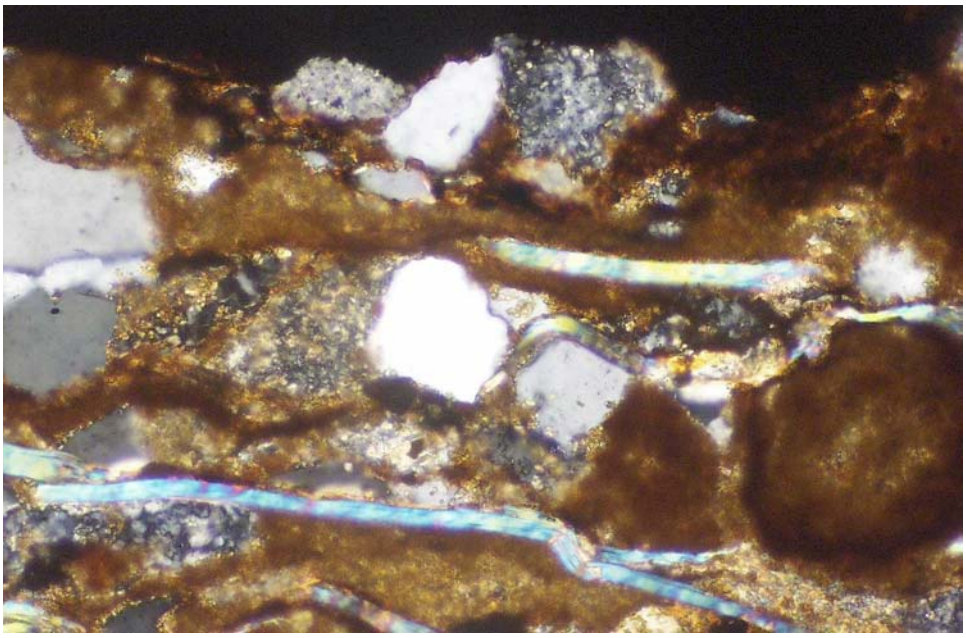


Figure 8.5b Crossed polars

Figure 8.6 Cormorant-1, 2773 m. Photomicrographs of a ripple cross-laminated, interbedded carbonaceous siltstone and very fine sandstone. 0.5 mm from a carbonaceous silt layer siderite is present, rimming the framework grains, but there is far less than in the silt band. The cross-polar image shows siderite as bright golden brown microspar (yellow circle) in contact with the allogenic quartz. Feldspars are completely altered to dense masses of kaolin (green circle).

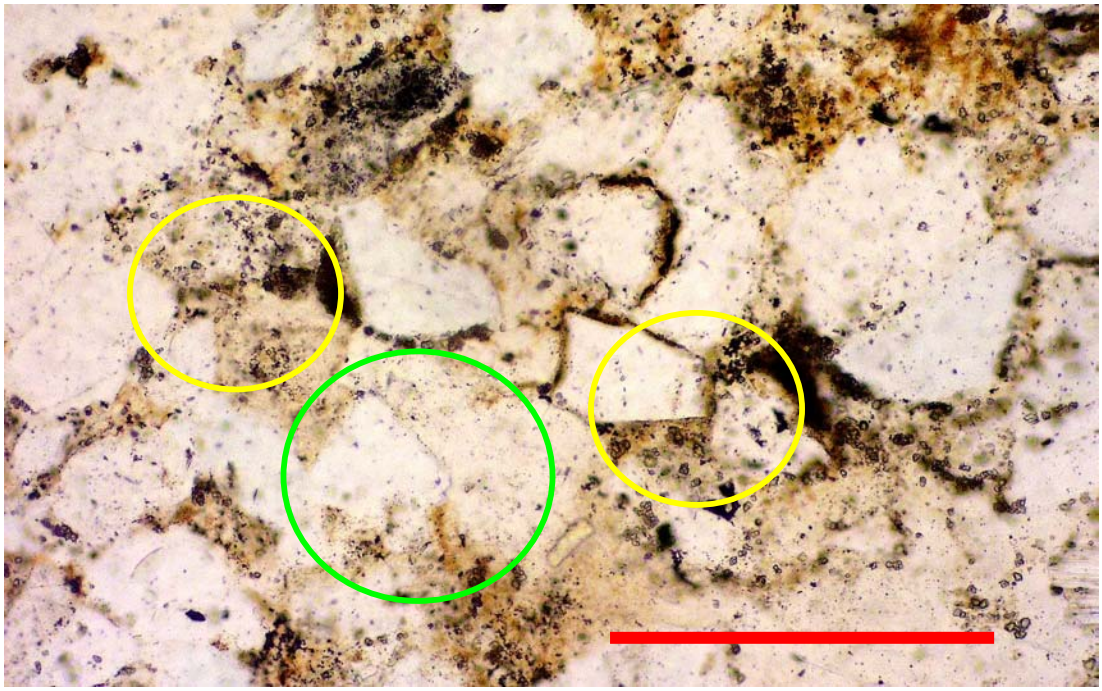


Figure 8.6a Plane polarised light (Scale bar 0.2 mm)

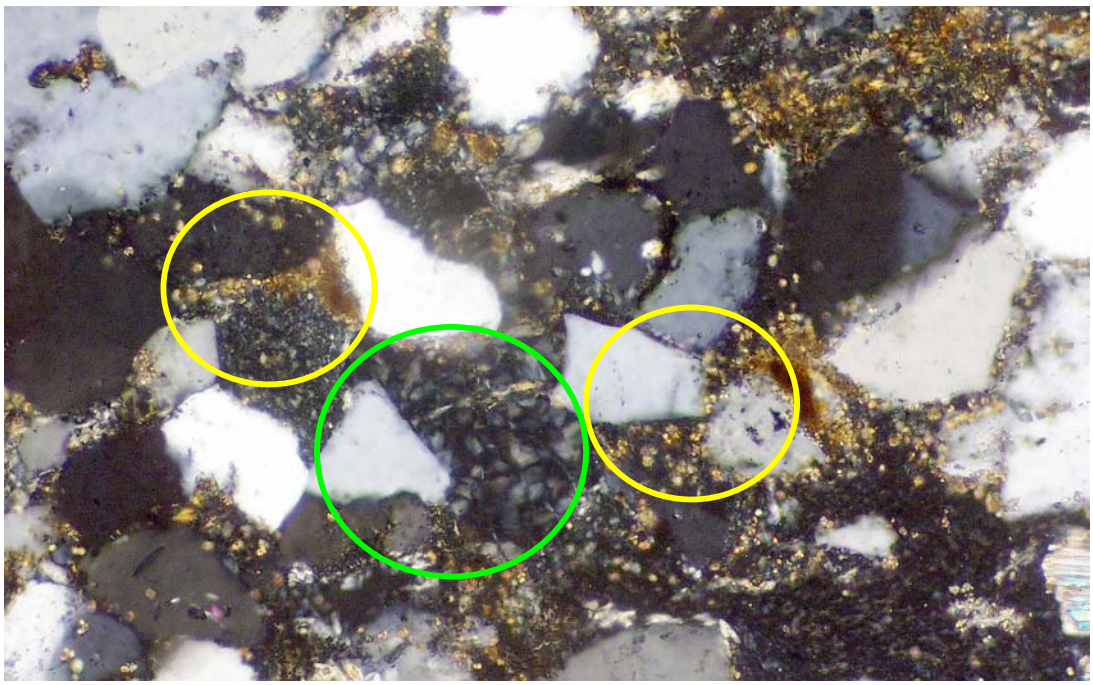


Figure 8.6b Crossed polars

Figure 8.7 Cormorant-1, 2773 m. Photomicrographs of a ripple cross-laminated, interbedded carbonaceous siltstone and very fine sandstnoe. Two millimetres from the nearest siltstone band, the amount of early siderite is minimal. This indicates that the reducing conditions associated with organic matter are essential in the precipitation of this cement phase. Feldspars are completed altered to areas of dense kaolin booklets (yellow circle) and rock fragments are altered to a mix of kaolin and illite (green circle).

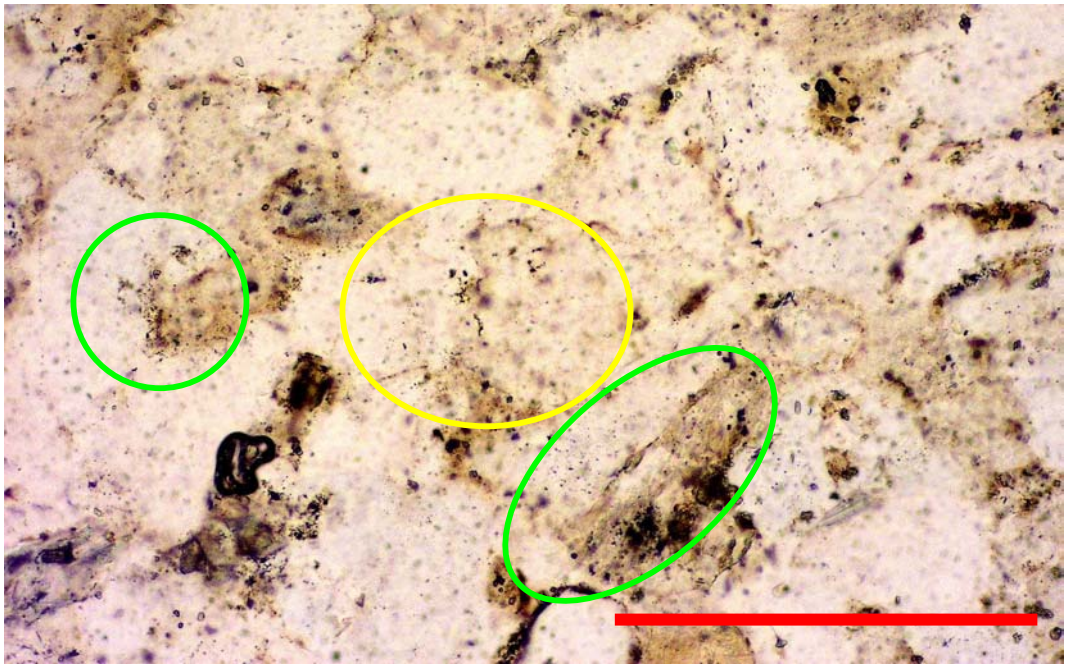


Figure 8.7a Plane polarised light (Scale bar 0.2 mm)

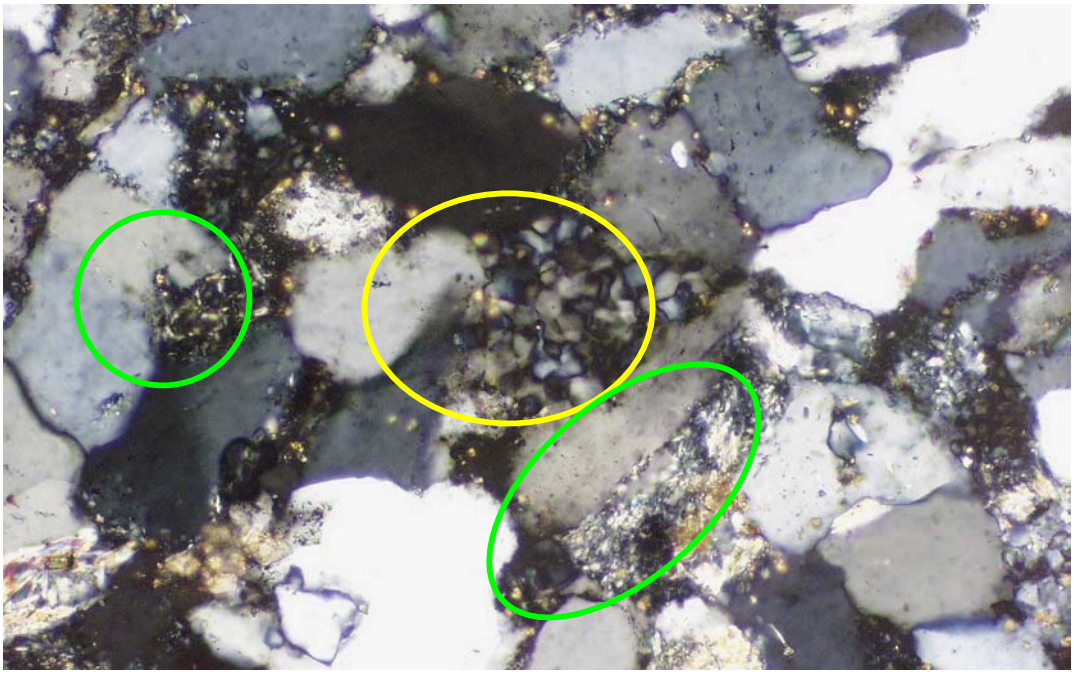


Figure 8.7b Crossed polars

Figure 8.8 Pelican-1, 2896.15 m. Mud rip-up clast conglomerate in medium to coarse sandstone. Microspar siderite growing within a deformed muscovite flake. The siderite post-dates compactional deformation.



Figure 8.8a Plane polarised light (Scale bar 0.2 mm)

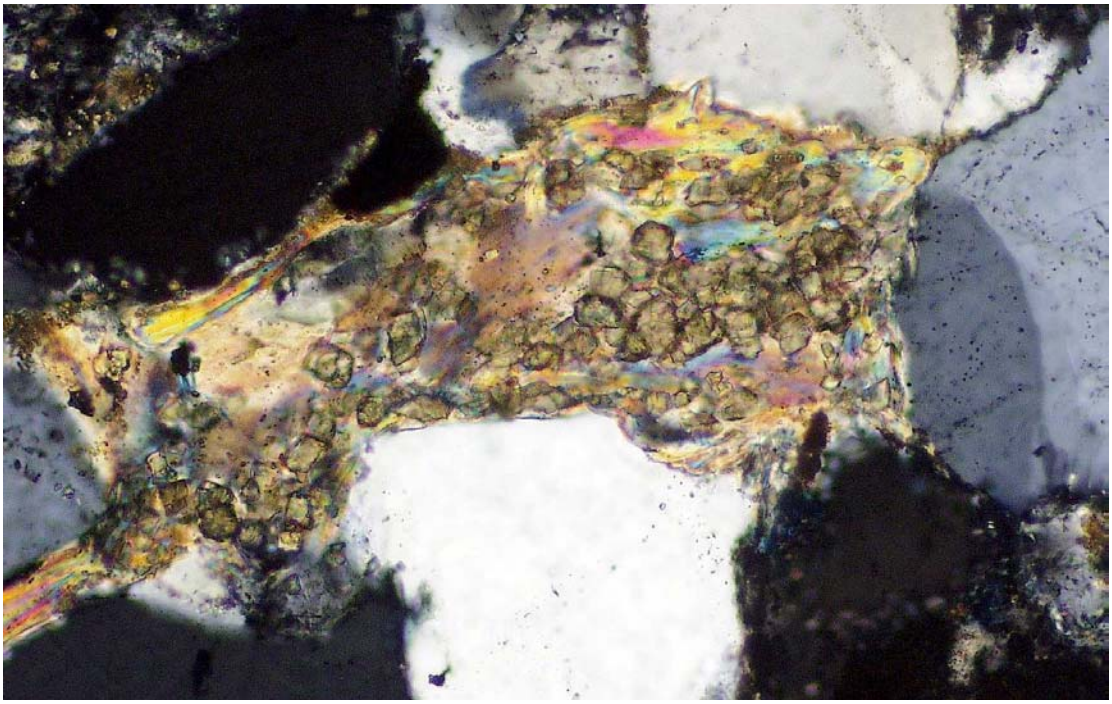


Figure 8.8b Crossed polars

Figure 8.9 Cormorant-1, 2773 m. Photomicrograph of ripple cross laminated, interbedded carbonaceous siltstone and very fine-grained sandstone. Detail in a silty layer shows the abundance of micritic and microspar siderite in association with organic matter. The siderite can form in clumps which replace the allogenic component of the rock (red circle) or scattered through the sample as a cement phase. The dark organic matter focuses dissolution of the silicate minerals, eventually forming stylolites (green circle). Muscovite flakes are deformed by compaction, sometimes altering to coarse-grained hydromuscovite or kaolin (yellow circle). The feature at centre left is an air bubble, an artifact of thin section preparation.

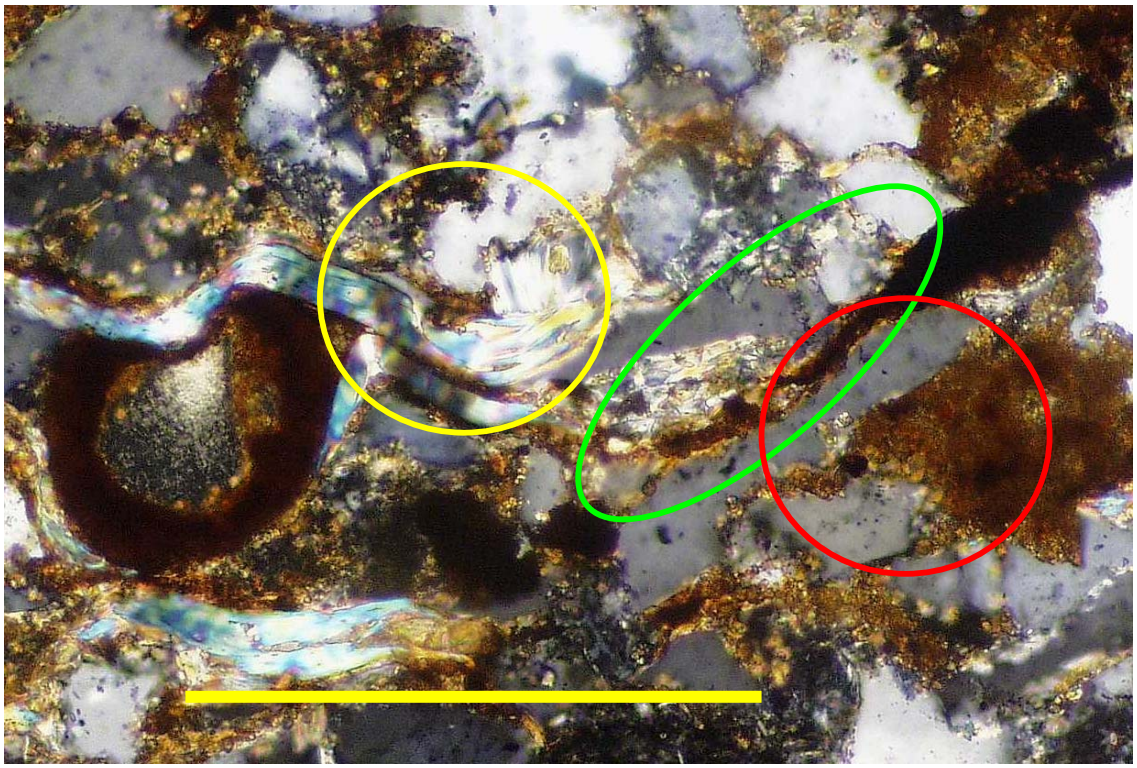


Figure 8.9 Crossed polars (Scale bar 0.2 mm)

Figure 8.10 Bass-2, 1441.26 m. Photomicrographs of a thin conglomerate layer within a sandy siltstone with mud rip-up clasts, possible floodplain deposits. Extensive low-Fe dolomite cement fills the porosity and etches quartz grains and their siderite rims (green circle) and dissolves feldspar grains (bright pale blue under CL). The dolomite appears to have been recrystallised as there is no obvious internal banding.



Figure 8.10a Plane polarised light (Scale bar 0.5 mm)

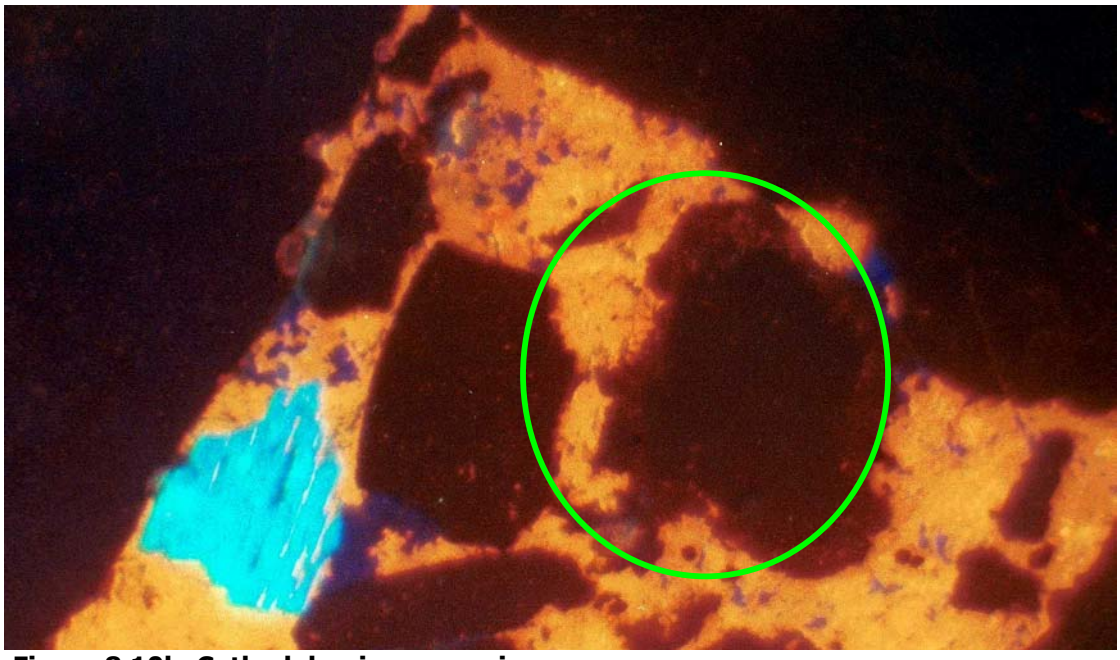


Figure 8.10b Cathodoluminescence image

Figure 8.11 Bass-2, 1441.26 m. Photomicrographs of a thin conglomerate layer within a sandy siltstone with mud rip-up clasts, possible floodplain deposits. Low-Fe dolomite completely fills pore space and dissolves a feldspar grain. Faint CL banding suggests a bright dolomite phase rimming the grains followed by a darker, pore-filling phase (green circle).

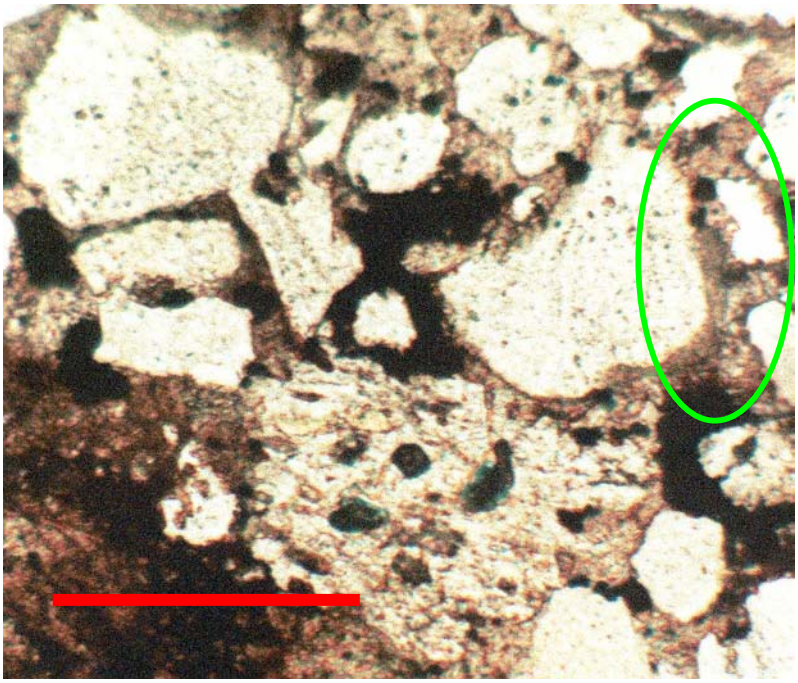


Figure 8.11a Plane polarised light (Scale bar 0.5mm)

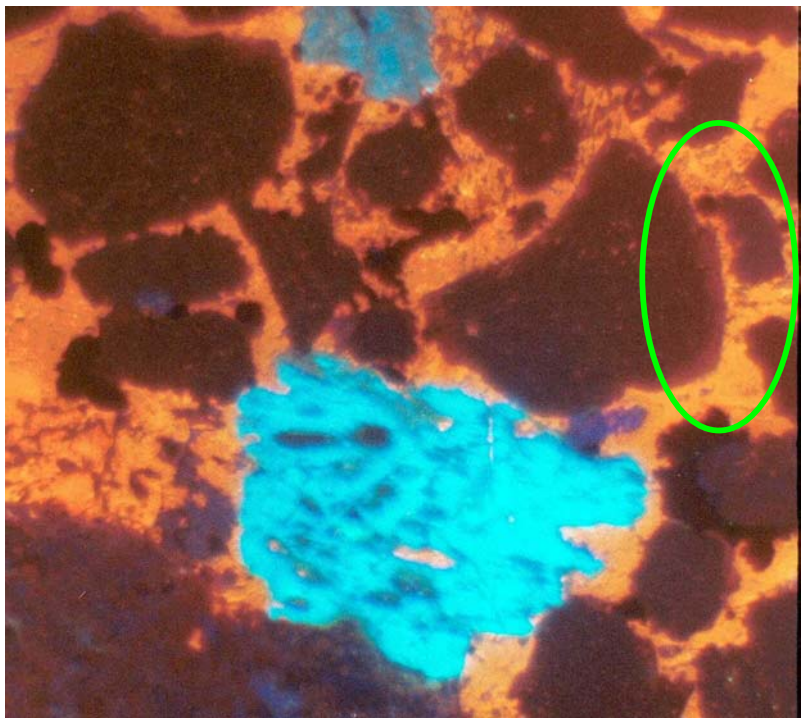


Figure 8.11b Cathodoluminescence image

Figure 8.12 Bass-1, 2108.54 m. Photomicrographs of siderite spare rhombs (dark in CL, yellow circle) grow on the edge of siderite micrite (dark in plane light) which cements and etches quartz silt. A composite granitic grain which was largely feldspar, has altered to a dense mass of kaolin (bright blue in CL). There was some feldspar dissolution prior to alteration to allow siderite cement against the odd-shaped quartz grain within the composite grain. Loose-packed kaolin grows away from the altered feldspar in pores among the framework grains.

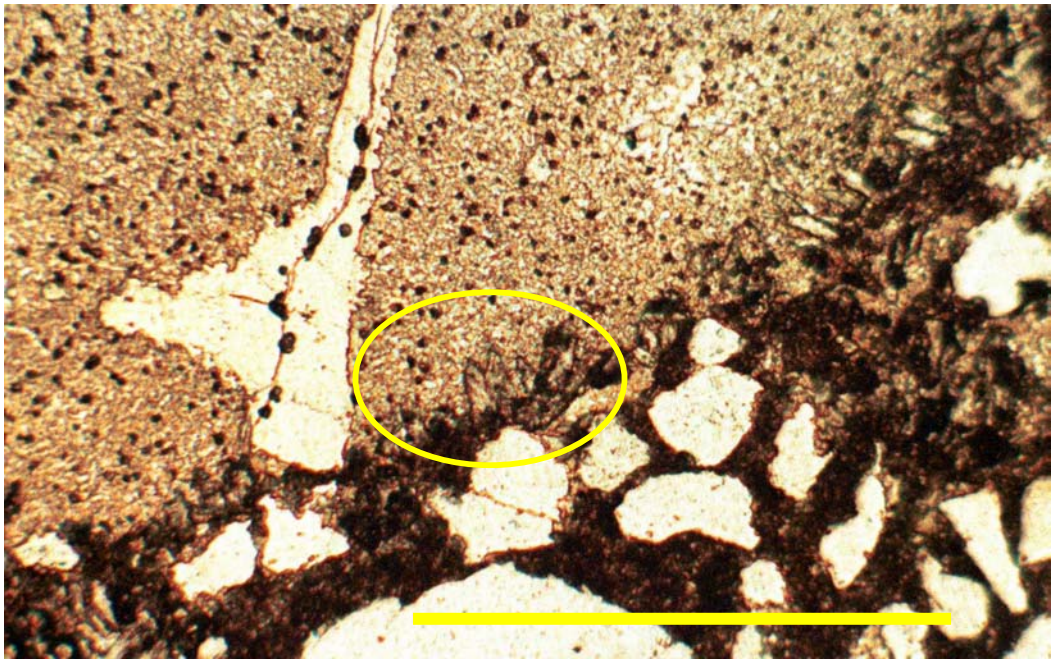


Figure 8.12a Plane polarised light (Scale bar 0.5 mm)

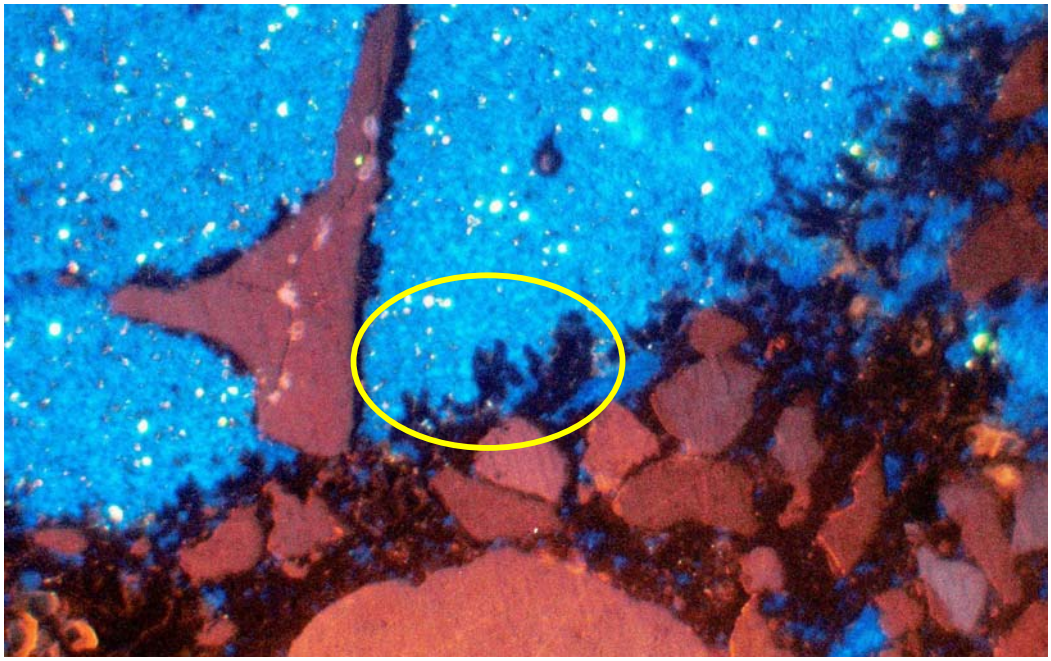


Figure 8.12b Cathodoluminescence image

Figure 8.13 Bass-2, 1441.26 m. Photomicrograph of a thin conglomerate layer within a sandy siltstone with mud rip-up clasts, possible flood plain deposits. Brightly luminescent dolomite partly fills porosity between quartz grains. There is extensive dissolution of dolomite (red circles) before the precipitation of kaolinite (speckled blue). Ankerite, or possible siderite rhombs (yellow circle) are clear under CL but the pitted surface of the slide make them hard to see in plain light.

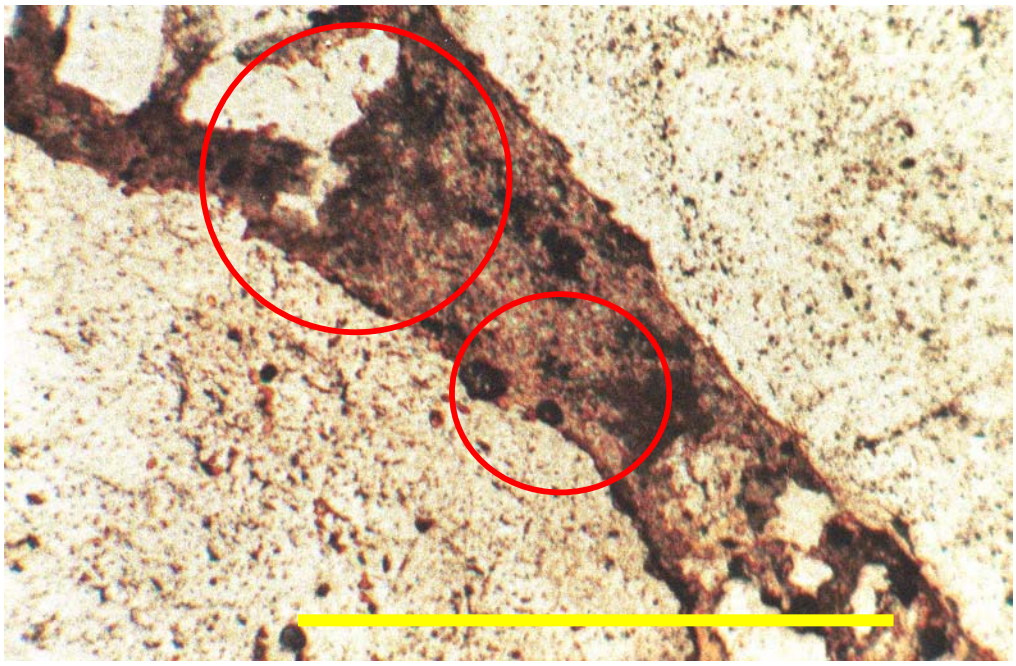


Figure 8.13a Plane polarised light (Scale bar 0.5 mm)

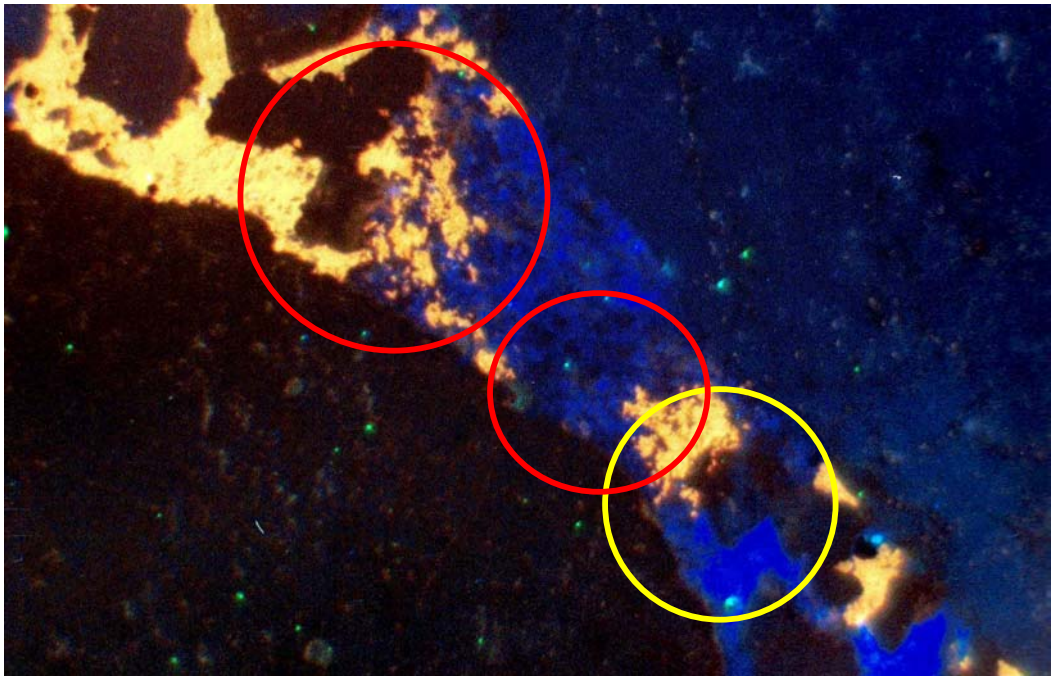


Figure 8.13b Cathodoluminescence image

Figure 8.14 Pelican-1, 2606.6 m. Photomicrographs of a fine sandstone with flaser bedding and trough cross bedding. These two images illustrate several points in the history of quartz diagenesis. The blue grain was fractured by early compaction then healed with quartz cement (pale brown in CL). The same cement rims most framework grains. Metamorphic quartz (reddish grains) has no overgrowth or only a thin rim. Most quartz rims have been subjected to local dissolution, probably by carbonate grains, which have been subsequently dissolved to give irregular outlines to the grains. The orange colours in plain light are burn marks in araldite resin from prolonged CL exposure.

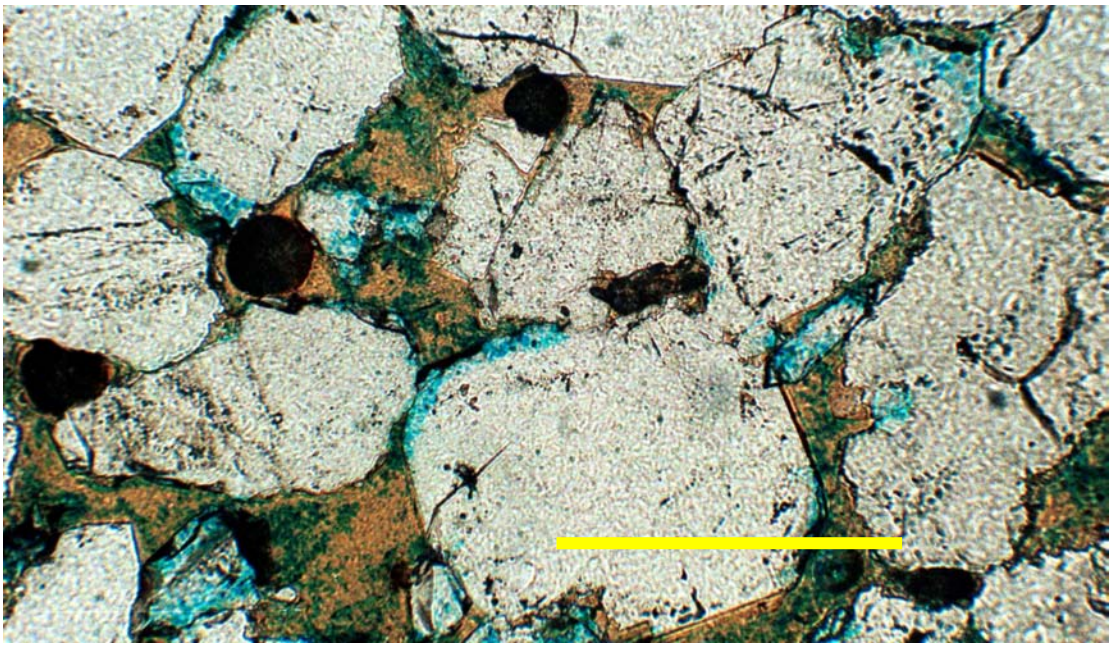


Figure 8.14a Plane polarised light (Scale bar 0.2 mm)

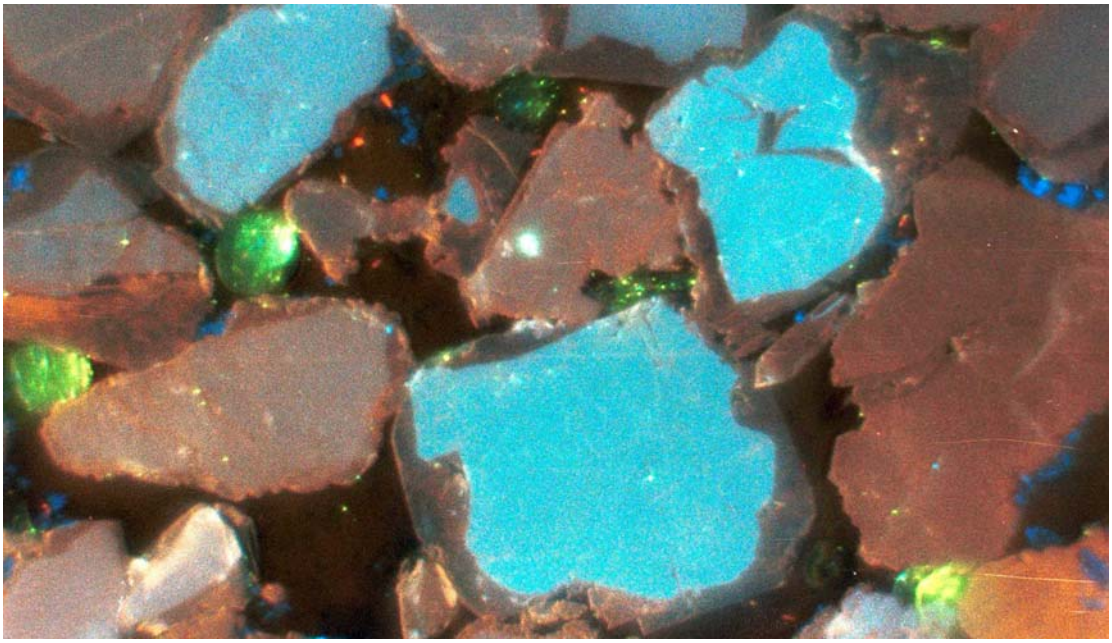


Figure 8.14b Cathodoluminescence image

Figure 8.15 Dondu-1, 2349 m. Photomicrographs of a coarse to very coarse-grained sand that appears to be a channel sandstone as the interval above is a lacustrine shoreline unit. Quartz cement fringes the framework quartz grains (pale purple in CL). Masses of kaolin (bright blue in CL) fill the pores. The jagged contact between the quartz cement and kaolin is a function of intergrowth of the two cements, indicating they are co-genetic. The fact that these two minerals grow together indicates a common origin, probably from the alteration and dissolution of feldspar. The mid-blue patches of kaolin under CL (circle) are the areas mixed with organic matter, possible recrystallised matrix.

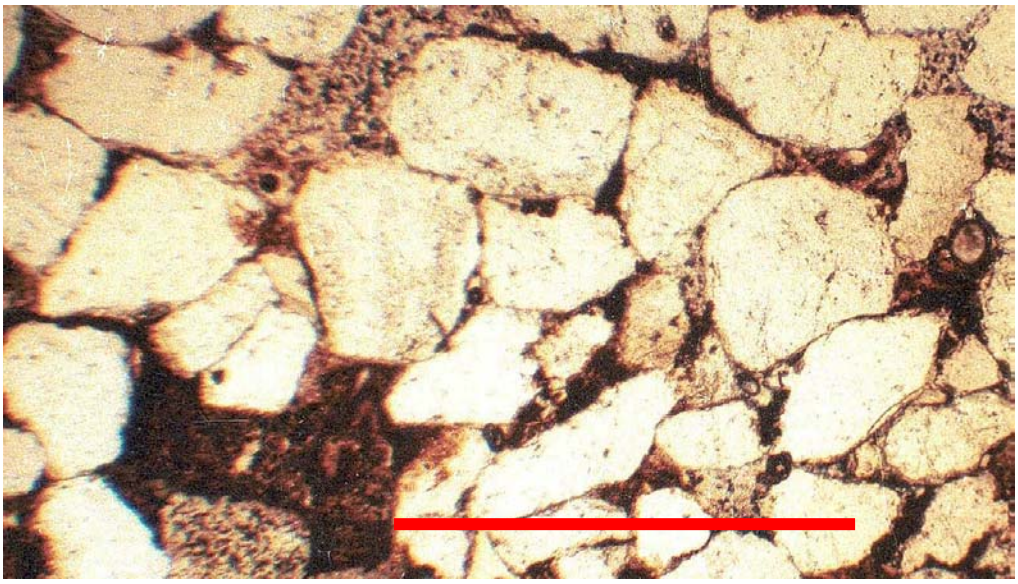


Figure 8.15a Plane polarised light (scale bar 0.5 mm)

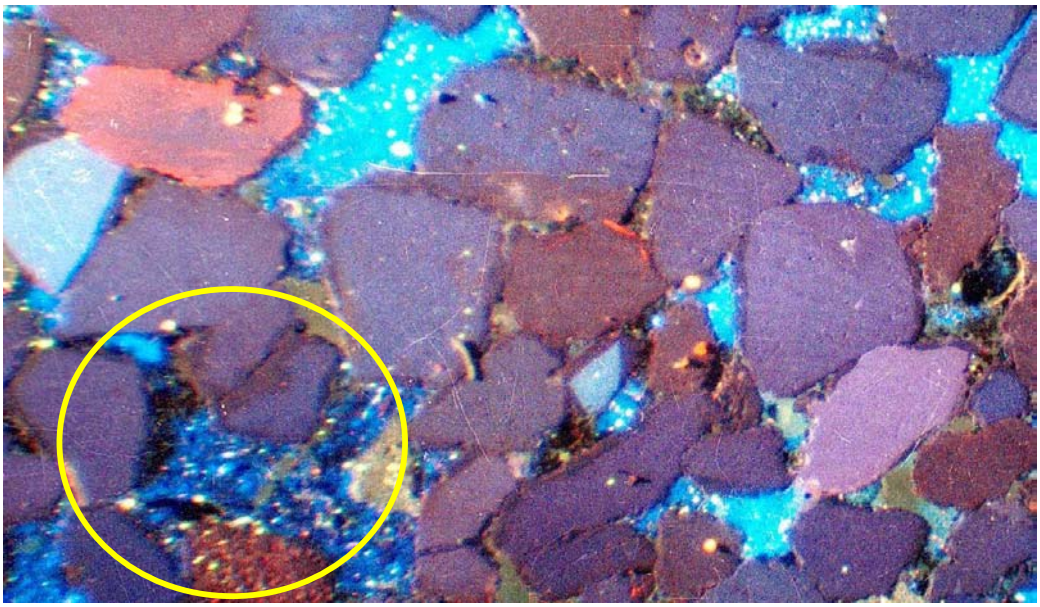


Figure 8.15b Cathodoluminescence image

Figure 8.16 Cormorant-1, 2640.2 m. Photomicrographs showing extensive siderite micrite rims that etch the framework grains. A feldspar grain (yellow circle) has been completed altered to a dense mat of kaolin. The ends of the feldspar are shown by minor siderite. Beyond the original grain, slightly coarser kaolin grows into primary porosity (red circle).

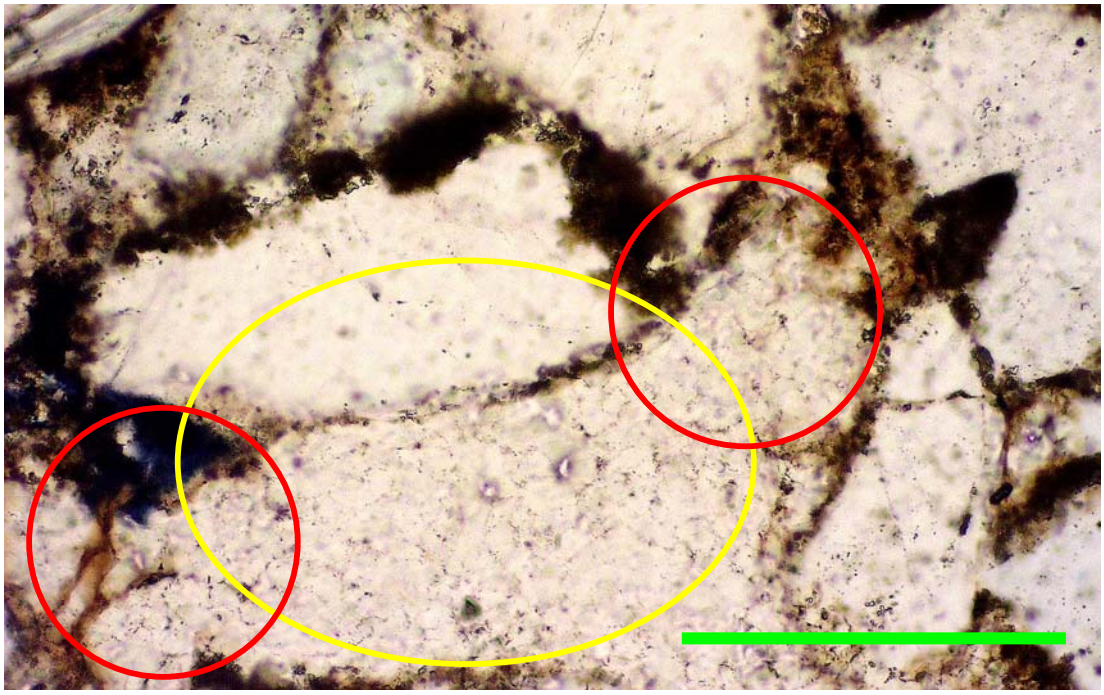


Figure 8.16a Plane polarised light (Scale bar 0.2 mm)

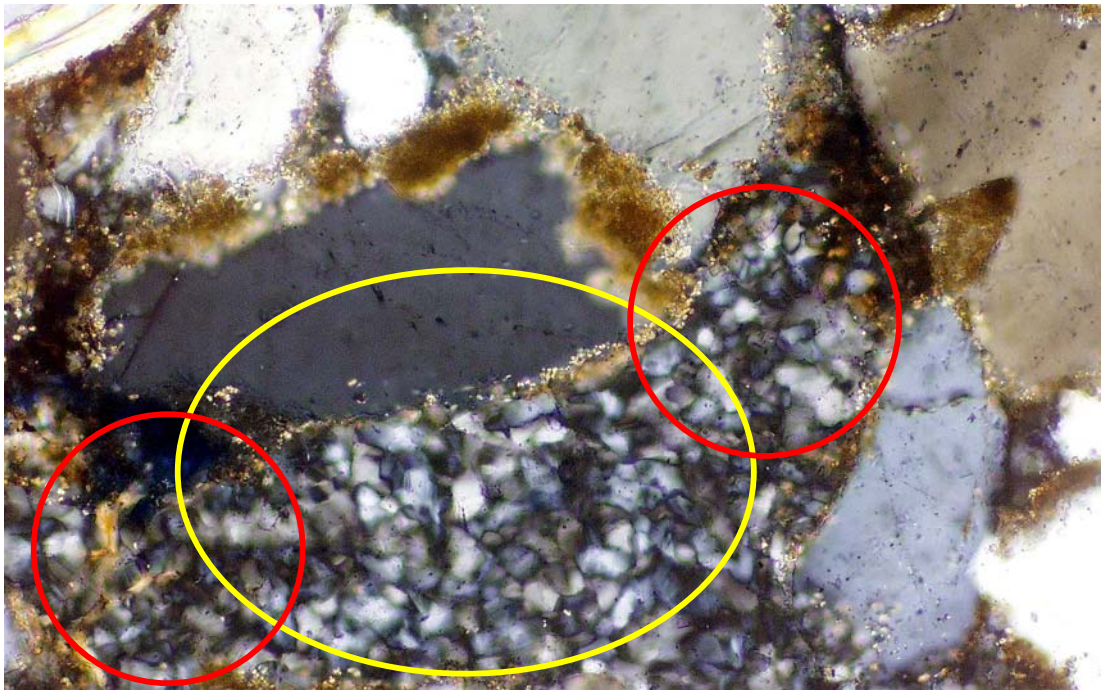


Figure 8.16b Crossed polars.

Figure 8.17 Dondu-1, 2349 m. Photomicrographs of a coarse sand to gravel in a channel. A shoreline connection, probably lacustrine, is suggested by the coarsening up, flaser bedded to flat bedded interval above. Euhedral quartz overgrowths (yellow circle) occur against open pore spaces. Where there is extensive kaolin growth (mottled grey tones), either as alteration of a feldspar or neoformed in the pore space adjacent, the authigenic quartz is intergrown with the kaolin. Dolomite (red cicle) shows dissolution prior to kaolin cement emplacement. The dolomite crystals in Figure 8.17b show zoned growth.

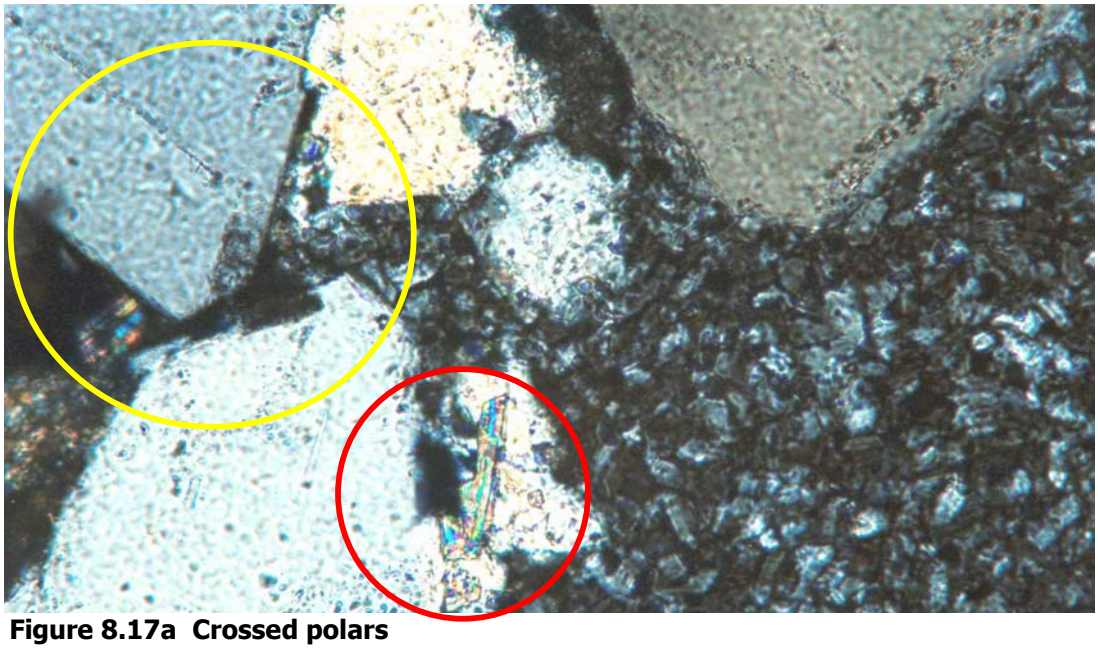


Figure 8.17a Crossed polars

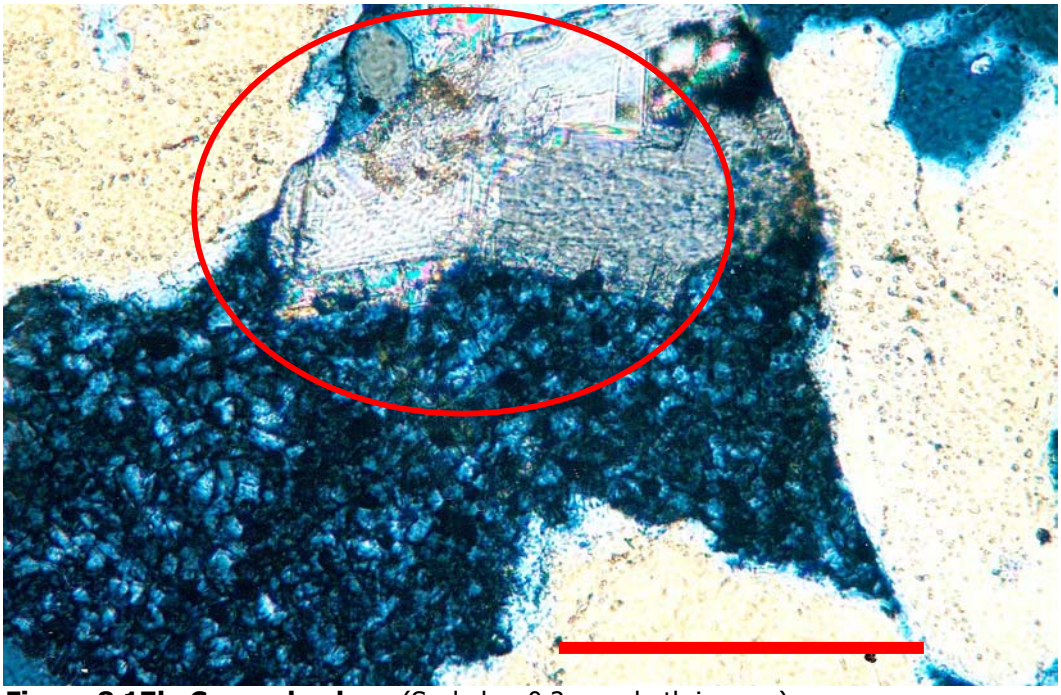


Figure 8.17b Crossed polars (Scale bar 0.2 mm, both images)

Figure 8.18 Pelican-1, 2896.15 m. Photomicrographs of a mud rip-up clast conglomerate in medium to coarse-grained sandstone. Thin siderite rims on framework grains predate extensive alteration of feldspars and rock fragments. The areas in these altered grains are then subject to considerable compaction which removes all porosity. Quartz-rich areas retain porosity. Thick quartz overgrowths (yellow circle) predate extensive compaction.

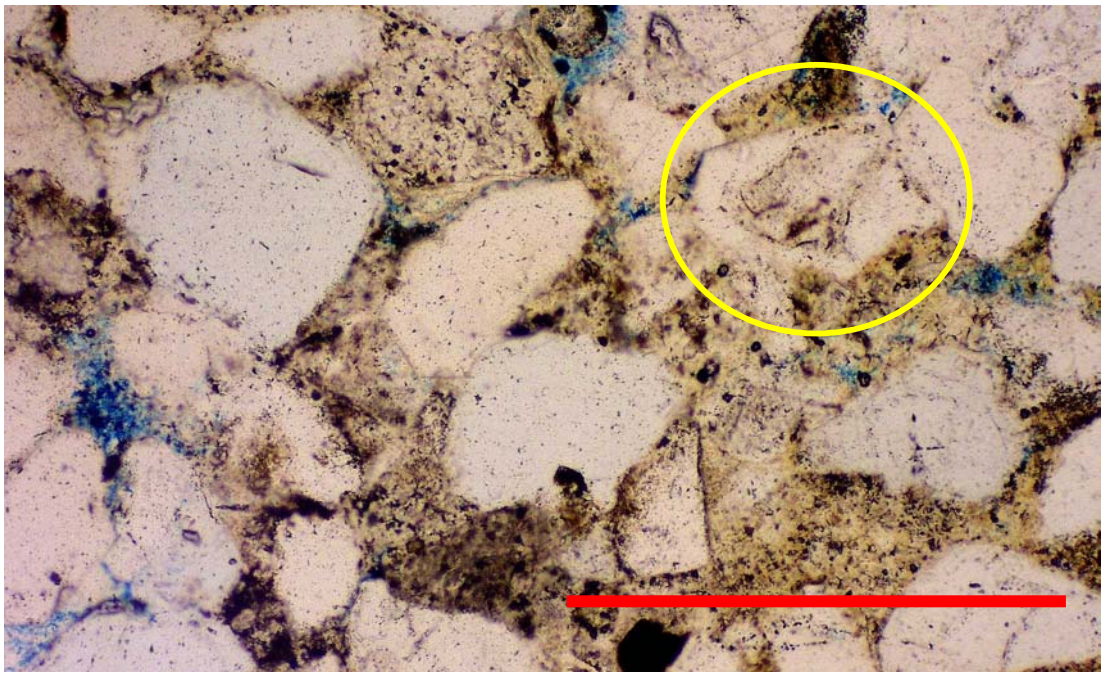


Figure 8.18a Plane polarised light (Scale bar 0.5 mm)

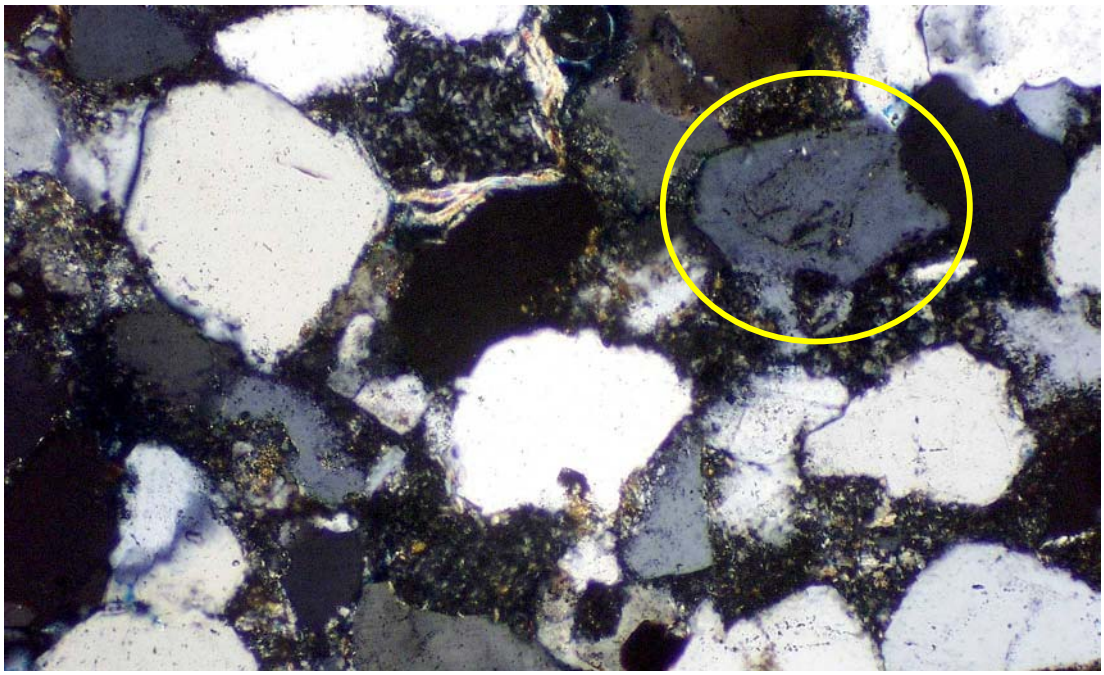


Figure 8.18b, Crossed polars

Figure 8.19 Pelican-1, 2896.15 m. Photomicrographs of a mud rip-up clast conglomerate in medium to coarse-grained sandstone. Detail of this image shows that some compaction has occurred after the quartz overgrowths formed. Plane light shows micritic siderite rimming and etching the framework grains. The porosity appears all secondary, created by the dissolution of a carbonate phase, probably dolomite, as siderite is still present.



Figure 8.19a Plane polarised light (scale bar, 0.5 mm)

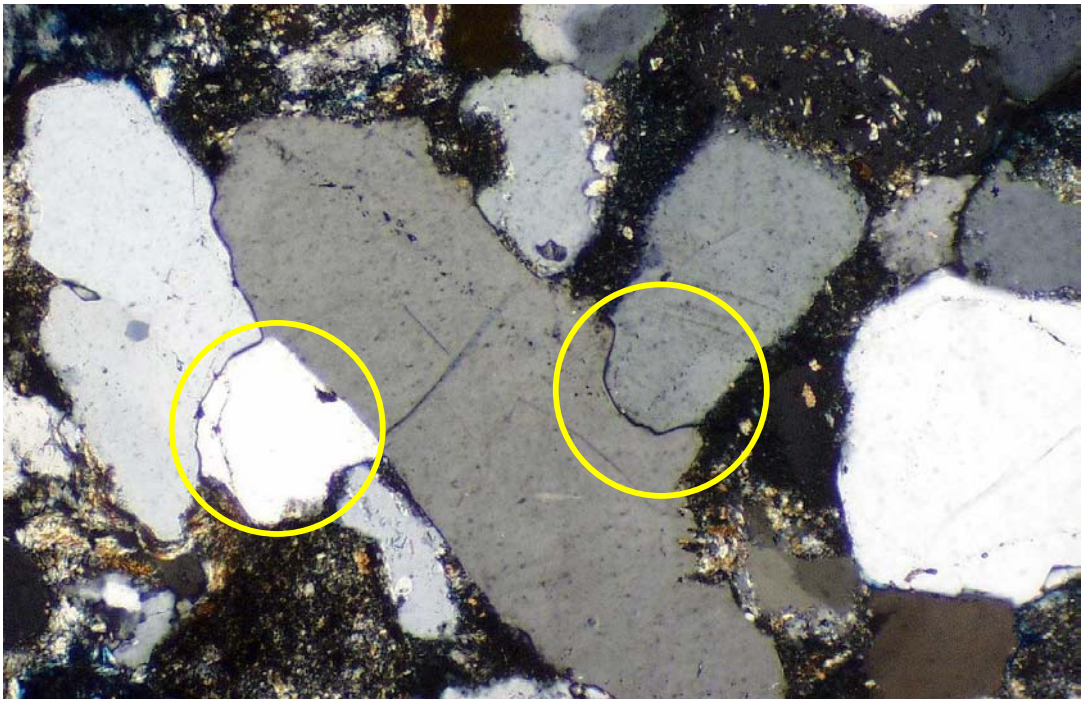


Figure 8.19b Crossed polars

Figure 8.20 Pelican-1, 2896.15 m. Photomicrographs of a mud rip-up clast conglomerate in medium to coarse-grained sandstone. Detail around the end of a quartz grain with thick overgrowth shows that some compaction occurred after the overgrowth was precipitated. A line of siderite micrite indicates the original edge of the grain.

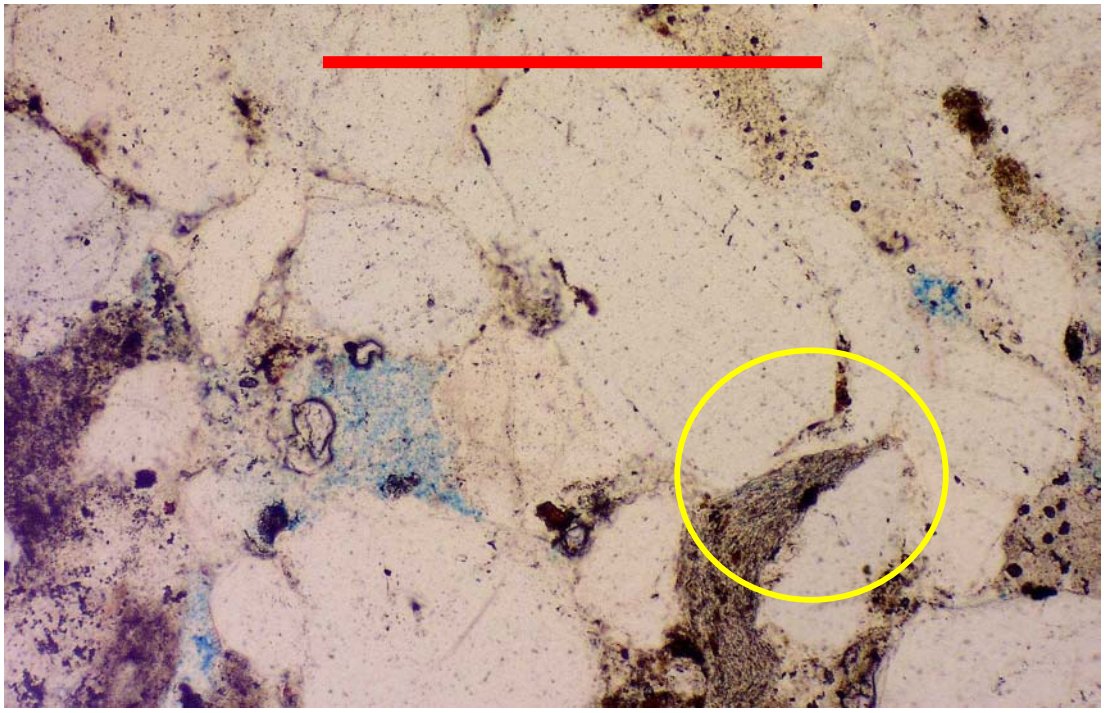


Figure 8.20a Plane polarised light (Scale bar 0.5 mm**)**

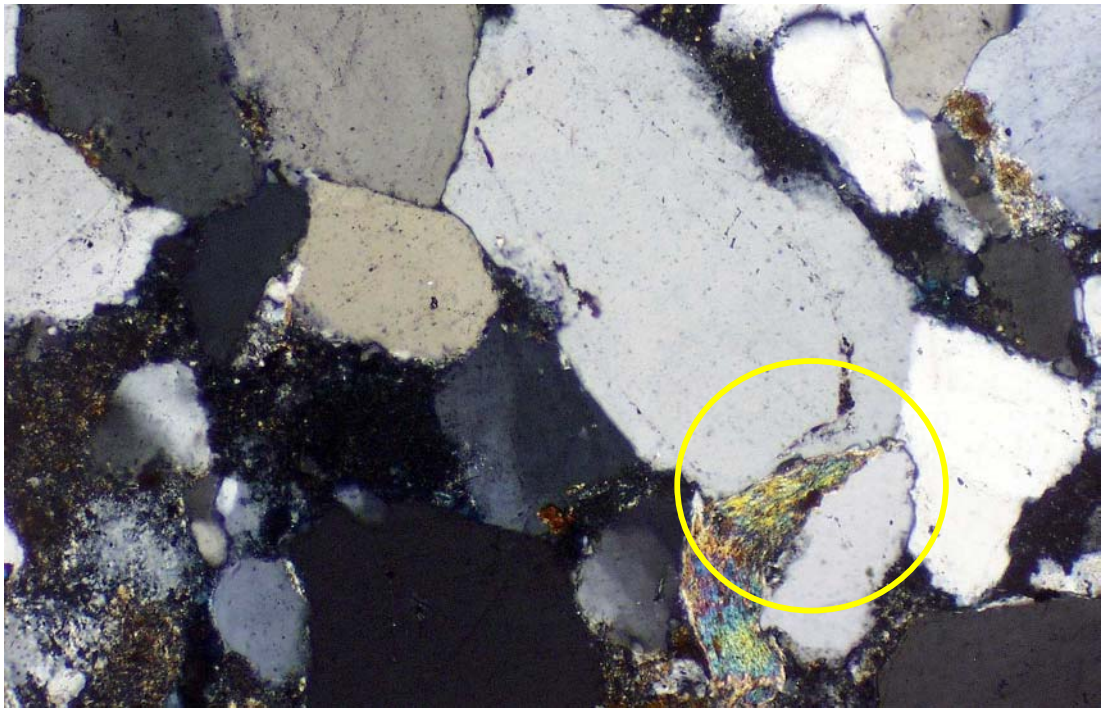


Figure 8.20b Crossed polars

Figure 8.21 Geothermal gradient as measured from the present day bottom hole temperatures. Contours are in degrees Celsius per kilometre (adapted from Cubitt, 1992).

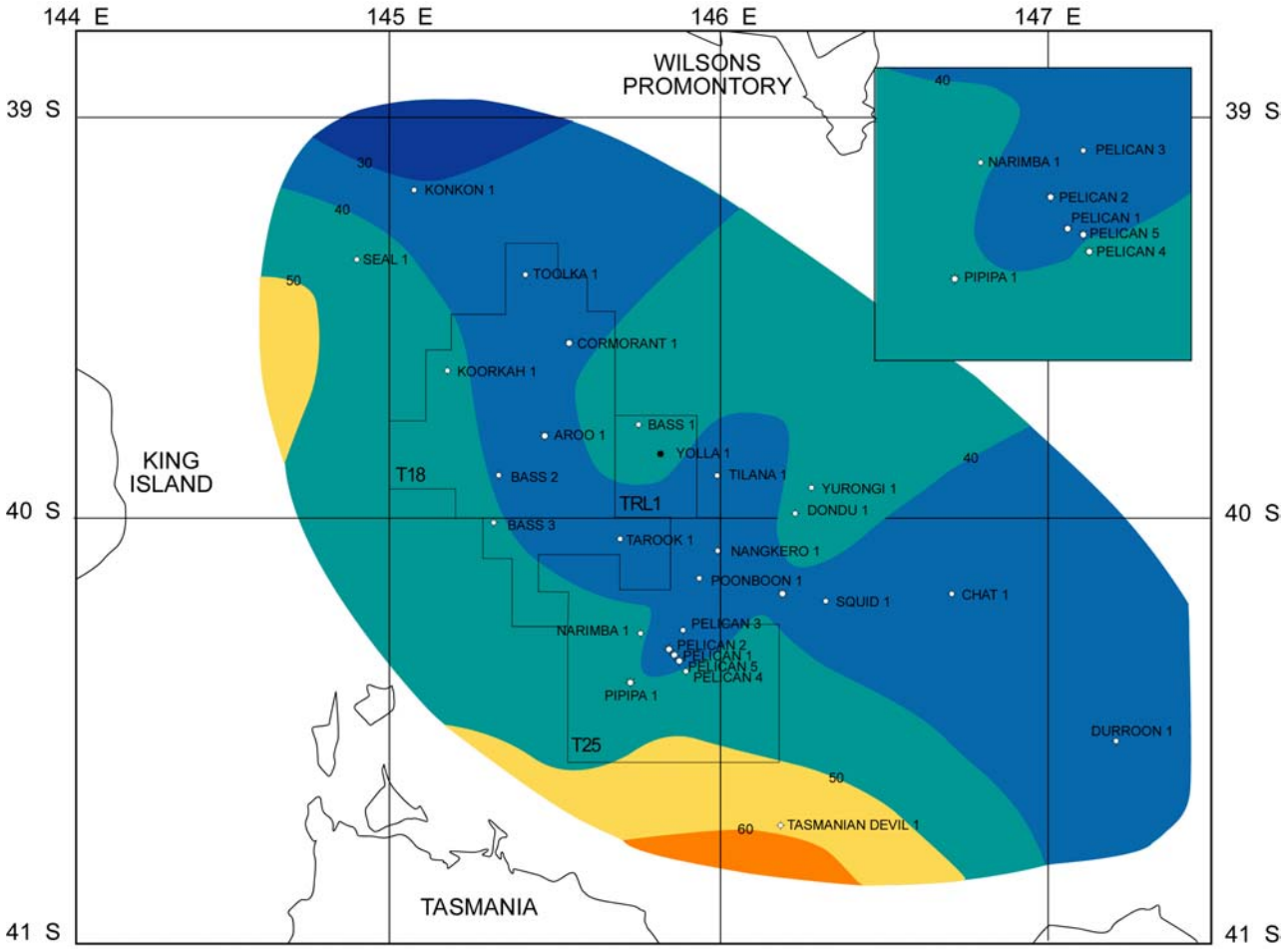


Figure 8.22 Isothermal map at a depth of 1000 m subsea. Contours are in degrees Celsius (adapted from Cubitt, 1992).

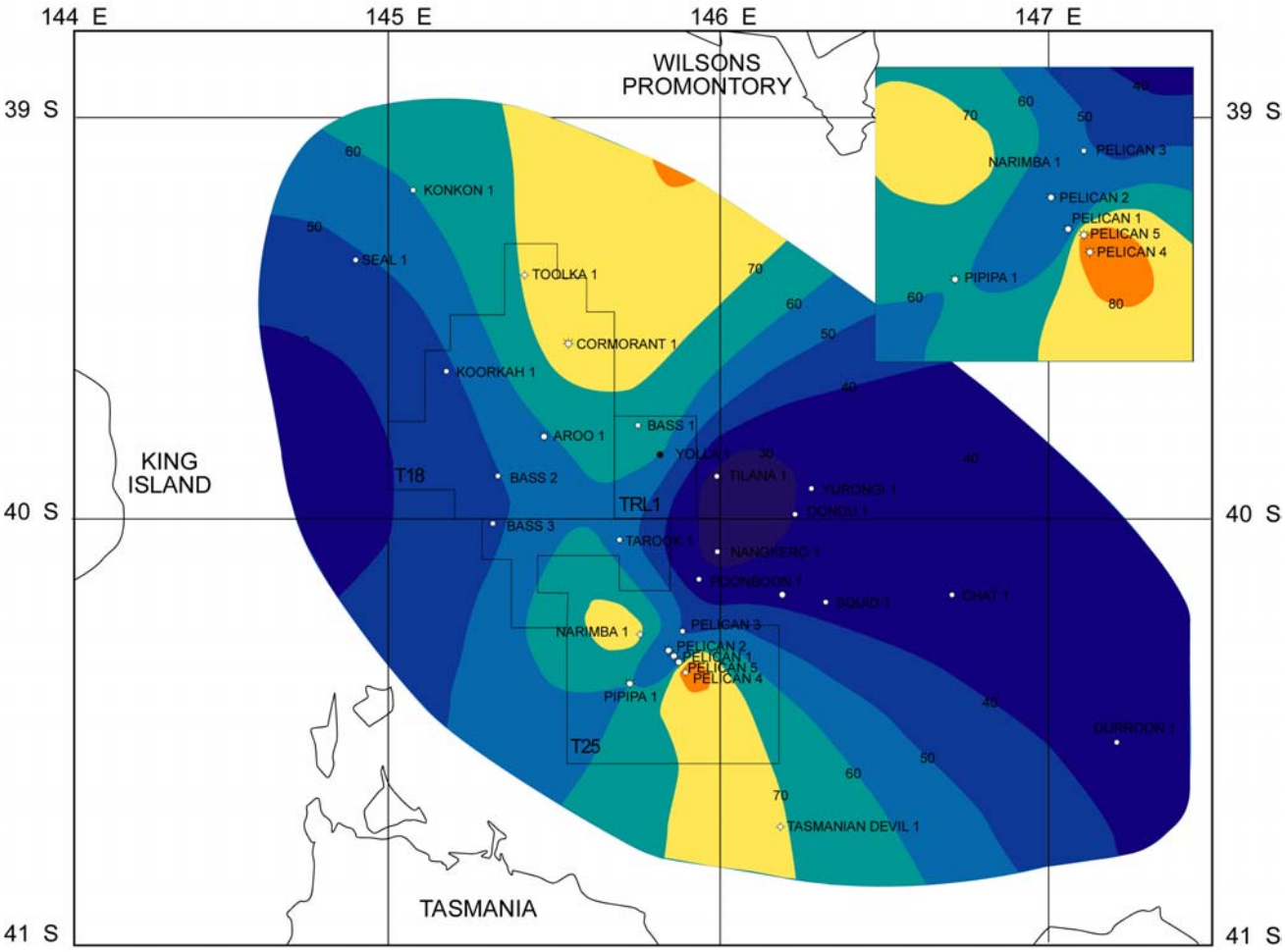
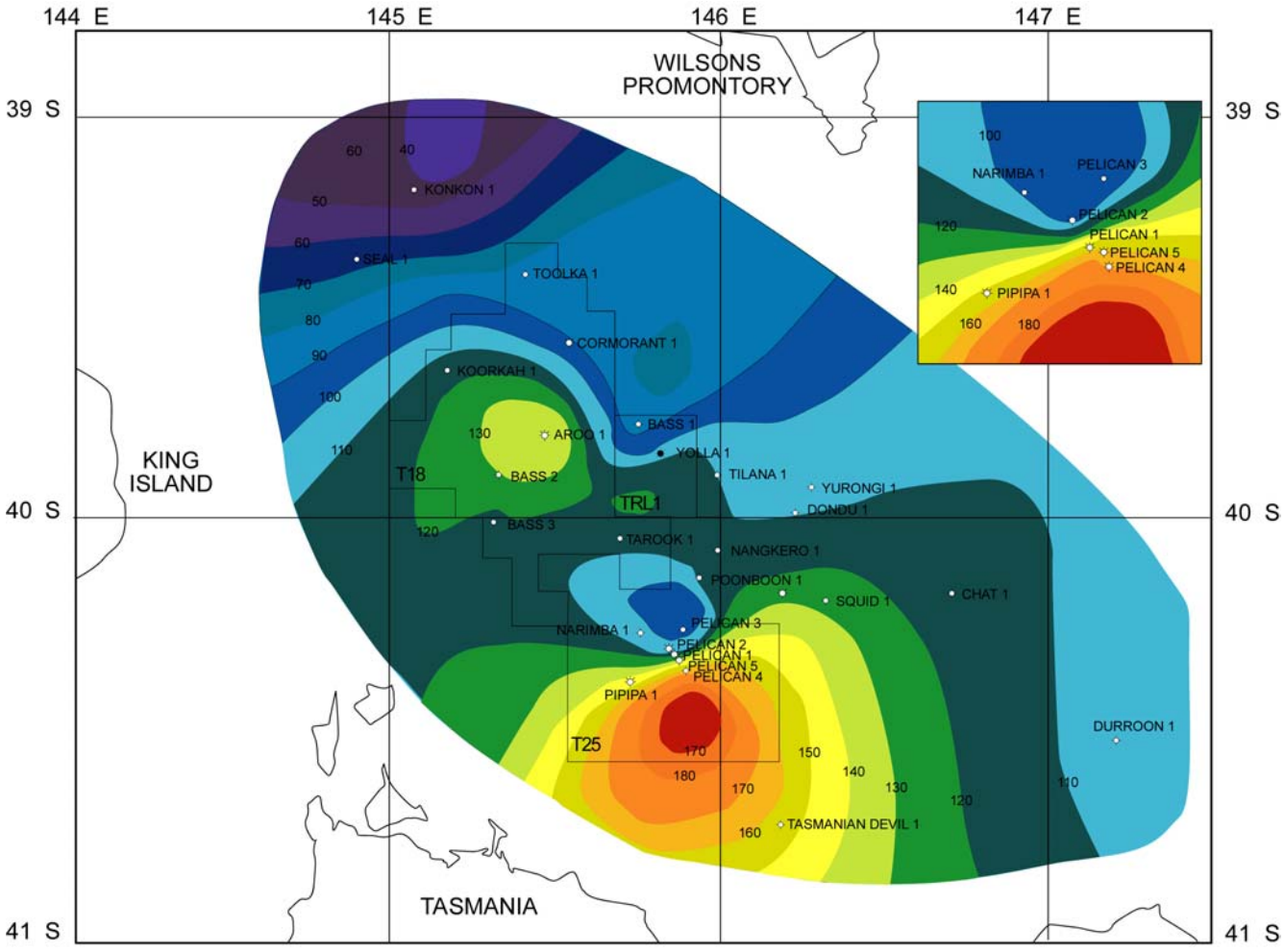


Figure 8.23 Isothermal map at the top of the *P. asperopolus* zone. Contours in degrees Celsius (adapted from Cubitt, 1992).



9. DEPOSITIONAL ENVIRONMENTS AND FACIES ANALYSIS

S. Lang and R. Root, National Centre for Petroleum Geology and Geophysics
J. McEachern, Simon Fraser University, British Columbia

9.1 KEY POINTS

- Based on new descriptions of 21 cores selected from nine wells, depositional environments in the Bass Basin ranged from fluvial channel belt and floodplain, to lacustrine and lacustrine delta. Lagoonal or interdistributary bay conditions, associated with a back-barrier marsh occur at several intervals, and foreshore, shoreface and shelf facies are also recognised. The overall setting is that of a land-locked alluvial and lacustrine basin, with an opening to the sea probably to the north or west that progressively became more important through time.
- Integration with palynological data supports the notion that the basin was well vegetated and dominated by peats that fringed extensive lakes and lagoons.
- Discrete channel belts were probably focused sub-parallel to basin-forming structures along fault relay zones.
- Several major lacustrine events associated with flooding surfaces can be recognised in the Upper Cretaceous to Eocene succession based on distinct stacking patterns and palynology. Freshwater lakes occurred within the Durroon (*P. mawsonii – T. apoxyexinus* zone), Tilana (Upper *F. longus* – Lower *L. balmei* zones*),* and Narimba sequences (Upper *L. balmei* – Middle *M. diversus* zones). Coastal lagoons and associated interdistributary bays (analogous with Lake Maracaibo, Venezuela) developed increasingly during the Middle to Late Eocene, associated with local flooding surfaces in the Aroo Sequence and the lower part of the Demons Bluff Sequence (Lower *N. asperus* zone).
- Wireline logs indicate alternating aggradational, retrogradational and progradational stacking patterns suggestive of cyclical variation in the balance between accommodation and sediment supply. Aggradational coaly intervals indicate a delicate balance between peat production and accommodation (especially during *P. asperopolus* zone).
- The highest ranking reservoir facies developed in coarse-grained sandstones within fluvial channels (meandering fluvial channel belt or distributary channels), possibly improved during low accommodation intervals associated with incised valley fill. Second ranking reservoir facies include the fine to medium-grained lacustrine shoreface and foreshore facies. The best reservoir potential exists within the *L. balmei* zone (Tilana and lower Narimba sequences).
- Deposition of the regional seal was associated with a regional transgressive bay/shallow marine event in the upper Demons Bluff Sequence (Anglesea Formation), however intra-formational seals within *L. balmei – N. asperus* zones offer excellent seal capacity, particularly in mudstones of the lower shoreface, lacustrine/lagoonal facies. Fine-grained abandoned channel fills, floodplain and coastal plain facies are moderate to poor seals.

- Optimum play conditions exist within coarse-grained fluvial channel belts or lacustrine shoreline/deltas sealed by lacustrine deposits within the *L. balmei* zone (Tilana and lower Narimba sequences). Higher risk plays occur within facies of fine-grained lacustrine or coastal lagoon shoreface sandstones, or in compositionally immature coarse-grained alluvial fan and proximal fluvial facies.

9.2 DEPOSITIONAL SETTING

The interpretation of depositional environments in the Bass Basin is based on a facies analysis of key wells (Figure 9.1), integrated with well log interpretations and the palynological results of Partridge (2002; Appendix C). In general, the Bass and Aroo megasequences (Late Cretaceous to Middle Eocene) are fluvial-lacustrine successions associated with peat-forming environments during the syn-tectonic and early thermal subsidence phases of basin development. From the Late Paleocene (Lower *M. diversus* zone) onwards, an increasing marine influence resulted in the formation of freshwater lakes and coastal lagoons within low-lying deltaic and coastal plain environments. Widespread thick coals developed from the early Middle Eocene onward (*P. asperopolus* to Lower *N. asperus* zones), as a result of steady slow subsidence (accommodation) across the basin. From the Middle to Late Eocene (Middle *N. asperus* zone) after widespread fluvial incision ('Boonah Sandstone'), the basin evolved into a protected estuarine and shallow marine embayment (Demons Bluff Sequence). Marine transgression continued through the Oligocene and Miocene, changing to cool-temperate shallow marine marl and limestone sedimentation (Torquay Sequence). Bioclastic carbonate sedimentation dominates through to the present day.

9.3 FACIES INTERPRETATIONS AND DESCRIPTIONS

The facies analysis is based on an interpretation of wireline log character from all available Bass Basin wells, with particular emphasis on new descriptions of 21 selected cores from nine key wells held at the Petroleum Data Repository, Geoscience Australia (Figure 9.1). The cores selected for logging are representative of both depositional facies and age range (Figure 9.2). Ichnofacies interpretations were determined from core photographs collected during the logging phase. The key for the graphic logs is shown in Figure 9.3, with graphic core log descriptions shown in Figures 9.13 to 9.21. A selection of core photos are included in Appendix M.

The following depositional environments were determined from the facies analysis:

- Alluvial fan and proximal fluvial system
- Alluvial plain (including fluvial channel belts and floodplain)
- Incised valley
- Peat mire
- Lacustrine delta/delta plain
- Lacustrine shoreface

- Freshwater lake
- Coastal lagoon/back barrier/interdistributary bay
- Barrier foreshore/shoreface
- Shallow marine/offshore bay

Alluvial Fan and Proximal Fluvial System

Although no cores intersected this facies, it is inferred based on the wedge-like progradational geometries observed in the seismic data across the Durroon Sub-basin (Figure 9.4, Durroon Sequence) and in the Cormorant Trough (Figure 9.5). The sediment composition is likely to reflect the local basement rock, along with mixing with sources farther inland. Coarse-grained sandstones and conglomerates are expected, and poor sorting associated with debris flows is also likely. The alluvial fan and proximal fluvial systems are located adjacent to fault scarps on the basin margin and in half graben within the depocentre.

Alluvial Plain (Fluvial Channel and Floodplain)

These facies are identified by medium to coarse-grained sandstone, ideally with evidence of fluvial channel fill (cross-bedded sandstones) and are not associated with marine fauna or micro-fossils. Good examples of these facies were observed at Durroon-1 (Figures 9.6 and 9.7), Yolla-2 (Figure 9.8), Poonboon-1 (Figures 9.9 to 9.11), Tilana-1 (Figure 9.12) and Pelican-5 (Figure 9.13), including local erosion surfaces, and fining-upward trends. Evidence of exposure (mudcracks, roots) in fine-grained overbank facies occurs in several cores and is interbedded with parallel-bedded and ripple-laminated crevasse splay sandstones. Some of the fluvial channel deposits may be distributary channels if associated with the top of a lacustrine deltaic succession (Poonboon-1, 2468-2470.6 m, Figure 9.11) or interbedded with lagoonal facies (Poonboon-1, 2684-2687 m, Figure 9.10). Fluvial channel deposits are common throughout the basin and appear to be the most optimum reservoir facies, especially within the *L. balmei* zone (Tilana and lower Narimba sequences). Porosity range up to 20%, and permeability typically between 10 and 300 mD, in some cases over 1000 mD based on core plug measurements.

Incised Valley Fill

Incised valley fill facies are more complex and the lowermost fluvial part was not intersected in the cores. However, based on the wireline log interpretation, the base of the "Boonah Sandstone" (Middle *N. asperus*, Demons Bluff Sequence) is a significant likely example of an incised valley fill. The "Boonah Sandstone" represents stacked sandy facies of variable thickness, that overlies a regional seismic-scale erosional unconformity. There is palynological evidence of estuarine conditions in Poonboon-1 (Core 1, 1953.8 and 1958.9 m) overlain by restricted marine to bay conditions (Partridge, 2002; Appendix C). The wireline log motif is typical of wave-dominated or mixed wave – tide-dominated incised valley fills, which have a sharp base (fluvial) fining-upward into shale (estuarine to central embayment) overlain by coarsening-upward, progradational motifs (marine transgressive foreshore and shoreface deposits) (Poonboon-1, Core 1, 1953-1960 m; Figure 9.11).

Peat Mire (Coal)

Peat, now coal, is common within the syn-rift and early post-rift successions, but is especially abundant in the *L. balmei* to *P. asperopolus* zones (Tilana, Narimba and Aroo sequences), where it forms thick extensive coals or thin localised coals. The most extensive coal-prone interval is an intra-Lower *N. asperus* package, lying within the uppermost part of the Aroo Sequence. Coal occurs less frequently in the "Boonah Sandstone" facies (Demons Bluff Sequence), within the confines of incised valleys. There is probably significant lateral variation in the peat systems, from forest peats to bogs or back-barrier marsh, to abandoned channel fill, all with specific geochemical character and hence different source potential (Boreham et al., 2003). Coals with relatively high hydrogen indices (HI) include coals in Poonboon-1 (3040.39-3040.54 m: HI 306) and Pelican-5 (2791.87-2792.00 m: HI 406.5). The sulphur content of the coals is generally very low (0.28 – 0.72%), although an anomalous coal with 2.46% sulphur, possibly indicative of marine influence, occurs in Pelican-5 (2034.00-2037.00m). Coal was also cored in Bass-1 (2261.4-2268.4 m; Figure 9.20).

Lacustrine Delta/Delta Plain

Lacustrine deltas are inferred from wireline log character (upward-cleaning progradational or aggradational cycles a few metres thick, often capped by emergent coals). In some cases distributary channels (Figure 9.10) can be interpreted within these cycles, identified by blocky, or fining-upward successions several metres thick. The main difficulty with the recognition of lacustrine deltas lies in distinguishing them from laterally extensive progradational lacustrine shorelines, which are typically cleaner, and lack distributary channels. A significant part of the succession represents upper or lower delta plain/coastal plain, especially in the western and southern parts of the basin. Lacustrine delta successions occur throughout the basin including the Durroon, Bass and Aroo sequences**.**

Lacustrine Shoreface

This facies is identified by clean, very fine to medium-grained, well-sorted sandstone, with a slight degree of coarsening-upward (e.g., Dondu-1, 2339-2356.5 m, Upper *L. balmei* to Lower *M. diversus* zones, Figure 9.16; Cormorant-1, 2222-2230.2 m, Upper *M. diversus* zone and 2773-2781.5 m, Lower *M. diversus* zone, Figure 9.17). The main sedimentary structures include parallel laminations, ripples, and small cross-beds. The lack of definitive marine palynomorphs suggests lacustrine shorelines or shorelines around coastal lagoons. Examples occur in both the Tilana, Narimba and Aroo sequences.

Freshwater Lake

Stacked fine-grained mudstones with high gamma log motifs are interpreted to be significant, but relatively shallow, lake successions, predominantly in the Narimba and Tilana sequences. Although rarely intersected in the cores (Poonboon-1, 3259-3255 m, Figure 9.9; Cormorant-1, 1994.2-1999.5 m, Figure 9.18), they range from massive to laminated mudstones, and represent periods of relatively high accommodation rates in the various half graben. Typically these are overlain by progradational log motifs. Lake successions are likely to occur throughout the basin especially within the Durroon, Bass and Aroo sequences.

Coastal Lagoon/Back Barrier/Interdistributary Bay

Weakly bioturbated very fine-grained sandstone interbedded with mudstone containing a marine-influenced microplankton (acritarchs including *Micrhystridium* spp., and dinocysts; see Partridge, 2002; Appendix C), and intercalated with back-barrier coal represent this facies (Figures 9.10, 9.14 and 9.15). Marine influence of these coastal lagoons (*Lower M. diversus* zone, Narimba Sequence) is thought to have been via restricted estuarine embayments that connected the shallow lakes to the sea. For further detail see Partridge (2002; Appendix C) who compares this facies with coastal lagoons similar to Lake Maracaibo in Venezuela. These facies are expected to merge into the lacustrine shorelines in a landward direction, and be difficult to distinguish in a seaward direction until full marine facies are confirmed. Ichnofauna identified are typical of a stressed, brackish coastal lagoon or interdistributary bay. For example in Pelican-5 (2864.9 m, *M. diversus* zone), heterolithic fine-grained sandstones and siltstones include *Planolites*, *Thalassinoides, Skolithos* and *fugichnia.* In Poonboon-1 (2688-2688.2 m; Lower *M. diversus* zone), heterolithic mudstone and fine-grained sandstone includes *Ophiomorpha, Paleophycus, Planolites, Teichichnus, Cylindrichnus,* and *Thallasinoides.* In Cormorant-1 (1998 m, Upper *M. diversus* zone), laminated siltstones includes *Planolites, Cylindrichnus, Paleophycus,* and *fugichnia.*

Barrier Foreshore/Shoreface

These include clean, marine influenced fine- to medium-grained sandstone in cleaning-upward cycles a few metres thick. These are most obvious in the upper part of the "Boonah Sandstone" (Demons Bluff Sequence) where the incised valley(s) was initially filled with estuarine, then shoreface sediments resulting from rising relative sea level. For examples, see Poonboon-1 (2683-2683.8 m, Figure 9.10; 1953-1960 m, Figure 9.11), and Cormorant-1 (1504-1512.5 m, Figure 9.19) which show transgressive barrier foreshore and shoreface deposits. Ichnofauna identified in Poonboon-1 (2683-2683.8 m, Lower *M. diversus* zone*,* Narimba Sequence) include *Ophiomorpha* and *Planolites.* A more abundant ichnofauna was identified in Cormorant-1 between 1054 and 1513.3 m (Lower *N. asperus,* Aroo Sequence). Ichnofossils include evidence of both rootlets and restricted marine bioturbation such as *Planolites, Cylindrichnus, Skolithos, Thallasinoides, Paleophycus, Lockeia,* and *fugichnia.*

Shallow Marine/Offshore Bay

This facies includes fine sandstone, siltstone and mudstone with marine microfauna, merging landward into glauconitic fine-sandstones. These facies represent the final stages of widespread marine flooding of the basin (Anglesea Formation; upper Demons Bluff Sequence), that lead to widespread transgressive embayment sedimentation (Bass-2, 1159-1165 m, Figure 9.21). Ichnofauna include an intensely bioturbated assemblage of *Arenicolites, Helminthopsis, Planolites,* and *Chondrites*, distinctly different from the more restricted assemblage of the coastal lagoon or interdistributary bay facies.

9.4 RELATIONSHIP BETWEEN FACIES AND RESERVOIR QUALITY

Reviews of the diagenesis of hydrocarbon reservoirs in the Bass Basin (Chapter 8) provides an overall summary of the diagenetic events in the basin. The primary relationship noted between reservoir quality and depositional facies is linked to the coarse grain size associated with specific facies, with a secondary link to dissolution of early-formed siderite associated with organic-rich facies.

Coarse-grained facies in the Bass Basin include the fluvial channels, some crevasse-splays and coarser-grained elements of the lacustrine/lagoonal shoreface or foreshore facies. The coarser-grained, arkosic or more quartzose rocks, particularly where the rock is clean with moderate to good sorting, have the best chance of retaining good reservoir quality even where deeply buried. Of these reservoirs, channels are the highest ranking, followed by the shoreface and foreshore facies.

Coarse-grained lithic rocks from Lower Cretaceous (Otway Megasequence) fluvial facies in Durroon-1 (3020-3024 m and 2552-2567 m; Figure 9.6) have generally poor reservoir permeability due to early compaction around lithic grains and diagenetic alteration of labile constituents. However, some good reservoir properties based on core-plug results occur in fluvial facies in Durroon-1 (1693.5-1696 m, Early Cretaceous; Figure 9.7). It is likely that undrilled alluvial fan or proximal fluvial coarse-grained or conglomeratic facies in the Upper Cretaceous Durroon Megasequence are also likely to have poor reservoir quality.

Within the Cainozoic succession, reservoir properties (>12% and up to 20% plug porosity and typically >10 mD to 300 mD based on core plugs) are preferentially developed within medium to coarse-grained fluvial channel, splay or distributary channel facies, as well as some fine- to medium-grained shoreface to foreshore facies. These facies were observed in the following core intervals examined for this study (listed from oldest to youngest):

***N. asperus* (Aroo and Demons Bluff sequences)**

Poonboon-1 (1953-1958 m, Middle *N. asperus* zone, shoreface; Figure 9.11)

Cormorant-1 (~1512 m, Lower *N. asperus* zone, shoreface; Figure 9.19)

***M. diversus* (Narimba and lower Aroo sequences)**

Poonboon-1 (2467-2472.5 m, Middle *M. diversus* zone, channels; Figure 9.11)

Pelican-5 (2871-2880.2 m, Lower *M. diversus* zone, channels; Figure 9.13)

Poonboon-1 (2684-2686.8 m, Lower *M. diversus* zone, channels; Figure 9.10)

***L. balmei* (Tilana and lower Narimba sequences)**

Yolla-2 (3033.5 – 3050.3 m, Lower *L. balmei*, zone, channels; Figure 9.8)

Poonboon-1 (3036 –3040 m, Lower *L. balmei* zone, channels; Figure 9.9)

Dondu-1 (2343.3-2356.4 m, Upper *L. balmei* zone, shoreface; Figure 9.16)*****

Tilana-1 (2789-2807.4 m, Upper *L. balmei* zone, channels; Figure 9.12)

** Dondu 1, 2349 m illustrated in Chapter 8 (Figures 8.15 and 8.17).*

Dissolution of early-formed micritic siderite (i.e., pre-compaction siderite) associated with slightly organic-rich facies is a secondary process linked to facies type that is associated with some improved reservoir properties (Chapter 8). The micritic siderite is formed by early reducing conditions in organic-rich, fine- or coarse-grained sandstone and siltstone (e.g., crevasse splays on the floodplain or lacustrine shoreface facies). An example is Cormorant-1 (2773 m, Lower *M. diversus* zone; Figure 9.17) (Chapter 8; Figures 9.6 to 9.8). Later dissolution of the siderite can lead to late compaction effects but modest secondary porosity can still be retained. Other diagenetic processes not directly related to facies type involve sediment composition (provenance), burial history and fluid interaction (Chapter 8).

A key observation by Cubitt (1992) is that the *L. balmei* zone interval (Tilana and Narimba sequences) has a predisposition to good reservoir quality even though it is represented mainly in deeper parts of the basin. From a facies perspective, this may be due to the relatively high-energy of the depositional systems when compared to the overlying succession. The intra-*L. balmei* unconformity event signals continued tectonic activity in the basin leading to increased depositional gradients. A combination of sediment composition, grain-size, early diagenetic history and subsequent burial history combine to maintain moderate to good reservoir quality despite deeper burial when compared with the overlying succession.

9.5 RELATIONSHIP BETWEEN FACIES AND SEAL CAPACITY

The relationship between depositional facies and seal capacity is mainly a function of grain-size, with fine-grained rocks from the lower and upper shoreface, lagoon, lacustrine or interdistributary bay, and stacked crevasse channel/floodplain having the most significant seal capacities (Chapter 7, Appendix L).

Of the MICP samples selected from cores examined for this study, the highest ranking sealing capacity was reported from mudstones of the lower shoreface facies (Dondu-1, 2342 m, Upper *L. balmei* zone, average oil column >1400 m). The other two lower shoreface samples from younger successions were siltstones with a predictably lower, but still good sealing capacity (Pelican-5, 2890.8 m, Lower *M. diversus* zone, average oil column 853 m; Poonboon-1, 1954.2 m, Middle *N. asperus* zone, average oil column 350 m).

The second highest ranking seal capacity was reported from finely laminated lagoonal or interdistributary bay mudstones (Cormorant-1, 1999.3 m, *P. asperopolus* - Upper *M. diversus* zones, average oil column ~1140 m). Other interdistributary bay or lacustrine facies also have good sealing capacities (Cormorant-1, 2231.6 m, Upper *M. diversus* zones, average oil column 797 m; Pelican-5, 2863.8 m, Lower *M. diversus* zones, average oil column 698 m; Poonboon-1 3259.8 m, Lower *L. balmei* zone, average oil column 568 m).

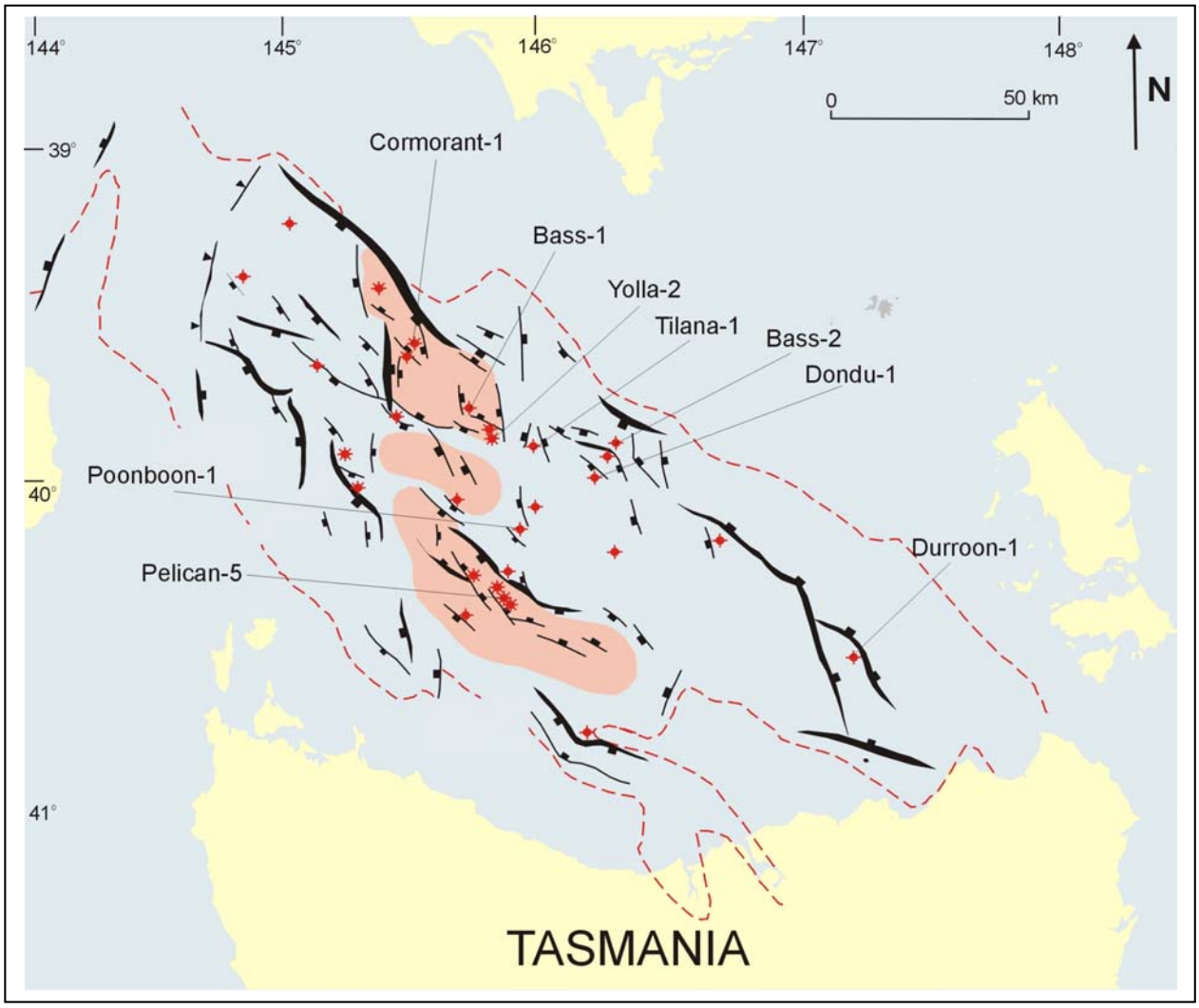
Other important sealing facies include fine-grained fluvial channel fills from Durroon-1 (3021.88 m, Early Cretaceous, 988m) and Tilana-1 (2800 m, Upper *L. balmei* zone, 898 m), both able to support an oil column

greater than 700 m. Coastal plain, fluvial overbank and back barrier berm deposits are the least significant sealing lithologies reported in the study, supporting <200 m oil columns. The only sample available from the regional seal, a shallow shelf or bay mudstone, had a modest to good sealing capacity (Bass-2, 1164.49 m, Upper *N. asperus* zone, 400 m).

A comparison of width/length aspect ratios for a variety of seal types suggest that lower lacustrine shoreface and lacustrine/lagoonal facies with high sealing capacity are also laterally extensive. Given that most of these samples were from intraformational units within the Tilana, Narimba or Aroo sequences (Eastern View Group), the potential to trap significant oil columns well below the regional seal is clear, provided other leakage pathways (faults, lateral seal failure) did not operate.

The *L. balmei* zone interval (Tilana and Narimba sequences) has both a predisposition for better reservoir quality for a given depth than the overlying succession, and contains good intraformational seals. Therefore the opportunity exists for significant stratigraphic and combined structural/stratigraphic traps in the deeper parts of the Bass Basin. Further work incorporating seal thickness, integrity and capacity is required to advance the evaluation of seals in the basin.

Figure 9.1 Map showing the location of wells with cores described and interpreted for this study.



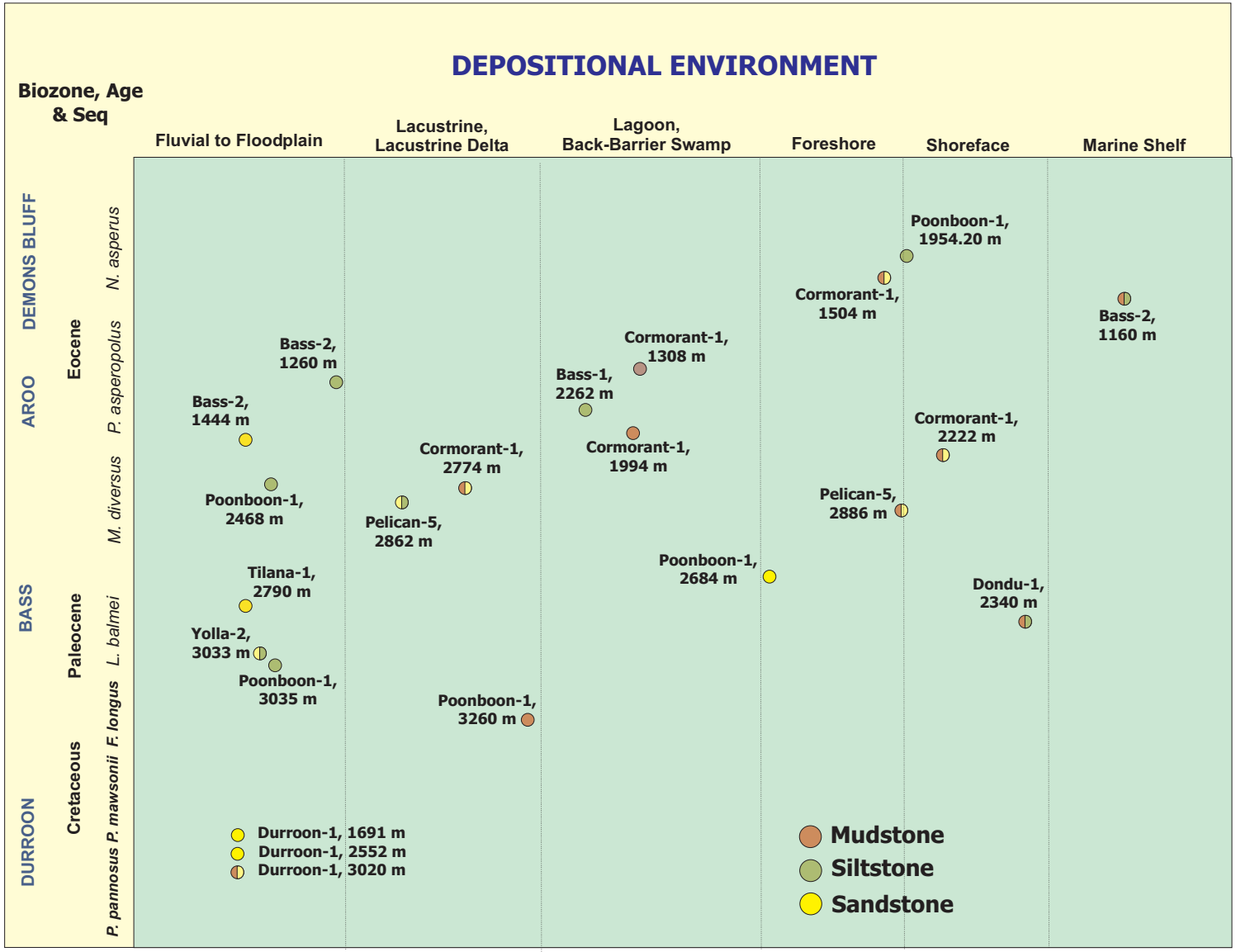
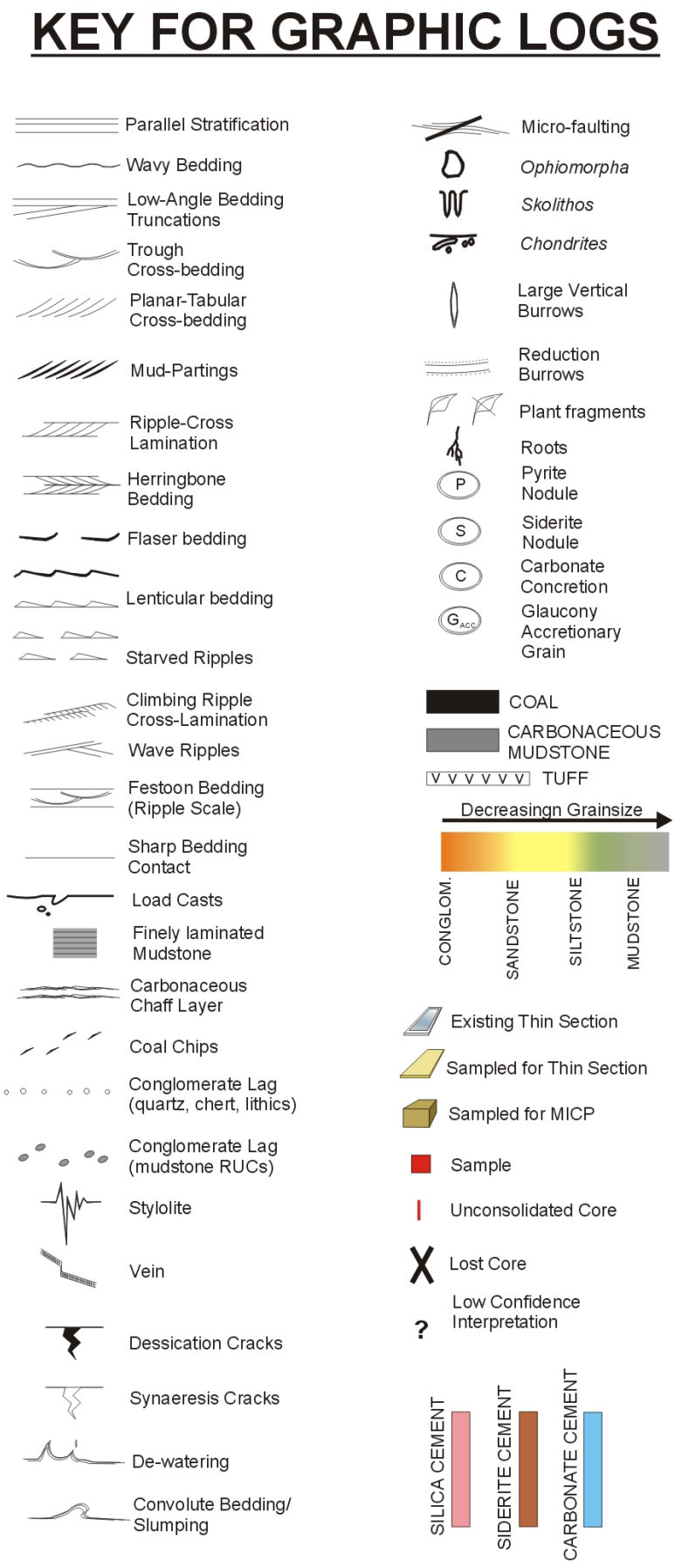


Figure 9.2 Depositional facies and spore/pollen biozones represented in selected cores in the Bass Basin.

Figure 9.3 Key for graphic logs showing the Figures 9.6 to 9.21.



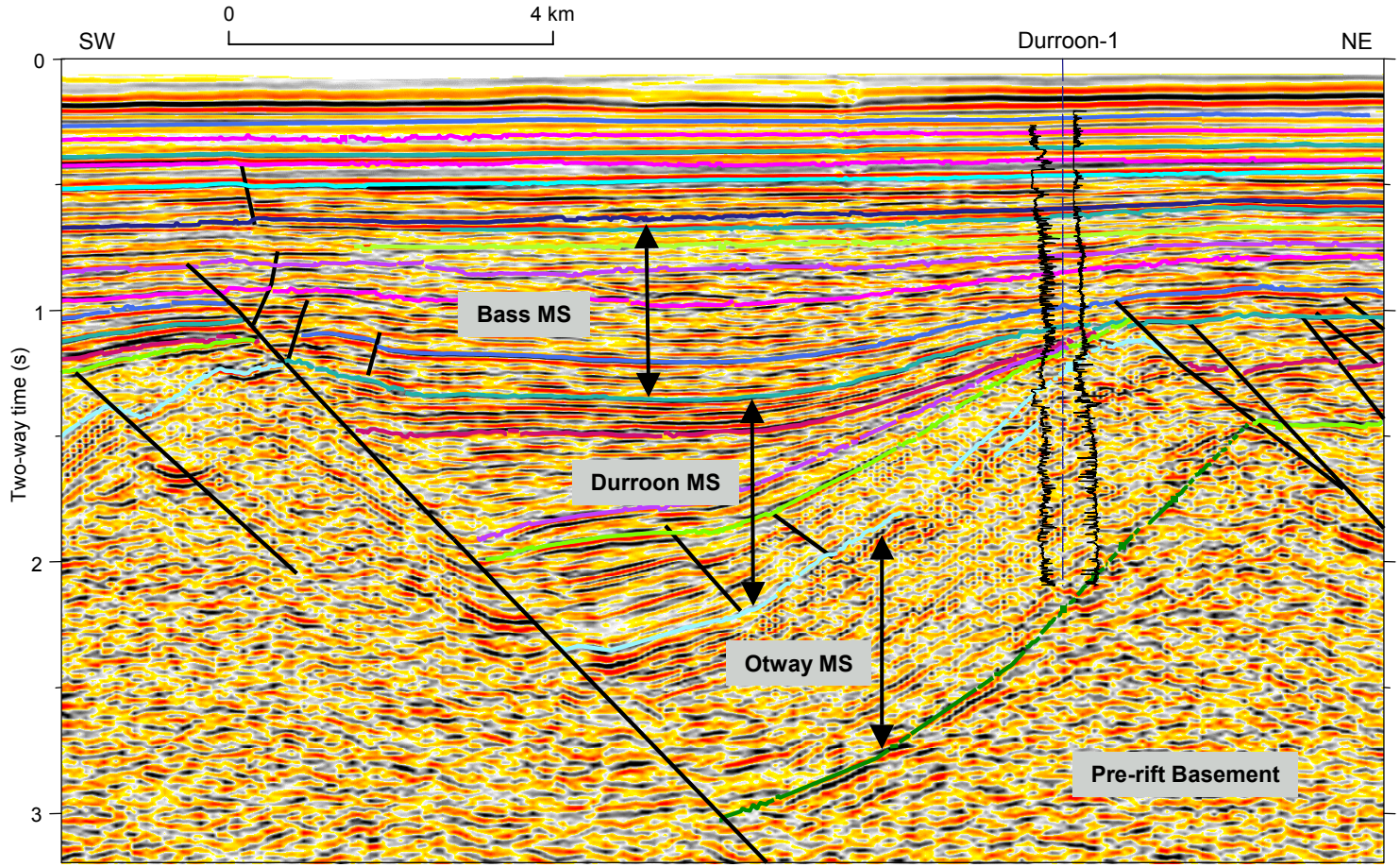


Figure 9.4 Geoscience Australia seismic line across part of the Durroon Sub-basin. This section shows in more detail the syn-tectonic successions intersected at the Durroon-1 well: the Early Cretaceous Otway Megasequence (Rift Phase 1) and the overlying early Late Cretaceous Durroon Megasequence (Rift Phase 2). Strata within the syn-rift succession has a wedge-like progradational geometry that is interpreted to contain fans. This seismic image is published with the permission of Fugro MCS.

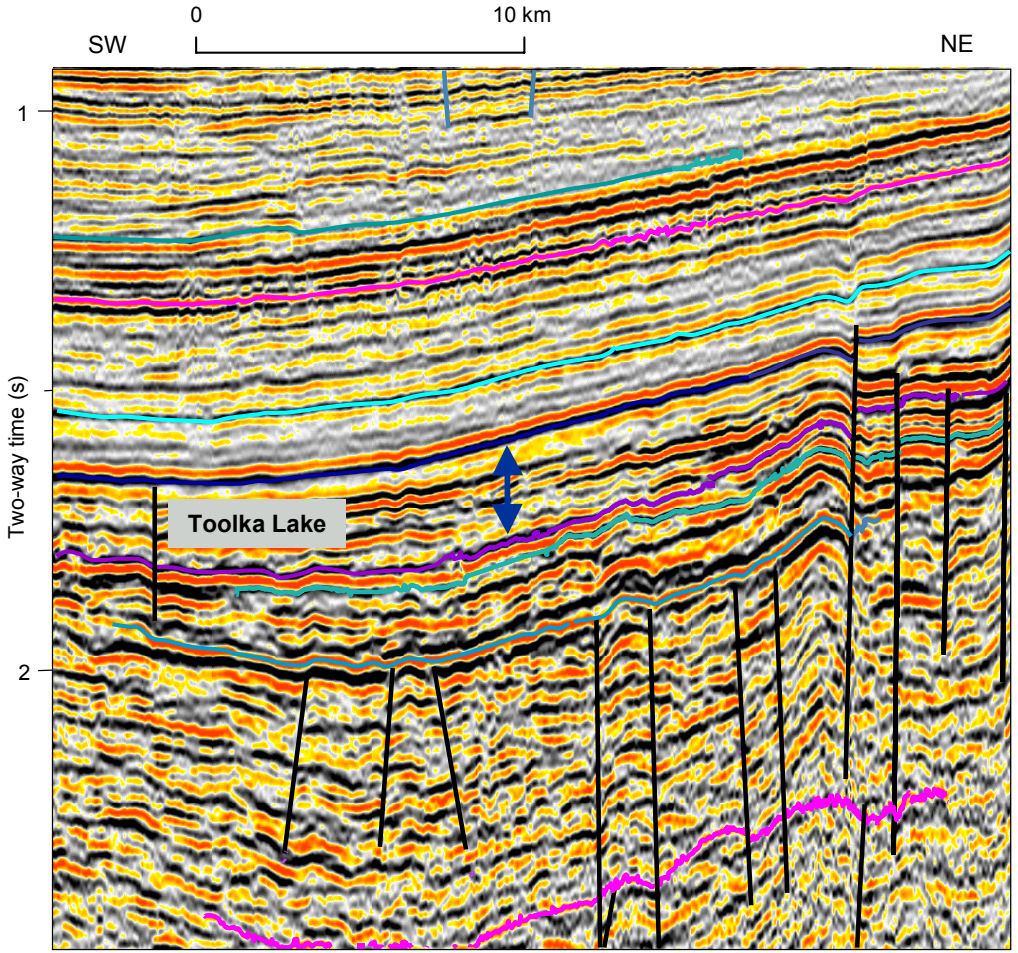


Figure 9.5 Geoscience Australia seismic line across the central Bass Basin showing the geometry and stratal character of sediments of Early to Middle Eocene age in the Cormorant Trough. The dark blue horizon marks the "Base of the Boonah Sand". This figure is published with the permission of Fugro MCS.

Figure 9.6 Fluvial channel deposits in Durroon-1 (3020-3024 m, 2552-2568 m) from the Lower Cretaceous Otway Megasequence (*P. pannosus* zone).

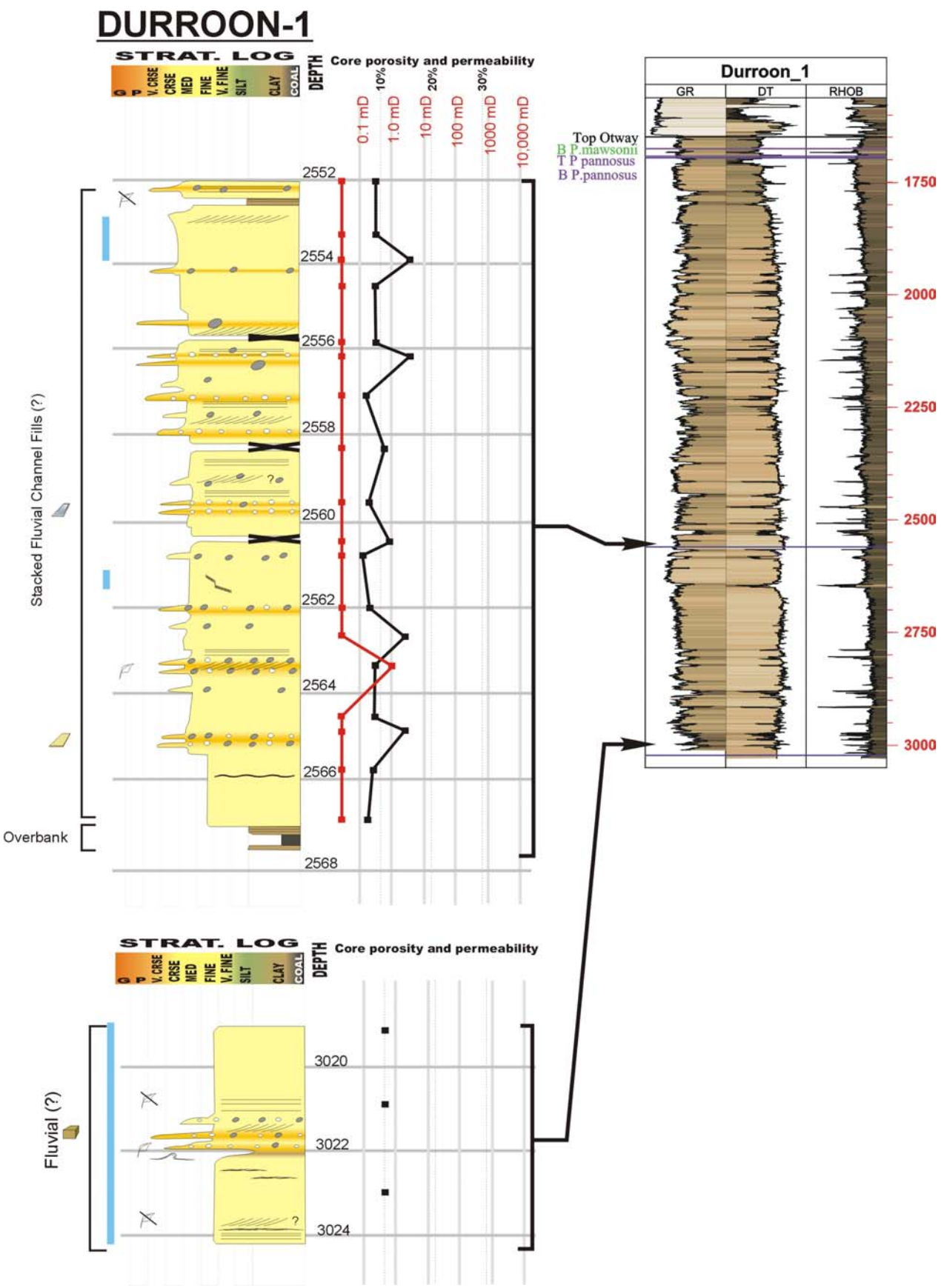


Figure 9.7 Fluvial channel and floodplain deposits in Durroon-1 (1691.3-1696.2 m) from the Lower Cretaceous Otway Megasequence (*P. pannosus* zone). Moderate porosity (>20%) and permeability (10-100 mD) occur in the fluvial channel-fill sandstones.

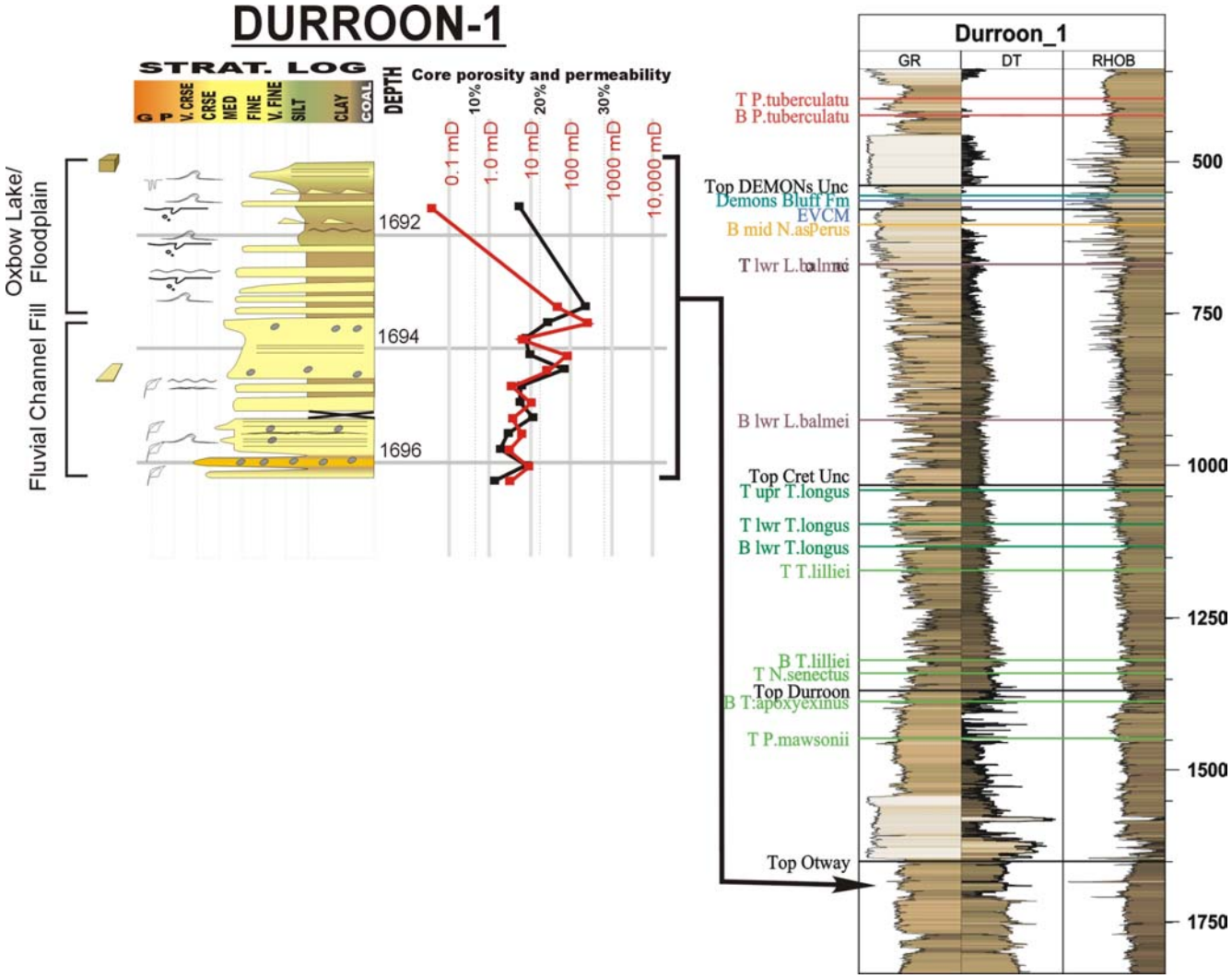


Figure 9.8 Example of stacked fluvial channels and overbank deposits in Yolla-1 (3033-3051 m) in the Tilana Sequence (Lower *L. balmei* zone).

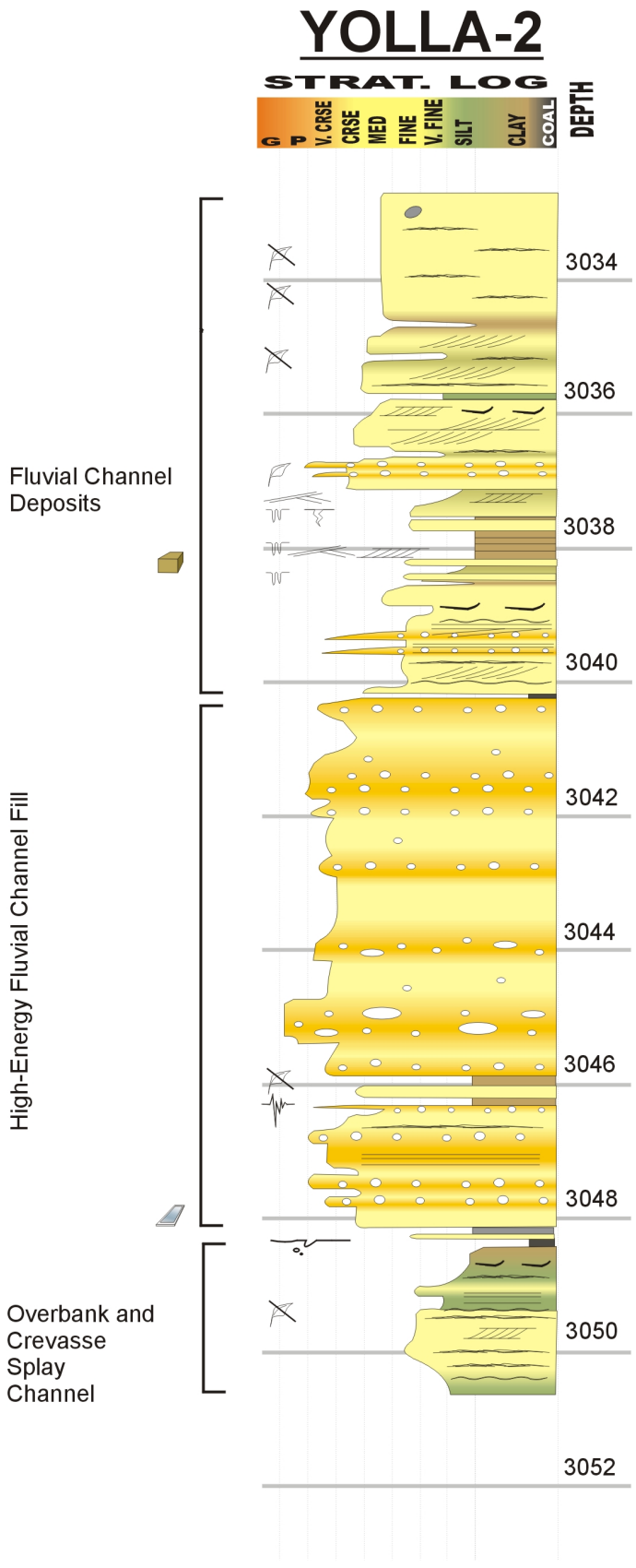


Figure 9.9 Poonboon-1 lacustrine (3259-3266 m; Upper *F. longus* zone) in the lowermost Tilana Sequence, and stacked fluvial channels or splays interbedded with overbank deposits and coal (3034-3042.6 m; Lower *L. balmei* zone) within the Tilana Sequence.

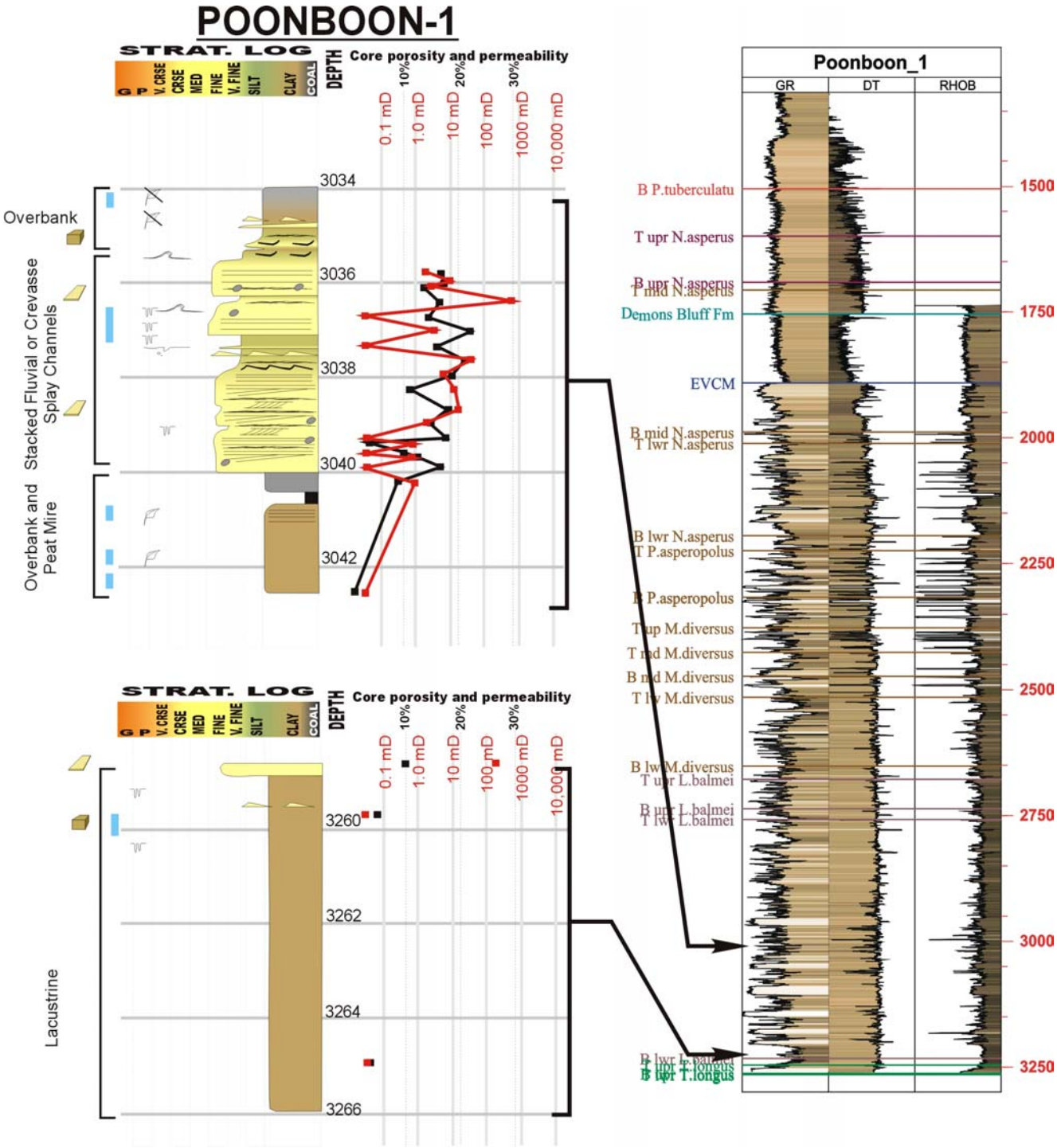


Figure 9.10 Poonboon-1 cores showing back-barrier berm and lagoon with crevasse splay deltas, distributary channels and foreshore lacustrine deltas forming part of an overall lower lacustrine delta plain succession (Core 3, 2683-2690.8 m). Palynology (Partridge, 2002; Appendix C) from core samples at 2688 and 2689.3 m record 33% and 50%, respectively, of the acritarch *Michystridium* spp., and the non-marine dinocyst *Morkallacysta* spp. Undifferentiated marine dinocysts (33%) are recorded at 2689.3 m supporting the interpretation of a coastal lagoon partially connected to the sea. This interval lies beneath a retrogradational fining-upward succession interpreted as a transgressive systems tract where a reliable marine dinocyst, *Apectodinium reburrus* is recorded (50%) in a sidewall core sample from 2678.6 m. The core lies within the Lower *M. diversus* zone, associated with the expansion of the "Koorkah" coastal lagoon to lake system identified by Partridge (2002; Appendix C), within the Narimba Sequence. Notice the moderate to good porosity and permeability of the fluvial succession (20-30% porosity, 100-1000 mD permeability). Also see Figure 9.14 and 9.15.

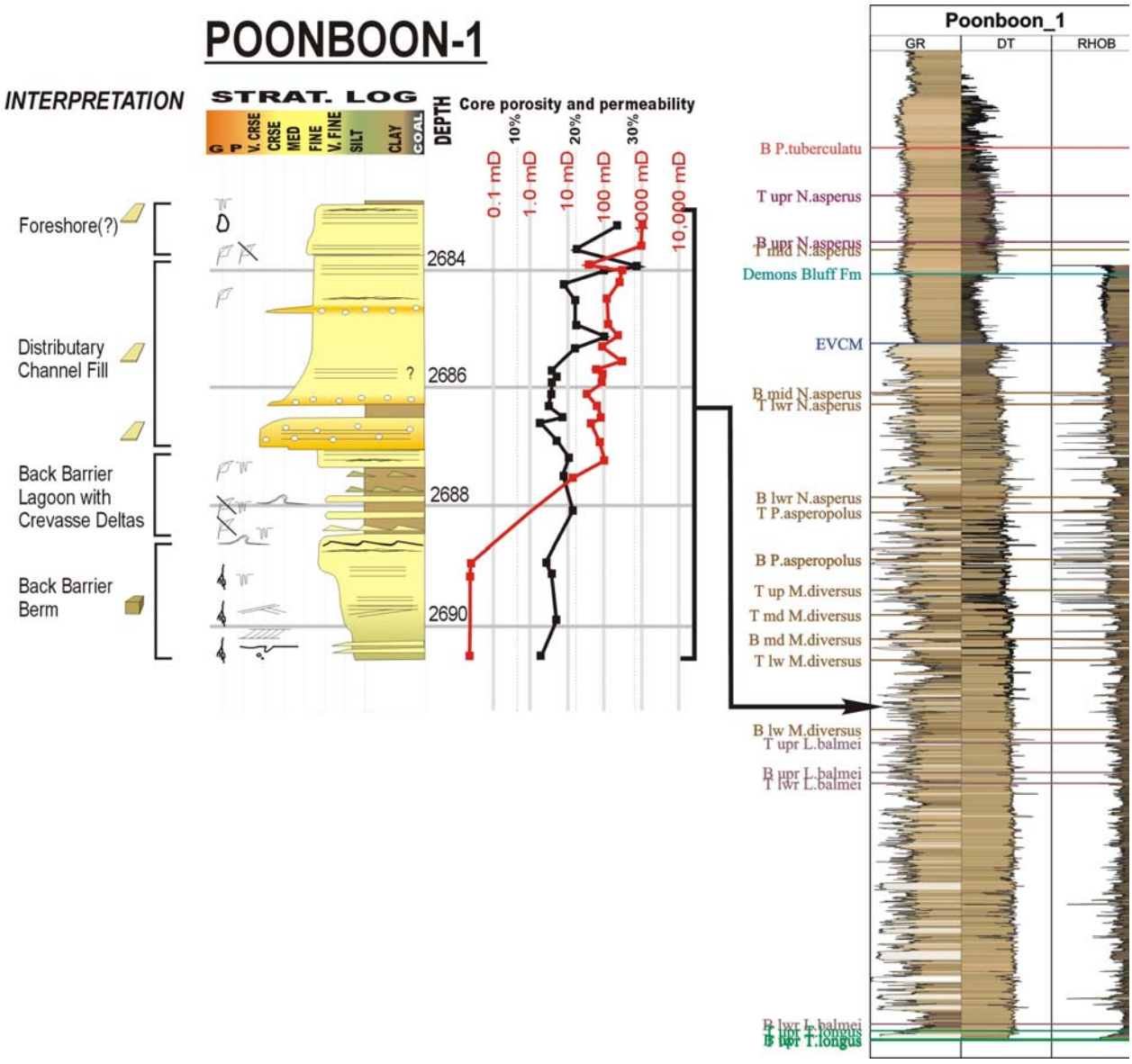


Figure 9.11 Poonboon-1 cores showing lacustrine foreshore to mid-shoreface (1953-1960.2 m) from the Demons Bluff Sequence (Middle *N. asperus* zone) and fluvial distributary channel-fill, splays and overbank deposits (2467-2474 m) from the Narimba Sequence (Middle *M. diversus* zone). Notice the development of moderate to good porosity and permeability of the fluvial succession (20-30% porosity, 100-1000 mD permeability).

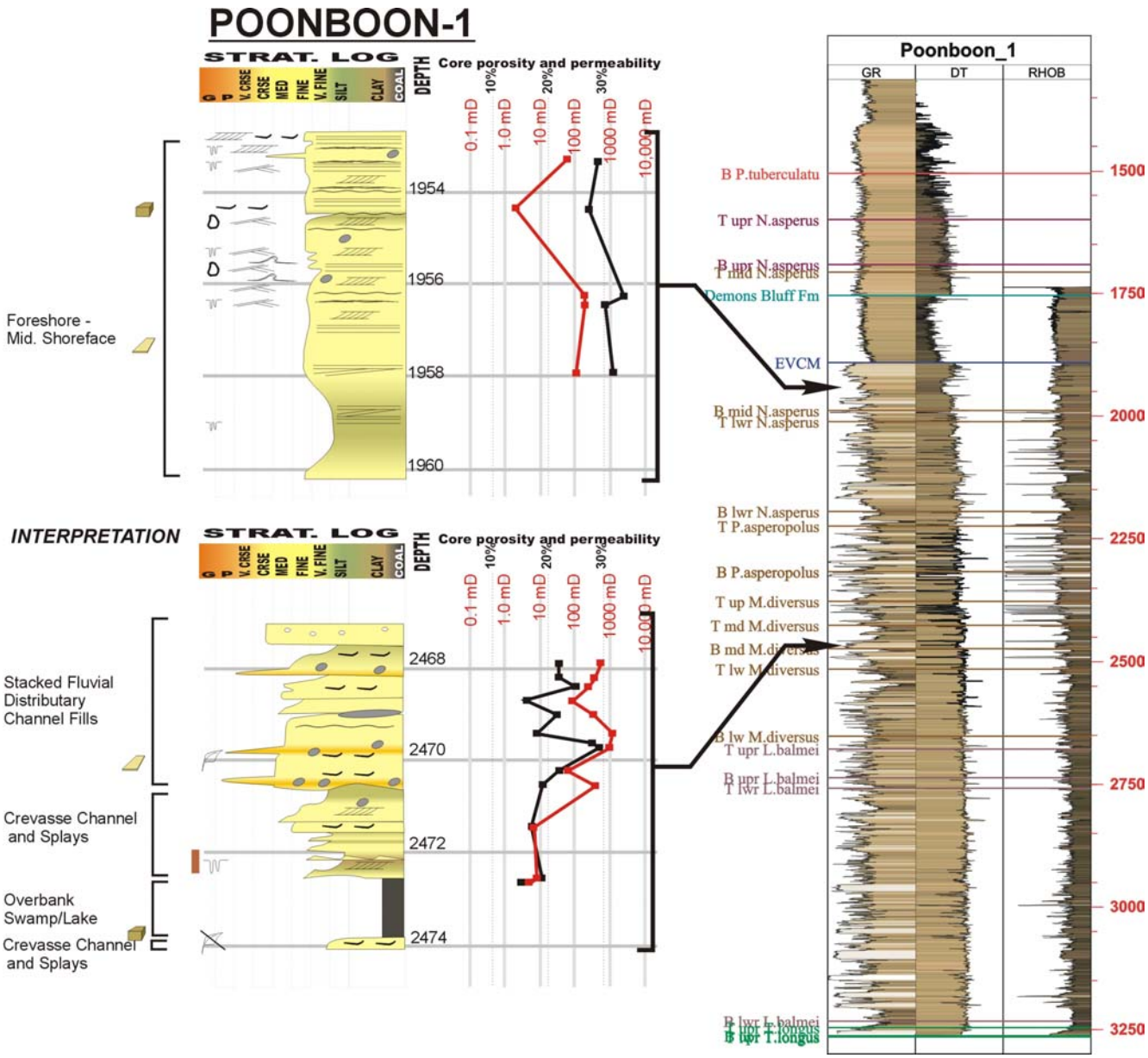


Figure 9.12 Tilana-1 core from 2789-2807.4 m showing fluvial distributary channels interbedded with lacustrine shoreface in the Narimba Sequence (Upper *L. balmei* to Lower *M. diversus* zones).

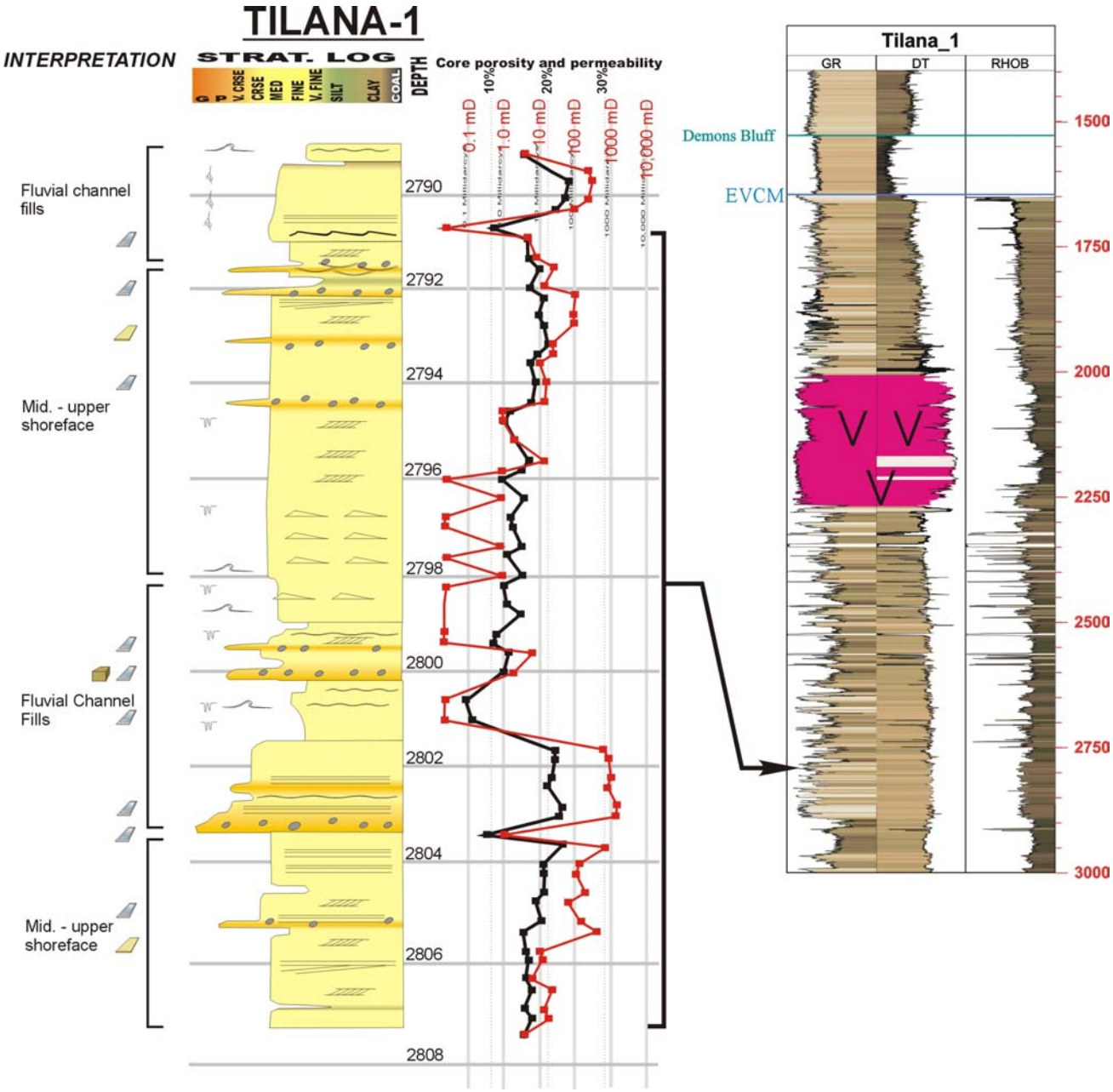


Figure 9.13 Pelican-5 core from 2862.2-2890.7 m showing lacustrine foreshore to shoreface overlain by stacked fluvial distributary channels topped by interdistributary bay facies. Porosity in the fluvial facies ranges from 10 to 20%, with pemeability from 5 to 12 mD, locally up to 300 mD. Good porosity (15-20%), but variable permeability (<0.1 to 200 mD) occurs in the lacustrine foreshore to shoreface. Part of a transgressive systems tract with increasingly isolated sandstone up section (Narimba Sequence; Middle *M. diversus* zone).

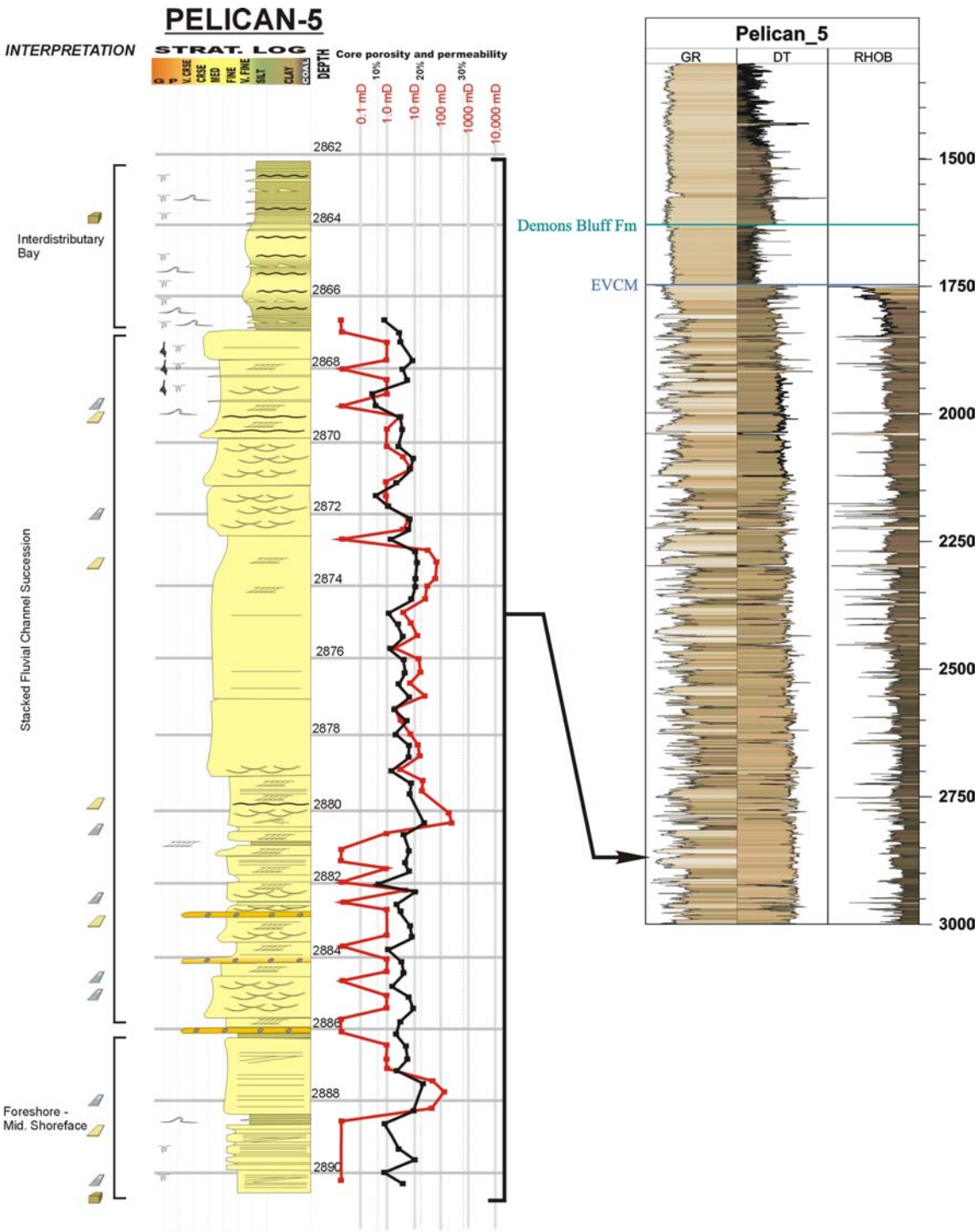


Figure 9.14 Lower part of Poonboon-1, Core 4, showing slightly bioturbated, tight, fine-grained sandstone with wave-influenced parallel lamination and rootlets (left) interpreted as back-barrier berm, overlain by coarsening-upward mudstones to fine-grained sandstones interpreted as back-barrier coastal lagoonal to lacustrine delta deposits (right). Acritarchs (*Micrhystridium* spp.) and dinocysts (*Morkallacysta* spp.) recorded from 2689.3 and 2688 m indicate a possible connection to the sea, supported by undifferentiated marine dinocysts recorded at 2689.3 m (Partridge 2002, Appendix C) (Lower *M. diversus* zone, Narimba Sequence).



Figure 9.15 Upper part of Poonboon-1, Core 4, showing reservoir facies interpreted as coarse-grained distributary channel sandstones with approximately 15-20% porosity and 100 mD permeability, overlying coarsening-upward mudstones to fine-grained sandstones interpreted as back-barrier coastal lagoonal deposits (left) at approximately 2686.8 m. Acritarchs and dinocysts recorded from 2688 m (blue dot) indicate a possible connection to the sea (Partridge, 2000, Appendix C) (Lower *M. diversus* zone, Narimba Sequence).



Figure 9.16 Example of lacustrine shoreface from Dondu-1 showing classic upward-coarsening, progradational log motif, with thinner backstepping parasequences at the top (2340-2356 m). Optimum reservoir conditions occur in the upper part of the cycle, with porosity ranging from 13-28% and permeability ranging from 1.0 to 500 mD (Upper *L. balmei* zone, lower Narimba Sequence).

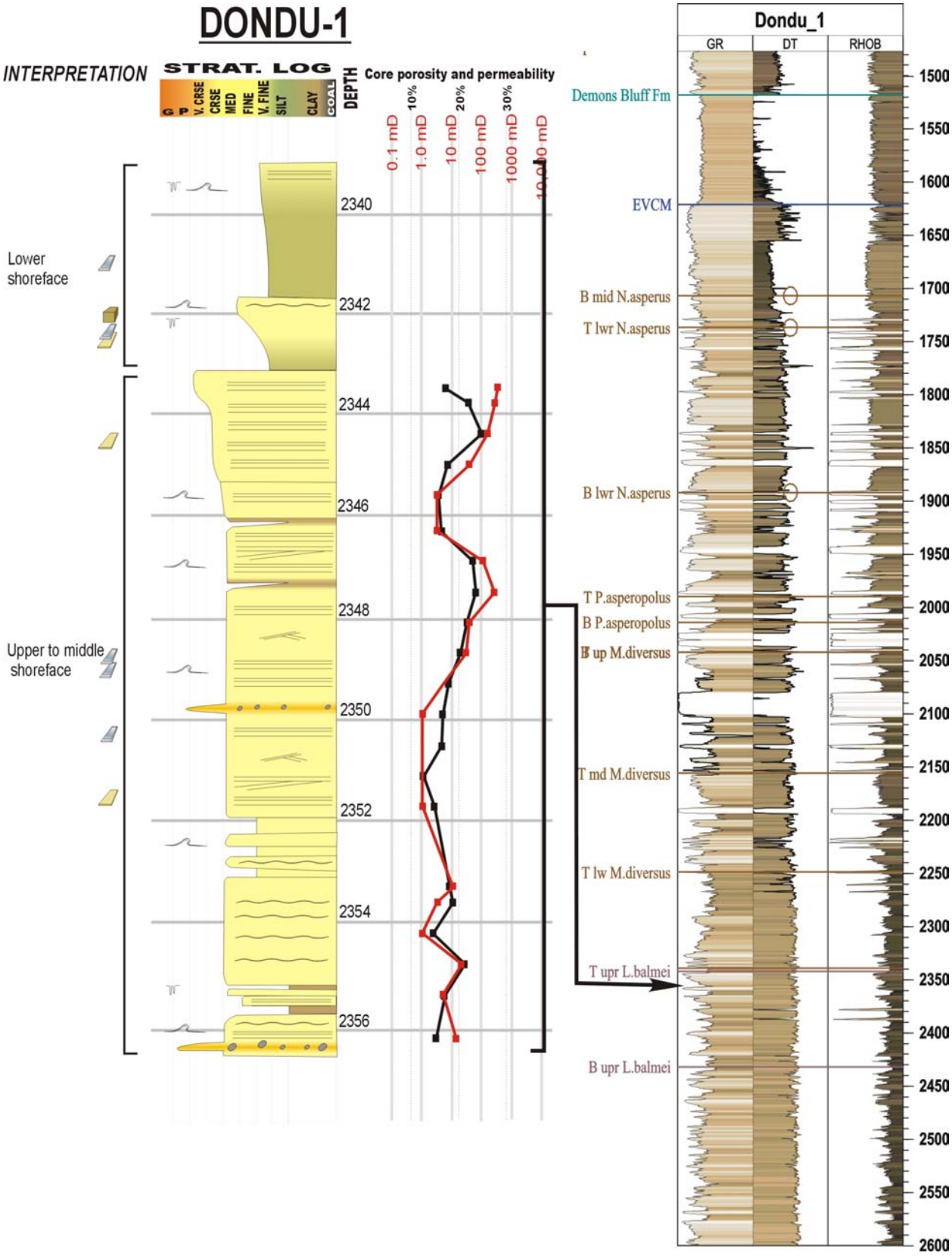


Figure 9.17 Cormorant-1 cores at 2222-2231.5 m, interpreted as peat mire and overlying lower shoreface (Upper *M. diversus* zone, lowermost Aroo Sequence), and 2773.2-2781.6 m interpreted as wave and tidally influenced lower delta plain, respectively (Lower *M. diversus* zone, Narimba Sequence).

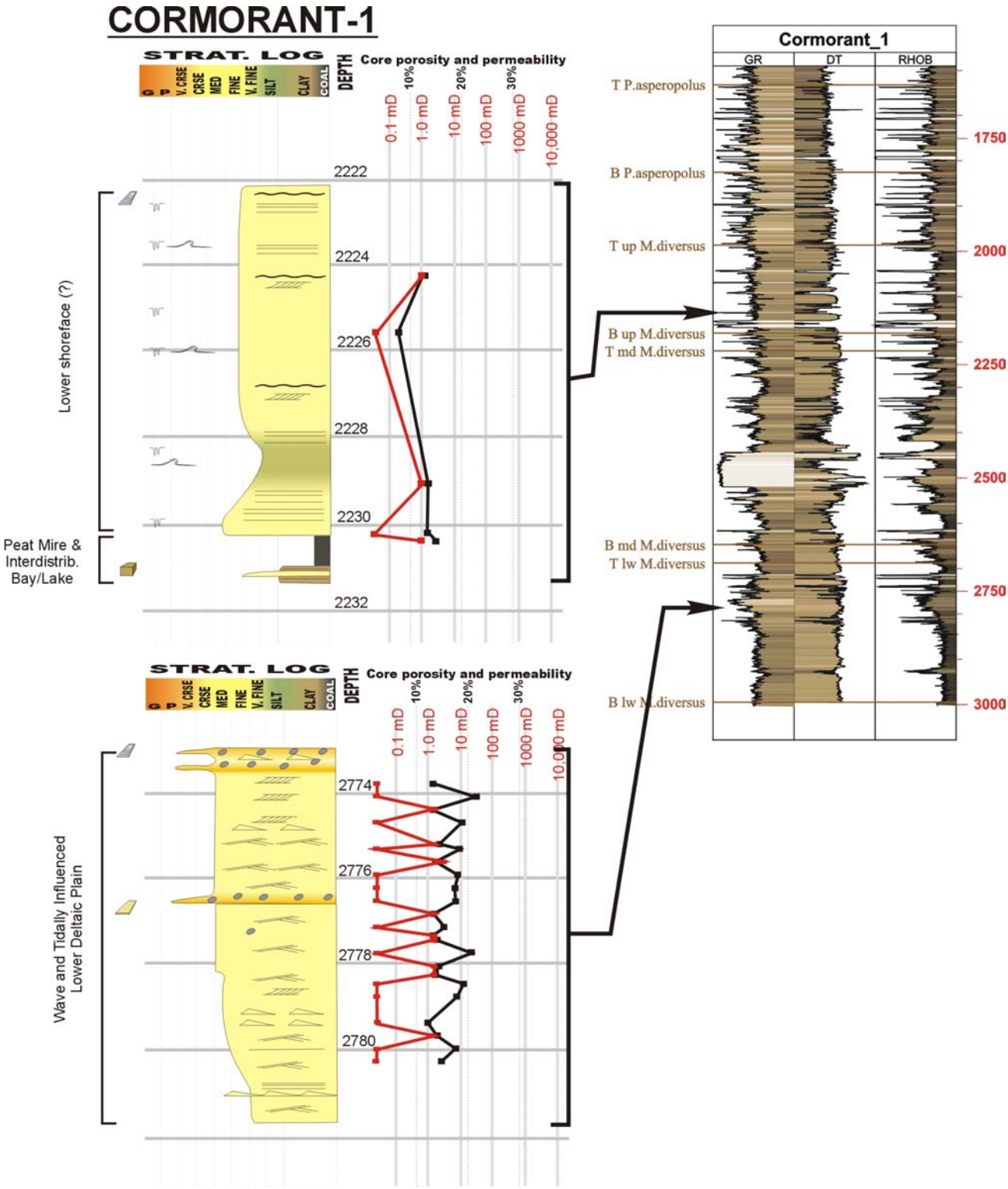


Figure 9.18 Cormorant-1 core 1994.2-2000.2 m interpreted as a lake or restricted coastal back barrier lagoon (Upper *M. diversus* zone, lowermost Aroo Sequence).

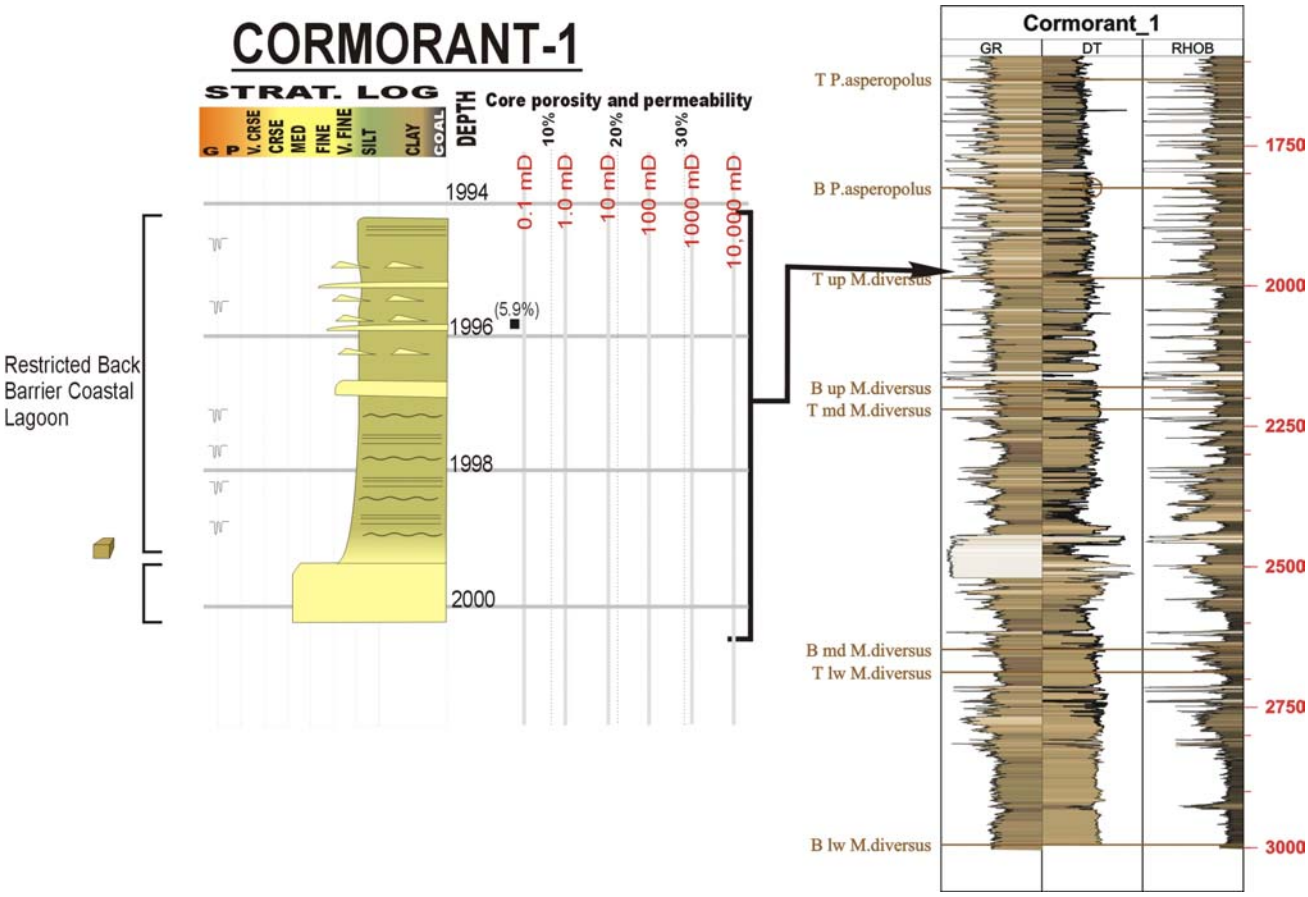


Figure 9.19 Cormorant-1 cores at 1307.2-1312.8 m interpreted as restricted coastal lagoon (Middle *N. asperus* zone, Demons Bluff Sequence) and 1503.8-1512.4 m interpreted as lacustrine shoreface and foreshore (Lower *N. asperus* zone, upper Aroo to lowermost Demons Bluff sequences).

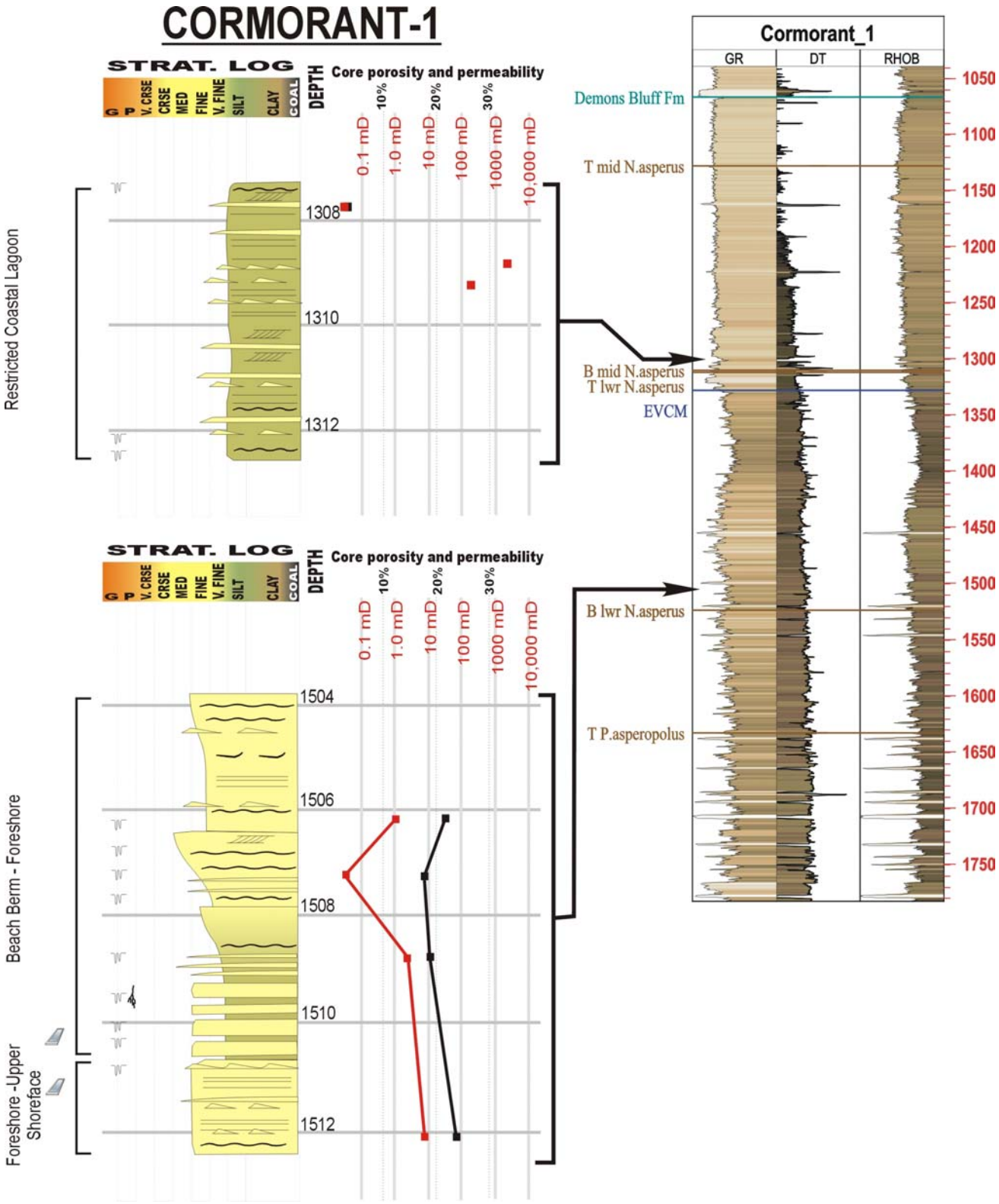


Figure 9.20 Bass-1 core at 2261.4-2268.5 m showing fine-grained shallow floodplain lake or inter-distributary bay deposits between peat mires (coals) (*P. asperopolus* zone; Aroo Sequence).

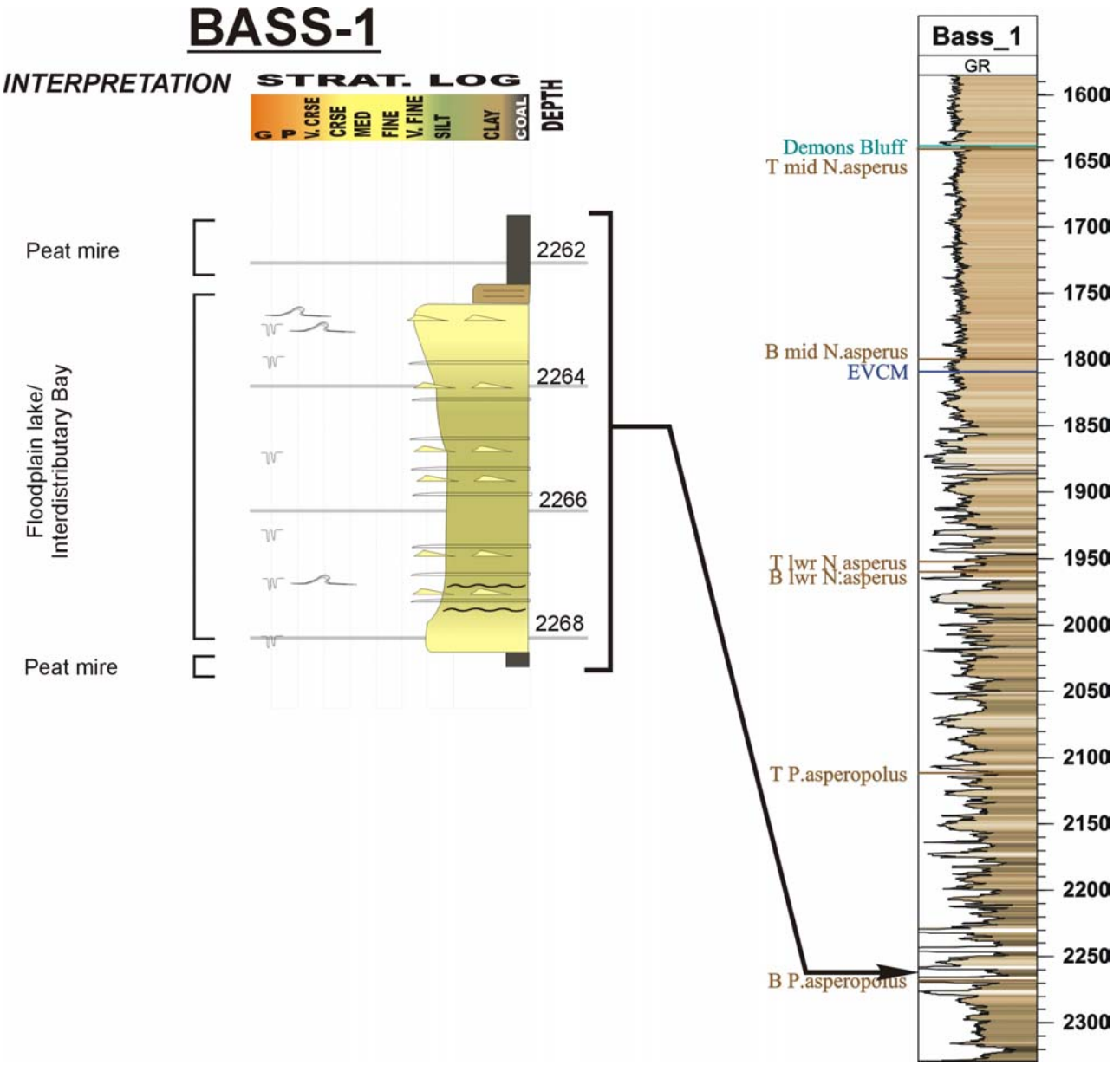
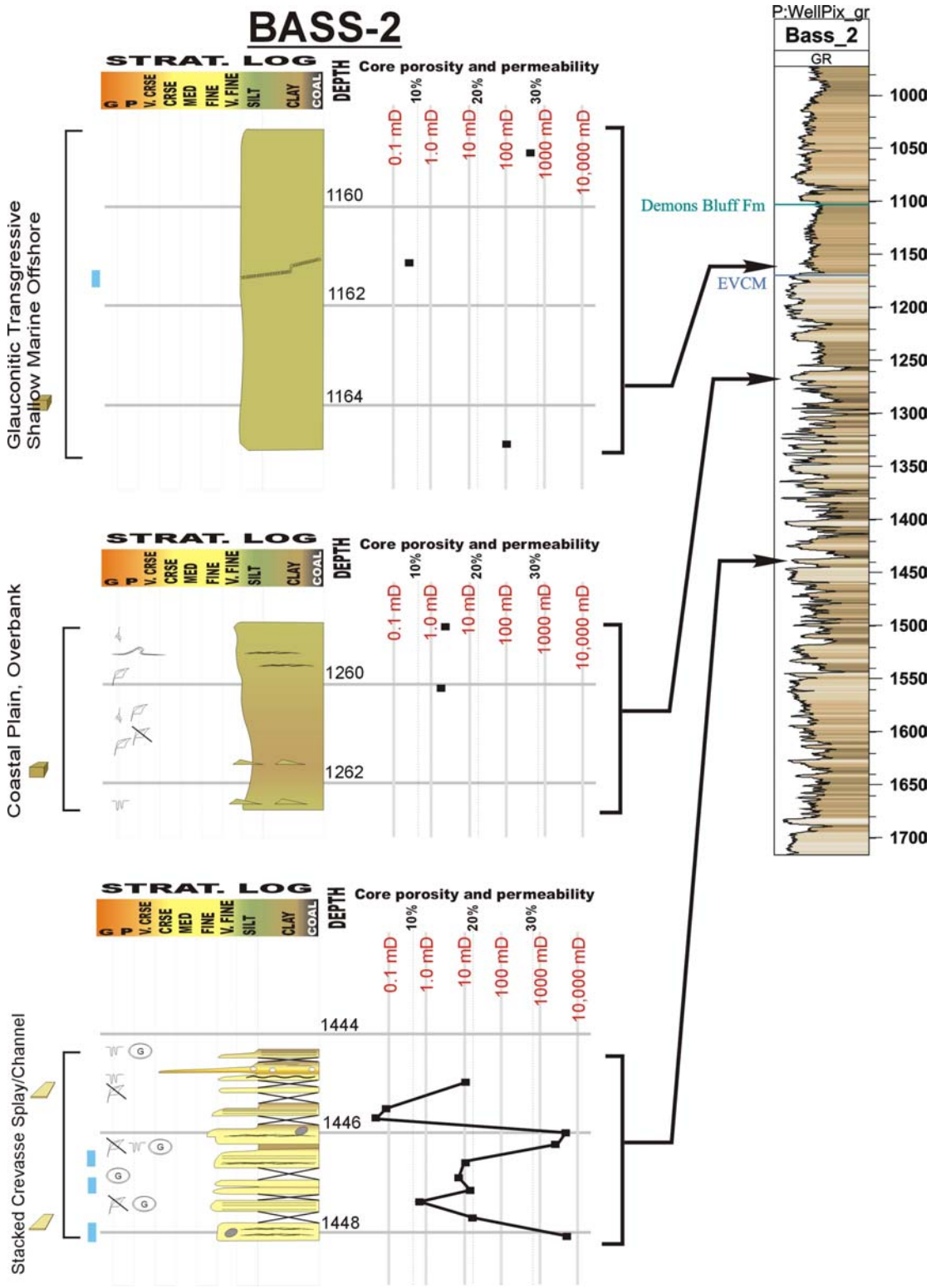


Figure 9.21 Bass-2 cores. Upper core (1159-1165 m) is glacuonitic siltstone forming part of the regional seal, interpreted as a transgressive shallow marine offshore deposit (Demons Bluff Sequence). Middle core (1259-1262.6 m) is coastal plain or overbank siltstones and very-fined grained sandstones (Aroo Sequence). Lower core (1444.4-1448.2 m) fine-grained sandstones, pebbly in places interpreted as crevasse splay deposits (Aroo to uppermost Narimba sequences).



10. PETROLEUM SYSTEMS AND PLAY ANALYSIS

10.1 KEY POINTS

- A geochemical correlation between recovered hydrocarbons and potential source rocks has shown that the Bass Basin hosts an effective, terrestrial-based petroleum system (coals and fluvio-deltaic facies). Lacustrine shales are likely to be more important as seal facies, rather than as potential source rocks. The Middle Eocene and younger marine succession shows low source potential and does not lie within the oil window. Prospective areas of the Bass Basin are included in the 2002 and 2003 Offshore Acreage Release Areas (Figure 10.1).
- Geohistory modelling has shown that the onset of the main oil generation phase (Paleocene to Early Eocene coals and shales) occurred from the Late Eocene to Early Miocene, post-dating the main periods of seal deposition and trap formation. The Miocene inversion occurred after the onset of generation in the basin, and has resulted in large structures along the northern basin margin.
- The critical factor in sourcing accumulations from the coaly succession appears to be effective primary and secondary expulsion from the source rock and the volume of charge. The accumulations at Cormorant, Yolla and Pelican confirm that generation and migration have occurred within the deeper depocentres. Recent fluid inclusion studies suggest a migration phase onto the flankings of these structures (e.g., Aroo-1 and Tilana-1; Kempton et al., 2002), possibly driven by late gas charge.
- Other areas of potential prospectivity include the "Tertiary Platform" (Lennon et al., 1999) in the vicinity of Poonboon-1 and Nangkero-1, sourced locally by hydrogen-rich coals of Late Paleocene to Early Eocene age (Chapter 5). In addition, plays along the flanks of the "Tertiary Platform" (e.g., Yurongi-1 and Chat-1) have yielded some evidence of migration or potential oil zones (Kempton et al., 2002).
- Untested plays include reservoir/seal pairs associated with times of maximum flooding events in the western Bass Basin (e.g., Lower *M. diversus* and "top" *P. asperopolus* MFS).
- The petroleum systems elements of the Durroon Sub-basin differ significantly from the Cape Wickham Sub-basin owing to the cessation of tectonically-driven subsidence in the eastern Bass Basin (Durroon Sub-basin) from the mid-Campanian onward.

10.2 EXPLORATION RISKS

The main exploration risks in the Bass Basin are reservoir quality, seal properties, trap integrity (trap and seal breach) and access to mature source rocks (hydrocarbon charge) (Trigg et al., 2003; Trigg and Blevin, 2003). In the early years of exploration in the Bass Basin, poor data quality was also considered a significant exploration risk due to poor imaging below the regional seal, and the prolific occurrence of coals and volcanic rocks in the basin succession. However, advances in technology and increased knowledge of the basin's geology have minimised this aspect of risk. The use of geophysical evidence, such as AVOs, as a proxy for detecting hydrocarbon accumulations/contacts should be used with caution because of the widespread occurrence of coals, sills/flows and the intrusion of volcanic fluids into porous/fractured strata.

Recent commercial reprocessing of the existing industry seismic dataset has upgraded much of the open-file seismic dataset (Fugro Multi Client Services).

An audit of all open-file exploration wells in the Bass Basin has been compiled as part of the WTRMP (Trigg et al., 2003). This report summarises information on exploration targets, drilling results and associated technical data. The report also presents "snapshots" of composite logs (gamma and sonic) and seismic data to show the structures drilled and general well lithology. A summary of well results from the audit is presented in Figures 10.2 and 10.3 (Trigg et al., 2003). Of the 32 wells drilled in the basin, six have been determined to be invalid tests as a result of being drilled off-structure, or the absence of structural closure at the target horizons (primarily due to the presence of volcanics and associated velocity problems).

In combination with data on shows and accumulations, the drilling results clearly show that mature source rocks have generated and expelled hydrocarbons in the Cormorant, Pelican, Yolla and White Ibis troughs. However, trap breach is a significant exploration risk along much of northern basin margin, particularly in the northwest, as confirmed by the breached accumulations detected at Cormorant-1 (Kempton et al., 2002). In addition, several oil and gas zones were recorded between 1500 and 2800 m (*P. asperpolous* to Lower *M. diversus* zones) at Cormorant-1, well below the crest of the anticlinal structure and the regional "Demons Bluff" sealing facies. This suggests that Miocene inversion resulted in fault reactivation and partial breaching of traps and intra-formational seals that were in place prior to the deformational event. Biodegradation of the Cormorant oil was detected during the geochemical analyses (Chapter 5). Failure to trap hydrocarbons at Koorkah-1 and Konkon-1 has also been attributed (in part) to seal breach, with Koorkah-1 recording shows from 2400 m to TD. Hydrocarbon charge may also be a factor in the failures at Koorkah-1 and Konkon-1.

The absence of commercial accumulations in the Pelican Trough has been attributed to poor reservoir quality, primarily low permeability. Although sediment deposition in the Pelican Trough was dominated by sand-rich facies from the Late Paleocene to Middle Eocene (*M. diversus* to Middle *N. asperus* zones), subsequent diagenetic events have hindered preservation of the initial reservoir quality. This may be due to a combination of factors, including lack of an early marine cementation phase, sediment compaction, structural deformation, and elevated palaeoheatflow in the Pelican Trough and surrounding areas (e.g., Flinders-1, Pelican-3) (Chapters 5, 6 and 8). These factors may have been less pronounced along the margins of the trough.

In the southwestern part of the basin, the accumulation at White Ibis-1 was probably sourced through updip migration from the flanking trough (Yolla/White Ibis Trough). This is supported by the high maturity of the hydrocarbons as detected during the geochemical analyses (Chapter 5). Some late stage reactivation associated with uplift of the ramp margin has enhanced structural closure over the fault block at higher stratigraphic levels, but has also probably partly breached the fault seal of the in-place White Ibis accumulation. Similar to White Ibis-1, the Tilana-1, Aroo-1 and Tarook-1 wells were also positioned to have

received hydrocarbon charge from flanking depocentres. A palaeo-hydrocarbon charge is supported by the results of recent fluid inclusion studies (Kempton et al., 2002). The deeper successions at Tilana-1 and Aroo-1 penetrated basaltic flows (3100 m to TD) which may act as seals. Migration above the volcanic succession will depend on faults to provided conduits to mature source rocks in the flanking depocentres. Failure of wells drilled on the "Tertiary Platform" (Lennon et al., 1999) may be due to lack of hydrocarbon charge (Dondu-1, Nangkero-1, Poonboon-1 and Yurongi-1).

10.3 SOURCE ROCKS

The principal potential source rocks in the Bass Basin are interbedded coals (ranging from 5 to 25 m thick), fluvio-deltaic and lacustrine shales of early Palaeogene age. Geochemical analyses (Chapter 5) show these source rocks have generated liquid and gaseous hydrocarbons, with the coals being the dominant source for the liquids (Boreham et al., 2003). The lacustrine shales have a low source potential, and geochemical analyses do not support a correlation of the potential source rock to recovered hydrocarbons. The largely terrestrial setting of the basin has meant that coals and fluvio-deltaic shales are present thoughout the pre-Oligocene succession. There were two peak periods of coal deposition as indicated by plots of source-richness (TOC) versus age (Chapter 5, Figures 5.1 to 5.8). These periods were Early to Late Eocene (54 to 35 Ma, Lower *M. diversus* to Middle *N. asperus* zones) and Maastrichtian to mid-Late Paleocene (70 to 59 Ma, mid-Lower *F. longus* to Lower *L. balmei* zones). The single well to penetrate the pre-Campanian succession (Durroon-1) indicates only minor occurrences of coal within the early rift section, although thin coaly intervals within the Aptian to Albian succession show good source potential (Chapter 5). The latest Eocene and younger succession (upper Demons Bluff and Torquay sequences) show poor source potential and are immature across the basin.

The older period of increased coal deposition (Maastrichtian to mid-Late Paleocene (70 to 59 Ma, mid-Lower *F. longus* to Lower *L. balmei* zone), coincided with the occurrence of deep lakes across the central and northwestern parts of the Bass Basin (Chapter 4; Partridge, 2002; Appendix C). These lakes began to form during the Maastrichtian, and persisted until the Early Eocene (Middle *M. diversus* zone). Coals deposited during this time probably accumulated in peat mires and lower delta plain environments that fringed the lakes and basin margin. Geochemical analyses have shown that the lacustrine shales have poor source potential (Chapter 5; Boreham et al., in press), and thus are probably more important as an intra-formational seal facies, rather than as a potential source rocks. The overall distribution of coals through time reflects the expansion and contraction of the lake systems and related environments. In general, areas of higher subsidence such as the Cormorant and Yolla troughs, recorded the deepening and shallowing of the lakes, while the fringing areas recorded the shifts between lacustrine and non-lacustrine environments.

The observed decrease in the frequence of coals during the ensuing Late Paleocene to earliest Eocene time (59 to 54 Ma; Chapter 5) does not appear to be an artefact of sampling or drilled section. Where penetrated, this succession consists of mostly sandstone with minor coal (e.g., Yurongi-1, Nangkero-1, Pelican-3), or thick lacustine shales with minor sandstone and very thin coal (e.g, Koorkah-1, Toolka-1A, Yolla-1, Aroo-1).

The lack of coals may be related to an overall expansion of the lake system and a related transgressive cycle that peaked during the Early Eocene (intra-Lower *M. diversus* MFS; Chapter 4). The only wells to penetrate coal-rich intervals of this age (mid-Lower *L. balmei* to Lower *M. diversus* zones) were Poonboon-1 and Bass-3. Analyses of the coal at Poonboon-1 (3042 m) show it to be one of the most hydrogen-rich coals in the basin (Chapter 5).

The younger period of increased coal deposition (54 to 35 Ma, Lower *M. diversus* to Middle *N. asperus* zones) coincided with a time of decreased accommodation across the Bass Basin due to a waning of tectonic-driven subsidence and sediment supply (Subsidence Phase 1). The increased frequency in coal deposition can be observed in almost every well in the basin (e.g., Toolka-1A, Dondu-1, Konkon-1, Cormorant-1), even those in the Pelican Trough, where deposition of sand-rich facies continued to be high. Within this younger period of increase coal deposition, coals younger than 39 Ma (Middle *N. asperus* zone and younger) show significantly less source potential than those within the underlying succession (see Figure 5.1). The younger coals were deposited during the time of overall marine flooding of the basin from the northwest, while the underlying coals (Middle *M. diversus* to Lower *N. asperus* zones) were associated with lagoonal environments and the shallower Lake Toolka lacustrine system (Chapter 4; Partridge, 2002; Appendix C). A hydrogen-rich coal analysed at Pelican-5 (2800 m; Middle M. diversus zone) was deposited following a time of peak transgression in the Early Eocene (intra-Lower *M. diversus* MFS; Chapter 4) and at the onset of a period of slower subsidence.

Oils in the Bass Basin are a single oil population sourced mainly from Early Eocene to Paleocene coals. Biodegradation of the Cormorant oil has resulted in a statistically separate oil family when compared to the Pelican and Yolla crudes. Much better oil-to-source correlations are found between the oils and the coals, than the claystones. Gases in the Bass Basin are wet and high in CO_2 content. The CO_2 is sourced from igneous intrusions. Gaseous hydrocarbons have a similar source to oils, but are generated over a wider maturity range. Analyses show that the White Ibis-1 gas is of higher maturity than Yolla-2 gas.

Geochemical analysis and modelling undertaken for this study has detemined that the basin-wide onset of oil generation and expulsion occurs at a depth of between 2450 to 3200 m (Chapters 5 and 6), with wireline data suggesting the occurrence of overpressure below a depth of approximately 2800 m (Miyazaki, 1995). The SANS results (Appendix H; Perlican-5 and Cormorant-1) show that the scattering intensity within samples decreases with depth, and is followed by a matrix reorganization and stabilization below 2800 to 2900 m depth. There is a permeability barrier below 2900 m which relates to a decrease in pore space, probably the result of oil moving from smaller to larger pore spaces. This depth correlates to approximately 0.7% VR, or the onset of primary migration (Appendix H). Igneous intrusions, mainly within Paleocene, Oligocene and Miocene sediments, have produced localised elevated maturity up to 5% VR. This study has determined that key events in the process of petroleum generation and migration from effective source rocks are:

- onset of oil generation occurred at a VR of 0.65% (2450 m in Pelican-5);

- onset of expulsion (primary migration) occurred at a VR of 0.75% (2700 to 3200 m in Bass Basin; 2850 m in Pelican-5);
- main oil window occurred between VR of 0.75% and 0.95% (2850 to 3300 m in Pelican-5); and
- main gas window occurred at VR>1.2% (>3650 m in Pelican-5).

The defined source rocks linked to hydrocarbon accumulations within the Bass Basin (Paleocene to Early Eocene coals) entered the oil generation window just prior to and following deposition of regional shaley facies of the Demons Bluff Sequence, and after the major trap forming structural events of the Late Cretaceous and Early Eocene. Paleocene to Early Eocene units continued to pass into the oil expulsion window during and after Miocene structural reactivation events. The base of the Pelican-5 well (~ 67 Ma, Maastrichtian) entered the main gas generation window (1.15 – 2.6 %Ro) around the start of the Miocene (~23 Ma). Paleocene to Early Eocene source rock intervals have not entered the main gas generation window. However, deeper undrilled sediments of the Durroon Megasequence (Tasman Rift Phase) may have entered the main gas generation window as early as the Paleocene. Migration from mature source rocks into available traps may have occurred via local fault-related conduits and intra-stratal fairways.

10.4 RESERVOIR ROCKS

Proven petroleum-bearing reservoirs in the Bass Basin occur mainly within the Paleocene (Upper and Lower *L. balmei* zones) and Lower Eocene (Lower M*. diversus* zone) succession (see Figure 2.2), and are predominantly fluvio-deltaic sandstones with net thicknesses of between 20 to 50 m. Some degraded oil was recovered at Cormorant-1 (1500 m depth) reservoired in much younger strata (*P. asperopolus* and Lower *N. asperus* zones), while an oil columnn at Yolla-1 was intersected within a Middle *N. asperus* age succession. The occurrence of oil in the younger succession at Cormorant-1 can possibly be attributed to upward migration from a deeper accumulation(s) that was breached during the Miocene inversion. Facies analysis and correlation of cores with wireline logs suggests that reservoir sandstones were deposited in a range of terrestrial, paralic and shallow marine environments (Baillie et al., 1991; Chapters 8 and 9). The lateral continuity of these facies is expected to vary widely. Porosity analyses on cores and sidewall cores at Cormorant-1 and Yolla-1 recorded average values of 15 to 25 percent.

At a field scale, the quality of the reservoir facies has been attributed to the textural maturity and grainsize, as well as diagenesis, depth of burial and heat flow within the basin (Chapter 8). Coarse-grained facies in the Bass Basin include fluvial channels, crevasse-splays, and coarser-grained facies deposited in lacustrine/lagoonal shoreface and foreshore environments (Chapters 8 and 9; Appendix L). The primary relationship between reservoir quality and depositional facies is linked to coarse grain size associated with specific facies, with a secondary link to dissolution of early siderite cementation phase associated with organic-rich facies. Early cementation by siderite served to preserve porosity and permeability during subsequent periods of compaction and deformation. The cement was later removed leaving behind good secondary intergranular porosity. Cubitt (1992) observed that the *L. balmei* interval has a predisposition to good reservoir quality even though it is represented mainly in deeper parts of the basin. The first "marine

influence" observed in the Bass Basin succession occurred in the Early Paleocene and coincided with deposition of the Lower *L. balmei* facies (Partridge, 2002; Appendix C). It was likely that the marine influence during sedimentation of *L. balmei* facies served to remove silt and provide some carbonate to act as an early cement. This maybe particularly true for wells formerly situated in more fluvial environments during the time of the lower Koorkah Lake succession (e.g., Yurong-1, Nangkero-1, Pelican-5, Chat-3, and Bass-3), along with the relatively high-energy of these depositional systems.

A study of the nature and distribution of porosity suggests that present-day reservoir quality is highest between 1900 and 2700 m subsea over the extent of the basin (Meszoly et al., 1986). In general, porosity declines fairly moderately with increasing depth (approximately 5.7 porosity units per 1000 meters; Meszoly et al., 1986), while permeabilities range from 16 to 308 mD. Two depth-related diagenetic zones have been recognised within the quartz-rich siliciclastics – an upper zone characterised by carbonate authigenesis from 1950 m to the base of the Demons Bluff shale facies; and, a lower zone lying below 2000 m, characterised by dissolution, compaction, quartz overgrowth cementation and authigenic illite and kaolinite (Meszoly et al., 1986).

10.5 SEALS

The MICP analysis of 15 selected samples from cores undertaken for this study has shown a wide variation in seal capacity (Chapter 7, Appendix L). It should be stressed that many of the cores taken during exploration drilling have focused on the recovery of reservoir facies, rather than seal facies. As such, the samples that were selected for seal analysis represent fine-grained intervals within the cores examined, but they are considered only a subset of all potential seal facies in the Bass Basin.

The highest capacity seal identified in this study occurred within a lower shoreface, carbonaceous mudstone in Dondu-1 (2342 m; average oil column >1400 m; Upper *L. balmei* zone). Other high capacity seal facies analysed (average oil column of 700 to 1150 m) were detected in lacustrine, lagoonal and interdistributary bay mudstones of latest Paleocene to Early Eocene age (Upper *L. balmei* to Middle *M. diversus* zones; Appendix L). The Late Paleocene to earliest Eocene was a period of low coal production (Section 10.3), and has been interpreted to coincide with an overall expansion of the Koorkah Lake system. A comparison of width/length ratios for a variety of seal types suggest that lower lacustrine shoreface and lacustrine/ lagoonal facies with high sealing capacity are also laterally extensive. The single sample to be analysed from the shaley facies of the "Demons Bluff" regional seal (Bass-2, 1164.69m, Upper *N. asperus* zone) yielded only modest to good sealing capacity (average oil column of 400 m). However, the low seal capacity result determined from the "Demons Bluff" regional seal may reflect secondary fracturing due to trap breaching or the influence of late volcanics, rather than primary seal properties. Further MICP analysis are required from potentially less-affected samples to determine a valid result for the "Demons Bluff" regional sealing facies.

10.6 PLAY CONCEPTS

Wells drilled to date in the western Bass Basin have tested a range of plays, including: 1) onlap onto or structural closure (drape) over the crest of intra-basin fault blocks located updip from deep flanking half-graben (White Ibis-1, Aroo-1 and Tilana-1); 2) Miocene and younger inversion structures and fault blocks associated the crestal collapse (Cormorant-1, Toolka-1A); 3) Eocene anticlines within the hanging wall of half graben and associated crestal collapse fault blocks (Pelican wells); 4) low-relief fault blocks within the basin associated with late-stage growth faults (Poonboon-1, Tarook-1), and, 5) footwall fault blocks along the basin margin with stratigraphic onlap (Tasmanian Devil-1; Flinders-1). Many of these plays have experienced late stage enhancement of structural closure (Eocene, Oligocene and Miocene) that may have partially breached in-place accumulations (White Ibis-1, Cormorant-1). The most successful plays have been those located updip or along the flanks of Cretaceous half graben where growth faulting continued until the Early Eocene. Prospective parts of the Bass Basin are offered in the 2002 and 2003 Release of Offshore Petroleum Exploration Areas – including areas overlying the Cormorant, White Ibis and Pelican troughs, as well as the prospective coal-rich areas around Poonboon-1 in the central basin.

The occurrence of the petroleum systems elements within the stratigraphic succession has been summarised in Figure 10.4. The main reservoirs within the basin that presently lie at drilling depths of 2800 to 3200 m are Paleocene or younger in age (Upper and Lower *L. balmei* zones). Within the deeper areas of the Cormorant, Yolla, Pelican and White Ibis troughs, where late stages of extension resulted in thicker Paleocene and Eocene sections, the target reservoirs are earliest Eocene and younger (Lower *M. diversus* and younger zones). Although deeper sections have been drilled (e.g., Pelican Trough), reservoir quality appears to be degraded below 3500 m. On the basin margins and shallower flanks of the troughs, Late Cretaceous reservoirs are also viable targets (Upper *F. longus* zone). The deposition of laterally extensive, intraformational and regional seal facies occurred during the Early to Late Paleocene ("Koorkah Lake" shales), Late Paleocene to Early Eocene (lower shoreface, carbonaceous mudstones; Dondu-1, 2342 m; Upper *L. balmei* zone; average oil column >1400 m), early Middle Eocene (associated with top *P. asperopolus* MFS), mid-Middle Eocene ("Toolka Lake" facies), and Late Eocene ("Demons Bluff" shale facies). The Maastrichtian to late Early Eocene was the main period of trap development across the basin (fault blocks; Upper *F. longus* to Middle *M. diversus* zones), with some traps developing locally during the late Early Eocene (growth faults and sediment loading) to mid-Middle Eocene (contraction deformation).

A geochemical correlation between recovered hydrocarbons and potential source rocks has shown that the Bass Basin hosts an effective, terrestrial-based petroleum system. The Middle Eocene and younger marine succession shows low source potential and does not lie within the oil window. A minor, intermittent marine influence in older rocks has been detected through biostratigraphic analyses, and is thought the be reflected in Eocene and Paleocene coals with locally high sulphur content (Poonboon-1). Geohistory modelling has shown that the onset of the main oil generation phase (Paleocene to Early Eocene coals and shales) occurred from the Late Eocene to Early Miocene, post-dating the main periods of seal deposition and trap formation. The Miocene inversion occurred after the onset of generation in the basin, and has resulted in

large structures along the northern basin margin. The critical factor in sourcing accumulations from the coaly succession appears to be effective primary and secondary expulsion from the source rock and the volume of charge. The accumulations at Cormorant, Yolla and Pelican confirm that generation and migration have occurred within the deeper depocentres. Recent fluid inclusion studies suggest a migration phase onto the flankings of these structures (e.g., Aroo-1 and Tilana-1; Kempton et al., 2002), possibly driven by late gas charge. Other areas of potential prospectivity include the "Tertiary Platform" (Lennon et al., 1999) in the vicinity of Poonboon-1 and Nangkero-1, sourced locally by hydrogen-rich coals of Late Paleocene to Early Eocene age (Chapter 5). In addition, plays along the flanks of the "Tertiary Platform" (e.g., Yurongi-1 and Chat-1) have yielded some evidence of potential oil zones (Kempton et al., 2002). A generalised map showing potential migration from mature source rocks is shown in Figure 10.5. Untested plays include reservoir/seal pairs associated with times of maximum flooding events in the western Bass Basin (e.g., Lower *M. diversus* and "top" *P. asperopolus* MFS). The petroleum systems elements of the Durroon Sub-basin differ significantly from the Cape Wickham Sub-basin owing to the cessation of tectonically-driven subsidence in the eastern Bass Basin (Durroon Sub-basin) from the mid-Campanian onward.

Figure 10.1 Location map of the Bass Basin and adjacent region, southeastern Australia. The basin outline, permits, well and field locations, including the 2002 (black) and 2003 (red) Acreage Release areas, are also shown.

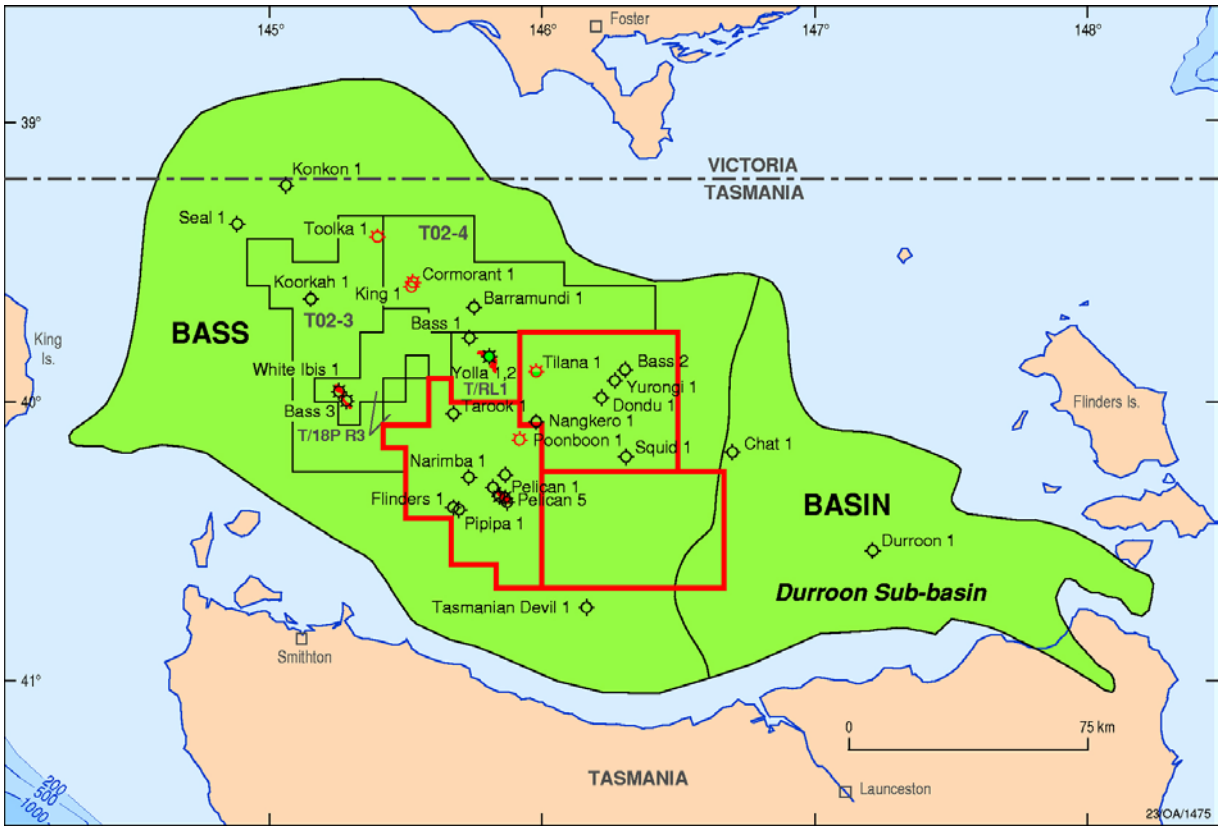


Figure 10.2 Chart summarising drilling results in the Bass Basin, and interpreted reasons for success and failures (from Trigg et al., 2003; Trigg and Blevin, 2003). A map showing the geographic distribution of these results is shown in Figure 10.3.

	Well	Operatror & year	Hydrocarbon Show	TD (m)	Rock Age at TD	Source Rock oil & gas potential	Invalid Structural Test	Reservoir Risk	Seal Risk	Charge Risk	Hydrocarbon Accumulation
Durroon Sub-basin	Chat 1	Bridge Oil Ltd, 1986	No significant	3104	Volcanic rock (*N. senctus*)	Immature to TD				Charge	
	Durroon 1	Esso E & P, 1972	No shows	3024	*P. notensis*	Generation & expulsion Below 3000m			No seal		
Cormorant Trough	Barramundi 1	Globex Far East, 1999	Carbon dioxide	2100	No data available	No data available			Seal Breach		
	Bass 1	Esso E & P, 1965	No shows	2352	Upper *M. diversus*	Immature to TD	Volcanic rock as primary objective				
	Cormorant 1	Esso E & P, 1970	Minor gas, trace oil	3001	Lower *M. diversus*	Generation: 1500-2250m Expulsion below 2500m			Seal Breach		
	King 1	SAGASCO, 1992	Fluroescence, gas, trace oil	2223	*M. diversus*	No data available			Seal Breach		
	Toolka 1	Esso E & P, 1974		2715	Volcanic rock Lower *M. diversus*	Generation below 2500m, but poor source richness/quality				Charge	
Pelican Trough	Flinders 1	SAGASCO, 1992	Minor gas	2723	Lower *L. balmei*	Localised high maturity due to igneous intrusion. Immature below 2400m	Volcanic rock as primary objective				
	Narimba 1	Esso E & P, 1973	Dry	3354	Lower *M. diversus*	Generation: below 2800m. Expulsion close to TD but poor source richness/quality				Charge	
	Pelican 1	Esso E & P, 1970	Condensate, gas	3178	Lower *M. diversus* Upper *L. balmei*	Elevated maturity. Poor sampling limits interpretation		Poor Permeability			
	Pelican 2	Esso E & P, 1970	Condensate, gas	3068	Lower *M. diversus*	Generation below 2700m		Poor Permeability			
	Pelican 3	Esso E & P, 1972	Minor gas	2907	Lower *L. balmei*	Elevated maturity. Poor sampling limits interpretation		Poor Permeability			
	Pelican 4	Hematite Petroleum, 1979	Condensate, gas	3051	No data available	Generation below 2700m. No expulsion to TD		Poor Permeability			
	Pelican 5	Amoco, 1985	Condensate, gas	4267	*T. lillei*	Generation: below 2450m Expulsion: 2850-3300m, >3650m (gas)		Poor Permeability			
	Pipipa 1	Hematite Petroleum, 1982	Fluorescence, trace gas	2115	Lower *N. asperus*	Localised high maturity due to igneous intrusion. Poor source richness/quality to TD				Charge	
	Tasmanian Devil 1	Weaver Oil & Gas, 1984	Dry	864	Volcanic rock (*P. tuberculatus*)	Limited data. Poor source richness/ quality and immature to TD	Volcanic rock as primary objective				
Western Bass	Konkon 1	Esso E & P, 1973		1537	Intra - *T. longus*	Immature to TD			Seal Breach		
	Koorkah 1	Amoco, 1985	Dry	3149	*T. lillei*	Generation: below 2800m. Expulsion: below 3000m			Seal Breach		
	Seal 1	Bridge Oil, 1986	No significant	1670	Volcanic rock Lower *L. balmei*	Limited data. Localised high maturity				Charge	
Central-western Bass	Bass 3	Esso E & P, 1967	Minor gas	2432	Lower *T. longus*	Immature to TD	Off structure				
	White Ibis 1	Premier Oil, 1998	Gas	2220	Volcanic rock	No data available			Partial Fault Seal Breach		Hydrocarbon Accumulation
Central-eastern Bass	Bass 2	Esso E & P, 1966	No shows	1801	Lower *L. balmei*	Immature to TD			No Seal		
	Dondu 1	Esso E & P, 1973	Dry	2927	Lower *L. balmei*	Generation & expulsion at 2784m				Charge	
	Nangkero 1	Hematite Petroleum, 1974	Dry	2877	Upper *L. balmei*	Generation: below 2300m. No expulsion to TD				Charge	
	Poonboon 1	Esso E & P, 1972	Trace gas	3266	Lower *T. longus*	Generation: below 2800m. Expulsion close to TD.				Charge	
	Squid 1	Weaver Oil & Gas, 1984	Dry	2922	Intra - *L. balmei*	Immature to TD			Trap integrity		
	Tilana 1	Amoco, 1985	Minor gas	3900	Volcanic rock (*T. longus*)	Generation: below 2500m. Expulsion: below 3000m (oil), >3900m (gas)	No structural closure			Charge	
	Yurongi 1	Esso E & P, 1973	No shows	2438	Lower *L. balmei*	Immature to TD				Charge	
Central Bass	Aroo 1	Hematite Petroleum, 1974	Fluorescence, minor gas	3692	Volcanic rock Lower *L. balmei*	Mature for liquids below 2900m	Volcanic rock as primary objective				
	Tarook 1	Esso E & P, 1972	No shows	2774	Volcanic rock (Middle *M. diversus*)	Generation at TD, but poor source richness/quality				Charge	
	Yolla 1	Amoco, 1985	Condensate, gas, oil	3347	Volcanic rock Lower *L. balmei*	Generation:1980-2580m. Expulsion: below 2500m					Hydrocarbon Accumulation
	Yolla 2	Premier Oil, 1998	Gas	3165	Volcanic rock	No data available					Hydrocarbon Accumulation

14-1/379

Figure 10.3 Map showing the geographic distribution of drilling results in the Bass Basin, and interpreted reasons for success and failures (from Trigg et al., 2003; Trigg and Blevin, 2003). A chart summarising this information is shown in Figure 10.2.

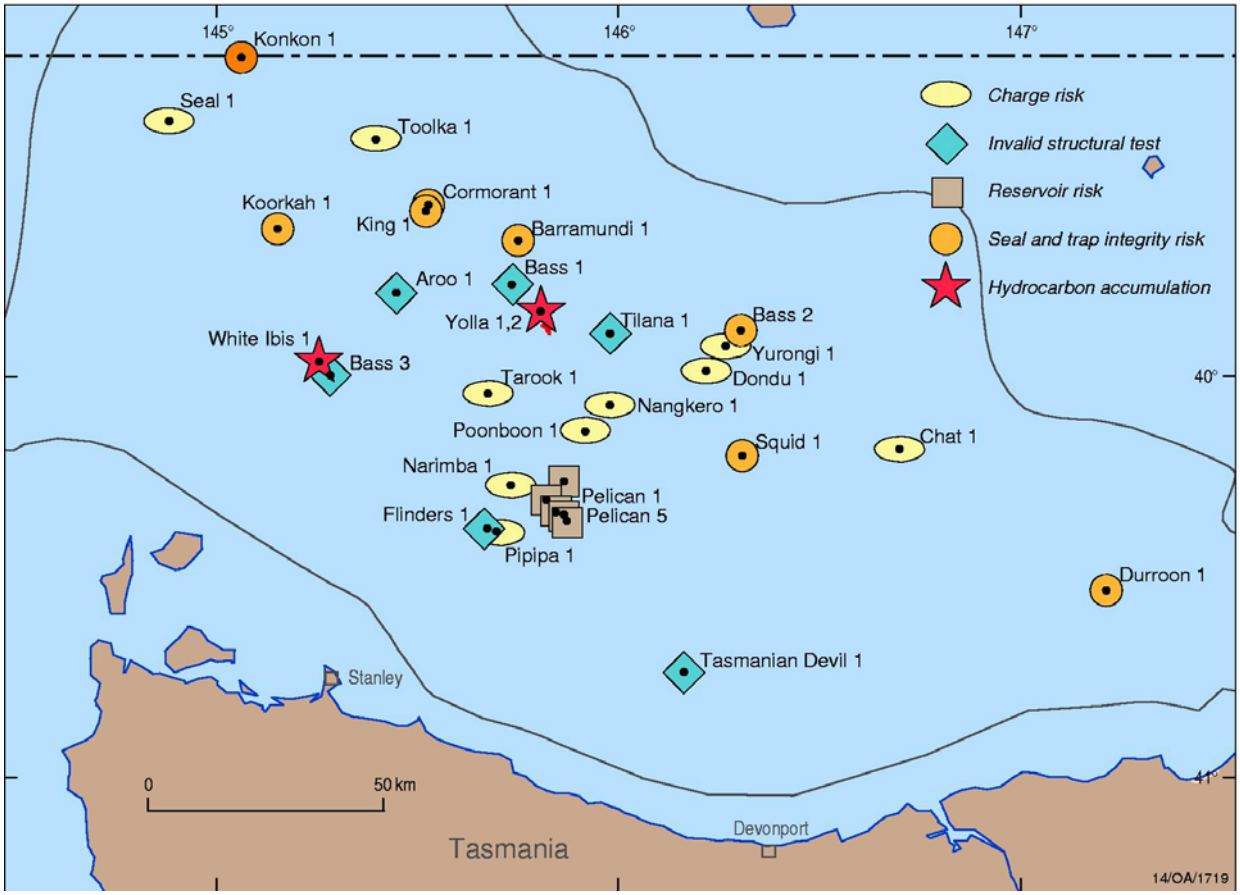


Figure 10.4 Stratigraphic column for the western Bass Basin showing the distribution of petroleum systems elements (reservoir, source, seal) and the overall timing of trap development. The terrestrial nature of the basin until the mid-Eocene (Middle N. asperus zone) means that elements of reservoir, source and seal occur mainly as interbedded (intra-formational) facies. Sealing shales deposited as part of the Koorkah and Toolka Lake cycles are thicker and more regional in nature. These shales are important as fault-seals (juxtaposition). Coals deposition increased across the basin from the late Early Eocene (Upper M. diversus) onward due to a decrease in the rate of tectonic-driven subsidence.

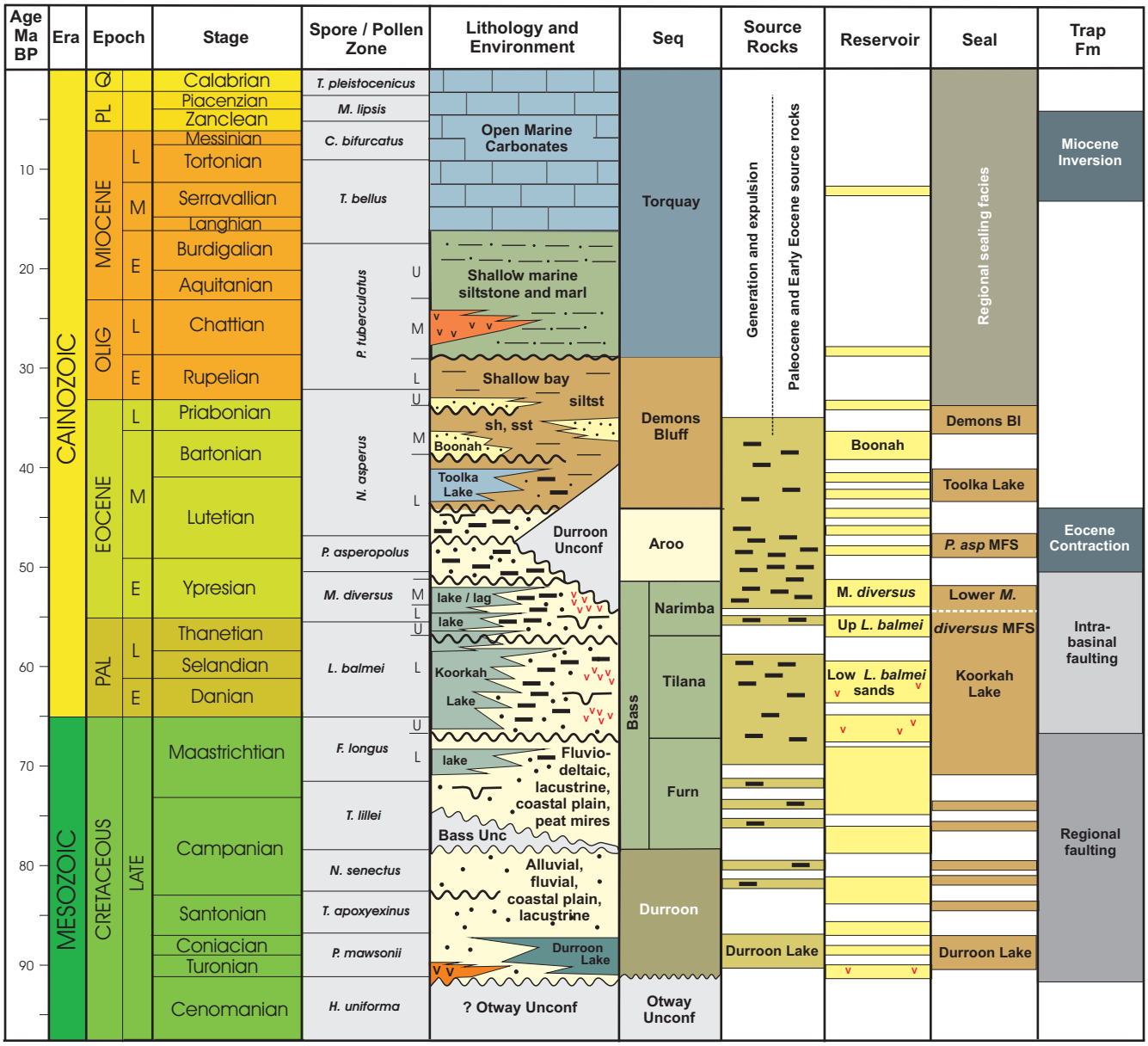
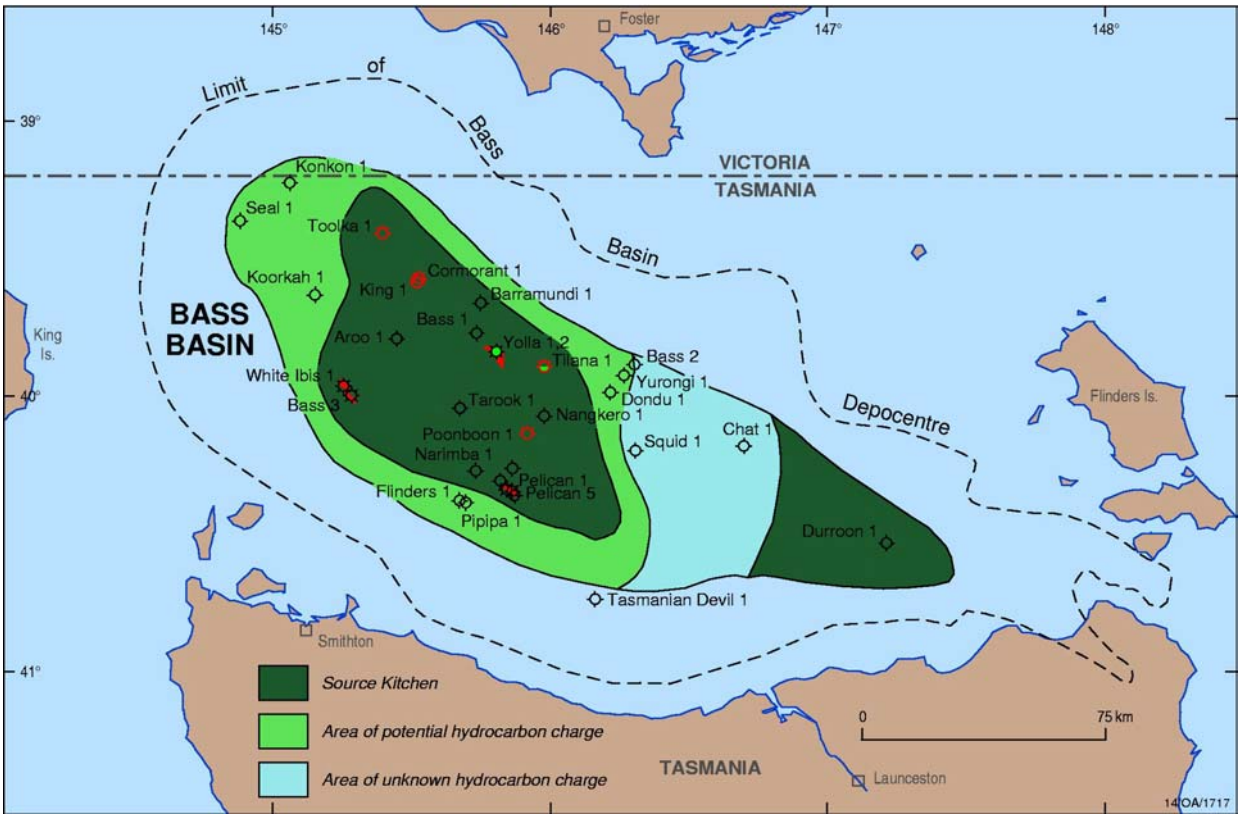


Figure 10.5 Generalised map showing the distribution of mature potential source rocks and areas of potential hydrocarbon charge in the Bass Basin. This map is based on the modelling of potential source rocks of Late Cretaceous to Early Eocene age, and evidence from fluid inclusion studies (Kempton et al., 2002).



11. ACKNOWLEDGEMENTS

Geoscience Australia and the National Centre for Petroleum Geology and Geophysics acknowledge the financial support provided by Mineral Resources Tasmania to undertake studies to enhance the understanding of the petroleum geology of the Bass Basin. The study was undertaken under the auspices of the Western Tasmanian Regional Minerals Program. Carol Bacon and Clive Calver are gratefully acknowledged for their support and coordination of the project. Fugro Multi Client Services are acknowledged for permission to use seismic images in numerous figures in this Record.

The MRT-funded Bass Basin project was undertaken as a collaborative effort by Geoscience Australia and the National Centre for Petroleum Geology and Geophysics (University of Adelaide). This project would not have been possible without the contributions of many others from both organisations who provided scientific input and a wide range technical support and expertise. The NCPGG acknowledges Igor Filipi, Nathan Ceglar and Catherine Gibson-Poole who assisted with drafting and computer support. Schlumberger is also thanked for access to GeoFrame training suite software at the NCPGG. Those from Geoscience Australia who are thanked for their scientific input over the course of this project include Chris Nicholson, Rosalie Pollock, and Barry West. In particular, Jennie Totterdell and Tony Stephenson are gratefully acknowledged for their editorial undertakings. Technical support for the Bass Basin Project was provided by Anne Fleming, Cameron Mitchell, Neville Montgomerie, Carmine Moscaritolo, Mark Webster, David Rowland and Alison Hancock - their professional contributions are gratefully acknowledged.

Murray Woods, Brian Pashley, Karin Weiss, Leanne McMahon, Silvio Mezzomo, Lindell Emerton and Terry Brown from Geoscience Australia are also acknowledged for the provision of cartography, graphic and report production services. Processing and preparation of biostratigraphic and SANS samples was undertaken at Geoscience Australia by Christian Thun, Andrew Kelman, Tony Watson and Richard Brown. Drs. Clinton Foster, Eric Monteil (Geoscience Australia) and Mike Macphail (Australian National University) provided additional input to the biostratigraphy. Organic geochemistry sample preparation and analyses were undertaken at the laboratories at Geoscience Australia by Janet Davenport, Paul Greenwood, Natalie Johns and Janet Hope. A sub-set of samples were analysed under contract for maturity properties by Dr. Jane Newman (Newman and Associates, New Zealand) and Dr. Alan Cook (Keiraville Konsultants). Access to all samples analysed for the Bass Basin Project was provided by the Petroleum Data Repositories at Geoscience Australia (Canberra) – Paula Cronin, Ben Miller, Eddie Resiak, Danny Britten are thanked for their assistance.

Reports commissioned from external companies on behalf of MRT, as well as all data generated from analyses carried out at Geoscience Australia and the National Centre for Petroleum Geology, are available through the Geoscience Australia website (www.ga.gov.au). Geochemical and biostratigraphic analysis are can be downloaded free-of-charge through the internet, while other reports have been lodged with the Petroleum Data Repositories at Geoscience Australia as Destructive Analysis Report. These reports can be ordered on the internet and are available at the cost-of-transfer.

12. REFERENCES

AGSO AND Geomark Research, 1996. The Oils of Western Australia. Proprietary Report, Canberra and Houston (unpublished).

Australian Financial Review, 2002. Gas competition on the boil (Corporate Focus Section). Friday, 6 December 2002, 62.

Baillie, P.W., 1992. Relationship of coal facies with sea level in the Bass Basin. Geological Society of Australia, Abstracts, 32, 116-117.

Baillie, P.W., 1993. Regional Geology. In: Maung, T.U, Miyazaki, S., Baillie, P.W., Lavering, I.H., Vuckovic, V., Stephenson, A.E., Williamson, P.E., Staunton, J., Radke, S.G., West, B.W., Gippespie, R.G., Resiak, E., and Temple, P.R., Eastern Bass Basin Petroleum Prospectivity Bulletin. Bureau of Resource Sciences, Petroleum Prospectivity Bulletin, 1993/2.

Baillie, P.W. and Bacon, C.A., 1989. Integrated sedimentological analysis, the Eocene of the Bass Basin. APEA Journal, 29 (1), 312-327.

Baillie, P.W. and Pickering, R., 1991. Tectonic evolution of the Durroon Basin, Tasmania. Exploration Geophysics, 22, 13-18.

Baillie, P.W., Tingate, P.R. and Stuart, W.J., 1991. Reservoir development and diagenesis in the Bass Basin, Tasmania. The APEA Journal, 33(1), 85-100.

Baillie, P.W. and Brown, A.V., 1984. Igneous rocks from Tasmanian Devil-1. Tasmanian Department of Mines, Unpublished Report 1984/74.

Blevin, J., 2001. Hydrocarbon prospectivity of Australia's remote frontier areas in offshore east and south-east Australia – examples from the basins of Lord Howe Rise. In: Hill, K.C. and Bernecker, T. (editors), Eastern Australasian Basins Symposium, A Refocused Energy Perspective for the Future, Petroleum Exploration Society of Australia, Special Publication, 25-35.

Blom, W.M. and Alsop, D.B., 1988. Carbonate mud sedimentation on a temperate shelf, Bass Basin, southeast Australia. Sedimentary Geology, 60, 269-280.

Boreham, C.J. and Powell, T.G., 1994. Petroleum source rock assessment of coal and associated sediments: qualitative and quantitative aspects. In: Law, B. and Rice, D. (editors), Hydrocarbons from Coal, AAPG Special Publication, 133-157.

Boreham, C.J. and DeBoer, R.A., 1998. Origin of Gilmore gas and oil, Adavale Basin, central Queensland. APPEA Journal, 38(1), 399-420.

Boreham, C.J. and Summons, R.E., 1999. New insights into the active petroleum systems in the Cooper and Eromanga basins, Australia. APPEA Journal 39(1), 263-96.

Boreham, C.J., Horsfield, B. and Schenk, H.J., 1999. Predicting the quantities of oil and gas generated from Australian Permian coals using pyrolytic methods. Marine and Petroleum Geology, 16, 165-188.

Boreham, C.J., Hope J.M. and Hartung-Kagi, B., 2001. Understanding source, distribution and preservation of Australian natural gas: a geochemical perspective. APPEA Journal, 41(1), 523-547.

Boreham, C.J., Blevin, J.E., Duddy, I., Newman, J., Liu, K., Middleton, H., Macphail, M.K. and Cook, A.C., 2002. Exploring the potential for oil generation, migration and accumulation in Cape Sorell-1, Sorell Basin, offshore west Tasmania. APPEA Journal 2002, 42(1), 405-435.

Boreham, C.J., Blevin, J.E., Radlinski, A.P. and Trigg, K.T., 2003. Coal as a source of oil and gas, a case study from the Bass Basin, Australia. APPEA Journal 2003, 43(1), 117-148.

Brown, B.R., 1976. Bass Basin, some aspects of the petroleum geology. In: Leslie, R.B., Evans, H.J. and Knight, C.L. (editors), Economic Geology of Australia and Papua New Guinea, 3. Petroleum, Monograph Series No. 7. The Australasian Institute of Mining and Metallurgy, 67-82.

Bryan, S.E., Constantine, A.E., Stephens, C.J., Ewart, A., Schon, R.W., and Parianos, J., 1997. Early Cretaceous volcano-sedimentary successions along the eastern Australian continental margin, implications for the break-up of eastern Gondwana. Earth and Planetary Science Letters 153, 85-102.

Burnham, A.K. and Sweeney, J.J., 1989. A chemical kinetic model of vitrinite maturation and reflectance. Geochimica et Cosmochimica Acta, 53, 2649-2657.

Cartwright, J.A. and Dewhurst, D.N., 1998. Layer-bound compaction faults in fine-grained sediments. GSA Bulletin (October 1998), 110, 1241-1257.

Chung, H.M., Gormly, J.R. and Squires, R.M., 1988. Origin of gaseous hydrocarbons in subsurface environments: theoretical considerations of carbon isotope distribution. Chemical Geology 71, 97-103.

Cook, C., 2002. Organic petrology of suites of samples from a number of petroleum exploration boreholes drilled in the Bass Basin, Australia. Keiraville Konsultants, Client report prepared for the National Centre for Petroleum Geology and Geophysics (unpublished) (included as Appendix I in this Geoscience Australia Record).

Core Laboratories, Inc., 1985. Core analysis report for Amoco Australia Petroleum Company, Durroon-1, Bass Basin, Victoria. Amoco Australia, Durroon-1, Well Completion Report.

Crist, R.P., Conolly, J.R. and Robinson, L.D., 2001. Barrimundi-1, A case history in fracture analysis and seal integrity in the Bass Basin. APPEA Journal, 41(1), 71-90.

Cubitt, C.J., 1992. Diagenetic controls and reservoir evaluation of the Eastern View Group, Bass Basin, Tasmania, Australia. Honours Thesis, National Centre for Petroleum Geology and Geophysics, University of Adelaide (unpublished).

Cummings, A.M., Hillis, R.R. and Tingate, P.R., 2002. Structural evolution and thermal maturation modeling of the Bass Basin. APPEA Journal 2002, 42(2), 175-191.

Das, P.K., 2001. Extensional subsidence, inversion and volumetric contraction in the Bass Basin of Australia, a seismic study. PhD Thesis, National Centre for Petroleum Geology and Geophysics, University of Adelaide (unpublished).

Das, P.K. and Lemon, N., 2000a. Flat spot anomaly; possible gas sands in the NW Bass Basin. PESA Journal, 28, 51-57.

Das, P.K. and Lemon, N., 2000b. A new model for the tectonic evolution of the southeastern Bass Basin, Australia (Poster Abstract). APPEA Journal, 40(1), 775-776.

Davidson, J.K. and Morrison, K.C., 1986. A comparison of hydrocarbon plays in the Bass, Gippsland, Otway and Taranaki Basins. In: Glenie, R.C. (editor), Second South-Eastern Australia Oil Exploration Symposium, PESA Symposium, Melbourne, 365-374.

Deighton, I.R., 1981. Burial and thermal geohistory analysis of the Bass Basin. Paltech Pty Ltd., Client report prepared for Cue Minerals N.L. (unpublished).

Duddy, I.R., 1992. Assessment of thermal history data from the Durroon-1 well, Bass Basin. Geotrack International Pty Ltd., Client report prepared for Bridge Oil (unpublished).

Duddy, I.R. and Erout, B., 2001. AFTA calibrated 2-D modeling of hydrocarbon generation and migration using Temispack, preliminary results from the Otway Basin. In: Hill, K.C. and Bernecker, T. (editors), Eastern Australasian Basins Symposium, A refocused energy perspective for the future, PESA Special Publication, 485-498.

Eadington, P. J., Lisk, M. and Kridger, F. W., 1996. Identifying oil well sites. United States Patent No. 5, 543-616.

Edwards, D.S., Struckmeyer, H.I.M., Bradshaw, M.T. and Skinner, J.E., 1999. Geochemical characteristics of Australia's southern margin petroleum systems. APPEA Journal 39(1), 297-321.

Edgerly, D.W. and Taylor, J., 1990. Seismic interpretation and basin analysis, Bass Basin T/15P. Petroconsultants Australasia Pty. Ltd. Report for Bridge Oil Ltd., (unpublished).

Etheridge, M.A., Branson, J.C. and Stuart-Smith, P.G., 1984. Structural interpretation of extensional sedimentary basins and its relevance to hydrocarbon exploration, examples from the Bass Strait region. Bureau of Mineral Resources, Canberra. Geological Society of Australia, Abstracts, 163-164.

Etheridge, M.A., Branson, J.C. and Stuart-Smith, P.G., 1985. Extensional basin-forming structures in Bass Strait and their importance for hydrocarbon exploration. The APEA Journal, 25(1), 344-361.

Etheridge, M.A., McQueen, H. and Lambeck, K., 1991. The role of intraplate stress in Tertiary (and Mesozoic) deformation of the Australian continent and its margins, a key factor in petroleum trap formation. Exploration Geophysics, 22, 123-128.

Exon, N.F., White, T.S., Malone, M.J., Kennett, J.P. and Hill, P.J., 2001. Petroleum potential of deepwater basins around Tasmania, insights from Ocean Drilling Program Leg 189. In: Hill, K.C. and Bernecker, T. (editors), Eastern Australasian Basins Symposium, A refocused energy perspective for the future, PESA Special Publication, 49-60.

Fardon, R., 2000. Western Tasmania Regional Minerals Program, Project 2, Digitisation of Tasmanian geological data. Ross Fardon and Associated Pty. Ltd., Consultants Report, Prepared for Mineral Resources Tasmania, 6 Sept 2000 (unpublished).

Faustmann, C., 1995. The seismic expression of volcanism in the Bass Basin referring to western Victorian analogues. Honours Thesis, The University of Adelaide (unpublished).

Fleming, A. and Blevin, J.E., 2003. Western Tasmania regional seismic data, selected reprocessed lines from seismic surveys T69A and T70A. An output of the Western Tasmanian Regional Minerals Program, Geoscience Australia Record 2003/6.

Geoscience Australia and Geomark Research, 2002. The oils of eastern Australia. Proprietary Report, Canberra and Houston (unpublished).

Gleadow, A.J.W. and Duddy, I.R., 1980. Early Cretaceous volcanism and the early breakup history of southeastern Australia, evidence from fission track dating of volcanoclastic sediments. In: Creswell, M.M. and Vellay, P. (editors), Gondwana V, Balkema Press, Rotterdam, 295-300.

Gretner, P.E., 1992. Geothermics, using temperature in hydrocarbon exploration. AAPG Education Course Notes Series 17, 170 p.

Gunn, P.J., Mitchell, J.N. and Meixner, T.J., 1996. The structure and evolution of the Bass and Durroon basins as delineated by aeromagnetic data. AGSO Record 1996/14.

Haq, B.U., Hardenbol, J. and Vail, P.R., 1988. Mesozoic and Cenozoic chronostratigraphy and eustatic cycles. In: Wilgus, C.K., Hastings, B.S., Kendall, C.G.St.C., Posamentier, H.W., Ross, C.A. and Van Wagoner, J.C. (editors), Sea-level changes, an integrated approach. Society of Economic Paleontologists and Mineralogists, Special Publication 42, 71-108.

Hayes, D.E. and Ringis, J., 1973. Seafloor spreading in the Tasman Sea. Nature, 243, 454-458.

Helby, R., Morgan, R. and Partridge, A.D., 1987. A palynological zonation of the Australian Mesozoic. Association of Australasian Palaeontologists, Memoir 4, 1-94.

Hill, K.A., Cooper, G.T., Richardson, M.J. and Lavin, C.J., 1994. Structural framework of the Eastern Otway Basin, inversion and interaction between two major structural provinces. Exploration Geophysics, 25, 79-87.

Hill, K.C., Hill, K.A., Cooper, G.T., O'Sullivan, A.J., O'Sullivan, P.B., and Richardson, M.J., 1995. Inversion around the Bass Basin, SE Australia. In: Buchanan, J.G. and Buchanan, P.G. (editors), Basin Inversion, Geological Society Special Publication 88, 525-547.

Hill, P.J., Moore, A.M.G. and Exon, N.F., 2001. Sedimentary basins and structural framework of the South Tasman Rise and East Tasman Plateau. In: Hill, K.C. and Bernecker, T. (editors), Eastern Australasian Basins Symposium, A refocused energy perspective for the future, PESA Special Publication, 37-48.

Holdgate, G.R., Smith, T.A.G., Gallagher, S.J. and Wallace, M.W., 2001. Geology of coal-bearing Palaeogene sediments, onshore Torquay Basin, Victoria. Australian Journal of Earth Sciences, 48, 657-679.

James, A.T., 1983. Correlation of natural gas by use of carbon isotopic distribution between hydrocarbon components. AAPG Bulletin, 67, 1176-1191.

James, A.T., 1990. Correlation of reservoired gases using the carbon isotopic compositions of wet gas components. AAPG Bulletin 74, 1441-1458.

Kaiko, A.R., 1998. Thermal history analysis of the Barrow and Dampier sub-basins, North West Shelf, Western Australia. PhD Thesis, The University of Adelaide (unpublished).

Kaldi, J.G., O'Brien, G.W. and Kivior, T., 1999. Seal capacity and hydrocarbon accumulation history in dynamic petroleum systems: the East Java Sea, Indonesia, and the Timor Sea, Australia. APPEA Journal, 39(1), 73-86.

Kempton, R.H., Liu, K., Boreham, C.J., Blevin, J.E. and Eadington, P.J., 2002. Hydrocarbon migration and accumulation in the Middle to Upper Eastern View Coal Measures of the Bass Basin, Tasmania, evidence from GOI™, QGF and QGF-E. CSIRO, Division of Petroleum Resources, Confidential Report 02-089 (unpublished).

Knowles, D.J., Suttill, R.J., and Migliucci, A.C., 1994. T/25P permit assessment project. SAGASCO Resources Ltd, (July 1994) (unpublished).

Lennon, R.G., Suttill, R.J., Guthrie D.A. and Waldron, A.R., 1999. The renewed search for oil and gas in the Bass Basin – results of Yolla-2 and White Ibis-1. APPEA Journal 39(1), 248-262.

Liu K., Kurusingal, J., Eadington, P.J. and Coghlan, D., 2001. Identify oil reservoirs. Australian Provisional Patent No. 16404/01.

Maung, T.U, Miyazaki, S., Baillie, P.W., Lavering, I.H., Vuckovic, V., Stephenson, A.E., Williamson, P.E., Staunton, J., Radke, S.G., West, B.W., Gippespie, R.G., Resiak, E., and Temple, P.R., 1993. Eastern Bass Basin Petroleum Prospectivity Bulletin. Bureau of Resource Sciences, Petroleum Prospectivity Bulletin, 1993/2.

Meszoly, G.F.J., Bodard, J.M., and Wall, V.J., 1986. Diagenesis and porosity in the Eastern View Group, Bass Basin. In: Glenie, R.C. (editor), Second South-Eastern Australia Oil Exploration Symposium, PESA Symposium, Melbourne, 303-315.

Middleton, M.F., 1982. The subsidence and thermal history of the Bass Basin, southeastern Australia. Tectonophysics, 87, 383-397.

Miyazaki, S., 1993. Source Rocks. In: Maung, T.U, Miyazaki, S., Baillie, P.W., Lavering, I.H., Vuckovic, V., Stephenson, A.E., Williamson, P.E., Staunton, J., Radke, S.G., West, B.W., Gippespie, R.G., Resiak, E., and Temple, P.R., Eastern Bass Basin Petroleum Prospectivity Bulletin. Bureau of Resource Sciences, Petroleum Prospectivity Bulletin, 1993/2.

Miyazaki, S., 1995. Oil generation from coals and carbonaceous claystones in the Bass Basin. PESA Journal, 23, 91-100.

Moore, W.R., Baillie, P.W., Forsyth, S.M., Hudspeth, J.W., Richardson, R.G. and Turner, N.J., 1984. Boobyalla Sub-basin, a Cretaceous onshore extension of the southern edge of the Bass Basin. APEA Journal, 24(1), 110-117.

Moore, A.M.G., Willcox, J.B., Exon, N.F. and O'Brien, G.W., 1992. Continental shelf basins on the west Tasmania margin. APEA Journal, 32(1), 231-250.

Mutter, J.C., Hegarty, K.A., Cande, S.C. and Weissel, J.K., 1985. Breakup between Australia and Antarctica, a brief review in light of new data. Tectonophysics, 114, 255-279.

Newman, J., 1997. New approaches to detection and correction of suppressed vitrinite reflectance. APPEA Journal, 37(1), 524-35.

Ozimic, S., Nicholas, E. and Pain, L., 1987. Bass Basin, Tasmania and Victoria. Bureau of Mineral Resources, Australian Petroleum Accumulations, Report 2.

Newman, J., Eckersley, K.M., Francis, D.A., and Moore, N.A., 2000. Application of vitrinite-inertinite reflectance and fluorescence to maturity assessment in the East Coast and Canterbury Basins of New Zealand. New Zealand Petroleum Conference, Proceedings, 314-333.

Nicholas, E., Lockwood, K.L., Martin, A.R., and Jackson, K.S., 1981. Petroleum potential of the Bass Basin. BMR Journal of Australian Geology and Geophysics, 6, 199-212.

Norvick, M.S. and Smith, M.A., 2001. Mapping the plate tectonic reconstruction of southern and southeastern Australia and implications for petroleum systems. APPEA Journal, 41(1), 15-35.

O'Sullivan, P.D. and Kohn, B.P., 1997. Apatite fission track thermochronology of Tasmania. AGSO Record 1997/35.

Partridge, A.D., 1999. Late Cretaceous to Tertiary geological evolution of the Gippsland Basin, Victoria. PhD thesis, La Trobe University, Victoria, 439 pp.

Partridge, A.D., 2001. Revised stratigraphy of the Sherbrook Group, Otway Basin. In: Hill, K.C. and Bernecker, T. (editors), Eastern Australasian Basins Symposium, A refocused energy perspective for the future, PESA Special Publication, 455-464.

Partridge, A.D., 2002. Bass Basin palynology project, unraveling a Late Cretaceous to Eocene geological history of large palaeolakes, coastal lagoons and marine bays. Biostrata Pty. Ltd, Biostrata Report 2002/13 (included as Appendix C in this Geoscience Australia Record).

Pittman, E. D. 1992. Relationship of porosity and permeability to various parameters derived from mercury injection, capillary pressure curves for sandstones. AAPG, Bulletin, 51, 191-198.

Purcell, W.R., 1949. Capillary pressures, their measurement using mercury and the calculation of permeability there from. Petroleum Transactions, American Institute of Mining, Metallurgical and Petroleum Engineers, 186, 39-48.

Powell, T.G. and Boreham, C.J., 1994. Terrestrially sourced oils, Where do they exist and what are our limits of knowledge? a geochemical perspective. In: Scott, A.C. and Fleet, A.J. (editors), Coal and coal-bearing strata as oil-prone source rocks? Geological Society Special Publication 77, 11-29.

Raggatt, H.G. and Crespin, I., 1952. Geology of Tertiary rocks between Torquay and Eastern View, Victoria. Australian Journal of Science, 14, 143-147.

Raggatt, H.G. and Crespin, I., 1955. Stratigraphy of Tertiary rocks between Torquay and Eastern View, Victoria. Proceedings of the Royal Society of Victoria, 67, 75-142.

Rezaee, M.R., Lemon, N.M. and Seggie, R.J., 1997. Tectonic fingerprints in siderite cement, Tirrawarra Sandstone, southern Cooper Basin, Australia. Geological Magazine, 134 (1), 99-112.

Robinson, V.A., 1974. Geologic history of the Bass Basin. APPEA Journal, 14(1), 45-49.

Royer, J-Y. and Rollet, N., 1997. Plate-tectonic setting of the Tasmanian region. Australian Journal of Earth Sciences, 44, 543-560.

Russell, N.J. and Baillie, P.W., 1989. Vitrinite palaeothermometry of offshore exploration wells, Tasmania. APPEA Journal, 29(1), 130-156.

Sayers, J., Symonds, P.A., Direen, N.G., and Bernardel, G., 2001. Nature of the continent-ocean transition on the non-volcanic rifted margin of the central Great Australian Bight. In, Wilson, R.C.L., Whitmarsh, R.B., Taylor, B., and Froitzheim, N., (editors), Non-Volcanic Rifting of Continental Margins; A Comparison of Evidence from Land and Sea. Geological Society, London, Special Publications, 187, 51-77.

Schowalter, T.T., 1979. Mechanics of secondary hydrocarbon migration and entrapment. AAPG Bulletin, 63, 723-760.

Schulz-Rojahn, J.P. and Phillips, S.E., 1989. Diagenetic alteration of Permian sandstone reservoirs in the Nappamerri Trough and adjacent areas, southern Cooper Basin. In: O'Neill, B.J. (editor), The Cooper and Eromanga Basins, Australia. Proceedings of Petroleum Exploration Society of Australia, Society of Petroleum Engineers, Australian Society of Exploration Geophysicists (SA Branches), Adelaide, 629-645.

Shaw, R. D., 1978. Sea-floor spreading in the Tasman Sea, a Lord Howe Rise-eastern Australia reconstruction. Bulletin Australian Society of Exploration Geophysics, 9(3), 75-81.

Siebert, R.M., Moncure, G.K. and Lahann, R.W., 1984. A theory of framework grain dissolution in sandstones. In: McDonald, D.A. and Surdam, R.C. (editors), Clastic Diagenesis, AAPG Memoir 37, 163-176.

Smit, R., 1988. A new tectonic model for the Bass Basin. Exploration Geophysics, 19, 163-168.

Smith, G.C., 1986. Bass Basin geology and petroleum exploration. In: Glenie, R.C. (editor), Second South-Eastern Australia Oil Exploration Symposium, PESA Symposium, Melbourne, 257-284.

Smith, J.W. and Pallasser, R.J., 1996. Microbiological origin of Australian coalbed methane. AAPG Bulletin, 80, 891-897.

Sneider, R.M., 1987. Practical petrophysics for exploration and development. AAPG Continuing Education Short Course Notes.

Stagg, H.M.J., Cockshell, C.D., Willcox, J.B., Hill, A., Needham, D.J.L., Thomas, B., O'Brien, G.W. and Hough, P., 1990. Basins of the Great Australian Bight region, geology and petroleum potential. Bureau of Mineral Resources, Australia, Continental Margins Program Folio 5.

Streit, J.E., 1994. Effects of fluid-rock interaction on shear zone evolution in Proterozoic granites on King Island, Tasmania. Honours Thesis, The Australian National University (unpublished).

Summons, R.E., 1996. Origin of petroleum from the Bass Basin. AGSO Professional Opinion with data from Oils of Australia, GeoMark Research Inc and the Australian Geological Survey Organisation (AGSO) (unpublished).

Surdam, R.C., Bosse, S.W. and Crossey, L.J., 1984. The chemistry of Secondary Porosity. In: McDonald, D.A. and Surdam, R.C., (editors) Clastic Diagenesis, AAPG Memoir 37, 127-150.

Sykes, R., 2001. Depositional and rank controls on the petroleum potential of coaly source rocks. In: Hill, K.C. and Bernecker, T., Editors, Eastern Australasian Basins Symposium: A Refocused Energy Perspective for the Future, Petroleum Exploration Society of Australia, Special Publication, 591-602.

Symonds, P.A., Colwell, J.B., Struckmeyer, H.I.M., Willcox, J.B. and Hill, P.J., 1996. Mesozoic rift basin development off eastern Australia. Mesozoic Geology of the Eastern Australia Plate Conference, Geological Society of Australia Inc., Extended Abstracts 43, 528-542.

Taylor, R., 2001. Horizon velocity analysis for depth conversion – A case study. ASEG 15th Geophysical Conference and Exhibition, August 2001, Brisbane, Extended Abstracts.

Teasdale, J.P., Pryer, L.L., Etheridge, M.A., Stuart-Smith, P.G., Loutit, T.S., Shi, Z., Vizy, J., and Henley, P., 2001. Regional potential field interpretation report, Bass and Durroon Basins. SRK Consulting (Energy Services), Report AG701, Non-exclusive client report commissioned by Geoscience Australia (now available as Geoscience Australia Record 2003/4).

Teasdale, J.P., Pryer, L.L., Stuart-Smith, P.G., Romine, K.K., Etheridge, M.A., Loutit, T.S. and Kyan, D.M., 2003. Structural framework and basin evolution of Australia's southern margin. APPEA Journal 2003, 43(1), 13-37.

The Australian Financial Review, 2002. Gas competition on the boil (Corporate Focus Section). Friday, 6 December 2002, 62.

Totterdell, J.T., Bradshaw, B.E. and Willcox, J.B., in press. Chapter 4: Structural and tectonic setting. In: O'Brien, G.W., Paraschivoiu, E. and Hibburt, J.E., Editors, Petroleum Geology of South Australia, Volume 5 – Great Australian Bight. Primary Industries and Resources South Australia.

Ting, F.T.C., 1978. Petrographic techniques in coal analysis. In: Karr, C. (editor), Analytical Methods for Coal and Coal Products, Volume I, Academic Press, New York, 3-26.

Trigg, K.T. and Blevin, J.E., 2003. Evaluation of exploration risk in the Bass Basin, results of a well audit study (Poster Abstract). APPEA Journal 2003, 43(1), 829-830.

Trigg, K.T., Blevin, J.E. and Boreham, C.J., 2003. An audit of exploration wells in the Bass Basin, 1965-1999. An output of the Western Tasmanian Regional Minerals Program, Geoscience Australia Record 2003/11.

Vavra, C.L., Kaldi, J.G. and Sneider, R.M. 1992. Geological applications of capillary pressure, a review. AAPG, Bulletin, 76, 840-850.

Veevers, J.J. and Ettreim, S.L., 1988. Reconstruction of Australia and Antarctica at breakup (95 ± 5 Ma) from magnetic and seismic data at the continental margin. Australian Journal of Earth Sciences, 35, 355-362.

Veevers, J.J., Powell, C.McA., and Roots, S.R., 1991. Review of seafloor spreading around Australia, I. Synthesis of the patterns of spreading. Australian Journal of Earth Sciences, 38, 373-389.

Waples, D.W., 1998. Basin modelling, how well have we done? In: Duppenbecker, S.J. and Iliffe, J.E. (editors), Basin Modelling; Practice and Progress. Geological Society of London, Special Publication 141, 1-14.

Waples, D.W. and Ramly, M., 2001. A statistical method for correcting log-derived temperatures. Petroleum Geoscience, 7, 231-240.

Waples, D.W., Kamata, H. and Suizu, M., 1992. The art of maturity modeling, Part 1, finding a satisfactory geological model. AAPG Bulletin, 76, 31-46.

Waples, D., Green, P., Hegarty, K. Duddy, I., 1996. Quantified thermal history reconstruction and basin modelling; essential aspects of basin modelling for oil and gas exploration. Geotrack International Pty Ltd., Workshop Course Notes, November 1996 (unpublished).

Wardlaw, N.C., 1980. The effects of pore structure on displacement efficiency in reservoir rocks and in glass micromodels. In: 1st Joint SPE/DOE Symposium on Enhanced Oil Recovery, SPE No. 8843, 345-352.

Wardlaw, N.C. and McKellar, M., 1981. Mercury porosimetry and the interpretation of pore geometry in sedimentary rocks and artificial models. Powder Technology, 29, 127-143.

Weissel, J.K. and Hayes, D.E., 1977. Evolution of the Tasman Sea reappraised. Earth and Planetary Science Letters, 36, 77-84.

Wilkins, R.W.T. and George, S.C., 2002. Coal as a source rock for oil, a review. International Journal of Coal Geology, 50, 317-361.

Willcox, J.B. and Stagg, H.M.J., 1990. Australia's southern margin, a product of oblique extension. Tectonophysics, 173, 269-281.

Williamson, P.E., Pigram, C.J., Colwell, J.B., Sherl, A.S., Lockwood, K.L. and Branson, J.C., 1985. Pre-Eocene stratigraphy, structure, and petroleum potential of the Bass Basin. APEA Journal, 25 (1), 362-381.

Williamson, P.E. and Pigram, C.J., 1986. Subsidence and maturation history of the Bass Basin from geohistory calculations. In: Glenie, R.C. (editor), Second South-Eastern Australia Oil Exploration Symposium, PESA Symposium, Melbourne, 285-299.

Williamson, P.E., Pigram, C.J., Colwell, J.B., Scherl A.S., Lockwood, K.L., and Branson, J.C., 1987. Review of stratigraphy, structure, and hydrocarbon potential of Bass Basin, Australia. AAPG. Bulletin, 71, 253-280.

Wood, T., 2003. BassGas project underway. Discovery, Victoria's Earth Resources Journal (February 2003). State Government Victoria, Department of Primary Industries, Minerals and Petroleum Division, 4.

Woodward-Clyde, 1999. Western Tasmanian Regional Minerals Program, Final Regional Development Plan. Report prepared for Department of Industry Science Resources, Mineral Resources Tasmania and Tasmanian Minerals Council. AGC Woodward-Clyde Pty Limited (unpublished).

Young, G.A. and Laurie, J.R. (Editors), 1996. An Australian Phanerozoic Timescale. Oxford University Press, Melbourne, 279 p.

Young, I.M., Trupp, M.A. and Gidding, M.J., 1991. Tectonic evolution of Bass Strait, origins of Tertiary inversion. Exploration Geophysics, 22, 465-468.

Zampatti, D., 1991. Diagenesis of the Eastern View Group sediments, Bass Basin, Tasmania. Honours Thesis, National Centre for Petroleum Geology and Geophysics, University of Adelaide (unpublished).

GEOSCIENCE AUSTRALIA RECORD 2003/19

PETROLEUM GEOLOGY OF THE BASS BASIN – INTERPRETATION REPORT

APPENDIX - VOLUME II

An Output of the Western Tasmanian Regional Minerals Program

Jane E. Blevin (Compiler)
Geoscience Australia
Petroleum and Marine Division

WITH CONTRIBUTIONS BY

Jane E. Blevin, Chris J. Boreham and Kathe R. Trigg, Geoscience Australia

Aaron Cummings, Ric Daniel, John Kaldi, Simon Lang, Nick Lemon, Rob Root and Peter Tingate, National Centre for Petroleum Geology and Geophysics, University of Adelaide

Alan D. Partridge, Biostrata Pty Ltd.

Canberra Australia 2003

Geoscience Australia

Chief Executive Officer: Neil Williams

Department of Industry, Tourism & Resources

Minister for Industry, Tourism & Resources: The Hon Ian Macfarlane MP
Parliamentary Secretary: The Hon Warren Entsch MP
Secretary: Mark Paterson

© Commonwealth of Australia 2003

This work is copyright. Apart from any fair dealings for the purposes of study, research, criticism or review, as permitted under the *Copyright Act*, no part may be reproduced by any process without written permission. Inquiries should be directed to the Communications Unit, Geoscience Australia, GPO Box 378, Canberra City, ACT, 2601

ISSN: 1448-2177
ISBN: 0 642 46777 3

Bibliographic references:

Blevin, J. (Compiler), 2003. Petroleum Geology of the Bass Basin - Interpretation Report, An Output of the Western Tasmanian Regional Minerals Program. Geoscience Australia, Record 2003/19.

Boreham, C., 2003. Petroleum geochemistry of source rocks, oils and gases. In: Blevin, J. (Compiler), Petroleum Geology of the Bass Basin – Interpretation Report, An Output of the Western Tasmanian Regional Minerals Program, Geoscience Australia Record 2003/19.

Geoscience Australia has tried to make the information in this product as accurate as possible. However, it does not guarantee that the information is totally accurate or complete. **Therefore, you should not rely solely on this information when making a commercial decision.**

Geoscience Australia Website: www.ga.gov.au

APPENDICES – VOLUME II (CD-ROM ONLY)

APPENDIX A. List of petroleum exploration wells in the Bass Basin (Jane Blevin, Geoscience Australia)

APPENDIX B: List of horizons interpreted in the Bass Basin wells (Jane Blevin, Geoscience Australia)

APPENDIX C. Biostratigraphy Reports (Alan Partridge, Biostrata Pty Ltd.)

- **C1.** Palynological analysis of Eocene interval 1380 to 2036 m in Cormorant-1, Bass Basin
- **C2.** Palynological review of Upper Cretaceous units in Durroon-1, Bass Basin
- **C3.** Palynological analysis of Eocene interval 1390 to 2036 m in King-1, Bass Basin
- **C4.** Quantitative palynological analysis of Paleocene to Middle Eocene interval Konkon-1, Bass Basin
- **C5.** Quantitative palynological analysis of eleven cuttings samples from 2266 to 3115 m in Koorkah-1, Bass Basin
- **C6.** Quantitative palynological analysis of Eastern View and Demons Bluff Groups in Poonboon-1, Bass Basin
- **C7.** Palynological analysis of Oligocene sandstones in Squid-1, Bass Basin
- **C8.** Bass Basin palynological project, unravelling a Late Cretaceous to Eocene geological history of large palaeolakes, coastal lagoons and marine bays

APPENDIX D. List of core and cuttings from the Bass Basin analysed for organic geochemistry (Chris Boreham, Geoscience Australia)

APPENDIX E. Vitrinite-inertinite reflectance and fluorescence (VRF™ or VIRF) results for Cormorant-1 and Pelican-5 (Jane Newman, Newman Pty Ltd.)

APPENDIX F. Palynology of coals and claystones from Cormorant-1 and Pelican-5 used for oil-source correlations (Mike Macphail, Australian National University)

APPENDIX G. List of oil and gases in the Bass Basin analysed for this study (Chris Boreham, Geoscience Australia)

APPENDIX H. Small Angle Neutron Scattering (SANS) study on low-ash coals from Cormorant-1 and Pelican-5 (Andrzej Radlinski, Alan Hinde and Chris Boreham, Geoscience Australia)

APPENDIX I. Organic petrology of selected samples from the Bass Basin (Alan Cook, Keiraville Konsultants Pty Ltd.)

APPENDIX J. Uncorrected bottom hole temperature data for Bass Basin wells (Aaron Cummings and Peter Tingate, National Centre for Petroleum Geology and Geophysics)

APPENDIX K. Kinetic modelling of Pelican-5 (Aaron Cummings, National Centre for Petroleum Geology and Geophysics)

APPENDIX L. Mercury injection capillary pressure test results and analytical equipment (Ric Daniel and John Kaldi, National Centre for Petroleum Geology and Geophysics)

APPENDIX M. Core photos of selected wells in the Bass Basin (Simon Lang and Rob Root, National Centre for Petroleum Geology and Geophysics)

APPENDIX A

LIST OF THE BASS BASIN PETROLEUM EXPLORATION WELLS AND DRILLING RESULTS

Jane Blevin, Geoscience Australia

Well Name, Operator and Year	Play Type and Target Horizon(s)	Results	Comments
Aroo-1 Hematite Petroleum 1974	Drape over basement high; Paleocene to Early Eocene sands	P&A Fluorescence, minor gas shows	Structural interpretation inaccurate due to the presence of volcanic rocks near target horizons.
Barramundi-1 Globex Far East 1999	Faulted rollover; Paleocene to Early Eocene sands	P&A CO^2 shows	Failure due to breach of regional seal.
Bass-1 Esso E & P Australia 1965	Carbonate reef complex	P&A No shows	Pre-drill interpreted reef structure was invalid. Intersected volcanic section of pyroclastic material.
Bass-2 Esso E & P Australia 1966	Anticlinal structure; Early Eocene sands	P&A No shows	No seal facies; igneous intrusion near TD.
Bass-3 Esso E & P Australia 1966	Anticlinal structure over basement fault block; Mid-Eocene sands	P&A Minor gas	Minor gas shows between 2054.05 to 2055.57 m. Deeper section was water wet. Later drilling of White Ibis-1 in 1998 showed that Bass-3 was not optimally located over the structure.
Chat-1 Bridge Oil Ltd 1986	Faulted dependent closure; Eocene and younger	P&A No shows	Lack of hydrocarbon charge; volcanics intersected near TD.
Cormorant-1 Esso E & P Australia 1970	Anticlinal structure; Paleocene to Early Eocene sands	P&A Minor gas and oil legs	Several pay zones encountered within the Eastern View Group, including a 2 m oil column, and 2 m and 3 m gas and condensate columns. Failure caused by ineffective seal due to late stage reactivation of trap.
Dondu-1 Esso E & P Australia 1973	Anticlinal structure; Paleocene to Early Eocene sands	P&A No shows	Dispersed minor gas shows associated with coals. Good reservoir quality sands above 2743 m.
Durroon-1 Esso E & P Australia 1972	Fault block with updip closure; Early Cretaceous	P&A No shows	No structural closure, lack of seal facies, variable porosity and permeability
Flinders-1 SAGASCO Resources 1992	Fault block; Early Eocene sands	P&A No shows	Water saturated; igneous intrusion near primary objective.
King-1 SAGASCO Resources 1992	Anticlinal structure; Paleocene to Early Eocene sands	P&A Fluorescence, gas shows, trace oil	Water saturated reservoir.
Konkon-1 Esso E & P Australia 1973	Four-way dip closed structure; Paleocene to Early Eocene sands	P&A No shows	Lack of reservoir and regional seal units.
Koorkah-1 Amoco Australia Exploration 1985	Anticlinal structure; Paleocene to Early Eocene sands	P&A No shows	Poor reservoir quality, possible lack of hydrocarbon charge.
Narimba-1 Esso E & P Australia 1973	Anticlinal structure; Early Eocene	P&A No shows	Lack of hydrocarbon charge.

Nangkero-1 Hematite Petroleum 1974	Fault block with overlying drape closure; Early to Middle Eocene sands	P&A No shows	Good reservoir and seal rocks encountered.
Pelican-1 Esso E & P Australia 1970	Anticlinal structure; Maastrichtian to Early Paleocene sands	P&A Gas and condensate discovery	Non-commercial accumulation with 12 gas/condensate-bearing sands between 2471 and 3162 m KB.
Pelican-2 Esso E & P Australia 1970	Anticlinal structure; Maastrichtian to Early Paleocene sands	P&A Gas and condensate	Appraisal well of gas/condensate discovery at Pelican-1. 16 gas/ condensate-bearing sands between 2272 and 3066 m KB.
Pelican-3 Esso E & P Australia 1972	Fault block; Late Paleocene sands	P&A Minor gas shows, weak fluorescence	Hydrocarbon-bearing sands encountered at Pelican-1 and -2 (Lower *M. diversus*) were absent at Pelican-3.
Pelican-4 Hematite Petroleum 1979	Anticlinal structure; Maastrichtian to Early Paleocene sands	P&A Gas and condensate shows	Further appraisal of gas/condensate-bearing sands at Pelican-1 and -2. Also aimed to test flow characteristics of reservoirs – however sands were too tight to conduct production tests. Three main gas/condensate-bearing intervals encountered, with minor gas and fluorescence recorded in thinner beds.
Pelican-5 Amoco Australia Exploration 1985	Faulted anticlinal structure; Maastrichtian to Early Eocene sands	P&A Gas and condensate flows (DST)	Further testing of Pelican structure. Six DSTs with 2 flows. Log evaluation indicates moveable hydrocarbons at various levels from 2750 to 4050 m KB. Low permeability reservoirs encountered.
Pipipa-1 Hematite Petroleum 1982	Faulted anticlinal structure; Early Eocene sands	P&A Trace gas, weak fluorescence	Good reservoir and seal rocks encountered. Water saturated.
Poonboon-1 Esso E & P Australia 1972	Anticlinal structure, drape over fault block; Late Paleocene to Eocene sands	P&A No shows	Good reservoir and seal rocks encountered. Water saturated. Minor gas kicks associated with coals.
Seal-1 Bridge Oil Ltd 1986	Anticlinal structure; Paleocene to Early Eocene sands	P&A No shows	Lack of hydrocarbon charge (access to mature source rocks).
Squid-1 Weaver Gas & Oil Corporation Australia 1984	Faulted anticlinal structure and overlying Oligocene sand lens; Late Cretaceous to Eocene sands	P&A No shows	Minor gas kicks associated with coals.
Tarook-1 Esso E & P Australia 1972	Low relief anticlinal structure; Early to Middle Eocene sands	P&A No shows	Good reservoir and seal rocks encountered.
Tasmanian Devil-1 Weaver Gas & Oil Corporation Australia 1984	Tilted fault block; Eocene and older sands	P&A No shows	Strata penetrated was significantly different to pre-drill prediction.
Tilana-1 Amoco Australia Exploration 1985	Anticlinal structure; Late Cretaceous to Eocene sands	P&A Minor oil and gas shows	Fluorescence recorded over intervals 3081 to 3096, 3260 and 3573 m KB. Overmature sediments may be due to local intrusions. Target sands had low permeability and porosity.
Toolka-1 Esso E & P Australia 1974	Anticlinal structure; Paleocene to Early Eocene sands	P&A Gas shows, Minor oil	Discontinuous reservoir sands.
White Ibis-1 Boral Energy Resources 1998	Anticlinal structure; Paleocene to Early Eocene sands	P&A Gas discovery	Suspended gas discovery.

Yolla-1 Amoco Australia Exploration 1985	Faulted basement high with dip and fault closure; Paleocene to Early Eocene sands	Suspended Condensate, gas and oil discovery	Production due to come on-line in 2004 (Origin Energy operated BassGas Project).
Yolla-2 Premier Oil Australasia 1998	Appraisal well of Yolla-1 downdip along anticline	P&A Gas shows	Successful in evaluating the Yolla accumulation.
Yurongi-1 Esso E & P Australia 1973	Anticlinal structure; Late Paleocene to Eocene sands	P&A No shows	Good reservoir and seal rocks encountered.
Narimba-1 Esso E & P Australia 1973	Anticlinal structure; Early Eocene	P&A No shows	Lack of hydrocarbon charge.

APPENDIX B.

LIST OF HORIZONS INTERPRETED IN THE BASS BASIN WELLS

Jane Blevin, Geoscience Australia

APPENDIX B. Summary of seismic horizons and sequences mapped for Bass Basin study.

Sequence	Horizon (Base)	Age (Ma) (Base)	Biozonation and Age (Base of Sequence)	Tectonostratigraphic or Depositional Event	Reference Well	Comments
Torquay	Torq-3	9	Planktic foraminifera Zone C, younger than latest Middle Miocene	Cessation of stong Miocene inversion	Cormorant-1 Konkon-1	Top of syn-inversion succession
Torquay	Torq-2	14.5	Planktic foraminifera Zone E1/D2, early Middle Miocene-to-mid-Middle Miocene	Onset of Middle Miocene inversion, End of polygonal faulting	Konkon-1 Cormorant-1 Toolka-1A	Base of syn-inversion succession
Torquay	Torq-1	17.5	Planktic foraminifera Zone G, latest Early Miocene	Polygonal faulting, Deepening marine environment	Pelican wells Durroon-1	Base of carbonate succession at Durroon-1
Torquay	Torq	28.0	Planktic foraminifera Zones I2 / I1, early Late Oligocene-to-Late Oligocene	Thermal subsidence, Mid-Oligocene unconformity, Polygonal faulting	Yurongi-1, Tarook-1, Pelican-2, -3, and -5, Aroo-1	Base of the Torquay Sequence; Regional lowstand unconformity; most continuous seismic horizon in the basin; Base of extrusive volcanic event in northern and western basin
Onset of Basin Phase – Thermal Subsidence 3, Base of Torquay Sequence (Top of Basin Phase – Thermal Subsidence 2)						
Demons Bluff	DBL-3	35	Middle *N. asperus,* early Late Eocene	Flooding surface	Nangkero-1, Narimba-1	Base of Demons Bluff shale (seal), regional flooding surface
Demons Bluff	DBL-2	39	Near base Middle *N. asperus*, late Middle Eocene	Fourth-order sequence boundary	Pelican-3, Squid-1	Base of Boonah Sandstone, local unconformity
Demons Bluff	DBL-1	42	Intra-Lower *N. asperus*, Middle Eocene	Base of Toolka Lake	Poonboon-1, Koorkah-1, Konkon-1	Base of the Toolka Lake cycle, flooding surface within the cycle can be mapped locally
Demons Bluff	DBL	43	Intra-Lower *N. asperus*, Middle Eocene	Thermal subsidence	Narimba-1, Poonboon-1, Aroo-1	Base of the Demons Bluff Sequence, unconformity
Onset of Basin Phase - Thermal Subsidence 2, Base of Demons Bluff Sequence (Top of Basin Phase – Thermal Subsidence 1)						

Sequence	Horizon (Base)	Age Ma (Base)	Biozonation and Age (Base of sequence)	Tectonostratigraphic or Depositional Event	Reference Well	Comments
Onset of Basin Phase - Thermal Subsidence 2, Base of Demons Bluff Sequence (Top of Basin Phase – Thermal Subsidence 1)						
Aroo	marker	47.5	Top *P. asperopolus*, early Middle Eocene	Flooding surface	Aroo-1	Regional flooding surface
Aroo	Aroo-1	50.5	Near base *P. asperopolus*, late Early Eocene	Fourth-order sequence boundary	Aroo-1	Unconformity
Aroo	Aroo	51.5 – 52.0	base of Upper *M. diversus*, mid-Early Eocene	Onset of post-rift subsidence. End of final stages of far-field, oblique extension, growth faulting and fault reactivation	Nangkero-1, Narimba-1, Cormorant-1	Base of the Aroo Sequence, unconformity, Most fault terminate at or near the base of the Aroo Sequence, thick coals are common at base of sequence
Onset of Basin Phase - Thermal Subsidence 1, Base of Aroo Sequence (Top of Basin Phase – Extension 3)						
Bass	marker	54.5	Intra-Lower *M. diversus*, earliest Early Eocene	Maximum flooding surface	Poonboon-1 Nangkero-1, Narimba-1	Regional flooding surface
Bass	Narimba	57	Near base Upper *L. balmei*, late Late Paleocene	Onset of growth faulting in the Pelican and Cormorant troughs, sediment loading	Pelican-5, Toolka-1A, Koorkah-1	Base of the Narimba Sequence, Volcanic intrusions into this succession are common, Koorkah Lake cycle
Bass	Tilana	68	Near base Upper *F. longus*, Late Maastrichtian	Onset of extensional phase in the western Bass Basin (Cape Wickham Sub-basin), growth faulting and sediment loading	Pelican-5, Poonboon-1, Koorkah-1	Base of the Tilana Sequence, Volcanic intrusions into this succession are common, Koorkah Lake cycle
Bass	Furneaux	77.5	Near base or Intra-*T. lillei*, mid-Campanian	Onset of extensional phase in the western Bass Basin	Pelican-5, Tilana-1	Base of the Bass Megasequence and Furneaux Sequence, unconformity
Onset of Basin Phase – Extension 3, Base of Bass Megasequence (Top of Basin Phase – Extension 2)						

Sequence	Horizon (Base)	Age Ma (Base)	Biozonation and Age (Base of sequence)	Tectonostratigraphic or Depositional Event	Reference Well	Comments
Onset of Basin Phase – Extension 3, Base of Bass Megasequence (Top of Basin Phase – Extension 2)						
Durroon	marker	81	*N. senectus*	Slow phase of syn-rift growth (transition)	Durroon-1	Breakup in the Tasman Basin at 83 Ma
Durroon	marker	83	*T. apoxyexinus*	Phase of syn-rift growth	Not interesected	Sediment of this age are absent at the Durroon-1 well, but inferred from seismic correlations
Durroon	marker	87	Intra-*P. mawsonii*	Phase of syn-rift growth	Durroon-1	Phase of syn-rift growth
Durroon	Base-2	91	Near base *P. mawsonii*	Onset of the main extensional phase in the Durroon Sub-basin	Durroon-1	Base of Durroon syn-rift succession
Onset of Basin Phase – Extension 2, Base of Durroon Megasequence (Top of Basin Phase – Extension 1)						
Otway	marker	97.5	*P. pannosus*	Top of Otway Megasequence; unconformity; pre-rift basement to the Bass Megasequence	Durroon-1	Cessation of extension was followed by Cenomanian uplift and erosion before the onset of Extension Phase 2.
Otway	Base 1	115 - 120 (inferred)	? Intra-Upper *F. wonthaggiensis*	Onset of rifting in the Bass Basin – probably localised movement along isolated fault segments	Durroon-1	Oldest sediments penetrated are Aptian (*P. notensis*, formerly *C. hughesii*)
Onset of Basin Phase - Extension 1, Base of Otway Megasequence (Pre-rift Basement)						

APPENDIX C.

BIOSTRATIGRAPHY REPORT FOR SELECTED BASS BASIN WELLS

Alan Partridge, Biostrata Pty. Ltd.

The following reports were commissioned by Geoscience Australia on behalf of Mineral Resources Tasmania, under the funding auspices of the Western Tasmanian Regional Minerals Program. Dr. Alan Partridge, Biostrata Pty Ltd, undertook the biostratigraphic analyses and prepared a series of eight reports (including a summary report). These reports have been reformatted for inclusion in this volume.

C1. Palynological analysis of Eocene interval 1380 to 2036 m in Cormorant-1, Bass Basin

C2. Palynological review of Upper Cretaceous units in Durroon-1, Bass Basin

C3. Palynological analysis of Eocene interval 1390 to 2036 m in King-1, Bass Basin

C4. Quantitative palynological analysis of Paleocene to Middle Eocene interval Konkon-1, Bass Basin

C5. Quantitative palynological analysis of eleven cuttings samples from 2266 to 3115 m in Koorkah-1, Bass Basin

C6. Quantitative palynological analysis of Eastern View and Demons Bluff Groups in Poonboon-1, Bass Basin

C7. Palynological analysis of Oligocene sandstones in Squid-1, Bass Basin

C8. Bass Basin Palynological Project, Unravelling a Late Cretaceous to Eocene geological history of large palaeolakes, coastal lagoons and marine bays

APPENDIX C1.

Palynological analysis of Eocene interval 1380 to 2036m in Cormorant-1, Bass Basin.

by

Alan D. Partridge

Biostrata Pty Ltd
A.B.N. 39 053 800 945

Biostrata Report 2002/06

20th June 2002

Palynological analysis of Eocene interval 1380 to 2036m in Cormorant-1, Bass Basin

by Alan D. Partridge

Introduction

This new palynological study of the uppermost 700 metres of the Eastern View Group in Cormorant-1 is a component of the Bass Basin Palynological Project coordinated by Geoscience Australia as part of the Western Tasmania Regional Minerals Program Offshore Collaborative Project, between Mineral Resources Tasmania, Geoscience Australia and the National Centre for Petroleum Geology and Geophysics to investigate aspects of the hydrocarbon prospectivity of the Bass and Sorell basins.

The interval of interest in Cormorant-1 covers the late Early Eocene to Middle Eocene (Upper *M. diversus* to Lower *N. asperus* Zones) which, from previous palynological studies, was known to contain marine dinocysts including a single specimen of the key index species *Charlesdowniea* (al. *Kisselovia*) *edwardsii* which had been reported from a sidewall core at 1825.8m. The objective of the study was to determine the abundance and diversity of the dinocysts in the palynological assemblages and to verify the presence of, and try and recover additional specimens of the key index species. If the latter were found it would provide better correlation of the Bass Basin succession to the Gippsland Basin, New Zealand and the international time scale. Unfortunately, this second objective was not achieved.

Materials and Methods

Nineteen samples comprising 8 conventional core and 11 cuttings samples were analysed in two batches (Stages 1 and 2). Laboratory processing of the samples was performed by Geoscience Australia. However, due to miscommunication the first batch of 16 samples were given an initial coarse filtration, which had the effect of separating a significant proportion of the organic-walled microplankton (mostly dinocysts) from the finer fraction of the residue containing the majority of angiosperm pollen. This rendered unreliable the counted ratio of dinocysts to the spore-pollen in the assemblages. Separate counts of slides from the two different residue size fractions revealed that the estimated abundance of the microplankton was low (mostly <1% of combined MP + SP count) and only rarely frequent (<10%). As these values were considered unlikely to significantly increase with reprocessing, the author decided to continue the study on the available slides. Collection and reprocessing of three of the cuttings samples in Stage 2 of the project, gave quantitative results close to the estimates derived from the first batch justifying the decision.

The palynological zones assigned to the samples, zone Confidence Ratings, key defining species and interpreted palaeoenvironments are provided in Table 1. Basic palynological data on organic residue yields, palynomorph concentrations in the residues, palynomorph preservation and species diversity in the samples are provided in Table 2. Species abundance and range data are provided in Tables 3 to 5. Author citation for spore-pollen species can be principally sourced for published species from Stover & Partridge (1973), and

for manuscript species from Partridge (1973). Author citation for dinocysts can be sourced from Williams *et al.* (1998), and for acritarchs, algal cysts and other microplankton from Fensome *et al.* (1990).

Geological Discussion

Notwithstanding difficulties with processing most samples analysed in Cormorant-1 have low concentrations of marine and non-marine dinocysts, which are used to environmentally subdivided the section as follows:

1. The most abundance and diverse marine dinocyst assemblages were recovered from the thick shale between 2012 and 2042m. The environment of deposition is suggested to be a large restricted marine lagoon. The presence of the mangrove pollen *Spinizonocolpites prominatus* (= modern *Nypa*) in the assemblages is evidence of tidal influence on the lagoon. This type of environment also applies to shales of similar thickness deeper in the well.
2. Assemblages from the interval of mixed thin coals, sands and shales between approximately 1620 and 2000m are characterised by lower concentrations of mainly cosmopolitan dinocysts. However, when all the species in the interval are listed the overall diversity is also moderate to high. The environment of deposition is also interpreted to be a large restricted marine lagoon. The thinner bedding through the interval, indicative of more rapid changes of environment, suggests the water depth in the lagoon was generally shallow. Falls in the lake water level thus frequently resulted in the deposition of widespread thin coals and thin fluvial/deltaic sands.
3. Assemblages from the cores 5 and 6 between 1505 and 1519m are characterised by mixed marine and non-marine dinocysts as well as some samples lacking any microplankton. This interval is interpreted to represent a shallow, at times ephemeral, lacustrine environments into which there were occasional marine incursions.
4. The shallowest cuttings samples from the distinctive gamma ray peak between 1322 and 1425m contain low abundance and diversity marine dinocyst assemblages which are interpreted to represent a return to a deeper lagoonal environments. This characteristic log interval is identified in eight wells in the northwest part of the basin and has informally been referred to as the Toolka unit (Partridge, 2002b). In contrast to the lagoonal environments of the underlying Early Eocene (Upper *M. diversus* to Lower *P. asperopolus* Zones) the unit lacks coals.

The hope to use marine dinocysts to further subdivide, and to improve the correlations both within and beyond the Bass Basin was not fulfilled by either this new study of Cormorant-1, or the complimentary study of the adjacent King-1 (Partridge, 2002a). Although key index species are present in the succession (eg. *Homotryblium tasmaniense* at 3033-36m and a single specimen of *Wetzeliella articulata* at 1902-05m) they are too rare to be consistently recovered by routine palynological analysis. Their further utilization awaits higher density sampling and much more intensive microscope analysis involving the searching multiple palynological slides per sample. Unfortunately these latter approaches were beyond the scope of this study.

Also unresolved from the study of this suite of samples is the issue of what part of the section in the Bass Basin corresponds to the duration of the cutting of the Marlin Channel in the Gippsland Basin, and the probable equivalent unconformity at the top of the Wangerrip Group in the Otway Basin. Aspects of the spore-pollen assemblages from cores 5 and 6 suggest that the whole package of rocks between 1425 and 1630m may not be represented in either of the adjacent basins.

Finally, at the bottom of the interval studied the shale between 2012 and 2042m is considered to correlate to the shale between 1980 and 2040m in King-1. The change, at about 2000m in both wells, from thicker shales

and thicker coals below to thinner shales and thinner coals above is considered to mark the ìrealî boundary between the Upper *M. diversus* and *P. asperopolus* Zones and may also be a significant sequence boundary.

Biostratigraphy

Upper *Malvacipollis diversus* spore-pollen Zone

Interval: 2024 to 2033 metres

Age: Early Eocene.

The two deepest cuttings samples analysed are assigned to the this zone on the presence of *Proteacidites pachypolus* and absence of younger index species of the overlying *P. asperopolus* Zone. Secondary species consistent with this zone assignment are the frequent occurrence of *Intratriporopollenites notabilis*, *Proteacidites obesolabrus* ms and *Spinizonocolpites prominatus* all recorded from the deeper sample.

The associated microplankton are diagnostic of the *Homotryblium tasmaniense* Zone, which was originally defined by Harris (1985) and has subsequently been modified by Partridge (1999).

***Proteacidites asperopolus* spore-pollen Zone**

Interval: 1621.5 to 1905 metres.

Age: Early Eocene.

This zone is recognised in seven cuttings and three core samples based on the presence of *Conbaculatisporites apiculatus* ms which has a First Appearance Datum (FAD) at 1902-50m, and the somewhat delayed FADs of *Sapotaceoidaepollenites rotundus* at 1716-19m and *Proteacidites asperopolus* at 1689.2m. The top of the zone has a high confidence pick in core-7 at 1682.5m which contains Last Appearance Datums (LADs) for *C. apiculatus*, *Proteacidites ornatus* and *S. prominatus* and also contains the only occurrence in the samples of *Clavastephanocolporites meleosus* Martin *et al*., 1996, which is considered to be restricted to the zone. The next shallower cuttings is also assigned to the zone, with lower confidence, based on the LAD of *Intratriporopollenites notabilis.* This latter sample is tentatively place in an informal upper subzone, based on the lack of other index species.

The associated dinocysts in the samples are broadly consistent with a late Early Eocene age but are not zone diagnostic. The most distinctive species are single specimens of *Hystrichokolpoma spinosum* Wilson 1988 recorded at 1868-72m and *Wetzeliella articulata* Eisenack 1938 recorded at 1902-05m. Unfortunately the occurrence of *Charlesdowniea* (al. *Wetzeliella*) *edwardsii* which had previously been reported from a sidewall core at 1825.8m (Partridge, 1973; p.4), and other related zone index species from the Subfamily Wetzelielloideae were not recovered in the samples. The frequent occurrence of the non-marine dinocyst genera *Saeptodinium* in the cuttings at 1786-89m is referred to the informal *Saeptodinium* facies.

Lower *Nothofagidites asperus* spore-pollen Zone

Interval: 1381 to 1519 metres

Age: Middle Eocene.

The top seven samples are referred to the Lower *N. asperus* Zone based on the increase in abundance of *Nothofagidites* pollen (typically to >30% of SP count), and rare presence of index species. The prominence of *Proteacidites leightonii* and absence of *Nothofagidites falcatus* in the samples from cores 5 and 6 may represent a hitherto undocumented transitional zone interval between the *P. asperopolus* and *N. asperus* Zone that warrants further investigation.

The associated microplankton comprise long ranging cosmopolitan marine dinocysts and undescribed possibly endemic non-marine dinocysts neither of which are currently age or zone diagnostic. Full description and illustration of the non-marine dinocysts is needed and recommended.

References

FENSOME, R.A., WILLIAMS, G.L., BARSS, M.S., FREEMAN, J.M. & HILL, J.M., 1990. Acritarchs and fossil Prasinophytes: An index to genera, species and infraspecific taxa. *AASP Contribution Series No. 25*, p.1-771.

HARRIS, W.K., 1985. Middle to late Eocene depositional cycles and dinoflagellate zones in southern Australia. **In** *Stratigraphy, Palaeontology, Malacology: Papers in Honour of Dr Nell Ludbrook,* J.M. Lindsay, editor, *Department of Mines and Energy South Australia Special Publication 5*, p.133-144.

MARTIN, M.A., MACPHAIL, M.K. & PARTRIDGE, A.D., 1996. Tertiary *Alangium* (Alangiaceae) in eastern Australia: evidence from pollen. *Review of Palaeobotany and Palynology, vol.94,* p.111-122.

PARTRIDGE, A.D., 1973. Revision of the Spore-Pollen Zonation in the Bass Basin. *Esso Australia Ltd Palaeontological Report 1973/4*, 22p. 6pls (2 May).

PARTRIDGE, A.D., 1999. Late Cretaceous to Tertiary geological evolution of the Gippsland Basin, Victoria. PhD thesis, La Trobe University, Bundoora, Victoria, p.i-xxix, p.1-439, 165 figs, 9 pls (unpubl.).

PARTRIDGE, A.D., 2002a. Palynological analysis of Eocene interval 1380 to 2036m in King-1, Bass Basin. *Biostrata Report 2002/08*, p.1-13.

PARTRIDGE, A.D., 2002b. Bass Basin Palynological Project: Unravelling a Late Cretaceous to Eocene geological history of large palaeolakes, coastal lagoons and marine bays. *Biostrata Report 2002/13*, p.1-36.

STOVER, L.E. & PARTRIDGE, A.D., 1973. Tertiary and late Cretaceous spores and pollen from the Gippsland Basin, southeastern Australia. Proceedings *Royal Society of Victoria, vol.85*, pt.2, p.237-286.

WILLIAMS, G.L., LENTIN, J.K. & FENSOME, R.A., 1998. The Lentin and Williams index of fossil dinoflagellates 1998 edition. *American Association of Stratigraphic Palynologists, Contributions Series, no. 34*, p.1-817.

Table-1. Interpretative Palynological Data from Cormorant-1

No.	Sample Type	Depth Metres	Depth Feet	Sample Origin	Spore-Pollen Zone	CR*	Microplankton Zone	CR*	Key Index Species	Palaeoenvironment
1	Cuttings	1380-84	4530-40	GA-1	Indeterminate					Indeterminate
2	Cuttings	1381-90	4530-60	GA-2	Lower *N. asperus* Zone	D4			FAD of *Nothofagidites falcatus*	Lagoonal - brackish
3	Core-5	1505.7	4940	GA-1	Lower *N. asperus* Zone	A4			FAD of *Tricolporites leuros*	Lagoonal - brackish
4	Core-5	1510.9	4957	GA-1	Lower *N. asperus* Zone	A4			FAD of *Matonisporites ornamentalis*	Lagoonal - brackish
5	Core-6	1513.3	4965	GA-1	Lower *N. asperus* Zone	A4			Frequent *Proteacidites leightonii*	
6	Core-6	1515.8	4973	GA-1	Lower *N. asperus* Zone	A4			Frequent *Proteacidites leightonii*	Lagoonal - brackish
7	Core-6	1519.0	4983.5	GA-1	Lower *N. asperus* Zone	A4			Frequent *Proteacidites recavus*	Lagoonal - brackish
8	Cuttings	1621.5	5320	GA-1	*P. asperopolus* Zone	D4			LAD of *Intratriporopollenites notabilis*	Lagoonal - brackish
9	Core-7	1682.5	5520	GA-1	*P. asperopolus* Zone	A1			LAD of *Spinizonocolpites prominatus*	Lagoonal - restricted marine
10	Core-7	1686.2	5532	GA-1	*P. asperopolus* Zone	A5				Coastal Plain - Deltaic
11	Core-7	1689.2	5542	GA-1	*P. asperopolus* Zone	A2			FAD of *Proteacidites asperopolus*	Lagoonal - restricted marine
12	Cuttings	1716-19	5630-40	GA-1	*P. asperopolus* Zone	D4			FAD of *Sapotaceoidaepollenites rotundus*	Lagoonal - restricted marine
13	Cuttings	1786-89	5860-70	GA-1	*P. asperopolus* Zone	D3	*Saeptodinium* Facies			Coastal Plain - Deltaic
14	Cuttings	1820-23	5970-80	GA-2	*P. asperopolus* Zone	D5			LAD of *Myrtaceidites tenuis*	Lacustrine - Fresh
15	Cuttings	1823-26	5980-90	GA-1	*P. asperopolus* Zone	D4				Lagoonal - restricted marine
16	Cuttings	1868-72	6130-40	GA-1	*P. asperopolus* Zone	D4				Lagoonal - restricted marine
17	Cuttings	1902-05	6240-50	GA-1	*P. asperopolus* Zone	D1			FAD of *Conbaculatisporites apiculatus*	Lagoonal - restricted marine
18	Cuttings	2024-33	6640-70	GA-2	Upper *M. diversus*	D4				Lagoonal - restricted marine
19	Cuttings	2033-36	6670-80	GA-1	Upper *M. diversus*	D2	*H. tasmaniense*	D3	FAD of *Homotryblium tasmaniense*	Lagoonal - restricted marine

ABBREVIATIONS

*CR = Confidence Ratings from STRATDAT

LAD = Last Appearance Datum

FAD = First Appearance Datum

GA-1 = Samples collected Stage-1 Work program

GA-2 = Samples collected Stage-2 Work program

CONFIDENCE RATINGS

Alpha Code Linked to Sample

A = Core

B = Sidewall core

C = Coal cuttings

D = Ditch cuttings

J = Junk basket

Numeric Code Linked to Palynomorph Assemblage

1 = Excellent confidence: High diversity assemblage **plus** key zone species.

2 = Good confidence: Moderately diverse assemblage **plus** key zone species.

3 = Fair confidence: Low diversity assemblage **plus** key zone species.

4 = Poor confidence: Moderate to high diversity **minus** key zone species.

5 = Very low confidence: Low diversity assemblage **minus** key zone species.

Table 2. Basic Palynological Data from Cormorant-1

No.	PalLab Spl.No.	Sample Type	Core No.	Top Feet	Base Feet	Top Metres	Base Metres	Visual Yield	Palynomorph Concentration	Palynomorph Preservation	No. SP Species	No. MP Species	Marine MP%	Other MP%	NED	Noth%
1	6405867	Cuttings		4530	4540	1380.7	1383.8	Low	Very Low	Fair	9	2				
2	6406875	Cuttings		4530	4560	1380.7	1389.9	Moderate	Moderate	Poor-Fair	41	2	<2%	<1%	19%	16%
3	6405868	Core	5		4940		1505.7	Moderate	Low	Poor-Fair	27	3	<1%	<1%	<3%	>40%
4	6405869	Core	5		4957		1510.9	Moderate	Low	Poor-Fair	24	2				
5	6405870	Core	6		4965		1513.3	Moderate	Low	Poor-Fair	30					
6	6405871	Core	6		4973		1515.8	High	Moderate	Fair-Good	49	3	<1%	<1%	<10%	>30%
7	6405872	Core	6		4983.5		1519.0	Moderate	Low	Poor-Fair	36	1		<1%		>40%
8	6405873	Cuttings		5320	5320	1621.5	1621.5	Moderate	Low	Poor-Fair	38	1	<1%			<20%
9	6405874	Core	7		5520		1682.5	High	Moderate	Fair-Good	36	2	<1%			
10	6405875	Core	7		5532		1686.2	Moderate	Low	Poor	18					
11	6405876	Core	7		5542		1689.2	Moderate	Low	Fair	46	1	<1%		<1%	<10%
12	6405877	Cuttings		5630	5640	1716.0	1719.1	Moderate	Low	Poor	20					
13	6405878	Cuttings		5860	5870	1786.1	1789.2	Low	Low	Poor	19	1				
14	6406876	Cuttings		5970	5980	1819.7	1822.7	Low	Very Low	Poor-Fair	33	2	4%		6%	19%
15	6405879	Cuttings		5980	5990	1822.7	1825.8	Moderate	Low	Poor	21	4				
16	6405880	Cuttings		6130	6140	1868.4	1871.5	Moderate	Low	Poor	31	2				
17	6405881	Cuttings		6240	6250	1902.0	1905.0	Moderate	Low	Poor-Good	32	5	<1%	<1%	<3%	<10%
18	6406877	Cuttings		6640	6670	2023.9	2033.0	Moderate	Moderate	Poor-Fair	21	6	10%		6%	16%
19	6405882	Cuttings		6670	6680	2033.0	2036.1	High	Moderate	Poor-Fair	30	6	>10%		>15%	<5%

ABBREVIATIONS

MP = Microplankton

SP = Spore-Pollen

NED = Neves Effect based on *Dilwynites/Araucariacites* Percentage

Noth% = Percentage of *Nothofagidites* in SP count.

Other MP = Brackish and fresh-water species

Table 3. Abundances of major palynomorph groups from Cormorant-1.

No.	Top Metres	Base Metres	Top Feet	Base Feet	Sample Type	Residue Filter	Gleicheniidites circinidites spores	ALL OTHER spores	Dilwynites and Araucariacites pollen	ALL OTHER gymnosperm pollen	Nothofagidites spp. pollen	ALL OTHER angiosperm pollen	FUNGAL microfossils	Reworked Spore-Pollen	**Total Terrestrial SUM**		Spore-Pollen Total	Microplankton Fresh-Brackish	Microplankton Marine	**SP + MP SUM**
1	1380.7	1383.8	4530	4540	Cuttings															
2	1380.7	1389.9	4530	4560	Cuttings	Fine	1%	9%	17%	18%	17%	30%	8%		330		98%	0%	2%	311
3		1505.7		4940	Core	Fine		8%	3%	15%	47%	23%	4%		116		97%	2%	1%	114
4		1510.9		4957	Core															
5		1513.3		4965	Core									X						
6A		1515.8		4973	Core	Fine		10%	7%	17%	31%	32%	3%		115		98%	1%	1%	114
6B		1515.8		4973	Core	Coarse		20%	14%	36%	4%	19%	7%	X	124		100%			115
7		1519.0		4983.5	Core	Fine	1%	2%	2%	16%	45%	30%	5%		119		99%	1%		114
8	1621.5	1621.5	5320	5320	Cuttings	Fine		7%	2%	4%	19%	57%	11%		143		100%			127
9		1682.5		5520	Core															
10		1686.2		5532	Core															
11		1689.2		5542	Core	Fine		13%	1%	11%	9%	58%	9%		139		100%			127
12	1716.0	1719.1	5630	5640	Cuttings															
13	1786.1	1789.2	5860	5870	Cuttings															
14	1819.7	1822.7	5970	5980	Cuttings	Fine	0.4%	12%	4%	7%	11%	22%	44%		276		96%		4%	162
15	1822.7	1825.8	5980	5990	Cuttings									X						
16	1868.4	1871.5	6130	6140	Cuttings															
17	1902.0	1905.0	6240	6250	Cuttings	Fine		6%	2%	5%	9%	48%	29%		143		99%	1%		102
18	2023.9	2033.0	6640	6670	Cuttings	Fine	0.3%	5%	3%	10%	9%	29%	43%		291		90%		10%	185
19	2033.0	2036.1	6670	6680	Cuttings	Fine	2%	40%	16%	12%	4%	27%	1%		113		75%	2%	23%	149

Table 4. Cormorant-1 well - spore-pollen distribution.

No.	Top Metres	Base Metres	Sample Type	Residue Filter	SPORE SPECIES	Baculatisporites spp.	Conbaculatisporites apiculatus ms	Cyathidites splendens	Cyathidites palaeospora	Foveotriletes balteus	Gleicheniidites circinidites	Ischyosporites spp.	Kuylisporites waterbolkii	Laevigatosporites major	Laevigatosporites ovatus	Latrobosporites crassus	Latrobosporites marginatus	Matonisporites ornamentalis	Peromonolites spp.	Polypodiidites/Verrucatosporites spp.	Polypodiaceoisporites varus ms	Retitriletes spp.	Rugulatisporites mallatus	Trilete spores undiff.	Tripunctisporis maastrichtiensis	Verrucosisporites kopukuensis	TOTAL SPORES
1	1380.7	1383.8	Cuttings					X				X								X						X	
2	1380.7	1389.9	Cuttings	Fine				1.0%	2.0%	0.3%	0.7%	0.3%			0.3%			0.3%	1.6%					3.3%		0.3%	10%
3		1505.7	Core	Fine					0.9%						6.3%					0.9%							8%
4		1510.9	Core			X		X	X	X	X			X	X			X							X	X	
5		1513.3	Core						X			X		X	X	X	X					X			X	X	
6A		1515.8	Core	Fine		X		X	2.7%			0.9%	X	X	1.8%		X					0.9%		1.8%		1.8%	10%
6B		1515.8	Core	Coarse		0.9%		1.7%	7.8%			3.5%			3.5%					X				1.7%	X	2.6%	22%
7		1519.0	Core	Fine				X	0.9%		0.9%	X			0.9%					X							3%
8	1621.5	1621.5	Cuttings	Fine		X		X	6.3%			X		X	1.6%					X						X	8%
9		1682.5	Core			X	X	X	X		X	X		X	X					X			X		X	X	
10		1686.2	Core			X		X												X							
11		1689.2	Core	Fine		1.6%		X	7.1%			X		X	4.7%	X				X				0.8%			14%
12	1716.0	1719.1	Cuttings			X		X	X			X	X	X	X											X	
13	1786.1	1789.2	Cuttings					X	X		X				X											X	
14	1819.7	1822.7	Cuttings	Fine				6.5%	6.5%		0.6%	0.6%			3.2%				0.6%				X	4.5%			23%
15	1822.7	1825.8	Cuttings					X	X		X	X								X						X	
16	1868.4	1871.5	Cuttings			X		X	X					X	X						X						
17	1902.0	1905.0	Cuttings	Fine			X	X	2.0%	X					5.9%					1.0%			X			X	9%
18	2023.9	2033.0	Cuttings	Fine				0.6%	4.2%		0.6%				1.2%				0.6%					1.8%		0.6%	10%
19	2033.0	2036.1	Cuttings	Fine		4.5%		11%	12%	0.9%	1.8%	2.7%		X	2.7%					2.7%	X		X	1.8%		2.7%	42%

ABBREVIATIONS

X = Present

C = Common

% = Percentage

Table 4. Cormorant-1 well - spore-pollen distribution.

No.	Top Metres	Base Metres	Sample Type	Residue Filter		GYMNOSPERM SPECIES	Gymnosperm pollen undiff.	Araucariacites australis	Dilwynites granulatus	Dilwynites tuberculatus	Lygistepollenites florinii	Microalatidites paleogenicus	Microcachryidites antarcticus	Phyllocladidites mawsonii	Podocarpidites spp.	Trichotomosulcites subgranulatus	TOTAL GYMNOSPERMS		ANGIOSPERM POLLEN SPECIES	Angiosperm pollen undiff.	Banksieaeidites arcuatus	Beaupreaidites elegansiformis	Beaupreaidites trigonalis ms	Beaupreaidites verrucosus	Clavastephanocolporites meleosus	Cupanieidites orthoteichus	Dicotetradites clavatus	Ericipites crassiexinus/scabratus
1	1380.7	1383.8	Cuttings					X	X																			
2	1380.7	1389.9	Cuttings	Fine			3.9%	6.6%	11%	0.7%	1.3%		0.3%	3.9%	9.5%	1.0%	38%			3.3%						0.7%	1.3%	1.0%
3		1505.7	Core	Fine					2.7%	X	1.8%		1.8%	2.7%	8.1%	0.9%	18%			1.8%			X					
4		1510.9	Core					X	X		X			X	X													X
5		1513.3	Core					X	X	X	X			X	X	X												
6A		1515.8	Core	Fine			0.9%	3.6%	2.7%	0.9%	3.6%	0.9%		5.4%	7.1%		25%			3.6%	0.9%							X
6B		1515.8	Core	Coarse				5.2%	9.6%		9.6%	X		17%	12%		54%			0.9%							1.7%	
7		1519.0	Core	Fine					0.9%	0.9%	X			11%	6.2%		19%							X		0.9%		
8	1621.5	1621.5	Cuttings	Fine				0.8%	0.8%	0.8%					4.7%	X	7.1%			0.8%				X		X	2.4%	X
9		1682.5	Core					X	X	X				X	X										X	X		
10		1686.2	Core								X			X	X							X				X		
11		1689.2	Core	Fine					0.8%	0.8%	2.4%	0.8%		2.4%	8		13%			0.8%				X			0.8%	
12	1716.0	1719.1	Cuttings						X	X					X												X	
13	1786.1	1789.2	Cuttings					X	X	X	X			X	X													
14	1819.7	1822.7	Cuttings	Fine			1.3%	2.6%	3.9%		0.6%		0.6%	1.3%	7.1%	1.9%	19%			2.6%				X		0.6%	0.6%	
15	1822.7	1825.8	Cuttings					X	X	X	X		X	X	X													
16	1868.4	1871.5	Cuttings					X	X	X	X			X	X													
17	1902.0	1905.0	Cuttings	Fine			1.0%	1.0%	1.0%	1.0%	X				5.9%	X	9.9%			5.9%				X		2.0%	1.0%	
18	2023.9	2033.0	Cuttings	Fine			2.4%	2.4%	3.6%		1.2%			1.8%	6.0%	6.0%	23%			4.2%						1.2%		
19	2033.0	2036.1	Cuttings	Fine				1.8%	8.9%	5.4%	1.8%				9.8%		28%									1.8%		

ABBREVIATIONS

X = Present

C = Common

% = Percentage

Table 4. Cormorant-1 well - spore-pollen distribution.

No.	Top Metres	Base Metres	Sample Type	Residue Filter	Haloragacidites harrisii	Ilexpollenites spp.	Intratriporopollenites notabilis	Liliacidites spp.	Lymingtonia sp.	Malvacipollis diversus	Malvacipollis robustus ms	Malvacipollis subtilis	Milfordia spp.	Myrtaceidites parvus/mesonesus	Myrtaceidites tenuis	Nothofagidites asperus	Nothofagidites brachyspinulosus	Nothofagidites deminutus	Nothofagidites emarcidus/heterus	Nothofagidites falcatus	Nothofagidites flemingii	Nothofagidites goniatus	Nothofagidites vansteenisii	Paripollis ochesis	Periporopollenites spp.	Polycolporopollenites esobalteus
1	1380.7	1383.8	Cuttings		X																X					
2	1380.7	1389.9	Cuttings	Fine	5.2%	0.7%						0.7%		1.0%		0.7%	5.9%	1.0%	7.5%	0.3%	2.6%	0.3%	0.3%		3.6%	
3		1505.7	Core	Fine	7.2%	0.9%		0.9%				0.9%				1.8%	1.8%		44%			1.8%				
4		1510.9	Core						X										X		X	X				
5		1513.3	Core		X											X			X		X	X				
6A		1515.8	Core	Fine	8.0%	0.9%		2.7%		0.9%		0.9%				0.9%	4.5%		27%							
6B		1515.8	Core	Coarse	7.0%				X		X	0.9%	X			X	1.7%		2.6%			X			0.9%	
7		1519.0	Core	Fine	8.8%	0.9%						X	0.9%				0.9%	0.9%	45%		X	X		X	0.9%	
8	1621.5	1621.5	Cuttings	Fine	11%	0.8%	X	3.9%						1.6%		0.8%	2.4%	1.6%	17%		X	X			1.6%	
9		1682.5	Core		X	X	X					X							X		X	X				
10		1686.2	Core		X	X	X												X							
11		1689.2	Core	Fine	17%		X	0.8%		X	X	1.6%		2.4%		0.8%	1.6%		7.1%		X	X				
12	1716.0	1719.1	Cuttings		X		X				X															
13	1786.1	1789.2	Cuttings		X							X			X											
14	1819.7	1822.7	Cuttings	Fine	3.9%			0.6%						6.5%			X	15%	2.6%		0.6%				0.6%	
15	1822.7	1825.8	Cuttings		X		X					X						X	X							
16	1868.4	1871.5	Cuttings		X		X				X	X							X		X					
17	1902.0	1905.0	Cuttings	Fine	24%	1%						4.0%		4.0%					12%		1.0%				1.0%	
18	2023.9	2033.0	Cuttings	Fine	18%			0.6%				4.8%		0.6%				16%							1.8%	
19	2033.0	2036.1	Cuttings	Fine	3.6%		1.8%				X	3.6%						1.8%	1.8%			X				2.7%

ABBREVIATIONS

X = Present

C = Common

% = Percentage

Table 4. Cormorant-1 well - spore-pollen distribution.

No.	Top Metres	Base Metres	Sample Type	Residue Filter	Proteacidites spp.	Proteacidites adenanthoides	Proteacidites alveolatus	Proteacidites annularis	Proteacidites asperopolus	Proteacidites differentipollis	Proteacidites biporus	Proteacidites crassus	Proteacidites grandis	Proteacidites incurvatus	Proteacidites kopiensis	Proteacidites latrobensis	Proteacidites leightonii	Proteacidites obesolabrus ms	Proteacidites obscurus	Proteacidites ornatus	Proteacidites pachypolus	Proteacidites prodigus ms	Proteacidites pseudomoides	Proteacidites recavus	Proteacidites reticuloscabratus	Proteacidites rugulatus
1	1380.7	1383.8	Cuttings															X								
2	1380.7	1389.9	Cuttings	Fine	9.2%																0.3%					
3		1505.7	Core	Fine	5.4%			0.9%													0.9%					
4		1510.9	Core		X													X						X		
5		1513.3	Core		X					X				X	X			X				X			X	
6A		1515.8	Core	Fine	9.8%			0.9%																		
6B		1515.8	Core	Coarse	4.3%			X					X			X		2.6%				X	X	X		
7		1519.0	Core	Fine	2.7%			6.2%									X	X	1.8%					0.9%		
8	1621.5	1621.5	Cuttings	Fine	4.7%	X									X									X		
9		1682.5	Core		X		X								X		C			X	X					
10		1686.2	Core		X												X									
11		1689.2	Core	Fine	15%	X		0.8%	0.8%	X					X	X	X	X			0.8%	X					
12	1716.0	1719.1	Cuttings		X								X				X									X
13	1786.1	1789.2	Cuttings		X												X	X	X							
14	1819.7	1822.7	Cuttings	Fine	12%		X						0.6%					X	0.6%							
15	1822.7	1825.8	Cuttings		X								X						X							
16	1868.4	1871.5	Cuttings		X						X	X					X			X	X					
17	1902.0	1905.0	Cuttings	Fine	5.0%			3.0%					X								1.0%					
18	2023.9	2033.0	Cuttings	Fine	11%																1.2%					
19	2033.0	2036.1	Cuttings	Fine	5.4%												4.5%	X			0.9%					

ABBREVIATIONS

X = Present

C = Common

% = Percentage

Table 4. Cormorant-1 well - spore-pollen distribution.

No.	Top Metres	Base Metres	Sample Type	Residue Filter	Proteacidites tuberculiformis	Proteacidites xestoformis ms	Pseudowinterapollis couperi	Santalumidites cainozoicus	Sapotaceoidaepollenites rotundus	Spinizonocolpites prominatus	Tricolp(or)ates spp.	Tricolpites phillipsii	Tricolporites adelaidensis	Tricolporites leuros	Tricolporites microreticulatus	Tricolporites paenestriatus	Tricolporites scabratus	Triporopollenites ambiguus	Triporopollenites simplis	TOTAL ANGIOSPERMS	**TOTAL SPORE-POLLEN COUNT**
1	1380.7	1383.8	Cuttings								X										
2	1380.7	1389.9	Cuttings	Fine				0.3%			5.6%									51%	305
3		1505.7	Core	Fine			X				5.4%			X			X			74%	111
4		1510.9	Core		X								X								
5		1513.3	Core						X						X						
6A		1515.8	Core	Fine							4.5%									65%	112
6B		1515.8	Core	Coarse		X			X		1.7%	X	X				X			24%	115
7		1519.0	Core	Fine				0.9%			7.1%		X			X				79%	113
8	1621.5	1621.5	Cuttings	Fine				3.9%			23%					10%				85%	127
9		1682.5	Core							X	X										
10		1686.2	Core					X			X		X		X	X		X			
11		1689.2	Core	Fine	X	X		1.6%			20%		X			0.8%				72%	127
12	1716.0	1719.1	Cuttings		X				X		X		X								
13	1786.1	1789.2	Cuttings								X		X		X						
14	1819.7	1822.7	Cuttings	Fine	X						10%									58%	155
15	1822.7	1825.8	Cuttings								X		X								
16	1868.4	1871.5	Cuttings								X		X					X			
17	1902.0	1905.0	Cuttings	Fine							13%					4.0%			X	81%	101
18	2023.9	2033.0	Cuttings	Fine							7.2%							0.6%		67%	167
19	2033.0	2036.1	Cuttings	Fine						0.9%	1.8%									30%	112

ABBREVIATIONS

X = Present

C = Common

% = Percentage

Table 5. Cormorant-1 well - microplankton distribution.

No.	Top Metres	Base Metres	Sample Type	Residue Filter	**MICROPLANKTON**	ACRITARCHS & ALGAE	Micrhystridium spp.	Botryococcus braunii	Pseudoschizaea spp.	ACRITARCHS & ALGAE SUM		NON-MARINE DINOCYSTS	Cubiculosphaera spp.	Morkallacysta spp.	Saeptodinium spp.	NON-MARINE DINOCYSTS SUM		MARINE DINOCYSTS	Dinocysts undiff.	Apectodinium spp.	Apteodinium sp.	Cleistosphaeridium spp.	Cordosphaeridium spp.	Eocladopyxis peniculata
1	1380.7	1383.8	Cuttings																					X
2	1380.7	1389.9	Cuttings	Fine				17%		17%									50%					
3		1505.7	Core	Fine			33%	33%		67%			33%			33%								
4		1510.9	Core																					
5		1513.3	Core																					
6A		1515.8	Core	Fine									50%			50%			50%					
6B		1515.8	Core	Coarse																				
7		1519.0	Core	Fine				100%		100%														
8	1621.5	1621.5	Cuttings	Fine																			X	
9		1682.5	Core																				X	
10		1686.2	Core																					
11		1689.2	Core	Fine										X										
12	1716.0	1719.1	Cuttings																					
13	1786.1	1789.2	Cuttings												X									
14	1819.7	1822.7	Cuttings	Fine															86%					
15	1822.7	1825.8	Cuttings					X					X											
16	1868.4	1871.5	Cuttings																					
17	1902.0	1905.0	Cuttings	Fine				X	X				100%		X	100%								
18	2023.9	2033.0	Cuttings	Fine															61%					
19	2033.0	2036.1	Cuttings	Fine									8%			8%			59%	2.7%	8%	3%		

ABBREVIATIONS

X = Present

C = Common

% = Percentage

Table 5. Cormorant-1 well -

No.	Top Metres	Base Metres	Sample Type	Residue Filter	Homotryblium tasmaniense
1	1380.7	1383.8	Cuttings		
2	1380.7	1389.9	Cuttings	Fine	
3		1505.7	Core	Fine	
4		1510.9	Core		
5		1513.3	Core		
6A		1515.8	Core	Fine	
6B		1515.8	Core	Coarse	
7		1519.0	Core	Fine	
8	1621.5	1621.5	Cuttings	Fine	
9		1682.5	Core		
10		1686.2	Core		
11		1689.2	Core	Fine	
12	1716.0	1719.1	Cuttings		
13	1786.1	1789.2	Cuttings		
14	1819.7	1822.7	Cuttings	Fine	
15	1822.7	1825.8	Cuttings		
16	1868.4	1871.5	Cuttings		
17	1902.0	1905.0	Cuttings	Fine	
18	2023.9	2033.0	Cuttings	Fine	
19	2033.0	2036.1	Cuttings	Fine	5%

ABBREVIATIONS
X = Present
C = Common
% = Percentage

Table 5. Cormorant-1 well - microplankton distribution.

No.	Top Metres	Base Metres	Sample Type	Residue Filter	Hystrichokolpoma spinosum	Kenleyia spp.	Paralecaniella indentata	Spinidinium spp.	Spiniferites spp.	Systematophora placanthum	Systematophora variable	Wetzeliella articulata	MARINE DINOCYSTS SUM		TOTAL MP COUNT
1	1380.7	1383.8	Cuttings				X								
2	1380.7	1389.9	Cuttings	Fine					33%				83%		6
3		1505.7	Core	Fine											3
4		1510.9	Core							X					
5		1513.3	Core												
6A		1515.8	Core	Fine									50%		2
6B		1515.8	Core	Coarse						X					
7		1519.0	Core	Fine											1
8	1621.5	1621.5	Cuttings	Fine											
9		1682.5	Core												
10		1686.2	Core												
11		1689.2	Core	Fine					X						
12	1716.0	1719.1	Cuttings												
13	1786.1	1789.2	Cuttings												
14	1819.7	1822.7	Cuttings	Fine			14%						100%		7
15	1822.7	1825.8	Cuttings								X				
16	1868.4	1871.5	Cuttings		X	X									
17	1902.0	1905.0	Cuttings	Fine								X			1
18	2023.9	2033.0	Cuttings	Fine		28%		6%	5.6%				100%		18
19	2033.0	2036.1	Cuttings	Fine		11%	X				2.7%		92%		37

ABBREVIATIONS

X = Present

C = Common

% = Percentage

APPENDIX C2.

Palynological review of Upper Cretaceous units in Durroon-1, Bass Basin.

by

Alan D. Partridge

Biostrata Pty Ltd
A.B.N. 39 053 800 945

Biostrata Report 2002/07

30th June 2002

Palynological review of Upper Cretaceous units in Durroon-1, Bass Basin.

by Alan D. Partridge

Introduction

A quantitative palynological study of the informal Furneaux Group and basal Eastern View Group in Durroon-1 has been undertaken as a component of the Bass Basin Palynological Project coordinated by Geoscience Australia as part of the Western Tasmania Regional Minerals Program Offshore Collaborative Project, between Mineral Resources Tasmania, Geoscience Australia and the National Centre for Petroleum Geology and Geophysics to investigate aspects of the hydrocarbon prospectivity of the Bass and Sorell Basins.

The Durroon-1 well, located in the southeastern extremity of the Bass Basin, penetrated a Tertiary succession of about 950 metres, an Upper Cretaceous succession of about 650 metres and over 1400 metres of Early Cretaceous sediment that had not been fully penetrated when the well was plugged and abandoned at a T.D. of 3024m. The focus of this study is solely on the Upper Cretaceous with the objectives of **1)** providing a quantitative reference section for the Upper Cretaceous palynological succession in the Bass Basin, **2)** quantifying the distribution, abundance and diversity of non-marine dinocysts and other microplankton, as indicators of lacustrine depositional environments, and **3)** documenting the presence and distribution of Neves effects within the terrestrial spore-pollen assemblages, as supporting palynological evidence for the presence of lacustrine depositional environments. The interval reviewed in the well represents an incomplete sequence from the Turonian *P. mawsonii* Zone to the Early Paleocene Lower *L. balmei* Zone and the spore-pollen zones are identified in a relatively good suite of sidewall core samples supplemented by 10 new cuttings samples. Although it was known beforehand that both the spore-pollen and the non-marine microplankton assemblages were worthy of full systematic description and illustration, such documentation was not the intent of this new study, and unfortunately was also beyond the scope of the overall project.

Materials and Methods

Assemblage counts were performed on 23 samples (15 SWCs and 8 cuttings samples), and species distributions were recorded for another five samples (3 SWCs and 2 cuttings), which were either unsuitable or unavailable for counting. One additional sidewall core in the sequence was barren, but is included in the samples reviewed for completeness. Most of the palynological slides examined are derived from the relinquished set prepared in the now closed laboratory operated by Esso Australia Ltd, and these were originally studied by Partridge (1973). New palynological slides needed to be prepared from the relinquished palynological residues for some samples where the original glycerin jelly mounting medium had desiccated making the slides unworkable. Two additional sidewall cores processed for the study by Morgan (1991) were also analysed. All the ten cuttings sample analysed were collected by Geoscience Australia personnel from their core library and prepared in their palynological laboratory. Three of these cuttings (at 1238-87m, 1323-29m and 1411-20m), due to miscommunication were given an initial coarse filtration, which had the effect of

separating a significant proportion of the larger palynomorphs from the finer fraction of the residue containing the majority of angiosperm pollen. Separate assemblage counts of the fine and coarse fractions were made and are recorded, but the results should be treated with caution.

The palynological zones assigned to the samples, zone Confidence Ratings, key defining species and interpreted palaeoenvironments are provided in Table 1. Basic palynological data on organic residue yields, palynomorph concentrations in the residues, palynomorph preservation and species diversity in the samples are provided in Table 2. Species abundance and range data are provided in Tables 3 to 5. Author citation for spore-pollen species can be principally sourced for published species from Dettmann (1963), Helby *et al.* (1987) and Stover & Partridge (1973), and for most of the manuscript species from Partridge (1973). Author citation for dinocysts can be sourced from Williams *et al.* (1998), and for acritarchs, algal cysts and other microplankton from Fensome *et al.* (1990).

Geological Discussion

Drilled in 1972, Durroon-1 is an extremely important well in the Bass Basin as it is the only well to fully penetrates the Upper Cretaceous, even though this succession is relatively thin (<650 metres) and contains significant time gaps. The interval investigated in this palynological study extends from the base of the Turonian Durroon Formation (deepest sample at 1533.1m), through the unconformably overlying Campanian to Maastrichtian section and stops at the deepest productive Paleocene sample at 925.1m. The thick sequence of older Otway Group sediments from 1646 to 3024m, the unnamed sandstones and volcanics between 1544 and 1646m, and the Tertiary succession above 900m where not re-examined.

The section of interest comprises the Furneaux Group and lower half of the overlying Eastern View Group. The currently informal Furneaux Group (name suggested by Peter Baillie *pers comm*.), is made up of the unnamed sandstones and volcanics from 1544 to 1646m, the Durroon Formation from 1370 to 1544m, and the Boobyalla unit from 1235 to 1370m. The Durroon Formation was originally proposed by Smith (1986; p.264) with its type interval specified as from 1374 to 1545m, which is herein redefined as the interval 1370 to 1544m. The informal Boobyalla unit is proposed in the final compilation report by Partridge (2002), and derives its name from the equivalent age sedimentary section present in the onshore Boobyalla Subbasin (Moore *et al*., 1984). The Eastern View Group between 582 and 1234m is all assigned to the informal Chat unit of Partridge (2002). Only the palynological samples from the bottom half of the latter unit have been re-examined or reviewed.

Palynological assemblages from the late Turonian age (middle *P. mawsonii* Zone) Durroon Formation are characterised by significant abundances of non-marine microplankton including dinocysts referred to *Morkallacysta* and algal cysts of the *Rimosicysta* Superzone recorded from the Kipper Shale in the adjacent Gippsland Basin (Partridge, 1999; Bernecker & Partridge, 2001). The associated spore-pollen assemblages are characterised by abundant *Dilwynites* pollen (average 30%) diagnostic of a Neves effect, which is the

tendency for certain more buoyant spores or pollen to have greater relative abundances in sediments deposited in more distal marine or lacustrine environments (Traverse, 1988; Partridge, 2002). The shallowest two sidewall cores from the formation are also characterised by a spike in the abundance of *Cupressacites* pollen (average 41%), which is interpreted to correlate with a similar spike in *Cupressacites* pollen in the Banoon Member at the top of the Flaxman Formation in the Otway Basin (Partridge, 2001). The 175 metre thick mudstone of the Durroon Formation is interpreted to have been deposited in distal fresh-water lacustrine facies (Palaeolake Durroon) which is coeval with the Flaxman Formation in the Otway Basin and the youngest part of the Kipper Shale in the Gippsland Basin. The moderate to high abundance of non-marine microplankton, the abundant *Dilwynites* and *Araucariacites* pollen indicating a strong Neves effect, and overall homogeneous nature of the mudstone lithology evidenced by the shaly gamma ray log and broad separation of the density and porosity logs, in combination is interpreted to mean that the Durroon Formation was deposited in a distal, and probably deep, fresh-water lacustrine environment.

The idea that the Durroon Formation was a significant fresh-water lacustrine facies was first proposed by Partridge (1973). Subsequently, in a study of cuttings samples Morgan (1985) gave an environmental range of brackish to fresh-water, which Baillie & Pickering (1991; p.14) interpreted as indicating *ì Ö the development of a least marginal marine conditionsî* . Because of this alternate interpretation it needs to be stressed that no definitive marine microplankton were found during this study, although several species or genera that were recorded are also found and can be abundant in both brackish and marine environments (eg. *Botryococcus braunii, Amosopollis cruciformis* and *Micrhystridium*). Further, the location of Durroon-1 on palaeogeographic reconstructions is remote from marine units of equivalent age to the Durroon Formation making any marine influence unlikely (eg. Partridge, 2002; fig.5).

The overlying Boobyalla unit, which is of Campanian age (upper? *N. senectus* to *T. lilliei* Zones), contains palynological assemblages characterised by *Nothofagidites* pollen (typically >20%), with markedly reduced abundances in the pollen of *Dilwynites* (average <5%) and *Cupressacites* (average <0.5%). Rare non-marine dinocysts and algae in this unit hint at the probable presence of more shaly lacustrine facies in the adjacent troughs (eg. Baillie & Pickering, 1991; fig.2). The significant time break of between 5 and 9 million years between the Durroon Formation and Boobyalla unit is correlated with the Longtom Unconformity identified in the Gippsland Basin by Bernecker & Partridge (2001).

Productive palynological samples from the Chat unit are divided between the Maastrichtian *F. longus* Zone and a single sample from the Paleocene Lower *L. balmei* Zone. The former are dominated by angiosperm pollen (notably *Nothofagidites* average 14%, *Proteacidites* average 9% and *Gambierina* average 5%), and the latter by gymnosperm pollen (notably *Phyllocladidites mawsonii* at 24%). Palynological evidence of lacustrine environments was insignificant except for the sidewall core at 1132.3m which contained indeterminate diaphanous dinocysts (identified solely by pigment spots) associated with a weak Neves effect (*Dilwynites* and *Araucariacites* pollen abundance of 16%). As this sample is associated with a distinct shale

character on the gamma ray and SP logs and has a broad separation of the bulk density and neutron porosity logs it may represent an important lacustrine ì flooding horizonî . In an attempt to more precisely locate the Cretaceous/Tertiary boundary in Durroon-1 similar shale horizons identified at 948-56m, 961-69m, 990-1005m and 1058-68m where sampled by the closest suitable cuttings. Unfortunately, these cuttings samples gave meager yields, containing only a few palynomorphs, and as those recorded were all long ranging species the samples could not be reliably assigned to either the *L. balmei* or *F. longus* Zones. Further, the two sidewall cores recovered from this interval at 977.2m and 1004m were composed of lithologies unfavourable for palynology. Of these only the shallower sample was processed and that proved to be barren.

An additional time break and unconformity is interpreted between the Boobyalla and Chat units placed at the log break at 1235m. This unconformity is correlated with the Seahorse Unconformity identified in the Gippsland Basin by Bernecker & Partridge (2001), and with one or more unconformities identified within the Timboon Sandstone in the Otway Basin by Partridge (2001).

Biostratigraphy

Lower *Lygistepollenites balmei* spore-pollen Zone

Sample at: 925.1 metres

Age: Paleocene.

The shallowest sidewall core examined is assigned to the Lower *L. balmei* Zone with low confidence based on the dominance of gymnosperm pollen in the assemblage (notably *Podocarpidites* spp at 31% and *Phyllocladidites mawsonii* at 24%), combined with the frequent occurrence of *Tetracolporites verrucosus* (1.2%) a species which is both inconsistent and rare above this zone. No species that commence their ranges within the *L. balmei* Zone were identified and this feature combined with rare occurrence of *Proteacidites clinei* ms suggests a position low in the zone.

Upper *Forcipites longus* spore-pollen Zone

Interval: 1040.9 to 1095.5 metres.

Age: Late Maastrichtian.

The shallower of the two sidewall cores is assigned to the Upper *F. longus* Zone on the FAD (First Appearance Datum) of the distinctive spore *Tripunctisporis maastrichtiensis*, the primary index species of the zone. In contrast, the deeper sidewall core is assigned to the zone on the secondary definition, an increase in the abundance of *Gambierina rudata* which in this case is 16% of spore-pollen count, based on the latest zone revision by Partridge (1999). Both samples are considered to be no younger than the Upper *F. longus* Zone based on the LADs (Last Appearance Datums) of *Battenipollis sectilis* and *Pseudowinterapollis wahooensis*. The bottom sample also contains the LADs in Durroon-1 of the additional index species *Tricolporites lilliei* and *Tricolpites confessus*.

Lower *Forcipites longus* spore-pollen Zone

Interval: 1132.3 to 1219.2 metres

Age: Early Maastrichtian.

The three sample are all assigned to Lower *F. longus* Zone on the presence of the eponymous species *Forcipites longus* and lack of younger features. Other index species recorded that are considered to range no older than this zone are *Tetracolporites verrucosus* and *Proteacidites reticuloconcavus* ms which are only recorded from the shallowest sample at 1132.3m. This latter sample also contains the common occurrence (10% of combined SP + MP counts) of small diaphanous dinocysts. These forms are identified in the counts by their ìpigment spotsî, and they cannot be assigned to any known genus as their morphology is not yet resolved.

***Tricolporites lilliei* spore-pollen Zone**

Interval: 1238 to 1311 metres

Age: Late Campanian.

Two cuttings and two sidewall cores are assigned to this zone on the presence of either the eponymous species *Tricolporites lilliei* or the accessory index species *Battenipollis sectilis* neither of which range below this zone (Helby *et al.*, 1987; fig.33). The consistent presence of *Gambierina rudata* (average 3%) and rarity of *Forcipites sabulosus* supports this zone assignment. The samples are dominated by *Nothofagidites* pollen (average >25%), spore of *Cyathidites* (average >10%) and occasional abundances of the gymnosperm pollen *Trichotomosulcites subgranulatus* (from <5% to >10%). The microplankton in the samples are not considered age diagnostic but they do include the youngest recorded occurrences of the genera *Morkallacysta* and *Rimosicysta* in Durroon-1.

***Nothofagidites senectus* spore-pollen Zone**

Interval: 1323 to 1366 metres and caved down to 1384 metres

Age: Early Campanian.

The spore-pollen assemblages from both sidewall cores and cuttings are confidently assigned to the *N. senectus* Zone on the common to abundant occurrence of *Nothofagidites* pollen (typically 5% to 30%), and consistent rare to frequent presence of *Forcipites sabulosus* (typically <1% to ~5%). A position high in the *N. senectus* Zone is favoured based on *Nothofagidites* pollen being significantly more abundant than *Forcipites sabulosus*. In the lower part the zone in both the Otway and Gippsland Basin the reverse relationship occurs with *Forcipites sabulosus* often >10% and *Nothofagidites* generally rare with abundances of <1%. None of the other species recorded are considered particularly zone diagnostic, but it is worth noting that the occurrence of *Coptospora pileolus* ms in two of the four samples is consistent with the youngest occurrence of this species in the Gippsland Basin. Morgan (1991) in contrast incorrectly treats the LAD of this species as a marker for the underlying *P. mawsonii* Zone. The microplankton in the samples are not considered age diagnostic, but they do include the interpreted lacustrine genera *Morkallacysta* and *Rimosicysta*.

***Phyllocladidites mawsonii* spore-pollen Zone**

Interval: 1374.6 to 1533.1 metres

Age: Turonian.

The spore-pollen assemblages are confidently assigned to *P. mawsonii* Zone based on the very rare presence of the eponymous species in six of the seven sidewall cores analysed. Index species indicating an age no younger than this zone are the occurrence of the spores *Appendicisporites distocarinatus* at 1432.6, *Verrucosisporites admirabilis* ms at 1411-20m, 1463m and 1493.5m, and the rare presence of *Crybelosporites striatus* between 1432.6 and 1533.1m. However, the overwhelming characteristic of the zone is the dominance of gymnosperm pollen *Dilwynites* (range 8% to 55%, average 30%), and *Cupressacites* (range <5% to 56%, average 21%). Abundance of these pollen types are characteristic of the middle part of the zone in Flaxman Formation in Otway Basin and Kipper Shale in the Gippsland Basin. A two-fold subdivision of the *P. mawsonii* Zone in Durroon-1 is evident on the ratio between *Dilwynites* and *Cupressacites* pollen with the latter showing dominance in the shallowest two sidewall cores at 1374.6 to 1386.8m. This peak in the abundance of *Cupressacites* pollen is interpreted to correlate with a similar abundance spike in the Banoon Member at the top of the Flaxman Formation in the Otway Basin (Partridge, 2001). A few angiosperm species show anomalous older range extensions in Durroon-1 compared to this zone in the adjacent Otway and Gippsland Basins. These are *Forcipites* sp. possibly related to *Forcipites stipulatus* Dettmann & Jarzen 1988, *Peninsulapollis gillii* (Cookson 1957), *P. askiniae* Dettmann & Jarzen 1988 and possible specimens of *Proteacidites palisadus* Couper 1953.

***Rimosicysta* microplankton Superzone**

Interval: 1374.6 to 1533.1 metres

Age: Turonian.

The samples from the Durroon Formation are also assigned to the *Rimosicysta* Superzone proposed by Partridge (1999) based on the unusual algal assemblage described from the Kipper Shale in the Gippsland Basin by Marshall (1989). The superzone is identified by the presence of either or both the algal genera *Rimosicysta* and *Wuroia*, which occur in all but the bottom sample in the interval assigned to the superzone in Durroon-1. A three-fold subdivision of the succession is apparent (Table 5). The deepest two sidewall cores are dominated by the algal cyst *Sigmopollis carbonis* (average ~75%), the middle three sidewall cores are characterised by *Rimosicysta* (average ~50%), while in the shallowest two sidewall cores the microplankton suite is overwhelmingly dominated by the non-marine dinocyst genus *Morkallacysta* (average >95%). Morgan (1991) proposes a finer subdivision of the microplankton succession, with emphasis on the LADs of species, but his splitting of the *Rimosicysta* species and restricted range given to *Wuroia* spp. was not supported by this study. It should also be noted that Morgan (1991) does not identify *Sigmopollis carbonis* which dominates a number of the assemblages. Testing of the biostratigraphic merits of these two alternative approaches to the subdivision of the microplankton succession through the Durroon Formation awaits the drilling of further exploration wells. In the meantime critical information for this future

exploration could be obtained from the full systematic description and illustration of these well-preserved and diverse non-marine microplankton assemblages.

References

BAILLIE, P.W. & PICKERING, R.L., 1991. Tectonic evolution of the Durroon Basin, Tasmania. *Exploration Geophysics, vol.22*, p.13-18.

BERNECKER, T., & PARTRIDGE, A.D., 2001. Emperor and Golden Beach Subgroups: The onset of Late Cretaceous sedimentation in the Gippsland Basin, SE Australia. **In** *Eastern Australian Basins Symposium. A Refocussed Energy Perspective for the Future,* K.C. Hill & T. Bernecker, editors, *Petroleum Exploration of Australia, Special Publication*, p.391-402.

COOKSON, I.C., 1957. On some Australian Tertiary spores and pollen grains that extend the geological and geographical distribution of living genera. *Proceedings of the Royal Society of Victoria, vol.69*, pt.1, p.41-53, pl.8-10.

COUPER, R.A., 1953. Upper Mesozoic and Cainozoic spores and pollen grains from New Zealand. *New Zealand Geological Survey Paleontological Bulletin 22,* p.1-77, pl.1-9.

DETTMANN, M.E., 1963. Upper Mesozoic microfloras from southeastern Australia. *Proceedings Royal Society Victoria 77*, p.1-148.

DETTMANN, M.E. & JARZEN, D.M., 1988. Angiosperm pollen from uppermost Cretaceous strata of southeastern Australia and the Antarctica Peninsula. *Memoir of the Association of Australasian Palaeontologists 5*, p. 217-237.

FENSOME, R.A., WILLIAMS, G.L., BARSS, M.S., FREEMAN, J.M. & HILL, J.M., 1990. Acritarchs and fossil Prasinophytes: An index to genera, species and infraspecific taxa. *AASP Contribution Series No. 25,* p.1-771.

HELBY, R., MORGAN, R. & PARTRIDGE, A.D., 1987. A palynological zonation of the Australian Mesozoic. **In** *Studies in Australian Mesozoic Palynology*, P.A. Jell, editor, *Memoir Association Australasian Palaeontologists 4,* p.1-94.

MARSHALL, N.G., 1989. An unusual assemblage of algal cysts from the late Cretaceous, Gippsland Basin, Southeastern Australia. *Palynology 13,* p.21-56.

MOORE, W. R., BAILLIE, P.W., FORSYTH, S.M., HUDSPERTH, J.W., RICHARDSON, R.G. & TURNER, N.J., 1984. Boobyalla Sub-basin: A Cretaceous onshore extension of the southern edge of the Bass Basin. *The APEA Journal, vol.24*, pt.1, p.110-117.

MORGAN. R., 1985. Palynology of Esso Durroon-1, Bass Basin. Unpublished report for Bridge Oil, 9p. 2 figs, 2 charts.

MORGAN. R., 1991. New palynology of the Durroon Mudstone, Durroon-1, Bass Basin. Unpublished report for Bridge Oil, 17p. 2 figs, 1 chart.

PARTRIDGE, A.D., 1973. Palynology of Durroon-1, Bass Basin. *Esso Australia Ltd Palaeontological Report 1973/1*, 11p. (31 January).

PARTRIDGE, A.D., 1973. Revision of the Spore-Pollen Zonation in the Bass Basin. *Esso Australia Ltd*

Palaeontological Report 1973/4, 22p. 6pls (2 May).

PARTRIDGE, A.D., 1999. Late Cretaceous to Tertiary geological evolution of the Gippsland Basin, Victoria. PhD thesis, La Trobe University, Bundoora, Victoria, p.i-xxix, p.1-439, 165 figs, 9 pls (unpubl.).

PARTRIDGE, A.D., 2001. Revised stratigraphy of the Sherbrook Group, Otway Basin. **In** *Eastern Australian Basins Symposium. A Refocused Energy Perspective for the Future,* K.C. Hill & T. Bernecker, editors, *Petroleum Exploration of Australia, Special Publication*, p.455-464.

PARTRIDGE, A.D., 2002. Bass Basin Palynological Project: Unravelling a Late Cretaceous to Eocene geological history of large palaeolakes, coastal lagoons and marine bays. *Biostrata Report 2002/13*, p.1-36.

SMITH, G.C., 1986, Bass Basin geology and petroleum exploration. **In** *Second South-Eastern Australia Oil Exploration Symposium,* R.C. Glenie, editor, Technical papers presented at PESA Symposium, 14-15 November, 1985, Melbourne, p.257-284.

STOVER, L.E. & PARTRIDGE, A.D., 1973. Tertiary and late Cretaceous spores and pollen from the Gippsland Basin, southeastern Australia. *Proceedings Royal Society of Victoria, vol.85,* pt.2, p.237-286.

TRAVERSE, A., 1988. *Paleopalynology*. Unwin Hyman Ltd, Boston, p.1-600.

WILLIAMS, G.L., LENTIN, J.K. & FENSOME, R.A., 1998. The Lentin and Williams index of fossil dinoflagellates 1998 edition. *American Association of Stratigraphic Palynologists, Contributions Series, no. 34*, p.1-817.

Table 1. Interpretative Palynological Data from Durroon-1

No.	Sample Type	Depth Metres	Depth Feet	Sample Origin	Spore-Pollen Zone	CR*	Microplankton Zone	CR*	Key Index Species	Palaeoenvironment
1	SWC 1/1	925.1	3035	Esso	Lower *L. balmei*	B4			LAD of *Tetracolporites verrucosus*	Non-marine - fluvial
2	Cuttings	963-72	3160-90	GA-1	Indeterminate					Non-marine - fluvial
3	SWC 30/2	977.2	3206	Esso	Barren					
4	Cuttings	1000-08	3280-310	GA-1	Indeterminate					Non-marine - fluvial
5	SWC 28	1040.9	3415	Esso	Upper *F. longus*	B1			FAD of *Tripunctisporis maastrichtiensis*	Non-marine - fluvial
6	Cuttings	1055-64	3460-90	GA-1	Indeterminate					Non-marine - fluvial
7	SWC 26	1095.5	3594	Esso	Upper *F. longus*	B4			*Gambierina rudata* common at 16%	Non-marine - fluvial
8	SWC 25	1132.3	3715	Esso	Lower *F. longus*	B2			FAD of *Proteacidites reticuloconcavus* ms	Non-marine - lacustrine
9	SWC 24	1171.7	3844	Esso	Lower *F. longus*	B3				Non-marine - fluvial
10	SWC 23	1219.2	4000	Esso	Lower *F. longus*	B3			FAD of *Forcipites longus*	Non-marine - fluvial
11	Cuttings	1238-87	4060-90	GA-1	*T. lilliei*	D2				Deltaic - Lacustrine
12	SWC 22	1249.7	4100	Esso	*T. lilliei*	B3			LAD of *Forcipites sabulosus*	Deltaic - Lacustrine
13	SWC 30/3	1287.2	4223	Esso	*T. lilliei*	B4				Deltaic - Lacustrine
14	Cuttings	1302-11	4270-300	GA-1	*T. lilliei*	D1			FAD of *Tricolporites lilliei*	Deltaic - Lacustrine
15	SWC 20	1310.6	4300	Morgan	Indeterminate					Deltaic - Fluvial
16	Cuttings	1323-29	4340-60	GA-1	*N. senectus*	D2				Deltaic - Lacustrine
17	SWC 19	1341.1	4400	Esso	*N. senectus*	B1				Deltaic - Lacustrine
18	SWC 18	1359.4	4460	Morgan	*N. senectus*	B2			FAD of *Nothofagidites senectus* in SWC	Non-marine - fluvial
19	Cuttings	1366-75	4480-510	GA-1	*N. senectus - P. mawsonii*		*Rimosicysta* Superzone	D3	LAD of common *Morkallacysta*	Lacustrine - fresh
20	SWC 17	1374.6	4510	Esso	*P. mawsonii*	B1	*Rimosicysta* Superzone	B3	Abundant *Morkallacysta*	Lacustrine - fresh
21	Cuttings	1375-84	4510-40	GA-1	Mostly caved *N. senectus*				Abundant *Morkallacysta*	Lacustrine - fresh
22	SWC 16	1386.8	4550	Esso	*P. mawsonii*	B1	*Rimosicysta* Superzone	B3	Abundant *Morkallacysta*	Lacustrine - fresh
23	Cuttings	1402-11	4600-30	GA-1	*P. mawsonii*	D2	*Rimosicysta* Superzone	D3	Abundant *Morkallacysta*	Lacustrine - fresh
24	Cuttings	1411-20	4630-60	GA-1	*P. mawsonii*	D2	*Rimosicysta* Superzone	D3	Abundant *Morkallacysta*	Lacustrine - fresh
25	SWC 14	1432.6	4700	Esso	*P. mawsonii*	B1	*Rimosicysta* Superzone	B3	LAD of *Appendicisporites distocarinatus*	Lacustrine - fresh
26	SWC 13	1463.0	4800	Esso	*P. mawsonii*	B1	*Rimosicysta* Superzone	B3		Lacustrine - fresh
27	SWC 12	1493.5	4900	Esso	*P. mawsonii*	B1	*Rimosicysta* Superzone	B3		Lacustrine - fresh
28	SWC 11	1510.3	4955	Esso	*P. mawsonii*	B1	*Rimosicysta* Superzone	B3	FAD of *Rimosicysta*	Lacustrine - fresh
29	SWC 10	1533.1	5030	Esso	*P. mawsonii*	B1	*Rimosicysta* Superzone	B4	Very abundant *Dilwynites* pollen	Lacustrine - fresh

ABBREVIATIONS

*CR = Confidence Ratings
LAD = Last Appearance Datum
FAD = First Appearance Datum
GA-1 = Samples collected Stage-1 Work program
Esso = Samples processed in Esso laboratory
Morgan = Samples processed in Roger Morgan's laboratory

CONFIDENCE RATINGS

Alpha Code Linked to Sample

A = Core
B = Sidewall core
C = Coal cuttings
D = Ditch cuttings
J = Junk basket

Numeric Code Linked to Palynomorph Assemblage

1 = Excellent confidence: High diversity assemblage **plus** key zone species.
2 = Good confidence: Moderately diverse assemblage **plus** key zone species.
3 = Fair confidence: Low diversity assemblage **plus** key zone species.
4 = Poor confidence: Moderate to high diversity **minus** key zone species.
5 = Very low confidence: Low diversity assemblage **minus** key zone species.

Table 2. Basic Palynological Data from Durroon-1

No.	PalLab Spl.No.	Sample Type	Core No.	Top Feet	Base Feet	Top Metres	Base Metres	Visual Yield	Palynomorph Concentration	Palynomorph Preservation	No. SP Species	No. MP Species	Other MP%	NED	Noth%	Cup%
1	NA	SWC	1/1		3035		925.1	Moderate	Moderate	Good	40			<1%	<3%	
2	6405895	Cuttings		3160	3190	963.2	972.3	Low	Low	Poor-Fair	17			<5%	~8%	
3	NA	SWC	30/2		3206		977.2	Barren	NA	NA						
4	6405896	Cuttings		3280	3310	999.7	1008.9	Very Low	Very Low	Poor	8					
5	NA	SWC	28		3415		1040.9	High	High	Fair-Good	40			11%	6%	<1%
6	6405897	Cuttings		3460	3490	1054.6	1063.8	Very Low	Very Low	Poor	3					
7	NA	SWC	26		3594		1095.5	High	High	Fair-Good	49	1	<1%	2%	19%	<1%
8	NA	SWC	25		3715		1132.3	Moderate	Moderate	Fair-Good	43	2	10%	16%	9%	1%
9	NA	SWC	24		3844		1171.7	Low	Low	Poor-Fair	32	1	<1%	<1%	23%	
10	NA	SWC	23		4000		1219.2	Moderate	Low	Poor-Fair	15					
11	6405898	Cuttings		4060	4090	1237.5	1246.6	High	Moderate	Fair	32	4	8%	9%	22%	
12	NA	SWC	22		4100		1249.7	Low	Low	Poor-Fair	17					
13	NA	SWC	30/3		4223		1287.2	Moderate	Moderate	Poor-Fair	38			1%	29%	<1%
14	6405899	Cuttings		4270	4300	1301.5	1310.6	High	High	Fair-Good	44	1	4%	4%	30%	
15	NA	SWC	20		4300		1310.6	Very Low	Very Low	Fair	13			8%	5%	
16	6405900	Cuttings		4340	4360	1322.8	1328.9	High	High	Poor-Good	33	3	4%	5%	16%	<1%
17	NA	SWC	19		4400		1341.1	Moderate	Moderate	Poor-Fair	35			<1%	34%	
18	NA	SWC	18		4460		1359.4	Very Low	Very Low	Fair-Good	18			6%	23%	
19	6405901	Cuttings		4480	4510	1365.5	1374.6	Moderate	Low	Poor-Fair	25		17%	24%	18%	<1%
20	NA	SWC	17		4510		1374.6	High	High	Poor-Good	45	10	42%	23%		27%
21	6405902	Cuttings		4510	4540	1374.6	1383.8	Moderate	Moderate	Poor-Fair	25	2	5%	6%	33%	
22	NA	SWC	16		4550		1386.8	High	High	Poor-Good	40	10	31%	21%		56%
23	6405903	Cuttings		4600	4630	1402.1	1411.2	High	High	Poor	22	4	47%	39%	2%	14%
24	6405904	Cuttings		4630	4660	1411.2	1420.4	Moderate	High	Poor-Fair	19	5	50%	41%	<1%	~10%
25	NA	SWC	14		4700		1432.6	Moderate	Moderate	Poor-Fair	50	9	4%	59%		19%
26	NA	SWC	13		4800		1463.0	Moderate	Moderate	Poor-Fair	43	12	7%	30%		17%
27	NA	SWC	12		4900		1493.5	Moderate	High	Poor-Fair	41	11	20%	51%		24%
28	NA	SWC	11		4955		1510.3	Moderate	Moderate	Poor-Fair	48	3	3%	16%		20%
29	NA	SWC	10		5030		1533.1	High	Very High	Poor-Good	40	5	27%	75%		4%

ABBREVIATIONS

NA = Not Available

MP = Microplankton

SP = Spore-Pollen

NED = Neves Effect based on *Dilwynites/Araucariacites* Pollen Percentage

Noth% = Percentage of *Nothofagidites* pollen in SP count.

Cup% = Percentage of *Cupressacites* pollen in SP count.

Table 3. Durroon-1 samples - abundances of major palynomorph groups.

No.	Depth Metres	Depth Feet	Sample Type	Gleicheniidites & Clavifera spores	ALL OTHER Spores	Dilwynites & Araucariacites pollen	ALL OTHER Gymnosperms	Nothofagidites species	ALL OTHER Angiosperms	FUNGAL microfossils	Reworked Spore-Pollen	**Total Terrestrial SUM**		SPORE-POLLEN TOTAL	MICROPLANKTON Fresh & Brackish	**SP + MP SUM**
1	925.1	3035	SWC 1/1	1.5%	10%	0.4%	74%	3%	11%			259		100%		259
2	963-72	3160-90	Cuttings		38%	3%	33%	7%	19%			58		100%		58
3	977.2	3206	SWC 30/2													
4	1000-08	3280-310	Cuttings													
5	1040.9	3415	SWC 28		16%	11%	36%	6%	30%	0.4%	0.7%	270		100%		267
6	1055-64	3460-90	Cuttings													
7	1095.5	3594	SWC 26	0.4%	17%	1.6%	25%	19%	36%		0.8%	256		100%	0.4%	255
8	1132.3	3715	SWC 25		26%	16%	23%	9%	24%	2.1%	0.4%	233		90%	10%	252
9	1171.7	3844	SWC 24	0.8%	27%	0.8%	27%	23%	20%	1.2%	1.2%	251		100%	0.4%	246
10	1219.2	4000	SWC 23													
11A	1238-87	4060-90	Cuttings		38%	3%	17%	21%	20%		1.1%	95		85%	15%	110
11B	1238-87	4060-90	Cuttings	0.4%	24%	11%	29%	22%	12%	0.4%	1.2%	259		95%	5%	268
12	1249.7	4100	SWC 22													
13	1287.2	4223	SWC 30/3		28%	1%	28%	29%	15%		0.4%	240		100%		239
14	1302-11	4270-300	Cuttings	0.4%	21%	4%	28%	30%	17%	0.4%		252		96%	4%	261
15	1310.6	4300	SWC 20		27%	8%	38%	5%	11%		11%	37		100%		33
16A	1323-29	4340-60	Cuttings		17%	4%	30%	31%	18%			122		100%		122
16B	1323-29	4340-60	Cuttings		45%	10%	41%	1.0%	4%			105		94%	6%	112
17	1341.1	4400	SWC 19													
18	1359.4	4460	SWC 18		23%	6%	21%	23%	24%		3.4%	119		100%		115
19	1366-75	4480-510	Cuttings		19%	23%	25%	18%	12%	2.2%	0.6%	180		83%	17%	212
20	1374.6	4510	SWC 17	0.5%	9%	23%	57%		10%			192		58%	42%	329
21	1375-84	4510-40	Cuttings		19%	6%	23%	33%	18%			219		95%	5%	231
22	1386.8	4550	SWC 16	0.4%	4%	21%	67%		7%			232		69%	31%	334
23	1402-11	4600-30	Cuttings	0.7%	4%	38%	52%	1.4%	2.9%	0.7%		140		53%	47%	264
24A	1411-20	4630-60	Cuttings		9%	40%	47%	0.9%	1.9%	0.9%		108		57%	43%	187
24B	1411-20	4630-60	Cuttings	1.9%	7%	43%	48%					54		34%	66%	161
25	1432.6	4700	SWC 14	0.6%	8%	58%	33%		0.6%			166		96%	4%	173
26	1463.0	4800	SWC 13	0.4%	13%	30%	55%		1.7%			236		93%	7%	253
27	1493.5	4900	SWC 12	0.5%	10%	50%	40%					199		82%	18%	244
28	1510.3	4955	SWC 11	0.4%	38%	16%	45%		0.4%			225		93%	7%	242
29	1533.1	5030	SWC 10	0.5%	1%	75%	23%		0.5%			183		73%	27%	249

SAMPLES WITH COUNTS ON DIFFERENT RESIDUE SIZE FRACTIONS

11A = Counts of slide with coarse fraction.
11B = Counts of slide with fine fraction.
16A = Counts of slide with fine fraction.
16B = Counts of slide with coarse fraction.
24A = Counts of slide with coarse fraction.
24B = Counts of slide with fine fraction.

Table 4. Durroon-1 - spore-pollen distribution.

No.	Depth Metres	Depth Feet	Sample Type	SPORE SPECIES	Aequitriradites spp.	Appendicisporites distocarinatus	Arcellites disciformis	Baculatisporites & Osmundacidites spp.	Balmeisporites glenelgensis	Balmeisporites holodictyus	Camarozonosporites bullatus	Camarozonosporites heskermensis	Camarozonosporites horrendus ms	Ceratosporites equalis	Cicatricosisporites/Ruffordiaspora spp.	Coptospora plieolus ms	Crybelosporites brenneriі	Crybelosporites striatus	Cyathidites splendens	Cyathidites spp. large >40µm	Cyathidites spp. small <40µm	Dictyophyllidites spp.	Foraminisporis asymmetricus	Foraminisporis dailyi	Foraminisporis wonthaggiensis	Gleicheniidites circinidites	Herkosporites elliottii	Laevigatosporites spp.	Latrobosporites amplus	Marattisporites scabratus	Monolete spores undiff.	Neoraistrickia truncata	Osmundacidites wellmanii	Peromonolites densus	Perotrilltes spp.	Retitrilletes spp.	Rugulatisporites mallatus
1	925.1	3035	SWC 1/1					1.2%			X										0.8%	1.2%				1.5%	1.2%	4.2%	X		0.4%		X	0.4%		0.4%	X
2	963-72	3160-90	Cuttings					1.7%													6.9%							26%			1.7%		X				
3	977.2	3206	SWC 30/2																																	
4	1000-08	3280-310	Cuttings																								X									
5	1040.9	3415	SWC 28					1.5%											X		3.4%	0.7%					1.9%	5.6%	X				X	X			
6	1055-64	3460-90	Cuttings																		X							X									
7	1095.5	3594	SWC 26					1.2%				X	X						X		1.2%				X	0.4%	0.8%	3.1%	X				X	X	0.8%	3.1%	
8	1132.3	3715	SWC 25					0.4%				X	X						X		2.2%	0.4%					3.1%	4.0%	0.9%				X	0.4%	4.0%	4.8%	
9	1171.7	3844	SWC 24					2.9%							0.8%				X	0.4%	4.1%					0.8%	1.2%	6.9%		1.2%						3.3%	
10	1219.2	4000	SWC 23																								X		X					X		
11A	1238-87	4060-90	Cuttings					1.1%												2.1%	18%							3.2%					X			6.4%	
11B	1238-87	4060-90	Cuttings		X			1.2%				X			1.2%					1.2%	12%					0.4%	0.4%	3.5%	0.4%					0.4%		1.2%	
12	1249.7	4100	SWC 22																								X							X	X	
13	1287.2	4223	SWC 30/3		X			2.1%					X		0.4%					1.3%	4.2%		0.4%				3.8%	6.7%					X		2.1%	4.6%	
14	1302-11	4270-300	Cuttings		0.4%		X			X					0.8%		X			0.4%	10%	0.4%	X			0.4%	0.4%	2.4%	X				X		X	2.4%	
15	1310.6	4300	SWC 20																	X	21%	3.0%						3.0%									
16A	1323-29	4340-60	Cuttings																		7.4%							5.7%			0.8%					0.8%	
16B	1323-29	4340-60	Cuttings					4.8%		X		X			3.8%	X			X	1.9%	16%		X			1.0%	1.9%		X			X		X	7.6%	
17	1341.1	4400	SWC 19		X			X						X	X	X					X				X	X	X	X		X				X	X	
18	1359.4	4460	SWC 18												X					1.7%	11%							8.7%								0.9%	
19	1366-75	4480-510	Cuttings					1.1%							0.6%					0.6%	8.6%						2.3%	2.9%							1.1%	0.6%	
20	1374.6	4510	SWC 17		X			0.5%				X		X	X	X				0.5%	3.1%	0.5%		X		0.5%	X	2.1%		0.5%					X	0.5%	
21	1375-84	4510-40	Cuttings					0.9%							X	X				1.4%	9.6%	0.9%	X					2.7%					X		X	1.4%	
22	1386.8	4550	SWC 16					0.4%						X	X	X				X	1.7%					0.4%	X	0.4%		0.9%		X			X	X	
23	1402-11	4600-30	Cuttings												X					0.7%	X	X				0.7%	0.7%	1.4%	X						X	1.4%	
24A	1411-20	4630-60	Cuttings																		6.5%						0.9%	1.9%								
24B	1411-20	4630-60	Cuttings					3.7%													1.9%	X				1.9%	X	X	X				X		X	1.9%	
25	1432.6	4700	SWC 14		X	X		1.8%				X		X	X			X		0.6%	2.4%		X			0.6%	X	0.6%					X		X	0.6%	
26	1463.0	4800	SWC 13					2.5%	X			X			0.8%	X		X		0.8%	1.7%		X		X	0.4%		2.5%		X		X	X		X	0.8%	
27	1493.5	4900	SWC 12					1.5%						X	X	X		X		1.5%	2.0%		X	X	X	0.5%	X	1.5%					X		X	1.0%	
28	1510.3	4955	SWC 11					7.1%						X	X					9.8%	4.4%	0.4%	X	X	X	0.4%		3.1%				X			X	2.2%	
29	1533.1	5030	SWC 10					0.5%						X	X	X		X		X	X		X		X	0.5%		X				X	X	X	X	

ABBREVIATIONS: X = Present % = Percentage cf. = Compare with

Table 4. Durroon-1 - spore-pollen distribution.

No.	Depth Metres	Depth Feet	Sample Type	Stereisporites antiquisporites	Stereisporites regium	Trilete spores undiff.	Triporoletes reticulatus	Tripunctisporis maastrichtiensis	Tuberculatosporites sp. A	Verrucosisporties admirabilis ms	**TOTAL Spores**	**GYMNOSPERM SPECIES**	Araucariacites australis	Corollina spp.	Cupressacites sp.	Dacrycarpites australiensis	Dilwynites spp.	Dilwynites tuberculatus	Lygistepollenites balmei	Lygistepollenites florinii	Microalatidites paleogenicus	Microcachryidites antarcticus	Phyllocladidites eunuchus ms	Phyllocladidites mawsonii	Phyllocalditides reticulosaccatus	Phyllocalditides verrucosus	Podocarpidites spp.	Trichotomosulcites subgranulatus	**TOTAL Gymnosperms**	**ANGIOSPERM SPECIES**	Angiosperm pollen undiff.	Aglaoreidia sp.	Australopollis obscurus	Battenipollis sectilis
1	925.1	3035	SWC 1/1	0.8%	X			X			12%					X	0.4%			1.5%	2.3%		1.9%	34%	0.4%	1.2%	31%	1.9%	74%		1.2%			
2	963-72	3160-90	Cuttings			1.7%					38%						3.4%			8.6%		1.7%		6.9%			16%		36%					
3	977.2	3206	SWC 30/2																															
4	1000-08	3280-310	Cuttings					X					X														X							
5	1040.9	3415	SWC 28	1.1%	0.7%	0.7%	0.4%	X			16%		9.4%		0.4%	0.4%	1.5%			1.9%		8.2%		4.9%	X		19%	2.2%	48%		0.4%			X
6	1055-64	3460-90	Cuttings																								X							
7	1095.5	3594	SWC 26	2.4%	2.8%	2.0%	X				18%		1.6%	0.4%	0.8%					0.4%		0.8%		9.4%	X	0.4%	11%	2.8%	27%		1.6%			4.3%
8	1132.3	3715	SWC 25	4.4%	X	1.3%	0.4%				26%		4.0%		1.3%	0.4%	13%					1.8%		8.4%		0.4%	11%	0.4%	41%		0.9%			1.3%
9	1171.7	3844	SWC 24	2.0%	1.6%	2.9%					28%						0.4%	0.4%				2.0%		11%		1.6%	11%	2.4%	29%		1.2%			X
10	1219.2	4000	SWC 23			X	X																	X									X
11A	1238-87	4060-90	Cuttings			4.3%	2.1%	1.1%			38%		1.1%				2.1%					1.1%		2.1%			8.5%	5.3%	20%		4.3%			
11B	1238-87	4060-90	Cuttings			2.4%	0.8%				25%		3.1%	X		0.8%	8.2%					1.2%		8.6%			7.1%	12%	41%		0.4%	0.4%		
12	1249.7	4100	SWC 22			X																		X	X		X						X
13	1287.2	4223	SWC 30/3		X	1.3%	0.8%				28%		0.8%		0.4%		0.4%					2.5%	X	5.4%			16%	3.3%	29%		0.8%		X	0.8%
14	1302-11	4270-300	Cuttings	X		1.6%	1.6%	0.4%			21%		1.6%	0.8%		0.4%	2.0%		X	0.4%		1.6%		5.6%			8.8%	11%	32%		2.4%			X
15	1310.6	4300	SWC 20		X	3.0%					30%						9.1%			3.0%		X		3.0%			36%		52%					
16A	1323-29	4340-60	Cuttings					2.5%			17%				0.8%		4.1%					2.5%		7.4%			8.2%	11%	34%		2.5%			
16B	1323-29	4340-60	Cuttings			1.9%	4.8%	1.0%			45%		4.8%			X	4.8%					1.0%	1.0%	6.7%			30%	1.9%	50%					
17	1341.1	4400	SWC 19	X			X						X			X						X		X		X	X	X					
18	1359.4	4460	SWC 18	0.9%							23%		1.7%				4.3%							13%			7.8%	0.9%	28%		0.9%			
19	1366-75	4480-510	Cuttings			0.6%	1.7%				20%		13%	0.6%	0.6%	X	11%					1.7%		10%		X	9.7%	2.9%	50%		0.6%			
20	1374.6	4510	SWC 17	X		1.6%	X		X		10%		3.6%	1.6%	27%	X	19%	0.5%				3.6%		1.0%		X	22%	1.6%	80%				X	
21	1375-84	4510-40	Cuttings			1.8%	0.5%				19%		2.7%				3.7%					2.7%		3.7%		X	13%	3.7%	30%		0.5%			
22	1386.8	4550	SWC 16	X	cf.	0.9%	X		X		5%		1.3%	X	56%	X	19%					3.0%		X		X	7.8%	X	88%				X	
23	1402-11	4600-30	Cuttings								5%		4.3%		14%		34%					12%					24%	2.9%	91%		0.7%		X	
24A	1411-20	4630-60	Cuttings								9%		0.9%		20%		39%					1.9%					24%	1.9%	88%					
24B	1411-20	4630-60	Cuttings							X	9%		11%		X		31%					7.4%					37%	3.7%	91%					
25	1432.6	4700	SWC 14	0.6%		1.2%	X		X		8%		13%	X	19%		46%					2.4%		X			10%	1.2%	91%				X	
26	1463.0	4800	SWC 13	2.5%		1.3%	X		X	X	14%		11%	2.5%	17%	X	19%					8.5%	X	0.4%			26%	X	85%				X	
27	1493.5	4900	SWC 12	1.0%		1.0%	X		X	X	10%		15%	2.0%	24%		36%					3.5%	X				9.5%	0.5%	90%					
28	1510.3	4955	SWC 11	4.9%		11	0.9%				38%		8.4%	3.1%	20%	X	7.6%					1.3%	X	X			20%	1.8%	61%					
29	1533.1	5030	SWC 10	X		X	X				1.1%		20%	X	4.4%		55%					2.7%	X	X		X	16%	X	98%					

ABBREVIATIONS: X = Present % = Percentage cf. = Compare with

Table 4. Durroon-1 - spore-pollen distribution.

No.	Depth Metres	Depth Feet	Sample Type	Concolpites leptos	Dicotetradites clavatus	Forcipites longus	Forcipites renmarkensis ms	Forcipites sabulosus	Forcipites sp.	Gambierina edwardsii	Gambierina rudata	Myrtaceidites parvus/mesonesus	Nothofagidites spp.	Nothofagidites brachyspinulosus	Nothofagidites endurus	Nothofagidites senectus	Peninsulapollis askiniae	Peninsulapollis gillii	Periporopollenites polyoratus	Proteacidites spp.	Proteacidites clinei ms	Proteacidites otwayensis ms	Proteacidites pallisadus	Proteacidites reticuloconcavus ms	Pseudowinterapollis wahooensis	Retimonocolpites peroreticulatus	Tetracolporites verrucosus	Tetradopollis securus ms	Tricolp(or)ates spp.	Tricolpites confessus	Tricolpites waiparaensis	Tricolporites lilliei	Triporopollenites spp.	**TOTAL Angiosperms**	**TOTAL SPORE-POLLEN COUNT**
1	925.1	3035	SWC 1/1								0.4%		2.3%		0.4%			1.5%	4.2%	1.9%	X						1.2%		0.8%					14%	259
2	963-72	3160-90	Cuttings								6.9%			1.7%	5.2%			1.7%	1.7%	5.2%									3.4%					26%	58
3	977.2	3206	SWC 30/2																																
4	1000-08	3280-310	Cuttings										X							X															
5	1040.9	3415	SWC 28	X	0.7%						2.2%	X		0.7%	5.2%			4.9%	1.5%	9.0%	0.4%				X		4.9%		6.0%	0.4%	X			36%	267
6	1055-64	3460-90	Cuttings																																
7	1095.5	3594	SWC 26		0.4%		X			X	16%				11%	7.9%		2.4%	0.4%	9.4%			X		X			X	1.2%	0.4%	X	X	0.4%	55%	254
8	1132.3	3715	SWC 25			X	X			X	2.2%				3.5%	5.3%		3.5%		11%		X	X	1.3%	X		X		2.6%	0.4%	0.9%	0.4%		33%	227
9	1171.7	3844	SWC 24			0.4%		0.4%			1.6%			X	8.6%	15%		4.5%		7.8%					0.4%				3.3%	X	0.4%			43%	245
10	1219.2	4000	SWC 23			X								X				X		X					X				X	X		X			
11A	1238-87	4060-90	Cuttings								1.1%				5.3%	16%		4.3%		5.3%									1.1%	2.1%		2.1%		41%	94
11B	1238-87	4060-90	Cuttings		0.4%						1.6%				2.0%	20%		1.2%	0.4%	5.1%									2.7%			X		35%	
12	1249.7	4100	SWC 22		X		X	X			X					X		X		X									X	X		X			
13	1287.2	4223	SWC 30/3				X	X		X	6.7%				4.2%	25%		0.8%		2.5%								0.4%	2.5%	X				44%	239
14	1302-11	4270-300	Cuttings					0.4%			5.6%		0.4%		X	29%		2.4%		4.0%						X			1.6%	X		0.8%		47%	251
15	1310.6	4300	SWC 20										6.1%		X	X		X		6.1%									6.1%					18%	33
16A	1323-29	4340-60	Cuttings					0.8%			1.6%		31%					4.9%		6.6%										1.6%				49%	122
16B	1323-29	4340-60	Cuttings					X			X		1.0%		X			1.0%		2.9%									X	X				5%	
17	1341.1	4400	SWC 19				X	X					X	X	X	X	X	X		X									X	X	X				
18	1359.4	4460	SWC 18					7.0%					22%		1.7%			8.7%		6.1%									2.6%					49%	115
19	1366-75	4480-510	Cuttings					1.1%					18%			X		4.6%		4.0%									1.1%	0.6%				30%	175
20	1374.6	4510	SWC 17						X								X	X		1.6%			cf.						8.3%				X	10%	192
21	1375-84	4510-40	Cuttings					0.5%			1.4%		33%			X		5.5%		2.7%									6.4%	0.9%				51%	219
22	1386.8	4550	SWC 16						X								X	X		X			cf.						7.3%	X				7.3%	232
23	1402-11	4600-30	Cuttings					X					1.4%			X		0.7%		0.7%									0.7%					4.3%	139
24A	1411-20	4630-60	Cuttings										0.9%																			1.9%		2.8%	107
24B	1411-20	4630-60	Cuttings													X		X		X									X						54
25	1432.6	4700	SWC 14						X											X			cf.						0.6%					0.6%	166
26	1463.0	4800	SWC 13															cf.		0.4%									1.3%				X	1.7%	236
27	1493.5	4900	SWC 12															cf.		X									X						199
28	1510.3	4955	SWC 11																										0.4%					0.4%	225
29	1533.1	5030	SWC 10																	X						X			0.5%					0.5%	183

ABBREVIATIONS: X = Present % = Percentage cf. = Compare with

Table 5. Durroon-1 - microplankton distribution.

No.	Depth Metres	Depth Feet	Sample Type	ACRITARCHS & ALGAE	Cymatisphaera spp.	Micrhystridium spp.	Amosopollis cruciformis	Botryococcus braunii	Circulisporites parvus	Rimosicysta spp.	Schizosporis spp.	Sigmopollis carbonis	Sigmopollis hispidis	Tetraporina sp.	Wuroia spp.	NON-MARINE DINOCYSTS	Cobricosphaeridium spp.	Morkallacysta spp.	Tetrachacysta sp.	Microplankton undiff.	TOTAL MP COUNT
1	925.1	3035	SWC 1/1																		
2	963-72	3160-90	Cuttings																		
3	977.2	3206	SWC 30/2																		
4	1000-08	3280-310	Cuttings																		
5	1040.9	3415	SWC 28																		
6	1055-64	3460-90	Cuttings																		
7	1095.5	3594	SWC 26			100%															1
8	1132.3	3715	SWC 25														12%			88%	25
9	1171.7	3844	SWC 24															100%			1
10	1219.2	4000	SWC 23																		
11A	1238-87	4060-90	Cuttings															19%		81%	16
11B	1238-87	4060-90	Cuttings							X	8%							8%		85%	13
12	1249.7	4100	SWC 22																		
13	1287.2	4223	SWC 30/3																		
14	1302-11	4270-300	Cuttings			10%				40%								20%		30%	10
15	1310.6	4300	SWC 20																		
16A	1323-29	4340-60	Cuttings																		
16B	1323-29	4340-60	Cuttings					29%		X	14%							X		57%	7
17	1341.1	4400	SWC 19																		
18	1359.4	4460	SWC 18																		
19	1366-75	4480-510	Cuttings					3%		3%								35%		59%	37
20	1374.6	4510	SWC 17			X	X	0.7%				1.5%	0.7%		X		X	97%	X		137
21	1375-84	4510-40	Cuttings															8%		92%	12
22	1386.8	4550	SWC 16				X		X	X		X					X	100%	X	X	102
23	1402-11	4600-30	Cuttings					X		1%								99%			125
24A	1411-20	4630-60	Cuttings													8%		91%		1%	80
24B	1411-20	4630-60	Cuttings					X		3%				X		4%	X	93%			107
25	1432.6	4700	SWC 14			X	X	43%		14%		43%			X				X	X	7
26	1463.0	4800	SWC 13			X	X	6%		65%	X	24%	X					X	X	6%	17
27	1493.5	4900	SWC 12		X	2%				73%		24%			X		X		X		45
28	1510.3	4955	SWC 11			24%				X		53%								24%	17
29	1533.1	5030	SWC 10			2%						95%								3%	66

ABBREVIATIONS: X = Present % = Percentage

APPENDIX C3.

Palynological analysis of Eocene interval 1380 to 2036m in King-1, Bass Basin.

by

Alan D. Partridge

Biostrata Pty Ltd

A.B.N. 39 053 800 945

Biostrata Report 2002/08

20th June 2002

Palynological analysis of Eocene interval 1380 to 2036m in King-1, Bass Basin

by Alan D. Partridge

Introduction

This palynological study of the Eastern View Group penetrated in King-1 is a component of the Bass Basin Palynological Project coordinated by Geoscience Australia as part of the Western Tasmania Regional Minerals Program Offshore Collaborative Project, between Mineral Resources Tasmania, Geoscience Australia and the National Centre for Petroleum Geology and Geophysics to investigate aspects of the hydrocarbon prospectivity of the Bass and Sorell Basins.

As no previous palynological work has been undertaken on King-1 this study has the dual objectives of providing initial age dating of the Eastern View Group, and investigating the abundance and diversity of marine dinocysts in the palynological assemblages from the latest Early Eocene and Middle Eocene (Upper *M. diversus* to Lower *N. asperus* Zones). The study is also intended to compliment a new palynological study of the equivalent interval in the adjacent Cormorant-1 well (Partridge, 2002a). Most of the samples analysed in King-1 are from conventional cores 1 to 4 cut between 1397 and 1440m, from the base of a distinctive shale interval between 1315 and 1455m informally named the Toolka unit (Partridge, 2002b). This latter unit lacks both conventional and sidewall cores in the adjacent Cormorant-1 well.

Materials and Methods

Twelve samples comprising 8 conventional core and 4 cuttings samples were analysed. Laboratory processing of the samples was performed by Geoscience Australia. However, due to an unfortunate misunderstanding or miscommunication the samples were given an initial coarse filtration, which had the effect of separating a significant proportion of the organic-walled microplankton (mostly dinocysts) from the finer fraction of the residue containing the majority of angiosperm pollen. This rendered unreliable the counted ratio of dinocysts to the spore-pollen in the assemblages. Separate counts of the two different residue size fractions gave a range of microplankton abundances of 1% to 21% (of combined MP + SP count) in the coarse fractions and zero to 4% in the finer fractions. These results are interpreted to indicate that the unbiased microplankton abundance would be in the range of <1% and <10%. As these values were considered unlikely to significantly increase with reprocessing, the author decided to completed the study on the available slides. Determination of the established zones, which are based on species ranges is not significantly affected by the skewed assemblages.

The palynological zones assigned to the samples, zone Confidence Ratings, key defining species and interpreted palaeoenvironments are provided in Table 1. Basic palynological data on organic residue yields, palynomorph concentrations in the residues, palynomorph preservation and species diversity in the samples is provided in Table 2. Species abundance and range data are provided in Tables 3 to 5. Author citation for

spore-pollen species can be principally sourced for published species from Stover & Partridge (1973), and for manuscript species from Partridge (1973). Author citation for dinocysts can be sourced from Williams *et al.* (1998), and for acritarchs, algal cysts and other microplankton from Fensome *et al.* (1990).

Geological Discussion

Notwithstanding the skewing of the assemblages by the initial coarse filtration, exacerbated by low concentration of palynomorphs on the slides, sparse microplankton assemblages were recorded from the majority of samples. The eight samples from the four cores over the narrow interval from 1398 to 1439m gave assemblages dominated in the finer fraction by *Nothofagidites* pollen (>30%) confirming assignment to Lower *N. asperus* Zone. The absence of the species *Nothofagidites falcatus* in the core assemblages suggests a position very low in the zone. The coarser fractions of the residues contained most of the microplankton, and these assemblages were dominated by the marine to brackish-water species *Paralecaniella indentata* or other undescribed species interpreted as non-marine dinocysts. The latter are assigned to the non-marine genera *Cubiculosphaera* and *Saeptodinium* described by Harris (1974) and the informal genus *Ceratertius.* The interval is interpreted to be predominantly a shallow lacustrine environment into which there were occasional marine incursions.

Three of the four deeper cuttings sample are assigned to the *P. asperopolus* Zone, while the deepest sample is assigned to the older Upper *M. diversus* Zone. Dinocysts in these samples are generally rarer but are overall of higher diversity and mostly represented by cosmopolitan marine species. The assemblages are therefore interpreted to represent a restricted marine environment typical of a large lagoon or lake. The thinly bedded aspect of the interval 1525 to 1980m is interpreted to reflect rapid changes of environment, suggesting the water depth in the lagoon was generally shallow. Falls in the lake water level thus frequently resulted in the deposition of widespread thin coals and thin fluvial/deltaic sands. The thicker 60 metre shale between 1980 and 2040m in King-1, which is sampled by the deepest cuttings is in contrast interpreted to represent a deeper lagoon. This bed is correlated with the interval 2012 to 2042m in Cormorant-1 as both shales contain the distinctive dinocyst *Homotryblium tasmaniense*.

Biostratigraphy

Upper *Malvacipollis diversus* spore-pollen Zone

Sample at: 2013-2017 metres

Age: Early Eocene.

The deepest cuttings analysed is assigned to the this zone on the presence of *Myrtaceidites tenuis* and absence of younger index species of the overlying *P. asperopolus* Zone. Secondary species recorded that are consistent with this zone assignment include *Intratriporopollenites notabilis*, *Proteacidites ornatus* and common *P. grandis*. The associated microplankton are diagnostic of the *Homotryblium tasmaniense* Zone, which was originally defined by Harris (1985), and has subsequently been modified by Partridge (1999).

***Proteacidites asperopolus* spore-pollen Zone**

Interval: 1614 to 1860 metres.

Age: Early-Middle Eocene.

The zone identified by the First Appearance Datum (FAD) of *Conbaculatisporites apiculatus* ms at 1857-60m and the Last Appearance Datums (LAD) of *Intratriporopollenites notabilis* at 1614-17m. Other key index species were not recorded. The associated marine dinocysts in the samples are broadly consistent with a late Early Eocene age but are not zone diagnostic.

Lower *Nothofagidites asperus* spore-pollen Zone

Interval: 1398 to 1439 metres.

Age: Middle Eocene.

The assemblages from the four conventional cores are all referred to the Lower *N. asperus* Zone based on the increase in abundance of *Nothofagidites* pollen (typically to >30% of SP count), and the rare presence of index species, including *Tricolporites leuros* at 1439m and *Anisotricolporites triplaxis* at 1407m. The prominence of *Proteacidites leightonii* and absence of *Nothofagidites falcatus* in these core may represent a hitherto undocumented transitional zone interval between the *P. asperopolus* and *N. asperus* Zone that warrants further investigation.

The associated microplankton comprise long ranging cosmopolitan marine dinocysts and undescribed possibly endemic non-marine dinocysts neither of which are currently age or zone diagnostic. Full description and illustration of the non-marine dinocysts is needed and recommended. The frequent occurrence of the marine to possibly brackish-water dinocyst *Paralecaniella indentata* in two of the core samples is referred to as the *Paralecaniella* facies.

References

FENSOME, R.A., WILLIAMS, G.L., BARSS, M.S., FREEMAN, J.M. & HILL, J.M., 1990. Acritarchs and fossil Prasinophytes: An index to genera, species and infraspecific taxa. *AASP Contribution Series No. 25,* p.1-771.

HARRIS, W.K., 1974 [imprint 1973]. Tertiary non-marine dinoflagellate cyst assemblages from Australia. **In** *Mesozoic and Cainozoic palynology: essays in honour of Isabel Cookson*, J.E. Glover & G. Playford, editors, *Geological Society of Australia Special Publication 4*, p.159-166.

HARRIS, W.K., 1985. Middle to late Eocene depositional cycles and dinoflagellate zones in southern Australia. **In** *Stratigraphy, Palaeontology, Malacology: Papers in Honour of Dr Nell Ludbrook*, J.M. Lindsay, editor, *Department of Mines and Energy South Australia Special Publication 5*, p.133-144.

PARTRIDGE, A.D., 1973. Revision of the Spore-Pollen Zonation in the Bass Basin. *Esso Australia Ltd Palaeontological Report 1973/4*, 22p. 6pls (2 May).

PARTRIDGE, A.D., 1999. Late Cretaceous to Tertiary geological evolution of the Gippsland Basin, Victoria.

PhD thesis, La Trobe University, Bundoora, Victoria, p.i-xxix, p.1-439, 165 figs, 9 pls (unpubl.).

PARTRIDGE, A.D., 2002a. Palynological analysis of Eocene interval 1380 to 2036m in Cormorant-1, Bass Basin. *Biostrata Report 2002/06*, p.1-16.

PARTRIDGE, A.D., 2002b. Bass Basin Palynological Project: Unravelling a Late Cretaceous to Eocene geological history of large palaeolakes, coastal lagoons and marine bays. *Biostrata Report 2002/13*, p.1-36.

STOVER, L.E. & PARTRIDGE, A.D., 1973. Tertiary and late Cretaceous spores and pollen from the Gippsland Basin, southeastern Australia. *Proceedings Royal Society of Victoria, vol.85,* pt.2, p.237-286.

WILLIAMS, G.L., LENTIN, J.K. & FENSOME, R.A., 1998. The Lentin and Williams index of fossil dinoflagellates 1998 edition. *American Association of Stratigraphic Palynologists, Contributions Series, no. 34*, p.1-817.

Table 1. Interpretative Palynological Data from King-1

No.	Sample Type	Depth Metres	Sample Origin	Spore-Pollen Zone	CR*	Microplankton Zone	CR*	Key Index Species	Palaeoenvironment
1	Core-1	1398	GA-1	Lower *N. asperus*	D2	*Paralecaniella* Facies		LAD of *Proteacidites asperopolus*	Lagoonal - brackish
2	Core-1	1400.31	GA-1	Lower *N. asperus*	D2				Lagoonal - fresh
3	Core-2	1404	GA-1	Lower *N. asperus*	D2				Lagoonal - fresh
4	Core-2	1407	GA-1	Lower *N. asperus*	D2				Lagoonal - fresh
5	Core-3	1425.38	GA-1	Lower *N. asperus*	D2				Lagoonal - fresh
6	Core-3	1430	GA-1	Lower *N. asperus*	D2				Lagoonal - brackish
7	Core-4	1435	GA-1	Lower *N. asperus*	D2	*Paralecaniella* Facies			Lagoonal - brackish
8	Core-4	1439	GA-1	Lower *N. asperus*	D2			FAD of *Tricolporites leuros*	Non-marine
9	Cuttings	1614-17	GA-1	*P. asperopolus*	D2	*H. tasmaniense*	D5	LAD of *Intratriporopollenites notabilis*	Lagoonal - restricted marine
10	Cuttings	1794-97	GA-1	*P. asperopolus*	D5				Lagoonal - restricted marine
11	Cuttings	1857-60	GA-1	*P. asperopolus*	D2			FAD of *Conbaculatisporites apiculatus* ms	Lagoonal - restricted marine
12	Cuttings	2013-17	GA-1	Upper *M. diversus*	D2	*H. tasmaniense*	D3	FAD of *Myrtaceidites tenuis*	Lagoonal - restricted marine

ABBREVIATIONS

*CR = Confidence Ratings

LAD = Last Appearance Datum

FAD = First Appearance Datum

GA-1 = Samples collected Stage-1 Work program

***CONFIDENCE RATINGS**

Alpha Code Linked to Sample

A = Core

B = Sidewall core

C = Coal cuttings

D = Ditch cuttings

J = Junk basket

Numeric Code Linked to Palynomorph Assemblage

1 = Excellent confidence: High diversity assemblage **plus** key zone species.

2 = Good confidence: Moderately diverse assemblage **plus** key zone species.

3 = Fair confidence: Low diversity assemblage **plus** key zone species.

4 = Poor confidence: Moderate to high diversity **minus** key zone species.

5 = Very low confidence: Low diversity assemblage **minus** key zone species.

Table 2. Basic Palynological Data from King-1

No.	PalLab Spl.No.	Sample Type	Core No.	Top Metres	Base Metres	Visual Yield	Palynomorph Concentration	Palynomorph Preservation	No. SP Species	No. MP Species	Marine MP%	Other MP%	NED	Noth%
1	6405883	Core	1		1398	Moderate	Low	Poor- good	38	5				
2	6405884	Core	1		1400.31	High	Moderate	Poor- good	46	4	<2%	<10%	<20%	>30%
3	6405885	Core	2		1404	High	Moderate	Fair-good	35	3				
4	6405886	Core	2	1407	1407.02	Moderate	Low	Fair-good	44	1		<1%	<20%	>30%
5	6405887	Core	3		1425.38	Moderate	Moderate	Fair-good	39	1		<1%	<10%	>40%
6	6405888	Core	3		1430	Moderate	Moderate	Fair-good	36	4	<1%	<10%	<10%	>40%
7	6405889	Core	4		1435	Moderate	Moderate	Fair-good	36	2	<1%	<1%	<5%	>30%
8	6405890	Core	4		1439	Moderate	Low	Good	23					
9	6405891	Cuttings		1614	1617	Moderate	Moderate	Fair-good	51	2	<1%		<15%	>30%
10	6405892	Cuttings		1794	1797	Moderate	Low	Poor- good	19	2	<1%			
11	6405893	Cuttings		1857	1860	Moderate	Moderate	Poor- good	33	6			<15%	<20%
12	6405894	Cuttings		2013	2017	Moderate	Moderate	Poor- good	31	4				

ABBREVIATIONS

MP = Microplankton

SP = Spore-Pollen

NED = Neves Effect based on *Dilwynites/Araucariacites* Percentage

Noth% = Percentage of *Nothofagidites* in SP count.

Other MP = Brackish and fresh-water species

Table 3. Abundance of major palynomorph groups from King-1.

No.	Top Metres	Base Metres	Sample Type	Residue Filter	Gleicheniidites spp. spores	ALL OTHER spores	Dilwynites and Araucariacites pollen	ALL OTHER gymnosperm pollen	Nothofagidites species	ALL OTHER angiosperm pollen	FUNGAL microfossils	Reworked Spore-Pollen	**Total Terrestrial SUM**		SPORE-POLLEN TOTAL	MICROPLANKTON fresh to brackish	MICROPLANKTON marine	**SP + MP SUM**
1		1398	Core															
2A		1400.31	Core	Fine		8%	1%	8%	31%	44%	9%		131		100%			119
2B		1400.31	Core	Coarse	2%	33%	26%	19%	3%	15%	1%	2%	107		79%	19%	2%	131
3		1404	Core															
4A	1407	1407.02	Core	Fine		6%	3%	7%	32%	46%	5%		111		100%			105
4B	1407	1407.02	Core	Coarse		46%	19%	9%	3%	19%	1%	3%	114		99%		1%	111
5A		1425.38	Core	Fine		3%		11%	44%	33%	8%	1%	123		100%			112
5B		1425.38	Core	Coarse	1%	17%	13%	41%	4%	19%	4%		113		98%		2%	110
6A		1430	Core	Fine		14%	2%	10%	42%	28%	5%		125		99%		1%	120
6B		1430	Core	Coarse	1%	48%	14%	6%	5%	23%		4%	110		80%	7%	14%	133
7		1435	Core	Fine		9%	2%	10%	35%	37%	6%		129		99%	1%		122
8		1439	Core															
9A	1614	1617	Cuttings	Fine		8%	3%	11%	35%	39%	4%		112		100%			107
9B	1614	1617	Cuttings	Coarse		47%	16%	10%	1%	27%			124		98%		2%	126
10	1794	1797	Cuttings															
11A	1857	1860	Cuttings	Fine		8%	1%	6%	25%	53%	7%		113		96%		4%	109
11B	1857	1860	Cuttings	Coarse	1%	43%	17%	9%	1%	26%	1%	2%	135		90%	1%	9%	144
12	2013	2017	Cuttings															

Table 4. King-1 samples - spore-pollen distribution.

No.	Top Metres	Base Metres	Sample Type	Residue Filter	SPORE SPECIES	Baculatisporites spp.	Camarozonosporites heskermensis	Conbaculatisporites apiculatus ms	Cyathidites splendens	Cyathidites palaeospora	Foveotriletes balteus	Gleicheniidites circinidites	Ischyosporites spp.	Kuylisporites waterbolkii	Laevigatosporites major	Laevigatosporites ovatus	Latrobosporites marginatus	Matonisporites ornamentalis	Monolites alveolatus	Peromonolites spp.	Polypodiaceoisporites varus ms	Polypodiidites/Verrucatosporites spp.	Retitriletes spp.	Ricciaesporites boxatus ms	Rugulatisporites mallatus	Trilete spores undiff.	Verrucatosporites attinatus ms	Verrucosisporites kopukuensis	TOTAL SPORES
1		1398	Core			X			X	X	X	X	X	X	X	X												X	
2A		1400.31	Core	Fine						5.0%				X		3.4%			X										8.4%
2B		1400.31	Core	Coarse		4.8%	X		1.9%	9.6%	X	1.9%	X		X	3.8%	X					2.9%	1.9%			6.7%		1.9%	36%
3		1404	Core			X			X	X	X	X			X		X	X		X		X						X	
4A	1407	1407.02	Core	Fine						5.7%															X	1.0%			6.7%
4B	1407	1407.02	Core	Coarse		4.5%			15%	18%					X	3.6%				0.9%		0.9%	0.9%			0.9%		3.6%	48%
5A		1425.38	Core	Fine						0.9%						1.8%						X						0.9%	3.6
5B		1425.38	Core	Coarse		5.6%			4.6%			0.9%	0.9%		X	1.9%												4.6%	19%
6A		1430	Core	Fine		X			X	8.4%			X			4.2%				0.8%						0.8%			14%
6B		1430	Core	Coarse		4.7%			12%	8.5%		0.9%	3.8%		X	8.5%						2.8%						9.4%	51%
7		1435	Core	Fine		0.8%			X	5.8%						1.7%				0.8%		X				0.8%	X	X	9.9%
8		1439	Core													X												X	
9A	1614	1617	Cuttings	Fine				0.9%		5.6%						1.9%													8.4%
9B	1614	1617	Cuttings	Coarse		2.4%	X	0.8%	12%	12%	X		X		X	8.9%				1.6%		X		X	X	7.3%		1.6%	47%
1O	1794	1797	Cuttings			X			X	X			X			X													
11A	1857	1860	Cuttings	Fine				1.0%		3.8%						2.9%					X					1.0%			8.6%
11B	1857	1860	Cuttings	Coarse		0.8%			8.5%	15%	X	0.8%	X		X	14%										2.3%	X	3.8%	45%
12	2013	2017	Cuttings			X			X	X		X			X	X									X			X	

ABBREVIATIONS

X = Present

C = Common

% = Percentage

Table 4. King-1 samples - spore-pollen distribution.

No.	Top Metres	Base Metres	Sample Type	Residue Filter	GYMNOSPERM SPECIES	Araucariacites australis	Cupressacites sp.	Dacrycarpites australiensis	Dilwynites granulatus	Dilwynites tuberculatus	Lygistepollenites florinii	Microalatidites paleogenicus	Microcachryidites antarcticus	Phyllocladidites mawsonii	Podocarpidites spp.	Trichotomosulcites subgranulatus	TOTAL GYMNOSPERMS		ANGIOSPERM SPECIES	Angiosperm pollen undiff.	Anisotricolporites triplaxis	Banksieaeidites arcuatus	Beaupreaidites verrucosus	Bluffopollis scabratus	Cupanieidites orthoteichus	Dicotetradites clavatus	Ericipites crassiexinus/scabratus	Gothanipollis bassensis	Haloragacidites harrisii	Ilexpollenites spp.
1		1398	Core			X			X		X		X	X	X								X		X				X	
2A		1400.31	Core	Fine					0.8%					2.5%	4.2%	1.7%	9.2%					0.8%			0.8%	0.8%			20%	3.4%
2B		1400.31	Core	Coarse		7.7%		1.0%	17%	1.9%	6.7%			1.9%	9.6%		46%										X		1.0%	
3		1404	Core			X			X	X	X			X	X														X	
4A	1407	1407.02	Core	Fine					2.9%			1.0%		2.9	3.8%		10%			1.0%	X			1.0%	1.9%				22%	1.9%
4B	1407	1407.02	Core	Coarse		4.5%			13%	2.7%	1.8%			0.9%	6.4%		29%			0.9%			X			0.9%			3.6%	
5A		1425.38	Core	Fine									1.8%	8.0%	1.8%		12%			2.7%					0.9%			X	13%	0.9%
5B		1425.38	Core	Coarse		4.6%	0.9%		8.3%	0.9%	12%			17%	13%		56%			0.9%					0.9%	0.9%			7.4%	
6A		1430	Core	Fine			0.8%		2.5%					0.8%	8.4%		13%					0.8%				1.7%			9%	
6B		1430	Core	Coarse		6.6%			5.7%	1.9%	1.9%			0.9%	3.8%		21%													
7		1435	Core	Fine		0.8%	0.8%		0.8%	0.8%			0.8%	2.5%	5.8%	0.8%	13%					1.7%			0.8%				12%	X
8		1439	Core																					X	X				X	X
9A	1614	1617	Cuttings	Fine					2.8%		0.9%			4.7%	5.6%		14%									0.9%			19%	0.9%
9B	1614	1617	Cuttings	Coarse		5.6%			6.5%	4.0%	1.6%		0.8%	1.6%	4.8%	0.8%	26%					0.8%				0.8%			2.4%	
10	1794	1797	Cuttings						X	X	X			X	X														X	
11A	1857	1860	Cuttings	Fine					1.0%		1.0%			1.9%	3.8%		7.6%					1.9%				1.0%			28%	1.0%
11B	1857	1860	Cuttings	Coarse		2.3%			10%	5.4%	0.8%			1.5%	6.9%		27%									0.8%			9.2%	
12	2013	2017	Cuttings						X		X				X										X				X	

ABBREVIATIONS

X = Present

C = Common

% = Percentage

Table 4. King-1 samples - spore-pollen distribution.

No.	Top Metres	Base Metres	Sample Type	Residue Filter	Intratriporopollenites notabilis	Liliacidites spp.	Lymingtonia sp.	Malvacipollis robustus	Malvacipollis subtilis	Myrtaceidites spp.	Myrtaceidites tenuis	Nothofagidites asperus	Nothofagidites brachyspinulosus	Nothofagidites deminutus	Nothofagidites emarcidus/heterus	Nothofagidites flemingii	Nothofagidites goniatus	Nothofagidites vansteenisii	Periporopollenites spp.	Polycolporopollenites esobalteus	Proteacidites spp.	Proteacidites adenanthoides	Proteacidites annularis	Proteacidites asperopolus	Proteacidites differentipollis	Proteacidites grandis	Proteacidites incurvatus	Proteacidites kopiensis	Proteacidites leightonii
1		1398	Core						X			X		X	X	X	X				X			X	X		X		C
2A		1400.31	Core	Fine					0.8%	1.7%				0.8%	28%	3.4%	2.5%				11%		X	0.8%					X	0.8%
2B		1400.31	Core	Coarse						1.9%					1.0%	1.9%					8.7%						X		2.9%
3		1404	Core				X								X	X					X						X		C
4A	1407	1407.02	Core	Fine					1.9%	1.0%		1.0%		1.0%	30%	1.9%		1.0%	1.0%		5.7%		1.0%						
4B	1407	1407.02	Core	Coarse					0.9%			0.9%					1.8%		0.9%		8.2%	X							1.8%
5A		1425.38	Core	Fine									1.8%	3.6%	40%	2.7%			1.8%	0.9%	6.3%		0.9%					X	
5B		1425.38	Core	Coarse					0.9%						2.8%	0.9%	0.9%		0.9%		0.9%		0.9%				X		
6A		1430	Core	Fine					2.5%			0.8%	0.8%	0.8%	34%	5.9%	0.8%	0.8%	0.8%		8.4%		0.8%						
6B		1430	Core	Coarse								0.9%	0.9%		0.9%	0.9%	0.9%				10%								11%
7		1435	Core	Fine				X	X			0.8%	1.7%	0.8%	28%	5.0%		0.8%	3.3%	X	9.1%		X				X		X
8		1439	Core												X	X			X	X	X	X	X						
9A	1614	1617	Cuttings	Fine		0.9%			2.8%	0.9%		0.9%	0.9%	1.9%	30%	2.8%				0.9%	4.7%		0.9%				X		
9B	1614	1617	Cuttings	Coarse	0.8%			X	0.8%							0.8%					10%				X	0.8%			5.6%
10	1794	1797	Cuttings													X					X				X				X
11A	1857	1860	Cuttings	Fine					1.0%	1.0%				2.9%	24%				1.9%		5.7%								
11B	1857	1860	Cuttings	Coarse	0.8%				0.8%						0.8%						5.4%					2.3%			3.1%
12	2013	2017	Cuttings		X			X	X		X				X	X			X		X	X			X	C			X

ABBREVIATIONS

X = Present

C = Common

% = Percentage

Table 4. King-1 samples - spore-pollen distribution.

No.	Top Metres	Base Metres	Sample Type	Residue Filter	Proteacidites nasus	Proteacidites obesolabrus ms	Proteacidites obscurus	Proteacidites ornatus	Proteacidites pachypolus	Proteacidites prodigus ms	Proteacidites pseudomoides	Proteacidites recavus	Proteacidites reticuloscabratus	Proteacidites rugulatus	Proteacidites tenuiexinus	Proteacidites tuberculiformis	Pseudowinterapollis couperi	Santalumidites cainozoicus	Sapotaceoidaepollenites rotundus	Tricolp(or)ates spp.	Tricolpites phillipsii	Tricolporites adelaidensis	Tricolporites leuros	Tricolporites microreticulatus	Tricolporites paenestriatus	Tricolporites scabratus	Triporopollenites ambiguus	Triporopollenites simplis	ANGIOSPERM SUM	SPORE-POLLEN TOTAL
1		1398	Core		X							X			X					X	X	X		X	X		X			
2A		1400.31	Core	Fine			X											2.5%		4.2%									82%	119
2B		1400.31	Core	Coarse			X				X									1.0%		X							18%	104
3		1404	Core				X			X		C				X				X		X								
4A	1407	1407.02	Core	Fine												X				10%				X		X		X	83%	105
4B	1407	1407.02	Core	Coarse								X						0.9%		1.8%									23%	110
5A		1425.38	Core	Fine			0.9%											2.7%		6.3%									85%	112
5B		1425.38	Core	Coarse								X								6.5%									25%	108
6A		1430	Core	Fine									X							4.2%	X							0.8%	73%	119
6B		1430	Core	Coarse								X								1.9%		X							28%	106
7		1435	Core	Fine													X	X		12%	X								77%	121
8		1439	Core									X						X	X	X		X	X	X		X				
9A	1614	1617	Cuttings	Fine					0.9%						X			0.9%		7.5%									78%	107
9B	1614	1617	Cuttings	Coarse		X						X								4.8%		X			X	X			27%	124
1O	1794	1797	Cuttings											X						X		X				X				
11A	1857	1860	Cuttings	Fine					1.0%											13%					1.9%				84%	105
11B	1857	1860	Cuttings	Coarse			0.8%													3.1%		X			0.8%				28%	130
12	2013	2017	Cuttings				X	X			X	X								X										

ABBREVIATIONS

X = Present

C = Common

% = Percentage

Table 5. King-1 samples - microplankton distribution.

No.	Top Metres	Base Metres	Sample Type	Residue Filter	ACRITARCHS & ALGAE	Botryococcus braunii	Pediastum sp.	SUM ACRITARCHS & ALGAE		NON-MARINE DINOCYSTS	Ceratertius gen. et sp. nov.	Cubiculosphaera spp.	Saeptodinium spp.	SUM NON-MARINE DINOCYSTS		MARINE DINOCYSTS	Dinocysts undiff.	Apectodinium spp.	Apteodinium sp.	Cordosphaeridium spp.	Diphyes colligerum	Eocladopyxis peniculata	Homotryblium tasmaniense	Hystrichokolpoma spinosum	Impagidinium spp.	Kenleyia spp.	Operculodinium centrocarpum	Paralecaniella indentata	Spinidinium spp.	Thalassiphora pelagica	SUM MARINE DINOCYSTS		**Total Microplankton**
1		1398	Core			X					X	X	X											X			X					
2A		1400.31	Core	Fine																													
2B		1400.31	Core	Coarse		11%		11%			11%	70%		81%														7%			7%		27
3		1404	Core									X																		X			
4A	1407	1407.02	Core	Fine																													
4B	1407	1407.02	Core	Coarse													100%														100%		1
5A		1425.38	Core	Fine																													
5B		1425.38	Core	Coarse													100%														100%		2
6A		1430	Core	Fine							X						100%											X			100%		1
6B		1430	Core	Coarse							26%	7%		33%			4%					X						63%			67%		27
7		1435	Core	Fine								100%		100%								X						C					1
8		1439	Core																														
9A	1614	1617	Cuttings	Fine																	X	X											
9B	1614	1617	Cuttings	Coarse													100%														100%		2
10	1794	1797	Cuttings															X									X						
11A	1857	1860	Cuttings	Fine													75%											25%			100%		4
11B	1857	1860	Cuttings	Coarse			7%	7%									93%		X					X		X					93%		14
12	2013	2017	Cuttings										X										C			C							

ABBREVIATIONS

X = Present

C = Common

% = Percentage

APPENDIX C4.

Quantitative palynological analysis of Paleocene to Middle Eocene interval Konkon-1, Bass Basin.

by

Alan D. Partridge

Biostrata Pty Ltd
A.B.N. 39 053 800 945

Biostrata Report 2002/09

30th June 2002

Quantitative palynological analysis of Paleocene to Middle Eocene interval Konkon-1, Bass Basin

by Alan D. Partridge

Introduction

A quantitative palynological study of the Paleocene to Eocene Eastern View Group in Konkon-1 has been undertaken as a component of the Bass Basin Palynological Project coordinated by Geoscience Australia as part of the Western Tasmania Regional Minerals Program Offshore Collaborative Project, between Mineral Resources Tasmania, Geoscience Australia and the National Centre for Petroleum Geology and Geophysics to investigate aspects of the hydrocarbon prospectivity of the Bass and Sorell Basins.

This new palynological study of the Konkon-1 well was initiated to investigate the abundance of marine microplankton in the more shaly northwestern part of the Bass Basin, which available data suggested was the most likely source direction from which marine influence entered the basin. The Konkon-1 well, drilled in 1973, was preferred to the nearby Seal-1 well, drilled in 1986, because it was better sampled by sidewall cores and the deep Paleocene section was less disturbed by igneous intrusions. The original palynological report by Stover (1973) also suggested Konkon-1 contained some of the most abundant and diverse marine microplankton assemblages recorded in the basin. Also predicted and found during this study are the presence of non-marine dinocysts and Neves effects amongst the spore-pollen assemblages. Both these features were recorded from the thick Paleocene shale section in the well. For this new study the original core and sidewall core samples between 1095.8 and 1494.7m were re-examined and six new samples collected and analysed. Although it was known beforehand that many of the microplankton assemblages were worthy of full systematic description and illustration, such documentation was not the intent of this new study, and unfortunately was also beyond the scope of the overall project.

Materials and Methods

Assemblage counts were performed on 25 samples comprising one conventional core and eighteen sidewall core samples from the relinquished set of original palynological slides, supplemented by six new infill samples. The latter, two conventional core and four cuttings samples, were collected by the author from the core library at Geoscience Australia and processed at their palynological laboratory. Most of the new samples were also counted by Dr Michael Macphail. In general the palynological slides contained high visual yields of organic residue (kerogen), and high concentrations of moderately well-preserved palynomorphs. An average of 283 specimens of both terrestrial and aquatic palynomorphs were counted per sample.

The palynological zones assigned to the samples, zone Confidence Ratings, key defining species and interpreted palaeoenvironments are provided in Table 1. Basic palynological data on organic residue yields, palynomorph concentrations in the residues, palynomorph preservation and species diversity in the samples

are provided in Table 2. Species abundance and range data are provided in Tables 3 to 5. Author citation for spore-pollen species can be principally sourced for published species from Stover & Partridge (1973, 1982), and for manuscript species from Partridge (1973). Author citation for dinocysts can be sourced from Williams *et al.* (1998), and for acritarchs, algal cysts and other microplankton from Fensome *et al.* (1990).

Geological Discussion

The interval studied in Konkon-1 extends from the first productive sidewall core above the dolerite intrusion intersected near the T.D. of the well, to the bottom sidewall core recovered from the base of the Anglesea Formation, which forms the regional seal for the sediments of the Boonah Formation and underlying Eastern View Group. This 400m thick interval from about 1095 to 1495m ranges in age from early Paleocene (or perhaps latest Maastrichtian) to basal Late Eocene, and represents the thinnest section of the Eastern View Group penetrated in the Bass Basin. The equivalent age section in more central wells in the basin can be over four times as thick (eg. Tilana-1).

The portion of the Eastern View Group penetrated in Konkon-1 from 1173 to 1525m is also unusual in that it is largely shale (>75%). Sandy intervals are only found at the base of the section penetrated (below 1474m), and over the interval 1213 to 1270m (>60% sandstone). In the middle of the latter section the occurrence of red, brown and yellow coloured quartz sands, recorded from both the cuttings and sidewall cores, is interpreted to be the manifestation of a significant unconformity. No similar coloured sands are found at an equivalent stratigraphic level in any other well in the Bass Basin. Overall, the predominance of ì shaleî in the Konkon-1 well suggests the section is more distal, relative to the more central wells in the basin, but at the same time the more attenuated succession relative to other wells suggests Konkon-1 may also contain significant missing section or hiatuses.

Undoubtedly, the most distinctive feature of the interval studied in Konkon-1 is the 137 metre thick shale unit from 1337 to 1474m (informally named the Koorkah unit in Partridge, 2002), which is broken only by two distinctive coal seams at 1352-55m and 1402-03m. The palynological assemblages from this shale contains both marine and non-marine microplankton and a strong Neves effect which together identify the Koorkah unit as deposited in a large lake or lagoon (Partridge, 2002). The Neves effect is identified in the terrestrial spore-pollen assemblages and refers to the tendency for certain more buoyant spores or pollen to have greater relative abundances in sediments deposited in more distal marine or lacustrine environments (Traverse, 1988; Partridge, 1999).

Also within this Koorkah unit occurs a marked change in the composition of the microplankton assemblages from exclusively non-marine dinocysts below 1400m, to an increasing abundance and diversity of cosmopolitan marine dinocysts above 1400m (Table 3). This change is interpreted to document the first major marine flooding of the Bass Basin, and represent a change from a largely landlocked and fresh-water fluvial to lacustrine regime, to that of a large marine coastal lagoon surrounded by deltaic and coastal plain

environments (Partridge, 2002). This environmental flip occurs in the Late Paleocene (Upper *L. balmei* Zone) and correlates with one or more major high stands of sea level during the Late Paleocene Thermal Maximum or LPTM (Aubry *et al.*, 1998). In Konkon-1 this boundary is considered to lie at a major sequence boundary located below the coal seam at 1402-03m.

The samples with non-marine dinocysts have low to moderate abundances (<1% to <25% MP relative to SP + MP count) and low diversities of microplankton (<5 species per sample), while samples with marine dinocysts have low to high abundances (<1% to >60%), with diversities of microplankton in the richer samples typically >10 species per sample (Table 2). Associated with both the marine and non-marine microplankton occurrences are the strong Neves effects amongst the spore-pollen. These Neves effects are represented by high abundance of gymnosperm pollen belonging to the species *Dilwynites granulatus*, *D. tuberculatus* and *Araucariacites australis*. The combined abundance of these three species is recorded as the NED% on Table 2, and varies from 9% to 51% (average 30%) of the spore-pollen count. Note that the NED% is <2% in the sidewall cores at 1354.8m and 1402.7m that sample the two coal seams, and averages only 10% in the two samples at 1359.4m and 1365.5m from the *Apectodinium hyperacanthum* marine transgression at the base of the Lower *M. diversus* Zone (Tables 1 & 2).

The low abundances of *Dilwynites* and *Araucariacites* pollen in the coals is considered typical of spore-pollen assemblages recovered from sediments deposited in lower coastal plain settings. The lower abundances of *Dilwynites* and *Araucariacites* pollen in the two samples at the base of the Lower *M. diversus* Zone have a different more complex explanation. The latter samples are considered to be representative of the *Apectodinium* Acme at the peak of the LPTM (Bujak & Brinkhuis, 1998; Crouch *et al*., 2001). During this short warm interval the parent plants producing the *Dilwynites* and *Araucariacites* pollen are believed to have reduced abundance in the hinterland vegetation thereby causing a proportional reduction in the NED% in the more distal lacustrine/lagoonal environments. It is considered probable based on palaeogeography that the samples at 1359.4m and 1365.5m are just as distal as the other microplankton rich samples in the Koorkah unit.

Indeed the only samples from the Koorkah unit that are considered proximal are the sidewall core samples from the two coal seams at 1354.8m and 1402.7m. The spore-pollen assemblages from these coals are characterised by with very high abundances of *Gleicheniidites circinidites* and *Clavifera triplex* spores (average >45%). Based on these very ì skewedî assemblages the coals are interpreted to represent low stands of sea level when the giant Palaeolake Koorkah drained and this part of the Bass Basin was replaced by extensive ì fern marshesî . Both coals undoubtedly overlie major sequence boundaries.

Samples analysed below the Koorkah unit (ie. SWCs at 1479.8m, 1490.5m and 1494.7m) lack microplankton or any recognisable Neves effect, and therefore this older interval is interpreted to have been deposited in a non-marine fluvial regime. The significant coal seams between 1474 and 1496m could however be

interpreted as deltaic or lower coastal plain facies lateral to Palaeolake Koorkah.
The Eastern View Group above the Koorkah unit can be divided into a 67 metre thick interval of interbedded shales and coals from 1270 to 1337m assigned to the Middle to Upper *M. diversus* Zones (Narimba unit of Partridge, 2002); a 57 metre thick sandy interval from 1257 to 1270m that is not adequately dated (equivalent to Cormorant and Poonboon units of Partridge, 2002); and a 40 metre thick shale unit from 1173 to 1213m assigned to the Lower *N. asperus* Zone (Toolka unit of Partridge, 2002). These units generally contain reduced microplankton abundances and lack any recognisable Neves effects, although this may partly reflect the limited number of palynological samples analysed.

The shaly Narimba unit may be more marine than the current sampling suggests and warrants further study. The deepest sidewall core at 1313.7m for example contains the important index dinocyst *Apectodinium homomorphum*. Unfortunately, the shallower sidewall core at 1283.2m is a coal and the lithology of the immediately overlying cuttings at 1274-80m is also coaly, and not surprisingly both samples contain non-marine palynomorph assemblages.

The overlying sandy interval from 1257 to 1270m is currently not adequately dated. The Lower *N. asperus* Zone assemblage extract from the cuttings sample collected from 1225-31m is interpreted to be largely caved. However, based on superposition, this 57 metre thick interval can be correlated with the Cormorant and Poonboon units identified in the Cormorant-1 and King-1 wells where the two units have a average thickness of over 550 metre (Partridge, 2002; fig.10). The marked difference in thickness is believed to be accounted for by a major time break or unconformity in Konkon-1. This is evidenced by recovery of ì brown to red-brown quartz sandstonesî from the sidewall cores at 1214.3m, 1240.5m and 1251.5m, and the subsequent observation by the author of yellow to orange coloured quartz grains in the cuttings below 1246m. This unconformity is interpreted to correlated to the Marlin Unconformity in the Gippsland Basin (Partridge, 1999).

The youngest unit of the Eastern View Group is the distinctive coarsening-up shale from 1173 to 1213m, which has been informally named the Toolka unit by Partridge (2002). Although the recorded microplankton abundances from this unit are low (<1%), and there is no appreciable Neves effect, the unit nevertheless contains a moderate diversity of cosmopolitan dinocysts and is therefore interpreted as deposited in a restricted marine lagoon, analogous to modern Lake Maracaibo (Partridge, 2002; fig.4). At its maximum extent the Palaeolake Toolka has a similar distribution, but shorter duration than the older Palaeolake Koorkah (Partridge, 2002; fig.9).

Only two samples have been analysed from the younger Demons Bluff Group and both belong to the Late Eocene Middle *N. asperus* Zone. The deeper is a cuttings sample at 1152-55m, which is believed to be representative of the shale spike at 1147-52m in the middle of the Boonah Formation. The shallower is the sidewall core at 1095.8m at the base of the Anglesea Formation. Both contain low abundances and low

diversity assemblages of cosmopolitan marine dinocysts and are interpreted as representative of restricted marine estuarine to bay environments of deposition.

Biostratigraphy

Upper *Forcipites longus* spore-pollen Zone or younger

Interval: 1490.4 to 1494.7 metres.

Age: Latest Maastrichtian to Paleocene.

The sidewall core at 1494.7m, which is also the deepest productive palynological sample in the well, was originally assigned to the *Forcipites* (al. *Tricolpites*) *longus* Zone by Stover (1973), but unfortunately the key index species recorded in the original study could not be confirmed. Based on the high abundance of *Phyllocladidites mawsonii* (30%), and frequent occurrence of *Tripunctisporis maastrichtiensis* (2%) in the assemblage a younger *L. balmei* Zone assignment is considered more likely. In contrast, the sample at 1490.4m, which was recorded as indeterminate by Stover (1973), is dominated by *Proteacidites* species (24%) and *Nothofagidites* pollen (16%) and has a more Cretaceous aspect. As neither sample contained any species whose ranges commence in the *L. balmei* Zone the interval is best treated as Upper *F. longus* Zone or younger based on the FAD (First Appearance Datum) of *T. maastrichtiensis*

***Lygistepollenites balmei* spore-pollen Zone**

Interval: 1371.6 to 1478.9 metres.

Age: Late Paleocene.

The eight sidewall cores over this 100 metre interval are assigned to the *L. balmei* Zone based on the consistent presence of *Gambierina rudata* and the eponymous species. Within the interval the base of the Lower *L. balmei* Zone can be confidently picked on the FAD of *Polycolpites langstonii* at 1478.9m and the top at the last consistent occurrence of *Tetracolporites verrucosus* at 1417.3m. The younger Upper *L. balmei* Zone can be confidently picked by the successive FADs of the following species: *Proteacidites annularis* in the coal at 1402.7m, *Matonisporites* (al. *Cyathidites*) *gigantis* at 1386.8m, and *Cupanieidites orthoteichus* at 1371.6m. The top of the zone is picked below the incoming of diagnostic species of the *M. diversus* Zone as in this well there appears to be range extensions or reworking of key *L. balmei* Zone index species into the overlying zone.

The associated microplankton assemblages between 1417.3 and 1463m are assigned to the informal *Morkallacysta* Facies based on the dominance of the eponymous genus in the assemblage. This association is representative of a lacustrine environment of deposition but is not considered age diagnostic. A descriptive study of the species assigned to this non-marine dinocyst genus needs to be undertaken to determine whether they have any biostratigraphic significance.

The top sample in the interval is assigned to the *Apectodinium reburrus* Acme Zone of Partridge (1999) based on the FAD of the eponymous species, even though the assemblage is still dominated by *Morkallacysta*.

Lower *Malvacipollis diversus* spore-pollen Zone

Interval: 1359.4 to 1365.5 metres.

Age: Early Eocene.

The assemblages from the two sidewall cores are assigned to the basal Lower *M. diversus* Zone based on the joint occurrence of *Spinizonocolpites prominatus*, *Crassoretitriletes vanraadshooveni* and *Proteacidites pachypolus*. These three species have variably disjunct ranges across the three Bass Strait basins, but all are first recorded associated with the *Apectodinium hyperacanthum* Zone marine incursion (Partridge, 1976, 1999). After this initial occurrence the species drop out of the palynological assemblages only to reappear later in the *M. diversus* Zone. The other distinctive feature of the two samples is the prominent occurrences of *Malvacipollis diversus/subtilis* (average 15%) and *Myrtaceidites parvus/mesonesus* (average 8%), which also can be considered diagnostic of the base of the Lower *M. diversus* Zone. The samples also contain abundant (average 30%) and diverse microplankton that are confidently assigned to the *Apectodinium hyperacanthum* Zone based on the prominent occurrence of the eponymous species.

Middle *Malvacipollis diversus* spore-pollen Zone

Interval: 1313.7 to 1354.8 metres.

Age: Early Eocene.

The shallowest sample a sidewall core at 1313.7m is confidently assigned to the Middle *M. diversus* Zone on the FAD of *Polycolporopollenites esobalteus*. Note however that Stover (1973) reports a older occurrence of this species at 1359.4m which was not confirmed in this study. The deeper samples from Core-1, and also the coal sampled by the sidewall core at 1354.8m, unfortunately lack key index species, and are only assigned to the Middle subzone on absence of *Matonisporites gigantis* and *Peninsulapollis gillii* which are not known to range above, or are not consistent above the Lower subzone in the Bass Basin (Partridge, 1973).

The associated microplankton are assigned to a revised concept of the *Apectodinium homomorphum* Zone proposed by Partridge (1999), which is defined as the interval from the LAD of *Apectodinium hyperacanthum* to the FAD of *Homotryblium tasmaniense*. Further, the abundant and diverse assemblages recovered from Core-1 are considered to correlate with a position high in zone based on the common occurrence of *Rhombodinium subtile* at 1352.4m

Upper *Malvacipollis diversus* spore-pollen Zone

Sample at: 1283.2 metres.

Age: Early Eocene.

The FAD of *Santalumidites cainozoicus* in the sidewall core sample at 1283.2m assigns this sample to the upper part of the Upper *M. diversus* Zone. Other key index species recorded are the disjunct reappearance of *Proteacidites pachypolus* and the FAD of *Myrtaceidites tenuis*. The immediately overlying cuttings at 1274-

80m contain a similar assemblage but lacks the index species. An age as young as the *P. asperopolus* Zone is considered possible for this sample.

Lower *Nothofagidites asperus* spore-pollen Zone

Interval: 1188.7 to 1231 metres.

Age: Middle Eocene.

Two cuttings and two sidewall cores are assigned to the Lower *N. asperus* Zone based on the increased abundance of *Nothofagidites* pollen to >20%, combined with the FADs of *Nothofagidites falcatus*, *Matonisporites ornamentalis* and *Tricolpites simatus*. In the original study by Stover (1973) the sidewall core at 1204m was incorrectly assigned to the older *P. asperopolus* Zone, based on the LAD of *Proteacidites asperopolus*, even though contemporary studies had shown that species as ranging through the Lower *N. asperus* Zone in the Bass Basin (Partridge, 1973). The associated microplankton are not considered zone diagnostic.

Middle *Nothofagidites asperus* spore-pollen Zone

Interval: 1095.8 to 1155 metres

Age: Late Eocene.

The cuttings that sample the thin shale parting in the Boonah Formation and the sidewall core from the base of the Anglesea Formation are both assigned to the Middle *N. asperus* Zone based on the presence of the key zone index species *Triorites magnificus*. The microplankton assemblage from the sidewall core can also be assigned to the *Corrudinium incompositum* Zone of Harris (1985) based on the presence of *Schematophora speciosus* and the manuscript species *Corrudinium corrugatum*.

References

AUBRY, M-P., LUCAS, S. & BERGGREN, W.A., editors, 1998. *Late PaleoceneñEarly Eocene Climatic and Biotic Events in the Marine and Terrestrial Records.* Columbia University Press, New York, 513p.

BUJAK, J.P. & BRINKHUIS, H., 1998. Global warming and dinocyst changes across the Paleocene/ Eocene epoch boundary. **In** *Late PaleoceneñEarly Eocene Climatic and Biotic Events in the Marine and Terrestrial Records.* M-P. Aubry, S. Lucas & W.A. Berggren, editors, Columbia University Press, New York, p.277-295.

CROUCH, E.M., HEILMANN-CLAUSEN, C., BRINKHUIS, H., MORGANS, H.E.G., ROGERS, K.M., EGGER, H. & SCHMITZ, B., 2001. Global dinoflagellate event associated with the late Paleocene thermal maximum. *Geology, vol.29*, p.315-318.

FENSOME, R.A., WILLIAMS, G.L., BARSS, M.S., FREEMAN, J.M. & HILL, J.M., 1990. Acritarchs and fossil Prasinophytes: An index to genera, species and infraspecific taxa. *AASP Contribution Series No. 25*, p.1-771.

HARRIS, W.K., 1985. Middle to late Eocene depositional cycles and dinoflagellate zones in southern Australia. **In** *Stratigraphy, Palaeontology, Malacology: Papers in Honour of Dr Nell Ludbrook,*

J.M. Lindsay, editor, *Department of Mines and Energy South Australia Special Publication 5*, p.133-144.

PARTRIDGE, A.D., 1973. Revision of the Spore-Pollen Zonation in the Bass Basin. *Esso Australia Ltd Palaeontological Report 1973/4*, 22p. 6pls (2 May).

PARTRIDGE, A.D., 1976. The geological expression of eustacy in the early Tertiary of the Gippsland Basin. *The APEA Journal, vol.16,* pt.1, p.73-79.

PARTRIDGE, A.D., 1999. Late Cretaceous to Tertiary geological evolution of the Gippsland Basin, Victoria. PhD thesis, La Trobe University, Bundoora, Victoria, p.i-xxix, p.1-439, 165 figs, 9 pls (unpubl.).

PARTRIDGE, A.D., 2002. Bass Basin Palynological Project: Unravelling a Late Cretaceous to Eocene geological history of large palaeolakes, coastal lagoons and marine bays. *Biostrata Report 2002/13*, p.1-36.

STOVER, L.E. & PARTRIDGE, A.D., 1973. Tertiary and late Cretaceous spores and pollen from the Gippsland Basin, southeastern Australia. Proceedings *Royal Society of Victoria, vol.85*, pt.2, p.237-286.

STOVER, L.E. & PARTRIDGE, A.D., 1982. Eocene spore-pollen from the Werillup Formation, Western Australia. *Palynology 6*, p.69-95.

TRAVERSE, A., 1988. *Paleopalynology*. Unwin Hyman Ltd, Boston, p.1-600.

WILLIAMS, G.L., LENTIN, J.K. & FENSOME, R.A., 1998. The Lentin and Williams index of fossil dinoflagellates 1998 edition. *American Association of Stratigraphic Palynologists, Contributions Series, no. 34*, p.1-817.

Table 1. Interpretative Palynological Data from Konkon-1

No.	Depth Metres	Depth Feet	Sample Type	Sample Origin	Spore-Pollen Zone	CR*	Microplankton Zone	CR*	Key Index Species	Palaeoenvironment
1	1095.8	3595	SWC 35	Esso	Middle *N. asperus*	B1	*C. incompositum*	B5	FAD of *Proteacidites rectomarginis*	Bay - restricted marine
2	1152-55	3780-90	Cuttings	GA-2	Middle *N. asperus*	D1			FAD of *Triorites magnificus*	Estuarine to Bay
3	1188.7	3900	SWC 27	Esso	Lower *N. asperus*	B1			FAD of *Tricolpites simatus*	Lagoonal - brackish
4	1192-201	3910-40	Cuttings	GA-2	Lower *N. asperus*	D1				Lagoonal - restricted marine
5	1204.0	3950	SWC 26	Esso	Lower *N. asperus*	B1			LAD of *Proteacidites asperopolus*	Lagoonal - brackish
6	1225-31	4020-40	Cuttings	GA-2	Lower *N. asperus*	D2			FAD of *Nothofagidites falcatus*	Lagoonal - brackish
7	1274-80	4180-200	Cuttings	GA-2	*P. asperopolus* or older	D5				Paralic to Non-marine
8	1283.2	4210	SWC 21	Esso	Upper *M. diversus*	B3			FAD of *Santalumidites cainozoicus*	Marsh - Peat swamp
9	1313.7	4310	SWC 19	Esso	Middle *M. diversus*	B2	*A. homomorphum*	B3	LAD of *Apectodinium homomorphum*	Lagoonal - brackish
10	1347.5	4421	Core 1	GA-2	Middle *M. diversus*	A4	*A. homomorphum*	A3		Lagoonal - restricted marine
11	1351.5	4434	Core 1	GA-2	Middle *M. diversus*	A4	*A. homomorphum*	A3		Lagoonal - restricted marine
12	1352.4	4437	Core 1	Esso	Middle *M. diversus*	A2	*A. homomorphum*	A1	FAD of *Rhombodinium subtile*	Lagoonal - restricted marine
13	1354.8	4445	SWC 17	Esso	Middle *M. diversus*	B4			*Glecheniidites/Clavifera* = 50% of SP	Marsh - Peat swamp
14	1359.4	4460	SWC 16	Esso	Lower *M. diversus*	B1	*A. hyperacanthum*	B2	LAD of *Apectodinium hyperacanthum*	Lagoonal - restricted marine
15	1365.5	4480	SWC 15	Esso	Lower *M. diversus*	B1	*A. hyperacanthum*	B2	FAD of *Spinizonocolpites prominatus*	Lagoonal - restricted marine
16	1371.6	4500	SWC 14	Esso	Upper *L. balmei*	B1	*A. reburrus* Acme	B3	FAD of *Apectodinium reburrus* ms	Lagoonal - restricted marine
17	1386.8	4550	SWC 13	Esso	Upper *L. balmei*	B2			FAD of *Matonisporites gigantis*	Lagoonal - brackish
18	1402.7	4602	SWC 12	Esso	Upper *L. balmei*	B2			*Glecheniidites/Clavifera* = 46% of SP	Marsh - Peat swamp
19	1417.3	4650	SWC 11	Esso	Lower *L. balmei*	B2	*Morkallacysta* Facies		LAD of *Tetracolporites verrucosus*	Lacustrine - fresh
20	1432.6	4700	SWC 10	Esso	Lower *L. balmei*	B2	*Morkallacysta* Facies			Lacustrine - fresh
21	1447.8	4750	SWC 9	Esso	Lower *L. balmei*	B2	*Morkallacysta* Facies			Lacustrine - fresh
22	1463.0	4800	SWC 8	Esso	Lower *L. balmei*	B2	*Morkallacysta* Facies		FAD of *Morkallacysta*	Lacustrine - fresh
23	1478.9	4852	SWC 7	Esso	Lower *L. balmei*	B2			FAD of *Polycolpites langstonii*	Non-marine - fluvial
24	1490.4	4890	SWC 6	Esso	Upper *F. longus* or younger	B4			LAD of *Forcipites* sp. nov.	Non-marine - fluvial
25	1494.7	4904	SWC 5	Esso	Upper *F. longus* or younger	B4			FAD of *Tripunctisporis maastrichtiensis*	Marsh - Peat swamp

ABBREVIATIONS

*CR = Confidence Ratings
LAD = Last Appearance Datum
FAD = First Appearance Datum
GA-2 = Samples collected Stage-2 Work program
Esso = Samples processed in Esso laboratory

CONFIDENCE RATINGS

Alpha Code Linked to Sample
A = Core
B = Sidewall core
C = Coal cuttings
D = Ditch cuttings
J = Junk basket

Numeric Code Linked to Palynomorph Assemblage
1 = Excellent confidence: High diversity assemblage **plus** key zone species.
2 = Good confidence: Moderately diverse assemblage **plus** key zone species.
3 = Fair confidence: Low diversity assemblage **plus** key zone species.
4 = Poor confidence: Moderate to high diversity **minus** key zone species.
5 = Very low confidence: Low diversity assemblage **minus** key zone species.

Table 2. Basic Palynological Data from Konkon-1

No.	PalLab Spl.No.	Sample Type	Core No.	Top Feet	Base Feet	Top Metres	Base Metres	Visual Yield	Palynomorph Concentration	Palynomorph Preservation	No. SP Species	No. MP Species	Marine MP%	Other MP%	NED	Noth%
1	NA	SWC	35		3595		1095.8	High	High	Fair-good	70	13	1%		3%	52%
2	6406889	Cuttings		3780	3790	1152.1	1155.2	High	High	Fair-good	42	4	3%		6%	26%
3	NA	SWC	27		3900		1188.7	High	High	Fair-good	60	6	<1%		11%	34%
4	6406890	Cuttings		3910	3940	1191.8	1200.9	Moderate	Moderate	Poor-fair	49	7	<1%		5%	43%
5	NA	SWC	26		3950		1204.0	Moderate	Moderate	Fair-good	60	1	<1%		2%	66%
6	6406891	Cuttings		4020	4040	1225.3	1231.4	Moderate	Low-Moderate	Fair	36	3	5%	<1%	5%	36%
7	6406892	Cuttings		4180	4200	1274.1	1280.2	Low	Low	Poor-fair	20	1		<1%	4%	26%
8	NA	SWC	21		4210		1283.2	Low	Low	Poor-fair	31				1%	20%
9	NA	SWC	19		4310		1313.7	High	High	Fair-good	46	1	2%		6%	14%
10	6406893	Core	1		4421		1347.5	High	High	Poor-fair	28	3	40%	<1%	21%	5%
11	6406894	Core	1		4434		1351.5	High	High	Poor-good	35	5	17%	1%	19%	8%
12	NA	Core	1		4437		1352.4	High	High	Poor	34	15	61%		29%	10%
13	NA	SWC	17		4445		1354.8	High	High	Fair-good	29	1		5%	1.9%	1%
14	NA	SWC	16		4460		1359.4	Low	Low	Fair	53	12	27%	1%	10%	2%
15	NA	SWC	15		4480		1365.5	Moderate	High	Poor-fair	48	12	33%	<1%	12%	1%
16	NA	SWC	14		4500		1371.6	High	High	Poor-fair	51	8	4%	1%	33%	6%
17	NA	SWC	13		4550		1386.8	High	High	Fair	42	1	1%		43%	6%
18	NA	SWC	12		4602		1402.7	High	High	Poor-fair	35				<0.5%	3%
19	NA	SWC	10		4650		1417.3	High	High	Fair-good	34	3		23%	49%	7%
20	NA	SWC	11		4700		1432.6	High	High	Fair-good	34	2		2%	40%	4%
21	NA	SWC	9		4750		1447.8	High	High	Fair-good	37	1		13%	48%	4%
22	NA	SWC	8		4800		1463.0	High	High	Fair-good	35	2		7%	53%	5%
23	NA	SWC	7		4852		1478.9	Moderate	Moderate	Fair	28				13%	24%
24	NA	SWC	6		4890		1490.5	Low	Low	Fair	27				11%	16%
25	NA	SWC	5		4904		1494.7	High	Very High	Poor	28					1%

ABBREVIATIONS

MP = Microplankton

SP = Spore-Pollen

NA = Not Available

NED = Neves Effect based on Dilwynites/Araucariacites Percentage

Noth% = Percentage of Nothofagidites in SP count.

Table 3. Konkon-1 - Abundances of major palynomorph groups.

No.	Top Metres	Base Metres	Top Feet	Base Feet	Sample Type	Gleicheniidites & Clavifera spores	ALL OTHER spores	Dilwynites & Araucariacites pollen	ALL OTHER gymnosperms	Nothofagidites species	ALL OTHER angiosperms	SPORE-POLLEN TOTAL	FUNGAL microfossils	Reworked Spore-Pollen	**Total Terrestrial SUM**		SPORE-POLLEN TOTAL	MICROPLANKTON fresh-brackish	MICROPLANKTON marine	**SP + MP SUM**
1		1095.8		3595	SWC 35		5%	3%	9%	47%	27%	91%	9%		260		99%		1.3%	240
2	1152.1	1155.2	3780	3790	Cuttings	0.3%	10%	3%	29%	25%	30%	98%	2%	0.3%	362		98%		2.2%	362
3		1188.7		3900	SWC 27	0.4%	5%	10%	20%	32%	25%	92%	8%		252		100%		0.4%	234
4	1191.8	1200.9	3910	3940	Cuttings	0.8%	7%	5%	10%	43%	33%	100%	0%		261		99%		0.8%	262
5		1204.0		3950	SWC 26		6%	1.4%	7%	38%	43%	96%	3%	0.7%	279		100%		0.4%	270
6	1225.3	1231.4	4020	4040	Cuttings	0.9%	6%	4.4%	22%	34%	25%	91%	8%	0.6%	338		95%	0.3%	4.9%	326
7	1274.1	1280.2	4180	4200	Cuttings	0.9%	7%	3.6%	23%	23%	31%	89%	10%	0.9%	112		99%		1.0%	101
8		1283.2		4210	SWC 21		1%	0.8%	3%	18%	69%	91%	9%		118		100%			107
9		1313.7		4310	SWC 19		4%	3.7%	4%	8%	36%	56%	44%		356		98%		2.0%	204
10		1347.5		4421	Core 1	2.9%	7%	16%	25%	4%	22%	77%	23%		244		59%	0.3%	40%	315
11		1351.5		4434	Core 1	1.4%	9%	16%	40%	7%	12%	85%	15%		280		82%	1.4%	17%	292
12		1352.4		4437	Core 1	5.7%	15%	28%	12%	9%	28%	98%	1.9%		158		39%		61%	393
13		1354.8		4445	SWC 17	50%	16%	1.9%	10%	1%	21%	100%			260		95%	4.8%		273
14		1359.4		4460	SWC 16	5.5%	20%	9%	8%	3%	47%	93%	6.3%	0.8%	237		73%	0.7%	27%	303
15		1365.5		4480	SWC 15	2.3%	13%	11%	10%	2%	53%	92%	7.9%	0.6%	177		67%	0.4%	32%	241
16		1371.6		4500	SWC 14	5.1%	11%	33%	26%	7%	15%	97%	2.6%		272		95%	1.1%	3.9%	279
17		1386.8		4550	SWC 13	7.1%	12%	41%	18%	6%	11%	95%	4.9%		266		99%		0.8%	255
18		1402.7		4602	SWC 12	42%	12%	0.4%	35%	3%	7%	100%			257		100%			257
19		1417.3		4650	SWC 11	2.9%	6%	47%	20%	7%	13%	95%	4.9%		204		77%	22%	1.2%	253
20		1432.6		4700	SWC 10	0.7%	4%	38%	29%	5%	19%	95%	5.3%		284		98%	2.2%		275
21		1447.8		4750	SWC 9	0.3%	5%	42%	19%	3%	18%	89%	11%		290		87%	13%		295
22		1463.0		4800	SWC 8	0.7%	5%	51%	21%	5%	13%	95%	4.8%		290		93%	7.1%		297
23		1478.9		4852	SWC 7		8%	11%	24%	21%	25%	89%	11%		256		100%			228
24		1490.5		4890	SWC 6	1.3%	13%	11%	26%	16%	32%	98%	2.1%		238		100%			233
25		1494.7		4904	SWC 5	5.3%	14%		51%	2%	28%	100%			264		100%			264

Table 4. Konkon-1 - spore-pollen distribution.

No.	Depth Metres	Sample Type	SPORES	Baculatisporites spp.	Camarozonosporites bullatus	Camarozonosporites heskermensis	Clavifera triplex	Cyathidites spp. large	Cyathidites spp. small	Dictyophyllidites spp.	Echinosporis echinatus	Gleicheniidites circinidites	Herkosporites elliottii	Ischyosporites spp.	Kuylisporites waterbolkii	Laevigatosporites spp.	Latrobosporites spp.	Marattisporites scabratus	Matonisporites gigantis comb. nov.	Matonisporites ornamentalis	Peromonolites spp.	Polypodiaceoisporites varus ms	Polypodiidites/Verrucatosporites spp.	Retitriletes spp.	Ricciaesporites boxatus ms	Rugulatisporites mallatus	Stereisporites antiquisporites	Stereisporites regium	Trilete spores undiff.	Tripunctisporis maastrichtiensis	Verrucosisporites kopukuensis	Total spores:	
1	1095.8	SWC 35				X		X	3.0%					X		1.7%					X			0.4%	X		0.4%		0.4%		X	6%	
2	1152-55	Cuttings		0.8%				1.4%	2.5%			0.3%				3.1%					0.3%		0.8%	0.3%			0.8%		0.6%			11%	
3	1188.7	SWC 27		0.9%					2.1%			0.4%	X			0.9%									X	X	0.4%		0.9%		X	6%	
4	1192-01	Cuttings		0.8%			0.4%		2.7%			0.4%				0.4%				0.4%	X		1.2%	0.4%			0.4%		0.8%		X	8%	
5	1204.0	SWC 26		0.4%				X	1.9%		0.7%			0.4%		1.1%				X	0.4%						0.4%		1.1%	0.4%	X	7%	
6	1225-31	Cuttings		0.3%				0.6%	0.3%			1.0%		1.0%		1.6%					1.0%	0.3%						0.3%	0.6%			7%	
7	1274-80	Cuttings						1.0%	1.0%			1.0%				1.0%													5.0%			9%	
8	1283.2	SWC 21																													0.9%	1%	
9	1313.7	SWC 19		0.5%				X	4.0%					0.5%	X	3.0%														X		8%	
10	1347.5	Core 1		0.5%			0.5%	0.5%	0.5%			3.2%									1.6%						1.1%		4.3%			12%	
11	1351.5	Core 1		1.3%					1.7%			1.7%		0.4%		4.6%					0.4%			0.4%			0.4%		1.3%			12%	
12	1352.4	Core 1		0.6%					9.0%			5.8%				0.6%											3.9%			0.6%		21%	
13	1354.8	SWC 17					5.4%		0.8%			45%				2.3%	1.2%										9.2%			0.4%	1.9%	66%	
14	1359.4	SWC 16		0.5%	X	X		4.1%	7.7%		0.9%	5.9%		0.9%		3.6%	0.5%					X		0.5%		X	1.4%	X	1.4%	X	X	27%	
15	1365.5	SWC 15						1.9%	8.0%			2.5%		0.6%		2.5%		0.6%	X			X				X			0.6%	X		17%	
16	1371.6	SWC 14		0.8%	X		0.4%	X	2.3%	0.4%		4.9%	X			1.1%			0.4%				0.4%	1.1%			3.8%	0.4%	0.8%	X		17%	
17	1386.8	SWC 13		0.8%	X			X	3.2%	0.4%		7.5%	X			3.6%			X		X						4.0%	X		0.8%		20%	
18	1402.7	SWC 12						1.2%	4.3%			42%	X			3.5%					X						1.9%		0.8%	X		54%	
19	1417.3	SWC 11		X				X	2.1%	0.5%		3.1%	X	0.5%		1.5%					X						2.1%			X		10%	
20	1432.6	SWC 10						X	3.0%	0.4%		0.7%	X								X		0.4%				0.4%			X		5%	
21	1447.8	SWC 9		0.4%				X	3.1%	0.8%		0.4%	0.4%			1.2%					X											6%	
22	1463.0	SWC 8		0.4%					1.8%	0.4%		0.7%	X			0.4%					0.7%						1.1%		0.4%	X		6%	
23	1478.9	SWC 7		0.9%						0.4%						6.1%					X		0.4%				0.9%			X		9%	
24	1490.5	SWC 6		0.4%					0.4%			1.3%	0.4%			9.4%		0.4%			0.4%			0.4%			0.4%	X	0.4%			14%	
25	1494.7	SWC 5						0.8%	0.4%			5.3%	X			4.2%							0.4%	1.5%			4.9%			1.9%		19%	

ABBREVIATIONS: X = Present % = Percentage

Table 4. Konkon-1 - spore-pollen distribution.

No.	Depth Metres	Sample Type	GYMNOSPERM POLLEN	Araucariacites australis	Cupressacites sp.	Dacrycarpites australiensis	Dilwynites granulatus	Dilwynites tuberculatus	Lygistepollenites balmei	Lygistepollenites florinii	Microalatidites paleogenicus	Microcachyridites antarticus	Phyllocladidites mawsonii	Phyllocaldidites reticulosaccatus	Phyllocaldidites verrucosus	Podocarpidites spp.	Trichotomosulcites subgranulatus	Total Gymnosperms:	ANGIOSPERM POLLEN	Angiosperm pollen undiff.	Arecipites spp.	Australopollis obscurus	Banksieaeidites arcuatus	Beaupreaidites elegansiformis	Beaupreaidites trigonalis ms	Beaupreaidites verrucosus	Bluffopollis scabratus	Concolpites leptos	Cupanieidites orthoteichus	Dicotetradites clavatus	Dryptopollenites semilunatus	Ericipites notensis	Ericipites crassiexinus/scabratus
1	1095.8	SWC 35		0.4%	0.4%	0.4%	2.1%	0.4%		0.8%			2.5%			5.5%	0.4%	13%						X			X		0.4%	X	X			X
2	1152-55	Cuttings		1.1%	0.6%		2.0%			3.7%	0.3%	0.6%	3.7%			19%	2.0%	33%			5.6%							X		0.3%		X		0.6%
3	1188.7	SWC 27		1.3%		X	8.6%	0.9%		2.6%		1.3%	12%			4.3%	1.3%	33%			0.4%			X	X	X	X			1.3%	0.4%		X	X
4	1192-01	Cuttings		1.2%	1.2%		3.5%	0.8%		1.5%		0.4%	3.1%			3.5%	0.4%	15%			1.2%									1.9%	0.4%			X
5	1204.0	SWC 26		0.4%			1.1%			2.6%	0.7%		2.2%			1.9%		9%			1.1%			X			X			1.9%	0.7%			0.4%
6	1225-31	Cuttings		1.3%			3.6%			1.0%	0.6%		2.3%			17%	3.6%	29%			2.9%									0.6%	0.3%			
7	1274-80	Cuttings		1.0%			3.0%					2.0%	12%			12%		30%			4.0%													
8	1283.2	SWC 21		0.9%						1.9%			X			0.9%		4%			0.9%									0.9%				
9	1313.7	SWC 19		0.5%			5.5%	0.5%		0.5%						5.5%	0.5%	13%												2.0%	2.5%	0.5%	X	
10	1347.5	Core 1		3.2%			18%			2.1%		0.5%	1.6%			22%	5.9%	54%			4.3%									0.5%				
11	1351.5	Core 1		2.5%	0.4%	0.4%	16%			3.8%		0.4%	2.5%			26%	13%	66%			3.4%	0.4%								0.4%			0.4%	
12	1352.4	Core 1		3.2%	1.3%		25%	1.3%		1.9%		0.6%	1.3%			5.2%	1.9%	41%			1.3%									X				
13	1354.8	SWC 17					1.9%			1.2%		1.2%	X			5.8%	1.9%	12%			1.2%						X							
14	1359.4	SWC 16		1.8%			8.2%			1.4%		0.5%	0.9%			5.5%	0.9%	19%			1.8%		X							X	0.5%		X	
15	1365.5	SWC 15		2.5%	3.7%		9.3%	0.6%	0.6%	1.2%			0.6%			4.9%		23%			0.6%	2.5%	1.9%							X			X	
16	1371.6	SWC 14		3.0%	9.4%		30%	0.4%	0.8%	0.8%	0.4%	0.4%	2.3%			9.8%	3.4%	61%			X		X							0.8%				
17	1386.8	SWC 13		1.2%	4.0%		39%	2.8%	0.4%	0.8%		0.8%	5.5%	0.4%		5.1%	1.6%	61%			0.4%		X											
18	1402.7	SWC 12					0.4%		X	1.9%	12%	2.3%	4.3%	X	X	14%	0.8%	36%			0.8%		0.4%											
19	1417.3	SWC 11		1.0%	6.2%		44%	3.6%	X	1.5%			0.5%	X		9.3%	3.1%	70%			X													
20	1432.6	SWC 10		3.0%	5.9%		36%	1.1%	0.7%	2.2%	0.7%	2.6%	1.1%	X		16%	1.5%	70%			1.5%													
21	1447.8	SWC 9		3.1%	3.1%	0.4%	43%	1.9%	X	1.6%	1.2%	2.3%	0.4%	X		12%	0.4%	70%			1.6%		X										0.4%	1.2%
22	1463.0	SWC 8		3.3%	6.5%		48%	2.2%	0.4%	1.8%		1.8%	2.9%	X	X	8.7%		75%			X										X			
23	1478.9	SWC 7		1.8%	0.9%		11%	0.4%			0.4%	0.4%	3.5%	1.3%	X	18%	2.2%	40%			0.4%													
24	1490.5	SWC 6		3.0%			7.7%			1.3%	0.4%	3.4%	0.4%			19%	1.7%	37%			1.7%													
25	1494.7	SWC 5							X	0.8%	0.4%	1.1%	30%	0.4%	X	16%	3.0%	51%			1.1%										11%			

ABBREVIATIONS: X = Present % = Percentage

Table 4. Konkon-1 - spore-pollen distribution.

No.	Depth Metres	Sample Type	Gambierina rudata/edwardsii	Haloragacidites harrisii	Ilexpollenites sp.	Juxtacolpus pieratus ms	Intratriporopollenites notabilis	Liliacidites spp.	Malvacipollis diversus	Malvacipollis subtilis	Milfordia spp.	Myrtaceidites parvus/mesonesus	Myrtaceidites tenuis	Myrtaceidites verrucosus	Nothofagidites asperus	Nothofagidites brachyspinulosus	Nothofagidites deminutus	Nothofagidites emarcidus/heterus	Nothofagidites endurus	Nothofagidites falcatus	Nothofagidites flemingii	Nothofagidites goniatus	Nothofagidites vansteenisii	Peninsulapollis gillii	Periporopollenites demarcatus	Periporopollenites polyoratus	Polycolpites langstonii	Polycolporopollenites esobalteus	Proteacidites spp.	Proteacidites annularis	Proteacidites crassus	Proteacidites grandis	Proteacidites incurvatus
1	1095.8	SWC 35		5.9%	0.4%			X		1.3%	X	5.1%		X	0.4%	3.8%	2.1%	43%		0.4%	0.4%	0.4%	1.7%		1.7%				3.0%	0.4%	X		X
2	1152-55	Cuttings		13%	0.6%			0.6%		0.8%		1.7%		X		3.7%	2.0%	19%	0.3%	0.6%					1.1%				2.0%	0.8%			
3	1188.7	SWC 27		7.3%					0.4%	0.4%		2.1%		X		6.0%	5.2%	20%		0.4%	1.7%	0.4%	0.4%		X	X			9.9%	1.7%	X		X
4	1192-01	Cuttings		12%	0.8%					1.2%		0.8%			0.8%	1.5%	4.6%	33%		1.2%	0.4%		1.5%		1.5%				5.4%	1.2%			
5	1204.0	SWC 26		10%	0.4%			X		1.9%	0.4%	3.3%			0.4%	1.1%	1.5%	31%			1.9%	1.1%	2.6%		0.4%	X			13%	1.5%	X	X	
6	1225-31	Cuttings		7.8%	0.3%			0.3%		1.0%		0.3%			0.6%	7.1%	2.3%	25%		0.6%	0.3%	0.3%	0.6%		2.6%			0.3%	3.6%	0.3%			
7	1274-80	Cuttings		12%				1.0%		1.0%						8.0%	8.0%	10%							1.0%				13%				
8	1283.2	SWC 21		20%	0.9%				3.7%	X			2.8%			0.9%	1.9%	17%							4.7%			0.9%	10%	6.5%	X	X	
9	1313.7	SWC 19		6.5%	1.0%		0.5%	1.0%	X	1.0%	1.0%	6.0%					1.0%	13%			0.5%		0.5%		X	X		X	15%	0.5%		X	
10	1347.5	Core 1		1.1%				1.6%				0.5%				1.1%	1.1%	2.1%			0.5%				2.1%				7.5%				
11	1351.5	Core 1		1.7%								0.4%				0.8%	0.8%	5.5%			0.8%	0.4%			1.7%				2.1%			0.8%	
12	1352.4	Core 1		3.9%					X	0.6%		0.6%				6.5%		1.3%			1.9%				2.6%	X			14%	1.3%		X	
13	1354.8	SWC 17		0.8%					X	X		3.5%						1.2%							X	X			2.7%	0.4%			X
14	1359.4	SWC 16	X	0.9%	0.5%		X		10%	5.5%		6.4%				0.9%		1.4%	0.5%		0.5%				0.5%	X			5.9%	X			
15	1365.5	SWC 15	0.6%	4.9%	0.6%			0.6%	11%	4.3%		9.9%						0.6%	0.6%		0.6%				0.6%				3.7%	X			X
16	1371.6	SWC 14	0.4%	0.4%	0.4%							X			0.4%	1.1%		2.6%	0.4%		2.3%			0.8%	0.4%	X	0.4%		7.2%	X			X
17	1386.8	SWC 13	0.8%	0.8%											0.4%	0.8%		1.6%	3.6%		0.4%			0.8%		X	0.4%		6.3%				
18	1402.7	SWC 12	X	X		X						X				0.4%		1.6%	0.8%		0.4%					X			1.9%	X			
19	1417.3	SWC 11	1.0%													1.5%		1.5%	3.6%		0.5%			X		X	X		8.2%				
20	1432.6	SWC 10	0.4%													0.4%		0.4%	4.1%					X		1.1%	X		7.8%				
21	1447.8	SWC 9	X		0.4%													0.4%	3.5%							1.6%	0.8%		7.0%				
22	1463.0	SWC 8	0.7%		0.4%				0.4%									2.9%	2.2%							0.7%	0.4%		5.1%				
23	1478.9	SWC 7														0.4%		0.4%	23%							1.8%	0.4%		20%				
24	1490.5	SWC 6																0.4%	16%							0.4%			24%				
25	1494.7	SWC 5	X					0.4%										0.4%	1.1%					3.8%		1.1%			6.1%				

ABBREVIATIONS: X = Present % = Percentage

Table 4. Konkon-1 - spore-pollen distribution.

No.	Depth Metres	Sample Type	Proteacidites kopiensis	Proteacidites latrobensis	Proteacidites leightonii	Proteacidites obesolabrus ms	Proteacidites obscurus	Proteacidites pachypolus	Proteacidites pseudomoides	Proteacidites recavus	Proteacidites rectomarginis	Proteacidites reticulatus	Proteacidites reticuloscabratus	Proteacidites rugulatus	Proteacidites tenuiexinus	Santalumidites cainozoicus	Sapotaceoidaepollenites rotundus	Spinizonocolpites prominatus	Tetracolporites multistrixus ms	Tetracolporites textus ms	Tetracolporites verrucosus	Tricolpate pollen undiff.	Tricolpites phillipsii	Tricolpites simatus	Tricolpites thomasii	Tricolporites adelaidensis	Tricolporites leuros	Tricolporites marginatus ms	Tricolporites paenestriatus	Triorites magnificus	Triporopollenites ambiguus	Triporopollenites simplis	Triporopollenites spp.	Total Angiosperms	Total Spore-Pollen Count
1	1095.8	SWC 35		X	X	X	0.8%	X		X	X	X	X		X	X	X					8.9%							X	X	0.4%	0.8%		81%	237
2	1152-55	Cuttings					0.3%	0.3%		0.3%						0.3%						1.7%									0.3%				56%	354
3	1188.7	SWC 27	X		X				X	X			X		X	X						2.6%	X	0.4%		X						0.4%		62%	233
4	1192-01	Cuttings					0.4%							X		0.4%						6.2%		0.4%		X					0.4%			77%	260
5	1204.0	SWC 26	X		0.4%	X	X	X	X				X		X	0.7%	0.4%					5.9%		0.4%	0.4%								0.7%	84%	269
6	1225-31	Cuttings																				6.8%												64%	309
7	1274-80	Cuttings																				3.0%												61%	100
8	1283.2	SWC 21			X	X	3.7%	X							X	X						8.4%				2.8%	3.7%		4.7%		X		0.9%	95%	107
9	1313.7	SWC 19			0.5%	X	0.5%		X				X									19%							1.5%				5.5%	79%	200
10	1347.5	Core 1																				11%												34%	187
11	1351.5	Core 1																				2.5%												22%	238
12	1352.4	Core 1			X	X	X		X				X									3.9%											0.6%	38%	155
13	1354.8	SWC 17					5.0%															7.3%									0.4%			22%	260
14	1359.4	SWC 16						X										0.9%	X			18%												54%	220
15	1365.5	SWC 15					X	0.6%	X									1.2%				14%						X	0.6%		X			60%	162
16	1371.6	SWC 14													X							3.0%						X					2.3%	23%	265
17	1386.8	SWC 13											X		X							0.4%						X					2.0%	19%	253
18	1402.7	SWC 12													X				X	3.5%		0.8%												11%	257
19	1417.3	SWC 11													X				X		0.5%	2.6%											1.0%	21%	194
20	1432.6	SWC 10											X									7.8%											1.5%	25%	269
21	1447.8	SWC 9													X						0.4%	4.3%						X			X		2.7%	24%	257
22	1463.0	SWC 8													X							3.6%											2.5%	19%	276
23	1478.9	SWC 7																				3.9%											1.3%	51%	228
24	1490.5	SWC 6																				6.0%											0.4%	49%	233
25	1494.7	SWC 5													X							4.5%											0.8%	30%	264

ABBREVIATIONS: X = Present % = Percentage

Table 5. Konkon-1 - microplankton distribution.

No.	Depth Metres	Sample Type	ACRITARCHS & ALGAE	Botryococcus braunii	Lecaniella sp.	Pediastrum sp.	Pseudoschizaea spp.	DINOCYSTS ó NON-MARINE	Cobricosphaeridium spp.	Morkallacysta spp.	DINOCYSTS ó MARINE	Dinocysts undiff.	Acomosphaera spp.	Apectodinium homomorphum	Apectodinium hyperacanthum	Apectodinium reburrus ms	Apteodinium spp.	Areoligera sp.	Batiacasphaera spp.	Cleistosphaeridium spp.	Cordosphaeridium spp.	Corrudinium corrugatum ms	Deflandrea spp.	Diphyes colligerum	Enneadocysta spp.	Fibrocysta bipolar	Glaphyrocysta spp.	Heteraulacacysta sp. A
1	1095.8	SWC 35										33%	X					X		X	X	X	X					33%
2	1152-55	Cuttings										63%													13%			
3	1188.7	SWC 27																X		X	X							
4	1192-01	Cuttings																										
5	1204.0	SWC 26										100%																
6	1225-31	Cuttings		6%								88%																
7	1274-80	Cuttings										100%																
8	1283.2	SWC 21																										
9	1313.7	SWC 19										50%		50%														
10	1347.5	Core 1		2%								98%																
11	1351.5	Core 1				7%						80%					2%						2%					
12	1352.4	Core 1										15%		X			11%	X		4%	5%			X		1%		
13	1354.8	SWC 17										100%																
14	1359.4	SWC 16		1%			1%					12%			27%			33%		1%	1%		4%	7%		X		
15	1365.5	SWC 15								1%		24%		6%	33%	1%		X		10%	1%			4%			11%	
16	1371.6	SWC 14								66%		18%				2%			5%	3%	2%							
17	1386.8	SWC 13										100%																
18	1402.7	SWC 12																										
19	1417.3	SWC 11			2%					93%		2%							3%									
20	1432.6	SWC 10							17%	83%																		
21	1447.8	SWC 9								100%																		
22	1463.0	SWC 8							14%	86%																		
23	1478.9	SWC 7																										
24	1490.5	SWC 6																										
25	1494.7	SWC 5																										

ABBREVIATIONS: X = Present % = Percentage

Table 5. Konkon-1 - microplankton distribution.

No.	Depth Metres	Sample Type	Heteraulacacysta sp. B	Hystrichokolpoma rigaudiae	Impagidinium spp.	Kenleyia spp.	Muratodinium fimbriatum	Operculodinium centrocarpum	Paralecaniella indentata	Phthanoperidinium comatum	Rhombodinium subtile	Rivernookia septata	Schematophora speciosus	Senegalinium dilwynensis	Spinidinium spp.	Spiniferites spp.	Systematophora spp.	Wetzeliella sp. cf W. symmetrica	Xenikodinium sp.	**Total Microplankton: (sum)**
1	1095.8	SWC 35		X				X	X	33%			X			X				3
2	1152-55	Cuttings			13%											13%				8
3	1188.7	SWC 27						X								100%				1
4	1192-01	Cuttings		50%												50%				2
5	1204.0	SWC 26																		1
6	1225-31	Cuttings			6%															17
7	1274-80	Cuttings																		1
8	1283.2	SWC 21																		
9	1313.7	SWC 19																		4
10	1347.5	Core 1																		66
11	1351.5	Core 1						4%								6%				54
12	1352.4	Core 1	22%			12%	X	1%	4%		7%					8%	4%	4%	1%	228
13	1354.8	SWC 17																		13
14	1359.4	SWC 16				X	X	4%				1%				8%				83
15	1365.5	SWC 15				X	X	3%				3%				3%				79
16	1371.6	SWC 14												5%	X					62
17	1386.8	SWC 13													X					2
18	1402.7	SWC 12																		
19	1417.3	SWC 11																		59
20	1432.6	SWC 10																		6
21	1447.8	SWC 9																		38
22	1463.0	SWC 8																		21
23	1478.9	SWC 7																		
24	1490.5	SWC 6																		
25	1494.7	SWC 5																		

ABBREVIATIONS: X = Present % = Percentage

APPENDIX C5.

Quantitative palynological analysis of eleven cuttings samples from 2266 to 3115m in Koorkah-1, Bass Basin.

by

Alan D. Partridge

Biostrata Pty Ltd
A.B.N. 39 053 800 945

Biostrata Report 2002/10

21st June 2002

Quantitative palynological analysis of eleven cuttings samples from 2266 to 3115m in Koorkah-1, Bass Basin

by Alan D. Partridge

Introduction

A quantitative palynological study of cuttings samples over the bottom 900 metres of the Eastern View Group penetrated in Koorkah-1 has been undertaken as a component of the Bass Basin Palynological Project coordinated by Geoscience Australia as part of the Western Tasmania Regional Minerals Program Offshore Collaborative Project, between Mineral Resources Tasmania, Geoscience Australia and the National Centre for Petroleum Geology and Geophysics to investigate aspects of the hydrocarbon prospectivity of the Bass and Sorell Basins.

This new palynological study of the Koorkah-1 well (drilled in 1985) is focussed on the thick shale unit identified between 2250 and 2692m, and the underlying interbedded sands and shale section from 2692 to 3149mTD. The upper shale unit contains only minor sandstones (<14% of section) and possibly three thin coal seams (at 2390m, 2428m and 2441m). The bottom interbedded unit is composed of approximately 56% shales and 44% sandstone and lacks any coal based on the sonic log and personal inspection of the cuttings. Rare, putative non-marine dinocysts recorded in the original palynological report by Morgan (1986), plus the similarity of the log character to the established lacustrine facies in the older Durroon Formation, in the southwest portion of the Bass Basin, and to the similar age Kipper Shale in the Gippsland Basin, suggested that the thicker shale intervals in Koorkah-1 could also represent significant lacustrine facies. The objective of the study was to quantify the abundance of the non-marine dinocysts and other microplankton through the older units in Koorkah-1 and to confirm whether the spore-pollen assemblages displayed Neves effects as had previously been found in the Durroon and Kipper formations.

Materials and Methods

The study was undertaken on eleven new cuttings samples as unfortunately neither the original palynological slides studied by Morgan (1986), nor any of the remaining sidewall cores from Koorkah-1 were available for re-examination. The new samples were collected by the author from the core library at Geoscience Australia and processed at their palynology laboratory. The samples which were comprised mostly of relatively homogeneous medium grey mudstone or shale, gave moderated yields of organic residue which contained generally high concentrations of very poorly preserved palynomorphs. An average of 250 specimens of both terrestrial and aquatic palynomorphs were counted per sample.

The palynological zones assigned to the samples, zone Confidence Ratings, key defining species and interpreted palaeoenvironments are provided in Table 1. Basic palynological data on organic residue yields, palynomorph concentrations in the residues, palynomorph preservation and species diversity in the samples are provided in Table 2. Brief lithological description of the samples are provided on Table 3. Species

abundance and range data are provided in Tables 4 to 6. Author citation for spore-pollen species can be principally sourced for published species from Stover & Partridge (1973), and for manuscript species from Partridge (1973). Author citation for dinocysts can be sourced from Williams *et al.* (1998), and for acritarchs, algal cysts and other microplankton from Fensome *et al.* (1990).

Geological Discussion

The interval studied in Koorkah-1 extends from the Early Maastrichtian to possibly the Late Paleocene (Lower *F. longus* to Upper *L. balmei* Zones). Microplankton abundances ranged from <1% to 27% (average 6%) of the combined spore-pollen and microplankton count. Although not particularly abundant both non-marine dinocysts (eg. *Morkallacysta*), and non-marine algae (eg. *Debarya*, *Pediastrum*, *Rimosicysta*) were recorded along with other genera known to occur in both environments (eg. *Amosopollis cruciformis* and *Horologinella*). Marine dinocysts were only identified from the shallowest cuttings at 2266-75m and are most likely caved. The associated spore-pollen assemblages are characterised by abundant *Dilwynites* and *Araucariacites* pollen (average 29%) that are interpreted to be representative of a strong Neves effect. The latter reflects the tendency for certain more buoyant spores or pollen to have greater relative abundances in sediments deposited in more distal marine or lacustrine environments (Traverse, 1988; Partridge, 2002b). The combination of these palynological features is interpreted to indicate a fresh-water lacustrine environments of deposition. The more pronounced Neves effect in the thicker shales is taken as evidence that the depositional environments were more distal and probably also deeper water.

It is also noted that the Well Completion Report placed an ì Intra Late Cretaceous Angular Unconformityî at 2690m at the base of the major shale section, and the presence of a major unconformity in the section is supported by the latest studies of the seismic data for the Bass Project. Although no obvious time break can be identified in the palynology succession the most likely position would be between the Upper and Lower *F. longus* Zones, and the palynological results would favour placing the boundary between these zones within the underlying interbedded unit rather than precisely at the base of the thickest shale. The preferred position for the zone boundary is below 2959m, where a sidewall core contains the oldest recorded occurrence by Morgan (1986) of the key index species *Tripunctisporis maastrichtiensis*.

The palynological data also indicates the Cretaceous/Tertiary boundary lies within the Koorkah unit but the precise position is equivocal. The boundary could lie above 2490m based on the youngest occurrence of *Battenipollis sectilis* and other secondary index species for the *F. longus* Zone, or alternatively deeper, just above youngest occurrence of the primary index species *Forcipites longus* at 2626m. The deeper pick is favour by the author based primarily on the similarity of the log character over the interval 2470 to 2692m to the thicker sections of the Kate Shale in the Gippsland Basin (Partridge, 1999a-b). The anomalous shallower occurrences of the secondary index species in the Koorkah-1 well being interpreted as younger extensions of the species ranges or reworking.

Biostratigraphy

***Forcipites longus* spore-pollen Zone**

Interval: 2677 to 3115 metres

Age: Maastrichtian.

The occurrence of multiple specimens of the eponymous species *Forcipites longus* in the deepest cuttings analysed is considered to be reliable evidence that Koorkah-1 has penetrated sediments no older than Early Maastrichtian. *Forcipites longus* is typically a rare species in assemblages and therefore is not normally recorded as either reworked or caved. The earlier study of Morgan (1986) recorded a similar range for the species from 2626 to 3148m, although it is noted that his deepest record is from the sidewall at 2728m. Similarly, the top of the zone is confidently placed at 2677m on the youngest occurrence of *F. longus* in the cuttings at 2677-80m, or perhaps slightly higher in the cuttings at 2626-35m examined by Morgan (1986). Shallower but less confident tops for the zone could lie at 2560-63m based on the LAD (Last Appearance Datum) of *Battenipollis sectilis*, or even higher at 2491m based on LAD of *Tricolpites confessus* recorded by Morgan (1986). Arguing against these shallower picks is the relative thinness of the *L. balmei* Zone (from ~2250 to 2470m) compared to other wells in the basin centre, and the similarity of the log character between 2470 and 2692m to that of the Kate Shale in the Gippsland Basin (Partridge, 1999a-b). The samples examined at 2560-63m and 2632-35m are therefore designated as undifferentiated *L. balmei* to *F. longus* Zones (Table 1).

Subdivision of the *F. longus* Zone is based on the FAD of *Tripunctisporis maastrichtiensis* which is first recorded at 2959m in a sidewall core by Morgan (1986), and from the shallower cuttings at 2731-34m in this study. Supporting a thick Upper subzone is the frequent to common occurrence of *Gambierina rudata* (average >6%) and mostly low abundances of *Nothofagidites*, which are normally more abundant in the lower subzone. Other key index species diagnostic of the broader zone recorded in the samples are *Grapnelispora evansii* at 2857-60m, and *Proteacidites palisadus, Pseudowinterapollis wahooensis* and *Tricolporites lilliei* at 2953-56m.

Lower *Lygistepollenites balmei* spore-pollen Zone

Interval: 2266 to 2491 metres.

Age: Early Paleocene.

The top of the zone is identified on the LADs of *Gambierina rudata* and *Lygistepollenites balmei* while the base of the zone is placed above the LADs of index species for the *F. longus* Zone. The shallowest sample at 2266-75m could however belong to the Upper *L. balmei* Zone as Morgan (1986) records *Proteacidites grandis*, a key index species for the Upper subzone, from the sidewall core at 2266.5m. The samples also contains the dinocysts *Apectodinium hyperacanthum* and *Diphyes colligerum*, but both are believed to be caved as the dinocyst assemblages is dominated by the non-marine genus *Morkallacysta*. The next deeper cuttings at 2338-41m has a higher confidence zone assignment based on the occurrence of *Polycolpites langstonii* which is not known to range below the upper part of the Lower subzone. The sample at 2488-91m

is probably still within the Lower subzone based on presence of *Haloragacidites harrisii,* but as this species is frequently caved the confidence in the zone assignment is low. Finally, the samples at 2560-63m and 2632-35m could belong to either the Lower *L. balmei* or *F. longus* Zones depending whether the rare occurrences of older index species are interpreted as reworked.

***Morkallacysta* Facies**

Notwithstanding the general low numbers of microplankton in the majority of the counts most assemblages are dominated by the non-marine dinocyst genus *Morkallacysta* originally described by Harris (1974). Although Morgan (1986) referred the specimens he recorded to the type species *Morkallacysta pyramidalis* the specimens recorded in this study have much less pronounced apical and antapical horns than the type species and have been left in open nomenclature pending illustration and description. Those samples were this genus is particularly prominent are referred to the *Morkallacysta* Facies. This facies is considered to be diagnostic of lacustrine depositional environments but does not as yet have demonstrable biostratigraphic significance. The *Morkallacysta* Facies may be more extensive than indicated on Table 1 as a large proportion of the microplankton in a number of the samples are too poorly preserved to be confidently identified.

Most significant of the other microplankton recorded in the samples the were specimens of the algal cyst *Rimosicysta*, which originally was described from Turonian age assemblages (Marshall, 1989) and has been previously been recorded in the Durroon Formation in the Bass (Partridge, 2002a). The occurrences in Koorkah-1 are believed to be a genuine extension in the range of this form and not a product of reworking.

References

FENSOME, R.A., WILLIAMS, G.L., BARSS, M.S., FREEMAN, J.M. & HILL, J.M., 1990. Acritarchs and fossil Prasinophytes: An index to genera, species and infraspecific taxa. *AASP Contribution Series No. 25*, p.1-771.

HARRIS, W.K., 1974 [imprint 1973]. Tertiary non-marine dinoflagellate cyst assemblages from Australia. **In** *Mesozoic and Cainozoic palynology: essays in honour of Isabel Cookson*, J.E. Glover & G. Playford, editors, *Geological Society of Australia Special Publication 4*, p.159-166.

MARSHALL, N.G., 1989. An unusual assemblage of algal cysts from the late Cretaceous, Gippsland Basin, Southeastern Australia. *Palynology 13,* p.21-56.

MORGAN, R., 1986a. Palynology Koorkah-1. Appendix 6 in Well Completion Report, 7p., 1 fig., 2 charts (unpubl.).

PARTRIDGE, A.D., 1973. Revision of the Spore-Pollen Zonation in the Bass Basin. *Esso Australia Ltd Palaeontological Report 1973/4*, 22p. 6pls (2 May).

PARTRIDGE, A.D., 1999a. Late Cretaceous to Tertiary geological evolution of the Gippsland Basin, Victoria. PhD thesis, La Trobe University, Bundoora, Victoria, p.i-xxix, p.1-439, 165 figs, 9 pls (unpubl.).

PARTRIDGE, A.D., 1999b. The Cretaceous/Tertiary boundary in Victoria. *Geological Society of Australia,*

Abstracts no.55, 13th Victorian Universities Earth Science Conferences, The University of Melbourne, September 1999, p.26-27.

PARTRIDGE, A.D., 2002a. Palynological review of Upper Cretaceous units in Durroon-1, Bass Basin. *Biostrata Report 2002/07*, p.1-16.

PARTRIDGE, A.D., 2002b. Bass Basin Palynological Project: Unravelling a Late Cretaceous to Eocene geological history of large palaeolakes, coastal lagoons and marine bays. *Biostrata Report 2002/13*, p.1-36.

STOVER, L.E. & PARTRIDGE, A.D., 1973. Tertiary and late Cretaceous spores and pollen from the Gippsland Basin, southeastern Australia. Proceedings *Royal Society of Victoria, vol.85*, pt.2, p.237-286.

TRAVERSE, A., 1988. *Paleopalynology*. Unwin Hyman Ltd, Boston, p.1-600.

WILLIAMS, G.L., LENTIN, J.K. & FENSOME, R.A., 1998. The Lentin and Williams index of fossil dinoflagellates 1998 edition. *American Association of Stratigraphic Palynologists, Contributions Series, no. 34*, p.1-817.

Table 1. Interpretative Palynological Data from Koorkah-1

No.	Sample Type	Depth Metres	Sample Origin	Spore-Pollen Zone	CR*	Microplankton Zone	CR*	Key Index Species	Palaeoenvironment
1	Cuttings	2266-75	GA-2	Lower *L. balmei*	D4	*Morkallacysta* Facies		LAD of *Gambierina rudata*	Lacustrine - brackish
2	Cuttings	2338-41	GA-2	Lower *L. balmei*	D1	*Morkallacysta* Facies		FAD of *Polycolpites langstonii*	Lacustrine - fresh
3	Cuttings	2488-91	GA-2	Lower *L. balmei*	D4				Lacustrine - fresh
4	Cuttings	2560-63	GA-2	*L. balmei/F. longus*	D5	*Morkallacysta* Facies		LAD of *Battenipollis sectilis*	Lacustrine - fresh
5	Cuttings	2632-35	GA-2	*L. balmei/F. longus*	D6	*Morkallacysta* Facies			Lacustrine - fresh
6	Cuttings	2677-80	GA-2	Upper *F. longus*	D1	*Morkallacysta* Facies		LAD of *Forcipites longus*	Lacustrine - fresh
7	Cuttings	2731-34	GA-2	Upper *F. longus*	D1			FAD of *Tripunctisporis maastrichtiensis*	Lacustrine - fresh
8	Cuttings	2857-60	GA-2	Upper *F. longus*	D1			*Grapnelispora evansii* present	Deltaic - Lacustrine
9	Cuttings	2953-56	GA-2	Upper *F. longus*	D4			FAD of common *Gambierina rudata*	Deltaic - Lacustrine
10	Cuttings	3022-25	GA-2	Lower *F. longus*	D1	*Morkallacysta* Facies?			Lacustrine - fresh
11	Cuttings	3112-15	GA-2	Lower *F. longus*	D1			FAD of *Forcipites longus*	Deltaic - Lacustrine

ABBREVIATIONS

*CR = Confidence Ratings

LAD = Last Appearance Datum

FAD = First Appearance Datum

GA-2 = Samples collected Stage-2 Work program

CONFIDENCE RATINGS

Alpha Code Linked to Sample

A = Core

B = Sidewall core

C = Coal cuttings

D = Ditch cuttings

J = Junk basket

Numeric Code Linked to Palynomorph Assemblage

1 = Excellent confidence: High diversity assemblage **plus** key zone species.

2 = Good confidence: Moderately diverse assemblage **plus** key zone species.

3 = Fair confidence: Low diversity assemblage **plus** key zone species.

4 = Poor confidence: Moderate to high diversity **minus** key zone species.

5 = Very low confidence: Low diversity assemblage **minus** key zone species.

Table 2. Basic Palynological Data from Koorkah-1

No.	PalLab Spl.No.	Sample Type	Top Metres	Base Metres	Visual Yield	Palynomorph Concentration	Palynomorph Preservation	No. SP Species	No. MP Species	Marine MP%	Other MP%	NED	Noth%	Gamb%
1	6406878	Cuttings	2266	2275	Moderate-High	High	Very poor	45	4	<2%	<3%	23%	8%	2%
2	6406879	Cuttings	2338	2341	Moderate-High	Moderate-high	Very Poor	33	2		<2%	44%	7%	2%
3	6406880	Cuttings	2488	2491	Moderate-High	Moderate-high	Poor	34	4		<2%	30%	3%	8%
4	6406881	Cuttings	2560	2563	Moderate-High	Moderate-high	Very poor	31	6		9%	38%	3%	7%
5	6406882	Cuttings	2632	2635	Moderate-High	High	Very poor	32	3		<1%	31%	2%	9%
6	6406883	Cuttings	2677	2680	Moderate-High	Moderate	Very poor	30	3		4%	42%	1%	7%
7	6406884	Cuttings	2731	2734	Moderate-High	Moderate-high	Very poor	32	1		3%	36%	5%	4%
8	6406885	Cuttings	2857	2860	Moderate-High	Moderate	Very poor	34	3		2%	18%	17%	4%
9	6406886	Cuttings	2953	2956	Moderate-High	High	Very very poor	32	4		6%	18%	8%	10%
10	6406887	Cuttings	3022	3025	Moderate-High	High	Very very poor	32	4		27%	28%	5%	6%
11	6406888	Cuttings	3112	3115	Moderate-High	Moderate	Very poor	29	1		2%	13%	20%	4%

ABBREVIATIONS

MP = Microplankton

SP = Spore-Pollen

NED = Neves Effect based on *Dilwynites/Araucariacites* Percentage

Noth% = Percentage of *Nothofagidites* in SP count.

Gamb% = Percentage of *Gambierina rudata/edwardsii* in SP count.

Table 3. Basic Sample Data from Koorkah-1

No.	SAMPLE TYPE	DEPTH Metres	Weight Grams	LITHOLOGY	SAMPLE TEXTURE
1	Cuttings	2266-75	17.0	SHALE: medium grey	Powder to fine
2	Cuttings	2338-41	18.0	SHALE: medium grey	Powder to medium
3	Cuttings	2488-91	17.0	SHALE: medium grey	Powder to medium
4	Cuttings	2560-63	17.5	SHALE: medium grey	Powder to medium
5	Cuttings	2632-35	18.5	SHALE: medium grey	Powder to medium
6	Cuttings	2677-80	20.5	SHALE: medium grey	Powder to medium
7	Cuttings	2731-34	23.7	SHALE 60%: medium-dark grey; SANDSTONE 40%: white, fine-grained.	Powder to medium
8	Cuttings	2857-60	27.7	SHALE 40%: medium grey; SANDSTONE 60%: white, fine-grained.	Powder to medium
9	Cuttings	2953-56	20.5	SHALE 70%: medium grey; SANDSTONE 30%: white, fine-grained.	Powder to medium
10	Cuttings	3022-25	20.4	SHALE 50%: medium grey; SANDSTONE 50%: white, fine-grained.	Powder to medium
11	Cuttings	3112-15	23.4	SHALE 80%: light-medium grey; SANDSTONE 20%: light-grey.	Powder to medium

Table 4. Abundances of major palynomorph groups from Koorkah-1.

No.	Depth Metres	Sample Type	Glecheniidites & Clavifera spores	ALL OTHER spores	Dilwynites & Araucariacites pollen	ALL OTHER gymnospoerm pollen	Nothofagidites spp.	Gambierina spp.	ALL OTHER angiospoerm pollen	**SPORE-POLLEN TOTAL**	Total fungal microfossils	Reworked Spore-Pollen	**TOTAL TERRESTRIAL SUM**		**SPORE-POLLEN TOTAL**	**MICROPLANKTON TOTAL**	SP + MP COUNT
1	2266-75	Cuttings	12%	14%	23%	18%	8%	2%	12%	90%	10%	0.4%	252		95%	4.6%	238
2	2338-41	Cuttings	4%	16%	44%	19%	7%	2%	6%	98%	2%	0.4%	256		98%	1.6%	255
3	2488-91	Cuttings	3%	9%	30%	32%	3%	8%	15%	98%	2%		262		98%	1.5%	262
4	2560-63	Cuttings	1%	15%	38%	15%	3%	7%	16%	95%	5%		245		91%	9.0%	256
5	2632-35	Cuttings	2%	9%	31%	30%	2%	9%	12%	95%	5%	0.4%	264		99%	0.8%	253
6	2677-80	Cuttings	0.4%	18%	42%	16%	1%	7%	13%	98%	2%	0.4%	248		96%	4.3%	253
7	2731-34	Cuttings	1%	14%	36%	14%	5%	4%	22%	96%	4%	0.4%	245		97%	2.9%	241
8	2857-60	Cuttings	1%	13%	18%	25%	17%	4%	19%	98%	2%	1%	240		98%	2.1%	239
9	2953-56	Cuttings	2%	18%	18%	22%	8%	9%	15%	91%	9%	1%	194		94%	6.4%	188
10	3022-25	Cuttings	1%	16%	28%	18%	5%	5%	20%	94%	6%		153		73%	26.9%	197
11	3112-15	Cuttings	2%	20%	13%	21%	20%	4%	15%	95%	5%		260		98%	2.4%	254

Table 5. Koorkah-1 - spore-pollen distribution

No.	Depth Metres	Sample Type	SPORES SPECIES	Ariadnaesporites sp.	Baculatisporites spp.	Camarozonosporites apiculatus ms	Cicatricosisporites spp.	Clavifera triplex	Cyathidites spp. large >40µm	Cyathidites spp. small <40µm	Dictyophyllidites spp.	Foraminisporis asymetricus	Foveotriletes balteus	Gleicheniidites circinidites	Grapnelispora evansii	Herkosporites elliottii	Laevigatosporites major	Laevigatosporites ovatus	Latrobosporites spp.	Latrobosporites amplus	Marattisporites scabratus	Osmundacidites wellmanii	Peromonolites densus
1	2266-75	Cuttings			1.3%			X	0.4%	4.8%			X	13.7%				0.9%	0.4%	X	0.4%		X
2	2338-41	Cuttings			0.8%			0.4%	0.4%	4.4%	0.8%			3.2%		X		2.0%		X			0.8%
3	2488-91	Cuttings			0.4%			0.4%		2.3%	0.8%			2.7%		1.2%		1.2%		X			
4	2560-63	Cuttings			1.7%				1.3%	2.1%	1.3%			0.9%		0.4%		1.3%					
5	2632-35	Cuttings			0.4%	X				0.8%	X			2.0%		1.2%		1.2%				0.4%	
6	2677-80	Cuttings		X	1.7%				0.4%	2.5%				0.4%		3.7%		0.8%		X		0.8%	
7	2731-34	Cuttings			2.6%				X	1.3%				0.9%		3.0%	X	1.7%		X		0.4%	
8	2857-60	Cuttings			0.9%				0.9%	2.6%		X		0.9%	0.4%	0.9%		1.3%	0.4%	X			
9	2953-56	Cuttings			X				0.6%	4.5%				1.7%		3.4%	X	1.1%	1.1%	X	0.6%	X	
10	3022-25	Cuttings			3.5%		X		0.7%	2.1%	1.4%			1.4%		0.7%		1.4%	0.7%	X			
11	3112-15	Cuttings			1.2%				1.6%	9.7%				2.4%		0.8%		0.8%	1.2%	X	0.4%	0.4%	

ABBREVIATIONS

X = Present

% = Percentage

Table 5. Koorkah-1 - spore-pollen distribution

No.	Depth Metres	Sample Type	Perotrilites spp.	Retitriletes spp.	Rugulatisporites mallatus	Stereisporites antiquisporites	Stereisporites regium	Stereisporites viriosus	Trilete spores undiff.	Triporoletes spp.	Tripunctisporis maastrichtiensis	TOTAL SPORES		**GYMNOSPERM SPECIES**	Gymnosperm pollen undiff.	Araucariacites australis	Cupressacites sp.	Dacrycarpites australiensis	Dilwynites granulatus	Dilwynites tuberculatus	Lygistepollenites balmei	Lygistepollenites florinii	Microalatidites paleogenicus
1	2266-75	Cuttings	X	0.4%		5.3%			1.8%		X	30%				4.4%	4.4%		22%	X	0.4%	0.9%	0.4%
2	2338-41	Cuttings		0.4%	X	4.0%			2.4%		0.4%	20%				5.2%	2.8%		40%	X	0.8%	0.8%	
3	2488-91	Cuttings		X		2.7%			0.4%		X	12%				2.3%	3.9%		28%	X		X	0.4%
4	2560-63	Cuttings		X	0.4%	5.6%			1.3%		X	16%				10.7%	1.3%		30%			0.4%	
5	2632-35	Cuttings	X	1.2%		2.0%	1.2%		1.6%		X	12%				3.2%	6.4%	X	30%		0.4%	X	
6	2677-80	Cuttings	X	1.2%		4.5%	X	X	2.5%			19%				20.2%	2.9%		23%		0.4%		
7	2731-34	Cuttings	X	1.7%		0.9%	0.4%		2.1%		0.9%	16%				17.9%	X		19%	X	0.4%		
8	2857-60	Cuttings	1.3%	1.7%		1.3%			1.7%	0.4%		15%				7.7%	0.4%	0.4%	11%		X		
9	2953-56	Cuttings	0.6%	1.7%		2.3%	1.7%		1.7%			21%				6.3%	1.7%		13%		0.6%		
10	3022-25	Cuttings	1.4%	1.4%		3.5%			0.7%			19%				1.4%	4.9%		28%		0.7%		
11	3112-15	Cuttings		0.4%		1.2%			2.8%	0.8%		24%			0.4%	3.2%	2.4%		10%		0.4%	0.4%	

ABBREVIATIONS

X = Present

% = Percentage

Table 5. Koorkah-1 - spore-pollen distribution

No.	Depth Metres	Sample Type	Microcachryidites antarcticus	Phyllocladidites mawsonii	Phyllocaldidites verrucosus	Podocarpidites spp.	Trichotomosulcites subgranulatus	TOTAL GYMNOSPERM POLLEN		**ANGIOSPERM SPECIES**	Angiosperm pollen undiff.	Australopollis obscurus	Battenipollis sectilis	Beaupreaidites orbiculatus	Dicotetradites clavatus	Forcipites longus	Gambierina rudata/edwardsii	Haloragacidites harrisii	Liliacidites spp.	Malvacipollis subtilis	Myrtaceidites parvus/mesonesus	Nothofagidites brachyspinulosus	Nothofagidites emarcidus
1	2266-75	Cuttings	0.4%	4.8%		7%	1.3%	46%				0.4%					1.8%	0.4%		0.4%	0.4%	2.2%	4.4%
2	2338-41	Cuttings		6.0%		8%	0.8%	64%			0.8%						2.4%	X				1.6%	2.4%
3	2488-91	Cuttings	0.8%	8.5%		17%	1.9%	63%							0.4%		7.8%	X	0.8%				
4	2560-63	Cuttings	0.4%	6.0%		7%	0.4%	56%			0.9%		0.4%	X			6.9%						
5	2632-35	Cuttings	0.8%	8.0%	0.8%	12%	2.4%	64%									9.2%	0.4%				0.4%	
6	2677-80	Cuttings	1.2%	4.5%		5%	1.7%	60%			0.8%					X	7.4%						
7	2731-34	Cuttings	0.4%	7.7%		5%	0.9%	52%			2.1%		1.3%				3.8%						
8	2857-60	Cuttings	0.9%	10.7%		10%	3.0%	44%			1.7%		1.7%				4.3%						
9	2953-56	Cuttings	0.6%	3.4%		16%	1.7%	43%			0.6%		1.1%				9.7%						
10	3022-25	Cuttings	0.7%	1.4%		10%	1.4%	49%					X			X	5.6%						
11	3112-15	Cuttings	0.4%	1.6%		14%	2.4%	35%			0.8%					1.2%	4.0%						

ABBREVIATIONS

X = Present

% = Percentage

Table 5. Koorkah-1 - spore-pollen distribution

No.	Depth Metres	Sample Type	Nothofagidites endurus	Nothofagidites flemingii	Nothofagidites senectus	Peninsulapollis gillii	Periporopollenites polyoratus	Polycolpites langstonii	Proteacidites spp.	Proteacidites clinei ms	Proteacidites palisadus	Pseudowinterapollis wahooensis	Tetracolporites verrucosus	Tetradopollis securus ms	Tricolp(or)ates spp.	Tricolpites waiparaensis	Tricolporites lilliei	Tricolporites marginatus ms	Triporopollenites spp.	TOTAL ANGIOSPERM POLLEN	**TOTAL spore-pollen COUNT**
1	2266-75	Cuttings	2.6%	X		1.3%	0.4%		8%						X				1.8%	25%	227
2	2338-41	Cuttings	3.2%			1.2%	0.4%	0.4%	3%						0.4%					16%	251
3	2488-91	Cuttings	1.9%		0.8%	5.0%			6%						2.3%				0.4%	25%	258
4	2560-63	Cuttings	3.0%		0.4%	5.6%			6%				0.4%		2.1%			X	1.3%	27%	233
5	2632-35	Cuttings	X		2.0%	2.0%			8%						2.4%					24%	251
6	2677-80	Cuttings	X		1.2%	3.7%			7%	0.4%					X				0.8%	22%	242
7	2731-34	Cuttings	4.3%		1.3%	4.3%			12%				0.4%		2.6%				0.9%	32%	234
8	2857-60	Cuttings	2.1%		15.0%	3.8%			9%					0.4%	0.9%	0.9%	0.4%		0.4%	41%	234
9	2953-56	Cuttings	6.3%		2.8%	4.5%			9%		X	0.6%			X	1.1%	X			36%	176
10	3022-25	Cuttings	1.4%		3.5%	5.6%			13%						2.8%	0.7%				32%	144
11	3112-15	Cuttings	2.4%		18.5%	1.2%			10%						2.8%				0.4%	41%	248

ABBREVIATIONS

X = Present

% = Percentage

Table 6. Koorkah-1 - microplankton and fungal distribution

No.	Depth Metres	Sample Type	MICROPLANKTON	ACRITARCHS & ALGAE	Micrhystridium spp.	Amosopollis cruciformis	Botryococcus braunii	Circulosporites parvus	Debarya sp.	Lecaniella sp.	Pediastum sp.	Sigmopollis carbonis	Rimosicysta sp.	DINOCYSTS	Dinocysts undiff.	Apectodinium hyperacanthum	Cleistosphaeridium spp.	Diphyes colligerum	Horologinella n.sp.	Morkallacysta spp.	TOTAL MP COUNT		Fungal spores & hyphae	Fungal fruiting bodies	Fungal germlins	Persavis sp.	REWORKED spores & pollen
1	2266-75	Cuttings													26%	5%		5%		63%	19		X	X	X		X
2	2338-41	Cuttings													50%		25%			25%	4		X				X
3	2488-91	Cuttings			25%	X	25%		25%											25%	4		X			X	
4	2560-63	Cuttings				X		X		X	5%				68%					26%	19		X	X			
5	2632-35	Cuttings				40%							X		20%					40%	5		X	X		X	X
6	2677-80	Cuttings					8%					8%			42%				8%	33%	12		X				X
7	2731-34	Cuttings					14%								86%						7		X				X
8	2857-60	Cuttings										20%			20%					60%	5		X				X
9	2953-56	Cuttings					8%					8%	X		85%					X	13		X				X
10	3022-25	Cuttings										6%	2%		70%		2%			21%	53		X				
11	3112-15	Cuttings													67%					33%	6		X				

ABBREVIATIONS

X = Present

% = Percentage

APPENDIX C6.

Quantitative palynological analysis of Eastern View and Demons Bluff Groups in Poonboon-1, Bass Basin.

by

Alan D. Partridge

Biostrata Pty Ltd
A.B.N. 39 053 800 945

Biostrata Report 2002/11

30th June 2002

Quantitative palynological analysis of Eastern View and Demons Bluff Groups in Poonboon-1, Bass Basin

by Alan D. Partridge

Introduction

A quantitative palynological study of the Eastern View and basal Demons Bluff Groups in Poonboon-1 has been undertaken as a component of the Bass Basin Palynological Project coordinated by Geoscience Australia as part of the Western Tasmania Regional Minerals Program Offshore Collaborative Project, between Mineral Resources Tasmania, Geoscience Australia and the National Centre for Petroleum Geology and Geophysics to investigate aspects of the hydrocarbon prospectivity of the Bass and Sorell Basins.

This new palynological study of the Poonboon-1well was initiated to **1)** establish a quantitative reference section for the palynological succession from Late Cretaceous to Miocene in the central part of the Bass Basin, **2)** help quantify the distribution, abundance and diversity of marine and non-marine dinocysts and other microplankton in the basin, to aid in mapping the geographic and temporal extend of lacustrine and marine palaeoenvironments, and **3)** document the presence and distribution of Neves effects within the terrestrial spore-pollen assemblages, as supporting palynological evidence for the presence of large palaeolakes and lagoons. The early Poonboon-1 well (spudded in 1972), was chosen because it was known to contain well-preserved microfloras and some of the best sidewall core sampling of all the wells in the basin, and was also believed to be unaffected by any volcanic intrusion, which disrupt the quality of the palynological successions in many of the other wells. In addition, relinquished palynological slides were available from the well and were immediately accessible. The interval reviewed in the well represents an essentially complete sequence from the latest Maastrichtian to Late Oligocene (Upper *F. longus* to Middle *P. tuberculatus* Zones). Although it was known beforehand that both the spore-pollen and microplankton assemblages were worthy of full systematic description and illustration, such documentation was not the intent of this new study, and unfortunately was also beyond the scope of the overall project.

Materials and Methods

Assemblage counts were performed on 65 samples and species lists were recorded for another eight samples from which the original palynological slides were either unsuitable or unavailable for quantitative analysis. Most of the material examined is derived from the relinquished palynological slides prepared in the now closed laboratory operated by Esso Australia Ltd and were originally studied by Partridge (1972). Materials re-examined from this original collection consists of 39 sidewall cores, 6 conventional core and 6 cuttings samples. The density of samples in some of the poorly sampled intervals in this early collection was improved by a new collection of an additional sample from conventional core-2 and 13 cuttings (GA-2 samples on Table 1). These samples were collected by the author from the core library at Geoscience Australia and processed at their palynological laboratory. The assemblages counts on most of the new samples were performed by Dr Michael Macphail. An average of 265 specimens of both terrestrial and

aquatic palynomorphs were counted per sample.

The palynological zones assigned to the samples, zone Confidence Ratings, key defining species and interpreted palaeoenvironments are provided in Table 1. Basic palynological data on organic residue yields, palynomorph concentrations in the residues, palynomorph preservation and species diversity in the samples are provided in Table 2. Species abundance and range data are provided in Tables 3 to 5. Author citation for spore-pollen species can be principally sourced for published species from Stover & Partridge (1973, 1982), or Helby *et al.* (1987), while many of the manuscript species can be found in Partridge (1973). Author citation for dinocysts can be sourced from Williams *et al.* (1998), and for acritarchs, algal cysts and other microplankton from Fensome *et al.* (1990).

Geological Discussion

The interval studied in Poonboon-1 has a thickness of 2030 metres extending from the bottom hole core at 3259 to 3266m to a sidewall core at 1233.2m, and ranges in age from latest Maastrichtian (Upper *F. longus* Zone) to Late Oligocene or possibly Early Miocene (Middle *P. tuberculatus* Zone or younger). The stratigraphic sequence analysed consists of 1272 metres of the Eastern View Group (containing 53 samples at an average spacing of 24 metres), all of the 590 metres thick Demons Bluff Group (containing 18 samples at an average spacing of 35 metres) and the basal 171 metres of the Torquay Group (containing just two samples at an average spacing of >85 metres).

The older Eastern View Group succession commences with interpreted fresh-water lacustrine shales at 3107-3140m and 3205-3245m near the bottom of the well. These shales represents the most southerly known extent of interbeds or tongues of the lacustrine Koorkah unit proposed by Partridge (2002d). The latter unit has been more fully analysed in Konkon-1 and Koorkah-1 (Partridge, 2002a-b). The remaining overlying Eastern View Group is comprised of 1113 metres of mixed sandstones, shales and coals (from 1994 to 3107m) that can be subdivided between the Narimba, Cormorant and Poonboon units proposed in Partridge (2002d). A predominantly lower coastal plain or deltaic depositional environment is indicated by the consistent presence of thin coal seams, and sporadic incursions of marine dinocysts. A total of 65 thin coal seams, from <1 to ~3 metres thick, with an average spacing ~19 metres, are evident on the sonic log. The coal seams are relatively widely spaced through the Paleocene to basal Early Eocene (*L. balmei* to Lower *M. diversus* Zones) and again through the Middle Eocene (Lower *N. asperus* Zone), and most closely spaced in the late Early Eocene (Middle *M. diversus* to *P. asperopolus* Zones).

The occurrences of non-marine and marine dinocysts through the Eastern View Group confirms the presence of short duration lacustrine, lagoonal and paralic palaeoenvironments. The most significant of these events are:

1. Non-marine dinocysts referred to the genus *Morkallacysta* Harris 1974 are recorded from the thicker shales (3107-3140m and 3205-3245m) near the bottom of the well that are associated with the most

prominent Neves effects. These shales are interpreted to be tongues of the lacustrine Koorkah facies extending into the southeastern part of the basin during episodes of maximum lake level.

2. Marine dinocysts recorded from sidewall cores that are diagnostic of the *Apectodinium reburrus* Acme Zone (2678.6m) and the succeeding *Apectodinium hyperacanthum* Zone (at 2651.8m). These zones represent the first major marine incursion into the Bass Basin at the time of the late Paleocene thermal maximum (LPTM), and have also been recorded in Konkon-1 (Partridge, 2002a)
3. Sporadic occurrences of the *Apectodinium homomorphum* Zone in the Lower and Middle *M. diversus* Zones. The older assemblage from a sidewall core at 2529.8m has an microplankton (MP) abundance of 3% and a low diversity of 5+ species. The younger from core-2 at 2472.5m has an MP abundance of 43% with a moderate diversity of 11+ species. The latter is tentatively correlated with the dinocyst assemblages recovered from between 1347.5 and 1352.4m in core-1 in Konkon-1 (Partridge, 2002a). With more detailed study these horizons could potentially be linked to microplankton flooding events within the Dilwyn Formation in the Otway Basin.
4. Sporadic occurrences of dinocysts diagnostic of the *Homotryblium tasmaniense* Zones are found through the Upper *M. diversus* and *P. asperopolus* Zones. Although both abundance and diversity are low (<6% and <5 species per sample) they nevertheless confirm that diluted marine influence had extended across most of the basin during the Early Eocene.

Prominent or strong Neves effects in the associated spore-pollen assemblages from the Eastern View Group were only recorded from distinctive shale (Koorkah unit) at the bottom of the well sampled between 3223.9 and 3262.3m. In the conventional and sidewall core samples from this section the combined abundance of the gymnosperm pollen *Dilwynites granulatus*, *D. tuberculatus* and *Araucariacites australis* have an average of 35% (referred to as the NED% in Table 2). This abundance spike is interpreted as a Neves effect, which is the tendency for certain more buoyant spores or pollen to have greater relative abundances in sediments deposited in more distal marine or lacustrine environments (Traverse, 1988; Partridge, 2002d). In the Bass Basin the joint occurrence in the thicker shales of non-marine dinocysts associated with strong Neves effects in the spore-pollen assemblages is interpreted to indicate distal lacustrine depositional environments for those shales (Partridge, 2002d). Weak Neves effects, represented by NED% of approximately 20% are also postulated to occur in the shale sampled (in ascending order) by the sidewall cores at 3116.9m, 2651.8m to 2678.6m, and core-2 at 2472.5m. Each of these events has associated peaks in the abundance or diversity of marine or non-marine dinocysts. The lower NED% being interpreted to indicate a somewhat more proximal environment of deposition within the palaeolake or lagoon.

The younger Demons Bluff Group succession can be subdivided into the 102 metre thick Boonah Formation (from 1892 to 1994m), the 137 metres thick Anglesea Formation (from 1755 to 1892m), and a 351 metre thick section assigned to an undifferentiated interval equivalent to both the Addiscot and Angahook Formation (from 1404 to 1755m). The use of these formation names follows the recent revision of the Demons Bluff Group in the adjacent Torquay Sub-basin by Holdgate *et al.* (2001). In contrast to the Eastern

View Group marine dinocysts are consistently recorded from the Late Eocene to Early Oligocene sediments of the Demons Bluff Group. Although the microplankton abundance (range <1% to 26%, average 7%) and diversity (range 1 to 11, average <6 species per sample) are both low the total recorded diversity through the section is >30 species (Table 5), and could easily be double that if greater effort was applied to the study of the microplankton. This consistent presence of marine dinocysts and lack of coals through the Demons Bluff Group indicates a markedly different depositional regime compared to the older Eastern View Group. Commencing with the Boonah Formation it is suggested that there is a progressive change in the deposition environments from estuarine to bay facies in the Anglesea Formation and then to a marginal marine sea in the younger formations. Surprisingly, even though palaeogeographic mapping indicates that the Anglesea and succeeding Addiscot/Angahook Formations represent large bays or marginal seas there is no obvious Neves effects observed in the spore-pollen assemblages (average NED% is <4%). The rise in abundance of *Nothofagidites* pollen to >50% of the spore-pollen could partly account for this as *Nothofagus* forests may have replaced the Araucariaceae forests (which produced the *Dilwynites* and *Araucariacites* pollen), as the dominant component of the hinterland vegetation.

At the top of the stratigraphic succession is the 1315m thick and carbonate-rich Torquay Group (from seafloor to 1404m) representing open marine sediments. Deposition of this unit could only have commenced after the Bass Strait became a through going marine seaway. Only two samples from the base of this unit were analysed, although significant caved sediments are also present in the underling cuttings at 1551-70m (Table 1). The assemblages examined contain abundant marine dinocysts (>25% of count) which are consistent with deposition in an open marine environment.

Biostratigraphy

Upper *Forcipites longus* spore-pollen Zone
Interval: 3223.9 to 3262.3 metres
Age: Late Maastrichtian.

The youngest Cretaceous spore-pollen zone is confidently identified in the bottom ~40 metres of Poonboon-1 but could potentially extend another ~160 metres higher through the interval 3066 to 3183.6m, which contain assemblages transitional with overlying *L. balmei* Zone. The presence of the distinctive spore *Tripunctisporis maastrichtiensis* in the bottom hole core confirms that the well did not penetrate deeper than the Upper *F. longus* Zone, while the LADs (Last appearance Datums) of *Ornamentifera sentosa*, *Quadraplanus brossus* and *Tricolporites lilliei* in the bottom core sample, *Grapnelispora evansii* and *Battenipollis sectilis* in the SWC at 3247.3m, and *Proteacidites reticuloconcavus* ms slightly higher in the SWC at 3223.9m confirms an age no younger than the zone following the latest revision by Partridge (1999). The possibility that the zone might extend higher is based on the shallower occurrences of *Nothofagidites senectus* to 3183.6m, and *Proteacidites clinei* ms and *Tricolpites waiparaensis* in core-4 at 3024.2m where they overlap with the FAD (First Appearance Datum) of *Haloragacidites harrisii* an index species for the *L. balmei* Zone.

Unfortunately, the assemblages in this transition interval are poorly preserved and not particularly diverse making confident zone assignments difficult. The samples between 3066 and 3183.6m are therefore given a composite *F. longus/L. balmei* Zone assignment pending more detailed study.

The sidewall cores at 3223.9m and 3233.3m contain common non-marine dinocysts that are assigned to the *Morkallacysta* facies which has also been recorded from similar age sediments in Koorkah-1 (Partridge, 2002b). These dinocysts are considered to be representative of lacustrine deposition but have not yet proved to be of biostratigraphic significance.

***Lygistepollenites balmei* spore-pollen Zone**
Interval: 2678.6 to 3042.2 metres
Age: Paleocene.
The suite of six conventional and sidewall core samples and ten cuttings samples can all be assigned to the broad *L. balmei* Zone on the consistent presence of the eponymous species (average <1%). The bottom of the zone is picked at the FAD of *Haloragacidites harrisii* while the top of the zone picked at the mutual extinctions or LADs of *Gambierina rudata, Nothofagidites endurus* and *Stereisporites regium.* In addition, the species *Lygistepollenites balmei* and *Australopollis obscurus* are last recorded from the basal sample of the Lower *M. diversus* Zone. This range extension of the last two species has traditionally been interpreted as reworking (eg. Partridge, 1973).

The Upper and Lower subdivision of the *L. balmei* Zone proposed by Partridge (1973) can be recognised but not the more detailed five-fold subdivision recently proposed in the Gippsland Basin by Partridge (1999). The lack of success in distinguishing the latter subdivisions is attributed to the rarity of the critical index species in the poorly preserved assemblages and limited number of core and sidewall cores available through the >400 metre thick zone. Unfortunately, all subdivisions of the zone are based primarily on FADs making them difficult to apply in cuttings. The top of the Lower *L. balmei* Zone is picked at 2737-40m on the LAD of *Tetracolporites verrucosus*, but it should be noted that the species is inconsistent and very rare through the zone, and as well this particular cuttings sample is also badly contaminated by caved Early Eocene species. The base of the overlying Upper *L. balmei* Zone is confidently identified in conventional core-3 by the oldest occurrences in the core samples of the species *Cupanieidites orthoteichus*, *Proteacidites grandis*, *P. incurvatus* and *Matonisporites* (al. *Cyathidites*) *gigantis*. The zone may extend to the next deeper cuttings but confidence in that assignment is low because of the likelihood of cavings.

Microplankton are represented through the *L. balmei* Zone by the sporadic occurrences of non-marine acritarchs, algae, and dinocysts (Table 5). The only reliable marine assemblage recorded is the occurrence of the *Apectodinium reburrus* Acme Zone in the sidewall core at 2678.6m, which is dominated by the eponymous species.

***Malvacipollis diversus* spore-pollen Zone**

Interval: 2362 to 2651.8 metres

Age: Latest Paleocene to Early Eocene.

A suite of 12 conventional and sidewall core samples, and three cuttings samples are assigned to the board *M. diversus* Zone. The assemblages are characterised by the consistent presence of *Haloragacidites harrisii* pollen (range <1% to 19%), and rare to common *Malvacipollis diversus* and *M. subtilis*. The Lower, Middle and Upper subzones are distinguished by the oldest and youngest occurrences of key species.

The base of the Lower *M. diversus* Zone is picked at 2651.8m on the FADs of *Spinizonocolpites prominatus* and *Crassoretitriletes vanraadshooveni*, while the most reliable pick for the top of the zone is at 2529.8m based on the LADs of *Matonisporites gigantis* and *Peninsulapollis gillii*, even though the zone could extend as high as the overlying less diagnostic sample at 2514.6m.

The base of the Middle *M. diversus* Zone is most confidently place at 2474.4m in core-2, based on the FAD of the principal index species *Proteacidites tuberculiformis*, although the zone could extend slightly deeper into the underlying cuttings (Table 1). The top of the zone is placed below the oldest occurrence of the index species for the overlying Upper *M. diversus* Zone, which are the FAD of *Myrtaceidites tenuis* in the cuttings at 2408-17m and the FAD of *Proteacidites pachypolus* in the next sidewall core at 2377.4m. The top of this subzone and the *M. diversus* Zone is placed at the sample below the incoming of index species of the *P. asperopolus* Zone.

Sporadic occurrences of marine microplankton occur through the *M. diversus* Zone. At 2651.8m from the base of the interval the *Apectodinium hyperacanthum* Zone is identified by the common occurrence of the eponymous species. In the sidewall core at 2529.8m and in the new sample from core-2 at 2427.5m the revised *Apectodinium homomorphum* Zone of Partridge (1999) is likewise identified on the presence of the eponymous species. The palynomorph assemblage from the latter sample is interesting because organic microforaminiferal liners are recorded associated with the marine dinocysts. Finally, from the cuttings at 2408-17m is assigned to the *Homotryblium tasmaniense* Zone of Harris (1985) based on the FAD of the eponymous species.

***Proteacidites asperopolus* spore-pollen Zone**

Interval: 2225 to 2317.1 metres

Age: Early Eocene.

The assemblages from the *P. asperopolus* Zone are characterised by highly diverse assemblages (typically >50 species per sample) containing common *Nothofagidites* (average 18%), *Haloragacidites harrisii* (average 13%), *Proteacidites* (average 17%), tricolpate/tricolporate pollen (average 17%) and *Myrtaceidites* (average 8%). The base of the zone is picked at 2317.1m on the FADs of *Proteacidites asperopolus* and *Conbaculatisporites apiculatus* ms, while the top of the zone is picked at the LADs of *Myrtaceidites tenuis* at

2225m and *Intratriporopollenites notabilis* in the underlying sidewall core at 2237.2m. No significant abundances or species of microplankton were recorded from this zone.

Lower *Nothofagidites asperus* spore-pollen Zone

Interval: 2009 to 2194.6 metres

Age: Middle Eocene.

The Lower *N. asperus* Zone is identified by the marked increase in the abundance of *Nothofagidites* pollen (average 35%) and decline in *Haloragacidites harrisii* (average 6%). The gymnosperm pollen *Phyllocladidites mawsonii* also becomes more common (range 4% to 19%, average 9%), compared to average abundance of <1% in the underlying zone. Index species supporting these gross assemblage changes are the FADs of *Matonisporites ornamentalis* at 2194.6m, *Tricolpites simatus* at 2047.6m, and *Proteacidites reflexus* at 2011.7m. Relative to the Gippsland Basin succession the FADs of *Nothofagidites vansteenisii* at 2047.6m, and *N. falcatus* at 1935.5m are both delayed. The top of the Lower subzone is placed at the sample below the incoming of index species for the Middle *N. asperus* Zone. No significant abundances or species of dinocysts were recorded from this zone.

Middle *Nothofagidites asperus* spore-pollen Zone

Interval: 1801.4 to 1988.8 metres

Age: Late Eocene.

The Middle *N. asperus* Zone shows similar gross characteristics to the Lower subzone, although *Nothofagidites* pollen is much more dominant (average 47%), and *Haloragacidites harrisii* very much secondary (average 8%). Also, with the cessation of coal deposition at the top of the Lower *N. asperus* Zone the gymnosperm pollen *Phyllocladidites mawsonii* is much less prominent (range 1% to 5%, average 2%). The zone is identified on the total range of the primary index species *Triorites magnificus* which is recorded from four of the seven samples. Other important markers are the FAD of *Proteacidites rectomarginis* at 1859.3m and the LADs of *Anacolosidites sectus* and *Proteacidites pachypolus* in the shallowest sample assigned to the zone.

Marine microplankton occur in all samples in the zone, varying in abundance from <1% to 26% (average 8%) of the combined SP and MP count (Table 3). Unfortunately recorded diversity in the standardised counts and slide scanning employed in this study only recorded a low average diversity of <5 species per sample (Table 2), and consequently the assemblages could not be confidently assigned to established zones. Although I am confident more diverse assemblages could be extracted by examining more microscope slides per sample, this could not be accomplished in the time allocated to the project.

Upper *Nothofagidites asperus* spore-pollen Zone

Interval: 1600.2 to 1767.8 metres

Age: Latest Eocene? to Early Oligocene.

The Upper *N. asperus* Zone has always been difficult to precisely identify because it represents a zone interval defined by negative criteria. These are the extinction of a group of key species at the top of the Middle *N. asperus* Zone, and the first appearance of the distinctive spore *Cyatheacidites annulatus* at the base of the overlying *P. tuberculatus* Zone (Stover & Partridge, 1973). In Poonboon-1 the identification of the zone is made more difficult by the reworking of Eocene spore-pollen, including many of the marker species for the base of the zone. Similar reworking has been recorded from this zone in Squid-1 (Partridge, 2002c). Identification of the zone is therefore based on secondary index species, which can be very rare or have poorly known stratigraphic ranges (Partridge, 1973). Applying these in Poonboon-1 the base of the zone is picked at 1767.8m on the FADs of *Granodiporites nebulosus*, *Proteacidites stipplatus* and the spore *Verrucosisporites cristatus*, while the top of the zone is picked below the FAD of *Cyatheacidites annulatus* in the sidewall core at 1505.7m. The FADs of *Foveotriletes crater* at 1737.4m and *Malvacipollis grandis* ms at 1600.2m are in general consistent with these picks. The assemblages are dominated by *Nothofagidites* pollen (average 58%), with secondary *Haloragacidites harrisii* (average 6%) and *Myrtaceidites* pollen (average 5%).

With the exception of the low recovery sidewall cores at 1691.6m and 1722.1m marine microplankton were recorded in all samples. Although both abundance (range <1% to 7%, average <4%) and recorded species diversity is low (average 6 species sample, excluding caved cuttings assemblage), some of the samples can be assigned to established zones based on the occurrence of key index species. The samples at 1706.9m and 1763m are assigned to the *Phthanoperidinium comatum* Acme Zone based on the common occurrence of the eponymous species, while the samples between 1505.7 and 1670m are assigned to the *Fromea leos* Zone based on the presence of the manuscript species *Fromea leos* and *Fromea neochytra* (Table 5).

***Proteacidites tuberculatus* spore-pollen Zone**

Interval: 1233.2 to 1505.7metres

Age: Early to Late Oligocene.

The three shallowest sidewall cores analysed are assigned to the *P. tuberculatus* Zone based on the FAD of *Cyatheacidites annulatus* at 1505.7m following the original zone definition of Stover & Partridge (1973). This sample is no younger than the Lower *P. tuberculatus* Zone based on the LAD of *Tripunctisporis maastrichtiensis*, while the shallowest sidewall core at 1233.2m is no older than the Middle *P. tuberculatus* Zone based on the FAD of *Cyathidites subtilis*. The assemblages are again dominated by *Nothofagidites* (average 38%), but they also contain common *Myrtaceidites* pollen (average 10%).

Marine dinocysts characteristic of the *Operculodinium* Superzone are abundant in all the samples (average >25%). The two shallower samples from the Torquay Group are dominated by *Spiniferites* while the sample at 1505.7m from the top of the Demons Bluff Group is dominated by undifferentiated dinocysts.

References

FENSOME, R.A., WILLIAMS, G.L., BARSS, M.S., FREEMAN, J.M. & HILL, J.M., 1990. Acritarchs and fossil Prasinophytes: An index to genera, species and infraspecific taxa. *AASP Contribution Series No. 25,* p.1-771.

HARRIS, W.K., 1985. Middle to late Eocene depositional cycles and dinoflagellate zones in southern Australia. **In** *Stratigraphy, Palaeontology, Malacology: Papers in Honour of Dr Nell Ludbrook,* J.M. Lindsay, editor, *Department of Mines and Energy South Australia Special Publication 5*, p.133-144.

HELBY, R., MORGAN, R. & PARTRIDGE, A.D., 1987. A palynological zonation of the Australian Mesozoic. **In** *Studies in Australian Mesozoic Palynology*, P.A. Jell, editor, *Memoir Association Australasian Palaeontologists 4,* p.1-94.

HOLDGATE, G.R., SMITH, T.A.G., GALLAGHER, S. & WALLACE, M.W., 2001. Geology of coal-bearing Palaeogene sediments, onshore Torquay Basin, Victoria. *Australian Journal of Earth Sciences, vol.48*, p.657-679.

PARTRIDGE, A.D., 1972. The Palynology of Poonboonñ1, Bass Basin. *Esso Australia Ltd Palaeontological Report 1972/19*, 8p. (6 December).

PARTRIDGE, A.D., 1973. Revision of the Spore-Pollen Zonation in the Bass Basin. *Esso Australia Ltd Palaeontological Report 1973/4*, 22p. 6pls (2 May).

PARTRIDGE, A.D., 1999. Late Cretaceous to Tertiary geological evolution of the Gippsland Basin, Victoria. PhD thesis, La Trobe University, Bundoora, Victoria, p.i-xxix, p.1-439, 165 figs, 9 pls (unpubl.).

PARTRIDGE, A.D., 2002a. Quantitative palynological analysis of Paleocene to Middle Eocene interval Konkon-1, Bass Basin. *Biostrata Report 2002/09*, p.1-18.

PARTRIDGE, A.D., 2002b. Quantitative palynological analysis of eleven cuttings samples from 2266 to 3115m in Koorkah-1, Bass Basin. *Biostrata Report 2002/10*, p.1-15.

PARTRIDGE, A.D., 2002c. Palynological analysis of Oligocene sandstones in Squid-1, Bass Basin. *Biostrata Report 2002/12*, p.1-18.

PARTRIDGE, A.D., 2002d. Bass Basin Palynological Project: Unravelling a Late Cretaceous to Eocene geological history of large palaeolakes, coastal lagoons and marine bays. *Biostrata Report 2002/13*, p.1-36.

STOVER, L.E. & PARTRIDGE, A.D., 1973. Tertiary and late Cretaceous spores and pollen from the Gippsland Basin, southeastern Australia. *Proceedings Royal Society of Victoria, vol.85,* pt.2, p.237-286.

STOVER, L.E. & PARTRIDGE, A.D., 1982. Eocene spore-pollen from the Werillup Formation, Western Australia. *Palynology 6*, p.69-95.

WILLIAMS, G.L., LENTIN, J.K. & FENSOME, R.A., 1998. The Lentin and Williams index of fossil dinoflagellates 1998 edition. *American Association of Stratigraphic Palynologists, Contributions Series, no. 34*, p.1-817.

Table 1. Interpretative Palynological Data from Poonboon-1

No.	Depth Metres	Depth Feet	Sample Type	Sample Origin	Spore-Pollen Zone	CR*	Microplankton Zone	CR*	Key Index Species	Palaeoenvironment
1	1233.2	4046	SWC 27a	Esso	Middle *P. tuberculatus*	B2	*Operculodinium* Sz	B2	FAD of *Cyathidites subtilis*	Open Marine
2	1325.9	4350	SWC 26a	Esso	*P. tuberculatus*	B4	*Operculodinium* Sz	B2	FAD of *Foraminisporis ozotus* ms	Open Marine
3	1505.7	4940	SWC 24a	Esso	Lower *P. tuberculatus*	B1	*F. leos*	B3	FAD of *Cyatheacidites annulatus*	Open Marine
4	1551-70	5090-150	Cuttings	GA-2	*P. tuberculatus* (caved)	D1	*P. simplex* (caved)	D4		Open Marine
5	1600.2	5250	SWC 23a	Esso	Upper *N. asperus*	B1	*F. leos*	B5	FAD of *Malvacipollis grandis* ms	Marginal Marine
6	1652-70	5420-80	Cuttings	GA-2	Upper *N. asperus*	D4	*F. leos*	D2	FAD of *Fromea leos* ms	Marginal Marine
7	1691.6	5550	SWC 22a	Esso	Upper *N. asperus*	B4			LAD of *Dryptopollenites semilunatus*	Marginal Marine
8	1706.9	5600	SWC 21a	Esso	Upper *N. asperus*	B1	*P. comatum* Acme	B3	LAD of *Phthanoperidinium comatum*	Marginal Marine
9	1722.1	5650	SWC 20a	Esso	Upper *N. asperus*	B5				Marginal Marine
10	1737.4	5700	SWC 19a	Esso	Upper *N. asperus*	B4			FAD of *Foveotriletes crater*	Marginal Marine
11	1749.6	5740	SWC 18a	Esso	Upper *N. asperus*	B4				Marginal Marine
12	1763.0	5784	SWC 16a	Esso	Upper *N. asperus*	B4	*P. comatum* Acme	B3	LAD of *Deflandrea heterophlycta*	Bay - restricted marine
13	1767.8	5800	SWC 15a	Esso	Upper *N. asperus*	B4			FAD of *Granodiporites nebulosus*	Bay - restricted marine
14	1801.4	5910	SWC 14a	Esso	Middle *N. asperus*	B1			LAD of *Triorites magnificus*	Bay - restricted marine
15	1859.3	6100	SWC 12a	Esso	Middle *N. asperus*	B1			LAD of *Proteacidites pachypolus*	Bay - restricted marine
16	1889.8	6200	SWC 30	Esso	Middle *N. asperus*	B1				Bay - restricted marine
17	1935.5	6350	SWC 6a	Esso	Middle *N. asperus*	B1			FAD of *Anacolosidites sectus*	Estuarine to Bay
18	1953.8	6410	Core 1	Esso	Middle *N. asperus*	B1				Estuarine to Bay
19	1958.9	6427	Core 1	Esso	Middle *N. asperus*	B4			Common *Enneadocysta pectiniformis*	Estuarine to Bay
20	1988.8	6525	SWC 4a	Esso	Middle *N. asperus*	B1			FAD of *Triorites magnificus*	Estuarine to Bay
21	2009-18	6590-620	Coal Cts	Esso	Lower *N. asperus*	D5				Marsh - Peat swamp
22	2011.7	6600	SWC 26	Esso	Lower *N. asperus*	B1			LAD of *Proteacidites asperopolus*	Coastal Plain - Deltaic
23	2047.6	6718	SWC 25	Esso	Lower *N. asperus*	B1			LAD of *Proteacidites reflexus*	Coastal Plain - Deltaic
24	2072.6	6800	SWC 24	Esso	Lower *N. asperus*	B5				Coastal Plain - Deltaic
25	2091-97	6860-80	Coal Cts	Esso	Lower *N. asperus*	B4				Marsh - Peat swamp

Table 1. Interpretative Palynological Data from Poonboon-1

No.	Depth Metres	Depth Feet	Sample Type	Sample Origin	Spore-Pollen Zone	CR*	Microplankton Zone	CR*	Key Index Species	Palaeoenvironment
26	2134.8	7004	SWC 22	Esso	Lower *N. asperus*	B4			LAD of *Proteacidites obesolabrus*	Coastal Plain - Deltaic
27	2169.6	7118	SWC 21	Esso	Lower *N. asperus*	B4			Common *Phyllocladidites mawsonii*	Coastal Plain - Deltaic
28	2194.6	7200	SWC 20	Esso	Lower *N. asperus*	B4			FAD of *Matonisporites ornamentalis*	Lacustrine -fresh?
29	2225.0	7300	SWC 19	Esso	*P. asperopolus*	B1			LAD of *Myrtaceidtes tenuis*	Coastal Plain - Lagoonal
30	2237.2	7340	SWC 18	Esso	*P. asperopolus*	B1			LAD of *Intratriporopollenites notabilis*	Coastal Plain - Deltaic
31	2257.3	7406	SWC 17	Esso	*P. asperopolus*	B2				Coastal Plain - Lagoonal
32	2287.2	7504	SWC 16	Esso	*P. asperopolus*	B1				Coastal Plain - Deltaic
33	2317.1	7602	SWC 15	Esso	*P. asperopolus*	B1			FAD of *Proteacidites asperopolus*	Coastal Plain - Lagoonal
34	2362-74	7750-90	Cuttings	GA-2	Upper *M. diversus*	D2				Coastal Plain - Lagoonal
35	2377.4	7800	SWC 13	Esso	Upper *M. diversus*	B1			FAD of *Proteacidites pachypolus*	Coastal Plain - Lagoonal
36	2408-17	7900-30	Cuttings	GA-2	Upper *M. diversus*	D2	*H. tasmaniense*	D3	FAD of *Homotryblium tasmaniense*	Coastal Plain - Lagoonal
37	2426.2	7960	SWC 11	Esso	Middle *M. diversus*	B1			*Spinizonocolpites prominatus* present	Coastal Plain - Lagoonal
38	2438.4	8000	SWC 10	Esso	Middle *M. diversus*	B4			FAD of *Proteacidites nasus*	Coastal Plain - Lagoonal
39	2472.5	8112	Core 2	GA-2	Middle *M. diversus*	A1	*A. homomorphum*	B3	Rare microforaminiferal liners present!	Lagonal - restricted marine
40	2474.4	8118	Core 2	Esso	Middle *M. diversus*	A1			FAD of *Proteacidites tuberculiformis*	Coastal Plain - Lagoonal
41	2499-508	8200-30	Cuttings	GA-2	Middle *M. diversus*	D4			FAD of *Polycolporopollenites esobalteus*	Coastal Plain - Lagoonal
42	2499.4	8200	SWC 8	Esso	Indeterminate					Coastal Plain - Deltaic
43	2514.6	8250	SWC 7	Esso	Lower *M. diversus*	B5			FAD of *Intratriporopollenites notabilis*	Coastal Plain - Deltaic
44	2529.8	8300	SWC 6	Esso	Lower *M. diversus*	B1	*A. homomorphum*	B3	LAD of *Matonisporites gigantis*	Coastal Plain - Lagoonal
45	2560.3	8400	SWC 5	Esso	Indeterminate					Fluvial?
46	2590.8	8500	SWC 4	Esso	Indeterminate					Fluvial?
47	2624.3	8610	SWC 3	Esso	Lower *M. diversus*	B4				Coastal Plain - Deltaic
48	2651.8	8700	SWC 2	Esso	Lower *M. diversus*	B1	*A. hyperacanthum*	A3	FAD of *Spinizonocolpites prominatus*	Coastal Plain - Lagoonal
49	2678.6	8788	SWC 1	Esso	Upper *L. balmei*	B1	*A. reburrus* Acme	A3	LAD of *Gambierina rudata*	Coastal Plain - Lagoonal
50	2688.0	8819	Core 3	Esso	Upper *L. balmei*	A1			FAD of *Cupanieidites orthoteichus*	Coastal Plain - Deltaic
51	2689.3	8823	Core 3	Esso	Upper *L. balmei*	A1			FAD of *Proteacidites grandis*	Coastal Plain - Deltaic
52	2713-25	8900-40	Cuttings	GA-2	Upper *L. balmei*	D4			FAD of *Matonisporites gigantis*	Coastal Plain - Deltaic

Table 1. Interpretative Palynological Data from Poonboon-1

No.	Depth Metres	Depth Feet	Sample Type	Sample Origin	Spore-Pollen Zone	CR*	Microplankton Zone	CR*	Key Index Species	Palaeoenvironment
53	2737-40	8980-90	Coal Cts	Esso	Lower *L. balmei*	C3			LAD of *Tetracolporites verrucosus*	Marsh - Peat swamp
54	2758-61	9050-60	Coal Cts	Esso	Lower *L. balmei*	C4				Marsh - Peat swamp
55	2795-801	9170-90	Cuttings	GA-2	Lower *L. balmei*	D4				Coastal Plain - Deltaic
56	2838-44	9310-30	Cuttings	GA-2	Lower *L. balmei*	D4				Coastal Plain - Deltaic
57	2847-50	9340-50	Coal Cts	Esso	Lower *L. balmei*	C4			*Phyllocadidites mawsonii* 43% of SP	Marsh - Peat swamp
58	2877-80	9440-50	Coal Cts	Esso	Lower *L. balmei*	C4			*Phyllocadidites mawsonii* 32% of SP	Marsh - Peat swamp
59	2896-902	9500-20	Cuttings	GA-2	Lower *L. balmei*	D4				Non-marine - fluvial
60	2951-57	9680-700	Cuttings	GA-2	Lower *L. balmei*	D5				Non-marine - fluvial
61	2975-84	9760-90	Cuttings	GA-2	Lower *L. balmei*	D4				Non-marine - fluvial
62	2995.6	9828	SWC 28	Esso	Lower *L. balmei*	B5			Reworking common 19% of SP	Non-marine - fluvial
63	2997.4	9834	SWC 27	Esso	Lower *L. balmei*	B3			*Phyllocadidites mawsonii* 69% of SP	Non-marine - fluvial
64	3042.2	9981	Core-4	Esso	Lower *L. balmei*	A1			FAD of *Haloragacidites harrisii*	Non-marine - fluvial
65	3066-69	10060-70	Cuttings	GA-2	*L. balmei/F. longus*	D4				Non-marine - fluvial
66	3116.9	10226	SWC 22	Esso	*L. balmei/F. longus*	B4				Lacustrine -fresh
67	3154.7	10350	SWC 18	Esso	*L. balmei/F. longus*	B4			*Proteacidites clinei* present	Non-marine - fluvial
68	3183.6	10445	SWC 12	Esso	*L. balmei/F. longus*	B4			LAD of *Nothofagidites senectus*	Non-marine - fluvial
69	3223.9	10577	SWC 33	Esso	Upper *F. longus*	B2	*Morkallacysta* Facies		LAD of *Proteacidites reticuloconcavus*	Lacustrine -fresh
70	3231-40	10600-30	Cuttings	GA-2	Upper *F. longus*	D4				Non-marine - fluvial
71	3233.3	10608	SWC 5	Esso	Upper *F. longus*	B3	*Morkallacysta* Facies			Lacustrine - fresh
72	3247.3	10654	SWC 34	Esso	Upper *F. longus*	B1			LAD of *Grapnelispora evansii*	Lacustrine - fresh
73	3262.3	10703	Core 5	Esso	Upper *F. longus*	B1			FAD of *Tripunctisporis maastrichtiensis*	Lacustrine - fresh

ABBREVIATIONS

*CR = Confidence Ratings

LAD = Last Appearance Datum

FAD = First Appearance Datum

GA-2 = Samples collected Stage-2 Work program

Esso = Samples processed in Esso laboratory

Sz = Superzone

CONFIDENCE RATINGS

Alpha Code Linked to Sample

A = Core

B = Sidewall core

C = Coal cuttings

D = Ditch cuttings

J = Junk basket

Numeric Code Linked to Palynomorph Assemblage

1 = Excellent confidence: High diversity assemblage **plus** key zone species.

2 = Good confidence: Moderately diverse assemblage **plus** key zone species.

3 = Fair confidence: Low diversity assemblage **plus** key zone species.

4 = Poor confidence: Moderate to high diversity **minus** key zone species.

5 = Very low confidence: Low diversity assemblage **minus** key zone species.

Table 2. Basic Palynological Data from Poonboon-1

No.	PalLab Spl.No.	Sample Type	Core No.	Top Feet	Base Feet	Top Metres	Base Metres	Visual Yield	Palynomorph Concentration	Palynomorph Preservation	No. SP Species	No. MP Species	Marine MP%	Other MP%	NED	Noth%
1	NA	SWC	27a		4046		1233.2	Moderate	High	Poor-good	30	10	20%	4%	9%	26%
2	NA	SWC	26a		4350		1325.9	Moderate	High	Poor-good	27	8	31%	11%	4%	22%
3	NA	SWC	24a		4940		1505.7	Moderate	High	Poor-fair	58	10	20%	2%	11%	41%
4	6406894	Cuttings		5090	5150	1551.4	1569.7	High	High	Poor-good	41	18	47%		12%	42%
5	NA	SWC	23a		5250		1600.2	Moderate	High	Poor-fair	62	7	5%	<1%	1%	50%
6	6406895	Cuttings		5420	5480	1652.0	1670.3	High	High	Poor-fair	40	14	16%		7%	60%
7	NA	SWC	22a		5550		1691.6	Low	Low	Poor-fair	41					
8	NA	SWC	21a		5600		1706.9	High	High	Fair-good	57	5	5%		1%	56%
9	NA	SWC	20a		5650		1722.1	Low	Low	Poor-fair	24	1				
10	NA	SWC	19a		5700		1737.4	Moderate	Moderate	Fair	53	1	<1%		2%	67%
11	NA	SWC	18a		5740		1749.6	High	High	Fair-good	53	6	<1%		2%	70%
12	NA	SWC	16a		5784		1763.0	High	High	Fair-good	55	9	7%		2%	47%
13	NA	SWC	15a		5800		1767.8	High	Very High	Poor-good	58	8	4%	1%	3%	47%
14	NA	SWC	14a		5910		1801.4	High	High	Fair-good	47	9	8%		7%	53%
15	NA	SWC	12a		6100		1859.3	High	High	Good	49	11	16%		5%	55%
16	NA	SWC	30		6200		1889.8	High	High	Poor-good	51	2	2%		4%	58%
17	NA	SWC	6a		6350		1935.5	High	High	Fair-good	47	1	1%		1%	47%
18	NA	Core	1		6410		1953.8	Moderate	Low	Poor-good	52	1	2%		2%	29%
19	NA	Core	1		6427		1958.9	Moderate	Moderate	Poor	27	9	26%	2%	3%	26%
20	NA	SWC	4a		6525		1988.8	High	High	Fair-good	64	1	1%		1%	49%
21	NA	Cuttings		6590	6620		2017.8	High	High	Fair	33					50%
22	NA	SWC	26		6600		2011.7	High	High	Poor-good	64				1%	20%
23	NA	SWC	25		6718		2047.6	Moderate	High	Poor-fair	56	1	<1%		6%	32%
24	NA	SWC	24		6800		2072.6	Low	Very Low	Poor-fair	11					
25	NA	Cuttings		6860	6880		2097.0	High	High	Fair	31				1%	50%
26	NA	SWC	22		7004		2134.8	High	High	Fair-good	45				2%	21%

Table 2. Basic Palynological Data from Poonboon-1

No.	PalLab Spl.No.	Sample Type	Core No.	Top Feet	Base Feet	Top Metres	Base Metres	Visual Yield	Palynomorph Concentration	Palynomorph Preservation	No. SP Species	No. MP Species	Marine MP%	Other MP%	NED	Noth%
27	NA	SWC	21		7118		2169.6	High	High	Fair-good	34					17%
28	NA	SWC	20		7200		2194.6	High	High	Fair	54	2		1%	1%	29%
29	NA	SWC	19		7300		2225.0	High	High	Fair	49	1		<1%	1%	12%
30	NA	SWC	18		7340		2237.2	High	High	Fair-good	65	1	<1%		2%	18%
31	NA	SWC	17		7406		2257.3	Moderate	High	Poor-fair	57	1		<1%	2%	21%
32	NA	SWC	16		7504		2287.2	Low	Low	Poor	26				1%	5%
33	NA	SWC	15		7602		2317.1	Moderate	Moderate	Poor-fair	50	1		<1%	3%	18%
34	6406896	Cuttings		7750	7790	2362.2	2374.4	Moderate	Moderate	Poor -fair	30	6	4%		2%	8%
35	NA	SWC	13		7800		2377.4	Moderate	Moderate	Fair	47	2	1%		2%	17%
36	6406897	Cuttings		7900	7930	2407.9	2417.1	Moderate	Moderate	Poor -fair	29	3	6%		6%	10%
37	NA	SWC	11		7960		2426.2	Moderate	Moderate	Fair	49	5	3%	4%	11%	29%
38	NA	SWC	10		8000		2438.4	High	High	Fair-good	46	1		<1%	13%	8%
39	6406898	Core	2		8112		2472.5	High	Moderate	Very Poor-Poor	34	11	43%		19%	9%
40	NA	Core	2		8118		2474.4	Moderate	Moderate	Poor -fair	42	1				
41	6406899	Cuttings		8200	8230	2499.4	2508.5	High	High	Poor -fair	35	4	22%		9%	20%
42	NA	SWC	8		8200		2499.4	Very Low	Very Low	Poor	5					
43	NA	SWC	7		8250		2514.6	Low	Low	Poor	21					
44	NA	SWC	6		8300		2529.8	High	High	Fair	41	5	3%	1%	11%	17%
45	NA	SWC	5		8400		2560.3	Very Low	Very Low	Poor	3					
46	NA	SWC	4		8500		2590.8	Very Low	Very Low	Poor	4					
47	NA	SWC	3		8610		2624.3	Low	Low	Poor	33	1		<1%	13%	15%
48	NA	SWC	2		8700		2651.8	Moderate	Moderate	Poor	44	1	5%		23%	2%
49	NA	SWC	1		8788		2678.6	Moderate	High	Poor -fair	49	6	4%	<1%	19%	10%
50	NA	Core	3		8819		2688.0	High	High	Poor	51	2		1%	19%	18%
51	NA	Core	3		8823		2689.3	Moderate	Moderate	Poor	34	2	<1%	1%	16%	13%
52	6406900	Cuttings		8900	8940	2712.7	2724.9	High	Moderate	Poor	30	1	2%		10%	10%

Table 2. Basic Palynological Data from Poonboon-1

No.	PalLab Spl.No.	Sample Type	Core No.	Top Feet	Base Feet	Top Metres	Base Metres	Visual Yield	Palynomorph Concentration	Palynomorph Preservation	No. SP Species	No. MP Species	Marine MP%	Other MP%	NED	Noth%
53	NA	Cuttings		8980	8990	2737.1	2740.2	High	High	Poor	36				<1%	19%
54	NA	Cuttings		9050	9060	2758.4	2761.5	High	High	Poor	33				1%	23%
55	6406901	Cuttings		9170	9190	2795.0	2801.1	Moderate	Moderate	Very Poor	30	2	7%		15%	9%
56	6406902	Cuttings		9310	9330	2837.7	2843.8	Moderate	Low	Very Poor	28	2	5%	<1%	10%	3%
57	NA	Cuttings		9340	9350	2846.8	2849.9	High	High	Poor	16					3%
58	NA	Cuttings		9440	9450	2877.3	2880.4	High	High	Poor	33	2		<1%	<2%	7%
59	6406903	Cuttings		9500	9520	2895.6	2901.7	Low	Low	Very Poor	29	1		2%	11%	8%
60	6406904	Cuttings		9680	9700	2950.5	2956.6	High	Moderate	Poor	25	1		<1%	9%	2%
61	6406905	Cuttings		9760	9790	2974.8	2984.0	High	High	Poor	23	1		<1%	2%	4%
62	NA	SWC	28		9828		2995.6	Low	Very Low	Poor	20	1		1%	11%	15%
63	NA	SWC	27		9834		2997.4	Moderate	Moderate	Poor	20					3%
64	NA	Core	4		9981		3042.2	High	Moderate	Poor -fair	33	2		1%	6%	5%
65	6406906	Cuttings		10060	10070	3066.3	3069.3	High	Moderate	Poor	28	1		2%	6%	2%
66	NA	SWC	22		10226		3116.9	High	High	Poor	35	2		1%	23%	3%
67	NA	SWC	18		10350		3154.7	High	High	Poor	32	1		1%	12%	9%
68	NA	SWC	12		10445		3183.6	Moderate	Low	Poor	20				1%	9%
69	NA	SWC	33		10577		3223.9	High	Moderate	Poor	27	2		13%	22%	4%
70	6406907	Cuttings		10600	10630	3230.9	3240.0	High	Moderate	Poor	26	1		<1%	3%	3%
71	NA	SWC	5		10608		3233.3	High	Moderate	Poor	28	4		5%	44%	2%
72	NA	SWC	34		10654		3247.3	High	High	Poor	32				29%	1%
73	NA	Core	5		10703		3262.3	High	High	Poor	43	3		2%	44%	

ABBREVIATIONS

MP = Microplankton

SP = Spore-Pollen

NA = Not Available

NED = Neves Effect based on *Dilwynites/Araucariacites* pollen percentage

Noth% = Percentage of *Nothofagidites* pollen in SP count.

Table 3. Poonboon-1 — abundances of major palynomorph groups.

No.	Depth metres	Depth feet	Sample Type	Gleicheniidites & Clavifera spores	ALL OTHER Spores	Dilwynites & Araucariacites pollen	ALL OTHER Gymnosperms	Nothofagidites species	ALL OTHER Angiosperms	FUNGAL microfossils	Reworked Spore-Pollen	**Total Terrestrial SUM**		SPORE-POLLEN TOTAL	MICROPLANKTON Fresh & Brackish	MICROPLANKTON Marine	**SP + MP SUM**
1	1233.2	4046	SWC 27a	0.8%	15%	11%	4.7%	29%	26%	14%		253		75%	4%	20%	288
2	1325.9	4350	SWC 26a	2.3%	13%	4.1%	12%	25%	28%	14%	0.9%	221		57%	11%	31%	327
3	1505.7	4940	SWC 24a		8.0%	12%	7.0%	45%	19%	8.5%		201		78%	0.8%	22%	237
4	1551-70	5090-150	Cuttings	0.7%	19%	12%	10%	41%	14%	2.9%		139		53%	0.4%	47%	256
5	1600.2	5250	SWC 23a	0.5%	4.9%	2.0%	12%	51%	28%	1.5%		203		95%	0.5%	5%	211
6	1652-70	5420-80	Cuttings	0.5%	5.9%	6.8%	9.1%	60%	17%	1.4%		220		84%		16%	257
7	1691.6	5550	SWC 22a														
8	1706.9	5600	SWC 21a	2.1%	5.0%	1.7%	5.4%	57%	26%	2.9%		240		95%		5%	246
9	1722.1	5650	SWC 20a														
10	1737.4	5700	SWC 19a	1.6%	11%	2.0%	10%	67%	8%			254		100%		0.4%	255
11	1749.6	5740	SWC 18a	0.5%	4.1%	2.3%	9.6%	70%	13%	0.5%		218		100%		0.5%	218
12	1763.0	5784	SWC 16a	0.4%	14%	1.6%	13%	47%	23%	1.2%		250		93%		7%	265
13	1767.8	5800	SWC 15a		7.4%	3.5%	10%	50%	24%	4.9%		284		95%	1.1%	4%	285
14	1801.4	5910	SWC 14a	0.4%	8.1%	7.3%	7.7%	53%	23%	0.4%	0.4%	248		92%		8%	268
15	1859.3	6100	SWC 12a		8.8%	5.5%	9.9%	55%	21%		0.4%	273		84%		16%	322
16	1889.8	6200	SWC 30	0.7%	5.6%	4.5%	11%	60%	16%	3.0%		267		98%		2%	264
17	1935.5	6350	SWC 6a		6.0%	0.7%	6.3%	47%	38%	1.9%		268		99%		0.8%	265
18	1953.8	6410	Core 1	0.5%	12%	1.5%	13%	29%	43%	1.5%		195		98%		2%	195
19	1958.9	6427	Core 1		1.5%	3.6%	4.6%	28%	54%	8.8%		194		72%	2%	26%	247
20	1988.8	6525	SWC 4a		3.8%	1.5%	9.6%	51%	31%	3.1%		260		99%		0.8%	254
21	2009-18	6590-620	Coal cts		1.9%		13%	50%	35%			266		100%			266
22	2011.7	6600	SWC 26	0.4%	12%	1.1%	22%	21%	42%	2.5%		285		100%			278
23	2047.6	6718	SWC 25	0.4%	9.7%	5.8%	22%	32%	29%	1.2%		259		100%		0.4%	257
24	2072.6	6800	SWC 24														
25	2091-97	6860-80	Coal cts		1.2%	0.8%	9.6%	50%	38%	0.4%		260		100%			259
26	2134.8	7004	SWC 22		4.3%	2.4%	16%	27%	20%	29%	0.4%	255		100%			180
27	2169.6	7118	SWC 21	0.8%	10%		29%	17%	43%			259		100%			259
28	2194.6	7200	SWC 20	0.8%	5.1%	1.6%	29%	31%	23%	7.9%	1.2%	253		99%	1.3%		233
29	2225.0	7300	SWC 19	0.7%	1.8%	1.1%	9.6%	14%	59%	13%	0.4%	271		100%	0.4%		235
30	2237.2	7340	SWC 18		12%	2.3%	9.5%	18%	54%	4.6%		263		100%		0.4%	252
31	2257.3	7406	SWC 17	0.4%	5.7%	1.9%	4.2%	21%	65%	1.5%		261		100%	0.4%		258
32	2287.2	7504	SWC 16	0.9%	6.3%	0.9%	3.6%	5.4%	73%	9.8%		112		100%			101
33	2317.1	7602	SWC 15		3.0%	3.3%	3.3%	22%	51%	17%	0.7%	269		100%	0.5%		221
34	2362-74	7750-90	Cuttings		8.9%	1.5%	12%	5.2%	34%	39%		269		96%		4%	172
35	2377.4	7800	SWC 13	0.4%	3.9%	1.8%	8.9%	17%	68%		0.4%	281		99%		1.1%	283
36	2408-17	7900-30	Cuttings	0.3%	2.6%	3.8%	11%	6.2%	34%	41%		340		93%		7%	214
37	2426.2	7960	SWC 11	0.4%	7.2%	11%	8.8%	29%	43%	0.4%	0.4%	251		93%	4%	3%	267
38	2438.4	8000	SWC 10	3.8%	8.7%	15%	11%	8.7%	42%	9.9%	0.4%	263		100%	0.4%		237

Table 3. Poonboon-1 — abundances of major palynomorph groups.

No.	Depth metres	Depth feet	Sample Type	Gleicheniidites & Clavifera spores	ALL OTHER Spores	Dilwynites & Araucariacites pollen	ALL OTHER Gymnosperms	Nothofagidites species	ALL OTHER Angiosperms	FUNGAL microfossils	Reworked Spore-Pollen	**Total Terrestrial SUM**		SPORE-POLLEN TOTAL	MICROPLANKTON Fresh & Brackish	MICROPLANKTON Marine	**SP + MP SUM**
39	2472.5	8112	Core 2	1.8%	12%	18%	3.6%	8.5%	50%	6.7%		165		59%		41%	259
40	2474.4	8118	Core 2														
41	2499-508	8200-30	Cuttings	0.3%	4.9%	8.2%	21%	16%	31%	18%		305		76%		24%	327
42	2499.4	8200	SWC 8														
43	2514.6	8250	SWC 7														
44	2529.8	8300	SWC 6	5.2%	6.4%	12%	12%	18%	46%	1.9%		267		96%	0.7%	3%	273
45	2560.3	8400	SWC 5														
46	2590.8	8500	SWC 4														
47	2624.3	8610	SWC 3	3.6%	4.4%	13%	35%	15%	28%	0.4%	0.8%	250		100%	0.4%		248
48	2651.8	8700	SWC 2	5.8%	14%	23%	26%	2.4%	28%		1.0%	206		95%		5%	215
49	2678.6	8788	SWC 1	17%	17%	19%	20%	10%	15%	1.5%	0.4%	264		96%	0.4%	4%	271
50	2688.0	8819	Core 3	13%	7.7%	19%	21%	18%	20%	0.7%	0.7%	272		99%	0.7%		270
51	2689.3	8823	Core 3	7.3%	13%	16%	27%	13%	23%	0.8%		262		99%	0.8%	0.4%	263
52	2713-25	8900-40	Cuttings	0.9%	12%	6.9%	28%	7.5%	17%	29%		319		98%		2%	233
53	2737-40	8980-90	Coal Cts	0.8%	9.0%	0.4%	47%	20%	22%	0.8%		244		100%			242
54	2758-61	9050-60	Coal Cts	2.8%	24%	0.8%	39%	23%	10%	0.4%		253		100%			252
55	2795-801	9170-90	Cuttings	1.4%	17%	14%	41%	7.8%	19%	0.7%		281		93%		7%	266
56	2838-44	9310-30	Cuttings	3.7%	24%	9.5%	47%	3.3%	12%	0.8%		241		95%	0.4%	5%	244
57	2847-50	9340-50	Coal Cts		1.6%		91%	3.2%	4.3%			253		100%			253
58	2877-80	9440-50	Coal Cts	2.8%	7.9%	1.6%	66%	7.5%	14%			253		99%	0.8%		255
59	2896-902	9500-20	Cuttings	3.4%	18%	9.7%	42%	6.9%	5.0%	15%		319		98%		2%	278
60	2951-57	9680-700	Cuttings	0.3%	13%	6.9%	43%	5.5%	6.9%	24%		290		99%		0.9%	222
61	2975-84	9760-90	Cuttings	0.5%	5.3%	1.3%	68%	3.7%	4.0%	17%		375		99%		0.6%	313
62	2995.6	9828	SWC 28	4.4%	8.8%	11%	33%	16%	7.0%	1.8%	18%	114		99%		1.1%	93
63	2997.4	9834	SWC 27	1.7%	1.7%		85%	3.4%	7.8%			232		100%			232
64	3042.2	9981	Core-4	1.6%	7.1%	6.3%	40%	5.1%	28%	13%		254		99%	0.9%		224
65	3066-69	10060-70	Cuttings	1.0%	6.5%		64%	1.6%	8.1%	19%		308		98%		2.3%	256
66	3116.9	10226	SWC 22	0.7%	15%	23%	29%	2.8%	27%	1.4%	0.7%	281		99%	0.7%	0.7%	279
67	3154.7	10350	SWC 18	1.6%	9.1%	12%	36%	8.7%	32%		0.8%	253		99%	1.2%		254
68	3183.6	10445	SWC 12	2.0%	3.5%	1.6%	67%	9.4%	16%			256		100%			256
69	3223.9	10577	SWC 33	0.5%	21%	22%	21%	4.2%	31%			189		86%	12%	1.4%	219
70	3231-40	10600-30	Cuttings	0.3%	6.1%	5.8%	58%	2.3%	8.7%	19%		309		99%	0.8%		252
71	3233.3	10608	SWC 5	0.4%	15%	44%	14%	2.4%	23%	0.8%		247		95%	5%	0.4%	258
72	3247.3	10654	SWC 34	0.4%	3.6%	29%	42%	0.7%	23%	0.7%	0.4%	277		100%			274
73	3262.3	10703	Core 5	4.0%	17%	44%	8.8%		26%			251		98%	2%		255

Table 4. Poonboon-1 — spore-pollen distribution. spore-pollen distribution.

No.	Depth metres	Depth feet	Sample Type	SPORE SPECIES	Baculatisporites spp.	Camarozonosporites bullatus	Camarozonosporites heskemensis	Clavifera triplex	Contaculatisporites apiculatus ms	Crassoretitriletes vanraadshooveni	Cyatheacidites annulatus	Cyathidites splendens	Cyathidites subtilis	Cyathidites spp. small <40µm	Densoisporites pellis ms	Dictyophyllidites spp.	Echinosporis echinatus	Foraminisporis ozotus ms	Foveotriletes balteus	Foveotriletes crater	Foveotriletes palaequetrus	Gleicheniidites circinidites	Grapnelispora evansii	Herkosporites elliottii	Ischyosporites spp.	Kuylisporites waterbolkii	Laevigatosporites major	Laevigatosporites ovatus	Latrobosporites amplus	Latrobosporites crassus	Latrobosporites ohaiensis	Marattisporites scabratus	Matonisporites gigantis	Matonisporites ornamentalis	Monolites alveolatus	Oramentifera sentosa	Peromonolites densus	Peromonolites vellosus	Peroltriletes spp.	Polypodiaceoisporites varus ms	Polypodiidites/Verrucatosporites spp.	Reltriletes spp.	Ricciaesporites boxatus ms	Rotverrusporites stellatus ms	Rugulatisporites mallatus	Rugulatisporites trophus
1	1233.2	4046	SWC 27a		1.4%						0.5%		X	7.8%								0.9%					0.5%	1.8%		X															
2	1325.9	4350	SWC 26a											9.6%		3.2%		X				2.7%						1.1%						X										X	
3	1505.7	4940	SWC 24a		0.5%						0.5%			6.5%					X	X	X				0.5%		X	0.5%						X								X		X	
4	1551-70	5090-150	Cuttings		X		X				X	0.7%	X	14%		0.7%		X				0.7%		X	0.7%		X	2.2%												X			X		
5	1600.2	5250	SWC 23a		X							0.5%		4.5%		X		X		X		0.5%		X	X	X				X			X							X			X		
6	1652-70	5420-80	Cuttings		0.5%						X			2.3%		0.9%					X	0.5%			0.5%		X	X													X				X
7	1691.6	5550	SWC 22a																					X	X								X					X				X		
8	1706.9	5600	SWC 21a		X							0.9%		1.3%		X						2.1%			0.4%	X		X		X				X							0.4%			X	
9	1722.1	5650	SWC 20a											X								X			X								X								X			X	
10	1737.4	5700	SWC 19a		0.4%							0.4%		5.5%						X		1.6%		X	0.8%			1.2%				0.4%				X			X		0.4%			
11	1749.6	5740	SWC 18a		0.5%							0.5%		1.8%								0.5%			0.9%	X	X	0.5%						X						X	X				
12	1763.0	5784	SWC 16a		1.6%									8.1%	X							0.4%		X	2.4%		X	0.4%		X				X							0.4%	X			
13	1767.8	5800	SWC 15a		0.7%							0.4%		3.3%					X		X			X	1.9%							0.4%		X						X	X		X	X
14	1801.4	5910	SWC 14a		0.4%									5.3%								0.4%			0.4%		X	0.8%				0.4%						0.4%						X	
15	1859.3	6100	SWC 12a									X		6.3%											1.1%		0.4%	0.7%													0.4%			X	
16	1889.8	6200	SWC 30		1.2%					X				1.5%								0.8%			0.4%		0.4%	1.5%															X		X	
17	1935.5	6350	SWC 6a											1.5%											0.8%		0.4%	1.9%										0.4%					X			
18	1953.8	6410	Core 1		1.6%							0.5%		1.0%			1.0%					0.5%			X			4.2%		X				X						1.0%					
19	1958.9	6427	Core 1									0.6%																							X										
20	1988.8	6525	SWC 4a		0.4%							X		0.8%											X			0.8%		X				X				0.4%			0.8%				
21	2009-18	6590-620	Coal cts											0.4%														0.8%													0.4%				
22	2011.7	6600	SWC 26		0.4%							0.7%		2.9%								0.4%			X		0.7%	5.4%										0.4%			0.4%			X	
23	2047.6	6718	SWC 25		1.2%							1.6%		0.8%								0.4%					0.4%	2.3%		X				X			0.8%						X	X
24	2072.6	6800	SWC 24																											X														
25	2091-97	6860-80	Coal cts																									0.8%																
26	2134.8	7004	SWC 22		0.6%							0.6%		2.8%			X					0.8%			1.1%			0.6%		X														
27	2169.6	7118	SWC 21									1.5%		1.2%					X			0.8%			0.4%			6.6%						X							0.4%			
28	2194.6	7200	SWC 20		0.4%							0.4%		1.7%	X							0.9%			0.4%	X		1.3%		X				X			X				0.9%	0.4%			
29	2225.0	7300	SWC 19				X		X					0.4%								0.9%				X		0.4%																
30	2237.2	7340	SWC 18		0.4%				0.4%			0.4%		5.2%												0.8%	0.4%	4.0%		X													X		
31	2257.3	7406	SWC 17						1.2%			X		1.2%					X			0.4%			X			3.5%							X										
32	2287.2	7504	SWC 16									1.0%		2.0%								1.0%			2.0%		X	1.0%													1.0%			
33	2317.1	7602	SWC 15		0.5%				X					0.9%												X		1.4%															X	
34	2362-74	7750-90	Cuttings		0.6%							4.2%		3.0%														3.0%													0.6%			
35	2377.4	7800	SWC 13		0.4%							X		0.7%								0.4%				0.4%		1.8%		0.4%		0.4%												
36	2408-17	7900-30	Cuttings		0.5%							1.0%		1.5%								0.5%																0.5%						
37	2426.2	7960	SWC 11		2.0%							0.4%		2.4%			0.4%					0.4%						1.2%		0.4%													X	
38	2438.4	8000	SWC 10		2.1%			0.4%				2.5%		3.0%								3.8%			0.4%			1.7%																
39	2472.5	8112	Core 2		0.6%			0.6%				1.9%		3.9%					X			1.3%						1.9%												0.6%				
40	2474.4	8118	Core 2		X					X		X													X				X										X			X	
41	2499-508	8200-30	Cuttings									0.4%		2.4%								0.4%						0.4%													0.4%			
42	2499.4	8200	SWC 8																																									
43	2514.6	8250	SWC 7		X							X					X																									X	
44	2529.8	8300	SWC 6		0.4%							X		2.3%								5.3%						0.4%					X										X	

Table 4. Poonboon-1 — spore-pollen distribution.

No.	Depth metres	Depth feet	Sample Type	Stereisporites antiquisporites	Stereisporites regium	Striamonoletes diglatoides	Triletе spores undiff.	Tripunctisporis maastrichtiensis	Verrucatosporites attinatus ms	Verrucosisporites cristatus	Verrucosisporites kopukuensis	TOTAL Spores	GYMNOSPERM SPECIES	Araucariacites australis	Cupressacites sp.	Dacrycarpites australiensis	Dilwynites granulatus	Dilwynites tuberculatus	Lygistepollenites balmei	Lygistepollenites florinii	Microalatidites paleogenicus	Microcachryidites antarcticus	Phyllocladidites mawsonii	Phyllocladidites reticulosaccatus	Phyllocladidites verrucosus	Podocarpidites spp.	Podocarpidites exiguus	Trichotomosulcites subgranulatus	TOTAL Gymnosperms	ANGIOSPERM SPECIES	Angiosperm pollen undiff.	Aglaoreidia qualumis	Anacolosidites luteoides	Anacolosidites sectus	Anisocolporites triplex	Australopollis obscurus	Banksieaeidites arcuatus	Banksieaeidites elongatus	Battenipollis sectilis	Beaupreaidites elegansiformis	Beaupreaidites verrucosus	Clavatipollenites glarius	Concolpites leptos	Cupanieidites orthoteichus	Cyperaceaepollis neogenicus
1	1233.2	4046	SWC 27a	3.7%			1.4%					18%		2.3%	2.8%		10%			0.5%			0.5%			1.8%			18%		0.5%								0.5%					
2	1325.9	4350	SWC 26a	0.5%			1.1%					18%		1.6%	2.7%	0.5%	3.2%			2.1%			1.6%			7.4%			19%		1.6%													
3	1505.7	4940	SWC 24a	X				X		X		9%		3.8%	1.6%	0.5%	9.2%	0.5%		1.1%	0.5%		1.1%			2.7%			21%		1.1%	X					X							
4	1551-70	5090-150	Cuttings	1.5%								21%		4.4%	1.5%	X	7.4%			1.5%			1.5%			5.9%			22%		1.5%	X						X						
5	1600.2	5250	SWC 23a						X	X	X	6%			1.0%	X	1.5%	0.5%		3.0%			4.0%			4.0%		0.5%	15%		2.5%	1.0%												
6	1652-70	5420-80	Cuttings	0.9%			0.5%				0.5%	6%		2.3%	1.4%		4.6%			1.8%			1.8%			3.2%		0.9%	16%		1.8%	0.9%									0.5%			
7	1691.6	5550	SWC 22a					X	X	X	X												X			X						X										X	
8	1706.9	5600	SWC 21a	1.3%			0.9%				X	7%		0.4%	0.9%	X	1.3%			1.7%	0.4%		1.7%			0.9%			7%		1.3%	0.9%					X					X	
9	1722.1	5650	SWC 20a								X			X			X			X		X				X															X	
10	1737.4	5700	SWC 19a				2.0%			X	X	13%		1.6%	0.8%		0.4%			1.6%			2.8%			4.3%		0.8%	12%			X					X					X	
11	1749.6	5740	SWC 18a	X				X		X	X	5%		0.9%	0.5%		1.4%		RW	1.8%		0.9%	2.3%			3.2%		0.9%	12%		1.8%	0.9%											
12	1763.0	5784	SWC 16a	0.4%			0.8%	X			X	15%		0.4%	1.2%		1.2%			1.2%			5.7%			4.5%		0.4%	15%		0.8%	0.4%							X	X		0.4%	X	
13	1767.8	5800	SWC 15a					X		X	3	8%		1.9%	3.0%	0.4%	1.9%			0.7%	0.7%	0.4%	1.9%			3.7%			14%									X				0.4%	
14	1801.4	5910	SWC 14a				0.4%		X		X	9%		3.7%			3.7%			2.4%		0.4%	2.4%			2.4%			15%		0.8%	0.4%		X				X						0.4%
15	1859.3	6100	SWC 12a						X		X	9%		0.4%			5.1%			2.2%	0.4%	0.7%	2.9%			3.3%		0.4%	15%		1.1%			X			0.4%			X				X	
16	1889.8	6200	SWC 30	0.4%			0.4%	X	X		X	7%		1.5%	0.4%		2.3%	0.8%		1.5%	0.8%	0.4%	1.5%			6.6%			16%		0.4%			X			X	X					X	
17	1935.5	6350	SWC 6a								1.1%	6%		0.4%			0.4%			4.2%			0.8%			1.5%			7%		2.3%			X			0.8%					0.4%	1.5%	
18	1953.8	6410	Core 1				0.5%				2.1%	13%			0.5%		1.6%			2.6%		1.0%	4.7%			3.6%		0.5%	15%		1.0%				X		2.1%			X		1.0%	X	
19	1958.9	6427	Core 1								1.1%	2%		1.1%	0.6%		2.3%	0.6%		0.6%			1.7%			2.3%			9%		1.1%						0.6%			1.7%		0.6%	
20	1988.8	6525	SWC 4a	0.4%				X			0.4%	4%		0.8%	0.4%		0.8%			1.2%			3.2%			4.8%		0.4%	12%		1.2%						1.6%				X		0.4%	
21	2009-18	6590-620	Coal cts								0.4%	2%								1.5%	3.4%		3.8%			2.3%		2.3%	13%		0.4%													
22	2011.7	6600	SWC 26				0.4%	0.4%	X		0.4%	12%		0.4%	0.7%		0.7%			1.4%		0.7%	12%			7.2%		1.1%	24%		0.7%						X					0.4%	
23	2047.6	6718	SWC 25				0.8%	0.4%			1.6%	10%		0.4%	0.4%		4.7%	0.8%		2.0%		0.8%	15%			3.5%			28%								0.4%					0.4%	
24	2072.6	6800	SWC 24								X															X																	
25	2091-97	6860-80	Coal cts								0.4%	1%		0.4%			0.4%			2.3%	0.8%		3.9%			2.3%		0.4%	10%		0.8%							0.8%					1.2%	
26	2134.8	7004	SWC 22	0.6%				X			X	6%		0.6%	0.6%		2.2%	0.6%			0.6%	0.6%	4.4%			16%		0.6%	26%		0.6%												0.6%	
27	2169.6	7118	SWC 21									11%											19%			8.5%		2.3%	29%		0.4%						1.5%						
28	2194.6	7200	SWC 20					X			X	7%		0.9%	0.4%	0.9%	0.9%			0.9%	1.3%	1.7%	5.7%			18%		3.5%	34%		0.4%						0.4%				0.4%		
29	2225.0	7300	SWC 19				0.4%				0.9%	3%					0.9%	0.4%		0.9%	0.9%	1.3%	3.0%			5.1%			12%		1.7%						2.1%					0.9%	
30	2237.2	7340	SWC 18				0.4%				0.4%	12%			0.4%		1.6%	0.8%		1.2%	0.8%	0.4%	0.8%			5.2%		1.2%	12%		0.4%						0.4%	X				0.4%	
31	2257.3	7406	SWC 17								X	6%		0.4%	0.4%		1.2%	0.4%					1.6%			2.3%			6%		1.9%						X			X		1.6%	
32	2287.2	7504	SWC 16									8%		1.0%						1.0%			1.0%			2.0%			5%		1.0%						1.0%					2.0%	
33	2317.1	7602	SWC 15				0.5%				0.5%	4%		0.9%			2.3%	0.9%		1.4%						2.7%			8%		0.9%						X					X	
34	2362-74	7750-90	Cuttings	0.6%			2.4%					15%		2.4%		0.6%						1.2%	4.2%			9.1%		4.2%	22%		12%												1.2%	X
35	2377.4	7800	SWC 13									4%		0.4%			1.4%			1.1%	0.4%		0.4%			5.7%		1.4%	11%		0.4%		X				X	X				1.8%	
36	2408-17	7900-30	Cuttings				1.0%					5%		1.0%	0.5%		4.5%	1.0%		0.5%			1.5%			13%		4.0%	26%		6.5%												
37	2426.2	7960	SWC 11				0.4%	X			X	8%		2.4%	0.4%		7.6%	1.2%		1.2%			1.6%			4.8%		0.8%	20%				X										X	
38	2438.4	8000	SWC 10								X	14%		0.8%			15%	0.4%		0.8%		0.4%				9.7%		1.7%	29%		1.3%							X					0.8%	
39	2472.5	8112	Core 2	2.6%			1.3%					15%		4.5%			14%	0.6%		0.6%		0.6%				1.9%		0.6%	23%		1.9%												1.3%	
40	2474.4	8118	Core 2			X		X			X								RW				X			X						X										X	
41	2499-508	8200-30	Cuttings				2.4%					6%		2.0%			6.8%	1.2%		2.8%		0.8%	4.4%			17%		1.2%	36%		8.0%												X	
42	2499.4	8200	SWC 8																RW							X																	
43	2514.6	8250	SWC 7								X								RW							X																X	
44	2529.8	8300	SWC 6	2.7%			0.4%	0.4%			X	12%		1.1%	0.8%		10%	0.8%		0.8%		1.1%	0.8%			6.1%		2.3%	24%									X						

Table 4. Poonboon-1 — spore-pollen distribution.

No.	Depth metres	Depth feet	Sample Type	Dicotetradites clavatus	Dryadopollenites retequetrus	Dryptopollenites semilunatus	Elphedripites notensis	Ericipites crassiexinus/scabratus	Gambierina edwardsii	Gambierina rudata	Granodiporites nebulosus	Gothanipollis bassensis	Haloragacidites harrisii	Ilexpollenites spp.	Intratriporopollenites notabilis	Liliacidites spp.	Malvacipollis diversus	Malvacipollis grandis ms	Malvacipollis robustus ms	Malvacipollis subtilis	Milfordia incerta	Milfordia homeopunctatus	Monosulcites uvatus ms	Myrtaceidites parvus/mesonesus	Myrtaceidites tenuis	Myrtaceidites verrucosus	Nothofagidites asperus	Nothofagidites brachyspinulosus	Nothofagidites deminutus	Nothofagidites emarcidus/heterus	Nothofagidites endurus	Nothofagidites falcatus	Nothofagidites flemingii	Nothofagidites goniatus	Nothofagidites senectus	Nothofagidites vansteenisii	Paripollis ochesis	Peninsulapollis gillii	Periporopollenites demarcatus	Periporopollenites polyoratus	Periporopollenites vesicus	Polycolporopollenites esobalteus	Polycolpites langstonii	Polyorificites oblatus	Proteacidites spp.	Proteacidites adenanthoides
1	1233.2	4046	SWC 27a					0.5%					6.5%							0.5%		0.5%		12%			0.9%		1.4%	29%		1.8%				1.4%							1.8%	
2	1325.9	4350	SWC 26a										8.5%							0.5%		0.5%		12%					0.5%	26%		0.5%	2.7%										2.7%	
3	1505.7	4940	SWC 24a									X	3.3%	0.5%					X	X		0.5%		4.9%		X	0.5%	0.5%	6.0%	40%		0.5%	0.5%	0.5%		0.5%			X					2.2%	
4	1551-70	5090-150	Cuttings										4.4%	X										2.2%				0.7%	0.7%	37%		1.5%	1.5%			0.7%								1.5%	
5	1600.2	5250	SWC 23a					X					5.0%	0.5%		X	RW	X			X	X		7.0%			0.5%		6.5%	43%		0.5%	0.5%	0.5%		0.5%			0.5%	0.5%				2.5%	
6	1652-70	5420-80	Cuttings	0.5%									6.5%	X		2								2.3%		X	0.9%	0.5%	2.8%	49%		2.8%	0.9%			3.7%				X				0.5%	
7	1691.6	5550	SWC 22a		X	X		X					X							X		X		X		X	X	X	X	X		X	X	X		X							X	
8	1706.9	5600	SWC 21a					X					7.3%	0.9%		X				0.9%				7.7%		X	0.9%	0.4%	13%	42%		0.4%	0.4%	0.4%		0.4%			X		X			1.7%	
9	1722.1	5650	SWC 20a										X														X		X	X						X							X	
10	1737.4	5700	SWC 19a									X	6.7%	X		X			X	X		X		0.4%		X	0.4%	0.4%	3.5%	46%		2.0%	2.4%	0.4%		12%			0.4%					0.4%	RW
11	1749.6	5740	SWC 18a	0.5%				X					1.8%	0.9%		0.5%			X	X				1.8%			0.5%	0.5%	22%	45%		0.5%	0.5%	0.5%		0.5%								1.4%	
12	1763.0	5784	SWC 16a	X			X	X					5.7%	0.8%						X				6.9%		X	0.8%	2.0%	4.5%	35%		0.4%	3.6%	0.8%		0.4%					X			1.2%	
13	1767.8	5800	SWC 15a					0.7%			X		7.0%			X			X	1.1%				11%		X	0.7%	2.2%	2.2%	37%		2.2%	3.3%	1.5%		3.0%			0.4%					0.4%	X
14	1801.4	5910	SWC 14a										8.5%	0.8%					X	2.0%				1.6%			0.4%		3.3%	41%		1.2%	1.2%	0.4%		5.3%								2.8%	X
15	1859.3	6100	SWC 12a					X					6.3%	0.4%						3.7%				0.7%		X	1.8%		3.3%	43%		1.8%	0.4%			4.8%			1.1%					3.3%	X
16	1889.8	6200	SWC 30										6.2%	0.4%						1.2%	0.4%			2.3%			1.2%	0.4%	5.0%	50%		3.1%	0.4%	0.4%		1.2%			X					1.9%	
17	1935.5	6350	SWC 6a	X									9.5%			X	0.4%			2.3%			X	6.5%				1.5%	3.0%	39%		0.8%	2.7%	0.4%		0.8%			0.8%	0.4%				6.8%	
18	1953.8	6410	Core 1	1.0%			0.5%						11%	2.1%						2.1%		0.5%		5.2%				0.5%	3.6%	20%			1.6%	0.5%		3.1%			X					7.3%	X
19	1958.9	6427	Core 1	0.6%				0.6%					10%							0.6%				16%		X			2.8%	22%						5.6%								7.3%	
20	1988.8	6525	SWC 4a	0.4%				X					4.8%	1.2%						1.2%	0.4%		X	4.4%		X	0.4%	2.8%	4.4%	40%			2.0%	0.4%		2.8%			0.8%	0.4%				7.1%	X
21	2009-18	6590-620	Coal cts	0.4%				0.8%					7.9%	0.8%		0.4%				0.4%			0.8%	0.8%					0.8%	47%			2.3%						1.5%					4.9%	
22	2011.7	6600	SWC 26	5.8%		0.7%						X	8.3%	0.4%			X		X	1.8%	0.4%							0.7%	1.8%	15%			2.2%	0.4%		0.7%			1.1%	0.4%		0.7%		8.3%	X
23	2047.6	6718	SWC 25	0.8%									9.0%	0.4%					X	2.3%				0.8%			0.4%	0.4%	2.3%	25%			2.7%	0.4%		1.2%			0.8%	0.4%		X		7.0%	X
24	2072.6	6800	SWC 24										X				X											X		X													
25	2091-97	6860-80	Coal cts										12%			0.8%								0.4%			0.4%		1.5%	47%			1.9%						1.2%			0.4%		5.8%	
26	2134.8	7004	SWC 22	1.1%		0.6%							2.2%	X						0.6%				1.1%				2.2%	2.8%	24%			8.9%	1.1%					1.1%			X		13%	
27	2169.6	7118	SWC 21	3.9%				X					0.8%							X							0.4%	0.4%		12%			3.9%						0.4%					31%	X
28	2194.6	7200	SWC 20	0.9%		0.4%							1.7%	0.4%						1.3%				0.9%			2.2%	0.9%	0.4%	20%			9.6%	0.9%					0.4%	0.4%				13%	X
29	2225.0	7300	SWC 19	1.3%		0.4%	X	X					4.7%	0.4%						0.9%				21%	X			0.4%		15%			0.9%						0.9%			1.3%			7.3%	X
30	2237.2	7340	SWC 18	2.4%			X	X					9.6%	0.4%	0.4%				X	1.2%		0.4%		3.6%	X			3.6%	1.6%	12%			2.0%						1.6%			X			10%	X
31	2257.3	7406	SWC 17	0.4%		1.2%						0.8%	8.2%	X		X	X		X	1.2%		0.4%		10%	X			0.8%		21%									3.5%			X			8.9%	X
32	2287.2	7504	SWC 16	2.0%									28%							X				1.0%	X			1.0%	2.0%	3.0%														37%	
33	2317.1	7602	SWC 15	0.5%		0.5%							13%	0.9%	0.5%		X		X	1.8%		0.9%		4.1%	1.8%	X		1.4%	0.5%	24%			0.5%	0.5%					2.3%			0.9%		X	10%	X
34	2362-74	7750-90	Cuttings										8.5%	0.6%		1.8%				1.8%		0.6%		3.6%	X				8.5%										2.4%						12%	
35	2377.4	7800	SWC 13	0.7%		0.7%							5.0%	X	0.4%		X		X	1.8%				19%		X			5.0%	11%			0.4%						1.4%	0.4%					8.6%	X
36	2408-17	7900-30	Cuttings	2.0%									8.5%				0.5%			4.0%				5.5%	0.5%			0.5%	8.0%	2.0%									2.5%						9.5%	
37	2426.2	7960	SWC 11	0.8%									8.0%		X	0.8%	2.4%			1.6%				5.6%				0.4%	0.4%	26%			2.0%	0.4%					0.4%	X					7.2%	X
38	2438.4	8000	SWC 10	1.7%		0.8%							3.8%		0.4%		2.1%		X	3.0%		0.4%		11%				1.7%	0.4%	6.4%			1.3%						0.8%	0.4%					7.6%	
39	2472.5	8112	Core 2										19%				4.5%		X	7.8%				X				0.6%		7.1%			1.3%						0.6%						7.8%	X
40	2474.4	8118	Core 2	X									X		X		X			X				X				X		X			X	X					X	X					X	X
41	2499-508	8200-30	Cuttings	0.4%									6.0%		0.4%	0.4%				1.6%				2.8%				1.2%	16%	0.4%			0.8%	0.8%		0.4%			0.8%	0.8%		0.4%			7.2%	
42	2499.4	8200	SWC 8										X				X																												
43	2514.6	8250	SWC 7	X									X		X		X							X				X		X			X											X	X
44	2529.8	8300	SWC 6	0.8%			0.4%						5.3%	1.9%			0.8%			2.7%				6.5%				0.4%		11%			6.1%	0.4%				0.4%	1.1%					10%	

Table 4. Poonboon-1 — spore-pollen distribution. **spore-pollen distribution.**

No.	Depth metres	Depth feet	Sample Type	Proteacidites alveolatus	Proteacidites angulatus	Proteacidites annularis	Proteacidites asperopolus	Proteacidites biporus	Proteacidites carobelindiae	Proteacidites clinei ms	Proteacidites confragosus	Proteacidites crassus	Proteacidites grandis	Proteacidites incurvatus	Proteacidites kopiensis	Proteacidites latrobensis	Proteacidites leighlonii	Proteacidites nasus	Proteacidites obesolabrus ms	Proteacidites obscurus	Proteacidites ornatus	Proteacidites otwayensis ms	Proteacidites parvus	Proteacidites pachypolus	Proteacidites pallisadus	Proteacidites prodigus ms	Proteacidites pseudomoides	Proteacidites recavus	Proteacidites rectomarginis	Proteacidites reflexus	Proteacidites reticulatus	Proteacidites reticuloconcavus ms	Proteacidites reticuloscabratus	Proteacidites rugulatus	Proteacidites stipplatus	Proteacidites tenuexinus	Proteacidites tuberculatus	Proteacidites tuberculiformis	Proteacidites truncatus	Proteacidites xestiformis ms	Pseudowinterapollis couperi	Quadraplanus brossus	Santalumiditles cainozoicus	Sapotaceoidaepollenites rotundus	Schizocolpus marlinensis	Schizocolpus ranus ms
1	1233.2	4046	SWC 27a			0.5%																																						
2	1325.9	4350	SWC 26a			0.5%																																						
3	1505.7	4940	SWC 24a			X																				X		X						X		X						X		
4	1551-70	5090-150	Cuttings			X																						0.7%																
5	1600.2	5250	SWC 23a			0.5%														X						X		0.5%						X		X					X	X	
6	1652-70	5420-80	Cuttings			0.9%																																						
7	1691.6	5550	SWC 22a														RW									X		X													X		X		
8	1706.9	5600	SWC 21a			0.4%											RW			0.4%								X						X		X								
9	1722.1	5650	SWC 20a																									X																
10	1737.4	5700	SWC 19a											RW						X							RW	X								X								
11	1749.6	5740	SWC 18a			X	RW											RW		X						X		X					RW	X									
12	1763.0	5784	SWC 16a			X														X								X		X											0.4%			
13	1767.8	5800	SWC 15a											RW						0.4%								X		X				X				X						
14	1801.4	5910	SWC 14a			0.4%										X	0.4%			0.4%				1.2%				X	X															
15	1859.3	6100	SWC 12a			0.7%								X		X	X							X				X		X											X			
16	1889.8	6200	SWC 30					X				X		X										X			X																	X
17	1935.5	6350	SWC 6a								X	X			X					0.4%				X										X								X		
18	1953.8	6410	Core 1				0.5%					X			X					0.5%				X			X	X													0.5%			
19	1958.9	6427	Core 1			1.1%																		0.6%																				
20	1988.8	6525	SWC 4a			0.8%						X		0.4%	X	X	X			0.4%				0.4%			X	X						X		X				X		0.4%			
21	2009-18	6590-620	Coal cts			1.1%											0.4%			0.4%													X						0.4%		1.1%			
22	2011.7	6600	SWC 26			2.2%	1.1%		X			X		X	X	X		X		0.4%			X	X	X		X	X	X												0.4%	0.4%		
23	2047.6	6718	SWC 25			0.4%	X										X							X			X	X			X	X		X						0.8%			
24	2072.6	6800	SWC 24														X																											
25	2091-97	6860-80	Coal cts			1.5%														0.8%								X													0.4%			0.8%
26	2134.8	7004	SWC 22			X		X						X			0.6%		X													X								0.6%			
27	2169.6	7118	SWC 21												X		0.8%	X					X			X	X								X					X			
28	2194.6	7200	SWC 20				X							X	X		X	X		0.4%																X					X			
29	2225.0	7300	SWC 19			0.4%	0.4%					X			X		0.4%			0.9%				0.4%									X					X			1.7%	0.4%	X	X
30	2237.2	7340	SWC 18			0.4%	X					X	X		X		0.4%		X	0.8%	X		X	0.4%			X						X			X					1.2%	0.4%		
31	2257.3	7406	SWC 17	X		X	0.4%					X	X				0.4%		X	0.8%			X	0.4%		X										X					0.4%			
32	2287.2	7504	SWC 16			1.0%	1.0%																	1.0%									X										
33	2317.1	7602	SWC 15			1.4%	X						X				0.5%		X	1.8%				0.5%			X																
34	2362-74	7750-90	Cuttings																					0.6%																				
35	2377.4	7800	SWC 13														X	X						2.5%												X					0.4%			X
36	2408-17	7900-30	Cuttings										0.5%							0.5%																								
37	2426.2	7960	SWC 11			0.8%							2.0%				X			0.8%																	X							
38	2438.4	8000	SWC 10	X									0.4%					X								X	X								X								X	
39	2472.5	8112	Core 2			0.6%							0.6%							0.6%																								
40	2474.4	8118	Core 2										X	X						X	X																X		X					X
41	2499-508	8200-30	Cuttings										1.6%							0.4%																								
42	2499.4	8200	SWC 8																																									
43	2514.6	8250	SWC 7										X																															X
44	2529.8	8300	SWC 6			0.8%							0.4%							0.8%															X									

Table 4. Poonboon-1 —

No.	Depth metres	Depth feet	Sample Type	Spinizonocolpites prominatus	Tetracolporites multistrixus ms	Tetracolporites textus ms	Tetracolporites verrucosus	Tetradopollis securus ms	Tricolp(or)ates spp.	Tricolpites confessus	Tricolpites incisus	Tricolpites phillipsii	Tricolpites simatus	Tricolpites waiparaensis	Tricolporites (Cunoniaceae?)	Tricolporites adelaidensis	Tricolporites leuros	Tricolporites lilliei	Tricolporites marginatus ms	Tricolporites paenestriatus	Tricolporites scabratus	Triorites magnificus	Triporopollenites ambiguus	Triporopollenites chnosus	Triporopollenites heloslus ms	Triporopollenites simplis	Triporopollenites spp.	TOTAL Angiosperms	TOTAL SP COUNT
1	1233.2	4046	SWC 27a						5.5%											0.9%								64%	217
2	1325.9	4350	SWC 26a						4.8%											2.1%								63%	188
3	1505.7	4940	SWC 24a						8.2%			X	X							0.5%						X	X	70%	184
4	1551-70	5090-150	Cuttings						3.7%											0.7%								57%	135
5	1600.2	5250	SWC 23a						7.5%								X			0.5%							X	80%	200
6	1652-70	5420-80	Cuttings						1.8%											0.5%								77%	217
7	1691.6	5550	SWC 22a						X				X			X	X						X			X			
8	1706.9	5600	SWC 21a						5.2%							X	X											85%	233
9	1722.1	5650	SWC 20a						X							X													
10	1737.4	5700	SWC 19a						0.4%							X	X				X							75%	254
11	1749.6	5740	SWC 18a						3.2%							X										0.5%		83%	217
12	1763.0	5784	SWC 16a						4.9%							X										1.6%		71%	247
13	1767.8	5800	SWC 15a						3.3%							X	X			0.4%						0.4%	0.4%	78%	270
14	1801.4	5910	SWC 14a						2.4%											0.4%		X	X			0.4%		76%	246
15	1859.3	6100	SWC 12a						2.9%				0.4%			X	X					X						76%	272
16	1889.8	6200	SWC 30						3.5%			X				X												78%	259
17	1935.5	6350	SWC 6a						5.7%			X	X			X				0.4%							0.4%	87%	263
18	1953.8	6410	Core 1						6.8%												X	X	X				1.0%	73%	192
19	1958.9	6427	Core 1						18%											0.6%								89%	177
20	1988.8	6525	SWC 4a						6.0%			X	X									X	X					85%	252
21	2009-18	6590-620	Coal cts						9.4%							0.8%				1.9%						0.8%	0.4%	85%	266
22	2011.7	6600	SWC 26						9.0%				X			0.7%					X		X	X				64%	278
23	2047.6	6718	SWC 25						5.5%							X				0.4%			0.4%					62%	256
24	2072.6	6800	SWC 24																				X						
25	2091-97	6860-80	Coal cts						4.6%						3.1%	0.4%				2.3%							1.2%	88%	259
26	2134.8	7004	SWC 22						6.7%			X				X												68%	180
27	2169.6	7118	SWC 21						4.6%							X										0.4%		60%	259
28	2194.6	7200	SWC 20						3.5%							X											0.9%	60%	230
29	2225.0	7300	SWC 19						18%							X				3.8%							X	85%	234
30	2237.2	7340	SWC 18	X					16%		0.4%					0.4%	0.4%			2.0%			0.4%				2.4%	75%	251
31	2257.3	7406	SWC 17						21%							X				1.6%			X		X	2.3%	X	88%	257
32	2287.2	7504	SWC 16						6.9%																			87%	101
33	2317.1	7602	SWC 15						14%		X				3.2%	X				0.5%			X				1.8%	88%	220
34	2362-74	7750-90	Cuttings						9.7%											0.6%								64%	165
35	2377.4	7800	SWC 13						20%							0.4%				1.8%					X		3.2%	85%	280
36	2408-17	7900-30	Cuttings						18%																			69%	200
37	2426.2	7960	SWC 11	0.8%					8.8%							0.4%				0.4%						X	2.0%	72%	249
38	2438.4	8000	SWC 10						6.8%						3.8%					0.4%			X			X	1.3%	57%	236
39	2472.5	8112	Core 2						5.8%											1.3%							0.6%	62%	154
40	2474.4	8118	Core 2	X												X				X									
41	2499-508	8200-30	Cuttings						7.2%											0.4%								58%	250
42	2499.4	8200	SWC 8																										
43	2514.6	8250	SWC 7																										
44	2529.8	8300	SWC 6						9.9%						2.3%					0.4%							1.9%	65%	262

Table 4. Poonboon-1 — spore-pollen distribution. **spore-pollen distribution.**

No.	Depth metres	Depth feet	Sample Type	SPORE SPECIES	Baculatisporites spp.	Camarozonosporites bullatus	Camarozonosporites heskemensis	Clavifera triplex	Contaculatisporites apiculatus ms	Crassoretitriletes vanraadshooveni	Cyatheacidites annulatus	Cyathidites splendens	Cyathidites subtilis	Cyathidites spp. small <40µm	Densoisporites pellis ms	Dictyophyllidites spp.	Echinosporis echinatus	Foraminisporis ozotus ms	Foveotriletes balteus	Foveotriletes crater	Foveotriletes palaequetrus	Gleicheniidites circinidites	Grapnelispora evansii	Herkosporites elliottii	Ischyosporites spp.	Kuylisporites waterbolkii	Laevigatosporites major	Laevigatosporites ovatus	Latrobosporites amplus	Latrobosporites crassus	Latrobosporites ohaiensis	Marattisporites scabratus	Matonisporites gigantis	Matonisporites ornamentalis	Monolites alveolatus	Oramentifera sentosa	Peromonolites densus	Peromonolites vellosus	Perotriletes spp.	Polypodiaceoisporites varus ms	Polypodiidites/Verrucatosporites spp.	Reitriletes spp.	Ricciaesporites boxatus ms	Rotverrusporites stellatus ms	Rugulatisporites mallatus	Rugulatisporites trophus
45	2560.3	8400	SWC 5																																										
46	2590.8	8500	SWC 4																																											
47	2624.3	8610	SWC 3		0.4%									2.4%								3.6%			0.4%														0.4%					
48	2651.8	8700	SWC 2		1.5%			0.5%		X		2.0%		5.9%			X					5.4%			1.0%			1.5%		0.5%							0.5%					X	X	
49	2678.6	8788	SWC 1		0.4%			1.5%				1.2%		1.9%		0.4%			0.4%			16%		0.4%	0.4%			6.9%			X		0.4%			0.4%			0.4%	0.4%				
50	2688.0	8819	Core 3		1.5%			0.7%				X		0.7%								12%		0.4%	X			2.6%	X	X			X						0.4%	0.4%				
51	2689.3	8823	Core 3		1.2%			0.8%				0.8%		2.3%					0.4%			6.5%		0.4%				3.1%					0.4%						1.5%					
52	2713-25	8900-40	Cuttings					1.3%				2.6%		4.8%		0.4%												0.9%					0.4%						0.9%					
53	2737-40	8980-90	Coal Cts		2.1%			0.4%						0.8%								0.4%						6.2%	X	X														
54	2758-61	9050-60	Coal Cts		2.4%	X		0.4%				1.6%		1.2%								2.4%					0.4%	15%				X												
55	2795-801	9170-90	Cuttings		1.6%		0.4%	0.4%				4.4%		2.4%								1.2%						2.4%																
56	2838-44	9310-30	Cuttings		2.6%							5.2%		6.1%		0.4%						3.9%						0.9%		0.4%														
57	2847-50	9340-50	Coal Cts		0.8%									0.8%																						X							
58	2877-80	9440-50	Coal Cts		0.4%			0.8%				0.4%		3.2%		0.4%						2.0%						2.8%		0.4%										0.4%			X	
59	2896-902	9500-20	Cuttings		1.5%							2.9%		1.8%					X			4.0%						1.8%													0.7%			
60	2951-57	9680-700	Cuttings		1.4%							1.4%		2.3%								0.5%						2.3%																
61	2975-84	9760-90	Cuttings		0.6%							1.0%		0.3%								0.6%		0.3%				0.6%																
62	2995.6	9828	SWC 28		1.1%			1.1%						3.3%								4.3%						1.1%								1.1%							
63	2997.4	9834	SWC 27																			1.7%						1.3%															
64	3042.2	9981	Core-4		0.5%							X		1.4%		0.5%						1.8%		1.4%				0.5%													0.5%			
65	3066-69	10060-70	Cuttings		0.8%							1.2%		0.8%								1.2%						2.0%																
66	3116.9	10226	SWC 22		0.4%							0.7%		1.8%								0.7%		5.1%				3.3%			X								0.4%		1.1%			
67	3154.7	10350	SWC 18		1.6%							0.4%		0.4%								1.6%		0.8%				1.2%											0.8%					
68	3183.6	10445	SWC 12				X					0.4%				X						2.0%		1.6%				0.8%	X		X									X		X		
69	3223.9	10577	SWC 33		2.6%		X					1.6%		3.2%		0.5%						0.5%		3.2%				X	0.5%		X									0.5%				
70	3231-40	10600-30	Cuttings		0.4%																	0.4%						3.2%															
71	3233.3	10608	SWC 5		1.2%									1.6%								0.4%		1.6%				1.6%	0.4%		0.4%								0.8%				
72	3247.3	10654	SWC 34		0.4%							0.4%		0.4%								0.4%	X	0.4%				1.1%	X		X									0.4%				
73	3262.3	10703	Core 5		2.4%			0.4%				0.8%		3.2%		0.4%						3.6%		0.8%				1.6%	X		X									1.6%			X	

ABBREVIATIONS: X = Present % = Percentage RW = Reworked **ABBREVIATIONS:** X = Present

Table 4. Poonboon-1 — spore-pollen distribution.

No.	Depth metres	Depth feet	Sample Type	Stereisporites antiquisporites	Stereisporites regium	Striamonoletes diglatoides	Triletе spores undiff.	Tripunctisporis maastrichtiensis	Verrucatosporites attinatus ms	Verrucosisporites cristatus	Verrucosisporites kopukuensis	TOTAL Spores	GYMNOSPERM SPECIES	Araucariacites australis	Cupressacites sp.	Dacrycarpites australiensis	Dilwynites granulatus	Dilwynites tuberculatus	Lygistepolenites balmei	Lygistepollenites florinii	Microalatidites paleogenicus	Microcachryidites antarcticus	Phyllocladidites mawsonii	Phyllocaldidites reticulosaccatus	Phyllocaldidites verrucosus	Podocarpidites spp.	Podocarpidites exiguus	Trichotomosulcites subgranulatus	TOTAL Gymnosperms	ANGIOSPERM SPECIES	Angiosperm pollen undiff.	Aglaoreidia qualumis	Anacolosidites luteoides	Anacolosidites sectus	Anisocolporites triplex	Australopollis obscurus	Banksieaeidites arcuatus	Banksieaeidites elongatus	Battenipollis sectilis	Beaupreaidites eleganslformis	Beaupreaidites verrucosus	Clavatipollenites glarius	Concolpites leptos	Cupanieidites orthoteichus	Cyperaceaepollis neogenicus
45	2560.3	8400	SWC 5																							X																
46	2590.8	8500	SWC 4																							X																
47	2624.3	8610	SWC 3				0.4%	0.4%			X	8%		2.8%	0.8%		10%	0.8%		0.8%	0.8%	0.4%	4.9%			26%	X	2.0%	49%		0.8%												
48	2651.8	8700	SWC 2	0.5%			1.0%				X	20%		4.4%			13%	5.4%	0.5%	1.5%		1.5%	0.5%			17%		5.4%	50%		2.5%					RW					0.5%	
49	2678.6	8788	SWC 1	2.7%	X			0.4%			0.4%	34%		2.7%	2.3%		15%	1.5%	0.4%			0.8%	1.5%		0.8%	12%	1.2%	1.9%	40%							4.6%						
50	2688.0	8819	Core 3	1.9%	X			X			X	21%		3.4%	0.4%		16%		2.6%	0.4%		2.2%	4.1%			10%		1.5%	41%							0.7%					0.4%	
51	2689.3	8823	Core 3	2.7%							0.4%	20%		1.5%	4.2%		14%	0.8%	2.3%	1.9%	0.4%		3.1%			12%	1.5%	1.9%	44%		1.2%											
52	2713-25	8900-40	Cuttings	0.4%			5.7%					18%		3.9%			5.7%			1.3%		1.3%	3.5%			25%		7.9%	49%		5.3%					1.3%						
53	2737-40	8980-90	Coal Cts								X	10%					0.4%		0.4%	2.5%	0.4%	1.7%	4.5%			25%		13%	48%													
54	2758-61	9050-60	Coal Cts	3.6%								27%					0.4%	0.4%	0.8%	6.3%		1.2%	4.0%			23%		3.6%	40%							0.4%						
55	2795-801	9170-90	Cuttings	0.4%			7.7%					21%		5.2%	0.4%		10%		2.8%			1.2%	2.0%		1.2%	32%		6.5%	62%		1.2%					1.2%						
56	2838-44	9310-30	Cuttings	1.3%			8.2%					29%		3.5%	0.4%		6.5%		0.4%	1.3%		1.3%	2.2%		0.4%	35%		7.8%	59%		0.9%											
57	2847-50	9340-50	Coal Cts									2%							0.8%	0.8%		7.1%	46%		2.8%	22%		11%	91%													
58	2877-80	9440-50	Coal Cts									11%					1.2%	0.4%	0.4%	2.0%	0.4%	3.2%	34%	0.4%	1.2%	11%		15%	68%													
59	2896-902	9500-20	Cuttings	3.7%			8.8%					25%		2.2%			8.8%	0.4%	0.4%	0.4%			4.4%		1.5%	35%		7.7%	61%		2.6%					0.4%						
60	2951-57	9680-700	Cuttings	2.7%			7.3%	0.5%				18%		2.3%			6.8%		0.5%	0.5%		0.5%	2.7%		0.9%	45%		6.4%	65%		1.8%					0.9%						
61	2975-84	9760-90	Cuttings	1.3%			2.3%					7%		0.3%	0.3%		1.3%		0.3%			0.6%	14%		3.2%	44%		20%	84%		0.6%											
62	2995.6	9828	SWC 28	3.3%			1.1%					16%		5.4%			8.7%		1.1%				11%			23%		6.5%	55%													
63	2997.4	9834	SWC 27	0.4%								3%							0.9%	2.2%		1.7%	69%	0.4%	0.4%	7.3%		3.4%	85%													
64	3042.2	9981	Core-4	2.3%				1.4%				10%		4.1%	0.5%		3.2%		0.5%		0.5%	1.4%	10%	1.4%	0.9%	30%		0.5%	53%		0.5%											
65	3066-69	10060-70	Cuttings	1.2%			2.0%					9%		1.2%	0.8%		5.6%			0.4%		0.4%	14%		0.4%	37%		18%	79%		1.6%					0.4%						
66	3116.9	10226	SWC 22	1.5%	X		0.7%	0.7%				16%		2.9%	4.4%		20%	0.7%	X	1.1%	0.4%	0.7%	7.3%	0.4%		14%		1.1%	53%		1.8%											
67	3154.7	10350	SWC 18	3.2%			0.8%					11%		2.0%	3.2%		10%			0.8%	0.4%	2.4%	4.8%	1.2%	0.4%	20%		3.6%	49%													
68	3183.6	10445	SWC 12	0.8%				X				5%		0.4%	X		1.2%				1.6%	1.2%	25%	0.8%	2.0%	34%		2.3%	69%													
69	3223.9	10577	SWC 33	6.9%	X		1.6%	X				21%		6.9%	1.6%		15%					X	5.8%			14%			43%													
70	3231-40	10600-30	Cuttings	1.6%			2.4%					8%		1.2%	0.4%		6.0%			0.4%		0.4%	4.8%		0.4%	39%		26%	78%		0.4%											
71	3233.3	10608	SWC 5	3.7%			1.6%	1.6%				15%		6.1%			38%					0.4%	1.2%			11%		1.2%	59%													
72	3247.3	10654	SWC 34	0.4%			0.4%	X				4%		7.3%	1.8%		22%		X	0.7%		0.7%	19%		1.1%	15%		4.7%	72%								X					
73	3262.3	10703	Core 5	5.2%	X		0.4%	0.8%				21%		18%	0.4%		25%	0.4%	X			X	2.0%			5.6%		0.8%	53%													

% = Percentage RW = Reworked

ABBREVIATIONS: X = Present % = Percentage RW = Reworked

Table 4. Poonboon-1 — spore-pollen distribution.

No.	Depth metres	Depth feet	Sample Type	Dicotetradites clavatus	Dryadopollenites retequetrus	Dryptopollenites semilunatus	Elphedripites notensis	Ericipites crassiexinus/scabratus	Gambierina edwardsii	Gambierina rudata	Granodiporites nebulosus	Gothanipollis bassensis	Haloragacidites harrisii	Ilexpollenites spp.	Intratriporopollenites notabilis	Liliacidites spp.	Malvacipollis diversus	Malvacipollis grandis ms	Malvacipollis robustus ms	Malvacipollis subtilis	Milfordia incerta	Milfordia homeopunctatus	Monosulcites uvatus ms	Myrtaceidites parvus/mesonesus	Myrtaceidites tenuis	Myrtaceidites verrucosus	Nothofagidites asperus	Nothofagidites brachyspinulosus	Nothofagidites deminutus	Nothofagidites emarcidus/heterus	Nothofagidites endurus	Nothofagidites falcatus	Nothofagidites flemingii	Nothofagidites goniatus	Nothofagidites senectus	Nothofagidites vansteenisii	Paripollis ochesis	Peninsulapollis gillii	Periporopollenites demarcatus	Periporopollenites polyoratus	Periporopollenites vesicus	Polycolporopollenites esobalteus	Polycolpites langstonii	Polyorificites oblatus	Proteacidites spp.	Proteacidites adenanthoides
45	2560.3	8400	SWC 5										X																														
46	2590.8	8500	SWC 4										X																														
47	2624.3	8610	SWC 3										1.6%	0.4%										0.4%				6.5%		7.7%			0.4%	0.4%				0.4%	0.4%	2.0%					7.7%	
48	2651.8	8700	SWC 2	X		X							2.5%				2.0%			1.0%				0.5%				0.5%		1.5%			0.5%											8.8%	X
49	2678.6	8788	SWC 1	0.4%						0.4%			1.2%							X							0.4%	3.1%		4.2%	1.2%		1.5%					0.8%		0.4%				3.5%	
50	2688.0	8819	Core 3	0.7%					X	0.4%			1.1%	0.4%						0.4%							0.4%	3.0%		5.2%	9.3%		0.7%					0.4%		0.4%			0.4%		9.0%	X
51	2689.3	8823	Core 3							1.9%														1.2%				0.8%		2.3%	9.2%		0.4%					3.1%		0.4%					10%	
52	2713-25	8900-40	Cuttings										0.9%							0.4%				4.4%				0.4%		0.4%	8.8%		0.9%											6.1%	
53	2737-40	8980-90	Coal Cts	0.8%		0.4%							3.7%	0.4%			X			1.7%								0.8%		2.9%	16%		0.4%						0.4%	0.4%					2.5%	
54	2758-61	9050-60	Coal Cts	0.8%					X				0.8%	0.4%														0.4%		0.8%	21%		0.4%				0.8%			0.4%				0.4%	
55	2795-801	9170-90	Cuttings							1.2%														0.8%				0.8%		0.4%	7.3%		0.4%											2.8%	
56	2838-44	9310-30	Cuttings							0.9%			1.3%																		3.5%								0.4%						3.0%	
57	2847-50	9340-50	Coal Cts																									0.4%			2.8%						0.4%			0.4%					
58	2877-80	9440-50	Coal Cts	X			0.4%			0.4%			1.2%	0.4%																0.4%	7.1%										0.4%				2.0%	
59	2896-902	9500-20	Cuttings	0.4%					X	0.4%														0.4%							6.6%		1.5%												1.5%	
60	2951-57	9680-700	Cuttings							X																					7.3%								0.5%						0.9%	
61	2975-84	9760-90	Cuttings							0.3%																		0.3%			4.2%														1.6%	
62	2995.6	9828	SWC 28							2.2%																					20%								2.2%		1.1%					
63	2997.4	9834	SWC 27					1.7%	X	1.3%			0.4%																		3.4%										0.4%				3.0%	
64	3042.2	9981	Core-4							14%			X														0.5%	0.5%		0.9%	4.1%								2.7%						9.9%	
65	3066-69	10060-70	Cuttings				0.4%			0.4%																					2.0%														1.2%	
66	3116.9	10226	SWC 22	0.7%					X	5.1%																		1.5%			1.5%								5.5%		0.4%				8.0%	
67	3154.7	10350	SWC 18							6.8%																					8.8%								10%						7.2%	
68	3183.6	10445	SWC 12							3.5%																					9.4%								6.3%						5.9%	
69	3223.9	10577	SWC 33							2.6%																					3.7%				0.5%				4.8%						17%	
70	3231-40	10600-30	Cuttings							1.2%				0.4%																	2.8%								0.4%						2.0%	
71	3233.3	10608	SWC 5							2.4%																					2.4%								6.5%						11%	
72	3247.3	10654	SWC 34							3.6%																		0.4%							0.4%				7.7%						6.9%	
73	3262.3	10703	Core 5				0.8%			5.2%						0.4%																							4.0%						11%	

ABBREVIATIONS: X = Present % = Percentage RW = Reworked

Table 4. Poonboon-1 — spore-pollen distribution. **spore-pollen distribution.**

No.	Depth metres	Depth feet	Sample Type	Proteacidites alveolatus	Proteacidites angulatus	Proteacidites annularis	Proteacidites asperopolus	Proteacidites biporus	Proteacidites carobelindiae	Proteacidites clinei ms	Proteacidites confragosus	Proteacidites crassus	Proteacidites grandis	Proteacidites incurvatus	Proteacidites kopiensis	Proteacidites latrobensis	Proteacidites leighlonii	Proteacidites nasus	Proteacidites obesolabrus ms	Proteacidites obscurus	Proteacidites ornatus	Proteacidites otwayensis ms	Proteacidites parvus	Proteacidites pachypolus	Proteacidites pallisadus	Proteacidites prodigus ms	Proteacidites pseudomoides	Proteacidites recavus	Proteacidites rectomarginis	Proteacidites reflexus	Proteacidites reticulatus	Proteacidites reticuloconcavus ms	Proteacidites reticuloscabratus	Proteacidites rugulatus	Proteacidites stipplatus	Proteacidites tenuiexinus	Proteacidites tuberculatus	Proteacidites tuberculiformis	Proteacidites truncatus	Proteacidites xestiformis ms	Pseudowinterapollis couperi	Quadraplanus brossus	Santalumiditles cainozoicus	Sapotaceoidaepollenites rotundus	Schizocolpus marlinensis	Schizocolpus ranus ms
45	2560.3	8400	SWC 5																																									
46	2590.8	8500	SWC 4																	X																									
47	2624.3	8610	SWC 3										0.4%							0.8%																									
48	2651.8	8700	SWC 2										0.5%	X												X									X									
49	2678.6	8788	SWC 1										0.8%	0.4%												X																		
50	2688.0	8819	Core 3										0.4%	X												X							X											
51	2689.3	8823	Core 3										0.4%																															
52	2713-25	8900-40	Cuttings																																									
53	2737-40	8980-90	Coal Cts			0.8%							0.4%											0.8%																				
54	2758-61	9050-60	Coal Cts																																									
55	2795-801	9170-90	Cuttings																																									
56	2838-44	9310-30	Cuttings																																									
57	2847-50	9340-50	Coal Cts																																									
58	2877-80	9440-50	Coal Cts																																									
59	2896-902	9500-20	Cuttings																																									
60	2951-57	9680-700	Cuttings																																									
61	2975-84	9760-90	Cuttings																																									
62	2995.6	9828	SWC 28																																									
63	2997.4	9834	SWC 27																																									
64	3042.2	9981	Core-4							0.5%																																			
65	3066-69	10060-70	Cuttings																																									
66	3116.9	10226	SWC 22		1.1%					X																																		
67	3154.7	10350	SWC 18																																									
68	3183.6	10445	SWC 12																																									
69	3223.9	10577	SWC 33																													X				X								
70	3231-40	10600-30	Cuttings																																									
71	3233.3	10608	SWC 5																													0.4%												
72	3247.3	10654	SWC 34							0.4%																																		
73	3262.3	10703	Core 5							X													X			X															0.4%				

ABBREVIATIONS: X = Present % = Percentage RW = Reworked **ABBREVIATIONS:** X = P

Table 4. Poonboon-1 —

No.	Depth metres	Depth feet	Sample Type	Spinizonocolpites prominatus	Tetracolporites multistrixus ms	Tetracolporites textus ms	Tetracolporites verrucosus	Tetradopollis securus ms	Tricolp(or)ates spp.	Tricolpites confessus	Tricolpites incisus	Tricolpites phillipsii	Tricolpites simatus	Tricolpites waiparaensis	Tricolporites (Cunoniaceae?)	Tricolporites adelaidensis	Tricolporites leuros	Tricolporites lilliei	Tricolporites marginatus ms	Tricolporites paenestriatus	Tricolporites scabratus	Triorites magnificus	Triporopollenites ambiguus	Triporopollenites chnosus	Triporopollenites helosus ms	Triporopollenites simplis	Triporopollenites spp.	TOTAL Angiosperms	TOTAL SP COUNT
45	2560.3	8400	SWC 5																										
46	2590.8	8500	SWC 4																										
47	2624.3	8610	SWC 3						11%																	2.0%	43%	247
48	2651.8	8700	SWC 2	X					9.8%																		30%	204
49	2678.6	8788	SWC 1						2.3%			X														0.4%	25%	259
50	2688.0	8819	Core 3						3.7%			0.4%														1.5%	39%	268
51	2689.3	8823	Core 3						2.3%																	1.9%	35%	260
52	2713-25	8900-40	Cuttings						4.4%																	0.4%	34%	228
53	2737-40	8980-90	Coal Cts			0.8%	0.8%		7.4%														0.4%			0.4%	43%	242
54	2758-61	9050-60	Coal Cts			0.4%			5.6%																	0.4%	33%	252
55	2795-801	9170-90	Cuttings						0.8%																	0.4%	17%	248
56	2838-44	9310-30	Cuttings						2.2%																		12%	231
57	2847-50	9340-50	Coal Cts			2.0%			1.6%																		8%	253
58	2877-80	9440-50	Coal Cts						8.7%																	0.4%	21%	253
59	2896-902	9500-20	Cuttings						0.4%																		14%	272
60	2951-57	9680-700	Cuttings						5.0%																		16%	220
61	2975-84	9760-90	Cuttings				X		2.3%																		9%	311
62	2995.6	9828	SWC 28		X				2.2%																	1.1%	28%	92
63	2997.4	9834	SWC 27						0.9%																		11%	232
64	3042.2	9981	Core-4						1.4%					0.9%												1.8%	37%	222
65	3066-69	10060-70	Cuttings				X		5.6%																	0.4%	12%	250
66	3116.9	10226	SWC 22						4.0%										X							1.5%	31%	275
67	3154.7	10350	SWC 18				X		4.8%																	2.8%	41%	251
68	3183.6	10445	SWC 12		X		0.4%		0.4%																	X	26%	256
69	3223.9	10577	SWC 33				1.1%		3.7%																	2.1%	35%	189
70	3231-40	10600-30	Cuttings						5.6%																	0.8%	14%	250
71	3233.3	10608	SWC 5				0.8%		1.6%																	0.4%	26%	245
72	3247.3	10654	SWC 34				X	X	4.4%																		24%	274
73	3262.3	10703	Core 5				0.8%		2.8%	X				0.4%				X								0.8%	26%	251

resent % = Percentage RW = Reworked

Table 5. Poonboon-1 - microplankton distribution.

No.	Depth metres	Depth feet	Sample Type	ACRITARCHS & ALGAE	Acritarchs & Algae undiff.	Cymatisphaera sp. (polygonal)	Horologinella incurvata	Micrhystridium spp.	Amosopollis cruciformis	Botryococcus braunii	Crassosphaera concinnia	Pediastum sp.	Pseudoschizaea spp.	NON-MARINE DINOCYSTS	Cobricosphaeridium spp.	Morkallacysta spp.	Saeptodinium spp.	MARINE DINOCYSTS	Dinocysts undiff.	Apteodinium australicum	Apectodinium homomorphum	Apectodinium hyperacanthum	Apectodinium reburrus ms	Batiacasphaera spp.	Cannosphaeropsis sp.	Cleistosphaeridium spp.	Cooksonidium capricornum	Cordosphaeridium spp.	Cyclopsiella vieta	Dapsilidinium pseudocolligerum	Deflandrea heterophlycta	Deflandrea leptodermata	Deflandrea phosphoritica	Deflandrea spp.
1	1233.2	4046	SWC 27a							17%									11%										6%					
2	1325.9	4350	SWC 26a							26%									16%					X						6%					
3	1505.7	4940	SWC 24a				6%	X		4%									51%						X										
4	1551-70	5090-150	Cuttings					26%		1%									12%	3%										3%					
5	1600.2	5250	SWC 23a			X		7%		7%	7%								36%																
6	1652-70	5420-80	Cuttings				5%	35%											10%	5%										3%					
7	1691.6	5550	SWC 22a																																
8	1706.9	5600	SWC 21a			X													21%																3%
9	1722.1	5650	SWC 20a			X																													
10	1737.4	5700	SWC 19a																100%																
11	1749.6	5740	SWC 18a			X													100%																
12	1763.0	5784	SWC 16a																20%									1%			11%	1%	1%	1%
13	1767.8	5800	SWC 15a							9%		5%							14%																
14	1801.4	5910	SWC 14a																18%								4%	4%					4%	7%
15	1859.3	6100	SWC 12a																18%									40%						
16	1889.8	6200	SWC 30																60%															
17	1935.5	6350	SWC 6a																															
18	1953.8	6410	Core 1																100%															
19	1958.9	6427	Core 1					6%		1%									13%							4%		4%						
20	1988.8	6525	SWC 4a																															
21	2009-18	6590-620	Coal cts																															
22	2011.7	6600	SWC 26																															
23	2047.6	6718	SWC 25																100%															
24	2072.6	6800	SWC 24																															
25	2091-97	6860-80	Coal cts																															
26	2134.8	7004	SWC 22																															
27	2169.6	7118	SWC 21																															
28	2194.6	7200	SWC 20										33%				67%																	
29	2225.0	7300	SWC 19														100%																	
30	2237.2	7340	SWC 18																100%															
31	2257.3	7406	SWC 17							100%																									
32	2287.2	7504	SWC 16																															
33	2317.1	7602	SWC 15					100%																											
34	2362-74	7750-90	Cuttings																71%															
35	2377.4	7800	SWC 13																		67%													
36	2408-17	7900-30	Cuttings																43%															
37	2426.2	7960	SWC 11					6%								56%			28%															

Table 5. Poonboon-1 - microplankton distribution.

No.	Depth metres	Depth feet	Sample Type	Diphyes colligerum	Distatodinium ellipticum	Enneadocysta spp.	Fibrocysta bipolaris	Fromea blysma ms	Fromea leos ms	Fromea neochytra ms	Glaphrocysta spp.	Heteraulacacysta spp.	Homotryblium tasmaniense	Hystrichokolpoma rigaudiae	Impagidinium spp.	Kenleyia spp.	Lingulodinium machaerophorum	Operculodinium centrocarpum	Palaeocystodinium golzowensis	Paralecaniella indentata	Pentadinium laticinctum	Phthanoperidinium comatum	Phthanoperidinium spp.	Protoellipsodinium simplex ms	Protoellipsodinium spp.	Pyxidinopsis pontus ms	Reticulatosphaera stellata	Samlandia reticulifera	Spinidinium spp.	Spiniferites spp.	Systematophora placanthum	Tectatodinium sp.	Turbiosphaera filosa	TOTAL MICROPLANKTON COUNT
1	1233.2	4046	SWC 27a												3%		3%	6%						13%		1%				34%		7%		71
2	1325.9	4350	SWC 26a											19%				9%									4%			19%	1%			139
3	1505.7	4940	SWC 24a						X	21%							X													9%	9%			53
4	1551-70	5090-150	Cuttings							1%				X	X		X	6%	X	X	X			2%	X		X			45%		1%		121
5	1600.2	5250	SWC 23a							29%							7%													7%				14
6	1652-70	5420-80	Cuttings						15%	10%								3%							8%					8%				40
7	1691.6	5550	SWC 22a																															
8	1706.9	5600	SWC 21a															3%				15%	41%							18%				34
9	1722.1	5650	SWC 20a																															
10	1737.4	5700	SWC 19a																															1
11	1749.6	5740	SWC 18a					X										X												X	X	X		1
12	1763.0	5784	SWC 16a					1%									1%	4%				39%	1%							16%				74
13	1767.8	5800	SWC 15a		5%										5%			9%					32%		5%			5%		14%				22
14	1801.4	5910	SWC 14a			4%		7%						7%	4%		7%	4%												29%	4%			28
15	1859.3	6100	SWC 12a	2%				8%										8%		12%										12%				50
16	1889.8	6200	SWC 30																	20%										20%				5
17	1935.5	6350	SWC 6a																											100%				2
18	1953.8	6410	Core 1																															3
19	1958.9	6427	Core 1			46%						3%		1%									1%							20%				70
20	1988.8	6525	SWC 4a																											100%				2
21	2009-18	6590-620	Coal cts																															
22	2011.7	6600	SWC 26																															
23	2047.6	6718	SWC 25																															1
24	2072.6	6800	SWC 24																															
25	2091-97	6860-80	Coal cts																															
26	2134.8	7004	SWC 22																															
27	2169.6	7118	SWC 21																															
28	2194.6	7200	SWC 20																															3
29	2225.0	7300	SWC 19																															1
30	2237.2	7340	SWC 18																															1
31	2257.3	7406	SWC 17																															1
32	2287.2	7504	SWC 16																															
33	2317.1	7602	SWC 15																															1
34	2362-74	7750-90	Cuttings										14%			14%																		7
35	2377.4	7800	SWC 13																											33%				3
36	2408-17	7900-30	Cuttings										50%			7%																		14
37	2426.2	7960	SWC 11																	6%										6%				18

Table 5. Poonboon-1 - microplankton distribution.

No.	Depth metres	Depth feet	Sample Type	ACRITARCHS & ALGAE	Acritarchs & Algae undiff.	Cymatisphaera sp. (polygonal)	Horologinella incurvata	Micrhystridium spp.	Amosopollis cruciformis	Botryococcus braunii	Crassosphaera concinnia	Pediastum sp.	Pseudoschizaea spp.	NON-MARINE DINOCYSTS	Cobricosphaeridium spp.	Morkallacysta spp.	Saeptodinium spp.	MARINE DINOCYSTS	Dinocysts undiff.	Apteodinium australicum	Apectodinium homomorphum	Apectodinium hyperacanthum	Apectodinium reburrus ms	Batiacasphaera spp.	Cannosphaeropsis sp.	Cleistosphaeridium spp.	Cooksonidium capricornum	Cordosphaeridium spp.	Cyclopsiella vieta	Dapsilidinium pseudocolligerum	Deflandrea heterophlycta	Deflandrea leptodermata	Deflandrea phosphoritica	Deflandrea spp.
38	2438.4	8000	SWC 10					100%																										
39	2472.5	8112	Core 2																9%		58%					3%								
40	2474.4	8118	Core 2																															
41	2499-508	8200-30	Cuttings																94%		4%													
42	2499.4	8200	SWC 8																															
43	2514.6	8250	SWC 7																															
44	2529.8	8300	SWC 6					9%		9%									9%		9%					27%								
45	2560.3	8400	SWC 5																															
46	2590.8	8500	SWC 4																															
47	2624.3	8610	SWC 3					100%																										
48	2651.8	8700	SWC 2																36%			64%												
49	2678.6	8788	SWC 1							8%									8%				50%					8%						8%
50	2688.0	8819	Core 3					50%								50%																		
51	2689.3	8823	Core 3					33%								33%			33%															
52	2713-25	8900-40	Cuttings																100%															
53	2737-40	8980-90	Coal Cts																															
54	2758-61	9050-60	Coal Cts																															
55	2795-801	9170-90	Cuttings																100%															
56	2838-44	9310-30	Cuttings						8%										92%															
57	2847-50	9340-50	Coal Cts																															
58	2877-80	9440-50	Coal Cts							50%						50%																		
59	2896-902	9500-20	Cuttings																100%															
60	2951-57	9680-700	Cuttings																100%															
61	2975-84	9760-90	Cuttings																100%															
62	2995.6	9828	SWC 28					100%																										
63	2997.4	9834	SWC 27																															
64	3042.2	9981	Core-4										50%			50%																		
65	3066-69	10060-70	Cuttings													100%																		
66	3116.9	10226	SWC 22													50%			25%															
67	3154.7	10350	SWC 18													100%																		
68	3183.6	10445	SWC 12																															
69	3223.9	10577	SWC 33		3%					3%						83%			10%															
70	3231-40	10600-30	Cuttings													100%																		
71	3233.3	10608	SWC 5						8%	23%					8%	54%			8%															
72	3247.3	10654	SWC 34																															
73	3262.3	10703	Core 5		25%										50%	25%																		

ABBREVIATIONS: X = Present % = Percentage

Table 5. Poonboon-1 - microplankton distribution.

No.	Depth metres	Depth feet	Sample Type	Diphyes colligerum	Distatodinium ellipticum	Enneadocysta spp.	Fibrocysta bipolaris	Fromea blysma ms	Fromea leos ms	Fromea neochytra ms	Glaphrocysta spp.	Heteraulacacysta spp.	Homotryblium tasmaniense	Hystrichokolpoma rigaudiae	Impagidinium spp.	Kenleyia spp.	Lingulodinium machaerophorum	Operculodinium centrocarpum	Palaeocystodinium golzowensis	Paralecaniella indentata	Pentadinium laticinctum	Phthanoperidinium comatum	Phthanoperidinium spp.	Protoellipsodinium simplex ms	Protoellipsodinium spp.	Pyxidinopsis pontus ms	Reticulatosphaera stellata	Samlandia reticulifera	Spinidinium spp.	Spiniferites spp.	Systematophora placanthum	Tectatodinium sp.	Turbiosphaera filosa	TOTAL MICROPLANKTON COUNT
38	2438.4	8000	SWC 10																															1
39	2472.5	8112	Core 2	1%			1%				2%					16%				3%										7%			1%	117
40	2474.4	8118	Core 2																															
41	2499-508	8200-30	Cuttings																											3%				77
42	2499.4	8200	SWC 8																															
43	2514.6	8250	SWC 7																															
44	2529.8	8300	SWC 6	18%																										18%				11
45	2560.3	8400	SWC 5																															
46	2590.8	8500	SWC 4																															
47	2624.3	8610	SWC 3																															1
48	2651.8	8700	SWC 2																															11
49	2678.6	8788	SWC 1																	8%										8%				12
50	2688.0	8819	Core 3																															2
51	2689.3	8823	Core 3																															3
52	2713-25	8900-40	Cuttings																															5
53	2737-40	8980-90	Coal Cts																															
54	2758-61	9050-60	Coal Cts																															
55	2795-801	9170-90	Cuttings																															18
56	2838-44	9310-30	Cuttings																															13
57	2847-50	9340-50	Coal Cts																															
58	2877-80	9440-50	Coal Cts																															2
59	2896-902	9500-20	Cuttings																															6
60	2951-57	9680-700	Cuttings																															2
61	2975-84	9760-90	Cuttings																															2
62	2995.6	9828	SWC 28																															1
63	2997.4	9834	SWC 27																															
64	3042.2	9981	Core-4																															2
65	3066-69	10060-70	Cuttings																															6
66	3116.9	10226	SWC 22																										25%					4
67	3154.7	10350	SWC 18																															3
68	3183.6	10445	SWC 12																															
69	3223.9	10577	SWC 33																															30
70	3231-40	10600-30	Cuttings																															2
71	3233.3	10608	SWC 5																															13
72	3247.3	10654	SWC 34																															
73	3262.3	10703	Core 5																															4

ABBREVIATIONS: X = Present % = Percentage

APPENDIX C7.

Palynological analysis of Oligocene sandstones in Squid-1, Bass Basin.

by

Alan D. Partridge

Biostrata Pty Ltd
A.B.N. 39 053 800 945

Biostrata Report 2002/12

30th June 2002

Palynological analysis of Oligocene sandstones in Squid-1, Bass Basin.

by Alan D. Partridge

Introduction

This palynological study of the Oligocene sandstones intersected in Squid-1 is a component of the Bass Basin Palynological Project coordinated by Geoscience Australia as part of the Western Tasmania Regional Minerals Program Offshore Collaborative Project, between Mineral Resources Tasmania, Geoscience Australia and the National Centre for Petroleum Geology and Geophysics to investigate aspects of the hydrocarbon prospectivity of the Bass and Sorell Basins.

The interval under investigation in Squid-1 is the 360 metre thick sandstone unit between 1425 and 1785m which overlies the Anglesea Formation. The age of this unit was not adequately determined in the original palynological reports on Squid-1, and further it was desirable to know whether the sandstone could be interpreted as filling a large channel entrenched into the top of the Anglesea Formation, or alternatively represented a lateral facies (ie. proximal strandline) of the shaly sediments overlying the Anglesea Formation in other wells. Analysis of both bulk and picked cuttings in Squid-1 and comparison with the sequence above the Anglesea Formation in Poonboon-1 are found to favour the second interpretation.

Materials and Methods

Unfortunately no conventional cores were cut and no sidewall cores were shot in the Squid-1 well so the new palynological analyses needed to rely solely on cuttings. Initially six bulk cuttings were analysed, but once these were discovered to be confused by both caved and reworked palynomorphs an additional four cuttings were collected and given alternative processing. The latter consisted of a pre-treatment with dilute HCl followed by sieving to breakdown and remove any of the calcareous shales and marls caved from between the 13-3/8" casing shoe at 1240m and top of the sand at 1425m. The assemblages extracted from this second batch of samples referred to as the ì picked cuttingsî provided significant help in understanding the section.

The palynological zones assigned to the samples, zone Confidence Ratings, key defining species and interpreted palaeoenvironments are provided in Table 1. Basic palynological data on organic residue yields, palynomorph concentrations in the residues, palynomorph preservation and species diversity in the samples are provided in Table 2. Species abundance and range data are provided in Tables 3 to 5. Author citation for spore-pollen species can be principally sourced for published species from Stover & Partridge (1973, 1982), and for manuscript species from Partridge (1973). Author citation for dinocysts can be sourced from Williams *et al.* (1998), and for acritarchs, algal cysts and other microplankton from Fensome *et al.* (1990).

The nine cuttings analysed all gave moderate to high organic residue yields, which contained moderate to high concentration of generally well-preserved palynomorphs. Recorded spore-pollen diversity was a high 44 species per sample, but this does include a significant number of reworked species. Microplankton diversity

was a moderate 15 species per sample, but would likely double if a thorough systematic study of the assemblages was undertaken.

Geological Discussion

The geological problem under investigation in Squid-1 was the age and correlation of the 360 metre thick sandstone unit between 1425 and 1785m, which is herein informally referred to as the Squid sandstone. The unit was presumed to have an Oligocene age as it overlies the Late Eocene Anglesea Formation, the regional seal to the Eastern View Group. However, no samples had been analysed from the Squid sandstone in the original palynological reports by Martin (1985) and Morgan (1986), nor were any studies made of the foraminiferal faunas from either this unit or the overlying Torquay Group. Two alternative lithological correlations of the sandstones also seemed possible. The Squid sandstone could represent a thicker development of the thin sands occurring immed-iately above the Anglesea Formation in other wells (eg. Cormorant-1 and King-1), or alternatively could wholly or partly represent a lateral facies of marine shales and marls in the other wells.

In anticipation that the palynological assemblages recovered from the Squid sandstone could give poor or equivocal results, samples were also analysed from the overlying marls assigned to the Torquay Group, and from the top of the underlying Anglesea Formation. A Late Eocene Middle *N. asperus* Zone age could be assigned to the latter formation based on slightly deeper cuttings samples that had previously been analysed by Martin (1985) and Morgan (1986). A fortuitous occurrence that assisted in the analysis was the presence of the 13-3/8" casing shoe at 1240m. The presence of this casing point meant that there was only 185 metres of open-hole section of the Torquay Group above the top of the Squid sandstone. Notwithstanding this limited exposure the soft marls of latter group caved extensively into the underlying sand section and confused the interpretation on the initial five bulk samples analysed (Table 1). This problem was partly overcome by a selective resampling and pre-treating the cuttings to remove or reduce the contamination from the caved marls.

From the Torquay Group samples were collected and analysed from a short distance below the casing point at 1275-80m, and from near the base of the marls at 1395-1400m. Within the Squid sandstone samples were collected a short distance below the top of the sandstone at 1445-70m, from an interval where thin coaly or carbonaceous beds were interbedded with the sandstone (samples at 1500-20m, 1530-50m), from immediately below the thin shale at 1586 to 1588m (samples at 1585-1600m, 1595-1600m), and from the middle of the lower massive sandstone section at 1670-85m. Finally the deepest sample at 1790-1800m is representative of the lithological change at the top of the Anglesea Formation.

Results of the new palynological study of Squid-1 indicate that the basal Torquay Group is Late Oligocene (Middle? *P. tuberculatus* Zone), the Squid sandstone Early Oligocene (Upper *N. asperus* to Lower? *P. tuberculatus* Zones), while the top of the Anglesea Formation is considered to be no younger than Late

Eocene (Middle *N. asperus* Zone). The palynomorph assemblages recovered from the Torquay Group are dominated by chorate dinocysts (principally *Spiniferites* spp.) which are recorded as caved to a greater or lesser extent in all the deeper cuttings. The other samples are dominated by angiosperm pollen (principally *Nothofagidites* spp.), as is typical of the broad *N. asperus* Zone. Finally, the top of the Anglesea Formation is characterised by a increased abundance of spores and the incoming of a significant number of typical Eocene dinocysts.

Because confidence in the identification of the spore-pollen zones is biased to FADs (First Appearance Datums) of species there is always some residual uncertainty in the spore-pollen zone assignments derived from cuttings. Fortunately, the associated microplankton assemblages contain species with important LADs (Last Appearance Datums) that provide additional age control.

Most critical to the age dating of the Squid sandstone in this report is the identification of the *Fromea leos* microplankton Zone from the cuttings between 1585 and 1600m that sample the interval at and just below the distinctive gamma ray shale spike at 1586 to 1588m. The as yet unpublished *F. leos* Zone has only previously been documented from the Gippsland Basin (eg. Partridge, 1994), where it is generally represented by less than 20 metres of open-marine marl at the base of the Seaspray Group, and forms part of the enigmatic ìEarly Oligocene Wedgeî that is irregularly distributed across the distal offshore portion of that basin (Bernecker & Partridge, 2001; appendix). The *F. leos* Zone in Squid-1 probably extends to the near the top of the Squid sandstone based on the occurrence of related species of *Fromea* in the cuttings at 1445-70m.

Age dating of the three cuttings samples between 1445 and 1550m from the upper part of the Squid sandstone is complicated by both cavings and significant reworking. Cuttings examined between the top of sandstone at 1425m and about 1550m where observed to be dominated by light to medium grey marl (interpreted as caved), with secondary loose quartz sand, and minor (<10%) black carbonaceous shale or coal. The last is interpreted to come from the ìcoalyî spikes on the sonic log between 1441 and 1535m, and is believed to be the principal source of *in situ* palynomorphs. The bulk of the recorded spore-pollen assemblages from the three cutting samples analysed between 1445 and 1550m were composed of long ranging species, but there was a conspicuous component, perhaps as high as 20% of spore-pollen assemblages, that is interpreted as reworked, based on well-established species ranges throughout southeast Australia. The most conspicuous reworked species recorded are *Proteacidites leightonii*, *P. asperopolus*, *P. pachypolus* and *Dicotetradites clavatus*. In combination these species indicate the source of the reworking was from sediments belonging to an interval extending from the *P. asperopolus* to basal Lower *N. asperus* Zones, implying an age range of late Early to early Middle Eocene. Although similar reworking has been recorded in other wells in the Bass Basin, at about the equivalent stratigraphic horizon above the Anglesea Formation, the numbers of reworked specimens is much lower (est. <1%). The postulated provenance of the reworking is to the south-east where the appropriate age sediments are at shallower depths (eg. Chat-1), or

are suspected to have been eroded (eg. Durroon-1). Unfortunately the microplankton recorded from the three samples between 1445 and 1550m are not particularly diagnostic as most are interpreted as caved from the overlying Torquay Group.

The only cuttings from the sandstone interval below the shale spike with the *F. leos* Zone is also interpreted as badly contaminated and therefore not diagnostic. The next older *Phthanoperidinium comatum* microplankton Acme Zone could be anticipated to occur in this part of the sandstone based on electric log correlation to Poonboon-1 (Partridge 2002a-b), but except for the questionable identification of an endocyst of *Deflandrea heterophlycta* nothing new was recorded in the assemblage.

The next change in the spore-pollen and microplankton assemblages occurs in the deepest sample examined, which was collected from the top of the Anglesea Formation. The assemblage recorded contains common *Phthanoperidinium comatum* and mixed with key Eocene dinocysts and is assigned to the next older *Stoveracysta kakanuiensis* microplankton Zone. Although the eponymous species of the zone is purported to have a basal Oligocene age in New Zealand (Clowes & Morgan, 1984), data from the adjacent Gippsland Basin favours placing the zone in the latest Eocene (Partridge, 1999). The associated spore-pollen which are considered diagnostic of the Middle *N. asperus* Zone support this age assignment.

The palynological results from Squid-1, and a new palynological study of the equivalent interval in Poonboon-1 (Partridge, 2002a), when integrated with electric log correlation between the two wells (Partridge, 2002b; fig.11) refutes the interpretation that the thick Squid sandstone is filling a large channel entrenched into the top of the Anglesea Formation. Rather, the Squid sandstone represents a lateral sandy facies of the more shaly sediments overlying the Anglesea Formation in other wells. Reviewing the electric logs and limited palynological data in the wells across the basin from the Pelican field wells in the SW, through Poonboon-1 and Nangkero-1 in the middle of the basin, to Dondu-1, Yourongi-1 and Bass-2 in the NE, reveals that the equivalent sections in these wells all belong to the more shaly facies found in Poonboon-1. However, similar but thinner sands have been found to overlie the distinctive Anglesea Formation directly to the east in the Chat-1 well (1072-1132m), and to the SE in the Durroon-1 well (458-540m). Unfortunately, there is no reliable age dating of the sands in the latter two wells, but as the base of these sands are significantly shallower (650m in Chat-1 and 1245m in Durroon-1) they potentially could be much younger.

Based on the above well control and analogy to palaeoshorelines identified in other parts of Bass Strait (eg. Partridge, 1999; Holdgate *et al.*, 2002) the Squid sandstone is interpreted to be a barrier sandstone body with a probably SSW to NNE orientation that was largely deposited in a shoreface environment. The shale spike at 1586 to 1588m in Squid-1 representing a flooding horizon and the overlying thin coaly beds representing regressive back-barrier marsh environments.

Biostratigraphy

***Proteacidites tuberculatus* spore-pollen Zone and**
***Operculodinium* microplankton Superzone**
Interval: 1275 to 1400 metres.
Age: Early? to Late Oligocene.

Following the original zone definition of Stover & Partridge (1973) the two samples from the Torquay Group are confidently assigned to the *P. tuberculatus* Zone based on the presence of multiple specimens of the spore *Cyatheacidites annulatus*. In addition the presence of the spore *Cyathidites subtilis* in the next deepest cuttings at 1445-70m (where it is interpreted as caved), suggests that the marls below the 13-3/8" casing shoe at 1240m extend into the Middle *P. tuberculatus* Subzone and are therefore partly or mostly Late Oligocene in age. The associated microplankton assemblages are dominated by chorate dinocysts and conform to the *Operculodinium* Superzone of Partridge (1999). *Spiniferites* spp. dominates the assemblages (average 58%), with *Operculodinium centrocarpum* (average 10%) the next most abundant species. The presence of both the manuscript species *Protoellipsodinium simplex* and *Tuberculodinium vancampoae* in the cuttings suggest that the two informal zones based on these species are present in the section below the casing point.

Upper *Nothofagidites asperus* spore-pollen Zone and
***Fromea leos* microplankton Zone**
Interval: ?1445 to 1600 metres
Age: Early Oligocene.

A confident identification of the Upper *N. asperus* Zone cannot be made in Squid-1 because of the nature of the zone definition, and instead age dating of these cuttings samples is largely dependant on the identification of the unpublished *F. leos* microplankton Zone. The problem with the spore-pollen zone definition is that it is based on negative criteria of the absence of index species for the immediately underlying and overlying zones (Stover & Partridge, 1973). Further, the abundance of the gymnosperm pollen *Phyllocladidites mawsonii* originally cited as secondary characteristic of zone in the Gippsland Basin is now recognised to be facies dependant and is not applicable beyond the coal measures sequences deposited in the onshore Gippsland Basin. Support for the zone assignment does however come from the presence of a number of rare species in the samples. These include *Proteacidites stipplatus, P. rectomarginis, Psilodiporites pertritus* ms and *Malvacipollis grandis* ms.

The *F. leos* Zone is identified on the total range of the eponymous species. In the Gippsland Basin the species has a first occurrence after the LAD of *Phthanoperidinium comatum*, and although it is the basal zone of the *Operculodinium* Superzone it generally occurs before the oldest super-abundant occurrence of *Spiniferites* spp. The FAD of the spore *Cyatheacidites annulatus* which defines the base of the *P. tuberculatus* Zone is documented in a few sections to occur within the *F. leos* Zone. Such subtleties

unfortunately cannot be confirmed in the contaminated cuttings analysed in Squid-1.

Middle *Nothofagidites asperus* spore-pollen Zone and
***Stoveracysta kakanuiensis* microplankton Zone**
Sample at: 1790-1800 metres
Age: Late Eocene.

The deepest cuttings sample analysed is assigned to the Middle *N. asperus* Zone based on the LADs of the secondary index species *Proteacidites recavus* and *P. tuberculiformis.* Unfortunately, the primary index species for the zone *Triorites magnificus* was not found, but is recorded from the slightly deeper cuttings at 1820-25m by Morgan (1986). Confidence in the zone assignment is somewhat reduced by the presence of extensive reworking in the overlying Squid sandstone including a number of key Eocene index species that normally have their LADs at the top of the Middle *N. asperus* Zone (eg. *Proteacidites pachypolus* and *Santalumidites cainozoicus*). Fortunately, strong independent support for the zone and age assignment is provided by the associated microplankton assemblage which is assigned to the *S. kakanuiensis* Zone based on the occurrence of the eponymous species. Although the latter species is considered to range into the basal Oligocene in New Zealand (Clowes & Morgan, 1984) it is not recorded above the Middle *N. asperus* Zone (or the Eocene) in the adjacent Gippsland Basin (Partridge, 1999).

References

BERNECKER, T. & PARTRIDGE, A.D., 2001. Emperor and Golden Beach Subgroups: The onset of Late Cretaceous sedimentation in the Gippsland Basin, SE Australia. **In** *Eastern Australian Basins Symposium. A Refocussed Energy Perspective for the Future,* K.C. Hill & T. Bernecker, editors, *Petroleum Exploration of Australia, Special Publication*, p.391-402.

CLOWES, C.D. & MORGAN, H.E.G., 1984. Micropaleontology of the Runangan-Whaingaroan (Eocene-Oligocene) Tortara Limestone, Kakanui River, New Zealand. *New Zealand Geological Survey record 3,* p.30-40.

FENSOME, R.A., WILLIAMS, G.L., BARSS, M.S., FREEMAN, J.M. & HILL, J.M., 1990. Acritarchs and fossil Prasinophytes: An index to genera, species and infraspecific taxa. *AASP Contribution Series No. 25*, p.1ñ771.

HOLDGATE, G.R., GALLAGHER, S. & WALLACE, M.W., 2002. Tertiary coal geology and stratigraphy of the Port Phillip Basin, Victoria. *Australian Journal of Earth Sciences, vol.49*, no.3, p.437-453.

MARTIN, H.A., 1985. The stratigraphic palynology of Squid #1 and Tasmanian Devil #1, Bass Basin. *Unpublished report for Kimberley Oil and Gas N.L.*, 6p., 2 figs, 1 table.

MORGAN, R., 1986. Palynology of Weaver Squid-1, Bass Basin, Australia. *Report to Bridge Oil Limited*, 12p. 2 charts (unpubl.).

PARTRIDGE, A.D., 1973. Revision of the Spore-Pollen Zonation in the Bass Basin. *Esso Australia Ltd Palaeontological Report 1973/4*, 22p. 6 pls (2 May).

PARTRIDGE, A.D., 1994. Palynological analysis of Blackback-3, Gippsland Basin. *Biostrata Report 1994/6*,

p.1-23, 2 charts.

PARTRIDGE, A.D., 1999. Late Cretaceous to Tertiary geological evolution of the Gippsland Basin, Victoria. PhD thesis, La Trobe University, Bundoora, Victoria, p.i-xxix, p.1-439, 165 figs, 9 pls (unpubl.).

PARTRIDGE, A.D., 2002a. Quantitative palynological analysis of Eastern View and Demons Bluff Groups in Poonboon-1, Bass Basin. *Biostrata Report 2002/11*, p.1-35.

PARTRIDGE, A.D., 2002b. Bass Basin Palynological Project: Unravelling a Late Cretaceous to Eocene geological history of large palaeolakes, coastal lagoons and marine bays. *Biostrata Report 2002/13*, p.1-36.

STOVER, L.E. & PARTRIDGE, A.D., 1973. Tertiary and late Cretaceous spores and pollen from the Gippsland Basin, southeastern Australia. Proceedings *Royal Society of Victoria, vol.85*, pt.2, p.237-286.

STOVER, L.E. & PARTRIDGE, A.D., 1982. Eocene spore-pollen from the Werillup Formation, Western Australia. *Palynology 6*, p.69-95.

WILLIAMS, G.L., LENTIN, J.K. & FENSOME, R.A., 1998. The Lentin and Williams index of fossil dinoflagellates 1998 edition. *American Association of Stratigraphic Palynologists, Contributions Series, no. 34*, p.1-817.

Table 1. Interpretative Palynological Data from Squid-1

No.	Sample Type	Depth Metres	Sample Origin	Spore-Pollen Zone	CR*	Microplankton Zone	CR*	Key Index Species	Palaeoenvironment
1	Bulk Cuttings	1275-1280	GA-1	*P. tuberculatus*	D2	*Operculodinium* Sz	D4		Open Marine
2	Bulk Cuttings	1395-1400	GA-1	*P. tuberculatus*	D2	*Operculodinium* Sz	D4	FAD of *Cyatheacidites annulatus*	Open Marine
3	Picked Cuttings	1445-1470	GA-2	*P. tuberculatus* to Upper *N. asperus*	D2	*F. leos* mixed with caved *P. simplex*	D4	LAD of *Fromea neochytra* ms	Marginal Marine
4	Picked Cuttings	1500-1520	GA-2	Upper *N. asperus* mixed with Early-Mid Eocene	D4	Indeterminate		Assemblage confused by both cavings and reworking.	Nearshore marine
5	Bulk Cuttings	1530-1550	GA-1	Upper *N. asperus* mixed with Early-Mid Eocene	D4	Indeterminate		Assemblage confused by both cavings and reworking.	Nearshore marine
6	Picked Cuttings	1585-1600	GA-2	Upper *N. asperus*	D4	*F. leos*	D3	Common *Fromea leos* ms	Marginal Marine
7	Bulk Cuttings	1595-1600	GA-1	Upper *N. asperus*	D4	*F. leos*	D3	FAD of *Fromea leos* ms	Marginal Marine
8	Picked Cuttings	1670-1685	GA-2	Indeterminate		Indeterminate		Assemblage entirely caved.	Nearshore marine
9	Bulk Cuttings	1790-1800	GA-1	Middle *N. asperus*	D4	*S. kakanuiensis*	D2	LAD of *Stoveracysta kakanuiensis*	Bay - restricted marine

ABBREVIATIONS

*CR = Confidence Ratings
LAD = Last Appearance Datum
FAD = First Appearance Datum
GA-1 = Samples collected Stage-1 Work program
GA-2 = Samples collected Stage-2 Work program

CONFIDENCE RATINGS

Alpha Code Linked to Sample
A = Core
B = Sidewall core
C = Coal cuttings
D = Ditch cuttings
J = Junk basket

Numeric Code Linked to Palynomorph Assemblage
1 = Excellent confidence: High diversity assemblage **plus** key zone species.
2 = Good confidence: Moderately diverse assemblage **plus** key zone species.
3 = Fair confidence: Low diversity assemblage **plus** key zone species.
4 = Poor confidence: Moderate to high diversity **minus** key zone species.
5 = Very low confidence: Low diversity assemblage **minus** key zone species.

Table 2. Basic Palynological Data from Squid-1

No.	PalLab Spl.No.	Sample Type	Top Metres	Base Metres	Visual Yield	Palynomorph Concentration	Palynomorph Preservation	No. SP Species	No. MP Species	Marine MP%	Other MP%	NED	Noth%
1	6405905	Bulk Cuttings	1275	1280	Moderate	Moderate to High	Fair-poor	25	17	66%		14%	17%
2	6405906	Bulk Cuttings	1395	1400	High	High	Poor-good	51	22	29%	<1%	17%	41%
3	6406909	Picked Cuttings	1445	1470	Moderate	Moderate	Poor	31	10	23%		4%	49%
4	6406910	Picked Cuttings	1500	1520	Moderate	Moderate	Poor-good	53	7	4%		2%	32%
5	6405907	Bulk Cuttings	1530	1550	High	High	Poor-good	55	7	6%		5%	44%
6	6406911	Picked Cuttings	1585	1600	High	High	Poor-good	36	14	22%	<1%	8%	57%
7	6405908	Bulk Cuttings	1595	1600	High	High	Poor-good	54	26	26%		14%	45%
8	6406912	Picked Cuttings	1670	1685	Moderate	Moderate	Fair	36	11	12%	<1%	10%	44%
9	6405909	Bulk Cuttings	1790	1800	High	Moderate	Poor-fair	53	24	12%		11%	29%

ABBREVIATIONS

MP = Microplankton

SP = Spore-Pollen

NED = Neves Effect based on *Dilwynites/Araucariacites* Percentage

Noth% = Percentage of *Nothofagidites* in SP count.

Table 3. Squid-1 — Abundances of major palynomorph groups.

No.	Top Metres	Base Metres	Sample Type	Gleicheniidites spores	ALL OTHER spores	Dilwynites and Araucariacites pollen	ALL OTHER gymnosperm pollen	Nothofagidites pollen	ALL OTHER angiosperm pollen	FUNGAL microfossils	Pre-Tertiary Spore-Pollen	**Total Terrestrial SUM**		SPORE-POLLEN TOTAL	MICROPLANKTON fresh to brackish	MICROPLANKTON marine	Microforaminiferal liners	Scolecodonts	**SP + Marine SUM**
1	1275	1280	Bulk Cuttings		39%	14%	17%	17%	11%	3%		109		33%		64%	3.1%	0.3%	325
2	1395	1400	Bulk Cuttings	2%	15%	16%	11%	40%	13%	5%	1.0%	200		71%	0.7%	28%	0.4%	0.4%	267
3	1445	1470	Picked Cutts		8%	4%	7%	44%	27%	9%	0.9%	224		77%		22%	0.8%		263
4	1500	1520	Picked Cutts		6%	2%	8%	29%	45%	9%		255		96%		4%			240
5	1530	1550	Bulk Cuttings	0.3%	6%	5%	6%	39%	34%	9%		295		93%		6%	1.0%		289
6	1585	1600	Picked Cutts		6%	7%	3%	51%	21%	11%		207		77%	0.4%	22%		0.4%	238
7	1595	1600	Bulk Cuttings	2%	10%	14%	10%	43%	18%	4%		197		71%	0.4%	25%	3.0%	0.4%	266
8	1670	1685	Picked Cutts	1%	7%	8%	4%	38%	28%	12%	0.4%	250		87%	0.4%	12%	0.4%		251
9	1790	1800	Bulk Cuttings		23%	10%	24%	28%	12%	1.4%	0.5%	222		88%	0.8%	12%			249

Table 4. Squid-1 well – spore-pollen distribution.

No.	Top Metres	Base Metres	Sample Type	SPORE SPECIES	Baculatisporites spp.	Camarozonosporites heskermensis	Conbaculites apiculatus ms	Cyatheacidites annulatus	Cyathidites spp. large >40µm	Cyathidites spp. small <40µm	Cyathidites splendens	Cyathidites subtilis	Dictyophyllidites arcuatus	Echinosporis echinatus	Foveotriletes balteus	Foveotriletes palaequetrus	Gleicheniidites circinidites	Herkosporites elliottii	Ischyosporites spp.	Laevigatosporites major	Laevigatosporites ovatus	Matonisporites ornamentalis	Peromonolites spp.	Polypodiaceoisporites varus ms	Polypodiidites/Verrucatosporites spp.	Retitriletes spp.
1	1275	1280	Bulk Cuttings		1.9%			0.9%	6.6%	16%								1.9%	X	X	1.9%				0.9%	X
2	1395	1400	Bulk Cuttings		2.6%	X		0.5%		5.8%			X		X	X	1.6%	X	X		1.6%	X	X		0.5%	X
3	1445	1470	Picked Cutts							4.5%		0.5%		0.5%							3.0%					
4	1500	1520	Picked Cutts		0.9%	X	RW		0.9%	1.7%				X					X		3.0%			RW		
5	1530	1550	Bulk Cuttings		X				1.5%	3.0%					X		0.4%		X	X	1.5%				0.4%	
6	1585	1600	Picked Cutts		1.1%	X	RW			1.1%								0.5%	X		1.1%					
7	1595	1600	Bulk Cuttings		1.1%			CV	0.5%	2.1%			X				1.6%		X	X	3.2%		X		X	
8	1670	1685	Picked Cutts		0.5%				0.5%	3.2%							0.9%				0.9%					0.5%
9	1790	1800	Bulk Cuttings		0.5%				0.5%	14%	X		X		X			X	5.0%	X	0.9%	X	X		X	

ABBREVIATIONS

% = Percentage
X = Present
CV = Caved
RW = Reworked

Table 4. Squid-1 well – spore-pollen distribution.

No.	Top Metres	Base Metres	Sample Type	Ricciaesporites boxatus ms	Rugulatisporites mallatus	Stereisporites antiquisporites	Trilete spores undiff.	Tripunctisporis maastrichtiensis	Verrucosisporites kopukuensis	TOTAL Spores		GYMNOSPERM SPECIES	Araucariacites australis	Cupressacites sp.	Dacrycarpites australiensis	Dilwynites granulatus	Dilwynites tuberculatus	Lygistepollenites florinii	Microalatidites paleogenicus	Microcachryidites antarcticus	Phyllocladidites mawsonii	Podocarpidites spp.	Trichotomosulcites subgranulatus	TOTAL Gymnosperm Pollen		ANGIOSPERM SPECIES	Angiosperm pollen undiff.
1	1275	1280	Bulk Cuttings			2.8%	6.6%			40%			6.6%		2.8%	6.6%	0.9%			2.8%	1.9%	9.4%	0.9%	32%			
2	1395	1400	Bulk Cuttings	X		3.2%	1.1%		X	17%			6.3%	0.5%	X	9.5%	0.5%	0.5%		0.5%	1.1%	9.0%		28%			
3	1445	1470	Picked Cutts			0.5%	0.5%			9%			3.0%			1.0%		1.0%			2.0%	4.0%	0.5%	11%			2.0%
4	1500	1520	Picked Cutts			0.4%			X	7%			0.9%			0.9%		0.9%	0.4%	1.3%	2.6%	3.9%		11%			0.9%
5	1530	1550	Bulk Cuttings		X	0.4%			X	7%			1.5%			3.0%	0.7%	0.4%			2.6%	3.4%	0.4%	12%			
6	1585	1600	Picked Cutts			2.2%	1.1%		X	7%			2.2%	X		6.0%		1.1%		X	1.6%	1.1%		12%			2.2%
7	1595	1600	Bulk Cuttings		X	1.1%	2.1%		X	12%			3.2%	X	0.5%	10%	1.1%	0.5%		0.5%	1.1%	7.4%	0.5%	25%			
8	1670	1685	Picked Cutts			0.5%	2.3%			9%			1.8%	X		6.8%	0.9%	0.5%			1.4%	3.2%		15%			2.3%
9	1790	1800	Bulk Cuttings		X	1.4%	1.8%	X	X	24%			5.5%		X	4.1%	0.9%	3.2%		0.5%	7.8%	12%	0.5%	35%			0.9%

ABBREVIATIONS

% = Percentage
X = Present
CV = Caved
RW = Reworked

Table 4. Squid-1 well – spore-pollen distribution.

No.	Top Metres	Base Metres	Sample Type	Aglaoreidia qualumis	Arecipites sp.	Banksieaeidites arcuatus	Banksieaeidites elongatus	Beaupreaidites elegansiformis	Beaupreaidites trigonalis ms	Cupanieidites orthoteichus	Cyperaceaepollis neogenicus	Dicotetradites clavatus	Dryadopollis retequetrus	Dryptopollenites semilunatus	Ericipites crassiexinus/scabratus	Gothanipollis bassensis	Haloragacidites harrisii	Ilexpollenites spp.	Intratriporopollenites notabilis	Liliacidites spp.	Limingtonia sp.	Malvacipollis grandis ms	Malvacipollis robustus	Malvacipollis subtilis	Margocolporites vanwijhei	Milfordia spp.
1	1275	1280	Bulk Cuttings														8.5%									
2	1395	1400	Bulk Cuttings	0.5%			X		X				X			X	19	X		X		X				
3	1445	1470	Picked Cutts	1.5%	1.5%							0.5%					17									0.5%
4	1500	1520	Picked Cutts							1.3%		2.2%		0.4%	0.4%	X	28	0.4%		0.9%		X	X	1.3%		X
5	1530	1550	Bulk Cuttings	0.7%		0.4%				0.7%	0.4%	0.7%			X		28	0.4%		1.1%	X		X	0.7%		
6	1585	1600	Picked Cutts	1.1%						0.5%	0.5%						15			X				0.5%		
7	1595	1600	Bulk Cuttings	1.1%						X							18	1.1%	RW					1.1%	X	
8	1670	1685	Picked Cutts	0.9%						0.5%		1.4%					14	0.5%		0.9%				1.4%		
9	1790	1800	Bulk Cuttings	0.9%				X			X	0.5%			X		6.0%							0.9%		0.5%

ABBREVIATIONS

% = Percentage
X = Present
CV = Caved
RW = Reworked

Table 4. Squid-1 well – spore-pollen distribution.

No.	Top Metres	Base Metres	Sample Type	Myrtaceidites parvus/mesonesus	Myrtaceidites tenuis	Nothofagidites asperus	Nothofagidites brachyspinulosus	Nothofagidites deminutus	Nothofagidites emarcidus/heterus	Nothofagidites falcatus	Nothofagidites flemingii	Nothofagidites goniatus	Nothofagidites vansteenisii	Periporopollenites spp.	Polycolpites langstonii	Proteacidites spp.	Proteacidites adenanthoides	Proteacidites annularis	Proteacidites asperopolus	Proteacidites biporus	Proteacidites grandis	Proteacidites incurvatus	Proteacidites kopiensis	Proteacidites leightonii	Proteacidites nasus	Proteacidites obesolabrus ms
1	1275	1280	Bulk Cuttings			0.9%		0.9%	14%	0.9%						0.9%										
2	1395	1400	Bulk Cuttings			0.5%		4.8%	34%	0.5%	0.5%	0.5%	0.5%	X	RW	0.5%		X			RW					
3	1445	1470	Picked Cutts	2.5%		0.5%	2.5%	5.0%	38%	1.0%	1.5%		0.5%			4.5%								2.0%		
4	1500	1520	Picked Cutts	3.5%		0.4%	0.4%	3.0%	25%	0.4%	2.6%		0.4%			12%	RW	X	0.9%	RW			X	0.4%		
5	1530	1550	Bulk Cuttings	1.1%		3.7%		2.2%	36%	0.4%	0.4%		0.4%	1.9%		10%	RW	0.4%	2.2%				X	1.5%		RW
6	1585	1600	Picked Cutts	3.3%	0.5%	0.5%		4.3%	50%	2.2%	0.5%					2.7%		0.5%	0.5%					0.5%		
7	1595	1600	Bulk Cuttings	X		1.1%	0.5%	2.6%	35%	1.1%	2.1%	0.5%	1.6%			3.7%		0.5%	RW					RW	RW	
8	1670	1685	Picked Cutts	3.7%			1.4%	3.7%	36%	0.9%	1.4%		0.5%			4.6%		X						0.5%		
9	1790	1800	Bulk Cuttings			0.9%		0.9%	22%	0.5%	4.1%	0.5%				0.5%						X				

ABBREVIATIONS

% = Percentage
X = Present
CV = Caved
RW = Reworked

Table 4. Squid-1 well – spore-pollen distribution.

No.	Top Metres	Base Metres	Sample Type	Proteacidites obscurus	Proteacidites pachypolus	Proteacidites recavus	Proteacidites rectomarginis	Proteacidites reticuloscabratus	Proteacidites stipplatus	Proteacidites tuberculatus	Proteacidites tuberculiformis	Psilodiporites pertritus ms	Santalumidites cainozoicus	Sapotaceoidaepollenites rotundus	Schizocolpus marlinensis	Tetrapollis campbellbrownii	Tricolp(or)ates spp.	Tricolpites thomasii	Tricolporites adelaidensis	Tricolporites paenestriatus	Tricolporites scabratus	Triporopollenites simplis	Triporopollenites spp.	TOTAL Angiosperm Pollen	TOTAL SP COUNT
1	1275	1280	Bulk Cuttings														1.9%			X				28%	106
2	1395	1400	Bulk Cuttings				0.5%			X				X		X	1.6%		X		X			55%	189
3	1445	1470	Picked Cutts	0.5%	0.5%								0.5%				4.5%			1.0%			X	79%	202
4	1500	1520	Picked Cutts	X	0.4%		X						0.4%				8.7%		0.9%	2.2%		0.9%		82%	231
5	1530	1550	Bulk Cuttings		0.7%	RW	X						0.4%				3.0%	0.4%	X					81%	268
6	1585	1600	Picked Cutts	X				X				X					2.2%			X				81%	184
7	1595	1600	Bulk Cuttings		RW				X	X				X			1.6%		X	X				63%	189
8	1670	1685	Picked Cutts	0.9%	0.5%												7.8%			0.5%				76%	219
9	1790	1800	Bulk Cuttings	X		X	X				X				X		2.3%		X					41%	218

ABBREVIATIONS

% = Percentage
X = Present
CV = Caved
RW = Reworked

Table 5. Squid-1 – microplankton distribution.

No.	Top Metres	Base Metres	Sample Type	ACRITARCHS and ALGAE	Cymatisphaera sp. (polygonal)	Cymatisphaera sp. (zigzag)	Horologinella incurvata	Micrhystridium spp.	Botryococcus braunii	Crassosphaera concinnia	Lecaniella sp.	Pediastum sp.	DINOCYST SPECIES	Dinocysts undiff.	Achomosphaera spp.	Apectodinium australiense	Arachnodinium antarcticum	Batiacasphaera spp.	Chiropteridium dispersum	Cooksonites spp.	Cordosphaeridium spp.	Dapsilidinium pseudocolligerum	Deflandrea heterophlycta	Deflandrea phosphoritica	Enneadocysta pectiniformis	Eocladopyxis peniculata	Fromea leos ms	Fromea neochytra ms
1	1275	1280	Bulk Cuttings			0.5%		6%						12%		1%			X	0.5%								
2	1395	1400	Bulk Cuttings				X		1%		1%			17%	X	X				X		1%						1%
3	1445	1470	Picked Cuttings		3%			51%						8%														2%
4	1500	1520	Picked Cuttings					22%						11%				11%				X						
5	1530	1550	Bulk Cuttings											17%								6%						
6	1585	1600	Picked Cuttings				2%	23%	2%	X				15%								X					28%	4%
7	1595	1600	Bulk Cuttings							X		1%		13%		1%			CV	X		3%		X		X	1%	X
8	1670	1685	Picked Cuttings				3%	32%	3%					6%								X	X				10%	
9	1790	1800	Bulk Cuttings						3%			3%		10%	X		X			X	X		3%	X	X			

ABBREVIATIONS

% = Percentage

X = Present

CV = Caved

RW = Reworked

Table 5. Squid-1 – microplankton distribution.

No.	Top Metres	Base Metres	Sample Type	Homotryblium plectilum	Hystrichokolpoma rigaudiae	Impagidinium spp.	Impletosphaeridium severinii	Lingulodinium machaerophorum	Lingulodinium solarum	Operculodinium centrocarpum	Palaeocystodinium golzowense	Paralecaniella indentata	Phenidinium sp.	Phthanoperidinium comatum	Protoellipsodinium simplex ms	Protoellipsodinium spp.	Pyxidinopsis pontus ms	Reticulatosphaera stellata	Samlandia reticulifera	Selenophemphix spp.	Spiniferites spp.	Stephanodinium spiniferum	Stoveracysta kakaniensis	Systematophora placacanthum	Tectatodinium spp.	Thalassiphora pelagica	Tuberculodinium vancampoae	TOTAL MP COUNT
1	1275	1280	Bulk Cuttings		1%	0.5%	X	0.5%		7%					1%	1%				X	67%			1%	X			208
2	1395	1400	Bulk Cuttings	X	3%	X		4%		13%	X	X			X	1%		4%		X	50%	X		3%			X	76
3	1445	1470	Picked Cuttings		3%			2%		7%								2%			20%			2%				59
4	1500	1520	Picked Cuttings							11%											44%							9
5	1530	1550	Bulk Cuttings		X			6%		17%					X						56%			X			X	18
6	1585	1600	Picked Cuttings		4%					4%					X	X					19%			X		X		53
7	1595	1600	Bulk Cuttings		X			X		13%		X			1%	X	1%	X		X	62%	X		1%		X		68
8	1670	1685	Picked Cuttings		X					16%					3%			X			26%							31
9	1790	1800	Bulk Cuttings		X			3%	X	13%	X		X	23%	X				X		39%		3%	X		X		31

ABBREVIATIONS

% = Percentage

X = Present

CV = Caved

RW = Reworked

APPENDIX C8.

BASS BASIN PALYNOLOGICAL PROJECT
Unravelling a Late Cretaceous to Eocene geological history of large palaeolakes, coastal lagoons and marine bays.

by

Alan D. Partridge

Biostrata Pty Ltd
A.B.N. 39 053 800 945

Biostrata Report 2002/13

10th June 2002

BASS BASIN PALYNOLOGICAL PROJECT

Unravelling a Late Cretaceous to Eocene geological history of large palaeolakes, coastal lagoons and marine bays.

by Alan D. Partridge

TABLE OF CONTENTS

Summary .....

Introduction .....

Selection of wells for review .....

Palaeoenvironments .....

Stratigraphic framework .....

Palaeolakes and Lagoons .....

Geological Results of Palynological Studies .....

Durroon-1 .....

Koorkah-1 .....

Konkon-1 .....

Poonboon-1 .....

Cormorant-1 and King-1 .....

Squid-1 .....

Conclusions and Recommendations .....

References .....

Figures

Figure 1. Matrix of Palaeoenvironmental Indicators

Figure 2. Illustration of Neves effect

Figure 3. Stratigraphic framework for the Bass Basin

Figure 4. Locality map for Lake Maracaibo

Figure 5. Turonian palaeogeography of the Bass Strait

Figure 6. Abundances of significant palynomorphs in Durroon-1

Figure 7. Abundances and ranges of significant palynomorphs in Koorkah-1

Figure 8. Abundances of significant palynomorphs in Konkon-1

Figure 9. Late Paleocene palaeogeography of Bass Strait

Figure 10. Palynological and log correlation between King-1 and Cormorant-1

Figure 11. Palynological and log correlation between Poonboon-1 and Squid-1

BASS BASIN PALYNOLOGICAL PROJECT
Unravelling a Late Cretaceous to Eocene geological history of large palaeolakes, coastal lagoons and marine bays.

by Alan D. Partridge

Summary

Until the establishment of the marine seaway through the Bass Strait in the latest Oligocene or early Miocene the Bass Basin has essentially been an intracratonic or landlocked sedimentary basin. During the Late Cretaceous and early Paleocene the palaeogeography of the basin is typified by large fresh-water palaeolakes surrounded by deltaic environments, although periodically this facies pattern was interrupted by episodes of more fluvial deposition. Marine waters appear to have first entered the basin from the north-west in the Paleocene at the time of the late Paleocene thermal maximum (LPTM). The then existing Palaeolake Koorkah and subsequent Early and Middle Eocene palaeolakes are interpreted as large coastal lagoons comparable in size to Lake Maracaibo the largest modern coastal lagoon. The thickest and most extensive coal seams, and highest percentage of coal, in the stratigraphic succession correlate to this episode of coastal lagoons, and both coal deposition and the coastal lagoon environments were terminated in the latest Middle Eocene by the widespread deposition of the sands of the Boonah Formation and subsequent finer-grained facies of the overlying Anglesea Formation. The consistent occurrence of diverse cosmopolitan dinocysts through these latter two units suggest deposition in estuarine to restricted marine bay environments, analogous to the modern Port Phillip, albeit at a much grander scale.

The palynological studies have focussed on improving the age framework and providing supporting evidence for the identification of lacustrine, lagoonal and marine environments. Distinguishing between these environments is derived from the study of abundance and diversity of organic-walled microplankton, and identification of Neves effects within the terrestrial spore-pollen component of the palynological assemblages. Microplankton identified include marine and non-marine dinocysts, acritarchs, and colonial and single-celled algae. The Neves effects are the tendency for certain pollen types to be dominant in more distal depositional environments and their presence and distribution in the Bass Basin is supportive of the presence of large and often deep palaeolakes in the basin.

New palynological analyses from the 360 metre sandstone section overlying the Anglesea Formation in Squid-1 confirm both an Early Oligocene age and correlation of the unit to marine shales in the central basin that are assigned to the Addiscot and Angahook Formations. This Squid sandstone is interpreted to have been deposited in a shoreface environment adjacent to a palaeoshoreline oriented SSW to NNE.

Introduction

Biostratigraphic analysis of the most prospective Late Cretaceous to Eocene section in the Bass Basin is entirely dependant on palynology as this part of the succession is largely depauperate in biogenic calcium carbonate making the search for and use of calcareous microfossil unproductive. Most of the 32 wells drilled in the offshore Bass Basin were also spudded prior to the mid-1980s, and although the palynological reports are typical of their vintage there has been little revision of the palynological data since then. In general, the older reports lack detailed range charts, comprehensive recording of dinocysts assemblages and quantitative assemblage counts required for modern sequence and facies analysis. In contrast to the early reports, the five most recent exploration wells drilled in the past decade lack palynological studies or have very skimpy analyses of a limited number of cuttings samples.

In consideration of the above limitations on the available biostratigraphy a Bass Basin Palynological Project component was initiated as part of the Western Tasmania Regional Minerals Program Offshore Collaborative Project, between Mineral Resources Tasmania, Geoscience Australia and the National Centre for Petroleum Geology and Geophysics, which had the ultimate objective of improving the hydrocarbon prospectivity of the Bass and Sorell Basins. The palynological studies have been focussed on the Bass Basin and had the following principal objectives:

1. To establish a composite quantitative reference section for the palynological succession from Late Cretaceous to basal Oligocene.
2. To quantify the distribution, abundance and diversity of marine and non-marine dinocysts and other microplankton in the basin, to aid in the identification in time and space of lacustrine and marine palaeoenvironments in the basin.
3. To document presence and distribution of Neves effects within the terrestrial spore-pollen assemblages, as supporting palynological evidence for existence of large palaeolakes.
4. To resolve the age limits and distribution of the Oligocene sandstones observed to locally overlie the regional seal formed by the Anglesea Formation.

Selection of wells for review

The timetable and budget for the project restricted the palynological study to selected intervals in just seven of the 32 wells drilled in the basin. The early wells Poonboon-1 and Durroon-1, both spudded in 1972, were chosen to construct a composite quantitative reference section as they were known to contain well-preserved microfloras and some of the best sidewall core sampling of any wells in the basin. The interval reviewed in Durroon-1 was the Upper Cretaceous (*P. mawsonii* to *F. longus* Zones), while in Poonboon-1 an essentially complete sequence from the latest Maastrichtian to basal Miocene (Upper *F. longus* to *P. tuberculatus* Zones) was re-examined. Other factors contributing to the choice of these wells was that Durroon-1 is the only well in the basin penetrating an extended section of the middle Cretaceous (ie. *P. mawsonii* to *T. lilliei* Zones), while the section penetrated in Poonboon-1 was believed to be unaffected by any volcanic intrusion.

The latter have carbonised and degraded parts of the palynological succession in many of the other wells. Finally, relinquished palynological slides were known to be available from these two wells, in contrast to more recent wells drilled through the 1980s and 1990s where the original palynological slides and what remains of the sidewall cores are not generally available.

To investigate the timing of the commencement and the subsequent distribution of marine influence across the basin additional studies were made of Konkon-1 and the close together Cormorant-1 and King-1 wells. Konkon-1 was chosen as the original palynological report by Stover (1973) suggested this well contained some of the most abundant and diverse marine microplankton assemblages recorded in the basin. The well is also located in the northwest portion of the basin which all the available data suggested was the direction from which marine influence entered the basin. In the Cormorant-1 and King-1 wells only the latest Early Eocene and Middle Eocene section was analysed. This interval is much thicker than in Konkon-1, and was also known to contain the very rare occurrence of key dinocyst index species in Cormorant-1. It was hoped to recover additional dinocyst index species in Cormorant-1 and King-1 so as to be able to apply the more detailed microplankton zonation developed in the Gippsland Basin. Unfortunately, as discussed below this objective was not achieved.

To investigate the presence of large palaeolakes and lagoons interpreted to be present at different times through the Bass Basin succession, new palynological studies were performed on thick shale units identified on the gamma ray logs in a number of wells. The oldest palaeolake identified, the Turonian Durroon Formation in Durroon-1, has always been regarded as a lacustrine unit based on the occurrence of non-marine algae and dinocysts (Partridge, 1973, 1996; Smith 1986). The issue was whether any lacustrine character could be identified in younger palynological assemblages in other wells. Identified as possible candidates were thick latest Cretaceous to Paleocene or Early Eocene shales in wells in the north-western portion of the basin (eg. Koorkah unit) , and a distinctive unit on the gamma log at the top of the Eastern View Group (eg. Toolka unit). The older shales were investigated as part of the studies of Konkon-1 and Poonboon-1, and by collection and analysis of fresh cuttings samples in Koorkah-1. Unfortunately, neither the original palynological slides, nor any of the sidewall cores from Koorkah-1 were available for this study. The younger unit was investigated as part of the reviews of Konkon-1 and Cormorant-1.

Study of the Oligocene sandstones was centred on the 360 metre thick sandstone found overlying the Anglesea Formation in Squid-1. The age of this unit was not adequately determined in the original palynological reports on Squid-1 and it was desirable to know whether the sandstone could be interpreted as filling a large channel entrenched into the top of the Anglesea Formation, or represented a lateral facies (ie. proximal strandline) of the shaly sediments overlying the Anglesea Formation in other wells. Analysis of both bulk and ì pickedî cuttings in Squid-1 and comparison with the sequence above the Anglesea Formation in Poonboon-1 were found to favour the second interpretation.

Palaeoenvironments

In the Bass Basin the analysis of stratigraphic units and palaeoenvironments at a broad scale is largely dependant on the distribution and proportion of the principal lithologies, shales, sandstones and coals. In general, the succession lacks either diagnostic mineral (eg. glauconite) or environmentally explicit lithologies (except of course for coal). As the stratigraphic succession being studied is entirely subsurface the basic lithological data comes from the cuttings descriptions, supplemented by a moderate density of sidewall cores and a relatively limited number of conventional cores. The electric logs provide additional information on the relative proportions of the principal lithologies, their distribution across the basin, and changes in the bedding thickness and stacking patterns. When this data is combined with knowledge of modern sedimentary environments, and modern analogues various facies associations and palaeoenvironments can be postulated.
Interpreting the palaeoenvironments in the Bass Basin also draws extensively on the more densely drilled and intensively studied Gippsland Basin. In the latter basin mapping the maximum seaward extent of coals in successive palynological zones has allowed the identification of the approximate positions of palaeoshorelines through time (Partridge, 1999a). When combined with palaeogeographic mapping the resulting improved understanding the distribution of both sedimentary parameters (lithologies, bed thickness etc) and fossils (dinocysts, mangrove pollen, Neves effects) with respect to these palaeoshorelines can be applied to the interpretation of palaeoenvironments in the Bass Basin. An empirical matrix for variety of environments identified and the parameters on which they are based is summarised in Figure 1.

In terms of the fossil content, generally all that is available are palynomorphs. As previously stated calcareous microfossils are absent from the Eastern View and Furneaux Groups, and generally rare and sporadic through the lower part of the Demons Bluff Group. The most important information that can be gleaned from the palynology are the abundances of microplankton and the identification of Neves effects amongst the spore-pollen.

Microplankton. The palynological assemblages in the Bass Basin contain a mixture of organic-walled microplankton including dinocysts, acritarchs and single-celled and colonial algae. The dinocysts can be divided between cosmopolitan marine forms (eg. *Apectodinium*, *Spiniferites*), and widely accepted non-marine forms (eg. *Morkallacysta, Saeptodinium*). Classification the latter as non-marine genera was first proposed by Harris (1974), notwithstanding the caveat that they can always be washed down-stream into marine environments. Also interpreted as non-marine are the suite of endemic single-celled algae (eg. *Rimosicysta, Wuroia*), originally described from the Kipper Shale in the Gippsland Basin by Marshall (1989), and also recorded from the Durroon Formation in Durroon-1. Colonial algae, represented by *Botryococcus* and *Pediastrum,* are mostly rare throughout the succession but their occurrences are consistent with the postulated environments of the sediments in which they are found. Acritarchs are mostly rare and only occasionally common in the succession, and because their modern affinities are unknown they are spilt between marine and non-marine types based solely on the environmental assignments of the associated microplankton.

Figure 1. Matrix of Palaeoenvironmental Indicators in Bass Basin and examples of their application to wells studied.

ENVIRONMENTS & FACIES versus LITHOLOGICAL & PALYNOLOGICAL CRITERIA

	Alluvial-Fluvial	**Upper Coastal Plain**	**Lower Coastal Plain**	**Proximal or Shallow Water**	**Distal or Deep Water**
Lithological Characteristics	No coals Sand >> Shale Conglomerates	Coals thin & infrequent Sand > Shale	Coals thickest & common Shale > Sand	Shale >> Sand Bedding thin Coals rare	Shale >>> Sand Bedding thick
Terrestrical Spore-pollen	SP diversity lowest often with notable species absences	SP moderate diversity Assemblages skewed by local abundances	SP diversity high Assemblages skewed or homogeneous	SP diversity high homogeneous assemblages + mangrove pollen	SP diversity often low assemblages skewed by Neves effects
Non-marine Microplankton (algae + dinocysts)	Rare and atypical eg. *Pseudoschizaea Circulisporites parvus*	Very sporadic and unusual if common eg. *Saeptodinium*	Uncommon with low diversity & abundnace eg. *Saeptodinium*	Low diversity <3 species but often abundant eg. *Morkallacysta*	Moderate diversity 3 to 10 species mostly abundant eg. *Rimosicysta* and *Wuroia*
Marine Microplankton (mainly dinocysts)	Absent	Absent	Often monospecific with high abundance ie. "dinocyst blooms" eg. *Apectodinium Paralecaniella*	Diversity moderate 5-10+ species MP abundance >5% to <20% eg. *Homotryblium*	Diversity high 10-30+ species MP abundance >20% Common *Spiniferites*

EXAMPLES FROM MAJOR UNITS AND WELLS STUDIED

Torquay Group **Open Marine Carbonates**	Facies not intersected	Facies not intersected	Facies not intersected	Facies not intersected	Abundant + diverse dinocysts in carbonates + weak Neves effect eg. Poonboon-1
Demons Bluff Group **Marine Clastics Bay/Estuarine**	Facies not intersected	Facies not intersected	Diverse SP + low MP assemblages from coaly shales in Squid sandstone	Diverse SP + variably abundant MP from Boonah Fm. Konkon-1, Poonboon-1	Some MP assemblages in Anglesea Fm in Poonboon-1 but Neves effect weak
Upper Eastern View Group **Lagoonal – Brackish to Restricted Marine**	This age facies not analysed in study	Moderately diverse SP assemblages, no MP, few coals, Poonboon unit in Poonboon-1	Diverse SP, infrequent MP abundances Narimba & Cormorant units in Poonboon-1	Diverse SP with mangrove pollen, MP diversity high Cormorant unit in King-1 & Cormorant-1	Possibly low diversity MP assemblages in Toolka unit but Neves effect weak
Lower Eastern View and Furneaux Groups **Lacustrine to Fresh-water**	Low diversity SP from conglomerates in Boobyalla Subbasin	Low diversity SP assemblages, no MP, few coals, Narimba in Pelican field wells	Moderate diversity SP rare non-marine MP, coaly lower Narimba unit in Poonboon-1	Weak Neves effect mostly rare MP in Palaeolake Koorkah tongue in Poonboon-1	Strong Neves effect rare to abundant MP assemblages in Palaeolakes Koorkah & Durroon

Neves Effect. Amongst the spore-pollen assemblages unusual high abundance of gymnosperm pollen belonging to the fossil genera *Dilwynites* and *Araucariacites* are interpreted as Neves effects (Traverse, 1988), and the sediments in which they found are interpreted to have been deposited in distal marine and lacustrine environments. The modern affinity of *Dilwynites* pollen is with the recently discovered Wollemi pine, a member of the family Araucariaceae.

The concept of the Neves effect (Figure 2), is derived from empirical observation of spore-pollen abundances in modern sedimentary environments, and is defined as the tendency for certain more buoyant spores or pollen to have greater relative abundances in sediments deposited in more distal marine or lacustrine environments. Typical of a Neves effect is for pine pollen from trees growing in the hinterland to have high relative abundance in the most distal offshore environments (Line 4). In contrast pollen and spores from coastal plain and shoreline vegetation tends to have greater absolute and relative abundance in deltaic and nearshore environments (Lines 1 & 2). Part of the reason for the effect is the relative differences in surface areas. Proximal sediments are generally dominated by spores and pollen from the local area which often represents a limited geographic area. In contrast, distal sediments provide a more regional spore-pollen spectrum and therefore tend to be dominated by spore-pollen derived from the geographically much larger hinterland.

Stratigraphic Framework

A summary of a new stratigraphic framework for the Bass Basin is provided in Figure 3. The scheme is a mixture of established formation names that can be applied to the Bass Basin (eg. Durroon, Boonah, Anglesea, Addiscot formations) and informal names proposed to facilitate discussion of the relationships of the major lithological and facies units identified. Additional testing and discussions of the utility of this stratigraphic framework is required before the formal description of the units as either formations or sequences can be made.

At the highest rank the succession is divided into four groups, the Turonian to early Maastrichtian Furneaux Group, the late Maastrichtian to Middle Eocene Eastern View Group, the Late Eocene to Early Oligocene Demons Bluff Group and Late Oligocene to Recent Torquay Group. The Eastern View Group is distinguished from the underlying and overlying groups by the presence of extensive coals, while the Torquay Group represents the commencement of carbonated deposition in the basin.

The currently informal Furneaux Group (name proposed by Peter Baillie *pers comm*.), is comprised of sandstones and shales deposited in lacustrine, deltaic and fluvial environments. The succession is only fully penetrated in Durroon-1 where it is subdivided into an unnamed basal volcanic and sandstone unit, the Durroon Formation defined by Smith (1986), and the informal Boobyalla unit. A significant time gap occur between the latter two units which is correlated to the Longtom Unconformity identified in the Gippsland

Figure 2. Illustration of Neves effect adapted from Traverse (1988).

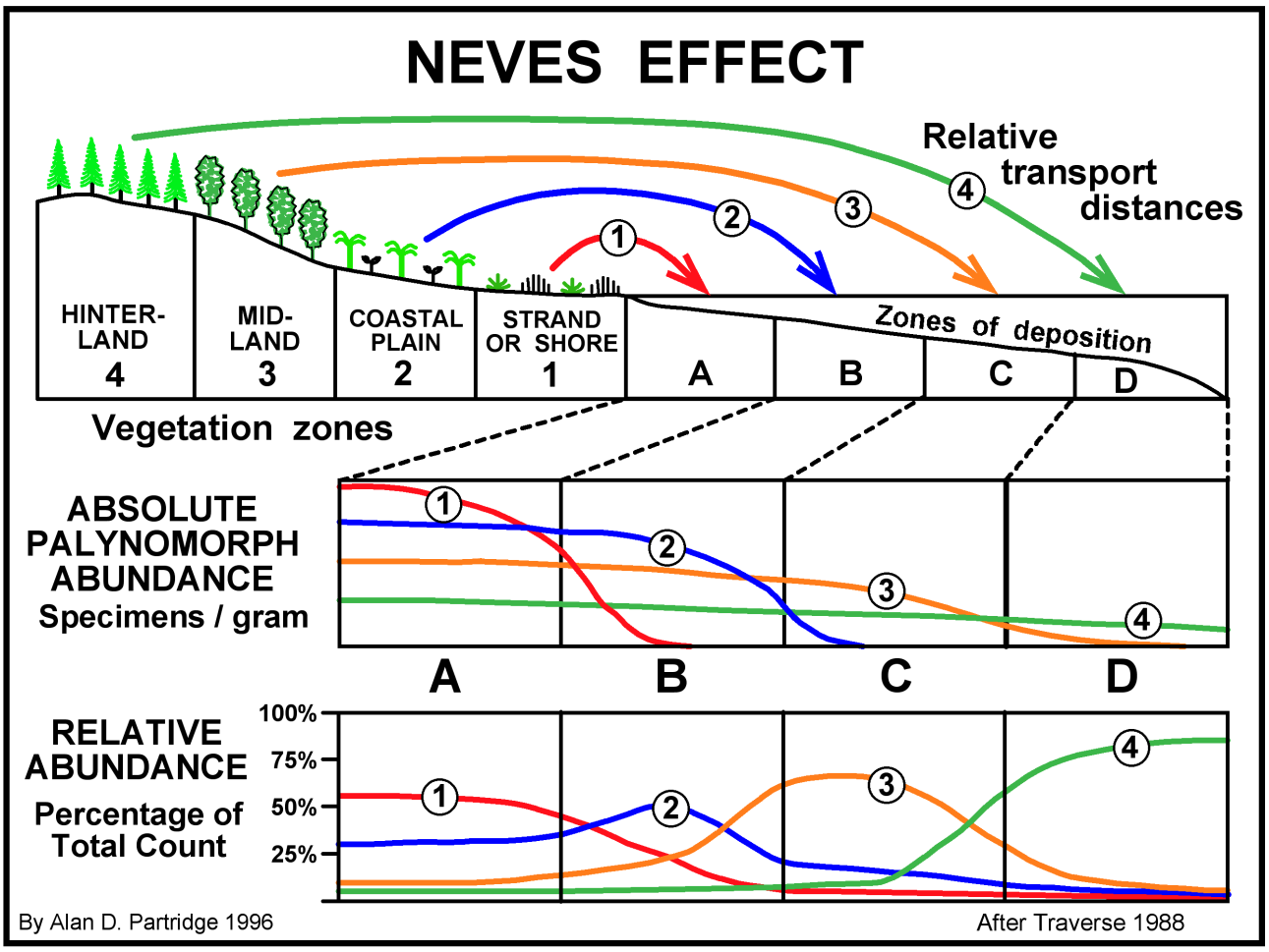
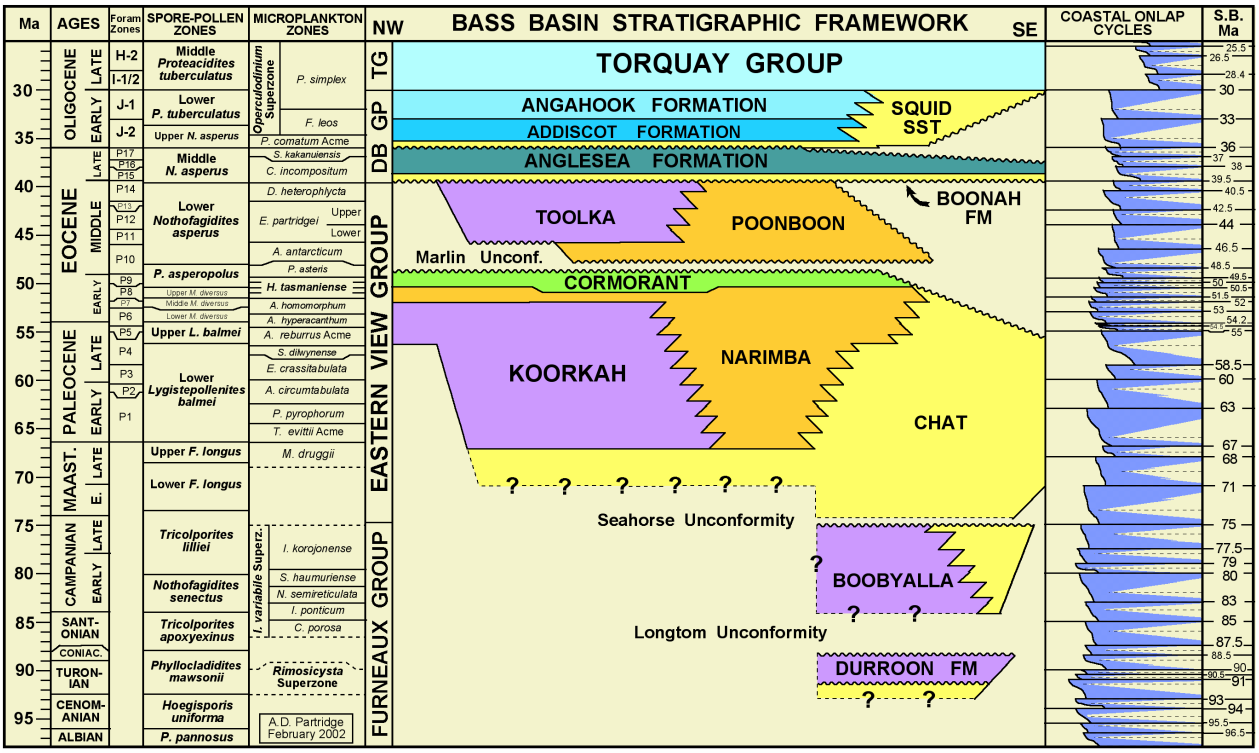


Figure 3. Proposed stratigraphic framework for the Bass Basin. Palynological zones and correlation to timescale of Haw et al. (1987) adapted from Partridge (1999a). Demons Bluff Group abbreviated to DB GP, and Torquay Group to TG. Except for those labelledas formations, new unit names are informal as is Furneaux Group.



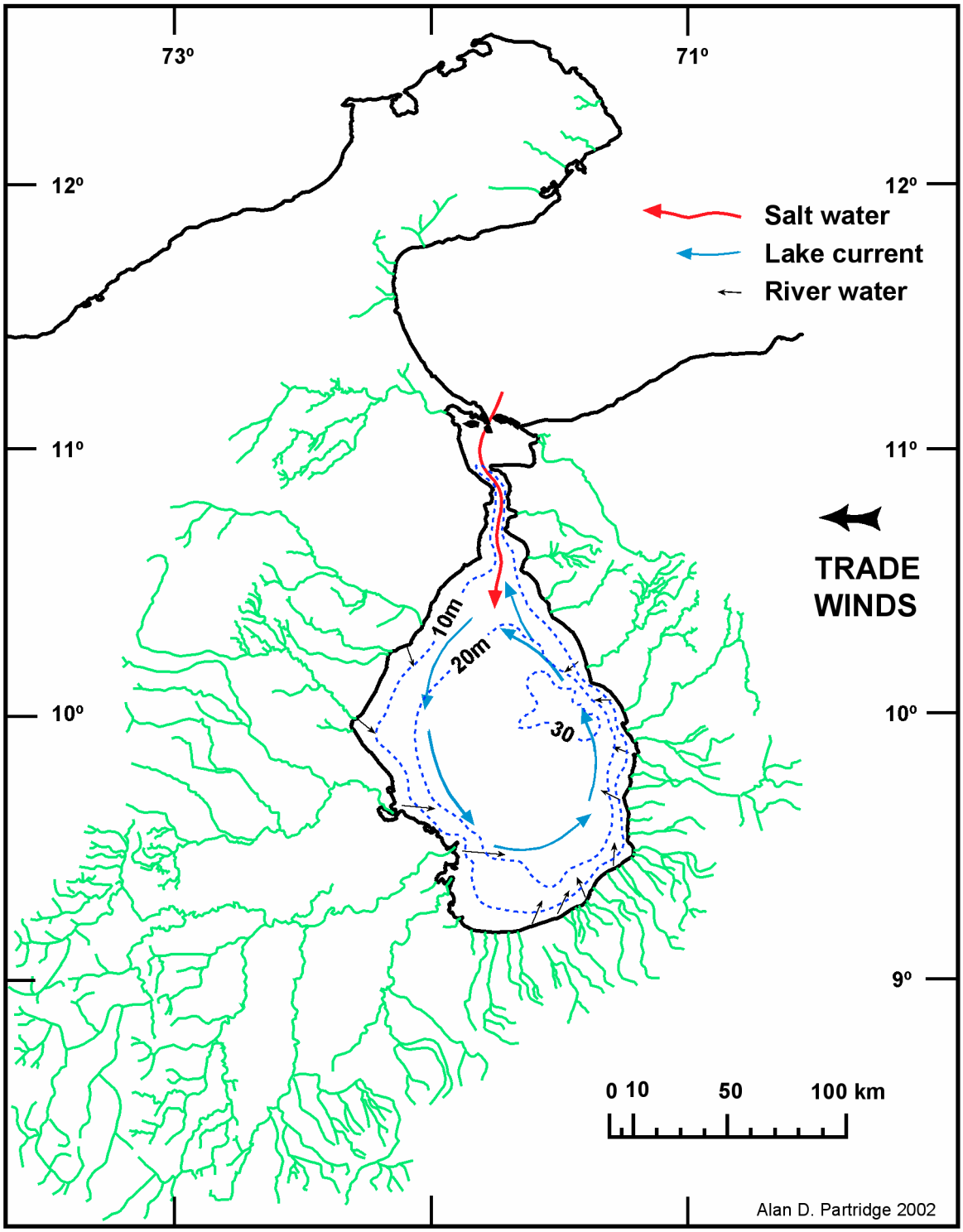
Basin by Bernecker & Partridge (2001). An unconformity also separates the Furneaux Group from the overlying Eastern View Group, but its precise age and stratigraphic position is uncertain. It is place between the *T. lilliei* and Lower *F. longus* Zones in Durroon-1 but may be lie within the Chat unit in other wells (eg. Koorkah-1). This unconformity is tentatively correlated with the Seahorse Unconformity identified in the Gippsland Basin by Bernecker & Partridge (2001), and with one or more unconformities identified within the Timboon Sandstone in the Otway Basin by Partridge (2001). The Eastern View Group, a contraction of the Eastern View Coal Measures, currently lacks a formal lithological subdivision of named formations. Seven informally named units are therefore proposed to facilitate the discussion of the facies relationships identified within the group (Figure 3). The subdivision is based largely on a NW to SE cross-section through the wells Konkon-1, Toolka-1, Cormorant-1, Koorkah-1, Poonoon-1, Squid-1, Chat-1 and Durroon-1. Key to the subdivision is the recognition of two thickly bedded shaly lacustrine facies referred to as the Koorkah and Toolka units, which are largely restricted to wells in the northwest portion of the basin (ie. Konkon-1, Seal-1, Toolka-1, Cormorant-1, Koorkah-1, and Aroo-1).

Laterally age equivalent to these lake or lagoonal facies are coastal plain to deltaic facies containing coals that are assigned to the Narimba and Poonboon units. These latter units are typified by the sequence in the Poonboon-1 well, and have been identified in the surrounding a circle of wells in the middle of the basin (ie. Tarook-1, Narimba-1, Pelican-1 to 5, Squid-1, Yurongi-1 and Tilana-1). The coaly coastal plain facies of the Narimba unit grades laterally into more sandy fluvial/alluvial sediments lacking coal in the most southeasterly Chat-1 and Durroon-1 wells. These non-marine sediments are referred to the Chat unit, and the name is also applied to sediments underlying the Koorkah and Narimba units, which also lack coal. It is surmised that coal deposition only started in the Bass Basin upon the initiation of Palaeolake Koorkah in the northwest portion of the basin. The younger Poonboon unit is still represent by coal measures in Chat-1, but is eroded or was never deposited in Durroon-1.

Between the major lacustrine facies of the Koorkah and Toolka units lies the Cormorant unit and parts of the Narimba and Poonboon units. The Cormorant unit is typically thinly bedded with a higher density of thin coal seams interbedded with restricted marine shales, and generally only rare sands. The thin bedding throughout the Cormorant unit suggests frequent and extensive changes in the environment of deposition as is likely to have occurred in a very shallow water lagoon, like modern Lake Maracaibo (Figure 4). In contrast, the thicker and more thickly bedded shales in the Koorkah and Toolka are interpreted to be more distal, and thus deeper water lacustrine or lagoonal facies. The intervening Narimba unit is considered to be transitional between the Koorkah and Cormorant units.

Correlation of the spore-pollen succession between the Bass and Gippsland Basins suggests the Cormorant unit is separated from the overlying Poonboon unit by missing Middle Eocene section correlated with the Marlin Unconformity of Partridge (1999a). This unconformity is based on missing dinocyst zones in the Gippsland Basin microplankton succession compared to more complete microplankton sequences in New

Figure 4. Locality map for Lake Maracaibo, Venezuela South America.



Zealand (Partridge, 1999a). Although identification in the Bass Basin of section equivalent to the Marlin Unconformity in the Gippsland Basin was a secondary objective of the palynological project, this correlation problem could not be solved in the wells analysed and additional palynological studies are still required.
The next major subdivision of the Bass Basin succession is assigned to the revised Demons Bluff Group of Holdgate *et al.* (2001), described from the Torquay Basin. This group represents the interval from the end of coal deposition to and commencement of widespread carbonate deposition.

Based on Holdgate *et al.* (2001) the main seal unit in the Bass Basin is now known as the Anglesea Formation. This unit was previously referred to as either the Upper Eocene Shale (Robinson, 1974) or Demons Bluff Formation (Baillie & Bacon, 1989). Also, the local name Konkon Sandstone of Baillie & Bacon (1989) is now recognised as a junior synonym of the Boonah Formation. Palynological data also confirms the correlation of the slightly calcareous marine sediments overlying the Anglesea Formation to the type sections of the Addiscot and Angahook Formations in the Torquay Basin. But as there is no clear electric log break, and little apparent change in lithology, between these formations in the Bass Basin a single name may be more appropriate. Further analysis of this interval is required. The widespread occurrence of cosmopolitan marine dinocysts, and absence of coal (except perhaps in Squid-1), in the formations of the Demons Bluff Group indicates deposition in marginal to restricted marine environments ranging from estuarine to bay facies.

The youngest major subdivision comprises the carbonate-rich sediments that are assigned to the Torquay Group, originally established in the Torquay Basin (Raggatt & Crespin, 1955). The group contains calcareous shales, marls, calcarenites and local volcanic piles, which have not yet been subdivided into formations or informal units. Torquay Group deposition commences in the Late Oligocene when the Bass Basin finally became an open-marine strait between the Otway and Gippsland Basins and extends through to the Pleistocene when the Bass Basin was again temporarily a large bay during the glacial periods.

Palaeolakes and Lagoons

Identification of palaeolakes and lagoons is integral to the interpretation of the stratigraphy and palynology of the Bass Basin presented in this report. According to the *Glossary of Geology* (Bates & Jackson, 1980; p.366) a lake is defined as any inland body of open standing water, that is sufficiently large and deep enough to sustain waves capable of producing somewhere on its periphery a barren wave swept shore. The term lagoon is restricted to shallow bodies of seawater separated from the adjacent sea by a low, narrow and elongate strip of land. Lagoons generally extend parallel to the coast, have irregular communication with the sea and may be little affected by tides (Bates & Jackson, 1987; p.365). The palaeolakes and lagoons postulated in the Bass Basin are identified from a combination of palynological, lithological and palaeogeographic evidence, and conform to definition of large lakes given by Herdendorf (1982) in having surface areas greater than 500 km^2. There are only 253 modern large lakes conforming to this definition (Herdendorf, 1982).

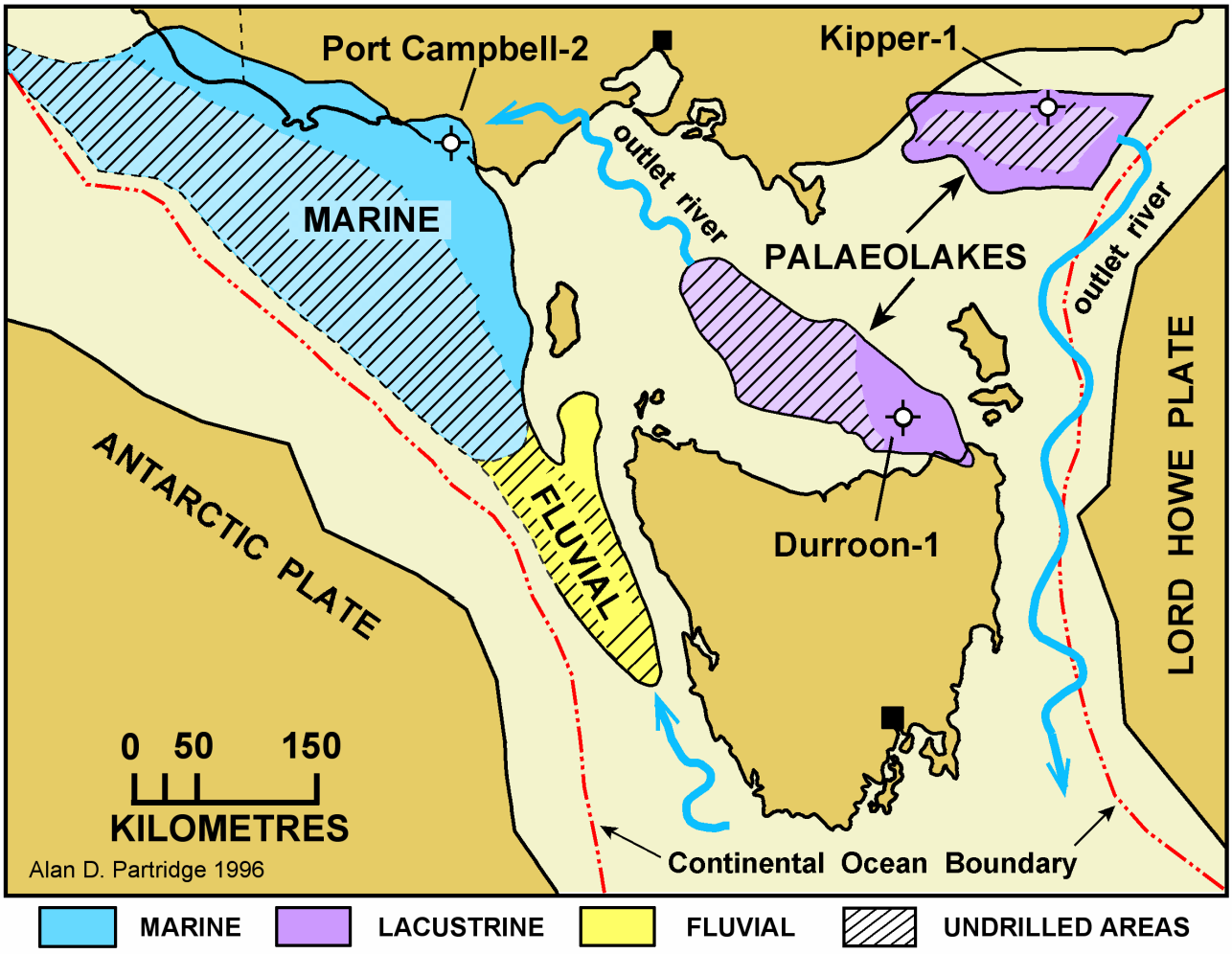
Palaeolake Durroon, even though only intersected in a single well, is the oldest acknowledged and perhaps best accepted palaeolake in the Bass Basin, because of the occurrence of an equivalent Turonian palaeolake in the adjacent Gippsland Basin (Partridge, 1973, 1996, 1999a; Bernecker & Partridge, 2001). The latter Palaeolake Kipper represented by the Kipper Shale is recognised on the basis of thick sequences of homogenous fine-grained clastics, the common occurrence of endemic non-marine microplankton and presence of Neves effects amongst the spore-pollen, the same criteria used to identify the Durroon Formation as a lacustrine facies. The features observed in Palaeolakes Kipper and Durroon also compare favourably with the general model of rift-valley lake sedimentation developed by Le Fournier (1980) and Johnson (1984) from studies of the great lakes along the East African Rift, and therefore these lakes are interpreted to have been relatively deep-water.

The palaeogeographic map for the Bass Strait region during the Turonian (Figure 5) shows the postulated extent of these two large lakes, as well as the extent of the marine transgression of the Otway Basin by the equivalent Waarre and Flaxman Formations. Also shown are the hypothetical overflow outlets for both lake systems. Because the Bass Strait region was at high palaeolatitudes during the Turonian based on continental reconstructions (eg. Veevers *et al.*, 1991; fig.6) there would have been a surfeit of precipitation over evaporation (Johnson, 1984; p.182) that would cause both lakes to fill their respective basins to capacity and overflow out to the ocean.

The latest Maastrichtian to Early Eocene Palaeolake Koorkah, the next major lacustrine facies that can be confidently identified in the Bass Basin, also displays most of the same characteristics as the older Turonian lakes. These include thick homogeneous shales, occurrence of known non-marine dinocysts and the same type of Neves effect. The similar high latitudinal position of the basin, and temperate rainforest vegetation indicated by the palynology, means that there was once again a surfeit of precipitation over evaporation, and the lake would have been filled to capacity and must have outflowed to the ocean. The influx of marine dinocysts from the northwest, documented in the Konkon-1 well, indicates that the outlet was in that direction.

Based on the surfeit of precipitation over evaporation and availability of plenty of geological time both Palaeolakes Durroon and Koorkah are likely to have had surface water levels close to the prevailing sea level. This conclusion is derived from the observation that with the exception of those tectonically formed lakes that are remote from the oceans (eg. East African Rift lakes, Lake Baikal) most modern perched lakes are Holocene glacial lakes and in the fullness of geological time their outlets will erode down to sea level. Under this model it should not be a surprise that the first major influx of marine dinocysts into the Bass Basin is found to correlate with high stands of sea level associated with the late Paleocene thermal maximum (LPTM).

Figure 5. Turonian palaeogeography of the Bass Strait.



Following the establishment of a permanent marine connection, in the Late Paleocene, the subsequent lacustrine facies in the Bass Basin are more analogous with modern Lake Maracaibo, situated at a latitude of 10°S in northern South America (Figure 4). This largest of all modern lagoons is comparable in size to the postulated Eocene lagoons (Cormorant and Toolka units), is relatively shallow (mean depth ~20 metres), and has a regular oval shape maintained by trade winds. Further, the modern Lake Maracaibo morphology can only have been established during the last 12,000 years, and considering the annual rainfall of >100 cm, and abundant rivers draining into the lagoon, it is easy to envisage the lagoon being quickly filled in course of geological time, so therefore its current morphology must also be partly controlled by the underlying geology.

With the cessation of coal deposition at the top of the Eastern View Group (top Middle Eocene) all the younger sediments of the Demons Bluff Group show a significantly greater marine character. The basin was nevertheless still mostly landlocked as there was no connection into the Gippsland Basin until Late Oligocene or Miocene at the earliest. A more appropriate model for deposition during this time is a large marine bay, analogous to modern Port Phillip only much larger. It needs to be remembered that all wells drilled to date in the Bass Basin are centrally located and coastal plain facies may have been deposited on the flanks of the basin as occurs in the Gippsland Basin at this time (Partridge, 1999a). The possibility of a thin succession of Early Oligocene coastal plain facies in the southeast portion of the basin is hinted at by the age of the Squid sandstone.

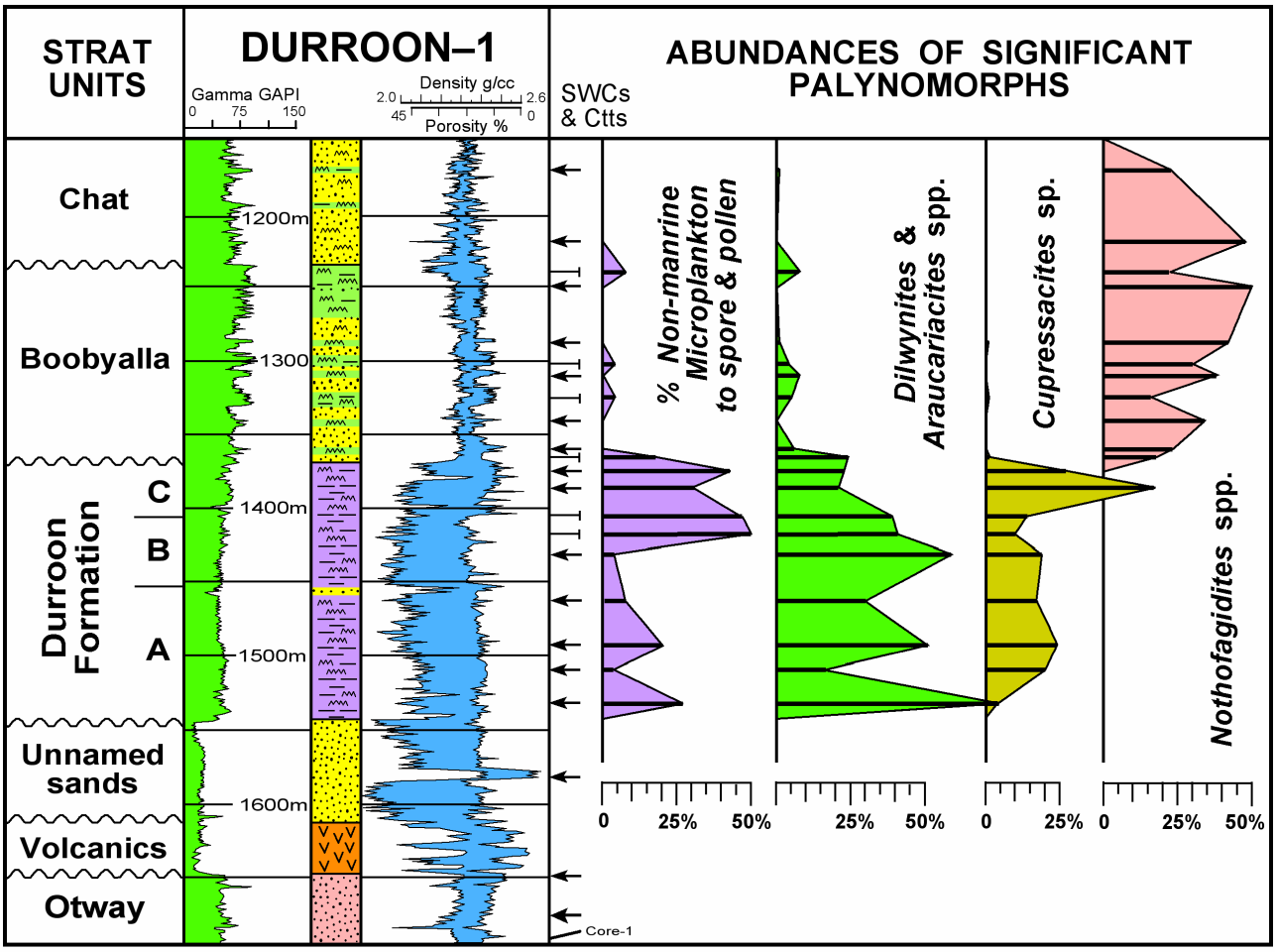
Geological Results of Palynological Studies.

Durroon-1.

Drilled in 1972, Durroon-1 is the only well in the basin that fully penetrates the upper Cretaceous Furneaux Group (Figure 3). Fortunately the well was sufficiently well-sampled by sidewall cores to serve as the quantitative palynological reference section over the interval Turonian to Maastrichtian (Figure 6; Partridge, 2002b). The interval investigated in the palynological study consists of the Turonian Durroon Formation, and the overlying informal Boobyalla and Chat units of Campanian to Maastrichtian age. The thick sequence of older Otway Group (1646-3024m), the unnamed sandstones and volcanics between 1545 and 1646m, and Tertiary sequence above 900m where not re-examined.

The Durroon Formation originally proposed by Smith (1986; p.264) for the interval 1374 to 1545m (here redefined as 1370 to 1544m) is of late Turonian age (*P. mawsonii* Zone), and is characterised by significant abundances of non-marine microplankton including dinocysts referred to *Morkallacysta* and algal cysts of the *Rimosicysta* Superzone recorded from the Kipper Shale in the adjacent Gippsland Basin (Partridge, 1999a; Bernecker & Partridge, 2001). The associated spore-pollen assemblages contain abundant *Dilwynites* pollen diagnostic of a Neves effect, and in the upper part of the formation (Unit C) a spike in the abundance of *Cupressacites* pollen is also present. This can be correlated with similar spike in *Cupressacites* pollen in

Figure 6. Abundances of significant palynomorphs in Upper Cretaceous in Durroon-1.



the Banoon Member at the top of the Flaxman Formation in the Otway Basin (Partridge, 2001). The 175 metre thick mudstone of the Durroon Formation is interpreted to have been deposited in distal fresh-water lacustrine facies (Palaeolake Durroon) which is coeval with the Flaxman Formation in the Otway basin and the youngest part of the Kipper Shale in the Gippsland Basin. The moderate to high abundance of non-marine microplankton, the abundant *Dilwynites* and *Araucariacites* pollen indicating a strong Neves effect, and overall homogeneous nature of the mudstone lithology evidenced by even gamma ray log and broad separation of the density and porosity logs, in combination are interpreted to mean that the Durroon Formation was deposited in a distal and probably deep fresh-water lacustrine environment.

The Durroon Formation is separated by a significant time break of between 5 and 9 million years from the overlying Boobyalla unit which is of Campanian age (*N. senectus* to *T. lilliei* Zones). Rare non-marine dinocysts and algae in this unit hint at the probable presence of more shaly lacustrine facies in the adjacent troughs. Equivalent age conglomerates and interbedded sandstones and mudstones are present in the onshore Boobyalla Subbasin (Moore *et al*., 1984), hence the derivation of the informal name for the unit. At the top of the diagram the informal Chat unit consists of non-marine fluvial sediments which lack any non-marine microplankton. Both these younger units represent much more fluvial to deltaic environments relative the unconformably underlying Durroon Formation. unfortunately, no reliable palynological dating has ever been obtained from the "Unnamed sands and volcanics" lying below the Durroon Formation. The original sidewall cores processed from this interval did not yield datable assemblages (Partridge, 1973), and subsequent studies of sidewall core material and cuttings by Morgan (1990) are here interpreted as unreliable due to contamination by material caved from higher in the well.

From the Chat unit new cuttings samples were collected and analysed over the interval 963 to 1008m in an attempt to more precisely define the position of the Cretaceous/Tertiary boundary. These analyses were unsuccessful as they gave a very low yield of palynomorphs which did not provide a reliable age.

Koorkah-1

The new palynological study of the Koorkah-1 well (drilled in 1985) was focussed on the thick shaly unit identified between 2250 and 2692m (Koorkah unit), and the underlying interbedded sands and shale section from 2692 to 3149mTD (Chat unit). A summary of the results obtained is provided in Figure 7. The interval was found to extends from the Early Maastrichtian Lower *F. longus* Zone to Late Paleocene Upper *L. balmei* Zone, with the latter identified in the sidewall cores at 2241m and 2266.5m previously analysed by Morgan (1986a). The thick shales were interpreted, from log character and the original palynological study, to represent probable lacustrine facies, and the objective was to provide additional supporting evidence from the palynology. As neither the original palynological slides, nor any of the remaining sidewall cores from Koorkah-1 were available for re-examination eleven new cuttings samples were collected and analysed (Partridge, 2002e).

Microplankton ranged from <1% to 27% of the combined spore-pollen and microplankton count in the cuttings samples, and although not particularly abundant are mainly represented by known non-marine dinocysts (eg. *Morkallacysta* Harris 1974). Marine dinocysts were only identified from the shallowest cuttings at 2266-75m and are most likely caved. The associated spore-pollen assemblages are characterised by abundant *Dilwynites* and *Araucariacites* pollen (average 29%) that are interpreted to be representative of a strong Neves effect. The combination of these palynological features is interpreted to indicate a fresh-water lacustrine environments of deposition. The more pronounced Neves effect in the thicker shales is taken as evidence that the depositional environments were more distal and probably also deeper water.

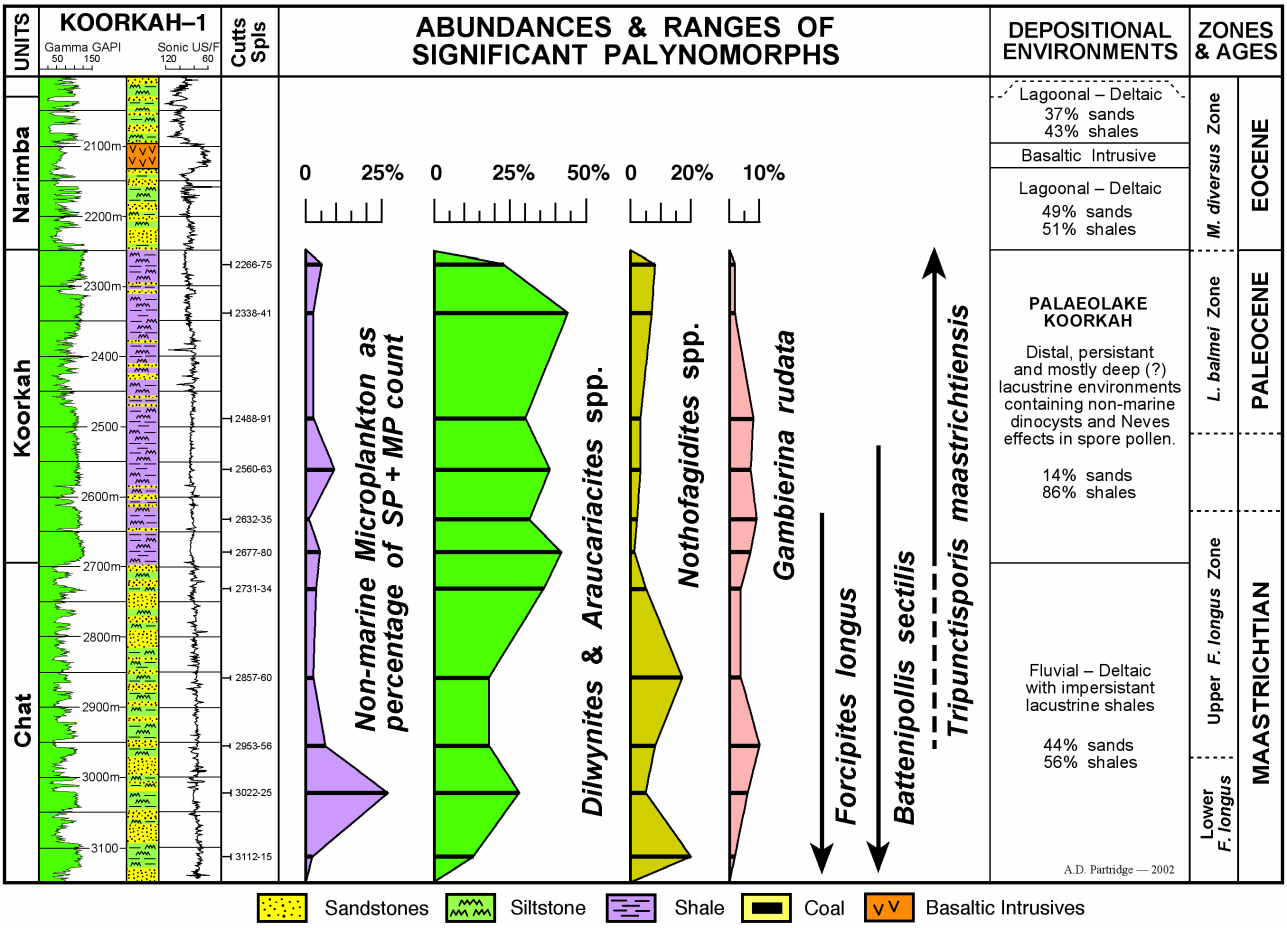
The Well Completion Report placed an "Intra Late Cretaceous Angular Unconformity" at 2690m at the base of the major shale section, and the presence of a major unconformity in the section is supported by the latest studies of the seismic data for the Bass Project. Although no obvious break can be identified in the palynology succession the most likely position would be between the Upper and Lower *F. longus* Zones and lie within the Chat unit rather than at the base of the Koorkah unit. The position of the zone boundary is based on the oldest occurrence of the spore *Tripunctisporis maastrichtiensis*, which is rare and inconsistent in the cuttings and only recorded by Morgan (1986a) from a single sidewall core at 2959m in the Chat unit. An unconformity at the equivalent stratigraphic level is identified within the Timboon Sandstone in the Otway Basin (Partridge, 2001).

The palynological data also indicates the Cretaceous/Tertiary boundary lies within the Koorkah unit but the precise position is equivocal. The boundary could lie above 2490m based on the youngest occurrence of *Battenipollis sectilis* and other secondary index species for the *F. longus* Zone, or alternatively deeper, just above youngest occurrence of the primary index species *Forcipites longus* at 2626m. The deeper pick is favour by the author based solely on the similarity of the log character over the interval 2470 to 2692m to the thicker sections of the Kate Shale in the Gippsland Basin (Partridge, 1999a-b). The anomalous shallower occurrences of the secondary index species in the Koorkah-1 well being interpreted as younger extensions of the species ranges or reworking.

Konkon-1

The new study of Konkon-1 was made to investigate the abundance of marine microplankton in the more shaly northwestern part of the Bass Basin, which available data suggested was the most likely source direction from which marine incursions entered the basin. The Konkon-1 well, drilled in 1973, was preferred to the later Seal-1 well, drilled in 1986, because it was better sampled by sidewall cores and the deep Paleocene section was less disturbed by igneous intrusions. The original palynological report by Stover (1973) also suggested this well contained some of the most abundant and diverse marine microplankton assemblages recorded in the basin. The original core and sidewall core samples between 1095.8 and 1494.7m were re-examined and six new samples collected and analysed by Partridge (2002d).

Figure 7. Abundances and ranges of significant palynomorphs through the Maastrichtian and Paleocene in Koorkah-1.



The distinctive feature of the section reviewed in Konkon-1 (Figure 8) is the thick shale unit from 1337 to 1474m (Koorkah unit) which is broken only by two distinctive coal seams at 1352-55m and 1402-03m. The palynological assemblages from the shale contains both microplankton and a strong Neves effect. The change in the microplankton assemblages from non-marine dinocysts below 1400m, to an increasing abundance and diversity of cosmopolitan marine dinocysts above 1400m, is interpreted to represent a change from a fresh-water lake to a marine coastal lagoon, and to represent the first major marine flooding of the Bass Basin. This change occurs in the Late Paleocene (Upper *L. balmei* Zone) and correlates with one or more major high sea level during the late Paleocene thermal maximum (LPTM). Sidewall core samples at 1354.8m and 1402.7m from the two coal seams are characterised by spore-pollen assemblages with very high abundances of *Gleicheniidites circinidites* and *Clavifera triplex* spores. These assemblages suggest the coals represent low stands of sea level when the lakes drained and this part of the basin was replaced by ìfern marshesî. The palaeolake and lagoon are referred to as Palaeolake Koorkah which is interpreted to have covered the northwestern half of the Bass Basin at its maximum extent (Figure 9). A modern analogue for the later lagoonal phase of Palaeolake Koorkah is Lake Maracaibo the largest modern coastal lagoon (Figure 4). In Konkon-1 the Palaeolake Koorkah is identified over the interval 1336 to 1474m and ranges in age from Early Paleocene to Early Eocene (Lower *L. balmei* to Middle *M. diversus* Zone).

No comparable abundances of microplankton or evidence of a Neves effect were recorded from either the older Chat unit or younger Narimba, Cormorant and Poonboon units, although this may largely reflect the limited number of palynological samples analysed, especially in the case of the Narimba unit. Marine dinocysts are next recorded in the succession from the Toolka unit between 1173 and 1213m. Although abundances are low (<1% to 5%) the presence of a low to moderate diversity of cosmopolitan dinocysts marks this as another lacustrine or lagoonal unit which has a similar distribution to the older Palaeolake Koorkah.

The approximately 320 metres of the Paleocene to Middle Eocene portion of the Eastern View Group penetrated in Konkon-1 is the most condensed section of the group so far encountered by any well drilled in the basin. It compares with an average thickness of over 1000 metres for the equivalent section in all other wells, and a maximum thickness of about 1800m penetrated in Tilana-1. The condensed nature and more basin margin location of the section in Konkon-1 would suggest the lacustrine sedimentation is representative of those intervals of time when the palaeolakes reached their maximum extent. In comparison to the lacustrine facies the other units in Konkon-1 are thinner and also more condensed, and when compared to the other wells they are also more incomplete. Thinnest are the Cormorant and Poonboon units which are more sandy and lack the coals found in these units in the rest of the basin (eg. Cormorant-1 and King-1). In addition, a major unconformity is postulated between the Early and Middle Eocene based on red and yellow weathered sandstones recorded in both the sidewall cores and cuttings. This unconformity is correlated to the Marlin Unconformity in the Gippsland Basin (Bernecker & Partridge, 2001; fig.2).

Figure 8. Abundances of significant Paleocene to Eocene palynomorphs in Konkon-1.

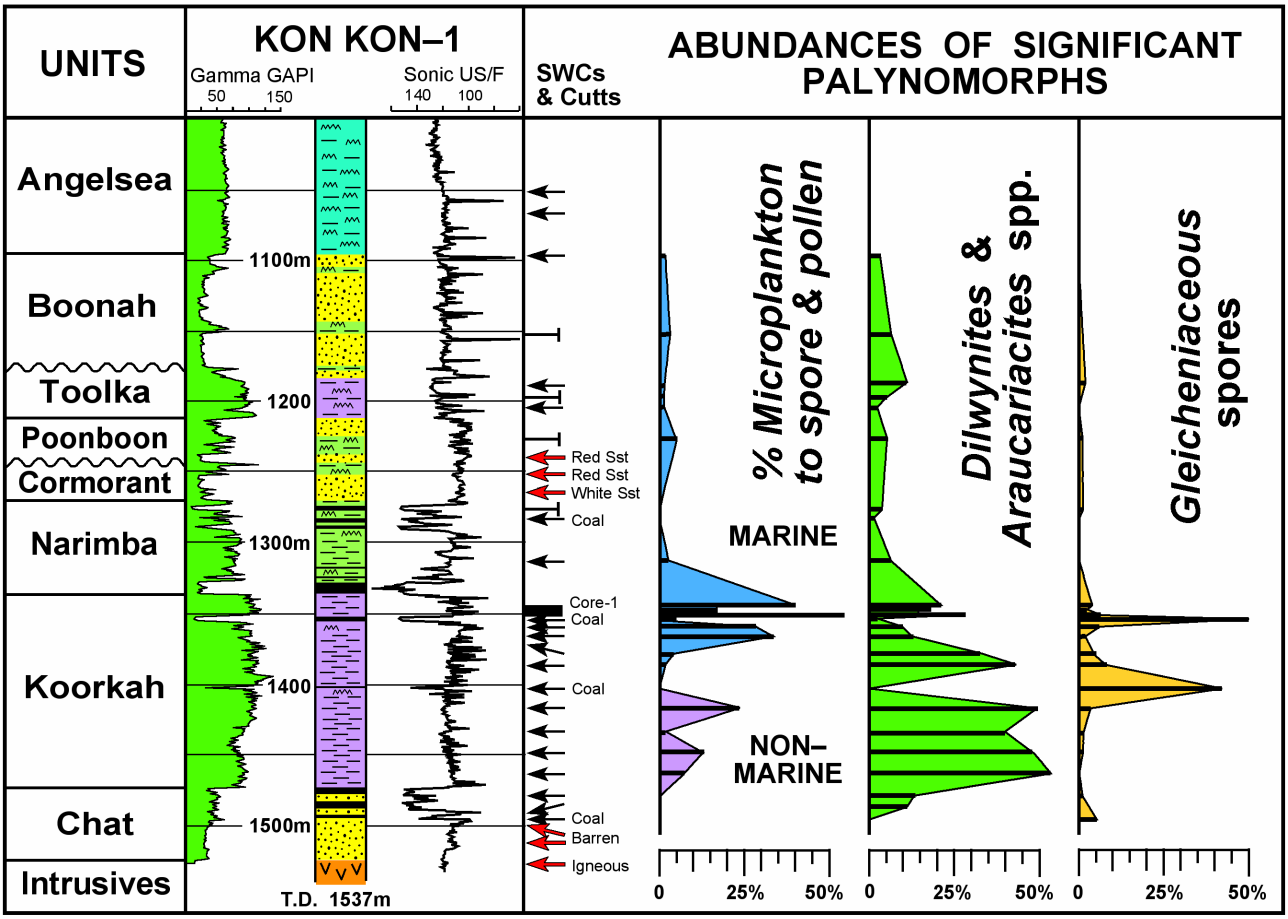
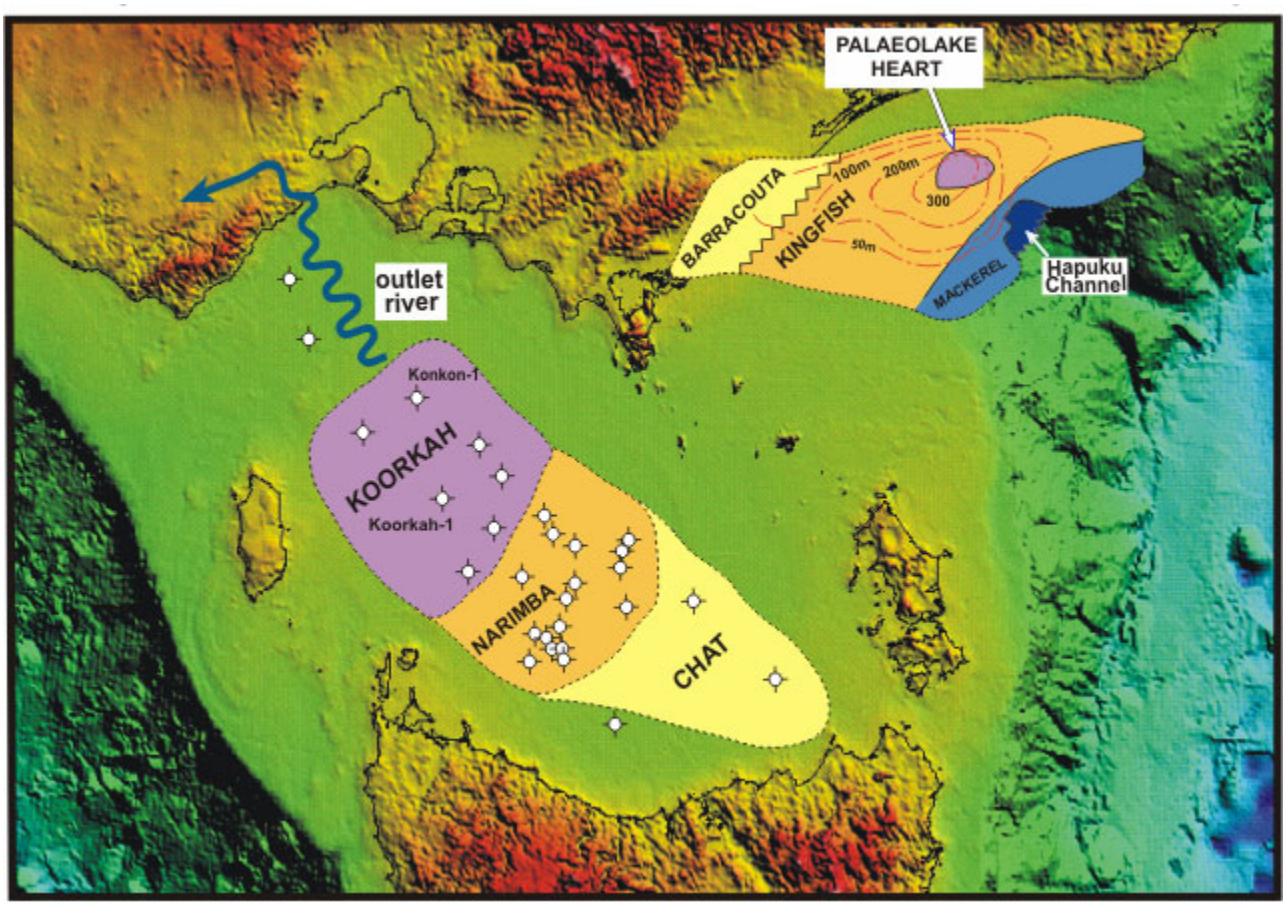


Figure 9. Late Paleocene palaeogeography of Bass Strait.



Palynological samples analysed from the younger Toolka unit and succeeding Boonah and Anglesea Formations, somewhat surprisingly only contained low abundances (<1% to 5%) of microplankton in the assemblage count. The assemblages also lack any obvious Neves effect. However, based on their low to moderate diversity of cosmopolitan dinocysts the assemblages are nevertheless interpreted as restricted marine. The Toolka unit is envisaged to have been deposited in a coastal lagoon, while the Boonah and Anglesea Formations are more likely deposited in estuarine or bay environments.

Poonboon-1

The early Poonboon-1 well, drilled in 1972, was chosen to be the principal quantitative reference section for the interval latest Maastrichtian to basal Miocene (Upper *F. longus* to *P. tuberculatus* Zones). The well is located near the centre of the basin, and contains the best sidewall core sampling through the Eastern View Group, and none of the palynological assemblages are obviously effected by igneous intrusions. Assemblage counts were made on 65 samples comprising 39 sidewall cores, 6 conventional core and 6 cuttings from the original palynological study by Partridge (1972), and a new collection of 13 cuttings and 1 core sample selected to increase the sample density through poorly sampled intervals. Data was recorded from an additional 8 samples which were not counted. Results of this new work is given in Partridge (2002f), and only a brief summary is provided here.

In Poonboon-1 significant abundances of marine dinocysts are only consistently recorded from Late Eocene and younger sediments above 1994m (ie. Boonah, Anglesea and younger formations), while a Neves effect is only identified from Maastrichtian age shale (*F. longus* Zone) intersected over the bottom 60 metres of the well (below 3204m). The latter is interpreted to represents the most southerly known extent of Palaeolake Koorkah. The intervening 1210 metres of Eastern View Group from 1994 to 3204m was predominantly deposited in lower coastal plain or deltaic environments as attested by the consistent presence of thin coal seams through the section. The sporadic occurrence of non-marine and marine dinocysts through this interval confirm short duration lacustrine or lagoonal palaeoenvironments (paralic facies) within the succession. The most significant of these events are:

1) Non-marine dinocysts referred to the genus *Morkallacysta* Harris 1974 recorded from the thicker shales (3107-3140m and 3205-3245m) near the bottom of the well that are associated with the most prominent Neves effects. These shales are interpreted to be tongues of the lacustrine Koorkah facies extending into the southeastern part of the basin during episodes of maximum lake level.
2) Marine dinocysts recorded from sidewall cores that are diagnostic of the *Apectodinium reburrus* Acme Zone (2678.6m) and the succeeding *Apectodinium hyperacanthum* Zone (at 2651.8m). These zones represent the first major marine incursion into the Bass Basin at the time of the late Paleocene thermal maximum (LPTM).
3) Sporadic occurrences of the *Apectodinium homomorphum* Zone in the Lower and Middle *M. diversus* Zones. The deeper from a sidewall core at 2529.8m has an microplankton (MP) abundance of 3% and

a low diversity of 5+ species. The shallower from core-2 at 2472.5m has an MP abundance of 43% with a moderate diversity of 11+ species. With more detailed study these horizons could potentially be linked to MP flooding events in the Dilwyn Formation in the Otway Basin.

4) Sporadic occurrences of dinocysts diagnostic of the *Homotryblium tasmaniense* Zones are found through the Upper *M. diversus* and *P. asperopolus* Zones. Although both abundance and diversity are low (<6% and <5 species per sample) they nevertheless confirm that a diluted marine influence has extended across most of the basin by the end of the Early Eocene.

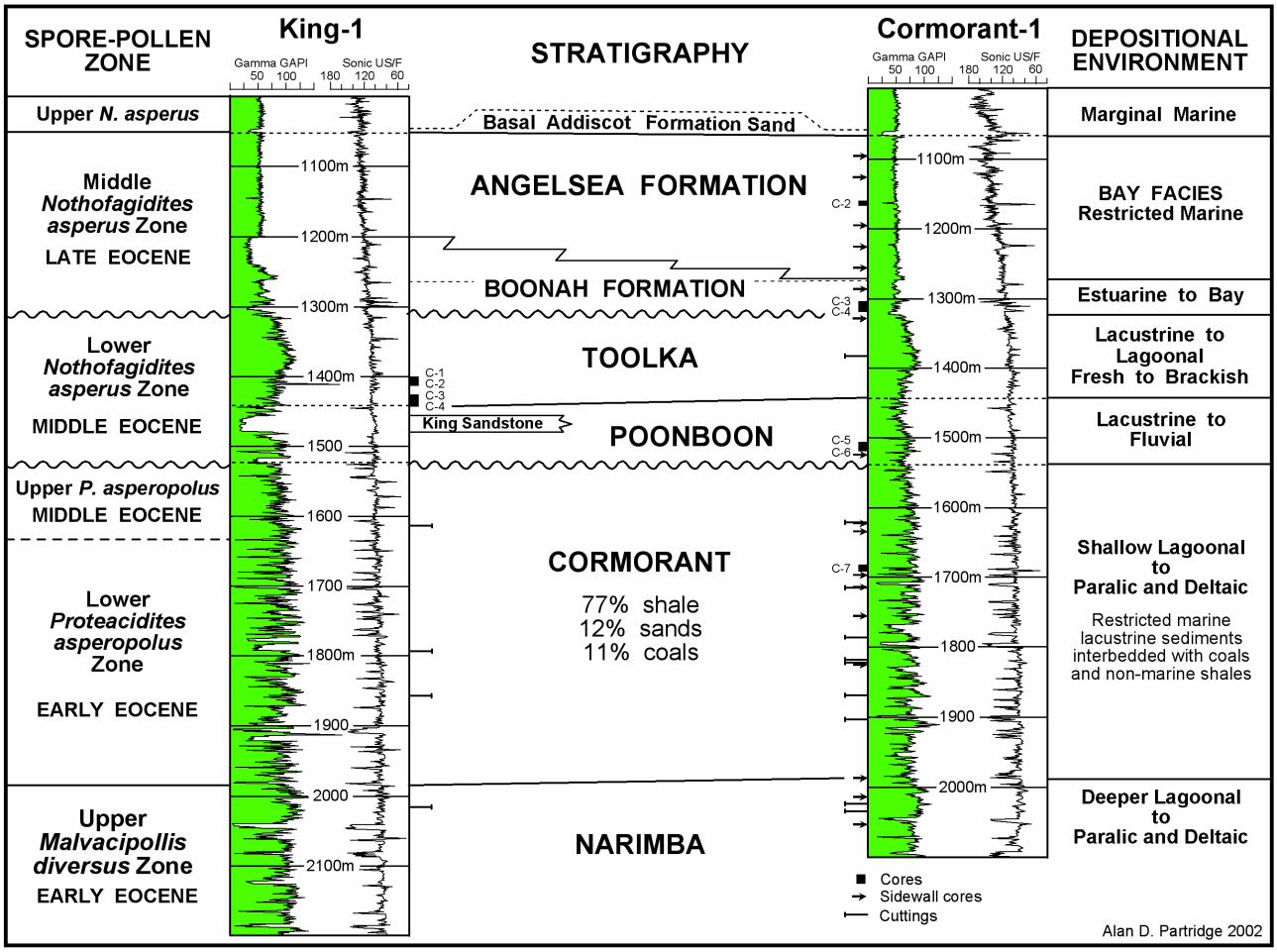
Cormorant-1 and King-1.

Palynological studies were conducted in Cormorant-1 and King-1 to investigate the expanded section from late Early Eocene through Middle Eocene (uppermost Upper *M. diversus* to Lower *N. asperus* Zones). The original palynological data indicated that this interval in Cormorant-1 contained marine dinocysts including the zone index *Charlesdowniea* (al. *Kisselovia*) *edwardsii* which had been reported from a sidewall core at 1825.8m. The objective of the study was to quantify the abundance and diversity of the microplankton present (both marine and non-marine), and determine whether other short ranging index species from the Subfamily Wetzelielloideae could be found in the section. Samples from the adjacent King-1 were analysed because this well had no previous palynological studies, and contained conventional cores at a stratigraphic level not previously sampled in Cormorant-1 (Figure 10).

Unfortunately the results of the search for microplankton were disappointing (Partridge, 2002a & c). Although overall composite species diversity through the intervals studied was high, in individual samples both abundance and species diversity was mostly low (abundance generally <10% and diversity <5 species per sample). Non-marine to brackish dinocysts were generally the most abundant species, but this group requires considerable taxonomic study before they will be of much stratigraphic use. The search for key index dinocysts was also unsuccessful. The presence of *Charlesdowniea edwardsii* in Cormorant-1 could not be confirmed, and *Wetzeliella articulata* was the only other species in this subfamily recorded. The original record of *C. edwardsii* must now be considered suspect, and perhaps can be interpreted as introduced into the sample as a laboratory contaminant. The study revealed that routine application of dinocyst for age dating and correlation within the upper Eastern View Group will be difficult. It requires an increase in both the density of sampling for palynology and much more intensive (and time consuming) searching of the palynological slides under the microscope to find the diagnostic index species.

The sections studied in Cormorant-1 and King-1 do help provide a better understanding of the stratigraphy and environment of deposition through the upper part of the Eastern View Group. In both wells the interval over which samples were examined extends from the upper part to the Narimba unit into the Toolka unit (Figure 10). Most of the samples analysed were from the Cormorant unit which is comprised of >75% shaly sediments on gross log character, with secondary sandstones and coals (each <15%). The section is characteristically thinly bedded (all beds <10 metres thick), with the shales consistently containing a

Figure 10. Palynological and log correlation between King-1 and Cormorant-1.



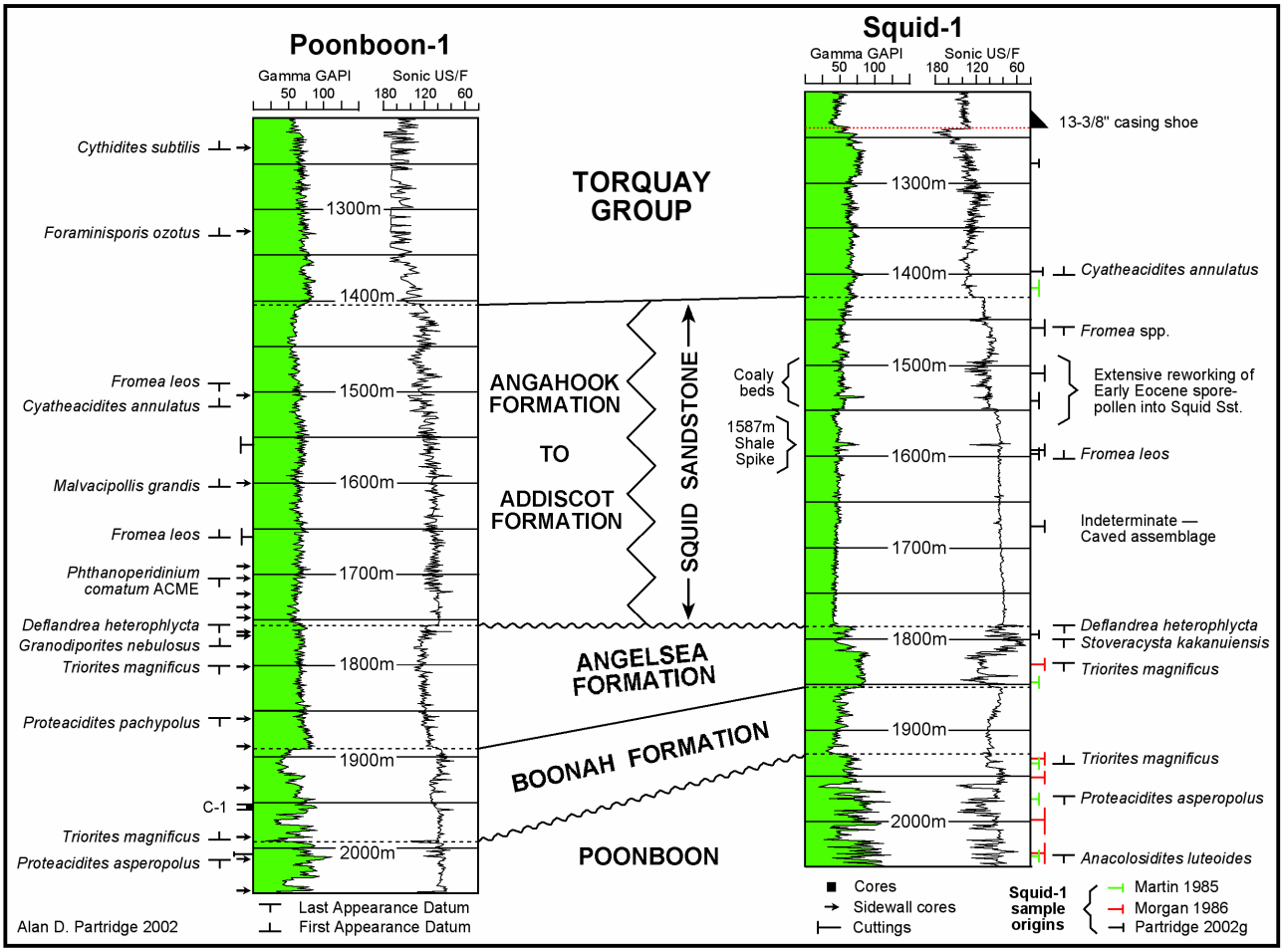
diversity of mainly marine dinocyst, but in low abundance (typically <1% to 5%). The associated spore-pollen assemblages contain rare specimens of the mangrove pollen *Spinizonocolpites prominatus* (= modern *Nypa* palm), but lack any significant development of a Neves effect. The environment of deposition is interpreted to be predominantly a shallow-water, restricted marine lagoon, which is periodically and frequently being replaced by coastal plain marshes. The presence of only minor sands through the unit suggests that the local Cormorant-1 and King-1 area is temporarily remote from any deltaic source or stabilised lake edge where strand-line sands could be developed. The suggested analogue for the Cormorant unit would be the modern Lake Maracaibo (Figure 4).

The underlying Narimba unit is distinguished from the Cormorant unit by containing thicker shales (typically >10 metres thick) and this is interpreted to mean that the lagoon or palaeolake facies was in general deeper.
In the overlying Poonboon and Toolka units the palynological assemblages are distinguished by a decline in the overall diversity of cosmopolitan marine dinocysts and an increase in brackish or non-marine types including undescribed species that might be endemic. Non-marine genera include *Saeptodinium* Harris 1974, *Cubiculosphaera* Harris 1974, while the possible brackish-water species *Paralecaniella indentata* (Deflandre & Cookson 1955) is the dominant species in some samples. Diversity remains low in individual samples (1 to 5 species), while abundances are <1% except in samples dominated by non-marine dinocysts. The shaly sediments of the Poonboon and Toolka units are thus also interpreted to represent predominantly lacustrine to lagoonal environments, although more brackish to fresh-water than the preceding Cormorant unit. This subtle change in facies is suggested to be indicative of a unconformity at the top of the Cormorant unit that correlates with the Marlin Unconformity in the Gippsland Basin (Partridge, 1999a). The presumed fluvial King sandstone in King-1 (Figure 10) may be reflective of a more fluvial regime in the Bass Basin at the time of the Marlin Unconformity.

Squid-1.

Palynological studies of Squid-1 were focussed on the 360 metre thick Oligocene sand unit from 1425 to 1785m (Figure 11). This unit had not been analysed in the original palynological reports by Martin (1985) and Morgan (1986b), nor was there any foraminiferal analysis from the interval or in the well. The geological problem was the age of this sand and whether it correlated with just the thin sands seen in some wells immediately above the Anglesea Formation (eg. Cormorant-1 and King-1), or alternatively was wholly or partly a lateral facies of the overlying marine shales and marls. Unfortunately, no conventional cores or sidewall cores were cut in Squid-1 so the palynological analysis needed to rely solely on cuttings. Initially six bulk cuttings were analysed, but once these were discovered to be confused by both caved and reworked palynomorphs an additional four cuttings were collected and given alternative processing. The latter consisted of a pre-treatment with dilute HCl followed by sieving to breakdown and remove any of the calcareous shales and marls caved from between the 13-3/8" casing shoe at 1240m and top of the sand at 1425m. The second batch of samples clarified and complimented the initial results, and the palynological analysis of both batches of samples are documented in Partridge (2002g).

Figure 11. Palynological and log correlation between Poonboon-1 and Squid-1.



Results from the new palynological study indicate that the Squid sandstone section is entirely Early Oligocene in age (Upper *N. asperus* to Lower *P. tuberculatus* Zones), and is a lateral facies of more shaly facies in wells to the northwest as illustrate by the palynological and electric log correlation to Poonboon-1 (Figure 11). The correlation relies principally on the identification of the *Fromea leos* microplankton Zone originally documented from the base of the Seaspray Group in the Gippsland Basin (Partridge, 1994). The *F. leos* Zone is identified in both bulk and pre-treated cuttings covering the distinctive gamma ray shale spike at 1586 to 1588m in Squid-1, and from sidewall cores and cuttings over the interval 1505.7m to 1670m in Poonboon-1. The next older *Phthanoperidinium comatum* microplankton Acme Zone is recorded over the interval 1706.9 to 1763m in Poonboon-1. However, the equivalent interval at the base of the sandstone in Squid-1 was not sampled as none of the cuttings were deemed to be suitable for analysis. No change in lithology or new shaly material was observed in the Squid-1 cuttings between 1600m and the next obvious log break at 1785m. Below the latter break the microplankton assemblages from the top samples from the Anglesea Formation in both wells are characterised by the LAD of the dinocyst *Deflandrea heterophlycta*. In the marly sediments above the Squid sandstone the microplankton assemblages are dominated by the dinocysts *Spiniferites* spp. and *Operculodinium centrocarpum* which are diagnostic of the *Operculodinium* Superzone. This latter interval equates to the Torquay Group. The spore-pollen assemblages support these correlations but the differentiation of the zones is less clear because the First Appearance Datums (FADs) on which the zone definitions depend are much less reliable in cuttings. Note especially that the FAD of the spore *Cyatheacidites annulatus*, the marker species for the base of the *P. tuberculatus* Zone, is found to occur **within** the *F. leos* Zone in other sections sampled by sidewall cores (eg. Partridge, 1994).

Another distinct feature of the new palynological analysis of Squid-1 is the discovery of a substantial reworking event in the upper part of the Squid sandstone. Cuttings examined between 1430 and 1550m where observed to be dominated by light to medium grey marl (interpreted as caved), with secondary loose quartz sand, and minor (<10%) black carbonaceous shale or coal. The last is interpreted to come from the ì coalyî spikes on the sonic log between 1441 and 1535m, and is believed to be the principal source of *in situ* palynomorphs. The bulk of the recorded spore-pollen assemblages from the three cutting samples analysed between 1445 and 1550m were composed of long ranging species (Partridge, 2002g), but there was a conspicuous component, perhaps as high as 20% of spore-pollen assemblage, that is interpreted as reworked, based on well-established species ranges throughout southeast Australia. The most conspicuous reworked species recorded are *Proteacidites leightonii*, *P. asperopolus*, *P. pachypolus* and *Dicotetradites clavatus*. In combination these species indicate the source of the reworking was from sediments belonging to an interval extending from the *P. asperopolus* to basal Lower *N. asperus* Zone, implying an age range of late Early to early Middle Eocene. Although similar reworking has been recorded in other wells in the Bass Basin, at about the equivalent stratigraphic horizon above the Anglesea Formation, the numbers of reworked specimens is much lower (est. <1%). The postulated provenance of the reworking is to the south-east where the appropriate age sediments are at shallower depths (eg. Chat-1), or are suspected to have been eroded (eg. Durroon-1).

The palynological age dating obtained in Squid-1 and the palynological and log correlation established to Poonboon-1, refutes the interpretation that the thick Squid sandstone is filling a large channel entrenched into the top of the Anglesea Formation. Rather, the Squid sandstone represents a lateral sandy facies of the more shaly sediments overlying the Anglesea Formation in other wells. Reviewing the electric logs and limited palynological data in the wells across the basin from the Pelican field wells in the SW, through Poonboon-1 and Nangkero-1 in the middle of the basin, to Dondu-1, Yurongi-1 and Bass-2 in the NE, reveal that the equivalent section in these wells all belong to the more shaly facies found in Poonboon-1. However, similar but thinner sands are known to overlie the distinctive Anglesea Formation directly to the east in the Chat-1 well (1072-1132m), and to the SE in the Durroon-1 well (458-540m). Unfortunately, there is no reliable age dating of the sands in the latter two wells, but as the base of these sands are significantly shallower (650m in Chat-1 and 1245m in Durroon-1, compared to 1785m in Squid-1) they potentially could be much younger.

Based on the above well control and analogy to palaeoshorelines identified in other parts of Bass Strait (eg. Partridge, 1999a; Holdgate *et al.*, 2002) the Squid sandstone is interpreted to be a barrier sandstone body with a probably SSW to NNE orientation that was largely deposited in a shoreface environment. The shale spike at 1586 to 1588m in Squid-1 representing a flooding horizon and the overlying thin coaly beds representing regressive back-barrier marsh environments.
Also based on the new analyses the thin sandstones (typically <10 metres thick) immediately overlying the Anglesea Formation in some other wells (eg. Cormorant-1 and King-1; Figure 10) can only be age equivalent to oldest part of the Squid sandstone. However, since they directly overlie the unconformity and sequence boundary postulated at the top of the Anglesea Formation they still may be related to entrenchment at this surface.

The 360 metre thick Squid sandstone and the equivalent section in other wells in the Bass Basin is an **expanded** section of an interval that is both poorly represented and poorly understood in other basins in southeast Australia. Based on my own unpublished palynological studies the interval is equivalent to both the Addiscot and Angahook Formations of the Demons Bluff Group in the onshore Torquay Basin where it has a maximum thickness of about 50 metres (Holdgate *et al.*, 2001; fig.15). In the Gippsland Basin the equivalent section is involved with the enigmatic "Early Oligocene Wedge" and broader issues about the appropriate definition of the top of Latrobe Unconformity (Bernecker & Partridge, 2001; appendix). For example, in the distal offshore Gippsland Basin the time-interval is either missing or represented by less than 20 metres of open-marine marl at the base of the Seaspray Group (eg. Partridge, 1994), whereas in the onshore Gippsland Basin the time-interval is represented by up to 150 metres of coal measure facies of the Burong Formation overlain by about 10 metres of Cunningham Greensand (Bernecker & Partridge, 2001; Partridge, 1999a).

In the Otway Basin and more westerly St Vincent Basin the precise correlation is less clear largely because

of a lack of detailed palynological studies of basal Oligocene strata. Correlations of the better known Late Eocene palynological sequences suggests that the distinctive log break mapped at the top of the Anglesea Formation in most wells in the Bass Basin is a sequence boundary unconformity that correlates to the commencement of the Chinaman Gully regression of McGowran *et al.* (1992). The succeeding, essentially non-marine Chinaman Gully Formation in the St Vincent Basin is correlated with part of the Squid sandstone, but exactly how much is uncertain. The problem revolves around how to correlate the succeeding ìtransgressive eventsî recognised by McGowran *et al.* (1992) into the Bass Basin. These are the Aldinga transgression (representing the restoration of neritic carbonate at the base of the Aldinga Member), the Ruwarung maximum flooding surface at the base of the Ruwarung Member, and the sequence boundary at Willungan/Janjukian Stage boundary. The current interpretation as shown in Figure 11 is that the Squid sandstone and laterally equivalent sediments assigned to the combined Addiscot and Angahook Formation in the more central parts of the basin are equivalent to the entire Early Oligocene. The overlying carbonate sediments are assigned to a currently undifferentiated Torquay Group and are Late Oligocene and younger in age.

Conclusions and Recommendations

The new palynological studies of selected intervals from only one-fifth of the wells drilled in the Bass Basin provide critical new information towards construction of a better stratigraphic framework and more comprehensive models for depositional processes in the basin. The core objective of providing a quantitative reference section for the palynological succession, although little discussed in this report, will ultimately prove its worth as the palynological data is upgraded in other wells to the same quality.

The principal immediate results from the project has been obtaining a quantitative picture of the distribution of marine and non-marine dinocysts and other microplankton in the basin, and the identification of Neves effects amongst the spore-pollen. This information has allowed better models to be formulated for the duration and geographic extent of palaeolakes and lagoons in the basin.

Notwithstanding these achievements more detailed palynological studies of wells in the Bass Basin are required as the density and quality of biostratigraphic data compares unfavourably with palynological techniques and approaches applied in other hydrocarbon bearing basin around Australia. Indeed lack of this type of data has probably contributed to perception that the Bass Basin has low productivity.

The following additional studies are recommended as a contribution to rectifying these perceptions:

1. Description and further study of the non-marine dinocysts to better understand the environmental controls on their distribution and potential source contribution.
2. Re-examination of Maastrichtian portion of Chat unit to better understand the boundary relationship between the Furneaux and Eastern View Groups.
3. Further study of sections crossing Early to Middle Eocene boundary to improve correlations with

adjacent basins and confirm or disprove the existence of a fluvial system in the basin corresponding to the Marlin Unconformity in the Gippsland Basin.

4. Review of existing data and new palynological analysis of sections in the Torquay Basin to identify position of palaeolake outlet from Bass Basin postulated to have been present as far back as the Cretaceous.

References

BAILLIE, P.W. & BACON, C.A., 1989. Integrated sedimentological analysis: The Eocene of the Bass Basin. *The APEA Journal, vol.29*, pt.1, p.312-327.

BATES, R.L. & JACKSON, J.A., editors, 1987. *Glossary of Geology. Third Edition.* American Geological Institute, Alexandria, Virginia, p.1-788.

BERNECKER, T. & PARTRIDGE, A.D., 2001. Emperor and Golden Beach Subgroups: The onset of Late Cretaceous sedimentation in the Gippsland Basin, SE Australia. **In** *Eastern Australian Basins Symposium. A Refocussed Energy Perspective for the Future,* K.C. Hill & T. Bernecker, editors, *Petroleum Exploration of Australia, Special Publication*, p.391-402.

DEFLANDRE, G. & COOKSON, I.C., 1955. Fossil microplankton from Australian late Mesozoic and Tertiary sediments. *Australian Journal of Marine and Freshwater Research, vol.6*, no.2, p.242-313, pls 1-9.

HARRIS, W.K., 1974 [imprint 1973]. Tertiary non-marine dinoflagellate cyst assemblages from Australia. **In** *Mesozoic and Cainozoic palynology: essays in honour of Isabel Cookson*, J.E. Glover & G. Playford, editors, *Geological Society of Australia Special Publication 4*, p.159-166.

HERDENDORF, C.E., 1982. Large lakes of the world. *Journal Great Lakes Research, vol.8,* pt.3, p.379-412.

HOLDGATE, G.R., SMITH, T.A.G., GALLAGHER, S. & WALLACE, M.W., 2001. Geology of coal-bearing Palaeogene sediments, onshore Torquay Basin, Victoria. *Australian Journal of Earth Sciences, vol.48*, p.657-679.

HOLDGATE, G.R., GALLAGHER, S. & WALLACE, M.W., 2002. Tertiary coal geology and stratigraphy of the Port Phillip Basin, Victoria. *Australian Journal of Earth Sciences, vol.49*, no.3, p.437-453.

JOHNSON, T.C., 1984. Sedimentation in large lakes. *Annual Review of Earth and Planetary Science, vol.12,* p.179-204.

LE FOURNIER , J., 1980. DÈpÙts de prÈouverture de líAtlantique Sud. Comparaison avec la sÈdimentation actuelle dans la branche occidentale de Rifts Est-Africains. *Recherches Geologiques en Afrique 5*, p.127-130.

MARSHALL, N.G., 1989. An unusual assemblage of algal cysts from the late Cretaceous, Gippsland Basin, Southeastern Australia. *Palynology 13,* p.21-56.

MARTIN, H.A., 1985. The stratigraphic palynology of Squid #1 and Tasmanian Devil #1, Bass Basin. *Unpublished report for Kimberley Oil and Gas N.L.*, 6p., 2 figs, 1 table.

MCGOWRAN, B., MOSS, G. & BEECROFT, A., 1992. Late Oligocene and Early Oligocene in Southern Australia: Local neritic signals of global oceanic changes. **In** *Eocene-Oligocene Climatic and Biotic Evolution*, D.R. Pothero & W.A. Berggren, editors, Princetown University Press, p.178-201.

MOORE, W. R., BAILLIE, P.W., FORSYTH, S.M., HUDSPERTH, J.W., RICHARDSON, R.G. & TURNER, N.J., 1984. Boobyalla Sub-basin: A Cretaceous onshore extension of the southern edge of the Bass Basin. *The APEA Journal, vol.24*, pt.1, p.110-117.

MORGAN, R., 1986a. Palynology Koorkah-1. Appendix 6 in Well Completion Report, 7p., 1 fig., 2 charts (unpubl.).

MORGAN, R., 1986b. Palynology of Weaver Squid-1, Bass Basin, Australia. *Report to Bridge Oil Limited*, 12p. 2 charts (unpubl.).

MORGAN, R., 1990. New palynology of the Durroon Mudstone, Duroon-1, Bass Basin. *Report to Bridge Oil Limited* (unpubl.).

MOSS, G. & MCGOWRAN, B., 1993. Foraminiferal turnover in neritic environments: the end-Eocene and mid-Oligocene events in southern Australia. *Memoir Association Australasian Palaeontologists 15,* p.407-416.

PARTRIDGE, A.D., 1972. The Palynology of Poonboon-1, Bass Basin. *Esso Australia Ltd Palaeontological Report 1972/19,* 8p. (6 December).

PARTRIDGE, A.D., 1973. Palynology of Durroon-1, Bass Basin. *Esso Australia Ltd Palaeontological Report 1973/1*, 11p. (31 January).

PARTRIDGE, A.D., 1996. Large Break-up lakes of the Bass Strait. *Gippsland Basin Symposium 1996, Stratigraphy, Hydrogeology, Seismic Analyses, Hydrocarbon Plays, Prospects and Developments. Friday, 22nd November 1996, School of Earth Sciences, University of Melbourne. Program & Extended Abstracts,* S. Gallagher, compiler, p.3-6.

PARTRIDGE, A.D., 1994. Palynological analysis of Blackback-3, Gippsland Basin. *Biostrata Report 1994/6*, p.1-23, 2 charts.

PARTRIDGE, A.D., 1999a. Late Cretaceous to Tertiary geological evolution of the Gippsland Basin, Victoria. PhD thesis, La Trobe University, Bundoora, Victoria, p.i-xxix, p.1-439, 165 figs, 9 pls (unpubl.).

PARTRIDGE, A.D., 1999b. The Cretaceous/Tertiary boundary in Victoria. *Geological Society of Australia, Abstracts no.55, 13th Victorian Universities Earth Science Conferences, The University of Melbourne, September 1999,* p.26ñ27.

PARTRIDGE, A.D., 2001. Revised stratigraphy of the Sherbrook Group, Otway Basin. **In** *Eastern Australian Basins Symposium. A Refocussed Energy Perspective for the Future,* K.C. Hill & T. Bernecker, editors, *Petroleum Exploration of Australia, Special Publication*, p.455-464.

PARTRIDGE, A.D., 2002a. Palynological analysis of Eocene interval 1380 to 2036m in Cormorant-1, Bass Basin. *Biostrata Report 2002/06*, p.1-16.

PARTRIDGE, A.D., 2002b. Palynological review of Upper Cretaceous units in Durroon-1, Bass Basin. *Biostrata Report 2002/07*, p.1-16.

PARTRIDGE, A.D., 2002c. Palynological analysis of Eocene interval 1380 to 2036m in King-1, Bass Basin. *Biostrata Report 2002/08*, p.1-13.

PARTRIDGE, A.D., 2002d. Quantitative palynological analysis of Paleocene to Middle Eocene interval Kon Kon-1, Bass Basin. *Biostrata Report 2002/09*, p.1-18.

PARTRIDGE, A.D., 2002e. Quantitative palynological analysis of eleven cuttings samples from 2266 to 3115m in Koorkah-1, Bass Basin. *Biostrata Report 2002/10*, p.1-15.

PARTRIDGE, A.D., 2002f. Quantitative palynological analysis of Eastern View and Demons Bluff Groups in Poonboon-1, Bass Basin. *Biostrata Report 2002/11*, p.1-35.

PARTRIDGE, A.D., 2002g. Palynological analysis of Oligocene sandstones in Squid-1, Bass Basin. *Biostrata Report 2002/12*, p.1-18.

RAGGATT, H.G. & CRESPIN, I.C., 1955. Stratigraphy of Tertiary rocks between Torquay and Eastern View, Victoria. *Proceedings Royal Society of Victoria, vol.67,* pt.1, p.75-142.

ROBINSON, V.A., 1974. Geological history of the Bass Basin. *The APEA Journal, vol.14*, pt.1, p.44-49.

SMITH, G.C., 1986, Bass Basin geology and petroleum exploration. **In** *Second South-Eastern Australia Oil Exploration Symposium,* R.C. Glenie, editor, Technical papers presented at PESA Symposium, 14ñ 15 November, 1985, Melbourne, p.257-284.

STOVER, , L.E., 1973. Palynological determinations for Kon Kon-1 well, Bass Basin. *Esso Production Research Co. Report EPR.58 ES.73; ESOA Report 1973/6*, 5p., 4 charts, data sheet.

TRAVERSE, A., 1988. *Paleopalynology*. Unwin Hyman Ltd, Boston, p.1-600.

VEEVERS, J.J., POWELL, C.McA. & ROOTS, S.R. 1991. Review of seafloor spreading around Australia. I. Synthesis of the patterns of spreading. *Australian Journal of Earth Science, vol.38,* no.4, p.373-389.

APPENDIX D.

LIST OF CORE AND CUTTINGS FROM THE BASS BASIN ANALYSED FOR ORGANIC GEOCHEMISTRY

C. Boreham, Geoscience Australia

Geoscience Australia No.	Palynology Laboratory No.	Well	Sample Depth Top m	Sample Depth Base m	Sample Type	Lithology	VRF	Kinetics	SANS
20010060	6405386	Cormorant 1	910.30	910.45	Core	shale	yes		
20010061	6405387	Cormorant 1	1160.08	1160.24	Core	shale	yes		
20010062	6405388	Cormorant 1	1310.96	1311.11	Core	shale	yes		
20010346	6405910	Cormorant 1	1444.77	1450.87	Cutt	coal			yes
20010347	6405913	Cormorant 1	1478.30	1487.44	Cutt	coal			yes
20010063	6405389	Cormorant 1	1518.46	1518.47	Core	shale	yes		
20010064	6405390	Cormorant 1	1519.75	1519.90	Core	coal	yes	yes	
20010065	6405391	Cormorant 1	1520.31	1520.36	Core	shale	yes	yes	yes
20010348	6405914	Cormorant 1	1530.11	1536.21	Cutt	coal			yes
20010349	6405915	Cormorant 1	1633.75	1639.84	Cutt	coal			yes
20010350	6405916	Cormorant 1	1661.18	1667.28	Cutt	coal			yes
20010066	6405392	Cormorant 1	1685.31	1685.39	Core	shale	yes		
20010067	6405393	Cormorant 1	1685.56	1685.72	Core	coal	yes	yes	yes
20010068	6405394	Cormorant 1	1686.58	1686.63	Core	shale	yes		
20010351	6405917	Cormorant 1	1725.19	1728.24	Cutt	coal			yes
20010352	6405918	Cormorant 1	1777.01	1780.05	Cutt	coal			yes
20010344	6405919	Cormorant 1	1829.53	1829.58	Core	coal			yes
20010353	6405920	Cormorant 1	1877.59	1883.69	Cutt	coal			yes
20010069	6405395	Cormorant 1	1950.74	1959.89	Cutt		yes		yes
20010354	6405921	Cormorant 1	2005.61	2011.70	Cutt	coal			yes
20010355	6405922	Cormorant 1	2042.18	2048.28	Cutt	coal			yes
20010356	6405923	Cormorant 1	2090.95	2097.05	Cutt	coal			yes
20010070	6405396	Cormorant 1	2154.96	2167.15	Cutt	coal	yes		yes
20010357	6405924	Cormorant 1	2215.92	2222.02	Cutt	coal			yes

20010345	6405925	Cormorant 1	2232.38	2232.53	Core	coal			yes
20010358	6405926	Cormorant 1	2276.88	2279.93	Cutt	coal			yes
20010071	6405397	Cormorant 1	2340.89	2353.08	Cutt	coal	yes		yes
20010359	6405927	Cormorant 1	2377.47	2383.56	Cutt	coal			yes
20010360	6405928	Cormorant 1	2414.05	2420.14	Cutt	coal			yes
20010361	6405929	Cormorant 1	2444.53	2447.57	Cutt	coal			yes
20010362	6405930	Cormorant 1	2478.05	2484.15	Cutt	coal			yes
20010363	6405931	Cormorant 1	2539.01	2545.11	Cutt	coal			yes
20010364	6405932	Cormorant 1	2563.40	2569.50	Cutt	coal			yes
20010365	6405933	Cormorant 1	2593.88	2599.98	Cutt	coal			yes
20010366	6405934	Cormorant 1	2621.31	2627.41	Cutt	coal			yes
20010367	6405935	Cormorant 1	2651.79	2654.84	Cutt	coal			yes
20010368	6405936	Cormorant 1	2688.37	2691.42	Cutt	coal			yes
20010369	6405937	Cormorant 1	2715.80	2718.85	Cutt	coal			yes
20010072	6405398	Cormorant 1	2758.47	2770.67	Cutt	coal	yes		yes
20010370	6405938	Cormorant 1	2792.00	2798.10	Cutt	coal			yes
20010371	6405939	Cormorant 1	2819.43	2822.48	Cutt	coal			yes
20010372	6405940	Cormorant 1	2831.63	2837.72	Cutt	coal			yes
20010373	6405941	Cormorant 1	2843.82	2849.91	Cutt	coal			yes
20010374	6405942	Cormorant 1	2941.36	2944.40	Cutt	coal			yes
20010073	6405399	Cormorant 1	2990.12	2996.22	Cutt	shale	yes		
20010081	6405407	Konkon 1	1280.18	1286.27	Cutt	coal		yes	
20010082	6405408	Konkon 1	1341.14	1344.18	Cutt	coal		yes	
20010083	6405409	Konkon 1	1344.87	1344.89	Core	shale			
20010084	6405410	Konkon 1	1345.17	1345.28	Core	coal			
20010085	6405411	Konkon 1	1345.68	1345.73	Core	shale			
20010086	6405412	Konkon 1	1353.33	1356.38	Cutt	coal			
20010047	6405373	Pelican 5	1700	1705	Cutt	shale	yes		
20010375	6405943	Pelican 5	1899.00	1905.00	Cutt	coal			yes
20010048	6405374	Pelican 5	2028	2031	Cutt	shale	yes		
20010049	6405375	Pelican 5	2034.00	2037.00	Cutt	coal	yes	yes	yes
20010376	6405944	Pelican 5	2190.00	2193.00	Cutt	coal			yes
20010377	6405945	Pelican 5	2304.00	2307.00	Cutt	coal			yes
20010378	6405946	Pelican 5	2409.00	2412.00	Cutt	coal			yes
20010050	6405376	Pelican 5	2418.00	2424.00	Cutt	shale	yes	yes	

20010379	6405947	Pelican 5	2502.00	2505.00	Cutt	coal			yes
20010380	6405948	Pelican 5	2592.00	2595.00	Cutt	coal			yes
20010051	6405377	Pelican 5	2640.00	2643.00	Cutt	shale	yes		
20010381	6405949	Pelican 5	2721.00	2724.00	Cutt	coal			yes
20010052	6405378	Pelican 5	2791.87	2792.00	Core	coal	yes		yes
20010053	6405379	Pelican 5	2792.10	2792.20	Core	shale	yes		
20010382	6405950	Pelican 5	2799.00	2802.00	Cutt	coal			yes
20010383	6405951	Pelican 5	2958.00	2601.00	Cutt	coal			yes
20010054	6405380	Pelican 5	3015.00	3018.00	Cutt	shale	yes		
20010384	6405952	Pelican 5	3063.00	3066.00	Cutt	coal			yes
20010385	6405953	Pelican 5	3162.00	3165.00	Cutt	coal			yes
20010386	6405954	Pelican 5	3246.00	3249.00	Cutt	coal			yes
20010055	6405381	Pelican 5	3399.00	3405.00	Cutt	shale	yes		
20010387	6405955	Pelican 5	3414.00	3417.00	Cutt	coal			yes
20010388	6405956	Pelican 5	3567.00	3570.00	Cutt	coal			yes
20010056	6405382	Pelican 5	3630.00	3636.00	Cutt	shale	yes		
20010389	6405957	Pelican 5	3702.00	3705.00	Cutt	coal			yes
20010057	6405383	Pelican 5	3810.00	3816.00	Cutt	shale	yes		
20010390	6405958	Pelican 5	3822.00	3825.00	Cutt	coal			yes
20020024	6406736	Pelican 5	3891.00	3906.00	Cutt	coal			yes
20010391	6405959	Pelican 5	3960.00	3963.00	Cutt	coal			yes
20010058	6405384	Pelican 5	4044.00	4055.00	Cutt	shale	yes		
20020025	6406737	Pelican 5	4227.00	4257.00	Cutt	coal			yes
20010059	6405385	Pelican 5	4251.00	4257.00	Cutt	shale	yes		
20010392	6405960	Pelican 5	4257.00	4260.00	Cutt	coal			yes
20010074	6405400	Poonboon 1	2398.81	2407.95	Cutt	coal		yes	
20010075	6405401	Poonboon 1	2472.54	2472.57	Core	shale			
20010076	6405402	Poonboon 1	2473.10	2473.18	Core	coal			
20010077	6405403	Poonboon 1	2473.94	2474.04	Core	shale		yes	
20010078	6405404	Poonboon 1	3040.39	3040.54	Core	coal		yes	
20010079	6405405	Poonboon 1	3041.48	3041.56	Core	shale		yes	
20010080	6405406	Poonboon 1	3127.29	3133.38	Cutt	coal		yes	
20010087	6405413	Tilana 1	2319.00	2325.00	Cutt	coal			
20010088	6405414	Tilana 1	2346.00	2352.00	Cutt	coal			
20010089	6405415	Tilana 1	2376.00	2379.00	Cutt	coal			

APPENDIX E.

VITRINITE-INERTINITE REFLECTANCE AND FLUORESCENCE (VRF™ or VIRF) RESULTS FOR CORMORANT-1 AND PELICAN-5

Jane Newman, Newman Pty. Ltd.

Table E1. Summarised VIRF data for Cormorant-1. Ro (normal) is calculated from actual measurements on indigenous vitrinite of normal chemistry. Ro (inferred) describes the potential range of Ro (normal) values suggested by the overall VIRF profile of a sample, and is important when normal vitrinite is absent or biased. Shaded rows indicate paired coal/shale samples.

Depth (m)		Type	Ro (normal)			Hydrothermal features
top	base		Measured	std dev	inferred	
910.30	910.45	core	**0.34** (n=19)	0.063	0.25 - 0.40	
1160.08	1160.24	core	**0.35** (n=2)	0.016	0.25 - 0.45	
1310.96	1311.11	core	**0.36** (n=17)	0.043	0.30 - 0.45	
1518.45	1518.47	core	**0.46** (n=24)	0.044	0.40 - 0.55	
1519.75	1519.90	core	**0.48** (n=22)	0.036	0.40 - 0.55	
1520.31	1520.36	core	**0.51** (n=37)	0.043	0.40 - 0.55	
1685.31	1685.39	core	**0.51** (n=17)	0.025	0.40 - 0.55	
1685.56	1685.72	core	**0.49** (n=20)	0.037	0.40 - 0.55	
1686.58	1686.63	core	**0.50** (n=8)	0.051	0.40 - 0.55	
1950.74	1959.89	cuttings	**0.56** (n=21)	0.044	0.45 - 0.60	coal has shrinkage cracks
2154.96	2167.15	cuttings	**0.65** (n=14)	0.084	0.50 - 0.65	coal has shrinkage cracks, thermally altered
2340.89	2353.08	cuttings	**0.71** (n=13)	0.052	*	coke, baked zs, thermally altered coal
2758.47	2770.67	cuttings	**1.02** (n=13)	0.038	0.80 - 1.10	igneous material, coke, baked zs - ?caved
2990.12	2996.22	cuttings	**1.00** (n=12)	0.066	0.80 - 1.10	microbreccia, coke, hydrothermal minerals

** inferred value cannot be determined due to inadequate inertinite*

Figure E1. The reflectance profile for Cormorant-1, based on VIRF analysis.

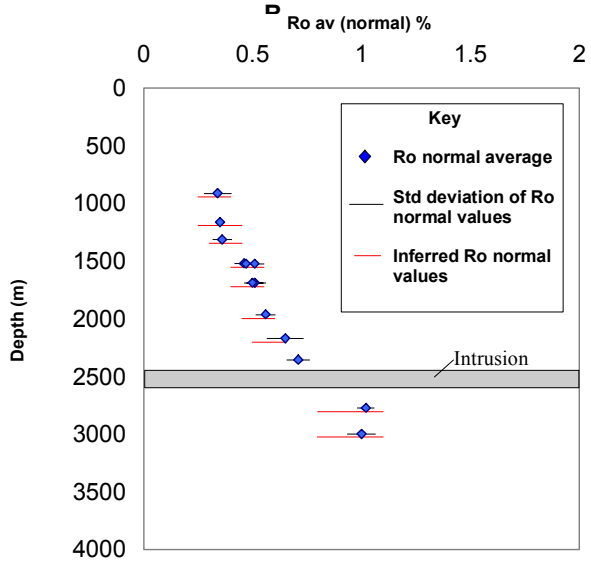
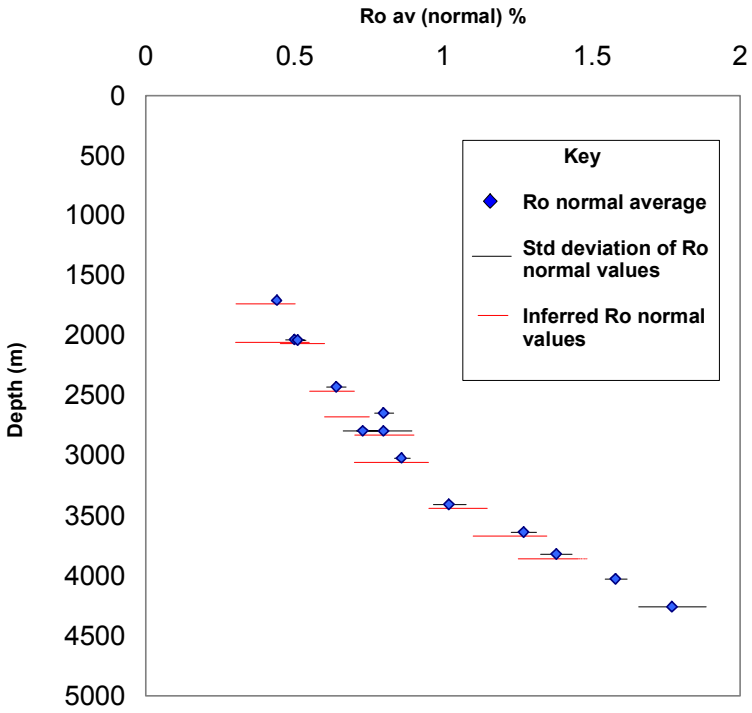


Table E2. Summarised VIRF data for Pelican-5. Ro (normal) is calculated from actual measurements on indigenous vitrinite of normal chemistry. Ro (inferred) describes the potential range of Ro (normal) values suggested by the overall VIRF profile of a sample, and is important when normal vitrinite is absent or biased. Shaded rows indicate paired coal/shale samples.

Depth		Type	Ro (normal)			Hydrothermal features
Top	base		*Measured*	*Std dev*	*Inferred*	
1700	1705	cuttings	**0.44** (n=15)	0.029	0.30 - 0.50	Rare, reworked
2028	2031	cuttings	**0.50** (n=50)	0.061	0.30 - 0.55	Abundant, indigenous
2034	2037	cuttings	**0.52** (n=39)	0.049	0.45 - 0.60	Very rare - coal sample
2418	2424	cuttings	**0.64** (n=19)	0.064	0.55 - 0.70	Rare; iron-stained carbonate
2640	2643	cuttings	**0.80** (n=24)	0.062	0.60 - 0.75	Rare
2791.87	2792	core	**0.73** (n=15)	0.138	0.70 - 0.90	Very rare - coal sample
2792.1	2792.2	core	**0.80** (n=2)	0.186	0.70 - 0.90	Rare, possibly reworked
3015	3018	cuttings	**0.86** (n=22)	0.056	0.70 - 0.95	Moderately abundant
3399	3405	cuttings	**1.02** (n=10)	0.112	0.95 - 1.15	Abundant, diverse
3630	3636	cuttings	**1.26** (n=9)	0.086	1.10 - 1.35	Abundant, diverse
3810	3816	cuttings	**1.38** (n=8)	0.107	1.25+	Abundant, diverse
4044	4050	cuttings	**1.58** (n=8)	0.074	-[1]	Very abundant, pervasive
4251	4257	cuttings	**1.77** (n=17)	0.227	-	Very abundant, pervasive

[1] inferred ranges cannot be determined above 1.30% Ro (normal)

Figure E2. The reflectance profile for Pelican-5, based on VIRF analysis.



APPENDIX F.

PALYNOLOGY OF COALS AND CLAYSTONES FROM THE CORMORANT-1 AND PELICAN-5 WELLS USED FOR OIL SOURCE CORRELATION

Mike Macphail , Australian National University

Appendix F. Palynology on coals and claystones from Cormorant-1 and Pelican-5 used for oil-source correlation.										
AGE	**WELL**	**DEPTH (m)**		**RAW COUNTS**						
(**from WCR)**		**top**	**base**	gymnosperms	angiosperms	ferns/allies	fungi	marine dinos	f/w algae	recycled
Oligocene	Cormorant-1	910.3	910.45	82	177	16	15	23	3	0
Late Eocene	Cormorant-1	1160.08	1160.24	131	148	58	0	35	0	0
Late Eocene	Cormorant-1	1162.1	1162.12	96	375	13	33	0	1	0
Middle-Late Eocene	Cormorant-1	1310.96	1311.11	94	59	94	8	2	0	0
Middle Eocene	Cormorant-1	1381	1390	117	149	31	25	5	1	0
Middle Eocene	Cormorant-1	1444.77	1450.87	43	296	10	82	0	0	0
Middle Eocene	Cormorant-1	1478.3	1487.44	58	220	12	54	0	0	0
Middle Eocene	Cormorant-1	1510.9	1510.93	101	313	24	35	0	0	0
Middle Eocene	Cormorant-1	1518.46	1518.74	139	109	29	23	0	4	1
Middle Eocene	Cormorant-1	1519.75	1519.9	152	213	7	25	0	1	0
Middle Eocene	Cormorant-1	1520.31	1520.36	118	193	12	3	0	0	0
Middle Eocene	Cormorant-1	1530.11	1536.21	72	241	7	85	0	0	0
Late Early Eocene	Cormorant-1	1633.75	1639.84	26	274	3	174	0	0	0
Late Early Eocene	Cormorant-1	1661.18	1667.28	30	245	9	79	0	0	0
Late Early Eocene	Cormorant-1	1685.31	1685.39	81	152	60	40	6	0	2
Late Early Eocene	Cormorant-1	1685.56	1685.72	26	311	2	85	0	0	0
Late Early Eocene	Cormorant-1	1686.58	1686.63	72	138	78	75	0	0	10
Late Early Eocene	Cormorant-1	1725.19	1728.24	50	251	5	160	0	0	0
Late Early Eocene	Cormorant-1	1777.01	1780.05	54	234	3	116	0	0	0
Late Early Eocene	Cormorant-1	1820	1823	30	90	35	121	7	0	0
Late Early Eocene	Cormorant-1	1829.53	1829.58	1	0	0	0	0	0	0
Late Early Eocene	Cormorant-1	1877.59	1883.69	2	1	0	0	0	0	0
Late Early Eocene	Cormorant-1	1950.74	1959.89	26	149	1	39	0	0	0
Late Early Eocene	Cormorant-1	1999.3	1999.33	83	217	31	110	16	15	0
Late Early Eocene	Cormorant-1	2005.61	2011.7	2	1	2	8	0	0	0
Late Early Eocene	Cormorant-1	2024	2033	39	112	16	124	19	0	0
Late Early Eocene	Cormorant-1	2042.18	2048.28	0	2	0	3	0	0	0
Late Early Eocene	Cormorant-1	2090.95	2097.05	0	5	0	0	0	0	0
Late Early Eocene	Cormorant-1	2154.96	2167.15	58	229	8	434	0	0	1
Late Early Eocene	Cormorant-1	2215.92	222.02	0	1	0	0	0	0	0
Mid. Early Eocene	Cormorant-1	2232.38	2232.53	86	219	7	75	0	0	0
Mid. Early Eocene	Cormorant-1	2232.8	2232.83	20	316	12	405	0	0	0

AGE	WELL	DEPTH (m)		RAW COUNTS						
(**from WCR**)		**top**	**base**	gymnosperms	angiosperms	ferns/allies	fungi	marine dinos	f/w algae	recycled
Mid. Early Eocene	Cormorant-1	2276.88	2279.93	0	1	1	2	0	0	0
Mid? Early Eocene	Cormorant-1	2340.89	2353.08	20	151	4	147	1	0	0
Mid? Early Eocene	Cormorant-1	2377.47	2383.56	31	226	3	203	0	0	0
Mid? Early Eocene	Cormorant-1	2414.05	2420.14	29	194	1	64	0	0	1
Mid? Early Eocene	Cormorant-1	2444.53	2447.57	0	0	0	3	0	0	0
Mid? Early Eocene	Cormorant-1	2478.05	2484.15	0	16	0	22	0	0	0
Mid? Early Eocene	Cormorant-1	2539.01	2545.11	38	195	5	170	1	18	7
Mid? Early Eocene	Cormorant-1	2563.4	2569.5	0	0	0	1	0	0	0
Mid? Early Eocene	Cormorant-1	2593.88	2599.98	73	225	3	132	0	1	0
Mid? Early Eocene	Cormorant-1	2621.31	2627.41	29	243	0	400	1	0	0
Mid? Early Eocene	Cormorant-1	2648.1	2648.12	7	19	14	54	0	1	2
Mid? Early Eocene	Cormorant-1	2651.79	2654.84	16	162	32	460	0	0	0
Early Early Eocene	Cormorant-1	2688.37	2691.42	66	195	4	115	0	0	1
Early Early Eocene	Cormorant-1	2715.8	2718.5	1	1	0	0	0	0	0
Early Early Eocene	Cormorant-1	2758.47	2770.67	21	132	0	62	0	0	0
Early Early Eocene	Cormorant-1	2792	2798.1	0	0	0	3	0	0	0
Early Early Eocene	Cormorant-1	2819.43	2822.48	0	0	0	0	0	0	0
Early Early Eocene	Cormorant-1	2831.63	2837.72	6	20	1	43	0	0	0
Early Early Eocene	Cormorant-1	2843.82	2849.91	13	199	2	154	0	0	0
Early Early Eocene	Cormorant-1	2941.36	2944.4	0	0	0	0	0	0	0
Early Early Eocene	Cormorant-1	2990.12	2996.22	47	7	11	36	0	0	0
Middle-Late Eocene	Kon Kon-1	1152	1152	116	197	39	7	10	0	0
Late Early Eocene	Kon Kon-1	1225	1231	89	188	22	22	16	1	0
Late Early Eocene	Kon Kon-1	1247	1280	30	61	9	11	1	0	0
Late Early Eocene	Kon Kon-1	1280.18	1286.27	22	35	3	0	0	0	0
Late? Early Eocene	Kon Kon-1	1341.14	1344.18	81	133	3	56	0	1	0
Late? Early Eocene	Kon Kon-1	1344.87	1344.89	76	53	20	50	250	0	0
Late? Early Eocene	Kon Kon-1	1345.17	1345.28	89	130	2	31	0	0	0
Late? Early Eocene	Kon Kon-1	1345.68	1345.73	201	46	42	74	1	288	0
Late Early Eocene	Kon Kon-1	1347.5	1347.5	101	64	23	57	128	1	0
Late Early Eocene	Kon Kon-1	1351.5	1351.5	156	51	29	42	50	4	0
Late? Early Eocene	Kon Kon-1	1351.7	1351.72	162	180	9	115	2	0	0
Mid. Early Eocene	Kon Kon-1	1353.33	1356.38	125	143	86	16	0	0	0
Early Oligocene	Pelican-5	1700	1705	119	203	38	45	30	1	0

AGE	WELL	DEPTH (m)		RAW COUNTS						
(**from WCR**)		**top**	**base**	gymnosperms	angiosperms	ferns/allies	fungi	marine dinos	f/w algae	recycled
Middle Eocene	Pelican-5	1899	1905	1	5	0	2	0	0	0
Middle Eocene	Pelican-5	2028	2031	47	52	15	4	0	0	0
Middle Eocene	Pelican-5	2034	2037	268	164	8	131	0	0	0
Middle Eocene?	Pelican-5	2049	2412	0	0	0	0	0	0	0
Late Early Eocene	Pelican-5	2190	2193	2	1	0	4	0	0	0
Late Early Eocene	Pelican-5	2418	2424	7	25	4	16	0	0	0
Late Early Eocene	Pelican-5	2502	2505	5	42	0	1	0	4	0
Late? Early Eocene	Pelican-5	2592	2595	6	0	0	3	0	0	0
Mid. Early Eocene	Pelican-5	2640	2643	90	37	38	34	1	0	1
Mid. Early Eocene	Pelican-5	2721	2724	113	25	13	48	0	1	0
Mid. Early Eocene	Pelican-5	2791.7	2791.72	3	22	32	7	0	0	0
Mid. Early Eocene	Pelican-5	2791.87	2792	77	64	112	9	0	0	0
Mid. Early Eocene	Pelican-5	2792.1	2792.2	82	52	16	43	0	0	1
Mid. Early Eocene	Pelican-5	2799	2802	46	64	11	165	0	0	0
Early Early Eocene	Pelican-5	2806.6	2806.7	112	102	51	38	15	0	0
Early Early Eocene	Pelican-5	2890.8	2890.83	44	12	45	19	1	0	0
Early Early Eocene	Pelican-5	2958	2601	15	7	8	28	0	0	0
Early Early Eocene	Pelican-5	3015	3018	37	19	5	64	0	0	1
Early Early Eocene	Pelican-5	3063	3066	84	22	147	20	0	0	0
Late? Paleocene	Pelican-5	3162	3163	78	22	114	27	0	0	0
Late? Paleocene	Pelican-5	3246	3249	45	4	26	13	0	0	0
Late? Paleocene	Pelican-5	3399	3405	90	31	48	34	0	0	1
Late? Paleocene	Pelican-5	3414	3417	11	1	6	4	0	0	0
Maastrichtian	Pelican-5	3567	3570	13	2	3	6	0	0	0
Maastrichtian	Pelican-5	3630	3636	50	13	42	29	0	0	0
Maastrichtian	Pelican-5	3702	3705	2	39	14	11	0	0	0
Maastrichtian	Pelican-5	3891	3906	8	75	22	35	0	2	0
Maastrichtian	Pelican-5	3960	3963	8	56	30	1	0	0	1
Campanian	Pelican-5	4227	4257	0	10	20	3	0	0	4
Late Early Eocene	Poonboon-1	2362	2374	36	105	24	105	7	0	0
Late? Early Eocene	Poonboon-1	2398.81	2407.95	92	271	15	38	0	0	0
Late? Early Eocene	Poonboon-1	2408	2417	52	138	10	140	14	0	0
Mid. Early Eocene	Poonboon-1	2472.54	2472.57	77	105	35	49	132	0	1
Mid. Early Eocene	Poonboon-1	2473.1	2473.18	41	85	202	125	0	0	0

AGE	WELL	DEPTH (m)		RAW COUNTS						
(**from WCR**)		**top**	**base**	gymnosperms	angiosperms	ferns/allies	fungi	marine dinos	f/w algae	recycled
Mid. Early Eocene	Poonboon-1	2473.94	2474.04	135	73	22	310	107	0	3
Mid Early Eocene	Poonboon-1	2499	2508	90	140	16	55	77	0	0
Late? Paleocene	Poonboon-1	2713	2725	111	77	41	91	5	0	0
Early Paleocene	Poonboon-1	2795	2801	153	43	52	52	18	0	0
Early Paleocene	Poonboon-1	2838	2844	134	31	66	28	12	1	2
Early Paleocene	Poonboon-1	2896	2902	165	38	69	47	6	0	0
Early Paleocene	Poonboon-1	2951	2957	144	36	40	70	2	0	0
Early Paleocene	Poonboon-1	2975	2984	260	29	22	64	2	0	0
Early Paleocene	Poonboon-1	3040.39	3040.54	12	1	11	174	0	0	0
Early Paleocene?	Poonboon-1	3041.48	3041.56	165	70	64	108	0	0	5
Early Paleocene?	Poonboon-1	3041.8	3041.81	193	97	50	72	0	1	0
Early Paleocene?	Poonboon-1	3066	3069	195	31	23	58	6	0	0
Early Paleocene?	Poonboon-1	3127.29	3133.38	268	11	44	11	0	1	0
Maastrichtian	Poonboon-1	3231	3240	195	34	18	59	2	0	0
Early? Eocene	Tilana-1	2319	2325	0	0	0	0	0	0	0
Early? Eocene	Tilana-1	2346	2352	2	30	3	33	0	0	0
Early? Eocene	Tilana-1	2376	2379	11	22	2	32	0	0	0

WELL	PREDICTED VEGETATION INPUT	DEPOSITIONAL ENVIRONMENT
Cormorant-1	Woody angiosperms + gymnopserms	Marginal marine
Cormorant-1	Gymnosperms + woody angiosperms	Marginal marine
Cormorant-1	Woody angiosperms + minor gymnosperms	Freshwater peat swamp
Cormorant-1	Gymnosperms + ferns	Peat swamp with minor marine influence?
Cormorant-1	Woody angiopserms + gymnopserms	Peat swamp with marine influence
Cormorant-1	Woody angiosperms + gymnosperms	Freshwater peat swamp
Cormorant-1	Woody angiosperms + minor gymnosperms	Freshwater peat swamp
Cormorant-1	Woody angiosperms + gymnosperms	Freshwater peat swamp
Cormorant-1	Gymnosperms + woody angiosperms	Freshwater peat swamp
Cormorant-1	Woody angiosperms + gymnosperms	Freshwater peat swamp
Cormorant-1	Woody angiosperms + gymnosperms	Freshwater peat swamp
Cormorant-1	Woody angiosperms + minor gymnosperms	Freshwater peat swamp
Cormorant-1	Woody angiosperms	Freshwater peat swamp
Cormorant-1	Woody angiosperms	Freshwater peat swamp
Cormorant-1	Woody angiosperms + minor gymnosperms	Peat swamp with minor marine influence
Cormorant-1	Woody angiosperms	Freshwater peat swamp
Cormorant-1	Woody angiosperms + ferns	Peat swamp with possible marine influence
Cormorant-1	Woody angiosperms + minor gymnosperms	Freshwater peat swamp
Cormorant-1	Woody angiosperms + minor gymnosperms	Freshwater peat swamp
Cormorant-1	Woody angiosperms + ferns/gymnosperms	Peat swamp with possible marine influence
Cormorant-1	No prediction	(oxidative destruction of organic sediments)
Cormorant-1	No prediction	(oxidative destruction of organic sediments)
Cormorant-1	Woody angiosperms + minor gymnosperms	Freshwater peat swamp
Cormorant-1	Woody angiosperms + minor gymnosperms	Peat swamp with minor marine influence
Cormorant-1	No prediction	(oxidative destruction of organic sediments)
Cormorant-1	Woody angiopserms + minor gymnosperms	Peat swamp with marine influence
Cormorant-1	No prediction	(oxidative destruction of organic sediments)
Cormorant-1	No prediction	(oxidative destruction of organic sediments)
Cormorant-1	Woody angiosperms + minor gymnosperms	Freshwater peat swamp
Cormorant-1	No prediction	(oxidative destruction of organic sediments)
Cormorant-1	Woody angiosperm + gymnosperms	Freshwater peat swamp
Cormorant-1	Woody angiosperms + minor gymnosperms	Freshwater peat swamp

WELL	PREDICTED VEGETATION INPUT	DEPOSITIONAL ENVIRONMENT
Cormorant-1	No prediction	(oxidative destruction of organic sediments)
Cormorant-1	Woody angiosperms + minor gymnosperms	Peat swamp with possible marine influence
Cormorant-1	Woody angiosperms + minor gymnosperms	Freshwater peat swamp
Cormorant-1	Woody angiosperms + minor gymnosperms	Freshwater peat swamp
Cormorant-1	No prediction	(oxidative destruction of organic sediments)
Cormorant-1	Woody angiosperms?	(oxidative destruction of organic sediments)
Cormorant-1	Woody angiosperms + minor gymnosperms	Peat swamp with possible marine influence
Cormorant-1	No prediction	(oxidative destruction of organic sediments)
Cormorant-1	Woody angiosperms + minor gymnosperms	Freshwater peat swamp
Cormorant-1	Woody angiosperms + minor gymnosperms	Freshwater peat swamp
Cormorant-1	Woody angiosperms?	Freshwater peat swamp
Cormorant-1	Woody angiosperms + minor ferns	Freshwater peat swamp
Cormorant-1	Woody angiosperms + minor gymnosperms	Freshwater peat swamp
Cormorant-1	No prediction	(oxidative destruction of organic sediments)
Cormorant-1	Woody angiosperms + minor gymnosperms	Freshwater peat swamp
Cormorant-1	No prediction	(oxidative destruction of organic sediments)
Cormorant-1	No prediction	(oxidative destruction of organic sediments)
Cormorant-1	Woody angiosperms?	Freshwater peat swamp
Cormorant-1	Woody angiosperms + minor gymnosperms	Freshwater peat swamp
Cormorant-1	No prediction	(oxidative destruction of organic sediments)
Cormorant-1	Gymnosperms + minor ferns	Freshwater peat swamp
Kon Kon-1	Angiosperms + gymnosperms	Peat swamp with minor marine influence
Kon Kon-1	Angiosperms + gymnosperms	Peat swamp with minor marine influence?
Kon Kon-1	Angiosperms + gymnosperms	Freshwater peat swamp
Kon Kon-1	Woody angiosperms + gymnosperms?	Freshwater peat swamp?
Kon Kon-1	Woody angiosperms + minor gymnosperms	Freshwater peat swamp
Kon Kon-1	Dinocysts + minor gymnosperms and ferns	Marginal marine
Kon Kon-1	Woody angiosperms + gymnosperms	Freshwater peat swamp
Kon Kon-1	Freshwater dinocysts + gymnosperms	Freshwater lake
Kon Kon-1	Dinocysts + gymnosperms, angiosperms	Marginal marine (Neves Effect?)+Q20
Kon Kon-1	Gymnosperms + dinocysts, angiosperms	Marginal marine (Neves Effect?)
Kon Kon-1	Woody angiosperms + gymnosperms	Peat swamp with possible marine influence
Kon Kon-1	Woody angiosperms, gymnosperms, ferns	Freshwater peat swamp
Pelican-5	Woody angiosperms + gymnosperms	Marginal marine

WELL	PREDICTED VEGETATION INPUT	DEPOSITIONAL ENVIRONMENT
Pelican-5	No prediction	(oxidative destruction of organic sediment?)
Pelican-5	Woody angiosperms, gymnosperms, ferns	Freshwater peat swamp
Pelican-5	Gymnosperms + minor woody angiosperms	Freshwater peat swamp
Pelican-5	No prediction	(oxidative destruction of organic sediment)
Pelican-5	No prediction	(oxidative destruction of organic sediment)
Pelican-5	Woody angiosperms + minor gymnosperms	Freshwater peat swamp
Pelican-5	Woody angiosperms	Freshwater peat swamp?
Pelican-5	Gymnosperms?	(oxidative destruction of organic sediments)
Pelican-5	Gymnosperms + minor ferns	Peat swamp with minor marine influence?
Pelican-5	Gymnosperms + minor ferns	Freshwater peat swamp
Pelican-5	Ferns + woody angiosperms	Freshwater peat swamp
Pelican-5	Ferns + minor angiosperms, gymnosperms	Freshwater peat swamp
Pelican-5	Gymnosperms + woody angiosperms	Freshwater peat swamp
Pelican-5	Gymnosperms + woody Angiosperms	Freshwater peat swamp
Pelican-5	Woody angiosperms + gymnosperms	Peat swamp with marine influence
Pelican-5	Gymnosperms + ferns	Peat swamp with minor marine influence?
Pelican-5	Gymnosperms + ferns?	Freshwater peat swamp
Pelican-5	Gymnosperms + minor woody angiosperms	Freshwater peat swamp
Pelican-5	Ferns + minor gymnosperms	Freshwater peat swamp
Pelican-5	Ferns + minor gymnosperms	Freshwater peat swamp
Pelican-5	Gymnosperms + minor ferns	Freshwater peat swamp
Pelican-5	Gymnosperms + ferns	Freshwater peat swamp
Pelican-5	Gymnosperms + minor ferns?	(oxidative destruction of organic sediments)
Pelican-5	Gymnosperms + minor ferns?	(oxidative destruction of organic sediments)
Pelican-5	Ferns + gymnosperms	Freshwater peat swamp
Pelican-5	Woody angiosperms + minor ferns	Freshwater peat swamp?
Pelican-5	Woody angiosperms + minor ferns	Freshwater peat swamp?
Pelican-5	Woody? angiosperms + ferns	Freshwater peat swamp?
Pelican-5	Woody angiosperms + minor ferns	Freshwater peat swamp?
Poonboon-1	Angiosperms + minor gymnosperms	Peat swamp with minor marine influence
Poonboon-1	Woody angiosperms + minor gymnosperms	Freshwater peat swamp
Poonboon-1	Woody angiosperms + gymnosperms	Peat swamp with possible marine influence
Poonboon-1	Dinocysts + gymnosperms, angiosperms	Marginal marine
Poonboon-1	Ferns + minor angiosperms, gymnosperms	Freshwater peat swamp?

WELL	PREDICTED VEGETATION INPUT	DEPOSITIONAL ENVIRONMENT
Poonboon-1	Gymnosperms + dinocysts, angiosperms	Marginal marine
Poonboon-1	Gymnosperms + dinocysts, angiosperms	Marginal marine
Poonboon-1	Gymnosperms + minor ferns	Peat swamp (possible marine influence?)
Poonboon-1	Gymnosperms + minor ferns, dinocysts	Freshwater peat swamp
Poonboon-1	Gymnosperms + ferns	Freshwater peat swamp
Poonboon-1	Gymnosperms + ferns	Freshwater peat swamp
Poonboon-1	Gymnosperms + minor ferns, angiosperms	Freshwater peat swamp
Poonboon-1	Gymnosperms	Freshwater peat swamp
Poonboon-1	Gymnosperms + ferns?	Freshwater peat swamp?
Poonboon-1	Gymnosperms + minor angiosperms, ferns	Freshwater peat swamp
Poonboon-1	Gymnosperms + minor angiosperms, ferns	Freshwater peat swamp?
Poonboon-1	Gymnosperms + minor angiosperms, ferns	Freshwater peat swamp?
Poonboon-1	Gymnosperms + minor ferns	Freshwater peat swamp?
Poonboon-1	Gymnosperms + minor, angiosperms, ferns	Freshwater peat swamp?
Tilana-1	No prediction	(oxidative destruction of organic sediment)
Tilana-1	Woody angiosperms?	(thermal destruction of organic sediments)
Tilana-1	Woody angiosperms?	thermal destruction of organic sediments)

APPENDIX G.

LIST OF OIL AND GASES IN THE BASS BASIN ANALYSED IN THIS STUDY

Chris Boreham, Geoscience Australia

GA No.	Well	Top m	Test	Type
10037	Cormorant-1	1500.0	FIT 6	oil
19999150	Pelican-1	3161.4		oil
19999151	Pelican-2	2879.5	FIT 1	oil
10036	Yolla-1	1830.0	DST 2	oil
10035	Yolla-1	2824.0	DST 1	oil
20009241	White Ibis-1	2015.2		gas
20009247	White Ibis-1	2048.5		gas
20009248	Yolla-2	2802.0		gas
20009250	Yolla-2	2815.0		gas

APPENDIX H.

SMALL ANGLE NEUTRON SCATTERING (SANS) STUDY ON LOW-ASH COALS FROM CORMORANT-1 AND PELICAN-5, BASS BASIN

Andrzej Radlinski, Alan Hinde and Chris Boreham, Geoscience Australia

H1. SAMPLE SELECTION AND PREPARATION

Small Angle Neutron Scattering (SANS) analysis was performed on low ash coals obtained by the flotation of cuttings or, where available, sidewall core material (density less than 1.5 g/cm^3) from Cormorant-1 (30 samples) and Pelican-5 (12 samples). These cuttings were collected within the Eastern View Coal Measures (EVCM), at average intervals of about 50 m between the depths 1445 to 2945 m at Cormorant-1, and at average intervals of about 100 m between the depths 1899 to 3165 m at Pelican-5 (Table H1). The samples were prepared for SANS analysis by gentle crushing, sieving and then embedding the 0.355 - 0.475 mm particle size fraction in resin.

SANS data were acquired in December 2001 using the SAND instrument at IPNS, Argonne National Laboratory, USA. In some cases (4 Cormorant-1 samples, 2 Pelican-5 samples) there was only enough float material to prepare small diameter SANS samples (marked *small* in Table H1). SANS data collected from these samples proved to be unreliable under the experimental conditions used and are not included in this report.

H2. RESULTS AND INTERPRETATION – PELICAN-5

Figure H1 shows the SANS data for 20 coal samples from Pelican-5. The results are presented in a standard manner: scattering intensity, I(Q) in absolute units, versus the scattering vector Q. Scattering curves comprise a (1) broad feature monotonically increasing towards small Q-values, approximately linear on the log-log scale, (2) a broad band peaked at about Q = 0.2 Å^{-1} whose amplitude increases with coal rank, and (3) a small flat background of about 0.2 to 0.3 cm^{-1}. These three features correspond to (1) a broad distribution of the pore sizes, (2) the formation of polyaromatic sheets as the thermal maturity of kerogen increases, and (3) the incoherent scattering on hydrogen atoms and coherent scattering on small-scale (nearly molecular-size) inhomogeneities in the coal matrix, respectively.

The scattering data at each sample depth are used to derive (i) the pore size distribution, (ii) specific surface area (Radlinski, et al., 2001), and (iii) the repeat distance of the polyaromatic sheets in the coal matrix. The data are then used to quantify the evolution of the pore space geometry with depth (maturity) in the pore size range 80 Å to 1000 Å (0.008 μm to 0.1 μm) and to infer the onset of hydrocarbon generation from kerogen.

The results shows there is a significant and systematic variation of the scattering intensity with depth. This is illustrated in Figure H2 for scattering intensity measured at Q=0.01 $Å^{-1}$, which corresponds to the pore size 2.5/Q = 0.025μm +/-50%. The SANS intensity at Q=0.01$Å^{-1}$ decreases by a factor of 4.5 within the depth range 1899 to 2792 m, and then increases by a factor of 2 at depth 2998 m and remains unchanged down to depth 3165m.

The pore size distributions, f(r), calculated for various depths from the full SANS curves (Figure H3) indicate there is a significant change of the micro-geometry of the pore space between depths from 2410 to 2593 m. For depths shallower than 2410 m the f(r) values (blue symbols) fall on a common curve with a characteristic kink at pore size of about 120 Å. For depths below 2593 m the f(r) values (red symbols) fall on a common curve (a power law distribution, linear on the log-log scale), which has no kink and lies above the distribution curves for shallower depths. The f(r) curve for depth 2499.5 m (black full circles) coincides with the "shallow" curve for small pore sizes and with the "deep" curve for large pore sizes. This trend indicates that re-arrangement of the pore space as depth increases first occurs for larger pores and gradually progresses towards the smaller ones.

A close analysis of the variation of the number density of pores (proportional to the pore size distribution f(r)) with depth indicates a significant and nearly stepwise increase of micro-porosity within the depth interval 2400 - 2600 m (Figure H4). This transition occurs within the vitrinite reflectance interval 0.55% to 0.65%.

The specific surface area (SSA) versus the probe size, calculated for various depths in Pelican-5 (in the units of cm^2/cm^3), is presented in Figure H5. (Note that 1 cm^2/cm^3 is equivalent to $0.714x10^{-4}$ m^2/g, assuming coal density of 1.4 g/cm^3). The extrapolated SSA in Pelican-5 for the probe size of several Å (*i.e.* , the linear size of methane or CO_2 molecule) varies from about 10,000 to 100,000 cm^2/cm^3, which corresponds to about 0.71 to 7.1 m^2/g. Figure H6 illustrates the variation of SSA with depth for the smallest measured probe size of 100 Å. The specific surface area systematically decreases with depth down to about 2800 m, then slightly increases at depths below 3000 m and stays relatively unchanged down to about 3150 m.

SANS curves in Figure H1 exhibit a weak broad band centered at the Q-value of about Q_o=0.2 $Å^{-1}$, whose intensity increases with the coal rank. This band corresponds to the scattering on the stacked poly-aromatic sheets within the coal matrix. The concentration of these sheets increases as the coal rank increases from sub-bituminous to anthracite (Radlinski and Radlinska, 1999). The position of the maximum of the peak corresponds to the mean stacking repeat distance of $2\pi/Q_o \approx 30$ Å.

Significance for hydrocarbon generation and expulsion: Pelican-5.

The intensity of SANS signal in coals is proportional to the specific surface area of the pore/matrix interface and to the scattering contrast between the coal matrix and the pore content. It is known that in the vitrinite reflectance range 0.3 -1.0%, the porosity (King and Wilkins, 1944) and the internal surface roughness of coals (Radlinski and Radlinska, 1999) decrease with rank, which results in a "structural" decrease of SANS

intensity with rank. The process of internal restructuring of coals can be particularly active in a narrow range of rank variation.

Superimposed on this "structural" decrease there is a variation of SANS signal caused by the onset of hydrocarbon generation, which results in the micropores being increasingly filled with bitumen. The scattering contrast between the bitumen and the coal macerals is low, which further decreases the "structural" scattering signal from a coal that has generated bitumen. In such coal, the bitumen partially filling the pore space is perceived by neutrons as part of the coal matrix. However, this "generation" decrease is limited to depths at which the bitumen is actually present in the pore space. Brine or gas have large SANS contrast with the coal matrix, which results in an increased scattering signal at depths directly above and below the generation window, where coal macerals have either not yet generated or the bitumen (or its components) has been expelled and/or cracked.

The pore size distribution (Figures H3 and H4) indicates that a significant re-distribution of the pore space takes place inside the coals of the Eastern View Coal Measures within the depth range 2400m to 2600 m, corresponding to the Ro range 0.55% to 0.65%. In particular, there is a significant increase of coal porosity within this depth interval, especially for pores larger than 100 Å in diameter. For pores of diameter 100 Å the change of porosity is much less pronounced (Figure H4). These changes are not reflected in the scattering intensity (Figure H2), which monotonically decreases down to the depth of 2800 m. This indicates that the rearrangement of the microstructure of the coal matrix does not affect the internal specific area beyond the usual decrease with rank.

Below depth 2800 m the scattering intensity increases stepwise by a factor of 2 at depth 2942 m and remains constant down to the maximum tested depth of 3162 m (Figure H2). There is no significant difference in pore size distribution in the depth range 2600 to 3126 m (Figures H3 and H4).

These results are used to interpret SANS data for Pelican-5 as graphically represented in Figure H7. Hydrocarbons are generated at depths around 2800 m and expelled upwards and sideways, but there is a permeability barrier located between depths 2800 and 2942 m. Data indicate that there is good communication at depths below 2942 m, and that the onset of hydrocarbon generation coincides with the region of structural re-arrangement in the depth range 2400 m to 2600 m.

Integration of the SANS results with independent geochemical data from Rock Eval analysis reveals much synergy. Figure H8 shows the depth plot of Hydrogen Index (HI) and Bitumen Index (BI). The HI parameter is a measure of the TOC-normalised residual hydrocarbon potential while the latter reflects the TOC-normalised yield of free hydrocarbons. The depth trend of increasing HI, reaching a maximum followed by a HI decrease is in response to increasing maturity. Sykes (2001) has seen the same maturity-driven HI trend in New Zealand coals of similar age and has used this feature to understand the key hydrocarbon generation and expulsion events. In Pelican-5, the onset of hydrocarbon (oil) generation corresponds to the rapid increase in HI at approximately 2450 m (Ro = 0.6%), consistent with the region of structural re-

arrangement seen in SANS. The onset of oil expulsion is identified at 2850 m (Ro = 0.74%) by the rapid decrease in HI immediately after the HI maximum. Over this range the BI shows a continual increase. The region in which the BI shows no further increase and remains fairly constant (SANS scattering intensity data is also constant; Figure H7), due to the maintenance of maximum saturation of the pore space with oil, occurs from 2850 to 3600 m (Ro = 0.74 – 1.13%) is defined as the oil window (Figure H8). This is in good agreement with the chemical maturity of the Bass Basin reservoired oils (Yolla-1 and Pelican-1 and -2) which indicates that the effective source rocks expelled oil over the Ro range from 0.75 to 0.95 % (main phase of oil generation). At depths > 3600 m, the BI begins to fall corresponding to removal (loss) of oil due either to increasing generation of primary gas resulting in more efficient expulsion of residual oil or the beginning of oil-to-gas cracking. This is consistent with maturity data on reservoired gases which suggests that gas was generated from source rocks at Ro > 1.3%.

H3. RESULTS AND INTERPRETATION – CORMORANT-1

Figure H9 shows SANS data for 20 coal samples (selected out of 30 coals analysed) in Cormorant-1 presented in the standard manner: scattering intensity, I(Q) in absolute units, versus the scattering vector Q. Scattering curves comprise of a (1) broad feature monotonically increasing towards small Q-values, approximately linear on the log-log scale, (2) a broad band peaked at about Q = 0.2 $Å^{-1}$ whose amplitude increases with coal rank, and (3) a small flat background of about 0.2 cm^{-1}. These three features correspond to (1) a broad distribution of the pore sizes, (2) formation of polyaromatic sheets as the thermal maturity of kerogen increases, and (3) incoherent scattering on hydrogen atoms and coherent scattering on small-scale (nearly molecular size) inhomogeneities in the coal matrix, respectively.

The scattering data have been used to derive for every depth (i) the pore size distribution, (ii) specific surface area (Radlinski et al., 2001), and (iii) the repeat distance of the polyaromatic sheets in the coal matrix. These data are used to quantify the evolution of the pore space geometry with depth (maturity) in the pore size range from 80 to 1000 Å (0.008 to 0.1 μm) and infer about the onset of hydrocarbon generation in the Eastern View Coal Measures.

There is a systematic decrease of the scattering intensity with depth. This is illustrated in Figure H10 for scattering intensity measured at Q=0.01 $Å^{-1}$, which corresponds to the pore size 2.5/Q = 0.025 μm +/-50%. For Cormorant-1 coals, SANS intensity decreases by a factor of 6 within the depth range 1445 to 2941.4 m.

The pore size distributions, f(r), calculated for various depths (Figure H11) indicate that there may be an onset of change of the micro-geometry of the pore space at depths below 2821 m. For depths shallower than 2821 m the f(r) curves (blue and red symbols) fall within a broad band with little apparent systematic variation with depth, apart from the general decrease of amplitude indicating a decrease of the porosity with depth. However, the pore size distribution curve for the deepest sample (2942.9 m) clearly lies outside of the band and indicates closing off (or clogging with bitumen) of pores smaller than about 100 Å across.

A close analysis of the variation of number density of pores (proportional to the pore size distribution f(r)) with depth indicates a significant increase of porosity for pores larger than about 100 Å across at depths below 2800 m (Figure H12). The transition occurs at the vitrinite reflectance value of about 0.80-0.85%.

The specific surface area versus the probe size, calculated for various depths in well Cormorant-1 (in the units of cm^2/cm^3), is presented in Figure H13. (Note that 1 cm^2/cm^3 is equivalent to $0.714x10^{-4}$ m^2/g, assuming coal density of 1.4 g/cm^3). The extrapolated specific surface area in Cormorant-1 for the probe size of several Å (*i.e.* , the linear size of the methane or CO_2 molecule) varies from about 10^3 to $4x10^5$ cm^2/cm^3, depending on coal rank, which corresponds to about 0.07 to 28 m^2/g. Figure H13 illustrates the variation of SSA with depth for the smallest measured probe size of 100 Å. The specific surface area systematically decreases with depth down to the maximum depth of about 2942.9 m.

SANS curves in Figure H9 exhibit a weak broad band centered at the Q-value of about Q_o=0.2 $Å^{-1}$, whose intensity increases with the coal rank. This band corresponds to the scattering on the stacked poly-aromatic sheets within the coal matrix. The concentration of these sheets increases as the coal rank increases from sub-bituminous to anthracite (Radlinski and Radlinska, 1999). The position of the maximum of the peak corresponds to the mean stacking repeat distance of $2\pi/Q_o \approx 30$ Å.

Significance for hydrocarbon generation at Cormorant-1

The intensity of SANS signal in coals is proportional to the specific surface area of the pore/matrix interface and to the scattering contrast between the coal matrix and the pore content. It is well known that in the vitrinite reflectance range 0.3 to 1.0%, the porosity (King and Wilkins, 1944) and the internal surface roughness of coals (Radlinski and Radlinska, 1999) decreases with rank, which is a "structural" decrease of SANS intensity with rank. The process of internal restructuring of coals can be particularly active in a narrow range of rank variation.

Superimposed on this "structural" decrease there is a variation of SANS signal caused by the onset of hydrocarbon generation, which results in the micropores being increasingly filled with bitumen. The scattering contrast between the bitumen and the coal macerals is very low, which further decreases the "structural" scattering signal from a coal that has generated bitumen. In such coal the bitumen partially filling the pore space is perceived by neutrons as part of the coal matrix. However, this "generation" decrease is limited to depths at which the bitumen is actually present in the pore space. Brine or gas have large SANS contrast with the coal matrix, which results in an increased scattering signal at depths directly above and below the generation window, where coal macerals have either not yet generated or the bitumen (or its components) has been expelled and/or cracked.

The pore size distribution (Figures H11 and H12) indicates that the onset of re-distribution of the pore space takes place inside the coals of the Eastern View Coal Measures below depth 2800 m, corresponding to Ro values larger than 0.85%. It is important to note that pores of diameter smaller than 100 Å practically disappear at these depths, which strongly indicates a possibility of clogging of these pores with liquid

bitumen. However, there is a significant increase of coal porosity for pores larger than 100 Å across at depths below 2800 m. These changes are not reflected in the scattering intensity (Figure H11), which monotonically decreases down to the maximum depth of 2943 m. This indicates that the rearrangement of the microstructure of the coal matrix does not affect the internal specific area beyond the usual decrease with rank.

These results are used to interpret SANS data for Cormorant-1 as graphically represented in Figure H15. Hydrocarbons are generated at depths around 2940 m and expelled upwards and sideways. Data indicate that there is good communication at all depths above 2942 m, and that the onset of hydrocarbon generation coincides with the region of structural re-arrangement in the depth range 2800 to 2940 m.

H4. VARIATION OF VITRINITE REFLECTANCE WITH DEPTH IN PELICAN-5 AND CORMORANT-1

Figure H16 shows the plot of vitrinite reflectance versus depth for wells Cormorant-1 and Pelican-5. Generally, the Ro data were measured on samples collected at different depths than these used for SANS measurements. Because of the scatter, it is convenient to fit a smooth curve to Ro data and use it to calculate the Ro-value at any depth rather than rely on the interpolation between the data points nearest to the depth of interest.

For Cormorant-1, the vitrinite reflectance versus depth in the interval 600 – 3000 m is well represented by the following second order polynomial:

$$Ro = 0.3403 - 7.5467 \times 10^{-5} D + 9.0932 \times 10^{-8} D^2 \quad (1)$$

where D is depth in metres. The correlation coefficient is R = 0.992.

For Pelican-5, the corresponding polynomial, valid in the depth interval 1800 to 4300 m is:

$$Ro = 0.6914 - 3.8912 \times 10^{-4} D + 1.425 \times 10^{-7} D^2 \quad (2)$$

and the correlation coefficient is R = 0.984.

It is possible to represent the vitrinite reflectance versus depth for both wells with one universal equation (Figure H17), using a third order polynomial:

$$Ro = 0.23371 + 9.798 \times 10^{-5} \Delta - 2.52 \times 10^{-8} \Delta^2 + 1.863 \times 10^{-11} \Delta^3 \quad (3)$$

where Δ = D for Pelican-5 and Δ = D + 300m for Cormorant-1, and D is depth in metres.

The correlation coefficient is 0.989.

This result could be interpreted that the maturity for Eastern View Coal Measures coals in Cormorant-1 is the same as for the Pelican-5 coals located 300m deeper. This could be caused either by different thermal history of the two wells or a different thermal transformation kinetics for the organic matter in each well, or a combination of the above. Formula 3 has been used to calculate the Ro values for SANS samples presented in Table H1.

H5. REFERENCES

King, J.G. and Wilkins, E.T., 1944. P*roc. Conf. Ultrafine. Struct. Coals Cokes, BCURA*, London, p.46; reproduced in Fig 4.1.1, p.70 in: N Berkowitz, *An Introduction to Coal Technology*, Academic Press, New York (1979), 345 pp.

Radlinski, A.P. and Radlinska, E.Z., 1999. The microstructure of pore space in coals of different rank, a small angle scattering and SEM study. In: *Coalbed Methane; Scientific, Environmental and Economic Evaluation*, Mastalerz, M., Glikson, M., and Golding, S.D. (eds), Kluwer Academic Publishers, Dodrecht, 329-365.

Radlinski, A.P., Mastalerz, M., Hinde, A.L., Hainbuchner, M., Rauch, H., Baron, M., Lin, J.-S., Fan, L., Thiyagarajan, P., 2001. Non-invasive measurements of pore size distribution in coal pellets using X-ray and neutron techniques". International Coalbed Methane Symposium 2001 Proceedings, The University of Alabama Tuscaloosa, Alabama, USA, 163-175.

Radlinski, A.P. and Hinde, A.L., 2002. Small angle neutron scattering and petroleum geology". *Neutron News* **13** (2), 11-17.

Sykes, R., 2001. Depositional and rank controls on the petroleum potential of coaly source rocks. Eastern Australasian Basins Symposium. PESA, 591-602.

Table H1. Basic data for low ash preparations used in the SANS analyses.

AGSO No.	SANS sample	Well	Top mRT	base mRT	Interval m	Ro% calc	Type	Lithology
20010346	normal	Cormorant-1	1444.77	1450.87		0.428	Cut	coaly
20010347	normal	Cormorant-1	1478.30	1487.44	35	0.435	Cut	coaly
20010064	normal	Cormorant-1	1519.75	1519.90	37	0.441	CORE 6	coal
20010348	normal	Cormorant-1	1530.12	1536.21	13	0.444	Cut	coaly
20010349	normal	Cormorant-1	1633.74	1639.84	3.6	0.465	Cut	coaly
20010350	normal	Cormorant-1	1661.18	1667.28	27	0.471	Cut	coaly
20010067	normal	Cormorant-1	1685.56	1685.72	21	0.475	CORE 7	coal
20010351	normal	Cormorant-1	1725.19	1728.24	41	0.484	Cut	coaly
20010352	normal	Cormorant-1	1777.01	1780.06	52	0.496	Cut	coaly
20010344	normal	Cormorant-1	1829.53	1829.59	51	0.508	CORE 8	coal
20010353	normal	Cormorant-1	1877.59	1883.69	51	0.521	Cut	coaly
20010069	normal	Cormorant-1	1950.74	1959.89	75	0.541	Cut	coal
20010354	normal	Cormorant-1	2005.61	2011.70	53	0.556	Cut	coaly
20010355	normal	Cormorant-1	2042.19	2048.28	37	0.566	Cut	coaly
20010356	normal	Cormorant-1	2090.95	2097.05	49	0.580	Cut	coaly
20010070	normal	Cormorant-1	2154.96	2167.15	67	0.602	Cut	coal
20010357	normal	Cormorant-1	2215.92	2222.02	58	0.619	Cut	coaly
20010345	normal	Cormorant-1	2232.38	2232.54	13	0.623	CORE 10	coal
20010358	normal	Cormorant-1	2276.88	2279.93	46	0.639	Cut	coaly
20010071	normal	Cormorant-1	2340.89	2353.09	69	0.664	Cut	coal
20010359	small	Cormorant-1	2377.47	2383.57	34	0.675	Cut	coaly
20010360	normal	Cormorant-1	2414.05	2420.14	37	0.689	Cut	coaly
20010361	normal	Cormorant-1	2444.53	2447.57	29	0.700	Cut	coaly
20010362	*none*	Cormorant-1	2478.05	2484.15		0.713	Cut	coaly
20010363	*none*	Cormorant-1	2539.02	2545.11		0.738	Cut	coaly
20010364	small	Cormorant-1	2563.40	2569.50	20	0.748	Cut	coaly
20010365	*none*	Cormorant-1	2593.88	2599.98		0.760	Cut	coaly
20010366	small	Cormorant-1	2621.31	2627.41	58	0.772	Cut	coaly
20010367	small	Cormorant-1	2651.79	2654.84	29	0.784	Cut	coaly
20010368	*none*	Cormorant-1	2688.37	2691.42		0.800	Cut	coaly
20010369	normal	Cormorant-1	2715.80	2718.85	64	0.812	Cut	coaly
20010072	normal	Cormorant-1	2758.47	2770.67	47	0.836	Cut	coal
20010370	*none*	Cormorant-1	2792.00	2798.10		0.849	Cut	coaly
20010371	normal	Cormorant-1	2819.43	2822.48	57	0.861	Cut	coaly
20010372	*none*	Cormorant-1	2831.63	2837.72		0.869	Cut	coaly
20010373	*none*	Cormorant-1	2843.82	2849.92		0.875	Cut	coaly
20010374	normal	Cormorant-1	2941.36	2944.40	123	0.923	Cut	coaly
20010375	normal	Pelican-5	1899	1905		0.458	Cut	coaly
20010049	normal	Pelican-5	2034	2037	135	0.486	Cut	coal
20010376	normal	Pelican-5	2190	2193	156	0.524	Cut	coaly
20010377	normal	Pelican-5	2304	2307	114	0.554	Cut	coaly
20010378	normal	Pelican-5	2409	2412	105	0.585	Cut	coaly
20010379	normal	Pelican-5	2502	2505	93	0.614	Cut	coaly
20010380	normal	Pelican-5	2592	2595	90	0.644	Cut	coaly
20010381	normal	Pelican-5	2721	2724	129	0.690	Cut	coaly
20010052	normal	Pelican-5	2791.87	2792	70	0.716	CORE 1	coal
20010382	small	Pelican-5	2799	2802	8	0.720	Cut	coaly
20010383	normal	Pelican-5	2958	2601	159	0.646	Cut	coaly
20010384	normal	Pelican-5	3063	3066	105	0.834	Cut	coaly
20010385	normal	Pelican-5	3162	3165	99	0.882	Cut	coaly
20010386	*none*	Pelican-5	3246	3249		0.925	Cut	coaly
20010387	*none*	Pelican-5	3414	3417		1.017	Cut	coaly
20010388	*none*	Pelican-5	3567	3570		1.110	Cut	coaly
20010389	small	Pelican-5	3702	3705	540	1.198	Cut	coaly
20010390	*none*	Pelican-5	3822	3825		1.282	Cut	coaly
20010391	*none*	Pelican-5	3960	3963		1.386	Cut	coaly
20010392	*none*	Pelican-5	4257	4260		1.634	Cut	coaly

Figure H1. SANS scattering intensity versus Z for 15 low ash coal samples from Pelican-5 within the Eastern View Coal Measures succession. Legend shows depth for each sample. Small diamtere samples are marked "sd".

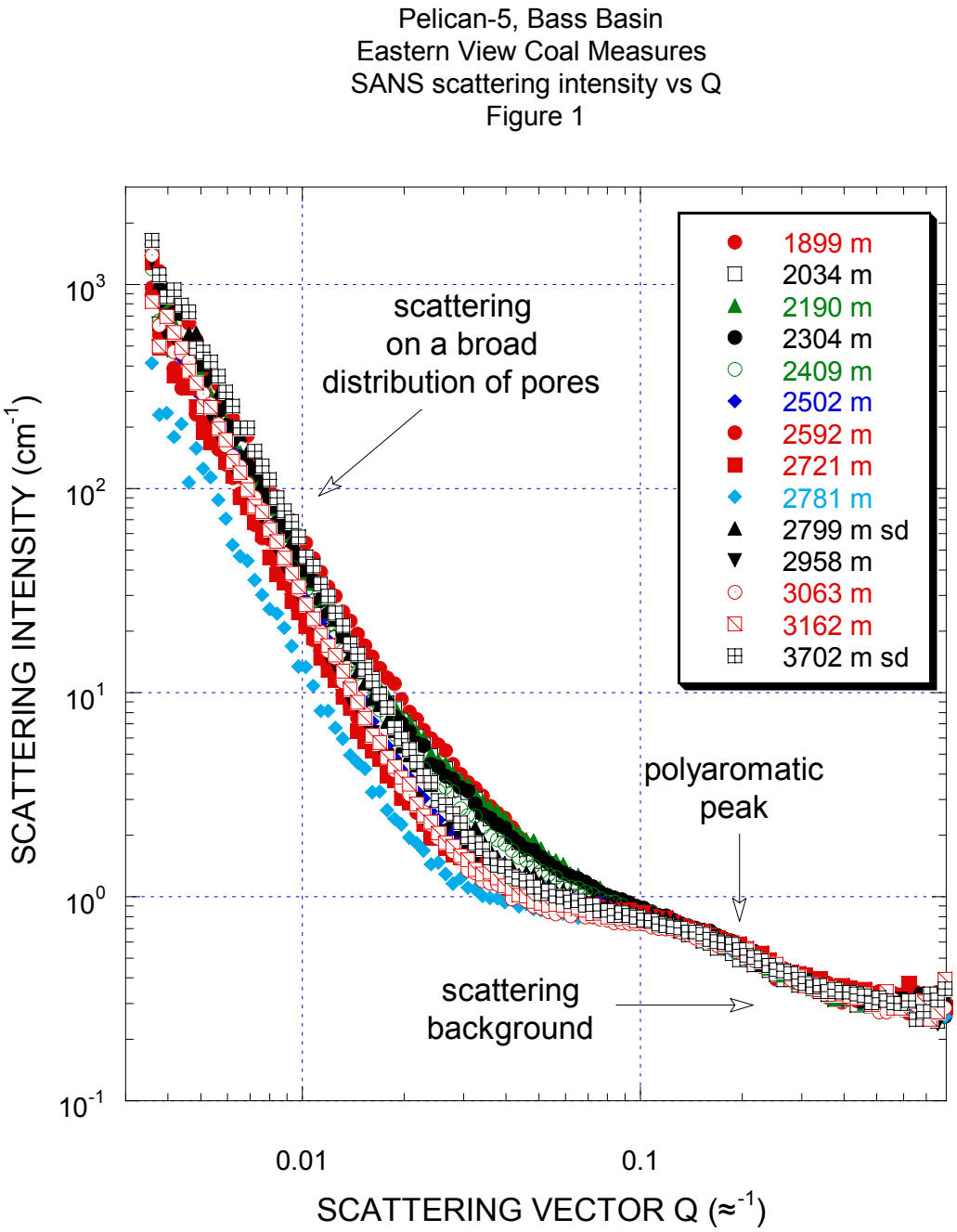


Figure H2. SANS intensity at Q=0.01 Å^{-1} versus depth for 12 low ash coal samples from Pelican-5.

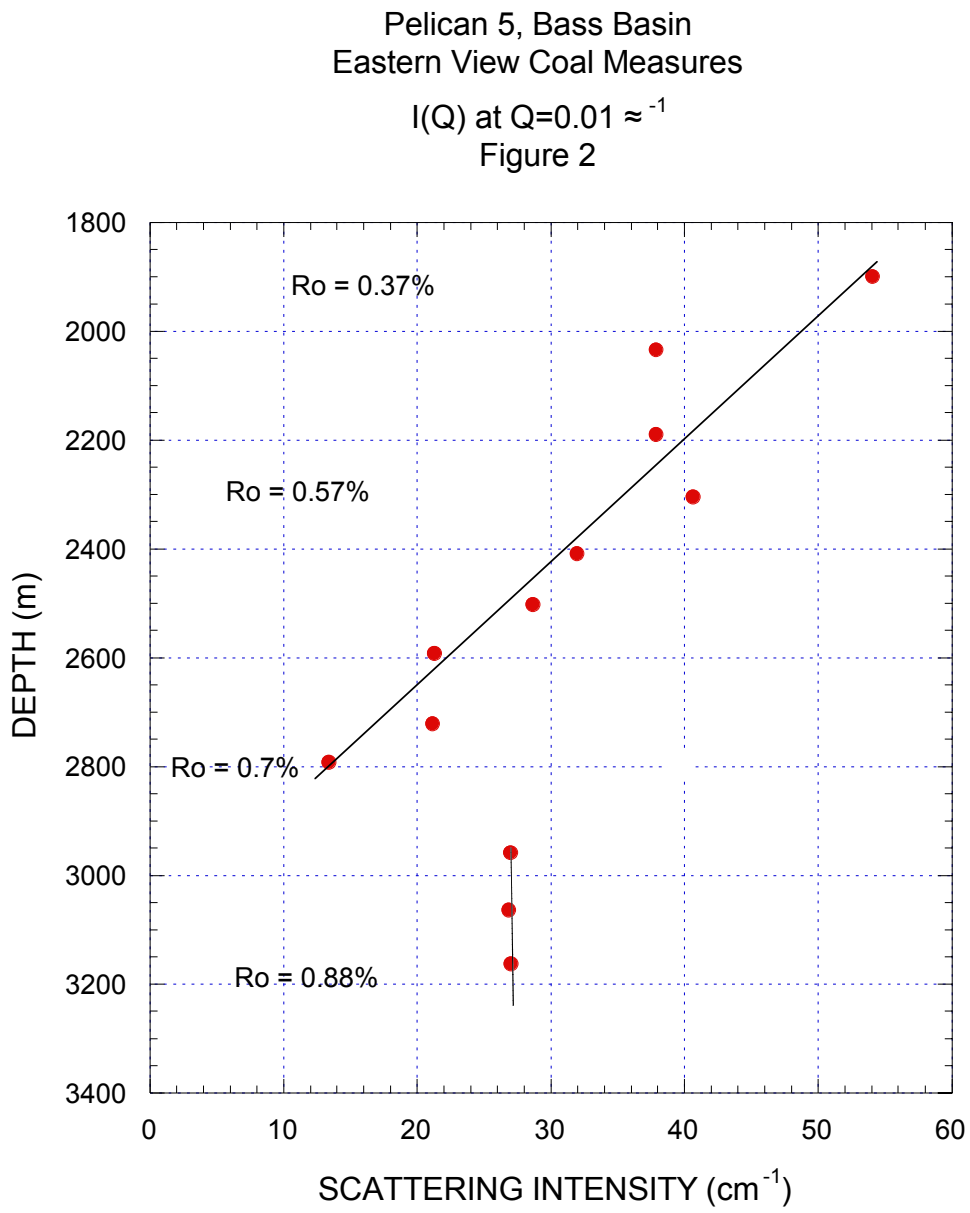


Figure H3. Variation of the pore size distribution with depth for low ash coal samples from Pelican-5. Only pores of diameter in the range of 80 – 800 Å are included.

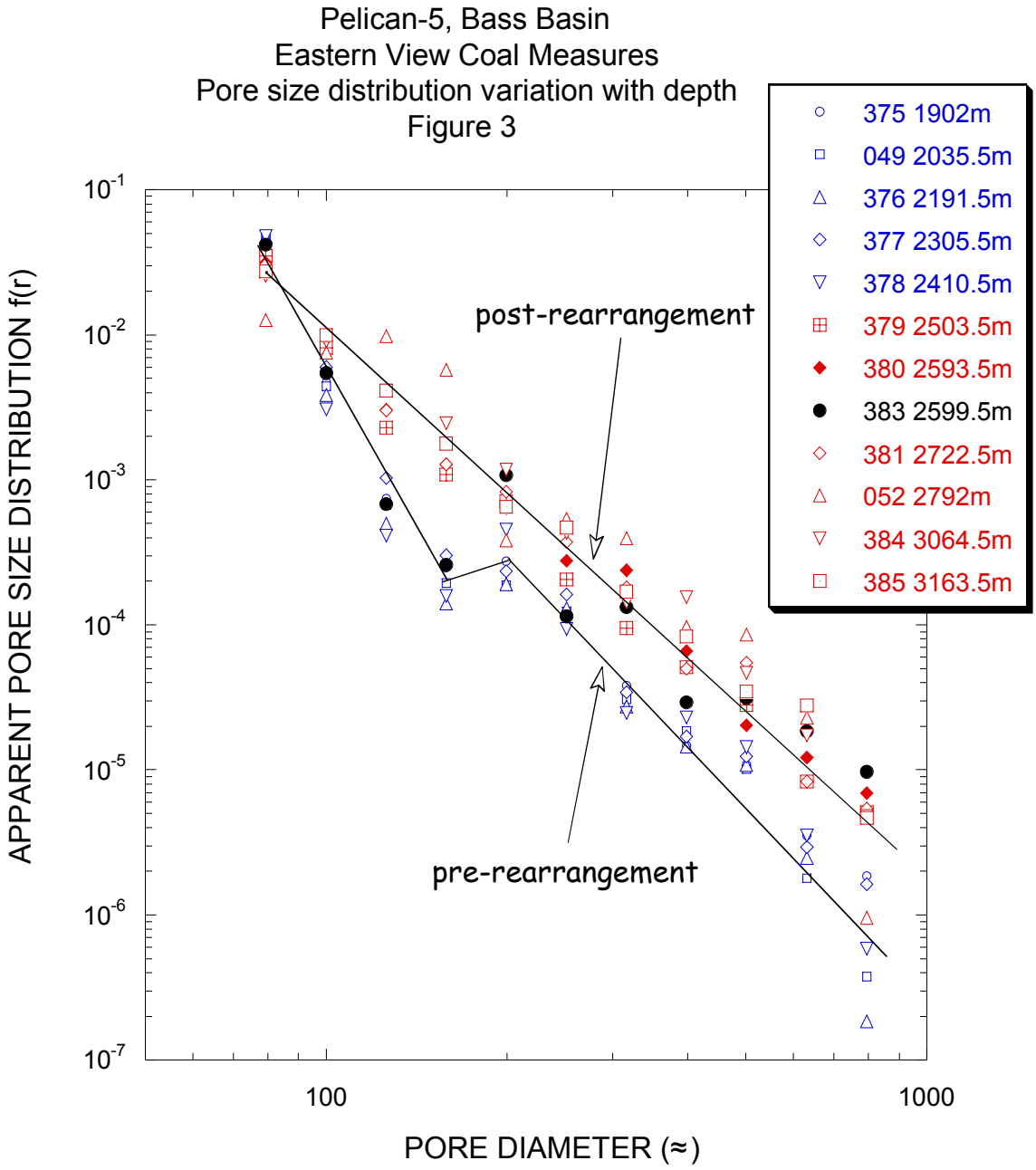


Figure H4. Variation of pore number density with depoth for three pore sizes: 100 A, 316 Å and 630 Å in Pelican-5, Eastern View Coal Measures, low ash preparations.

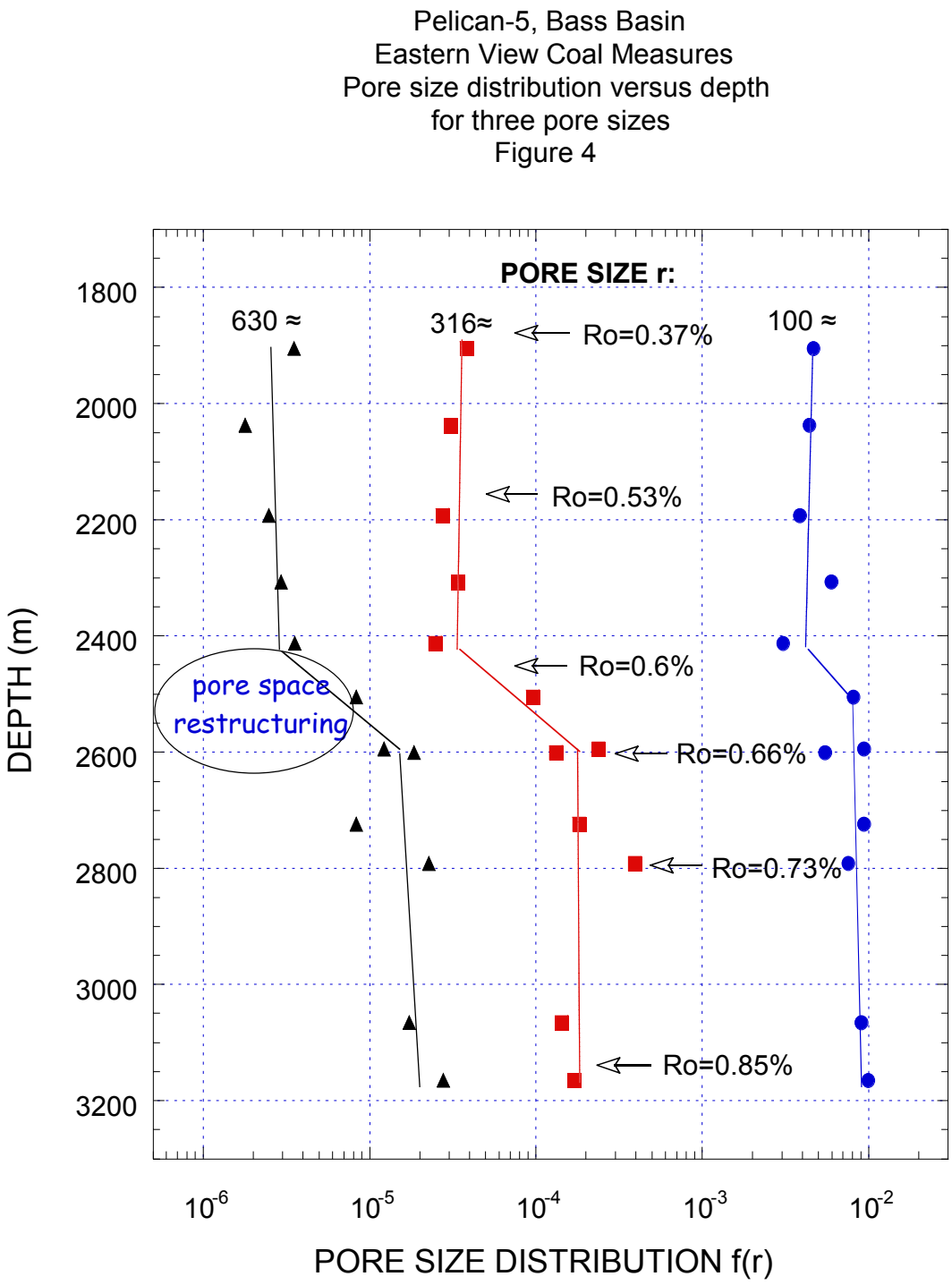


Figure H5. Specific internal surface area versus probe diameter calculated for 12 low ash coals from Pelican-5.

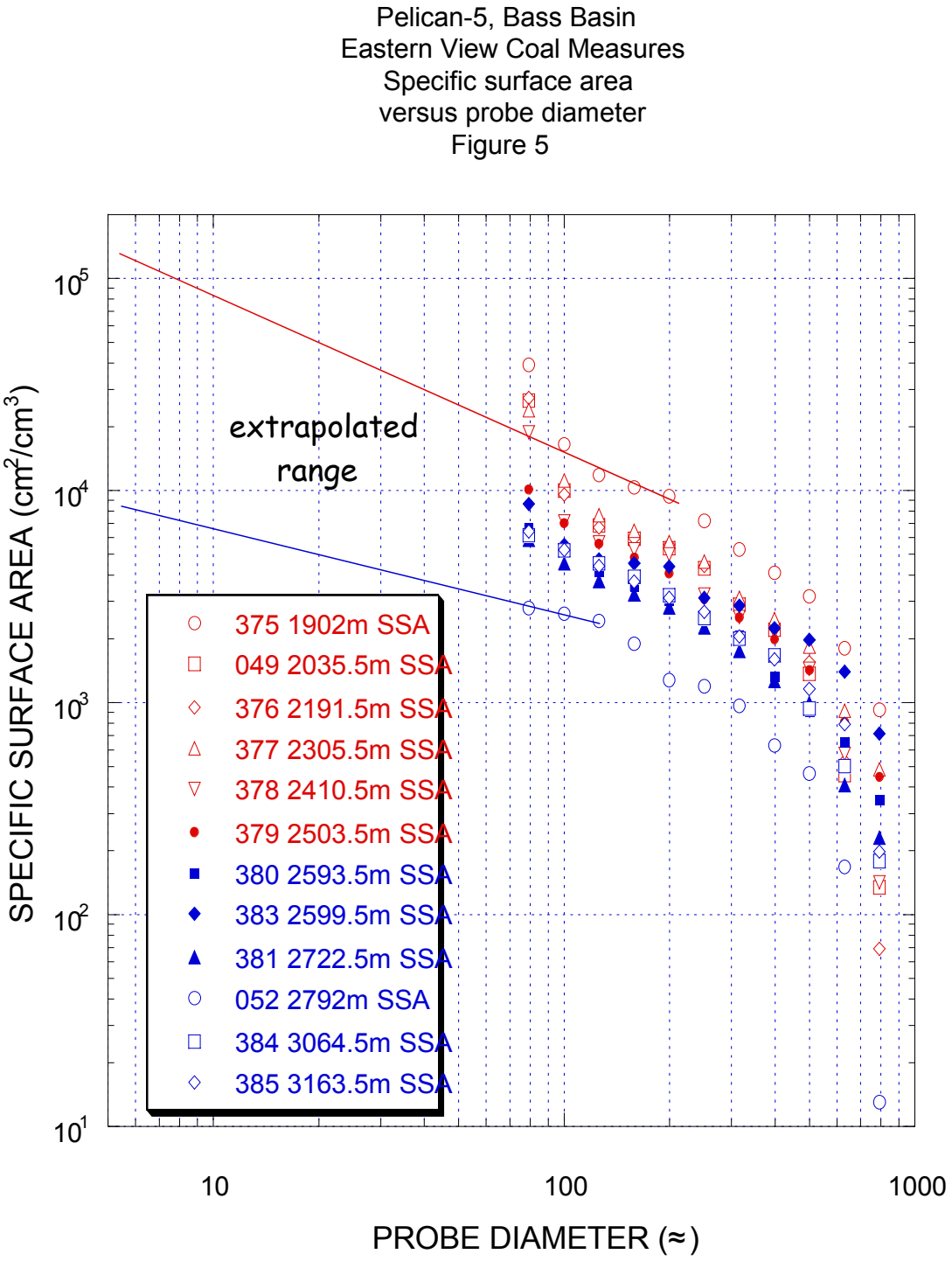


Figure H6. The variation of the specific surface area with depth for probe size 100 Å, Pelican -5, low ash preparations, Eastern View coals Measures.

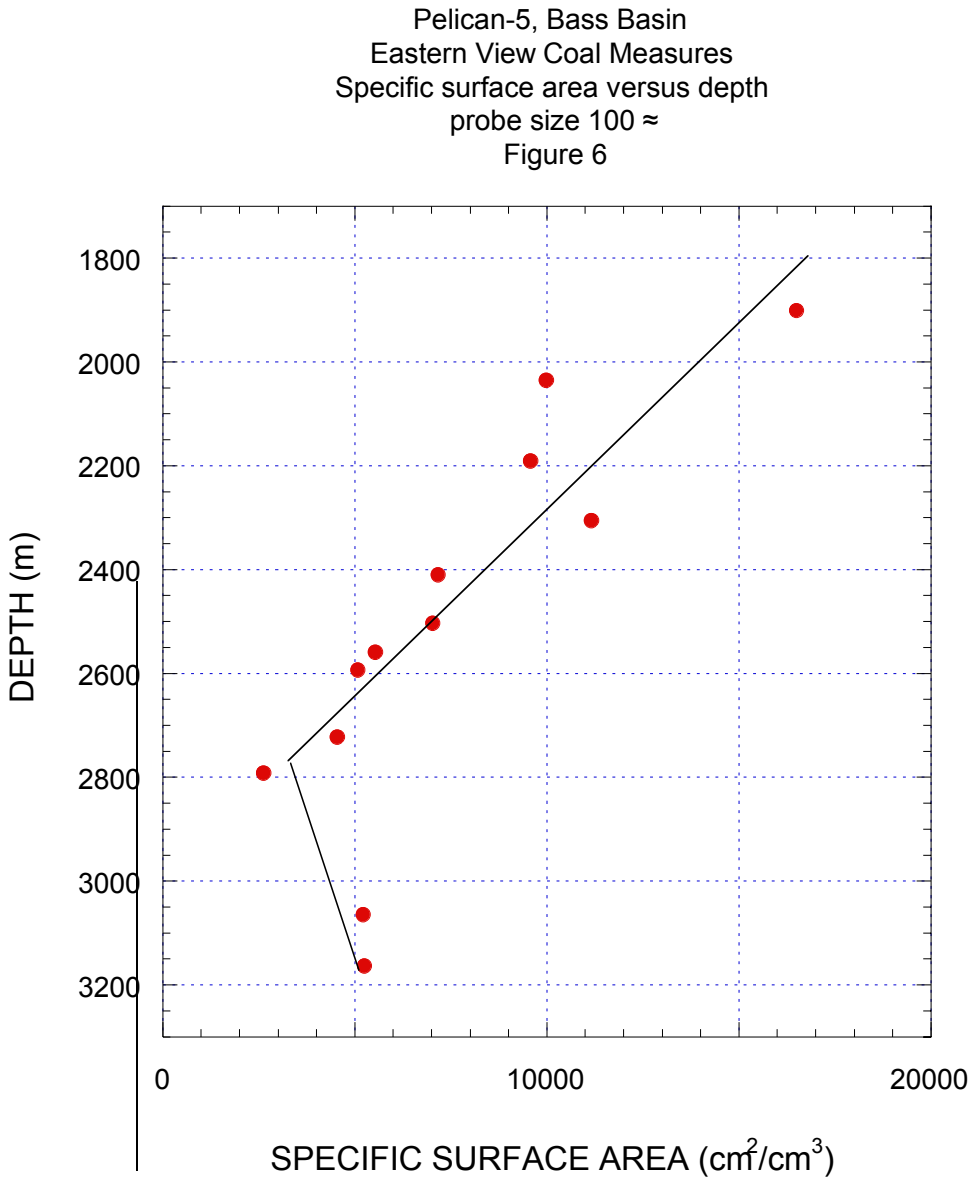


Figure H7. Interpretation of SANS data for Pelican-5, micro-structural events, hydrocarbon generation and expulsion.

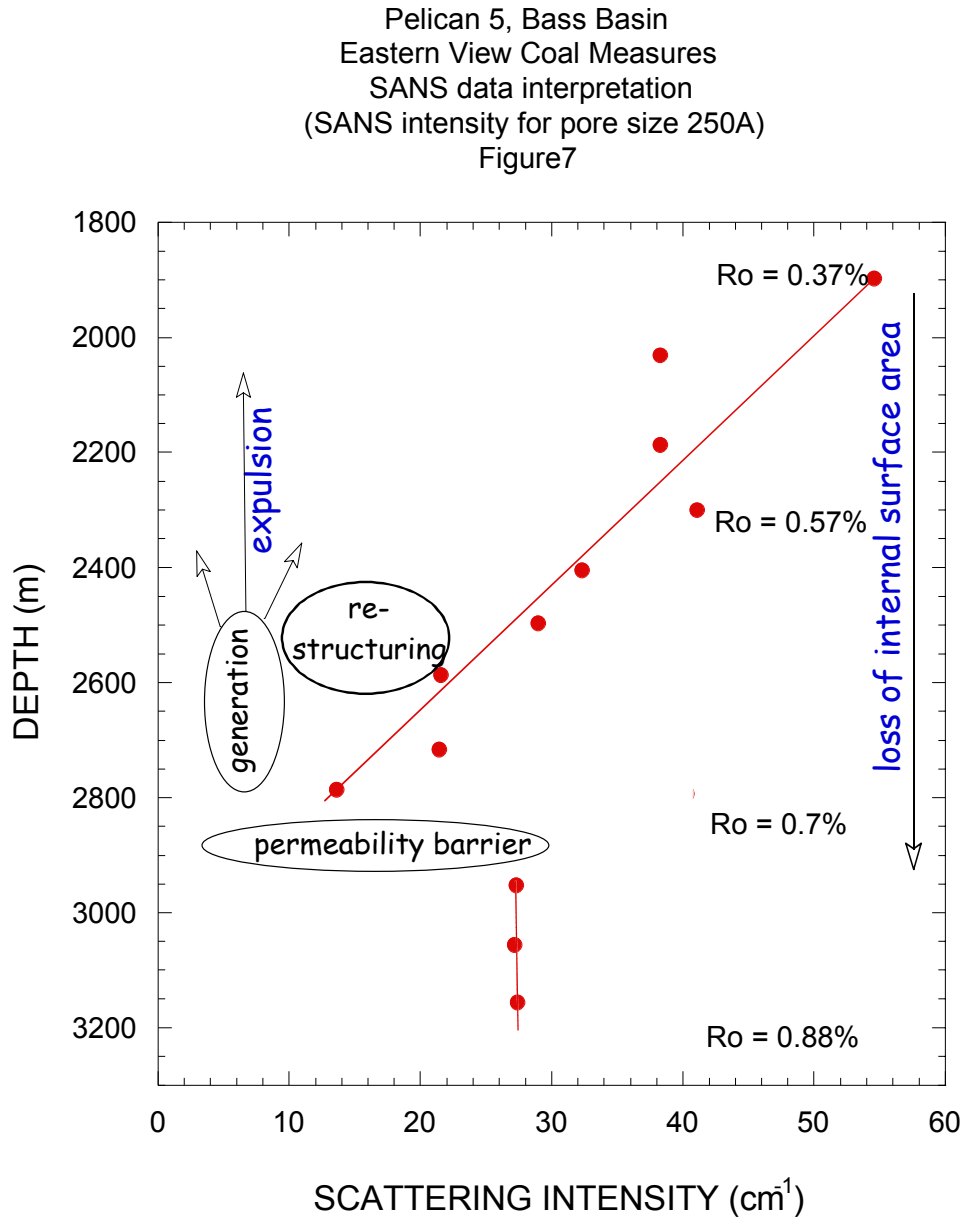


Figure H8. Depth plot of Hydrocarbon Index and Bitumen Index for low-ash coals from Pelican-5.

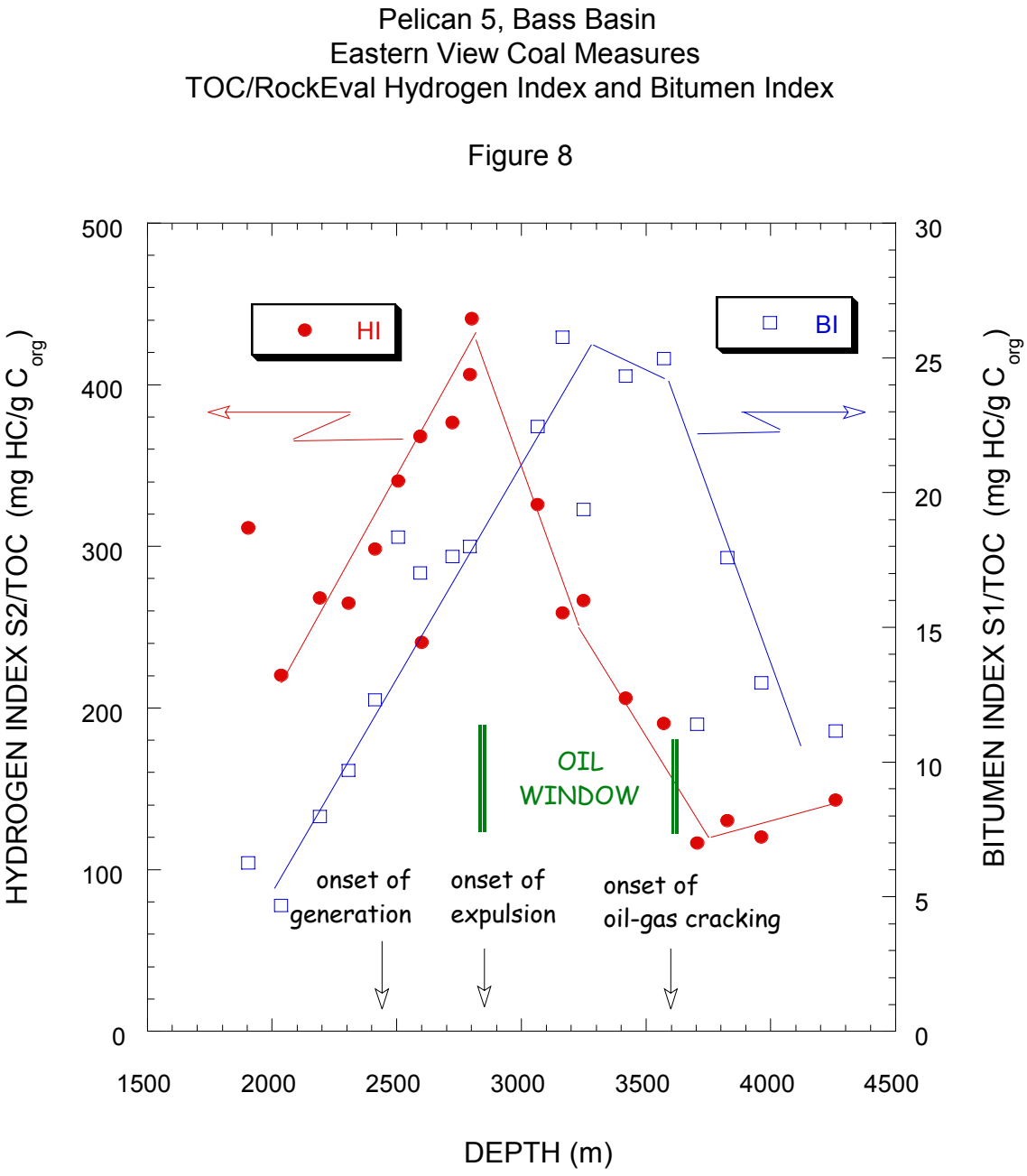


Figure H9. SANS scattering intensity versus Z for 20 low ash coal samples from Eastern View coal Measures, Cormorant-1. The legend shows depth of each sample.

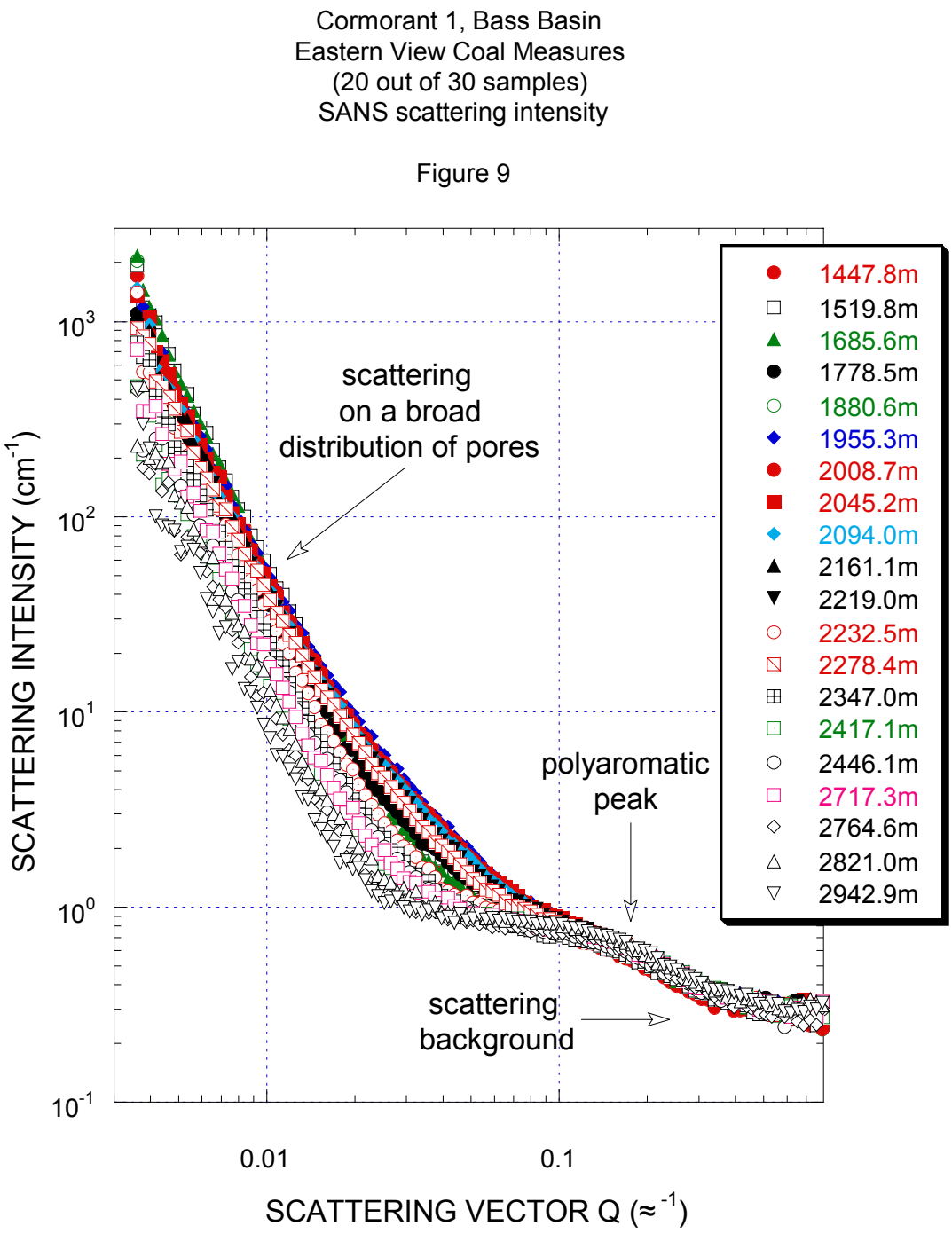


Figure H10. SANS ontensity at Q=0.01 Å^{-1} versus depth for 26 low ash coal samples from Cormorant-1. Data points for sidewall samples are marked "C".

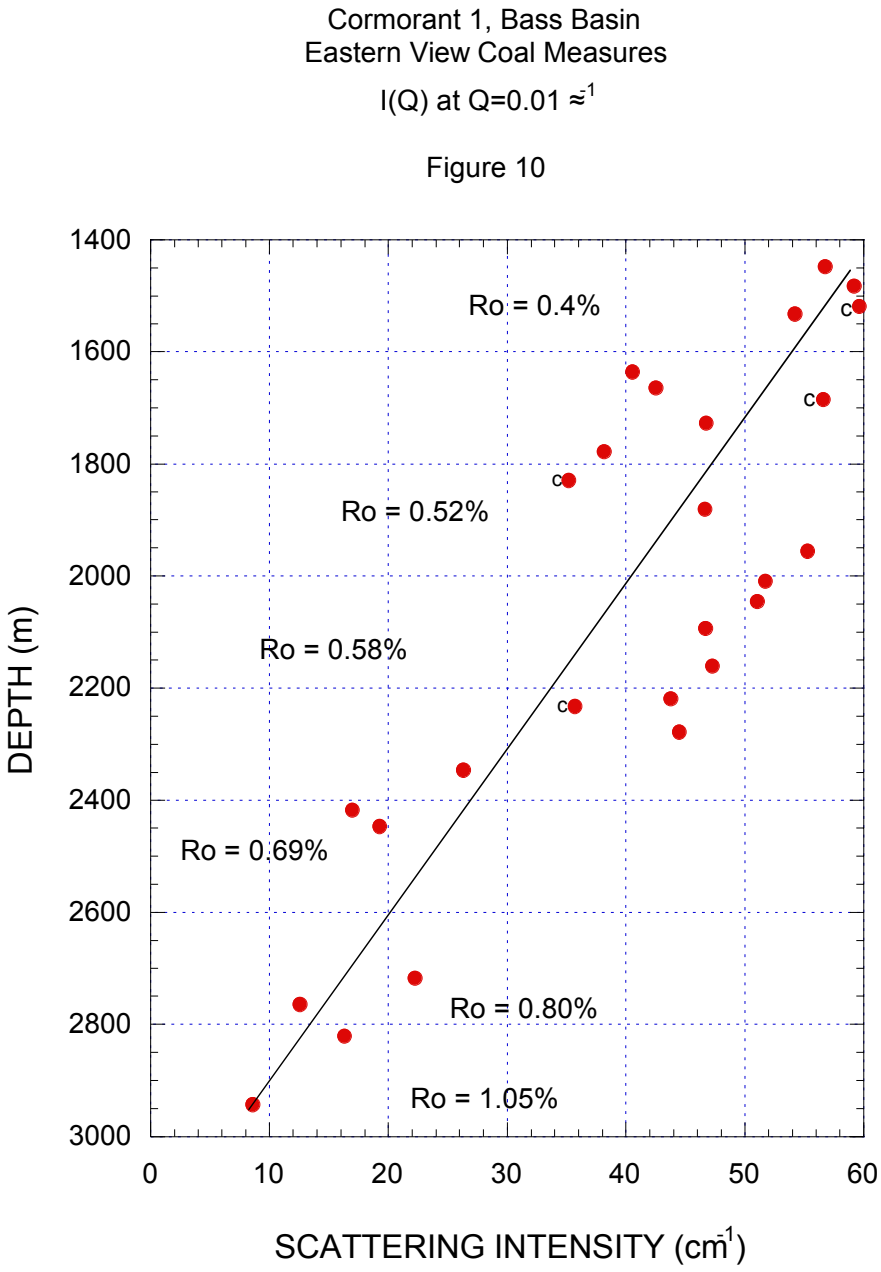


Figure H11. Variation of the pore size distribution with depth for low ash coal samples from Cormorant-1. Only pores of diameter in the range 80 – 800 Å are included.

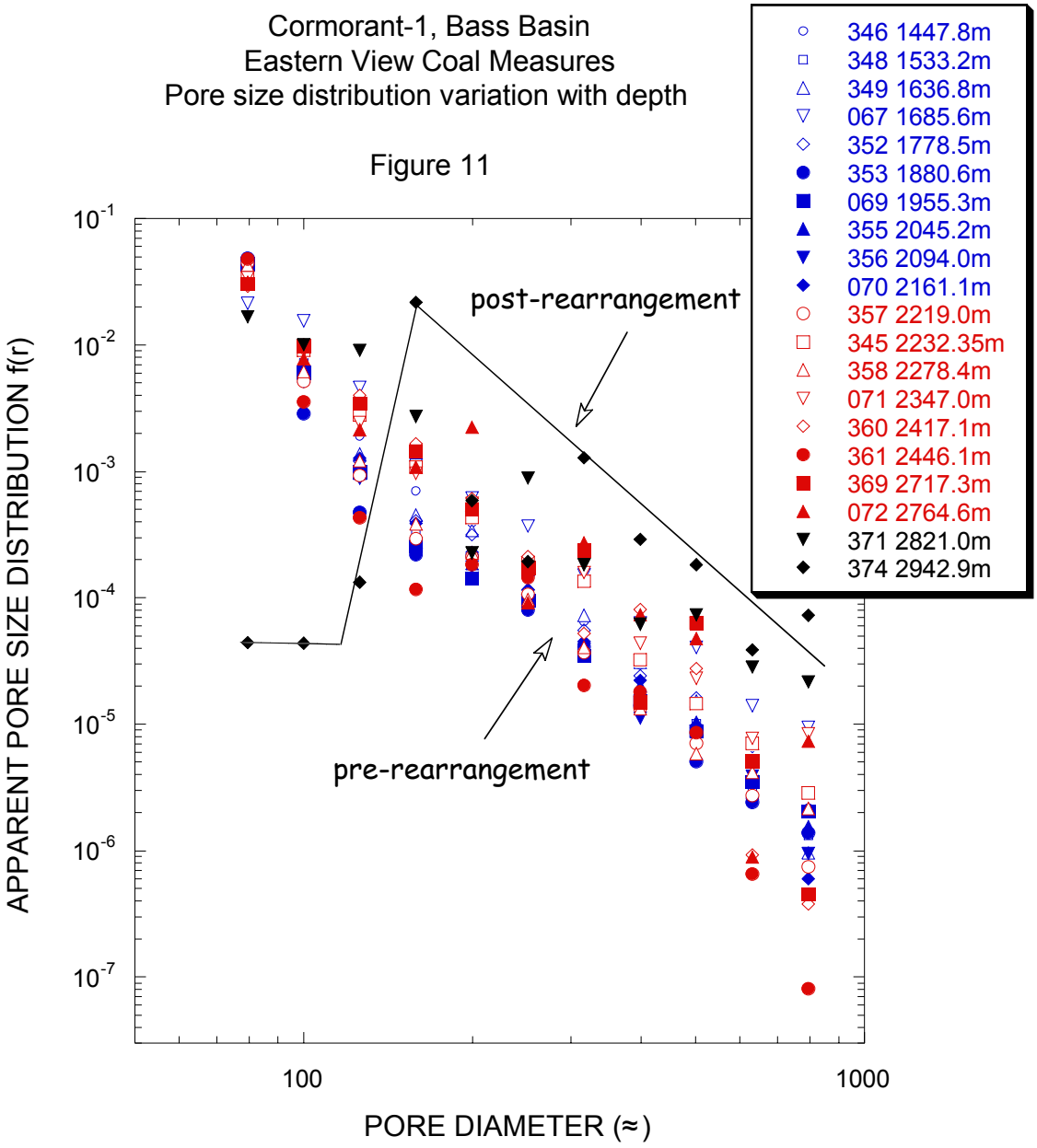


Figure H12. Variation of pore number density with depth for three pore sizes: 100 Å, 316 Å, and 630 Å, in Cormorant-1, Eastern View Coal Measures, low ash preparations.

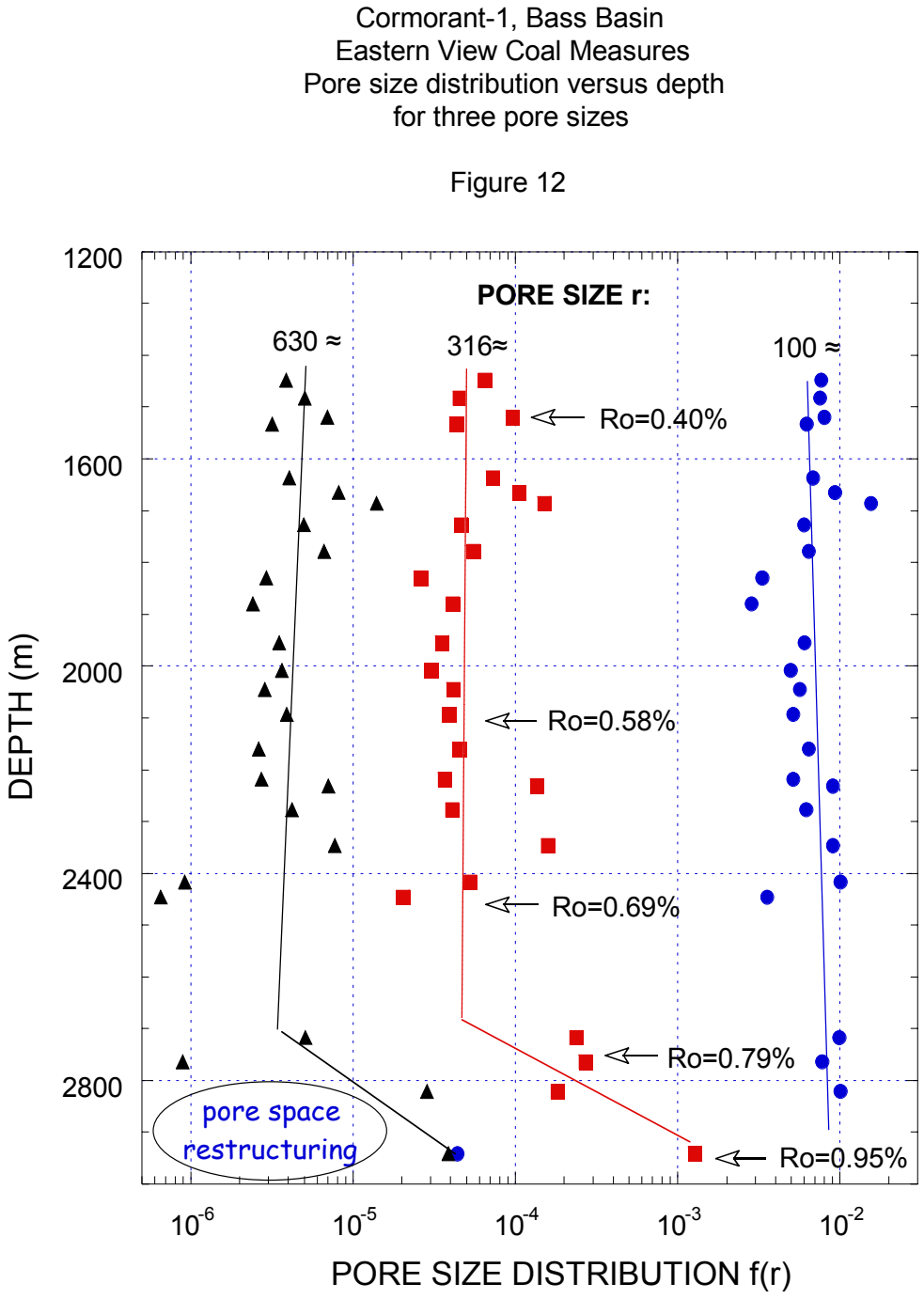


Figure H13. Specific internal surface area versus probe diameter calculated for 12 low ash coals from Cormorant-1.

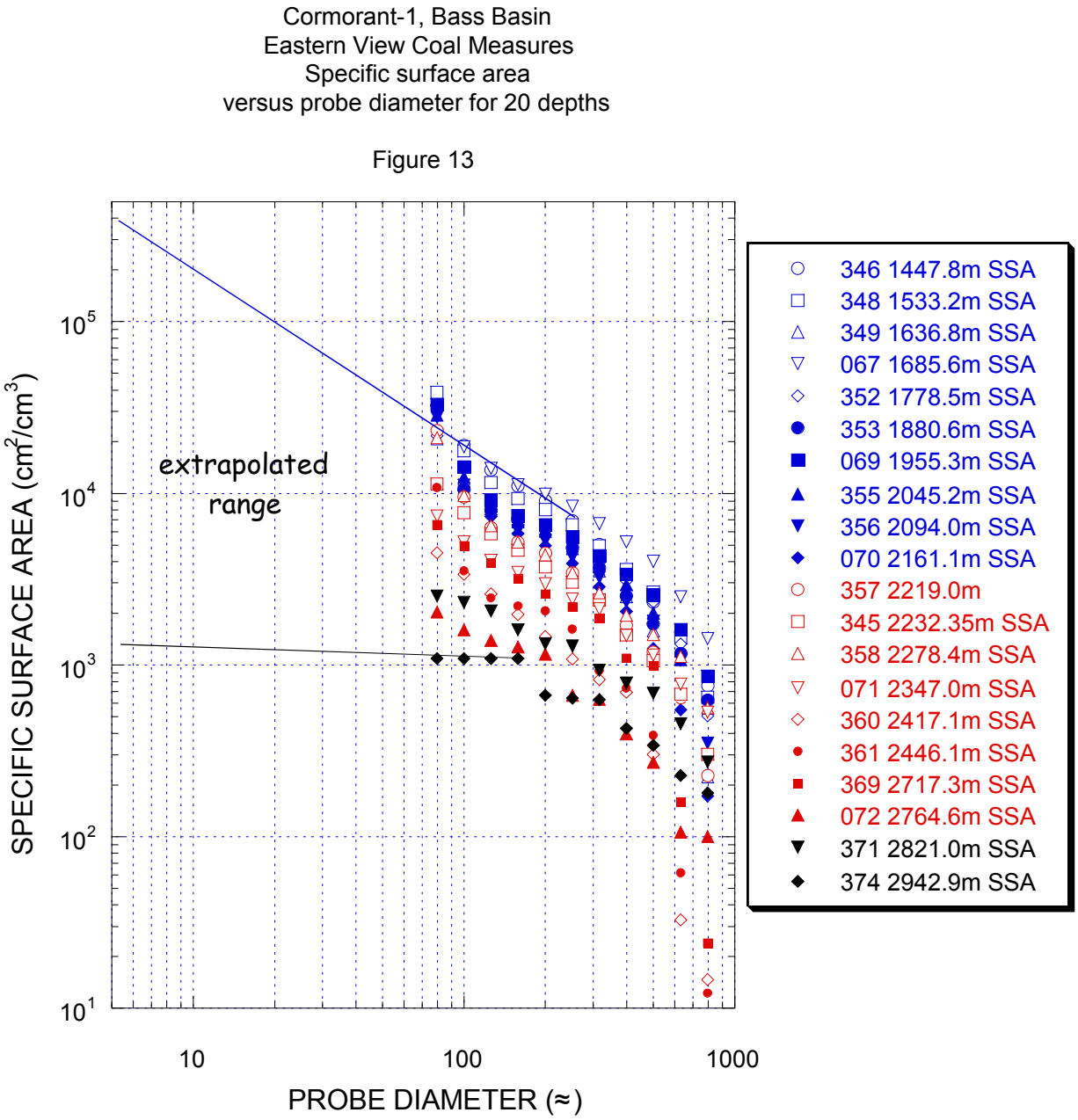


Figure H14. The variation of the specific surface area with depth for probe size 100 Å, low ash preparations, Eastern View Coal Measures, Cormorant-1.

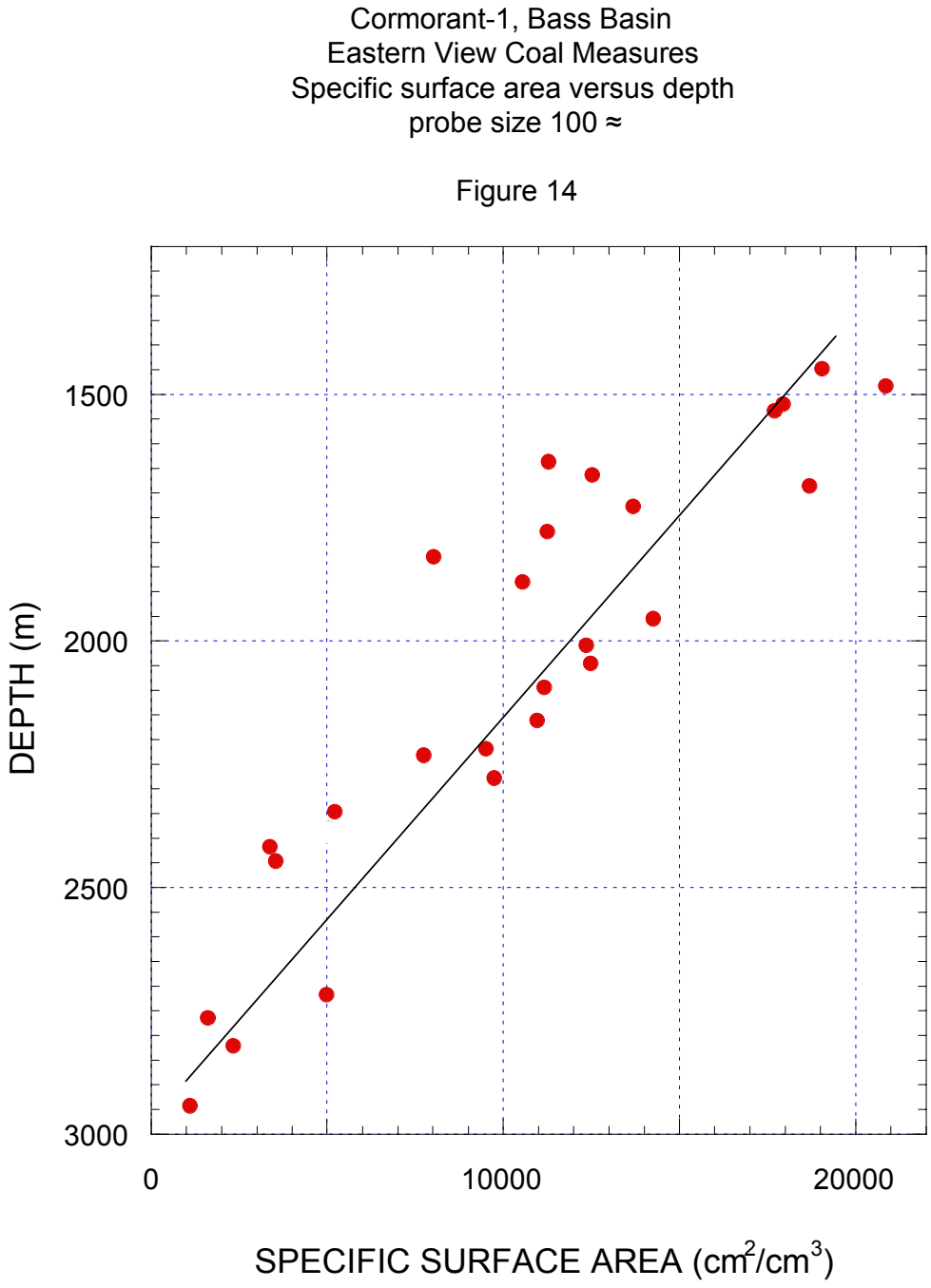


Figure H15. Interpretation of SANS data for Cormorant-1, micro-structural events, hydrocarbon generation and expulsion.

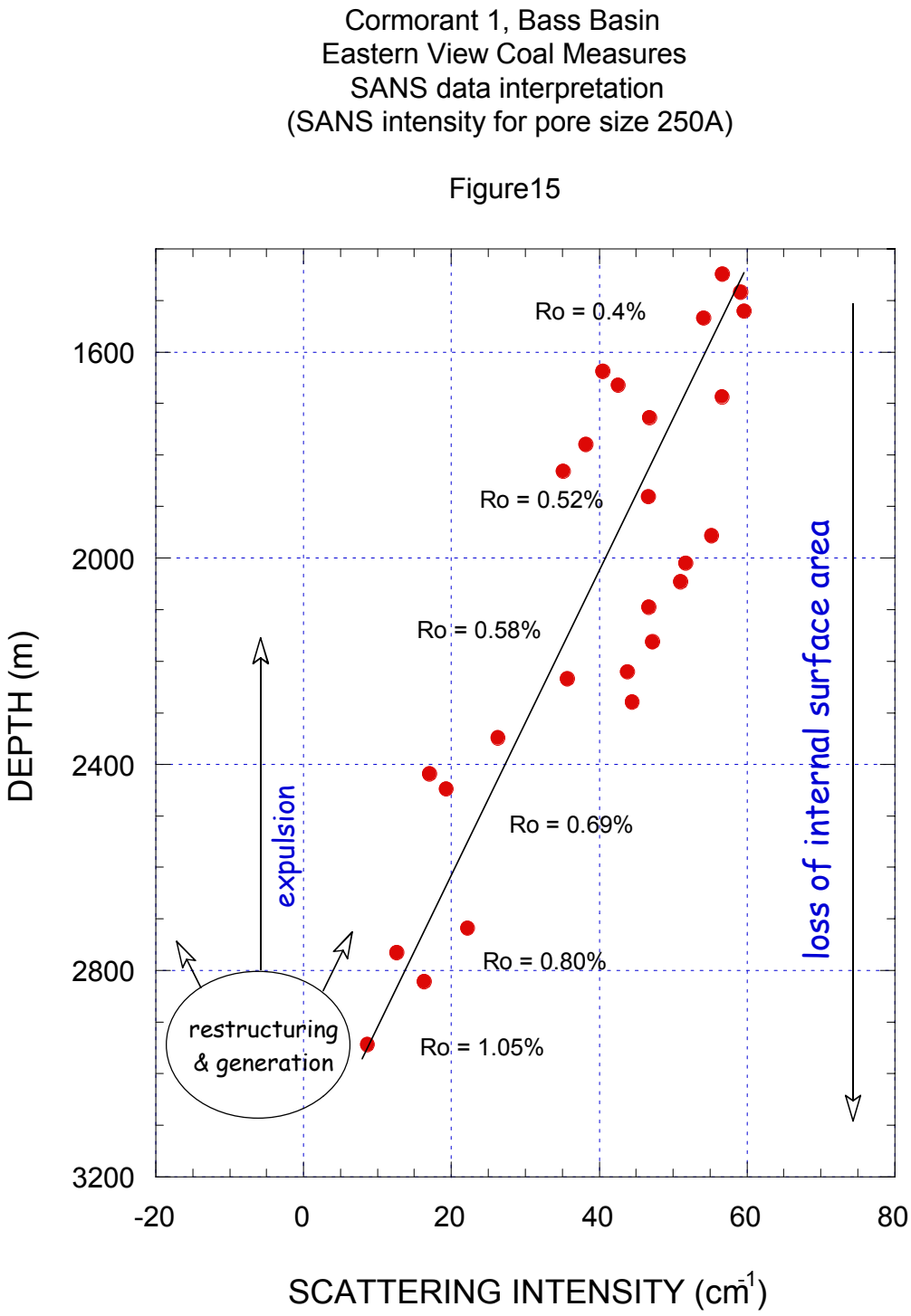


Figure H16. Vitrinite reflectance versus depth for Cormorant-1 and Pelican-5. The legends show parameters for second order polynomial fits.

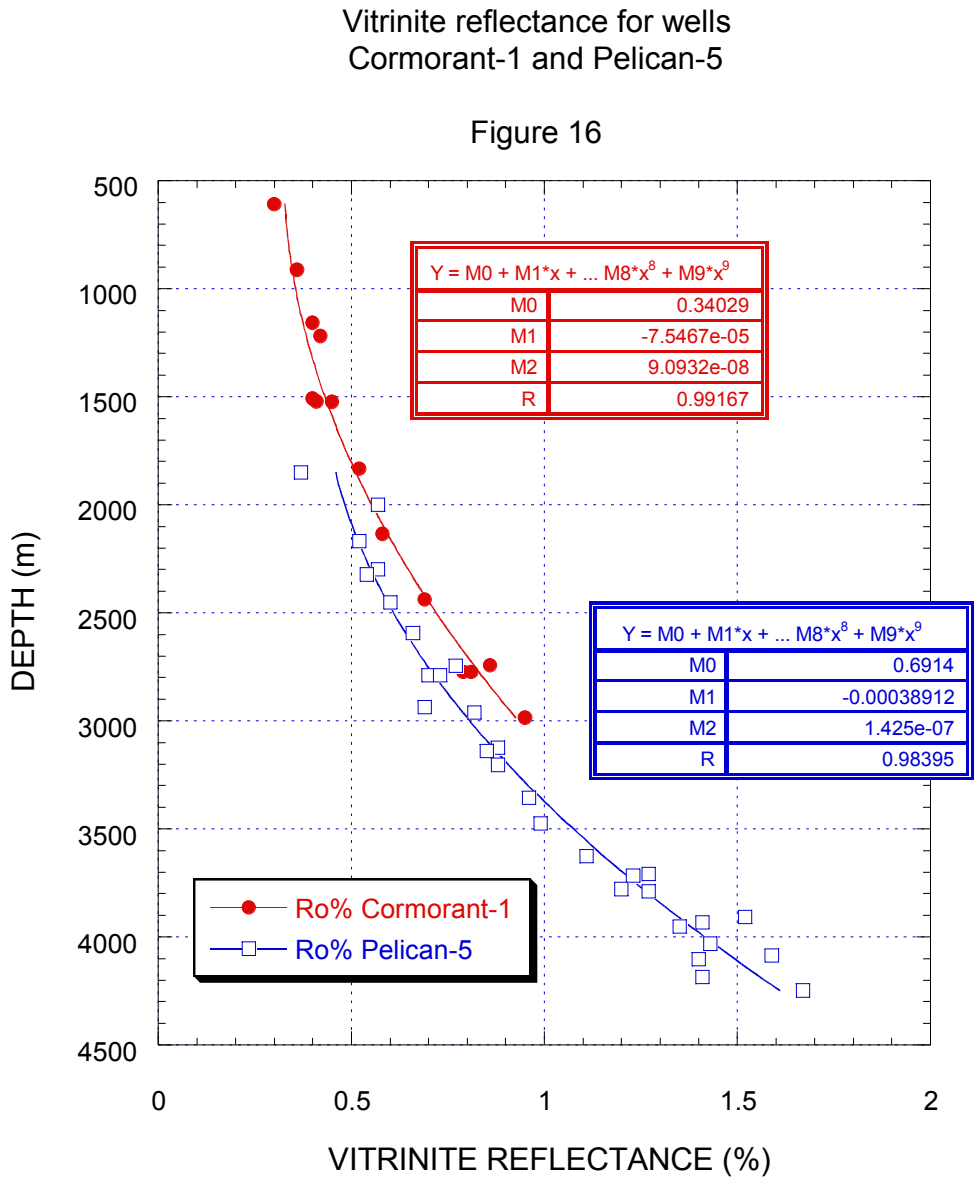
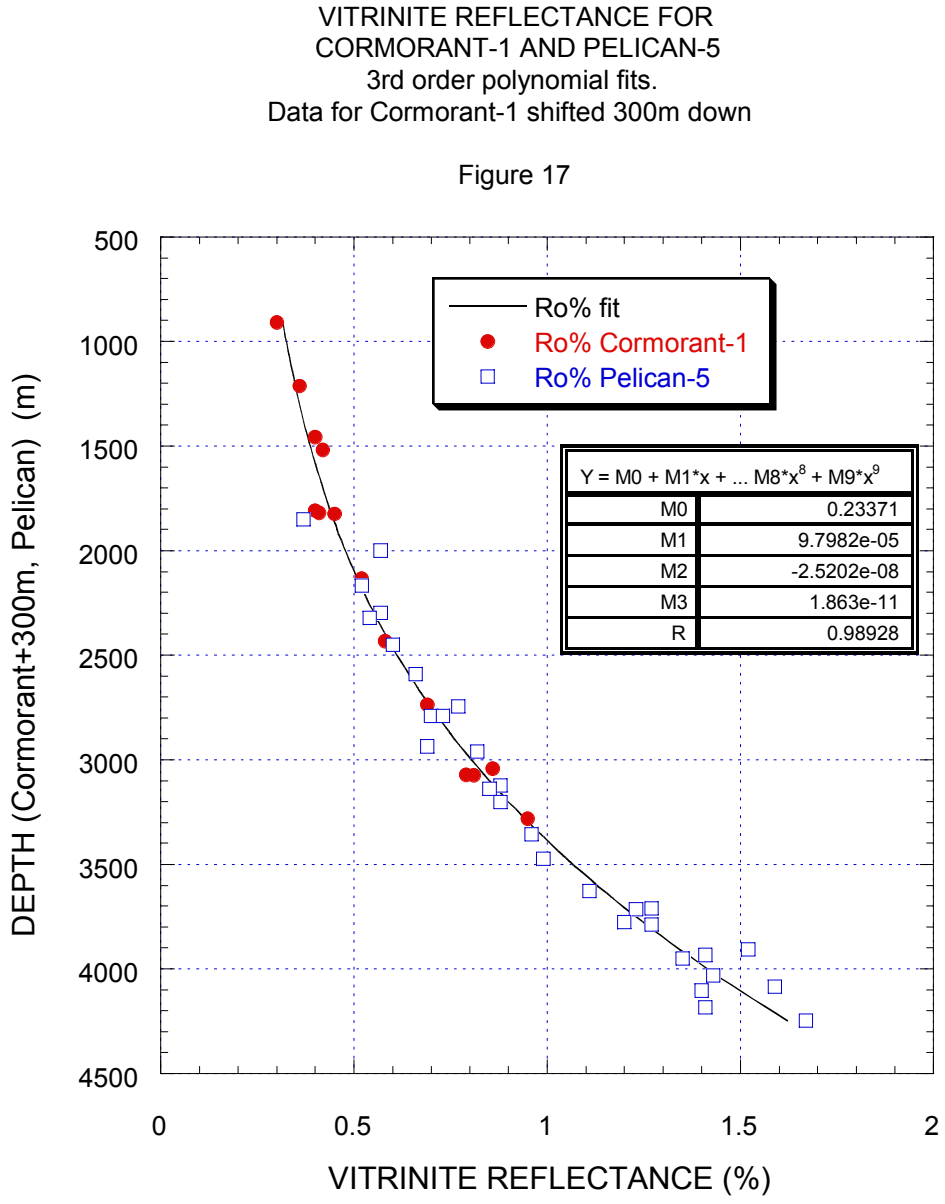


Figure H17. Universal representation for vitrinite reflectance versus effective depth for Cormorant-1 and Pelican-5. The legend shows parameters for a universal third order polynomial fit.



APPENDIX I.

ORGANIC PETROLOGY OF SUITES FROM A NUMBER OF PETROLEUM EXPLORATION BOREHOLES DRILLED IN THE BASS BASIN (MARCH 2002)

Alan Cook, Keiraville Konsultants Pty. Ltd., 7 Dallas Street, Keiraville NSW 2500

Note: The format of this report has been altered. The contents are unchanged.

AROO-1, p 1

KK # / Ref #.	Depth (ft) /Type	$\overline{R}_v$max	Range	N	Sample description including liptinite fluorescence, maceral abundances, mineral fluorescence
					Lower Torquay Group (Early / Late Oligocene)
T8310	5740-5770	0.48	0.40-0.58	28	Rare lamalginite and liptodetrinite yellow to orange. (Siltstone>
Ctgs	$\overline{R}_I$max	0.74	0.62-1.00	5	carbonate. Dom sparse, V>L>L. Vitrinite sparse, inertinite and liptinite rare. Fossil fragments sparse. Mineral fluorescence patchy weak orange to absent. Iron oxides abundant. Pyrite common.)
					Upper Eastern View Coal Measures (Mid / Late Eocene)
T8311	6860-6880	0.56	0.47-0.65	28	Rare resinite and sporinite orange, rare *Botryococcus*-related
Ctgs	$\overline{R}_I$max	0.96	0.75-1.24	17	telalginite yellow. (Siltstone>carbonate. Dom abundant, I>V>L. Inertinite and vitrinite abundant, liptinite rare. Mineral fluorescence patchy weak orange to absent. Iron oxides abundant. Pyrite common.)
					Upper Eastern View Coal Measures (Mid Eocene)
T8312	7370-7380	0.55	0.50-0.65	27	Sparse cutinite orange to weak brown, sparse resinite greenish
Ctgs	$\overline{R}_I$max	0.83	0.77-0.91	6	yellow, sparse sporinite orange to dull orange, rare lamalginite, orange rare suberinite dull orange to weak brown, rare liptodetrinite orange to dull orange, rare exsudatinite, orange. (Siltstone>carbonate>coal. Coal abundant, duroclarite>vitrite> vitrinertite, V>>L>I. Maceral group composition of coal (mf):: vitrinite-95.0%, inertinite-1.0%, liptinite-4.0%. Dom common, V>L>I. Vitrinite common, liptinite and inertinite sparse. Mineral fluorescence patchy weak dull orange to absent. Iron oxides common. Pyrite sparse.)
					Upper Eastern View Coal Measures (Early / Mid Eocene)
T8313	7910-7920	0.64	0.53-0.72	28	Sparse cutinite orange to weak brown, sparse resinite greenish
Ctgs	$\overline{R}_I$max	0.99	0.81-1.38	5	yellow to orange, sparse sporinite yellow to dull orange, rare lamalginite orange, rare suberinite dull orange to weak brown, rare liptodetrinite yellow to dull orange. (Siltstone>carbonate> coal. Coal abundant, vitrite>clarite, V>>L>I. Maceral group composition of coal (mf): vitrinite-97.0%, inertinite-0.2%, liptinite-2.8%. Dom common, V>L>I. Vitrinite and liptinite sparse, inertinite rare. Coals belong to the Upper Eastern View facies with most of the inertinite being sclerotinite rather than inertodetrinite and semifusinite. Mineral fluorescence patchy dull orange to absent. 'Frypanned' rims on coal rare but some strong alteration noted. Iron oxides abundant. Pyrite sparse.)

					Mid/Upper Eastern View Coal Measures (Early Eocene)
T8314	8880-8890	0.67	0.57-0.77	33	Sparse sporinite orange, rare cutinite, resinite and lamalginite
Ctgs	$\overline{R}_I$max	1.23	0.90-1.67	10	orange, rare liptodetrinite yellow to dull orange. (Siltstone> carbonate>coal. Coal sparse, duroclarite>vitrinertite. V>I>L. Maceral group composition of coal (mf): vitrinite-59.0%, inertinite-40.0%, liptinite-1.0%. Dom common, V>I>L. All three maceral groups sparse. The coal shows a change in organic facies to the Lower Eastern View B facies. Mineral fluorescence patchy dull orange to absent. 'Fry panned' rims on coal rare and relatively weak. Iron oxides abundant. Pyrite common.)
					Mid Eastern View Coal Measures (Upper Cretaceous)
T8315 Ctgs	11690-11700	-	-	-	Fluorescing liptinite absent. (Igneous rock fragments, doleritic. textures, but some grains strongly altered and with rosette structures. Dom absent, all maceral groups absent. Mineral fluorescence absent. Iron oxides major. Pyrite sparse.)

The Torquay Group sample is immature to marginally mature and contains sparse vitrinite. The next four samples are from the Eastern View Coal Measures and are early mature to mid-mature. T8311 to T8313 contain coals that belong to the Upper Eastern View organic facies of Smith and Cook (1984). T8314 belongs to the Lower Eastern View organic facies of Smith and Cook (1984). The deepest sample represents an igneous rock that is interpreted as being an intrusion although some strongly altered grains were noted that may be more consistent with a volcanic origin. No evidence of contact alteration was found in T8314 but it is nearly 3000' above the igneous horizon and effects would not normally be expected at this distance. Some frypanning effects were noted in coal grains. The rims of such grains and cracks within them, show higher reflectances, but the cores may show lower vitrinite reflectance values due probably to migration of tars into the coals. Some occurrences show relatively pervasive alteration rather than having the raised reflectances confined to rims and fractures. The presence of pervasive alteration and the lowering effects of heat alteration can make it difficult to assess the original reflectance of the vitrinite.

NOTE: "Frypanning" is the term given to a process where the sample has been raised during the initial drying process (usually at the rig site) to a temperature where the organic matter oxidizes. In coals it is apparent by the presence of high reflecting rims. In siliciclastic sediments, frypanning is generally seen either as zones where liptinite lack fluorescence or mineral fluorescence is weak or absent. The temperatures to cause heat alteration are variable but of the order of 300^{o}C plus. Any temperatures over 400^{o}C cause rapid heat alteration and may support continued combustion where the TOC is over about 30%. The exact temperatures at which alteration occurs depend in part on organic matter type and rank and in part on the duration of the heating. With coals, excessive heating produces an offensive odour that usually causes the process to be stopped. With other sediment types, the odour may not be as severe and heating effects are potentially more severe.

Frypanning has the effect of reducing TOC, raising reflectances (except where lower values are found within core zones) and lowering fluorescence intensity. The effects on Rock-Eval analyses are more difficult to predict. This is because the carbonaceous residue shows much higher Tmax and lower HI, but the tar devolatilization products driven into the grains ahead of the oxidation front are likely to show lower Tmax and higher HI values. Data from bulk analysis methods cannot readily be corrected for the effects of frypanning. Microscope analyses attempt to exclude the effects of the alteration that has occurred. Microscope methods are the normal method of detecting that samples have been affected by excessive temperatures during drying.

BASS-2

KK # Ref #.	Depth (ft) /Type	$\overline{R}_v$max	Range	N	Sample description including liptinite fluorescence, maceral abundances, mineral fluorescence
					Upper Eastern View Coal Measures (Late Eocene)
T8317	3811.5	0.49	0.41-0.63	31	Rare cutinite, resinite and liptodetrinite yellow to dull orange,
Core	$\overline{R}_I$max	0.78	0.65-0.90	5	rare sporinite and lamalginite yellow to orange. (Siltstone. Dom sparse, V>I>L. Vitrinite sparse, inertinite and liptinite rare. Oil drops rare greenish yellow. Mineral fluorescence weak to absent. Iron oxides abundant. Pyrite abundant.)

BASS-3

KK # Ref #.	Depth (ft) /Type	$\overline{R}_v$max	Range	N	Sample description including liptinite fluorescence, maceral abundances, mineral fluorescence
					Upper Eastern View Coal Measures (Late Eocene)
T8318	5300-5320	0.52	0.41-0.62	29	Rare lamalginite orange, rare sporinite orange. (Siltstone>
Ctgs	$\overline{R}_I$max	0.85	0.68-1.47	10	carbonate. Dom sparse, V>I>L. Vitrinite sparse, inertinite and liptinite rare. Fossil fragments sparse. Mineral fluorescence patchy weak dull orange to absent. Iron oxides abundant. Pyrite abundant.)

The Bass-2 and Bass-3 samples are marginally mature and contain sparse dom.

CHAT-1

KK # Ref #.	Depth (ft) /Type	$\overline{R}_v$max	Range	N	Sample description including liptinite fluorescence, maceral abundances, mineral fluorescence
					Upper Eastern View Coal Measures (Late Eocene)
T8319	3966.5-4025.5	0.46	0.39-0.51	18	Fluorescing liptinite absent. (Carbonate>claystone>sandstone.. Dom rare, V>I. Vitrinite and inertinite rare, liptinite absent.
Ctgs	$\overline{R}_I$max	0.68	0.60-0.77	4	Rare yellow oil inclusions within quartz grains. Mineral fluorescence absent. Iron oxides sparse. Pyrite common.)
					Mid ECVM (Late Cretaceous/Maastrichtian)
T8320	7667.2-7677.1	0.49	0.39-0.62	31	Sparse cutinite yellow to dull orange, sparse lamalginite yellow to orange, sparse sporinite orange to dull orange, rare resinite
Ctgs	$\overline{R}_I$max	1.28	1.01-1.54	5	greenish yellow to dull orange, rare liptodetrinite yellow to dull orange. Coal abundant, vitrite>duroclarite, V>I>>L. Maceral group composition of coal (mf): vitrinite-70.0%, inertinite-28.0%, liptinite-2.0%. Dom common, V>L>I. Vitrinite and liptinite sparse, inertinite rare. Lower Eastern View facies. Mineral fluorescence patchy orange to dull orange. Iron oxides sparse. Pyrite rare.)

The Chat-1 samples are immature but rare oil inclusions were noted in some quartz grains. Frypanning was not a prominent feature of these samples.

NANGKERO-1

KK # Ref #.	Depth (ft) /Type	$\overline{R}_v$max	Range	N	Sample description including liptinite fluorescence, maceral abundances, mineral fluorescence
					Upper Eastern View Coal Measures (Mid / Late Eocene)
T8321	6440-6460	0.52	0.45-0.62	28	Sparse cutinite orange dull orange to weak brown, sparse
Ctgs	$\overline{R}_I$max	0.80	0.74-0.92	6	sporinite orange, sparse resinite yellow, sparse liptodetrinite orange to dull brown, rare suberinite dull orange to dull brown. (Carbonate>siltstone>coal. Coal abundant, clarite>vitrite. V>>L>I. Maceral group composition of coal (mf): vitrinite-93.0%, inertinite-1.0%, liptinite-6.0%. Dom common, V>L>I. All three maceral groups sparse. Mineral fluorescence patchy weak dull orange to absent. 'Frypanned' coal sparse. Iron oxides abundant. Pyrite sparse.)
					Mid EVCM (Cretaceous / Paleocene Boundary)
T8322	8290-8300	0.57	0.48-0.66	32	Sparse resinite greenish yellow to orange, sparse sporinite yellow
Ctgs	$\overline{R}_I$max	0.85	0.82-0.89	5	to orange, sparse cutinite dull orange to weak brown, rare liptodetrinite orange to dull orange, rare suberinite dull orange to dull brown. (Calcareous siltstone>coal. Coal abundant, clarite> vitrite. V>>L>I. Maceral group composition of coal (mf): vitrinite-91.0%, inertinite-1.0%, liptinite-8.0%. Dom sparse, V>I>L. Vitrinite and inertinite sparse, liptinite rare. 'Frypanned' coal common. Mineral fluorescence patchy orange to absent. Iron oxides abundant. Pyrite sparse to common.)

The two samples are early mature and both appear to belong to the Upper Eastern View Facies although the deeper sample may be transitional to the Lower Eastern View facies. Frypanning is present in both samples.

NARIMBA-1

KK # Ref #.	Depth (ft) /Type	$\overline{R}_v$max	Range	N	Sample description including liptinite fluorescence, maceral abundances, mineral fluorescence
					Mid Upper Eastern View Coal Measures (Early Eocene)
T8323	7810-7820	0.59	0.51-0.66	31	Sparse cutinite dull orange to weak brown, sparse sporinite
Ctgs	$\overline{R}_I$max	1.55	1.19-1.83	3	orange to dull orange, sparse resinite greenish yellow to dull orange, rare lamalginite orange, rare liptodetrinite orange to dull orange. (Carbonate>siltstone>coal. Coal abundant, vitrite> clarite. V>>L>I. Maceral group composition of coal (mf): vitrinite-92.0%, inertinite-<0.1%, liptinite-8.0%. Dom common, V>L>I. Vitrinite common, liptinite sparse, inertinite rare. Upper Eastern View facies. Mineral fluorescence patchy orange to absent. Iron oxides abundant. Pyrite common.)

The sample is early mature and the coal belongs to the Upper Eastern View facies.

PELICAN-3

KK # Ref #.	Depth (ft) /Type	$\overline{R}_v$max	Range	N	Sample description including liptinite fluorescence, maceral abundances, mineral fluorescence
					Upper Eastern View Coal Measures (Late Eocene)
T8324	5820-5880	0.51	0.41-0.59	27	Rare sporinite orange, rare lamalginite and liptodetrinite yellow
Ctgs	$\overline{R}_I$max	0.73	0.70-0.78	4	to orange. (Claystone>carbonate. Dom sparse, V>I>L. Vitrinite sparse, inertinite and liptinite rare. Oil drops rare greenish yellow. Mineral fluorescence patchy orange to absent. Iron oxides abundant. Pyrite common.)
					Upper Eastern View Coal Measures (Mid / Late Eocene)
T8325	6210-6240	0.53	0.44-0.65	27	Common cutinite orange to weak brown, sparse resinite greenish
Ctgs	$\overline{R}_I$max	0.88	0.75-1.10	6	yellow to dull orange, sparse suberinite dull orange to weak brown, sparse sporinite yellow to dull orange, rare liptodetrinite orange to dull orange. (Siltstone>>coal. Coal abundant, clarite> vitrite. V>>L>I. Maceral group composition of coal (mf): vitrinite-87.0%, inertinite-3.0%, liptinite-10.0%. Dom sparse, V>I>L. Vitrinite sparse, inertinite and liptinite rare. 'Frypanned' coal common. Mineral fluorescence absent. Iron oxides abundant. Pyrite abundant.)
					Upper Eastern View Coal Measures (Early Eocene)
T8326	7190-7200	0.59	0.49-0.67	31	Abundant suberinite dull orange to weak brown, abundant
Ctgs	$\overline{R}_I$max	0.97	0.83-1.07	6	resinite greenish yellow to dull orange, abundant sporinite yellow to dull orange, abundant cutinite orange to weak brown, common liptodetrinite orange to dull orange. (Coal>>claystone> carbonate. Coal dominant, clarite>vitrite>liptite. V>>L>I. Maceral group composition of coal (mf): vitrinite-83.0%, inertinite-1.0%, liptinite-16.0%. Dom sparse, V>L>I. Vitrinite sparse, liptinite and inertinite rare. 'Frypanned' coal rare. Mineral fluorescence absent. Iron oxides sparse. Pyrite rare.)

The three sample are all early mature and the organic facies is the Upper Eastern View facies.

SEAL-1

KK # Ref #.	Depth (ft) /Type	$\overline{R}_v$max	Range	N	Sample description including liptinite fluorescence, maceral abundances, mineral fluorescence
					Base of Demons Bluff Formation
T8327	3280.8-3313.6	0.43	0.40-0.49	26	Rare cutinite orange to dull orange, rare resinite yellow to dull orange, rare sporinite orange, rare liptodetrinite yellow to dull
Ctgs	$\overline{R}_I$max	1.03	0.70-1.40	6	orange. (Carbonate>siltstone>sandstone>coal. Coal sparse, duroclarite> clarite>vitrite. V>>L>I. Dom sparse, V>L>I. Vitrinite sparse, liptinite and inertinite rare. Higher plant inertinite prominent. Rare yellow oil inclusions within quartz grains. Glauconite rare. Mineral fluorescence patchy orange to absent. Iron oxides common. Major siderite. Pyrite common.)

The section sampled is immature but rare oil inclusions were noted within quartz grains.

TAROOK-1

KK # Ref #.	Depth (ft) /Type	$\overline{R}_v$max	Range	N	Sample description including liptinite fluorescence, maceral abundances, mineral fluorescence
					Top Upper Eastern View Coal Measures (Late Eocene)
T8328	6100-6160	0.52	0.44-0.58	18	Rare cutinite dull orange, rare liptodetrinite orange to dull
Ctgs	$\overline{R}_I$max	0.83	0.73-1.15	9	orange. (Siltstone>>carbonate. Dom sparse, I>V>L. Inertinite and vitrinite sparse, liptinite rare. Mineral fluorescence patchy dull orange to absent. Iron oxides common. Pyrite abundant.)
					Upper Eastern View Coal Measures (Mid Eocene)
T8329	6860-6870	0.53	0.46-0.61	28	Sparse cutinite and suberinite dull orange weak brown, sparse
Ctgs	$\overline{R}_I$max	0.86	0.75-1.00	5	resinite yellow to dull orange, rare sporinite yellow to dull orange, rare liptodetrinite orange to dull orange. (Calcareous siltstone>carbonate>siltstone>coal. Coal abundant, clarite> vitrite. V>>L>I. Maceral group composition of coal (mf): vitrinite-91.0%, inertinite-<0.1%, liptinite-9.0%. Dom sparse, V>I>L. Vitrinite and inertinite sparse, liptinite rare. Exsudatinite rare, yellow to orange. Mineral fluorescence patchy orange to absent. Iron oxides common. Pyrite abundant.)
					Upper Eastern View Coal Measures (Early Eocene)
T8330	7400-7430	0.54	0.46-0.61	27	Sparse cutinite and suberinite dull orange to weak brown, sparse
Ctgs	$\overline{R}_I$max	0.96	0.90-1.06	5	resinite greenish yellow to orange, sparse sporinite orange to dull orange, rare lamalginite and liptodetrinite orange to dull orange. (Siltstone>carbonate>coal. Coal abundant, duroclarite>clarite> vitrite. V>>I>L. Maceral group composition of coal (mf): vitrinite-88.6%, inertinite-1.4%, liptinite-10.0%. Dom common, V>L>I. All three maceral groups sparse. Oil drops rare, greenish yellow, some green oil haze developed on standing. 'Frypanned' coal sparse, effects widespread and penetrative. Mineral fluorescence patchy orange to absent. Iron oxides common. Pyrite abundant.)
					Upper Eastern View Coal Measures (Early Eocene)
T8331	7820-7850	0.58	0.50-0.67	27	Sparse cutinite dull orange weak brown, sparse resinite greenish
Ctgs	$\overline{R}_I$max	1.02	0.85-1.17	5	yellow to dull orange, sparse sporinite orange to dull orange, rare liptodetrinite orange to dull orange. (Siltstone>carbonate> coal. Coal abundant, clarite>vitrite. V>>I>L. Maceral group composition of coal (mf): vitrinite-95.8%, inertinite-0.2%, liptinite-4.0%. Dom common, V>L>I. All three maceral groups sparse. Fossil fragments rare. 'Frypanned' coal common and effects are penetrative. Mineral fluorescence patchy orange to absent. Iron oxides abundant. Pyrite common.)
					Upper Eastern View Coal Measures (Early Eocene)
T8332	8340-8380	0.61	0.50-0.67	29	Sparse cutinite orange to dull orange, sparse suberinite dull
Ctgs	$\overline{R}_I$max	0.98	0.85-1.10	5	orange to dull brown, sparse resinite and sporinite yellow to dull orange, sparse lamalginite orange to dull orange, sparse *Botryococcus*-related telalginite orange, rare liptodetrinite orange to dull orange. (Siltstone>carbonate>coal. Coal abundant, clarite >vitrite>duroclarite. V>>I>L. Maceral group composition of coal (mf): vitrinite-91.9%, inertinite-0.1%, liptinite-8.0%. Dom abundant, V>L>I. Vitrinite abundant, liptinite common, inertinite rare. 'Frypanned' coal sparse. Mineral fluorescence patchy orange to absent. Iron oxides abundant. Pyrite common.)

Frypanning of samples has been extensive and although oxidized rims were excluded and care was taken to exclude grains where the whole grains had elevated reflectances, it is possible that the vitrinite reflectance values for T8330 and T8331 are too high, possibly by about 0.04%. The section sampled ranges from early to mid-mature and all belong to the Upper Eastern View facies.

TOOLKA-1a

KK # Ref #.	Depth (ft) /Type	$\overline{R}_v$max	Range	N	Sample description including liptinite fluorescence, maceral abundances, mineral fluorescence
					Upper Eastern View Coal Measures (Late Eocene)
T8333 Ctgs	4880-4900	0.60	0.49-0.70	28	Sparse cutinite orange to weak brown, sparse suberinite dull orange to weak brown, rare resinite yellow to dull orange, rare sporinite and liptodetrinite yellow to dull orange, rare lamalginite dull orange. (Siltstone>carbonate>coal. Coal abundant, vitrite> clarite. V>>L>I. Maceral group composition of coal (mf): vitrinite-97.0%, inertinite-<0.1%, liptinite-3.0%. Dom common, V>I>L. Vitrinite common, inertinite and liptinite rare. 'Frypanned' coal abundant and effects are penetrative. Mineral fluorescence absent. Iron oxides abundant. Pyrite common.)
					Upper Eastern View Coal Measures (Early / Mid Eocene)
T8334	5580-5600	0.57	0.46-0.70	26	Sparse cutinite and resinite yellow to dull orange, sparse
Ctgs	$\overline{R}_I$max	1.00	0.95-1.05	5	suberinite dull orange to weak brown, rare sporinite yellow to dull orange, rare liptodetrinite orange to dull orange. (Siltstone> calcareous siltstone>coal. Coal abundant, vitrite>clarite, V>>L>I. Maceral group composition of coal (mf): vitrinite-95.0%, inertinite-2.0%, liptinite-3.0%. Dom common, V>L>I. Vitrinite common, inertinite and liptinite sparse. Exsudatinite rare, yellow. 'Frypanned' coal common and effects are penetrative. Mineral fluorescence patchy orange to absent. Iron oxides abundant. Pyrite common.)
					Mid/Upper Eastern View Coal Measures (Early Eocene)
T8335	6090-6100	0.58	0.50-0.72	30	Sparse resinite greenish yellow to dull orange, sparse cutinite
Ctgs	$\overline{R}_I$max	1.00	0.87-1.15	6	and suberinite dull orange to weak brown, sparse lamalginite orange to dull orange, rare sporinite yellow to dull orange, rare liptodetrinite orange to dull orange. (Siltstone>coal. Coal abundant, vitrite>clarite. V>>L>I. Maceral group composition of coal (mf): vitrinite-95.9%, inertinite-0.1%, liptinite-4.0%. Dom abundant, V>L>I. Vitrinite abundant, liptinite common, inertinite rare. Facies is generally Upper Eastern View but may be transitional to Lower Eastern View facies.. 'Frypanned' coal rare. Mineral fluorescence patchy dull orange to absent. Iron oxides abundant. Pyrite sparse.)

The value for the shallowest of the samples may be higher due to the effects of frypanning, but a corrected value is not less than 0.55%. T8335 is probably the least affected of the three. The section sampled is marginally mature.

YURONGI-1

KK # Ref #.	Depth (ft) /Type	$\overline{R}_v$max	Range	N	Sample description including liptinite fluorescence, maceral abundances, mineral fluorescence
					Upper Eastern View Coal Measures (Mid / Late Eocene)
T8336 Ctgs	4710-4740	0.41	0.36-0.50	31	Abundant resinite yellow to dull orange, common cutinite dull orange, common suberinite dull orange to weak brown, sparse sporinite yellow to orange, sparse *Botryococcus*-related telalginite bright orange, sparse liptodetrinite yellow to dull orange. (Coal>siltstone>carbonate. Coal dominant, vitrite> clarite. V>>L>I. Maceral group composition of coal (mf): vitrinite-90.0%, inertinite-<0.1%, liptinite-10.0%. Dom sparse, V>L>I. Vitrinite and liptinite sparse, inertinite rare. Exsudatinite sparse, yellow. Mineral fluorescence absent. Iron oxides common. Pyrite sparse.)
					Upper Eastern View Coal Measures (Early Eocene)
T8337	5580-5600	0.60	0.46-0.70	30	Sparse suberinite and cutinite dull orange to weak brown, sparse
Ctgs	$\overline{R}_I$max	0.97	0.90-1.05	6	resinite and sporinite yellow to dull orange, rare liptodetrinite orange to dull orange. (Carbonate>sandstone.coal. Coal major, duroclarite>vitrite. V>>I>L. Maceral group composition of coal (mf): vitrinite-85.0%, inertinite-11.0%, liptinite-4.0%. Dom rare, V>L>I. All three maceral groups rare. 'Frypanned' coal abundant and effects are extensive and intensive so that unaltered coal is difficult to find. It appears that the dom may be less affected. Mineral fluorescence patchy dull orange to absent. Iron oxides common. Pyrite sparse.)

The difference in vitrinite reflectance between the two samples may have been exaggerated by the effects of frypanning. T8336 is immature and T8337 is probably best interpreted as marginally mature.

Samples collected for vitrinite analyses, 23-25 October 2001, Petroleum Data Repositories, Geoscience Australia. Stratigraphic Codes: DB – Demons Bluff Formation, EVCM – Eastern View Coal Measures

Well	Sample	Inverval/s				Sample Type	Stratigraphic Location	Strat Tops m (KB)
		Depth (KB) m		Depth (KB) ft				
		Top	Base	Top				
Aroo-1	**1**	1749.6	1758.7	5740	5770	Cuttings	Lower Torquay Group (Early/Late Oligocene)	DB = 1814m
	2	2090.9	2097.0	6860	6880	Cuttings	Upper EVCM - Mid/Late Eocene	EVCM = 2052m
	3	2246.4	2249.4	7370	7380	Cuttings	Upper EVCM - Mid Eocene	
	4	2411.0	2414.0	7910	7920	Cuttings	Upper EVCM - Early/Mid Eocene	
	5	2706.6	2709.7	8880	8890	Cuttings	Mid/Upper EVCM - Early Eocene	
	6	3563.1	3566.2	11690	11700	Cuttings	Mid EVCM - Upper Cretaceous	
Bass-2	**1**	1161.7		3811.5		Core	Upper EVCM - Late Eocene	DB = 1103m EVCM = 1170m
Bass-3	**1**	1615.4	1618.5	5300	5310	Cuttings composite over two intervals	Upper EVCM - Late Eocene	DB = 1434m
		1618.5	1621.5	5310	5320			EVCM = 1170m
Chat-1	**1**	1209	1218	3966.5	3996.0	Cuttings composite over two intervals	Upper EVCM - Late Eocene	DB = 1071m
		1218	1227	3996.0	4025.5			EVCM = 1181m
	2	2337	2340	7667.2	7677.1		Mid EVCM - Late Cretaceous (Maastrictian)	
Nangkero-1	**1**	1962.9	1969.0	6440	6460	Cuttings	Upper EVCM - Mid/Late Eocene	DB = 1752m
	2	2526.8	2529.8	8290	8300	Cuttings	Mid EVCM - Cretaceous/Palaeoce Boundary	EVCM = 1881m
Narimba-1	**1**	2380.5	2383.5	7810	7820	Cuttings	Mid/Upper EVCM - Early Eocene	DB = 1654m EVCM = 1793m
Pelican-3	**1**	1773.9	1783.1	5820	5850	Cuttings composite over two intervals	Upper EVCM - Late Eocene	DB = 1665m
		1783.1	1792.2	5850	5880			EVCM = 1786m
	2	1892.8	1902.0	6210	6240	Cuttings	Upper EVCM - Mid/Late Eocene	
	3	2191.5	2194.6	7190	7200	Cuttings	Upper EVCM - Early Eocene	
Seal	**1**	1000	1010	3280.8	3313.6	Cuttings	Base of Demons Bluff Fm	DB = 885m EVCM = 1004m

Tarook-1	**1**	1859.3	1865.4	6100	6120	Cuttings composite over three intervals	Top Upper EVCM - Late Eocene	DB = 1726m
		1865.4	1871.5	6120	6140			EVCM = 1862m
		1871.5	1877.6	6140	6160			
	2	2090.9	2094.0	6860	6870	Cuttings composite over two intervals	Upper EVCM - Mid Eocene	
		2094.0	2097.0	6870	6880			
	3	2255.5	2258.6	7400	7410	Cuttings composite over three intervals	Upper EVCM - Early Eocene	
		2258.6	2261.6	7410	7420			
		2261.6	2264.7	7420	7430			
	4	2383.5	2386.6	7820	7830	Cuttings composite over three intervals	Upper EVCM - Early Eocene	
		2386.6	2389.6	7830	7840			
		2389.6	2392.7	7840	7850			
	5	2542.0	2545.1	8340	8350	Cuttings composite over four intervals	Upper EVCM - Early Eocene	
		2545.1	2548.1	8350	8360			
		2548.1	2551.2	8360	8370			
		2551.2	2554.2	8370	8380			
Toolka-1A	**1**	1487.4	1493.5	4880	4900	Cuttings	Upper EVCM - Late Eocene	DB = 1104m
	2	1700.8	1706.9	5580	5600	Cuttings	Upper EVCM - Earl/Mid Eocene	EVCM = 1330m
	3	1856.2	1859.3	6090	6100	Cuttings	Mid/Upper EVCM - Early Eocene	
Yurongi-1	**1**	1435.6	1444.8	4710	4740	Cuttings	Upper EVCM - Mid/Late Eocene	DB = 1302m
	2	1700.8	1706.9	5580	5600	Cuttings	Upper EVCM - Early Eocene	EVCM = 1379m

APPENDIX J.

UNCORRECTED BOTTOM HOLE TEMPERATURE DATA FOR BASS BASIN WELLS

Aaron Cummings and Peter Tingate, National Centre for Petroleum Geology and Geophysics

Well	Depth m	Temperature °C	Time Since Circulation (hrs)	Circulation Time (hrs)
Aroo-1	923.54	121.11	-	-
	2951.99	106.11	-	-
	3222.35	121.11	-	-
	3429.30	121.11	-	-
	3649.37	127.22	-	-
	3652.11	138.89	-	-
Bass-1	701.04	40.00	3	-
	1952.85	75.00	4	-
	2349.40	96.67	3	-
Bass-2	640.08	36.67	2	-
	640.08	36.67	4	-
	1687.37	68.33	4	-
	1800.45	72.22	4	-
Bass-3	853.74	46.11	3	-
	1900.43	83.33	2	-
	1900.43	86.11	3	-
	2411.27	96.11	2	-
	2433.83	97.78	3	-
Chat-1	3107.00	98.90	8	1.92
	3107.00	104.40	16.25	1.62
Cormorant-1	915.01	38.89	4	-
	915.01	40.00	6	-
	2640.48	80.00	5	-
	3000.76	92.22	5	-
	3000.76	71.11	9	-
	3000.76	114.44	19	-
Dondu-1	2577.08	115.56	7	-
	2577.08	108.89	7.5	-
	2695.96	111.11	11	-
	2926.99	92.22	3.5	-
	2926.99	116.67	4	-
	2926.99	119.44	6	-
	2926.99	126.67	11	-
Durroon - 1	933.60	35.56	7	-
	933.60	35.56	12	-
	1838.00	63.89	16	-
	1838.00	63.89	10.5	-
	1838.00	62.78	5	-
	3021.50	80.00	5	-
	3021.50	91.11	11	-

Flinders-1	1252.00	48.30	7.9	2.9
	2718.80	116.70	13.6	1.3
	2718.80	123.30	20.6	1.3
	2718.80	126.10	38.1	1.3
King-1	1239.20	56.70	10	2
	2225.20	83.30	10	3.5
	2225.20	88.30	14.1	3.5
	2225.20	92.20	26.4	3.5
	2225.20	100.00	34.1	3.5
	2225.20	102.20	38.4	3.5
	1486.00	63.70	14.5	2.5
	1436.25	62.00	16.8	2.5
	1460.00	64.30	21.2	2.5
	2122.00	88.30	26.7	2.5
Konkon-1	1537.11	76.11	4.5	-
	1537.11	65.56	5.5	-
	1537.11	68.89	7.5	-
Koorkah-1	1598.98	58.89	4	-
	3146.15	98.89	7.5	-
	3149.19	120.00	18	-
	3146.15	125.56	23.5	-
	3146.15	131.67	33	-
Nangkero-1	1005.84	44.44	3	-
	1005.84	44.44	6	-
	990.60	41.11	5	-
	2877.31	86.67	5	-
	2877.31	93.89	11	-
	2877.31	97.78	18	-
Narimba-1	2684.68	120.00	9	-
	2686.20	85.00	5	-
	2686.20	92.78	8	-
	2686.20	108.33	25	-
	2914.19	107.78	2.5	-
	2914.19	113.89	7	-
	3018.74	114.44	4	-
	3018.74	117.78	6	-
	3169.92	128.89	13	-
	3170.53	127.78	17	-
	3353.71	129.44	7.5	-
	3353.71	130.00	9.5	-
	3353.71	138.89	17	-
Pelican-1	2602.99	120.00	5	-
	2612.14	86.11	5	-
	2612.14	96.11	15	-
	2621.28	84.44	2.5	-
	2621.28	98.89	9	-
	3178.45	114.44	2.5	-
	3178.45	114.44	3	-
	3178.45	112.78	3.5	-
	3178.45	112.78	4	-

Pelican-2	2838.30	87.78	8	-
	2879.45	92.22	3	-
	2894.08	107.22	5	-
	2894.08	98.33	7	-
	2932.18	87.78	4.5	-
	3068.12	90.00	3	-
	3068.12	87.78	4	-
	3068.12	92.22	10	-
Pelican-3	2864.21	100.00	6.5	-
	2902.00	93.89	5	-
	2905.96	95.56	6	-
Pelican-4	872.95	37.78	3	-
	872.95	43.33	6	-
	2552.09	88.33	6	-
	2869.08	97.78	6	-
	2869.08	97.78	9	-
	2869.08	97.78	15	-
	2869.08	112.22	6	-
	2869.08	112.22	9	-
	2869.08	113.89	15	-
	3050.74	108.89	11	-
	3050.74	106.11	11.5	-
	3050.74	115.56	14	-
Pelican-5	1776.07	64.44	18	-
	3002.28	95.56	7.5	-
	3002.28	104.44	9.5	-
	3002.28	104.44	12	-
	3002.28	111.67	16.5	-
	3002.28	135.00	57	-
	3020.26	102.22	7.5	-
	3647.24	131.11	7.5	-
	3647.24	131.11	11	-
	3647.24	138.89	11	-
	3647.24	130.00	12	-
	3647.24	143.33	14.5	-
	3647.24	135.00	30.5	-
	3647.24	146.11	21	-
	4029.15	161.67	19.5	-
	4267.20	170.00	7	-
	4267.20	172.78	8.5	-
	4267.20	175.56	16.8	-
	4267.20	170.56	48	-
	4267.20	177.78	52	-
Pipipa-1	879.96	39.44	5.5	-
	2115.01	76.67	8.5	-
	2115.01	86.11	8.5	-
	2115.01	83.33	12.5	-
	2115.01	86.11	18	-

Poonboon-1	2690.47	98.89	8	-
	2690.47	100.00	18	-
	3198.27	106.67	6	-
	3198.27	113.33	12	-
	3258.31	108.89	2.5	-
	3258.31	120.00	12	-
	3259.23	112.78	12	-
	3267.46	115.56	3	-
Seal-1	1669.00	68.30	5.67	0.85
	1669.00	74.40	9.75	0.85
Squid-1	-	-	-	-
Tarook-1	2773.68	91.11	6	-
	2773.68	94.44	7	-
Tilana-1	1661.16	60.00	5	-
	3066.29	103.89	7.5	-
	3900.22	111.11	10	-
	3900.22	115.56	19.5	-
Toolka-1A	2714.85	101.11	6	-
	2714.85	104.44	7	-
	2714.85	106.67	18	-
	2714.85	106.67	23	-
Yolla-1	1759.00	75.00	10	-
	1982.11	72.22	5.5	-
	1982.11	78.89	9	-
	2022.96	78.89	14.5	-
	3347.01	121.11	9.5	-
	3347.01	132.22	18	-
	3347.01	140.00	18	-
	3347.01	143.33	24	-
	3347.01	137.78	31	-
Yurongi-1	2438.40	83.33	4.5	-
	2438.40	89.44	5.5	-
	2438.40	105.56	21	-

APPENDIX K.

KINETIC MODELLING OF PELICAN-5

Aaron Cummings, National Centre for Petroleum Geology and Geophysics

Kinetics calibration in Pelican-5

The interpreted depth to onset of oil expulsion in the previous chapter was modelled based upon source rock kinetic data described in Chapter 5 of this Record (Figure 5.17; Boreham et al., 2003). The range in source rock kinetic behaviour can be approximated by two end members that have been termed "Bass Resistive" and "Bass Labile" based upon coals analysed in Cormorant-1 (1686 m) and Konkon-1 (1280 m) respectively. A model was made for Pelican-5 where coals with end member kinetics were sited at different stratigraphic levels. Oil expulsion versus time plotted with maturity was carried out for a hypothetical coal at the base of the Paleocene (Middle EVCM) within Pelican-5. The saturation level of 0.8 gave the best fit to give expulsion at a vitrinite level of 0.75%. This value is high but coals typically need greater oil saturation levels prior to expulsion than shales.

Using a saturation value of 0.8 for oil and 0.1 for gas prior to expulsion, the base of Pelican-5 (*Upper T. longus*) was also plotted to display oil (Figure K1) and gas expulsion behaviour (Figure K2) over a wider maturity range. Mixed Type II/III kinetic parameters, based on BasinMod default values, give a reasonable approximation to the labile and resistive kinetic behaviour for oil expulsion. Kinetic parameters are given in Appendix III.

Figure K1. Plot of coal source rock oil expulsion and maturity versus time based upon kinetic descriptions of coal source rocks from the basal Paleocene horizon, Pelican-5 well. The end member kinetic behaviour brackets the range of coal expulsion behaviour for Bass Basin coals. A saturation of ~ 0.8 is required prior to expulsion for coals to expell oil at a vitrinite reflectance value of 0.75%. See Appendix K for kinetic parameters.

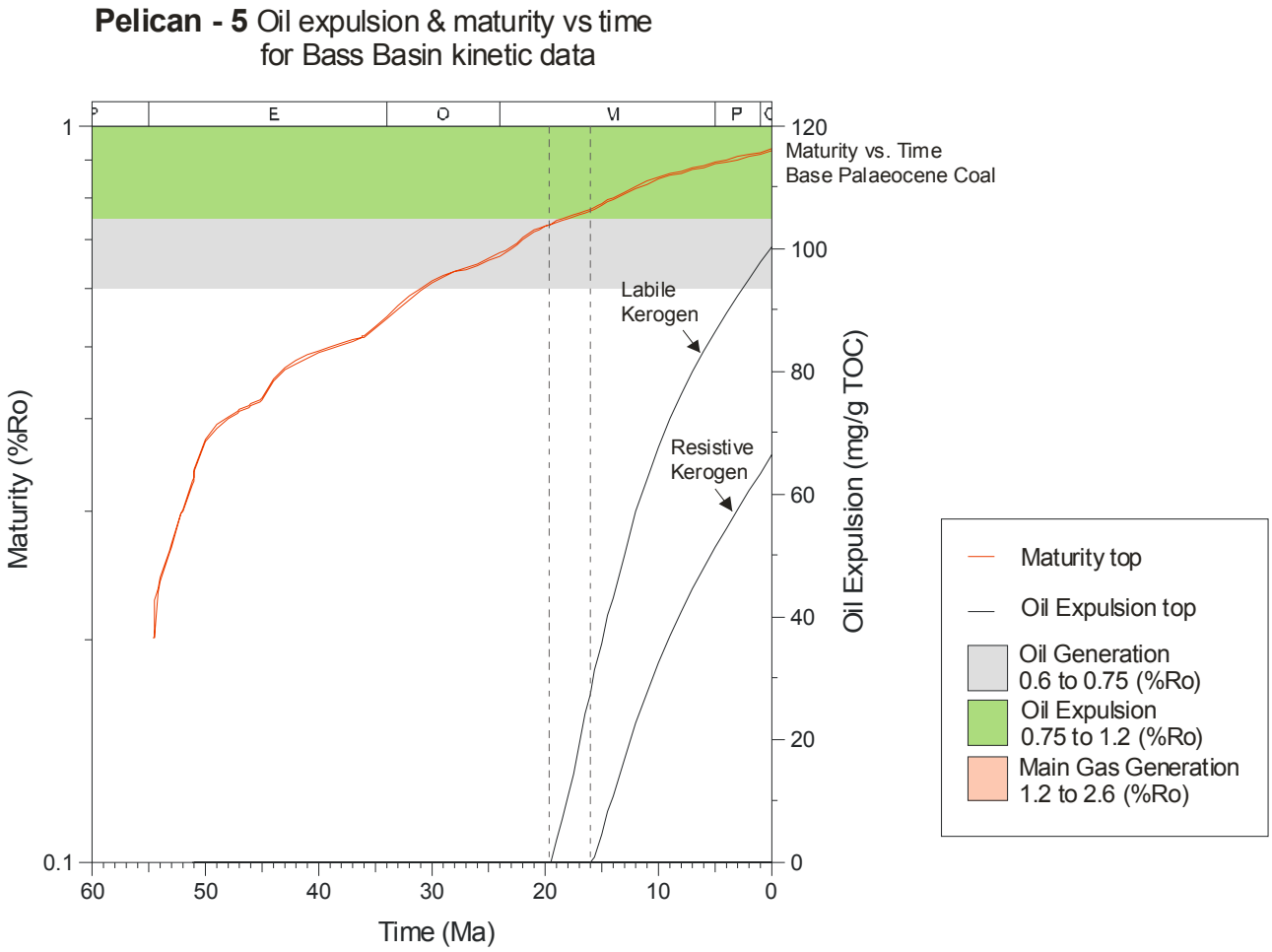
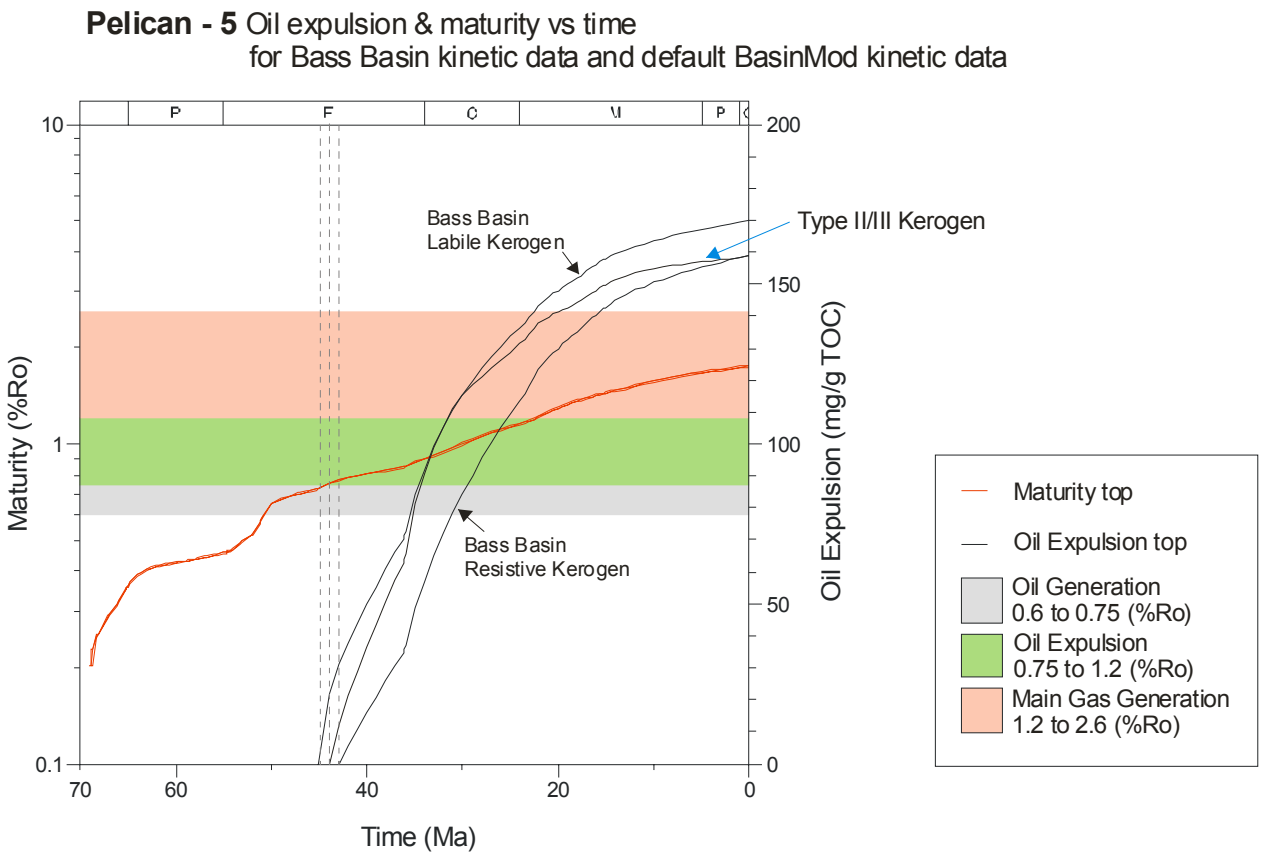


Figure K2. Comparison of oil expulsion versus time between end member coal kinetics and a mixture of BasinMod default Type II and Type III kinetics over a wider maturity range. The mixed Type II and Type III kinetic model approximates Bass Basin coal source rock behaviour reasonably well.



APPENDIX L

REPORT ON MERCURY INJECTION CAPILLARY PRESSURE TEST RESULTS

Ric Daniel and John Kaldi, National Centre for Petroleum Geology and Geophysics

This appendix contains the complete version of the "Hydrocarbon Seal Evaluation Study, Bass Basin, Tasmania" report as prepared for Mineral Resources Tasmania by the National Centre for Petroleum Geology and Geophysics (2002). This report has been formatted for inclusion in this appendix.

HYDROCARBON SEAL EVALUATION STUDY,

BASS BASIN,

TASMANIA

REPORT PREPARED FOR

MINERAL RESOURCES TASMANIA,

GEOSCIENCE AUSTRALIA,

NATIONAL CENTRE FOR PETROLEUM GEOLOGY AND GEOPHYSISCS

BY

RIC DANIEL

JOHN KALDI

2002

National Centre for Petroleum Geology and Geophysics

THE UNIVERSITY OF ADELAIDE, SOUTH AUSTRALIA

DISCLAIMER

The NCPGG shall not be liable or responsible for any loss, cost, damages or expenses incurred by the client, or any other person or company, resulting from any information or interpretation given in this report. In no case shall the NCPGG be responsible for failure to meet deadlines and lost production arising from this report.

EXECUTIVE SUMMARY

This report details the results of a study to determine seal capacity of potential seal rocks in the Bass Basin, Offshore Tasmania. Samples from eight wells were analysed using mercury injection capillary pressure (MICP) techniques.

A correlation of depositional environments to seal capacities reveal that environments with significant sealing capacity include fine-grained rocks from the lower and upper shoreface, interdistributary bays, lagoon and stacked crevasse channels/flood plains. Sensitivities to variations in contact angle (θ, interfacial tension (IFT) and subsurface fluid densities were included in the analysis. Capillary pressure results were used to determine seal capacities (hydrocarbon height retention), as well as pore-throat size distributions and height above free water level (HAFWL) versus water saturation (Sw). Hydrocarbon column heights for oil and gas were calculated for each sample. The sensitivities, in turn, were averaged for both oil and gas. Average sealing capacity for all samples were determined. The average column height of oil (density 0.735g/cc) able to be sealed is 605 metres. A column height of 262 metres of gas (density 0.1 g/cc) can be held. The highest oil column (>1400m) is supported by muds from the lower shoreface in Dondu 1. Lagoonal muds from Cormorant 1 will support an ~1140m column of oil, while the fluvial channel fills from Durroon 1 and Tilana 1 support > 700m oil column. Coastal plain, fluvial overbank and back barrier berm deposits are the least significant sealing lithologies in this study, supporting <200m oil columns.

L1. INTRODUCTION

Mineral Resources Tasmania, Geoscience Australia, and the National Centre for Petroleum Geology and Geophysics (NCPGG), University of Adelaide, undertook a joint study on petroleum systems in the Bass Basin. The NCPGG conducted the seal evaluation component of the study. Eight wells from the Bass Basin, offshore Tasmania were examined, and samples were taken from conventional cores. The aim of this part of the study is to assess the sealing capacity of specific mudstone/ siltstones, which are potential seals within the Bass Basin. Samples were analysed by Mercury Injection Capillary Pressure (MICP) Porosimetry.

Details on the operation and quality control of the porosimeter are described in Section L4. Individual plot of wells results follow this discussion. The Excel spreadsheets containing the MICP analytical data are not inlcuded in this PDF file. These spreadsheets are available in the "Seal Analyses Results" folder on the CD-ROM and should be accessed using Windows Explorer.

Samples from Bass Basin wells analysed by MICP

Well Name	Depth, metres	Sample type	Rock type
Bass-2	1164.5	Core	Carbonaceous laminated siltstone/mudstone
Bass-2	1261.0	Core	Carbonaceous laminated siltstone
Cormorant-1	1687.0	Core	Laminated siltstone/mudstone
Cormorant-1	1999.3	Core	Laminated mudstone
Cormorant-1	2231.6	Core	Very-fine grained sandstone/siltstone
Cormorant-1	2685.3	Core	Very-fine grained sandstone, carbonaceous siltstone
Dondu-1	2342.0	Core	Carbonaceous mudstone/siltstone
Durroon-1	3021.9	Core	Mudstone, very-fine grained sandstone
Pelican-5	2805.2	Core	Mudstone cemented
Pelican-5	2863.8	Core	Siltstone/sandstone
Pelican-5	2890.8	Core	Laminated siltstone
Poonboon-1	1954.2	Core	Siltstone
Poonboon-1	2473.8	Core	Carbonaceous laminated siltstone
Poonboon-1	2689.6	Core	Very-fine grained sandstone
Poonboon-1	3035	Core	Siltstone
Poonboon-1	3259	Core	Mudstone
Tilana-1	1667	Core	Carbonaceous siltstone, very-fine grained sandstone
Tilana-1	2800	Core	Carbonaceous mudstone
Yolla-2	3039	Core	Siltstone, very-fine grained sandstone

L2. METHODOLOGY

Mercury Injection Capillary Pressure (MICP)

The theory of the mercury porosimeter is based on the physical principle that a non-reactive, non-wetting liquid will not penetrate pores until sufficient pressure is applied to force its entrance. The relationship between the applied pressure and the pore size into which mercury will intrude is given by the Washburn equation:

$$PD = -4 \gamma \cos \theta$$

Where P is the applied pressure, D is the diameter, γ is the surface tension of mercury (480 dyne cm^{-1}) and θ is the contact angle between mercury and the pore wall, usually near 140°. This equation assumes that all pores are right circular cylinders. As pressure increases, the instrument senses the intrusion volume of mercury by the change in capacitance between the mercury column and a metal sheath surrounding the stem of the penetrometer. As the mercury column shortens, the pressure and volume data are continuously acquired by an attached personal computer. Mercury porosimetry is a technique, which is rate limited, as predicted by the Darcy equation. This describes the general function of pressure drop vs. flowrate.

Where p_1 is the upstream pressure, p_2 is the downstream pressure, L is the pore length, $1/\alpha$ is the permeability coefficient, μ is the fluid viscosity, V is the superficial velocity of fluid and g_c is a dimensional constant. The velocity of flow in a viscous liquid such as mercury is proportional to the pressure drop and inversely proportional to the length and surface area of the pore. Hence, given a specific limited flow velocity, the complete filling of a porous network will be a function of time. The larger the volume of pores the more time is required to fill the total pore volume completely. Therefore mercury porosimetry is most accurate when mercury is allowed to fill all the available pores, at equilibration.

The mercury injection porosimetry analyses for this study were carried out using a Micromeritics Autopore 9410 instrument (Section L4). This is composed of two separate systems, one for low pressure runs and the second for the high pressure runs. The low pressure run must always be done first, followed quickly by the high pressure run, to preclude the possibility of extra mercury intrusion into the sample by capillary action while the sample is held at atmospheric pressure at the conclusion of the low pressure run.

The system operates using the equilibration by time method - after the required pressure for a reading is attained it is held for twenty seconds to allow the amount of mercury entering the pores to stabilise. This is done because the process of mercury filling the pores is not an instantaneous one. Mercury begins entering the pores as soon as the pressure exceeds the value required for the pore throats' diameter, but the time required to fill the pores depends on the volume and shape of the pores. The equilibration by time process allows the pores to fill. If equilibration is not allowed, then the filling may not be complete when the reading is taken, which leads to estimation of lower pore volumes and smaller pore sizes than is actually the case.

Readings of mercury intrusion are taken by measuring the electrical capacitance of the penetrometer. This varies as the mercury is intruded from the precision bore stem into the pore space of the sample by the increasing pressure.

Each sample is washed in alcohol and dried at 60°C for 24 hours, weighed and placed into a penetrometer (a glass chamber attached to a precision bore nickel-plated glass tube) and the entire assembly weighed. This is placed in the low pressure port and evacuated to 0.05 torr. This vacuum is held for thirty minutes to ensure that no vapour remains in the sample. After this time the penetrometer is filled with mercury and the low pressure run is carried out. The pressure is increased incrementally from 2 psia to 28.94 psia, with a reading taken after 20 seconds of equilibration at each pressure. At the end of the low pressure run the penetrometer returns to atmospheric pressure. It is removed from the instrument and weighed to obtain its weight plus that of the mercury.

The penetrometer is then placed in the high pressure chamber, which uses hydraulic oil to take the pressure incrementally from 28.94 psia to 60,000 psia. Again readings are taken after a twenty second equilibration period. The pressure then decreases incrementally from 60,000 psia to 20 psia, with readings taken after the equilibration period. The sample is removed from the penetrometer and weighed.

Capillary Pressure

The samples were analysed using the Mercury Injection Capillary Pressure (MICP) techniques described in the above section on Methodology. MICP involves forcing a non-wetting fluid (mercury) into the pore system of a cleaned and dried core sample. The mercury displaces the wetting phase (air) that initially saturated the pores within the rock. Surface forces oppose the entrance of the mercury and pressure must be exerted to enable the mercury to enter the pores and thereby displace the air (Purcell, 1949). The smaller the pore throats, the greater the pressure required for the mercury enter the rock. Mercury saturation is commonly plotted as a function of mercury injection pressure.

Capillary pressure can be expressed as the relationship:

1) $Pc = 2\sigma \cos \tilde{\theta} r$

Where:

- Pc = Capillary Pressure (psi)
- σ = interfacial tension (dynes/cm)
- θ = contact angle (degrees)
- r = radius of capillary (microns)

MICP Plots

MICP plots of the side wall cores and cuttings samples are presented in the first two graphs in each set of analyses. These display the data in a lognormal format from 0-60,000 psi against volume of mercury injected into the sample (the lognormal format is useful for differentiating data points in the low-pressure

regime when analysing reservoir lithologies). The second graph displays plots of pressure against volume of mercury injected as a percentage (this is used for calculating the water saturation graphs).

Pore Throat Size

Using the following data for the air mercury system from (Vavra et al, 1992), capillary pressure data were converted to effective pore throat size:

Air/mercury contact angle (θa/m) = 140°, and
interfacial tension (σa/m) = 480 dynes/cm.
σ(a/m) cos θ(a/m)= 370
1 cm = 10,000 µm, (microns)
1 psi = 69035 dynes/cm2

Solving for r in equation results in the following relationship of capillary pressure to pore throat size:

1 psi = (approx.) 100 microns
10 psi = (approx.) 10 microns
100 psi = (approx.) 1 micron
1000 psi = (approx.) 0.1 micron

The cumulative pore-throat size distributions for the samples are presented in the third figure of the sample analysis set as lognormal size distribution.

Water Saturation

While MICP studies done solely for the purpose of determining pore throat radius and pore throat size distribution are valuable, there is, perhaps, even greater benefit in using these analyses to relate the rock types to saturations as a function of height above the FWL.

The mercury/air capillary pressure system is used to replicate static distribution of hydrocarbons in the subsurface. The initial pressure at which the mercury first displaces the air is referred to as "displacement pressure" (Pd). In the subsurface, buoyancy pressure drives hydrocarbon (the non-wetting phase) movement and forces it into the pore throats of a rock, displacing water (the wetting phase). Buoyancy is simply the density difference between hydrocarbon and brine multiplied by the column height and a constant (k) gravitational factor, which is 0.433. The greater the column thickness, the greater the buoyancy pressure driving the hydrocarbon.

Pd in the reservoir system is the pressure at which hydrocarbon first entered the pore system by displacing the water. Different rocks with different pore throat sizes will have different displacement pressures and different saturations as a function of height (h) above the free water level (FWL). Thus, in any given reservoir section, the lowest indication of live (vs residual) hydrocarbon in a particular rock type approximates the displacement pressure (Pd) for that rock. The Pd can thus be considered as the

hydrocarbon – water contact *for that particular rock type*. It should be remembered that a reservoir may have several hydrocarbon water contacts (as a function of pore properties controlled by rock type), but will have only one FWL. It is therefore of significance to determine the FWL.

In order to do this, capillary pressure data must first be converted to height above free water level information by using the equation:

2. $Pcb/o = h(\rho b-\rho o) \times 0.433$

   Where: Pcb/o = Capillary Pressure (psi) reservoir brine/oil system
   h = height (in ft.)
   ρb = rine density (gm/cc)
   ρo = density (gm/cc)

In order to use the capillary pressure relationships to interpret real subsurface data in such a way, the data must first be converted from the air/mercury system used in the laboratory to the hydrocarbon/brine system in the reservoir. Laboratory analyses of fluid samples from well completion reports indicate the following reservoir fluid parameters for the wells:

Gas Density - 0.1 gm/cc
Oil Density – 0.735 to 0.797 gm/cc
Brine Density – 1.01- 1.05 gm/cc

No measurements for Contact Angle and Interfacial Tensions were available, so based on existing data from other samples in the region the following values were considered reasonable:

System	Contact angle (θ)	Interfacial tension (σ)
Brine/oil	5	15 dynes/cm
Brine/gas	0°	30 dynes/cm
Air/mercury	140°	485 dynes/cm

Once the capillary pressure values have been converted to h (height in metres), a plot of height versus mercury (non-wetting phase) saturations can be constructed. However, conversion of mercury (non-wetting phase) to hydrocarbon (non-wetting phase) will now result in a height versus hydrocarbon saturation plot. Since water (wetting phase) saturation is more commonly used in the oil and gas industry, the non-wetting

phase saturation needs to be converted to water (wetting-phase) saturation (Schowalter, 1979). This is done using the simple conversion:

3) Sw = 1 – Snw
here: Sw = wetting phase (water) saturation
nw = non-wetting phase (hydrocarbon) saturation

Combining equations (2) and (3) results in a plot of height (above FWL) versus water saturation.

Saturation height functions were calculated using input parameters of the brine and hydrocarbon densities indicated in well completion reports (above). The conversion was run using a brine density value (1.01 to 1.05 gm/cc) and the oil density (0.735 to 0.797 gm/cc). and the Sw versus height functions were plotted on the fourth and fifth graph (linear and semi log formats, respectively) for each sample analysis. The column height versus water saturation curves for each well were also plotted on a single graph for comparison, both in linear and semi-log format (see combined colour plots below)

L3. SEAL CAPACITY

A summary of the water saturation curves for the samples from the Bass basin is presented in the following coloured composite graphs of normal (linear) and lognormal parameters. The average hydrocarbon height is highlighted on each graph. The lognormal graphs are more definitive as a result of larger scale values in the lower height range. Sensitivities determined for the study were determined from Bass Basin well completion reports and corroborated with data from adjacent areas. Tables and corresponding plots of the various sensitivities are presented, following the composite water saturation curves.

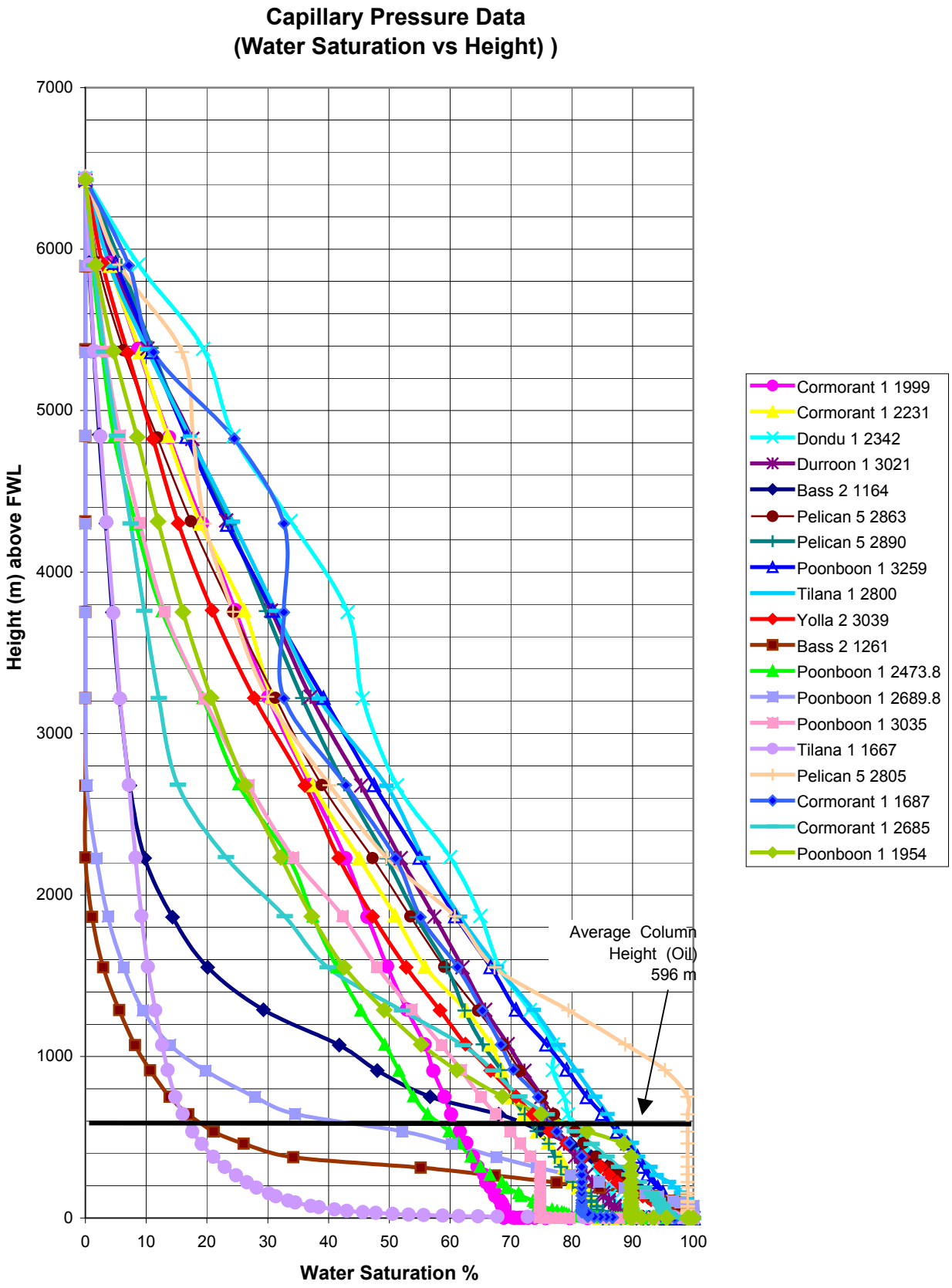
The threshold or displacement pressure of the samples from the Bass Basin, averages **5835 psia at 596** metres above free water level. This means that the average sealing lithology will support a **596 metre column of oil** with a density of ~ 0.735 gm/cc (or a **263 metre column of gas** with a density of 0.1 gm/cc).

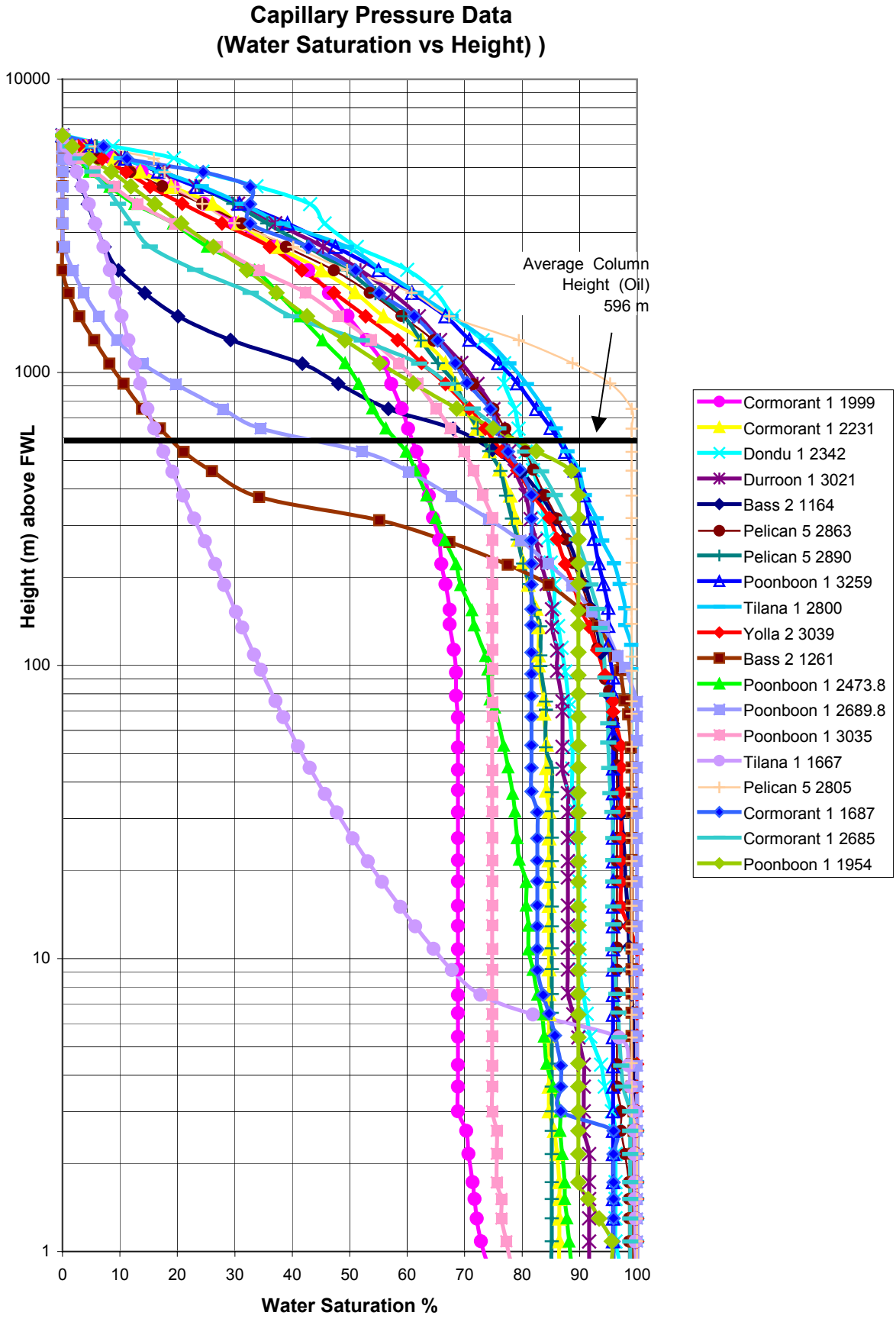
The results and interpretation of the analyses on sediments from the these wells can be viewed in terms of minimum hydrocarbon heights that can be supported by the sealing lithologies. The seal lithological samples are derived from a variety of depositional environments, which are highlighted in the following graphs and are shown below. Plots of length versus width and area versus thickness of ancient and modern analogues of seal depositional environments (mudstone and siltstone lithologies) are presented. These highlight the spatial extent of the various depositional environments attributed to the potential sealing lithologies analysed in this study.

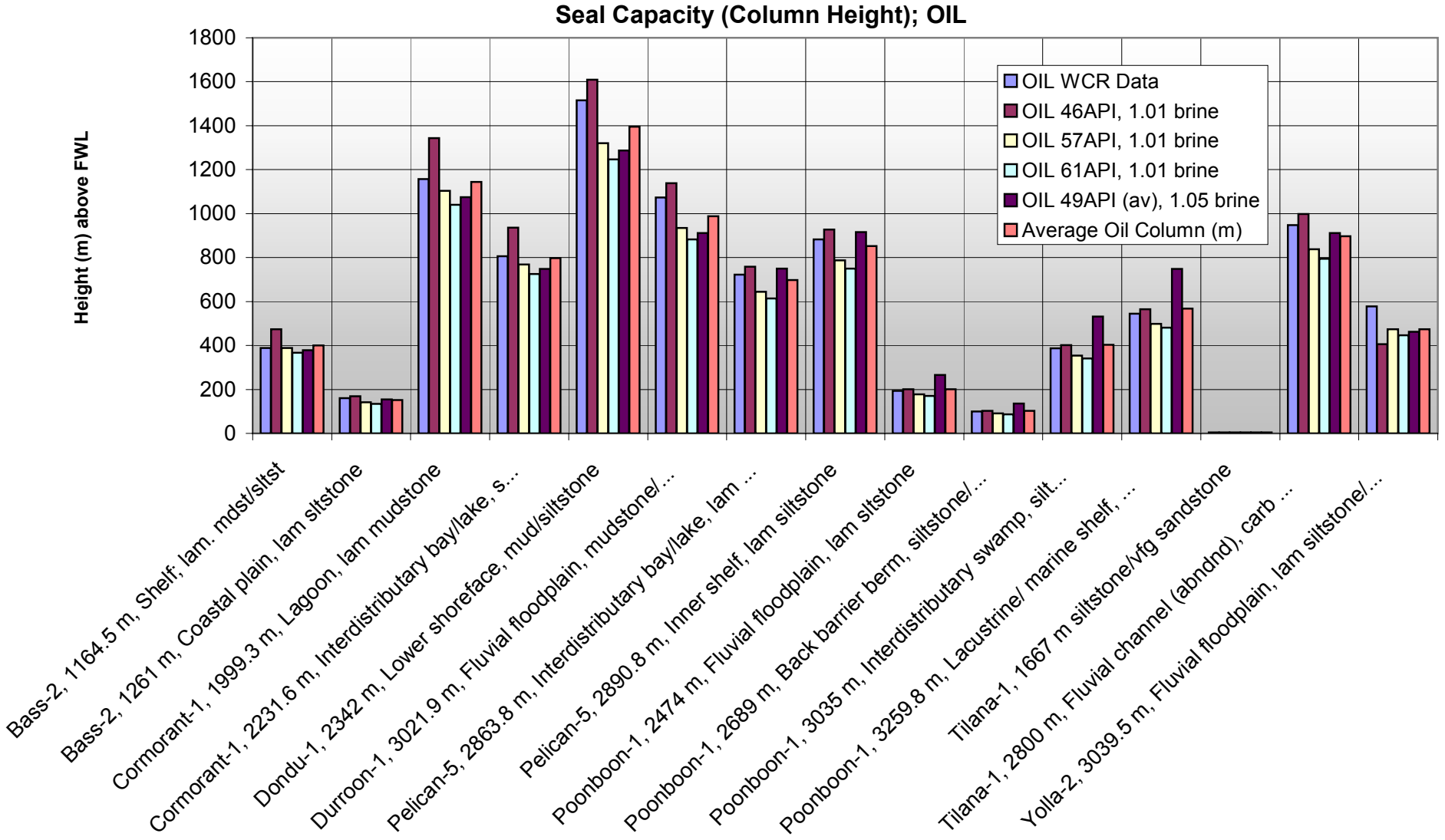
DEPOSITIONAL ENVIRONMENT
Shelf
Lower Shoreface
Foreshore - Upper Shoreface
Back Barrier Lagoon/Lake
Lacustrine or Marine (shelf)
Back Barrier Berm
Coastal Plain (?)
Interdistributary Bay/Lake
Interdistributary Swamp/Marsh
Fluvial Channel
Fluvial Overbank
Stacked Crevasse Channel
Fluvial Overbank; Crevasse Splays/Channels

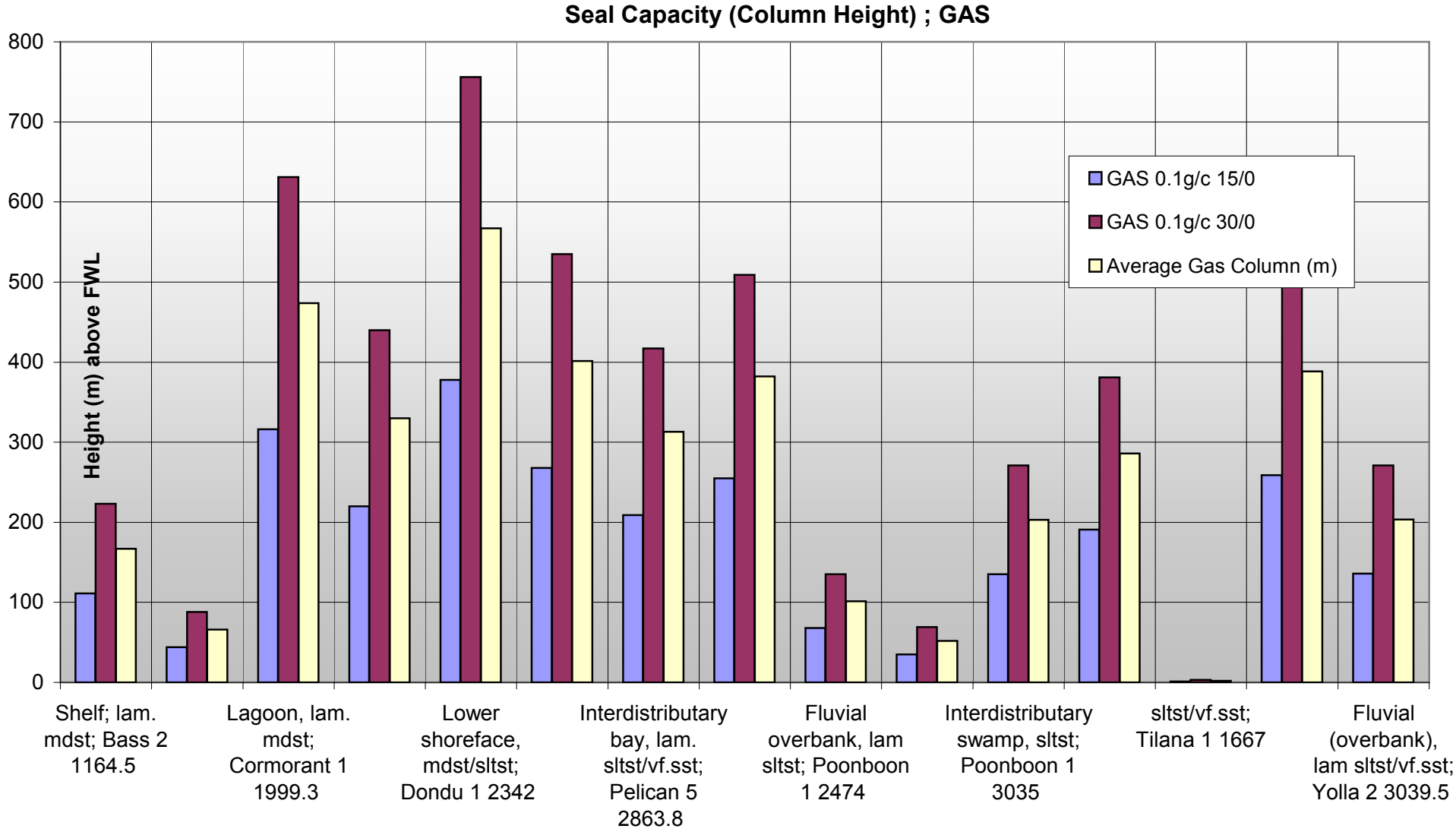
Significant seal depositional environments determined from this study are the lower shore face (muds) lagoons (silty muds) and abandoned channel fill (silty muds). The areal distribution of these environments are >1,000 km^2, 10-1000 km^2 and 1 km^2, with thicknesses 1-30 m, 2-1-50 m and 5-10 m respectively.

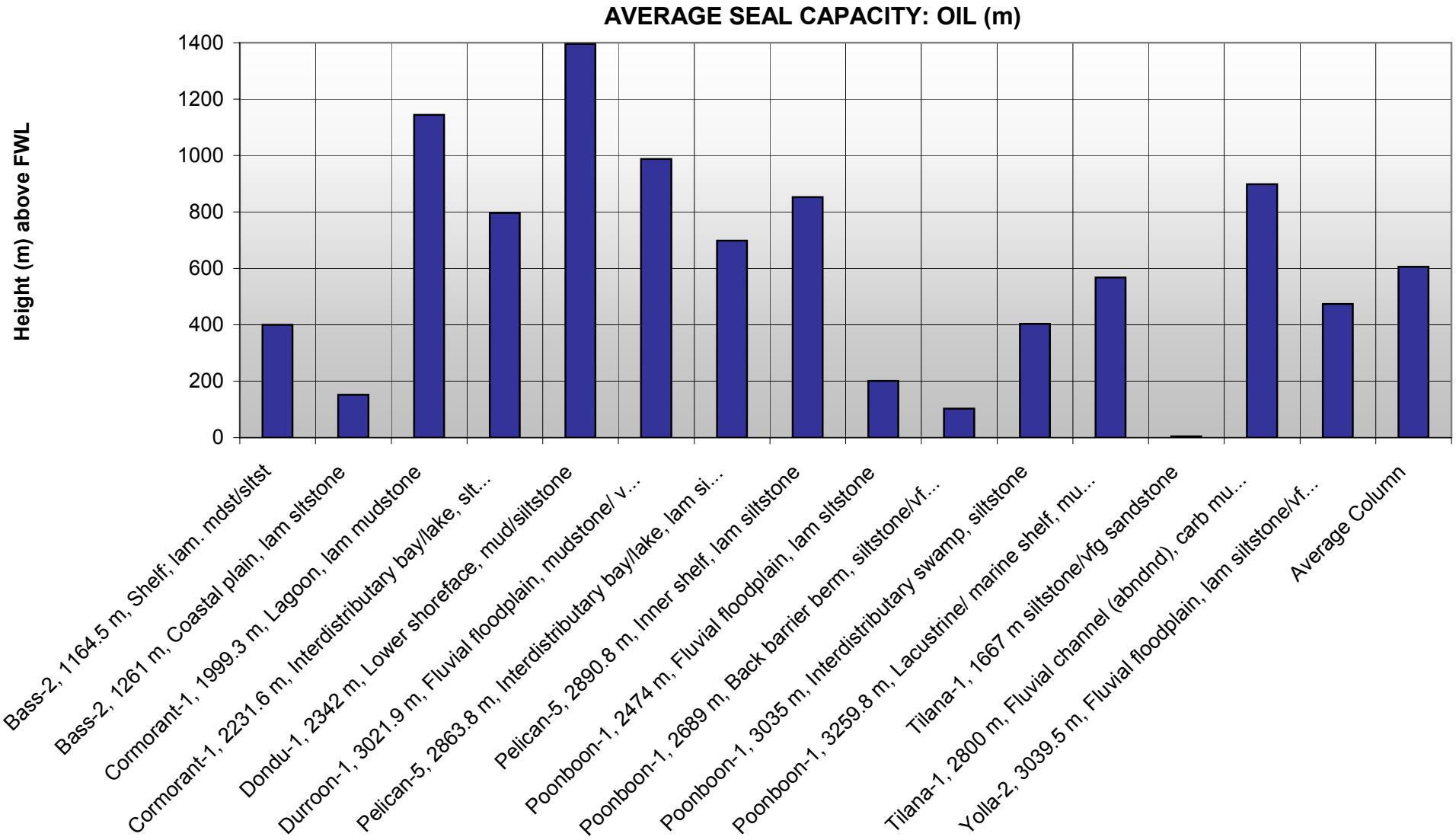
The highest oil column (>1400 m) is supported by mudsones from the lower shoreface in Dondu 1. Lagoonal mudstones from Cormorant 1 will support an ~1140 m column of oil, while the fluvial channel fill mudstones from Durroon 1 and Tilana 1 support > 700 m oil column. Coastal plain, fluvial overbank and back barrier berm deposits are the least significant sealing lithologies in this study (siltstones to very fine sandstones), supporting <200 m oil columns.

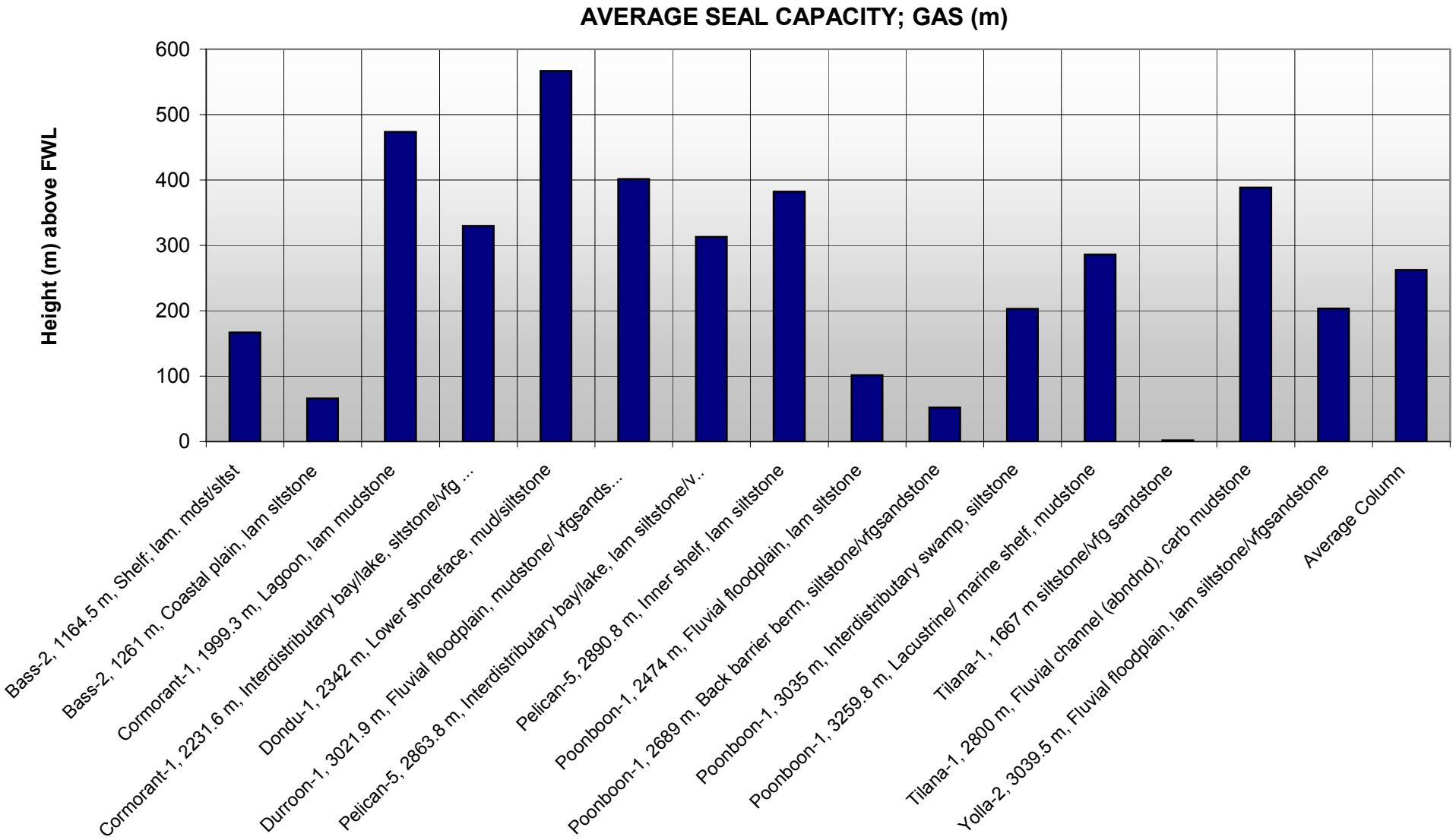

Capillary Pressure Data
(Water Saturation vs Height))
Height (m) above FWL
7000
6000
5000
4000
3000
2000
1000
0
0
10
20
30
40
50
60
70
80
90
100
Water Saturation %
Average Column Height (Oil) 596 m
Cormorant 1 1999
Cormorant 1 2231
Dondu 1 2342
Durroon 1 3021
Bass 2 1164
Pelican 5 2863
Pelican 5 2890
Poonboon 1 3259
Tilana 1 2800
Yolla 2 3039
Bass 2 1261
Poonboon 1 2473.8
Poonboon 1 2689.8
Poonboon 1 3035
Tilana 1 1667
Pelican 5 2805
Cormorant 1 1687
Cormorant 1 2685
Poonboon 1 1954

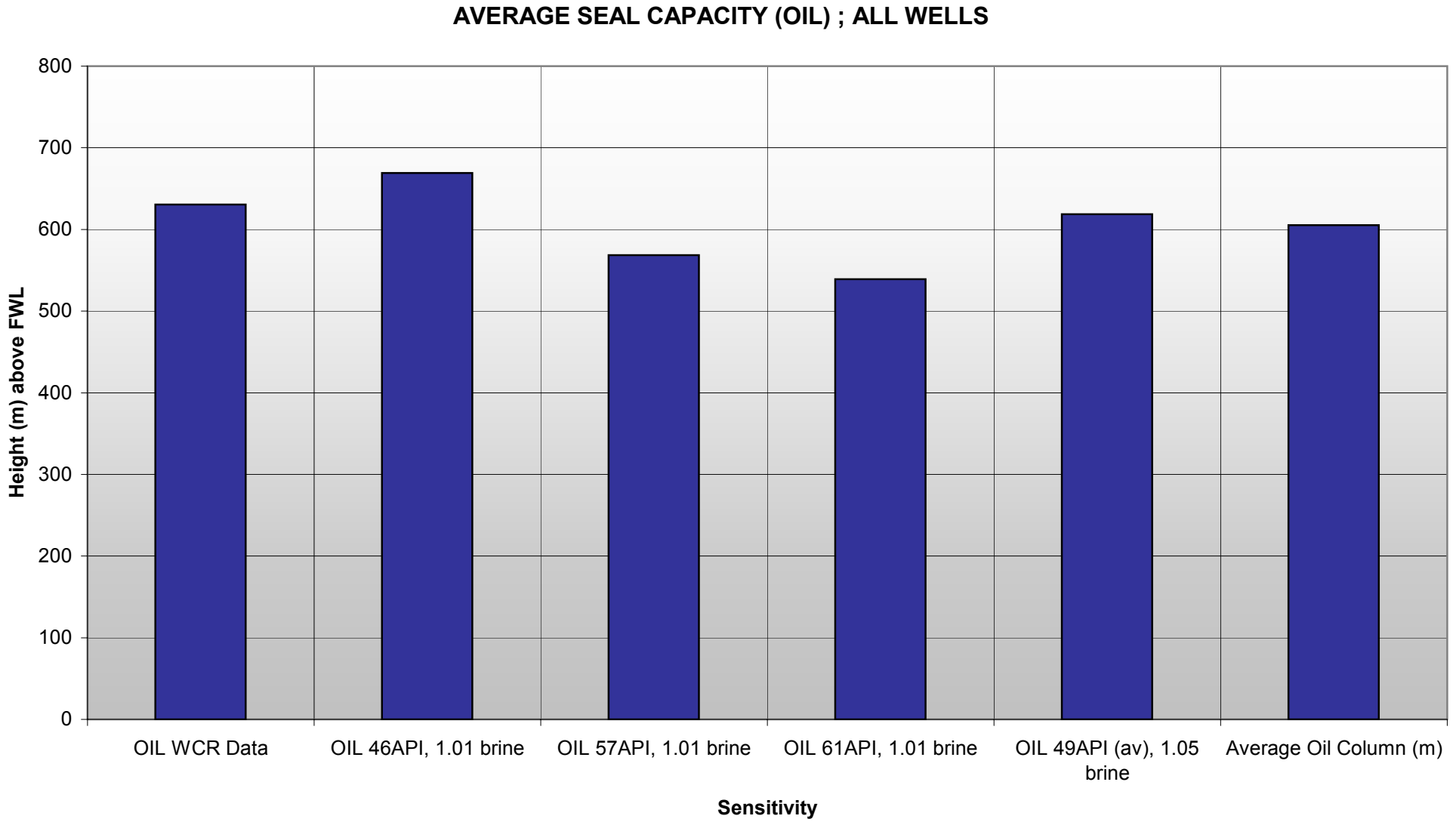

Capillary Pressure Data
(Water Saturation vs Height))
Height (m) above FWL
10000
1000
100
10
1
0
10
20
30
40
50
60
70
80
90
100
Water Saturation %
Average Column
Height (Oil)
596 m
Cormorant 1 1999
Cormorant 1 2231
Dondu 1 2342
Durroon 1 3021
Bass 2 1164
Pelican 5 2863
Pelican 5 2890
Poonboon 1 3259
Tilana 1 2800
Yolla 2 3039
Bass 2 1261
Poonboon 1 2473.8
Poonboon 1 2689.8
Poonboon 1 3035
Tilana 1 1667
Pelican 5 2805
Cormorant 1 1687
Cormorant 1 2685
Poonboon 1 1954

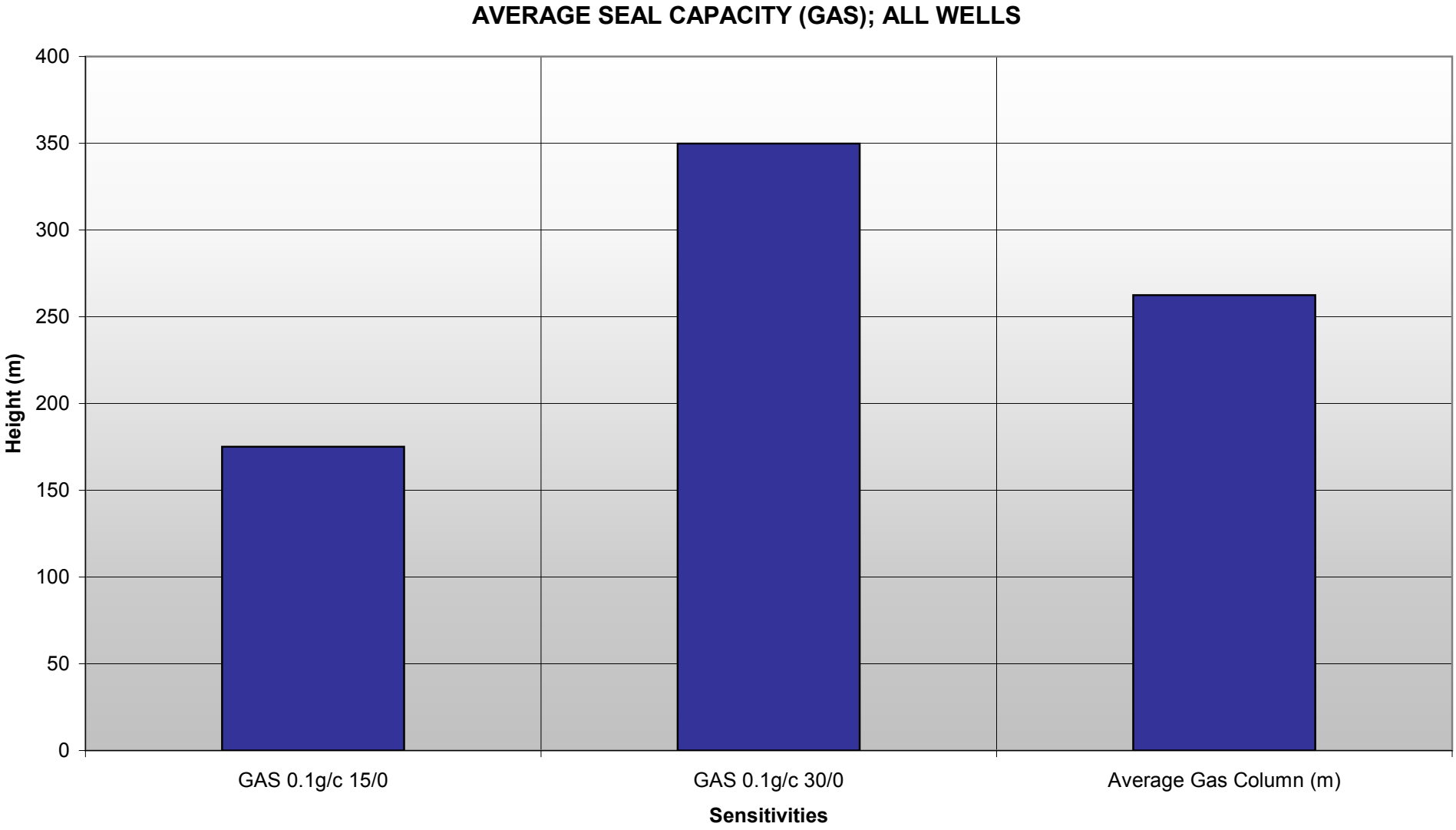

Seal Capacity (Column Height); OIL
Height (m) above FWL
1800
1600
1400
1200
1000
800
600
400
200
0
OIL WCR Data
OIL 46API, 1.01 brine
OIL 57API, 1.01 brine
OIL 61API, 1.01 brine
OIL 49API (av), 1.05 brine
Average Oil Column (m)
Bass-2, 1164.5 m, Shelf; lam. mdst/sltst
Bass-2, 1261 m, Coastal plain, lam sltstone
Cormorant-1, 1999.3 m, Lagoon, lam mudstone
Cormorant-1, 2231.6 m, Interdistributary bay/lake, s...
Dondu-1, 2342 m, Lower shoreface, mud/siltstone
Durroon-1, 3021.9 m, Fluvial floodplain, mudstone/...
Pelican-5, 2863.8 m, Interdistributary bay/lake, lam ...
Pelican-5, 2890.8 m, Inner shelf, lam siltstone
Poonboon-1, 2474 m, Fluvial floodplain, lam sltstone
Poonboon-1, 2689 m, Back barrier berm, siltstone/...
Poonboon-1, 3035 m, Interdistributary swamp, silt...
Poonboon-1, 3259.8 m, Lacustrine/ marine shelf, ...
Tilana-1, 1667 m siltstone/vfg sandstone
Tilana-1, 2800 m, Fluvial channel (abndnd), carb ...
Yolla-2, 3039.5 m, Fluvial floodplain, lam siltstone/...


Seal Capacity (Column Height) ; GAS
Height (m) above FWL
800
700
600
500
400
300
200
100
0
GAS 0.1g/c 15/0
GAS 0.1g/c 30/0
Average Gas Column (m)
Shelf; lam. mdst; Bass 2 1164.5
Lagoon, lam. mdst; Cormorant 1 1999.3
Lower shoreface, mdst/sltst; Dondu 1 2342
Interdistributary bay, lam. sltst/vf.sst; Pelican 5 2863.8
Fluvial overbank, lam sltst; Poonboon 1 2474
Interdistributary swamp, sltst; Poonboon 1 3035
sltst/vf.sst; Tilana 1 1667
Fluvial (overbank), lam sltst/vf.sst; Yolla 2 3039.5


AVERAGE SEAL CAPACITY: OIL (m)
Height (m) above FWL
1400
1200
1000
800
600
400
200
0
Bass-2, 1164.5 m, Shelf; lam. mdst/sltst
Bass-2, 1261 m, Coastal plain, lam sltstone
Cormorant-1, 1999.3 m, Lagoon, lam mudstone
Cormorant-1, 2231.6 m, Interdistributary bay/lake, slt...
Dondu-1, 2342 m, Lower shoreface, mud/siltstone
Durroon-1, 3021.9 m, Fluvial floodplain, mudstone/ v...
Pelican-5, 2863.8 m, Interdistributary bay/lake, lam si...
Pelican-5, 2890.8 m, Inner shelf, lam siltstone
Poonboon-1, 2474 m, Fluvial floodplain, lam sltstone
Poonboon-1, 2689 m, Back barrier berm, siltstone/vf...
Poonboon-1, 3035 m, Interdistributary swamp, siltstone
Poonboon-1, 3259.8 m, Lacustrine/ marine shelf, mu...
Tilana-1, 1667 m siltstone/vfg sandstone
Tilana-1, 2800 m, Fluvial channel (abndnd), carb mu...
Yolla-2, 3039.5 m, Fluvial floodplain, lam siltstone/vf...
Average Column


AVERAGE SEAL CAPACITY; GAS (m)
Height (m) above FWL
600
500
400
300
200
100
0
Bass-2, 1164.5 m, Shelf; lam. mdst/sltst
Bass-2, 1261 m, Coastal plain, lam sltstone
Cormorant-1, 1999.3 m, Lagoon, lam mudstone
Cormorant-1, 2231.6 m, Interdistributary bay/lake, sltstone/vfg ...
Dondu-1, 2342 m, Lower shoreface, mud/siltstone
Durroon-1, 3021.9 m, Fluvial floodplain, mudstone/ vfgsands...
Pelican-5, 2863.8 m, Interdistributary bay/lake, lam siltstone/v..
Pelican-5, 2890.8 m, Inner shelf, lam siltstone
Poonboon-1, 2474 m, Fluvial floodplain, lam sltstone
Poonboon-1, 2689 m, Back barrier berm, siltstone/vfgsandstone
Poonboon-1, 3035 m, Interdistributary swamp, siltstone
Poonboon-1, 3259.8 m, Lacustrine/ marine shelf, mudstone
Tilana-1, 1667 m siltstone/vfg sandstone
Tilana-1, 2800 m, Fluvial channel (abndnd), carb mudstone
Yolla-2, 3039.5 m, Fluvial floodplain, lam siltstone/vfgsandstone
Average Column


AVERAGE SEAL CAPACITY (OIL) ; ALL WELLS
800
700
600
500
400
300
200
100
0
Height (m) above FWL
OIL WCR Data
OIL 46API, 1.01 brine
OIL 57API, 1.01 brine
OIL 61API, 1.01 brine
OIL 49API (av), 1.05 brine
Average Oil Column (m)
Sensitivity


AVERAGE SEAL CAPACITY (GAS); ALL WELLS
Height (m)
400
350
300
250
200
150
100
50
0
GAS 0.1g/c 15/0
GAS 0.1g/c 30/0
Average Gas Column (m)
Sensitivities

APPENDIX L. SENSITIVITIES, BASS BASIN WELL SAMPLES, AVERAGE COLUMN HEIGHTS													
	OIL WCR Data	OIL 46API, 1.01 brine	OIL 57API, 1.01 brine	OIL 61API, 1.01 brine	OIL 49API (av), 1.05 brine	Average Oil Column (m)	GAS 0.1g/c 15/0	GAS 0.1g/c 30/0	Average Gas Column (m)	GAS 0.1g/c 15/0	GAS 0.1g/c 30/0	Average Gas Column (m)	Average Oil Height (m)
Bass-2, 1164.5 m, Shelf; lam. mdst/sltst	389	474	389	367	379	400	111	223	167	111	223	167	400
Bass-2, 1261 m, Coastal plain, lam sltstone	160	169	142	135	154	152	44	88	66	44	88	66	152
Cormorant-1, 1999.3 m, Lagoon, lam mudstone	1157	1344	1103	1040	1075	1144	316	631	474	316	631	474	1144
Cormorant-1, 2231.6 m, Interdistributary bay/lake, sltstone/vfg siltone	806	936	768	725	749	797	220	440	330	220	440	330	797
Dondu-1, 2342 m, Lower shoreface, mud/siltstone	1515	1609	1320	1246	1287	1395	378	756	567	378	756	567	1395
Durroon-1, 3021.9 m, Fluvial floodplain, mudstone/ vfgsandstone	1073	1139	935	882	911	988	268	535	402	268	535	402	988

Pelican-5, 2863.8 m, Interdistributary bay/lake, lam siltstone/vfg sandstone	**723**	**759**	**645**	**614**	**750**	**698**	**209**	**417**	**313**	**209**	**417**	**313**	**698**
Pelican-5, 2890.8 m, Inner shelf, lam siltstone	**882**	**927**	**788**	**750**	**916**	**853**	**255**	**509**	**382**	**255**	**509**	**382**	**853**
Poonboon-1, 2474 m, Fluvial floodplain, lam sltstone	**193**	**201**	**177**	**170**	**266**	**201**	**68**	**135**	**102**	**68**	**135**	**102**	**201**
Poonboon-1, 2689 m, Back barrier berm, siltstone/vfgsandstone	**99**	**103**	**91**	**87**	**136**	**103**	**35**	**69**	**52**	**35**	**69**	**52**	**103**
Poonboon-1, 3035 m, Interdistributary swamp, siltstone	**387**	**401**	**354**	**341**	**532**	**403**	**135**	**271**	**203**	**135**	**271**	**203**	**403**
Poonboon-1, 3259.8 m, Lacustrine/ marine shelf, mudstone	**545**	**565**	**499**	**481**	**749**	**568**	**191**	**381**	**286**	**191**	**381**	**286**	**568**
Tilana-1, 1667 m siltstone/vfg sandstone	**4**	**5**	**4**	**4**	**5**	**4**	**1**	**3**	**2**	**1**	**3**	**2**	**4**
Tilana-1, 2800 m, Fluvial channel (abndnd), carb mudstone	**947**	**998**	**838**	**795**	**911**	**898**	**259**	**518**	**389**	**259**	**518**	**389**	**898**
Yolla-2, 3039.5 m, Fluvial floodplain, lam siltstone/vfgsandstone	**578**	**406**	**474**	**447**	**462**	**473**	**136**	**271**	**204**	**136**	**271**	**204**	**473**
Average Column	**631**	**669**	**568**	**539**	**619**	**605**	**175**	**350**	**262**	**175**	**350**	**262**	**605**

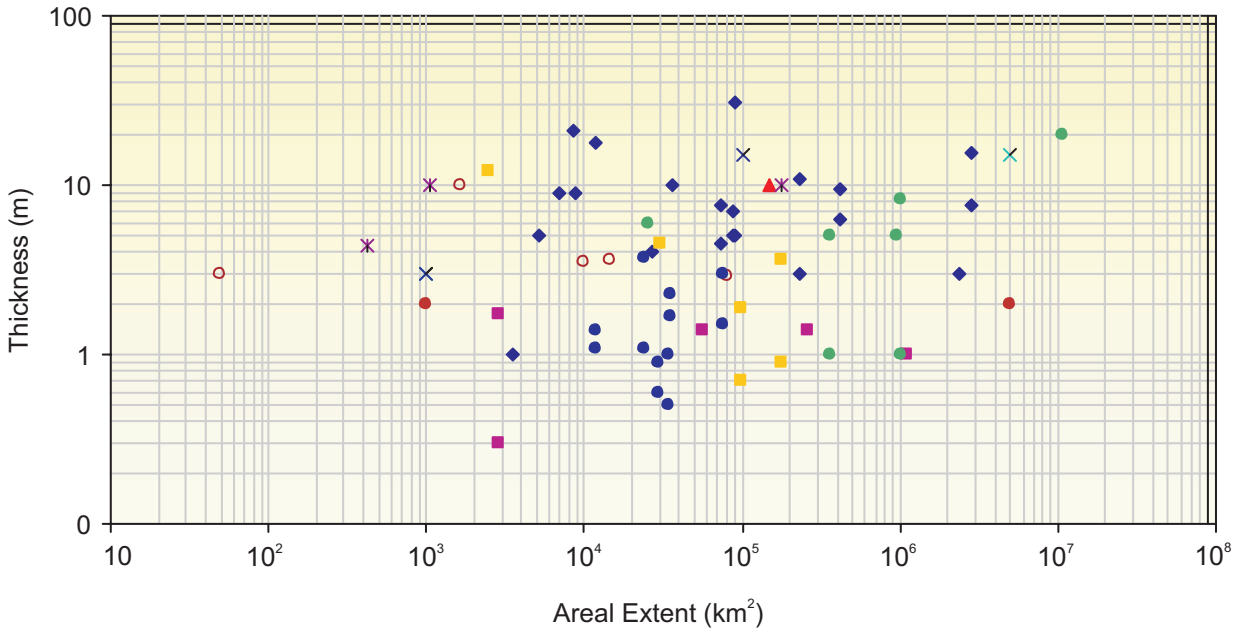
APPENDIX L. SEAL ANALYSIS RESULTS, BASS BASIN WELLS

WELL NAME	DEPTH		Seal Capacity (m)	LITHOLOGY	DEPOSITIONAL ENVIRONMENT	BIOZONE	Expected Length	Expected Width	Length/Width& Orientation
	METRES	*FEET*							
Bass-2	1164.49	3820.50	400	Carbonaceous, finely-laminated mudstone-siltstone	Shelf	*(?) P. asperopolus - Upper N. Asperus*	Several 10,000's to several 100,000s	Several 10,00's to a few 100,000's	~5 parallel w/ shoreline
Bass-2	1261.87	4140.00	152	Finely laminated siltstone, w/ carbonaceous chaff	Coastal plain, Interdistributary floodplain	*(?) P. asperopolus - Upper N. Asperus*	n/a	n/a	n/a
Cormorant-1	1999.30	6559.38	1144	Finely laminated mudstone	Back barrier lagoon/lake	*P. asperopolus - Upper M. diversus*	Few 1000's to a few 10,000's	A few 1000's to ~10,000	~3 parallel w/ shoreline
Cormorant-1	2231.60	7321.52	797	Interbedded siltstone and very fine-grained sandstone--starved and lenticular bedding, bioturbation	Interdistributary bay/lake	*Upper M. diversus*	Few 10,000's to several 10,000's	~10,000 to a few 10,000's	~2 parallel w/ shoreline
Cormorant-1	2648.10	8687.99	ts/micp	Carbonaceous mudstone w/ rare interbedded very fine-grained sandstone--starved ripple bedding	n/a	*Middle M. diversus*	n/a	n/a	n/a
Cormorant-1	2685.30	8810.04	ts/micp	Finely interbedded, very fine-grained sandstone and variably carbonaceous mudstone--biotrubated	n/a	*Middle M. diversus*	n/a	n/a	n/a
Dondu-1	2342.00	7683.73	1395	Moderately carbonaceous mudstone-siltsone	Lower shoreface	*Upper L. balmei*	Few 10,000's to several 10,000's	several 100 to several 1000's	~9 parallel w/ shoreline

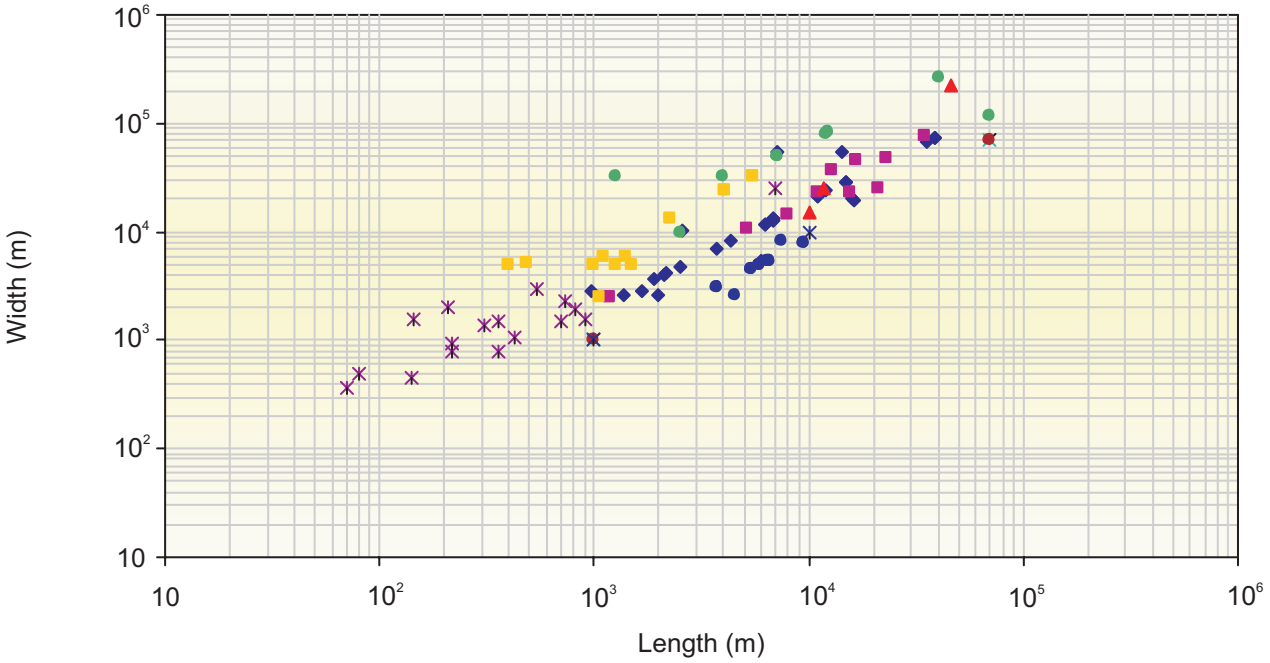
WELL NAME	DEPTH		Seal Capacity (m)	LITHOLOGY	DEPOSITIONAL ENVIRONMENT	BIOZONE	Expected Length	Expected Width	Length/Width& Orientation
	METRES	*FEET*							
Durroon-1	1690.73	5547.00	ts/micp	Very fine- to fine-grained sandstone	Fluvial overbank	*P. mawsonii*	Few 100 to several 100	Several 100 to several 1000's(?)	~10 parallel to main channel orientation
Durroon-1	3021.88	9914.30	988	Cemented, mudstone and fine-grained sandstone	Fluvial floodplain associated with stacked crevasse channels	*Early Cretaceous*	Few 100 to several 100	Several 100 to several 1000's(?)	~10 parallel to main channel orientation
Pelican-5	2805.20	9203.41	micp	Cemented(?) mudstone	n/a	*M. diversus*	n/a	n/a	n/a
Pelican-5	2863.80	9395.67	698	Very finely interbedded siltstone and very fine-grained sandstone--ripple laminated and bioturbated	Interdistributary bay/lake	*M. diversus*	Few 10,000's to several 10,000's	~10,000 to a few 10,000's	~2 parallel w/ shoreline
Pelican-5	2890.80	9484.25	853	Finely-laminated siltstone	Lower shoreface-inner-shelf and foreshore/upper shoreface	*M. diversus*	Few 10,000's to several 10,000's	several 100 to several 1000's	~9 parallel w/ shoreline
Poonboon-1	1954.20	6411.42	ts/micp	Siltstone	Lower shoreface-inner-shelf and foreshore/upper shoreface	*Middle N. asperus*	Few 10,000's to several 10,000's	several 100 to several 1000's	~9 parallel w/ shoreline
Poonboon-1	2473.80	8116.14	201	Finely laminated siltstone, w/ carbonaceous chaff	Fluvial floodplain	*Middle M. diversus*	Few 100 to several 100		~10 parallel to main channel orientation
Poonboon-1	2689.60	8824.15	136	Parallel stratified and ripple cross-laminated very fine-grained sandstone--bioturbated	Back-barrier beach berm	*Lower M. diversus*	n/a	n/a	n/a

WELL NAME	DEPTH		Seal Capacity (m)	LITHOLOGY	DEPOSITIONAL ENVIRONMENT	BIOZONE	Expected Length	Expected Width	Length/Width& Orientation
	METRES	*FEET*							
Poonboon-1	3035.00	9957.35	403	Siltstone--root traces	Interdistributary swamp/marsh	*Lower L. balmei*	n/a	n/a	n/a
Poonboon-1	3259.80	10694.88	568	Massive mudstone	Lacustrine or marine shelf	*Lower L. balmei*	Several 10,000's to several 100,000s	Several 10,00's to a few 100,000's	n/a
Tilana-1	1667.40	5470.47	4	Siltstone to very fine-grained sandstone w/ carbonaceous chaff	n/a	*Upper L. balmei*	n/a	n/a	n/a
Tilana-1	2800.00	9186.35	898	Massive, fissile, carbonaceous mudstone	Fluvial channel (abandoned)	*Upper L. balmei*	Several 1000's to several 10,000's (?)	Few 100 to a few 1000's	~15 parallel to channel orientation
Yolla-2	3039.45	9971.95	473	very finely interbedded siltstone and very fine-grained sandstone--ripple laminated	Fluvial floodplain	n/a	Few 100 to several 100	Several 100 to several 1000's(?)	~10 parallel to main channel orientation

Analogue Data: Thickness/Areal Extent for Seal Depositional Environments



Analogue Data: Width/Length for Seal Depositional Environments



- Back-Barrier Lagoon
- Fluvial Overbank
- Marsh/Swamp, Coastal Plain
- Interdistributary Bay
- Abandoned Channel
- Tidal Flats
- Lacustrine
- Prodelta
- Upper Deltaic Plain
- Lower Deltaic Plain
- Shelf

L4. ANALYTICAL EQUIPMENT DETAILS, MICROMERITICS AUTOPORE 9410, MERCURY INJECTION POROSIMETER

General Arrangement of the System

The Autopore 9410 machine is composed of two separate systems, one for low pressure runs and the second for the high pressure runs. The low pressure run must always be done first, followed quickly by the high pressure run, to preclude the possibility of extra mercury intrusion into the sample by capillary action while the sample is held at atmospheric pressure at the conclusion of the low pressure run.

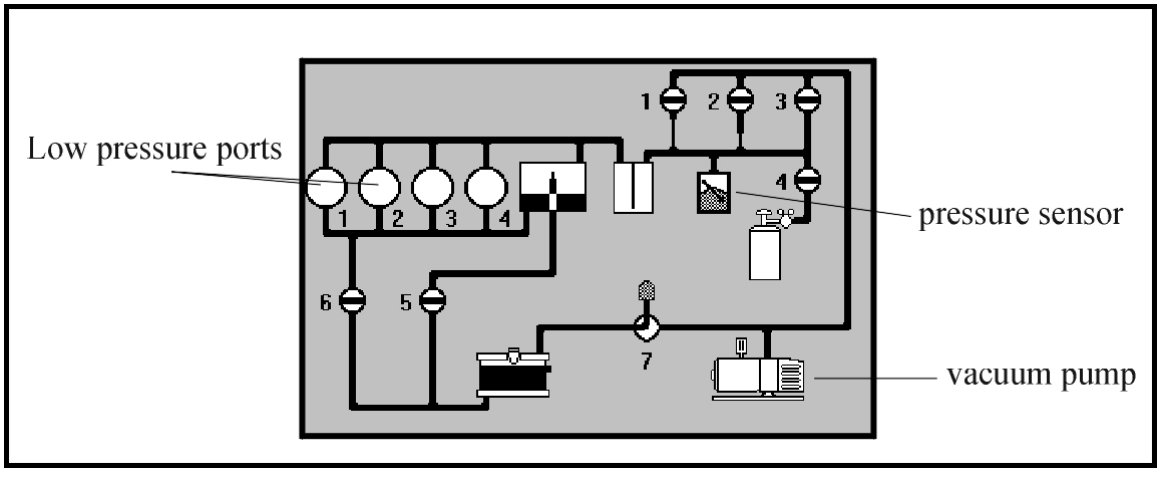
The system can operate using either the equilibration by time method - after the required pressure for a reading is attained it is held for twenty seconds to allow the amount of mercury entering the pores to stabilise – or the equilibration by intrusion rate method – the sample is held at the required pressure until the mercury volume has stabilised. This is done because the process of mercury filling the pores is not an instantaneous one. Mercury begins entering the pores as soon as the pressure exceeds the value required for the pore throats' diameter, but the time required to fill the pores depends on the volume and shape of the pores. The equilibration by time process allows the pores to fill. If equilibration is not allowed then the filling may not be complete when the reading is taken, which leads to estimation of lower pore volumes and smaller pore sizes than is actually the case. It is this method which is generally used here.

The system is controlled by a personal computer running the proprietary Micromeritics Autopore software under Windows 95. The program is simple to run, but can fail at times due to electrical problems and occasional unknown causes.

Low Pressure System

The low pressure system consists of two sample ports, a vacuum pump, a mercury reservoir and associated mercury fill chamber, an air pump, a pressure sensor and the associated valves, switches, electronics and piping (Figure L1).

Figure L1. Schematic layout of a Micromeritics Autopore porosimeter low pressure section.



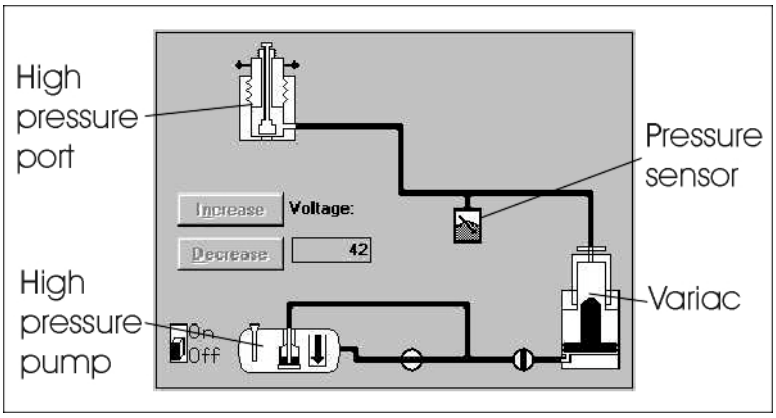
To operate the system, a weighed sample is placed in a penetrometer which is sealed and then placed in a low pressure port. The vacuum pump is switched on and the program is initiated. Any modifications to the running parameters are made at this point, and the run file, which lists the selected pressures for intrusion readings, is chosen. The particulars of the sample are then entered and the evacuation of the system is carried out to a vacuum of 0.5 torr. Once this value is reached the vacuum is held for a previously chosen period, usually five minutes. At the end of this time mercury is pumped from the reservoir to the fill chamber, from which it fills the penetrometer. The excess mercury is then drained back to the reservoir. The low pressure readings are taken from 2 psia up to a maximum of 50 psia (40 psia is the currently used pressure)and the sample is returned to atmospheric pressure at the conclusion of the run. Once atmospheric pressure is reached the penetrometer is removed from the low pressure port and weighed (this is the 'assembly weight'), the data being entered when starting the high pressure run. The low pressure run is then complete.

High Pressure System

The high pressure system (Figure L2.) consists of a high pressure port, a pump, a variac, pressure sensors and the associated valves, piping and electronics. The high pressure system can operate to pressures of 60,000 psia.

Data, including the name of the low pressure run data file and the assembly weight is entered. The penetrometer is placed in the high pressure port which is then closed and screwed down tight. The seal is closed and the run is commenced, at pressures from 45 psia to 60,000 psia and then back down to atmospheric pressure, with 20 second equilibration. The penetrometer is then removed from the high pressure port.

Figure L2. Schematic layout of a Micromeritics Autopore porosimeter high pressure section.



General Layout of the System

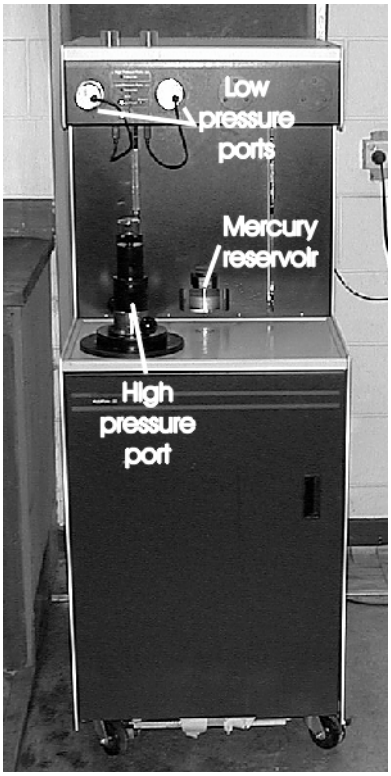
The mercury porosimetry instrument is located in Room H1-10b, immediately off H1-10. The desktop computer which controls the instrument is located in Room H1-10a adjacent to the mercury laboratory. The instrument and the computer are connected by a cable which travels via the ceiling and connects to them

via 9 pin 'D' connectors. On the computer connection is made via the COM1 port. There is only one port on the instrument. The main power switch is located at the lower right rear of the instrument, near the power connection. The vacuum pump runs at all times when the instrument is turned on.

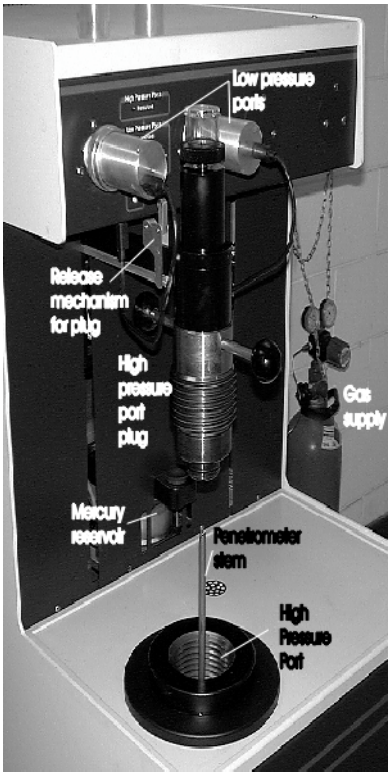
The instrument (Appendix Figures 1.3 and 1.4) is arranged with the two low pressure ports above and behind the high pressure port. Below the tray bearing the high pressure port are the vacuum pump, the high pressure pump and the variac. The mercury reservoir is situated above and behind the tray, with the filling hole located in front of it. There is a viewing window in the reservoir for checking the mercury level. The gas supply to the low pressure system is located on the wall to the right of the machine, connected by a copper gas line to a port on the left rear of the machine, next to the computer interface connection. Between the two low pressure ports are the warning lamps for mercury up, low pressure system pressurised and high pressure system pressurised.

The low pressure ports consist of a tube embedded in the machine with rubber seals inside an inner tube, which is threaded at the outer end with a machined grip ring which accepts the cap. This cap, which contains the electrode for taking the capacitance readings, is connected to the body of the machine by a cable. The high pressure ports consist of a pressure vessel which has an electrode in the base and which contains the hydraulic fluid used for pressurisation, a large threaded plug which screws into the pressure vessel and a vent with a small Perspex cup and lid on top. The top of the plug is able to rotate to ensure better centering of the penetrometer and the plug.

The Micromeritics Autopore 9410 mercury injection porosimeter.



A closer view of the Micromeritics Autopore 9410 mercury injection porosimeter.



L5. INJECTION ANALYSIS DATA FOR BASS BASIN WELLS

The following graphs are water saturation curves for the samples presented as a series of composite coloured graphs of normal (linear) and lognormal parameters. The average hydrocarbon height and displacement pressure is highlighted on each graph. The log normal graphs are more definitive as a result of larger scale values in the lower height range. Sensitivities used for the study were determined from Bass Basin well completion reports, corroborated with data from adjacent areas. Results for the following well samples are shown. Note that the Excel spreadsheets containing the MICP analystical data are not included in this PDF file. These spreadsheets are available in the "Seal Analyses Results" folder on the CD-ROM and should be access using Windows Explorer.

Samples from Bass Basin wells analysed by MICP

Well Name	Depth, metres	Sample type	Rock type
Bass-2	1164.5	Core	Carbonaceous laminated siltstone/mudstone
Bass-2	1261.0	Core	Carbonaceous laminated siltstone
Cormorant-1	1687	Core	Laminated siltstone/mudstone
Cormorant-1	1999	Core	Laminated mudstone
Cormorant-1	2231	Core	Very-fine grained sandstone/siltstone
Cormorant-1	2685	Core	Very-fine grained sandstone, carbonaceous siltstone
Dondu-1	2342	Core	Carbonaceous mudstone/siltstone
Durroon-1	1690	Core	Mudstone, very-fine grained cemented sandstone
Durroon-1	3021	Core	Mudstone, very-fine grained sandstone
Pelican-1	2805	Core	Mudstone cemented
Pelican-5	2863	Core	Siltstone/sandstone
Pelican-5	2890	Core	Laminated siltstone
Poonboon-1	1954	Core	Siltstone
Poonboon-1	2474	Core	Carbonaceous laminated siltstone
Poonboon-1	2689	Core	Very-fine grained sandstone
Poonboon-1	3035	Core	Siltstone
Poonboon-1	3259	Core	Mudstone
Tilana-1	1667	Core	Carbonaceous siltstone, very-fine grained sandstone
Tilana-1	2800	Core	Carbonaceous mudstone
Yolla-2	3039	Core	Siltstone, very-fine grained sandstone

L6. REFERENCES

Kaldi, J.G., G. O'Brien, and T. Kivior. 1999. Seal capacity and hydrocarbon accumulation history in dynamic petroleum systems: the East Java Sea, Indonesia, and the Timor Sea, Australia. APPEA Journal V.39.

Pittman, E. D. 1992. Relationship of porosity and permeability to various parameters derived from mercury injection - capillary pressure curves for sandstones. American Association of Petroleum Geologists Bulletin, 51, 191-198.

Purcell, W.R., 1949. Capillary pressures – their measurement using mercury and the calculation of permeability there from. Petroleum transactions, American Institute of Mining, Metallurgical and Petroleum Engineers, v. 186, p. 39 – 48.

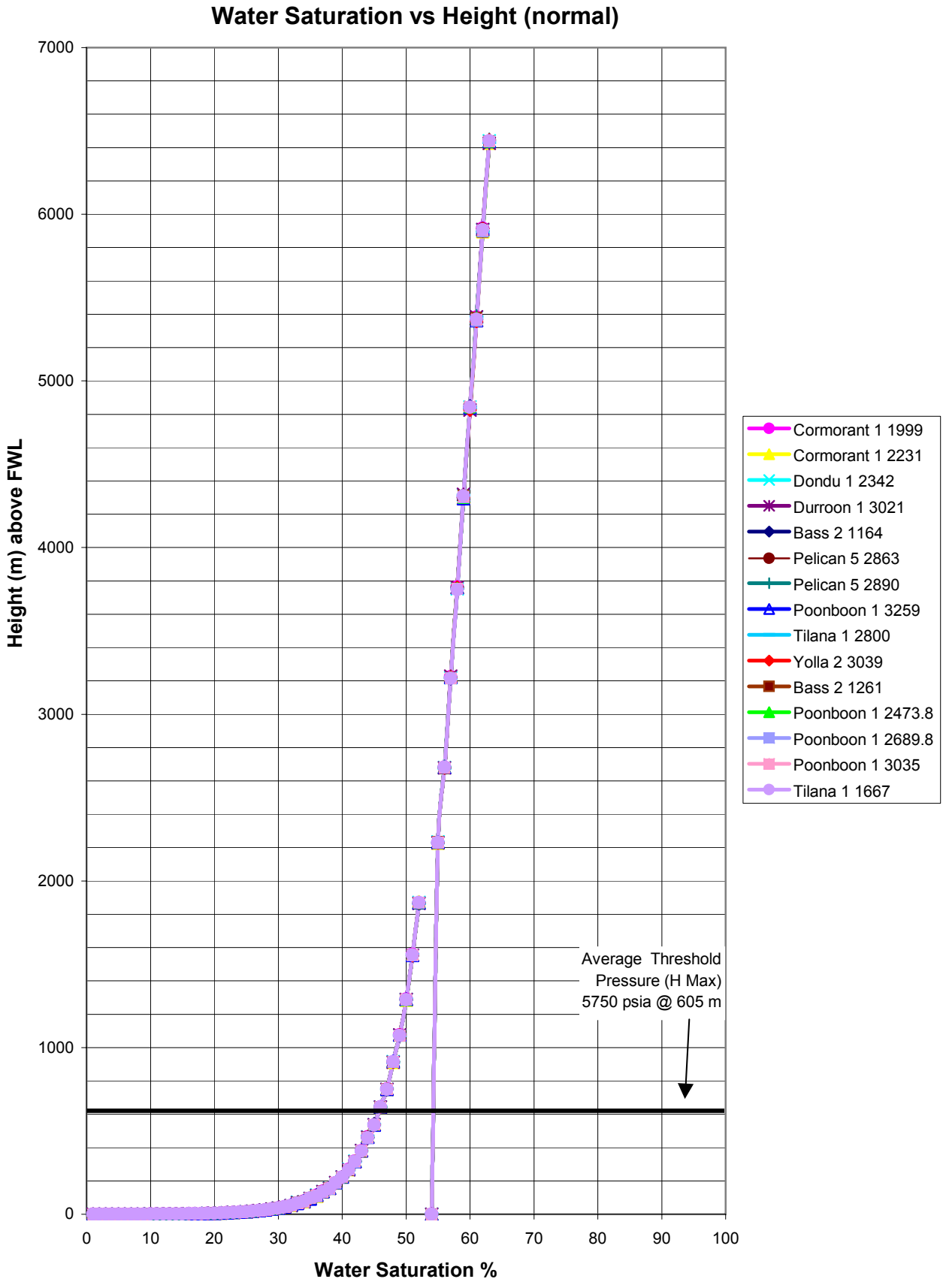
Schowalter, T.T., 1979. Mechanics of secondary hydrocarbon migration and entrapment. AAPG Bulletin v. 63, p. 723 – 760.

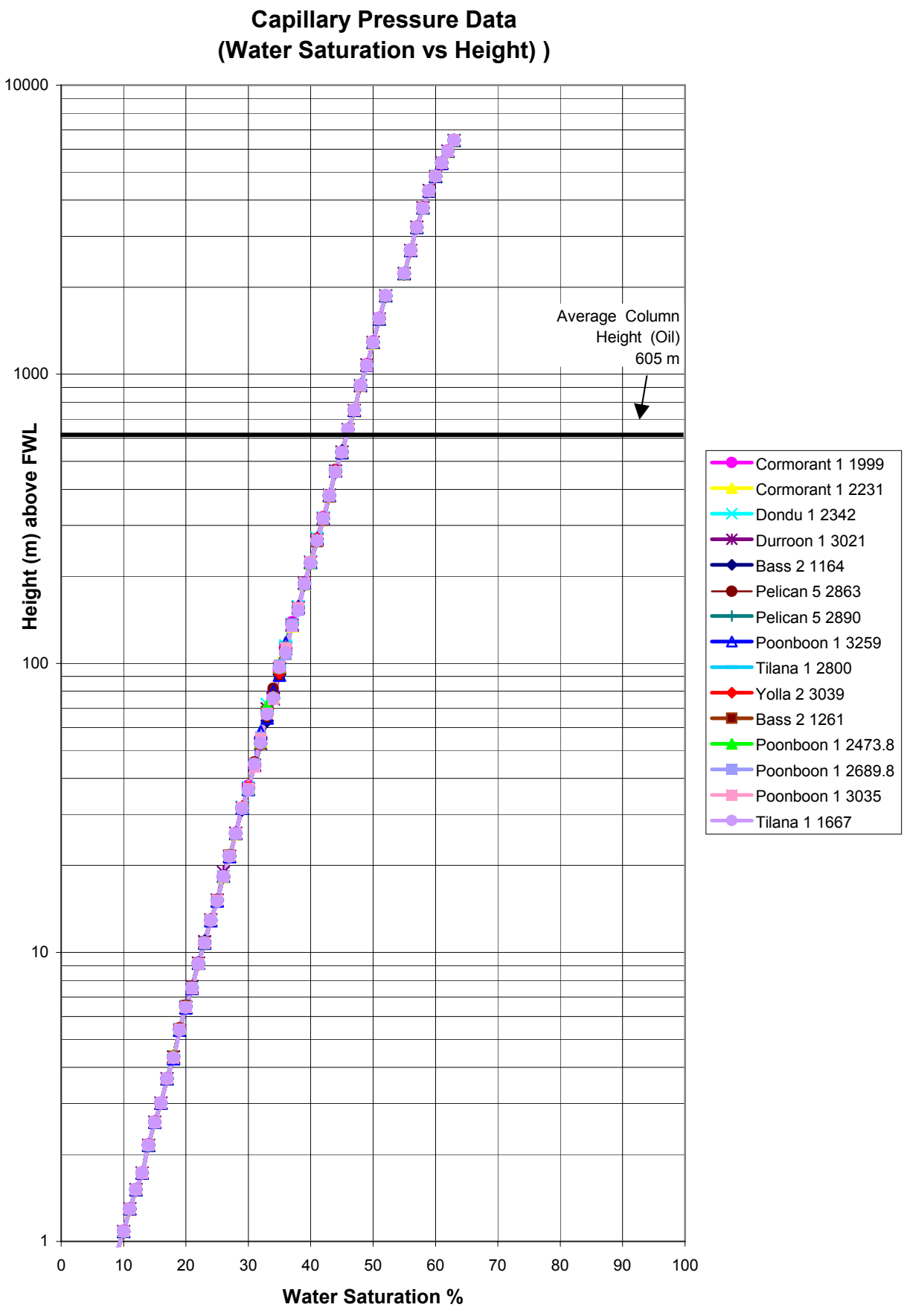
Sneider, R.M.., 1987. Practical petrophysics for exploration and development. AAPG Continuing Education Short Course Notes.

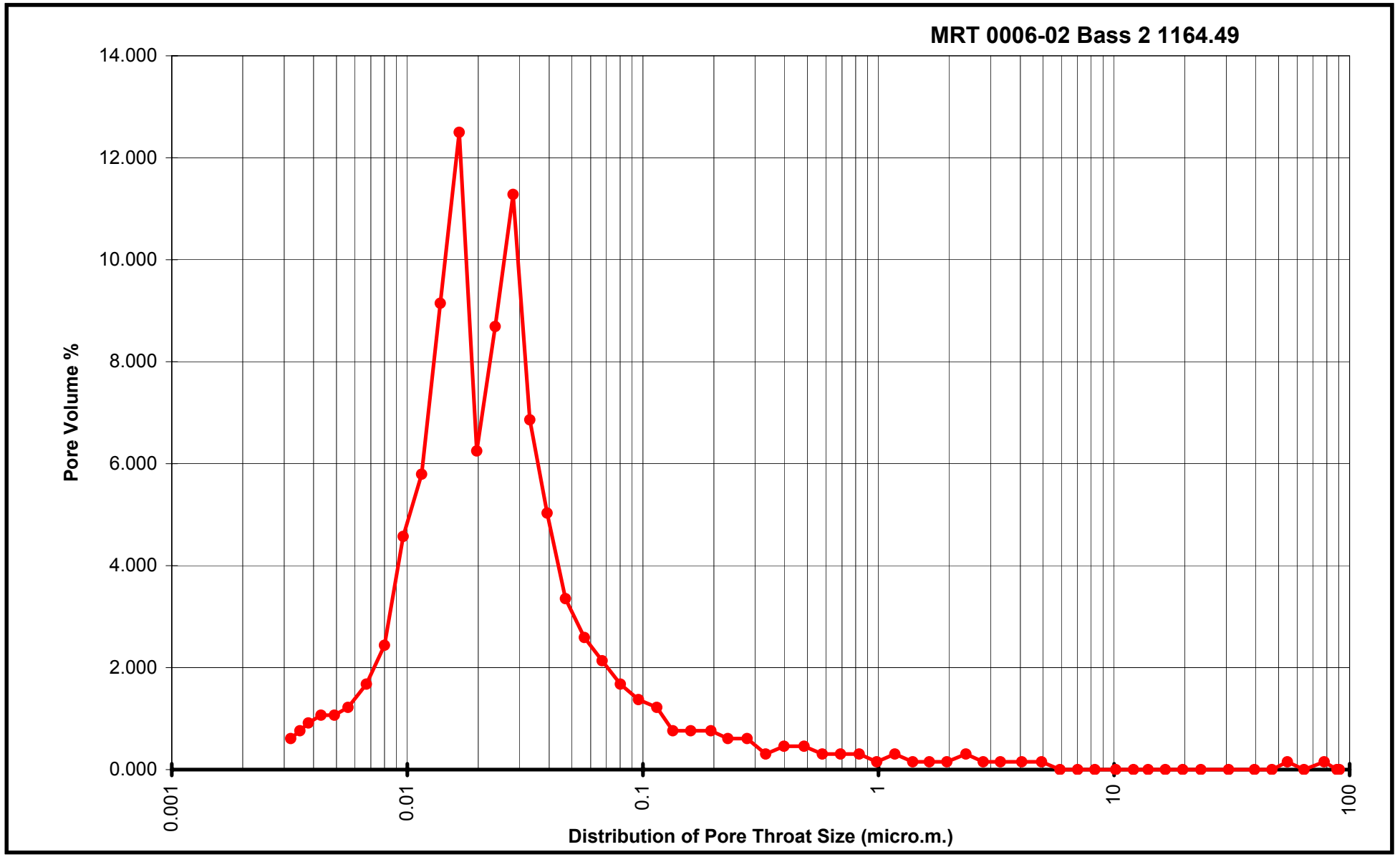
Vavra, C. L., Kaldi, J. G. and Sneider, R. M. 1992. Geological Applications of Capillary Pressure: A Review. American Association of Petroleum Geologists Bulletin, 76, 840-850.

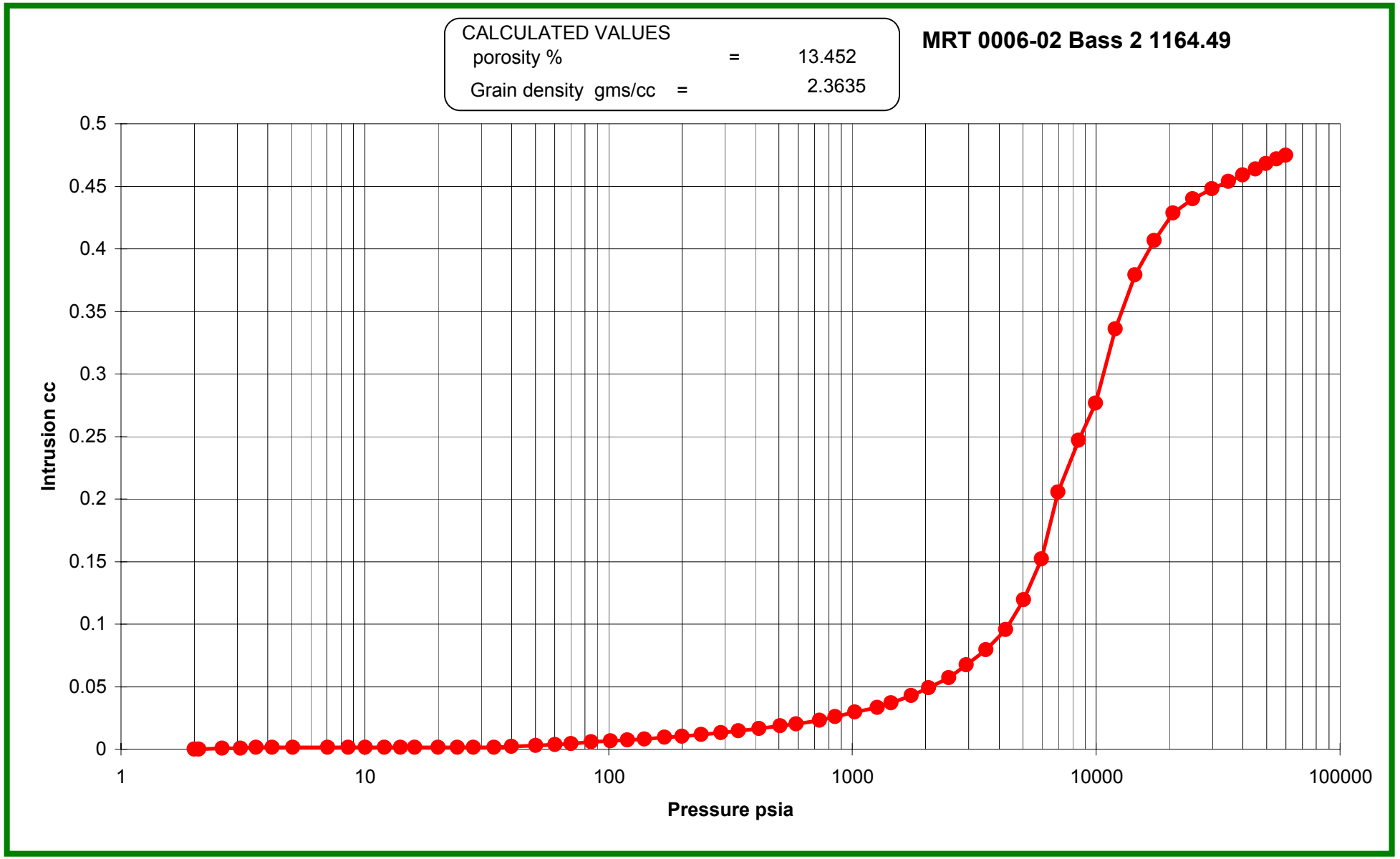
Wardlaw, N.C., 1980. The effects of pore structure on displacement efficiency in reservoir rocks and in glass micromodels. In: 1st joint SPE/DOE Symposium on Enhanced Oil Recovery, SPE no. 8843, p. 345 – 352.

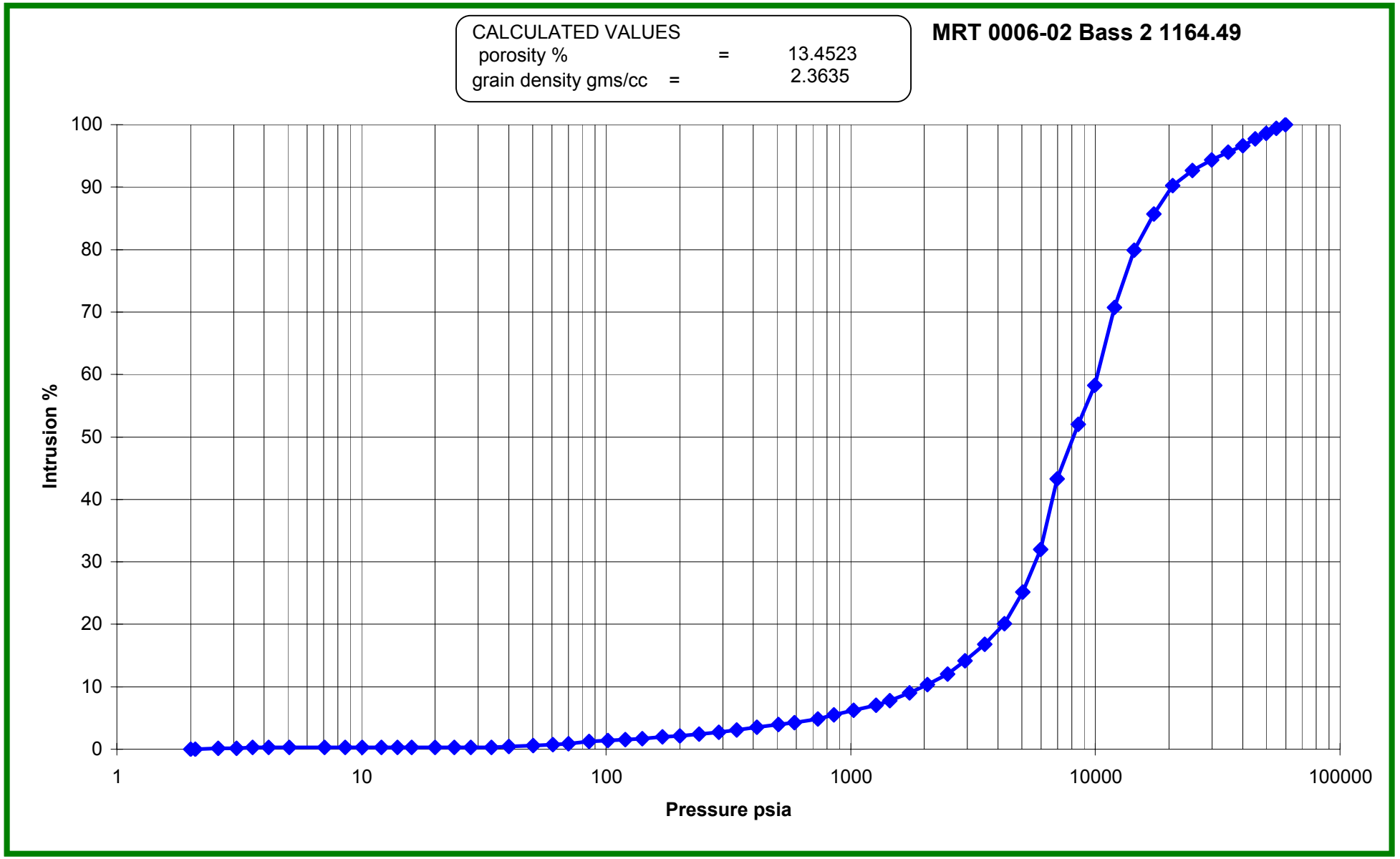
Wardlaw, N.C., and M. McKellar, 1981. Mercury porosimetry and the interpretation of pore geometry in sedimentary rocks and artificial models. Powder Technology v. 29, p. 127 – 143.

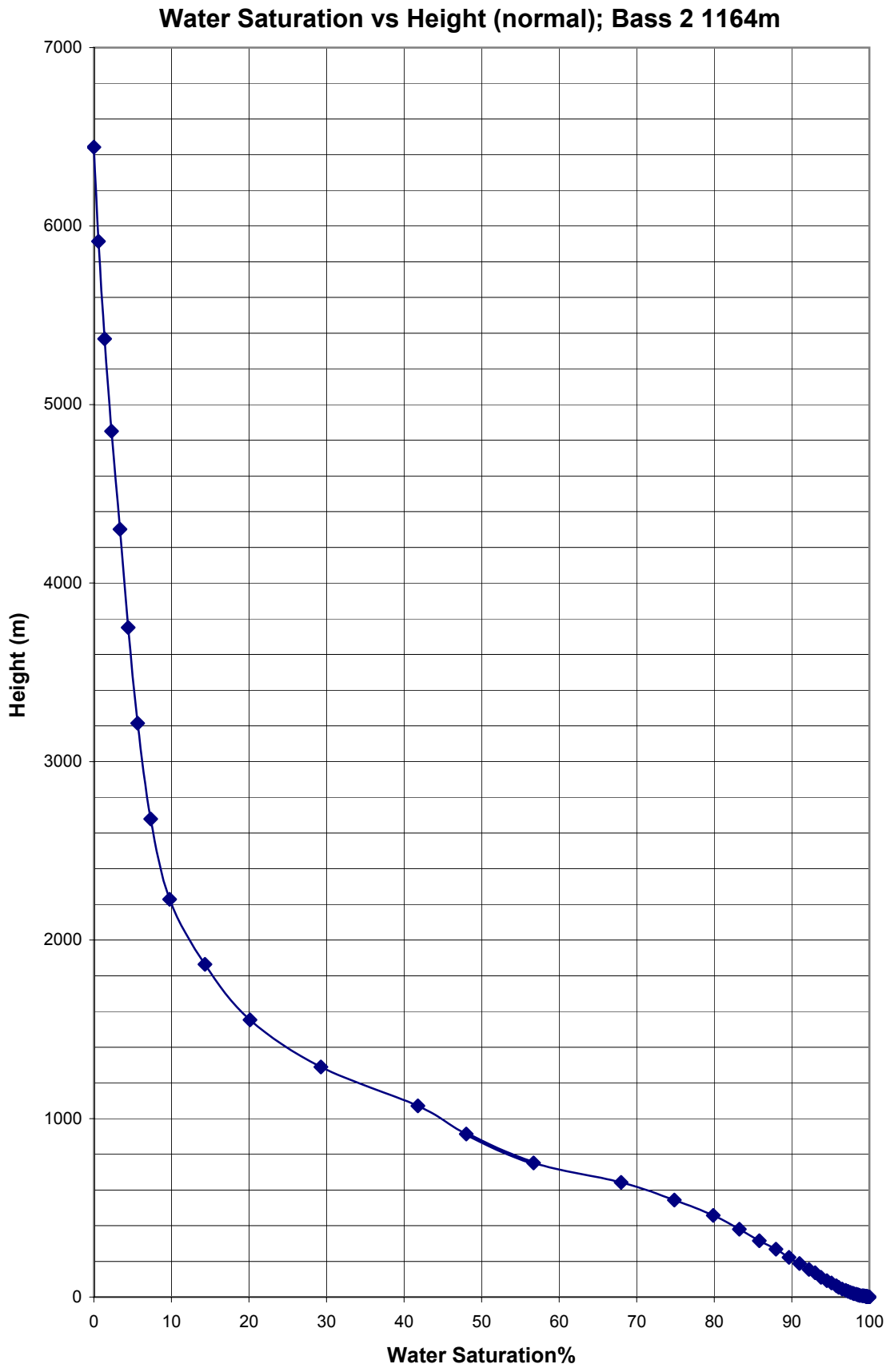

Water Saturation vs Height (normal)
Height (m) above FWL
7000
6000
5000
4000
3000
2000
1000
0
0
10
20
30
40
50
60
70
80
90
100
Water Saturation %
Average Threshold
Pressure (H Max)
5750 psia @ 605 m
Cormorant 1 1999
Cormorant 1 2231
Dondu 1 2342
Durroon 1 3021
Bass 2 1164
Pelican 5 2863
Pelican 5 2890
Poonboon 1 3259
Tilana 1 2800
Yolla 2 3039
Bass 2 1261
Poonboon 1 2473.8
Poonboon 1 2689.8
Poonboon 1 3035
Tilana 1 1667

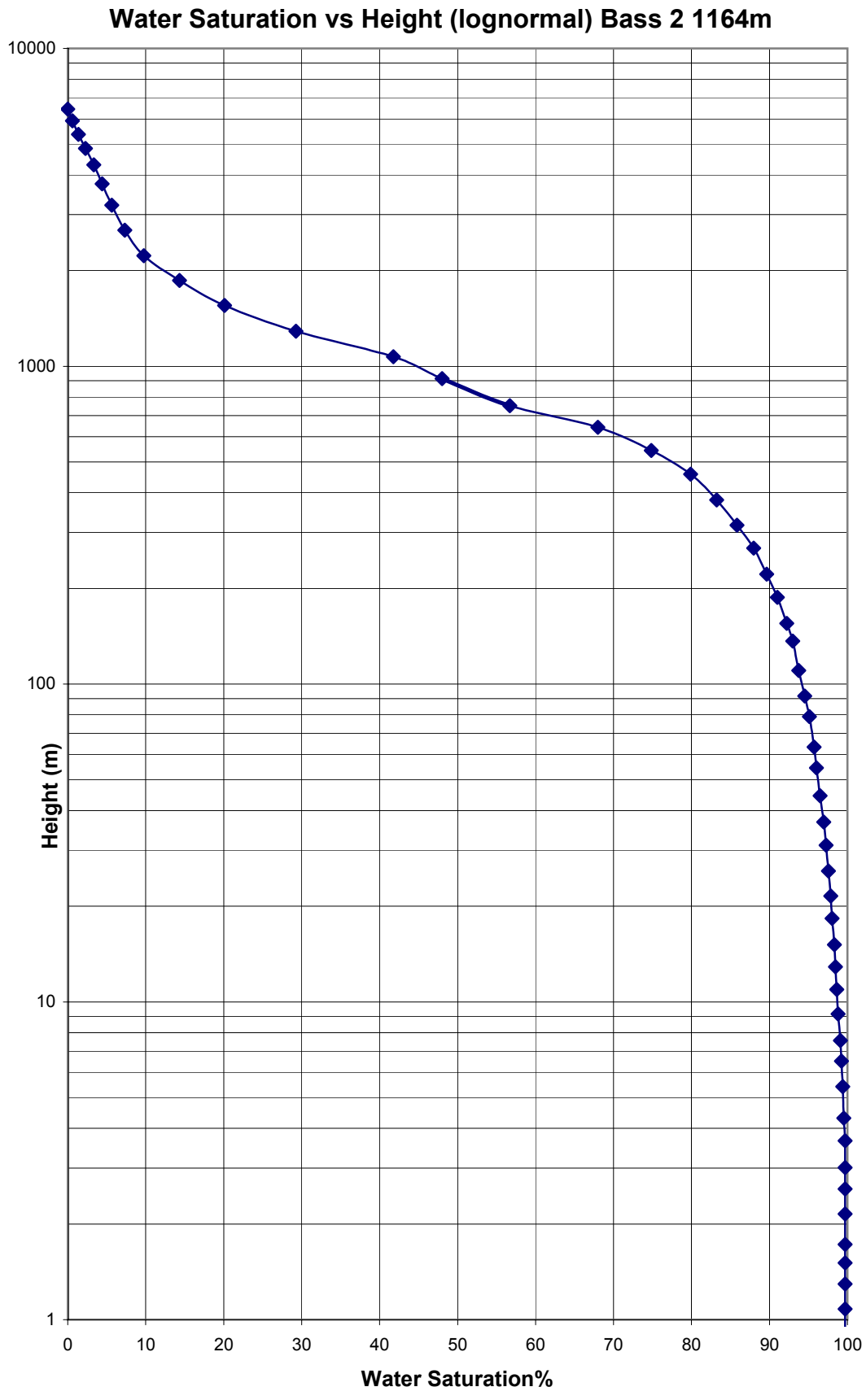

Capillary Pressure Data
(Water Saturation vs Height))
10000
1000
100
10
1
Height (m) above FWL
0
10
20
30
40
50
60
70
80
90
100
Water Saturation %
Average Column
Height (Oil)
605 m
Cormorant 1 1999
Cormorant 1 2231
Dondu 1 2342
Durroon 1 3021
Bass 2 1164
Pelican 5 2863
Pelican 5 2890
Poonboon 1 3259
Tilana 1 2800
Yolla 2 3039
Bass 2 1261
Poonboon 1 2473.8
Poonboon 1 2689.8
Poonboon 1 3035
Tilana 1 1667

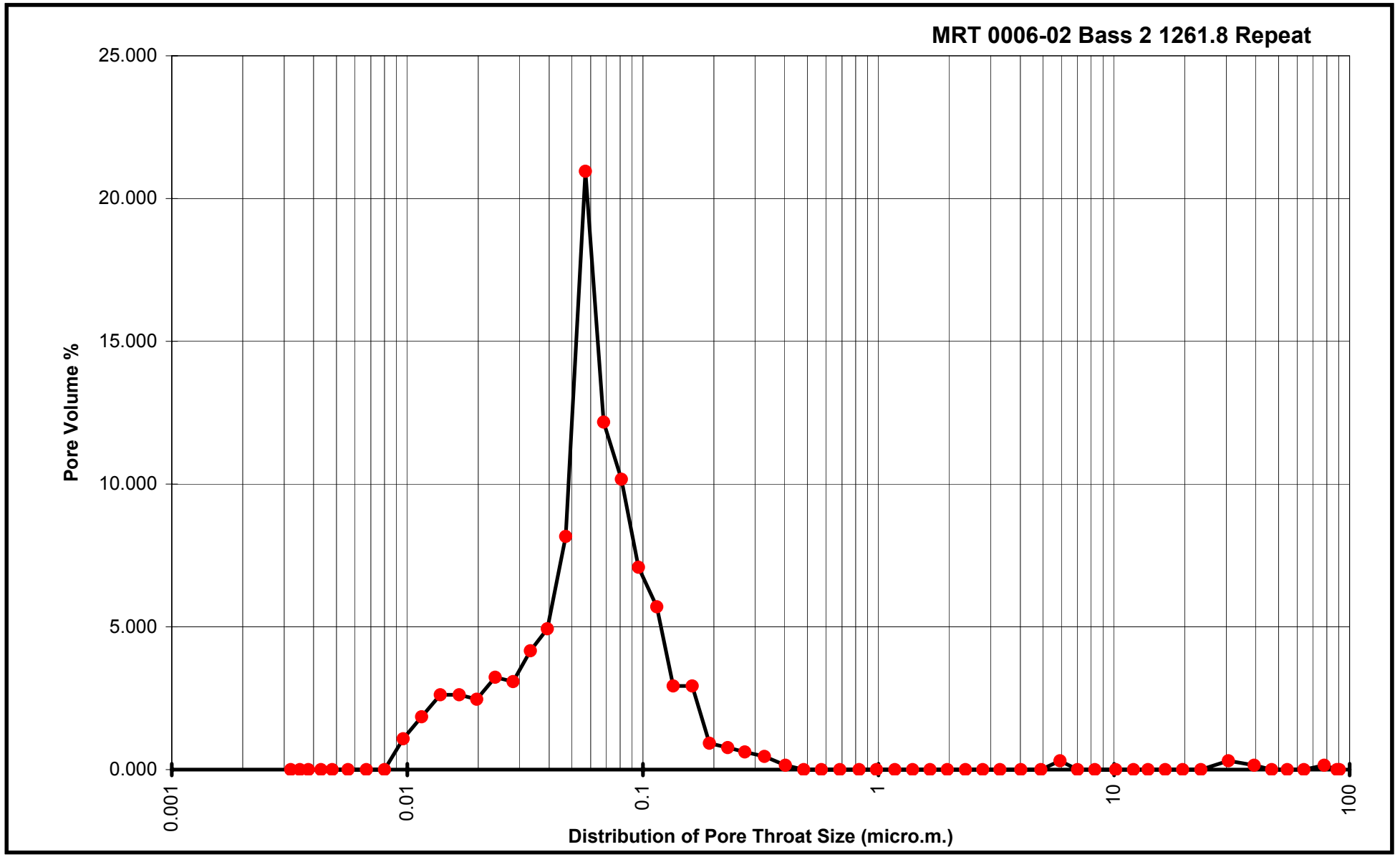

MRT 0006-02 Bass 2 1164.49
Pore Volume %
14.000
12.000
10.000
8.000
6.000
4.000
2.000
0.000
0.001
0.01
0.1
1
10
100
Distribution of Pore Throat Size (micro.m.)

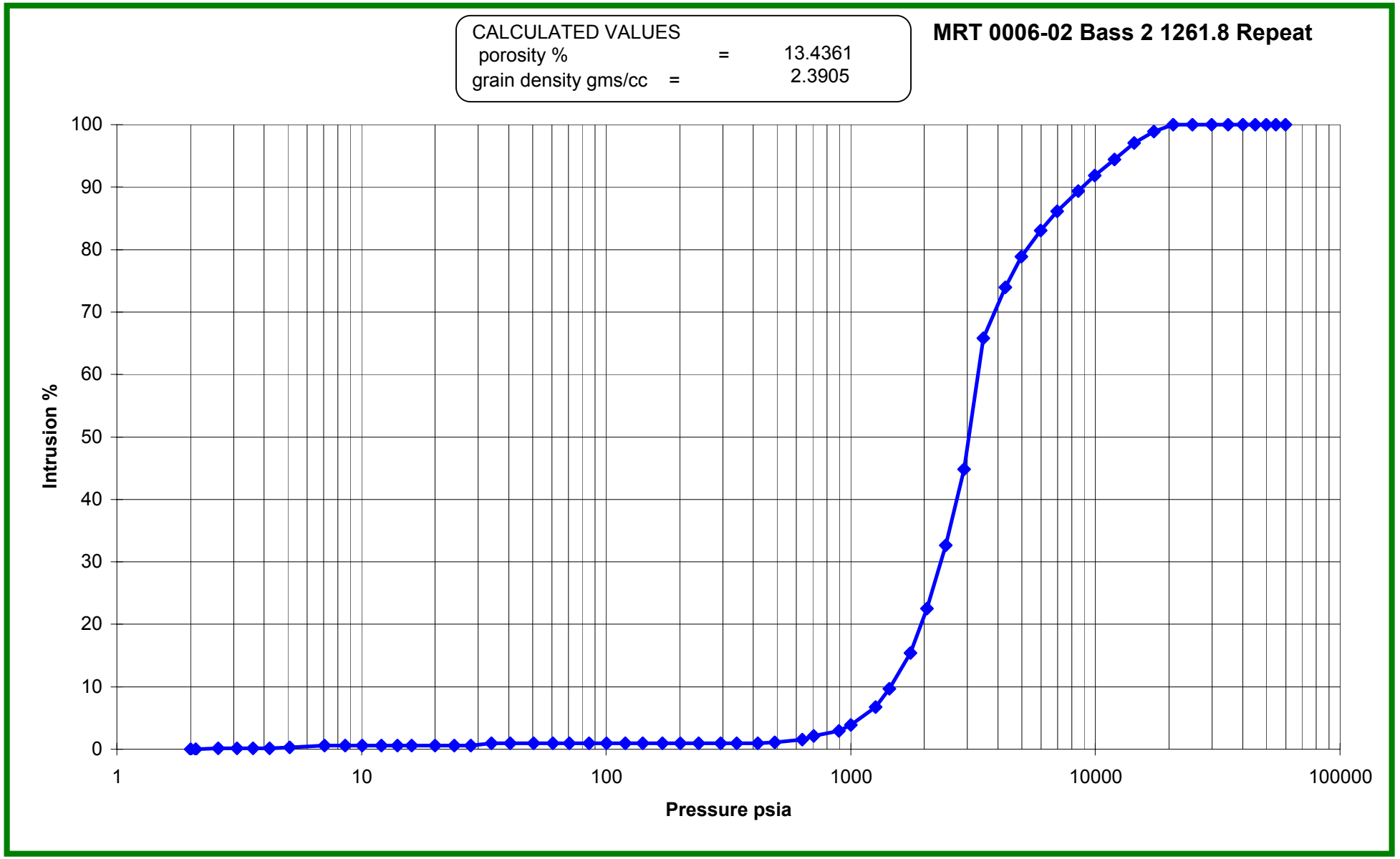

CALCULATED VALUES
porosity % = 13.452
Grain density gms/cc = 2.3635
MRT 0006-02 Bass 2 1164.49
Intrusion cc
0.5
0.45
0.4
0.35
0.3
0.25
0.2
0.15
0.1
0.05
0
1
10
100
1000
10000
100000
Pressure psia

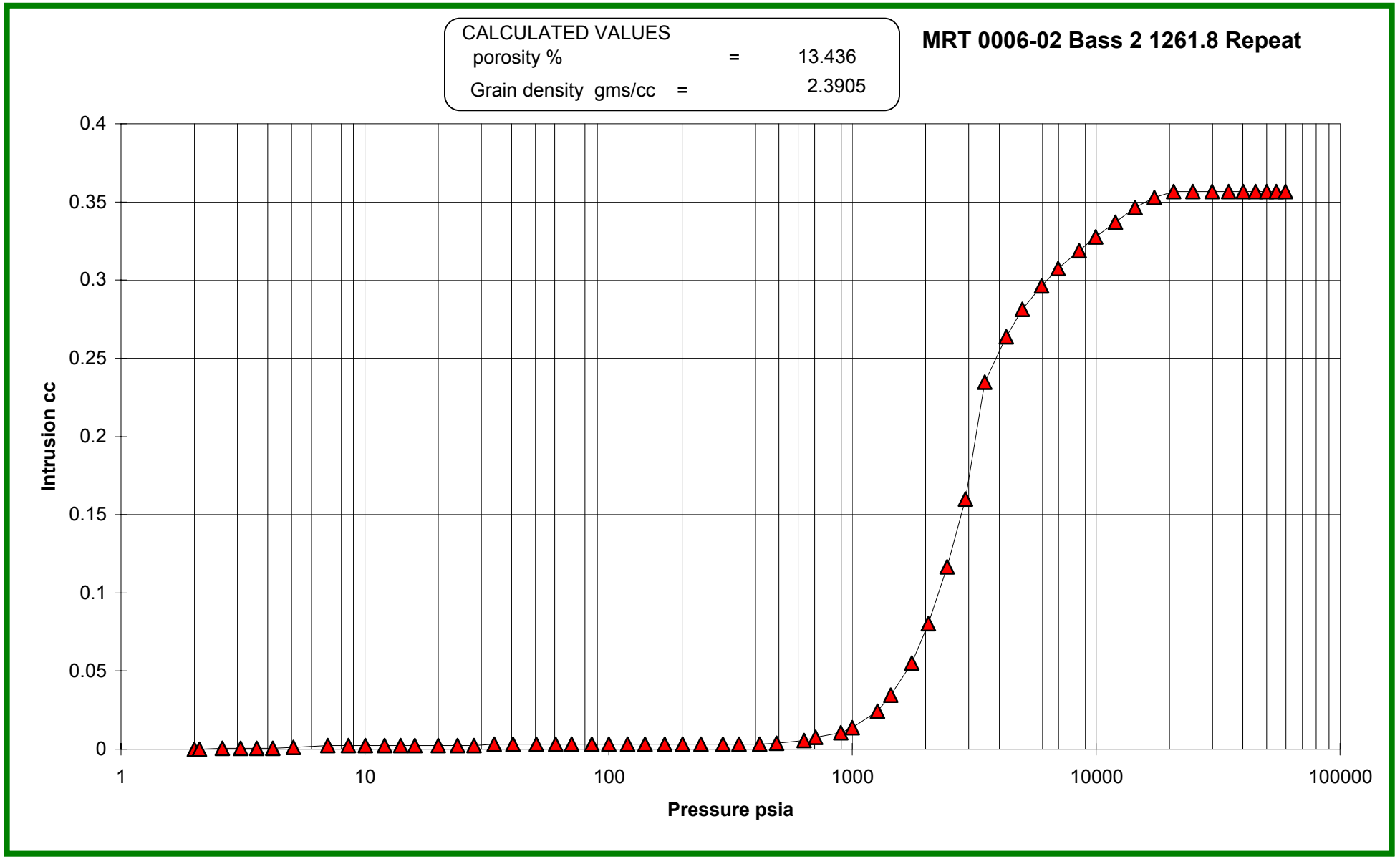

CALCULATED VALUES
porosity % = 13.4523
grain density gms/cc = 2.3635
MRT 0006-02 Bass 2 1164.49
Intrusion %
100
90
80
70
60
50
40
30
20
10
0
1
10
100
1000
10000
100000
Pressure psia

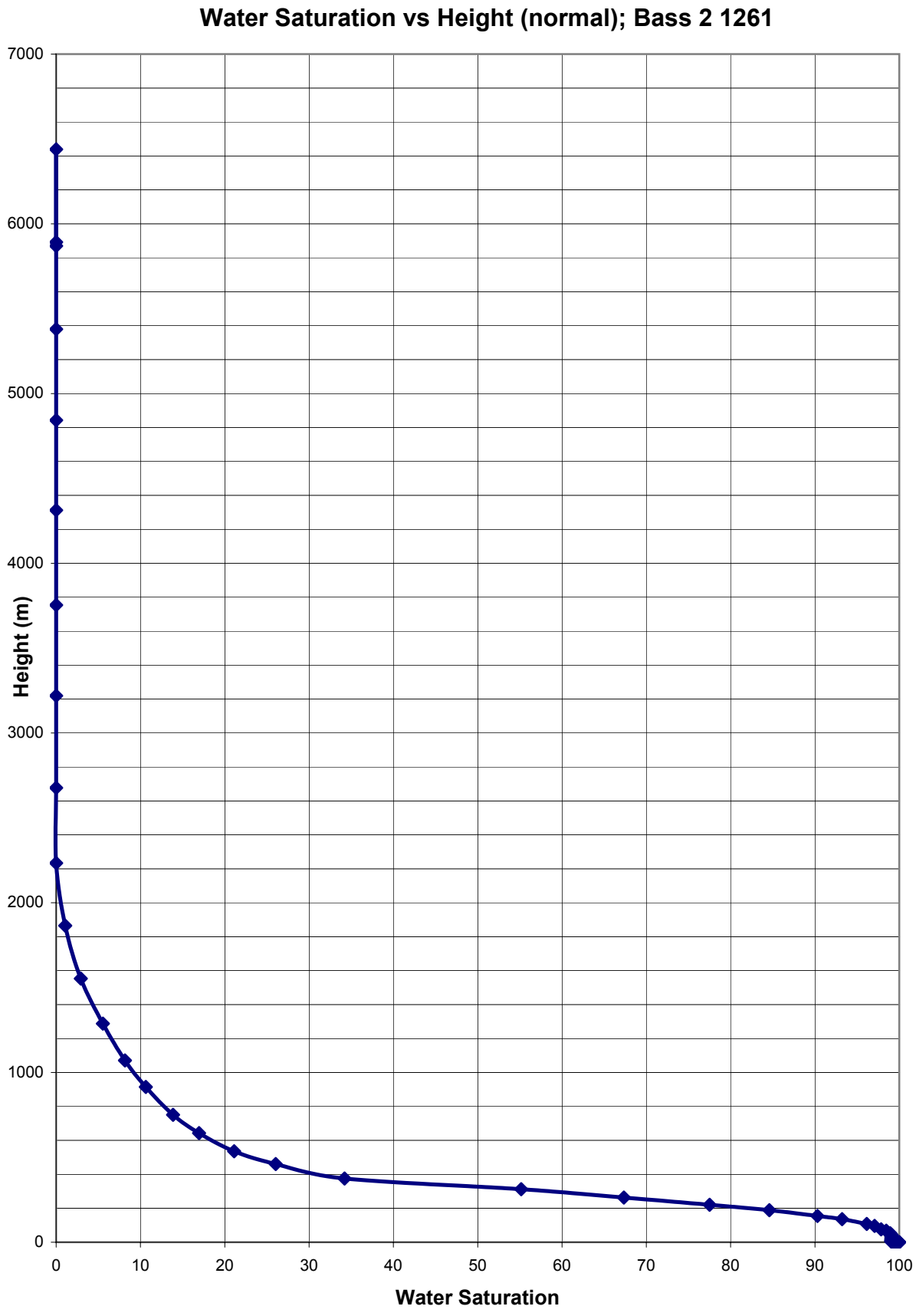

Water Saturation vs Height (normal); Bass 2 1164m
Height (m)
7000
6000
5000
4000
3000
2000
1000
0
0
10
20
30
40
50
60
70
80
90
100
Water Saturation%

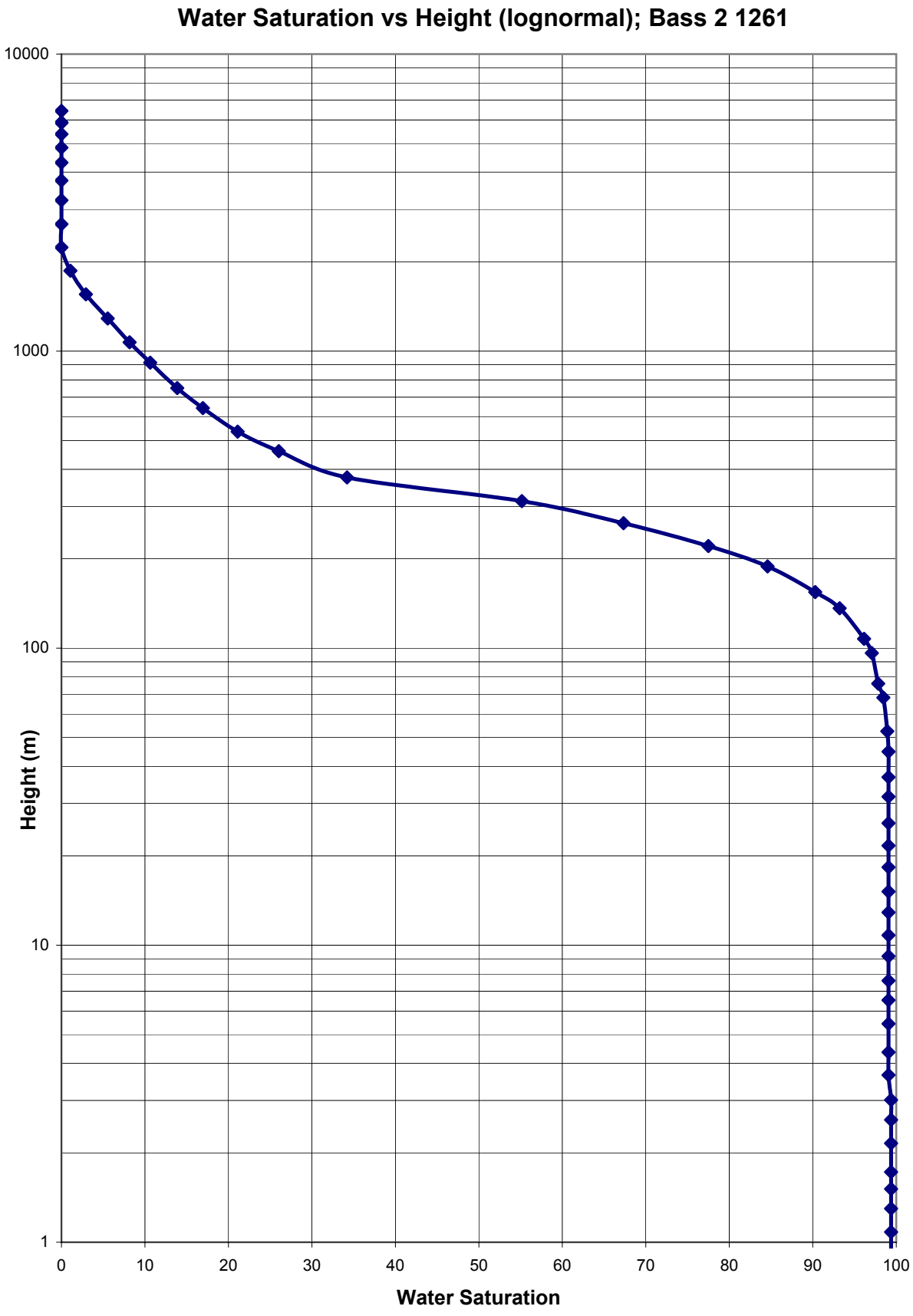

Water Saturation vs Height (lognormal) Bass 2 1164m
10000
1000
100
10
1
Height (m)
0
10
20
30
40
50
60
70
80
90
100
Water Saturation%

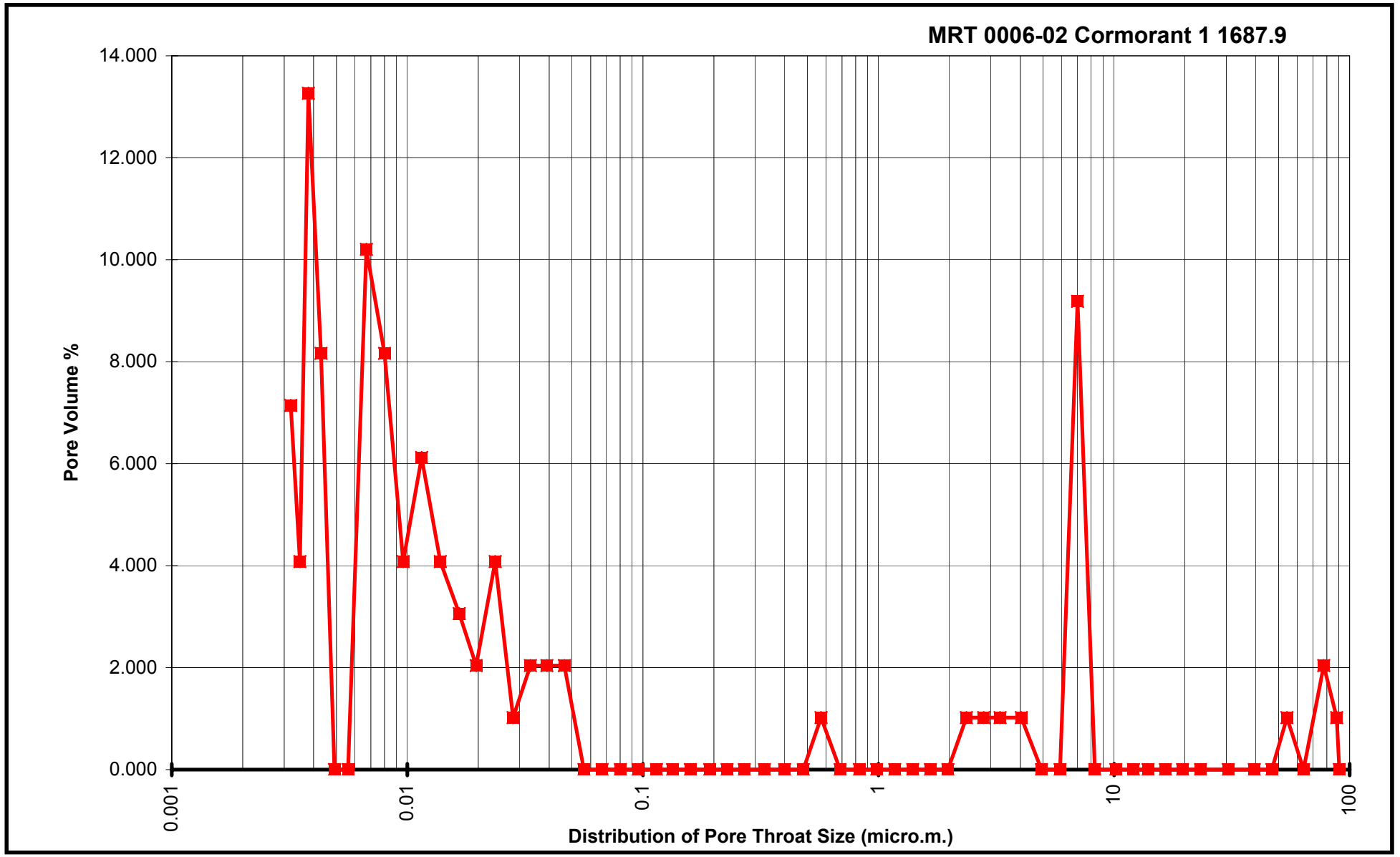

MRT 0006-02 Bass 2 1261.8 Repeat
25.000
20.000
15.000
10.000
5.000
0.000
Pore Volume %
0.001
0.01
0.1
1
10
100
Distribution of Pore Throat Size (micro.m.)

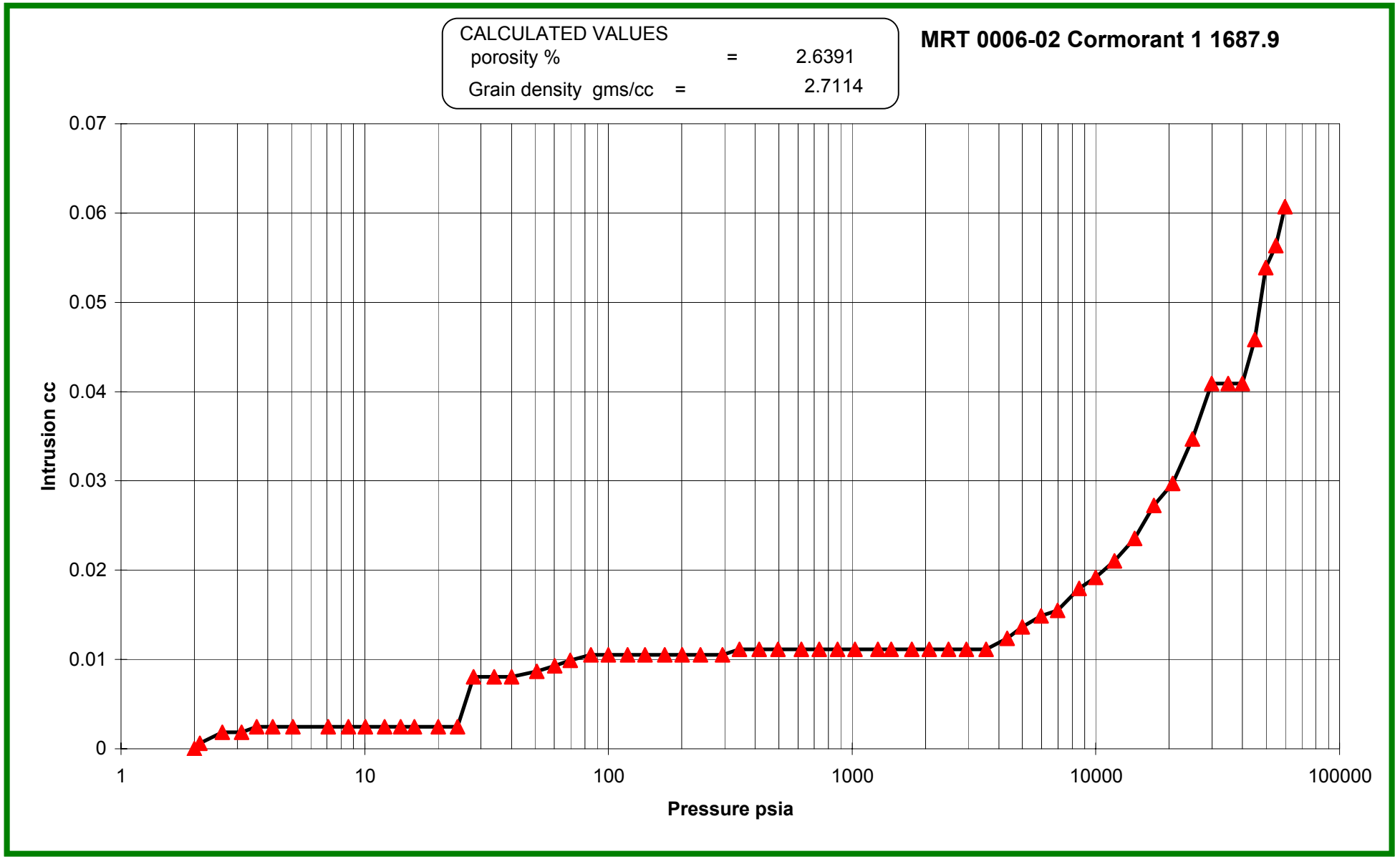

CALCULATED VALUES
porosity % = 13.4361
grain density gms/cc = 2.3905
MRT 0006-02 Bass 2 1261.8 Repeat
Intrusion %
100
90
80
70
60
50
40
30
20
10
0
1
10
100
1000
10000
100000
Pressure psia

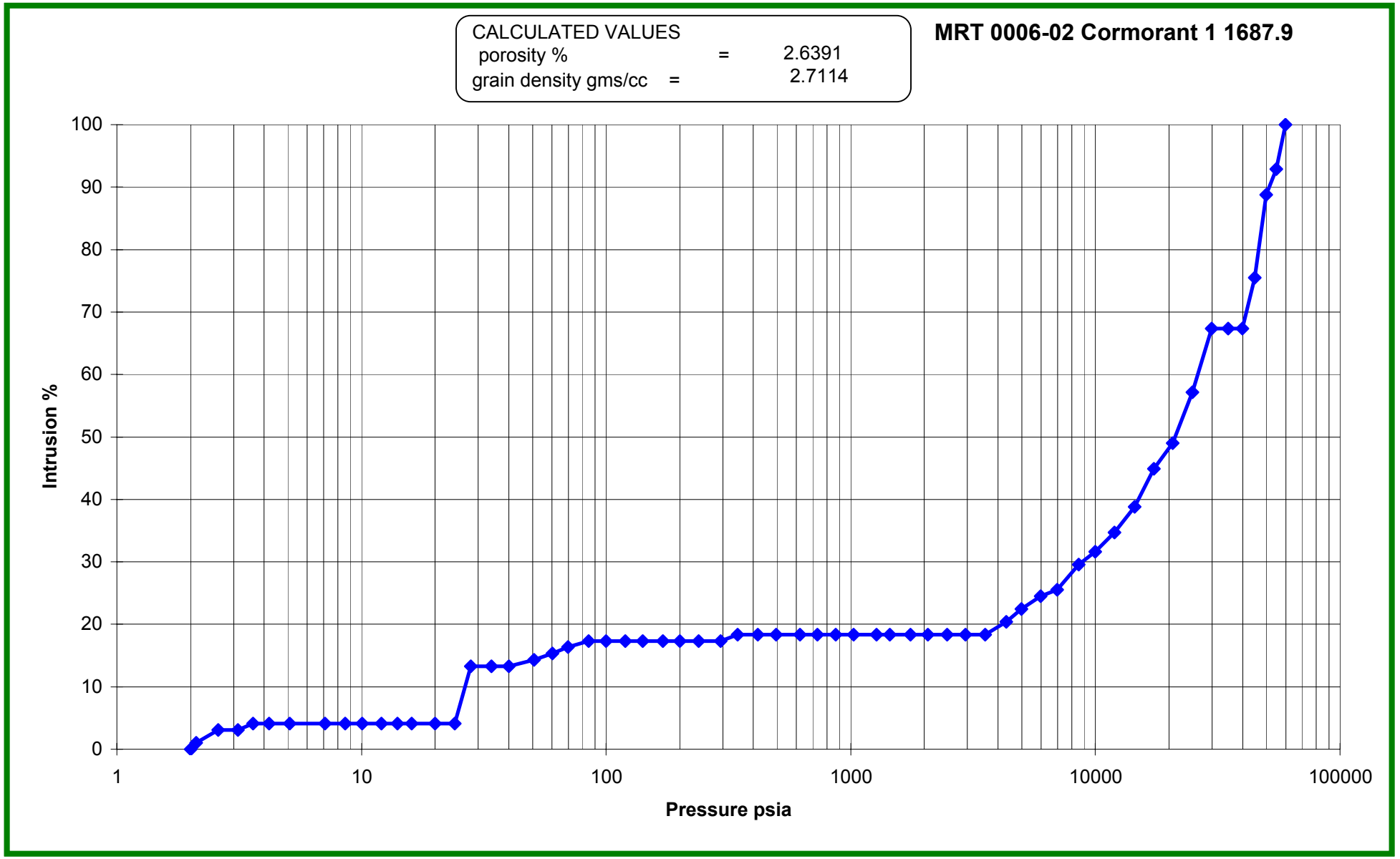

CALCULATED VALUES
porosity % = 13.436
Grain density gms/cc = 2.3905
MRT 0006-02 Bass 2 1261.8 Repeat
Intrusion cc
0.4
0.35
0.3
0.25
0.2
0.15
0.1
0.05
0
1
10
100
1000
10000
100000
Pressure psia

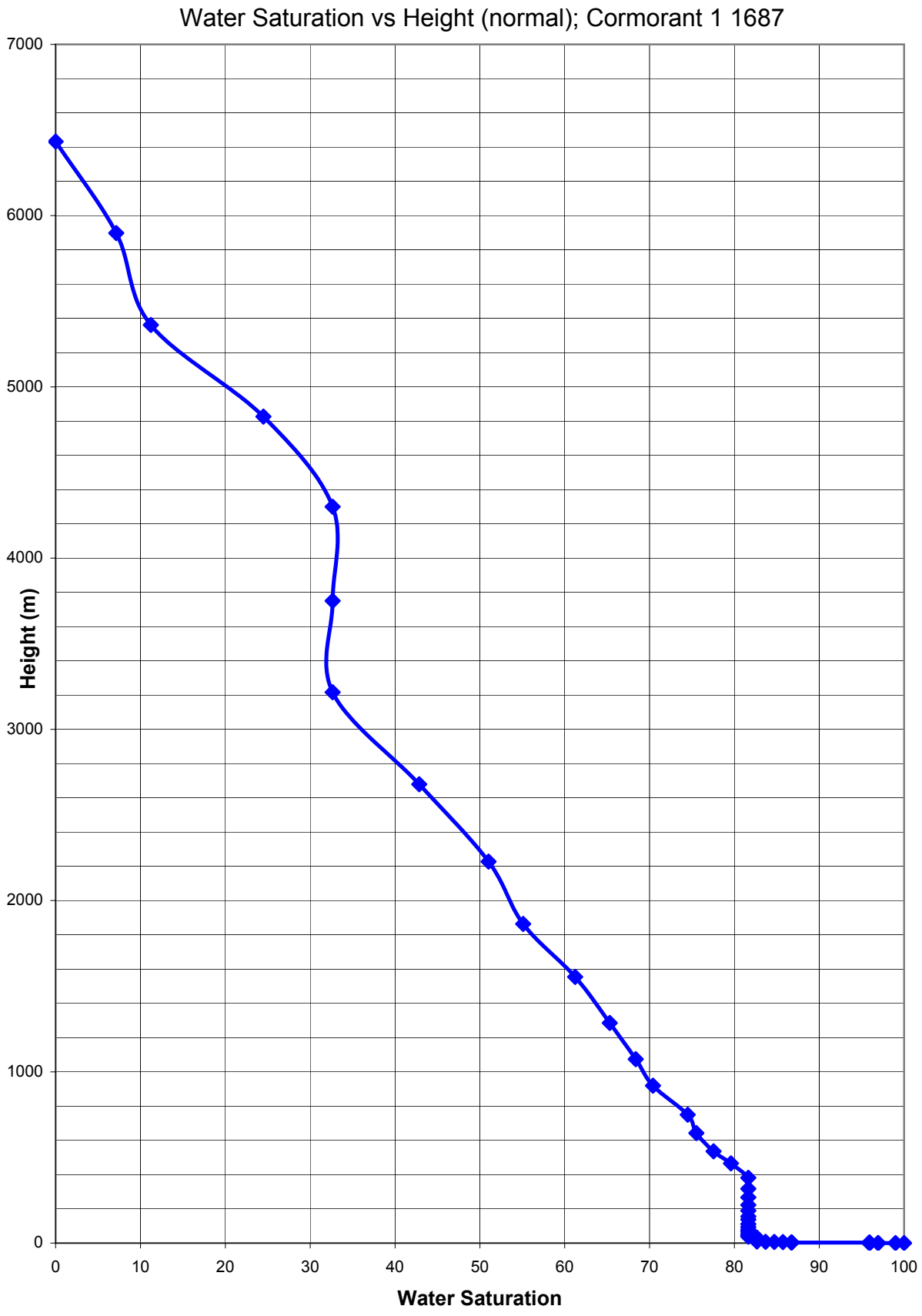

Water Saturation vs Height (normal); Bass 2 1261
7000
6000
5000
4000
3000
2000
1000
0
Height (m)
0
10
20
30
40
50
60
70
80
90
100
Water Saturation

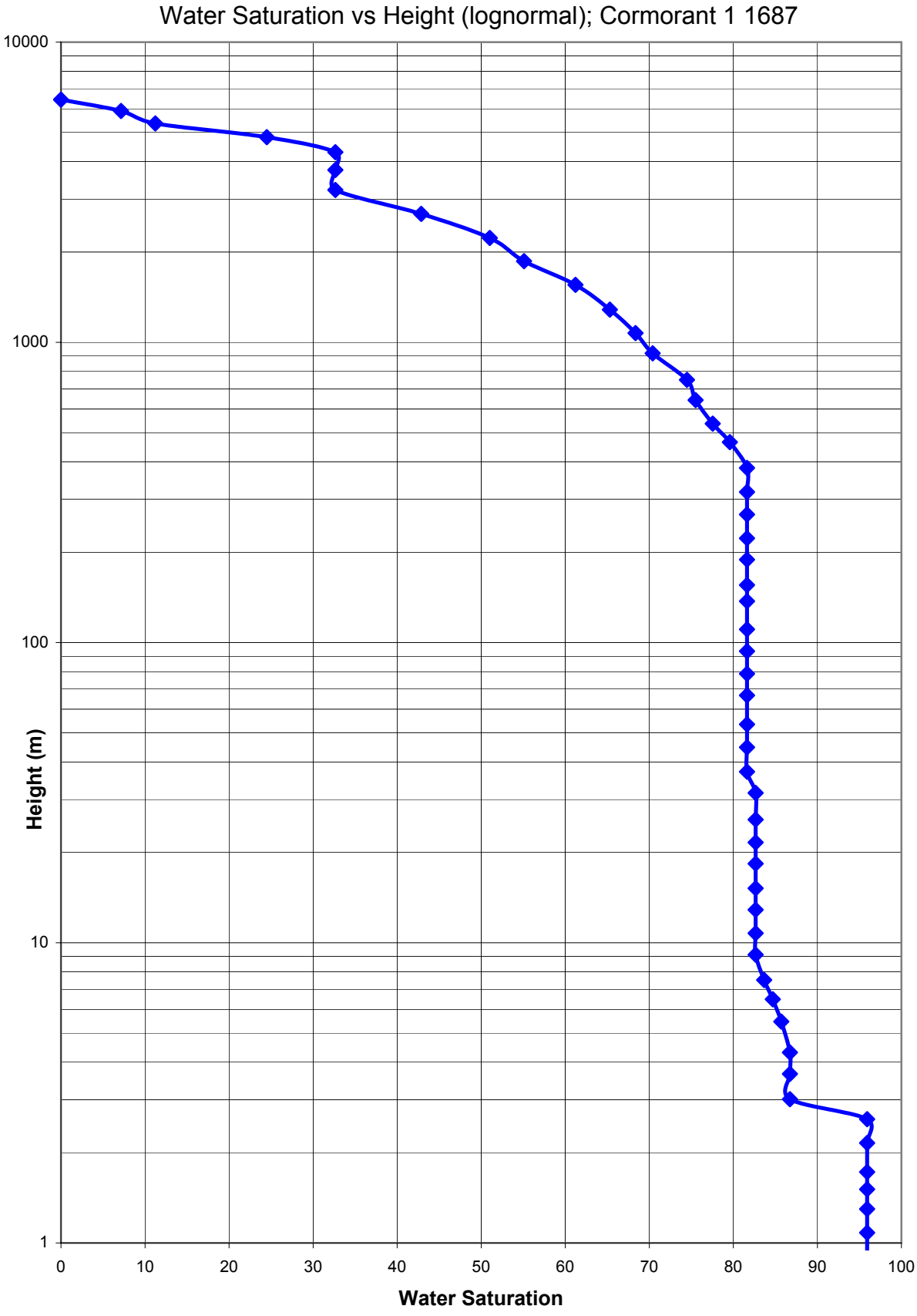

Water Saturation vs Height (lognormal); Bass 2 1261
10000
1000
100
10
1
Height (m)
0
10
20
30
40
50
60
70
80
90
100
Water Saturation

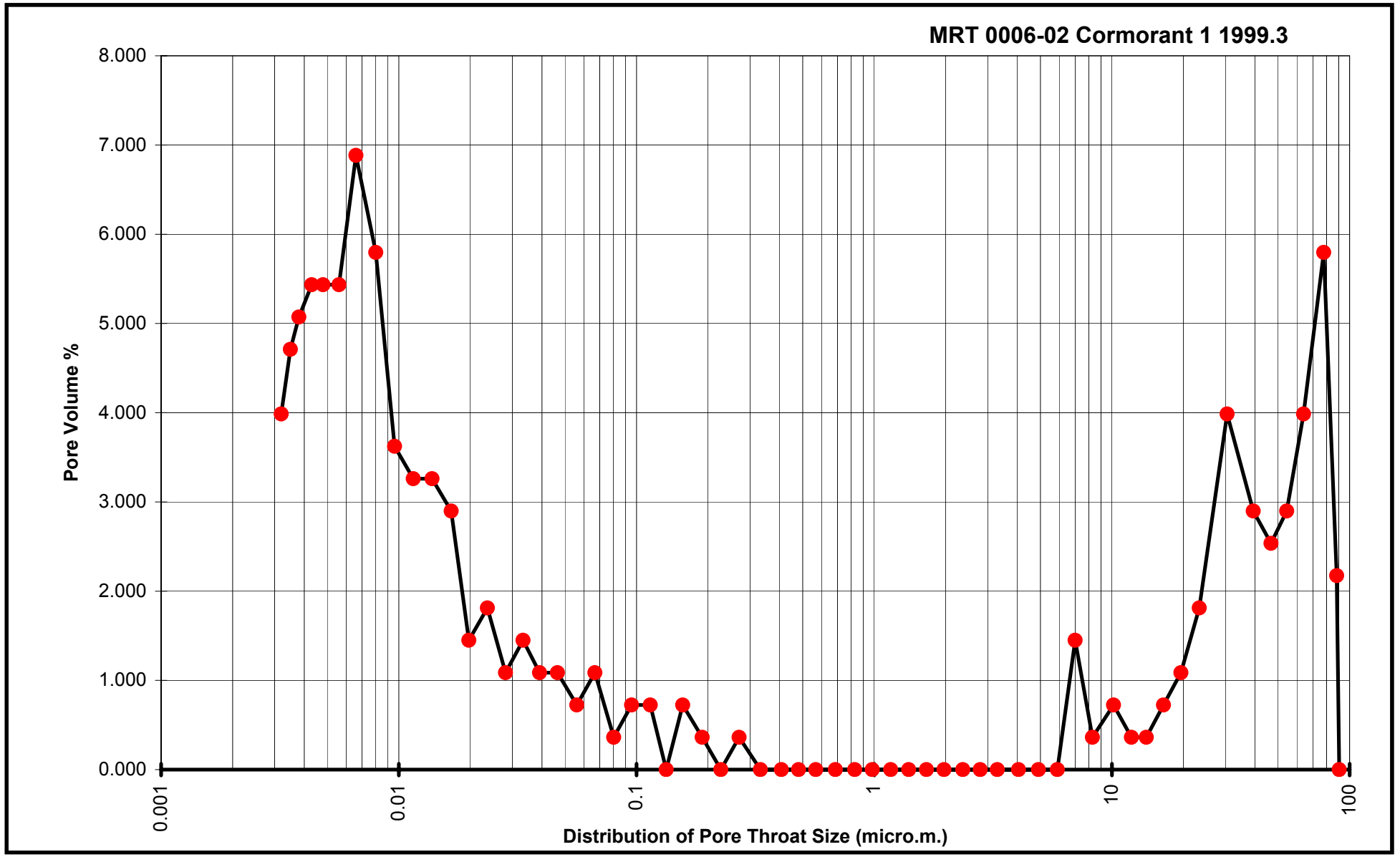

MRT 0006-02 Cormorant 1 1687.9
Pore Volume %
14.000
12.000
10.000
8.000
6.000
4.000
2.000
0.000
0.001
0.01
0.1
1
10
100
Distribution of Pore Throat Size (micro.m.)

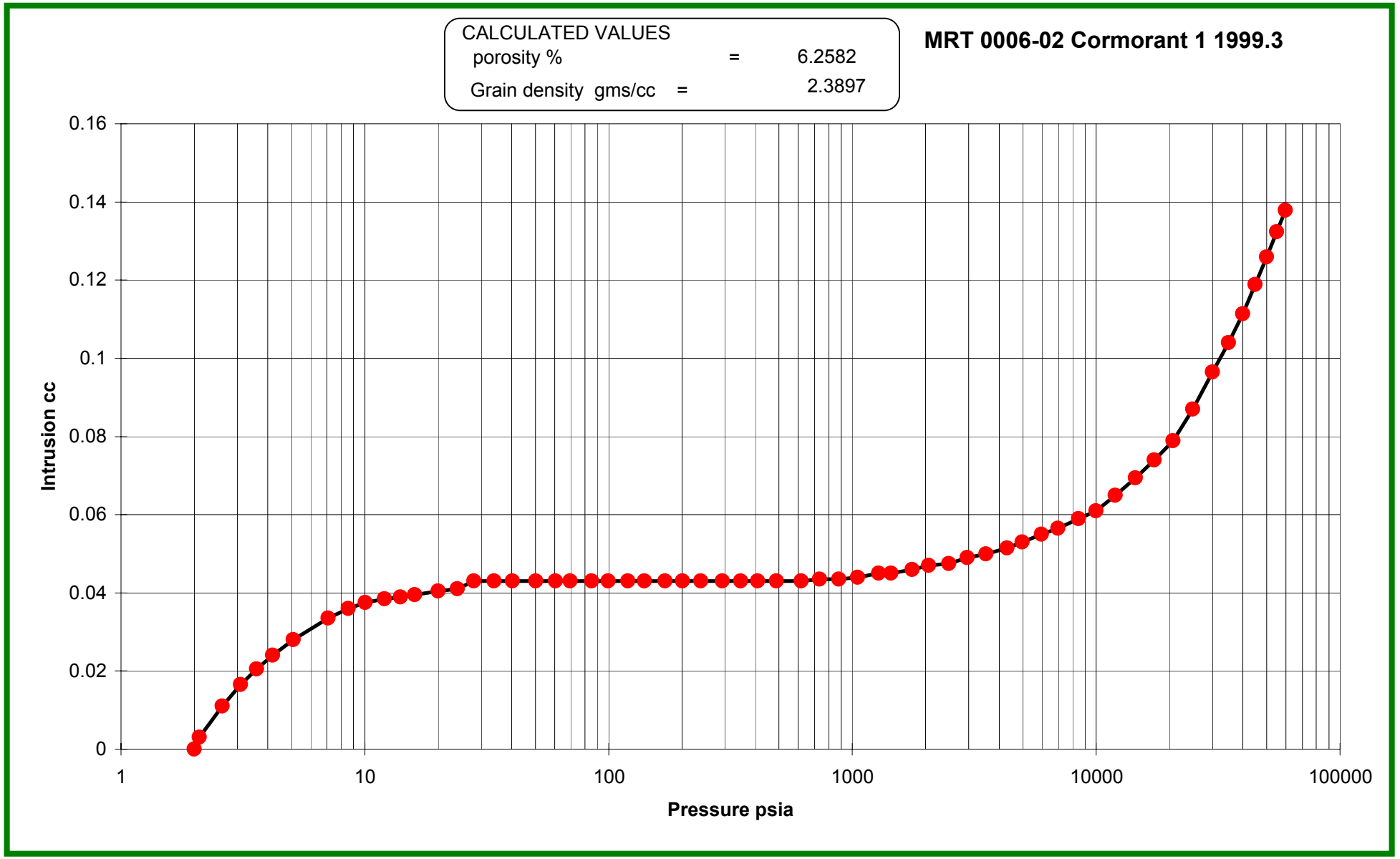

CALCULATED VALUES
porosity % = 2.6391
Grain density gms/cc = 2.7114
MRT 0006-02 Cormorant 1 1687.9
Intrusion cc
0.07
0.06
0.05
0.04
0.03
0.02
0.01
0
1
10
100
1000
10000
100000
Pressure psia

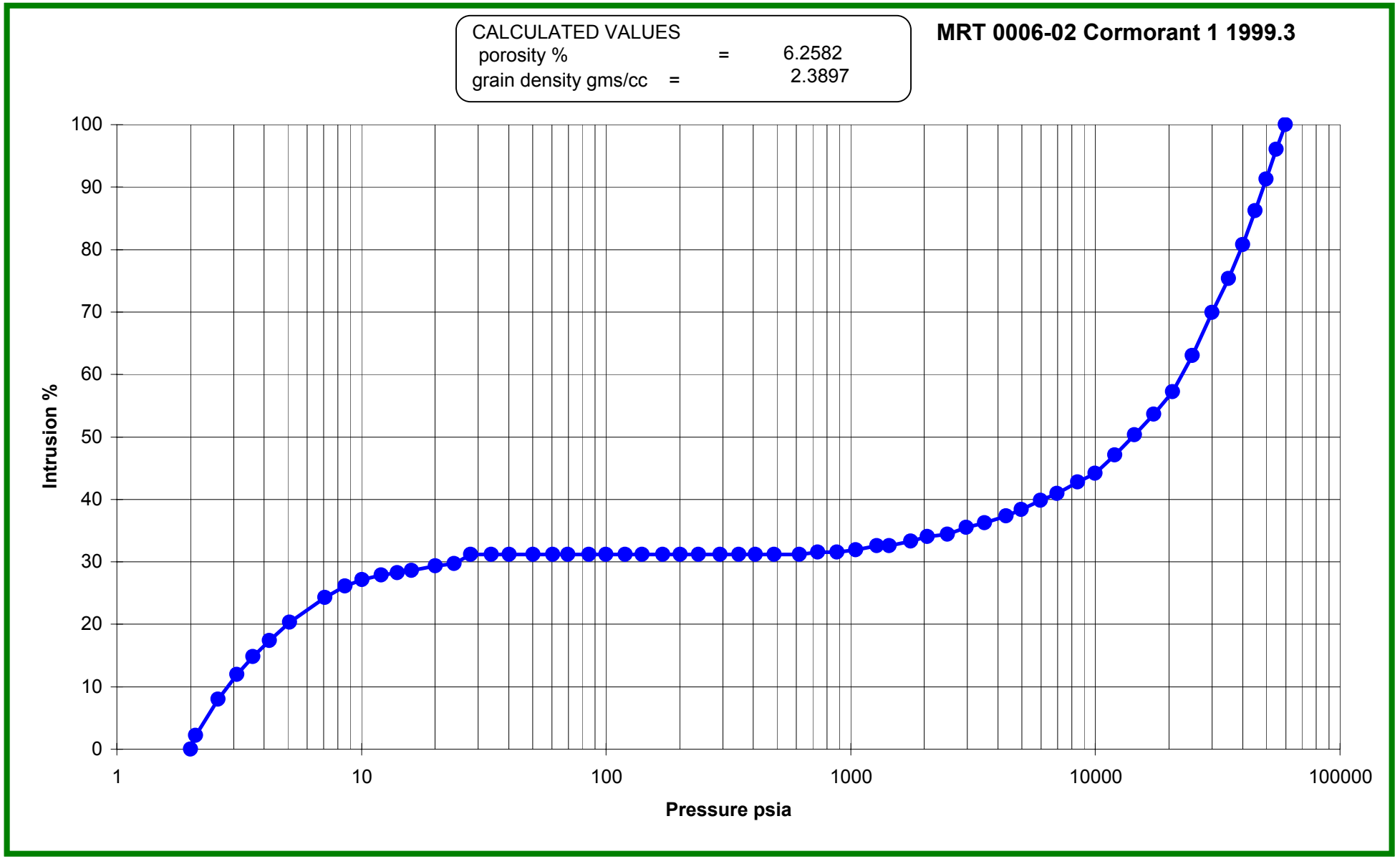

CALCULATED VALUES
porosity % = 2.6391
grain density gms/cc = 2.7114
MRT 0006-02 Cormorant 1 1687.9
Intrusion %
100
90
80
70
60
50
40
30
20
10
0
1
10
100
1000
10000
100000
Pressure psia

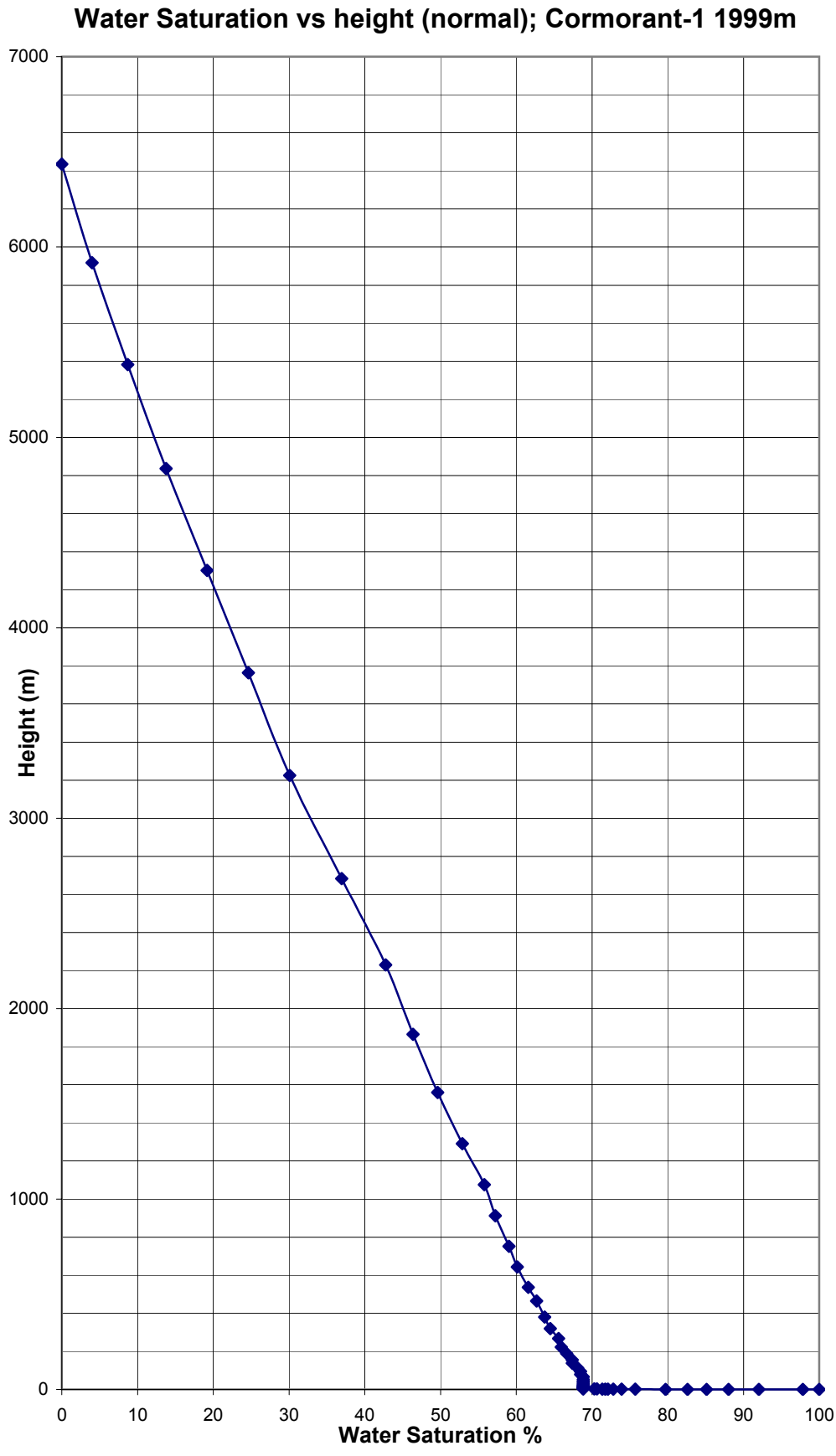

Water Saturation vs Height (normal); Cormorant 1 1687
7000
6000
5000
4000
3000
2000
1000
0
Height (m)
0
10
20
30
40
50
60
70
80
90
100
Water Saturation

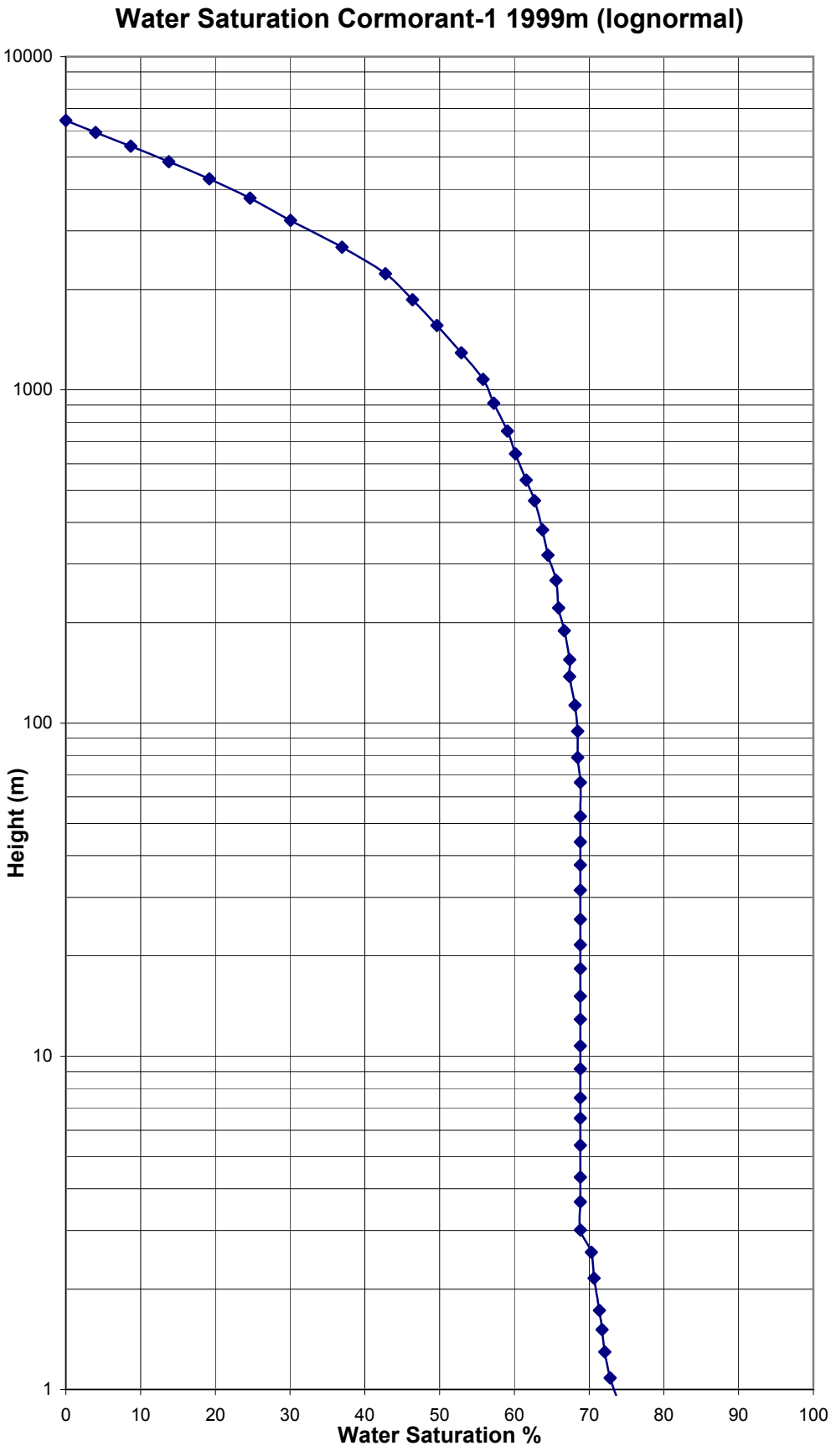

Water Saturation vs Height (lognormal); Cormorant 1 1687
10000
1000
100
10
1
Height (m)
0
10
20
30
40
50
60
70
80
90
100
Water Saturation


MRT 0006-02 Cormorant 1 1999.3
Pore Volume %
8.000
7.000
6.000
5.000
4.000
3.000
2.000
1.000
0.000
0.001
0.01
0.1
1
10
100
Distribution of Pore Throat Size (micro.m.)

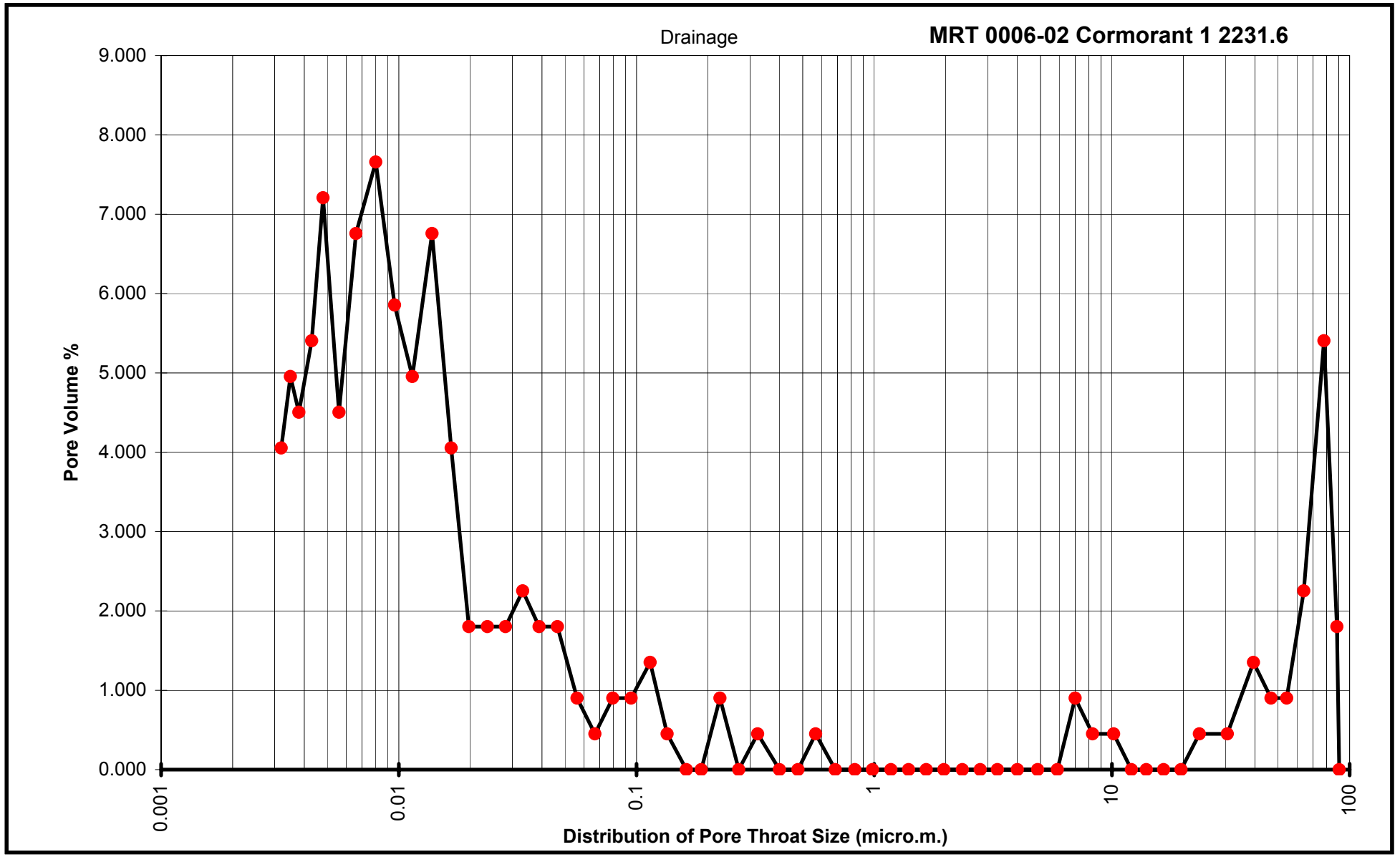

CALCULATED VALUES
porosity % = 6.2582
Grain density gms/cc = 2.3897
MRT 0006-02 Cormorant 1 1999.3
Intrusion cc
0.16
0.14
0.12
0.1
0.08
0.06
0.04
0.02
0
1
10
100
1000
10000
100000
Pressure psia

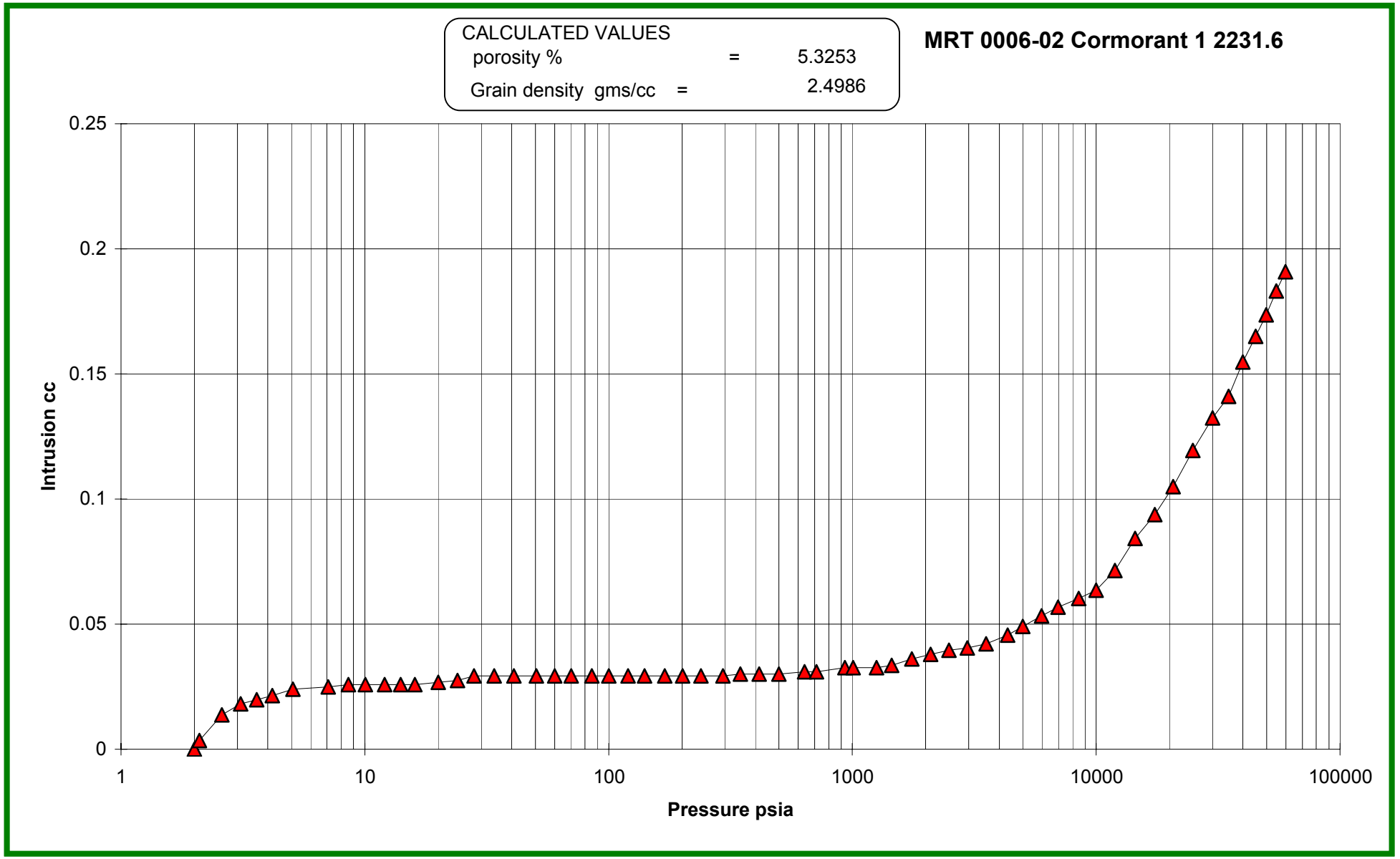

CALCULATED VALUES
porosity % = 6.2582
grain density gms/cc = 2.3897
MRT 0006-02 Cormorant 1 1999.3
Intrusion %
100
90
80
70
60
50
40
30
20
10
0
1
10
100
1000
10000
100000
Pressure psia


Water Saturation vs height (normal); Cormorant-1 1999m
Height (m)
7000
6000
5000
4000
3000
2000
1000
0
0
10
20
30
40
50
60
70
80
90
100
Water Saturation %


Water Saturation Cormorant-1 1999m (lognormal)
10000
1000
100
10
1
Height (m)
0
10
20
30
40
50
60
70
80
90
100
Water Saturation %

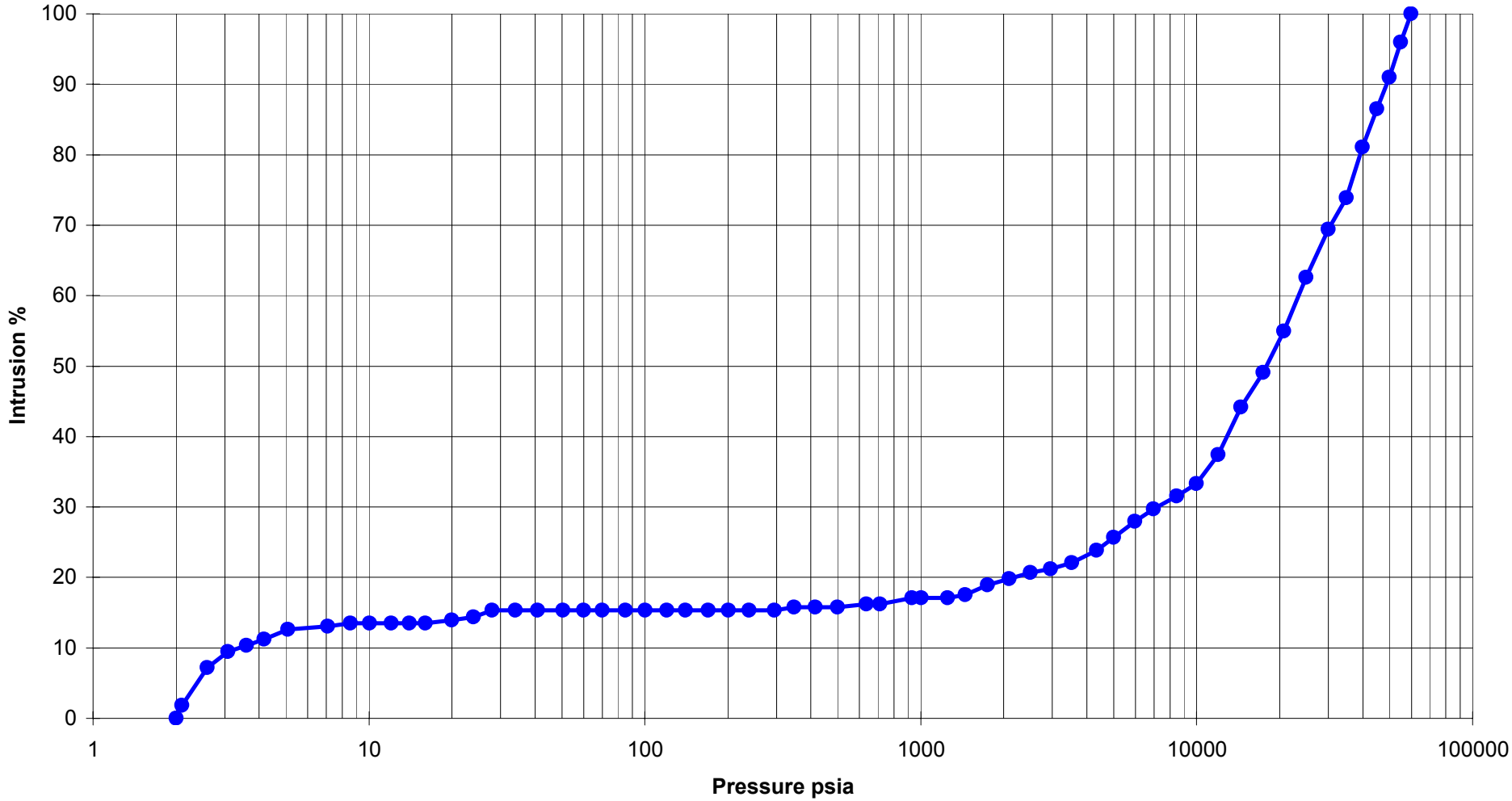
Cormorant_1_2231m.xls



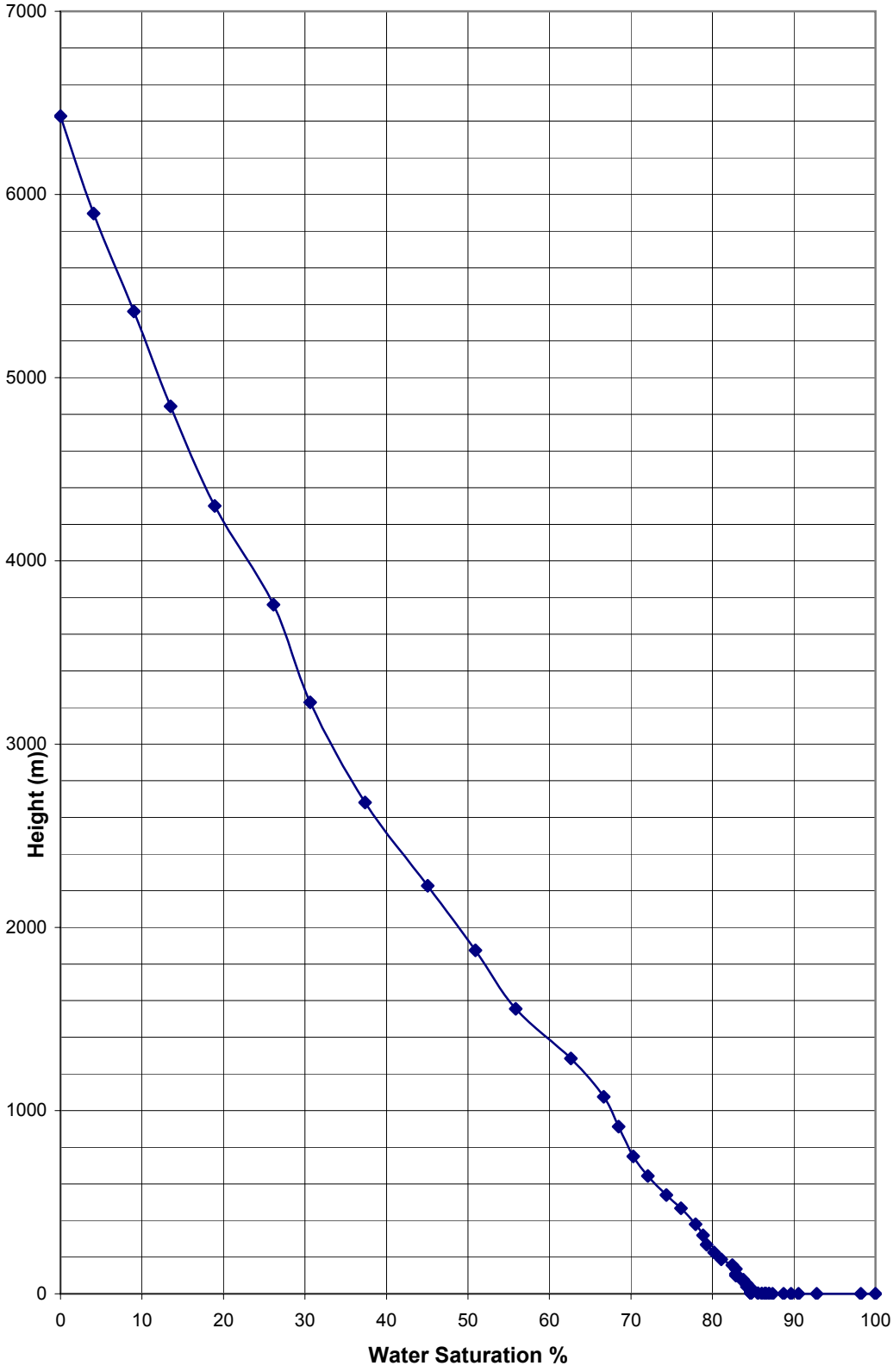

CALCULATED VALUES
porosity % = 5.3253
Grain density gms/cc = 2.4986
MRT 0006-02 Cormorant 1 2231.6
Intrusion cc
0.25
0.2
0.15
0.1
0.05
0
1
10
100
1000
10000
100000
Pressure psia

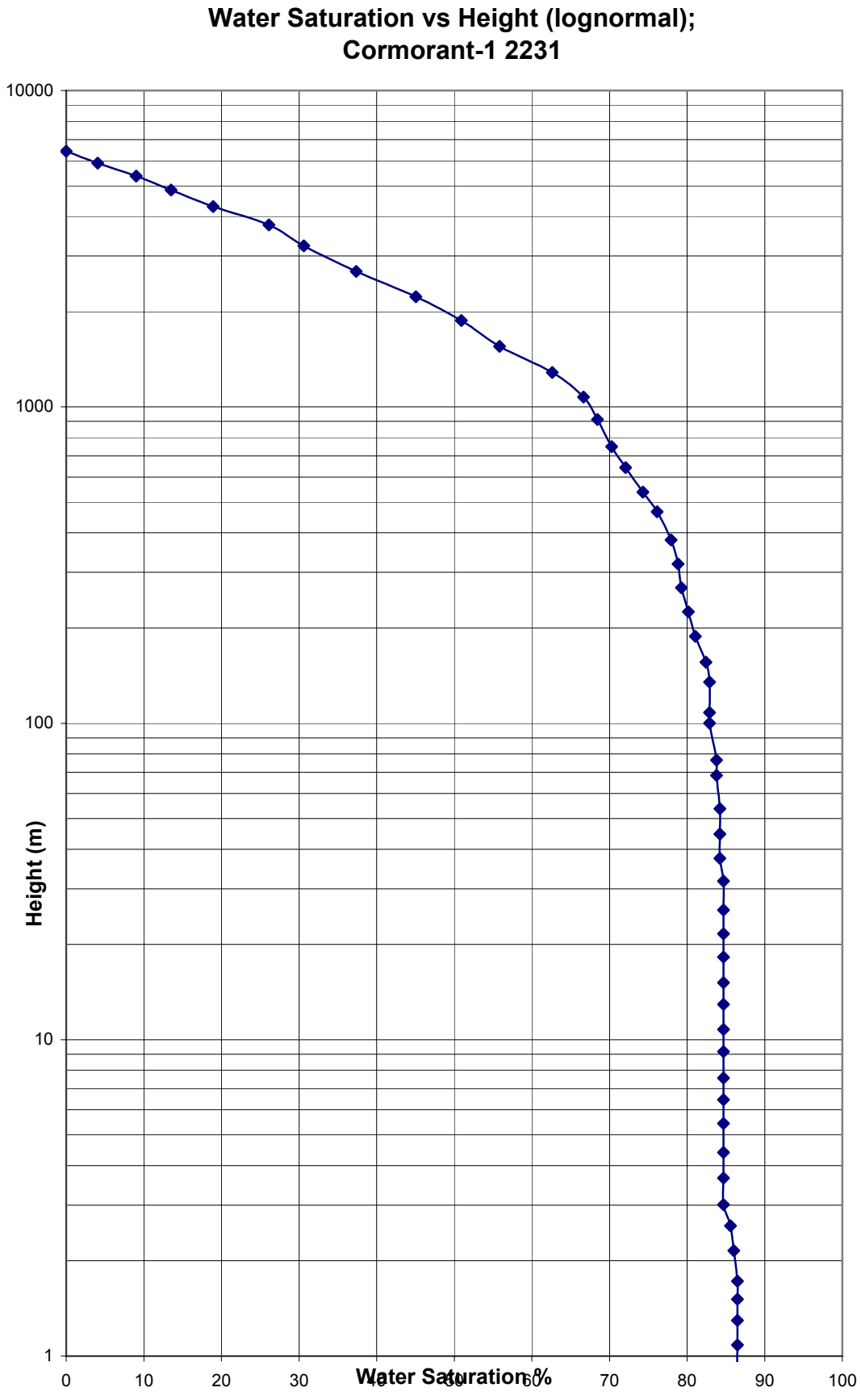
CALCULATED VALUES
porosity % = 5.3253
grain density gms/cc = 2.4986

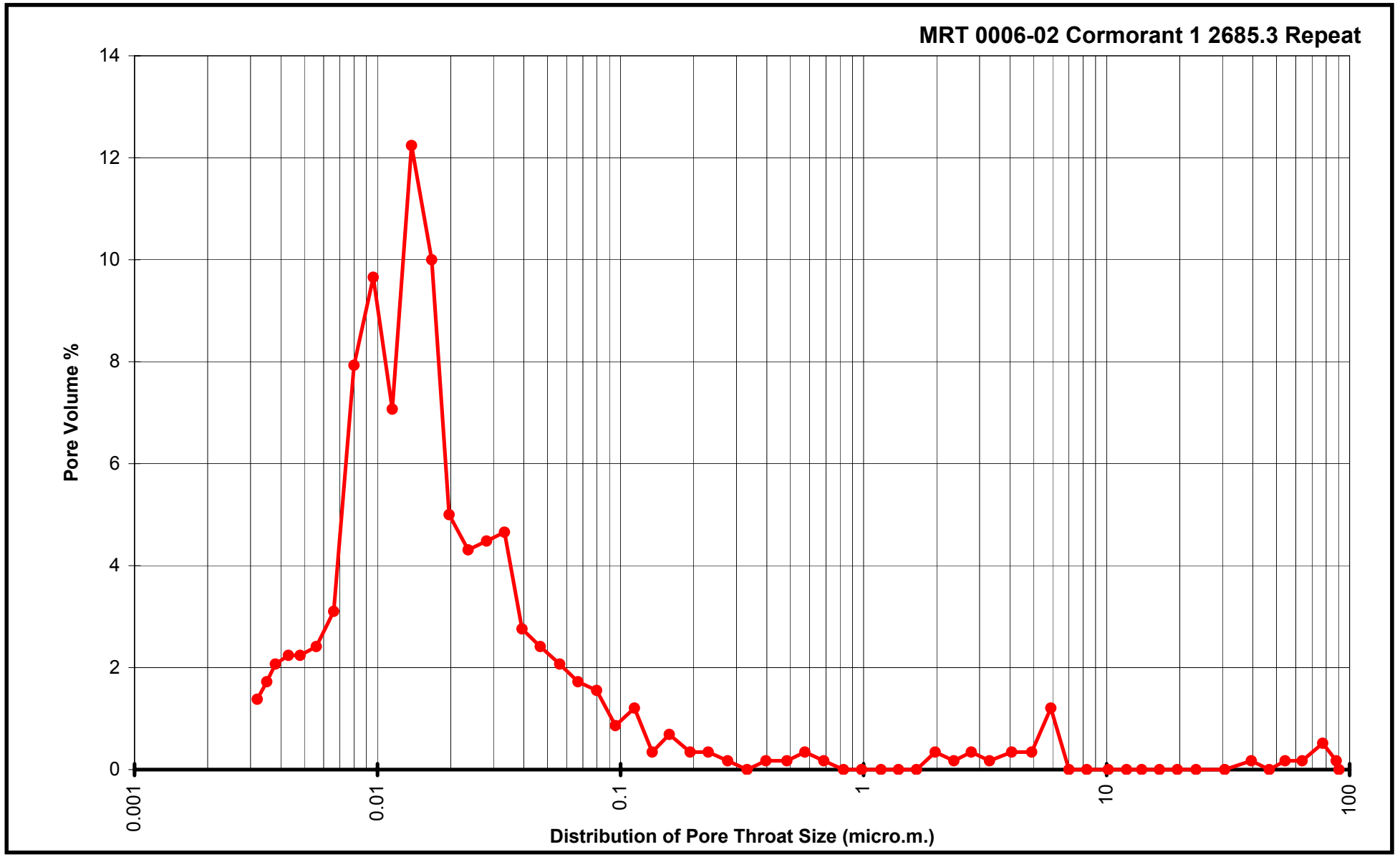
MRT 0006-02 Cormorant 1 2231.6

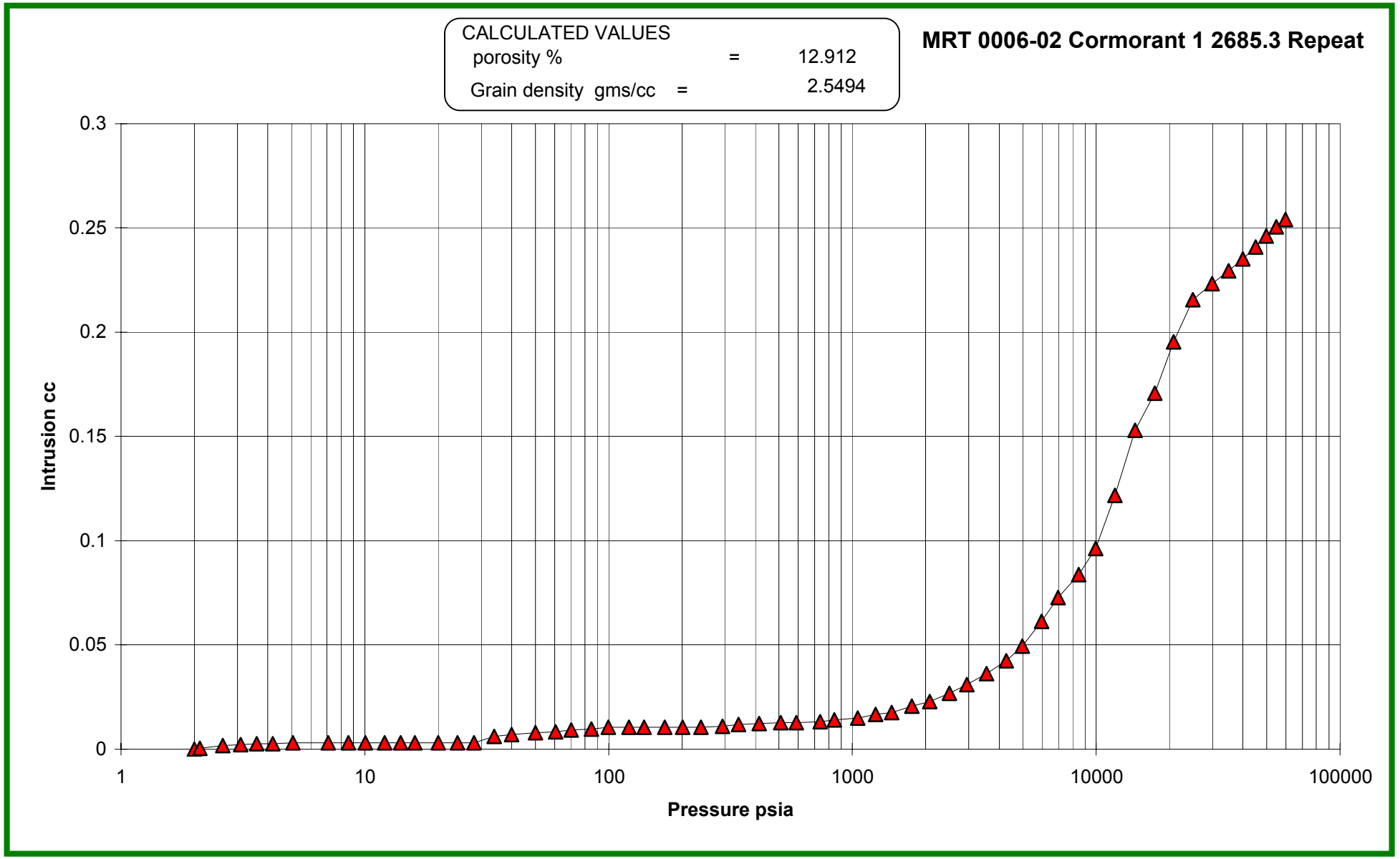


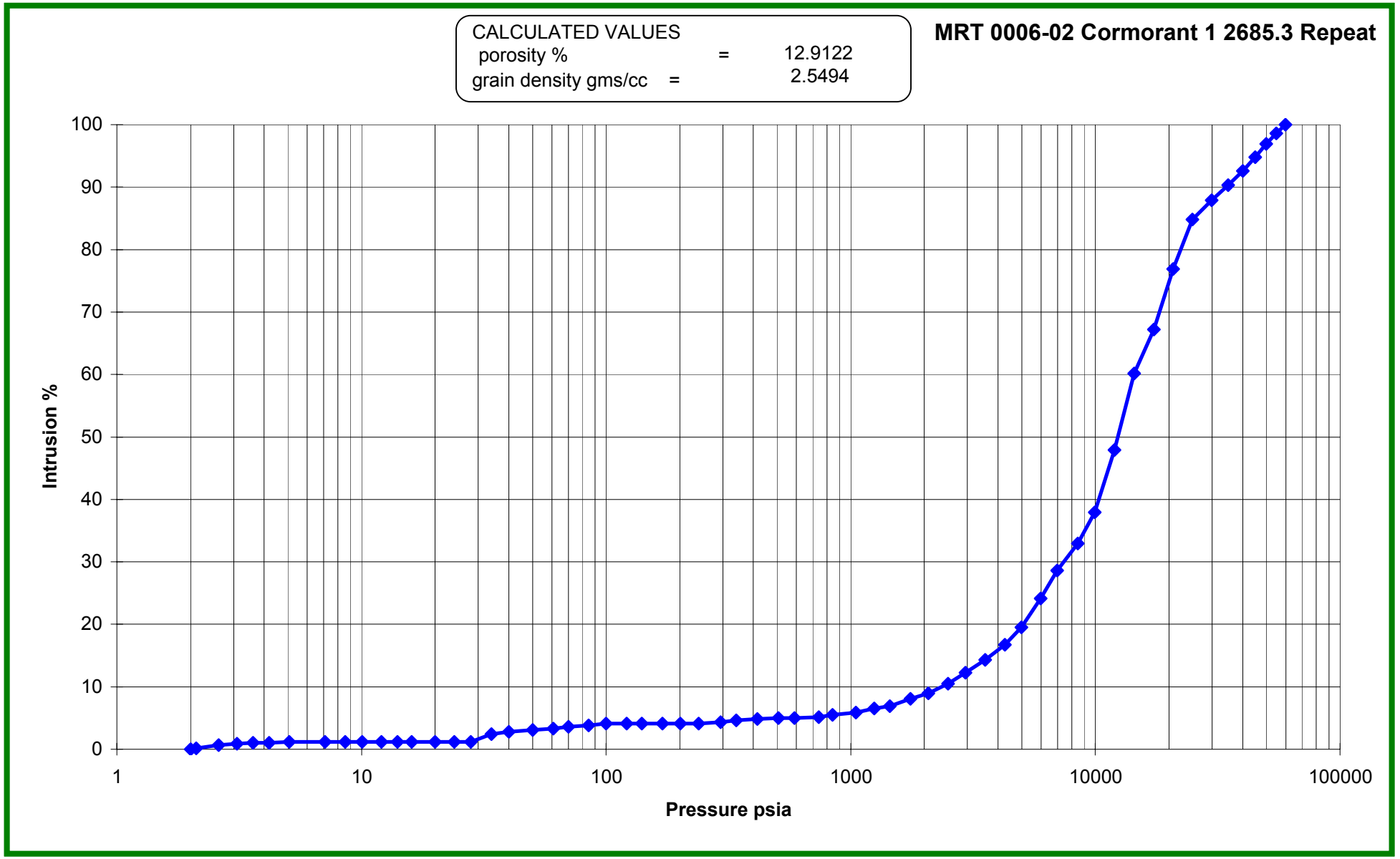
Water Saturation vs Height (normal); Cormorant-1 2231

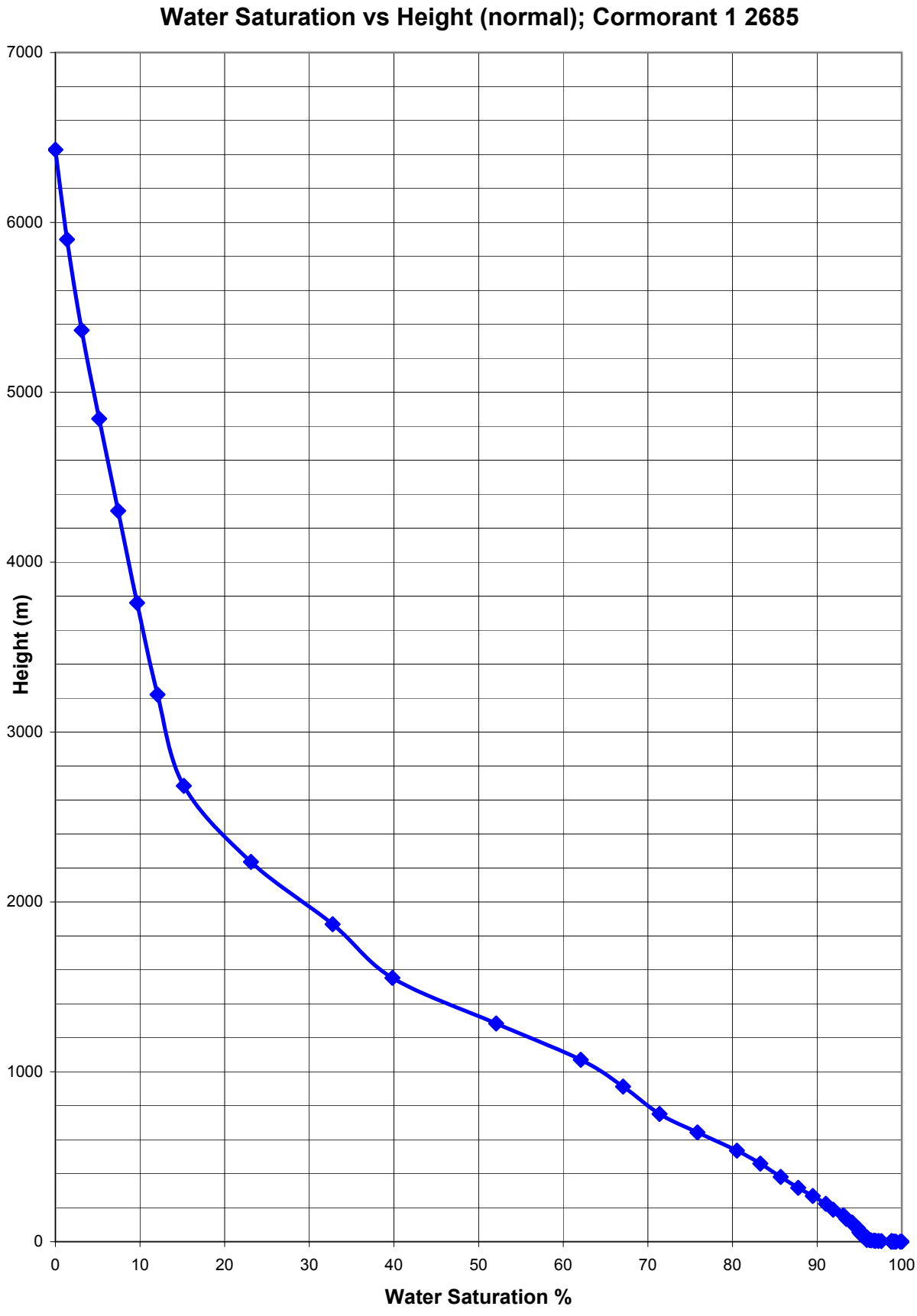


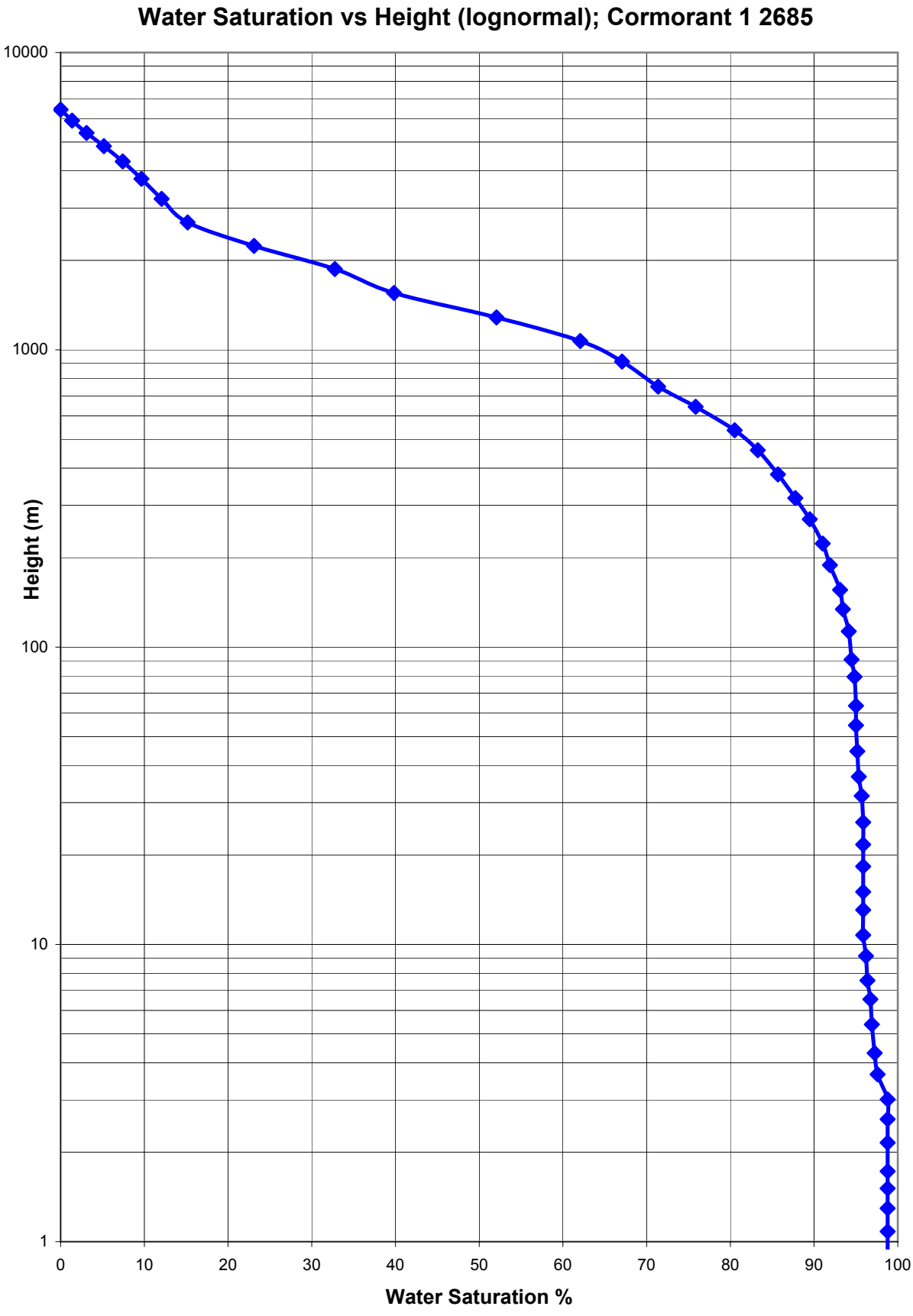

Water Saturation vs Height (lognormal);
Cormorant-1 2231
10000
1000
100
10
1
Height (m)
0
10
20
30
40
50
60
70
80
90
100
Water Saturation, %


MRT 0006-02 Cormorant 1 2685.3 Repeat
Pore Volume %
14
12
10
8
6
4
2
0
0.001
0.01
0.1
1
10
100
Distribution of Pore Throat Size (micro.m.)

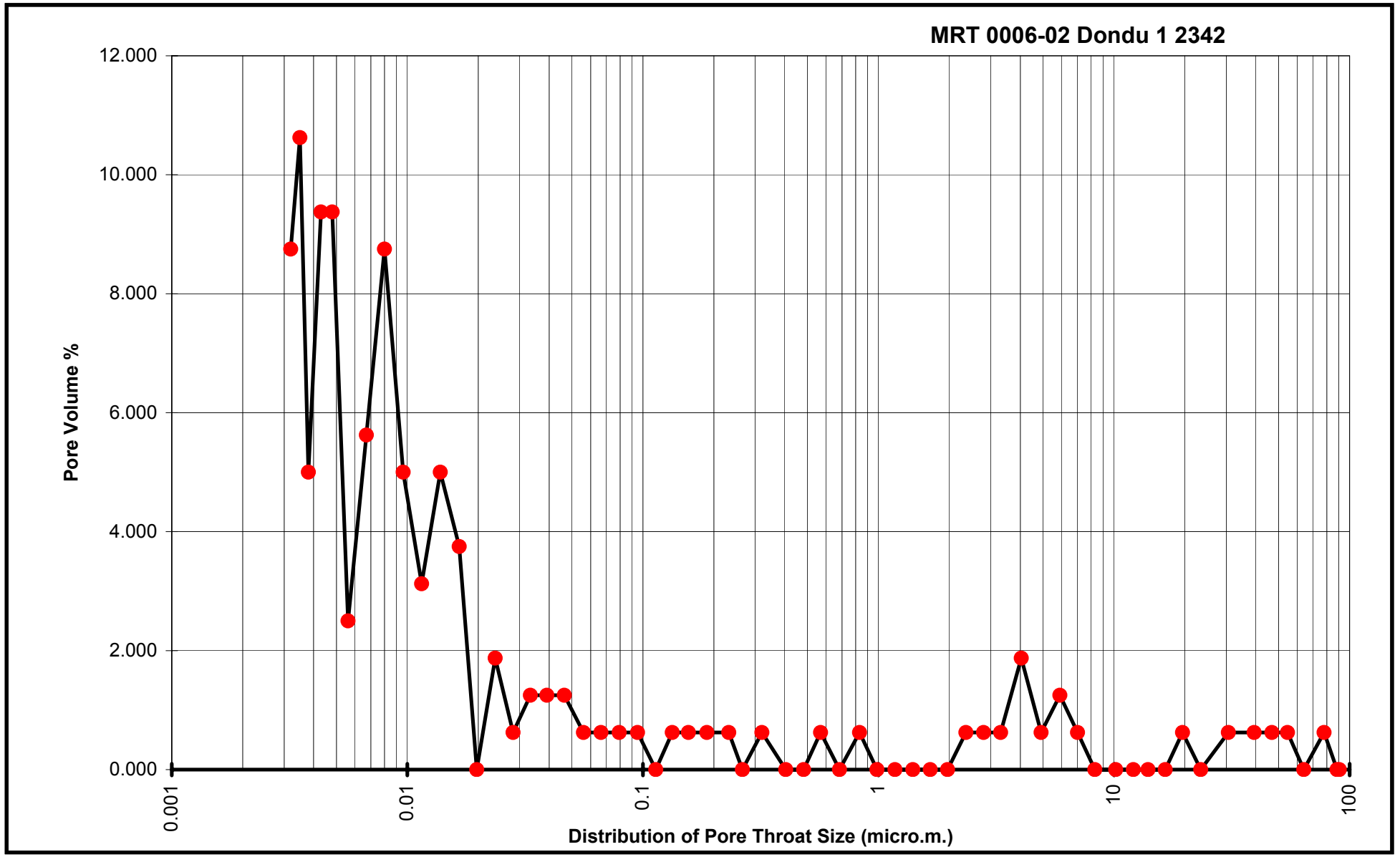

CALCULATED VALUES
porosity % = 12.912
Grain density gms/cc = 2.5494
MRT 0006-02 Cormorant 1 2685.3 Repeat
Intrusion cc
0.3
0.25
0.2
0.15
0.1
0.05
0
1
10
100
1000
10000
100000
Pressure psia


CALCULATED VALUES
porosity % = 12.9122
grain density gms/cc = 2.5494
MRT 0006-02 Cormorant 1 2685.3 Repeat
Intrusion %
100
90
80
70
60
50
40
30
20
10
0
1
10
100
1000
10000
100000
Pressure psia


Water Saturation vs Height (normal); Cormorant 1 2685
Height (m)
7000
6000
5000
4000
3000
2000
1000
0
0
10
20
30
40
50
60
70
80
90
100
Water Saturation %


Water Saturation vs Height (lognormal); Cormorant 1 2685
10000
1000
100
10
1
Height (m)
0
10
20
30
40
50
60
70
80
90
100
Water Saturation %

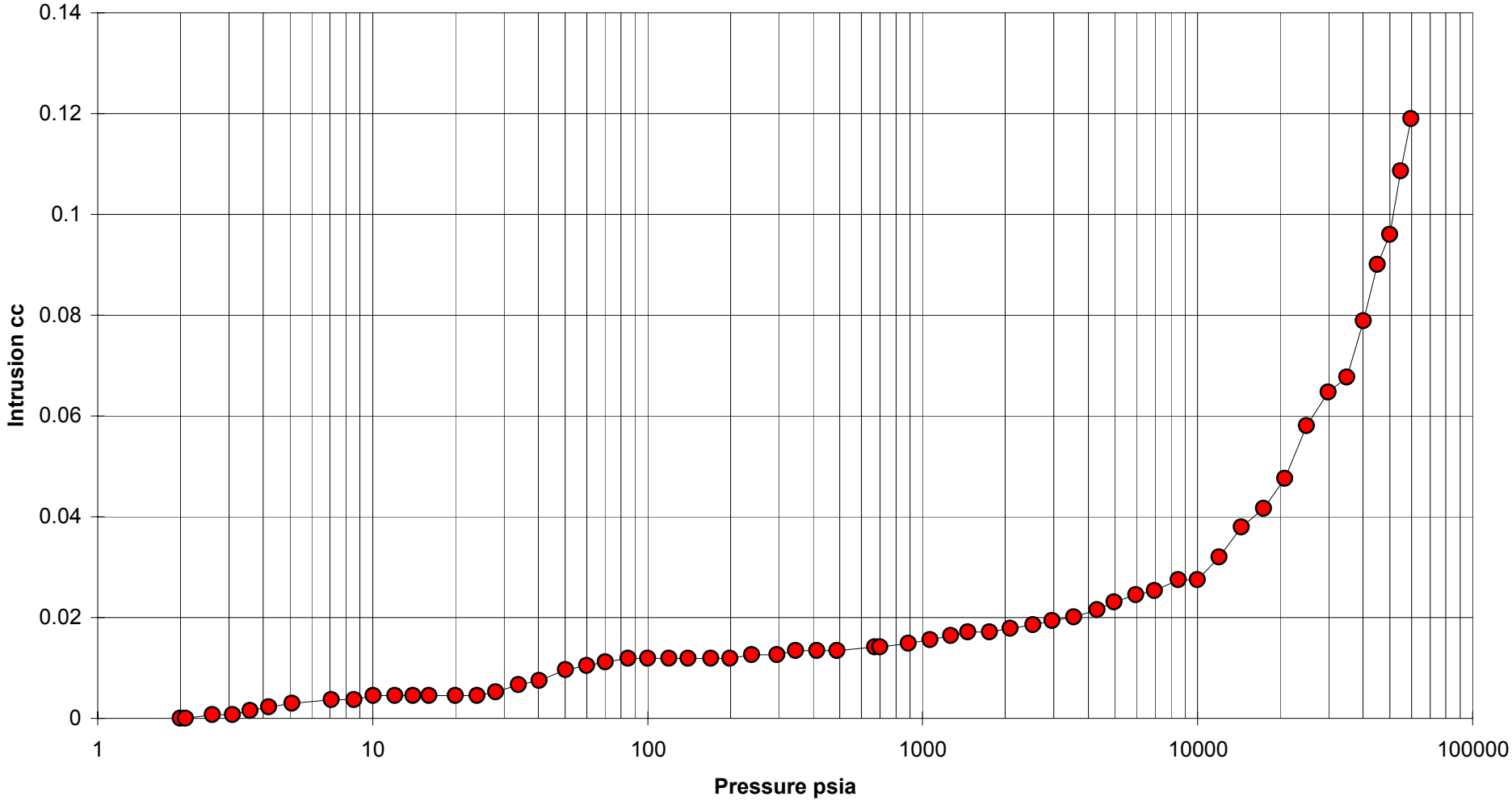
Dondu_1_2342m.xls

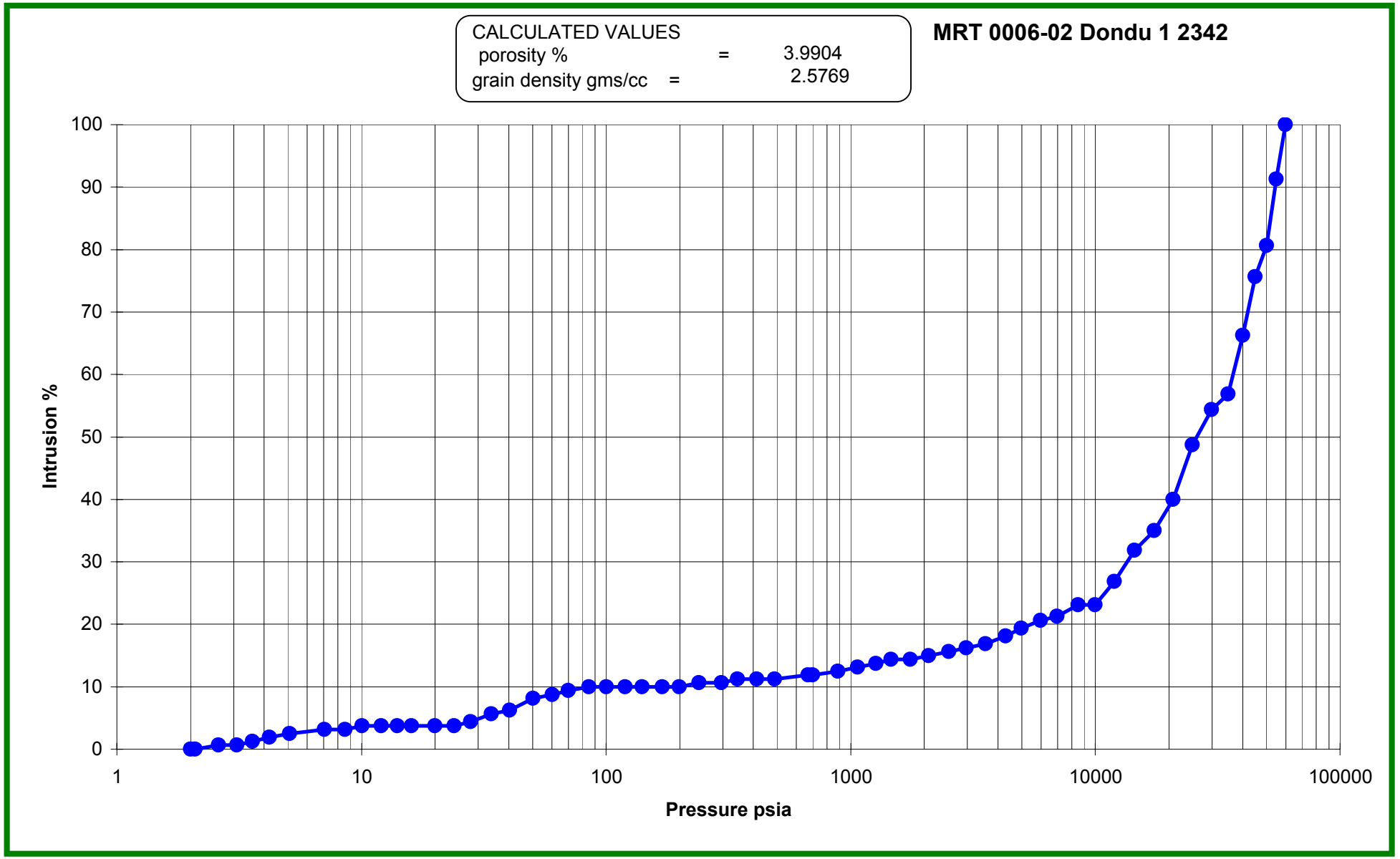


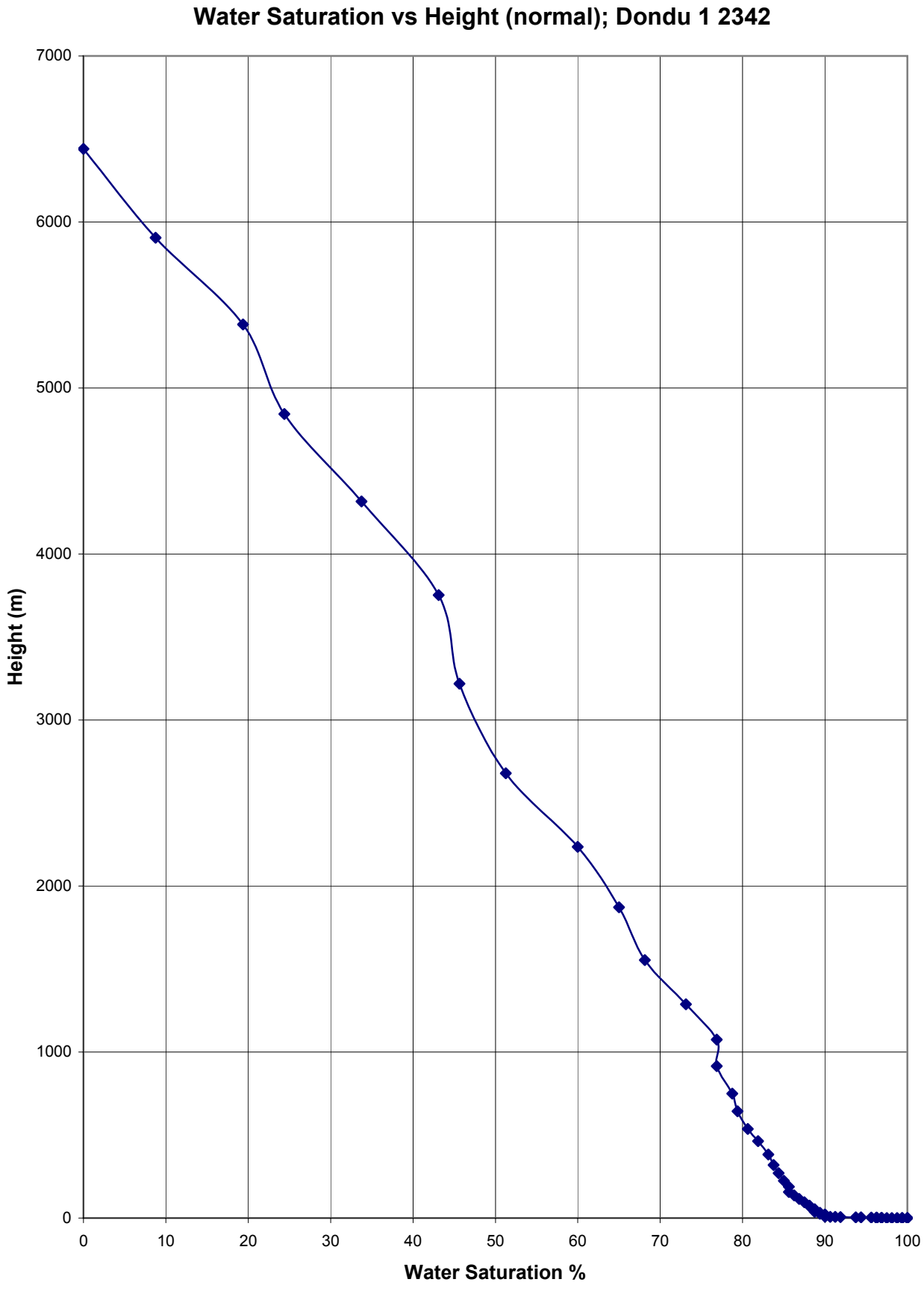
CALCULATED VALUES

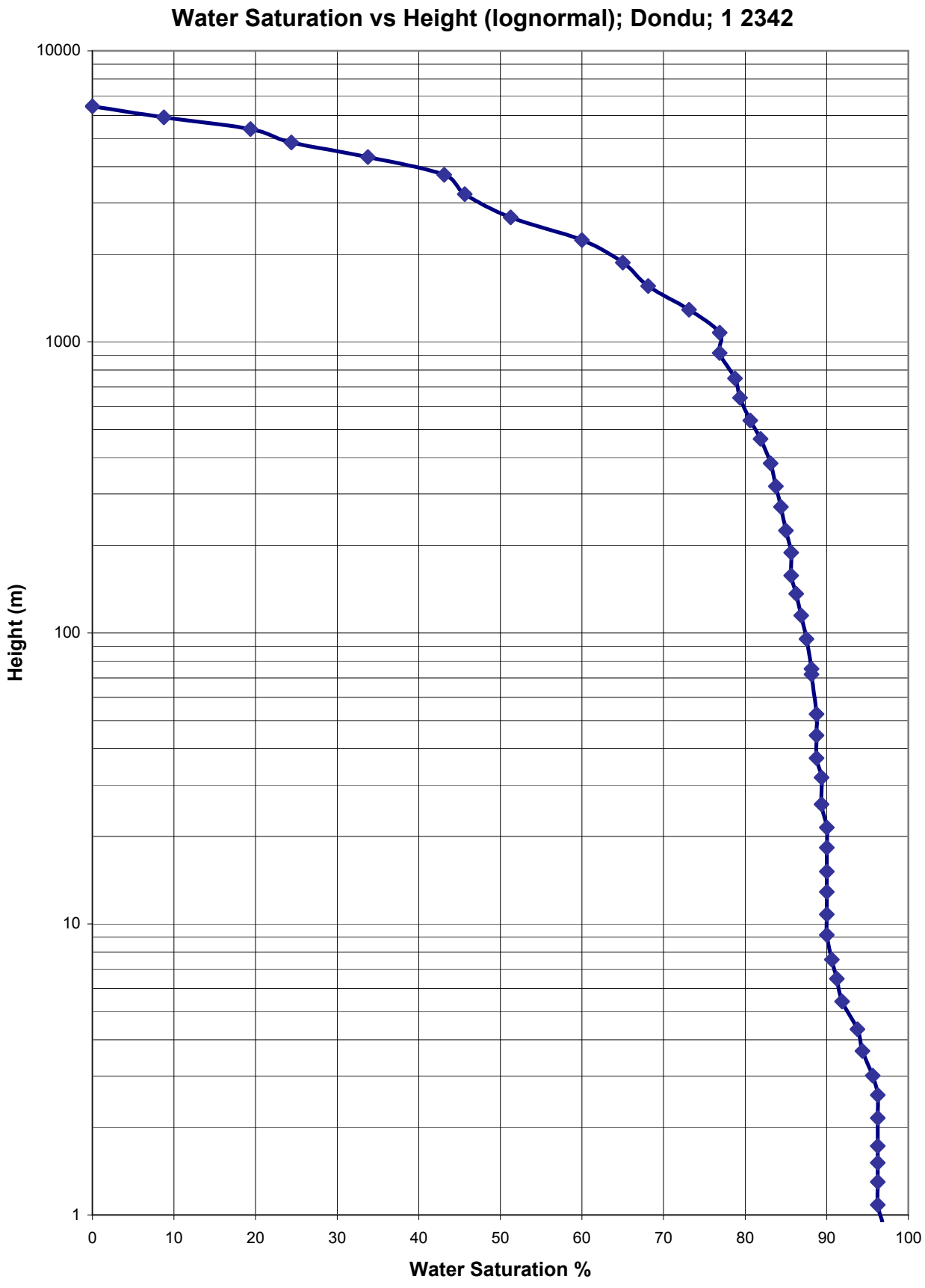
porosity %	=	3.9904
Grain density gms/cc	=	2.5769

MRT 0006-02 Dondu 1 2342

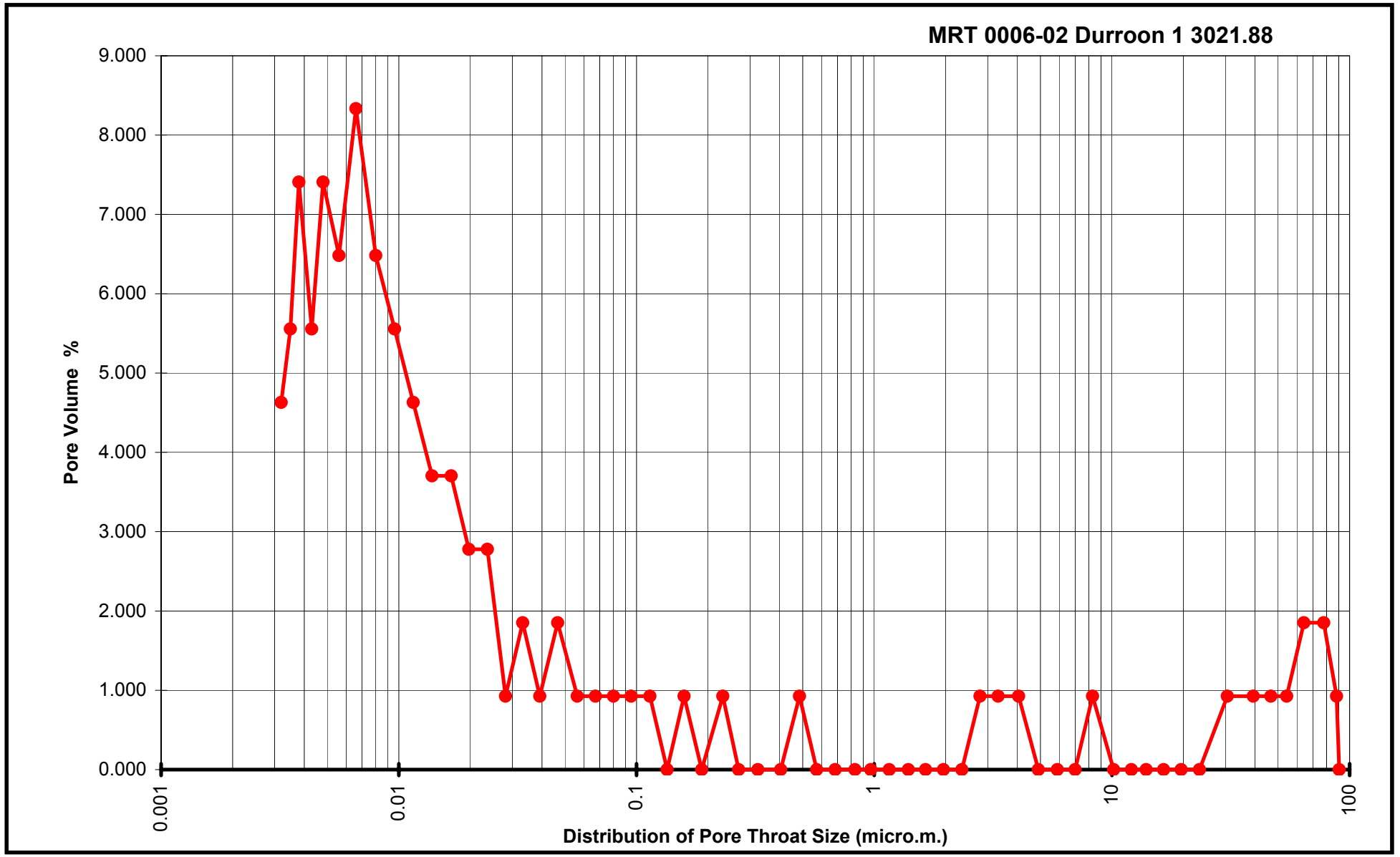


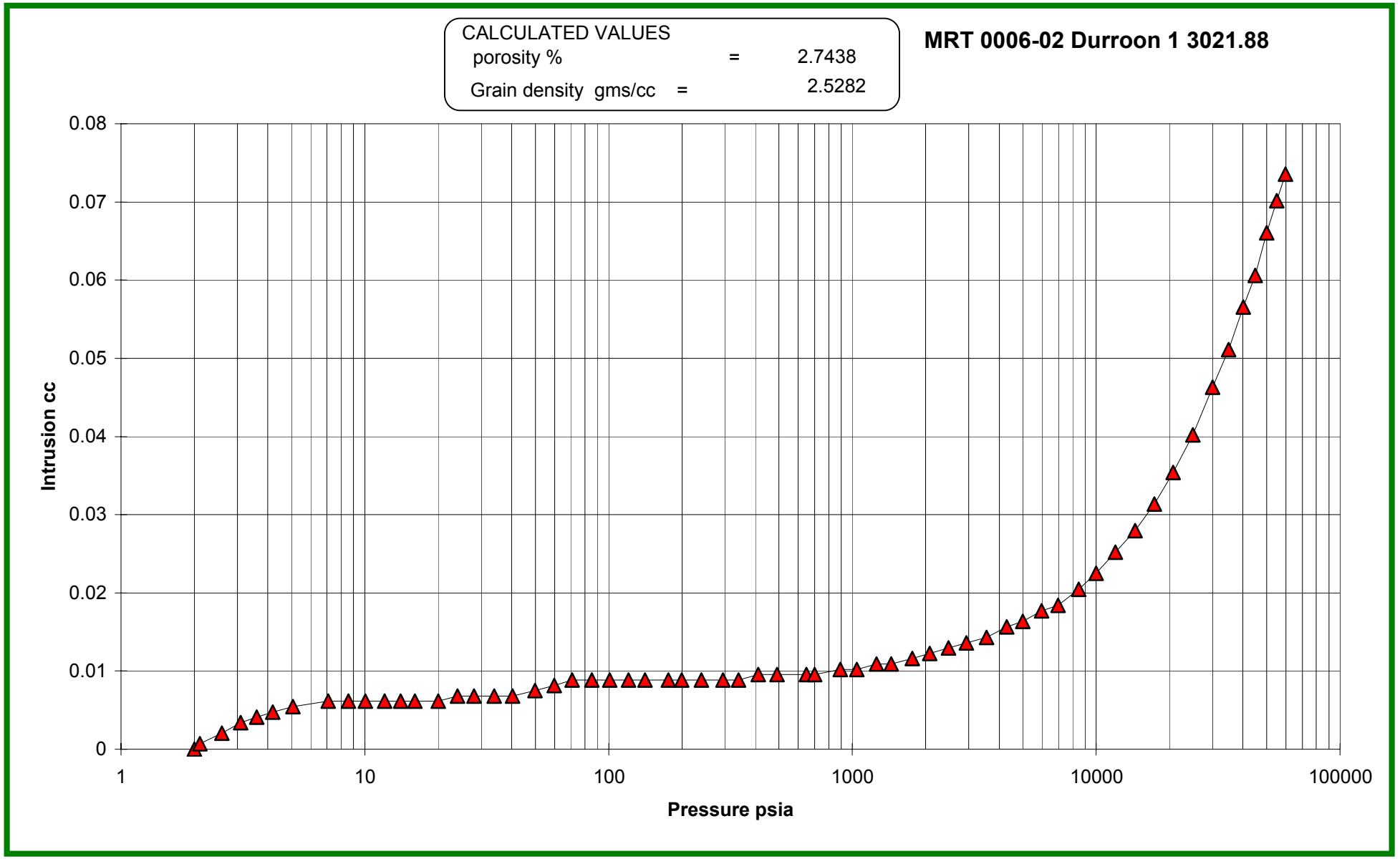

CALCULATED VALUES
porosity % = 3.9904
grain density gms/cc = 2.5769
MRT 0006-02 Dondu 1 2342
Intrusion %
100
90
80
70
60
50
40
30
20
10
0
1
10
100
1000
10000
100000
Pressure psia

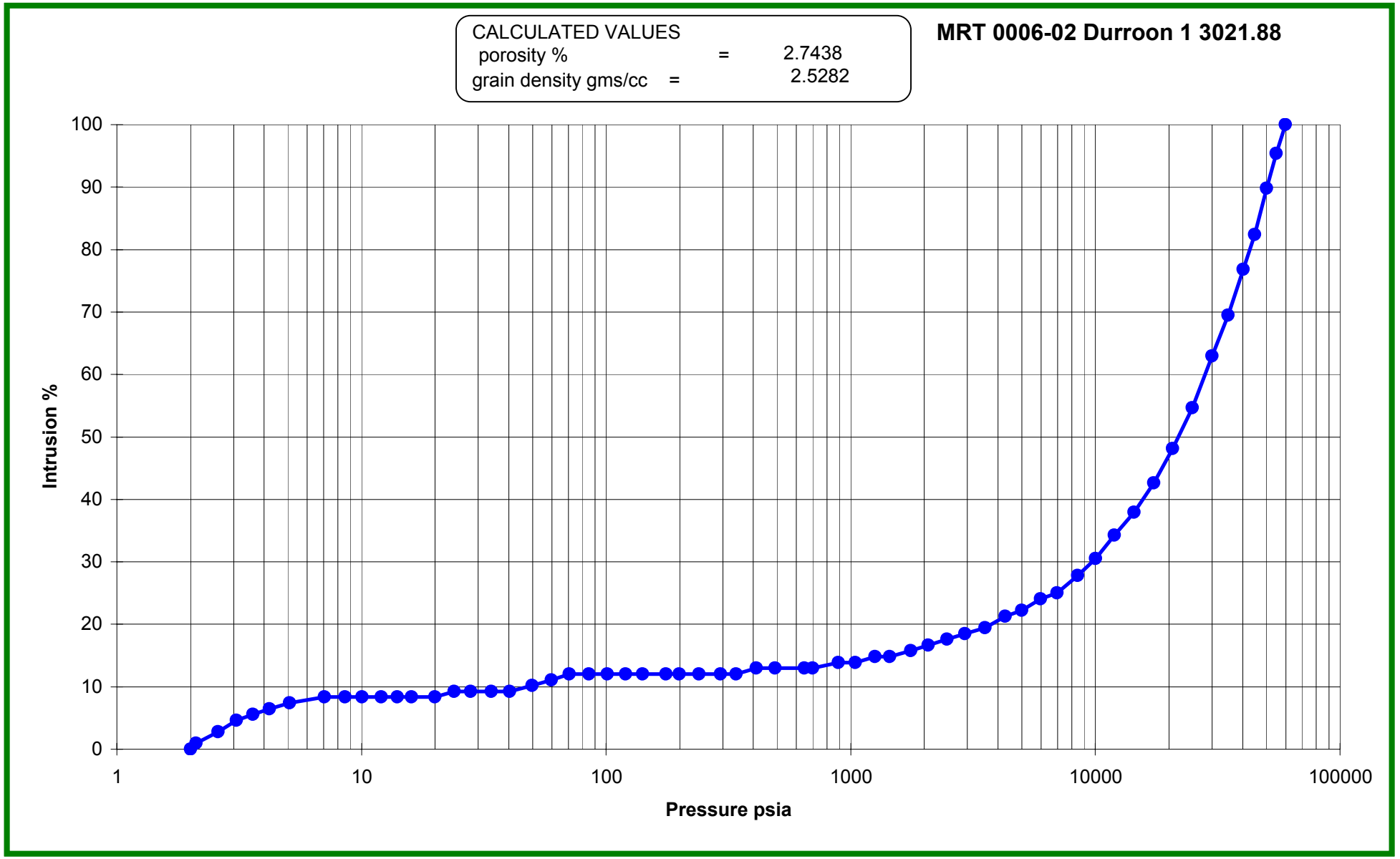

Water Saturation vs Height (normal); Dondu 1 2342
Height (m)
7000
6000
5000
4000
3000
2000
1000
0
0
10
20
30
40
50
60
70
80
90
100
Water Saturation %

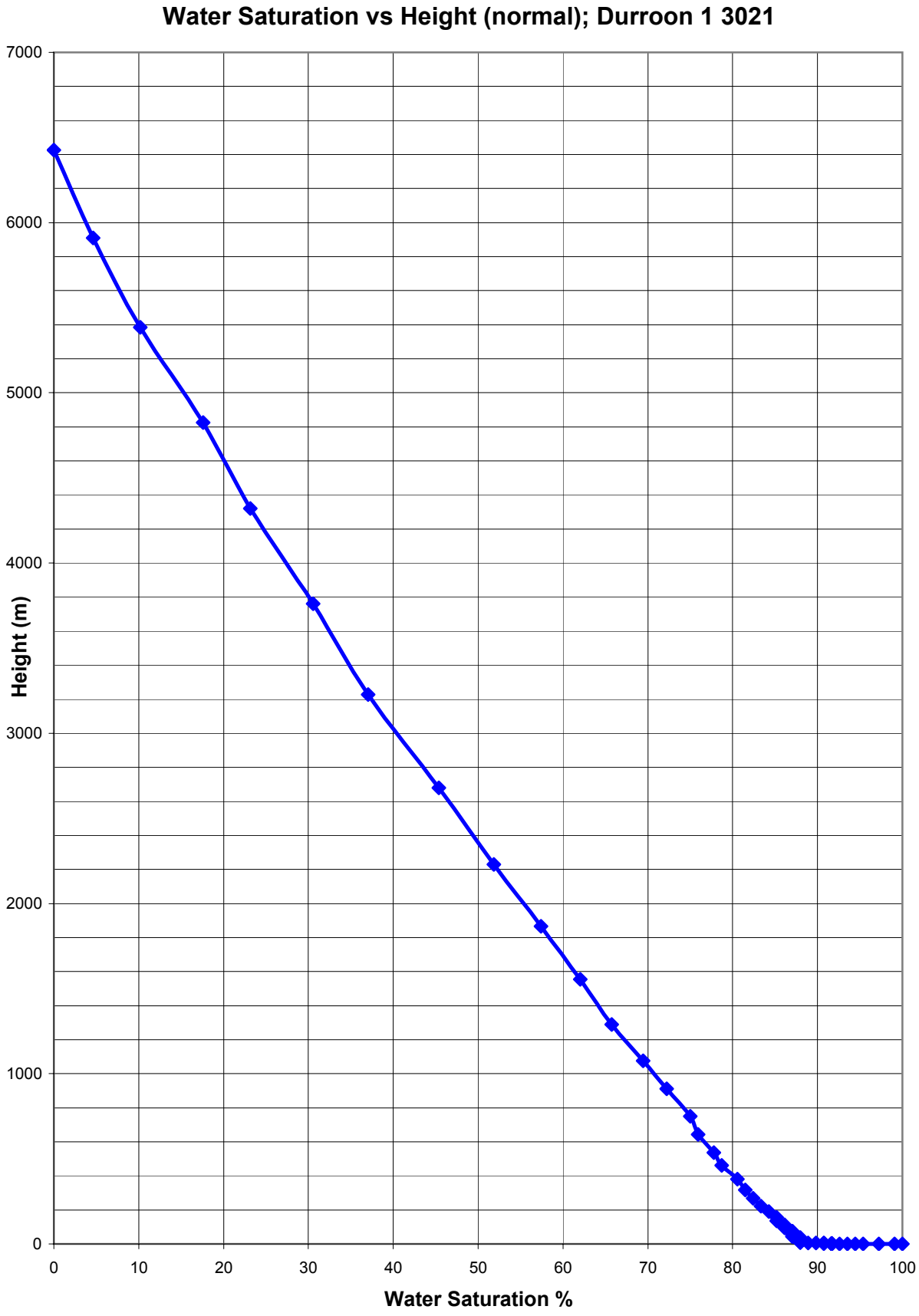

Water Saturation vs Height (lognormal); Dondu; 1 2342
Height (m)
10000
1000
100
10
1
0
10
20
30
40
50
60
70
80
90
100
Water Saturation %

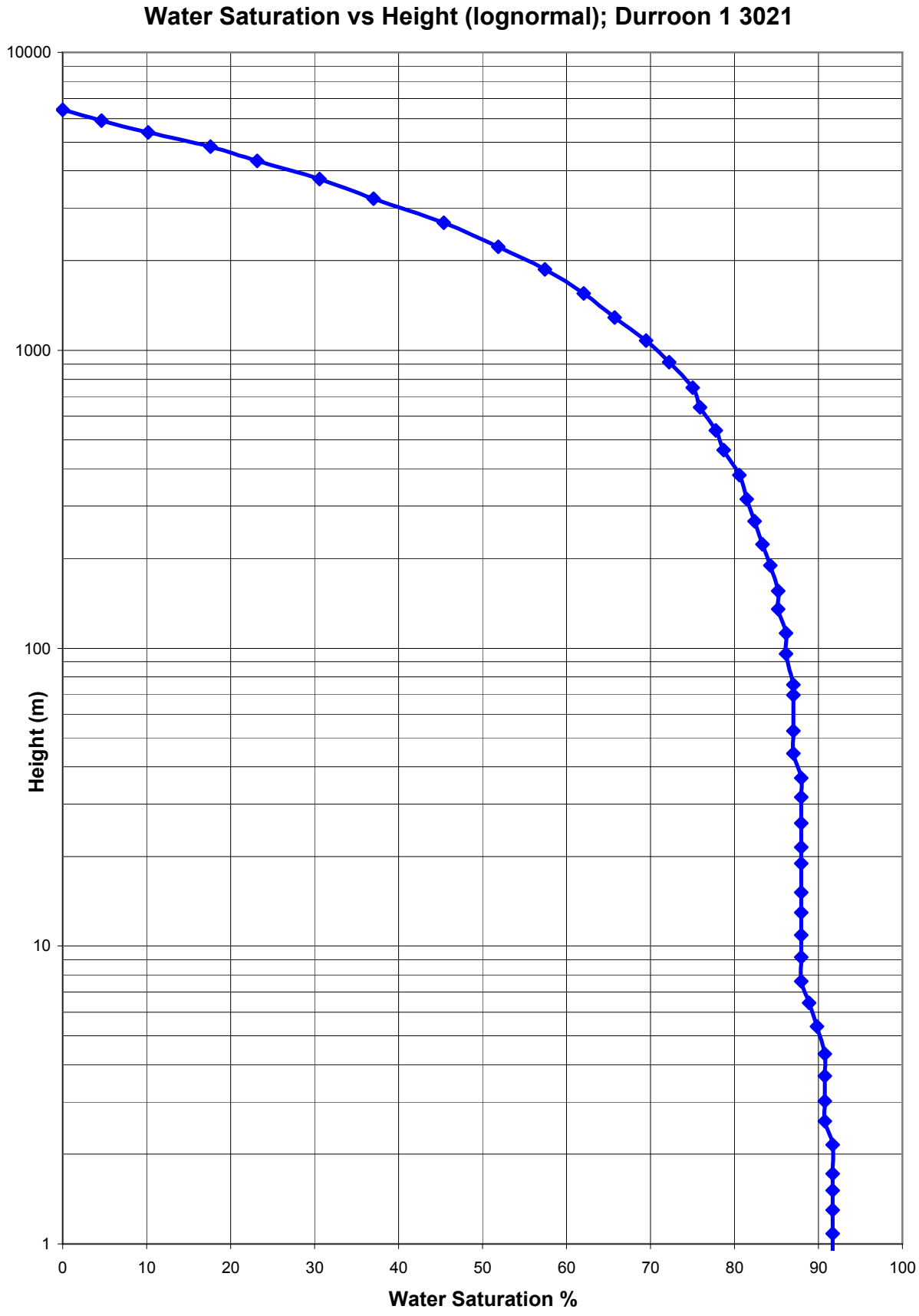
Durroon_1_3021m.xls

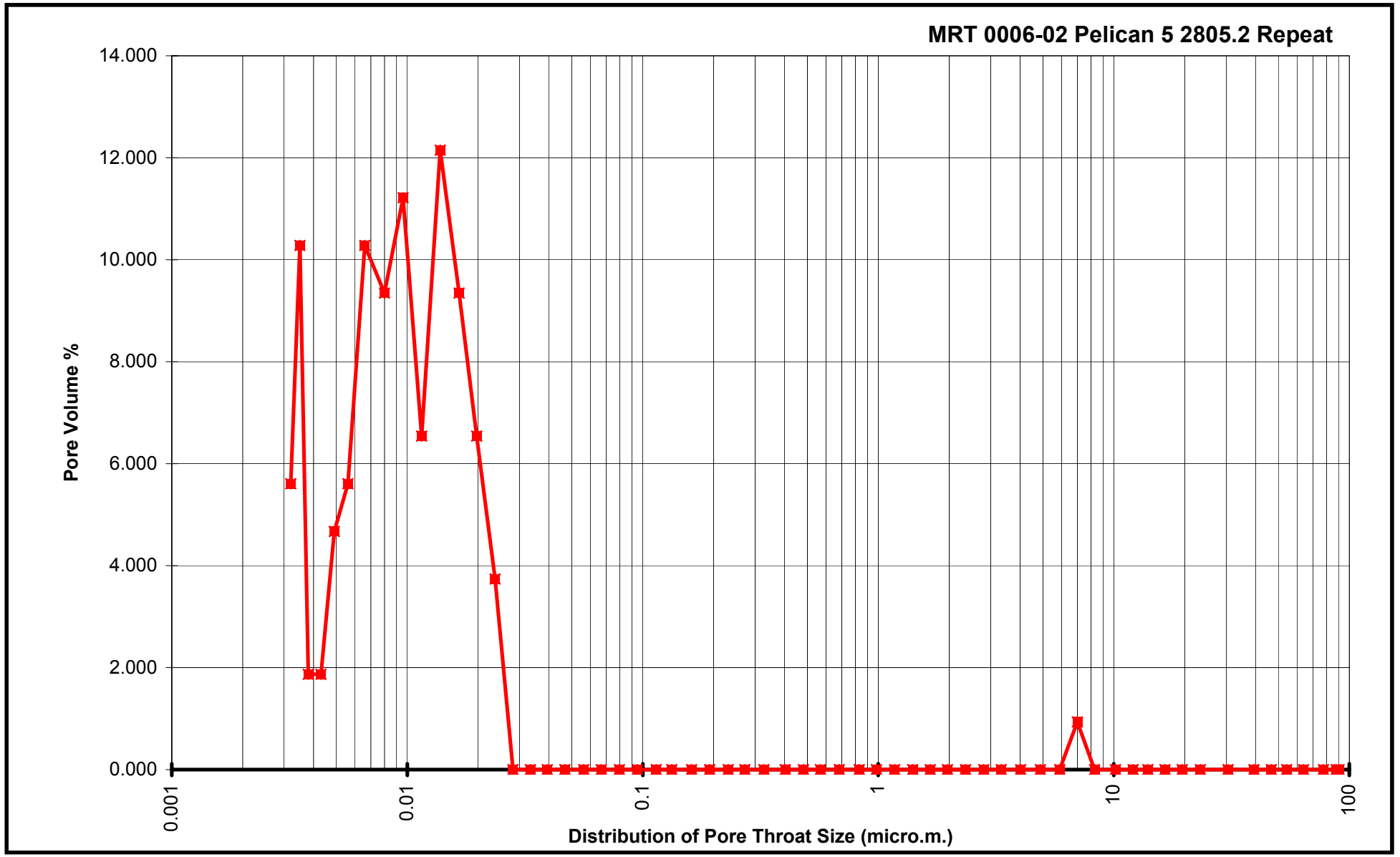


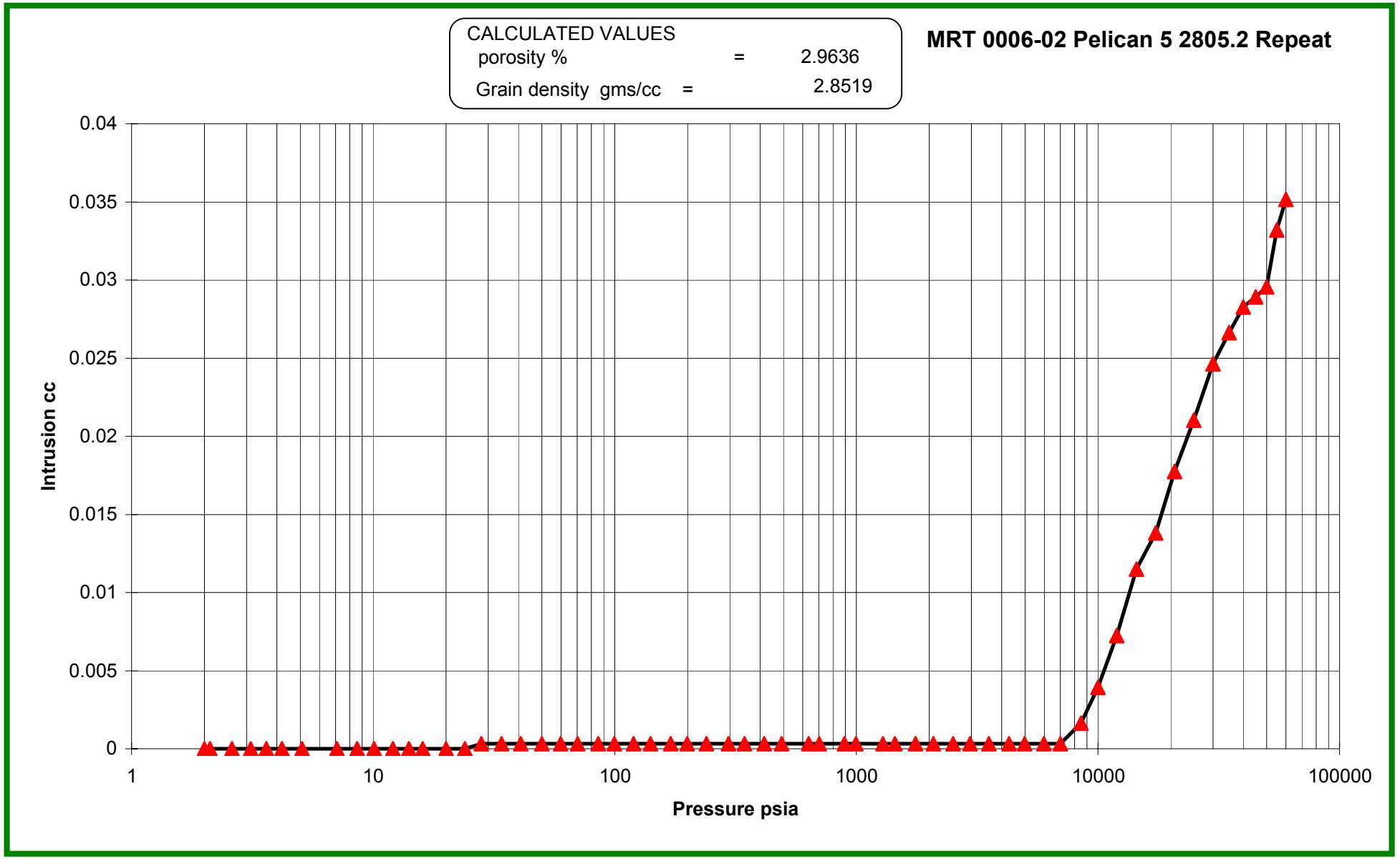

CALCULATED VALUES
porosity % = 2.7438
Grain density gms/cc = 2.5282
MRT 0006-02 Durroon 1 3021.88
Intrusion cc
0.08
0.07
0.06
0.05
0.04
0.03
0.02
0.01
0
1
10
100
1000
10000
100000
Pressure psia

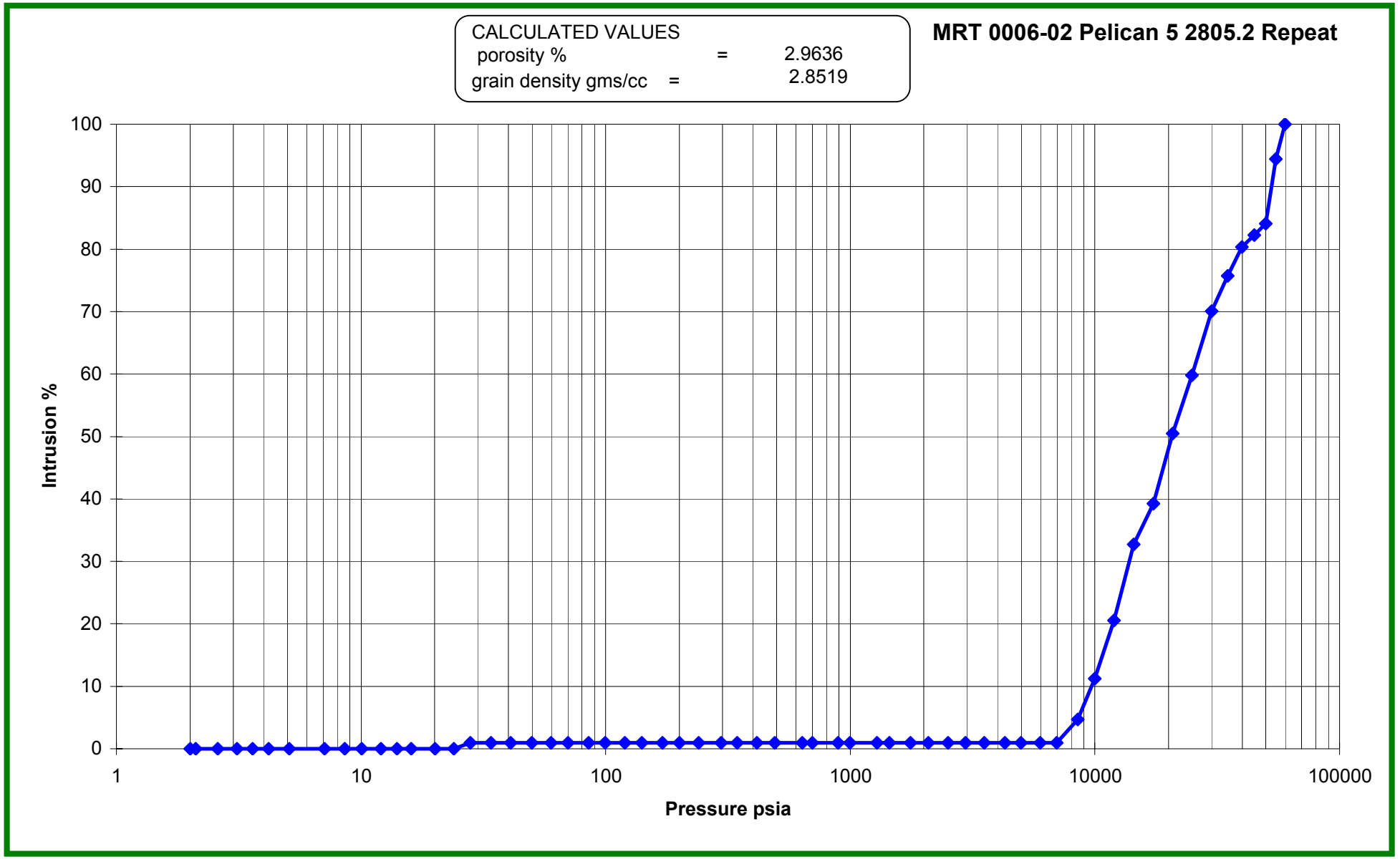

CALCULATED VALUES
porosity % = 2.7438
grain density gms/cc = 2.5282
MRT 0006-02 Durroon 1 3021.88
Intrusion %
100
90
80
70
60
50
40
30
20
10
0
1
10
100
1000
10000
100000
Pressure psia

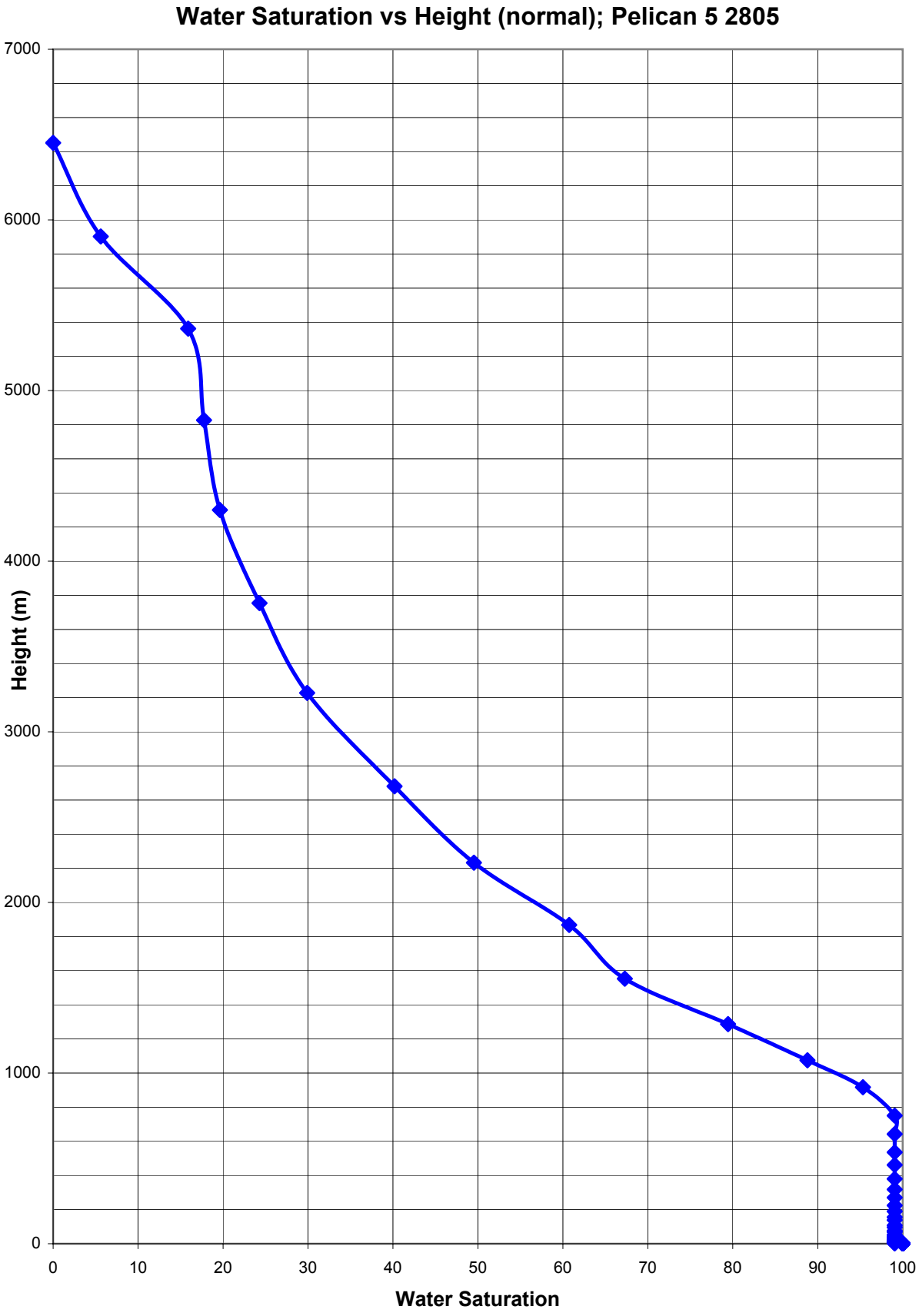

Water Saturation vs Height (normal); Durroon 1 3021
Height (m)
7000
6000
5000
4000
3000
2000
1000
0
0
10
20
30
40
50
60
70
80
90
100
Water Saturation %

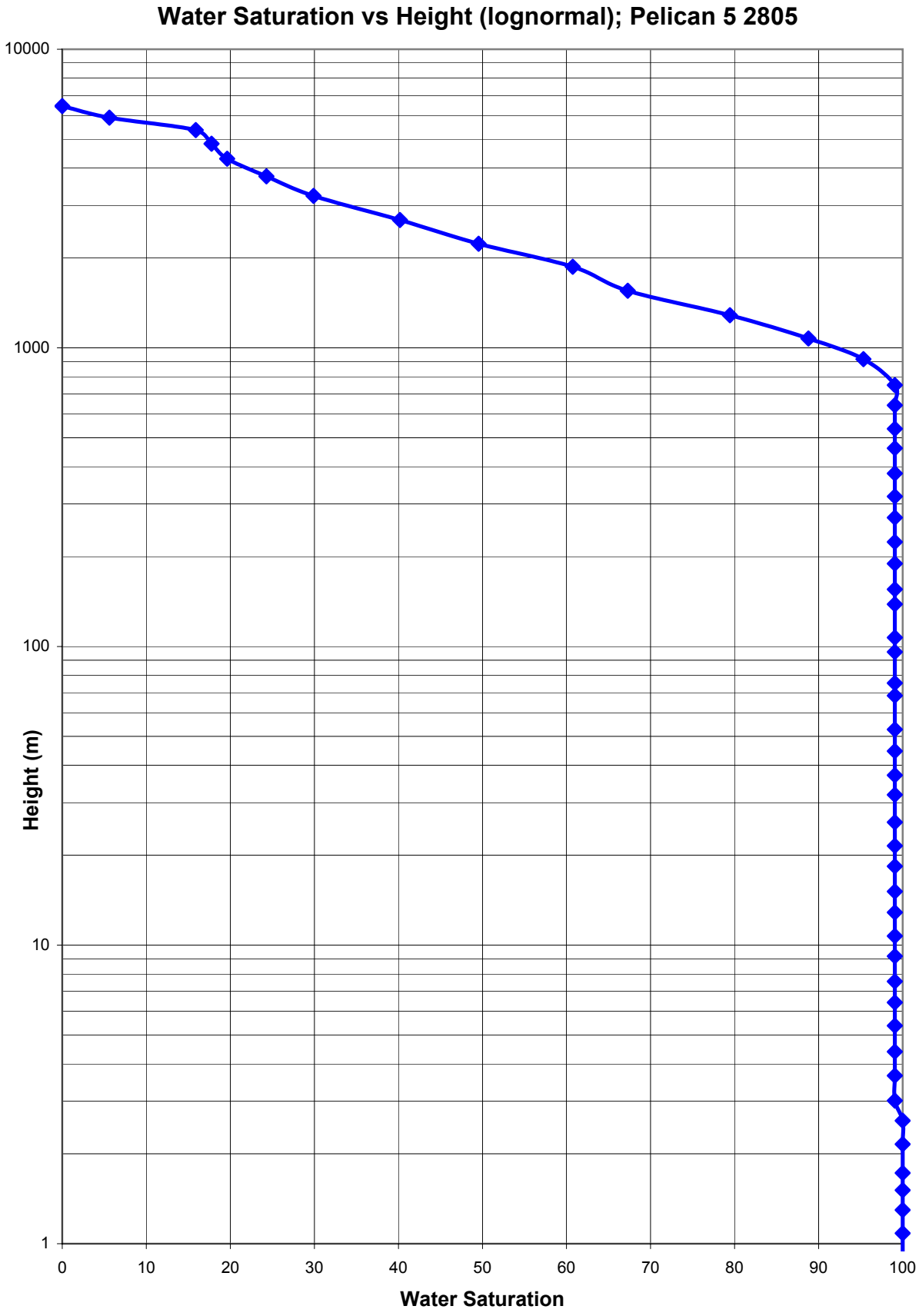

Water Saturation vs Height (lognormal); Durroon 1 3021
10000
1000
100
10
1
Height (m)
0
10
20
30
40
50
60
70
80
90
100
Water Saturation %


MRT 0006-02 Pelican 5 2805.2 Repeat
14.000
12.000
10.000
8.000
6.000
4.000
2.000
0.000
Pore Volume %
0.001
0.01
0.1
1
10
100
Distribution of Pore Throat Size (micro.m.)

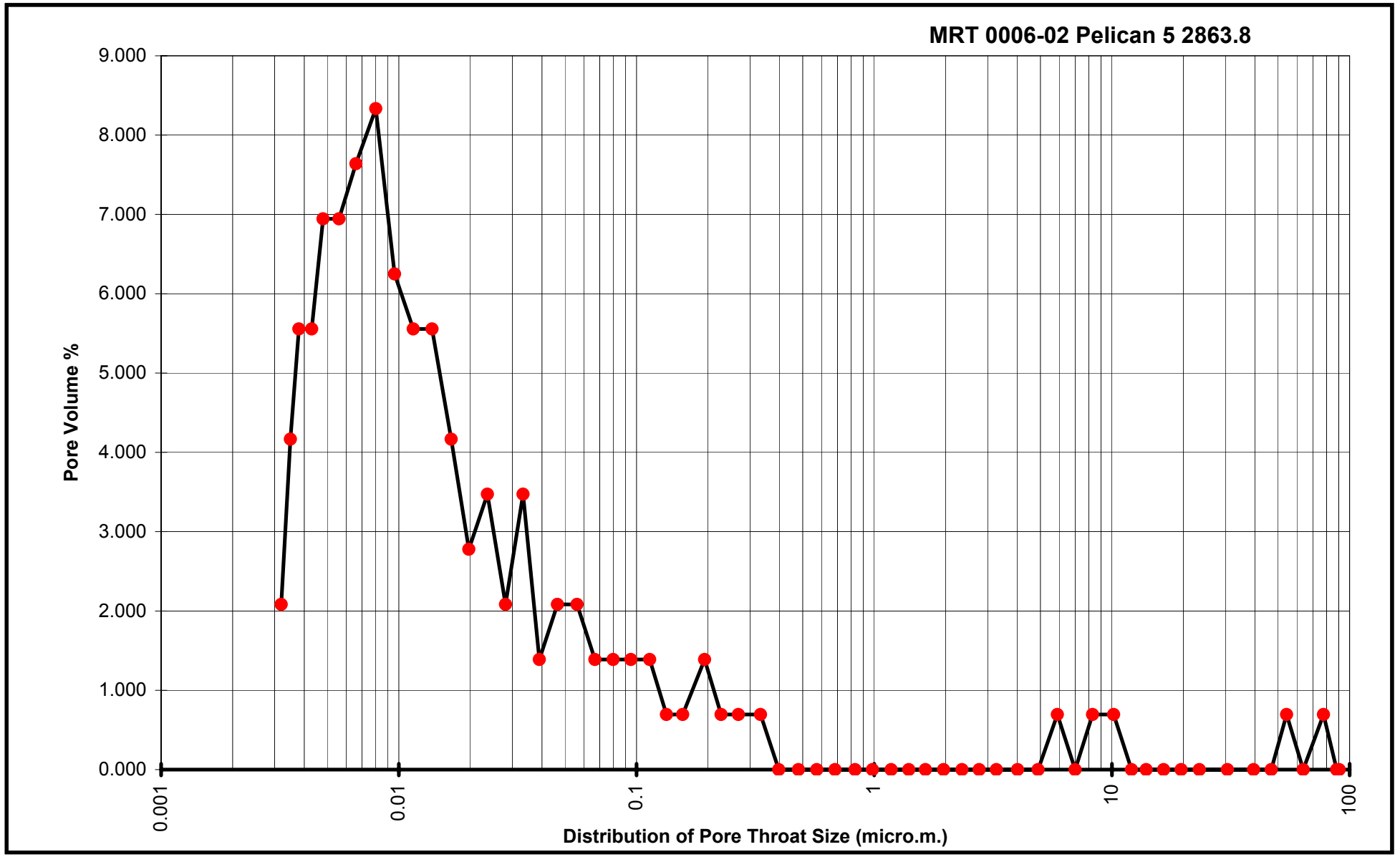

CALCULATED VALUES
porosity % = 2.9636
Grain density gms/cc = 2.8519
MRT 0006-02 Pelican 5 2805.2 Repeat
Intrusion cc
0.04
0.035
0.03
0.025
0.02
0.015
0.01
0.005
0
1
10
100
1000
10000
100000
Pressure psia

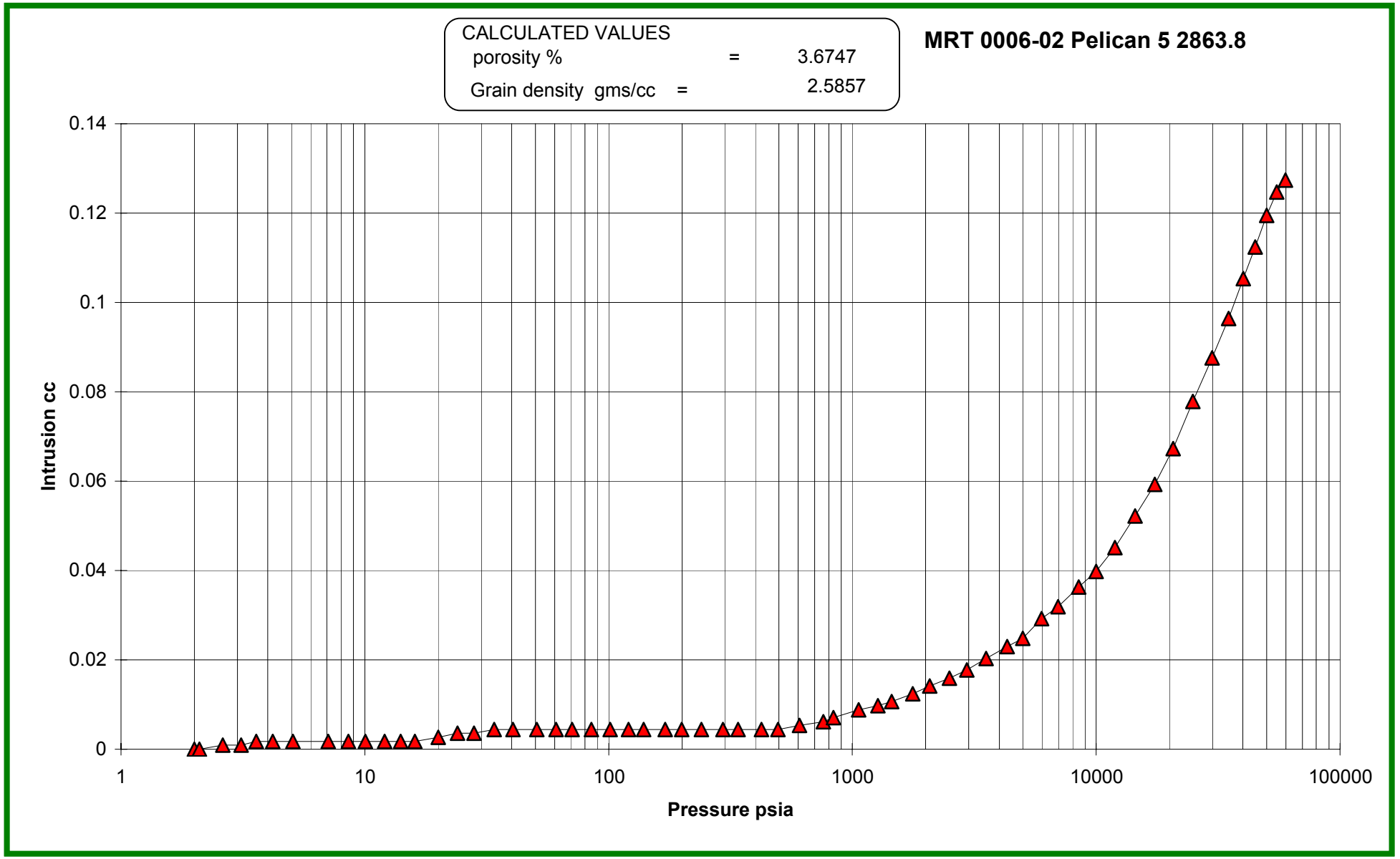

CALCULATED VALUES
porosity % = 2.9636
grain density gms/cc = 2.8519
MRT 0006-02 Pelican 5 2805.2 Repeat
Intrusion %
100
90
80
70
60
50
40
30
20
10
0
1
10
100
1000
10000
100000
Pressure psia


Water Saturation vs Height (normal); Pelican 5 2805
Height (m)
7000
6000
5000
4000
3000
2000
1000
0
0
10
20
30
40
50
60
70
80
90
100
Water Saturation


Water Saturation vs Height (lognormal); Pelican 5 2805
10000
1000
100
10
1
Height (m)
0
10
20
30
40
50
60
70
80
90
100
Water Saturation

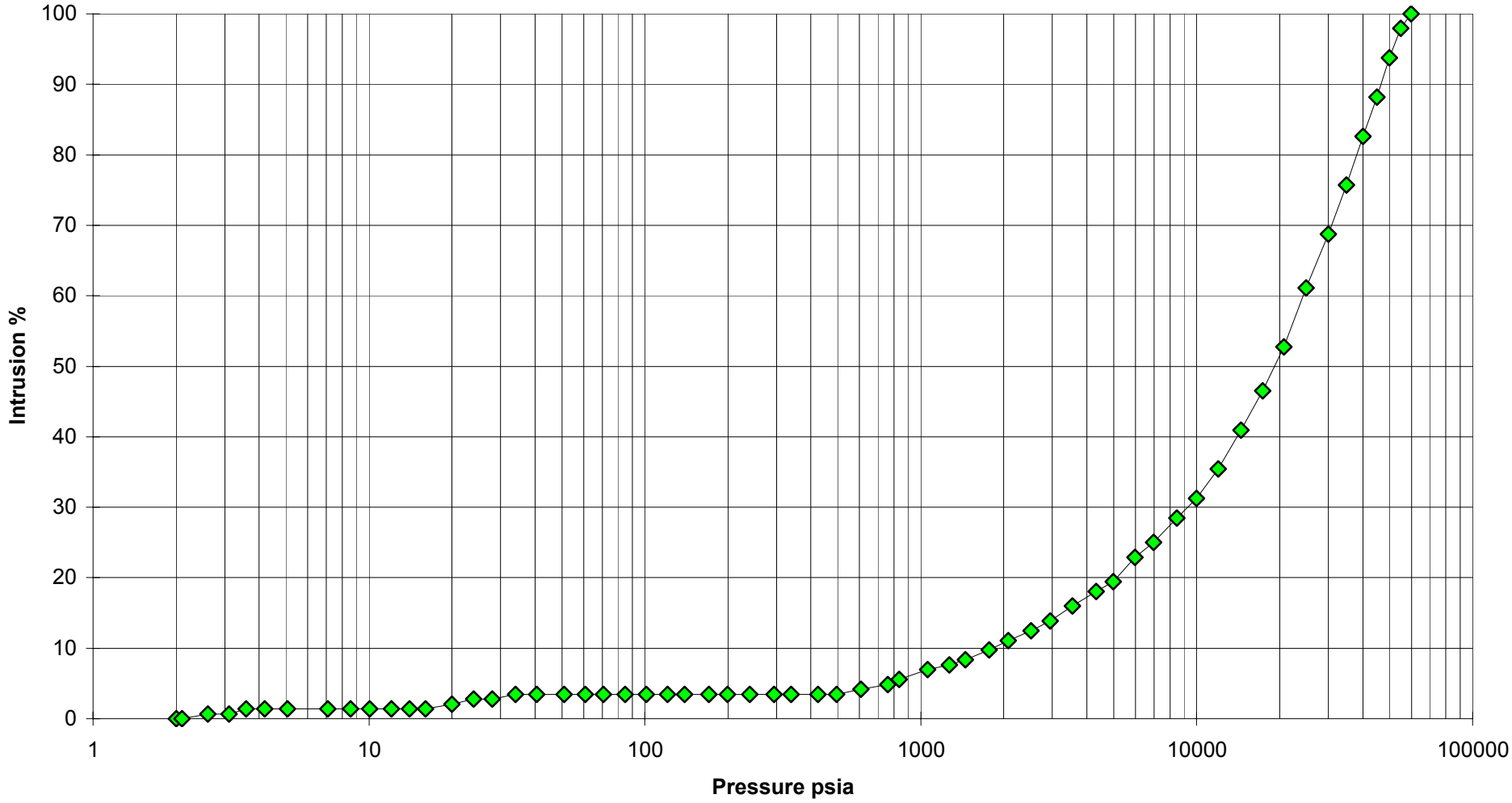
Pelican_5_2863m.xls

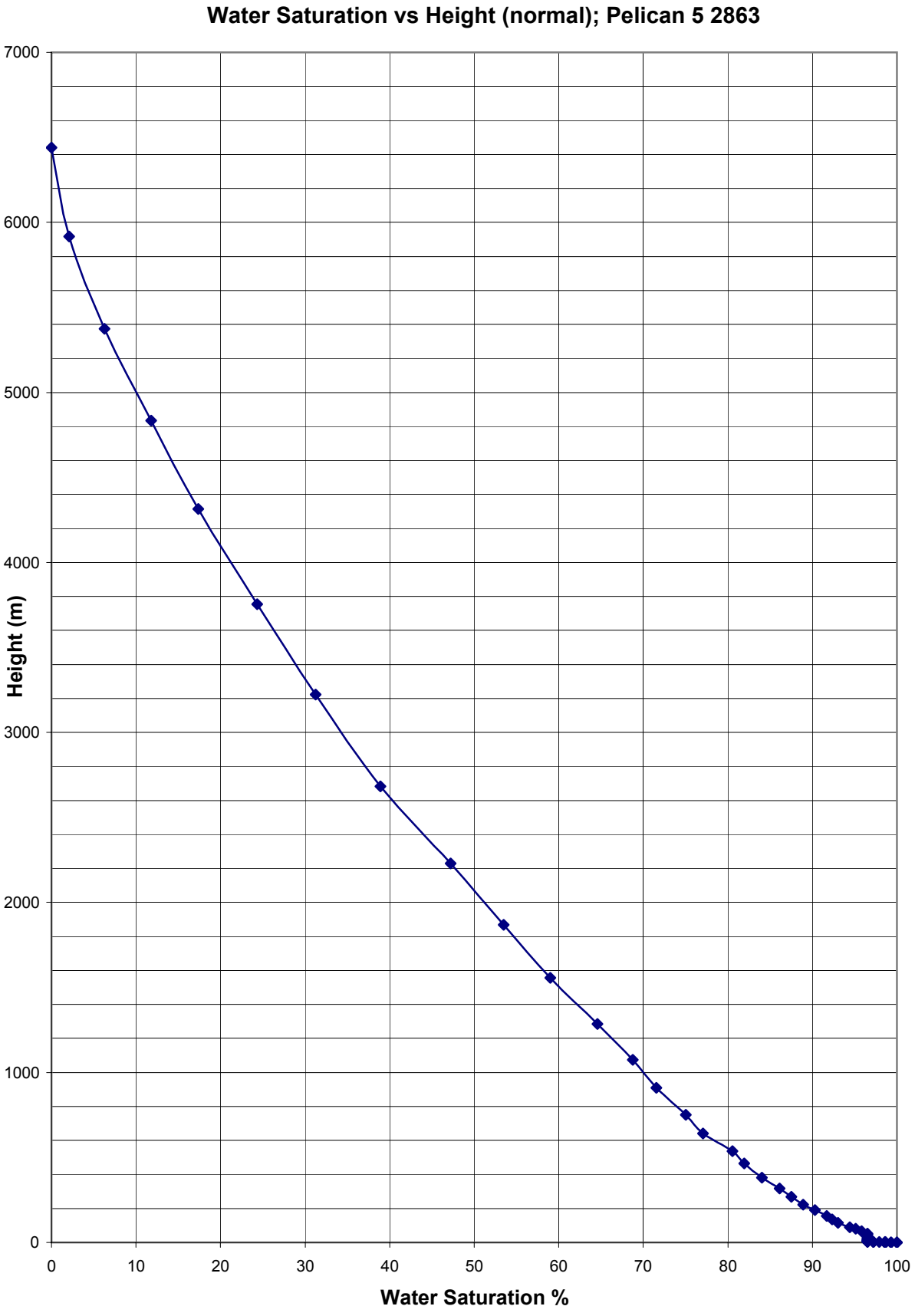


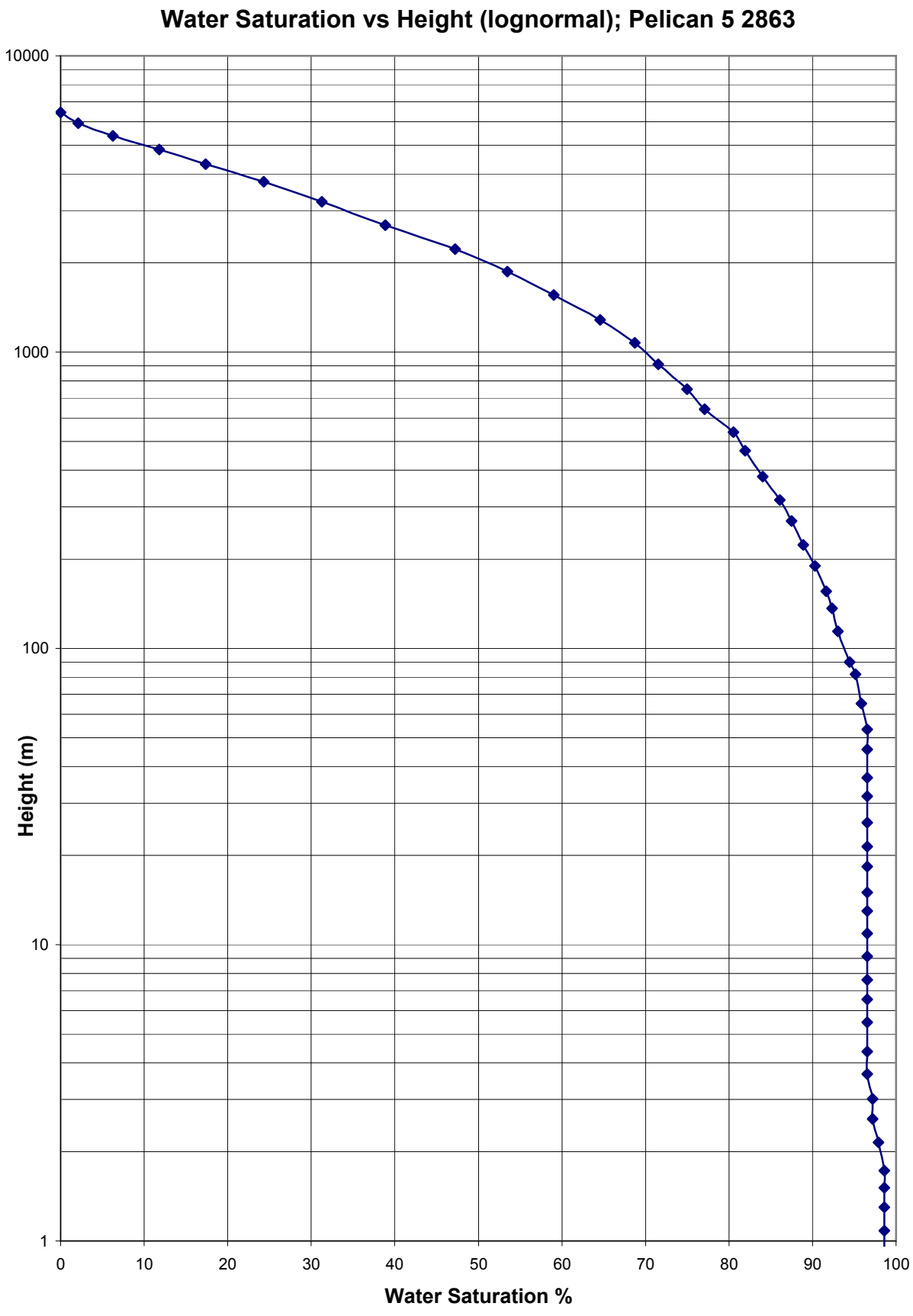

CALCULATED VALUES
porosity % = 3.6747
Grain density gms/cc = 2.5857
MRT 0006-02 Pelican 5 2863.8
Intrusion cc
0.14
0.12
0.1
0.08
0.06
0.04
0.02
0
1
10
100
1000
10000
100000
Pressure psia

CALCULATED VALUES
porosity % = 3.6747
grain density gms/cc = 2.5857

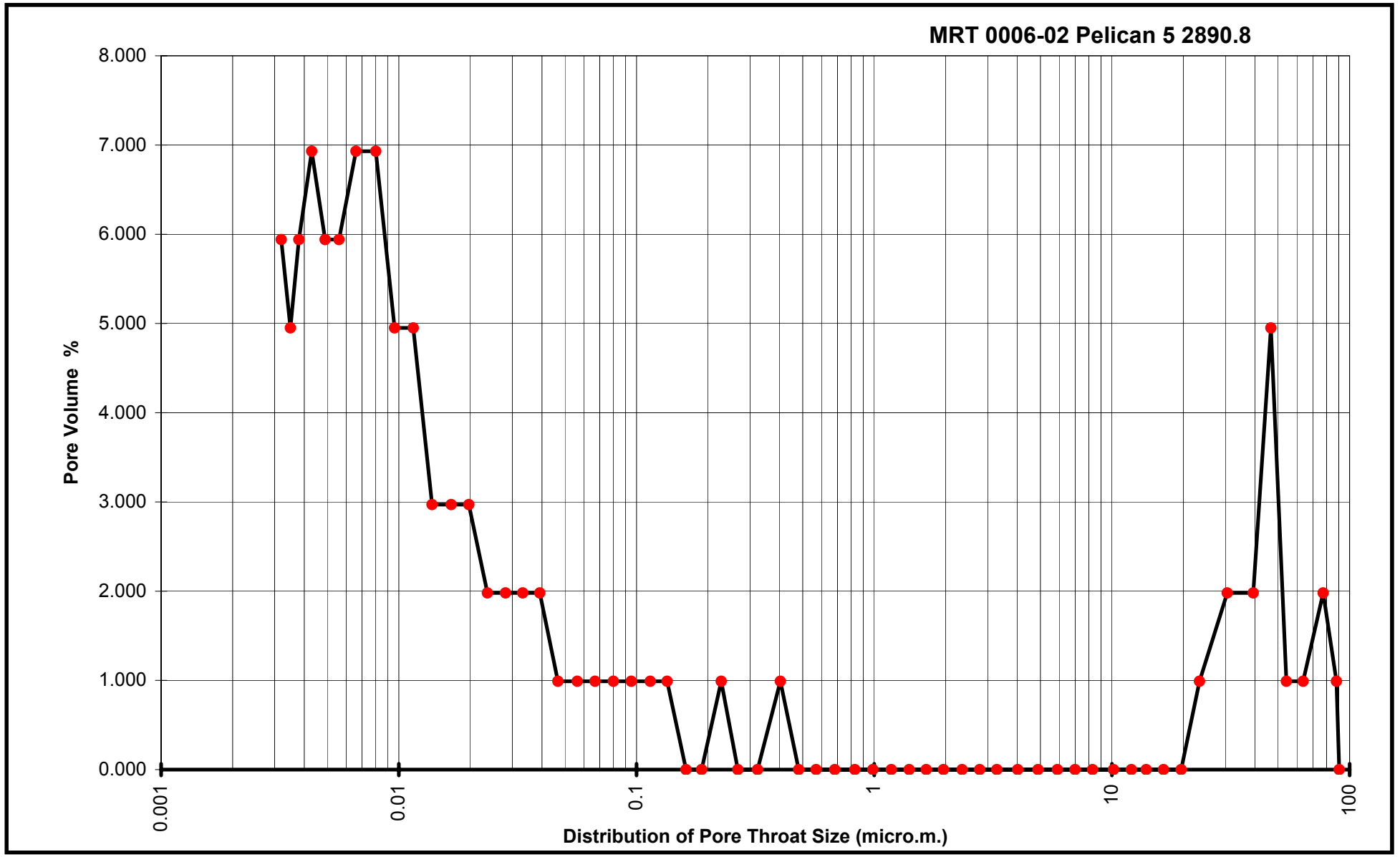
MRT 0006-02 Pelican 5 2863.8

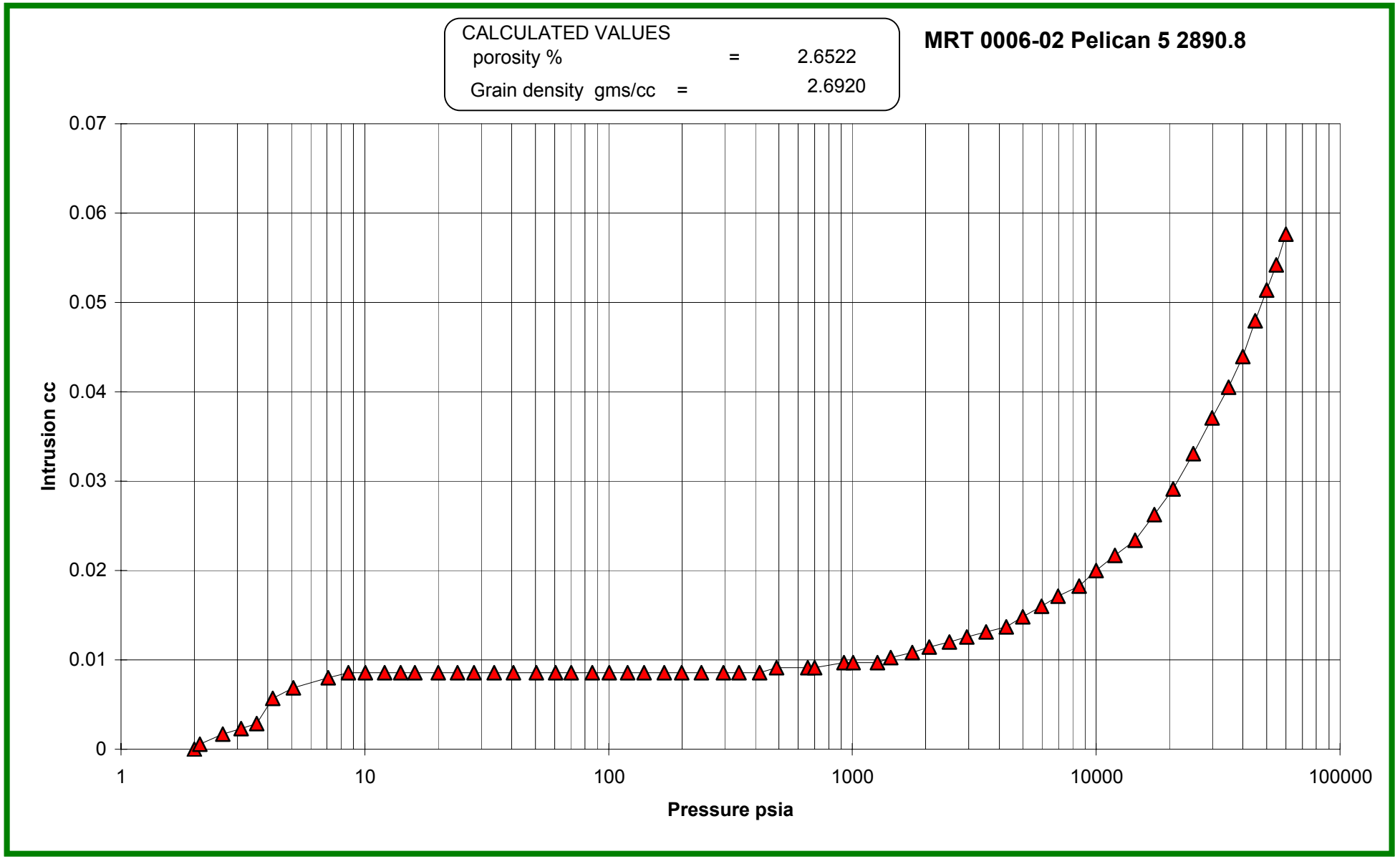


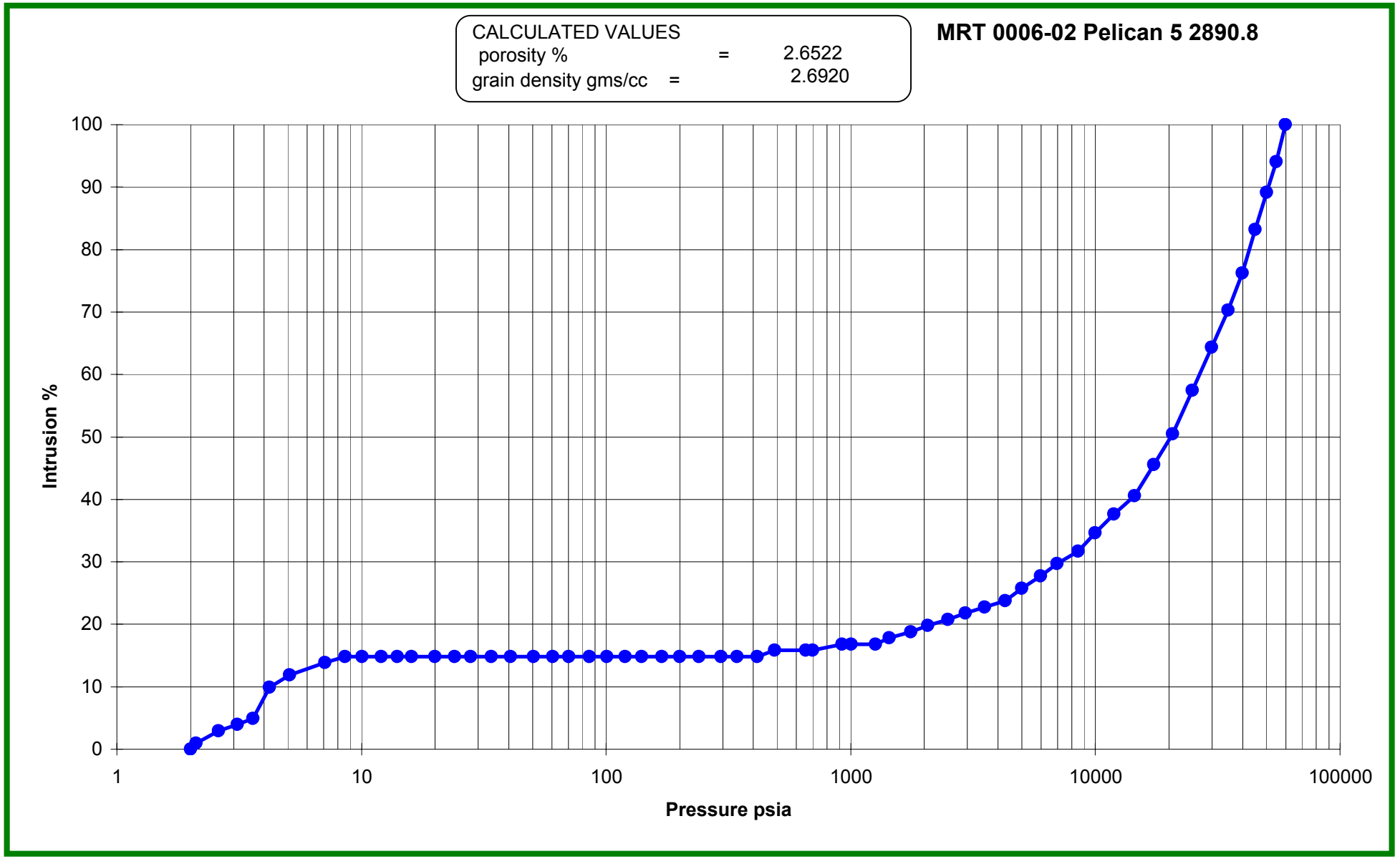

Water Saturation vs Height (normal); Pelican 5 2863
Height (m)
7000
6000
5000
4000
3000
2000
1000
0
0
10
20
30
40
50
60
70
80
90
100
Water Saturation %

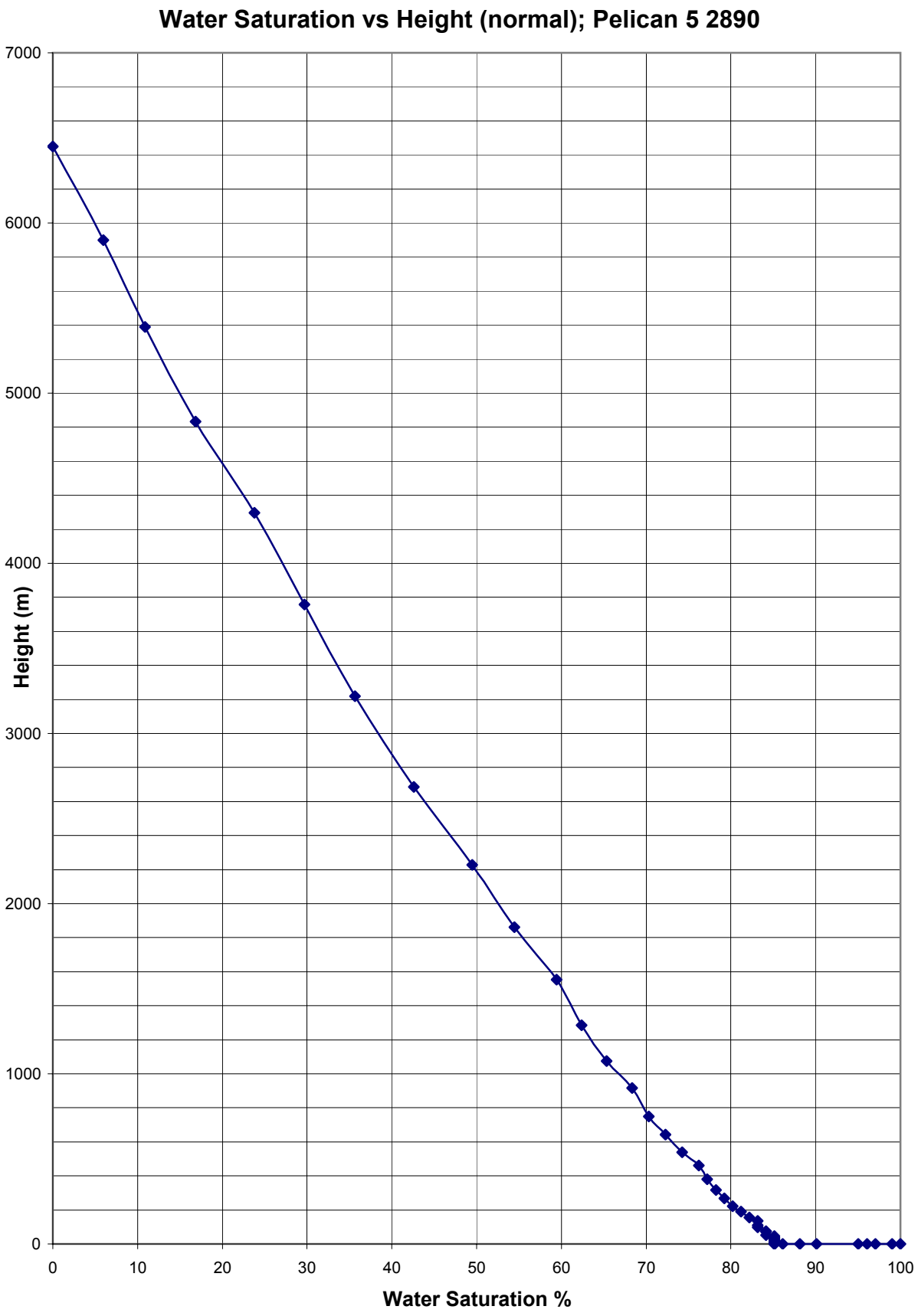

Water Saturation vs Height (lognormal); Pelican 5 2863
10000
1000
100
10
1
Height (m)
0
10
20
30
40
50
60
70
80
90
100
Water Saturation %

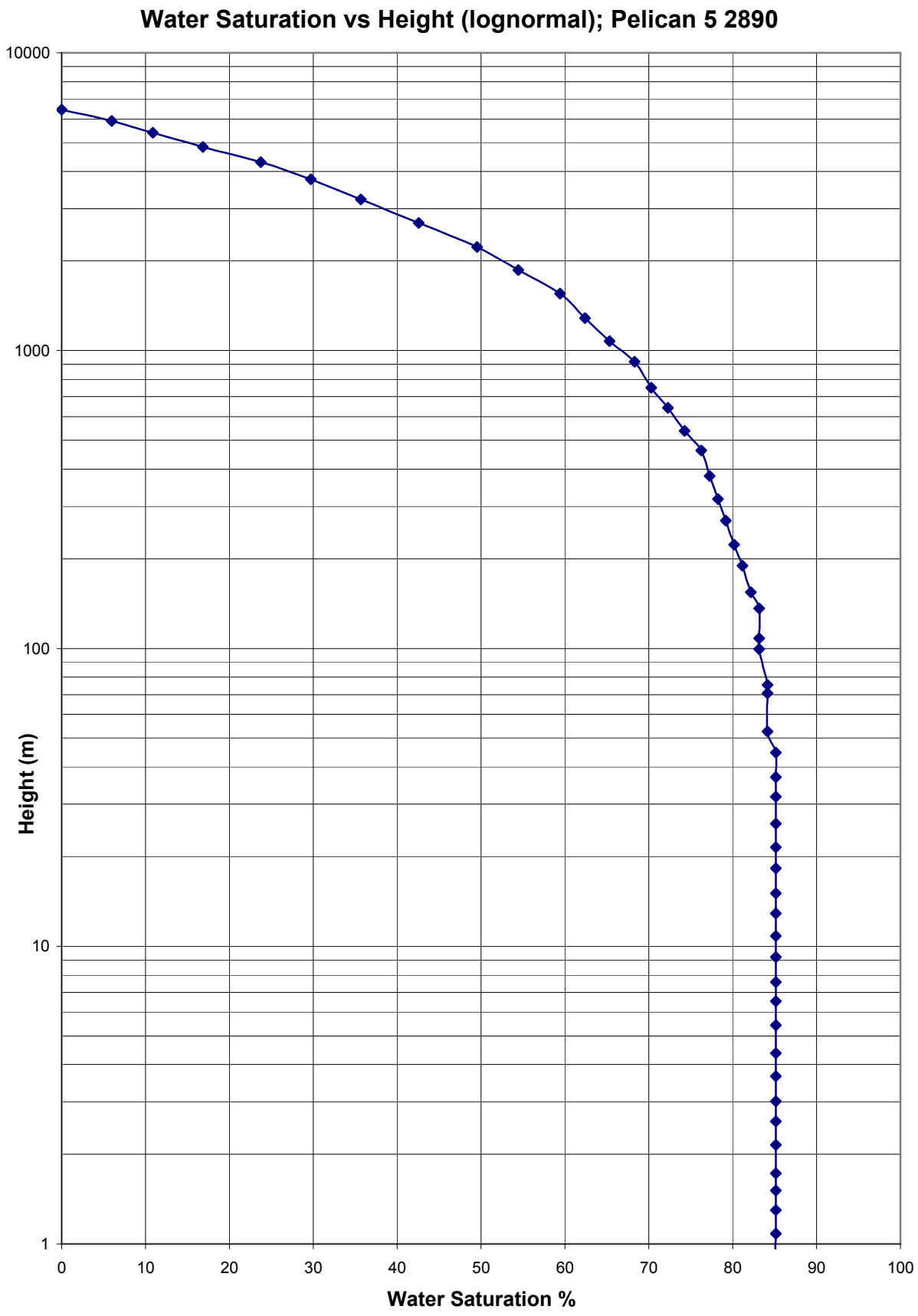
Pelican_5_2890m.xls

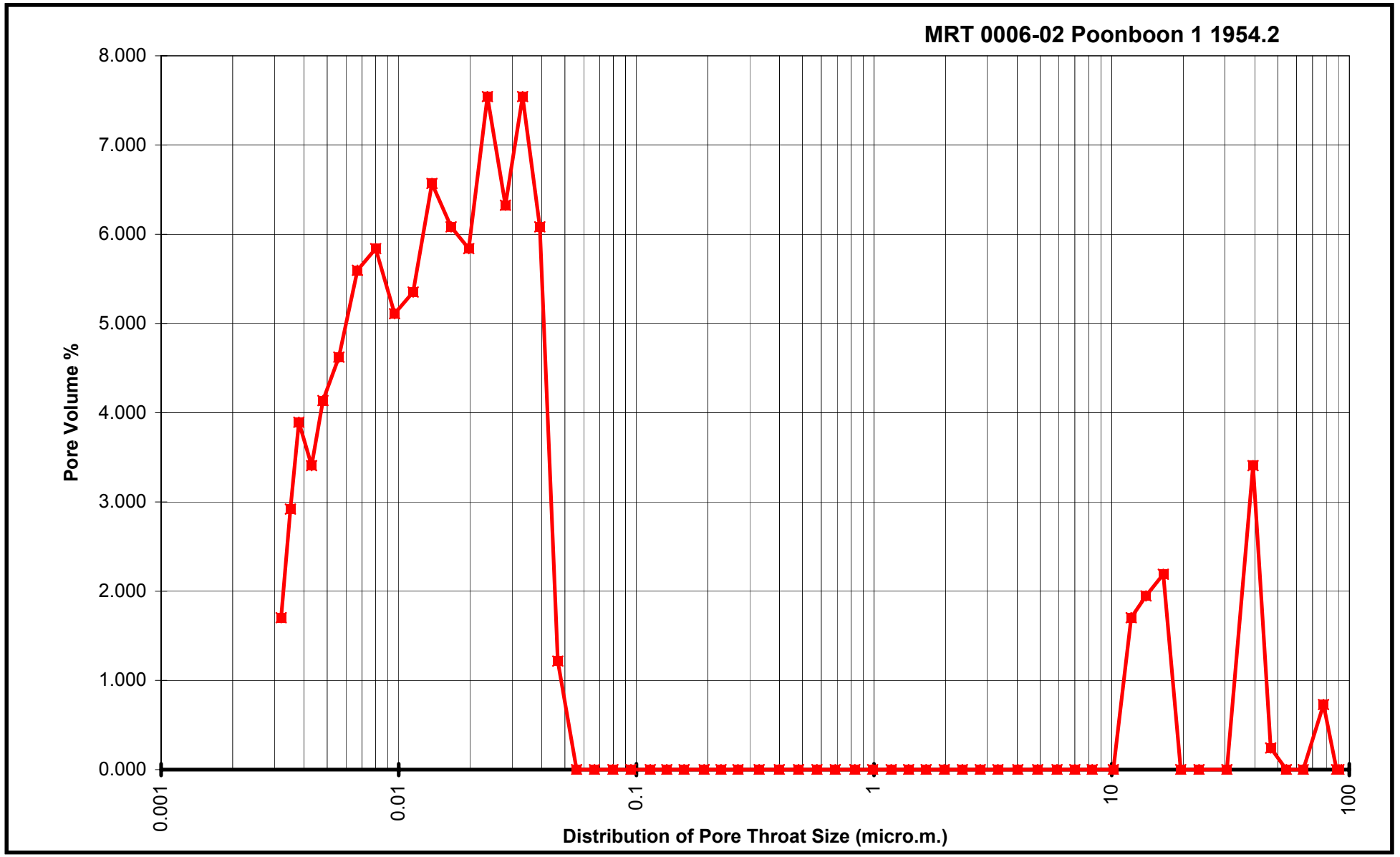


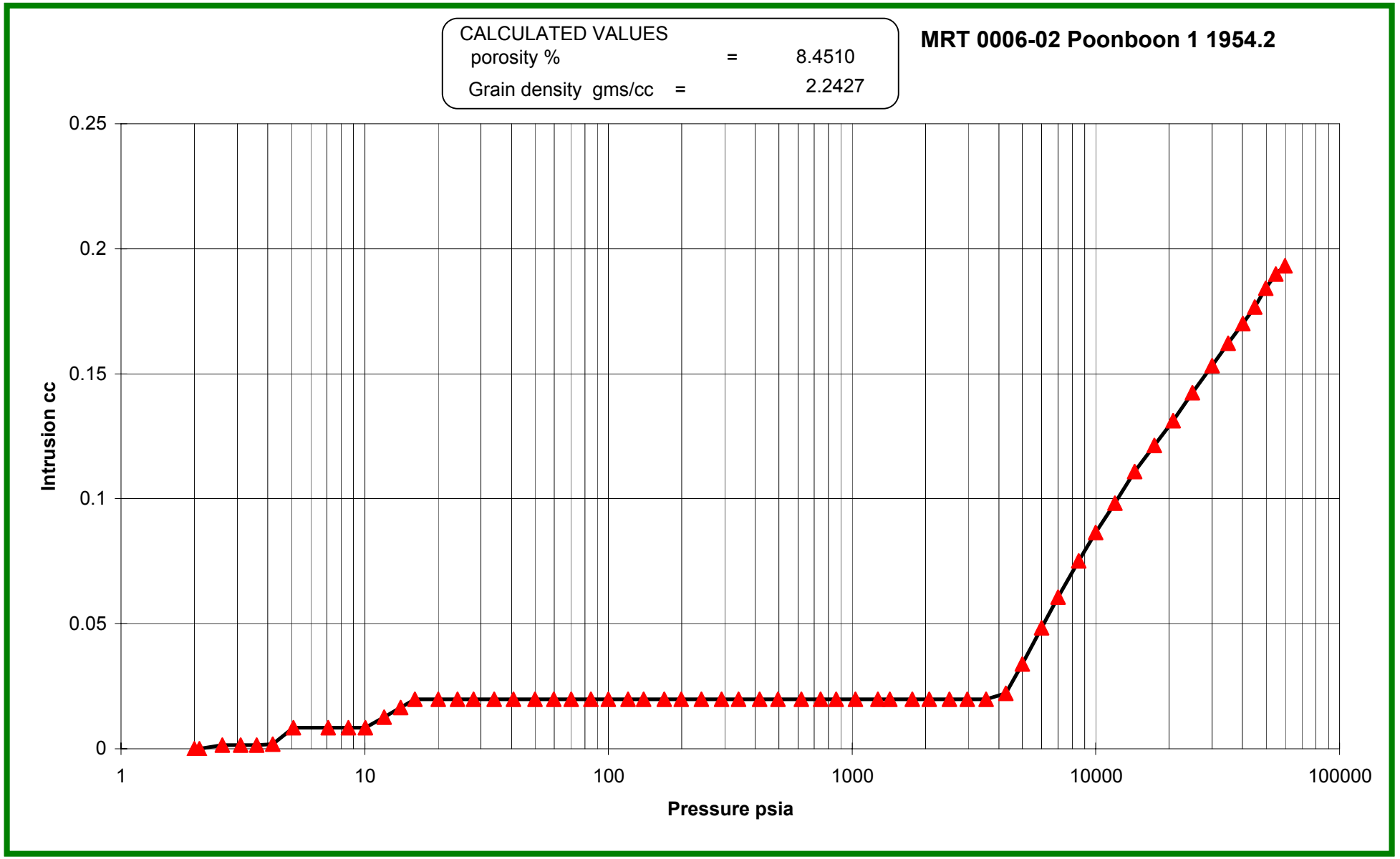

CALCULATED VALUES
porosity % = 2.6522
Grain density gms/cc = 2.6920
MRT 0006-02 Pelican 5 2890.8
Intrusion cc
0.07
0.06
0.05
0.04
0.03
0.02
0.01
0
1
10
100
1000
10000
100000
Pressure psia

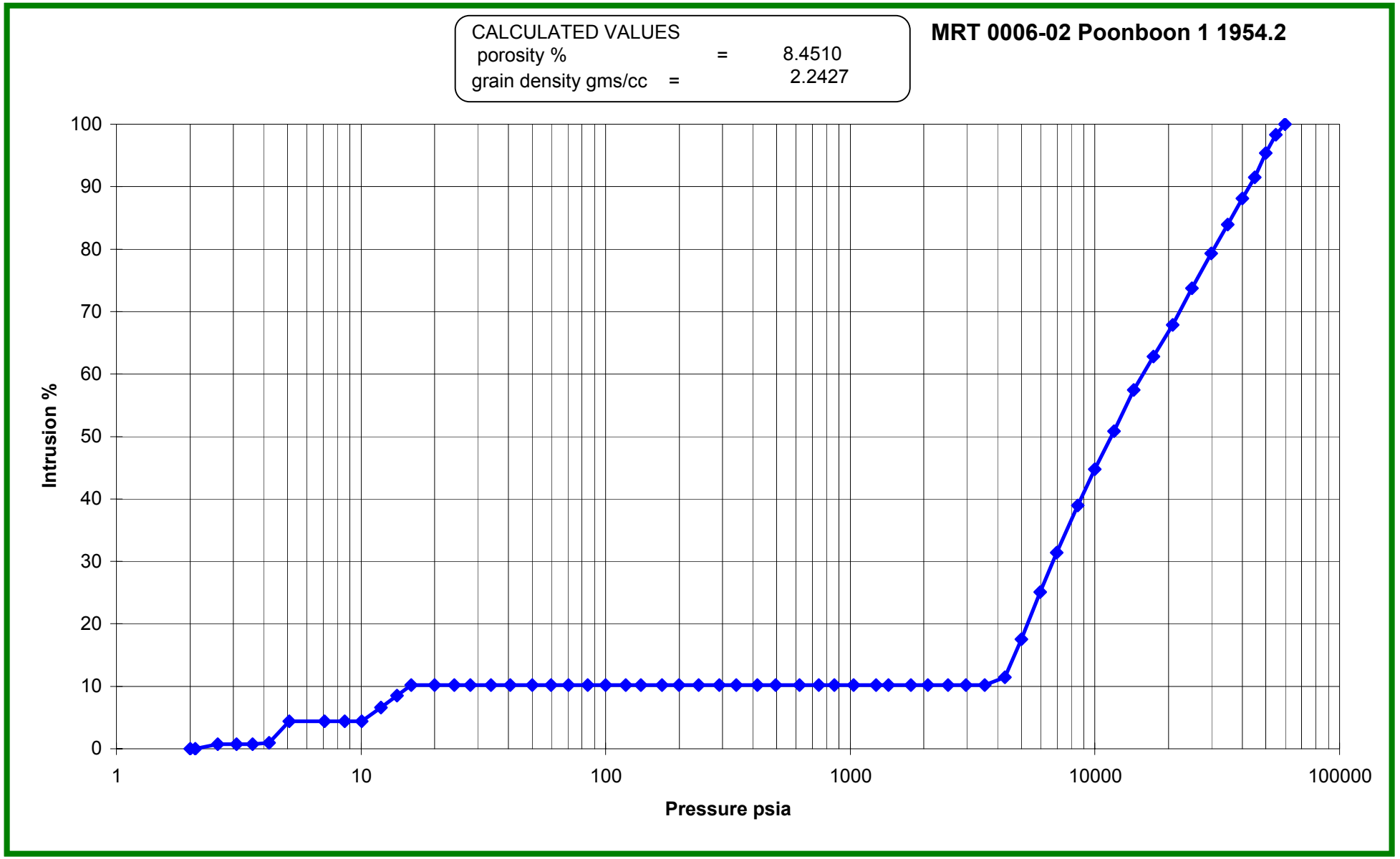

CALCULATED VALUES
porosity % = 2.6522
grain density gms/cc = 2.6920
MRT 0006-02 Pelican 5 2890.8
Intrusion %
100
90
80
70
60
50
40
30
20
10
0
1
10
100
1000
10000
100000
Pressure psia

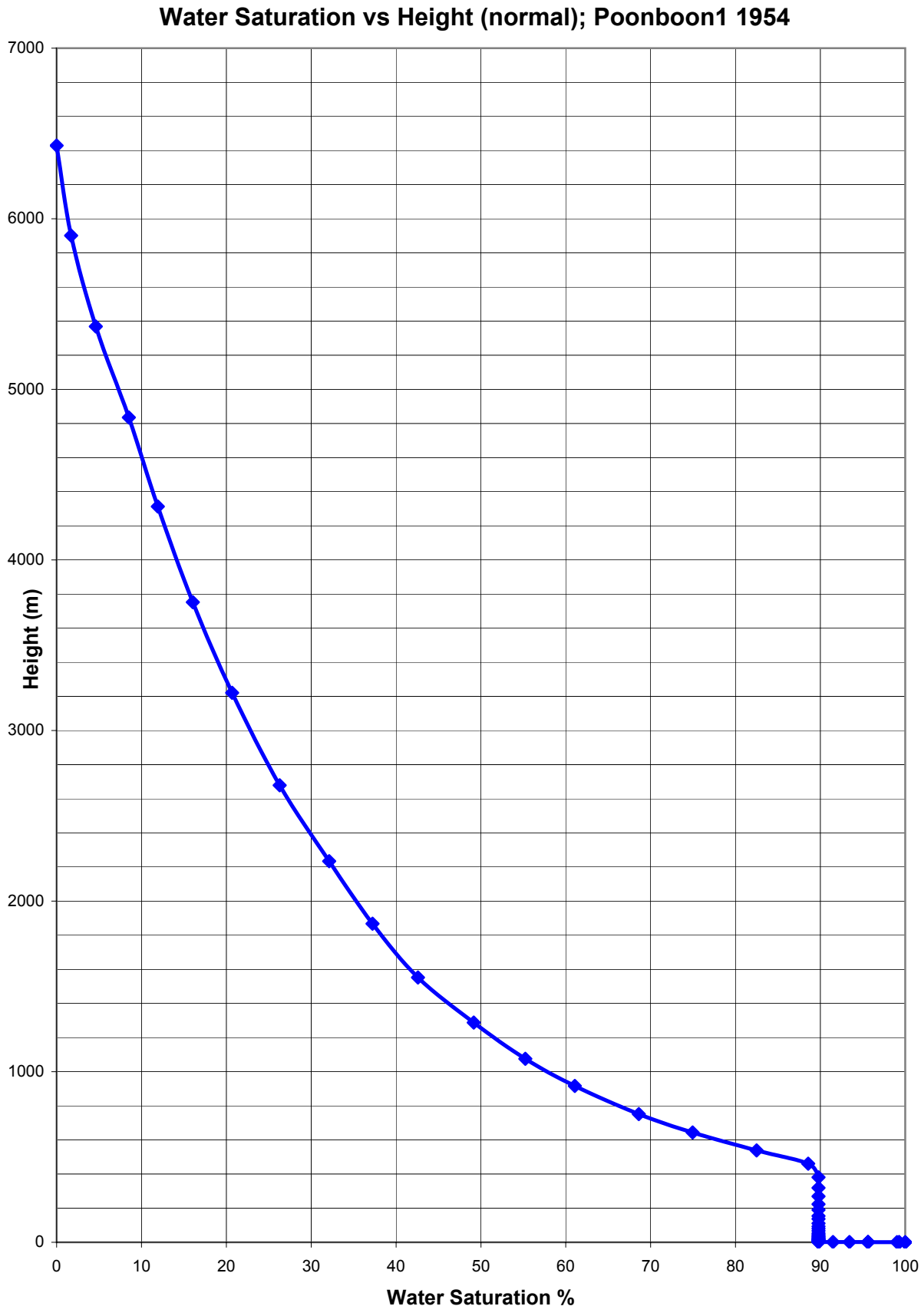

Water Saturation vs Height (normal); Pelican 5 2890
Height (m)
7000
6000
5000
4000
3000
2000
1000
0
0
10
20
30
40
50
60
70
80
90
100
Water Saturation %

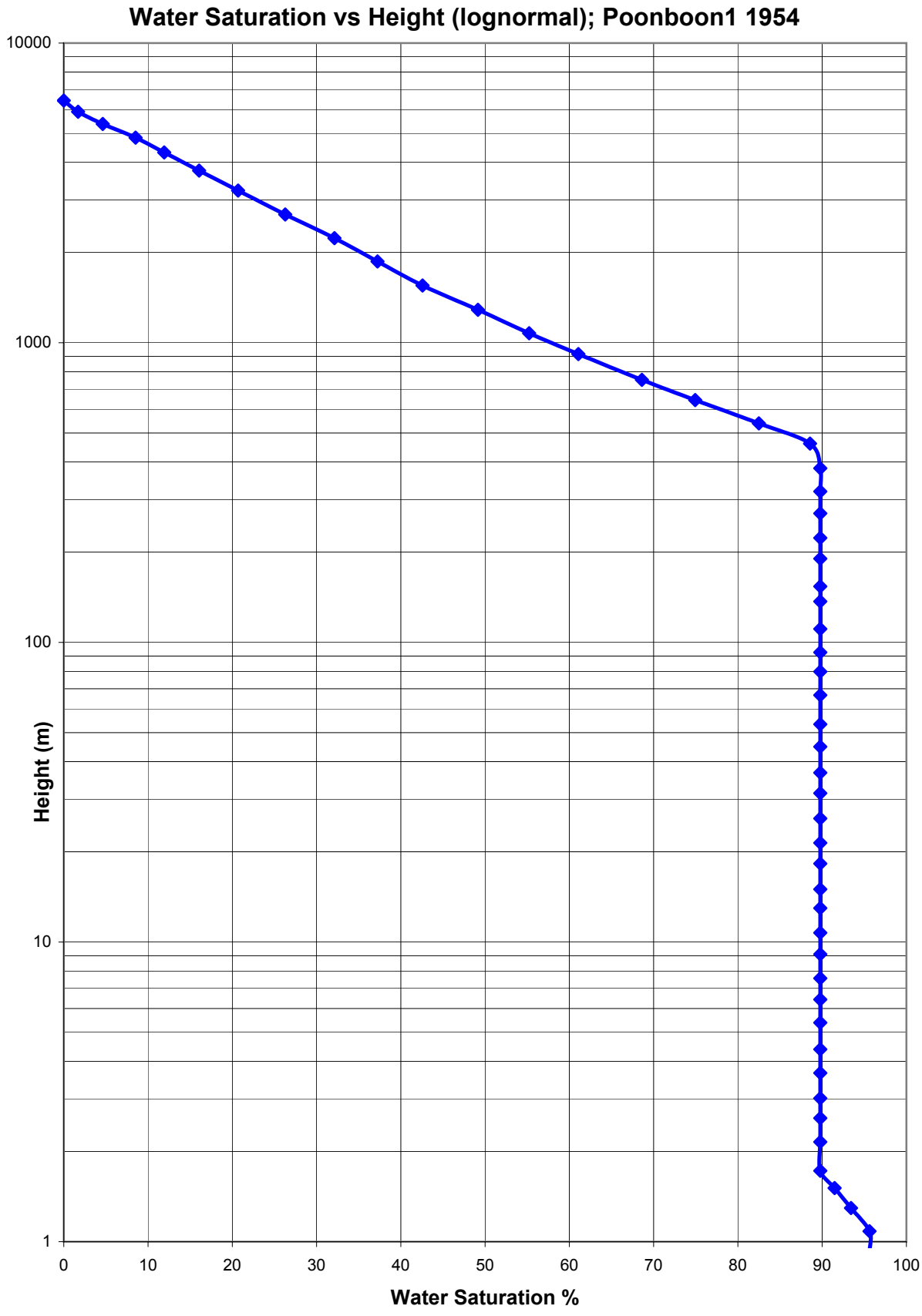

Water Saturation vs Height (lognormal); Pelican 5 2890
10000
1000
100
10
1
Height (m)
0
10
20
30
40
50
60
70
80
90
100
Water Saturation %

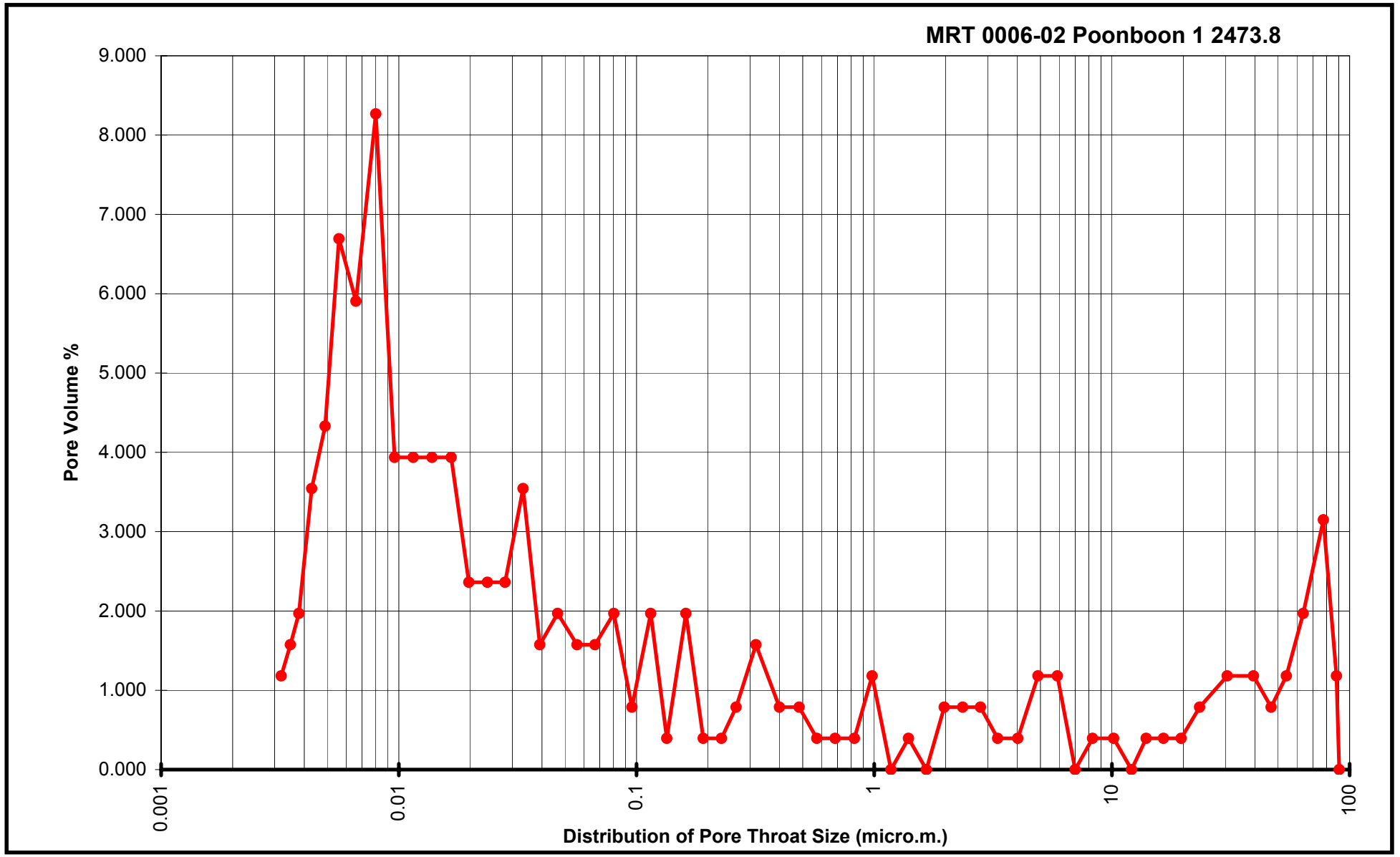

MRT 0006-02 Poonboon 1 1954.2
Pore Volume %
8.000
7.000
6.000
5.000
4.000
3.000
2.000
1.000
0.000
0.001
0.01
0.1
1
10
100
Distribution of Pore Throat Size (micro.m.)

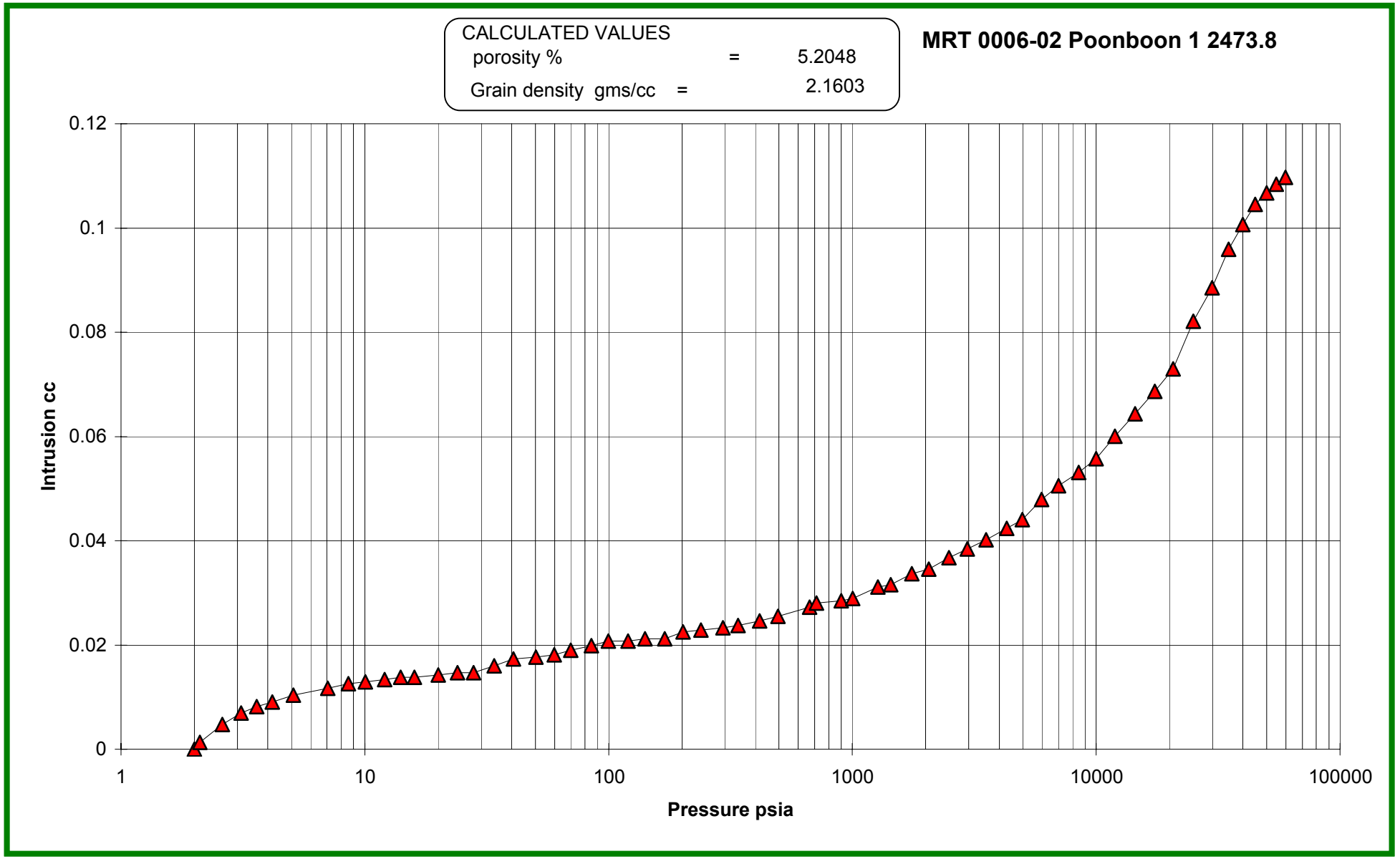

CALCULATED VALUES
porosity % = 8.4510
Grain density gms/cc = 2.2427
MRT 0006-02 Poonboon 1 1954.2
Intrusion cc
0.25
0.2
0.15
0.1
0.05
0
1
10
100
1000
10000
100000
Pressure psia

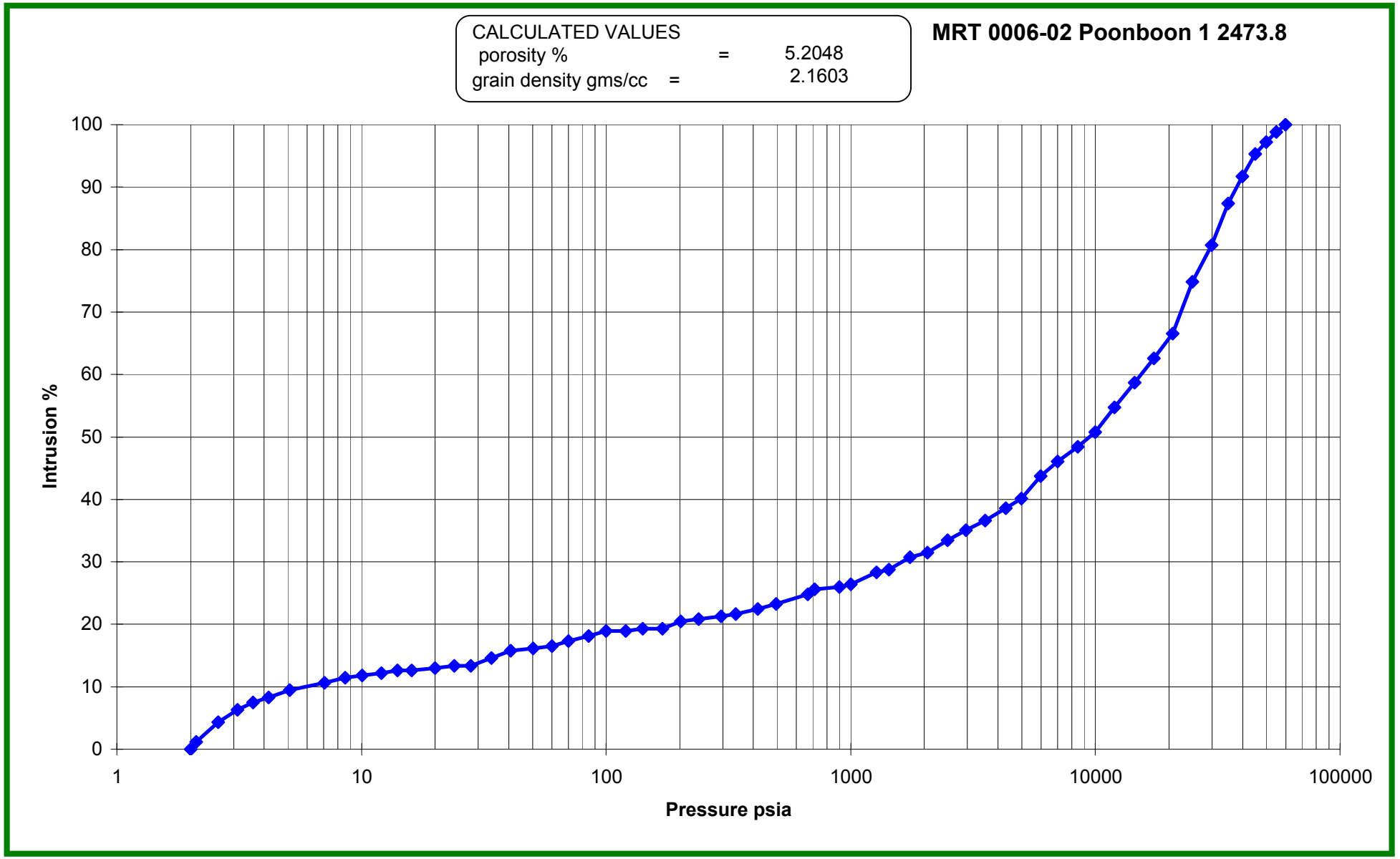

CALCULATED VALUES
porosity % = 8.4510
grain density gms/cc = 2.2427
MRT 0006-02 Poonboon 1 1954.2
Intrusion %
100
90
80
70
60
50
40
30
20
10
0
1
10
100
1000
10000
100000
Pressure psia

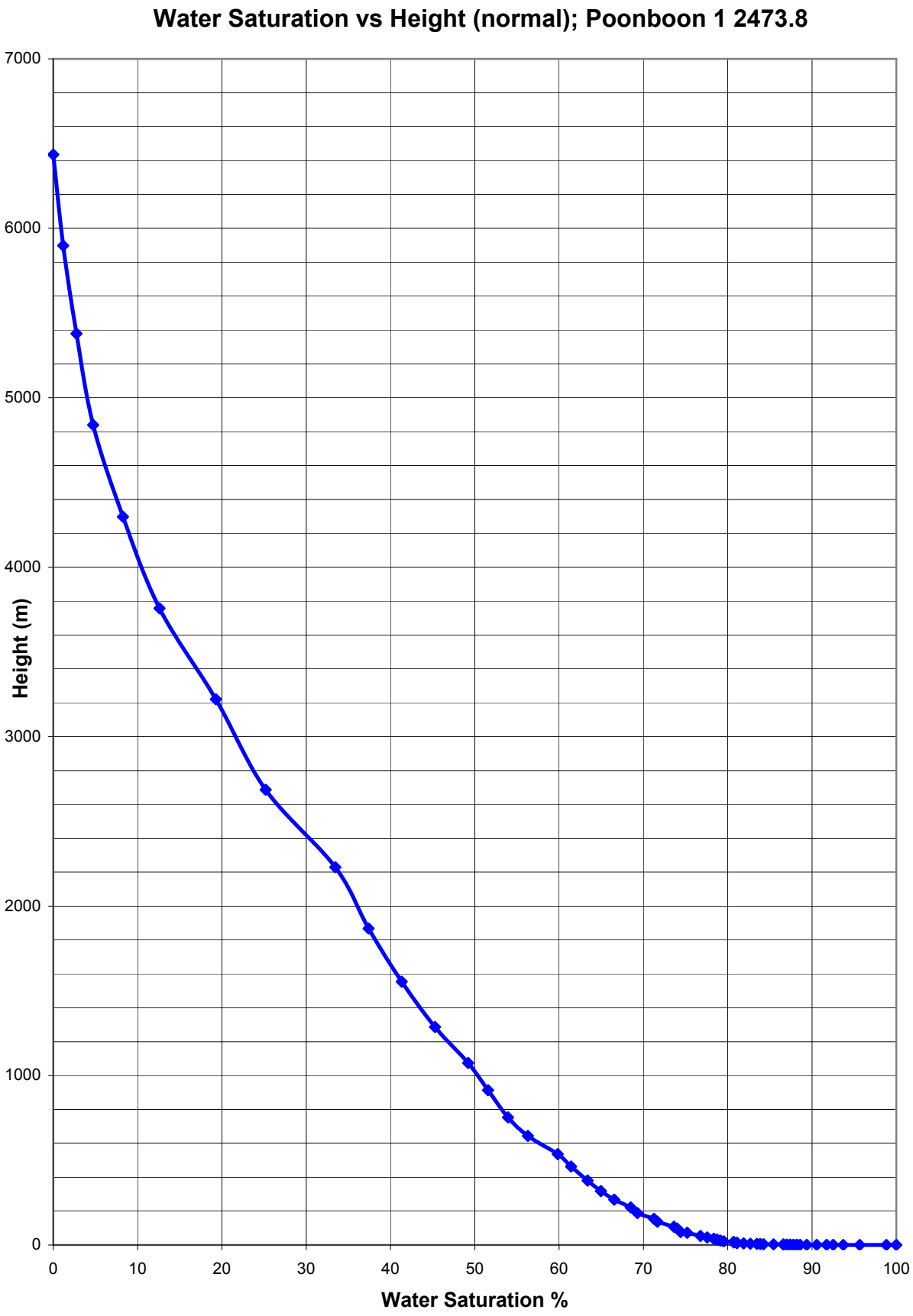

Water Saturation vs Height (normal); Poonboon1 1954
7000
6000
5000
4000
3000
2000
1000
0
Height (m)
0
10
20
30
40
50
60
70
80
90
100
Water Saturation %

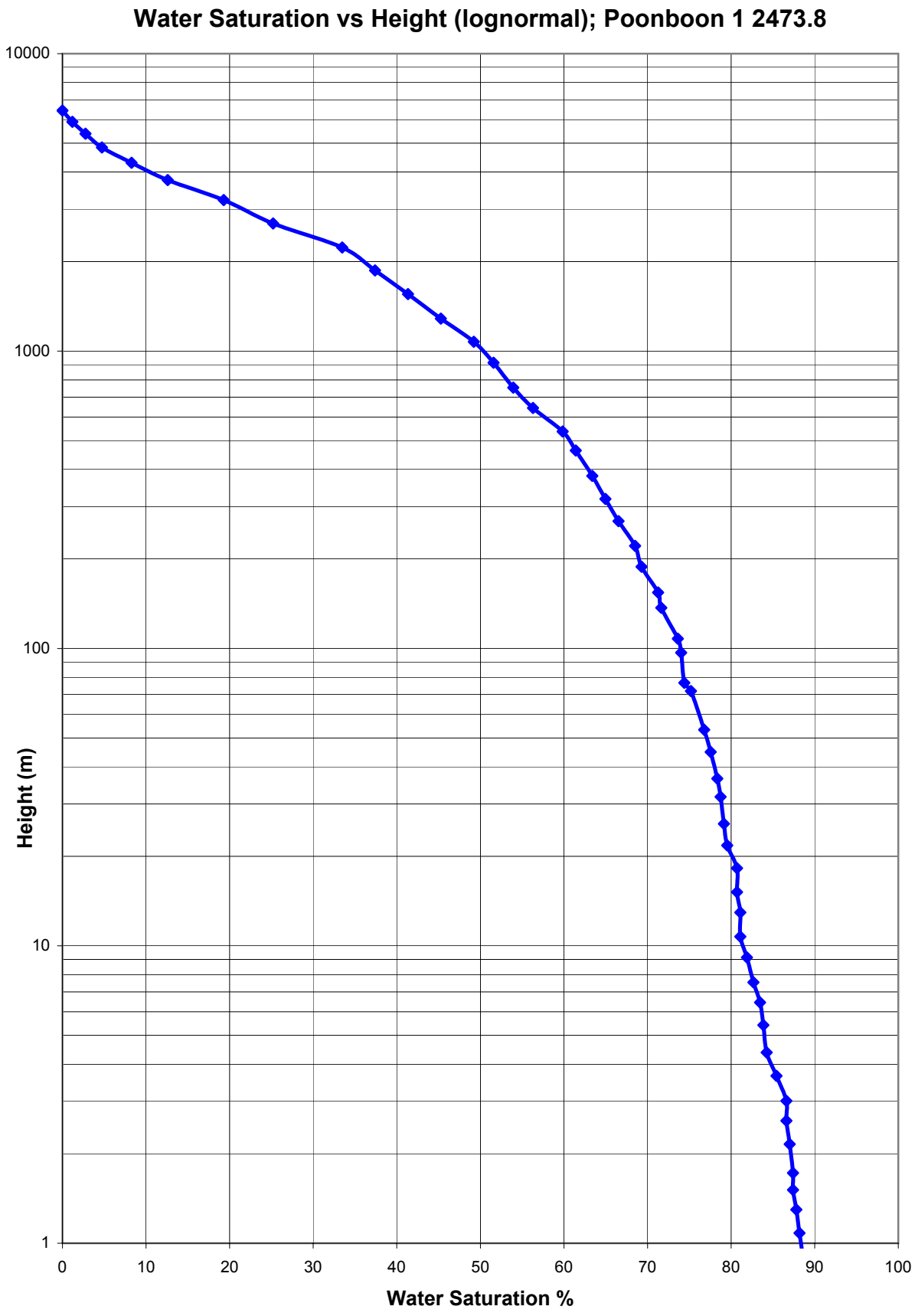

Water Saturation vs Height (lognormal); Poonboon1 1954
10000
1000
100
10
1
Height (m)
0
10
20
30
40
50
60
70
80
90
100
Water Saturation %

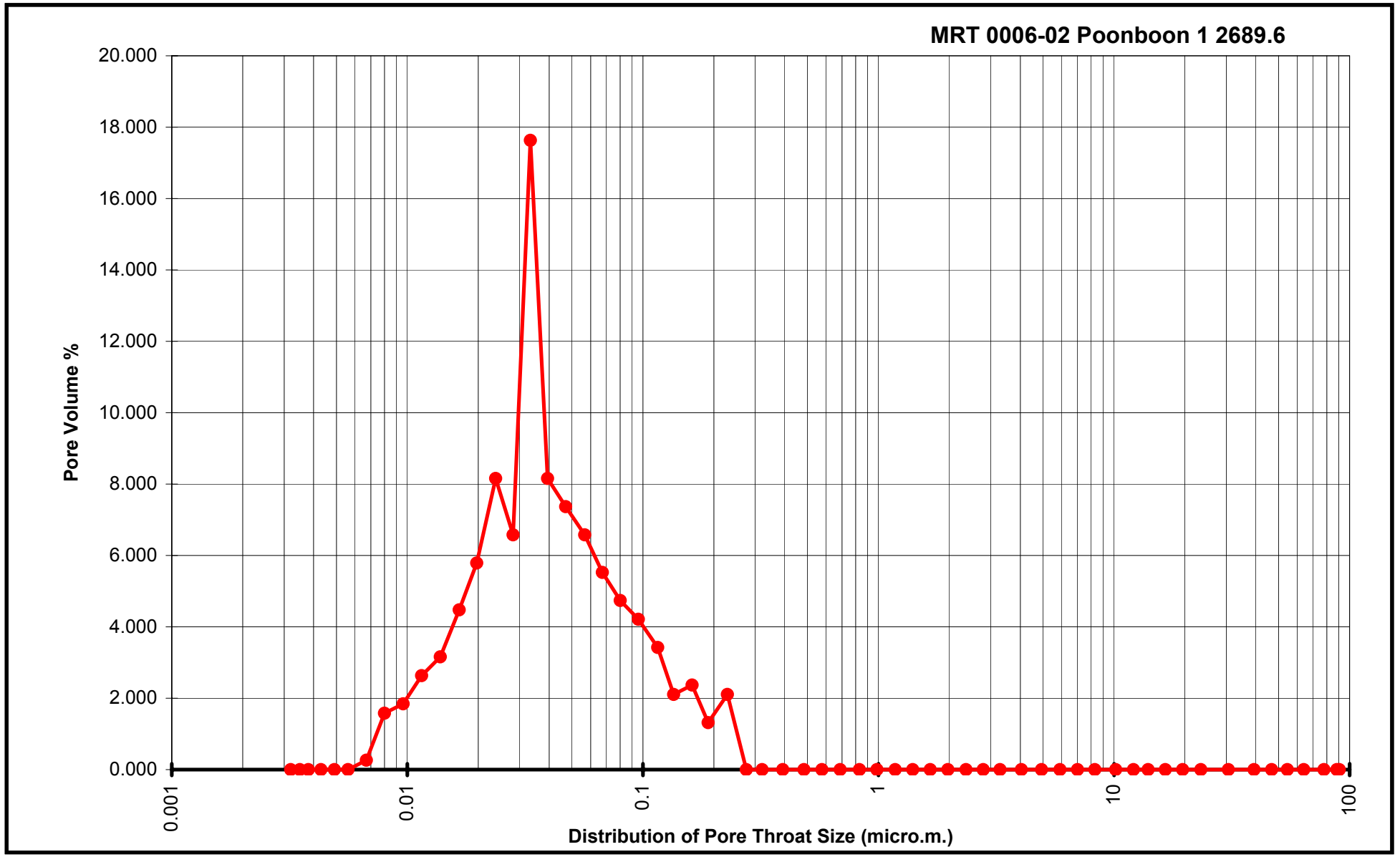

MRT 0006-02 Poonboon 1 2473.8
Pore Volume %
9.000
8.000
7.000
6.000
5.000
4.000
3.000
2.000
1.000
0.000
0.001
0.01
0.1
1
10
100
Distribution of Pore Throat Size (micro.m.)

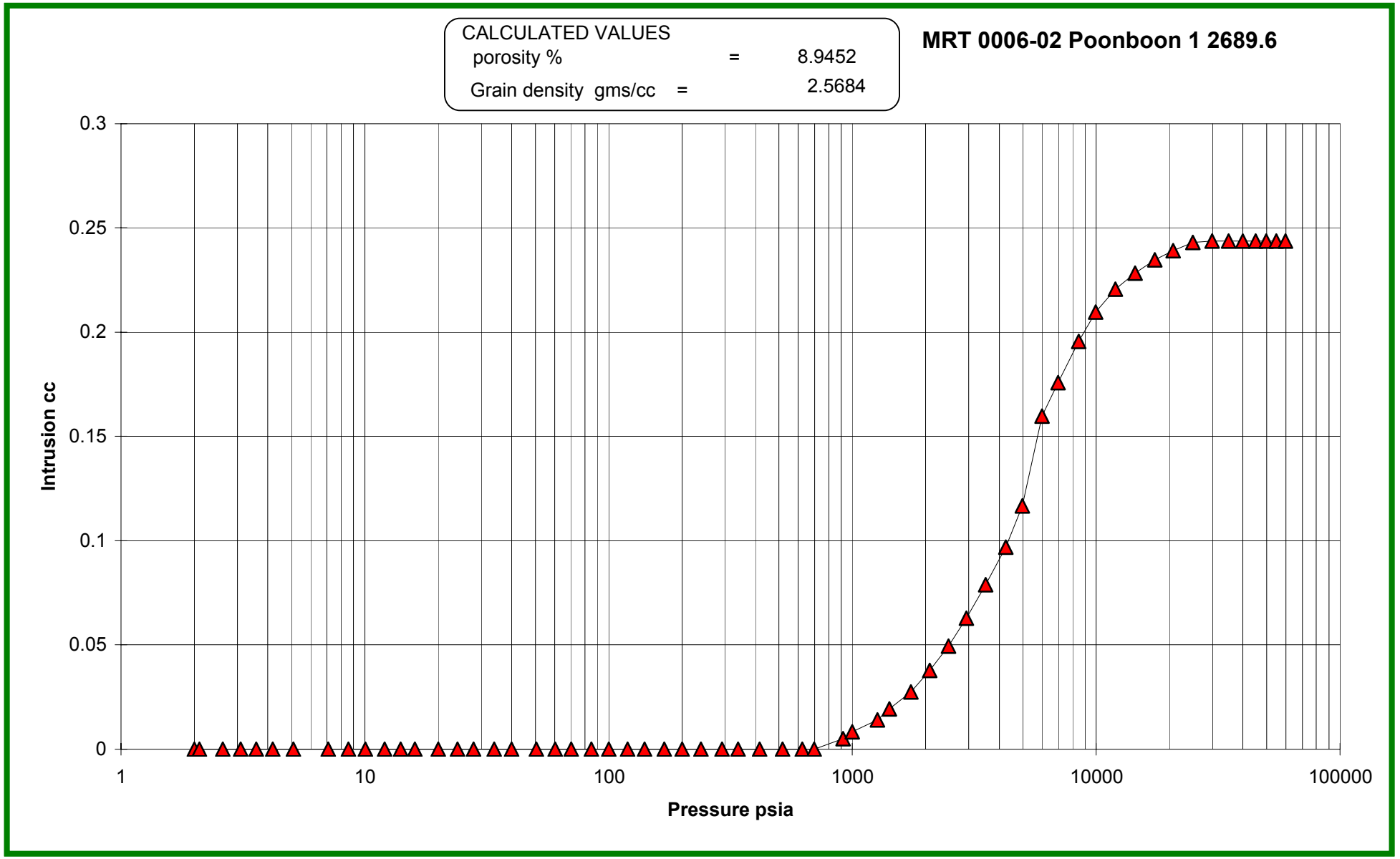

CALCULATED VALUES
porosity % = 5.2048
Grain density gms/cc = 2.1603
MRT 0006-02 Poonboon 1 2473.8
Intrusion cc
0.12
0.1
0.08
0.06
0.04
0.02
0
1
10
100
1000
10000
100000
Pressure psia

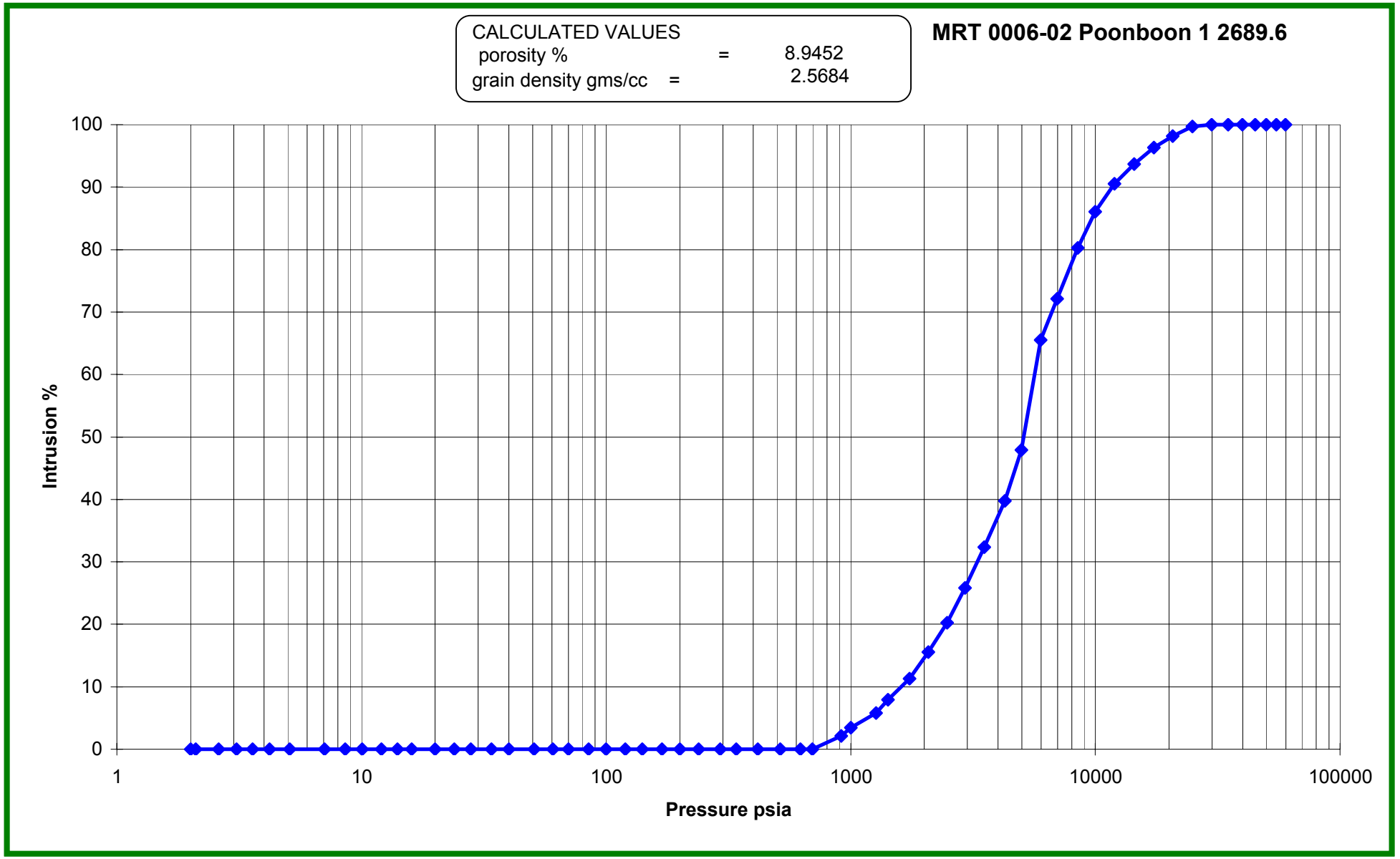

CALCULATED VALUES
porosity % = 5.2048
grain density gms/cc = 2.1603
MRT 0006-02 Poonboon 1 2473.8
Intrusion %
100
90
80
70
60
50
40
30
20
10
0
1
10
100
1000
10000
100000
Pressure psia

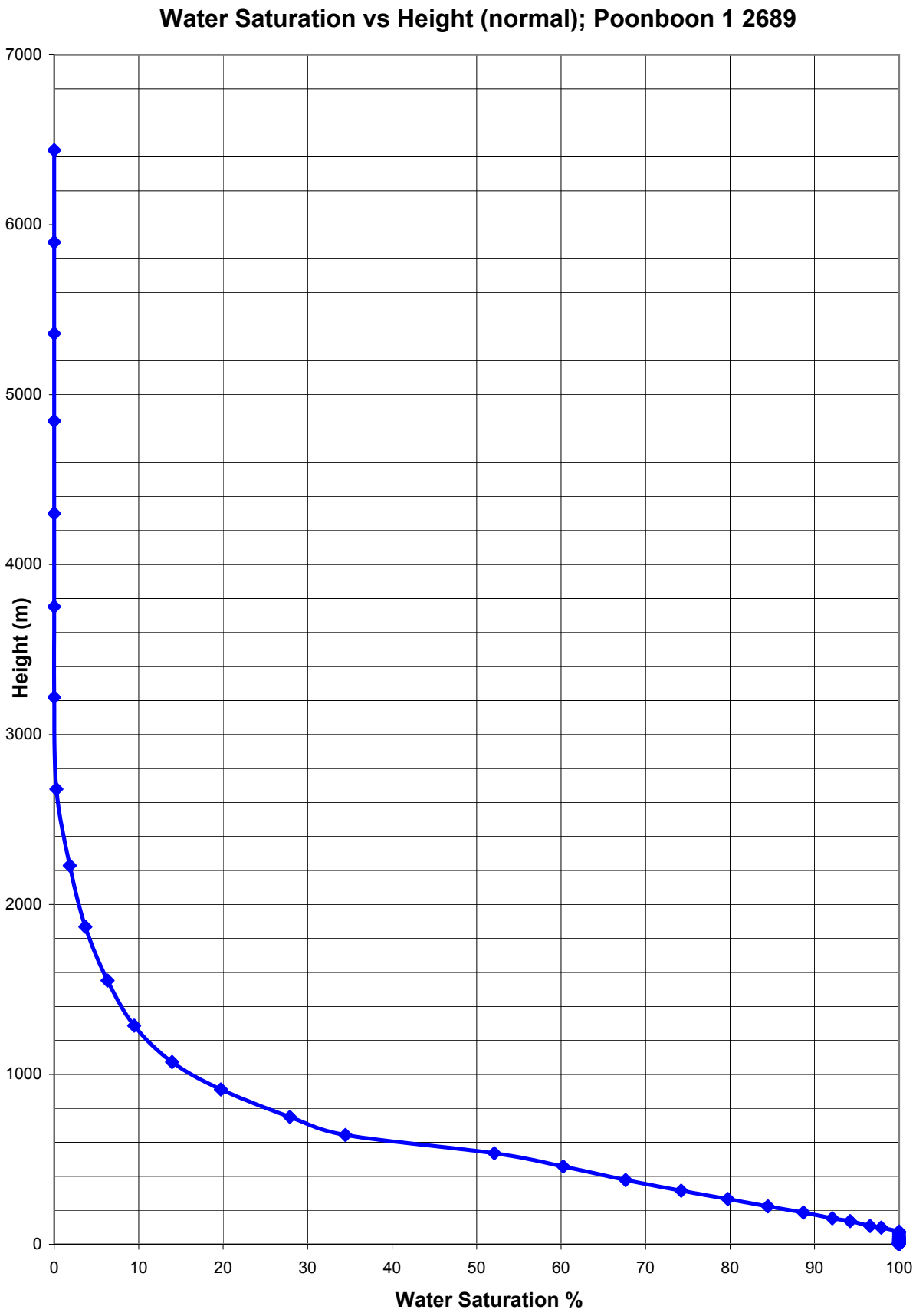

Water Saturation vs Height (normal); Poonboon 1 2473.8
Height (m)
7000
6000
5000
4000
3000
2000
1000
0
0
10
20
30
40
50
60
70
80
90
100
Water Saturation %

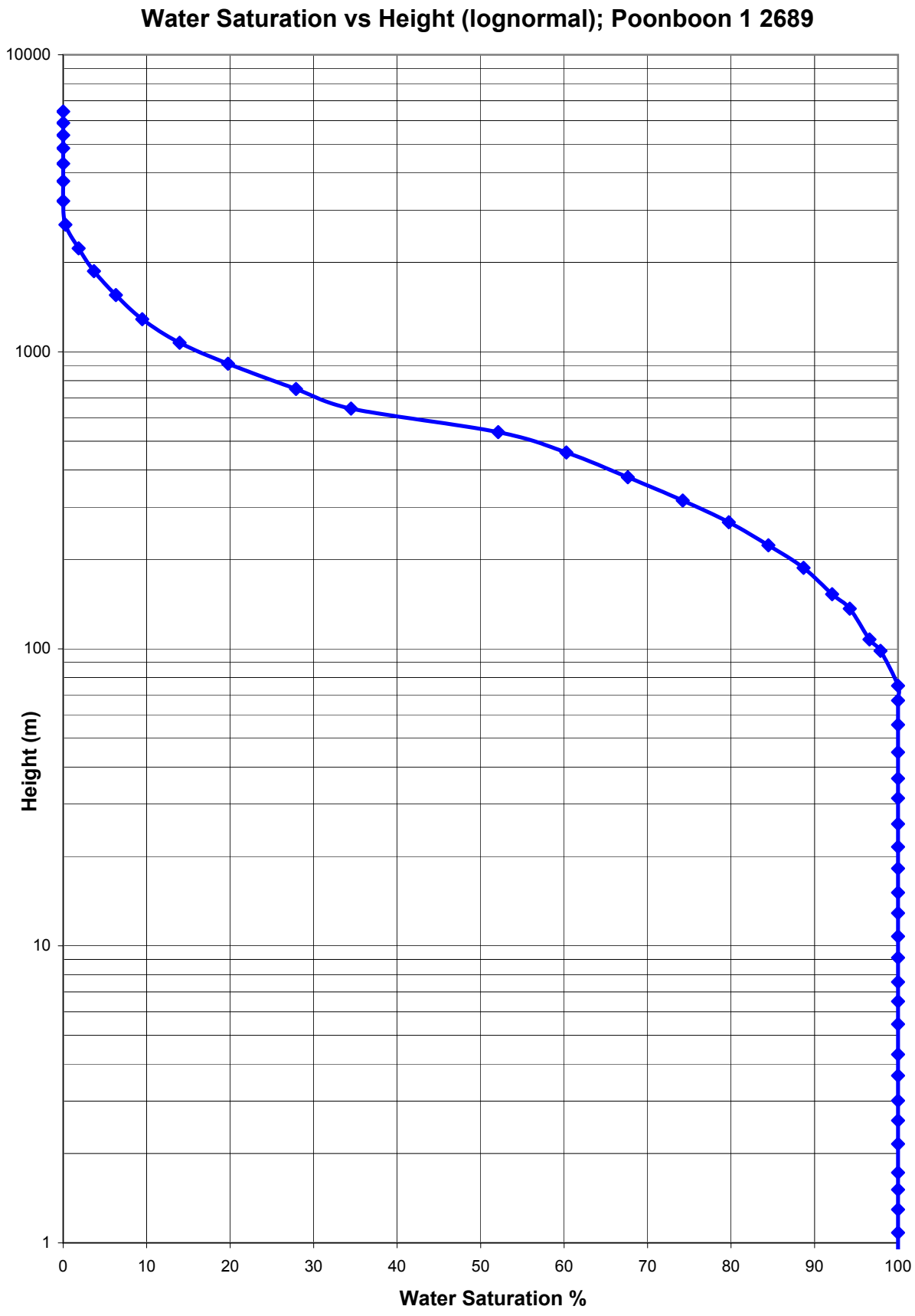

Water Saturation vs Height (lognormal); Poonboon 1 2473.8
10000
1000
100
10
1
Height (m)
0
10
20
30
40
50
60
70
80
90
100
Water Saturation %

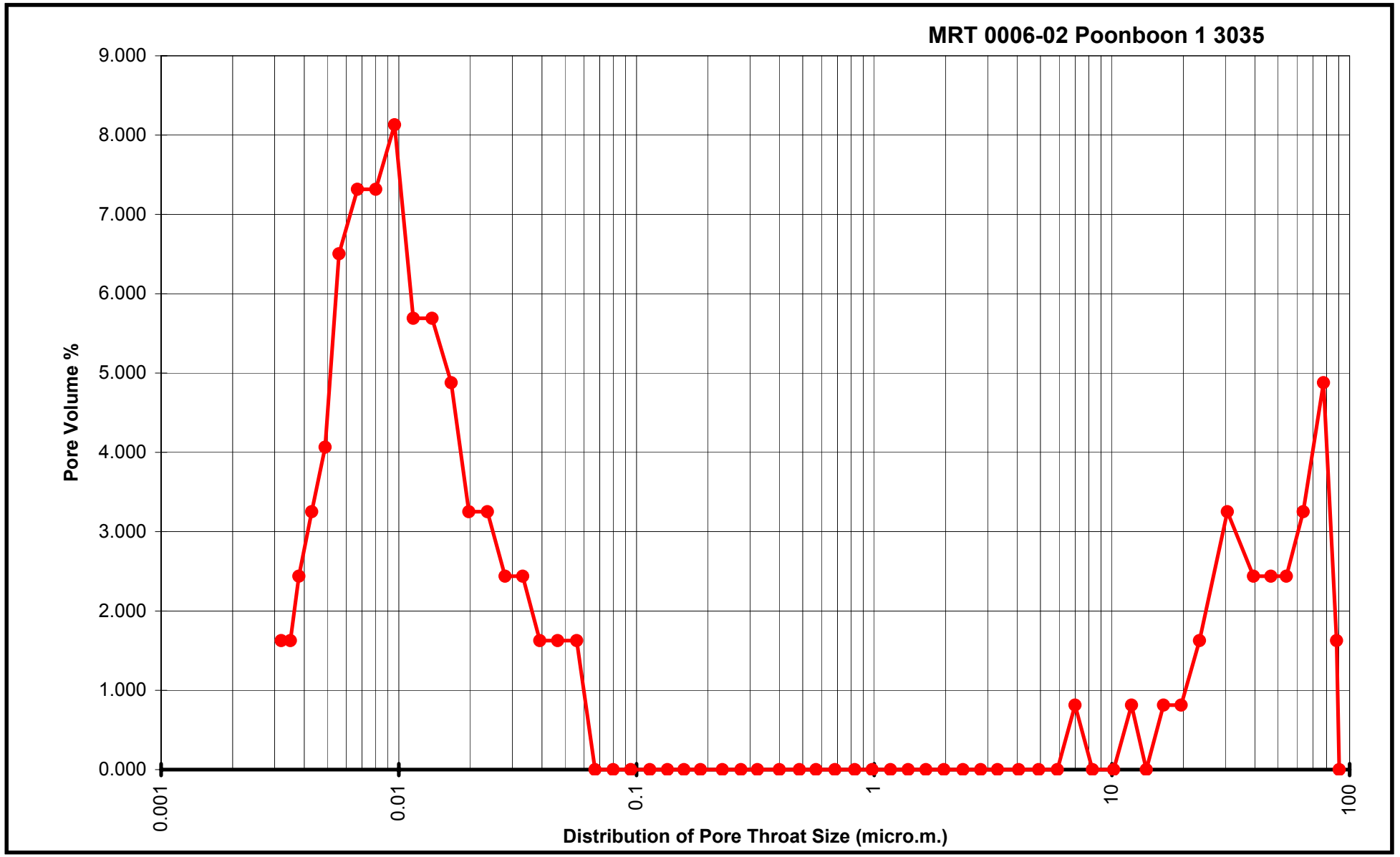

MRT 0006-02 Poonboon 1 2689.6
Pore Volume %
20.000
18.000
16.000
14.000
12.000
10.000
8.000
6.000
4.000
2.000
0.000
0.001
0.01
0.1
1
10
100
Distribution of Pore Throat Size (micro.m.)

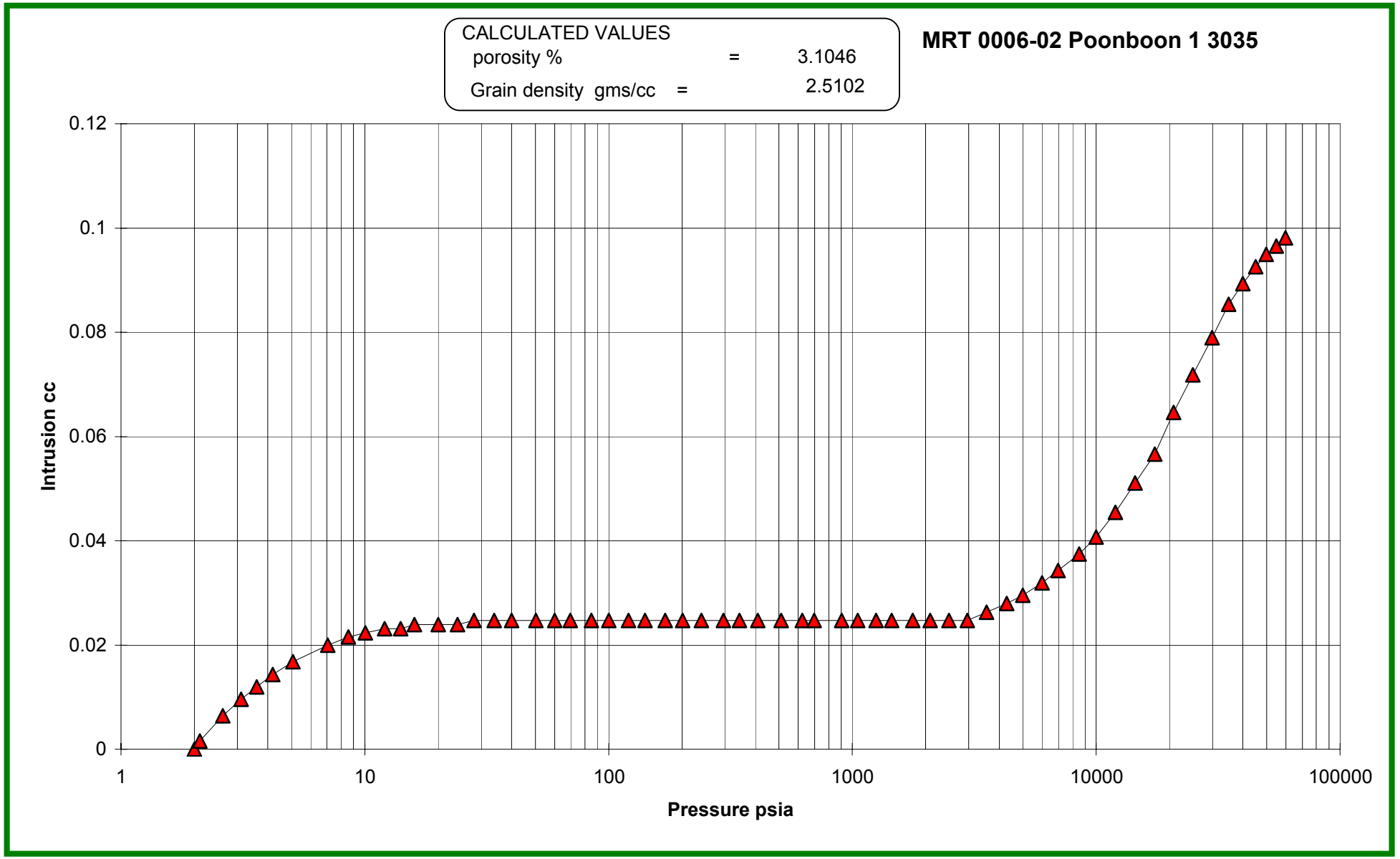

CALCULATED VALUES
porosity % = 8.9452
Grain density gms/cc = 2.5684
MRT 0006-02 Poonboon 1 2689.6
Intrusion cc
0.3
0.25
0.2
0.15
0.1
0.05
0
1
10
100
1000
10000
100000
Pressure psia

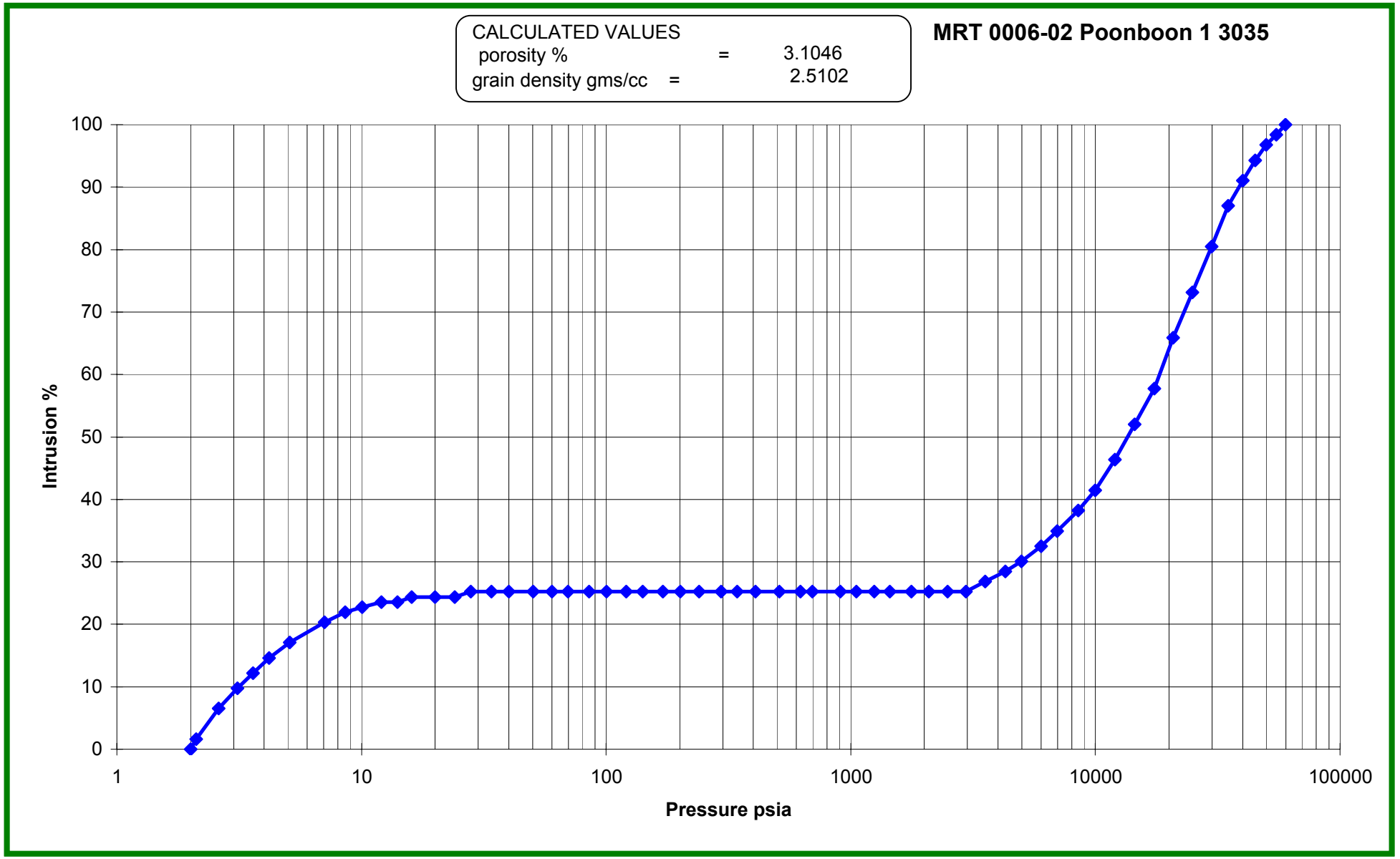

CALCULATED VALUES
porosity % = 8.9452
grain density gms/cc = 2.5684
MRT 0006-02 Poonboon 1 2689.6
Intrusion %
100
90
80
70
60
50
40
30
20
10
0
1
10
100
1000
10000
100000
Pressure psia

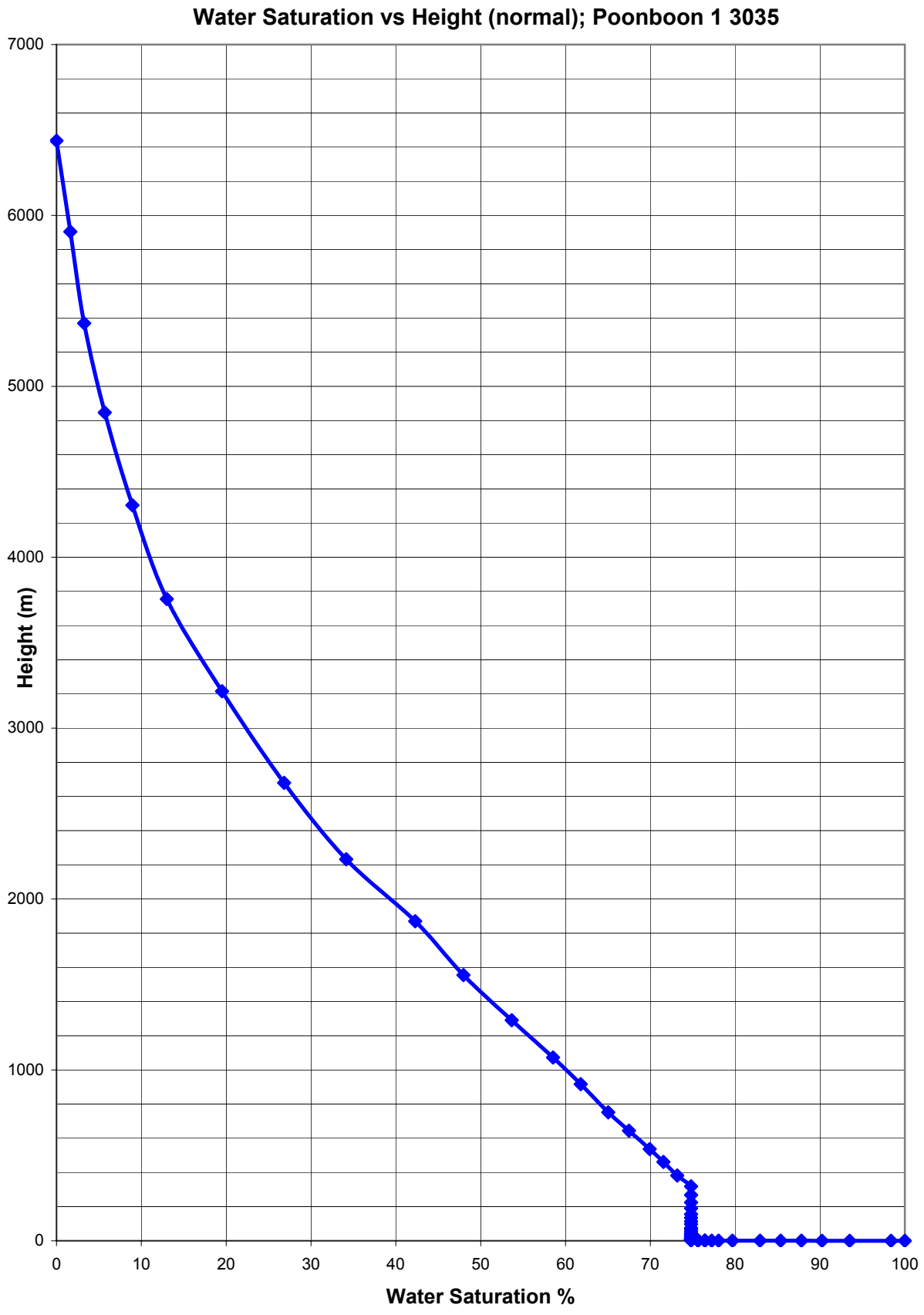

Water Saturation vs Height (normal); Poonboon 1 2689
Height (m)
7000
6000
5000
4000
3000
2000
1000
0
0
10
20
30
40
50
60
70
80
90
100
Water Saturation %

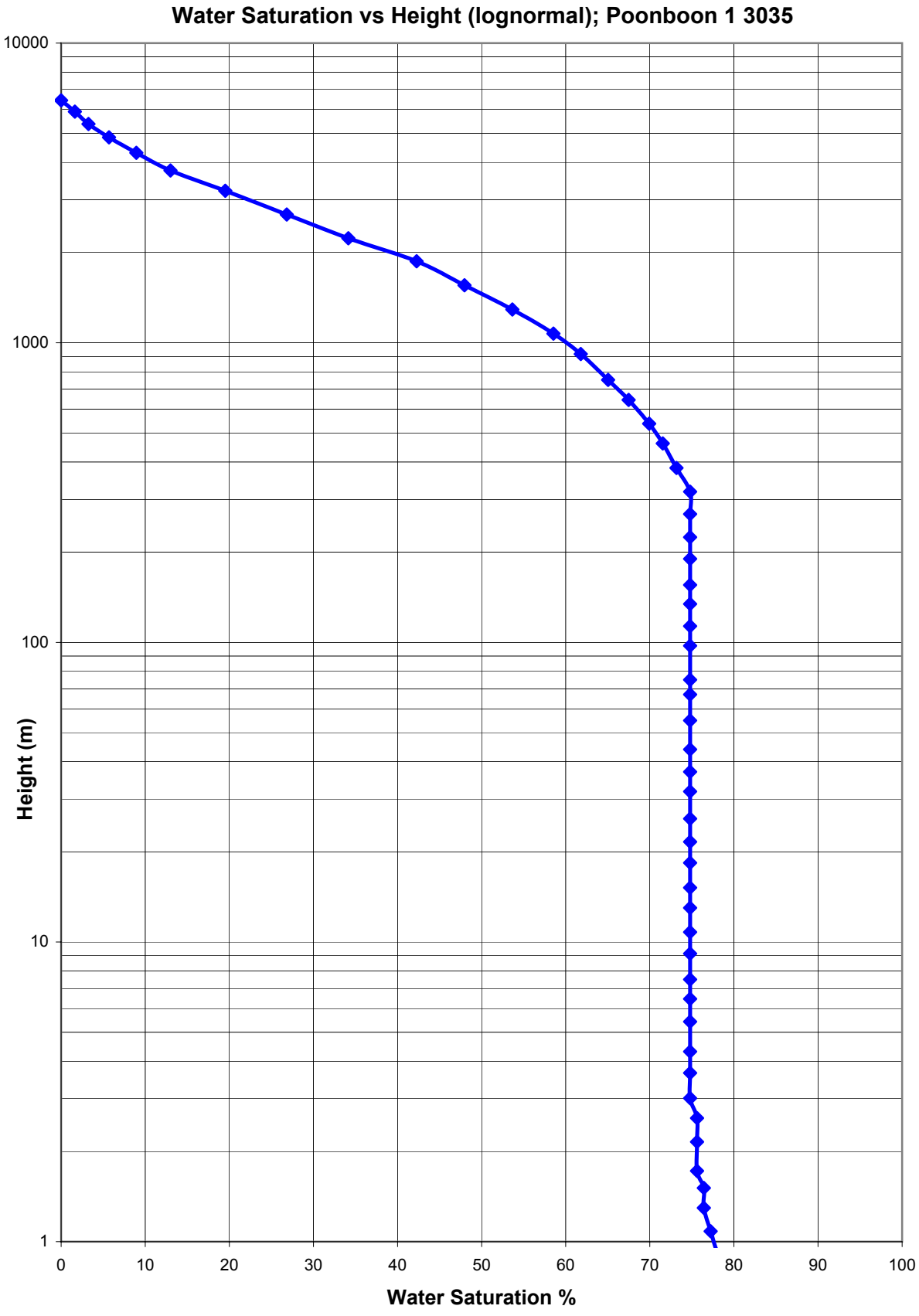

Water Saturation vs Height (lognormal); Poonboon 1 2689
10000
1000
100
10
1
Height (m)
0
10
20
30
40
50
60
70
80
90
100
Water Saturation %


MRT 0006-02 Poonboon 1 3035
Pore Volume %
9.000
8.000
7.000
6.000
5.000
4.000
3.000
2.000
1.000
0.000
0.001
0.01
0.1
1
10
100
Distribution of Pore Throat Size (micro.m.)

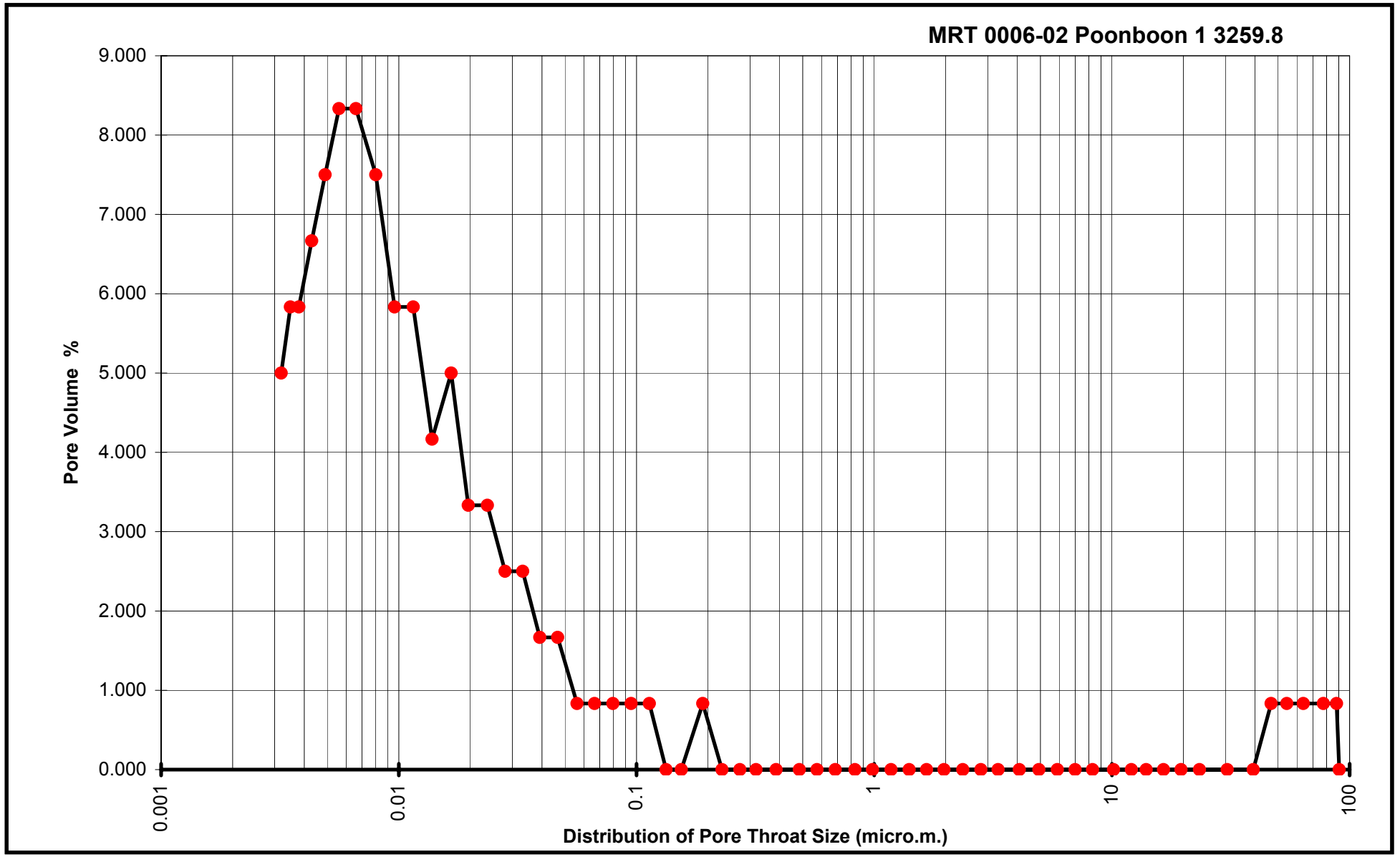

CALCULATED VALUES
porosity % = 3.1046
Grain density gms/cc = 2.5102
MRT 0006-02 Poonboon 1 3035
Intrusion cc
0.12
0.1
0.08
0.06
0.04
0.02
0
1
10
100
1000
10000
100000
Pressure psia

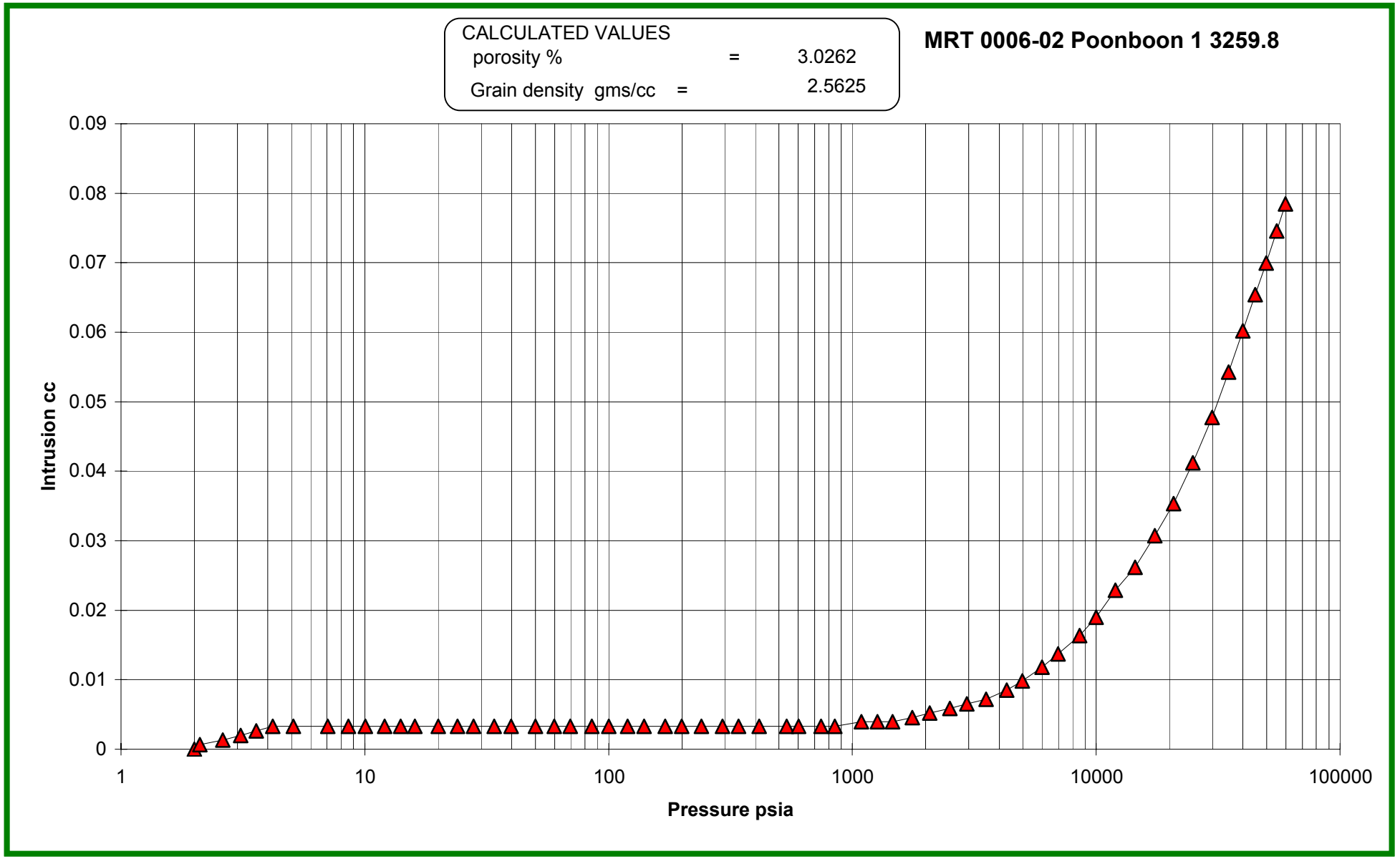

CALCULATED VALUES
porosity % = 3.1046
grain density gms/cc = 2.5102
MRT 0006-02 Poonboon 1 3035
Intrusion %
100
90
80
70
60
50
40
30
20
10
0
1
10
100
1000
10000
100000
Pressure psia

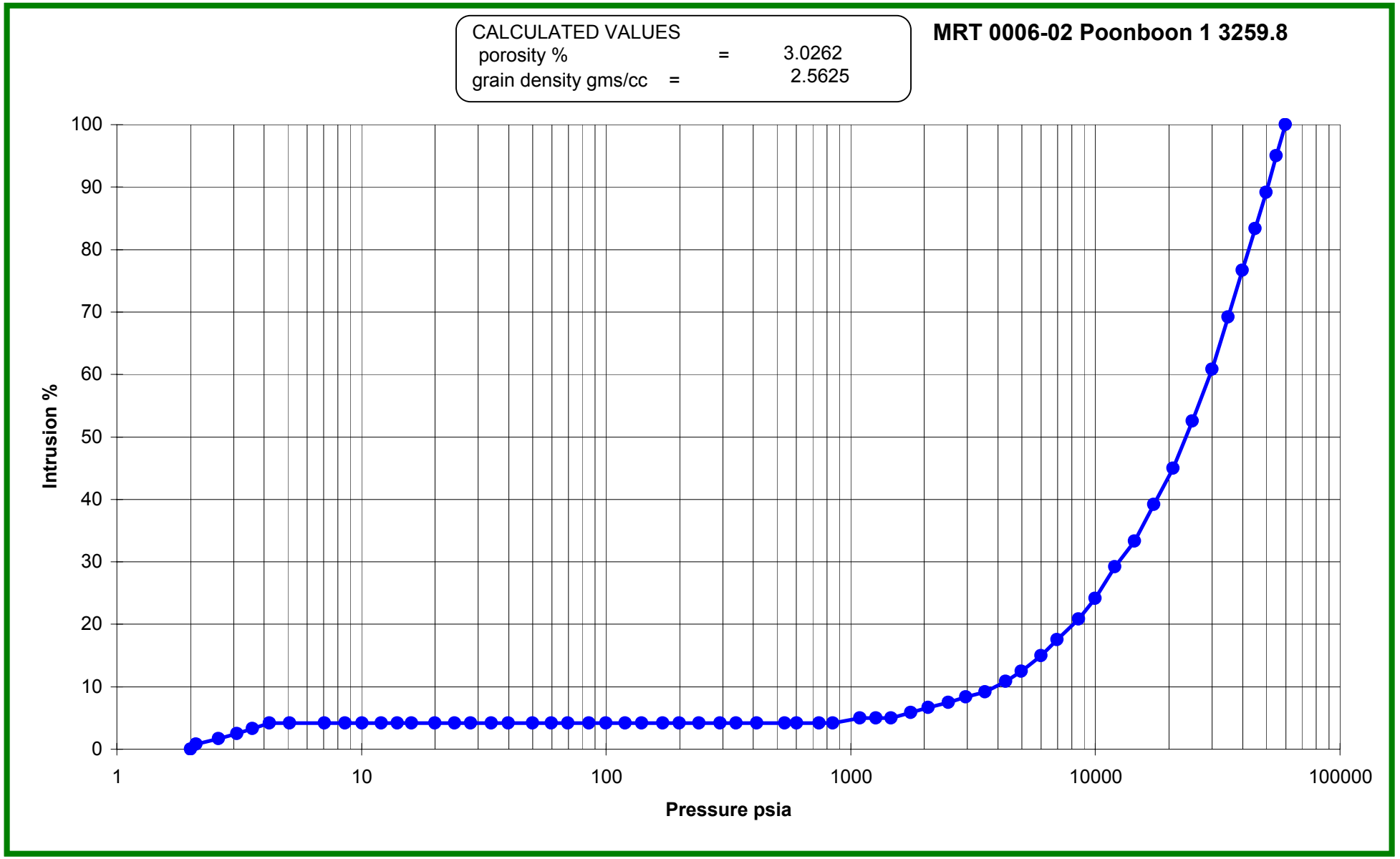

Water Saturation vs Height (normal); Poonboon 1 3035
Height (m)
7000
6000
5000
4000
3000
2000
1000
0
0
10
20
30
40
50
60
70
80
90
100
Water Saturation %

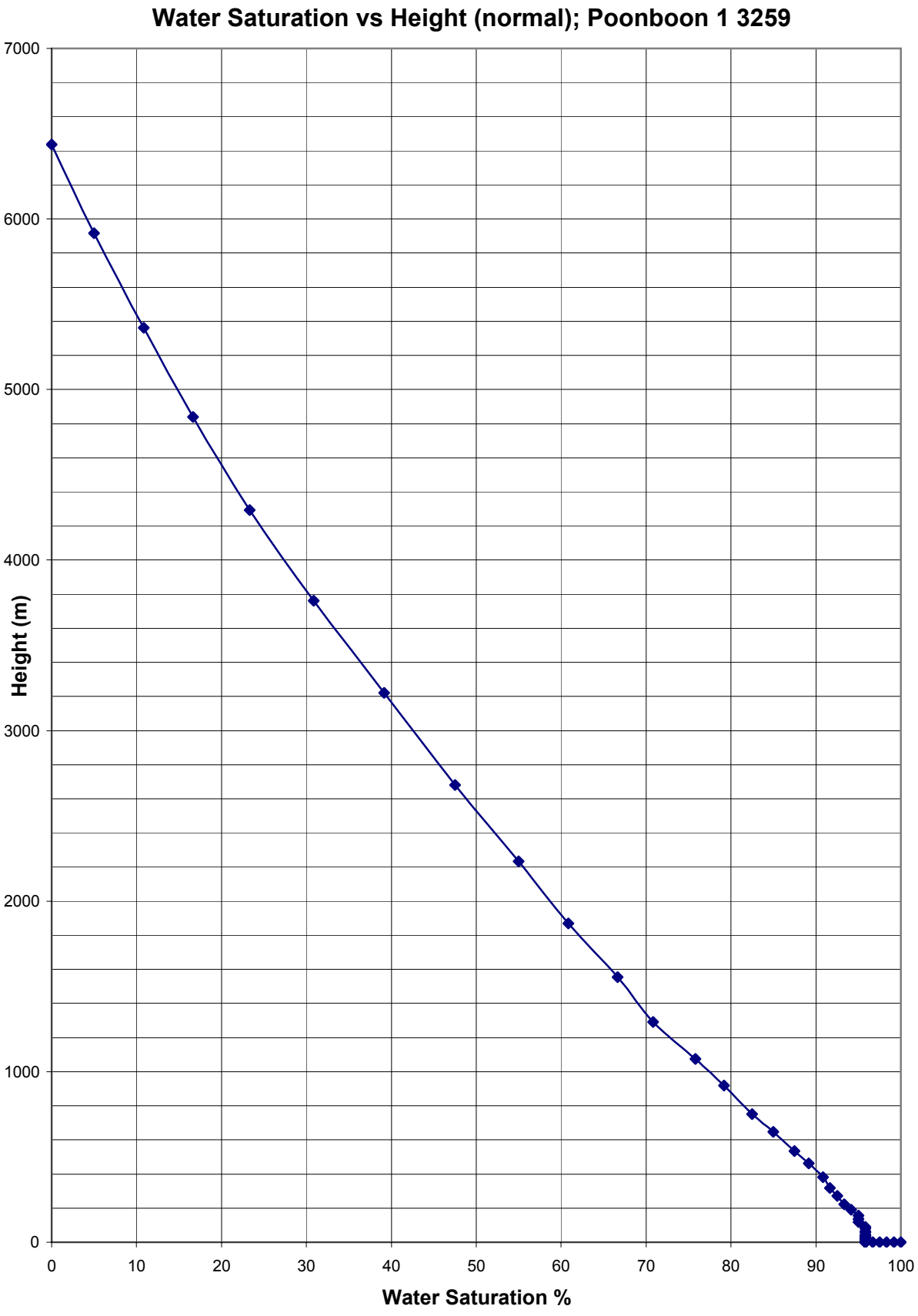

Water Saturation vs Height (lognormal); Poonboon 1 3035
10000
1000
100
10
1
Height (m)
0
10
20
30
40
50
60
70
80
90
100
Water Saturation %

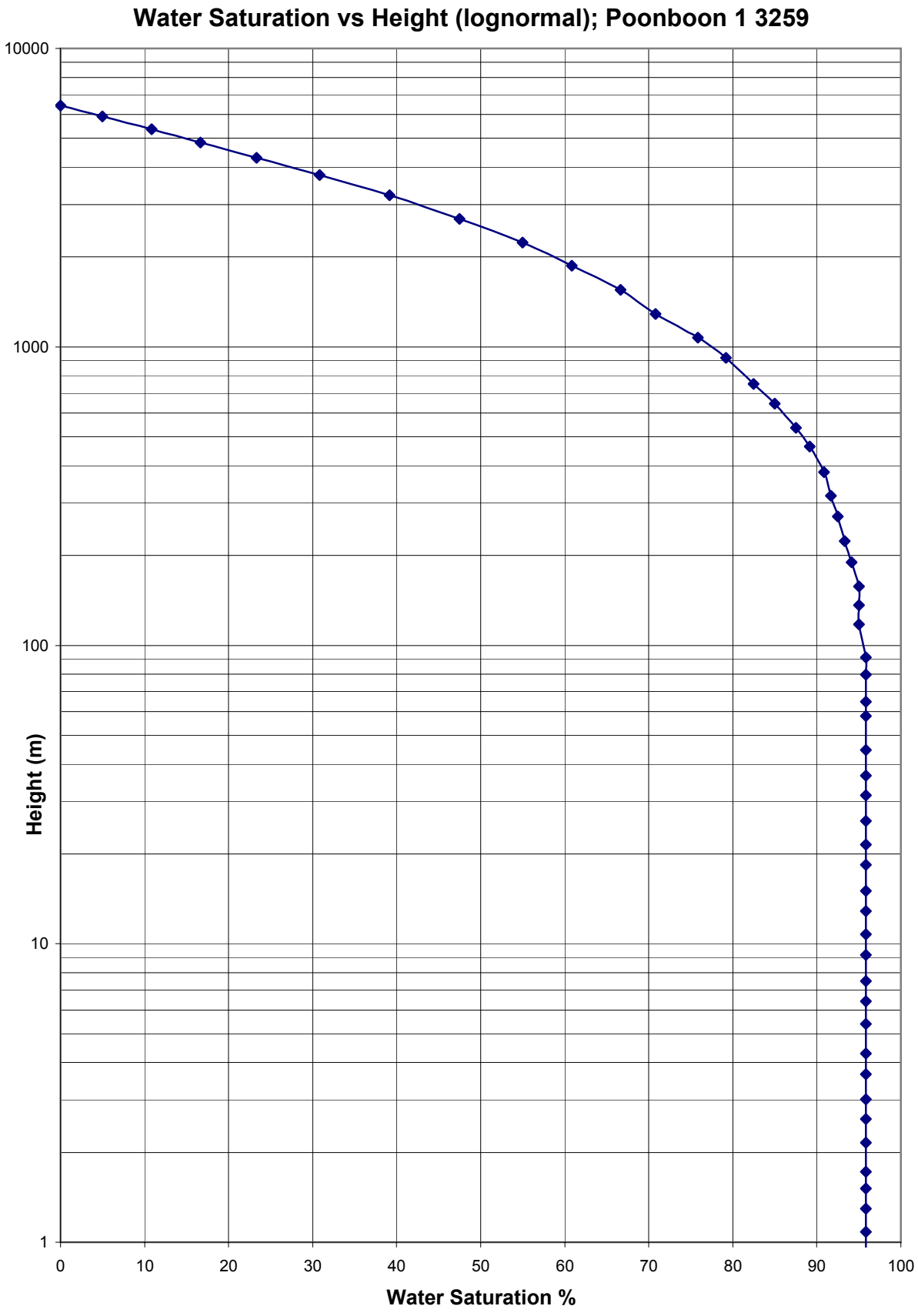
Poonboon_1_3259m.xls

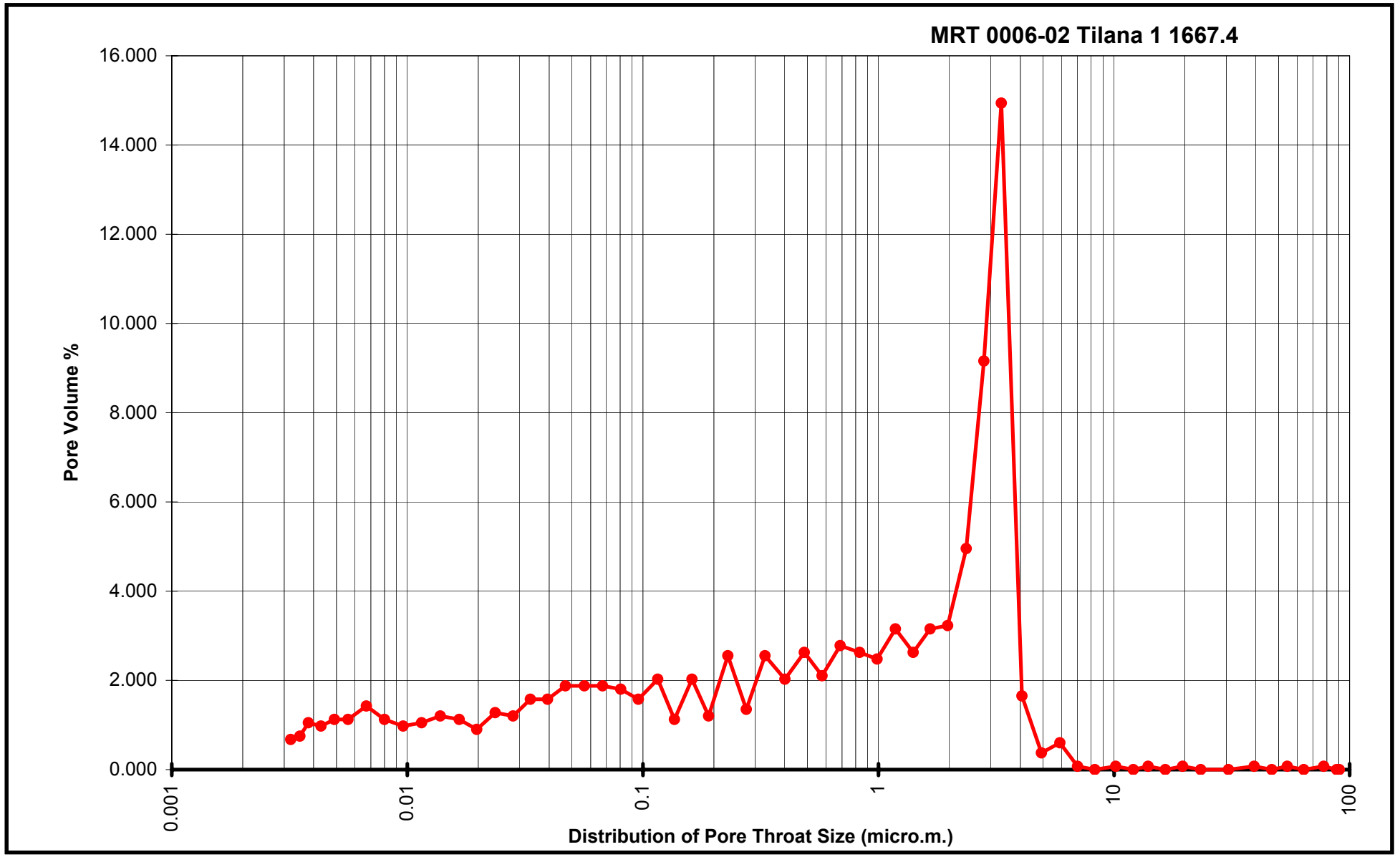


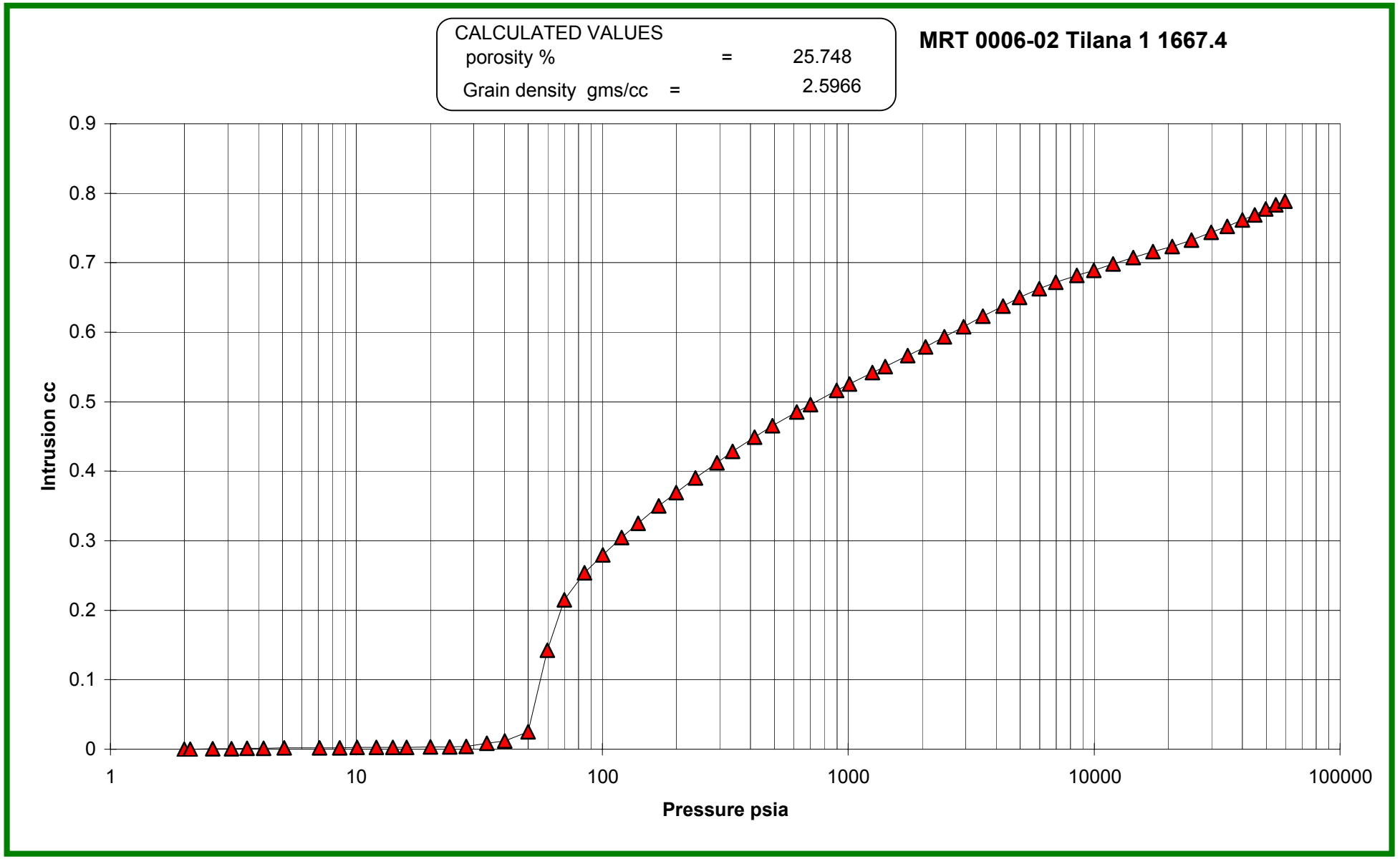

CALCULATED VALUES
porosity % = 3.0262
Grain density gms/cc = 2.5625
MRT 0006-02 Poonboon 1 3259.8
Intrusion cc
0.09
0.08
0.07
0.06
0.05
0.04
0.03
0.02
0.01
0
1
10
100
1000
10000
100000
Pressure psia


CALCULATED VALUES
porosity % = 3.0262
grain density gms/cc = 2.5625
MRT 0006-02 Poonboon 1 3259.8
Intrusion %
100
90
80
70
60
50
40
30
20
10
0
1
10
100
1000
10000
100000
Pressure psia


Water Saturation vs Height (normal); Poonboon 1 3259
Height (m)
7000
6000
5000
4000
3000
2000
1000
0
0
10
20
30
40
50
60
70
80
90
100
Water Saturation %

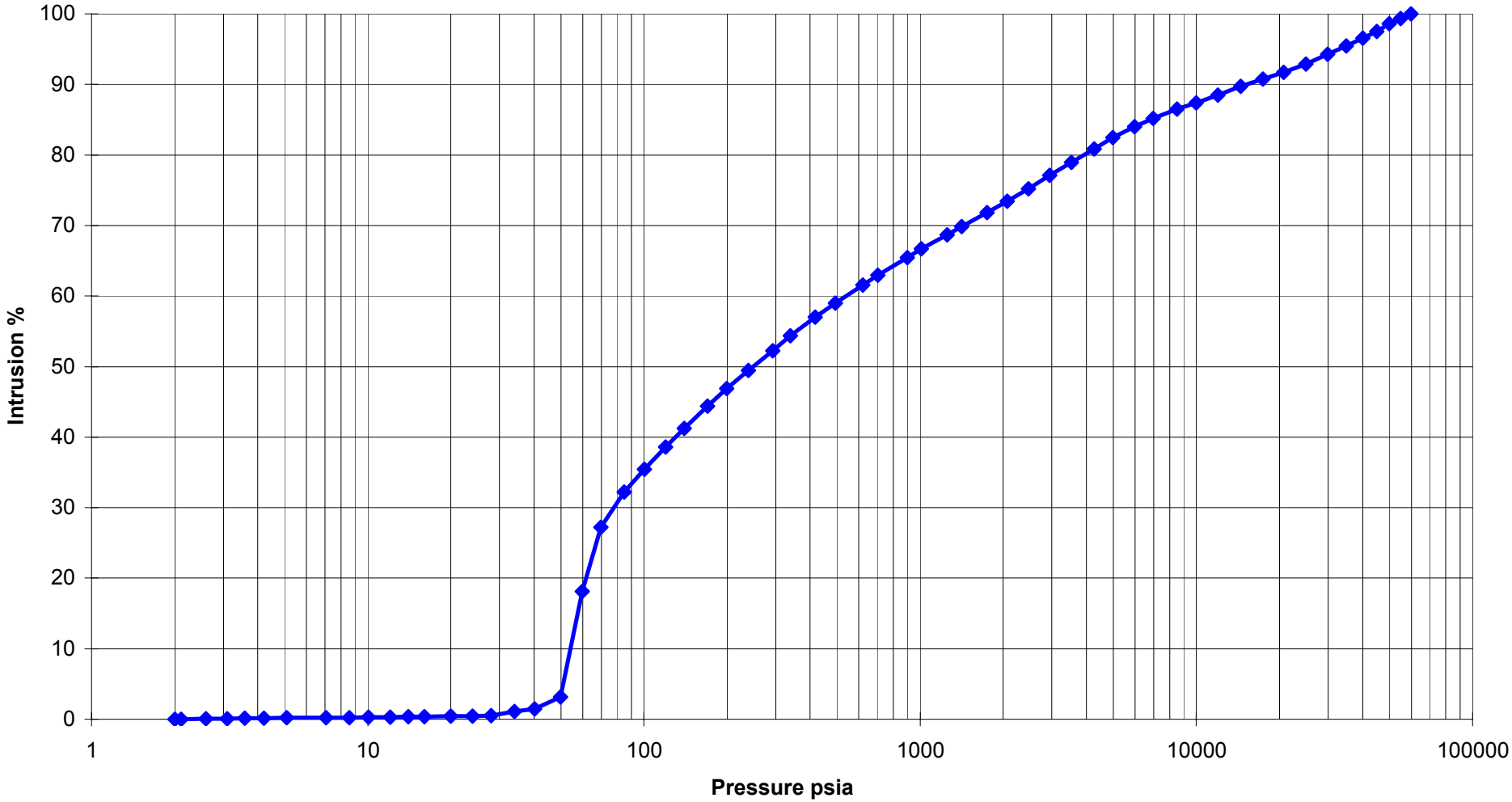

Water Saturation vs Height (lognormal); Poonboon 1 3259
10000
1000
100
10
1
Height (m)
0
10
20
30
40
50
60
70
80
90
100
Water Saturation %

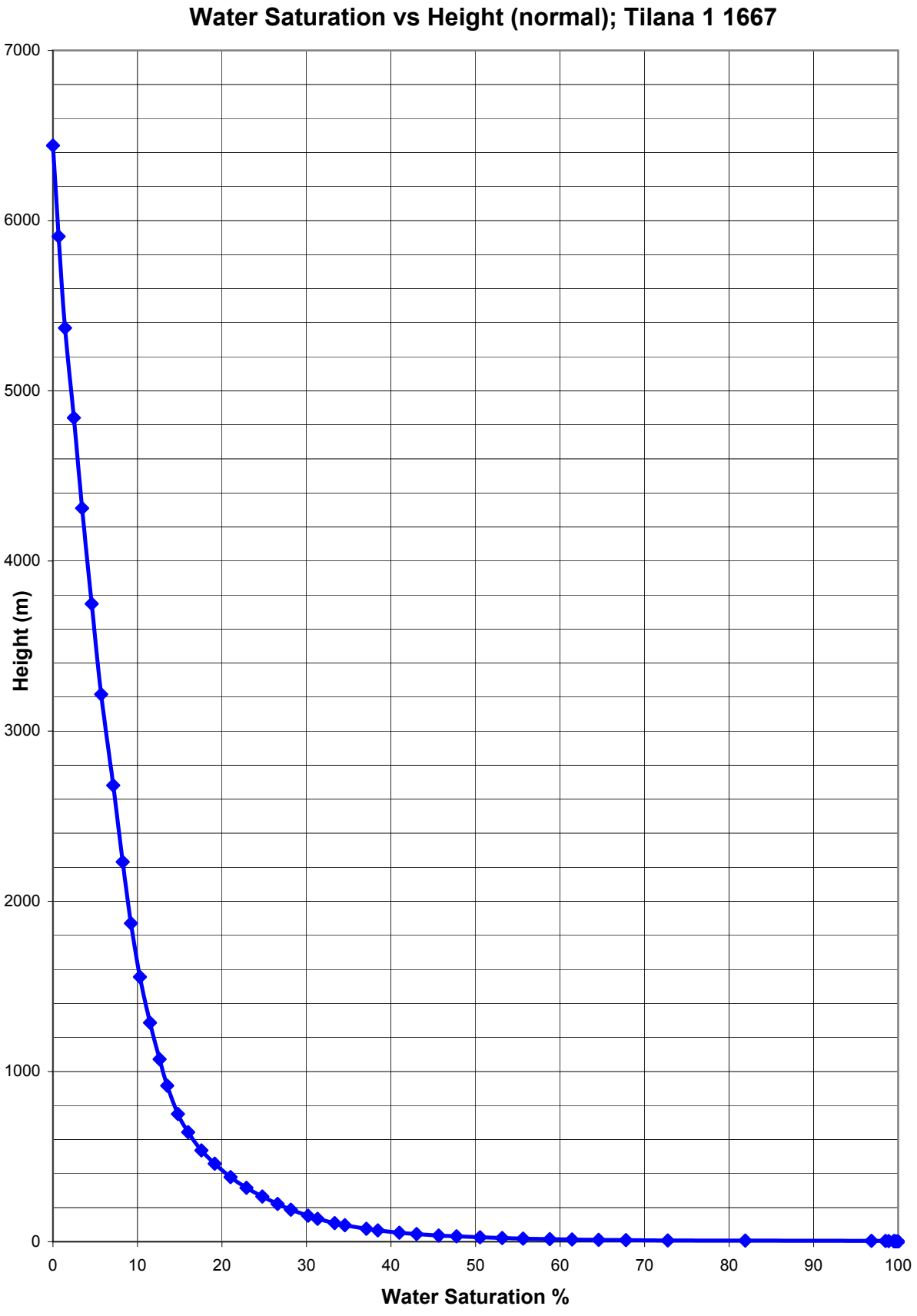

MRT 0006-02 Tilana 1 1667.4
16.000
14.000
12.000
10.000
8.000
6.000
4.000
2.000
0.000
Pore Volume %
0.001
0.01
0.1
1
10
100
Distribution of Pore Throat Size (micro.m.)

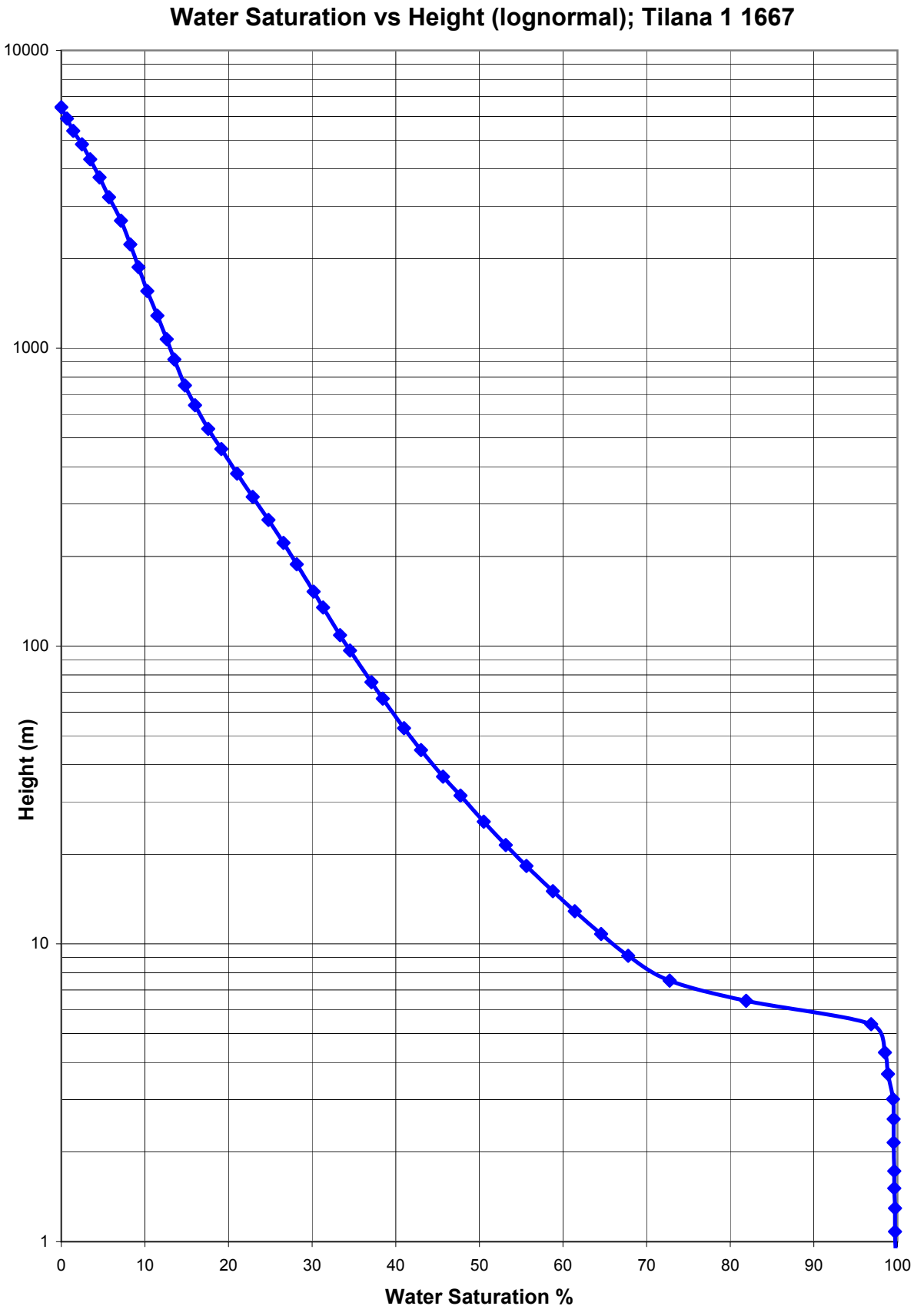

CALCULATED VALUES
porosity % = 25.748
Grain density gms/cc = 2.5966
MRT 0006-02 Tilana 1 1667.4
Intrusion cc
0.9
0.8
0.7
0.6
0.5
0.4
0.3
0.2
0.1
0
1
10
100
1000
10000
100000
Pressure psia

CALCULATED VALUES
porosity % = 25.7483
grain density gms/cc = 2.5966

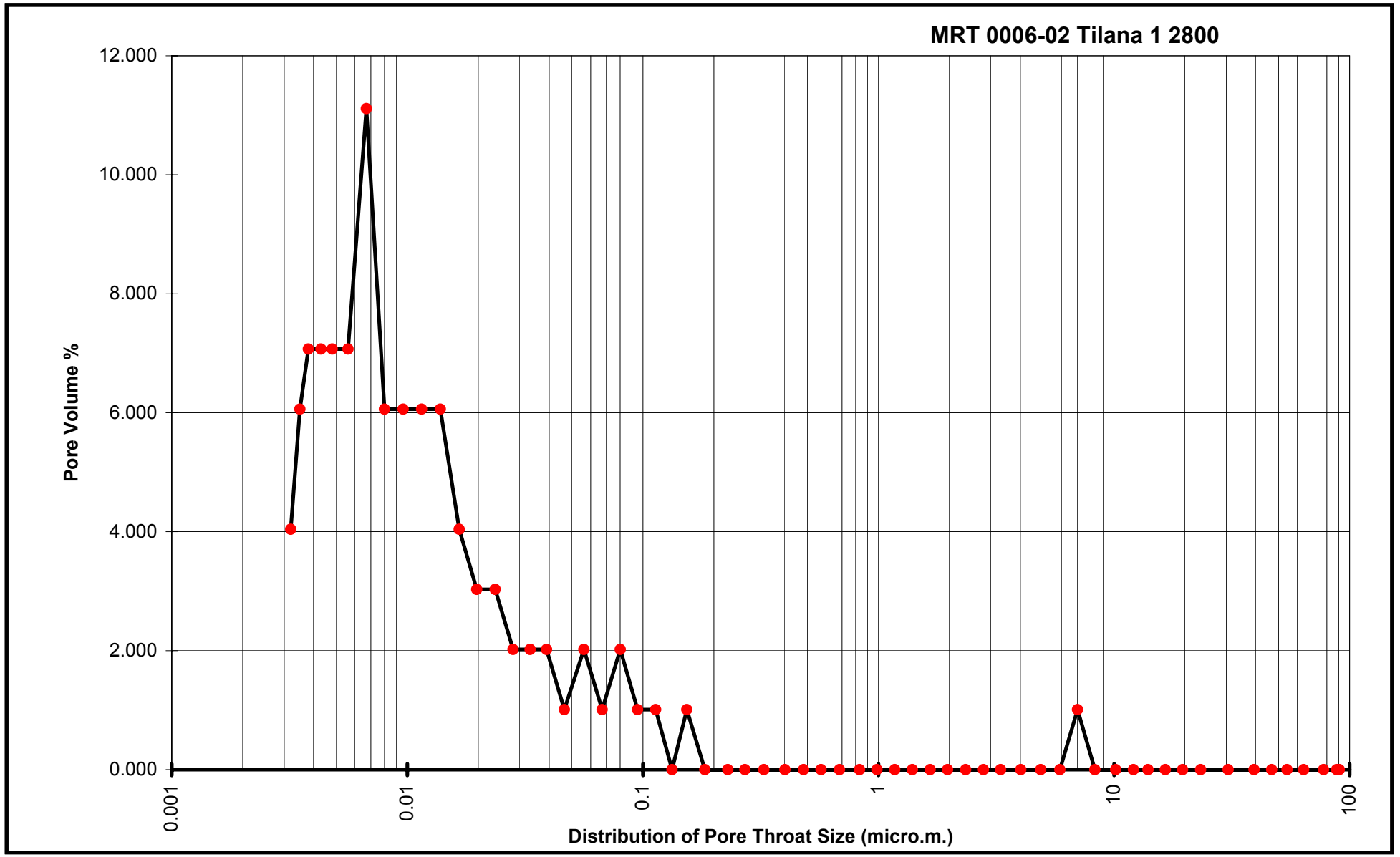
MRT 0006-02 Tilana 1 1667.4



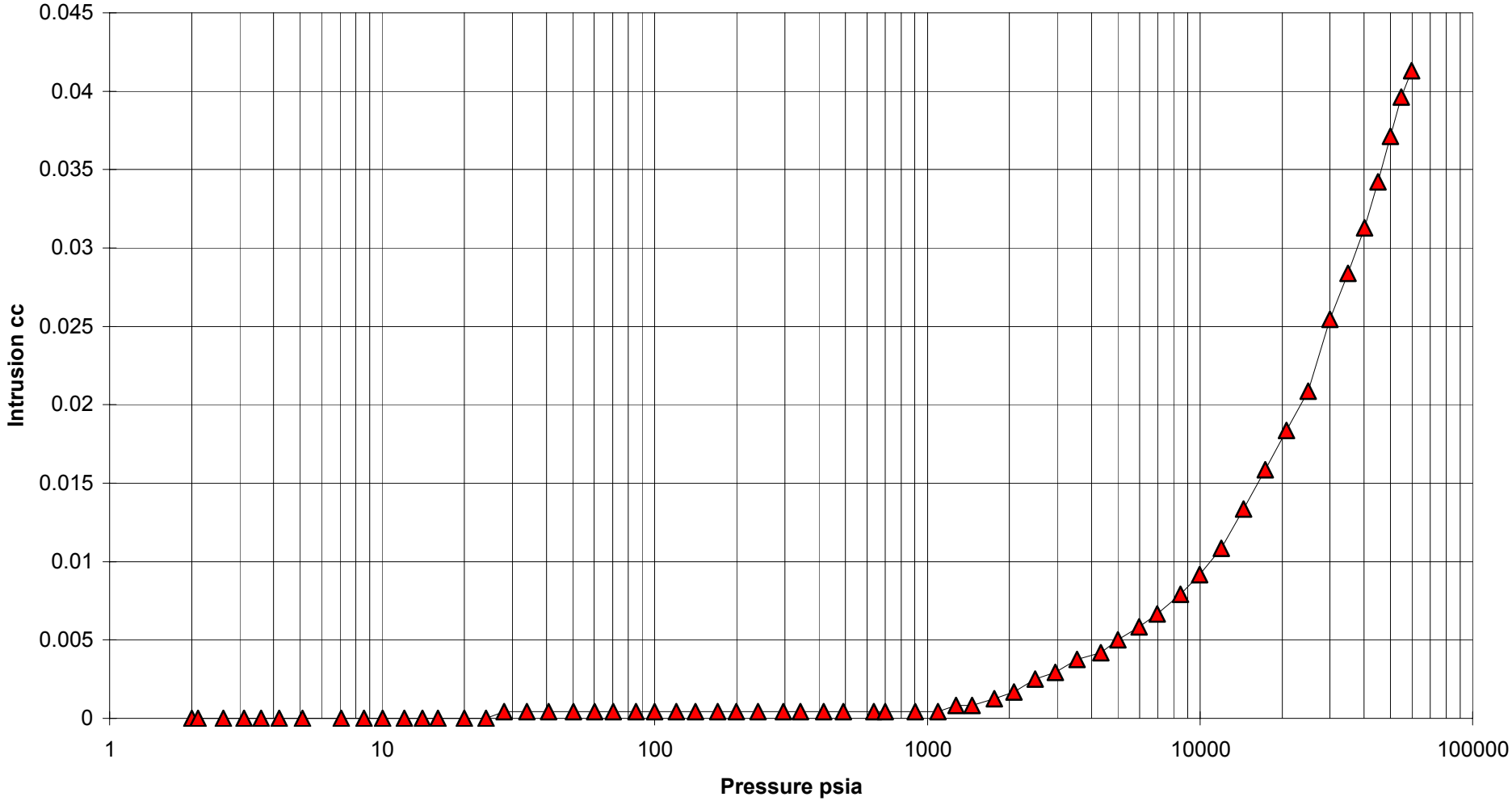

Water Saturation vs Height (normal); Tilana 1 1667
Height (m)
7000
6000
5000
4000
3000
2000
1000
0
0
10
20
30
40
50
60
70
80
90
100
Water Saturation %


Water Saturation vs Height (lognormal); Tilana 1 1667
10000
1000
100
10
1
Height (m)
0
10
20
30
40
50
60
70
80
90
100
Water Saturation %

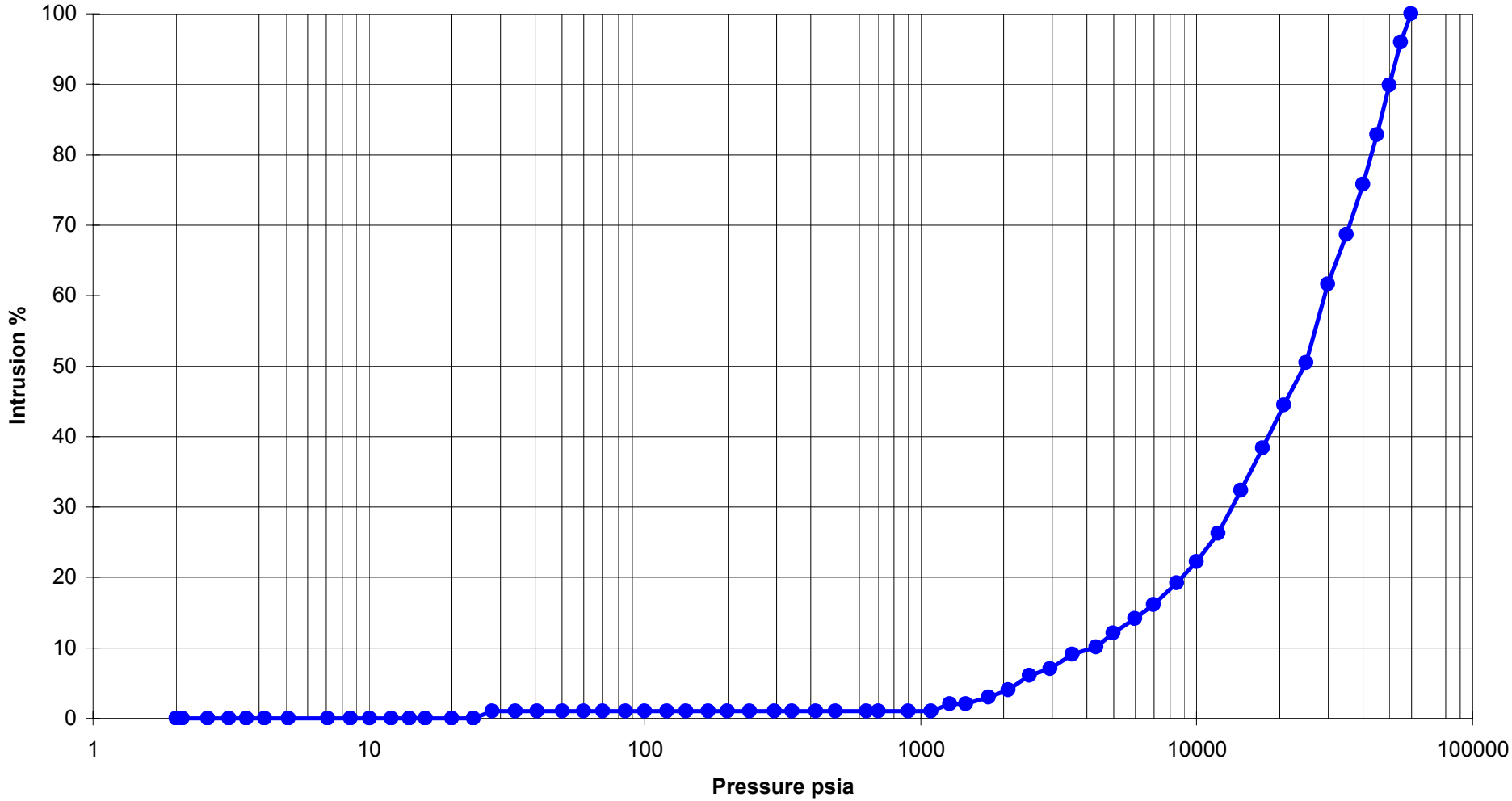
Tilana_1_2800m.xls

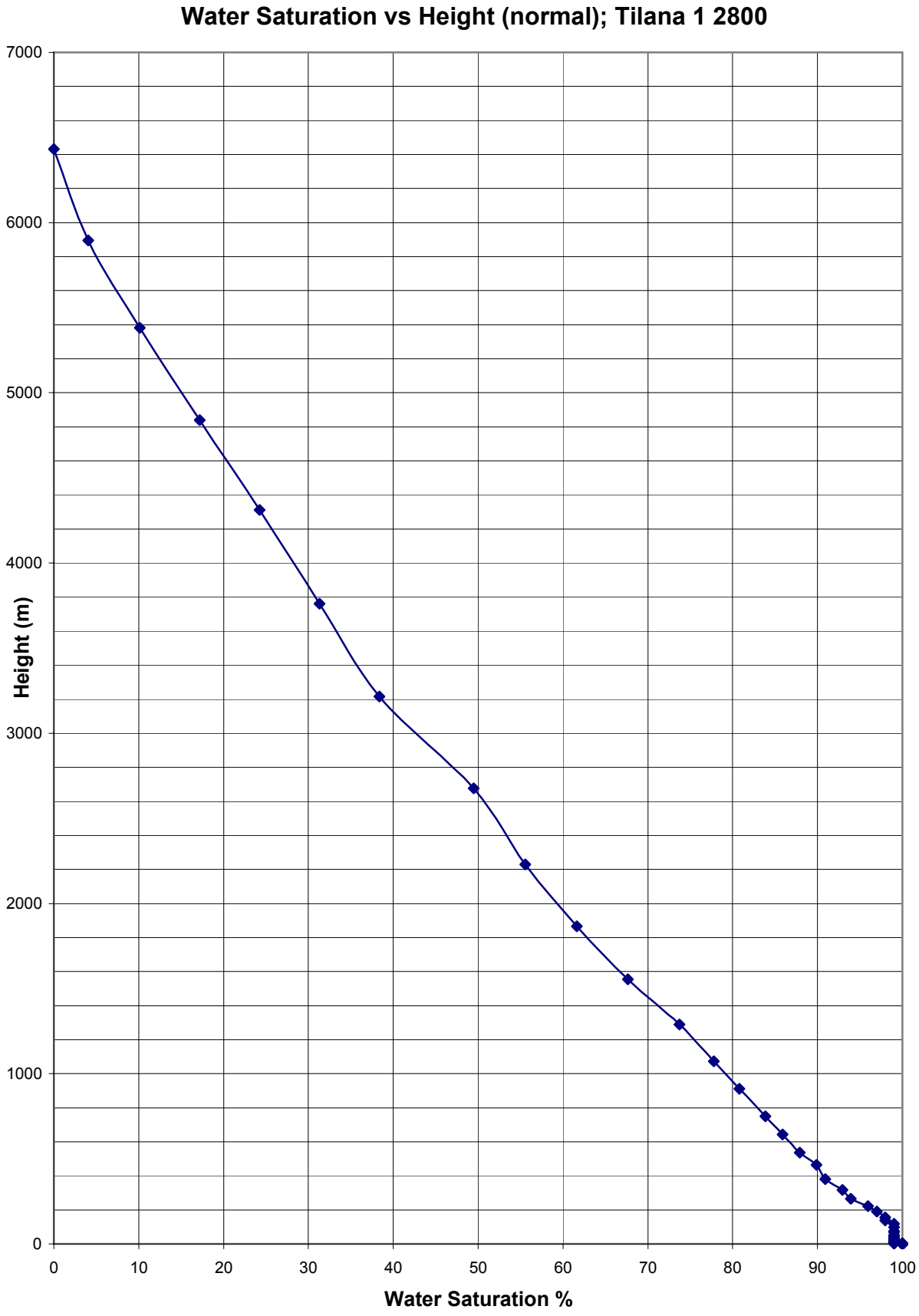


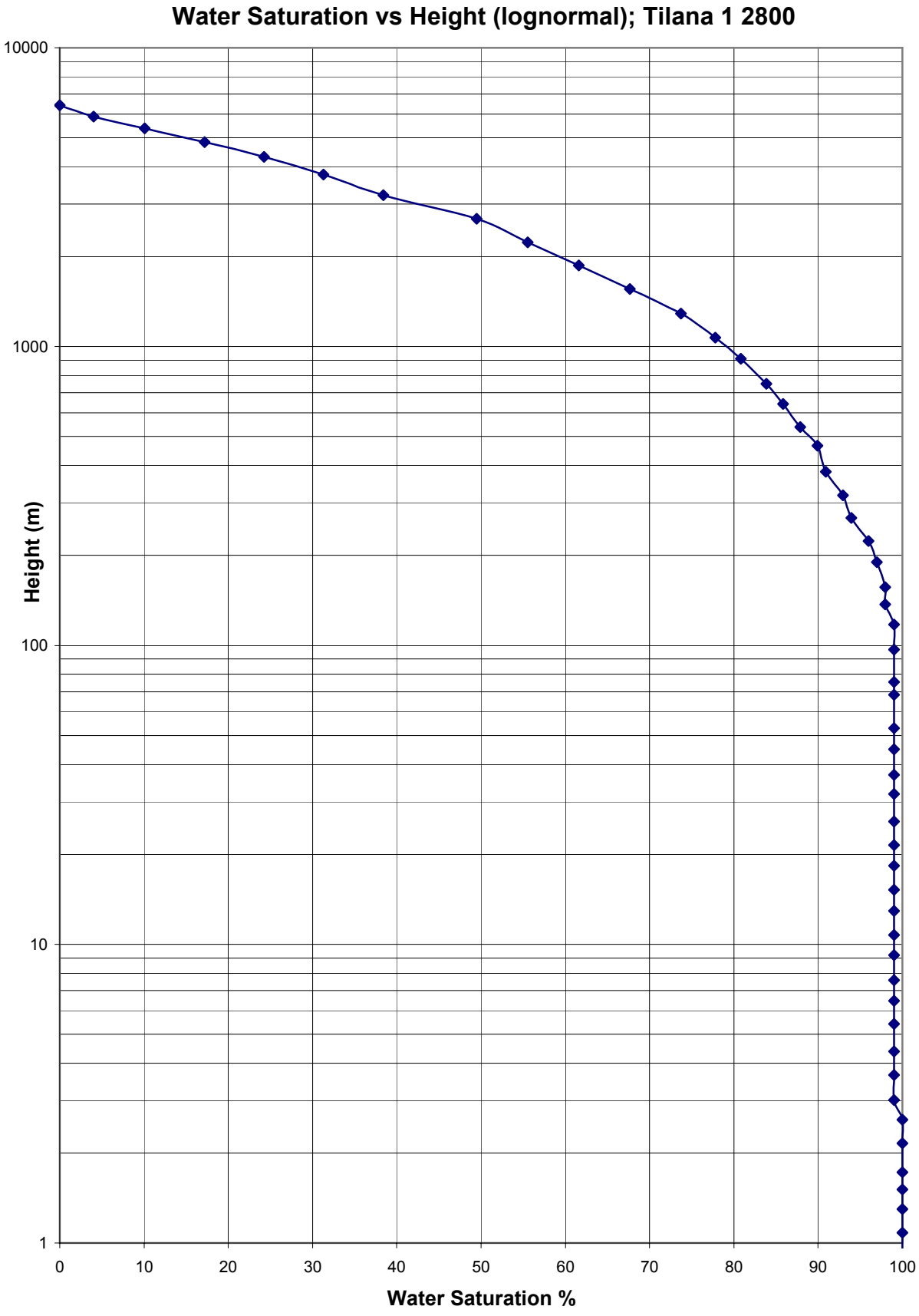
CALCULATED VALUES
porosity % = 2.5484
Grain density gms/cc = 2.5727



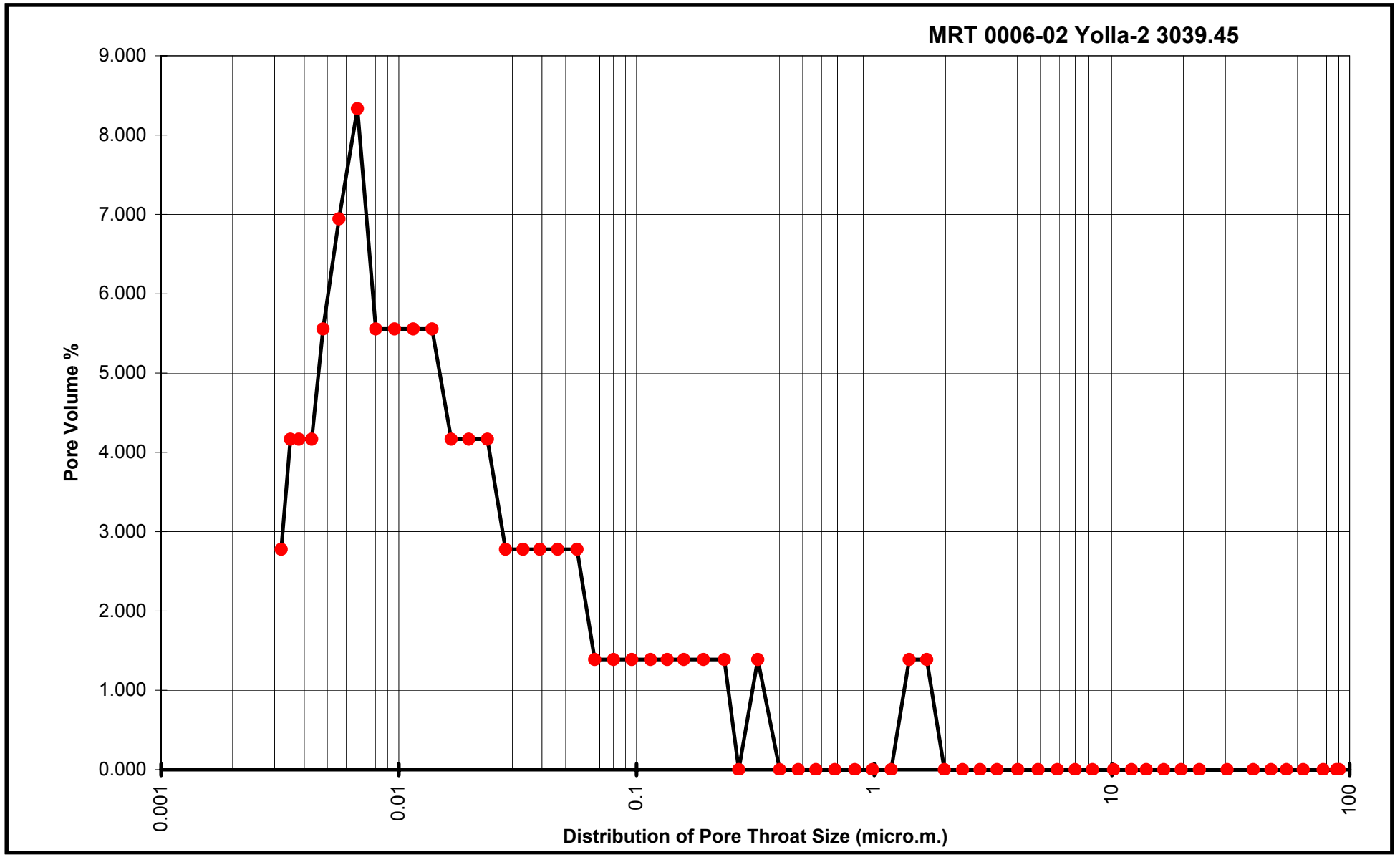
CALCULATED VALUES
porosity % = 2.5484
grain density gms/cc = 2.5727

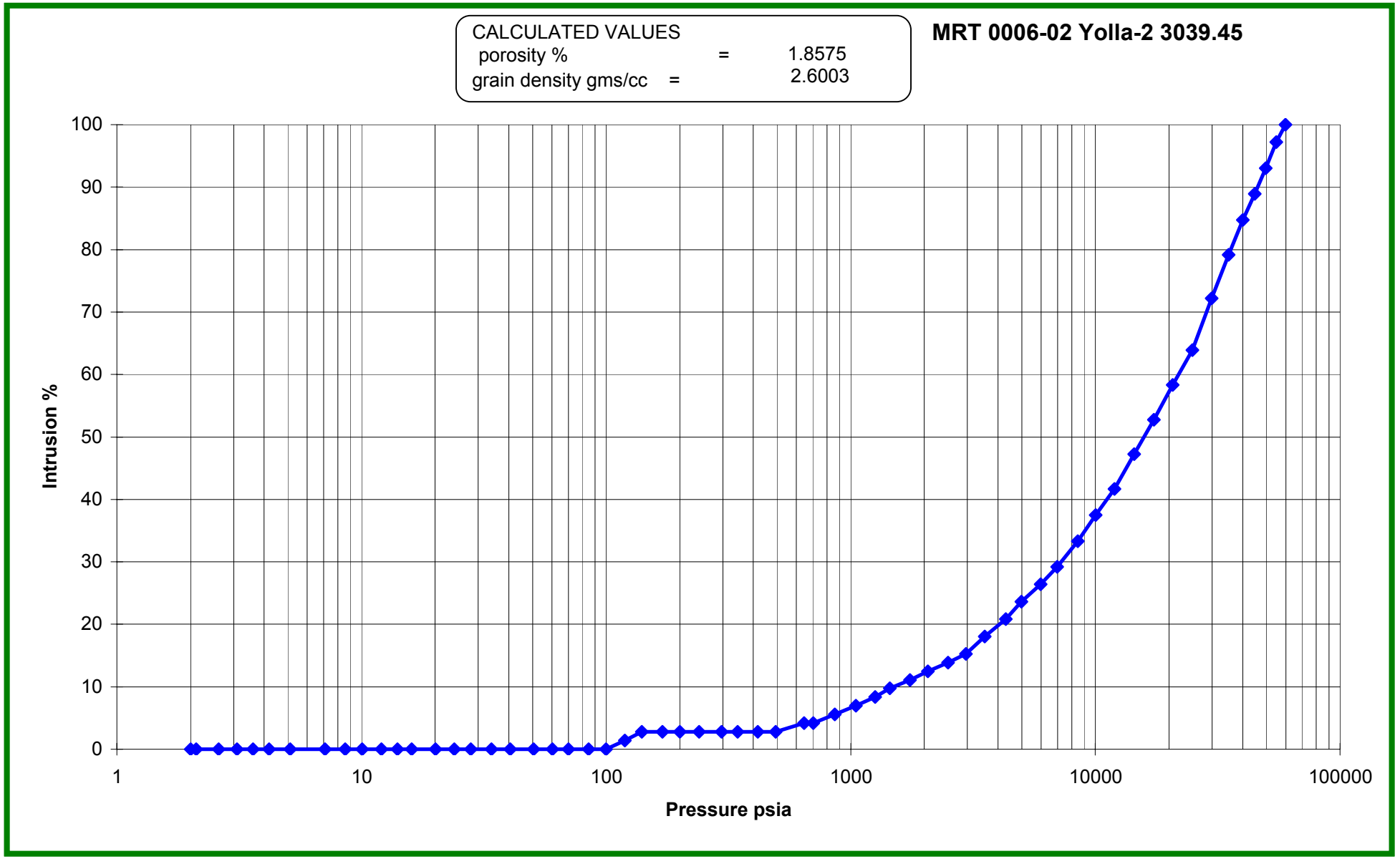


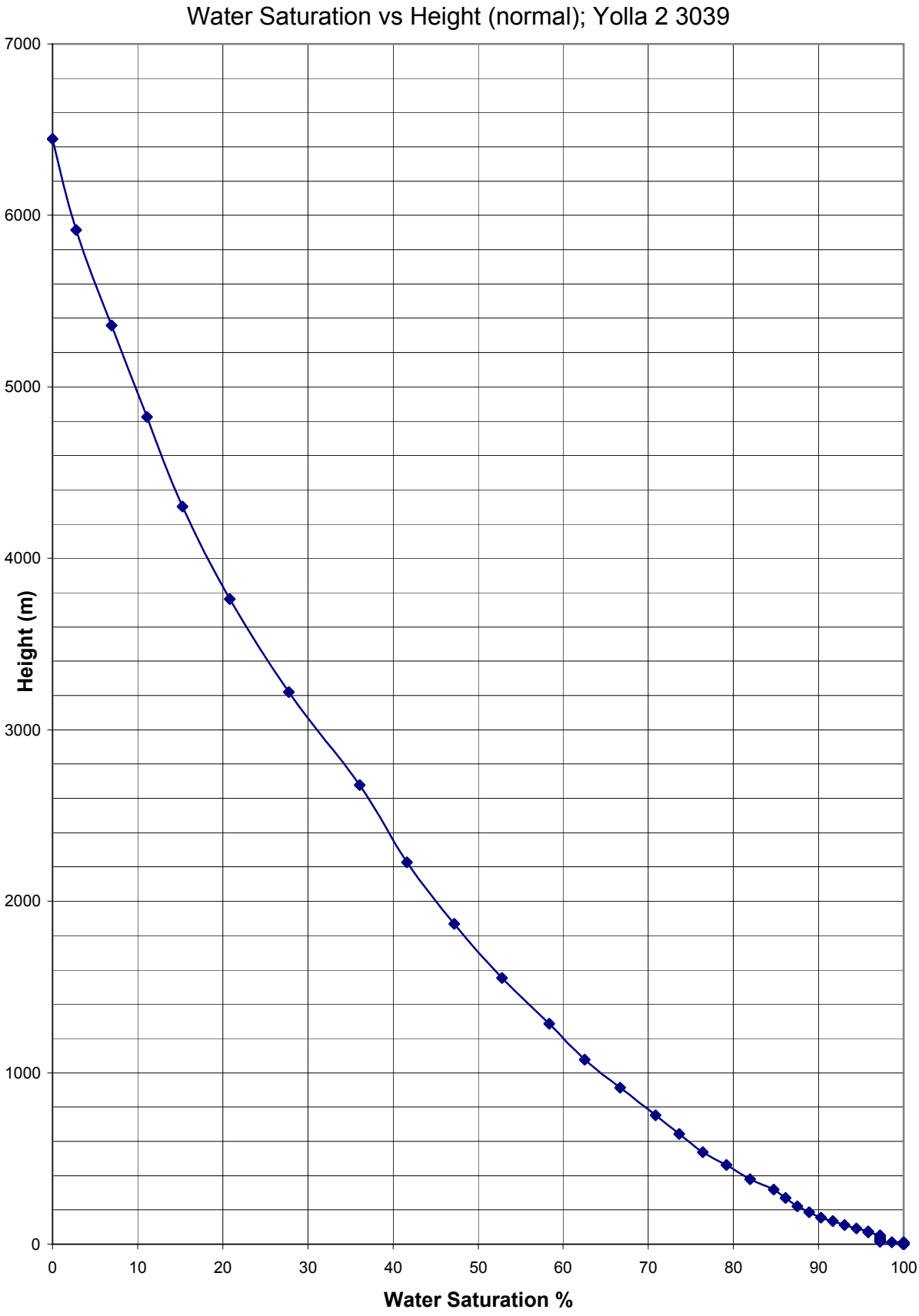

Water Saturation vs Height (normal); Tilana 1 2800
Height (m)
7000
6000
5000
4000
3000
2000
1000
0
0
10
20
30
40
50
60
70
80
90
100
Water Saturation %

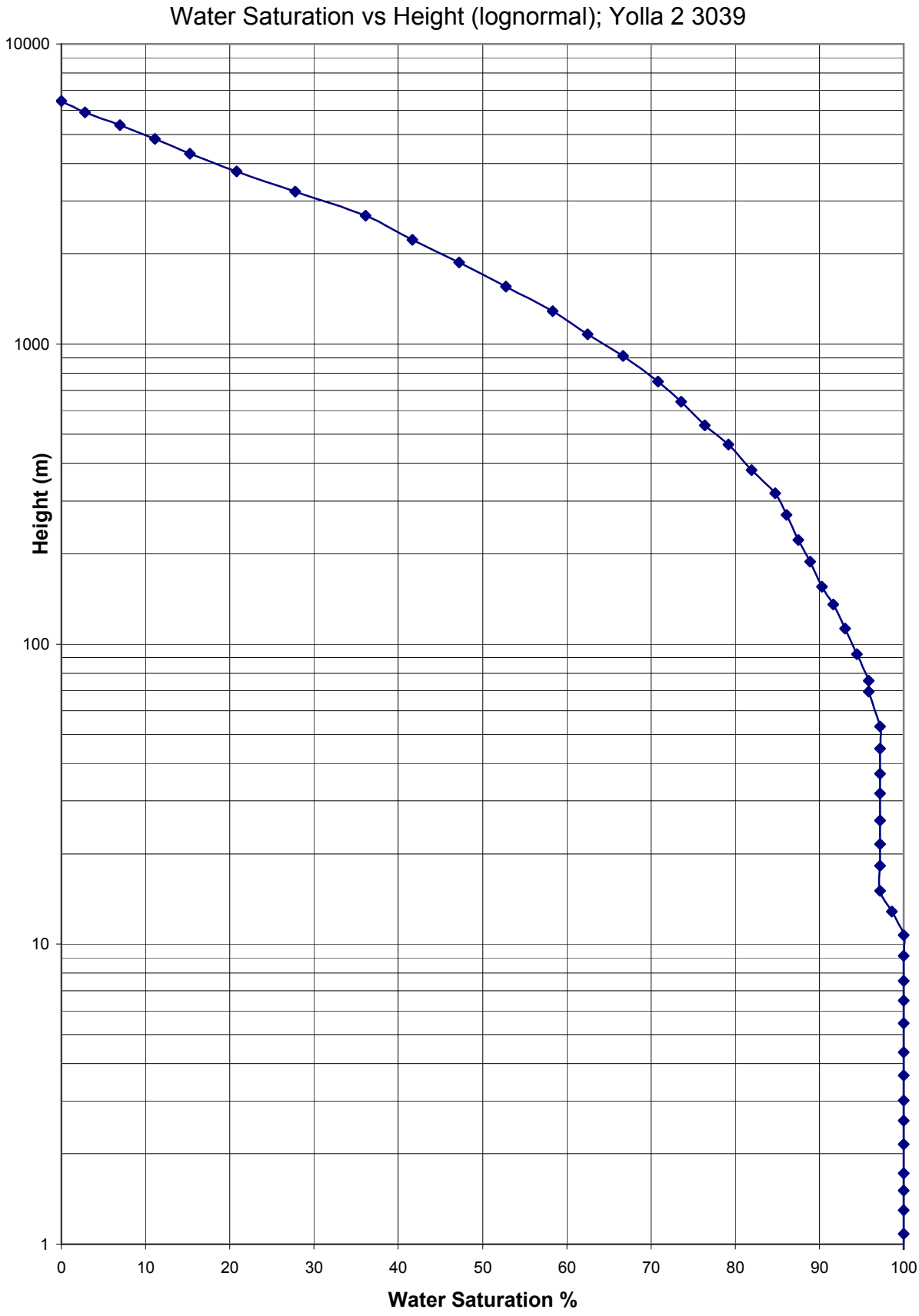

Water Saturation vs Height (lognormal); Tilana 1 2800
10000
1000
100
10
1
Height (m)
0
10
20
30
40
50
60
70
80
90
100
Water Saturation %

Yolla_2_3039m.xls




CALCULATED VALUES
porosity % = 1.8575
grain density gms/cc = 2.6003
MRT 0006-02 Yolla-2 3039.45
Intrusion %
100
90
80
70
60
50
40
30
20
10
0
1
10
100
1000
10000
100000
Pressure psia


Water Saturation vs Height (normal); Yolla 2 3039
7000
6000
5000
4000
3000
2000
1000
0
Height (m)
0
10
20
30
40
50
60
70
80
90
100
Water Saturation %


Water Saturation vs Height (lognormal); Yolla 2 3039
10000
1000
100
10
1
Height (m)
0
10
20
30
40
50
60
70
80
90
100
Water Saturation %

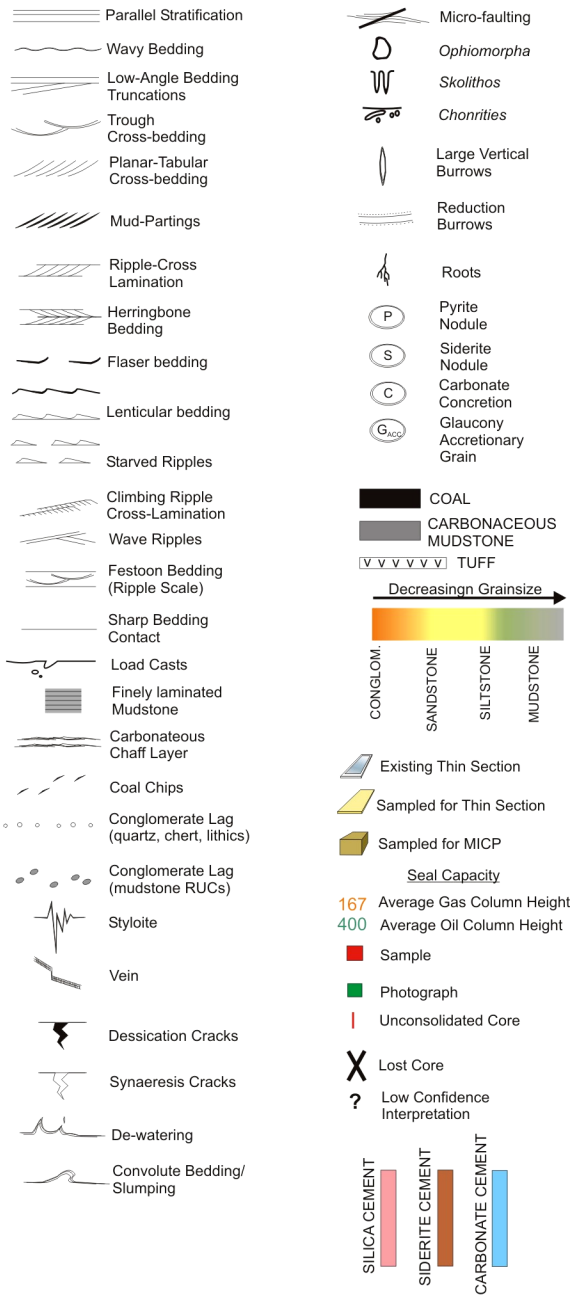
APPENDIX M.

DESCRIPTIONS AND PHOTOGRAPHS OF SELECTED CORES FROM THE BASS BASIN

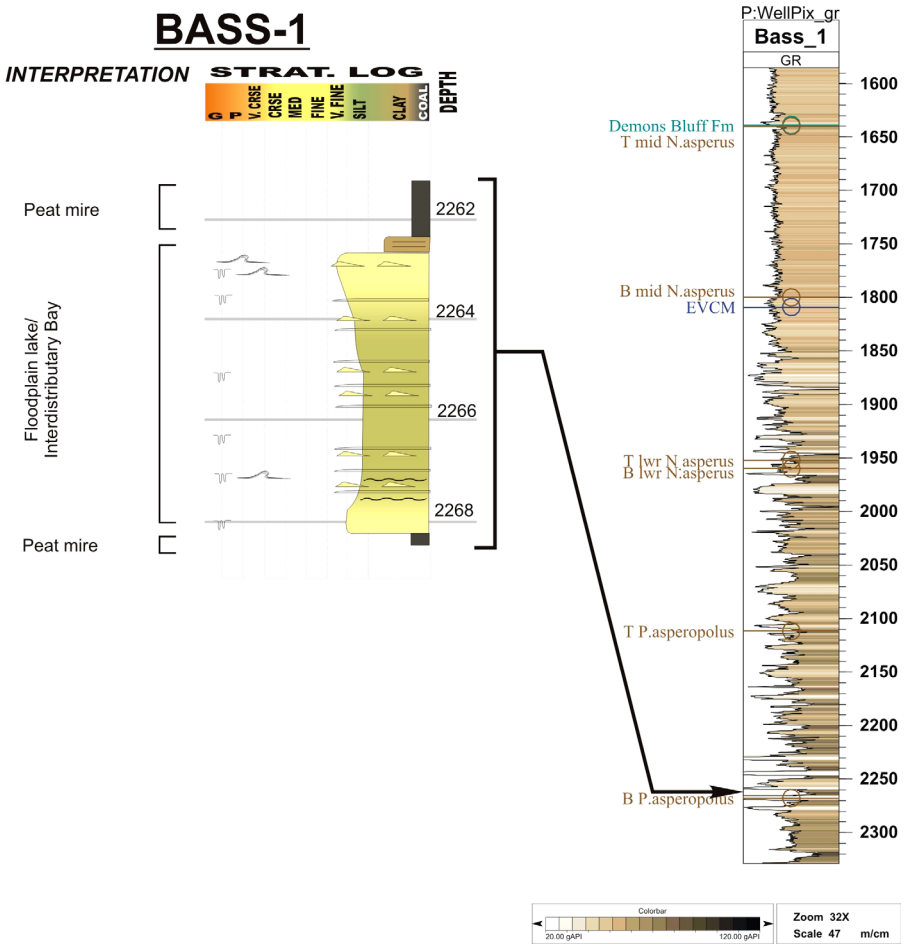
Simon Lang and Rob Root, National Centre for Petroleum Geology and Geophysics

Key for Interpreted Well Log (Gamma Ray)

KEY FOR GRAPHIC LOGS



Bass-1 Interpreted Well Log (Gamma Ray)



Bass-1 Core Photos

Core 11, 1793.14 – 1794.36 m



Core 11, 1798.02 m



Core 12, 1952.55 – 1943.38 m

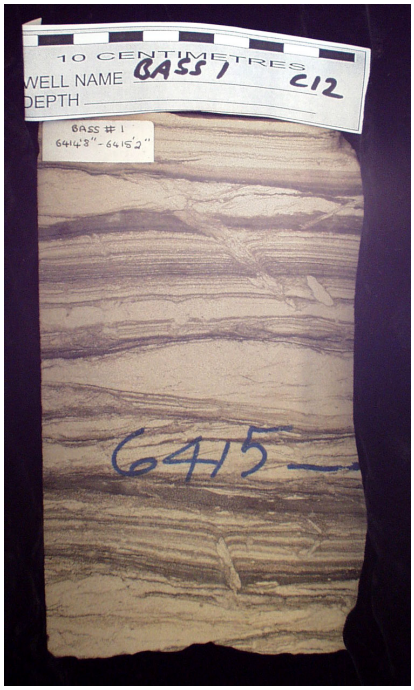


Core 12, 1953.46 –1955.29 m



Bass-1 Core Photos

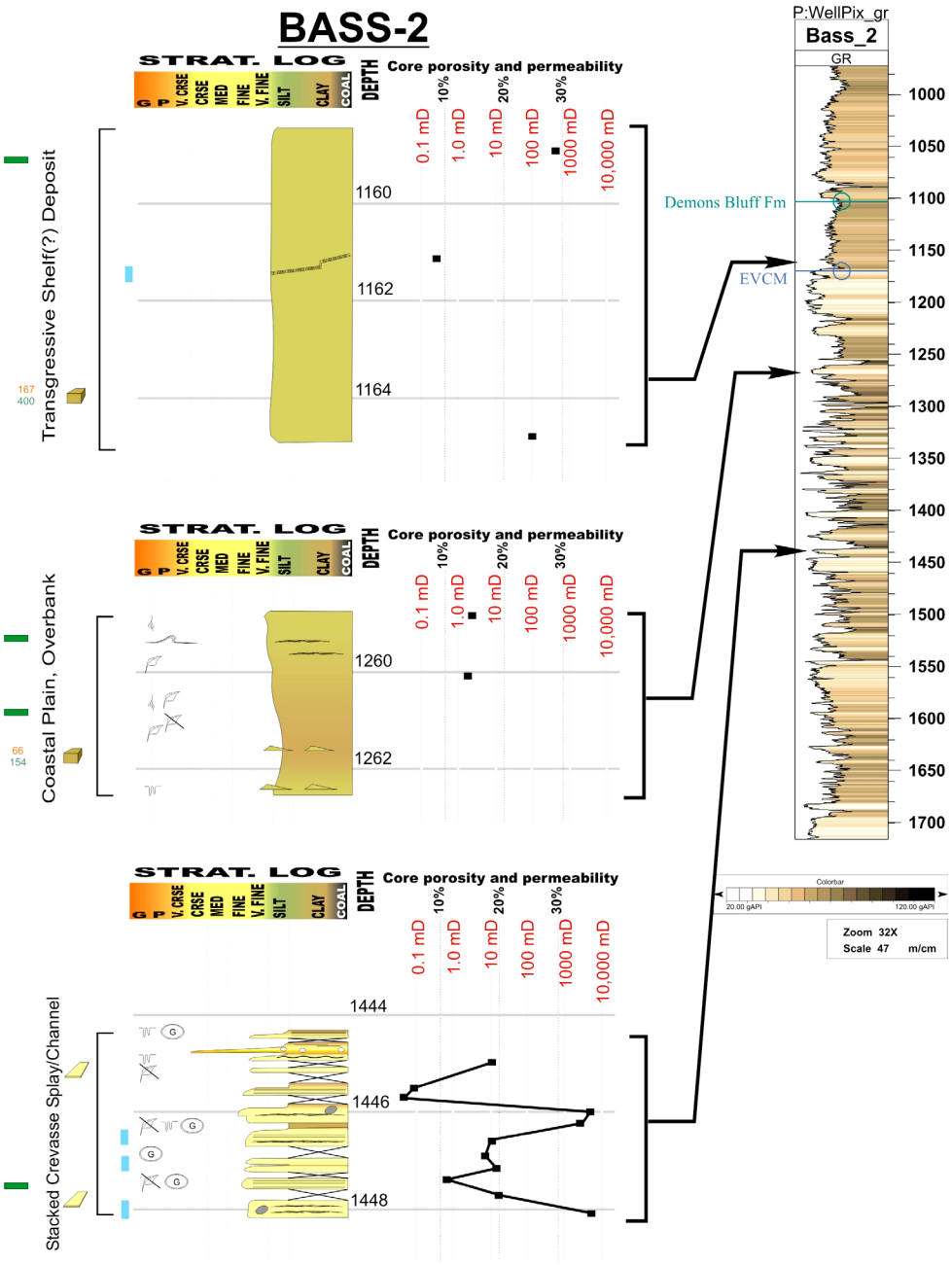
Core 12, 1955.29 m



Core 12, 1956.5 – 1958.34 m



Bass-2 Interpreted Well Log (Gamma Ray)

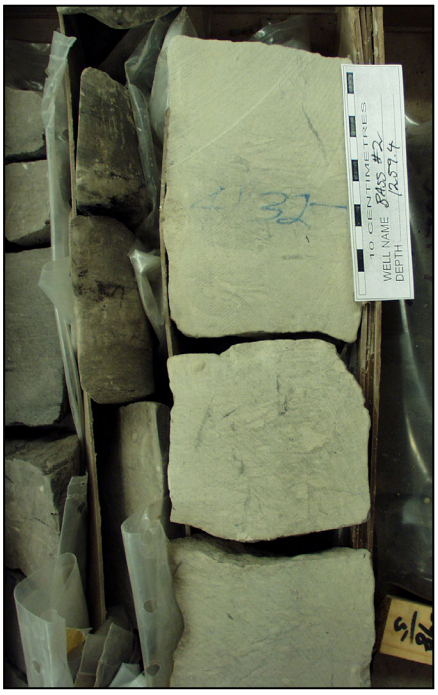


Bass-2 Core Photos

Core 4, 1159.62 m



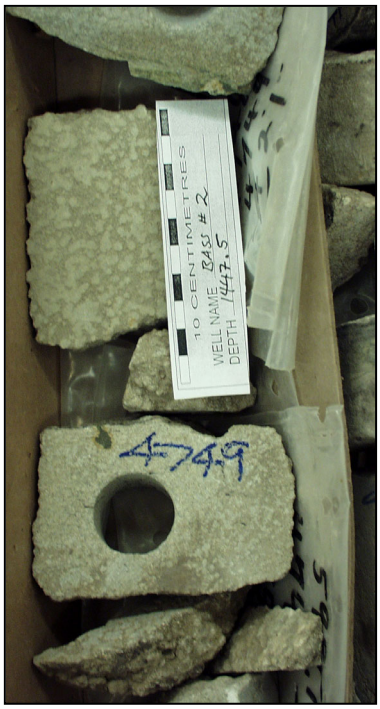
Core 5, 1259.4 m



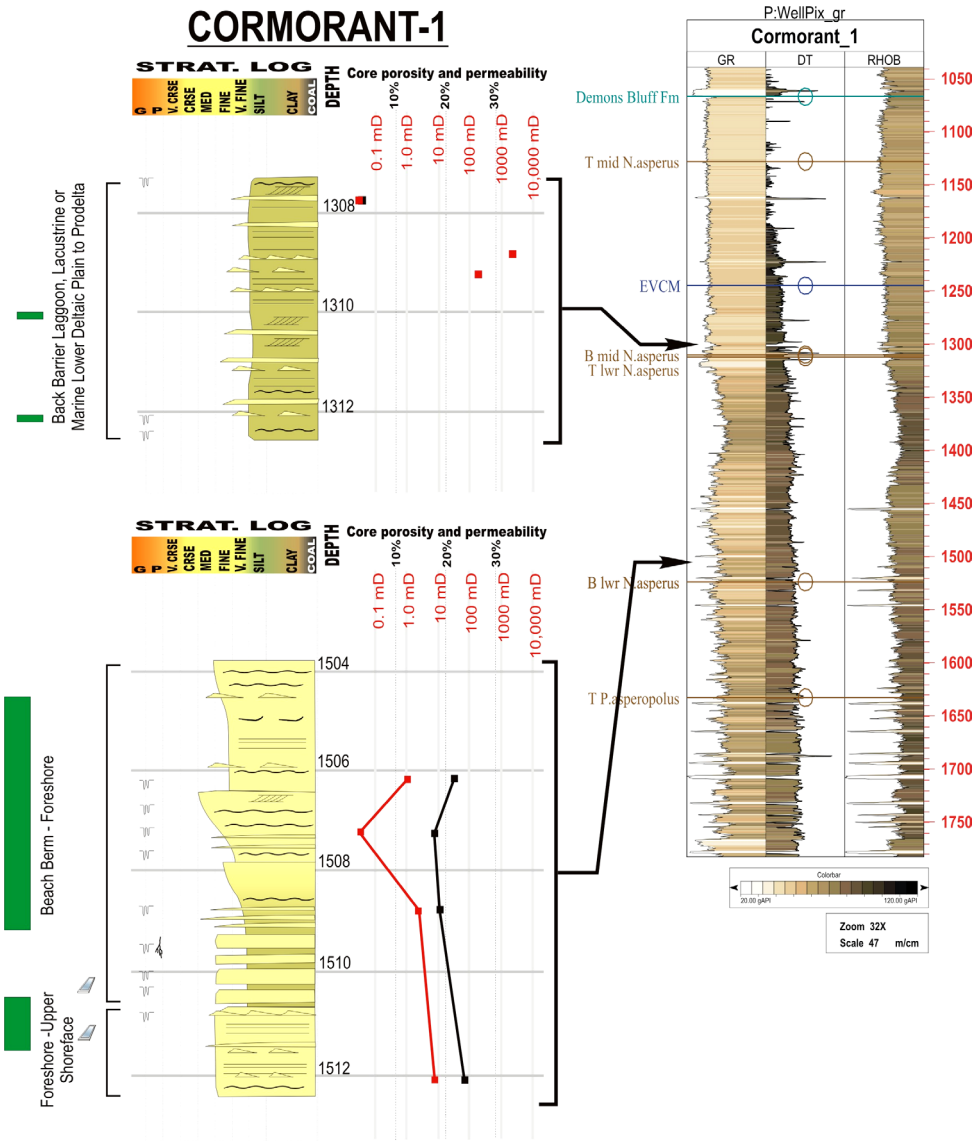
Core 5, 1260.9 m



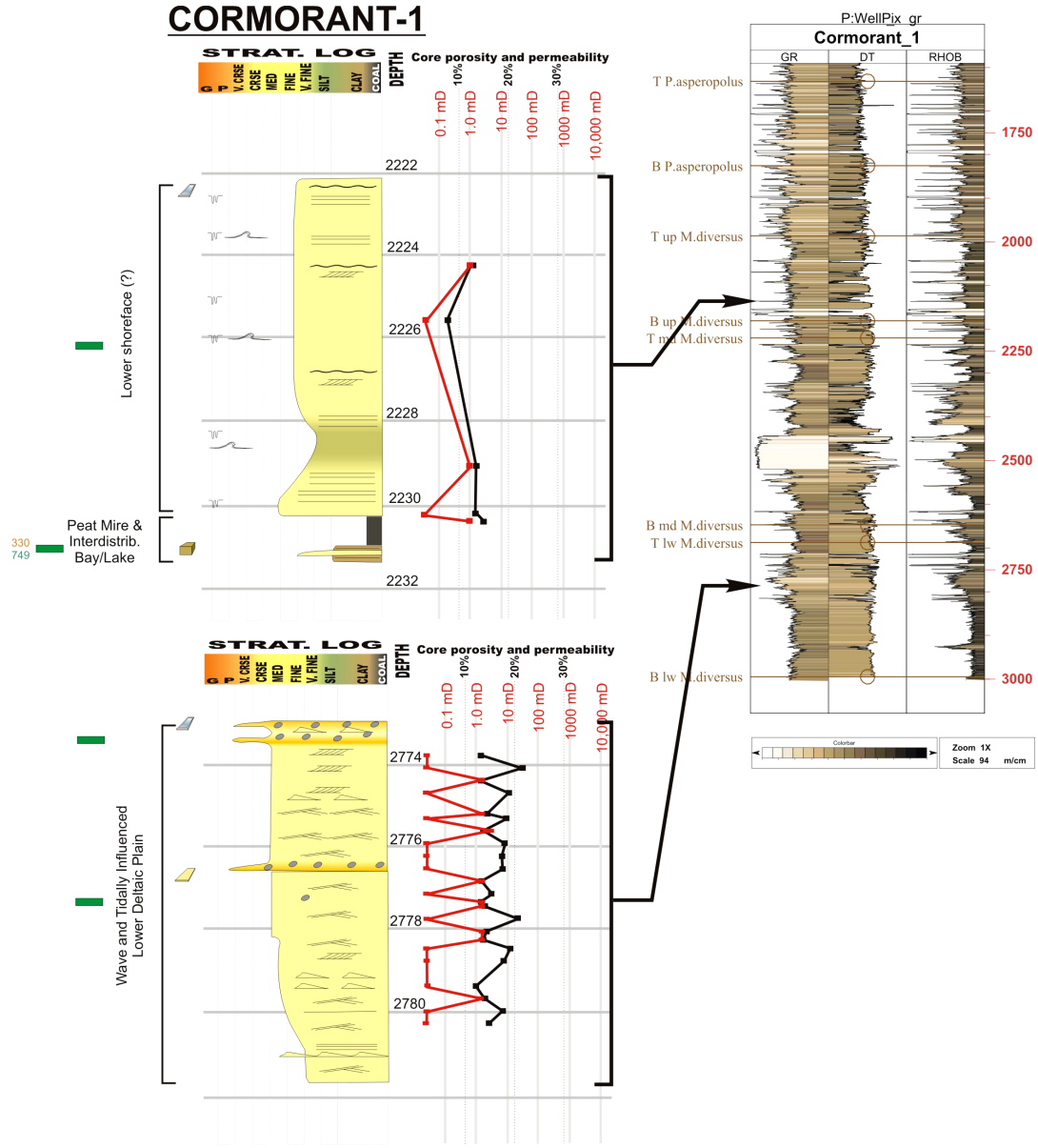
Core 7, 1447.5 m



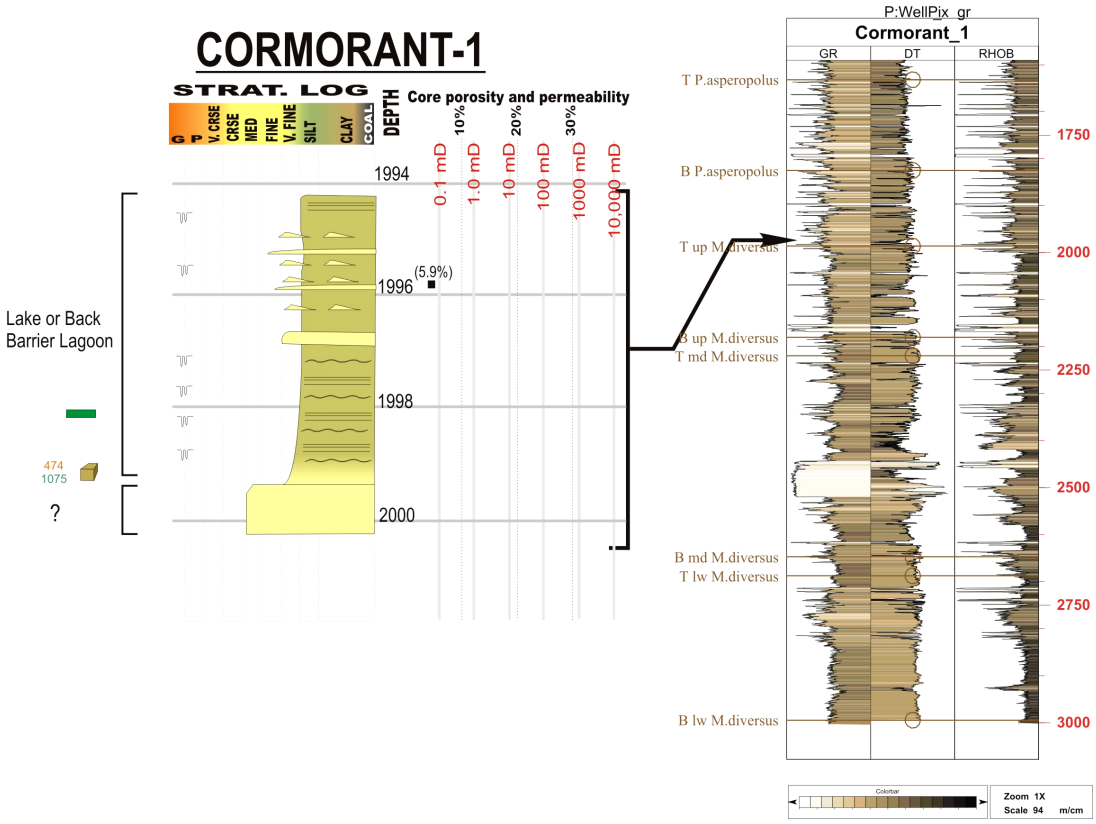
Cormorant-1 Interpreted Well Log (Gamma Ray)



Cormorant-1 Interpreted Well Log (Gamma Ray)



Cormorant-1 Interpreted Well Log (Gamma Ray)

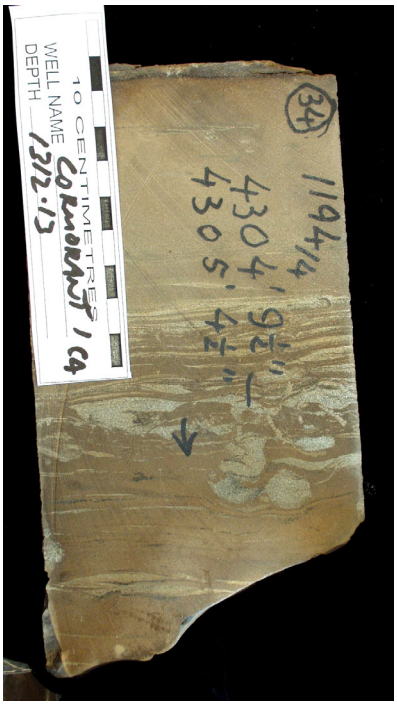


Cormorant-1 Core Photos

Core 3, 1310.33 m



Core 4, 1312.13 m



Core 5, 1504.49 – 1506.93 m



Core 5, 1505.71 – 1507.88 m



Cormorant-1 Core Photos

Core 5, 1507.54 – 1509.2 m



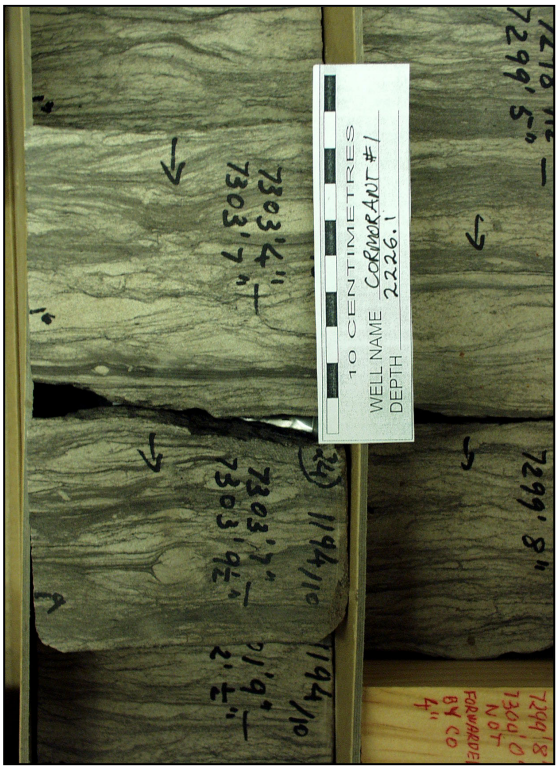
Core 5, 1510-57 – 1511.5 m



Core 9, 1998.2 m

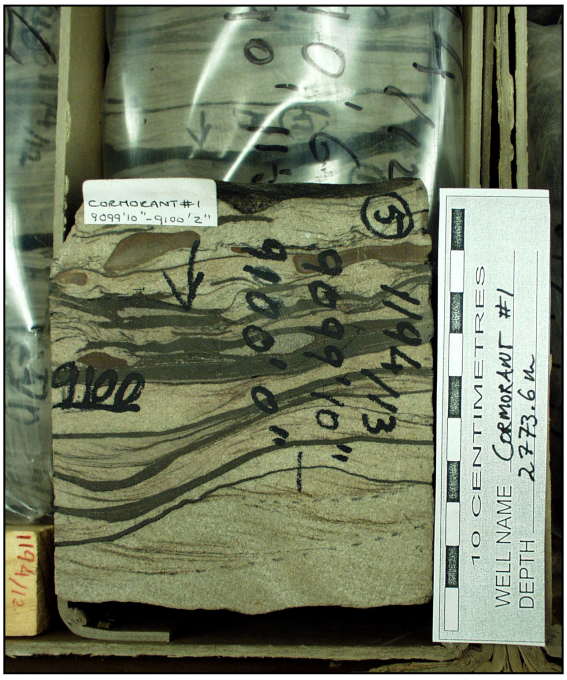


Part Core, 2226.1m

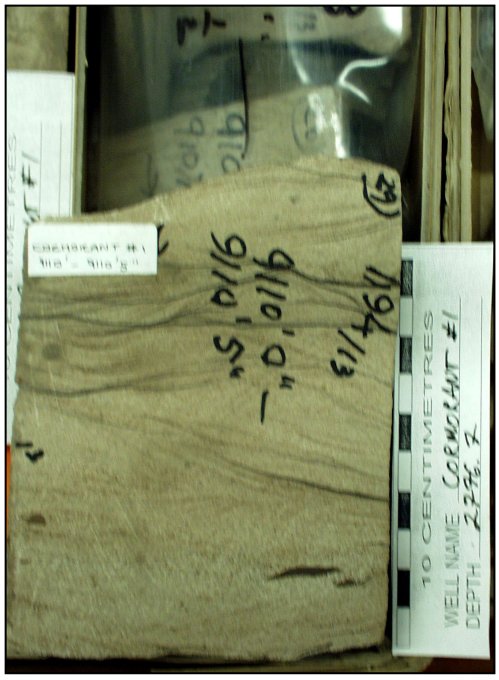


Cormorant-1 Core Photos

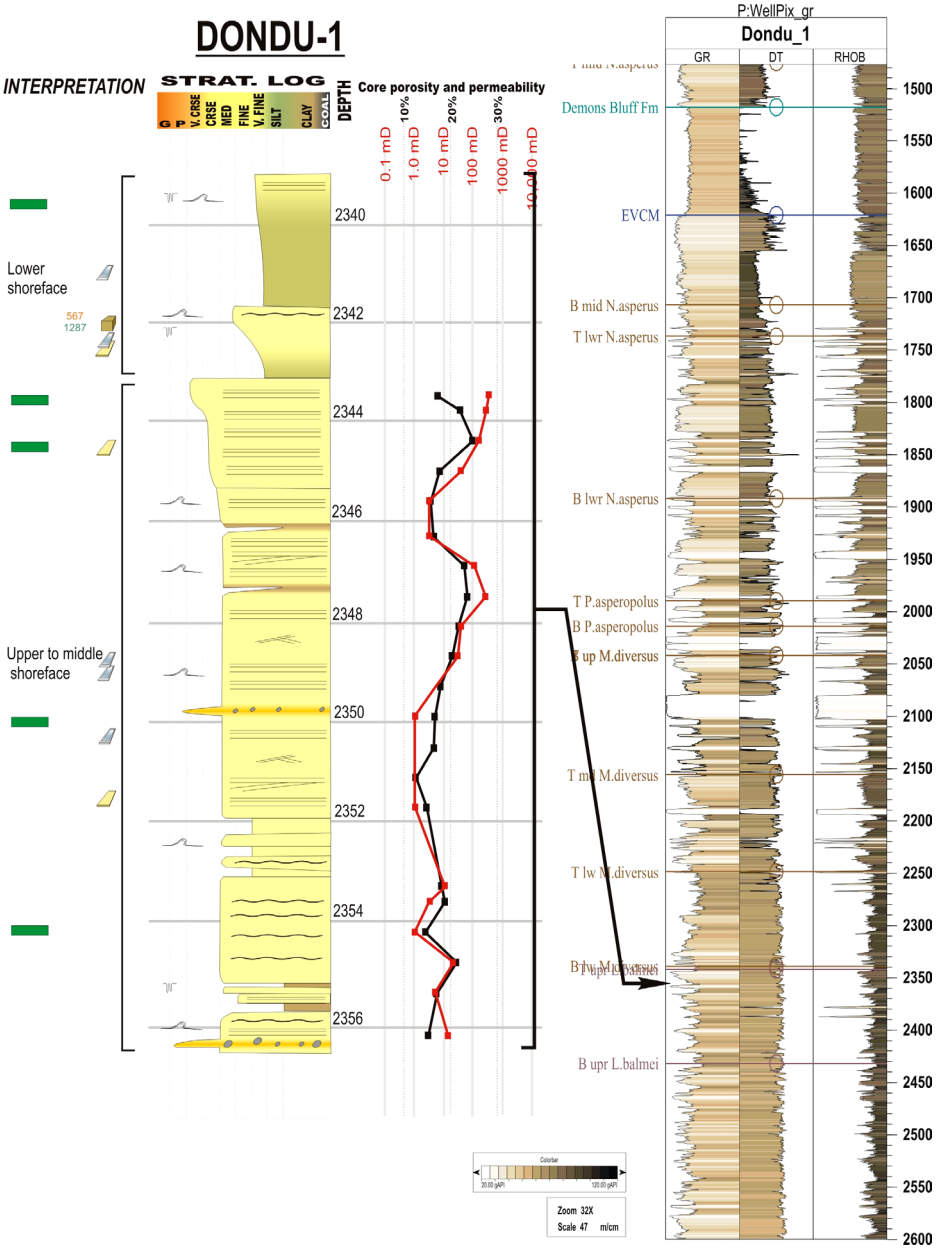
Core 12, 2773.6 m



Core 12, 2776.7 m

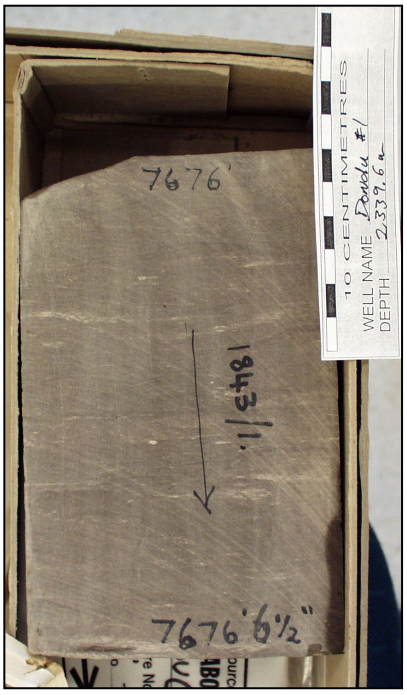


Dondu-1 Interpreted Well Log (Gamma Ray)

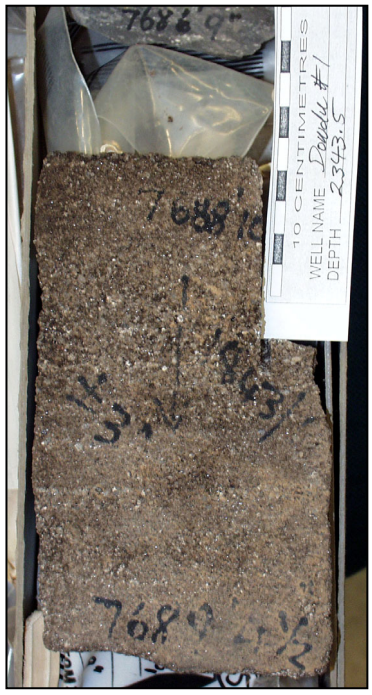


Dondu-1 Core Photos

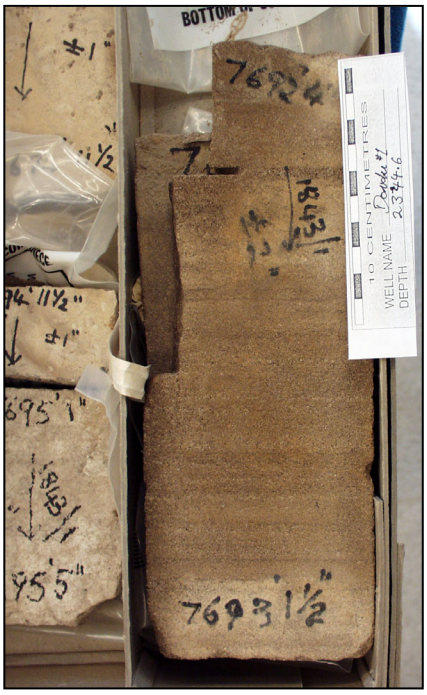
Core 1, 2339.6 m



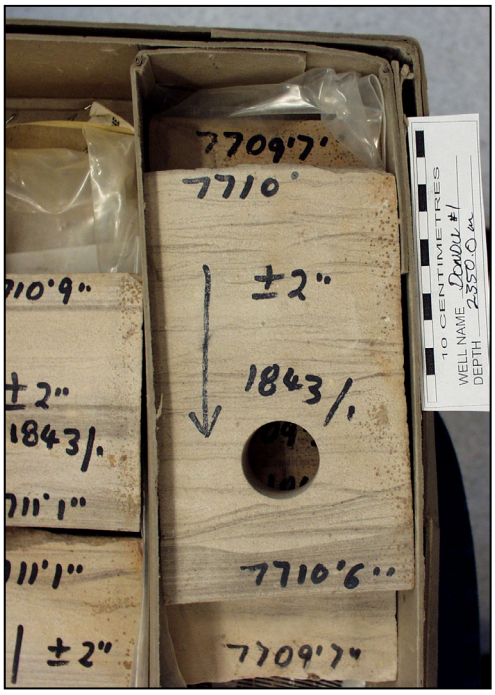
Core 1, 2343.5 m



Core 1, 2344.6 m

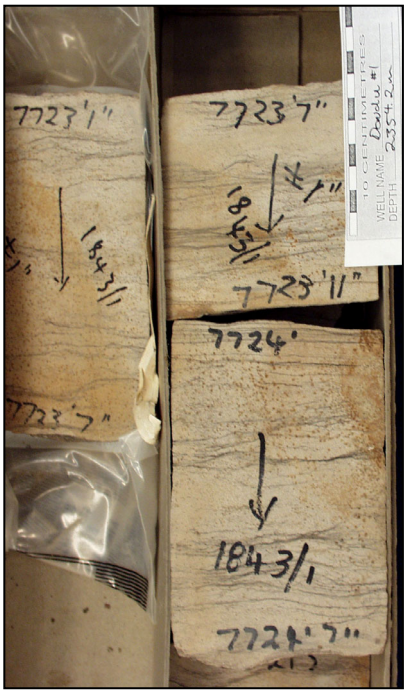


Core 1, 2350.0 m

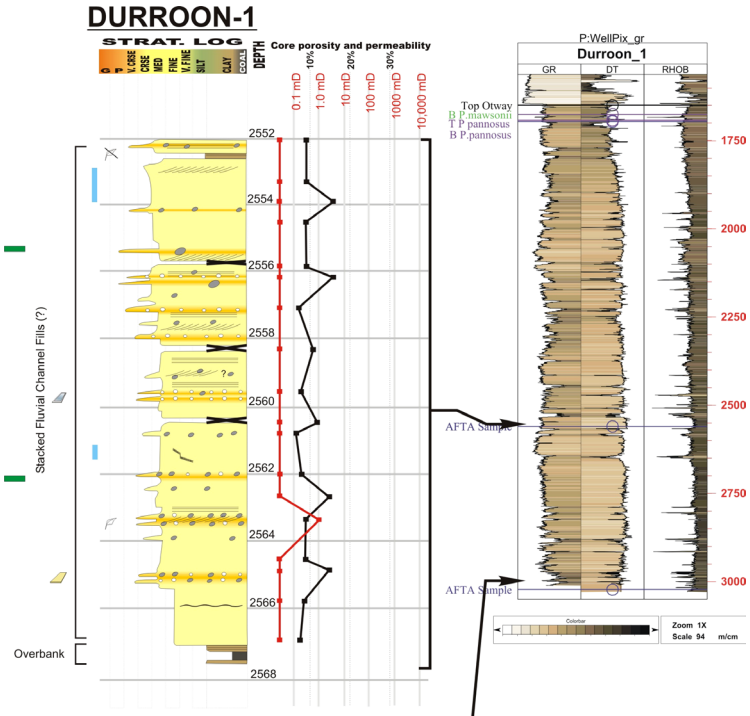


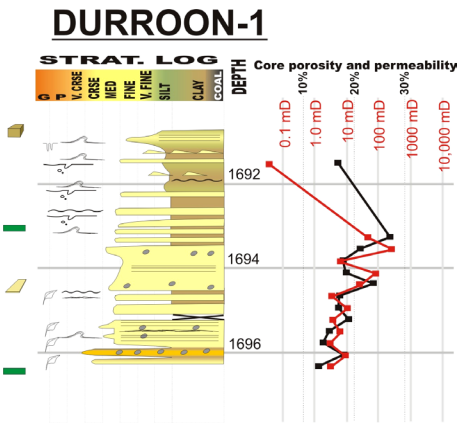
Dondu-1 Core Photos

Core 1, 2354.2 m



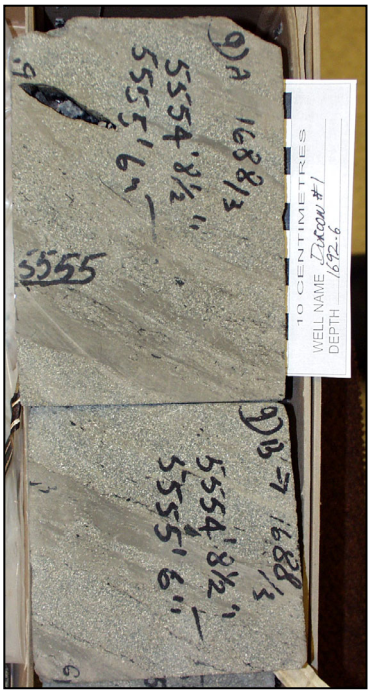
Durroon-1 Interpreted Well Log (Gamma Ray)





Durroon-1 Core Photos

Core 3, 1693.16 m



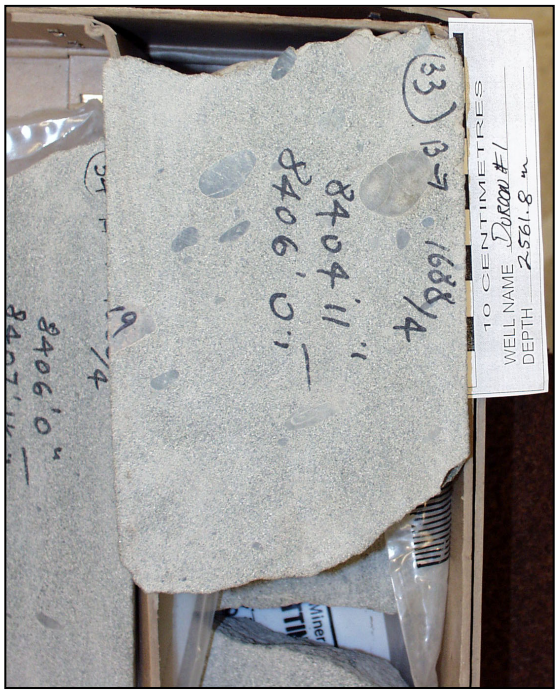
Core 3, 1696.5 m



Core 4, 2555.4 m



Core 4, 2562.15 m

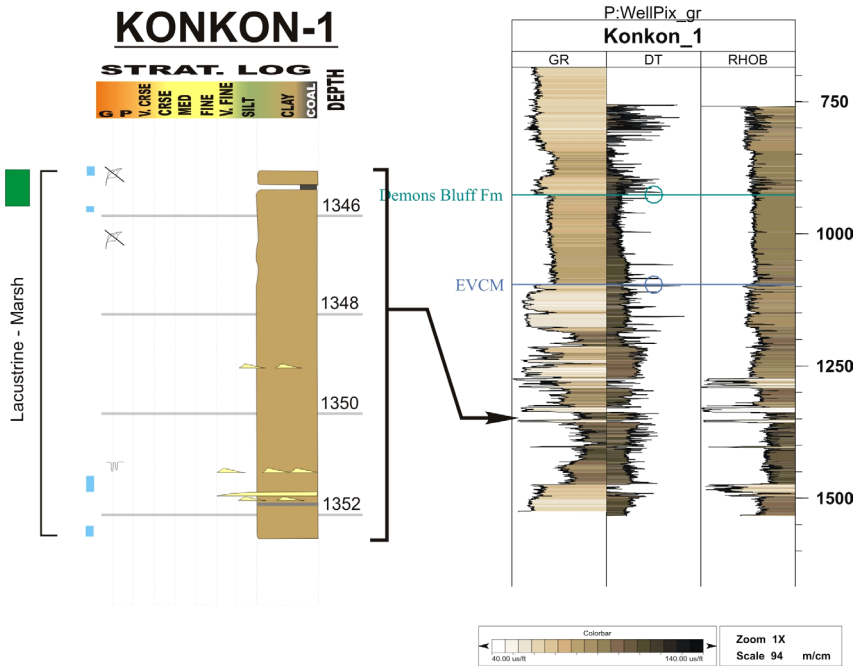


Durroon-1 Core Photos

Core 5, 3021.5 m



Konkon-1 Interpreted Well Log (Gamma Ray)



Konkon-1 Core Photos

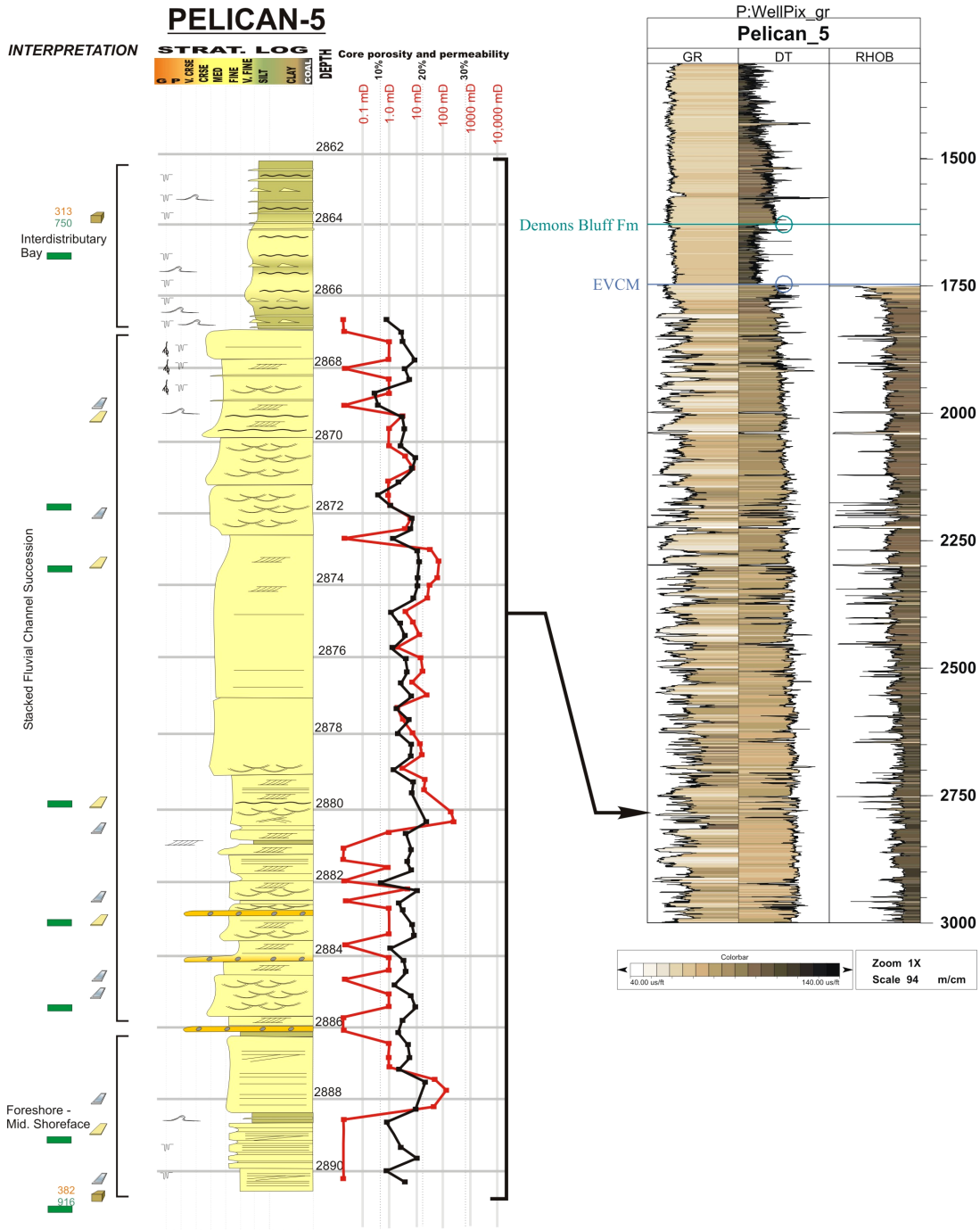
Core 1, 1345.1 m



Core 1, 1345.8 m

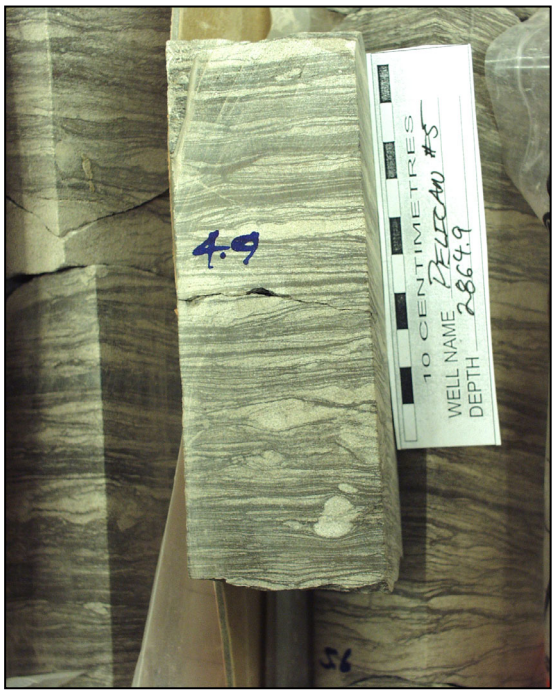


Pelican-5 Interpreted Well Log (Gamma Ray)

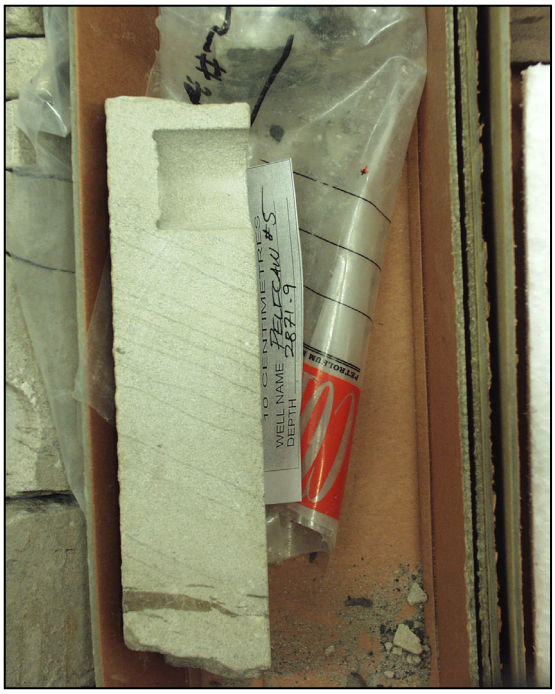


Pelican-5 Core Photos

Core 2, 2864.9 m



Core 2, 2871.9 m



Core 2, 2873.6 m

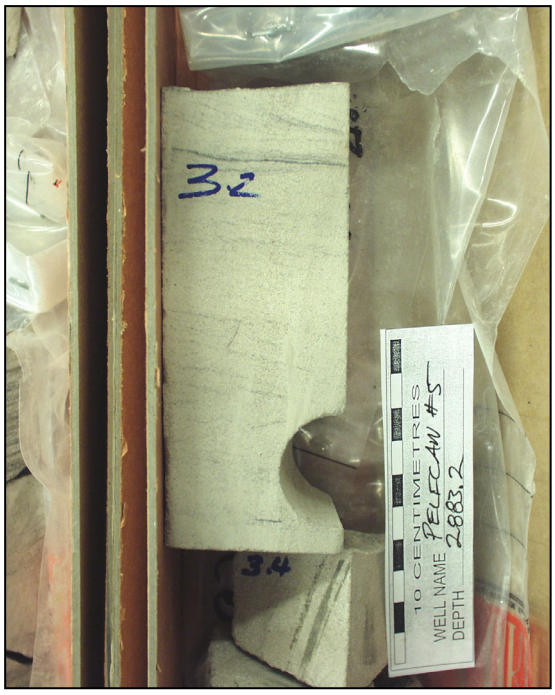


Core 2, 2879.8 m



Pelican-5 Core Photos

Core 3, 2883.2 m



Core 3, 2885.5 m



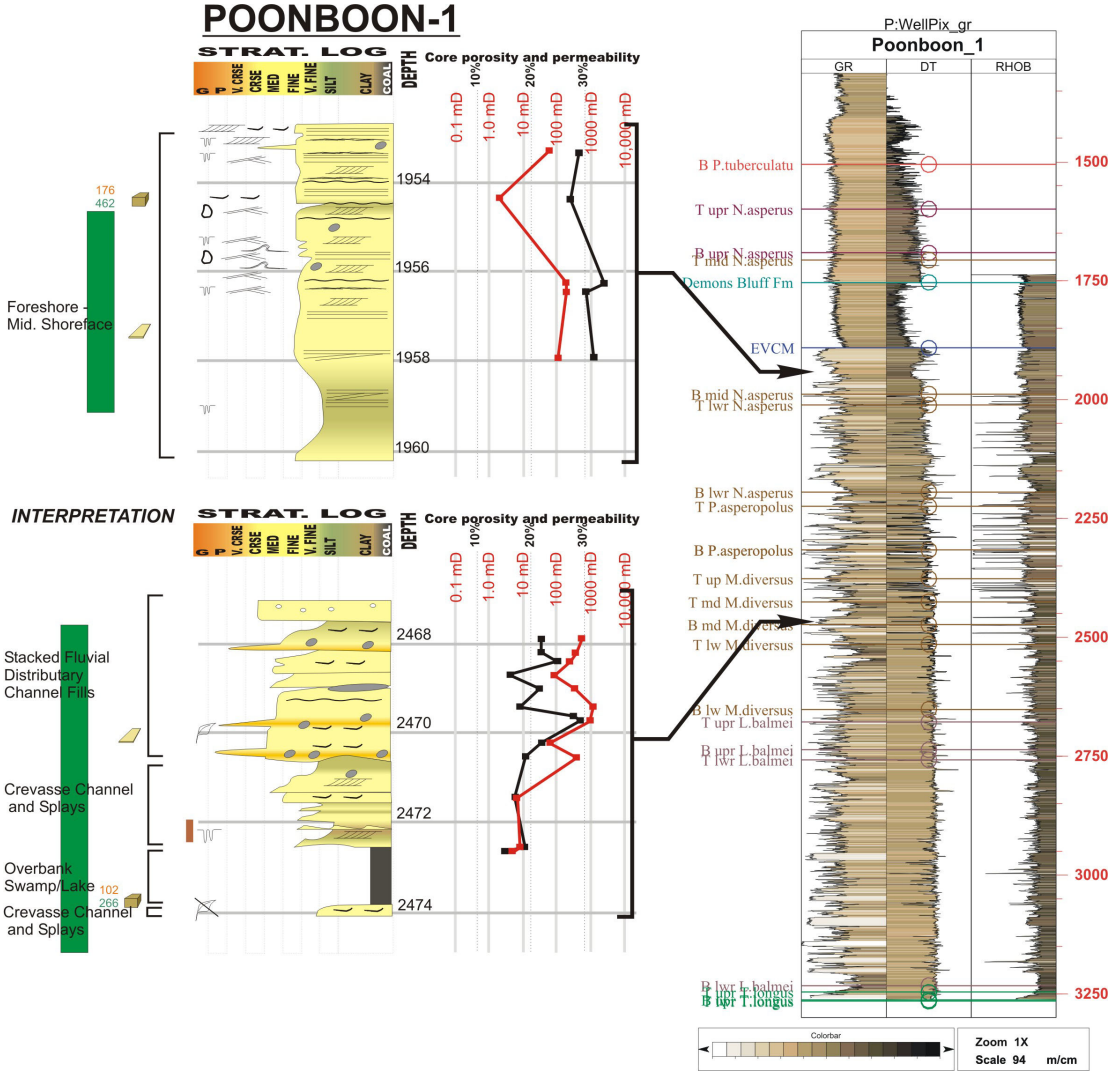
Core 3, 2889.2 m



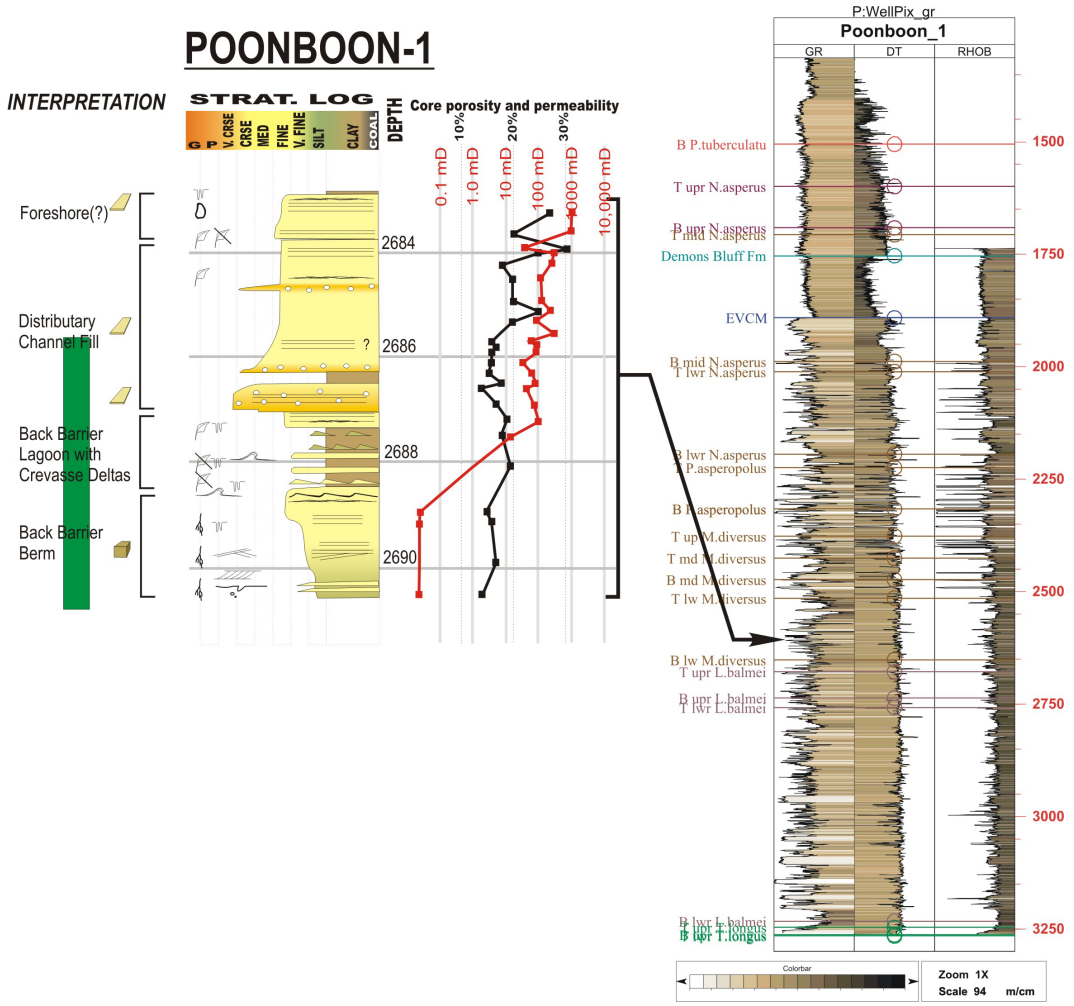
Core 3, 2891.1 m



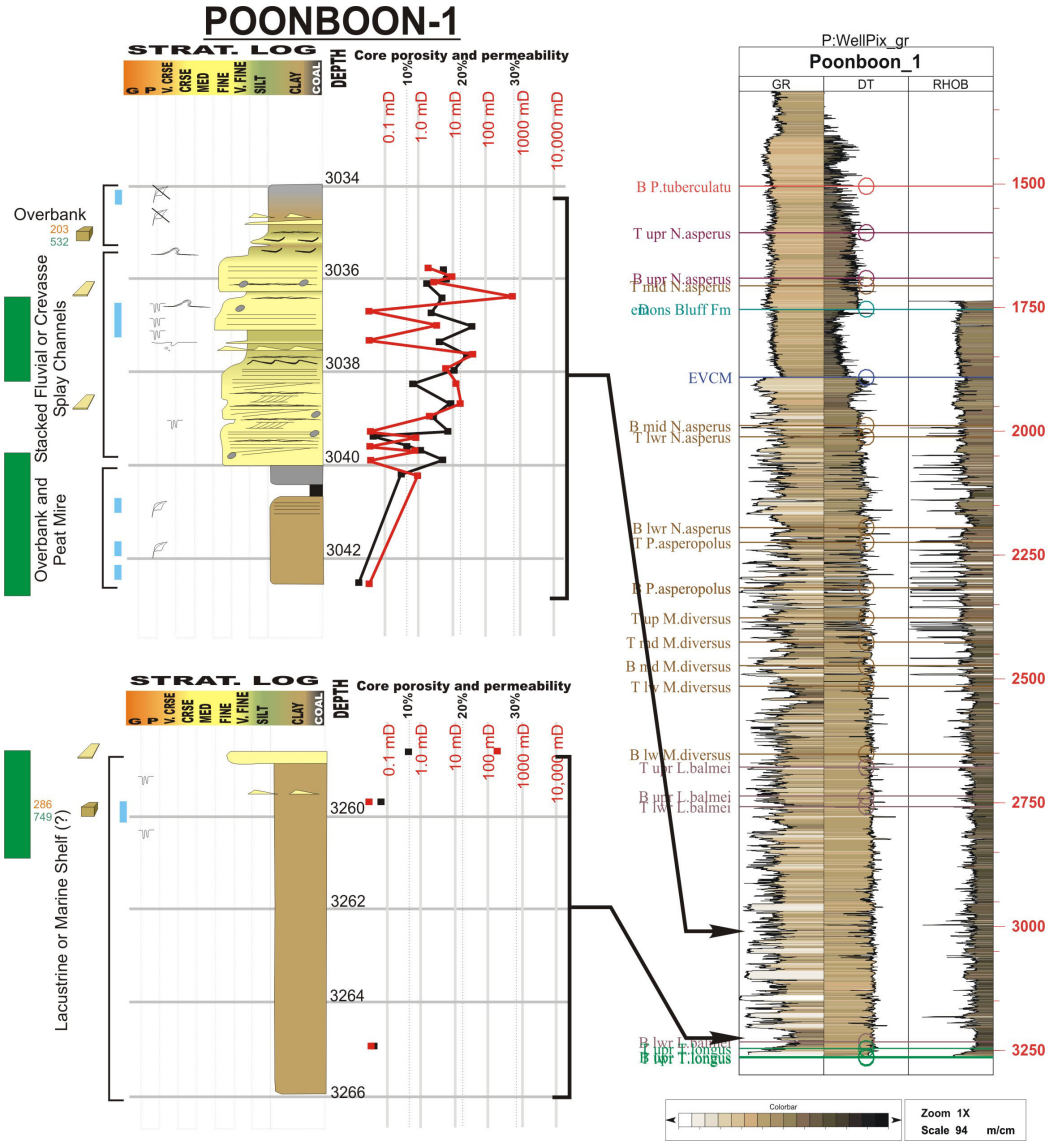
Poonboon-1 Core Photos



Poonboon-1 Core Photos



Poonboon-1 Core Photos



Poonboon-1 Core Photos

Core 1, 1954.77 – 1959.2 m



Core 2, 2467.66 – 2469.79 m



Core 2, 2469.79 – 2474.2 m



Core 3, 2685.6 – 2688.3 m



Poonboon-1 Core Photos

Core 3, 2688.03 – 2690.47 m



Core 4, 3036.41 – 3038.24m



Core 4, 3039.77 – 3041.59 m



Core 4, 3041.59 – 3042.51m

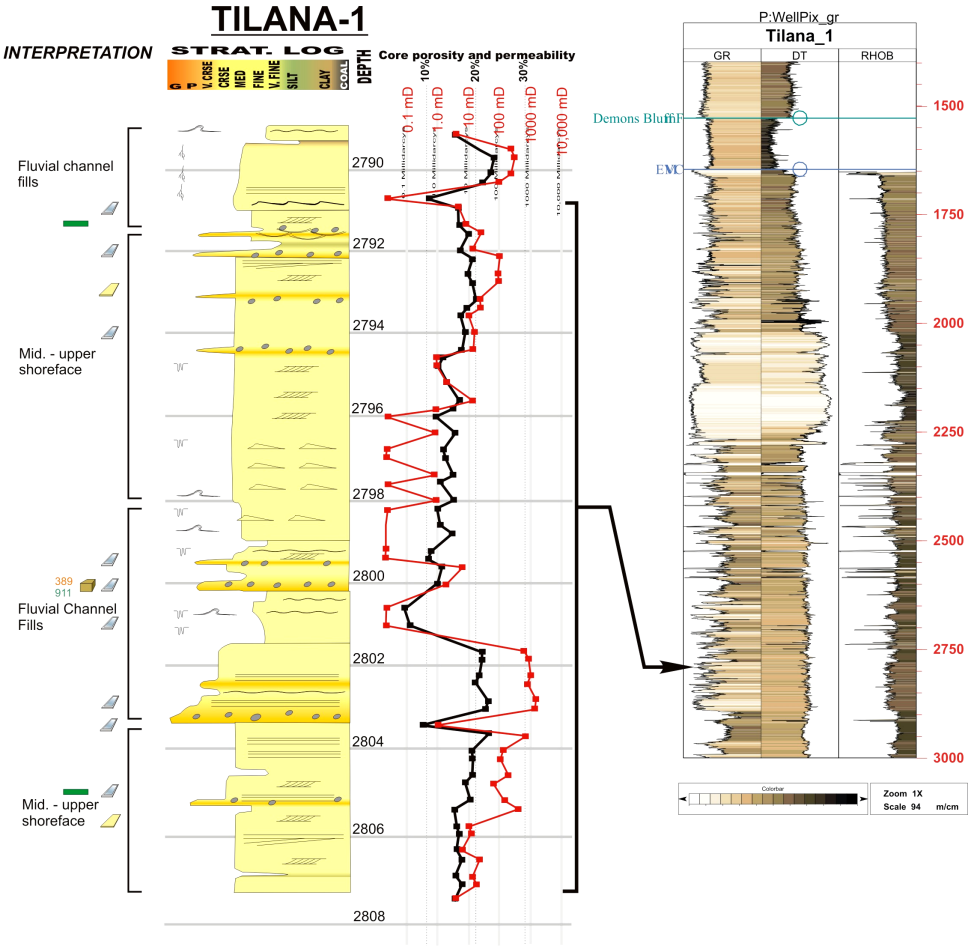


Poonboon-1 Core Photos

Core 5, 3258.61 – 3261.05 m



Tilana-1 Interpreted Well Log (Gamma Ray)

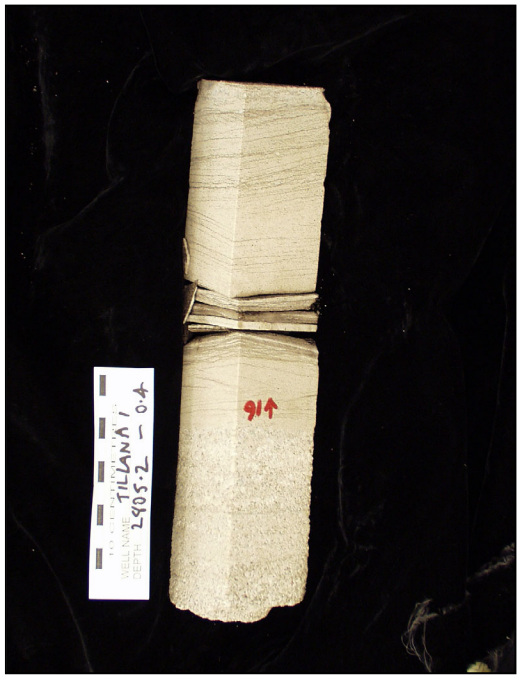


Tilana-1 Core Photos

Core 2, 2791.43 – 2791.44 m

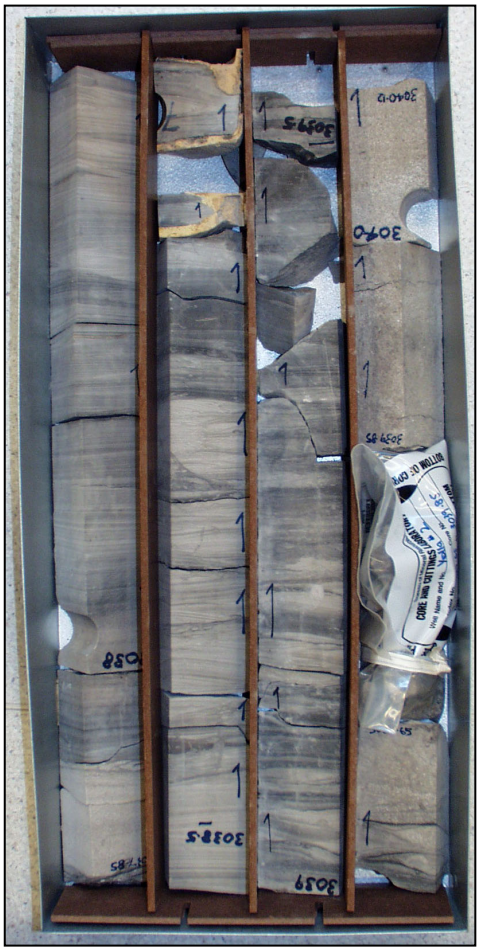


Core 2, 2805.2 – 2805.4 m



Yolla-2 Core Photos

Core 1, 3037.85 – 3040.0 m



Core 1, 3047.5 – 3049.23 m

